William R. Corliss

Scientific
Satellites

NATIONAL AERONAUTICS AND SPACE ADMINISTRATION

Scientific
Satellites

Scientific Satellites

William R. Corliss

FOREWORD

The Space Age began in 1957, with an 83-kilogram Russian satellite beeping greetings to a startled world.

Since that spectacular beginning, intensive effort has gone into the scientific exploration of space and into preparation for manned exploration of the Moon. The early steps have passed into history, and much equipment and instrumentation have already been replaced by later, more complex forms. In the hustle of progress, few men have had opportunity to describe what they have done or used.

There is grave danger that the line of development of space equipment and instrumentation may be lost if care is not given to its preservation. Much information is contained in in-house reports, but, as in all active fields, the records are scattered, often incomplete, and sometimes silent on important points. In time, personnel, too, can be expected to begin to scatter. While it can still be recovered, it is important that this information be recorded. Otherwise, in the future much of the usefulness of present-day measurements could be jeopardized. As future investigators try to assess past results and to combine them with their own, they will need to know accurately how the results were obtained.

Mr. Corliss has undertaken to search out and study the records of equipment and instrumentation on unmanned spacecraft, and to put his findings in usable form. He has gone back to ultimate sources, even to the personnel involved, in NASA, in the U.S. Air Force, and among many of their contractors. He has tried to uncover the actual designs used. For his task, he is well prepared. An engineer by profession, he is engaged in a successful technical-writing career. The space effort and the space scientist are in his debt for his efforts.

This book, accurate, well organized, and truly readable, should interest layman, engineer, and scientist. Each will be able to

see for himself the fascinating growth of the vehicles and instruments that have brought unmanned space science to its present position.

John E. Naugle
Deputy Associate Administrator (Sciences)
Office of Space Science and Applications
National Aeronautics and Space Administration

CONTENTS

Part I

PRESENT STATUS AND HISTORY

Chapter 1

STATUS AND OBJECTIVES OF SATELLITE SCIENCE

1–1.   Advantages of the Satellite Instrument Platform

More than 600 Earth satellites have been orbited since October 4, 1957, when Sputnik 1 first circled the globe.   Almost every one of these satellites has carried a cargo of scientific instruments, even though military or engineering objectives have sometimes been foremost.   Typical satellite-borne sensors are micrometeoroid microphones, magnetometers, plasma probes, and the ubiquitous radiation detectors.   Radio signals from these miniature, unmanned observatories and the study of scientific capsules ejected from them have enabled scientists to map partly the complex fluxes of radiation and micrometeoroids that crisscross a vast Earth-centered region stretching from an altitude of 150 kilometers to beyond the Moon's orbit.   Satellites also serve as platforms for astronomical instruments that image the Sun and stars at wavelengths that cannot penetrate the Earth's atmospheric shield.

The scientific value of the Earth satellite stems from four generic properties that are possessed imperfectly or not at all by high-altitude balloons and sounding rockets:

(1) Long-term immersion in the space medium, permitting direct measurements of the space environment

(2) Long-term location of a relatively stable instrument platform high above the absorbing, distorting, and noisy atmosphere of the Earth, opening up the electromagnetic spectrum from five to 18 decades ($\sim$3 km to $\sim$3$\times$10^{-5} Å).   (See fig. 1–1.)   The charged-particle shielding effectiveness of the Earth's magnetic field is also reduced at satellite distances, particularly for those elliptic orbits that penetrate the magnetopause.

TABLE 1–1.—*Typical Satellite Research Areas* [a]

Field or discipline	Research opportunities due to long-term immersion in the space medium	Research opportunities due to removal of absorption and distortion effects	Research opportunities due to the unique position and environment
Aeronomy [b]	Direct measurement of temperatures, densities, winds, turublence, and populations of neutral and ionized species.	-------	Ground observation of drag effects and calculation of density. Direct measurement of Earth's energy budget.
Ionospheric and auroral physics.	Global surveys of electron concentration as a function of time. Direct measurement of irregularities and interactions with solar phenomena. Auroral particle densities and identities. Precipitation rate from radiation belts. Origin of auroras.	Ultraviolet and infrared spectroscopy of auroras.	Electron density by topside sounding. Electron density by measurement of Doppler and Faraday effects on satellite transmissions. (Signal scintillations indicate turbulence.) Shape, transients, and photometry of auroras from new vantage points.
Trapped radiation	Direct measurement of fluxes and compositions as functions of time and space.	-------	
Geomagnetism	Direct measurement of Earth's field and its fluctuations. Determination of shape of magnetopause and "wakes" of Earth and Moon.	Direct measurement of undistorted interplanetary field outside shielding of magnetopause.	

Geodesy			Inference of Earth's shape, mass, and internal structure from observations of satellites.
Meteoritics	Direct measurements of fluxes, sizes, velocities, and compositions.		
Solar physics	Direct measurement of solar wind and the extension of the corona.	Solar processes as revealed by ultraviolet radiation, X-rays, radio noise, and infrared radiation.	Macrostructure of solar wind, plasma tongues, and magnetic field as Earth moves around the Sun.
Stellar astronomy		Same as above, but extended to quasars, neutron stars, etc.	
Interstellar physics		Ultraviolet reddening law. Study of zodiacal light at short and long wavelengths. Detection of molecular hydrogen.	
Cosmic-ray physics		Measurement of fluxes and compositions above the atmosphere.	
Cosmology		Secular changes in gravitation constant.	Velocity dependence of gravitation constant. Time dilation.
Biology	Detection of indigenous life at high altitudes. Evidence for or against panspermia.		Effects of zero-g, space radiation, and lack of 24-hr cycle on organisms.

[a] Note the abundant "mapping" opportunities.
[b] Meteorological applications not included.

Solar plasma

Some cosmic rays

Magnetopause

Satellite range

Radio waves

Photons, energetic cosmic rays

H_2O O_3

H_2O CO_2 O_2

Sounding-rocket range

Ionosphere

Molecules

Molecules, atoms, nuclei

Atmospheric absorption mechanisms

Radio window

Optical window

Ground level

1km   1m   1cm   1μ   100Å   1Å   1x

Visible

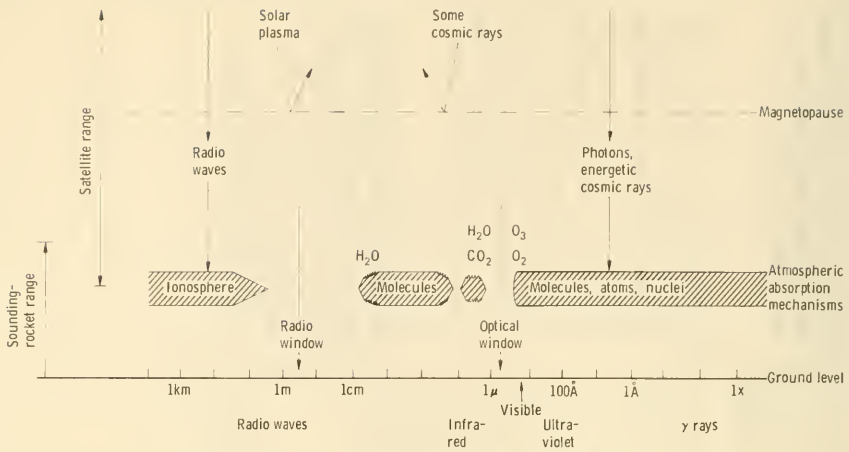Radio waves   Infra-red   Ultra-violet   γ rays

FIGURE 1–1.—The Earth's magnetosphere and atmosphere prevent most photonic and particulate radiation that arrives from outer space from reaching instruments on the ground. Satellites provide stable, long-lived instrument platforms above these insulating and interfering phenomena. See additional information on near-Earth environments in figures 1–2 through 1–13.

(3) Advantage of position. There is scientific utility in observing the Earth from afar (meteorology) and, in turn, watching satellites from the ground (geodesy and ionospheric research).

(4) The unique aspects of the space environment—zero gravity, radiation, absence of the Earth's 24-hour rhythm—present opportunities to study life from new vantage points.

In short, the availability of satellite instrument platforms has immensely stimulated many scientific disciplines. Table 1–1 shows in more detail how the special advantages of the satellite are being employed by science.

Some Disadvantages.—The lengthy list of inviting research opportunities in table 1–1 should not be allowed to obscure the disadvantages of satellite research, which are:

(1) Extreme weight, volume, and power limitations

(2) The separation of the experimenter and his equipment by hundreds of kilometers, making maintenance impossible and experimental adjustments difficult

(3) The need for much higher equipment reliability than in Earth-based laboratories

(4) The sensitive electromagnetic, mechanical, spatial, and other interfaces that exist between each experiment and the rest of the spacecraft

(5) Hard vacuum, space radiation, the traumatic launch environment, and so on

(6) The restrictive problems of working within a large, highly integrated, rigorously scheduled enterprise

(7) The gamble of appreciable time and effort against the perversity of rocket and machine.   The possibility of failure through the fault of someone else.

All experimenters recognize that Earth-based research is itself not completely free from these problems.   The existence of the problems has not reduced the queue waiting for satellite space. The scientific payoff is well worth the gamble (ch. 10).

While most satellites carry scientific instruments, other objectives may predominate.   In addition to the military satellites and scientific satellites is a third class, the applications satellites, typified by weather and communication satellites.   A fourth class consists of the technology satellites, which are designed to test spacecraft materials and components under actual operating conditions.   Semantics notwithstanding, abundant valuable geophysical data have been obtained from military and applications satellites that have included scientific instruments among their payloads or from military spacecraft carrying piggyback instrument pods.   In fact, any satellite, even though instrumentally inert, helps us to measure better the figure of the Earth and the density of the upper atmosphere.

1–2.   Status of Satellite Science

Satellite science contains segments of several conventional scientific disciplines.   It is mostly geophysics, but certainly not all, because fields such as seismology are obviously excluded, save for where satellites relay data from remote, ground-based stations. Satellite science also embraces portions of astronomy, solar physics, cosmology, and even biology (table 1–2).   Scientific satellites are primarily research tools; consequently, satellite science includes only those parts of science where these tools perform better than sounding rockets, terrestrial observatories, and other means to the same ends.

The general purpose of this section is to outline very briefly the present state of satellite science in the fields listed in table 1–2. The primary purpose is to show what satellites have contributed already and where they will be valuable in the future.   For more thorough reviews of space science, see the journal *Space Science*

TABLE 1–2.—*The Extent of Satellite Science*

Fields where scientific satellites make major contributions	More inclusive disciplines
Aeronomy_____.	
Ionospheric and auroral physics _____.	
Trapped radiation_____	Geophysics
Geomagnetism_____	
Geodesy_____	
Meteoritics_____.	
Solar physics_____.	
Stellar astronomy_____	Astronomy and astrophysics
Interstellar physics_____.	
Cosmic-ray physics_____	Cosmology
Cosmology_____	
Biology_____.	Biology

Reviews, the several collections of COSPAR [1] papers published in volumes entitled *Space Research* (refs. 1–5), and *Sourcebook on the Space Sciences* (ref. 6).

Aeronomy.—The Earth's upper atmosphere is well and continuously explored by aircraft and balloons up to 150 kilometers. (See fig. 1–2.) (Ref. 7.)   Sounding rockets commonly carry instruments up to 250 kilometers and higher, but their periods of useful observation are measured in minutes.   The realm of the scientific satellite begins at 150 kilometers and extends outward several hundred thousand kilometers.   Onboard instruments directly measure temperature, density, the compositions of neutral and ionized populations, fluctuations in these parameters, and energy inputs from the Sun and Earth.   Furthermore, satellites can be observed from the Earth and inferences made concerning drag forces and air density.

Mapping the atmosphere is the primary function of an aeronomy satellite.   From point values of temperature, pressure, density, and composition, one draws graphs, such as figures 1–3 and 1–4, showing the average characteristics of the atmosphere.   Such maps are relatively constant in time below 100 kilometers.   Above this level, the solar ultraviolet radiation, plasma streams, and magnetohydrodynamic waves cause large variations in the parameters.   The density of the upper atmosphere, for example, may vary by a factor of 4 between the sunlit and dark sides of the Earth. Several hundred kilometers out, temperatures fluctuate hundreds of degrees as the Sun rotates in its 27-day period and

---

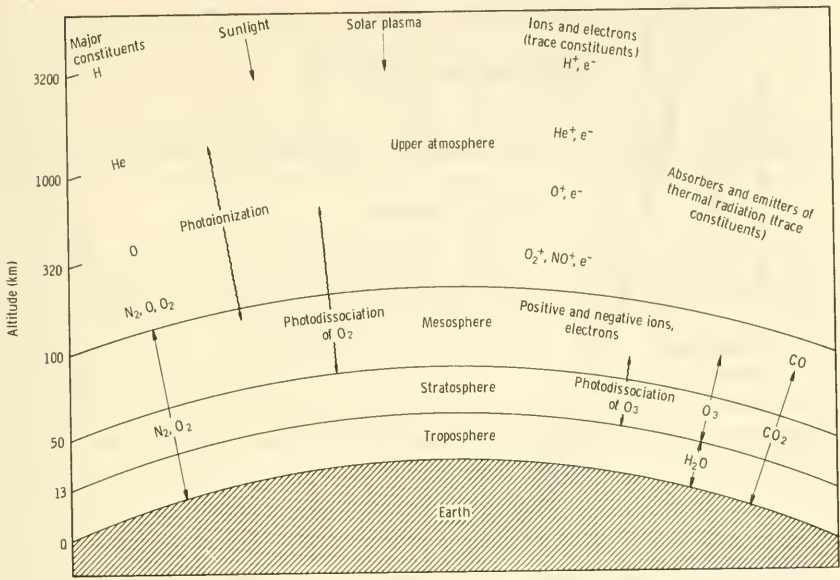[1] COSPAR=Committee on Space Research, an international committee of scientists.

FIGURE 1–2.—Structure and composition of the Earth's atmosphere and some of the physical phenomena that control its characteristics. (Adapted from ref. 7.)
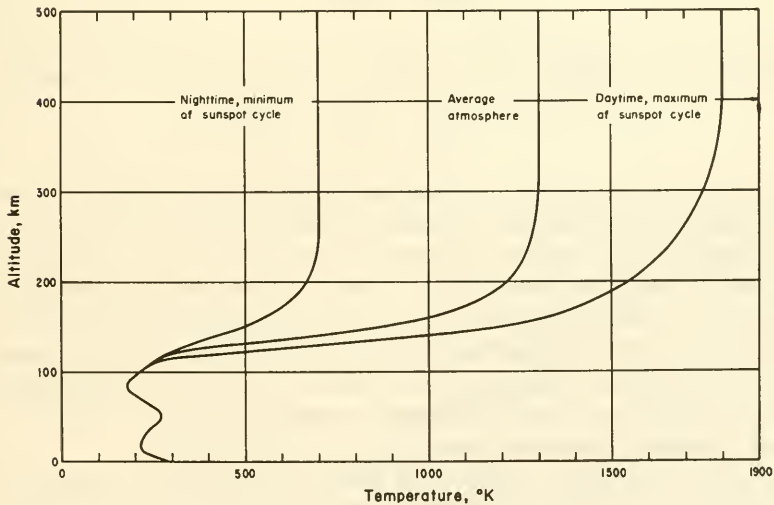

FIGURE 1–3.—Typical temperature distributions for nighttime conditions near sunspot minimum, for daytime conditions near sunspot minimum, and for an average situation. At high altitudes, the effects of solar forces are extremely large (ref. 8).
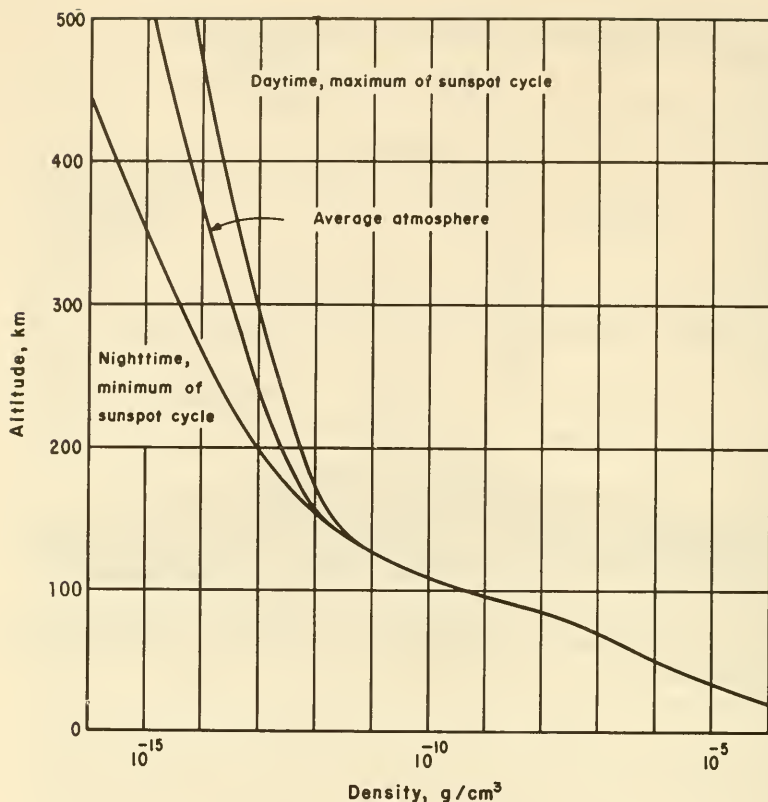
FIGURE 1-4.—Density of the Earth's atmosphere for the same conditions described in figure 1-3 (ref. 8).

active areas on its surface sweep the Earth with streams of ultraviolet photons and energetic particles (refs. 9–11).

A classical and typical illustration of the value of scientific satellites to aeronomy came when Nicolet, after careful studies of drag-induced perturbations of the Echo I orbit, postulated the existence of a layer of helium between the oxygen-nitrogen substratum and the hydrogen outer envelope (ref. 12). Subsequent studies by Bourdeau, using plasma probes on Explorer VIII, confirmed Nicolet's deduction (ref. 13). (See fig. 1–2.)

Scientific satellites not only are useful in refining our maps of the constantly shifting atmosphere but also, by virtue of their location, they can measure the ultraviolet flux of the Sun and the energy input from the solar wind. Here is a sensitive interface between aeronomy and the field of solar physics; it is discussed

further on page 18.   The Sun is the wellspring of energy that creates many of the phenomena we are endeavoring to map. Ideally, by measuring the thermal and ionizing forces impressed upon the atmosphere by the Sun, scientists could deduce the maps from first principles.   Unfortunately, we know even less about the upper atmosphere than we do about weather at low levels.

Future scientific satellites must play a twofold role: (1) make more detailed maps of the upper atmosphere, using direct sampling techniques, and (2) measure more precisely the forces that the Sun exerts.   From such data, scientists will construct better cause-and-effect models.

Ionospheric and Auroral Physics.—Beginning at about 50 kilometers, sounding rockets and satellites encounter the Earth's ionosphere, which is constituted of ever-changing regions of ionized gases created by solar ultraviolet and particulate radiation (figs. 1–5 and 1–6).   The ionosphere coexists with the neutral atmosphere and lies far below the belts of trapped radiation (refs. 11, 14, 15). (See fig. 1–7.)

The existence of ionized regions high above the Earth was suggested early in this century to explain anomalous transmissions of radio signals far beyond the line of sight.   By midcentury, ground-
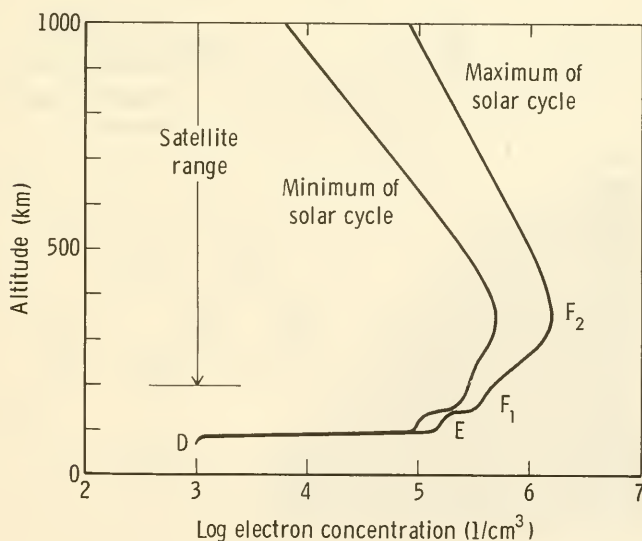

FIGURE 1–5.—Daytime electron concentration in the ionosphere at the extremes of the solar cycle. (Adapted from ref. 16.)
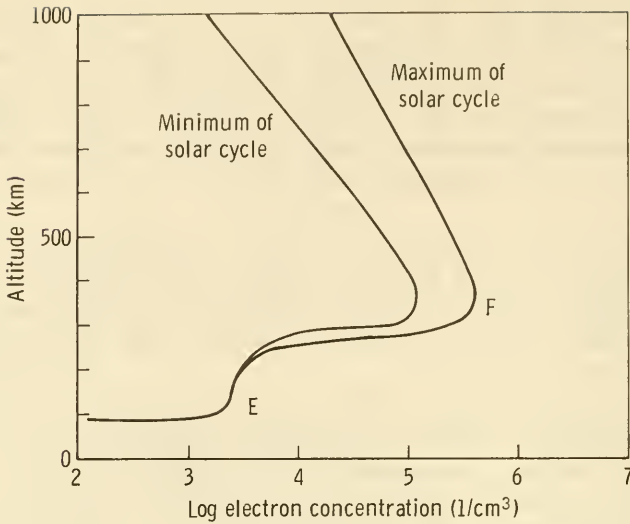
FIGURE 1–6.—Nighttime electron concentration in the ionosphere at the extremes of the solar cycle. Note that although electron concentration drops at very high altitudes, the fraction of the atoms ionized actually increases. (Adapted from ref. 16.)
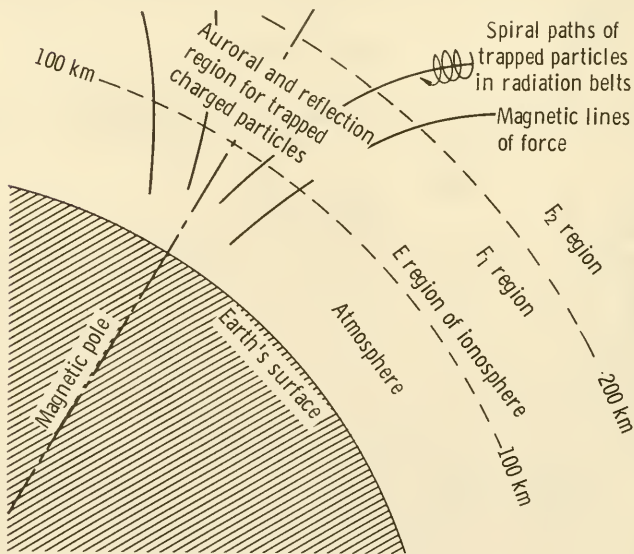

FIGURE 1–7.—Schematic drawing showing four strongly interacting components of the Earth's particulate envelope: the neutral atmosphere, the ionosphere, the auroras, and the trapped radiation zone.

based, radarlike ionosondes had obtained extensive data indicating the probable existence of four layerlike concentrations of electrons during the daytime: the D-, E-, F_1-, and F_2-layers, in ascending order. The apparent heights and concentrations of these electrified layers seemed to change with solar activity and from day to night. Sounding-rocket studies of the ionosphere in the 1940's and 1950's, showed no well-defined layers, however, but rather broad regions of electron concentration (figs. 1–5 and 1–6).

The reflection and refraction properties of the ionosphere, as they affect radio waves, depend upon electron concentration, which, in turn, depends upon solar forces. The positive ions that are also created by solar ultraviolet radiation, X-rays, and cosmic rays are much less mobile than the electrons and, because they interact only slightly with radio waves, play little part in determining radio transmission properties. It is of great scientific interest, though, to sample directly the ions that exist—O_2^+, N_2^+, O^+, NO^+, He^+—to identify ionization mechanisms and trace the complex chemical-reaction kinetics of this thin medium.

Scientific satellites may dip into the ionosphere to an altitude of 150 kilometers at perigee. Lower altitudes would radically shorten their lifetimes. Consequently, scientific satellites make direct measurements only at the upper fringe of the ionosphere, primarily in the F-regions. There are two other ways, however, in which satellites can add to ionosonde and sounding-rocket results. First, ground stations can record the Doppler shifts and polarizations of satellite radio signals that are caused by the ionosphere. For this reason, satellites often carry radio beacons transmitting at various frequencies. Scintillations, or fluctuations, of transmitted signals can be used to deduce irregularities or fine structure of the ionosphere. The second satellite technique depends upon ''topside sounding,'' as contrasted to the ''bottomside sounding'' carried out by terrestrial ionosondes. Sounding involves listening for radio echoes from regions of high electron density. Only satellites, obviously, possess the capability of continuously sounding the top of the ionosphere over wide geographical areas.

Auroral physics, like many other aspects of satellite science, possesses a surfeit of observational data. Many books and papers record the frequency, colors, shifting forms, and nuances of the often-beautiful auroral displays (refs. 17–20). But, even though we are a decade into the space age and regularly fly satellites through the polar zones, the exact origins of the auroras are still a mystery.

The greenish-white, sometimes red or violet, arcs, sheets, and shifting curtains of the auroras were first linked to magnetic storms, which were soon found to be due to solar activity. Modern spectroscopy has shown that most of the auroral light is composed of permitted and forbidden lines of neutral and ionized oxygen and nitrogen. Auroral activity centers on the Earth's magnetic poles, where the magnetic lines of force intersect the atmosphere (fig. 1–8). There is an obvious interface with the trapped-radiation zones that terminate about 100 kilometers above the magnetic poles. Probably, some trapped particles collide with and excite the atoms, ions, and molecules in the upper atmosphere, but the genesis of the auroras is an incomplete story. (Auroras can be and have been made artificially with high-altitude nuclear explosions, emphasizing the close link between auroras and trapped radiation.)

The value of the scientific satellite for studying auroras is apparent from figure 1–8: Instruments can be carried through the
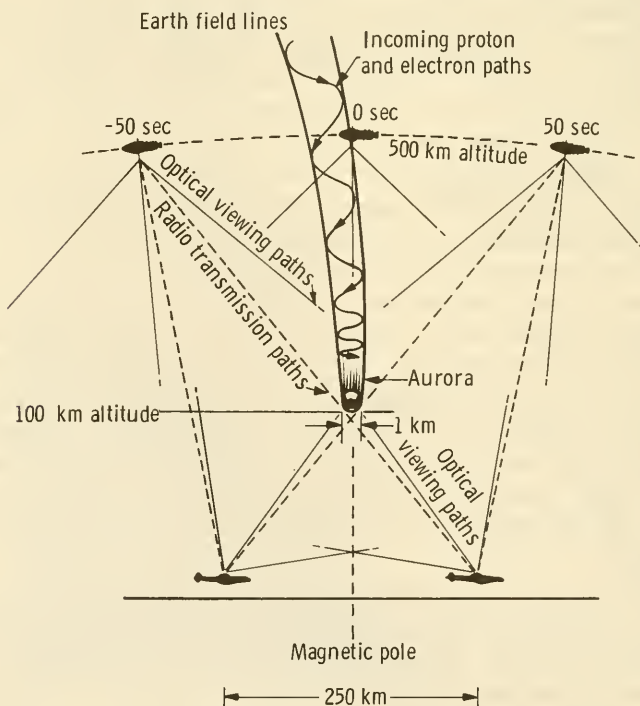

FIGURE 1–8.—Simultaneous measurements of the auroras can be made by polar satellites and aircraft (ref. 21).

auroras for direct measurements, and they can observe the displays with spectroscopes and photometers from positions well above the Earth and aircraft-based instruments.

Closely associated with the auroras is the airglow. At night, the airglow (called nightglow) consists of a faint continuum with superimposed emission lines, brightest just above the horizon. The red and green lines of atomic oxygen, which also appear in the auroras, are present, as well as lines from the hydroxyl radical and sodium. Lyman-α radiation is also observed. The source of energy for airglow excitation is the Sun, but apparently energy is stored chemically during the day and released during the night. Numerous chemical reactions have been suggested, but the origin of the airglow (including nightglow, dayglow, and twilight glow) remains incompletely explained. The role of the scientific satellite involves direct sampling of the environment as well as providing a platform for photometers and spectrometers in regions of the spectrum that do not reach the Earth's surface.

Trapped Radiation.—Above the envelopes of the neutral atmosphere and the ionosphere, but still within the cavity of the magnetosphere, lie the great radiation belts, frequently called the Van Allen Belts, after their discoverer, J. A. Van Allen (fig. 1–9).
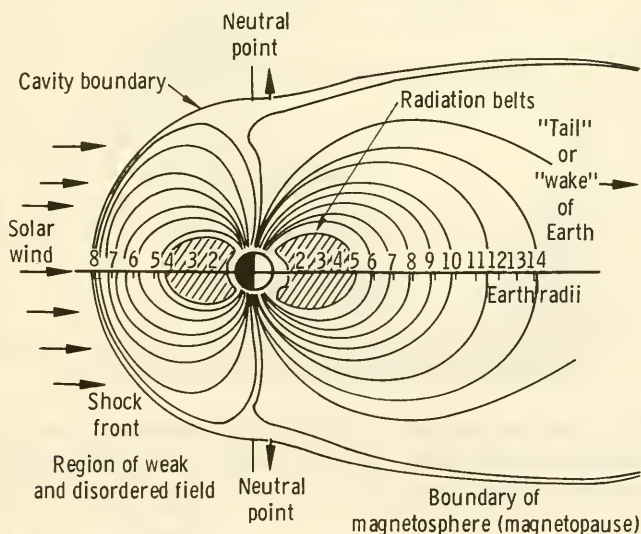

FIGURE 1–9.—Present view of the Earth's magnetosphere. On the Sunward side, a shock layer builds up where the solar wind contacts and compresses the magnetosphere. Leeward, the magnetic cavity tails off into space away from the Sun (but not along the orbital path).

The early satellite explorations above 200 kilometers, carried out primarily with Explorer and Vanguard satellites, first seemed to indicate two well-defined belts of magnetically trapped charged particles. Further experimentation, however, has shown that the region between the top of the ionosphere and the magnetopause is occupied by magnetically trapped, coexisting populations of electrons and protons, with minor fractions of heavier particles. Concentrations in space and energy do exist, but, except for protons, they are not well defined (figs. 1–9 and 1–10). Interaction with
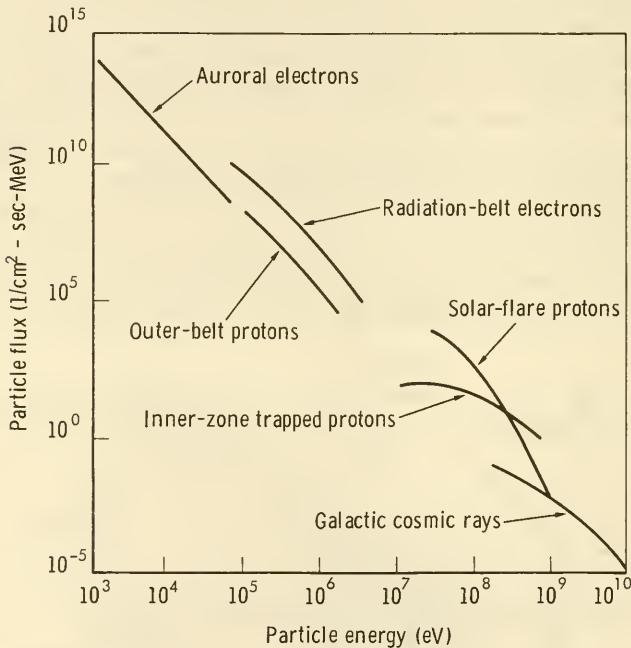

FIGURE 1–10.—Particle fluxes from various sources encountered by scientific satellites (ref. 24).

the solar wind molds the Earth's magnetosphere into an asymmetric, streamlined shape, with a "wake" that trails off into space in a direction away from the Sun for many Earth radii [2] (refs. 22–23).

Despite the many hundreds of satellite radiation instruments that have returned data since 1958, the precise origins and fates of charged particles trapped within the belts are not known. The

[2] Ness has concluded from Explorer-XVIII data that the Moon may have a similar wake (ref. 25).

neutron-albedo hypothesis certainly accounts for the origin of many protons and electrons. This theory holds that neutrons created during cosmic-ray reactions with nuclei in the Earth's upper atmosphere subsequently invade the radiation-belt region and decay into protons and electrons, which are then magnetically trapped (fig. 1–11). Many trapped particles are undoubtedly removed from the belts when they collide with atoms and molecules in the upper atmosphere. Other mechanisms for particle birth and death probably exist, but no theories regarding them have been generally accepted.

The shapes of the magnetosphere and the contained radiation zones are molded by the solar wind and its interaction with the Earth's magnetic field. An interface also exists between the trapped radiation and the auroras. Evidently, electrons continu-
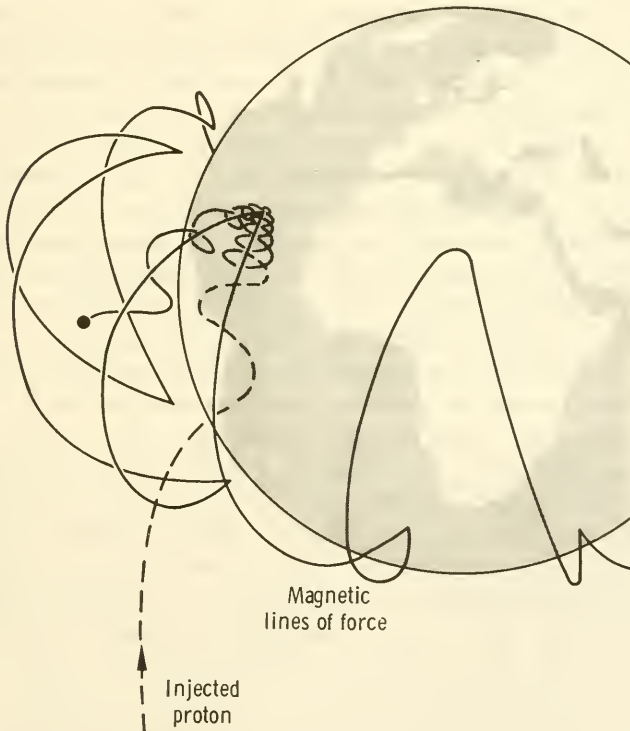

Magnetic
lines of force

Injected
proton

FIGURE 1–11.—Magnetic trapping of a charged particle. A proton, perhaps originating in the decay of an albedo neutron, spirals along the Earth's magnetic lines of force and is reflected back and forth from pole to pole.

ously precipitate into the auroral regions from the radiation belts. Some scientists feel that the auroras are created, at least in part, by these precipitating electrons.

Man himself experiments with the zones of trapped radiation by exploding nuclear weapons at high altitudes, an event that injects large quantities of electrons into the magnetic bottle formed by the Earth's field. Satellites also map these manmade phenomena (figs. 1–10 and 1–11).

Satellites, such as those in the Explorer class, can probe the entire region of trapped radiation, measuring particle flux, energy, direction, and identity. In addition to this mapping function, the larger satellites of the future will doubtless engage in active experiments, where charged particles are artificially injected into the radiation zones in a controlled manner. In this way, better insights into particle capture, storage, and loss mechanisms can be gained.

Geomagnetism.—The classical view of the Earth's magnetic field is that of a dipole located at the Earth's center, but tilted 11° from the axis of rotation. The field strength decreases as one moves away from the Earth, according to an inverse-cube law. The total surface field in the polar regions is about 50 000 γ (1 $\gamma = 10^{-5}$ gauss). Superimposed on the steady field are many short-term fluctuations as well as secular changes created in part by interactions with the streams of solar plasma. There are also departures from the dipole field owing to irregularities within the Earth itself. An earthbound observer would expect the classical dipole field to extend with decreasing strength out to infinity. It does not. Instead, the Earth's magnetic lines of force, and the trapped-radiation zones as well, are confined within the asymmetric cavity of the magnetopause (refs. 25–29). (See fig. 1–9.)

The magnetosphere is, in a sense, a magnetic bottle, diverting all but the most energetic cosmic rays on the outside, yet confining the radiation belts within. The magnetopause is closest to Earth on the sunlit side, where a shock front of solar plasma builds up and streams around the blunt end (fig. 1–9). The length of the leeward tail is not known. The magnetopause marks the transition zone between the bottled geomagnetic field and the weak spiral magnetic field pulled out of the Sun by the solar wind. For a distance of several Earth radii around the magnetosphere, there is a region of irregular, rapidly fluctuating magnetic fields. Satellite magnetometers penetrating this zone always record transients, some as high as 100 γ, before entering the relative calm of the interplanetary magnetic field, which has a strength of 5–10 γ.

The Sun does more than distort the magnetosphere with the solar wind. Solar storms apparently unleash immense tongues of plasma that sometimes envelop the Earth (fig. 1–12). The mag-
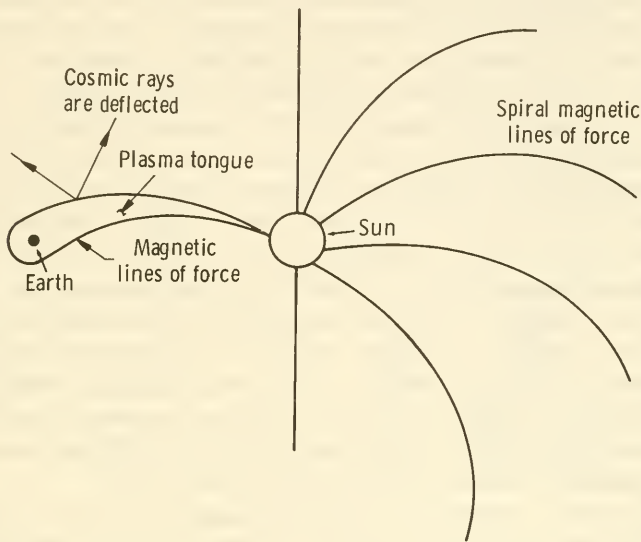
FIGURE 1–12.—On the right half of the sketch, spiral magnetic lines of force are pulled out of the Sun by the solar wind. On the left, a storm on the Sun shoots out a plasma tongue that envelops the Earth. The plasma tongue surrounds the Earth with a magnetic "bottle," deflecting some of the cosmic-ray flux and causing a Forbush decrease.

netic field carried along with the plasma tongue superimposes another magnetic field upon that of the Earth, deflecting still more cosmic rays. Decreases in cosmic-ray flux thus created by solar storms are called "Forbush decreases." The interplanetary "weather" outside the shelter of the magnetopause is dominated by these solar eruptions, and so, to a lesser extent, is the state of the Earth's radiation zones, ionosphere, and upper atmosphere.

The manifest value of the Earth satellite is in transporting magnetometers on eccentric orbits that regularly penetrate the magnetopause and map the fields within and without. Many satellites have carried such magnetometers, and abundant records exist showing the secular variations of the magnetosphere. Present emphasis is on studying the short-term fluctuations of the magnetic fields, the magnetospheric wakes of the Earth and Moon,

and the propagation of magnetohydrodynamic disturbances out from the Sun, past the tiny obstruction of the Earth, and on into interstellar space.

Geodesy.—If a satellite were launched into orbit around a perfectly spherical and homogeneous planet, its orbital plane, in the absence of perturbing forces, would remain fixed in inertial space. The Earth, however, is neither perfectly spherical nor homogeneous. The well-known equatorial bulge causes the orbital plane to rotate. By observing this induced rotation, scientists have inferred a 45-kilometer difference between the Earth's major and minor axes. Other perturbations to the orbit of an Earth satellite are caused by: (1) the Earth's slight pear shape, (2) a positive gravitational anomaly in the western Pacific, and (3) negative anomalies in the Indian Ocean and Antarctica. In other words, the Earth's physical shape and asymmetries in mass distribution beneath its surface can be deduced by analyzing the perturbations to satellite orbits. Of course, tracking, which is sometimes aided by flashing lights on satellites, must be precise. Drag forces and the effects of the Sun and Moon must also be accounted for if geodetic data are to be reliable (ref. 30).

Meteoritics.—Perhaps the least-explored dimension of the near-Earth environment is the flux of micrometeoroids encountered by satellites, probes, and high-altitude rockets. Not only are masses, velocities, densities, compositions, and origins of micrometeoroids uncertain, but their distribution within the solar system is poorly understood (refs. 31–33).

The best available picture of the micrometeoroid environment is that shown in figure 1–13. Almost all of the data used in making this graph came from microphone experiments, which record the number of impacts above a certain threshold and at the same time yield a signal proportional to some yet-undetermined function of particle mass and velocity. The abscissa in figure 1–13 is therefore in doubt. There are also regions in the graph where no measurements at all are available.

Satellites in eccentric orbits and space probes indicate that the micrometeoroid flux decreases with distance from the Earth, and may be 100 000 times weaker in interplanetary space. Just why the Earth should be surrounded by a stable cloud of dust has not been determined, although the Earth's gravitational field is an obvious factor. One hypothesis states that micrometeoroids are ejecta from meteoroid impacts on the Moon, and are thus naturally concentrated in Earth-Moon space, their point of origin.

Many micrometeoroids are bits of fluff, with densities of less than 1. A minority is composed of iron and nickel. The
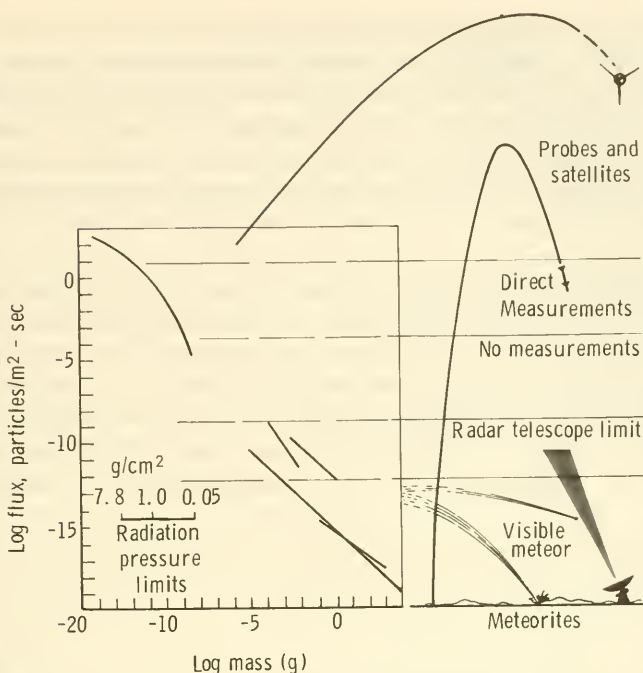
FIGURE 1–13.—Summary of micrometeoroid measurements made on spacecraft. Flux scale at left indicates cumulative flux.

velocities of micrometeoroids in orbit about the Sun would be between 11 and 72 km/sec,[3] relative to the Earth. Quite unexpectedly the Mars probe, Mariner IV, recorded a retrograde micrometeoroid impact, which makes the origin of micrometeoroids even more obscure. Suggested origins include (1) ejecta from the Moon, (2) cometary debris, and (3) asteroidal material.

Larger and more sophisticated satellites, such as Pegasus, have provided more accurate data on the magnitude of micrometeoroid flux as a function of position in the solar system. More elaborate micrometeoroid detectors will measure velocities directly, possibly by time-of-flight techniques.

Solar Physics.—The Sun, our nearest star, is frequently disparaged as a very common, yellow, Class G2 star, located in an inauspicious spot in our galaxy. In truth, the Sun is a magnificent incandescent sphere, with a visual diameter of about 1 400 000 kilometers, 108 times the diameter of the Earth. In the visible

---

[3] Solar-system escape velocity minus and plus the orbital velocity of the Earth.

region of the spectrum, which peaks at 5850 Å, the Sun appears quite stable. Photometers rarely show changes greater than 1 percent. But at the long- and short-wavelength ends of the spectrum, the radiation we receive varies by orders of magnitude. These variations, which are largely blocked by the atmosphere for Earth-based observers, plus the Sun's particulate radiations, provide many insights into the birth, stability, and death of all stars (fig. 1–14).

Sunlight is such an obvious terrestrial fact that it is logical to ask what advantages satellite-borne experiments have over Earth-based, rocket-, and balloon-borne experiments. The Sun, by creating the Earth's ionosphere and the ozone region in the upper atmosphere, prevents the passage of most of the electromagnetic spectrum. The solar wind and solar cosmic rays are also best studied by satellites outside the magnetosphere. High-altitude
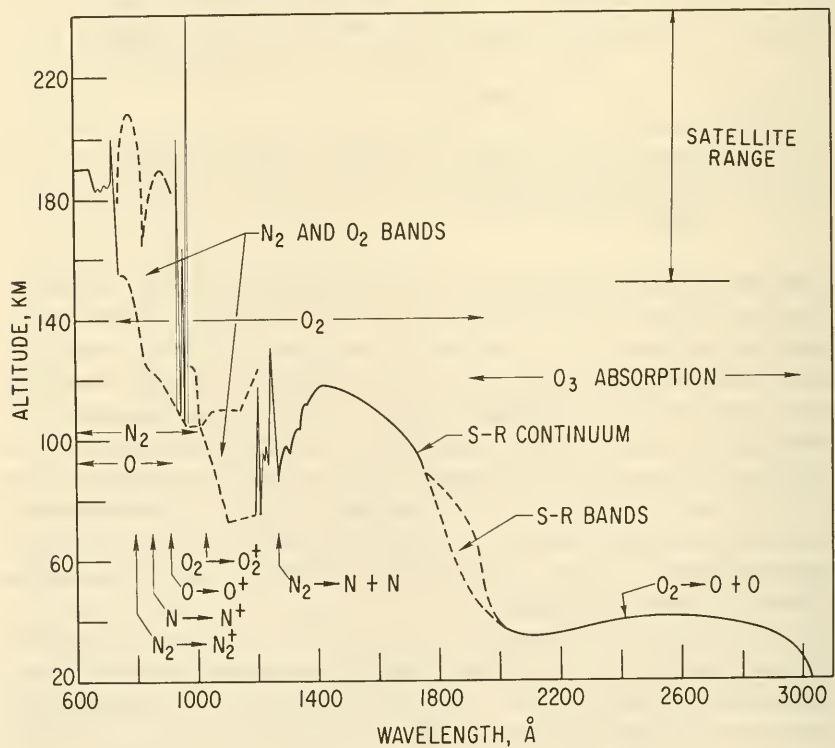
FIGURE 1–14.—The solar ultraviolet spectrum is rapidly attenuated by the Earth's atmosphere. The ordinate shows the altitude at which the flux has decreased by a factor of 2.718.

rockets, which have pioneered solar spectroscopy in the ultra-violet, provide only transitory instrument platforms.   A long-lived satellite observation platform, such as OSO, thus has great value to solar science.   Satellites, as they accompany the Earth in its orbit around the Sun, also make excellent solar probes that map the macrostructure of the solar plasma and solar magnetic field at 1 A.U.

The rich panorama of solar phenomena observable at satellite altitudes is too complex and extensive to describe here.   The non-technical reader should refer to the "General Bibliography" for key review works. Some technical background, though not a great deal, is necessary, however, for the discussion of solar instruments presented in chapter 12.   Pertinent characteristics of the Sun are described in table 1–3.

Stellar Astronomy.—Satellites give the astronomer an instrument platform high above the frustrations of the Earth's absorbing and distorting atmosphere.   The advantages and technology of astronomical satellites are therefore similar to those satellites assigned to solar research.   There are, however, two important differences:

(1) Millions of stars, galaxies, nebulae, and other astronomical targets exist.   The scientific satellite must select, from a field of many, a target much fainter than the Sun.   Furthermore, the instrument packages must be pointed more accurately and stably than for satellites used in solar research.

(2) The range of stellar phenomena is far greater, from neutron stars to quasars, and instrument types and ranges are correspondingly expanded.

The areas of stellar astronomy opened up by satellites, as in the case of the Sun, are in the short- and long-wavelength regions of the spectrum.   The inference is that satellites will be most useful in studying white dwarfs, quasars, and other stars that emit much of their radiation in wavelengths outside the visible.   More significant, though, is the strong likelihood that entirely new kinds of stars and totally different stellar processes will be found.   In a sense, scientists expect that unexpected phenomena will be the most important.   Whenever new dimensions have been opened up for scientific exploration, the unpredictable discoveries have usually overshadowed other findings; viz, the Earth's magnetopause and regions of trapped radiation.

Still, some direction must be given to experiment planning for astronomical satellites.   Interest now centers on the ultraviolet portion of the spectrum.   Rocket observations in that area have

TABLE 1–3.—*Pertinent Characteristics of the Sun*

Phenomenon	Features
Particulate radiation (refs. 34–35) ____	Low-energy cosmic rays emitted in conjunction with solar flares. These are primarily protons, with some alphas and heavier particles. (See fig. 1–10 and table 1–4.) Neutrons are also detected.
Plasma (ref. 36) _____	Solar wind has an average flux of $10^5/cm^2$-sec and a velocity between 300 and 600 km/sec. Composition: mostly hydrogen, possibly some helium and heavier particles. Tongues of plasma are superimposed on the steady-state solar wind.
Electromagnetic radiation (refs. 37, 38).	In the visible, there is a steady flux that is close to a blackbody spectrum peaking at 5850Å (5800° K). Power: about 1400 w/m^2 at the Earth's orbit. At short wavelengths, the solar flux decreases rapidly, but exceeds that expected from the blackbody law. X-rays and gamma rays are also emitted, especially during solar flares. Radiation mechanisms not known for certain. Ultraviolet, X-ray, and gamma-ray fluxes are highly variable. At long wavelengths, there is intense radio noise emitted from the solar corona, which has a blackbody temperature of up to 2 000 000° K. Radio emissions are also variable.
Visible features (ref. 39) _____	Sunspots, prominences, granules, and other fine structures are easily resolved in the visible range. Although their frequency, morphology, and evolution are best studied on the Earth, satellites can carry instruments to study the more diagnostic short wavelengths and obtain images with higher resolution.

already shown that many stars are not as bright in the ultraviolet region as present theory predicts. In addition, some stars are surrounded by strange ultraviolet nebulosities. A systematic photometric survey of stars in the ultraviolet is needed to help develop new stellar facts and theories. X-ray emissions are also of interest. To illustrate, scientists at the Naval Research Laboratory (NRL) have discovered with rocket instruments an intense X-ray source in Scorpius. Such short wavelengths may indicate the existence of so-called neutron stars (ref. 40).

In the radio region of the spectrum, the astronomer finds many knots to unravel. One of the most puzzling and stimulating is the quasar, or quasi-stellar radio source. There are also unexplained radio sources in the sky that are not correlated with any visible sources. Radio astronomy satellites using huge, extended antennas above the ionosphere should enlarge the observable spectrum considerably.

Interstellar Physics, Cosmic Rays, Cosmology, and Fundamental Physics.—Visible light tells us a great deal about our own galaxy and similar aggregations of stars nearby. The character of the "space" between the stars and galaxies is not as well known. There seems to be a weak interstellar magnetic field of about 1 γ. A tenuous plasma, with an average of perhaps 1 proton/cm^3, fills this space. There also seem to be concentrations of dust and gas that may be a prelude to the formation of stars. By placing ultraviolet and radio instrumentation on satellites, scientists hope to explore regions where little visible light is emitted. Some specific experiments that have been suggested involve (1) the measurement of the reddening of ultraviolet radiation by the scattering of interstellar matter, and (2) the search for ultraviolet emissions of molecular hydrogen at 1108 and 1008 Å. Atomic hydrogen is a known constituent of interstellar space, but no one has yet detected hydrogen molecules.

An Earth satellite is also in a favorable position to study galactic cosmic rays, which differ from solar cosmic rays in that their energies are much higher (fig. 1–10 and table 1–4). The nuclei involved are present in different amounts. Galactic cosmic rays consist of charged particles that are apparently uniformly distributed through space, but vary in flux according to the effects of the magnetic fields of the Sun and Earth. There is an 11-year cycle measured on the Earth's surface, and this cycle is 180° out of phase with solar activity. As the Sun's magnetic field builds up during the solar cycle, more and more cosmic rays are deflected away from the Earth. Superimposed upon this systematic behavior are the Forbush decreases, caused, as previously noted, by

magnetic fields generated by sporadic solar storms. Earth-based observations are hampered by the fact that the high-energy (up to 10^{20} eV), primary cosmic rays collide with nuclei in the upper atmosphere and generate showers of secondaries, which yield little direct information about primary cosmic rays. The value of satellite research here is obvious.

TABLE 1–4.—*Relative Abundance of Primary Cosmic-Ray Particles*

[From ref. 41]

Element	Galactic	Solar
Hydrogen	2500	([a])
Helium	360	1250
Lithium, beryllium, boron	11	0.3
Carbon	18	6
Nitrogen	8	2
Oxygen	10	10
Fluorine	1	0.4
Neon	3	1.5
$11 \leq Z \leq 18$	9	1.3

[a] Varies.

Cosmologists and those concerned with the physical fabric of the universe—as, for example, theories of relativity—have in the scientific satellite a tool of undetermined value. A few experiments have been suggested in table 1–1, but none is being actually designed for satellite use. Explorer XI, which carried a gamma-ray telescope, searched for gamma rays of galactic and extragalactic origin that might indicate the continuous creation of matter. The experiment recorded only a few gamma rays and is regarded as unfavorable to the steady-state theory of cosmology. Beyond this single experiment and the few ideas presented in table 1–1, satellites have seemed to offer little to cosmology directly.

Biology.—Satellites present the discipline of biology with two unusual opportunities. The first is an enlargement of the attainable biosphere to include the fringes of the atmosphere and nearby space. It is conceivable that there may be indigenous life, sustained by sunlight, in the high, thin regions of the atmosphere. It is also possible that, despite the discrediting of the panspermia theory, there is some kind of influx of minute life forms from outer space. The second area of satellite biology involves the unique physiological effects of zero gravity, space radiation, and

the lack of the 24-hour rhythm present on the Earth's surface. Scientific satellites, which in this book exclude manned spacecraft, have already invaded this new research area, using lower life forms, with the Discoverer and Biosatellite series. No one knows just what will be discovered when life is exposed to this radically new combination of environmental forces.

1-3. Content and Organization of the Book

Part II of this book, which follows two short introductory chapters, deals with the problems of placing an unmanned satellite in orbit, keeping it operational, and getting useful data back to the experimenters on Earth. Part III considers the scientific instruments placed on satellites and how their design is molded by experimental objectives and the often delicate interfaces that separate them from the remainder of the spacecraft.

Manned spacecraft are bypassed in this book. Do they not offer even better opportunities for research? The superior flexibility, adaptability, and decision-making capability of man are hard to deny. Gerathewohl and others have made strong cases for the manned, orbital research laboratory (ref. 42). In particular, man's ability to recognize completely new, unexpected situations seems a valuable asset in a realm where, through prejudgment, our instruments may be sampling only the expected portion of the environment. The proponents of manned spaceflight frequently cite the X-15 and other manned research vehicles in which man has been instrumental in saving many a mission through improvisations and the repair of faults. The Mercury and Gemini flights tend to support this view. Yet until man has a stronger foothold in space—say, as a regular passenger in orbital laboratories—unmanned, scientific satellites will continue to take most of the measurements. Even on Earth, we resort to unmanned, automated weather stations and oceanographic buoys to make synoptic, repetitive measurements. There is more urgency to do this in space, where danger is great and costs to sustain man soar.

The case for the unmanned scientific spacecraft has been forcefully put forth by Boyd (ref. 43). His argument runs like this:

(1) The presence of man will disturb many experiments through his movements (bad for precision telescope pointing), his vapors and exhalations (mass-spectrometer contamination), and his associated parasites (in biological experiments)

(2) Astronauts are likely to be under high stress, which may impair their judgment; viz, the difficulty in identifying the "snowflakes" seen during early manned spaceflight

(3) Manned missions are usually short; too short for most space experiments, unless crew changes are incorporated

(4) Parts of the space environment, such as the radiation zones, are dangerous to man

(5) Many scientists express little enthusiasm when it is suggested that astronauts might help tune or adjust delicate instruments

In other words, man is not necessarily a blessing to satellite science.

These arguments are in a sense more antiastronaut than pro-instrument. Counterarguments are easy to marshal: Instruments are unreliable and relatively inflexible; they cannot recognize new situations or repair themselves; and so on. Proponents of manned spaceflight can always point to the difficulties and disappointments of OGO I, OGO II, and OAO I, saying that these spacecraft were too far advanced for their time. And that they were less than complete successes because it is just too difficult to integrate and control properly more than a certain upper limit of scientific payload, as measured, say, in terms of kilograms, number of parts, or number of experiments. (See sec. 9–3.) Probably a complexity "bottleneck" does exist, but is the upper limit any higher for manned spacecraft? If necessary, NASA can always put up more "simple" Explorers and fewer "complex" Observatories.

Man and machine certainly complement each other in space science, just as observatories complement Explorers. The trade-offs in terms of dollars and scientific return remain to be worked out.

In any discussion of the competitors of scientific satellites, sounding rockets must not be ignored (ref. 44). Again, we find unique advantages: fast reaction time, low cost, easy physical recovery, preselection of time and place of launch, rapid sampling along a vertical profile, and short cycle time from instrument to flight to improved instrument. But sounding rockets have short lives, limited geographical coverage, and small payloads. Again, it is a case of one type of vehicle complementing another. Each mission has to be studied in view of its own special requirements.

The struggles to orbit the tiny Explorer I and Vanguard I are now far behind us. Research through use of satellites, though it does not receive the sums allotted to manned and military spacecraft, increases in scientific importance each year. Almost every satellite launched makes room for one or more scientific instruments. Scientists are great improvisers, and they hitchhike into orbit on many test vehicles that would otherwise have carried only

ballast. Space, barely touched by sounding rockets a decade ago, is now a well-traveled thoroughfare for the first few thousand kilometers.

References

1. KALLMAN BILL, H., ED.: Space Research (first of the COSPAR groups of papers). Interscience Publishers, 1960.
2. VAN DE HULST, H. C.; DE JAGER, C.; MOORE, A. F., EDS.: Space Research II. Interscience Publishers, 1961.
3. PRIESTER, W., ED.: Space Research III. John Wiley & Sons, Inc., 1963.
4. MULLER, P., ED.: Space Research IV. John Wiley & Sons, Inc., 1964.
5. KING-HELE, D. G.; MULLER, P.; AND RIGHINI, G., EDS.: Space Research V. John Wiley & Sons, Inc., 1965.
6. GLASSTONE, S.: Sourcebook on the Space Sciences. D. Van Nostrand Co., 1965.
7. WALKER, J. C. G.: The Upper Atmosphere. Space/Aero., vol. 42, Oct. 1964, p. 56.
8. ANON.: Significant Achievements in Planetary Atmospheres, 1958–1964. NASA SP–98, 1966.
9. RATCLIFFE, J.: Physics of the Upper Atmosphere. Academic Press, 1960.
10. SPENCER, N. W., ET AL.: New Knowledge of the Earth's Atmosphere From the Aeronomy Satellite (Explorer XVII). NASA X–651–64–114, 1964.
11. VAN ZANDT, T. E.; AND KNECHT, R. W.: The Structure and Physics of the Upper Atmosphere. *In* Space Physics, D. P. LeGalley and A. Rosen, eds., John Wiley & Sons, Inc., 1964.
12. NICOLET, M.: Helium, An Important Constituent in the Lower Exosphere. J. Geophys. Res., vol. 66, 1961, p. 2263.
13. BOURDEAU, R. E.: Ionospheric Research From Space Vehicles. Space Sci. Rev., vol. 1, 1962, p. 683.
14. BOURDEAU, R. E.: Research within the Ionosphere. Sci., vol. 148, Apr. 30, 1965, p. 585.
15. JOHNSON, F. S., ED.: Satellite Environment Handbook. Second ed., Stanford University Press (Palo Alto), 1965.
16. JOHNSON, F. S.: The Physical Properties of the Earth's Ionosphere. Vol. 1 of Progress in the Astronautical Sciences, S. F. Singer, ed., Interscience Publishers, 1962.
17. AKASOFU, S.: The Aurora. Sci. Am., vol. 213, Dec. 1965, p. 55.
18. CHAMBERLAIN, J. W.: Physics of the Aurora and Airglow. Academic Press, 1961.
19. CHAPMAN, S.: Aurora and Geomagnetic Storms. *In* Space Physics, D. P. LeGalley and A. Rosen, eds., John Wiley & Sons, Inc., 1964.
20. CHAPMAN, S.: Solar Plasma, Geomagnetism and Aurora. Gordon & Breach, 1964.
21. MEYEROTT, R. E.; AND EVANS, J. E.: Auroral Measurements and Upper Atmospheric Physics. AIAA J., vol. 2, July 1964, p. 1169.
22. HESS, W. N., ED.: Introduction to Space Science. Gordon & Breach, 1965.
23. O'BRIEN, B. J.: The Trapped Radiation Zones. *In* Space Physics, D. P. LeGalley and A. Rosen, eds., John Wiley & Sons, Inc., 1964.

24. HESS, W. N.: Lifetime and Time History of Trapped Radiation Belt Particles. *In* Space Research IV., P. Muller, ed., John Wiley & Sons, Inc., 1964. (Also available in NASA TN D–2303, 1964.)

25. NESS, N. F.: The Magnetohydrodynamic Wake of the Moon. J. Geophys. Res., vol. 70, Feb. 1, 1965, p. 517.

26. CAHILL, L. J.: Magnetic Fields in Interplanetary Space. Science, vol. 147, Feb. 26, 1965, p. 991.

27. CAHILL, L. J.: The Magnetosphere. Sci. Am., vol. 212, Mar. 1965, p. 58.

28. NESS, N. F.: Earth's Magnetic Field: A New Look. Science, vol. 151, Mar. 4, 1966, p. 1041.

29. SMITH, E. J.: Interplanetary Magnetic Fields. *In* Space Physics, D. P. LeGalley and A. Rosen, eds., John Wiley & Sons, Inc., 1964.

30. VEIS, G., ED.: The Use of Artificial Satellites for Geodesy. John Wiley & Sons, Inc., 1963.

31. ALEXANDER, W. M., ET AL.: Review of Direct Measurements of Interplanetary Dust From Satellites and Probes. *In* Space Research III, W. Priester, ed., John Wiley & Sons, Inc., 1963. (Also available in NASA TM X–54570, 1962.)

32. HAMERMESH, B.: Micrometeoroids. *In* Space Physics, D. P. LeGalley and A. Rosen, eds., John Wiley & Sons, Inc., 1964.

33. SCHMIDT, R. A.: A Survey of Data on Microscopic Extraterrestrial Particles. NASA TN D–2719, 1965.

34. MCDONALD, F. B.: Review of Galactic and Solar Cosmic Rays. NASA TM X–55245, 1965.

35. ANDERSON, K. A.: Energetic Solar Particles. *In* Space Physics, D. P. LeGalley and A. Rosen, eds., John Wiley & Sons, Inc., 1964.

36. BERNSTEIN, W.: The Solar Plasma—Its Detection, Measurement and Significance. *In* Space Physics, D. P. LeGalley and A. Rosen, eds., John Wiley & Sons, Inc., 1964.

37. FRIEDMAN, H.: X-Ray Astronomy. Sci. Am., vol. 210, June 1964, p. 36.

38. LARMORE, L.: Solar Physics and Solar Radiation. *In* Space Physics, D. P. LeGalley and A. Rosen, eds., John Wiley & Sons, Inc., 1964.

39. KUIPER, G. P., ED.: The Sun. Univ. of Chicago Press, 1953.

40. DEUTSCH, A. J.; AND KLEMPERER, W. B., EDS.: Space Age Astronomy. Academic Press, 1962.

41. LUDWIG, G. H.: Particles and Fields Research in Space. NASA SP–11, vol. 1, 1962, p. 129.

42. GERATHEWOHL, S. J.: Man's Role in Space. Int. Sci. and Tech., no. 45, Sept. 1965, p. 64.

43. BOYD, R. L. F.: In Space: Instruments or Man? Int. Sci. and Tech., no. 41, May 1965, p. 65.

44. HINES, C. O.: Sounding Rocket Resurgence. Astronaut. Aeron., vol. 4, Jan. 1966, p. 8.

Chapter 2

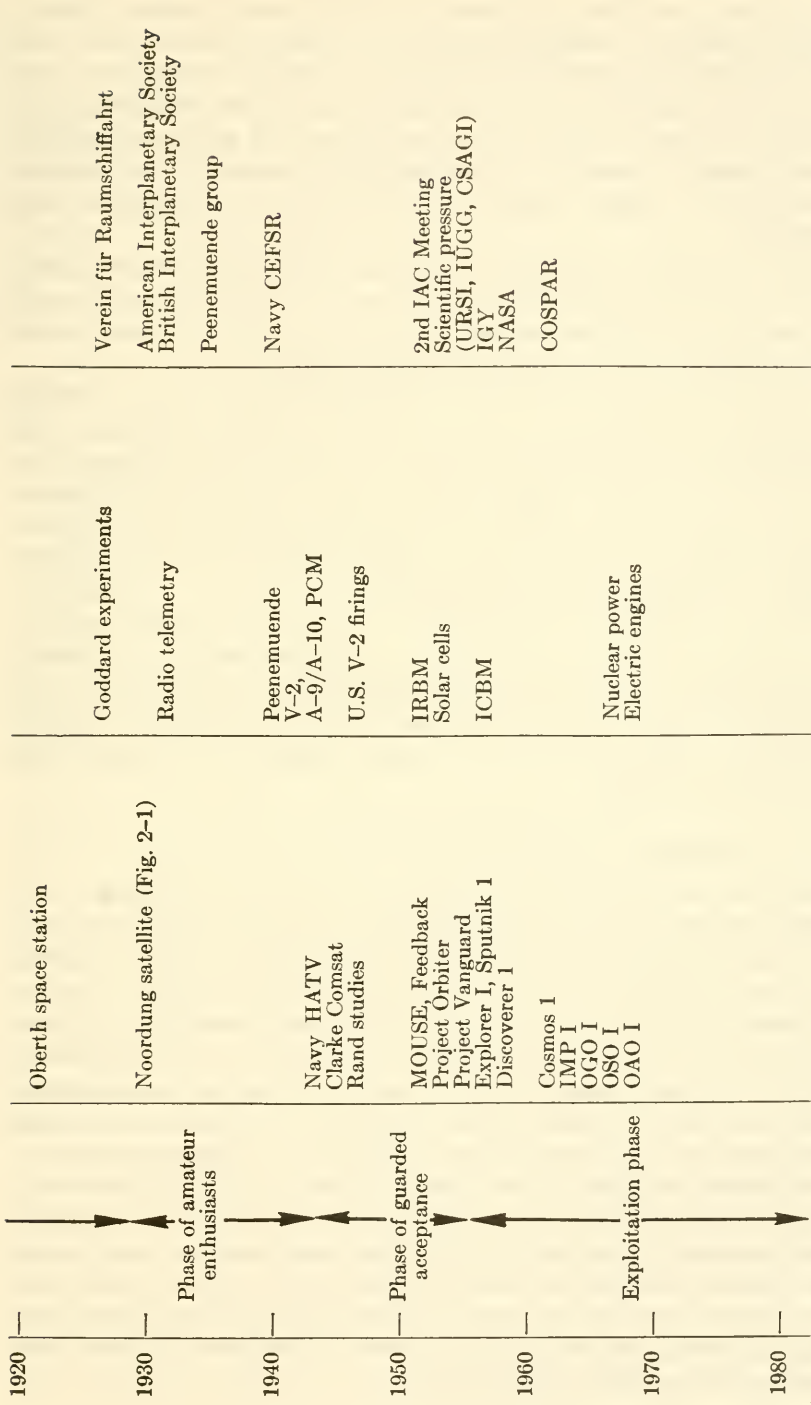## HISTORY OF SCIENTIFIC SATELLITES

2-1. Prolog

By January 1, 1966, more than 450 artificial satellites had been placed in orbit. Over 100 new satellites are launched each year, and old ones constantly crisscross the skies above us. Against this backdrop, it is difficult to project one's thoughts back that spare handful of years to the time when the satellite idea received only ridicule. What other modern technical idea has so rapidly made the transition from speculative pulp magazines to reputable scientific journals? Yet this symbol of the space age, the unmanned satellite, carrying only scientific instruments for payload, was also ignored by the great astronautical pioneers (ref. 1).

Before I tell this fascinating tale of scorned ideas, organizational jealousies, and international politics, consider what ingredients are necessary for the founding of a whole new technology. First, the idea must be born and promulgated; in this case, the concept of the scientific satellite itself. Then, the basic technical cornerstones must be laid in place, as exemplified by rocketry, ground support, power supplies, and radio telemetry. There must also be money and organizational support to convert ideas into hardware. The assignment of money, men, and other resources to an untried idea requires someone, frequently someone not caught up in the enthusiasm of the idea, to commit his reputation in the face of conflicting recommendations from advisers. Many a harried man has been found willing to sail his administrative ship into new seas, however, as the existence of the airplane, nuclear power, and the satellite amply prove.

The history of scientific satellites can, like those of many other technical developments, be broken down into the four phases delineated below and in table 2-1.

TABLE 2-1.—*Chronological Chart Showing the Evolution of the Satellite Idea and the Supporting Technology*

[See text for definitions of the abbreviations and acronyms]

Year	Phase	Evolution of the satellite idea	Evolution of technology	Evolution of organizations
1870		Hale's "Brick Moon"		
1880		Verne's gun		
1890		Lasswitz novel		
1900	Idea phase	Tsiolkovsky		
1910				

Year	Phase	Projects/Satellites	Technology	Organizations
1920				
	Phase of amateur enthusiasts	Oberth space station	Goddard experiments	Verein für Raumschiffahrt
1930		Noordung satellite (Fig. 2-1)	Radio telemetry	American Interplanetary Society / British Interplanetary Society / Peenemünde group
1940		Navy HATV / Clarke Comsat / Rand studies	Peenemünde V-2, A-9/A-10, PCM / U.S. V-2 firings	Navy CEFSR
1950	Phase of guarded acceptance	MOUSE, Feedback / Project Orbiter / Project Vanguard / Explorer I, Sputnik 1 / Discoverer 1	IRBM / Solar cells / ICBM	2nd IAC Meeting / Scientific pressure (URSI, IUGG, CSAGI) / IGY / NASA
1960	Exploitation phase	Cosmos 1 / IMP I / OGO I / OSO I / OAO I		COSPAR
1970			Nuclear power / Electric engines	
1980				

(1) *The Idea Phase.*—A lengthy period when isolated thinkers, including many amateurs, sketched out the sinews of the idea. The technical concept at this stage had precarious credibility and was usually dismissed as ridiculous by "competent authorities."

(2) *The Phase of the Enthusiasts.*—The first amateur societies were formed. Technological developments began to support the satellite idea. The military examined the concept to assess its war potential.

(3) *The Phase of Guarded Acceptance.*—The professional technical community agreed that the idea was sound, though many claimed it pointless and wasteful of money. At this stage, nearly all of the technical cornerstones were in place.

(4) *The Exploitation Phase.*—A trigger or catalyst was required to initiate this phase. In the case of scientific satellites, the catalyst was the desire to acquire cold-war prestige through the launch of a scientific satellite during the International Geophysical Year (IGY). In this phase, the idea was translated into hardware; large blocks of resources were committed; and formerly obscure "dreamers" became heroes.

Dilatory though the genesis and development of the satellite idea may now seem (table 2–1), it will now serve as a handy framework to support the historical sketches that follow. The emphasis in this chapter is on early history—say, up to 1960. More recent history of technical developments is intrinsic in the chapters that follow.

2–2. Tracking the Satellite Idea

In 1870, Edward Everett Hale, a most inventive author, published a story entitled "The Brick Moon," in the *Atlantic Monthly*. This story is also available in book form (ref. 2). In this surprisingly well-thought-out tale, huge waterpowered flywheels flung an artificial satellite into orbit along the Greenwich meridian. Hale's new moon was visible from Earth and helped make the determination of longitude easier for navigators. He also contemplated using it to aid communications. It was a very sophisticated idea at a time when the horse still had 30 years of supremacy ahead.

Scientists had long known that an object traveling in a circular path around the Earth could, if its velocity was correct, remain in orbit perpetually. After all, the Moon was there for everyone to see. But for man to place an artificial satellite in orbit around the Earth—that was preposterous. It could not be done, and what would be the use anyway? It was more absurd than that nonsense about machines flying like birds.

Two more fictional satellites followed Hale's into orbit. In 1879, Jules Verne wrote about launching small satellites with a gun possessing a muzzle velocity of 10 000 m/sec (ref. 3). The gun approach recurs periodically in the astronautical literature (ref. 4). Recent experiments by the Canadians, using long-barreled naval artillery, indicate that a few tens of kilograms can probably be placed successfully in orbit without rockets. The launch technique suggested by Kurd Lasswitz in his 1897 novel *Auf zwei Planeten* (*Of Two Planets*) is much farther from credibility (ref. 5). Lasswitz employed an "abaric," or antigravity, field to position a Martian spacecraft over the North Pole.

Perhaps gun launchers and antigravity will eventually come to pass, just as "The Brick Moon" foretold in a crude way the Transit navigation satellites. In over three millennia of literature, one can find almost any idea one looks for. Indeed, who would be overly surprised to learn that the ancient Greeks also thought of satellites? The pile of tailings from time's mine of imaginative literature, containing all those dead and truly impossible ideas, is always incomparably larger than the handful of rare nuggets that become reality.

After the novelists came the now-revered astronautical pioneers: Tsiolkovsky, Goddard, Esnault-Pelterie, von Pirquet, and Oberth. The scientific-satellite concept, however, did not germinate in their hands, for they were preoccupied with propelling man himself into space (ref. 1). An Earth satellite? Yes, it was possible and would be a good way station on the voyages to the Moon and planets (fig. 2–1). Tsiolkovsky mentioned satellites at the beginning of the century; so did Hermann Oberth, in his classic *Die Rakete zu den Planetraumen* (*Rocket into Planetary Space*), first published in 1923 (ref. 6). By the late 1920's the space-station idea was firmly entrenched, but mainly as a stepping-stone to the planets; scientific research was strictly a secondary objective.

Let us be fair to those who looked forward to manned space-flight to the exclusion of instrumented, automatic satellites probing at the fringes of the Earth's atmosphere. After all, beyond the atmosphere was only vacuum, and perhaps a few bits of meteoric material. Who had heard of the Van Allen Belts, the solar wind, or the magnetopause? Beyond that, the art of radio telemetry was still in its infancy. Here, ignorance was a formidable barrier to imaginative thinking (ref. 1). Without a means of transmitting data without wires, of what use was an unmanned, unrecoverable research satellite? Possibly someone, somewhere,

foresaw that simultaneous advances in telemetry and rocketry would make the scientific satellite possible, but he did not record his thoughts.

The era of the isolated, unappreciated dreamer who thought of man roaming the cosmos came to an end about 1927. In Germany, the United States, England, and other countries, small but enthusiastic groups began to coalesce. The largest were the Verein für Raumschiffahrt (VfR) in Germany, founded in 1927; the American Interplanetary Society in the United States, founded in 1930; and
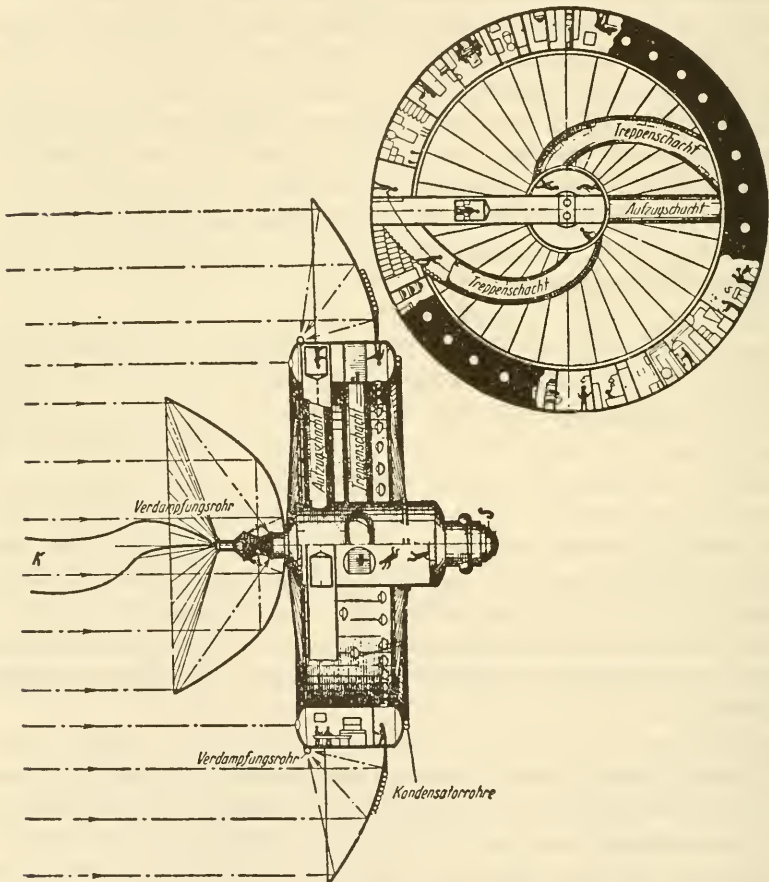
FIGURE 2–1.—Noordung conceived this manned space station in the late 1920's. It was to rotate slowly to provide artificial gravity and to obtain its power from solar concentrators. Kondensatorrohre = condenser pipes; Verdampfungsrohr = boiler pipe; Treppenschacht = stairwell; Aufzugschaft = elevator shaft (ref. 7).

the British Interplanetary Society in England, founded in 1933. These small organizations of dedicated amateurs wrote, published, evangelized, carried out experiments with small rockets, and dreamed of trips to the Moon and planets. They actually knew little of Goddard's trail-blazing experiments.[1] Tsiolkovsky's works were buried in obscure Russian publications. The military potential of the rocket, which in a scant 20 years was to become the major spur to the realization of spaceflight, was all but ignored (ref. 8). So was space science. Yet these small groups nurtured the concept of spaceflight and, in the face of ridicule, proclaimed (loudly) that men would someday escape the Earth in huge rockets. The enthusiasts were certain of their prognoses, but even they were pessimistic about the time scale.

To summarize, the situation was this in 1935: many ideas for manned spaceflight, much amateur enthusiasm, and a few rocket exeriments, but radio telemetry was rudimentary, and the idea of space research was neglected. Despite this unpromising climate, the foundations for satellite research were laid during the next 20 years, 1935 to 1955.

The necessary technological explosion was stimulated by warfare. First came the hot war, World War II, then the cold war. The hundreds of scientific satellites that have been launched since 1957 owe their existence directly and almost completely to military stimuli—hot and cold.

The first great upward surge of space technology took shape near the small Baltic village of Peenemuende (ref. 10). Here, Baron von Braun had gone duck hunting along the sandy beaches, and here his son, Wernher von Braun, went with the German Army in 1937 to develop and test the A/4, better known as Vengeance Weapon 2, the V–2.

Peenemuende is most famous for the V–2 rocket, but, as we shall see later, major advances were also made there in guidance and control, communications, ground support, and many other aspects of astronautics. Beyond the V–2 were studies of an ICBM (Intercontinental Ballistic Missile, the A–9/A–10 project), and space projects far exceeding immediate military necessity. Krafft Ehricke recalls that satellite studies continued up until 1943 (ref. 11). The impact of Peenemuende on the development of scientific satellites was not in the concept or the idea—no one had yet suggested the unmanned, purely scientific satellite—but

---

[1] Goddard was secretive about his work because the newspapers had ridiculed his 1919 paper (ref. 9), in which he suggested a Moon rocket. Rocketry was on a par with extrasensory perception in those days.

rather in the creation and refinement of supporting technology (fig. 2–2).

With the capture and transfer of the Von Braun group and their V–2 hardware [2] to the United States during Operation Paperclip, in 1945, the thread of the satellite story can be picked up in the activities of the American military services. Presumably, the Russians, who had captured many V–2 technicians but few engineers and research men, were also thinking about the potentialities of huge new rockets, but we know little of their early ICBM and satellite planning.

Before surveying the ups and downs of early U.S. satellite work in the 1945–1957 period, consider two pronouncements made in 1945. First, Arthur C. Clarke published his famous paper on unmanned communications satellites in *Wireless World* (ref. 12). To unhearing ears, he forecast both their feasibility and economic value. The second prediction came from Dr. Vannevar Bush, well known for his pioneer work on computers and the atomic bomb. Bush testified before Congress in December 1945 that ICBM's would not be feasible for many years to come and that people should stop thinking about them (ref. 13).

The first flurry of U.S. satellite studies came when the Navy and Army Air Force, stimulated by the V–2, tried to assess future military possibilities. In October 1945, the Navy Bureau of Aeronautics established the CEFSR (Committee for Evaluating the Feasibility of Space Rocketry). Later in the same month, the committee recommended launching a small satellite for scientific purposes (ref. 14). The Navy called the concept the HATV (High Altitude Test Vehicle). It was to have a half-ton payload and to be launched by a hydrogen-oxygen booster with a thrust of 46 000 kilograms (101 400 lb).

The Navy and Army Air Force held several joint meetings in late 1945 to explore the possibility of a common satellite program. No agreement was reached.

Subsequently, the Army Air Force asked the Rand Corp. to look at the satellite problem. On May 12, 1946, a prophetic report, entitled "Preliminary Design of an Experimental World-Circling Spaceship," was issued (ref. 15). The report stated that satellites could be:

(1) A scientific tool of great value

(2) A technical accomplishment that would inflame mankind.

---

[2] Actually, only two complete V–2's were assembled from the captured German parts. Missing components for others were manufactured in the United States.
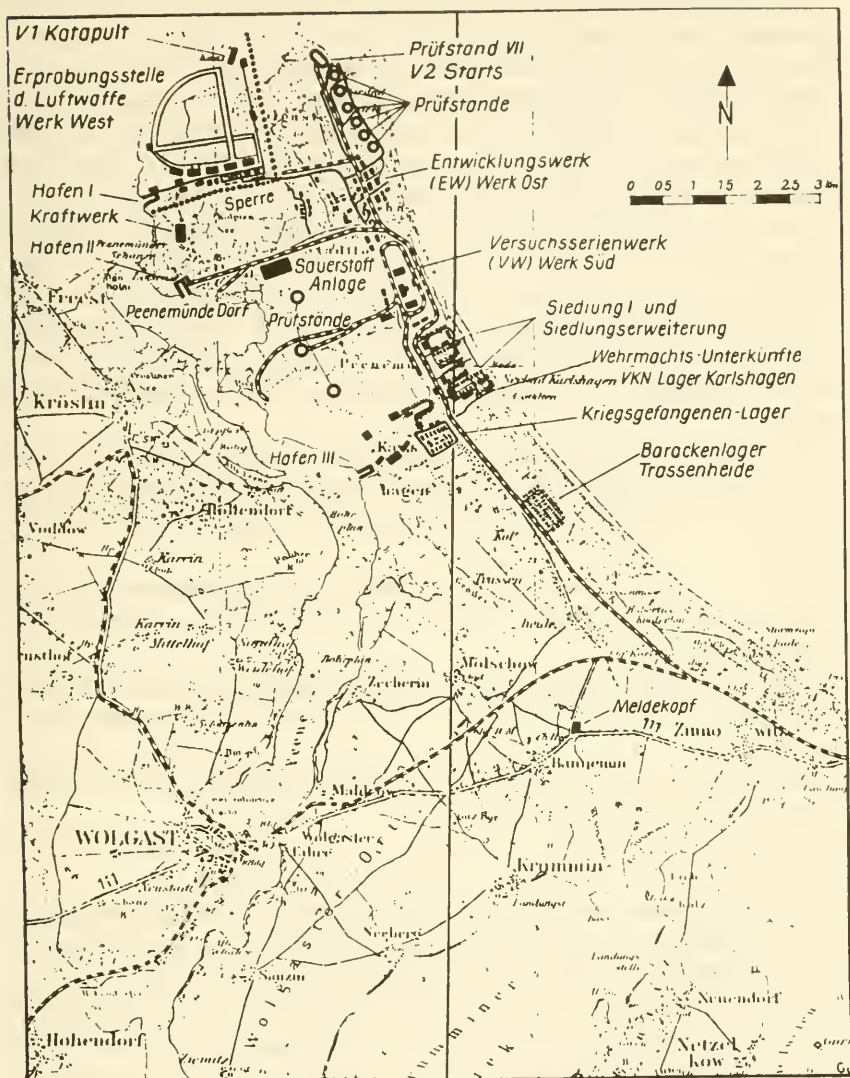
FIGURE 2–2.—German map of the Peenemuende V–2 launching facilities on the Baltic.

A quotation from the Rand report is pertinent here:

To visualize the impact on the world, one can imagine the consternation and admiration that would be felt here if the U.S. were to discover suddenly that some other nation had already put up a successful satellite.

The same report mentioned meteorological, communications, and biological satellites.

By the middle of 1946, the scientific-satellite idea was firmly and favorably established in the minds of many.   The second ingredient of a successful program, basic technology, had been pushed to high levels by the V–2 effort, although solar cells and miniaturized electronics had not yet arrived on the scene.   Firings of captured V–2's further substantiated the satellite idea.   But the third vital element needed, assigned resources, was still missing (table 2–1).

The first burst of excitement over satellites waned as postwar budgets choked off funds for all but a few minor studies.   After all, there was apparently no military value to satellites, and the Government had not begun to support basic science at levels that would countenance the construction of a large rocket and its supporting hardware.   Satellites were almost born in the 1945–1951 period.

As official U.S. support for satellites headed down into the trough that preceded the final crest, the amateurs again took over the burden.   Typical of these unofficial activities were the following:

(1) The stimulating paper written by Eric Burgess in 1949, ''The Establishment and Use of Artificial Satellites'' (ref. 16). (See fig. 2–3.)

(2) The second meeting of the International Astronautical Congress, held in London in 1951, and dedicated to the artificial satellite (ref. 17)

(3) The key paper, ''Minimum Satellite Vehicles,'' by Gatland, Kunesch, and Dixon, 1951 (ref. 18)

(4) MOUSE (Minimum Orbital Unmanned Satellite of the Earth), a concept suggested by Singer in 1953 (ref. 19)

Most significant about the new generation of technical papers was the realistic molding of the payload size to the capabilities of military launch vehicles, like the Redstone, then under development by Von Braun's group at Redstone Arsenal, near Huntsville, Ala.   The huge, manned, moonbound spaceships prophesied in the past now shared the limelight with unmanned, instrumented capsules weighing but a few kilograms.

By 1954, just about everyone admitted the scientific value of a small satellite circling the Earth for long periods, radioing back data about its environment.   The scientific satellite was now seen to be a logical extension of instrumented balloons and sounding rockets.   The V–2's fired from White Sands in the early 1950's carried radiation detectors, spectrographs, and micrometeoroid detectors.   The results whetted the scientific appetite for long-lived instrument platforms in outer space.
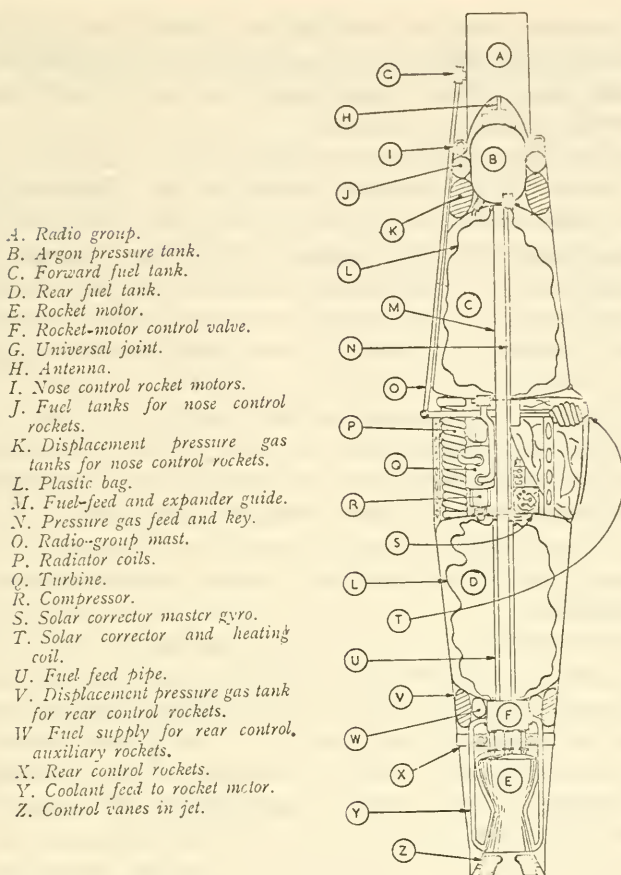
A. Radio group.
B. Argon pressure tank.
C. Forward fuel tank.
D. Rear fuel tank.
E. Rocket motor.
F. Rocket-motor control valve.
G. Universal joint.
H. Antenna.
I. Nose control rocket motors.
J. Fuel tanks for nose control rockets.
K. Displacement pressure gas tanks for nose control rockets.
L. Plastic bag.
M. Fuel-feed and expander guide.
N. Pressure gas feed and key.
O. Radio-group mast.
P. Radiator coils.
Q. Turbine.
R. Compressor.
S. Solar corrector master gyro.
T. Solar corrector and heating coil.
U. Fuel feed pipe.
V. Displacement pressure gas tank for rear control rockets.
W. Fuel supply for rear control auxiliary rockets.
X. Rear control rockets.
Y. Coolant feed to rocket motor.
Z. Control vanes in jet.

FIGURE 2–3.—The scientific satellite proposed by Burgess in 1949. Sun-heated steam was to be used for power instead of solar cells, which were not invented until 4 years later (ref. 16).

While amateurs and professionals continued their paper studies of small research satellites, the exigencies of the cold war forced the military back into the satellite picture. First, the Army was "bending metal" for the Redstone battlefield missile, and fired its first "round" in August 1953. The V–2 technology, itself a child of war, was being expanded. Redstone capabilities led directly to the launching of the first Explorer, in January 1958. The second military factor was the critical need for a reconnaissance vehicle. The Rand Corp. began to examine "spy-in-the-sky" satellites for the U.S. Air Force. Reconnaissance-satellite studies begun in the

late 1940's turned into Projects Feedback, Pied Piper, Big Brother, and WS–117L. Eventually, these programs moved into the hardware phase, and, as they did so, generated more basic technology to support the scientific satellite.

The cold war is not, of course, fought with threats of military weapons alone. One recalls the words of the 1946 Rand report relative to that new factor, international technical prestige—later half-jokingly called the International Scientific Olympic Games. The prestige factor, coupled with pressure from scientists looking ahead to the International Geophysical Year (IGY), scheduled for 1957–1958, inspired renewed Government interest in scientific satellites.

In 1954, the Ad Hoc Committee on Space Flight of the American Rocket Society proposed to the National Science Foundation that the United States sponsor the construction of a small satellite that would be launched by military rockets during the IGY.[3] The National Science Foundation accepted the suggestion, and its International Scientific Committee passed the thought on to other IGY participants.

In the fall of 1954, the U.S. Committee for the IGY formed a small study group, with Dr. Fred Whipple as chairman, to investigate the possibility of a U.S. IGY satellite. Whipple's group reported on a ''Long-Playing Rocket,'' or LPR, that used a 5-kilogram, white, spherical satellite, 50 centimeters in diameter, that could be observed visually from the Earth. The study group found the satellite idea both feasible and desirable, and on March 10, 1955, it adopted a resolution favoring the launching of an American IGY satellite.

From late summer 1954 to early 1955 was a great period for resolutions in favor of scientific satellites, as everyone climbed on the decade-old bandwagon. In addition to the committees and study groups mentioned above, the following three international organizations added their voices to the clamor:

(1) The International Scientific Radio Union (URSI)

(2) The International Union of Geodesy and Geophysics (IUGG)

(3) The Comité Spécial de l'Année Géophysique Internationale (CSAGI)

Such pressures had favorable results, for, on July 29, 1955, President Eisenhower announced that the United States would launch

---

[3] An interesting historical note: There had been plans to use Goddard's rockets for sounding the atmosphere during the Second Polar Year, in the 1930's.

"small, unmanned, Earth-circling satellites as a part of the U.S. participation in the IGY." The Soviet Union followed suit the next day. The third, and final, ingredient necessary for success was now present; money and manpower had been added to the technology (evolved from military programs) and the satellite idea itself (mainly the product of amateurs).

President Eisenhower's message signaled the start of the Vanguard program, authorized on September 9, 1955, by the Secretary of the Navy, managed by the Naval Research Laboratory, and funded by the National Science Foundation. This final definition of the Vanguard Program was preceded by rival proposals from the Army and Navy. The Navy suggestion, which necessitated the development of a new launch vehicle, based on the Viking sounding rocket, won out over the Army proposal to use the Redstone missile technology (ref. 20). By 1954, the Army, Navy, and Air Force were all back studying satellites again, with the last adhering rather closely to military missions. For many months, the Army and Navy pooled their efforts in Project Orbiter, which included contributions from von Braun's Huntsville organization, the Army's Jet Propulsion Laboratory (JPL), the Office of Naval Research (ONR), and several industrial companies. Project Orbiter, which was examining a modified Redstone with solid-propellant upper stages, was terminated in August 1955, soon after the White House announcement (ref. 21).

The Project Orbiter studies were not in vain, for when the

FIGURE 2–4.—Vanguard I, launched March 17, 1958, portrays early United States design thinking.
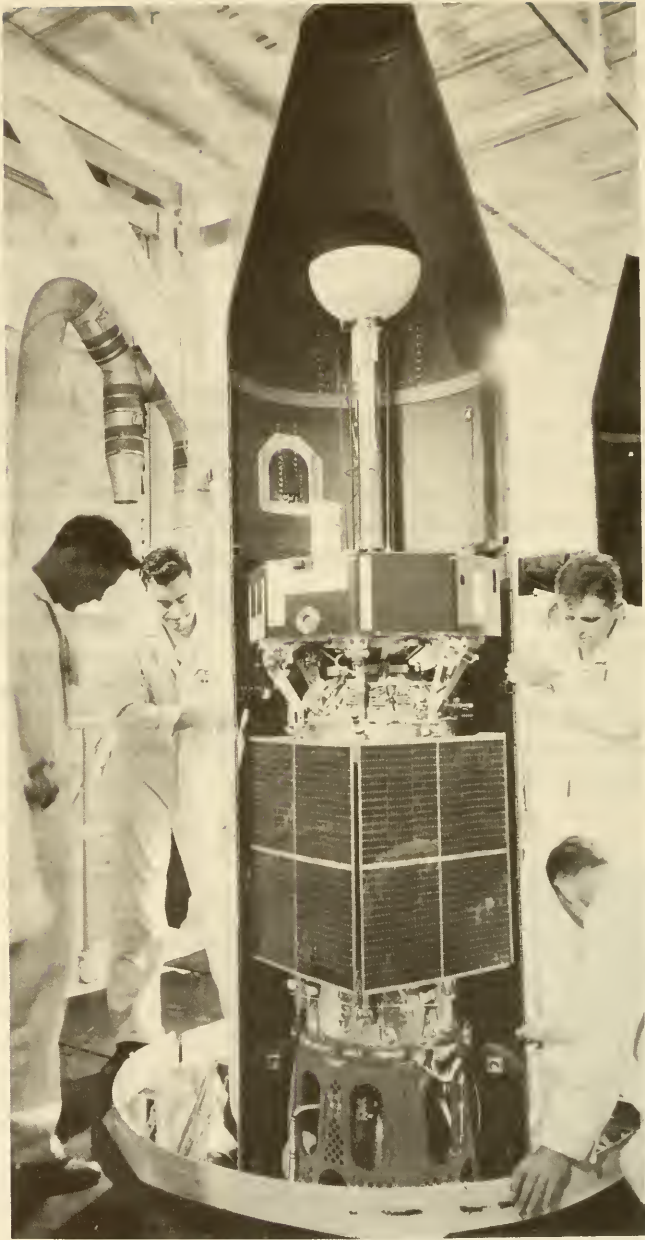
FIGURE 2–5.—IMP B shown being mated to the Delta launch vehicle and fitted with the shroud. IMP B, officially called Explorer XXI, was typical of many Explorer-class satellites launched between 1961 and 1966.
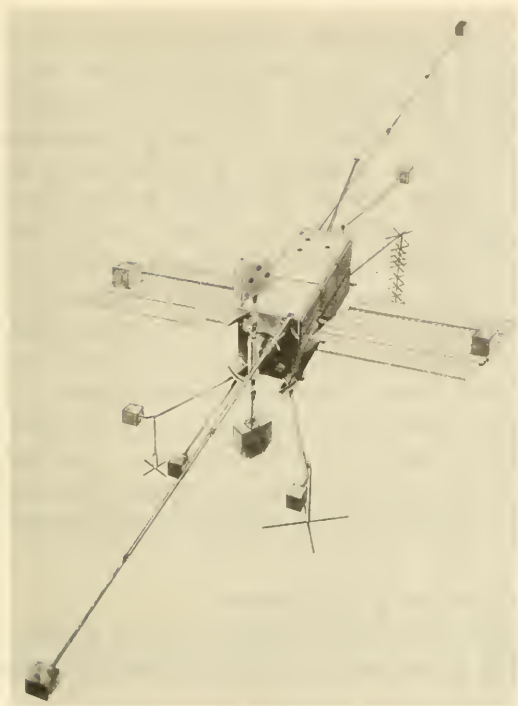
FIGURE 2–6.—Drawing of the OGO spacecraft, showing the many appendages typical of this series. The OGO typifies the Observatory class of satellites.

Vanguard Program seemingly faltered in 1957,[4] the prestigious pressure of the Sputnik 1 success on October 4, 1957, caused the Secretary of Defense to announce on November 8, 1957, that the Army was also to participate in the IGY satellite program.[5] Eighty-four days later, on January 31, 1958, the Army launched the first U.S. satellite, Explorer I, using a Juno I rocket—a modified Jupiter rocket, which, in turn, was derived from the Redstone, which, to complete the chain, owed much to V–2 technology (figs. 2–4, 2–5, and 2–6).

Vanguard I was finally orbited on March 17, 1958, but the very real technical success of the Vanguard program has always been overshadowed by Sputnik 1, Explorer I, and the well-publicized early Vanguard failures.

The development of the satellite idea did not end with Van-

[4] Actually, Vanguard experienced no more than the usual rocket-development problems.

[5] In making this decision, President Eisenhower permitted the Army to employ military rockets that had been specifically denied to the Vanguard Program because of the desire to keep the U.S. effort free from military overtones.

guard I and Explorer I. There has been considerable refinement and specialization of scientific satellites. The long Explorer series has evolved many specialized spacecraft, such as the Energetic Particles Explorer, the Topside Sounder, and the Atmosphere Explorer. Satellites have also been generalized, as illustrated by the orbiting Observatory series, which provides standardized environments for many different instruments. These trends, and other classes of satellites that have evolved primarily from the military space programs, are described in table 2–2. Crude as that categorization is, it helps illustrate the main lines of development. There is no reason to believe that this evolution has ended. The future will probably see more active (as distinguished from passive) satellite experiments in space, in which the space environment is altered artificially in a cause-and-effect fashion. One can imagine, for example, the deliberate injection of charged particles into the Earth's radiation belts and the launching of large masses of ices to simulate comets.

2–3.   Development of Satellite Technology

This section presents the historical unfolding of basic satellite technology, the second of the three essential, parallel developments outlined in table 2–1.

Satellite technology is a huge and many-faceted subject. Since it is the primary topic of this book, it is desirable to establish early a framework for discussion. Such a framework (the satellite subsystems and supporting launch-vehicle and Earth-based-facility systems) is the model of figure 2–8. The satellite system consists of 10 clear-cut subsystems, each with well-defined functions. (See table 3–1 for functional definitions.)

Short historical vignettes of the subsystems follow, in the order of their clockwise appearance on the model. Supplementing the text is table 2–3, a chronological chart illustrating the evolution of critical satellite technical developments.

The Communication Subsystem.—Willy Ley has pointed out how the concept of the unmanned scientific satellite was long retarded by the slow birth of radio telemetry (ref. 1). The early thinkers would undoubtedly be astounded at the avalanche of millions of bits of scientific and spacecraft-status data that a modern satellite can release in a burst to waiting ground antennas.

Marconi successfully demonstrated long-distance radio communication in 1895, but radio telemetry, where technical data are transmitted, did not see its first application until March 3, 1932, when the French physicists R. Beneau and P. Idrac received radio signals from instruments they had placed on balloons (radio-

TABLE 2-2.—*Evolution of Scientific Satellite Types* [a]

Type or class	Characteristics	Examples
Explorer class	Small, usually rather specialized satellites, used primarily in geophysical studies. Orbits are shaped to mission objectives. Timing is often set by known natural phenomena (solar cycle) or manmade events (high-altitude weapons). Logical extrapolations of sounding rockets.	Explorers, Vanguards, IMP's, Elektrons (figs. 2-4 and 2-5).
Observatory class	Large, generalized satellites, providing standardized experimental environment for many diverse instruments. Orbits less flexible than Explorers. Launched on a regular basis. Designed for long-term, systematic studies of space phenomena.	OGO, OSO, OAO (fig. 2-6).
Recoverable spacecraft	Large satellites with reentry capabilities. Generally placed in low orbits and caused to reenter after a few days or weeks. Experiments are usually biological in character; i.e., specimens and dosimeters.	Discoverers, Cosmos series, Bio-satellite, military-reconnaissance satellites (fig. 2-7).
Piggyback type	Satellites that are carried into orbit and "kicked off" other spacecraft, or satellite instrument capsules carried in lieu of ballast on test spacecraft. Scientific objectives are strictly secondary to primary mission, which is often military in nature. Standardized pods and capsules have been developed for use when opportunities arise, but many satellites are specially tailored to mission.	Injun 1, Grebs, TRS series, OV series.
All other satellites	Many geodetic and radio-transmission data of scientific importance are gathered from nonscientific satellites.	Echo, Tiros, Transit, Project West Ford, etc.

[a] See appendix for a list of all scientific satellites.
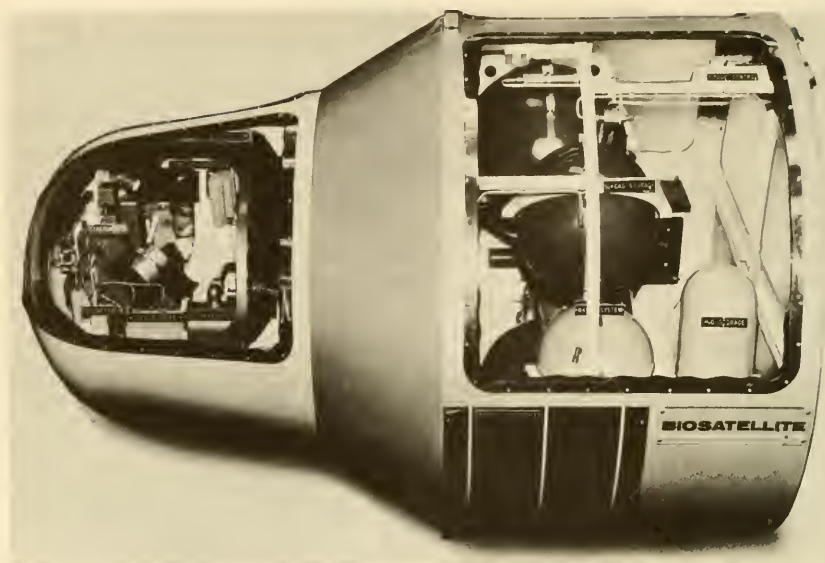
FIGURE 2–7.—Photograph of a model of a Biosatellite showing a primate experiment. Biosatellite is one of the very few recoverable scientific satellites launched by NASA.

sondes). Radio telemetry was, however, a logical extrapolation of wire telemetry, invented by the Dutchman, Olland, in 1877, for industrial purposes; i.e., the remote indication of switch positions, temperatures, and pressures. In addition, the radio control of unmanned boats and planes preceded radio telemetry by several years. In the United States, scientific radio telemetry began with the classic balloon studies of the stratosphere by A. V. Astin and L. F. Curtiss in 1936 (ref. 22).

With the feasibility of radio telemetry successfully demonstrated, engineers converged on the problem of what kind of telemetry was best. Amplitude modulation was tried first, but noise seriously degraded information during transmission. World War II saw the uncoordinated growth of a host of new pulse- and frequency-modulation techniques in secret projects. Commercial and military techniques unknowingly diverged and even used different terminology. Many postwar meetings of specialists were needed to kill this technological Hydra and standardize techniques and terminology.

During World War II, the Germans at Peenemuende had no choice but to develop telemetry to radio back data on what was happening in their V–2's. There were many early failures and it was almost impossible to find the cause of failure in the rubble of
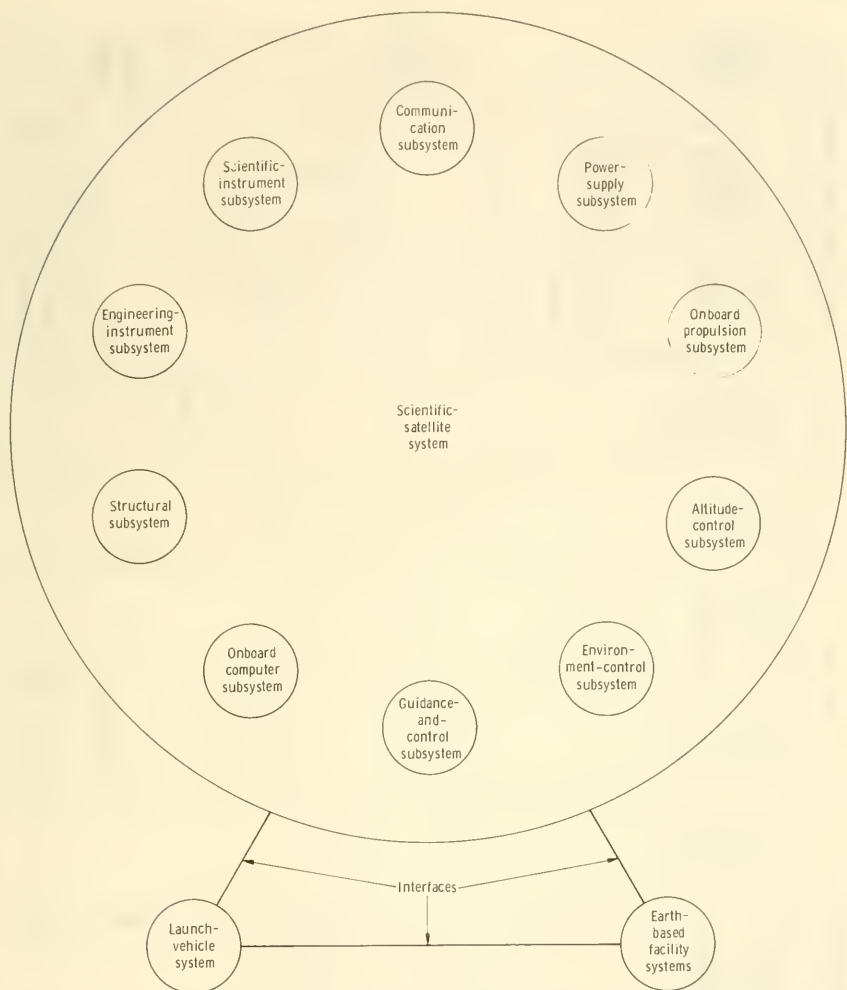
FIGURE 2–8.—Schematic showing the 10 subsystems of the generalized scientific satellite. The supporting launch-vehicle and Earth-based facility systems are also indicated.

a V–2 crater. Amplitude modulation was tried first, but a shift was soon made to frequency modulation. By the end of 1943, V–2 transmitters were pinpointing trouble spots in real time.

Many modulation schemes have been tried on scientific satellites, but the trend today is strongly in favor of some variety of pulse modulation. (See sec. 9–4.) The pressure forcing this trend comes from the superior communication efficiency of pulse modulation, on the one hand, and its better compatibility with digital computing machinery, on the other. Computers are essential if the tor-

TABLE 2–3.—Chronological Summary of Key Technical Developments in the History of Scientific-Satellite Technology

Year	Communication subsystem	Power-supply subsystem	Onboard propulsion subsystem	Attitude-control subsystem	Environmental control subsystem	Guidance-and-control subsystem	Onboard computer subsystem	Structural subsystem	Engineering instrument subsystem	Scientific-instrument subsystem	Launch-vehicle system	Earth-based facility system
1930	Radio telemetry									Goddard instruments	Goddard rockets	
1935										Radiosondes	V–2	Peenemuende
1940	Pulse techniques					Star tracker			V–2 status instruments			
1945		Solar furnaces used in designs								V–2 and sounding rockets	Viking	White Sands

Year											
1950						Sun-follower					Missile telemetry
1955	Minitrack	Redstone								Solar cells — Snap program, Radioisotopes first used	
1960		Atlas, Thor, Vanguard, Delta, Scout	Radiation detectors, Photometers, Spectrometers	Spheres, Cylinders, Balloons, Polygons, Booms, Pods, Boxes	Tape recorders, Specialized computers	Solar aspect, horizon scanners; Magnetometers	Paint patterns, Louvers, Electric heating	Spin stabilization, Cold-gas jets, Gravity gradient, Magnetic forces	Mono-propellants		Ascendancy of PCM
1965	STADAN	Saturn I, Titan 3	OAO telescope, RAE	RAE	Centralized computers				Electric propulsion?	Snap-10A test	
1970											Lasers

rent of satellite data is to be digested and converted into useful form. Many of today's satellites turn all analog signals into digital signals in the binary language before transmission to the Earth.[6] Only when the data are intended for human analysis are they converted back into decimal or analog form.

Another historical trend has been the shift to ever-higher radio-frequencies. A chronological list of transmitter frequencies shows a shift from tens of megacycles to thousands of megacycles. Now, lasers, which use optical frequencies, are being studied for communication.

Finally, it seems inevitable that the larger satellites, like those in the Observatory class, will carry some form of data compressor or selector on board. Thousands of miles of unanalyzed data tapes are being stored away today because there is no fast, electronic way of sorting the significant data from the endlessly repeated or slowly varying measurements that come from many space experiments.

The Power-Supply Subsystem.—When Oberth, Noordung, Clarke, and the early Navy and Army Air Force groups first studied the satellite problem, the Sun was the most obvious source of energy. It still is, and, with the exception of a small handful of battery or radioisotope-thermoelectric-powered satellites, all satellites are plastered with solar cells or encumbered with rather awkward solar-cell paddles. Solar cells are dominant on scientific satellites today because power demands are low and lifetimes short. There are no important competitors for these missions in sight. (See sec. 9-5.)

It was not always this way. Solar cells were not invented until 1953, during the course of semiconductor research at the Bell Telephone Laboratories (ref. 23). Before this discovery, spacecraft theoreticians relied upon solar furnaces, the commonplace battery, and solar thermoelectric power (figs. 2-1 and 2-3). Of course, when the potential of nuclear power became evident, at the end of World War II, nuclear reactors seemed destined to solve all spacepower problems. Project Feedback and other reconnaissance-satellite programs made the first feasibility studies of nuclear spacepower (ref. 24).

The simple solar cell was far simpler to develop for Vanguard and the later Explorers than solar collectors or radioisotopic power supplies. Once entrenched in the lead, solar cells have remained there. A brief period of doubt occurred in 1962, when the artificial radiation belts created by high-altitude nuclear ex-

---

[6] Explorer VI first used pulse-code modulation (PCM) in 1960.

plosions greatly reduced the performances of several orbiting solar-cell powerplants. The rapid introduction of radiation resistant $p–n$ cells to replace the older $n–p$ cells effectively solved this problem.

The development of nuclear space-power plants began in 1957, when the Atomic Energy Commission started the Snap (Systems for Nuclear Auxiliary Power) program. The first radioisotopic generator to be flown was a modified Snap 3, in 1959, which provided 2.7 watts of power to a prototype Transit navigation satellite. The first nuclear-reactor powerplant placed in orbit was a test version of the 500-watt Snap 10A, launched on April 3, 1965. Since present-day scientific satellites generally require less than a kilowatt of electrical power and often have lifetimes of less than a year,[1] nuclear power has not been needed. A radioisotopic power generator, Snap 19, was built for Explorer XVIII (IMP I—Interplanetary Monitoring Platform/Probe I) but was never used because its radiation interfered with sensors measuring environmental radiation.

Solar cells are often used in combination with chemical batteries, which power the satellite during shadow periods. Although batteries have been employed in technology for almost two centuries, there was little impetus to miniaturize them or adapt them to zero-g environments until the Space Age. When first used on satellites, batteries were notable for their leakiness and for the limited number of charge-discharge cycles they could survive as the satellite passed through the Earth's shadow zone. Most of these defects have now been remedied.

The history of spacepower presents an overabundance of ideas and intriguing schemes for power production, but, except for solar cells, fuel cells, and radioisotopic generators, no operational hardware. There continues to be much research and development of thermoelectric and thermionic converters, biological fuel cells, boiling-potassium nuclear reactors, ferroelectricity, and other advanced concepts. Solar cells themselves are being made of new semiconductor materials and are being fabricated in thin polycrystalline sheets. The greatest impact of these efforts will be felt mainly on the larger spacecraft, where the lack of kilowatt-sized powerplants has restricted mission planners.

The Onboard Propulsion Subsystem.—Onboard propulsion equipment is used on scientific satellites for orbit control, station keeping, and maneuverability. Thrust is also needed to deorbit recov-

---

[1] Timers are now included on many satellites to turn them off the air after 6 months or some other fixed period.

erable satellites in the Discoverer, Cosmos, and Biosatellite classes. (See sec. 9–6.)

The history of liquid and solid onboard chemical rockets is necessarily the same as that of their much larger cousins that power the launch vehicles. Discussion of launch-vehicle rocketry is found later in this section. Meanwhile, there are a few divergent but pertinent stems to this tree of rocket evolution.

First, the station-keeping function is often accomplished by cold-gas jets, which were first used as attitude-control devices in the early 1960's on Discoverer satellites. Second, interplanetary spacecraft, like Mariner II, in 1962, and some satellites have employed monopropellants, like hydrazine, to provide precisely measured impulses. In contrast, no major launch vehicles use monopropellants. A more recent innovation has been the fabrication of tiny rockets with a subliming material providing the expellant for attitude-control thrust. Finally, at some indeterminate future time, large, reliable electrical power supplies will be available to power ion and plasma engines for station keeping, attitude control, and orbit adjustment. Electrical propulsion was proposed as early as the 1930's, but its basic feasibility has only recently been proven on suborbital and satellite flights.

The Attitude-Control Subsystem.—The attitude control and stabilization of Earth satellites has proven to be a much more complex task than the astronautical pioneers anticipated. First of all, they hardly thought about it at all in their fascination with the booster problem. Neither did they foresee the perturbing effects of the atmosphere, solar pressure, gravity gradients, and internal-momentum changes. Probably the earliest clear statement of the problem was by Esnault-Pelterie in his *L'Astronautique*, in 1930; but problem statements are not solutions (ref. 25). And who in 1930 dreamed of unmanned satellite telescopes, whose attitude had to be remotely controlled to a minute of arc?

The first Earth satellites were not attitude controlled at all; that is, they were allowed to tumble and roll. This situation favored isotropic instrumentation, but the space environment turned out to be far from isotropic. In addition, Earth-pointing satellites were needed for meteorological studies.

Simple spin stabilization was suggested by Singer in 1954 (ref. 19). It was used on the first Pioneer probes and Explorer I in 1958, and on the Tiros series of weather satellites, starting in 1960. Spinup and spindown (despin) mechanisms [8] were included on many early satellites to adjust the spin rate. Spin stabilization

---

[8] The "yo-yo" despin device, described in sec. 9–7, is typical.

has been satisfactory for many geophysical experiments, especially where scientists wish to scan the environment.

The study of the Sun and stars, however, requires a very steady platform, which can be achieved only with complete and sophisticated attitude control. In 1955, Stuhlinger proposed the use of reaction flywheels for attitude control (ref. 26). To this suggestion were soon added chemical rockets, cold-gas jets, magnetic bars and coils, and inertia spheres. These active devices are described in detail in section 9–7. Most attitude-control schemes have been tried on one or more satellites. Where complete, precise stabilization is needed in inertial space, as with the OAO (Orbiting Astronomical Observatory), a combination of gyros (which are saturable; i.e., limited in the amount of angular momentum they can store) and cold-gas jets is commonly used. Electrical propulsion seems likely for attitude control in the future.

The cooperativeness of the satellite environment in promoting stabilization came as a surprise. Even today, it is intuitively hard to believe that the variations of the force of gravity and centrifugal force over the dimensions of a satellite can be useful. Yet, gravity gradients, solar pressure, atmospheric drag, and magnetic forces are all employed in passive stabilization of spacecraft. Gravity-gradient stabilization equipment, developed in the early 1960's by the Applied Physics Laboratory (APL) of Johns Hopkins University for the Transit satellites, is most common. It accounts for the elongated shapes and projecting masses on recent meteorological and communications satellites. Magnetic bars and coils have been installed on many of the later Explorers; viz, Explorer XXV.

The Environmental-Control Subsystem.—Here is a seemingly prosaic area of technology that has created many more headaches than anyone ever predicted during the youthful days of astronautics.

Thermal control of the satellite first comes to mind. Tsiolkovsky and Oberth realized that all heat generated on board and absorbed from the Sun had to be radiated away to maintain a spacecraft's temperature within reasonable limits. The real problem has not been one of recognition, but rather one of analysis (sec. 9–8). Even with detailed thermal models of a satellite, it is difficult to predict satellite temperatures to within 10° C. Frequently, local hot spots (or cold spots) will compromise equipment operation.

Passive temperature control by use of paint patterns began with Explorer I and has continued to this day, but the technique is limited, and, as just mentioned, precision is hard to attain.

Active thermal control involves the use of rotating vanes or louvers like venetian blinds. Louvers saw use as early as 1962, on Mariner II, and have become common equipment on large satellites, such as OGO I (Orbiting Geophysical Observatory), and on interplanetary spacecraft. Thermostatically actuated rotating vanes, though proposed for early satellites, have not been used operationally. Electrical heating or cooling (thermoelements) has been introduced.

Once a satellite was launched, no one expected that its mechanical environment (vibration and noise) would be important. Experience soon showed that apparently insignificant things, such as the closing of relays, could introduce spurious signals into the micrometeoroid-detection apparatus. Countermeasures here have been simple: mechanical insulation and the use of solid-state devices.

The Van Allen Belts create a radiation environment that must be controlled to lengthen the lives of the solar cells and sensitive electronic components. In addition, fluctuating currents throughout the satellite can cause electronic crosstalk between circuits. Finally, every satellite is itself the source of a magnetic field that must be reduced to near zero to insure accurate magnetometer data. Like the vibration problem mentioned above, these delicate satellite interfaces were not appreciated during the early days of astronautics. Recognition came only through experience in space. Perhaps, in view of the subtlety of satellite interfaces, it is unrealistic to have expected cognizance at a time when rockets and satellites themselves were still in the science-fiction category.

The Guidance-and-Control Subsystem.—If we restrict ourselves to the navigational guidance and control of the orbited satellite, superficially there would seem little for the satellite to do except sense its attitude (a form of navigation) and correct it. When one looks ahead, though, the maneuverable scientific satellite appears on the horizon, especially in connection with synchronous satellites. The history of this subsystem therefore draws on the full history of maneuverable spacecraft and their inertial and position-finding sensors.

Historically, the navigation, or position finding, of Earth satellites has been an Earth-based function. In other words, the satellite itself has carried no position-finding apparatus other than radio beacons to aid ground stations. For a history of the gyros,

radars, and accelerometers customarily carried by launch vehicles and deep-space probes and which eventually will probably be installed on maneuverable scientific satellites, the reader should refer to Draper and Farrior (refs. 27, 28). The evolution of Earth-based tracking equipment is covered later in this section.

Navigation for attitude control (orientation finding) and for inserting instrument-orientation information on scientific telemetry records is a prime satellite-based function. Attitude information for the first Explorers and Vanguards came in the form of periodic enhancement of the satellite-transmitter signal strength, caused as the spinning satellite swept the Earth with its antenna pattern. Next came solar-aspect sensors on Explorer VI (1959), which indicated only the intensity of sunlight, but which were useful for adding orientation information to scientific records. Solar sensors do not have the angular resolution needed for Sun-tracking in guidance and attitude control.

The next important satellite navigational device was the horizon scanner, first suggested by Stuhlinger in 1956,[9] along with a scheme for using the cosmic-ray-shadowing effect of the Earth for obtaining directional information (ref. 26). Horizon scanners are, of course, mainly employed by Earth-pointing meteorological and reconnaissance satellites. Their first recorded use was on Discoverer 2 in 1959. The larger scientific satellites, like OGO I, now use horizon scanners in conjunction with solar-aspect sensors to provide attitude information and help orient the solar panels.

The most difficult navigation tasks occur on the solar and astronomical satellites, the OSO's (Orbiting Solar Observatory) and OAO's. Although these satellites do not have to rotate continuously in inertial space, as the Earth-pointing types, they must track the Sun and stars with very high precision in the presence of disturbing torques, if the scientific instruments are to be effective. Such requirements have led to the development of sophisticated Sun and star trackers (sec. 9-9). The Sun and stars have been easily tracked from Earth for many years by simple telescope drives, but obviously these will not suffice for a satellite. Sun trackers, which are somewhat easier to design, were developed second. In 1950, the University of Colorado designed and built a Sunfollower that was used to take solar spectrograms from high-altitude rockets (fig. 2-9). MIT began work on star trackers for use on long-range bombers in 1945. The now-ancient Snark missile, built by Northrop Aviation Co., carried a star tracker.

---

[9] Quite likely, the horizon scanner was also suggested during reconnaissance-satellite studies around 1950.

Star trackers saw their first operational use in space on Mariner IV, in 1964, when the star Canopus was tracked during the flight to Mars. The first Earth satellite equipped with star trackers was OAO I, launched in 1966.
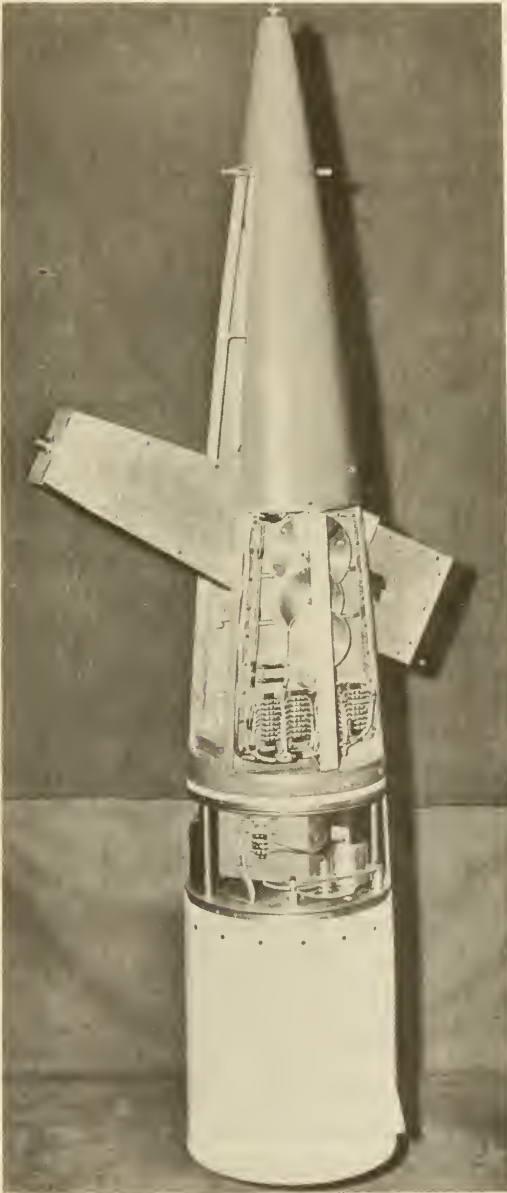
FIGURE 2–9.—The University of Colorado Sunfollower used in high-altitude-rocket solar research in the early 1950's. (Courtesy of the Univ. of Colo.)

So much for position and attitude sensing. One other aspect of satellite control remains, that of command. Here, again, the space pioneers bypassed remote and autonomous control and restricted their thinking to missions where man himself flipped the switches and turned the knobs. The history of scientific-satellite command thus has its origin in the radio-controlled boats and aircraft of the 1920's. Remote control and command were further developed by the military for use in drones and guided missiles. At the beginning of the Space Age, no one foresaw today's scientific satellite that, upon command, will change its attitude, play back recorded data, switch instruments on and off, and, in the case of Biosatellite, deorbit itself.

Since 1957, more and more controllable functions have been added to scientific satellites. The object, of course, is to increase the versatility and survivability of the machine. Sometimes, for example, a part failure may cause an unacceptable power drain on a satellite. If the offending component can be switched off by a command from Earth, the useful lifetime of the satellite will be greatly prolonged. This is an example of external control.

Internal control, which evolved concurrently with external control, is typified by the spacecraft clock, or timer. A spacecraft clock commands instrument booms and solar panels to deploy after launch and, at the end of the planned mission, it switches the satellite off the air, freeing its frequencies for other applications.

Speaking very generally, the trend in satellite control is toward more external control, in the direction of the classical Earth-based laboratory experiment, in which the investigator can make some (but not very many) manipulations and adjustments to his apparatus.

The Computer Subsystem.—Computers of the analog and digital types have long and venerable histories that need not be repeated here. Bernstein's delightful book, *The Analytical Engine*, recounts this story well (ref. 29). A word is necessary, though, on the application of computers on board scientific satellites.

Three tasks can be performed by onboard computers: arithmetic operations, logical operations, and data storage. The first satellites carried no computers at all. All computations were done on the ground. Gradually, highly specialized, decentralized computers were introduced by the experimenters themselves to convert sensor data into the digital form acceptable to the communication subsystem. Another early device was the tape recorder, first used on Explorer III, in 1958, to store data for burst transmission over ground stations. The concept of a centralized satellite-borne

computer is becoming more and more reasonable as the demand grows for some form of data selection and/or compression.

The Structural Subsystem.—Classically (and in science fiction), spacecraft are projectile shaped, often boasting wings like their atmospheric counterparts. To be sure, a streamlined fairing is needed for payload protection during the launch vehicle's ascent, but every schoolboy now knows that the satellite, once in space, can take the geometry best suited to the mission at hand.

Early satellites were simple spherical or cylindrical cans surrounding the instrument payload and sprouting antennas like whiskers. Solar cells often shingled the external surfaces. Cylindrical satellite geometry has persisted from Explorer I to this day. It derives from the application of spin stabilization, which favors a spin axis coincident with a spacecraft axis of symmetry. The desire for replaceable component and instrument packages next led to the common polygon cylinders, where each segment of the polygon forms an instrument bay. Explorer XII was the first scientific satellite to use this approach.

Some satellite shapes, like that of the OAO's, are dominated by their instruments. Others, such as Biosatellite, are shaped by the reentry requirements. If there is complete attitude control, rather than spin stabilization, configurations have tended to be boxlike.

The bifurcation in satellite design philosophy, discussed earlier, has led, on one hand, to small, specialized satellites and, on the other, to large, generalized spacecraft. In the first instance, the satellite structure has been specialized to the mission requirements (e.g., magnetometer booms). In the generalized satellites, an attempt is made to standardize experiment compartments and mountings.

There are few historical trends. One trend might be the inevitable shift to winglike solar paddles, rather than surface-mounted solar cells, as power requirements have risen beyond the capacities of satellite surfaces. The desire for instrument isolation has led to the profusion of quill-like booms that project from many satellites and deep-space probes (sec. 9–11). The structure of the scientific satellite has always been subservient to the demands of the instruments, the method of attitude control, the power supply, and the environment. Its history consequently shows continual adjustments to developments in these fields.

The Engineering-Instrument Subsystem.—Engineering instruments report back on a satellite's status,[10] or "health." Their

---

[10] In satellite engineering, "status" refers to the operational mode of the satellite as well as its temperatures, voltages, etc.

value is strictly utilitarian, helping to pinpoint trouble, actual or impending. They are closely akin to the fuel and temperature gages on a car. Because of their rather unromantic function, engineering instruments are seldom mentioned in today's astronautical literature and not at all in yesterday's.

Man's machines have always incorporated status indicators. They may be anything from steam-pressure gages on an ancient steam locomotive to the pattern of colored lights indicating valve positions in an oil refinery. Satellite engineering instrumentation is different only in the sense that such parameters as temperatures, switch positions, and power-supply voltages are relayed back from outer space by telemetry. Even this factor is hardly unique, because unmanned balloons, sounding rockets, oceanographic buoys, V–2 test rockets, and other radio-linked, unmanned equipments have been doing this since radio telemetry first became practical in the 1930's.

History here is a record of ever more sophisticated status instruments. Explorer I, for example, carried four temperature monitors at strategic spots. Six years later, a more advanced satellite, IMP I, relayed 15 status points back to Earth, including 9 temperature measurements and several critical voltages and currents. A satellite in the observatory series may radio back as many as 50 status measurements. The trend is toward more versatile scientific satellites that can be manipulated from Earth. More detailed status instrumentation has been the natural result.

The Scientific-Instrument Subsystem.—Every time that man has invaded a new environment, whether in person or by proxy, using an unmanned machine, he has included scientific instruments in the payload.

A famous instance is that of Torricelli, who in 1643 invented the mercury barometer and carried it up a mountain to record pressure changes with altitude. In 1749, kites carrying thermometers were flown in Glasgow. The urge to fly instruments at higher and higher altitudes caused Hargrove to build a powerful box kite that, in 1893, lifted temperature and pressure recorders (called meteorographs) to an altitude of 3 kilometers (10 000 feet). Balloons went even higher. The Frenchman Gay-Lussac measured temperatures, pressures, and electric fields at 7 kilometers (23 000 feet) in 1804. By 1893, unmanned balloons had reached 16 kilometers (53 000 feet). The next upward step was accomplished by the rocket. Goddard apparently was the first to put scientific instruments on rockets. On July 17, 1929, one of his liquid-fueled models lifted a barometer and a ther-

mometer to an inauspicious altitude of 30 meters (90 feet); nevertheless, it was a true sounding rocket. On April 16, 1946, the first American-fired V–2 carried in its payload a Geiger counter designed by J. A. Van Allen. The V–2's almost reached the Van Allen Belts. If they had, the discovery might have accelerated the evolution of scientific satellites.

Ostensibly, the purpose of the first satellites was purely scientific in nature. To be sure, Sputnik 1, Explorer I, and Vanguard I all returned significant scientific data from their experiments. History suggests, though, that political impact was perhaps more important than science at first. Many of the hundreds of satellites that have followed Sputnik 1 have been undeniably scientific.

Of the thousands of instruments that have been orbited, the largest fraction comprises the radiation detectors. The surprise of discovering the Van Allen Belts and the desire to map them have been partly responsible for this inequality of effort. Another factor has been the ready availability of radiation instrumentation (from nuclear engineering) suitable for space use. Magnetometers, plasma probes, micrometeoroid detectors, and other instruments required much more development work. Geophysical instruments, as a class, comprise perhaps 90 percent of all satellite instruments to date. Solar and stellar instruments, such as optical and ''X-ray'' telescopes, are now finding satellite platforms with acceptable stabilization and data-handling capability (chs. 12 and 13). Cosmological experiments, such as those calculated to check the general theory of relativity, are still in the development stage. Beyond these known fields of research undoubtedly lie undetected and unimagined phenomena that will require the design of radically new instruments.

The Launch-Vehicle System.—Of all the areas of space technology, rocketry has received the most attention from historians. So many histories exist, covering the several centuries from the Chinese war rocket to the V–2 war rocket, that reference to these, along with a few very specific comments, seems adequate (refs. 1, 13, 30).

War rockets, with minor modifications, launched Explorer I and Sputnik 1. In contrast, Vanguard I was orbited by a specially designed launch vehicle. When NASA was formed in 1958, it became obvious that the military launch vehicles, such as the Atlas and Titan series, would have to be used for the first scientific satellites, but that NASA would also need its own line of launch vehicles, particularly for manned missions. Military rockets had specialized applications and were often not adaptable to, or avail-

able for, NASA payloads. The Delta, Scout, Centaur, and Saturn launch-vehicle programs were the result (ch. 8). A glance at the table of scientific-satellite launchings (p. 264) will show, however, that military launch vehicles have been workhorses of considerable value.

A final comment concerns the piggyback and instrument-pod techniques employed by the Department of Defense on its many military satellites and launch-vehicle tests. A surprising number of scientific experiments have been placed in orbit as secondary objectives of military missions. The scientific "fallout" has been significant.

The Earth-Based Facility System.—The larger part of the space dollar manifests itself in the farflung Earth-based facilities that are essential to the testing, checkout, launching, tracking, data reception, and recovery of scientific satellites. These facilities will be described in more detail in chapter 7. Here, let us concentrate on historical evolution. Except for the launch and tracking facilities, it is recent history.

Probably the first rocket test range with any technical sophistication was the artillery range of the Royal Laboratory, at Woolwich, England, where Congreve experimented with his war rockets in 1802 (ref. 1). More than 100 years later, Goddard was not so fortunate. In the 1920's, he flew his experimental rockets from deserted fields near Auburn, Massachusetts. In 1930, he moved to Mescalero Ranch, near Roswell, N. Mex., about 100 miles east of White Sands, where there was more privacy and fewer restrictive local ordinances. While Goddard worked secretively in New Mexico, amateur organizations, particularly in the United States and Germany, were trying the tempers of local property owners by testing their frequently erratic small rockets at improvised sites.

World War II brought Peenemuende, and Peenemuende brought a surprisingly modern launch range. As Peenemuende was slowly built up from 1937 on, rocket test stands and a liquid-oxygen plant were built. There were tracking radars and checkout facilities—in short, many of the trappings of our Eastern and Western Test Ranges (fig. 2–10).

The White Sands Proving Grounds (later called White Sands Missile Range), in New Mexico, constituted the first American launch site of any size. Here, captured German V–2's, Private A's, WAC Corporals, and other military and high-altitude sounding rockets were fired from 1946 on.

A strange geographical coincidence occurred when the Eastern Test Range (ETR), at Cape Kennedy (then Cape Canaveral), was activated in 1950.[11] It was located only a few tens of miles from the spot where Jules Verne had his Baltimore Gun Club fire a manned projectile to the Moon in his novel *De la Terre à la Lune*. The Cape Kennedy site was selected over two other proposed sites in 1947. The competitors were spots near El Centro, Calif., and on the Washington coast. Favorable weather, a long island chain, and the presence of the deactivated Banana River Naval Air Station favored the Florida site. On May 11, 1949, President Truman signed Public Law 60, authorizing the Secretary of the Air Force to establish a joint missile-proving ground at Cape Canaveral.

The first nonfictional flight from the ETR took place on July 24, 1950, when a Project Bumper rocket, using a V–2 first stage and a WAC Corporal upper stage, was successfully fired. The ETR is now an immense facility, extending over 8000 kilometers along an arc of islands and deployed ships and terminating near Ascension Island.
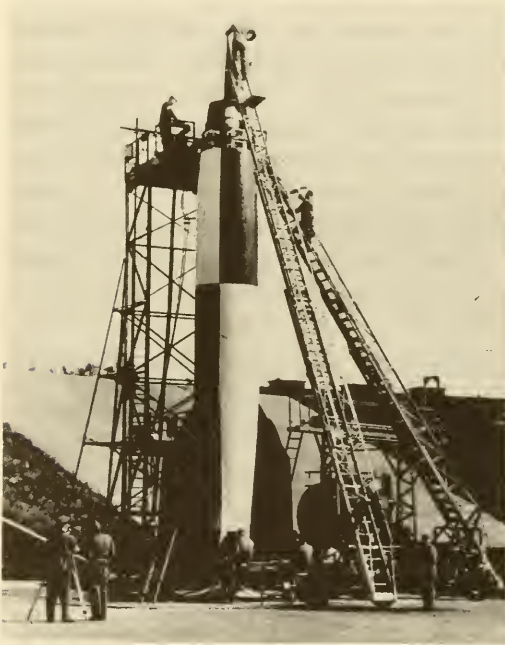
FIGURE 2–10.—A V–2 on a Peenemuende launch pad, a precursor of modern launch pads.

---

[11] The ETR was first called the AMR (Atlantic Missile Range).

Another major U.S. launch facility is the Western Test Range (WTR),[12] at Point Mugu, Calif., which was opened in 1958 and is used primarily for military space shots and scientific satellites requiring polar orbits (ch. 7). NASA also employs a smaller launch facility at Wallops Island, on the Virginia coast. The National Advisory Committee for Aeronautics (NACA) fired its first rocket from Wallops Island on July 4, 1945. The first satellite sent aloft from Wallops Island, Explorer IX, was launched on February 16, 1961. Since then, many scientific satellites, mainly using Scout launch vehicles, have been orbited from Wallops Island.

Successful satellites quickly pass out of the range of the last tracking/receiving station of the ETR or WTR. If satellite data are wanted frequently, along with many orbit fixes, a worldwide network of these stations is needed. The greater the geographical coverage of the net, the more often data can be radioed from the satellite.[13]

In the early days of the space program, there was considerable emphasis on optical tracking of satellites, because the accuracy and effectiveness of radio tracking had not been proven. The Moonwatch teams, each composed of a dozen or so amateur observers with small telescopes, were established in connection with the Vanguard Program. A network of Baker-Nunn cameras was also set up to supplement the Moonwatch groups.[14] Optical tracking is more precise than radio interferometry, and it can be used with "dark" (nontransmitting) satellites.

The first electronic tracking nets employed the Minitrack and Microlock concepts advanced by the (contending) Naval Research Laboratory and the Jet Propulsion Laboratory (JPL), respectively. The Navy Minitrack system evolved from tracking experience at White Sands and was made a part of the Vanguard program in 1955. Microlock, like Minitrack, was an interferometer system. It was used in conjunction with Minitrack for tracking the first few Army Explorers. NASA took over operation of the Minitrack stations in 1958 and has since established new stations. Collectively, the stations form STADAN (Satellite Tracking and Data Acquisition Network).

If anyone had suggested in 1955, just prior to the Vanguard Program, that 10 years later satellites would be sending back so

---

[12] Formerly, the PMR (Pacific Missile Range).

[13] Russia does not possess a worldwide network, but has been able to carry out ambitious space programs despite this lack.

[14] Excellent optical observations with theodolites, particularly of the bright Sputniks, have been made in other countries.

much data that a large fraction of it would go unanalyzed, that person would surely have been considered wildly imaginative. But it is a fact that tens of miles of magnetic tape are filled with satellite data every day.   An absolutely essential segment of ground-support equipment for a scientific-satellite program is an extensive bank of computers, indexes, archives, and other data-handling machinery.   The story of data processing, however, is hardly history, since it is still in the making.   The rapid developments in this field are summarized in chapters 5 and 7.

NASA also operates two other global tracking networks that are sometimes pressed into service for satellite tracking.   They are the Manned Space Flight Network and the Deep Space Net; the latter includes the Deep Space Instrumentation Facility (DSIF).

Parallel to the NASA tracking facilities are those constructed by the Department of Defense (DOD) for military purposes.   The DOD Space Track project, a centralized clearinghouse for all satellite tracking data, rather than a tracking net per se, was created in 1958 (ref. 31).   Space Track was the progenitor of SPADATS (Space Detection and Tracking System), which is also a data gathering and cataloging operation.   The details of the actual tracking and surveillance stations operated by DOD are obviously classified information.   Since military necessity dictates that dark satellites and warheads must be tracked, DOD facilities certainly include radars that can skin-track small objects at satellite altitudes.   All military-satellite tracking and cataloging operations feed data to the Air Force's NORAD (North American Air Defense Command).

2–4.   Organizational and Administrative History

The final essential ingredient in any large cooperative undertaking is organizational in character.   The history of the many private, national, and international astronautical groups that have formed and dissolved over the last few decades presents such a forest of acronyms and abbreviations that its presentation in text form would be unduly inconsiderate to the reader.   Therefore, another chronological chart has been prepared to show the evolution of the acronyms that we now use so freely but which, in the light of the past, are rather short-lived.   Table 2–4 is a much more detailed version of the right-hand segment of table 2–1.   (See ref. 32.)

TABLE 2–4.—*The Historical Evolution of Space-Oriented Organizations and Projects*

[See text for definition of abbreviations and acronyms]

| Year | Private and professional | U.S. Government organizations and programs | | International |
		Nonmilitary	Military	
1910				
		NACA formed		
1920	Verein für Raumschiffahrt			
	Goddard Guggenheim grant			

TABLE 2-4.—*The Historical Evolution of Space-Oriented Organizations and Projects*—Continued

[See text for definition of abbreviations and acronyms]

Year	Private and professional	U.S. Government organizations and programs		International
		Nonmilitary	Military	
1930	American Interplanetary Society			
	Institute for the Aeronautical Sciences			
	British Interplanetary Society			Peenemuende
	Von Kármán forms RRP (forerunner of JPL)			
1940			Project ORDCIT Paperclip, CEFSR White Sands Proving Grounds Rand and Navy satellite studies	

1950	American Astronautical Society	IRBM	First IAF meeting
	NSF funds Vanguard	ICBM Feedback, Pied Piper Project Orbiter	URSI, IUGG, CSAGI recommends IGY satellite IGY COSPAR formed First COSPAR meeting
1960	Vanguard, NASA formed NASA Explorers	Explorer I Discoverer program	
	Observatory program	Piggyback program Injun 1	ELDO Ariel 1, Alouette 1 IQSY ESRO formed
	AIAA formed Owl		
1970			

References

1. LEY, W.: Rockets, Missiles, and Space Travel. Viking Press, 1957.
2. HALE, E. E.: The Brick Moon and Other Stories. Little, Brown Co., 1899.
3. KRULL, A. R.: A History of the Artificial Satellite. Jet Propulsion, vol. 26, May 1956, p. 369.
4. STOIKO, M.; AND DORSEY, J. W.: Rocket Catapult Facts and Fables. Astronautics, vol. 5, July 1960, p. 30.
5. LASSWITZ, K.: Auf Zwei Planeten. (Leipzig), 1897.
6. OBERTH, H.: Die Rakete zu den Planetenraumen. R. Oldenburg (Munich), 1923.
7. NOORDUNG, H.: The Problems of Space Flight. R. C. Schmidt (Berlin), 1928.
8. MACMECHEN, R.: Rockets, the New Monsters of Doom. Liberty, vol. 8, Sept. 19, 1931, p. 16.
9. GODDARD, R. H.: A Method of Reaching Extreme Altitudes. Smithsonian Institution, 1919.
10. HUZEL, D. K.: Peenemuende to Canaveral. Prentice-Hall, Inc., 1962.
11. EHRICKE, K. A.: The Satelloid. Astronaut. Acta, vol. 2, 1956, p. 63.
12. CLARKE, A. C.: Extraterrestrial Relays. Wireless World, Oct. 1945.
13. EMME, E. M., ED.: The History of Rocket Technology. Wayne State Univ. Press (Detroit), 1964. (Also available in Technology and Culture, vol. 4, Fall 1963.)
14. HALL, R. C.: Early U.S. Satellite Proposals. Technology and Culture, vol. 4, Fall 1963, p. 410.
15. ANON.: Preliminary Design of an Experimental World-Circling Spaceship. Rand Corp., Santa Monica, May 1946. (Also available in Rpt. SM–11827, Douglas Aircraft Co., May 2, 1946.)
16. BURGESS, E.: The Establishment and Use of Artificial Satellites. Aeronautics, Sept. 1949, p. 70.
17. CARTER, L. J.: The Artificial Satellite: Proceedings of the Second International Congress on Astronautics. Brit. Interplanetary Soc., 1951.
18. GATLAND, K. W.; KUNESCH, A. M.; AND DIXON, A. E.: Minimum Satellite Vehicles. J. Brit. Interplanetary Soc., vol. 10, 1951, p. 287.
19. SINGER, S. F.: A Minimum Orbital Instrumented Satellite—Now. J. Brit. Interplanetary Soc., vol. 13, 1954, p. 74.
20. VON BRAUN, W.: A Minimum Satellite Vehicle Based on Components Available from Missile Development of the Army Ordnance Corps. Guided Missile Development Div., Ordnance Missile Lab., Redstone Arsenal, 1954.
21. PICKERING, W. H.: History of the Juno Cluster System. In Astronautical Engineering and Science, E. Stuhlinger et al., eds., McGraw-Hill Book Co., Inc., 1963.
22. MAYO-WELLS, W. J.: The Origins of Space Telemetry. Technology and Culture, vol. 4, Fall 1963, p. 499.
23. CHAPIN, D. M.; FULLER, C. S.; AND PEARSON, G. L.: A New Silicon p-n Junction Photocell for Converting Solar Radiation into Electrical Power. J. Appl. Phys., vol. 25, May 1954, p. 676.
24. CORLISS, W. R.; AND HARVEY, D. G.: Radioisotopic Power Generation. Prentice-Hall, Inc., 1964.

25. ESNAULT-PELTERIE, R.: L'Astronautique. A. Lahure (Paris), 1930.
26. STUHLINGER, E.: Control and Power Supply Problems of Instrumented Satellites. Jet Propulsion, vol. 26, May 1956, p. 364.
27. DRAPER, C. S.; WRIGLEY, W.; AND HOVORKA, J.: Inertial Guidance. Pergamon Press, 1960.
28. FARRIOR, J. S.: Inertial Guidance, Its Evolution and Future Potential. In Astronautical Engineering and Science. E. Stuhlinger et al., eds., McGraw-Hill Book Co., Inc., 1963.
29. BERNSTEIN, J.: The Analytical Engine: Computers—Past, Present, and Future. Random House, 1964.
30. ADAMS, C. C.: Space Flight. McGraw-Hill Book Co., Inc., 1958.
31. THOMAS, S.: Satellite Tracking Facilities. Holt, Rinehart & Winston, 1963.
32. ROSHOLT, R.: An Administrative History of NASA, 1958–1963. NASA SP–4101. National Aeronautics and Space Administration, 1966.

Part II

MISSIONS AND SPACECRAFT

Chapter 3

SATELLITE MODELS AND SUBSYSTEM
INTEGRATION

3-1. Definition of the Generalized Scientific Satellite

This is a chapter of definitions and models—foundation stones for the more detailed technical discussions that follow. Defining a spacecraft model is a precarious occupation. Every engineering group has its own way of categorizing the thousands of parts that constitute the modern scientific satellite. Nevertheless, a model, or reference framework, is essential to the definition of the subsystem interfaces, those partitions between interacting satellite subsystems that dominate the thoughts and calculations of satellite designers.

Not so many years ago, even as late as World War II, complex vehicles and weapons were merely assemblies of separately designed components (blackboxes) rather than thoughtfully integrated systems. Often component interfaces failed to match, reducing overall system performance. During the 1950's, systems design became a key concept. The design and manufacture of the B–58 supersonic bomber typified the upsurge in systems thinking, in which each subsystem is made subservient to system needs.

Scientific satellites have gone both toward and away from tightly integrated systems. The smaller, more specialized Explorer-class spacecraft exemplify the highly tuned, precisely integrated satellites. On the other hand, the original streetcar-satellite concept, represented by the Observatory series, showed the systems design pendulum swinging back toward reasonably tolerant spacecraft, in which interface matching was not quite so critical. By supplying standardized mounting racks and busbars, satellites like OGO do make it somewhat easier for experiment designers, who are frequently unaware of the more delicate interfaces surrounding

their apparatus.   Unfortunately, the Observatories were so complex that they had to be tightly integrated to make them operate satisfactorily.   Of course, tightly integrated satellites usually yield higher performance in terms of the fraction of the satellite weight devoted to instrumentation, but they oblige everyone, including the experimenter, to work harder.

A total satellite system is more than the spacecraft alone.   It includes all Earth-based facilities and the rocket launch vehicle as
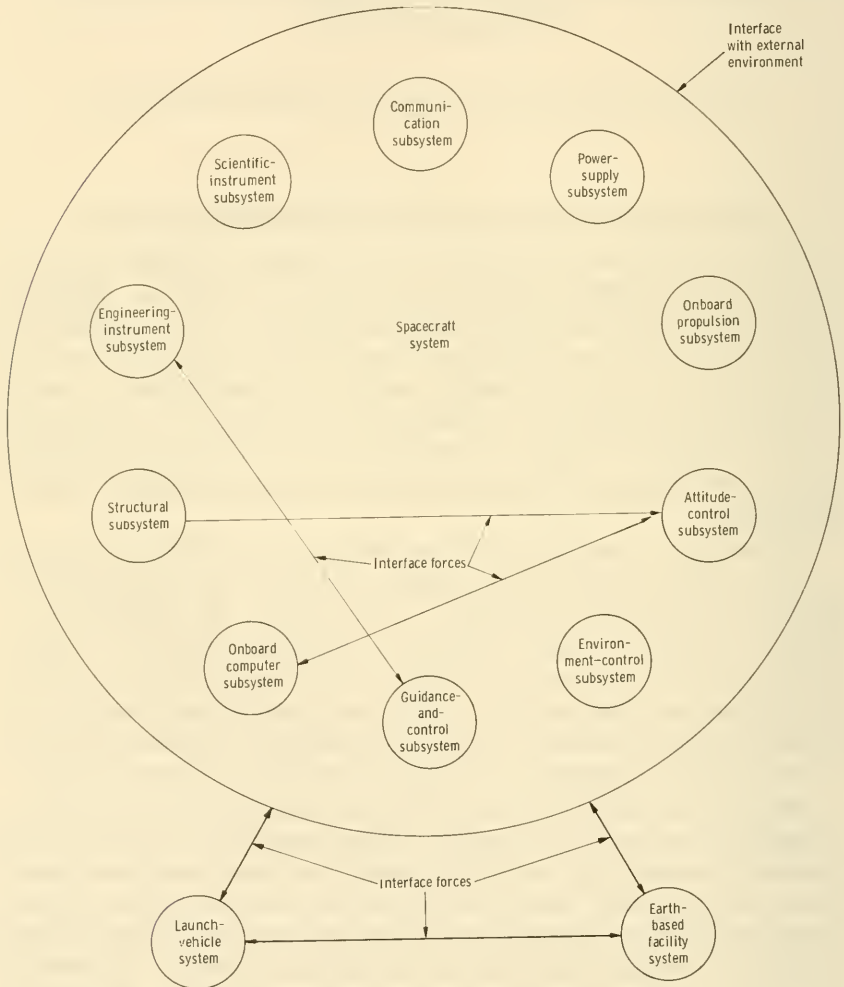
FIGURE 3–1.—Schematic of the scientific-satellite system, showing the spacecraft, launch-vehicle, and Earth-based facility systems. The external environment also imposes forces on the total system. See figure 3–2 for definitions of the different types of interfaces.

well. In figure 3–1, the word "system" is applied to three entities: the spacecraft, the Earth-based facilities, and the launch vehicle. Next in the hierarchy of definitions are the spacecraft subsystems. Ten in number, they are the primary subject of this book.   A typical subsystem is the satellite power supply, which nearly everyone recognizes as a separate, clean-cut classification (table 3–1).   The computer subsystem, on the other hand, cannot be defined with surgical precision, since many components on a satellite engage in manipulation of data and other functions commonly ascribed to computers.

The number of interfaces (or connections) existing between n subsystems is $n(n-1)/2$.   For the generalized scientific satellite, $n=10$, so that a total of 45 interfaces exist on the satellite alone. To these must be added the interfaces separating the satellite from the launch vehicle and the Earth-based facilities.   Many of these interfaces are sensitive and must be properly matched for good system performance.

To make the concept of the interface less abstract, consider the various types of interfaces that can connect any two subsystems. The most obvious of the nine types of interfaces shown in figure 3–2 are the electrical, mechanical, and thermal varieties.   For example, one would obviously not try to operate a dc motor with ac power.   Satellite interfaces are usually more subtle than this. Still speaking electrically, a better illustration might be the requirement for power at a voltage specified within narrow limits. The information interface requires that data and command words be in the correct format and properly coded when information is exchanged between subsystems.   The biological interface is perhaps the most subtle of all.   In practice, it means that one biological experiment should not contaminate another and that life-detection experiments, for example, must not be vitiated or poisoned by micro-organisms unintentionally carried along on other experiments.
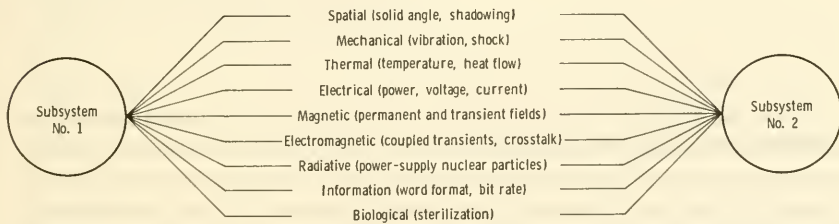
FIGURE 3–2.—The nine different types of interfaces that may exist between spacecraft subsystems.

TABLE 3–1.—*Definition of the Generalized Scientific Satellite*

Systems and subsystems	Functions
Spacecraft system_____	Carry instruments and experiments in satellite orbit and relay information back to Earth.
Communication subsystem_____	Relay information (data and commands) between Earth and satellite and, in concept, to and from other spacecraft.
Power-supply subsystem_____	Provide electrical power to all satellite subsystems.
Onboard propulsion subsystem_____	Provide thrust for orbit changes, station keeping, and deorbiting.
Attitude-control subsystem_____	Stabilize satellite attitude. Modify attitude upon command.
Environmental-control subsystem__	Maintain specified temperatures, radiation levels, electromagnetic environment, etc.
Guidance-and-control subsystem____	Receive commands from memory (including clocks and programmers) or from Earth and relay them to appropriate subsystems. Establish status of satellite, including attitude, position, and operating modes. Act to reduce deviations from desired performance.
Computer subsystem_____	Store information. Carry out computations for other subsystems.
Structure subsystem_____	Support and maintain satellite configuration under design loads.
Engineering-instrument subsystem_	Measure the status of the satellite, except attitude and position.
Scientific-instrument subsystem____	Measure scientific phenomena. Carry out active experiments.
Launch-vehicle system_____	Launch the satellite from the Earth's surface and inject it into the desired orbit.
Earth-based facility system_____	Provide all necessary services for launch vehicle and satellite; viz, testing, tracking, communication, data reduction, computation, decision-making, etc.

The magnitude of the interface-matching, or system-integration, problem now becomes apparent. Each of the 45 interfaces on the generalized satellite may be crossed by as many as 9 different types of "forces." In addition, some subsystems, particularly the scientific-instrument subsystem, may consist of several diverse pieces of apparatus (sub-subsystems), all separated by their own

interfaces. A satellite integrator must keep a careful eye on each interface, matching each as well as he can, while keeping the overall goal of maximizing system performance in mind (ref. 1).

3-2.   Measures of Satellite-System Performance

In maximizing the performance of any complex system, it is desirable to have a single figure of merit that integrates all aspects of performance into a single number, such as a cost-effectiveness parameter. This task is difficult in the case of scientific satellites because no one can really place a value on scientific information, which is the real product of the operation. Furthermore, the satellite might well uncover new and unexpected physical phenomena that would negate any prior assessment of an experiment's value. Data from satellite experiments tend to be repetitious and redundant, so that a figure of merit, such as bits of data received per dollar invested, is not particularly meaningful. Satellite research is a gamble in which the prize is often unpredictable and the odds for winning it difficult to compute.

Three important performance factors cut across most system interfaces and deserve separate mention. They are: weight, reliability, and cost. (See sec. 9-2 for additional material on reliability.) Once a mission goal is set—say, the mapping of the magnetohydrodynamic wake of the Earth—engineers try to maximize the scientific value of the mission within constraints that are fixed usually by nonscientific considerations. Satellite weight, for example, is usually set by the assigned launch vehicle or, if several launch vehicles are available, the amount of money the program can afford to assign. Another major performance factor—reliability—can also be purchased with money if the dollars are preferentially funneled into reliability and test programs rather than launch vehicles. The spacecraft designer soon finds that he does not want to pay for the reliability level that would probably give him 10 years of operation. In fact, as mentioned earlier, most satellites now incorporate timers that automatically shut off transmissions after 6 months, a year, or whatever time period seems appropriate to the mission objectives. The important point here is that all performance factors—cost, weight, reliability, etc.—are interrelated.

Given a specific mission, one first sets dollar budgets and goals for weight, reliability, and any other important factors. Halfway through a design, the weight goal may be achieved with room to spare,[1] so that an additional experiment can be incorporated,

---

[1] Few satellite-design histories show such good fortune.

thereby raising the overall scientific value of the mission. Or, possibly, the available weight would be put to better use by paralleling critical components (redundancy) to increase overall reliability. In chapter 9, this subject of engineering tradeoffs will be discussed further.

A measure of performance, such as reliability, is meaningful only when the satellite's external environment is fully defined. In other words, reliability is the probability that a given piece of equipment will operate at design levels, for a specified time period, under certain environmental conditions. During the launch, the external environment includes wind gusts, but not self-created vibrations. In orbit, space radiation, hard vacuum, insolation, and micrometeoroids constitute external environmental factors, but internal heat sources would be excluded. The external environment has been described briefly in the graphs and tables of chapter 1. Conceptually, the external environment may be thought of as an extra subsystem, which applies forces through the thermal, mechanical, and other interfaces that have already been defined (fig. 3–1). The role of the external environment in molding subsystem design will be covered in chapter 9.

The satellite-optimization process focuses attention on the $n(n-1)/2$ interfaces introduced in the preceding section. Each interface will be crossed by several interlocking parameters that physically and mathematically tie the system together. A thermal interface will involve parameters such as temperature and rate of heat flow. An electrical interface is bridged by voltage and current parameters. Finally, all subsystems are tied together at a still higher level of integration by weight, cost, and reliability. Thus, each parameter helps to bind the system into a well-performing whole. Each component and each experiment must work well when immersed in the welter of wires, solar cells, magnetometers, transistors, and thousands of other parts that make up the typical scientific satellite.

The age of the blackbox is long past. Every pound in orbit costs tens of thousands of dollars, and every hour of reliable operation is wrung from perverse equipment by painstaking design, development, and test. The subject of integration, or interface matching, pervades all chapters of this book. The purpose of this chapter is to set the stage.

3–3.   Integration Techniques

Satellite integration occupies a critical position in the development cycle of a scientific satellite (fig. 3–3). The successful inte-

gration of subsystems into a high-performance satellite transcends the disciplines of science and engineering. Components or experiments, no matter how well they work in unintegrated isolation, may be less than useless when mounted in the completed satellite. Spacecraft integration is achieved more through proper management of people and information than through mathematical analysis or sophisticated design. The essentials of program management for integration are:

(1) *Education.*—Make everyone concerned with the project aware of the nature of the integration problem and why its solution is essential to success. Experimenters, in particular, must be convinced of the necessity of the paperwork, meetings, and other coordinating that inevitably arise during the integration process.

(2) *Definition of the System.*—First, a model of the system must be established. Not only must each subsystem be defined, but all impressed forces (internal and external), the interfaces, and component specifications must be spelled out in detail. The formal specifications, interface documents, and compatibility documents may be voluminous and oppressive.

(3) *Organization.*—Some one person must be put in charge and held responsible for satellite program management, including the
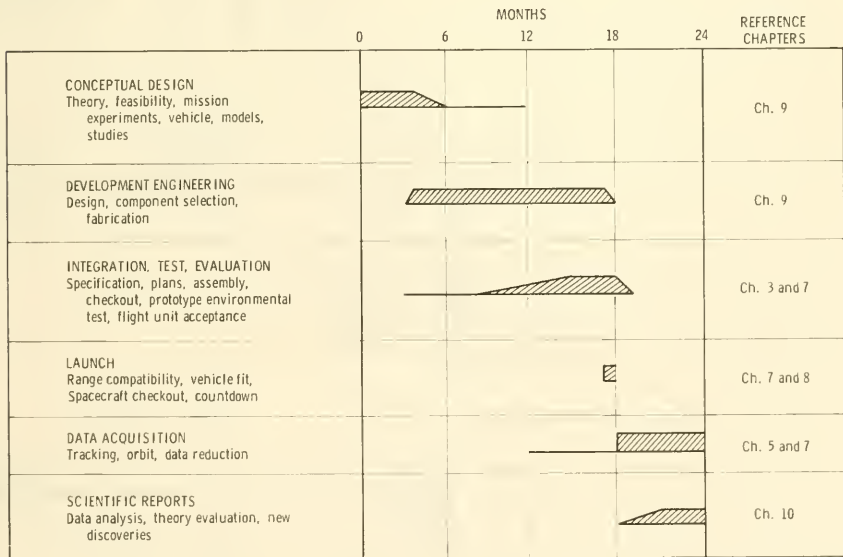
FIGURE 3–3.—A typical scientific-satellite development cycle (adapted from ref. 2).
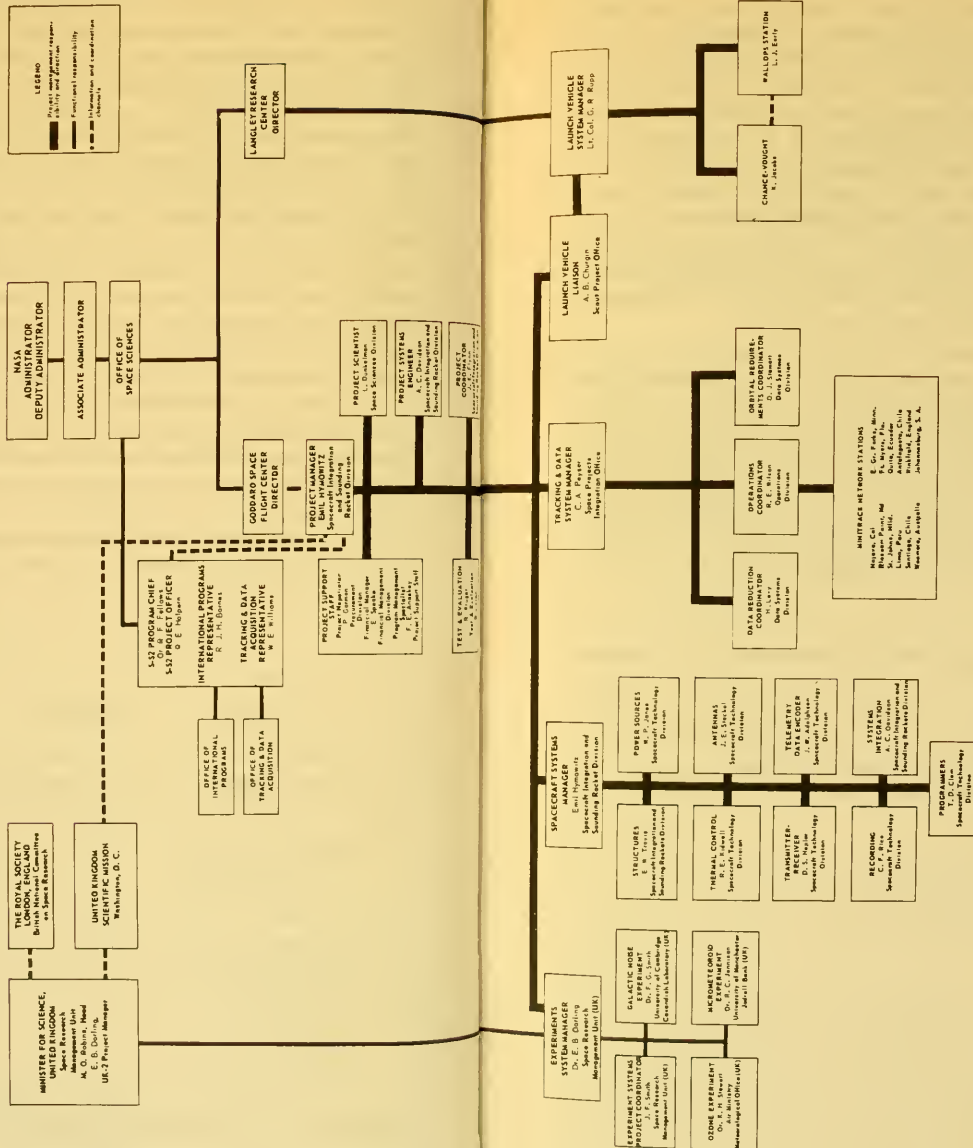
FIGURE 3–4.—Organization chart for the Ariel-2 satellite program (ref. 3).

enforcement of interface specifications. Specific liaison, coordination, and review functions must be defined and manned (fig. 3–4).

(4) *Communication.*—All definitions of subsystems and interfaces must be widely promulgated. The same is true for the inevitable design changes that plague complex engineering enterprises. There must be regular meetings of all participants to insure that subsystem interfaces are being properly matched.

(5) *Testing.*—The best and most foresighted management and engineering staffs cannot anticipate all interface problems. Extensive testing under simulated operating conditions is mandatory. Tests sometimes uncover unexpected interactions and crosstalk between experiments and subsystems that must be eliminated. Retesting is then required before final acceptance.

The effectiveness of the spacecraft integration process is measured by the success of the launch, the quality of the scientific data radioed back, and the attainment of design lifetime. Once orbit has been attained, the satellite designer moves on to the next satellite in the program, but, for the experimenter, the job is far from finished, because data must be assembled, reduced, interpreted, and the results made available to the scientific community. These extra dimensions of the experimenter's job are described in chapter 10, ''Satellite Science—An Overall View.''

References

1. KRUEGER, D. A.; AND FRANTA, A. L.: The Electronic Checkout and Integration of Orbiting Geophysical Observatory Experiments. NASA X–722–65–366, 1965.
2. NEW, J. C.: Achieving Satellite Reliability Through Environmental Tests. NASA TN D–1853, 1963.
3. FRANTA, A. L.; AND DAVIDSON, A. C.: Achieving Ariel II Design Compatibility. NASA TN D–3085, 1966.

Chapter 4

SATELLITE DYNAMICS

4-1. Prolog

Scientific satellites, like weather balloons, oceanographic buoys, and other unmanned instrument carriers, are launched upon a somewhat fickle sea of perturbing forces. The major force shaping the satellite orbit is, of course, gravity; but air drag, the pressure of sunlight, and irregularities in the shape of the Earth continuously distort an orbit, so that no two successive rotations about the Earth are precisely the same. Since a main function of the scientific satellite is the mapping of the fields and fluxes in nearby space, scientists must know the positions of their instruments and the directions in which they point at all times, regardless of orbital vicissitudes.

The role of satellite dynamics is several faceted, though mainly concerned with prediction:

(1) The prediction of the propulsive forces needed to launch a given satellite into a specified orbit at a certain point in time (sec. 4–3)

(2) The prediction of the effects of perturbing forces on satellite position and attitude (secs. 4–5 and 4–7)

(3) The prediction of the propulsive forces necessary to: (a) maintain a specified orbit (station keeping), (b) modify or trim an orbit, and (c) maintain or alter the attitude of a satellite (sec. 4–5)

(4) The prediction of the impulse vector required to deorbit a satellite and deposit it in a specified recovery area (sec. 4–6)

(5) The analysis of observed orbit perturbations in order to estimate the perturbing forces of importance to geodesy (sec. 11–7). This application of space dynamics assumes that our current inheritance of physical laws is correct.

(6) The analysis of observed orbit perturbations in order to confirm or deny present physical laws; i.e., the testing of the hypothesis of general relativity (ch. 13).

Over an idealized, flat Earth, any ballistic (or free-falling) projectile describes a parabola; but the Earth is spherical, and real projectiles follow elliptical paths, providing no forces, other than gravity, act upon them. If the elliptical trajectory does not intersect the solid Earth or the dense portions of the atmosphere, the projectile will make more than one planetary revolution and thus, by definition, become a satellite. Eventually, perhaps in hours or thousands of years, drag forces will slow down the satellite, its orbit will decay, and the mission will end in a fiery plunge into the upper atmosphere (fig. 4–1).

In principle, satellites can be launched by a single impulse applied at the Earth's surface—say, with a large cannon, à la Jules Verne (sec. 8–3). In practice, of course, almost all satellites are orbited by large, staged rockets that apply accelerating forces over a period of several minutes. A typical launch sequence is shown in figure 4–2. First, there is booster liftoff. After a minute or so of vertical ascent through the lower layers of the atmosphere, the launch vehicle is commanded to "pitch over" and carry the satellite downrange toward waiting tracking stations, strung along thousands of miles of islands and ships. There are usually several thrust-and-coast periods, sometimes alternating with discards of
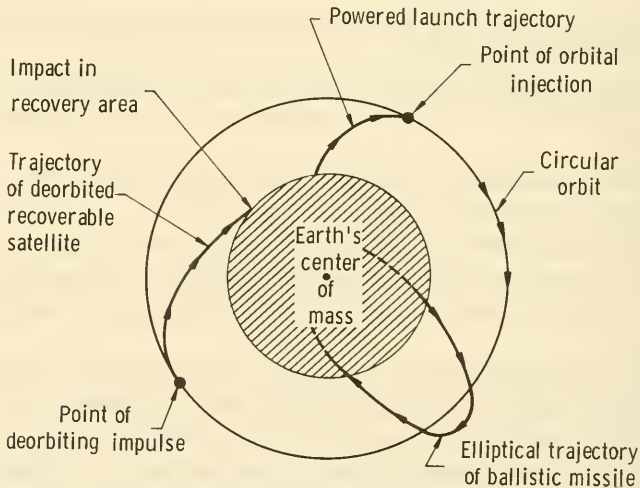
FIGURE 4–1.—Some features of satellite launch, deorbit, and reentry.
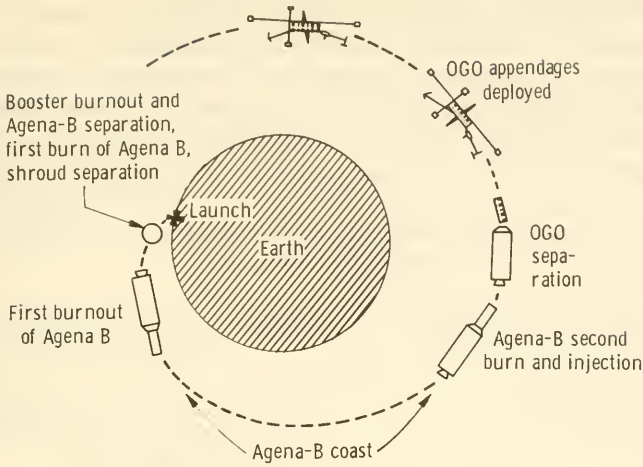
FIGURE 4–2.—OGO launch sequence, illustrating the
ascent, coast, injection, and appendage-deployment
phases.

spent rocket stages. When the desired altitude has been reached,
the final launch-vehicle stage will inject the satellite into orbit
with the proper velocity and angle. When an orbit is confirmed by
the worldwide tracking networks, the satellite goes through an
insectlike metamorphosis, during which instrument booms, solar-
cell panels, and telemetry antennas are erected on the satellite
surface. The satellite now orbits the Earth, pushed and pulled
slightly this way and that by electric fields, magnetic fields, radia-
tion pressure, micrometeoroid impacts, the attractions of the Sun
and the Moon, and the inhomogeneities in the Earth's gravita-
tional field.

This chapter presents short primarily nonmathematical descrip-
tions of launch trajectories, perturbed and unperturbed orbits,

satellite reentry paths, and satellite-attitude dynamics. These descriptions tie in closely with the later subjects of guidance, attitude control, onboard propulsion, and the overall optimization of system performance. Table 4–1 is introduced here to summarize the more important interactions between the descriptive discipline of satellite dynamics and the hardware of the satellite subsystems.

TABLE 4–1.—*Relationships Between Satellite Subsystems and Satellite Dynamics*

Systems and subsystems	Implications and constraints involving satellite dynamics [a]
Launch-vehicle system_____	Propulsion requirements should be minimized to increase payload on a given launch vehicle (ch. 8).
Earth-based facility system_____	Orbits should pass over established tracking and data-reception stations (sec. 7–4). Recoverable satellites should descend into designated recovery areas.
Spacecraft system:	
Communication subsystem____	Directional antennas must be aimed at the Earth (ch. 5).
Power-supply subsystem_____	Solar-cell panels must be aimed at Sun. Orbits should minimize time in shadow zone. Nuclear power supplies require restricted launch trajectories for safety reasons.
Onboard propulsion subsystem	Orbit corrections and station keeping should be minimized to save fuel. De-orbiting impulse should be minimized within constraints of aerodynamic heating and deceleration forces (sec. 4–6).
Attitude-control subsystem____	Minimize power and fuel used in stabilization and satellite attitude changes.
Environment-control subsystem.	Avoid lengthy shadow periods and, where the mission permits, fixed orientation with respect to the Sun (sec. 9–6). Minimize atmospheric heating and deceleration forces.
Guidance-and-control subsystem.	Maneuvers and pointing changes should be simple and few (ch. 6).
Computer subsystem_____	Minimize onboard navigation, guidance, and control computations to keep weight and power requirements low.
Structural subsystem_____	Avoid high accelerations during launch and reentry (sec. 9–10).
Engineering-instrument subsystem.	None.

TABLE 4–1.—*Relationships Between Satellite Subsystems and
Satellite Dynamics—Continued*

Systems and subsystems	Implications and constraints involving satellite dynamics [a]

Spacecraft system—Continued
    Scientific-instrument
  subsystem.
	Some typical mission requirements for various satellites follow:
	    Intersect atmosphere for drag measurements and sample collection.
	    Avoid atmosphere to prolong satellite lifetime.
	    Point satellite at the Sun, a specific star, or the Earth, or scan environment over large solid angle.
	    Anchor orbit around Moon.
	    Intersect Earth's magnetopause.
	    Intersect Earth's "wake."
	    Pass through Earth's auroral zones.
	    Cause orbit plane to rotate once a year to keep perpendicular to Sun.
	    Cause orbit to penetrate selected regions of Earth's radiation zones.

[a] Note the abundance of "maximize" and "minimize" functions associated with satellite dynamics.

4–2.   Mission Descriptions

Scientific-satellite missions are generally simple when compared to those of military spacecraft and planetary probes, which often include midcourse, terminal, and rendezvous maneuvers to worry the orbit analyst.   On some scientific-satellite studies, the orbit must be made to dip into the fringes of the atmosphere; on others, the orbit should take instruments beyond the magnetopause that shields the Earth from much of the interplanetary "weather." Relatively speaking, though, little maneuvering is done beyond establishing the orbit's initial conditions and letting nature take its course thereafter (table 4–2).

The attitude-control and stabilization of scientific satellites, on the other hand, may be an extremely challenging task; particularly when one undertakes a stellar survey, where thousands of stars must be found and focused in satellite instruments, despite the presence of many perturbing torques.

In other words, scientific-satellite orbits are usually not actively controlled, but instrument-pointing requirements frequently turn satellite attitude control into an engineering task of high order.

TABLE 4–2.—*Orbital and Attitude-Control Requirements for Various Scientific-Satellite Missions*

Technical field	Mission type [a]	Apogee	Perigee, km	Inclination [b]	Lifetime, mo.	Orbital adjustments	Deorbiting	Attitude control [c]
						Propulsive functions		
Aeronomy	Direct measurement	------	~200	All desired	>6	------	------	Usually none or spin-stabilized, satellites spherical.
	Ground-based observation of satellite.	------	~200	All desired	>12	------	------	
Ionospheric physics.	Direct measurement	------	~200	All desired	>6	------	------	One axis, minimum, Earth pointing.
	Topside sounding	------	>500	All desired	>6	------	------	
	Ground-based observation of satellite.	------	------	All desired	------	------	------	
Trapped radiation.	Direct measurement	Beyond magnetopause.	>300	All desired	>6	------	Recoverable capsules.	One axis, minimum.
Auroral physics.	Direct measurement	------	~200	Polar	>6	------	------	One axis, minimum.
	Observation; spectroscopy, etc.	------	>300	Polar	>6	------	------	Instrument pointing.

Geomagnetism	Direct measurement	To Moon and beyond	>300	All desired	>12	----		One axis, minimum.
Geodesy	Ground-based observation of satellite.	-------	>300	All desired	>12	----	----	One axis, minimum.
Meteoritics	Direct measurement	To Moon and beyond	>300	All desired	>6	----	Sample collecting.	One axis, minimum.
Solar physics	Observation; spectroscopy, etc.	Medium altitude.	>500	Polar preferred.	>12	Plane rotation.	----	Instrument pointing.
Stellar astronomy	Observation; spectroscopy, etc.	Medium altitude.	>500	----	>12	----	----	Instrument pointing.
Interstellar physics.	Observation; spectroscopy, etc.	Medium altitude.	>500	----	>12	----	----	Instrument pointing.
Cosmic rays	Direct measurement	Medium altitude.	>500	----	>12	----	Recoverable capsules.	One axis, minimum.
Cosmology	Ground-based observation of satellite.	Medium altitude.	>500	----	>12	----	----	One axis, minimum.
Biology	Direct measurement	Medium altitude.	Medium	----	<6	----	Recoverable capsules.	No spin, reentry.
	Life detection	~200 km	----	----	<6	----	----	Reentry.

a See table 1-2, for additional description of research opportunities.

b On most mapping missions, all inclinations are desired.

c Three-axis stabilization is often desirable, but many missions can produce good data with single-axis stabilization plus aspect sensors. Multiexperiment Observatories may have separately pointed instrument sections.

In table 4–2, representative scientific-satellite missions are categorized by discipline. Most missions destined to be performed before A.D. 2000 are included. In general, one discerns no urgent need for synchronous orbits and station-keeping functions in satellite science, though some missions would undeniably benefit from
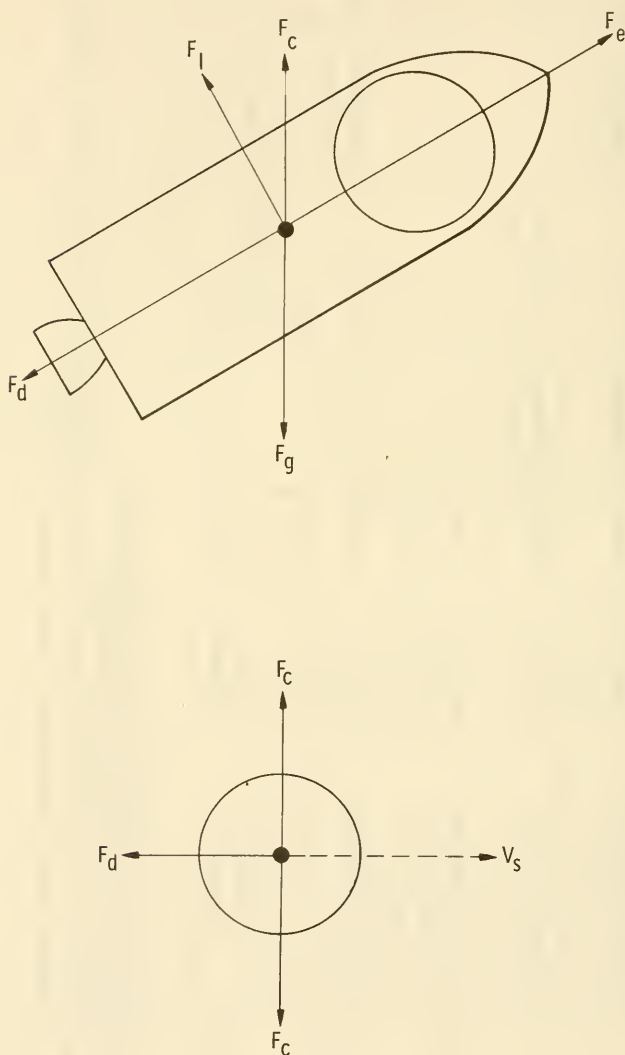
FIGURE 4–3.—Applied forces for an ascending launch vehicle and a satellite in orbit. F_e=engine thrust, F_d=drag force, F_l=lift, F_g=force due to gravity, F_c=centrifugal force, and V_s=satellite velocity.

them. The close relationship between table 4–2 and table 1–2, which lists typical satellite research areas, follows naturally from the four fundamental advantages of satellite orbits (sec. 1–1):

(1) The capability of making direct measurements in outer space

(2) The removal of the atmospheric and magnetospheric shields

(3) The positional advantage

(4) The unique biological environment in a satellite

4–3. Launch Dynamics

Hale's fictitious "brick moon," described in chapter 2, was flung into orbit by a huge, water-powered flywheel; today, rockets are the accepted launch technique. The intent of this section is a review of the dynamics of the rocket-launch process, which begins at liftoff and ends with the final-stage engine cutoff and the separation of the satellite from the launch vehicle.

Satellite Launch Requirements.—First, what must a launch vehicle do to create a satellite?

According to convention, a spacecraft becomes a satellite when it makes more than one circuit of the Earth without using thrust to counteract the pull of gravity. Thus, for a satellite in circular orbit, gravitational force counterbalances centrifugal force (fig. 4–3):

$$F_g = F_c$$

$$\frac{GmM}{R^2} = \frac{mV_s^2}{R}$$

So that

$$V_s = \sqrt{GM/R} \tag{4-1}$$

where

F_g = the force due to gravity (newtons)

F_c = the centrifugal force (newtons)

m = the satellite mass (kg)

R = the distance of the satellite from the center of the Earth (not altitude) (m)

V_s = the satellite velocity (m/sec)

M = the mass of the Earth (5.98×10^{24} kg)

G = the universal constant of gravitation (6.67×10^{-11} newton-m²/kg²)

The curves plotted in figure 4–4 are generated from equation (4–1) and the additional fact that the satellite period, T, is just distance divided by velocity, therefore:

$$T = \frac{2\pi R}{V_s} = 2\pi \sqrt{\frac{R^3}{GM}} \qquad (4\text{-}2)$$

From figure 4–4, it appears, at least in theory, that even a sea-level satellite is possible if an engine were used to overcome the immense drag forces at 7910 m/sec (Mach 6.5). No wings would be needed for lift. At higher altitudes, the horizontal velocity necessary to sustain a satellite becomes smaller as the force of gravity weakens. At an altitude of 35 800 kilometers (R=42 100 kilometers), the satellite rotates with the same period as the Earth itself, and we have a 24-hour, or synchronous, satellite. If it is in an equatorial orbit, the satellite will appear fixed above some point on the Equator. It is then termed "stationary." Above the synchronous altitude, satellites appear to have a retrograde motion to an observer on the Earth, because the Earth rotates faster than the satellites do.

Although horizontal injection velocities are lower at higher altitudes, disproportionately more fuel is used in doing work against the Earth's gravitational field during the ascent to higher satellite injection altitudes. Therefore, high-altitude orbits are more difficult to attain. At the limit, where the spacecraft escapes the Earth altogether, the altitude is infinite in our simple model, and the work done by the launch vehicle can be found by substituting the Earth's escape velocity of 11 200 m/sec in the kinetic-energy equation; the result is 6.25×10^7 joules/kg.
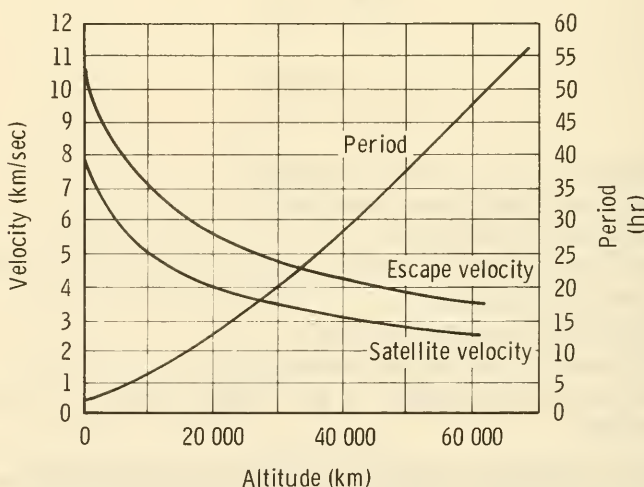
FIGURE 4–4.—Satellite velocity and period versus altitude for circular Earth orbits.

Returning to the satellite injection problem, if the horizontal injection velocity is less than $\sqrt{GM/R}$, the spacecraft will descend back to Earth along an ellipse with its apogee at the point of injection (fig. 4–5). If the horizontal injection velocity is greater than $\sqrt{GM/R}$, the orbit will again be elliptical, but with the perigee now at the injection point. Misalinement of the injection velocity vector will result in other ellipses, some of which will intersect the Earth and end the mission. Logic indicates that each orbital mission possesses ranges of acceptable injection velocities and angles—in other words, a velocity-injection-angle corridor.

The launch-dynamics problem, however, is considerably more difficult than the above presentation indicates. There are three categories of complications: (1) launch constraints, (2) departures from ideality (viz, a rotating Earth), and (3) data requirements of the scientists (users). In addition to these problems (elaborated upon below), efficiency insists that the launch process be optimized. That is, all pertinent parameters must be adjusted to maximize the payload in orbit or maximize some other figure of merit. (See sec. 3–2.)
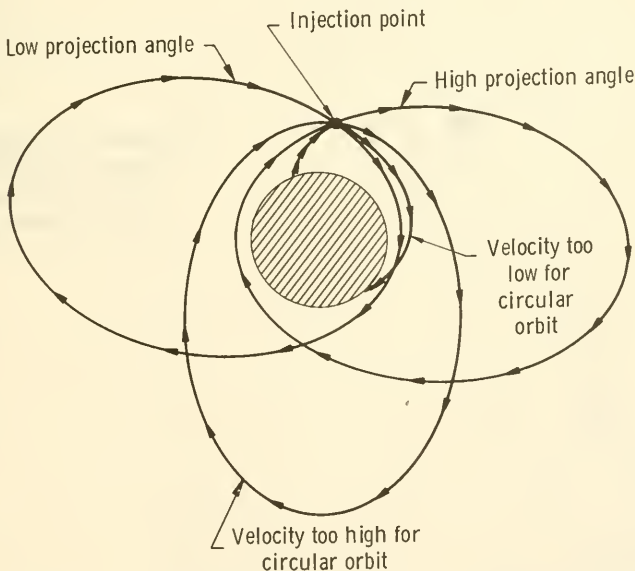
FIGURE 4–5.—Elliptical orbits resulting from the misalinement of injection angle and injection velocities above and below $\sqrt{GM/R}$ required for circular orbits.

Launch Constraints.—Launch trajectories are always constrained by safety regulations, the azimuths of downrange tracking stations, weather conditions, the time of day best suited for optical tracking, and the direction of the Earth's rotation. Launch vehicles are not propelled into space at random. To borrow a nautical term, there are "rules of the road." Launch-site rules of the road closely resemble those of an airport—only they are more narrow and, if overstepped, the consequences are generally catastrophic to the mission; e.g., the mission is aborted by destruction. At every
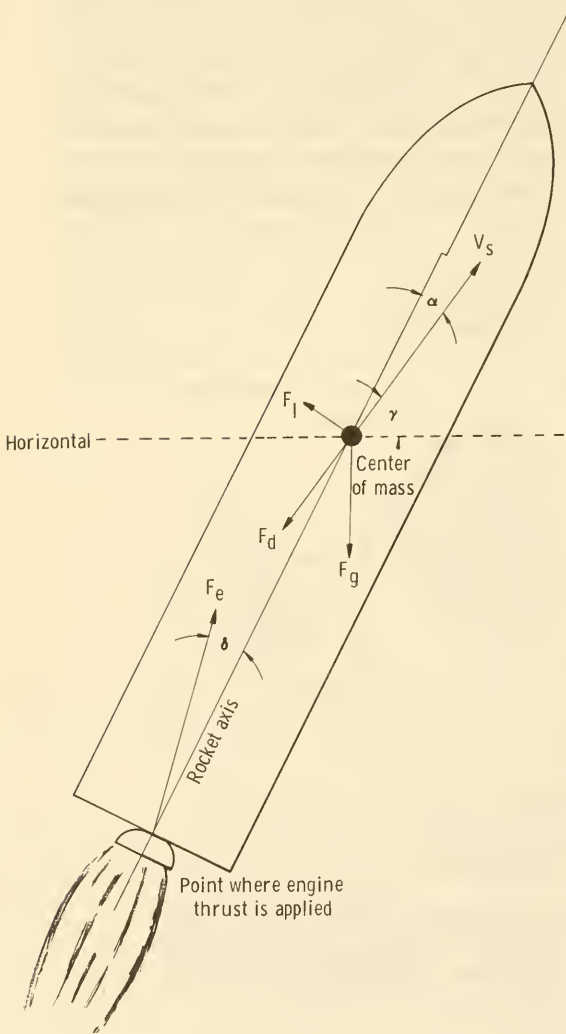
FIGURE 4-6.—Diagram of the forces acting upon a launch vehicle.

moment during launch, the range safety officer monitors the position, velocity, and predicted path of the launch vehicle and its payload. Departures from a previously specified corridor of acceptable flight parameters will cause him to demolish the aberrant machine. Corridors vary from mission to mission. They might, for example, be more narrow for the launch of a nuclear-powered satellite because of danger from accidentally released radioactivity.

Departures From Ideality.—The four important forces acting upon an ascending space vehicle are:

$F_e(h,t) =$ the engine thrust, which varies with altitude (h) and time (t). (Figs. 4-6 and 4-7 define the variables.)

$F_g(h) =$ the force due to gravity

$F_d(h,v,\alpha) =$ the aerodynamic-drag force, which varies with altitude (h), vehicle velocity (v), and the angle of attack (α)

$F_l(h,v,\alpha) =$ the lift force, which also varies with vehicle altitude, velocity, and angle of attack.
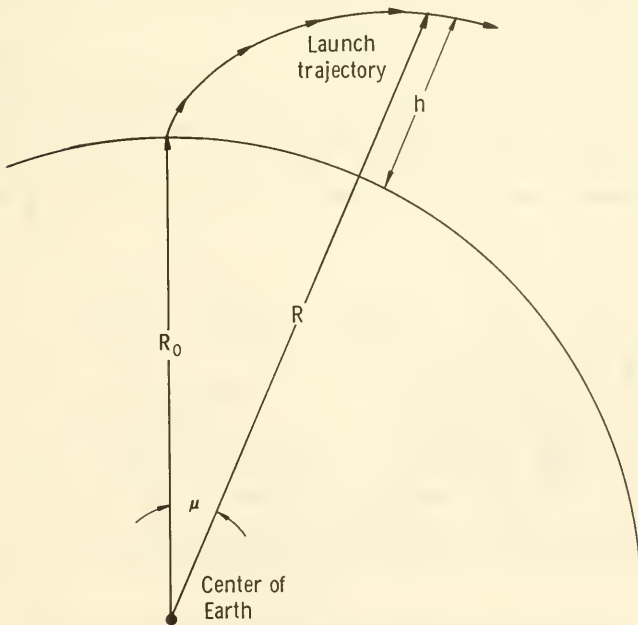
FIGURE 4–7.—Variables for a launch trajectory over a spherical Earth.

The lift and drag forces are given by:

$$F_l(h,v,\alpha) = \tfrac{1}{2}\rho(h)v^2 A C_l \qquad F_d(h,v,\alpha) = \tfrac{1}{2}\rho(h)v^2 A C_d$$

where $p(h) =$ air density.

In two-dimensional rectangular coordinates x and y, the differential equations describing the motion of the launch vehicle in local or *topocentric* coordinates are

$$\left.\begin{aligned}
\ddot{x} &= \frac{F_e(h,t)\ \cos\ [\theta(t)+\delta(t)]}{m(t)} - F_g(h)\ \sin\ \mu \\[4pt]
&\quad -\frac{F_d(h,v,\alpha)}{m(t)}\ \cos\ \gamma(t) - \frac{F_l(h,v,\alpha)}{m(t)}\ \sin\ \gamma(t) \\[10pt]
\ddot{y} &= \frac{F_e(h,t)\ \sin\ [\theta(t)+\delta(t)]}{m(t)} - F_g(h)\ \cos\ \mu \\[4pt]
&\quad -\frac{F_d(h,v,\alpha)}{m(t)}\ \sin\ \gamma(t) + \frac{F_l(h,v,\alpha)}{m(t)}\ \cos\ \gamma(t)
\end{aligned}\right\} \qquad (4\text{--}3)$$

where the variable μ is defined in figures 4–3 and 4–7, and $m(t) =$ the launch-vehicle mass, which diminishes with time as fuel and oxidizer are consumed by the engine.

Equations (4–3) must be integrated once to obtain the velocities, $\dot{x}$ and $\dot{y}$, and once more to describe the launch-vehicle trajectory in terms of x and y. With staged launch vehicles, the altitude, h, is a rather smooth function of time (fig. 4–8), but the total acceleration and velocity curves show sharp breaks at stage separation points.
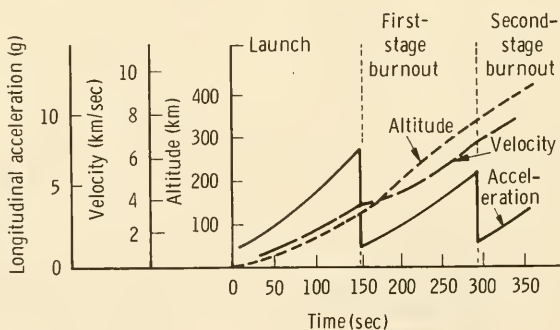
FIGURE 4–8.—Representative launch-vehicle trajectory parameters as functions of time after launch.

Equations (4–2) and (4–3) are intended to be instructive only. In actual trajectory calculations, the motion of the launch vehicle is described in three dimensions, taking into account the rotation of the Earth. More equations are introduced to describe the attitude changes of the launch vehicle as the applied torques vary. Vehicle pitching, rolling, and yawing motions are coupled to the foregoing differential equations through the angles in the arguments.

While feasibility studies of launch trajectories are sometimes done by hand, sophisticated computer programs are readily available that numerically integrate the differential equations of motion, including all the significant perturbation terms.

The differential equations themselves do not signal the fact that an orbit is achieved at injection. In fact, if properly formulated, the differential equations could be integrated to follow the satellite around in orbit after the last launch-vehicle stage has been jettisoned. The equations are that general. Usually, however, the computer shifts to a new set of differential equations, designed to take into account perturbation forces, such as solar pressure, that were unimportant in the launch-trajectory description. The final computation made using the launch-trajectory differential equations determines whether the satellite was injected within the acceptable orbit corridor, bounded by the velocity and injection-angle constraints.

User-Data Requirements.—After the differential equations of motion are set down and integrated, the graphs plotted, and other analytical tools sharpened, the results are still much too general, say, for a downrange tracking station that needs to know when and where to point its antennas. Computers must grind out launch-vehicle coordinates in local reference frames for all observers associated with a given launch. Indeed, target prediction in terms of local instrument-pointing coordinates is the computer's main task. Much as the differential equations help to summarize the physics involved, the data user still wants to know azimuth, elevation, slant range, and radial velocity as functions of time for his location, rather than gravitational force. Such information is not explicit in the integrated equations of motion. Coordinate-system origins and variables must be written down in terms of parameters that can be directly measured with ground-based instruments.

Another type of desired information is related to the difficulty of attaining different satellite orbits, as measured by the overall velocity that must be added to the satellite by the launch vehicle.
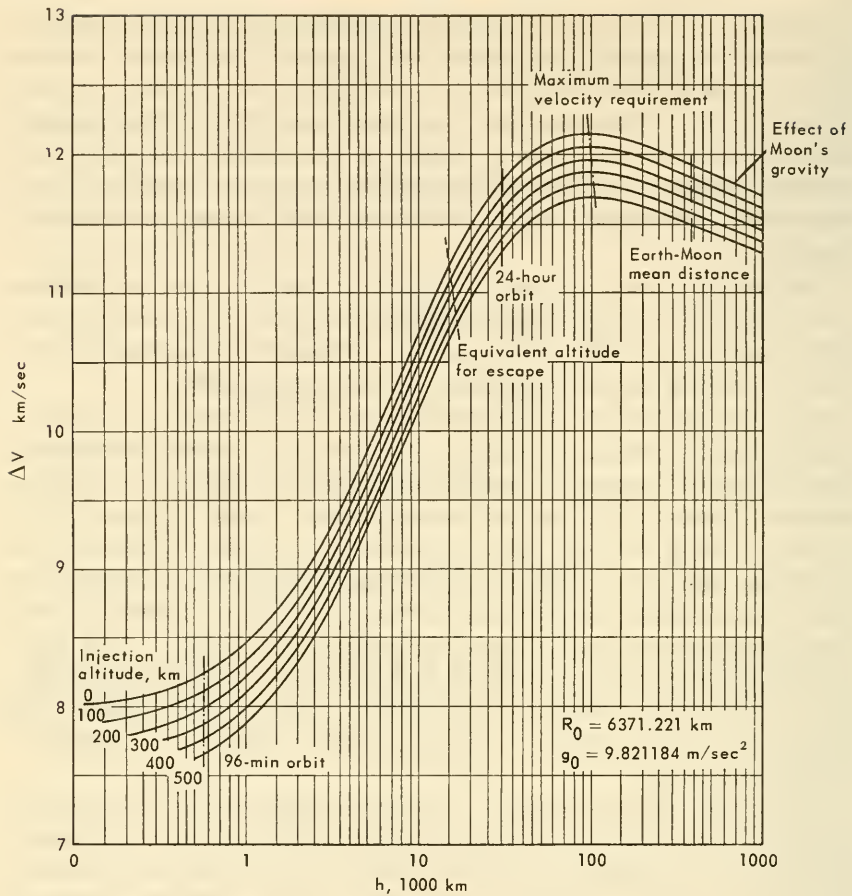
FIGURE 4–9.—Net velocity requirements versus orbital altitude, assuming a Hohmann (minimum-energy) ellipse during ascent. This figure shows general trends only and does not include drag effects, lift, etc. (Adapted from ref. 1. Used by permission of McGraw-Hill Book Co.)

Velocity-increment (Δv) graphs are customarily used by mission planners and rocket designers (fig. 4–9).

Launch Windows.—Launch windows are timespans during which it is relatively easy, in terms of existing launch-vehicle capabilities, to place a specific space vehicle in a specific trajectory. The width of a launch window is broadened when a more powerful booster becomes available for a satellite of fixed weight. The window is narrowed, however, when the required payload increases without concurrent increases in propulsion capabilities.

Launch windows obviously exist when a spacecraft is aimed at other planets in the solar system or intended to rendezvous with another satellite already in orbit. Whenever you shoot at a moving target, the trigger must be pulled at exactly the right instant. One satellite discussed in this book faces this kind of synchronization problem; it is the Anchored IMP spacecraft (IMP's D and E). (See fig. 4–10.) Lunar launch windows occur daily, in contrast to those of Mars, which open up about 2 years apart.

Anchored IMP Launch Sequence

Sequence No.	Time (sec)	Event
1	0	Stage I liftoff
2	148	Main engine cutoff
3	152	Stage II ignition signal
4	153	Stage I/II separation
5	215	Jettison fairing
6	542	Stage II cutoff
7	562	Start coast phase pitch program
8	1099	End coast phase pitch program
9	1104	Fire spin rockets (spinup)
10	1106	Jettison stage II-active retro system
11	1110	Stage III ignition
12	1132	Stage III burnout
13	1179	De-spin stage III/spacecraft
14	1227	Solar cell paddle release (4)
15	1229	Fluxgate boom release (2)
16	1234	Spacecraft/stage III separation-yo stage III
17		Spin stabilized coast
18	DBC	Command timer
19	DBC+T	Direct command stage IV ignition
20	DBC+T+22	Stage IV burnout
21	DBC+T+22+1200+	Separate stage IV
22		In orbit

T = timer
DBC = determined by computer

FIGURE 4–10.—A flight plan for Anchored IMP (IMP's D and E). The spacecraft must intercept the moving Moon and inject itself into a lunar orbit at precisely the right moment with an onboard, solid-fuel rocket engine.

A second kind of launch window exists when a satellite must be placed in a specific plane [1] for scientific purposes—say, for simultaneously obtaining geophysical data from conjugate points in orbit. Injecting a satellite in a specific plane is accomplished most easily at the moment when the target plane passes through the satellite injection point. If a hold during the launch-vehicle countdown delays the launch, an additional velocity increment will be needed to nudge the satellite into the target plane, which has since swept past the injection point; the longer the launch delay, the larger the additional velocity increment. Eventually, the propulsion penalty becomes intolerable, and the edge of the launch window is reached (fig. 4-11) (ref. 2).
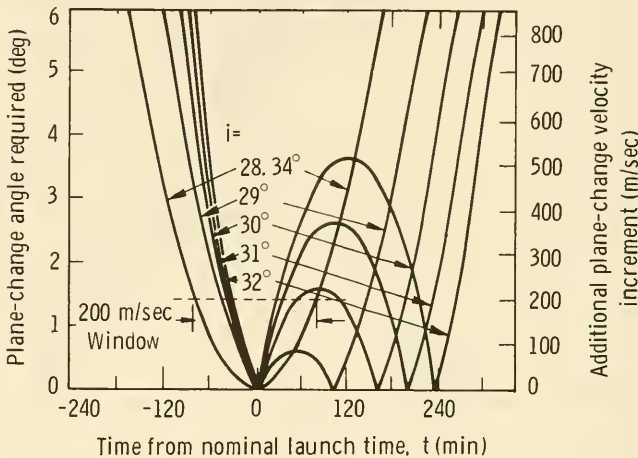
FIGURE 4-11.—Launch windows for orbital missions aimed at a specific plane. As the target plane sweeps past the plane of the launch site. more and more velocity must be added to the satellite to shift it out of the plane of the launch site into the desired plane, which draws steadily away as the Earth turns. The length of the window is determined by drawing a horizontal line through the curves at a level equal to the maximum extra velocity increment available. $i =$ target plane inclination, launch-site latitude, 28.34° N (ref. 2).

A third type of launch window occurs when eccentric, long-lived orbits are desired. When apogees are measured in hundreds of thousands of kilometers, as for Explorers VI and XVIII, per-

[1] Not merely a plane with the same inclination, but in a unique plane among the infinity of planes with the same inclination.

turbations by the Sun and Moon may depress the orbit perigee into the dense atmosphere and prematurely end the mission (ref. 3). By launching the satellite during a window in time, the perturbing forces can be lessened, perhaps even put to advantage, and the mission extended (fig. 4–12) (ref. 4).
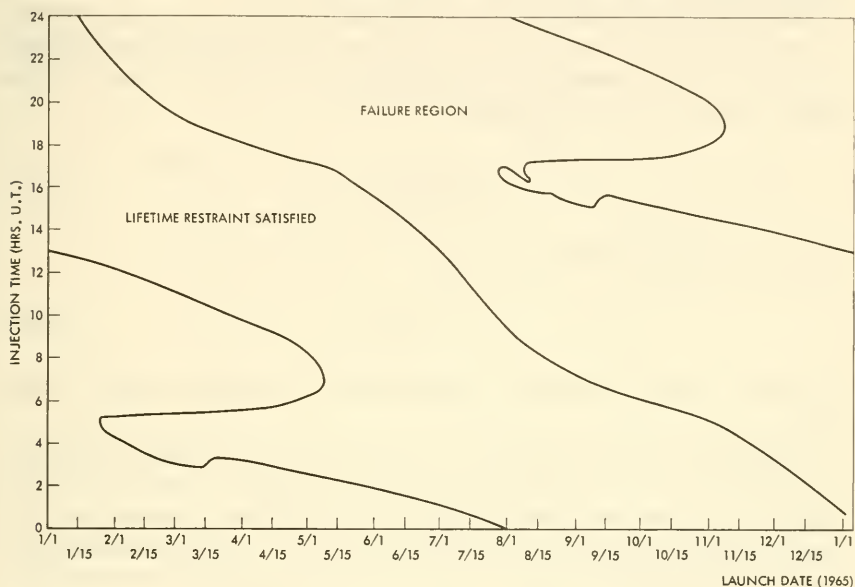
FIGURE 4–12.—Launch-window map for Explorer XXVIII (IMP C). To achieve a lifetime of 1 year, the perigee of this satellite could not drop below approximately 180 km. The peculiar shape of the map contours is due to the combination of several perturbing forces (ref. 4).

4–4. Orbital Dynamics of Unperturbed Satellites

When a command from the guidance equipment cuts off the thrust of the launch vehicle's final stage, and satellite separation has occurred, the path of the injected satellite is described by the equations of orbital dynamics, a subfield of astrodynamics and a major subject of this chapter.

The presentation first examines only idealized, stable orbits about an Earth represented by a point mass. Ideal orbits, like ideal launch trajectories, are educational, but many natural and artificial forces act upon a real satellite to upset ideality. The more practical, perturbed orbits are described in section 4–5.

Satellite Orbit Parameters.—The simple circular orbit associated with balancing of gravitational and centrifugal forces must now

be replaced by a second, more general conic section, the ellipse. The equation for the ellipse in polar coordinates is

$$R = \frac{a(i - e^2)}{1 + l \cos \phi} \tag{4-4}$$

where the variables are defined in figure 4–13.

The velocity of a satellite in an elliptical orbit is always greatest at perigee, where the gravitational and compensating centrifugal forces are the strongest. At apogee, the velocity is least. The general equation for velocity is

$$V_s = \sqrt{GM\left(\frac{2}{R} - \frac{1}{a}\right)} \tag{4-5}$$

The orbital period, T, is given by

$$T = 2\pi \sqrt{\frac{a^3}{GM}} \tag{4-6}$$

Equations (4–4) through (4–6) apply to circular orbits when $a = R$.

Equation (4–4) is expressed in variables that simplify the physical picture, but it does not involve coordinates tied either to a geocentric reference frame located at the Earth's center or to a topocentric reference frame with an origin at some tracking station on the Earth's surface. This deficiency will be corrected in a few pages.

Six variables, or orbital elements, are needed to specify a satellite orbit completely: three to define the position of the orbital plane relative to the Earth; the other three to describe the orbit itself. (Note that the position of the satellite in the orbit is not specified by orbital elements.) The "classical" set [2] of orbital elements is presented below:

Ω = the longitude of the node, measured in the plane of the equator from the direction of the vernal equinox to the direction of the ascending node, or intersection of the orbit with the equator (fig. 4–14)

i = the inclination, or angle between the plane of the orbit and the plane of the equator

ω = the argument of perigee, or angle between the direction of the ascending node and the direction of perigee

a = the semimajor axis

e = the eccentricity

T = the time of perigee passage

[2] Actually, any six independent orbital parameters suffice.

These orbital elements are geocentric in the sense that they are measured from the center of the Earth. Their frame of reference, however, does not rotate with the Earth, but is referred to the fixed stars. Consequently, a satellite's orbit seems to change as the Earth rotates.
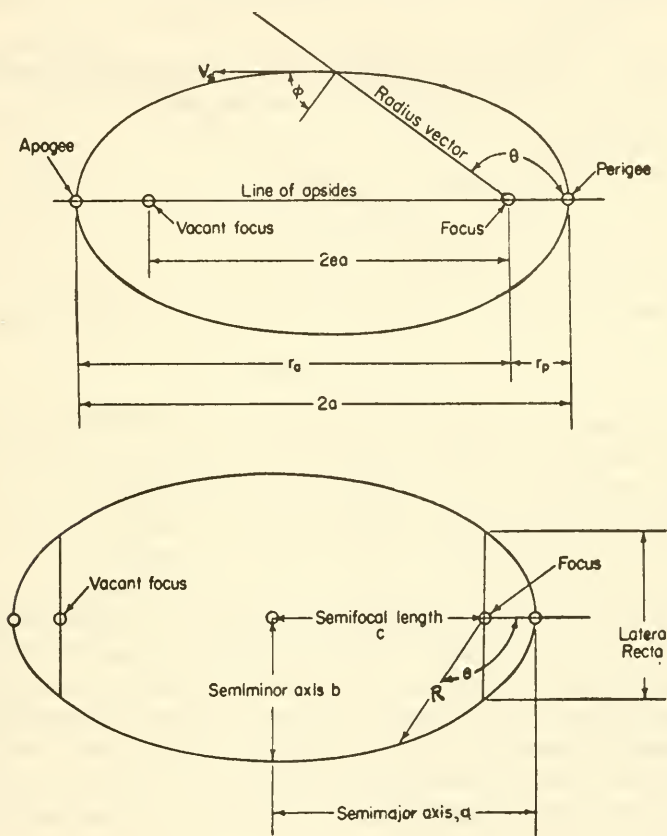
Semimajor axis a as noted on the diagram

Semiminor axis $b = a\sqrt{1 - e^2}$

Semifocal distance $c = \sqrt{a^2 - b^2}$

Radial distance $r = \dfrac{a(1 - e^2)}{1 + e \cos \theta}$

Semilatus rectum $l = a(1 - e^2)$

Eccentricity $e = c/a$

Aphelion or apogee distance $r_a = a + c = a(1 + e)$

Perihelion or perigee distance $r_p = a - c = a(1 - e)$

Position angle θ as noted on the diagram

FIGURE 4–13.—Definitions of ellipse parameters. The shaded areas in the bottom diagram illustrate one of Kepler's laws, which asserts that equal areas are swept out by radius vectors in equal times.
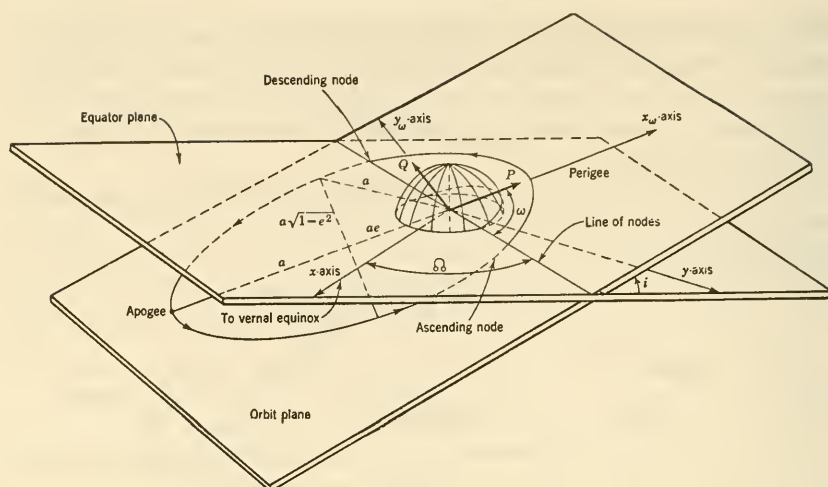
FIGURE 4–14.—The "classical" set of geocentric orbital parameters.

In astronautical parlance, especially satellite listings (see appendix), satellite orbits are described by an incomplete set of four, easily comprehended parameters: viz, perigee altitude and apogee altitude (both measured from the Earth's surface), orbital period, and orbital inclination. These four parameters give a "feel" for the orbit, but they say nothing about the orientation of the orbital axis. They are also redundant, because the orbital period can be computed if the apogee and perigee altitudes are known (eq. 4–6).

In summary, three sets of orbital parameters have been introduced so far: polar coordinates (for physical understanding); the classical, geocentric orbital elements (for the sake of completeness); and the common, "journalistic" parameters. Beyond these is a host of other possible sets of possible variables and coordinate systems, each possessing some special advantage for some special purpose (ref. 5).

In practical trajectory and orbit calculations, where data must be generated by computers for many ground stations and many satellites, mathematicians adopt rectangular coordinates with the point of origin fixed at the point of observation on the Earth's surface; i.e., a topocentric set. One would suppose that polar coordinates would be more "natural" for orbital description, but rectangular coordinates make the computation task much easier.

To illustrate the computational difficulty of going from one set of coordinates to another, a few pertinent equations are intro-

duced. Following Baker, the position of the observing station is first established in rectangular coordinates:

$$\mathbf{R}\begin{cases} X = -r_c \cos \phi' \cos \theta = -(C+H) \cos \phi \cos \theta \\ Y = -r_c \cos \phi' \sin \theta = -(C+H) \cos \phi \sin \theta \\ Z = -r_c \sin \phi' = -(S+H) \sin \phi \end{cases} \tag{4-7}$$

where

r_c = the geocentric distance of the station

ϕ' = the geocentric latitude

H = the height above a reference spheroid expressed in equatorial radii

ϕ = the geodetic latitude of the station

θ = the angle between the station and the direction of the vernal equinox measured at the Earth's center

$C = [1 - (2f - f^2) \sin^2 \phi]^{-\frac{1}{2}}$

$S = C(1-f)^2$

f = the flattening of the reference spheroid.

The rates of change of the station coordinates are:

$$\dot{\mathbf{R}}\begin{cases} \dot{X} = \omega(C+H) \cos \phi \sin \theta \\ \dot{Y} = -\omega(C+H) \cos \phi \cos \theta \\ \dot{Z} = 0 \end{cases} \tag{4-8}$$

where ω is the Earth's angular velocity. The vector $\mathbf{R}$ in figure 4–15 extends from the point X, Y, Z to the Earth's center.

The position of the satellite in terms of the same geocentric coordinate system is given by the point x, y, z, which is also the terminus of the vector $\mathbf{r}$. The topocentric coordinates of the satellite are defined as ξ, η, and ζ, which, in turn, define the vector $\boldsymbol{\rho}$. The relationships are:

$$\boldsymbol{\rho}\begin{cases} \xi = x + X \\ \eta = y + Y \\ \zeta = z + Z \end{cases} \qquad \dot{\boldsymbol{\rho}}\begin{cases} \dot{\xi} = \dot{x} + \dot{X} \\ \dot{\eta} = \dot{y} + \dot{Y} \\ \dot{\zeta} = \dot{z} + \dot{Z} \end{cases} \qquad \begin{aligned} \boldsymbol{\rho} &= \mathbf{r} + \mathbf{R} \\ \dot{\boldsymbol{\rho}} &= \dot{\mathbf{r}} + \dot{\mathbf{R}} \end{aligned}$$

The range from the tracking station to the satellite is now

$$\rho = (\xi^2 + \eta^2 + \zeta^2)^{\frac{1}{2}} \tag{4-9}$$

and the range rate, $\dot{\rho}$, is

$$\dot{\rho} = (\xi\dot{\xi} + \eta\dot{\eta} + \zeta\dot{\zeta})/\rho$$

To express the satellite altitude and azimuth in these terms, a topocentric unit vector, **L**, is first defined

$$L_{x_h} = \xi_h/\rho, \qquad L_{y_h} = \eta_h/\rho, \qquad L_{z_h} = \zeta_h/\rho$$

where:

$\xi_h = \xi \cos \theta \sin \phi + \eta \sin \phi \sin \theta - \zeta \cos \phi$
$\eta_h = \eta \cos \theta - \xi \sin \theta$
$\zeta_h = \xi \cos \theta \cos \phi + \eta \cos \phi \sin \theta + \zeta \sin \phi$

Then the elevation of the satellite, ϵ, is

$$\epsilon = \tan^{-1} [L_{z_h}/(L_{x_h}^2 + L_{y_h}^2)^{\frac{1}{2}}] = \sin^{-1} L_{z_h} \qquad (4\text{--}10)$$

and the azimuth, A, is

$$A = \tan^{-1} [L_{y_h}/L_{x_h}] \qquad (4\text{--}11)$$

The above equations are often used to generate local ephemerides for various stations and satellites. The Goddard Space Flight Center of NASA, for example, publishes the *Goddard Orbit Bulletin,* which describes the orbits of many satellites. In addition, NASA furnishes local ephemerides and viewing predictions for many scientific sites and several cities.

Orbit Determination.—The task of orbit determination from tracking data is the inverse of ephemeris generation. Tracking units often give the satellite elevation, azimuth, and range as a function of time (sec. 7–4). In terms of these particular parameters, the position of the satellite in terms of the unit vector **L** is:

$L_x = - \cos \theta \sin \phi \cos \epsilon \cos A + \cos \theta \cos \phi \sin \epsilon - \sin \theta \cos \epsilon \sin A$
$L_y = - \sin \theta \sin \phi \cos \epsilon \cos A + \sin \theta \cos \phi \sin \epsilon + \cos \theta \cos \epsilon \sin A$
$L_z = \cos \theta \cos \epsilon \cos A + \sin \phi \sin \epsilon \qquad (4\text{--}12)$

and

$$x = \xi - X, \qquad y = \eta - Y, \qquad z = \zeta - Z \qquad (4\text{--}13)$$

Equation (4–12), however, determines only the three coordinates of a single point in space and not the six measurements (called a minimal data set) needed to determine the orbit completely. At least two three-dimensional fixes from a single station are needed. Baker and Deutsch list several possible data sets that will completely determine an orbit (refs. 5, 6). Some possibilities are: three ranges from each of three different stations; three ranges
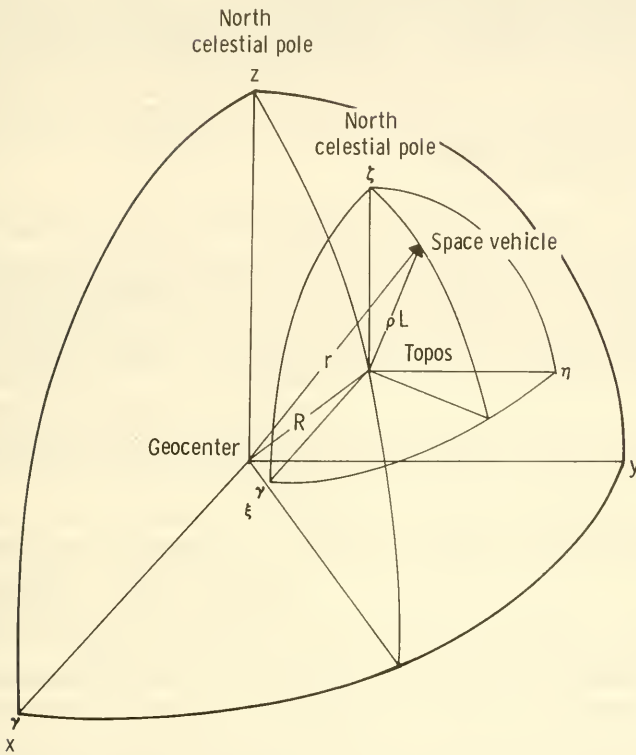
FIGURE 4–15.—Diagram defining a set of topocentric coordinates. Such coordinates can be measured directly from tracking-station instruments.

and three range rates from a single station; six ranges; six range rates; and so on. The variables employed depend upon the instruments installed at the tracking site. Radars, for example, can measure range and range rate quite accurately. Optical instruments have more precision when angles are being measured, but cannot measure range or range rate directly at all.

A single orbital determination from a minimal data set usually does not have the precision needed for scientific and long-term prediction requirements. Precision orbits are computed from many fixes made at many tracking stations over many satellite revolutions. Data from tracking sites (STADAN, sec. 7–4) are usually fed into a central computing facility, where they are processed to generate the local ephemerides and other predictions that are the practical results of orbit determination.

4–5.   Orbital Perturbation Forces and Their Effects

Once launched into an elliptical path, with the Earth's center of gravity at one of the foci, a satellite immediately begins to stray from that hypothetical, ideal, stable orbit fixed in the inertial reference frame of the stars. Such departures from perfection are termed "perturbations." Table 4–3 indicates that perturbations have several sources.

TABLE 4–3.—*Sources of Real and Apparent Orbital Perturbations*

Source of perturbation	Implications a
Earth's rotation_____	Satellite orbit plane rotates 15° west every hour. As a result a satellite scans much of the Earth's surface.
Relativity_____	Negligible advance of orbit's perigee.
Earth's bulge_____	Recession of nodes and advance of orbit's perigee.
Earth's pear shape_____	Long-term changes in orbit eccentricity.
Gravitational forces of Sun and Moon.	May raise or depress perigee and shorten or extend mission. Orbits can be "anchored" to Moon; i.e., lunar orbits.
Atmospheric drag _____	Varies with satellite cross section. Eventually causes reentry.
Magnetic drag_____	Negligible, except for huge satellites.
Radiation pressure_____	May raise or depress perigee for very large satellites.
Propulsion system_____	Under control of designer. Can overcome perturbating forces or maneuver satellite.

a See discussions in text.

Perturbations may be undesirable, say, when atmospheric drag prematurely ends the life of a satellite. On the other side of the coin, analysis of the same drag perturbations can yield estimates of the density of the upper atmosphere as a function of time. In other words, the orbits of Earth satellites need not drift aimlessly or uselessly in response to perturbating forces. Natural as well as artificial forces can be put to practical use.

Effects of the Earth's Rotation.—The Earth rotates on its axis approximately 15° each hour, a fact that causes the satellite orbit to shift continually in the eyes of a terrestrial observer. This might be called an "apparent" perturbation, since it is caused by the motion of the observer and not by "real" forces. Each equatorial pass of the satellite will show it shifted farther to the west
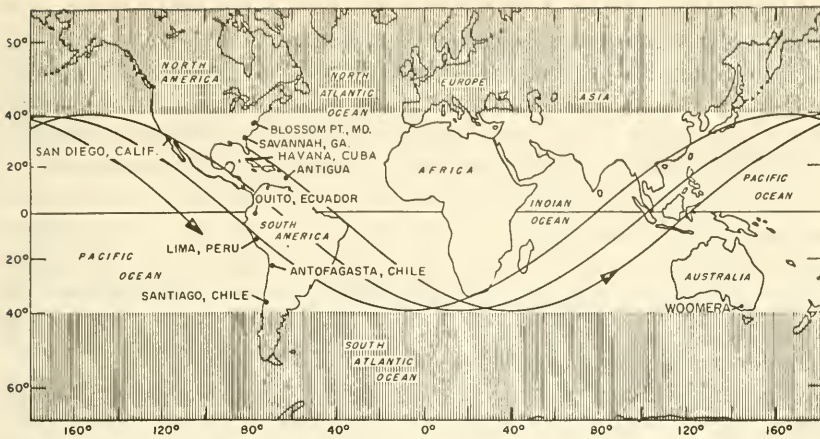
FIGURE 4–16.—Ground traces for an orbit of moderate inclination launched along the Eastern Test Range (ETR). The satellite crosses the equator approximately 15° farther west on each pass.

by about 15°. The result is the familiar pattern of satellite ground traces shown in figure 4–16.

Relativistic Effects.—Eccentric artificial-satellite orbits will show very small deviations from the orbital motion predicted by Newtonian mechanics. A more accurate description of nature, the general theory of relativity, predicts that there will be a small, continuous rotation of the satellite line of apsides (fig. 4–13). As a result, there is an advance of the perigee over and above that caused by the Earth's bulge and axial rotation. The advance of perigee, P, in seconds of arc per revolution is

$$P = \frac{1.73 \times 10^6}{a(1-e^2)}$$

where

e = eccentricity
a = semimajor axis (cm)

Calculations using the above equation predict perigee advances of only a few seconds per year for very eccentric satellites (ref. 5). This is a negligible effect. In fact, it is so small that an Earth satellite cannot be used effectively to test the hypothesis of the general theory of relativity, as has been done with the orbit of Mercury.

Note that Earth-satellite velocities are so small compared with that of light that the special theory of relativity predicts only negligible effects.

Asymmetry of the Earth.—The Earth's equatorial bulge and slight pear shape have been well publicized. There are also important anomalies in the gravitational fields in the western Pacific, the Indian Ocean, and Antarctica. As a result, the orbit of a real satellite is pulled away from the orbital path calculated under the assumption that the Earth can be represented by a point mass.

The asymmetry problem is attacked mathematically by expanding the gravitational potential function in a series of harmonics. In section 11–7, where the use of satellites in geodesy is discussed, this expansion is discussed in more detail. Here, it is sufficient to point out that various terms in the expansion can be identified with certain deformations of the figure of the Earth.

The major effect of the Earth's bulge is the regression of the nodes; that is, the orbital plane rotates slightly more westward on each revolution than would be expected from the rotation of the Earth alone. Physically speaking, as the satellite nears the equator on, for example, a southeast trace, the extra gravitational pull of the bulge deflects the satellite farther southward (fig. 4–17).
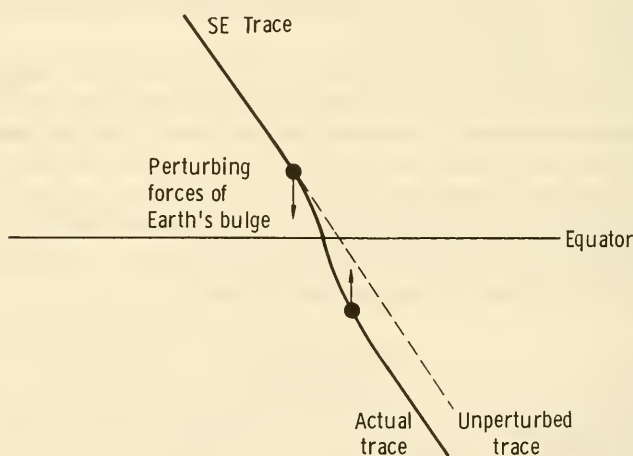
FIGURE 4–17.—The perturbing gravitational force of the Earth's bulge causes the orbital plane to regress westward.

After passing the equator, the satellite is pulled northward, back into its original direction of motion, but the ground trace has been offset slightly, and the satellite has crossed the equator slightly west of where it would if the Earth had no bulge. Riley and Sailor present the following equation (attributed to King-Hele) for the regression rate (ref. 7):

$$\Delta\Omega = \frac{k \cos i}{a^{7/2}(1-e^2)^2} \qquad (4\text{-}14)$$

where

$\Delta\Omega$=the regression rate (1/sec)
k=a constant based on the second harmonic of the Earth's field
i=the orbit inclination to the equator

A second effect of the bulge's perturbing force is the deflection of the satellite as it nears a perigee point near the equator. Taking a southeast-orbit trace again, with a perigee point near Cape Kennedy, there will be a slight overshoot of the previous perigee point as the satellite swings down toward perigee and, at the same time, is pulled toward the equator. The orientation of the whole orbit is thus rotated. In orbital terminology, there is a rotation of the line of apsides. The rotation rate is much higher than that due to relativistic effects:

$$\Delta\omega = \frac{k(2 - \frac{5}{2}\sin^2 i)}{a^{7/2}(1-e^2)^2} \qquad (4\text{-}15)$$

where $\Delta\omega$=the rotation rate in radians/sec.

Gravitational Effects of the Sun and Moon.—The gravitational fields of the Sun and Moon are overwhelmed by that of the Earth for close satellite orbits. In fact, the perturbation of the Earth's bulge is more important. At the apogee of a very eccentric elliptical orbit, however, when the satellite is hundreds of thousands of kilometers from Earth, the Sun and Moon may significantly affect the orbit. The classical instance is that of Explorer VI, where the Moon's attraction depressed the perigee so much that the satellite life was shortened. Conversely, proper positioning of the orbit can reverse the effect and prolong orbital lifetime.

Orbital perturbations involving three bodies—the satellite, the Earth, and the Moon or Sun—are difficult to generalize. Each case must be attacked separately. Several of the mathematical schemes described later in this section are applicable. A common approach involves calculating the forces on the satellite from all bodies, as obtained from Newton's law of gravitation and ephemerides, and integrating the differential equations of motion step by step in time.

A very special satellite depending upon the Moon's gravitational field to shape its orbit is the selenoid, or synodic, satellite. Klemperer has shown that there are five spots in the Earth-Moon plane where a small artificial satellite would be in dynamic equilibrium
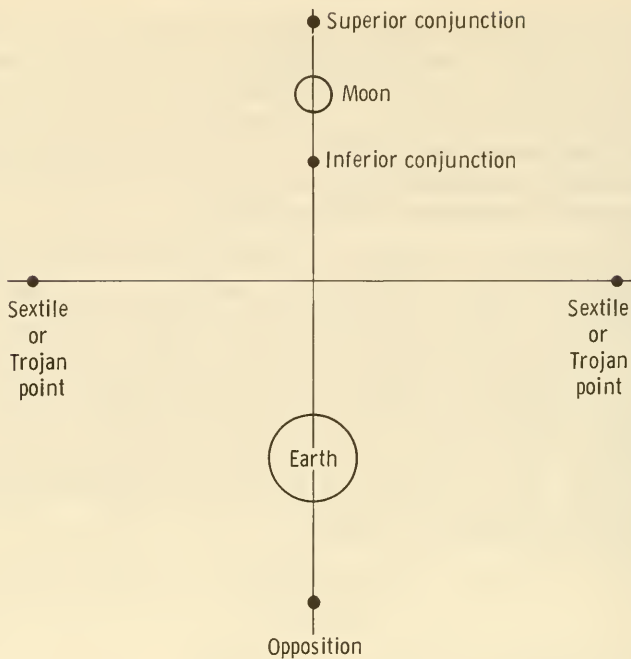
FIGURE 4–18.—Locations of the five dynamically stable points in the Earth-Moon system. Only the two sextile points are stable under small perturbations (ref. 8).

(fig. 4–18). The so-called sextile points, located at the corners of equilateral triangles formed by the Earth, Moon, and satellite, are the only ones that are stable under small perturbations. Similar stable points exist in the Sun-Jupiter system; these are called Trojan points. A number of small asteroids or planetoids have actually been observed at these points, preceding and following Jupiter around the Sun. Conceivably, an artificial satellite could be placed at the sextile points in the Earth-Moon system and rotate around the Earth once a month. At the moment, such a satellite would appear to offer no advantages over the Anchored IMP. From the standpoint of scientifically mapping the Earth-Moon plane, satellites physically fixed in the same relative positions would contribute little.

Atmospheric Drag.—The effects of atmospheric drag on satellite lifetime were greatly underestimated in the early days of astronautics. First, the atmosphere above 150 kilometers was denser than expected, by more than an order of magnitude. Second, the

Sun not only significantly expanded the sunlit side of the atmosphere with its heat but also injected large quantities of matter into the upper atmosphere. Lifetimes of satellite orbits were therefore much shorter than predicted, and orbital drag perturbations were stronger and more variable. Four major variations in drag—all Sun-caused—are now recognized:

(1) The diurnal effect due to the Sun-heated atmospheric bulge

(2) The 11-year cycle caused by the varying rate of particle injection by the Sun

(3) Erratic drag increases due to particle injection during solar storms

(4) The semiannual plasma effect that causes drag to peak around April and June (ref. 9)

Atmospheric drag decelerates a satellite, causing some of its kinetic energy to be converted into atmospheric heat. As the satellite slows down, its centrifugal force decreases and gravity pulls it farther into the atmosphere. The orbit is made more nearly circular in the process. The drag force is given by

$$F_d = \tfrac{1}{2}\rho A V_s^2 C_D$$

where the variables have already been defined in section 4–3. Assuming an exponential static atmosphere (for insight rather than precise estimates of lifetime) and integrating over a complete satellite orbit

$$\Delta E = - \oint \mathbf{F}_d \cdot \mathbf{R} \, d\theta$$

$$\cong - \pi C_D A G \bar{\rho} e^{-\beta(R-R_0)} \tag{4–16}$$

where

$\Delta E =$ the satellite kinetic-energy loss

$\bar{\rho} =$ the average density of the atmosphere

$\beta =$ the constant in the exponential representation of the atmosphere, $\rho = \bar{\rho} e^{-\beta(R-R_0)}$, sometimes called the scale height.

The orbital-energy equation is

$$E = \frac{GM}{2R}$$

Taking finite differences and using equation (4–16)

$$\frac{\Delta R}{\Delta n} = - \frac{2\pi R^2 \rho C_D A}{m} \tag{4–17}$$

where $n =$ the satellite lifetime measured in revolutions.

Equation (4–17) is only as accurate as the exponential, static atmosphere that is assumed. Ladner and Ragsdale, at the Marshall Space Flight Center, and Bruce have published curves that include the effects of solar atmospheric perturbations. The data of the former authors are suitable for planning purposes and are reproduced in part in figures 4–19 through 4–21 (ref. 10). Figure
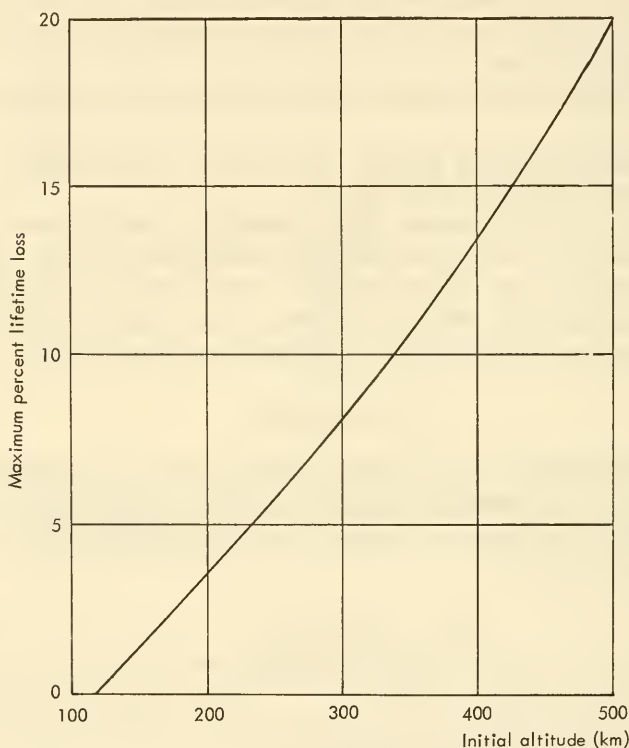
FIGURE 4–19.—Loss in satellite lifetime due to the Earth's diurnal atmospheric bulge (ref. 10).

4–19 takes into account the diurnal bulge effect. Figure 4–20 presents an estimate of the effects of the 11-year solar cycle. The timing and magnitude of solar storms are difficult to predict and are not included.

Magnetic Drag.—When a large satellite moves through the Earth's magnetic field, an electromotive force of about $10^{-8} HV_s$ volt/cm (H = the magnetic field strength in gauss) is established at right angles to the field and direction of satellite motion (ref. 11). This emf tends to drive the electrons to one end of the satellite
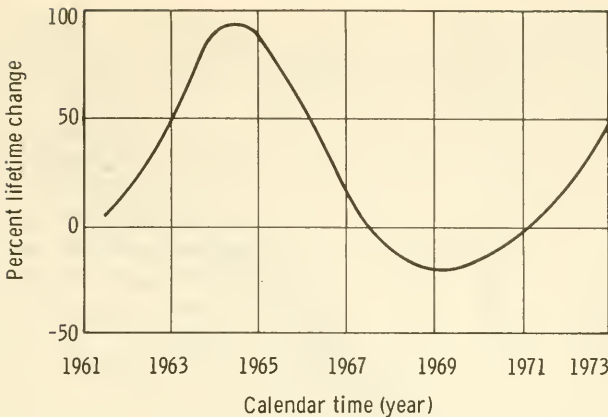
FIGURE 4–20.—Estimated satellite lifetime change due to density changes in the Earth's atmosphere resulting from the 11-year solar cycle (ref. 10).

and, in effect, polarizes the spacecraft. The electrostatic fields built up between the ends of the charged satellite will have negligible effect on the paths of the heavy ions intercepted by the satellite in its swath through the upper atmosphere, but the lighter electrons will be diverted toward the positively charged end of the satellite. This asymmetry of charge flow creates a current flow across the satellite body. The motorlike interaction of the current-carrying conductor with the magnetic field slows the satellite down. Beard and Johnson calculate that the magnetic drag is proportional to the cube of the satellite dimensions. For a satellite over 50 meters in diameter and above 1200 kilometers in altitude, where the density of charged particles is high, the magnetic drag can exceed aerodynamic drag.

The Effects of Solar-Radiation Pressure.—When a solar photon strikes a satellite surface and is reflected or absorbed, a tiny bit of momentum is transferred to the satellite. A pressure is produced that is proportional to the power in the Sun's rays. For normal incidence and complete reflection, the solar pressure at the Earth's orbit is 9.2×10^{-6} newtons/m². Small though this pressure is, it has caused the perigee of large, low-density satellites, such as those in the Echo series, to vary by hundreds of kilometers. Depending upon the shape and orientation of the orbit, the solar pressure may depress or elevate perigee. The perigee of Echo I, for example, has oscillated as the perigee point has rotated relative to the Sun under the influence of the equatorial bulge.
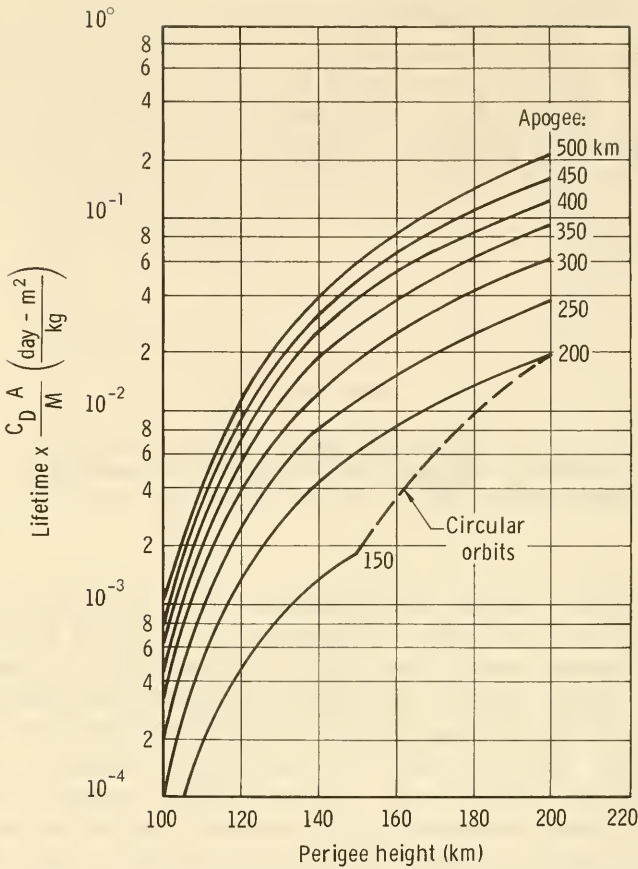
FIGURE 4–21.—Orbital lifetimes for various orbits (ref. 10).

Solar-pressure effects can be computed for simple, spherical satellites, but most scientific satellites are faceted, with surfaces possessing different reflectivities, and rotate at varying rates and inclinations. Earth shadowing and self-shadowing, say, by solar-cell paddles, make the analytical problem still less tractable. Fortunately, the effects are usually important only for balloon-type satellites in eccentric orbits. As a point of interest, Buckingham, Lim, and Miller have shown that a group of balloon-type satellites, initially placed in the same orbit together, can be angularly spaced and maintained at the desired spacing by solar pressure (ref. 12).

Active Orbit Control.—Scientific satellites, as they are presently conceived, orbit the Earth more or less at the mercy of perturbing

forces. Onboard propulsion equipment—an electrical engine, for example—might generate compensating thrusts to keep the satellite in the desired orbit. This is called station keeping. The important question here is: Why bother? Drag compensation would extend satellite lifetime, but the necessary propulsion equipment would displace scientific instruments when orbits of adequate lifetime are already easily achieved. The rotation of perigee could also be offset, but there seems to be no overwhelming need to do this, particularly when one wishes to scan as much space as possible. In other words, natural perturbations present no critical problems for most scientific satellites. In fact, they have positive value in geodesy and in missions that map fields and particles.

If, in some application, active compensation of perturbations seems desirable, the artificial force can be considered mathematically as another perturbing force and treated accordingly.

Military and applications satellites often demand intentional orbit modifications over and above those caused by natural forces— for satellite rendezvous, for example, or the nudging of a communication satellite into a stable, stationary orbit over the equator. Here again, active propulsion has not been justified for the great bulk of scientific satellites. If a scientist desires to explore space at a different altitude or orbit inclination, it is simpler and cheaper to launch a new satellite than to propel an old one to the new orbit.

Propulsion requirements for active orbit control have been worked out by many authors (refs. 13, 14), but there seems no need to reproduce their results here.

Perturbation-Computation Techniques.—Once a perturbing force has been estimated (the pressure of sunlight, for example), how is its influence on a specific orbit calculated? Two classes of techniques are recognized: special perturbations and general perturbations. The first class involves the numerical integration of the differential equations of motion, which are written to include all important perturbing forces. In the general-perturbations approach, the analytical statement of the perturbed orbit is expanded in a series, which is then integrated. The term "general" applies because different initial conditions can be substituted in the resulting integrated equations. In special perturbations, there is a unique "special" starting point for each case.

There are three principal procedures used in the area of special perturbations (ref. 5):

(1) *Cowell's Method.*—A step-by-step integration of the total acceleration, including that caused by the central force field (fig.
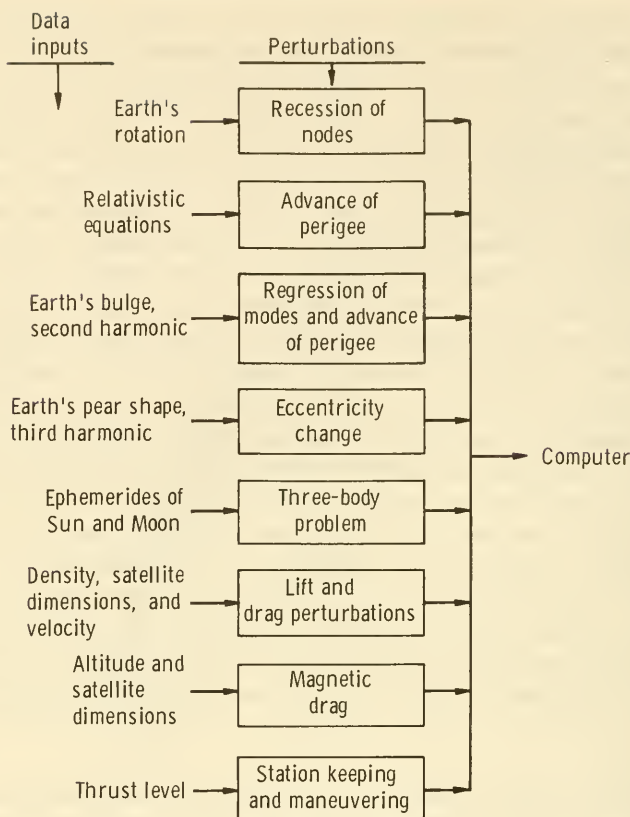
FIGURE 4–22.—Schematic diagram showing inputs and
perturbations affecting satellite orbits.

4–22). The force vectors from all sources are added to that due
to gravity, and the resulting motion of the satellite is computed
over a short time interval. A new position is calculated at the
end of the interval. Forces at the new position are again com-
puted and another segment of the orbit worked out. Cowell's
method is simple, flexible, and sometimes used in computing space-
probe trajectories. It is rarely used in satellite work because the
perturbing forces are very small compared with the central force
field, and errors increase quickly as the number of revolutions
increases.

(2) *Encke's Method.*—This is also a step-by-step method, but
here a reference orbit is established and the perturbations are
computed relative to it. Accuracy and calculational efficiency are

usually much improved over Cowell's method in orbital studies. When the perturbed orbit diverges too far from the reference orbit, however, errors and inefficiency become serious, and a new, or rectified, reference orbit must be constructed. The Encke method is well adapted to guidance studies.

(3) *The Variation-of-Parameters Method.*—This technique is similar to the Encke method, except that the reference orbit is continuously rectified. (The varying reference orbit is called osculating.) The results from the variation-of-parameters method are very accurate, but the need for constantly updating the reference orbit makes the mathematics cumbersome. With modern computers, though, the computing costs are not exorbitant.

When orbits must be followed over hundreds and thousands of revolutions, general perturbations are very useful; i.e., efficient and accurate. Since the technique involves analytically integrating [3] the series expansion of the pertinent accelerations, changes in the orbit can be easily related to the perturbing force that causes it (ref. 5). In contrast, when only tables of computer-printed data appear, cause and effect are difficult to discern. The pear shape of the Earth, for example, was discovered by the methods of general perturbations, when J. A. O'Keefe and A. Eckels related long-term changes in orbital eccentricity to terms originating in differences in the Northern and Southern Hemispheres. The reader should refer to basic astrodynamic texts for more details (refs. 5, 6).

4–6.   Intentional Reentry

Most scientific satellites are eventually slowed by drag forces and reenter the Earth's atmosphere in an uncontrolled manner. Aerodynamic heating completely consumes most of them. The only reentry trajectories important enough to describe here are those that escape the above fate—the recoverable scientific satellites, carrying dosimeters, biological specimens, and similar cargo back from orbit along a carefully controlled trajectory.

The physical parameters involved in the reentry of a scientific satellite are illustrated in figure 4–23. The sequence of events is this:

(1) The satellite (or capsule from a parent satellite) is deflected out of its orbit into an ellipse that intersects the dense portion of the Earth's atmosphere.

(2) The atmosphere is encountered and the kinetic energy of the satellite, which is several times the amount needed to melt the

---

[3] As opposed to numerical integration.
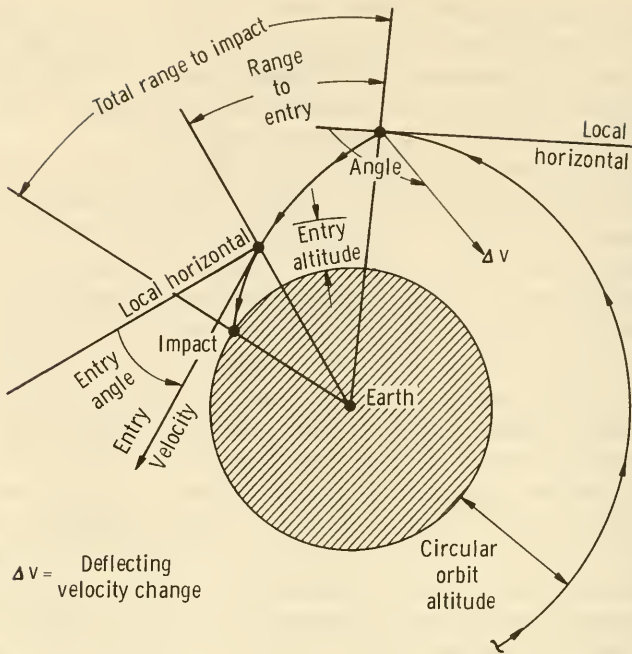
FIGURE 4–23.—Parameters describing the controlled deorbiting and reentry of a recoverable satellite.

satellite, is turned into heat. An ablating thermal shield protects the satellite from the high temperatures. Most of the reentry heat is carried away by the air and the gases released during shield ablation.

(3) A parachute is deployed to reduce the satellite velocity still further.

(4) The satellite is recovered in midair by aircraft or retrieved on land or sea.

The important things to know are the timing, magnitude, and direction of the retrothrust needed for recovery in a designated area.

The reentering satellite, like the ascending launch vehicle, is subjected to five forces: gravity, centrifugal force, lift, drag, and applied thrust. Not only is the trajectory shaped by these forces, but they will also determine the magnitudes of the deceleration and thermal heating. If the deceleration is too high, destruction of the payload may result. Too much lift might cause the satellite to skip out of the atmosphere like a flat stone on water. The acceptable reentry conditions for the "corridor" are shown in figure
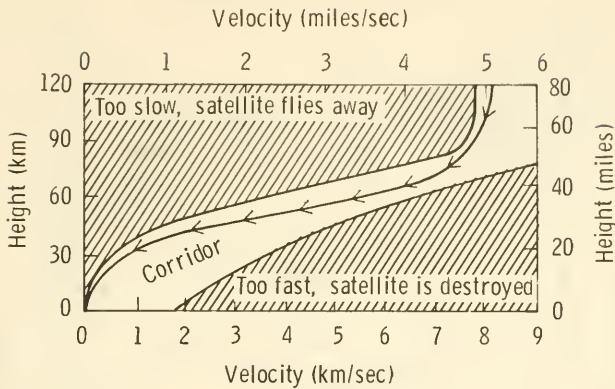
FIGURE 4–24.—A typical satellite reentry corridor (ref. 15).

4–24. The trajectories of "dumped" satellites, or capsules under-going controlled reentry, are generally steeper than drag-induced reentries.

Two kinds of reentry calculations are common. In the first, an atmospheric model is selected and the deceleration is derived analytically. Such an approach, plus the assumption of an exponential atmosphere, leads to the interesting fact that peak deceleration occurs when the satellite velocity equals $\dfrac{1}{\sqrt{e}}$ times the original velocity before deceleration (ref. 15). The information obtained from the above kind of analysis does not predict the actual trajectory, although it does provide design data of value. A second kind of analysis remedies this defect. It is similar in spirit and philosophy to the methods described in section 4–3 for launch trajectories. The equations must be the same as equation (4–3), because the same forces are involved. The only difference is that the launch vehicle is ascending under thrust, while the reentering satellite is descending under atmospheric braking. With these minor adjustments made, the differential equations of motion are integrated step by step, with the correct lift-and-drag forces inserted at each point.

Some results from such computations are presented in figures 4–25 and 4–26 (ref. 16). The particular parameters shown are those of interest to someone controlling the descent and recovery of a scientific satellite. Some obvious trends are:

(1) The steeper the descent, corresponding to a shorter range, the greater the deorbiting impulse needed—a fairly obvious point

(2) The direction of the deorbiting thrust, defined in figure
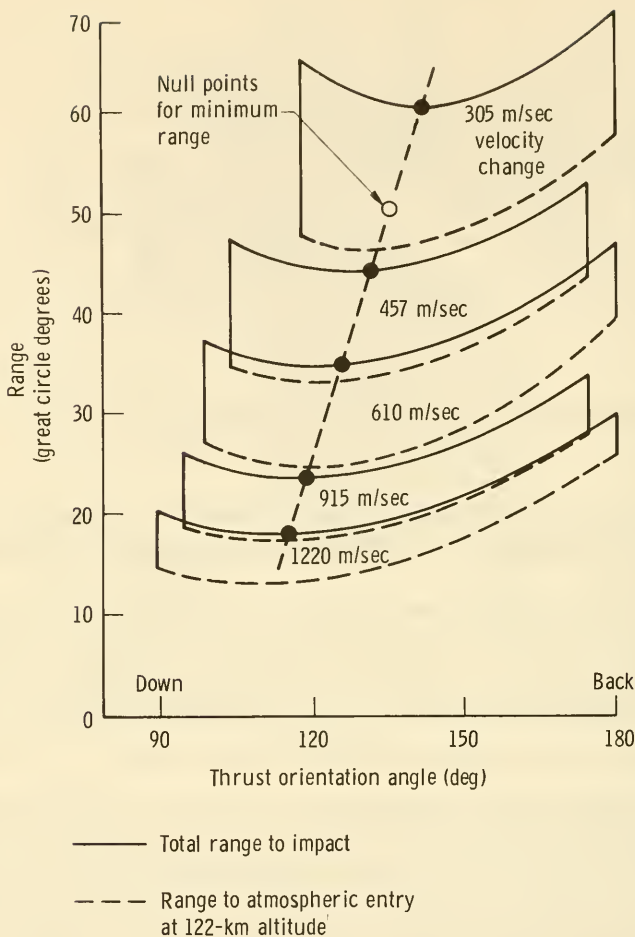
FIGURE 4-25.—Range to impact and point of reentry
for a 320-kilometer recoverable satellite as functions
of the deorbiting thrust vector (ref. 16).

4-23, is about 120° for minimum range; that is, down and opposed
to the direction of motion. Pure retrothrust in opposition to the
velocity vector is not the most efficient.

(3) The higher the orbit, the greater the range for a given
impulse—again, a physically obvious observation.

4-7.   Satellite-Attitude Dynamics

The bulk of this chapter has been devoted to the description of
the position of the satellite center of mass, as a function of time,
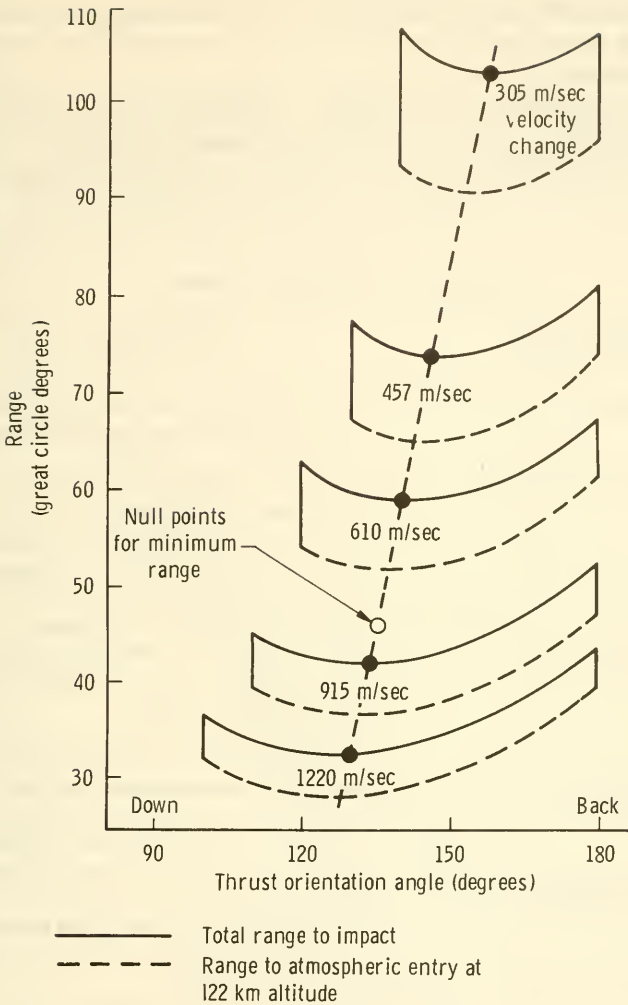
FIGURE 4–26.—Range to impact and point of reentry for a 640-kilometer recoverable satellite as functions of the deorbiting thrust vector (ref. 16).

under the influence of natural and artificial forces. Scientific satellites, though, are far from isotropic, so that satellite orientation, or attitude, must also be specified for the purposes of control and the interpretation of the scientific information telemetered back to Earth. Consider some of the anisotropies of scientific satellites:

(1) Many scientific instruments are directional and must be pointed at a target, or at least have their orientations telemetered to experimenters

(2) Most solar-cell power-supply subsystems rely upon some degree of attitude control for maximum power production

(3) Many satellite telemetry antennas have directional properties

TABLE 4–4.—*Satellite Torques*

Torque source	Particulars [a]
Unbalanced aerodynamic forces	Important below 500 km. Dominant below 300 km for many satellites (ref. 17).
Unbalanced radiation pressure	Pressure depends upon reflectivity and inclination of satellite surfaces. Surface characteristics change with time in space environment. Pressure is 9.2×10^{-6} newton/m² for perfect reflectivity and normal incidence.
Gravity gradients	Depends upon the radial dependence of gravitational and centrifugal forces. See equation (4–18).
Magnetic fields	If satellite has a permanent or induced magnetic field, interaction with Earth's field will create torques (ref. 18).
Propulsion units	Any thrust not directed through satellite center of mass will cause angular acceleration. Under control of designer.
Micrometeoroid impacts	Impacts with a non-zero moment arm to the center of mass can cause significant accelerations. Average effect should be small (ref. 19).
Ejected mass	Ejection of an instrument capsule, pod, or subsatellite (OV–4) can create a large change in angular momentum.
Emitted radiation	Antisotropic radiation of photons, say, from a power supply, can create a net torque. Under control of designer. Negligible.
Internal motion	Torques are created by gyros, motors, and other rotating equipment. Motion of instrument scanning platforms, extendable booms, and relays can cause attitude disturbances. Under control of designer.

[a] See fig. 4–27 for approximate magnitudes of torques for a specific satellite.

(4) Recoverable satellites must be properly oriented for retro-thrust

(5) Cylinders, polyhedrons, and other complex configurations are common satellite shapes. Therefore, the three satellite moments of inertia are not equal. Some satellites, such as the OSO's, are jointed, or articulated, instead of being rigid structures.

(6) If the satellite structure is anisotropic, there will be external, disturbing torques. (See table 4–4.)
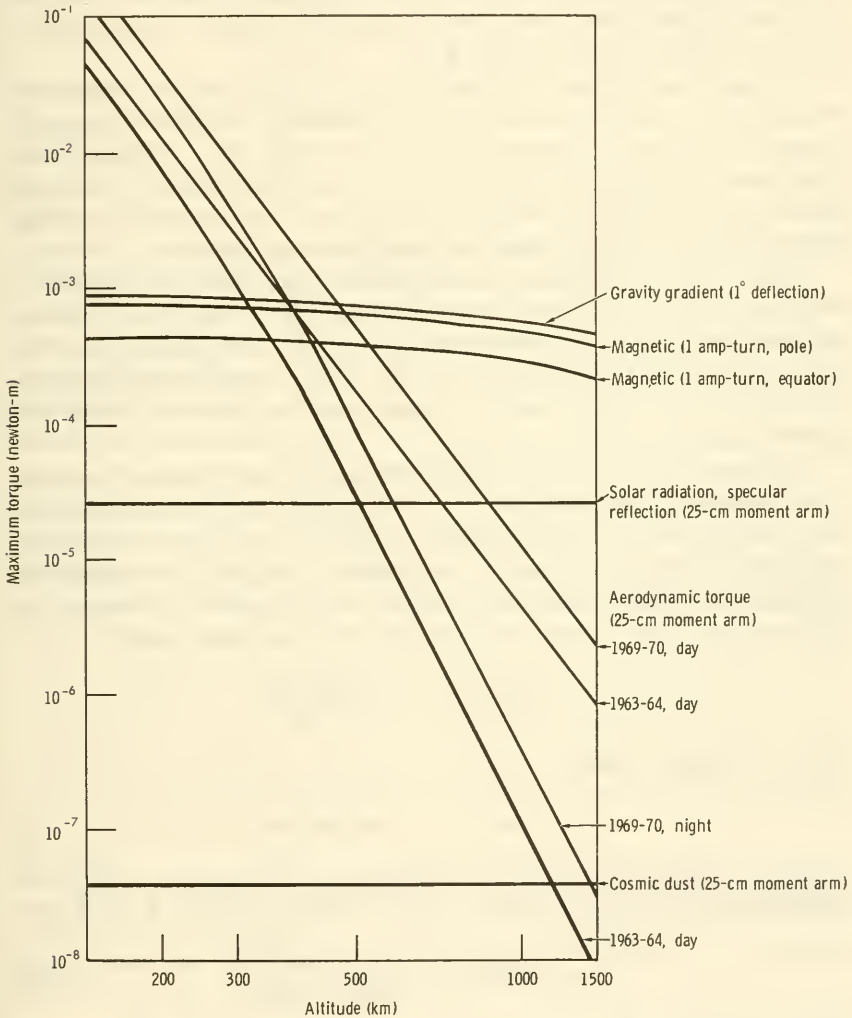
FIGURE 4–27.—Relative magnitudes of environmental torques on a satellite. Satellite used in calculations was a Discoverer, a 1.5 x 9-meter cylinder (ref. 20).

Anisotropy thus requires a reference frame in which to measure satellite attitude and a mathematical formulation of satellite motion in that frame. The purpose of this section is a simplified description of attitude dynamics that will be useful in treating the subject of attitude control (sec. 6–5) and the design of attitude-control subsystem hardware (sec. 9–8).

Sources of Disturbing Torques.—In the near-frictionless realm of outer space, the least internal motion or external torque accelerates a satellite into unwanted and undamped rotation. The list of offending but sometimes useful torques is lengthy and best presented in tabular form (table 4–4).

The satellite designer can control most of the torques, even those originating with the external environment. Satellite magnetic moments and mass asymmetries can be reduced. External surfaces can be adjusted to control or even usefully employ radiation pressure. In a similar vein, the extension of booms and antennas can be used to reduce unwanted satellite spin (ch. 9).

Figure 4–27 indicates that gravity-gradient and magnetic torques usually dominate above 400 kilometers. They are followed in importance by radiation-pressure torques. The weakness of the data presented in figure 4–27 is the lack of generality—the perturbing torques are all vehicle dependent—but the trends are still significant.

The derivation of the gravity-gradient-torque equation is pertinent because it illustrates how the variation of gravitational and centrifugal forces over the dimensions of the satellite, a seemingly negligible effect, can create important torques. Consider an idealized dumbbell satellite of length $2e$, like that portrayed in figure 4–28. The forces due to gravity on each end are

$$F_{g_1} = \frac{mg_0 R_0^2}{R_1^2} \qquad F_{g_2} = \frac{mg_0 R_0^2}{R_2^2}$$

The centrifugal forces

$$F_{c_1} = m\omega^2 R_1 \qquad F_{c_2} = m\omega^2 R_2$$

actually balance each other out because their moment arms are inversely proportional to their radii. The net torque, L, is then

$$L = mg_0 R_0^2 Re \, \sin \, \phi \left(\frac{1}{R_1^3} - \frac{1}{R_2^3} \right) \qquad (4\text{--}18)$$

where all of the variables are defined in figure 4–28. Further analysis shows that for small excursions, the undamped dumbbell satellite will swing, or librate, pendulumlike, with a period $\sqrt{3}$
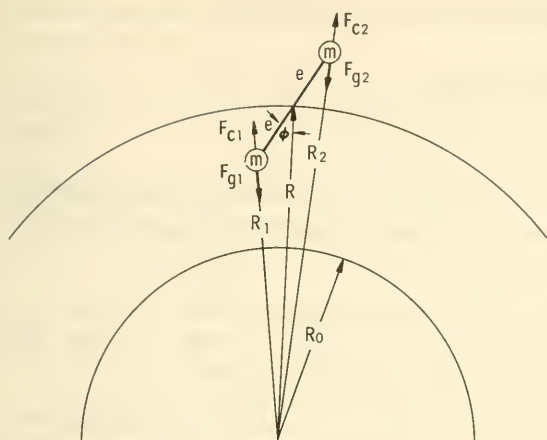
FIGURE 4–28.—Force diagram for deriving the gravity-gradient torque on a dumbbell satellite of mass $2m$ and length $2e$ (ref. 21).

times its orbital period. Our natural Moon librates in a similar fashion. In practice, gravity-gradient torques are strong enough to be used in stabilizing Earth-pointing satellites.

Coordinate Systems for Attitude Description.—Before writing down the equations of motion for a satellite, two coordinate systems must be defined. One set of coordinates will be embedded in the satellite itself, and will spin, tumble, and librate with it. The second, or reference, set of coordinates is usually fixed in inertial space, or associated with some mission function (fig. 4–29). In choosing the reference frame, the analyst is influenced by the factors of analytical simplicity, computational simplicity, the co-ordinates naturally associated with the attitude-determining sensors, and those coordinates that are most convenient in describing the satellite attitude during the mission; e.g., the reference frame of the fixed stars for astronomical satellites. The desired attitude of the satellite is described relative to the reference set of axes as a function of time. It is the task of the guidance-and-control subsystem to measure the actual satellite attitude, compare it with the desired attitude, establish corrective measures, and command the attitude-control subsystem to make the needed changes (refs. 22, 23).

Satellite Equations of Motion.—If Ω is the angular velocity of the satellite relative to the reference axes and ω is the angular velocity of the reference coordinate in inertial space,[4] the angular momentum, $\mathbf{H}$, of the satellite is:

$$\mathbf{H} = I_X(\Omega_X + \omega_X)\mathbf{e}_X + I_Y(\Omega_Y + \omega_Y)\mathbf{e}_Y + I_Z(\Omega_Z + \omega_Z)\mathbf{e}_Z \qquad (4\text{–}19)$$

[4] Many reference frames are possible (refs. 22, 23). If an inertial frame is selected, $\Omega = 0$.

where I_X, I_Y, I_Z = the satellite moments of inertia and $\mathbf{e}_X$, $\mathbf{e}_Y$, and $\mathbf{e}_Z$ are unit vectors.

If L is the external applied torque

$$\mathbf{L} = \dot{\mathbf{H}} + \omega \times \mathbf{H} \qquad (4\text{--}20)$$

in which $\mathbf{H}$ is the time rate of change of $\mathbf{H}$ as seen by an observer in the X, Y, Z set of axes. The components of equation (4–20) are:

$$
\begin{aligned}
I_X(\dot{\Omega}_X + \dot{\omega}_X) + (I_Z - I_Y)(\Omega_Y + \omega_Y)(\Omega_Z + \omega_Z) &= L_X \\
I_Y(\dot{\Omega}_Y + \dot{\omega}_Y) + (I_X - I_Z)(\Omega_Z + \omega_Z)(\Omega_X + \omega_X) &= L_Y \\
I_Z(\dot{\Omega}_Y + \dot{\omega}_Z) + (I_Y - I_X)(\Omega_X + \omega_X)(\Omega_Y + \omega_Y) &= L_Z
\end{aligned}
\qquad (4\text{--}21)
$$

Since many satellites are spin-stabilized in the reference frame of the fixed stars, where $\omega = 0$, a typical set of equations of motion is:

$$
\begin{aligned}
I_X\dot{\Omega}_X + (I_Z - I_Y)\Omega_Z\Omega_Y &= L_X \\
I_Y\dot{\Omega}_Y + (I_X - I_Z)\Omega_X\Omega_Z &= L_Y \\
I_Z\dot{\Omega}_Z + (I_Y - I_X)\Omega_Y\Omega_X &= L_Z
\end{aligned}
\qquad (4\text{--}22)
$$
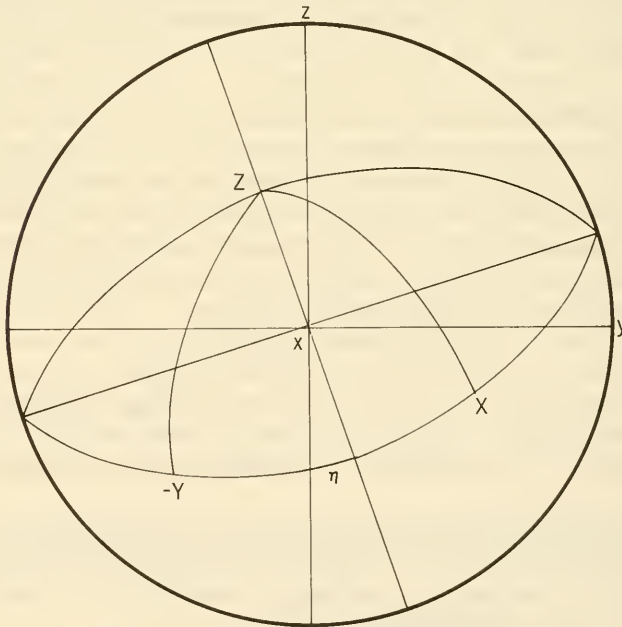
FIGURE 4–29.—Coordinate systems used in attitude dynamics. Frame x, y, z is the reference set of axes, and the attitude of the satellite, specified by frame X, Y, Z is measured relative to it.

These are the Euler equations for a body freely suspended at its center of mass.

Similar specialized cases can be worked out from the general equation of motion, equation (4–20).

References

1. CALLAWAY, R. C.: Powered Flight Through Atmospheres. *In* Handbook of Astronautical Engineering, H. H. Koelle, ed., McGraw-Hill Book Co., Inc., 1961.
2. MILSTEAD, A. H.: Launch Windows for Orbital Missions. USAF, AD 601072, 1964.
3. SHUTE, B.: Launch Windows for Highly Eccentric Orbits. *In* Celestial Mechanics and Astrodynamics, V. G. Szebehely, ed., Academic Press, 1964.
4. PADDACK, S. J.; AND SHUTE, B. E.: IMP–C Orbit and Launch Time Analysis. NASA TM X–55128, 1965.
5. BAKER, R. M. L.; AND MAKEMSON, M. W.: An Introduction to Astrodynamics. Academic Press, 1960.
6. DEUTSCH, R.: Orbital Dynamics of Space Vehicles. Prentice-Hall, Inc., 1963.
7. RILEY, F. E.; AND SAILOR, J. D.: Space Systems Engineering. McGraw-Hill Book Co., Inc., 1962.
8. KLEMPERER, W. B.; AND BENEDICT, E. T.: Synodic Satellites. Astronautics, vol. 3, Oct. 1958, p. 28.
9. BRUCE, R. W.: Satellite Orbit Sustaining Techniques. ARS J., vol. 31, Sept. 1961, p. 1237.
10. LADNER, J. E.; AND RAGSDALE, G. C.: Earth Orbital Satellite Lifetime. NASA TN D–1995, 1964.
11. BEARD, D. B.; AND JOHNSON, F. S.: Charge and Magnetic Field Interaction With Satellites. J. Geophys. Res., vol. 65, Jan. 1960, p. 1.
12. BUCKINGHAM, A. G.; LIM, Y. C.; AND MILLER, J. A.: Orbit Position Control Using Solar Pressure. J. Spacecraft and Rockets, vol. 2, Nov. 1965, p. 863.
13. EDELBAUM, T. N.: Propulsion Requirements for Controllable Satellites. ARS J., vol. 31, Aug. 1961, p. 1079.
14. LEVIN, E.: Low-Acceleration Transfer Orbits. *In* Handbook of Astronautical Engineering, H. H. Koelle, ed., McGraw-Hill Book Co., Inc., 1961.
15. VERTREGT, M.: Principles of Astronautics. Second ed., Elsevier Publishing Co. (Amsterdam), 1965.
16. SWET, C. J.: Biosatellite Recovery From Circular Orbits. Applied Physics Laboratory, AD 295851, 1962.
17. PEARSON, P.: Precession of UK–3 Satellite Due to Aerodynamic Torques. Spaceflight, vol. 8, Mar. 1966, p. 98.
18. HOHL, F.: The Electromagnetic Torques on Spherical Earth Satellites in a Rarefied Partially Ionized Atmosphere. NASA TR R–231, 1966.
19. MORGAN, S. P.; AND YU, E. Y.: Meteoric Disturbances of Gravitationally Oriented Satellites. J. Spacecraft and Rockets, vol. 2, Nov. 1965, p. 857.

20. WIGGINS, L. E.: Relative Magnitudes of the Space-Environment Torques on a Satellite. AIAA J., vol. 2, Apr. 1964, p. 770.
21. KLEMPERER, W. B.; AND BAKER, R. M.: Satellite Librations. Astronaut. Acta, vol. 3, 1957, p. 16.
22. ROBERSON, R. E.: A Unified Analytical Description of Satellite Attitude Motions. Astronaut. Acta, vol. 5, 1959, p. 347.
23. ROBERSON, R. E.: Principles of Inertial Control of Satellite Attitude. *In* Proc. of the IXth International Astronautical Congress, F. Hecht, ed., Springer-Verlag (Vienna), 1959.

Chapter 5

SATELLITE COMMUNICATION AND DATA HANDLING

5–1. Prolog

Passive, noncommunicating, "dark" satellites may be useful in geodetics and aeronomy, but a satellite's scientific utility is increased manyfold by adding telemetering equipment. Consequently, most scientific satellites are active. Like their predecessors, the sounding rockets, scientific satellites tie the experimenter to his experiment with electromagnetic waves.

The typical scientific satellite circles the Earth at an altitude of only a few hundred kilometers. Rarely do eccentric orbits swing out beyond the Moon. Over such short distances, communication is relatively easy. Communication problems still exist, but satellites do not operate at the threshold of communication feasibility, like the deep-space probes. Satellite-to-Earth communication is, in fact, so successful that one major task lies in coping with the flood of data that converges on the Earth from nearby space. An Observatory-class satellite, for example, may transmit bursts of data at a rate of 100 000 bits/sec, or, in more vivid terms, a book or two a minute. Recording, manipulating, storing, and somehow reducing this inundation to scientific meaning now pose a far larger problem than satellite communication per se. Many design choices and tradeoffs are strongly influenced by the data-handling problem.

Scientific satellites are basically information gatherers. Their instruments are extrapolations of man's senses. Information is the common currency involved here. The bulk of satellite-garnered information travels via electromagnetic waves, but, to be completely general, a second space-to-Earth information channel is created by the recoverable satellite and the data capsule deorbited from a parent satellite (fig. 5–1).
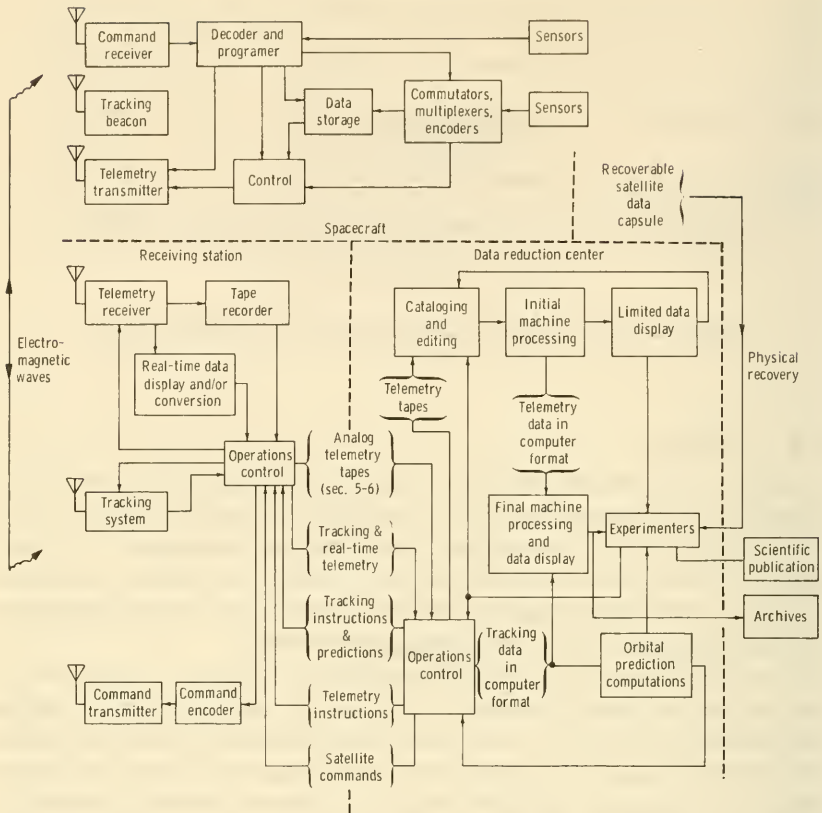
FIGURE 5–1.—Information-flow diagram for a scientific-satellite system. (Sensors may be experimental, status-indicating, or altitude-indicating.) (Adapted from ref. 1.)

Information in four distinct categories is transmitted from and to a scientific satellite:

(1) Scientific data, which often, but not always, make up the greatest part of the information exchanged

(2) Data conveying the "health," or status, of the satellite; i.e., temperatures and voltages. (Also called housekeeping or engineering data.)

(3) Commands sent from the Earth to the satellite

(4) Navigational information, including attitude and (rarely, for satellites) positional data. Often, navigational data will consist only of the output from solar-aspect sensors or magnetometers.

The flow of information between experiment and experimenter is far from direct and not all one-way. Interposed between the experimenter and his instrument are analog-to-digital (AD) converters, rf links, data-storage devices, data compressors, data-display equipment, and the like—all conversing among themselves by means of electrical signals as they modify and mold the raw sensor readings. The necessity for and extent of data handling support the basic contention of this chapter: Data handling is becoming a major determinant of satellite communication-subsystem design.

The satellite's communication subsystem is manifestly essential to mission success. It is, however, but one of 10 satellite subsystems and cannot be surgically excised from the system as a whole. The most sensitive interfaces are portrayed schematically in figure 5–2. Satellite subsystems also converse among themselves, usually with the communication subsystem serving as a hub. But these dialogs sometimes circulate in closed loops (feedback) and never reach Earth, especially where spacecraft-status information is involved.

What makes good communication? Low cost, high reliability, and system capaciousness, measured in bits/sec, are obviously important considerations, but only when considered in a systems context (ch. 3). This observation leads to the subject of design tradeoffs. One could, for example, increase the rate of information transfer by increasing the satellite transmitter power level. But a larger power supply means reducing the number of scientific experiments carried. The overall scientific value of the mission might be decreased rather than increased. The gist is that strict adherence to the bit-rate and transmitter-power equations (secs. 5–2 and 5–5) does not necessarily lead to the best design. The tradeoffs involve more subtle, equationless factors, such as the compatibility of the satellite communication subsystem with existing ground-based equipment.

Finally, this chapter deals only with the transmission and handling of satellite information. Equipment design is treated in chapter 9.

5–2. Information and Languages

The basic commodity of communication is information. To evaluate the performance of communication equipment, information must be quantified and made measurable. The unit of currency is the bit: represented by a 1 or a 0, a yes or no, a pulse or a no-pulse, or any other two-valued phenomenon. A bit is a digit

FIGURE 5–2.—Interface diagram showing the more important relation-
ships between the communication subsystem and the rest of the space-
craft. The dotted line shows one of the many other information links
that bypass the communication subsystem.

in the binary number system. Numbers in any system of counting
may be reduced to binary, which is based on the number 2 instead
of the usual 10. For example, the binary number 101 is a three-bit
number equivalent to 5 in the decimal system. Continuously vary-
ing analog data may also be approximated by a series of binary
numbers (fig. 5–3). The binary system of numbers is particularly
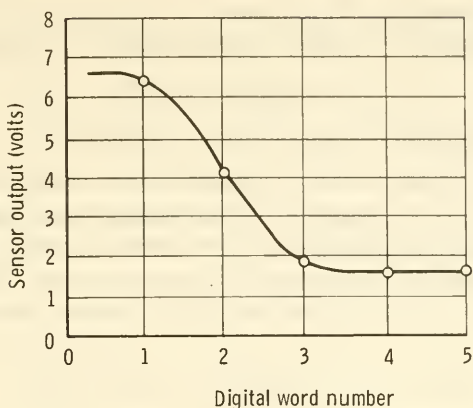
Data word no.	Decimal sensor reading	Three-bit data word	Four-bit data word
1	6.3	110	1101
2	4.1	100	1000
3	1.8	010	0100
4	1.6	010	0011
5	1.7	010	0011

FIGURE 5–3.—Analog signal represented by 3-bit and 4-bit data words. In the 3-bit word, each bit corresponds to 1 volt. When the scale is expanded, using 4-bit words, each bit then corresponds to 0.5 volt.

convenient to mechanize in terms of electronic components, mainly because nature has provided us with so many two-valued devices, such as relays and electronic switches. Much satellite communication relies on the binary language.[1] It is the *lingua franca* of machine communication.

Information is much like heat energy, in that it cannot be transferred from one place to another without being degraded to some extent. In fact, the laws describing information transfer have many of the trappings of thermodynamics. Information, for instance, possesses entropy. An important equation relates the rate

---

[1] Pulse code modulation (PCM), in particular, employs the binary system of counting. Other modulation schemes, such as pulse frequency modulation (PFM), do not necessarily use the binary language.

of information transfer, H, measured in bits/sec, to the bandwidth of the communication channel, B, measured in cycles/sec:

$$H = B \log_2 (1 + S/N) \qquad (5\text{--}1)$$

where S/N = the signal-to-noise ratio (table 5–1)

Nature introduces noise into all communications, making the comprehension of the transmitted information more difficult. The larger the signal-to-noise ratio, the more information one can receive and correctly decipher on a given channel. For threshold reception, $S/N = 1$, but in practice $S/N = 10$ or 15 for fair readability.

TABLE 5–1.—*Typical Information Rates*

[From ref. 3]

Type of message	Straight transmission (bits/sec)	With compression (bits/sec)
Color TV (commercial)_____	7×10^7	10^6
Black-and-white TV (commercial)_____	4×10^7	10^5 to 10^6
Speech_____	7×10^4	10^2
Facsimile_____	2.4×10^3	10^2
Coded English text (20 words/min)_____	10	2
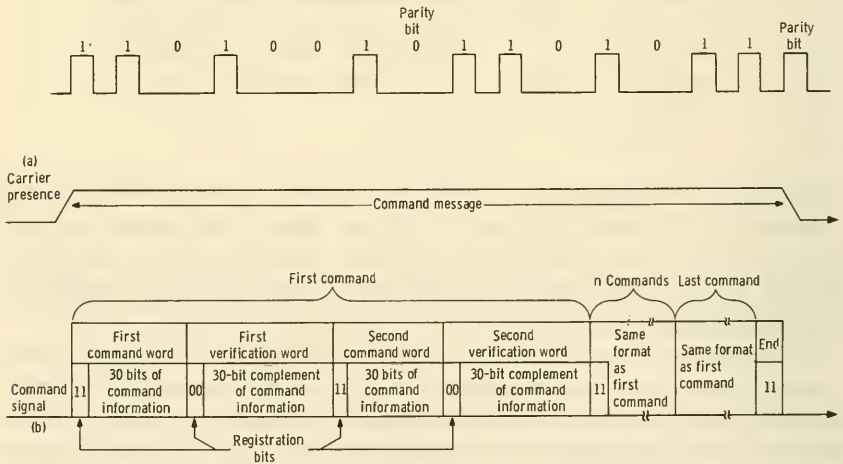
FIGURE 5–4.—Types of word structure: (*a*) two seven-bit words, 1101001 and 1101011, each followed by a parity bit; (*b*) the OAO command-message structure, showing command words and their complements (ref. 2).

Assume for the moment that all satellite conversation is translated into binary numbers represented by a string of bits (fig. 5–4(a). An ordered group of bits—representing a data point, a command, or a measurement of satellite attitude—is called a word. A data word may be of almost any length. One-bit words might represent the position of a switch. Four bits might be needed, as in figure 5–3, to represent an analog measurement to the accuracy desired. The OAO command word illustrated in figure 5–4(b) requires 32 bits. A word must be long enough to accommodate the probable dynamic range and the desired accuracy of the experiment. Word length may be variable, say, upon command from the ground, or by direction of a data-compression circuit that chops off useless leading zeros.

Three important features of digital telemetry illustrated in figure 5–4 are:

(1) The need to append an address to a command word so that the coded instruction [2] will be delivered to the proper satellite subsystem by the command decoder in the guidance-and-control subsystem

(2) The use of the complement of the command word for checking purposes. In a complement, each 1 or 0 in the command word is replaced by 0 or 1, respectively. Upon receipt of a critical command, the satellite guidance-and-control subsystem adds the command word and its complement together; if the result is not a string of 1's, the transmission has been garbled and must be retransmitted.

(3) The use of a parity bit at the end of a data word. A parity bit is 1 if there is an odd number of 1's in the data word; 0, otherwise. Incorrect parity bits indicate the loss of an odd number of bits during transmission; the loss of a single bit being the most likely occurrence.

The use of parity bits and word complements represents redundancy, an attractive, easily mechanized feature of digital operations. Redundancy occurs whenever data are repeated or its information content partially reiterated. Spoken languages always contain some redundancy. A missing word, for example, can often be inferred from context. An incorrect parity bit, like a missing spoken word, indicates an error in communication. No finite amount of redundancy can ever guarantee perfect data transmission. Fortunately, satellite instrument readings usually vary so slowly that the spurious data points are easy to spot

---

[2] Instructions may involve merely execution (switch throwing) or quantitative execution (roll 10°).

visually or by machine. The discarding and interpolation of supposedly bad data points are equivalent to correcting a message by context. Where erroneous data points are not obvious from context, error-correcting codes, such as those using parity bits, must be relied upon.

Scientific and engineering instruments on a satellite are usually scanned sequentially; that is, a magnetometer will be read, then a thermocouple, then a solar-aspect sensor, and so on, in an orderly, recurring fashion. This procedure is called commutation, or time-division multiplexing.[3] A commutator may be thought of as a rotating switch, on which each position corresponds to a telemetry channel. The resulting sequence of words is arrayed schematically in table 5–2 to illustrate a data frame. On large satellites, there may be more than one commutator, each with its own set of channels. Furthermore, subcommutators may sequentially change the data points inserted at various word positions in the frame, as indicated for OSO II in tables 5–2 and 5–3. Table 5–3, in fact, also illustrates the great variety of data points telemetered from a medium-sized satellite.

The telemetry format shown in table 5–2 is generally rigid; that is, each word has so many bits assigned to it. In this way, many zeros may be transmitted before the first significant bit is reached in each word. Such wasted space can be reduced by:

(1) Judiciously changing the word length upon command.

(2) Designing a data compressor that automatically eliminates leading zeros from the word.

Telemetry capacity may also be conserved by changing the sampling rate for experiments that are yielding data that vary slowly with time.

Data selection is different from data compression, which merely discards bits that are not significant. In automatic data selection, some judgment is exerted. Data points might be sent at a rate depending upon how fast they change in time. If, for example, magnetic-field sensors indicated a sudden change in field strength, the satellite circuits would recognize the situation and send magnetometer readings more frequently. In the inverse case, the data-transmission rate would be reduced. In automatic data selection, a degree of judgment is built into the spacecraft so that less, but more important, information is transmitted. In data com-

---

[3] Frequency-division multiplexing, where each channel is identified with a subcarrier of different frequency, is employed where there are relatively few data points to telemeter.

TABLE 5–2.—*The 32-Word OSO–II Data Frame.   The Sail and Wheel Subcommutators Sequentially Insert the Channels Listed in Table 5–3*

(1)	(2)	(3)	(4)
NRL experiment	Wheel subcommutator	Harvard experiment	Harvard experiment
(5)	(6)	(7)	(8)
NRL experiment	NRL experiment	Univ. of New Mexico experiment	Sail subcommutator
(9)	(10)	(11)	(12)
NRL experiment	NRL experiment	Harvard experiment	Harvard experiment
(13)	(14)	(15)	(16)
NRL experiment	Univ. of Minnesota experiment	Univ. of Minnesota experiment	Sail subcommutator
(17)	(18)	(19)	(20)
NRL experiment	Wheel subcommutator	Harvard experiment	Harvard experiment
(21)	(22)	(23)	(24)
NRL experiment	GSFC experiment No. 1	Univ. of New Mexico experiment	Sail subcommutator
(25)	(26)	(27)	(28)
NRL experiment	GSFC experiment No. 2	Harvard experiment	Harvard experiment
(29)	(30)	(31)	(32)
NRL experiment	Univ. of Minnesota experiment	Frame synchronization	Frame synchronization

TABLE 5-3.—*OSO-II Wheel- and Sail-Commutator Channel Assignments*

Channel	Wheel commutator	Channel	Sail commutator
1	Ames commutator	1	Elevation-position readout
2	Univ. of New Mexico Point No. 1	2	Elevation-scan monitor
3	Univ. of New Mexico Point No. 2	3	Elevation-PWM input signal
4	Univ. of New Mexico Point No. 3	4	Azimuth-PWM input signal
5	Univ. of Minnesota Point No. 1	5	Azimuth-position readout
6	Univ. of Minnesota Point No. 2	6	Azimuth-scan monitor
7	Univ. of Minnesota Point No. 3	7	Azimuth-current monitor
8	Univ. of Minnesota Point No. 4	8	Elevation-current monitor
9	Univ. of Minnesota Point No. 5	9	Elevation-position readout
10	Univ. of Minnesota Point No. 6	10	On-target signal
11	GSFC Point No. 1	11	+15 V reg. (linear amplifier)
12	GSFC Point No. 2	12	Azimuth-preamplifier monitor
13	GSFC Point No. 3	13	Azimuth-position readout
14	GSFC Point No. 4	14	+15 PWM monitor
15	GSFC Point No. 5	15	Elevation-preamplifier amplifier
16	Subcommutator 1 I.D.	16	Subcommutator 2 I.D.
17	Battery No. 3 temperature	17	Elevation-position readout
18	Battery No. 5 temperature	18	+19 volt day-pointed experiment power
19	Ames commutator	19	+19 volt (cont. sys.)/+15 volt (aux.)
20	Top-skin temperature	20	+15 volt reg. (scan circuits)
21	Bottom-skin temperature	21	Azimuth-position readout
22	Rim-skin temperature	22	Target intensity

23	Transmitter No. 1 temperature	23	Harvard voltage monitor
24	Battery No. 1 temperature	24	Power-amplifier box temperature
25	Slip-ring temperature	25	Elevation-position readout
26	Hub temperature	26	Elevation-scan monitor
27	Spin-box temperature	27	Linear-amplifier box temperature
28	+19 volt (battery)	28	Azimuth-casting temperatures
29	+19 volt day power; +19 volt night power	29	Azimuth-position readout
30	Despin and spin-backup arming monitor	30	Azimuth-scan monitor
31	Arm-release-and-lock monitor	31	Solar-cell-panel temperature
32	Transmitter select	32	Solar-cell-panel temperature
33	+15 volt reg. (spin circuits)	33	Elevation-position readout
34	+19 volt orbit power: UVS bypass open	34	Azimuth power-transistor temperature
35	Charge-rate monitor	35	Solar-cell-panel temperature
36	Spin-rate monitor	36	Solar-cell-panel temperature
37	Spin-gas pressure	37	Azimuth-position readout
38	Auto-spin in monitor	38	Sail-commutator temperature
39	Arm temperature	39	Pitch readout
40	Playback off; modulation on	40	Harvard temperature monitor
41	Spin gas-bottle temperature	41	Elevation-position readout
42	Pointed experiments on 1-year-timer bypass	42	NRL-voltage monitor
43	Magnetometer	43	P.B.U. reg. on/off
44	Encoder select	44	Pitch—man and B.U. arming
45	+15 volt reg. (aux.)	45	Azimuth-position readout
46	Tape-recorder select	46	Pitch gas pressure
47	Wheel-experiment monitor	47	Radiation and albedo-eye experiment
48	Sync. word	48	Sync. word

pression, the same amount of information is sent, but in a more compact form; that is, fewer bits. Take a string of 50 constant 8-bit data points. The same information could be sent in just two eight-bit words—a 50, plus the constant reading—leaving 48 words available for other information. In data compression and selection, the additional circuit complexity and its effect on overall reliability must be weighed against the increased amount of information received on Earth.

5–3. Data Transmission Media

Until now, conventional radio waves have been assumed to carry information from satellite to Earth, and vice versa. Radio telemetry is attractive because we have a half century of experience in implementing radio links. The radio spectrum, though, occupies only a few decades in the total electromagnetic spectrum, which stretches from radiofrequencies to gamma rays. In addition, commercial and military traffic always threatens to dispossess the scientific-research channels. The search for more bandwidth forces engineers to examine the rest of the electromagnetic spectrum and even beams of atomic particles for use as potential communication carriers. Looking is not finding, however, and radio waves are well entrenched as the basic information carrier for satellite science.

TABLE 5–4.—*Frequencies Available for Space Research* (*Mc*) [a]

10.003– 10.005	183.1 –184.1	5670–5725
19.990– 20.010	400.05– 401	8400–8500
15.762– 15.768	900 – 960	
18.030– 18.036	1427 –1429	*Gc*
30.005– 30.010	1700 –1710	15.25–15.35
39.986– 40.002	2110 –2120	31.0 –31.3
136 –137	2290 –2300	31.5 –31.8
137 –138	5250 –5255	31.8 –32.3
143.6 –143.65		34.2 –35.2

[a] Extraordinary Administrative Radio Conference, International Telecommunication Union, Geneva, 1963 (ref. 5).

Satellite communication presently employs frequencies between 10 and 10 000 megacycles, although the frequencies allotted to space research by international agreement extend up to 35.2 gigacycles (table 5–4). Frequencies lower than 10–15 Mc are reflected by the ionosphere and have to compete with terrestrial communications and severe radio noise (sec. 5–5), so that the low-frequency restrictions of table 5–4 are not significant. Besides, there is less

room for wide-bandwidth channels at low frequencies. Moving to higher frequencies, an opaque edge to the atmospheric radio window begins at the 50 gigacycles, beyond which satellite communication is difficult.

Another major communication window opens in the visible portion of the spectrum. Here, engineering interest has focused on the laser as a source of highly directional, extremely coherent electromagnetic radiation (ref. 4). A few megacycles of bandwidth are easy to find at optical frequencies of 10^{15} cycles/sec. Lasers can also generate intense, narrow beams that are suitable for tracking as well as communication.[4] Communication lasers are still in the development stage. Better modulation and detection schemes need to be perfected before the optical range is opened to satellite communication. Finally, the tremendous mass of data already flooding experimenters signifies no pressing need to expand our ability to transmit data from satellites.

Moving beyond the visible portion of the spectrum, ultraviolet radiation, X-rays, and gamma rays are strongly absorbed and distorted by the atmosphere. Directional, coherent, easily modulated radiation sources are not available at the very short wavelengths. Physical particles, such as protons and neutrons, are subject to the same criticisms, and, for the present, are ruled out for satellite communication.

In summary, widespread research-and-development efforts are opening up the optical frequencies for communication, but there seems little need for more information-carrying capacity in satellite research.

5-4.   Carrier Modulation

Once an information carrier has been selected—in all probability, a train of electromagnetic waves—some way of impressing information on it must be found. Primitive radiotelegraphy merely switched the carrier itself on and off in Morse code fashion. Later, the telemetry carrier was modulated in a more sophisticated fashion. To illustrate, the amplitude could be sequentially modulated at different frequencies, each frequency representing an output of a sensor. Frequency modulation and phase modulation quickly followed amplitude modulation (fig. 5-5). The rapidly expanding requirements of industrial and military telemetry gave birth to a host of modulation and coding schemes described by a maze of letter abbreviations. A pause to explain these abbreviations will save dozens of footnotes in this chapter.

There are three important carrier-modulation techniques: am-

---

[4] Laser signals have been reflected from Explorer XXII and detected at NASA's Wallops Island facility.

Amplitude modulation (AM)

Frequency modulation (FM)

Pulse-amplitude modulation (PAM)

Pulse-width modulation (PWM) or (PDM)

Pulse-position modulation (PPM)
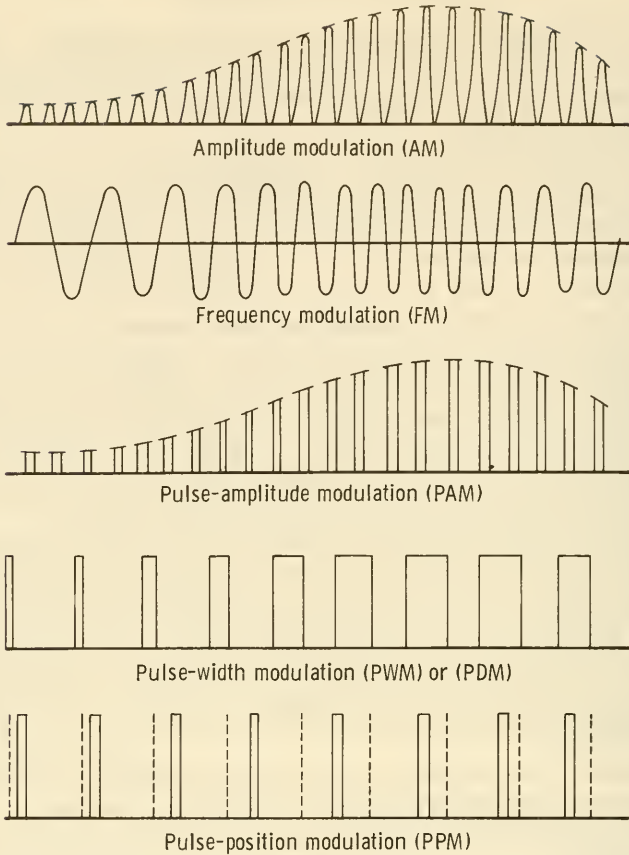
FIGURE 5–5.—Comparison of several kinds of telemetry modulation.

plitude modulation (AM), frequency modulation (FM), and phase modulation (PM). Such abbreviations are strung together like this: AM/AM, FM/AM, FM/FM, etc. The right-hand side refers to the method of carrier modulation; the left-hand side, to the modulation of subcarriers impressed upon the carrier. If only one term is used—i.e., AM or FM—it refers to the main carrier. With the advent of pulsed telemetry, the abbreviations explained in figures 5–5 and 5–6 appeared. Sometimes three abbreviations are merged. For example, PAM/FM/FM describes a telemetry system sampling AM pulses and frequency modulating the subcarriers of a frequency-modulated carrier. The conventions are summarized by the following arrangement: data encoding approach/subcarrier modulation/carrier modulation.

When no subcarriers are present, the middle term is dropped.
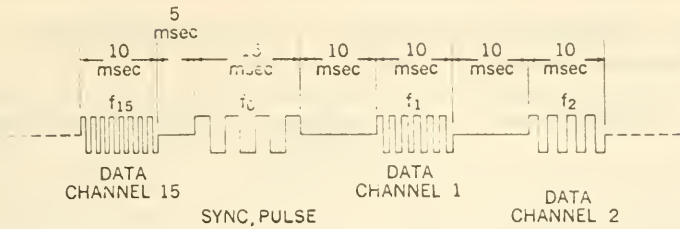
FIGURE 5-6.—Pulse-frequency modulation (PFM). The frequency of the pulses in each group carries the information (ref. 6).

When encoding methods are discussed, the left-hand abbreviations, such as PCM, are used alone.[5] To make matters worse, the conventions are not always followed.

Many telemetry schemes have been tried in space telemetry, but the most popular have been FM/FM, PFM, and PCM/FM. The first Explorer adopted FM/PM and FM/AM telemetry. Pulse-code modulation (PCM) appeared as early as 1959 on Explorer VI. The term "Telebit" was applied to the uncoded, binary PCM telemetry on Explorer VI. PCM techniques are rapidly gaining dominance, particularly on large satellites, a fact implying that figures of merit must exist for the intercomparison of the various modulation techniques.

Quantitative comparison of telemetry codes usually involves power, bandwidth, and information efficiency. Table 5-5 shows that the three PCM schemes all appear to—

(1) Use relatively little power. A valuable property on a power-limited satellite

(2) Use relatively little bandwidth, which is desirable when the spectrum is crowded

(3) Have relatively good information efficiencies

True, PCM is not the absolute best in any category, but it is a good compromise. Theoretical studies also show the PCM telemetry transmits information with less chance of error under conditions found in satellite telemetry. In other words, PCM provides good signal-to-noise ratios.

Beyond all these numerical measures of performance is a fact emphasized earlier: Only digital computers can effectively cope with the flood of satellite data. PCM is more nearly compatible with computers than other common modulation schemes. Other factors favoring PCM are:

[5] The Inter-Range Instrumentation Group (IRIG) sets the telemetry standards for space-research work in the United States.

TABLE 5–5.—*Comparison of Telemetry Systems*

Telemetry scheme	Rf power required [a] (relative to PPM/AM) [b]	Information efficiency [c]	Rf bandwidth (kc) [d]
PPM/AM	1	0.17	76
PCM/FM	1.7	.24	18
PCM/PM	2	.21	20
PCM/AM	3.4	.21	18
PAM/FM	8.3	.050	85
AM/FM	9.3	.045	93
PDM/FM [e]	9.3	.045	92
PDM/PM	11	.036	110
FM/FM	14	.030	140
AM/PM	15	.028	150
PAM/PM	15	.028	150
PDM/AM	16	.035	94
FM/AM	17	.055	50
FM/PM	18	.023	185
PAM/AM	250	.073	18
AM/AM	2300	.24	9.4

[a] Based on a signal-to-noise power ratio at threshold of 100 and a total information bandwidth of 1000 cycles/sec (ref. 7).

[b] Pulse-position modulation.

[c] A measure of the system's capability to transmit information at a given power level.

[d] For a given power level and signal-to-noise power ratio.

[e] Pulse-duration modulation.

(1) PCM circuitry can draw upon the computer industry's advances in miniaturization, redundancy techniques, and improvements in component reliability

(2) PCM telemetry can incorporate the parity and word-complement checks described earlier

(3) All kinds of information—data, commands, etc.—can be easily encoded

(4) PCM possesses unlimited accuracy; that is, words can be made any length, using as many significant bits as desired. In contrast, analog information is limited, with an accuracy of about one part in a thousand.

The case for PCM is very convincing, but there will always be special applications that can justify the selection of a different type of telemetry. PCM is complex. PCM equipment possesses significantly more components when compared with other kinds of modulation equipment. Status telemetry for the smaller launch vehicles, for example, finds FM/FM and other types of modulation

simpler and perfectly adequate. PFM is very common on Explorer-class satellites. In the case of space research, however, the standardization of data-reduction equipment and archiving systems accelerates the trend to digital codes.

5-5.   Constraints and Tradeoffs in Satellite Communication

Information, like electrical power, penetrates every nook and cranny of the scientific-satellite system, including those portions that remain behind on Earth. Major communication parameters—for instance, carrier frequency, word format, or reliability—cannot be selected without affecting other parts of the system. To prepare a foundation for chapter 9, the satellite "hardware" chapter, some important communication constraints and tradeoffs will now be explored.

The Choice of Carrier Frequency.—In section 5–3, the narrow electromagnetic windows in the atmosphere, radio noise, and the crammed radio spectrum were mentioned as constraints affecting the choice of the carrier frequency in satellite telemetry. The major factors involved are listed in table 5–6.

TABLE 5–6.—*Factors Affecting the Choice of Carrier Frequency* [a]

Factor	Troublesome frequency region	Table or figure reference
Atmospheric noise	<50 Mc	Figure 5–7.
Manmade noise	<1 Gc	None.
Cosmic noise	<4 Gc	Figure 5–7.
Terrestrial noise	<10 Gc	Figure 5–7.
Oxygen and water-vapor noise	>10 Gc	Figure 5–7.
Solar noise	<30 Gc	Figure 5–7.
Electron attenuation	<1 Gc	Figure 5–8.
Condensed water-vapor attenuation	>3 Gc	Figure 5–8.
Oxygen and water-vapor attenuation	>10 Gc	Figure 5–8.
Ionospheric refraction	<1 Gc	Figure 5–9.
Tropospheric refraction	<30 Gc	Figure 5–9.
Faraday rotation	<10 Gc	Figure 5–10.
Scintillation	<1 Gc	None.
International agreements	(table 5–4)	Table 5–4.
State of the art	<10 kc, >100 Gc	None.

[a] Adapted from ref. 8, used by permission of McGraw-Hill Book Co.

No regions of the electromagnetic spectrum are free and clear of impediments to satellite communication. Noise and attenuation can always be overcome by pumping more power into the satellite transmitter, but this obviously incurs a weight penalty. Atmospheric signal-path distortions imply tracking-antenna corrections.
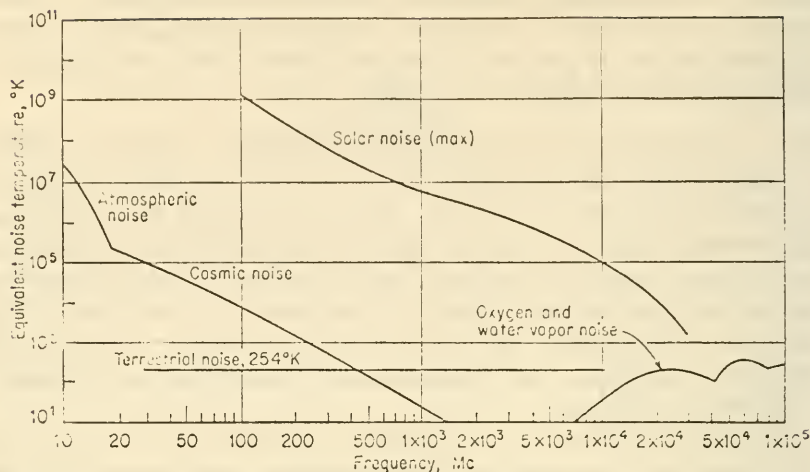
FIGURE 5–7.—Composite external-noise profile (ref. 8. Used by permission of McGraw-Hill Book Co.).

State of the art—a very real constraint—can be advanced with the application of money.

Taking noise first: noise is received from every object seen by the ground station's antenna pattern. Most of the noise plaguing satellite communication originates in the random motion of electrons in the noise source. It is not surprising to find the hot Sun a major noise producer (fig. 5–7). Happily, the Sun and the satellite will not be in the antenna pattern at the same time very often. Other, but much weaker, celestial-noise sources dot the sky, especially along the Milky Way. Communication will be degraded when these sources are intercepted by the antenna. Even the Earth generates noise. At low elevation angles, antennas pick up this low-temperature radiation.

Noise is conveniently described by assigning an effective blackbody temperature to the objects intercepted by the receiving antenna. The noise intensity is given as a function of frequency by the Stefan-Boltzmann law. The Earth's radio-noise spectrum peaks at about 254° K, while the Sun's corona has a radio temperature of millions of degrees. The composite external-noise profile, which excludes the Sun, shows a relatively transparent electromagnetic window between 1 and 10 gigacycles (fig. 5–7).

Electromagnetic waves are attenuated when carrier energy is extracted from them by molecules that are resonant near the carrier frequency. Attenuation is a function of the total mass of the atmosphere along the transmission path. Figure 5–8 illustrates
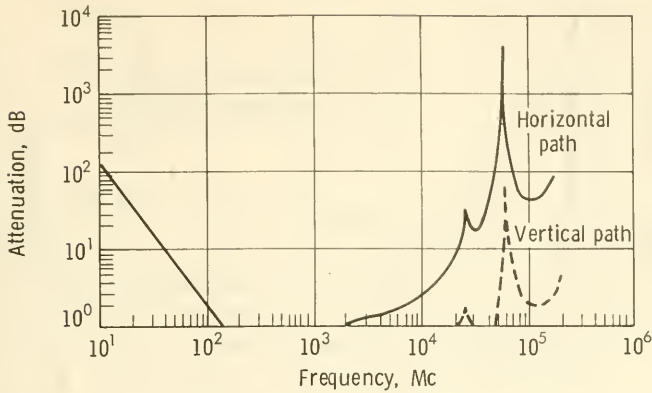
FIGURE 5–8.—Composite atmospheric attenuation profile for temperate-zone ground stations, with no precipitation (ref. 8; used by permission of the McGraw-Hill Book Co.).

the differences in attenuation for short vertical and long horizontal paths. High, arid spots make good telemetry-receiving stations, because there is less atmosphere above them and the air contains less water vapor. Electromagnetic waves are also attenuated when they cause ionosphere electrons to oscillate. The resonant, or "plasma," frequencies lie between 5 and 15 Mc. Ionospheric attenuation depends upon the total electron population along the transmission path, a property dependent upon solar activity. Attenuation leaves an open communications window between 100 megacycles and 10 gigacycles (fig. 5–8).

When Earth-based receiving antennas search for a satellite, they must adjust their aim for the refractive effects of the troposphere and ionosphere. The antennas see a slightly distorted view of the heavens, worst near the horizon, and much like the picture a fish sees of dry land. Tropospheric refraction depends upon the mass and composition of the air between the satellite and observing antenna, especially the concentration of water vapor. Refraction, like attenuation, depends upon elevation angle (fig. 5–9). Snell's law is operative here, for tropospheric refraction of radio waves is identical to the optical refraction. Below 30 Gc, tropospheric refraction is fairly constant and antenna compensation is easy.

In the ionosphere, radio waves travel faster as electron density increases. Refraction follows. Indeed, at low frequencies (5–15 megacycles), refraction turns into reflection and the ionosphere appears opaque. Since the ionospheric electron density is pro-
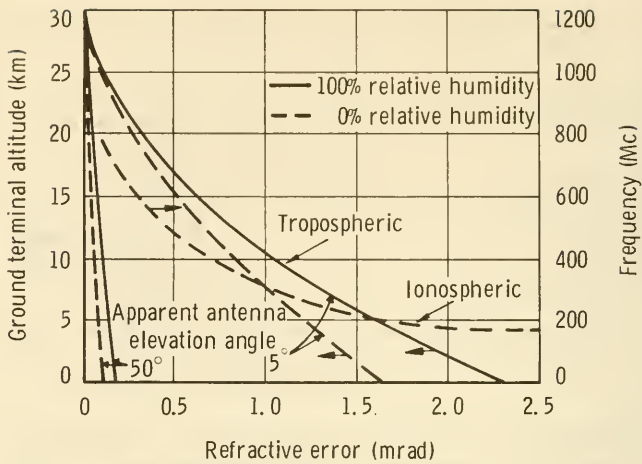
FIGURE 5–9.—Tropospheric and ionospheric refraction. Ionospheric refraction is frequency-dependent. Tropospheric refraction is fairly constant below 30 gigacycles (ref. 8; used by permission of the McGraw-Hill Book Co.).

foundly affected by solar activity, refraction there depends upon the time of day, the time position in the 11-year solar cycle, and solar storm activity. Again, the lower the elevation angle, the greater the amount of refraction. Unlike tropospheric refraction, ionospheric refraction is strongly frequency dependent at radio wavelengths (fig. 5–9). At satellite-telemetry frequencies, ionospheric refraction is only a minor problem in tracking and communication.

Two other phenomena occur as a radio wave passes through the Earth's ionosphere. First, the wave's plane of polarization is rotated as it interacts with the free electrons and magnetic field. Michael Faraday discovered a similar effect in certain crystals; so,. the analogous ionospheric phenomenon has been named the "Faraday effect." The amount of rotation varies as the inverse square of the carrier frequency and also depends upon the total electron content of the transmission path (fig. 5–10). Circularly polarized receiving antennas are deployed to reduce decoupling between transmitter and receiver. The Faraday effect is also a valuable scientific tool in determining the electron content of the ionosphere. Another ionospheric effect depends upon the fact that the propagation velocity of radio waves varies inversely with the frequency. The lower frequency waves move slightly ahead of the higher frequency waves, resulting in phase dispersion. In other
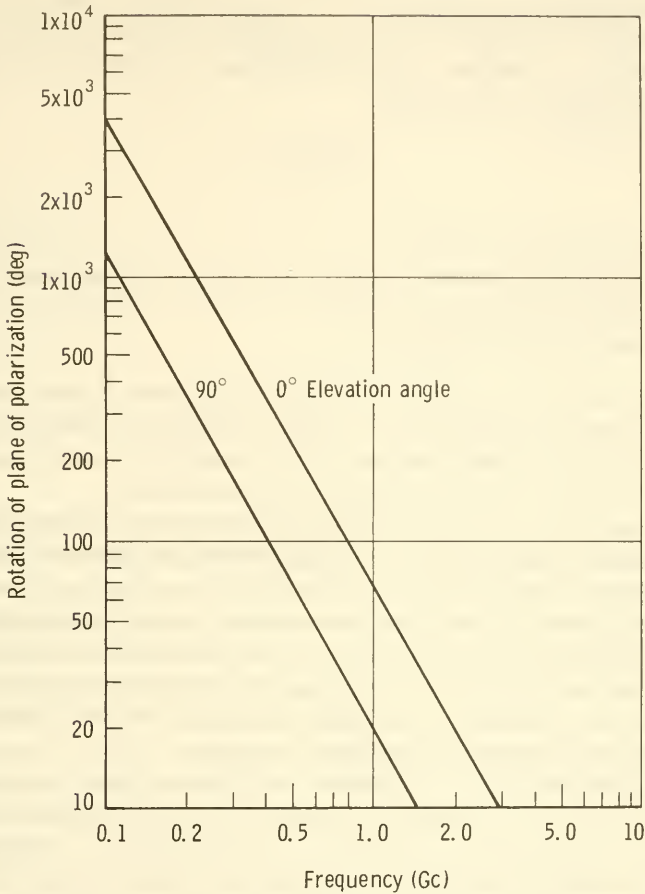
FIGURE 5–10.—Faraday effect as a function of frequency. This effect is discussed in chapter 11, relative to its value in measuring integrated electron density (ref. 8; used by permission of the McGraw-Hill Book Co.).

words, all portions of a frequency-modulated wave are not in phase. The amount of dispersion is inversely proportional to the square of the frequency, another point supporting the case of high-frequency carriers.

Scintillations, or fluctuations, of satellite signals are caused by irregularities in the atmosphere. The effect is most pronounced below 1 gigacycle. Like the Faraday effect, scintillations help diagnose atmospheric structure and constitution.

Another factor influencing carrier frequency, though it has

little bearing upon frequency selection, is the Doppler effect. The frequencies of satellite signals apparently increase and decrease as the satellite approaches and recedes from the ground station. The frequency shift is given by:

$$\Delta f = \frac{\dot{\rho} f_t}{c} \qquad (5\text{-}2)$$

where

Δf = the frequency shift
$\dot{\rho}$ = the radial satellite velocity relative to the station
f_t = the transmitter frequency
c = the velocity of light

Because satellite velocities are small compared to the velocity of light, frequency shifts are less than 1 part in 10 000. Ground-based receivers must increase their bandwidths over that of the signal to insure complete reception at all times.

The subject of signal fading concludes the list of important transmission phenomena. Satellite signals pulsate as the satellite rolls, pitches, and tumbles. No satellite transmitting antennas are perfectly isotropic, and, as the antenna pattern sweeps over the Earth, signals will pulsate at the spin frequency or some multiple of it. As the satellite moves along its elliptical path, there is also a longer term, fading effect superimposed on the pulsations as the transmitter distance to the Earth changes.

Summarizing, all transmission phenomena would indicate that the best transmitter frequencies are those between 1 and 10 gigacycles. The historical record (see appendix) indicates that scientific-satellite carrier frequencies have fallen below this "optimum" range, although they have moved upward steadily. Deep-space probes, such as Mariner IV, which have had to solve much more challenging transmission problems, have pioneered space communication above 1 gigacycle (2.3 gigacycles for Mariner IV). Satellites have not found it essential to go to these higher frequencies.

The Calculation of Transmitter Power Level.—Once the modulation scheme and carrier frequency have been chosen, the designer can calculate the transmitter power needed to overcome distance, signal attenuation, and noise. Success is achieved if a signal-to-noise ratio of 10 (preferably 15) is calculated at the receiver for the assigned power-input level. A simplified derivation follows:

The signal power, P_r (measured in dB) received at the receiver is:

$$P_r = P_t + G_t + G_r - L_p - L_x \qquad (5\text{-}3)$$

TABLE 5–7.—*Power Gains of Several Common Antennas* [a]

[From ref. 1]

Antenna type	Gain over an isotropic antenna
Isotropic	1
Infinitesimal dipole or loop	1.5
Half-wave dipole	1.64
Parabola of geometric area A	6.3 to 7.5 A/λ^2
Broadside array of area A	$4\pi A/\lambda^2$
Turnstile	1.15

[a] See ch. 9 for antenna-design discussion.

where

P_t = the transmitter power (dB)

G_t = the gain of the transmitting antenna relative to an isotropic antenna (dB) (table 5–7)

G_r = the gain of the receiving antenna relative to an isotropic antenna (dB)

L_p = the signal attenuation due to distance = $\log (4\pi\rho/\lambda)^2 = 32.5 + 20 \log f + 20 \log \rho$ (km) (dB)

L_x = signal losses due to atmospheric attenuation and other causes (dB)

f = frequency (cycles/sec).

The noise power, P_n, is found from

$$P_n = 204 + 10 \log B + 10 \log T_e \text{ (dB)}$$

where T_e = the effective temperature of all noise sources seen by the antenna.

One can then write:

$$P_r - P_n = 10 \log S/N = P_t + G_t + G_r$$
$$-L_p - L_x - 204 - 10 \log B - 10 \log T_e \quad (5\text{–}4)$$

where S/N = the signal-to-noise ratio, which should be >10.

Unlimited power is not available on scientific satellites, so that P_t will have a fixed upper limit. L_p, L_x, G_r, and T_e are under only partial control by the designer; i.e., through the choice of frequency, antenna, etc. (table 5–8). The bandwidth, B, cannot be reduced in order to improve S/N without also decreasing the bit rate (eq. 5–1).

TABLE 5-8.—*Typical Telemetry System Performance* [a]

[From ref. 1]

	Explorer I	OGO I	Pioneer V
Transmitter power, watts	0.01	5	5
Transmitter-antenna gain	1.64	16	1.15
Receiver-antenna gain	50	10 000	200 000
Wavelength, m	2.78	0.75	0.31
Distance of spacecraft, km	4800	96 000	32 000 000
Bandwidth, cycles	20	200 000	10
Signal-to-noise ratio	3	15	3

[a] Design values shown for OGO I.

Reliability Goals.—A satellite is all but useless to science if its communication subsystem fails. Furthermore, the communication subsystem boasts a large fraction of the total number of fallible parts in the satellite. Once a lifetime has been selected for a mission—say, 6 months—reliability and test engineers must analyze the circuits, choose and test parts, and decide where redundancy would be helpful to meet the reliability goals. Of course, the ground stations must also be included in the total reliability picture, since they are just as essential to successful communication. Reliability is covered more thoroughly in chapter 9, but it is so obvious a design constraint that it had to be mentioned.

Timing Satellite Transmissions.—The NASA Satellite Tracking and Data Acquisition Network (STADAN, sec. 7–5) is impressive, but the stations are widely scattered. Satellites, therefore, are commanded from Earth to transmit their store of information when over an appropriate receiving station. "Data dumping" and "burst transmission" are terms applied to these commanded transmissions. Satellites sometimes transmit continuously at low power in real time while they store simultaneously the same data for later burst transmissions. Scientists in other countries can then monitor the signals. Satellite beacons also transmit steadily so that scintillations and the Faraday effect can be studied.

Other Constraints.—The constraint of data-format compatibility has already been belabored. Another limitation is the cost of the ground-based facilities, in the sense that established frequencies, data formats, and site locations present inertia to change. Money limitations also affect the degree of attainable reliability, since more money can buy higher quality parts and accelerate the state of the art.

Some noteworthy interfaces with other satellite subsystems deserve comment. There is a pointing, or spatial, interface between the attitude-control and communication subsystems. Most satellites do not radiate isotropically. Communication can be greatly improved by pointing a directional antenna at the receiving station. This has to be done by deep-space probes. It is also a feature of some of the larger, more completely stabilized satellites, where dozens of experiments collect awesome quantities of data for concentrated burst transmissions.

5-6.   Data Handling

The data deluge, information flood, or whatever you choose to call it, is hard to measure in common terms. An Observatory-class satellite may spew out more than 10^{11} data words during its lifetime, the equivalent of several hundred thousand books. Data-rate projections, summed for all scientific satellites, prophesy hundreds of millions of words per day descending on Earth-based data-processing centers. These data must be translated to a common language, or at least a language widely understood by computers (viz, PCM), then edited, cataloged, indexed, archived, and made available to the scientific community upon demand. Obviously, the vaunted information explosion is not only confined to technical reports alone, but also to the data from which they are written. In fact, the quantity of raw data generally exceeds the length of the resulting paper by many orders of magnitude.

A short glossary at this point will indicate the things that are, or might be, done to the data received from satellites.

Data handling.—A general term, including all of the functions listed below

Data processing.—Another general term

Data reduction.—Translation of data into graphs, tables, or some more usable (and usually more compact) form

Data smoothing.—Reduction of data variability by running averages, or some other mathematical technique

Data compression.—Reduction of the total number of data bits; most commonly by logarithmic amplifiers, sampling, or interpolation (ref. 9)

Data selection.—Choice of the most significant pieces of data with an eye to reducing the total amount of data

Data editing.—Removal or correction of erroneous data points. Sometimes includes the adding of time, position, and attitude information
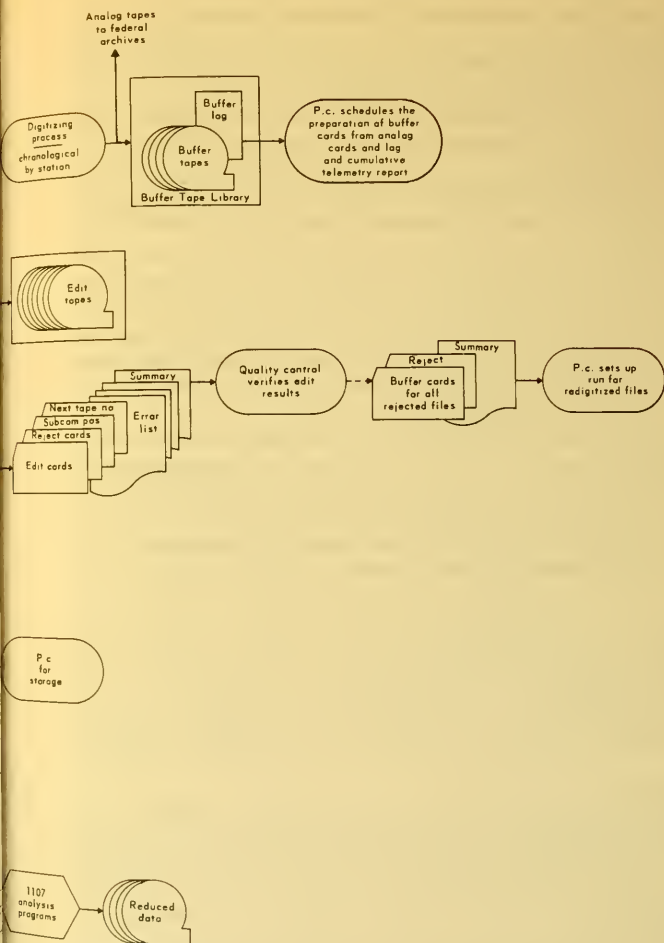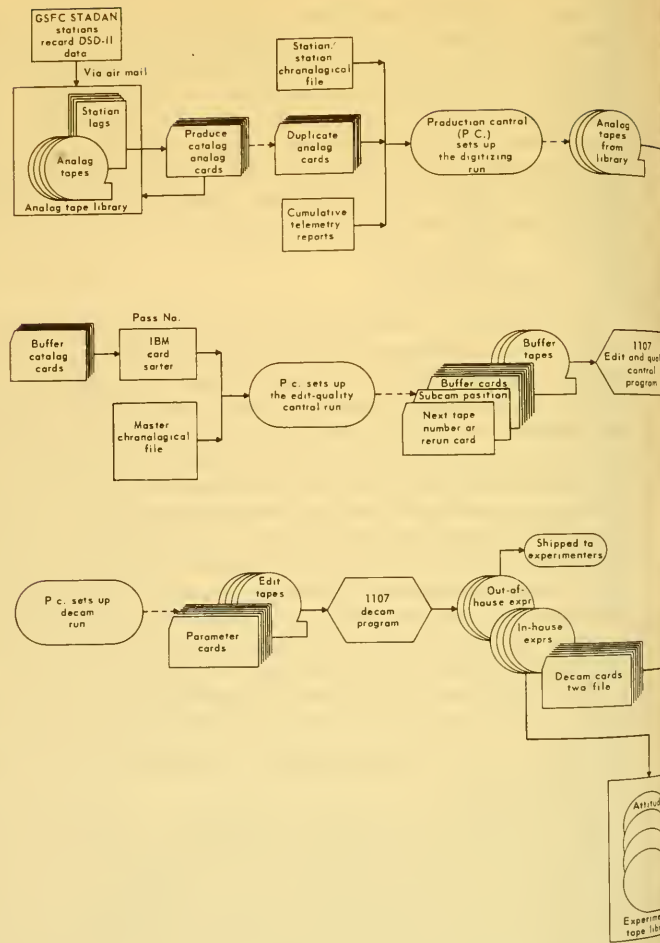
FIGURE 5–11.—The OSO data-processing flow chart.

Data cataloging.—Assignment of identifying information to data
   records
Data indexing.—Assignment of descriptors to data that will per-
   mit easy access and retrieval by users
Data archiving.—Permanent storage of data in retrievable form
Data formating.—Changing the word structure or the form of
   the data record
Data translation.—Changing one form of data into another,
   especially one type of telemetry into a form acceptable to
   computers

The intent of this section is to follow the flow of information
from NASA satellites from its points of reception (STADAN
stations) to the processing points, the experimenter, and the
archives. Figure 5–1 showed a very general view of this flow.
More details are presented in figure 5–11, where the flow of
OSO-II data is shown schematically.

Dangers Inherent in Mechanized Data Handling.—Some satellite
experimenters complain about the difficulty of experimenting with
instruments hundreds of kilometers away in orbit. Mechanized
data processing stimulates more displeasure, because raw data
may be judged by machines or persons possibly unaware of the
character and purpose of the experiment. Isolated data points
that are out of line may, for example, be cast out of the record,
when in reality they represent a physically real event of great
significance to a trained observer. Data editing, selection, and
smoothing are the procedures most likely to lead to the discarding
of valuable information. Data cataloging and indexing, if under-
taken without insight and experience, can bury data so deeply in
archives that they might as well have been discarded in the first
place.

Mechanization of data handling is a necessity in space science,
regardless of its dangers. The experimenter's only sure defense
is to intercept the raw data themselves—if the system even permits
that. A better approach for the experimenter is to insure that the
people and machines on the data-processing line truly understand
his experiment.

Forms of Data.—Despite trends toward PCM encoding, much
satellite data still need to be translated into digital form, if it is to
be consumed by a computer. Raw satellite data, however, consist
only of the carrier signals recorded—usually on magnetic tape—at
the receiving station. This signal must be decommutated, linear-
ized, "cleaned up," and otherwise changed into a usable form.
Even if the data are already digitized in a PCM format, they may

not be digestible by a computer because the word format and pulse widths are not correct.· Data handling necessitates a lot of ''bit fiddling'' just to prepare the data for editing and cataloging. Ultimately, all satellite data will probably end up in standard digital form.

The Data-Processing Line.—The best way to describe what happens to data from the time they are received and packaged for the experimenter is to describe a typical NASA data-processing line. OSO II, a satellite of moderate complexity, is selected here. The frame format is shown in table 5–2 and the processing line itself in figure 5–11.[6] The discussion follows the arrangement of the processing line.

Analog-Tape Recording.—Standard magnetic analog tape, 1.27 centimeters wide, was used to record satellite signals directly. Seven tracks on the tape recorded the following information:

(1) dc and a 14 400-cycle/sec clock signal

(2) Reference signals from Minitrack time-standard-control track generator

(3) Satellite PCM data from the station's signal conditioner

(4) Ten-kilocycle Minitrack reference frequency

(5) Satellite PCM data from the station's diversity combiner

(6) Serial decimal time from Minitrack time standard

(7) WWV [7] signal, audio command, or code

STADAN stations were instructed to record 2 minutes of low-speed OSO-II data before sending a fast-speed playback command to the satellite. Two satellite passes, each consisting of about 5 minutes of playback, were recorded on each analog reel. Tapes were then airmailed to the Analog Tape Library at Goddard Space Flight Center.

Data taken from the first 20 satellite passes over the Fort Meyers, Fla., STADAN station were processed as soon as received and made available to the experimenters immediately. This constitutes the experimenter's opportunity for a ''quick look'' at the data.

Analog-Tape Processing.—Buffer tapes were made at Goddard by running the data from the analog tape, which were still in the form of recorded PCM telemetry signals, through an analog-to-digital converter. The processed analog tapes were ultimately

---

[6] The data-handling functions shown in fig. 5–11 are performed by the NASA STARS (Satellite Telemetry Automatic Reduction System). (See refs. 10, 11.)

[7] The call letters for a radio station operated by the National Bureau of Standards in Washington, D.C.

sent to NASA's Space Data Center or some other storage facility. Buffer tapes have a special format, consisting of frames which contain the ground-station time, the still-commutated digital satellite data, synchronization words, and special inserted "flag" words to be used in later computer processing. A Buffer Tape Library accumulates all NASA tapes.

Buffer-Tape Processing.—An edit tape is prepared by running the buffer-tape information through a computer. The computer calculates universal time (UT) from the WWV signal and inserts it in the record. Next, the computer checks each synchronization word for bit errors. If bit errors occur, the data word in question is flagged as possibly erroneous. The edit tape is then written.

Edit-Tape Processing.—The edit tapes are now run through a computer to generate the experimenter tapes. Data points from the individual experiments are then separated out by decommutation. Separate tapes, each appropriately labeled with receiving-station and time identifications, are written for each experimenter. Except for the "quick-look" data mentioned above, regularly processed data are not available to the experimenter until about 1 month after they are recorded at the STADAN station.

Experimenter-Tape Processing.—For those OSO-II experimenters at Goddard Space Flight Center, additional tapes were prepared by a computer data-reduction program that displays the data in formats that are more convenient for study and analysis. Attitude tapes, describing the satellite's orientation in space, were also made available at this stage. Experimenters not at Goddard used their own computers and data-processing equipment according to their individual needs and tastes.

Comments on OSO-II Processing.—The procedures described above are fairly typical of today's data processing. The only things done to a non-NASA experimenter's data are analog-to-digital conversion and the flagging of out-of-sync words. No judgment function is performed. Experimenters receiving their tapes obviously need some sort of computer equipment to prepare printed, or perhaps automatically graphed, data.

Complex as the OSO-II data-processing line may appear, it still stops short of full automation, in which data would be judged, selected, and reduced by computer. The systematic handling of data and the careful accounting and labeling at each step are absolute necessities. OSO II is only one active satellite out of the many whose data (several analog tapes each) are shipped to Goddard daily. By multiplying the activities of the OSO-II production line by 10 to perhaps 100 times, the full scope and complexity of data processing from scientific satellites can be appreciated.

References

1. Ludwig, G. H.: Spacecraft Information Systems. NASA TN D–1348, 1962. (Also in Cosmic Rays, Solar Particles, and Space Research, B. Peters, ed., Academic Press, 1963.)
2. Lewis, T. B.: Primary Processor and Data Storage Equipment for the Orbiting Astronomical Observatory. IEEE Trans., EC–12, Dec. 1963, p. 677.
3. Pierce, J. R.; and Cutler, C. C.: Interplanetary Communications, Advances in Space Science. Vol. 1, 1959, p. 55.
4. Potter, P. D.; Stevens, R.; and Wells, W. H.: Radio and Optical Space Communications. NASA CR–50062, 1962.
5. Smith-Rose, R. L.: Allocation of Radio Frequencies for Space Science. COSPAR Info. Bull., no. 22, Feb. 1965.
6. Rochelle, R. W.: Pulse Frequency Modulation. NASA TN D–1421, 1962. (Also see NASA TR R–189, 1964.)
7. Nichols, M. H.; and Rauch, L. L.: Radio Telemetry. John Wiley & Sons, Inc., 1965.
8. Krassner, G. N.; and Michaels, J. V.: Introduction to Space Communications Systems. McGraw-Hill Book Co., Inc., 1964.
9. Hogg, G.: A Data Compression Primer. NASA TM X–55323, 1965.
10. Creveling, C. J.; Ferris, A. G.; and Stout, C. M.: Automatic Data Processing. IRE Trans., SET–8, June 1962, p. 124.
11. Habib, E. J.; Keipert, F. A.; and Lee, R. C.: Telemetry Processing for NASA Scientific Satellites. ISA Preprint 7.2–2–65, 1965. (Also issued as NASA TN D–3411, 1966.)

Chapter 6

SATELLITE NAVIGATION, GUIDANCE, AND CONTROL

6-1. Prolog

Satellite-control technology encompasses a wide spacecraft spectrum ranging from passive, unstabilized satellites, at one end, to complex, pointable orbiting observatories, at the other. In a sense, one can "drive" a large satellite, much as one drives an automobile, but using ground-communicated and internally stored commands instead of a steering wheel. Experiments can be switched on and off, data transmission rates changed, and new experimental targets acquired. Control circuits permeate every satellite subsystem, providing a flexibility that can adapt the satellite to the ever-changing environment, unexpected experimental opportunities, and equipment failures. The versatility and flexibility of the large satellites is purchased at a price paid in complexity. Small, less-flexible satellites succeed in narrow application niches by virtue of their greater simplicity and reliability.

Satellite-control functions fall into three broad classes:

(1) Orbit control, which is subdivided into injection control, orbit maintenance (station keeping) and modification, and re-entry control

(2) Attitude control including initial stabilization, initiation of search modes, and target acquisition and locking

(3) Status control, or the control of the operational mode of the satellite. Included here are housekeeping functions, stored commands that extend solar-cell paddles, antennas, and experiments.

The word "control" describes a chain of events that begins with the measurement of some performance attribute—for example,
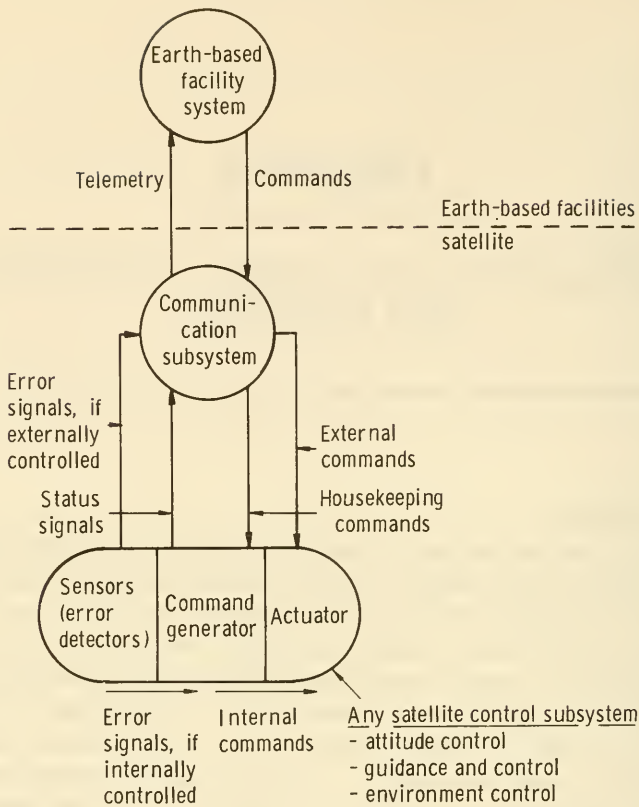
FIGURE 6–1.—Generalized block diagram of a satellite guidance-and-control subsystem. Internal and external control approaches are illustrated.

satellite attitude or battery voltage (fig. 6–1). This measurement is compared to the desired value of the parameter, which is specified by stored or communicated references. Any disparity above or below present limits causes control circuitry to direct a corrective command to the appropriate subsystem actuator. In closed-loop, or feedback, control, error signals are fed back until the performance deviation has been corrected. In open-loop control, commands are executed but there is no feedback; e.g., extension of the satellite solar-cell panels.

Specialized terms have evolved, particularly in orbit control. Table 6–1 defines these terms and establishes semantic boundaries between the three different control areas delineated above.

TABLE 6–1.—*Satellite-Control Terminology* [a]

Control function	Control areas		
	Orbit control	Attitude control	Status control
Error detection (need for change).	Navigation information is provided by ground-tracking and/or onboard inertial and optical equipment (sec. 6–2).	Attitude information is provided by inertial, magnetic, and/or optical equipment in the attitude-control subsystem.	Error data provided by a variety of sensors (voltmeters, etc). Control signals also generated by timers, stored programs, and ground-based operators (sec. 9-9).
Generation of corrective command.	Guidance signals are generated by the guidance-and-control subsystem.	Attitude-correcting signals generated by the attitude-control subsystem (sec. 6–5).	Corrective signals generated by the guidance-and-control subsystem, ground-originated commands, or stored commands.
Actuation (command execution).	The *actuator* is the onboard propulsion subsystem for orbit and reentry control.	Gyros, gas jets, inertia wheels, gravity-gradient-devices, etc., in the attitude-control subsystem make the necessary attitude changes.	Actuators, such as switches, exist in all subsystems.

[a] See table 3–1, for definitions of satellite-subsystem functions.

From table 6–1, it appears that the signals to the actuators—the commands—may originate from several points:

(1) From an operator on the ground who determines the need for a command from telemetry signals or a schedule of events. Most such commands fall in the open-loop category.

(2) From programs or instructions stored in the satellite memory (timers, bimetallic switches, tapes, computer memories). These are also usually open loop in character.

(3) From the onboard guidance-and-control, attitude-control, and environment-control subsystems that autonomously issue commands consistent with the need; i.e., closed-loop controls.

There are also many self-regulating, closed-loop control circuits in spacecraft; viz, thermostats and voltage regulators.

With control circuits embedded in every subsystem, a clear-cut guidance-and-control subsystem is hard to extricate for study. In addition, the attitude-control and environment-control subsystems carry out specialized control functions that by custom are kept separate. The guidance-and-control subsystem is defined by exception; that is, it performs those control functions not assigned to the attitude-control and environment-control subsystems. To elucidate further the relationships between the three control subsystems, the interface diagram (fig. 6–2), delineates the flow of error and command information between subsystems. Of course, many subsystems possess closed loops that do not show up on this limited picture; power-supply voltage regulators, for example.

The sections that follow deal, first, with navigation (orbit measurement), then orbit control, attitude control, and satellite-status control. All but the last area are well represented in the literature of space technology as confirmed in the bibliography.

6–2.   Satellite Tracking

When satellite navigational information is obtained from Earth-based equipment alone, with limited assistance from satellite beacons and transponders, the process is termed "tracking." Tracking is distinct from navigation employing the onboard, self-contained equipment covered in the next section.

Satellites, their launch vehicles, and reentry capsules are tracked during ascent, while in orbit, and during reentry. Here, emphasis is on orbit tracking, which produces information for the following purposes:

(1) Orbit definition, resulting in orbital elements and ephemerides

(2) Orbit perturbation analysis and the inference of environmental forces important to science

(3) The timing of deorbit thrust for reentry

(4) The guidance of the satellite during orbital maneuvering and station keeping

(5) Satellite identification and accounting by military surveillance systems that must detect hostile objects in space

What orbit parameters of a high, fast-moving, often invisible satellite can be conveniently and accurately measured from the ground? Tracking systems can be divided into three classes according to what they are tracking: (1) naturally illuminated satellites, (2) beacon-carrying satellites, and (3) artificially illumi-
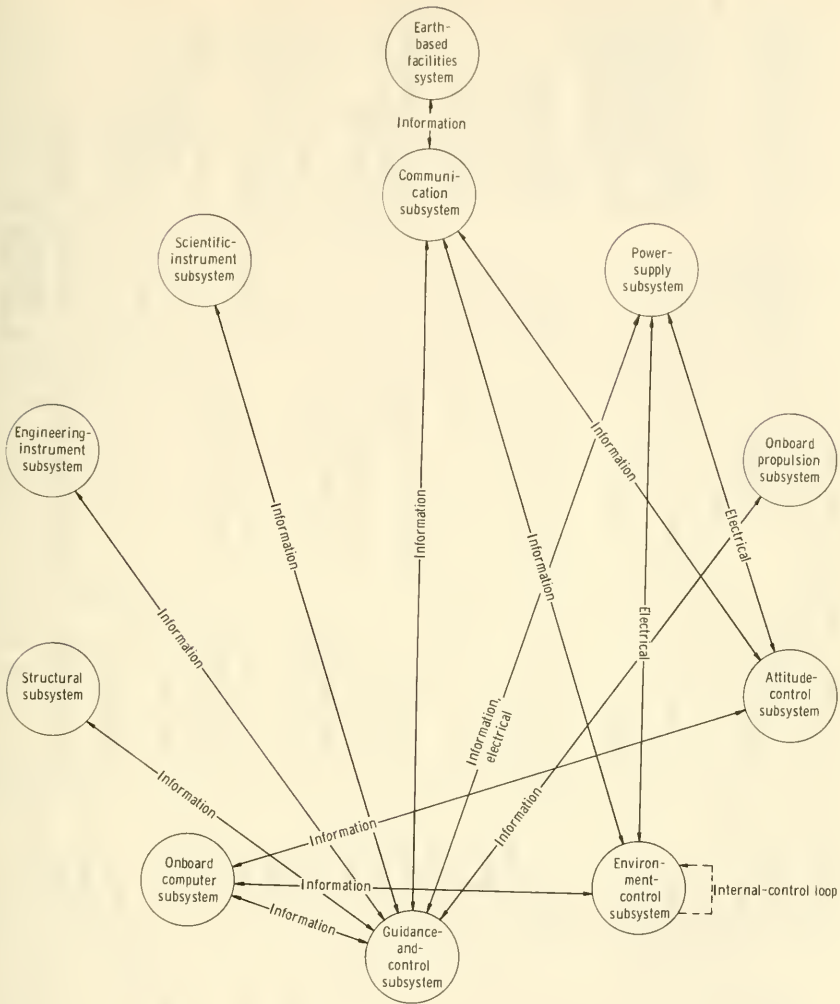
FIGURE 6–2.—Interface diagram showing the more important relationships between the three satellite-control subsystems and the remainder of the spacecraft. The information interface includes the transmission and reception of error and navigational information as well as commands.

nated or radio-triggered satellites (table 6–2). In all three cases, the satellite first has to be visible in some part of the electromagnetic spectrum to ground-based instruments. Reflected sunlight and self-contained optical and electromagnetic beacons make the satellite visible to cameras, the human eye, and radio antennas,

TABLE 6–2.—*Principal Tracking Concepts*

Tracking concept	Ground-based transmissions	Satellite signal source	Ground-based signal analysis	Parameters measured	Approximate accuracy	Typical hardware
Radio interferometry	None	Beacon	Interferometer	Direction cosines	20″	Minitrack, Microlock, DIANE, ESTRAC.
Doppler-tracking	None	Beacon	Doppler	Δf vs. time		Doploc, TRANET, U.S.S.R. network (?).
Big-dish tracking	None	Beacon	Receiver only	Direction cosines	Fair	Jodrell Bank.
Optical telescope	None	Reflected light.	Telescope	Direction cosines	0.1°–1.0°	Moonwatch.
Ballistic camera	None	Reflected light.	Ballistic camera	Direction cosines	10″	Wild BC–4.
Baker-Nunn camera	None	Reflected light.	Baker-Nunn camera.	Direction cosines	2″	Baker-Nunn camera, SAO network.
Conventional radar	Pulsed, narrow beam	Reflected signal.	Echo-timing, Doppler effect.	Range, range rate, direction cosines.	1°	BMEWS.
Radar interferometry	Pulsed, fan-shaped beam.	Reflected signal.	Interferometer	Direction cosines	6°	Satellite detection fence (SPASUR).
Radar transponder	Pulsed, narrow beam	Transponder.	Signal-timing, Doppler effect.	Range, range rate, direction cosines.	(Table 6–3)	FPS–16.
Side tone	Continuous beam with side tones.	Transponder.	Phase analysis of side tones.	Range, range rate	±15 m, ±0.1 m/sec.	NASA Range-and-Range-Rate System.
Radar interferometry with transponder.	Pulsed, narrow beam	Transponder.	Interferometer	Direction cosines	1′	MISTRAM.
Sequential collation of range.	Pulsed, narrow beams (4 stations).	Transponder.	Phase analysis	Ranges from stations	For locating ground stations.	SECOR.

all of which can be made directionally sensitive.   An important word is "directionally," because observations of satellites in classes (1) and (2) generally yield only angular information, such as elevation and azimuth.   The only exception is the Doppler analysis of satellite signals, which produces satellite velocity and range. If the satellite is illuminated by a radar or laser beams, or triggered by ground signals, range and range rate as well as angular position may be directly measured.

In chapter 4, the methods of determining orbital elements from tracking data were described.   Note that the use of ephemerides for satellite acquisition is the inverse of tracking for purposes of orbit determination.   The six classical orbital elements can be found from angular measurements alone, from ranges and range rates alone, or from many other combinations of six independent observations.   Precision orbits, however, are obtained only from many measurements from many sites over a long period of time (ch. 4).

With today's farflung, overlapping networks of civilian, military, and foreign tracking stations, all satellites are constantly scrutinized by all manner of instruments.   With more than 200 satellites in orbit at any moment, and navigational information pouring in from as many different tracking sites, emphasis has shifted from the 1957 problem of mere acquisition to coping with the abundance of tracking data and keeping the satellites sorted out. Note the similarity to the telemetry data-handing problem.

A more conventional tracking problem owes its existence to atmospheric and ionospheric distortion of the satellite signals. The subjects of attenuation, reflection, refraction, polarization, and scintillation were treated in chapter 5.   Fortunately, the practical effects are small at high frequencies, and tracking corrections are easily made.   At low frequencies—viz, the first Sputniks, which transmitted at 20 megacycles—satellite signals are sometimes heard when the satellite is on the opposite side of the Earth.   Beacon tracking under such conditions is meaningless. The satellite must be well above the horizon.

The purpose of this section is the description of the principles employed in the different tracking systems.   The facilities themselves and their worldwide networks are covered in the next chapter.

Radio-Interferometer Tracking.—Satellite radio interferometry came into being with the Navy Vanguard and Army Explorer

$$Cos\ \alpha = \frac{2\pi\phi\lambda}{L}$$
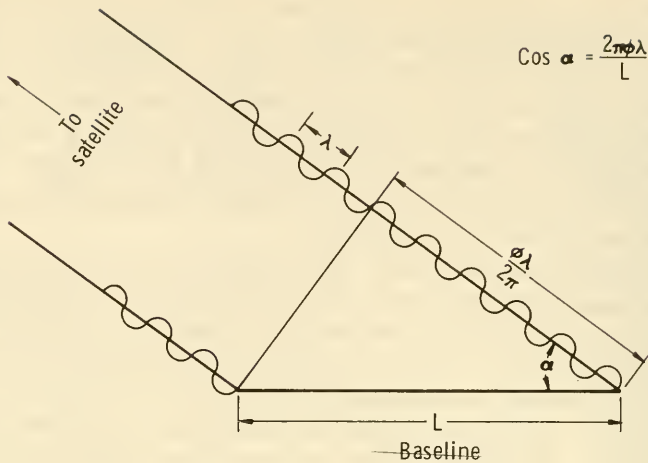
FIGURE 6–3.—An interferometer measures the angle of a transmitting or reflecting satellite by measuring the phase difference between the radio waves received at different points. Since the number of whole wavelengths along the side of the triangle cannot be counted by a single interferometer installation, ambiguity-resolving receiver arrays must be added, as in figure 6–4.

programs. The Navy Minitrack differed from the Army Microlock primarily in the ability of the latter to lock onto satellite beacon signals electronically. Both measured the phase differences between signals received at separate antennas. Both were simple, accurate, and inexpensive in terms of ground facilities, and required the satellite to carry only a tiny beacon transmitter. The Minitrack stations were the first to be deployed operationally throughout the world. They have survived, in improved form, as integral parts of the NASA STADAN (Satellite Tracking and Data Acquisition Network). A few Microlock stations were installed, but they were taken out of service as Minitrack became the major tracking system for U.S. scientific satellites. The French DIANE and the ESRO[1] ESTRACK networks also employ interferometry.

The interferometer principle is this: If plane wavefronts are intercepted and detected at two antennas separated by a baseline, L, and a phase difference, ϕ, is measured between them, the direc-

---

[1] ESRO is the European Space Research Organization.

tion of the satellite, α (subject to atmospheric and ionospheric corrections), is given by

$$\alpha = \cos^{-1} \frac{2\pi\phi\lambda}{L} \qquad (6\text{--}1)$$

where $\lambda =$ the wavelength of the satellite beacon signal. $\lambda = 2.2$ meters at the present Minitrack frequency of 136 megacycles (initially, it was 108 megacycles) (fig. 6–3).

In Minitrack, an array of ground-based antennas measures two of the direction cosines of the line joining the satellite and the ground station (fig. 6–4).   Since the reference baselines for the
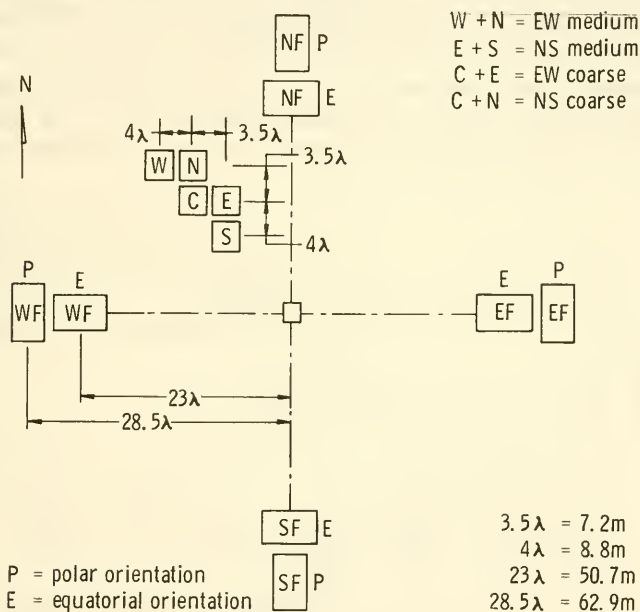
FIGURE 6–4.—Antenna field for a 136-megacycle Minitrack interferometer station.   Several sets of antennas with different baselines are used to eliminate ambiguities that arise when $\phi\lambda > 2\pi$.

two angular measurements are perpendicular, the third direction cosine is automatically known.   A minimum of three separate fixes from a single Minitrack station will provide the six orbital elements.   Accuracy, however, comes only with time and measurements from many coordinated stations.   Even with its manifest simplicity, Minitrack data lead to very accurate orbital elements. Minitrack accuracy is approximately 20 arcseconds.

Successful though Minitrack is with many satellites, it lacks precision on eccentric orbits, such as those of the IMP's, where small angular displacements may correspond to large segments of the orbital trajectory. Interferometry is also of little use in tracking stationary (synchronous) satellites. The STADAN Minitrack equipment is therefore complemented by NASA Range-and-Range-Rate tracking equipment (covered later). Minitrack is of no use at all in tracking "dark," nontransmitting satellites. Interferometer systems with accompanying ground-based radars remedy this defect; viz, SPASUR, the Navy Space Surveillance network.

Doppler Tracking of Transmitting Satellites.—The motion of fast Earth satellites causes a Doppler shift in the frequencies of the signals received on the ground. At the Minitrack frequency of 136 megacycles, Doppler shifts may be several kilocycles. The qualitative picture seen by a receiving station is portrayed in figure 6–5. At the point of closest approach, the satellite has a
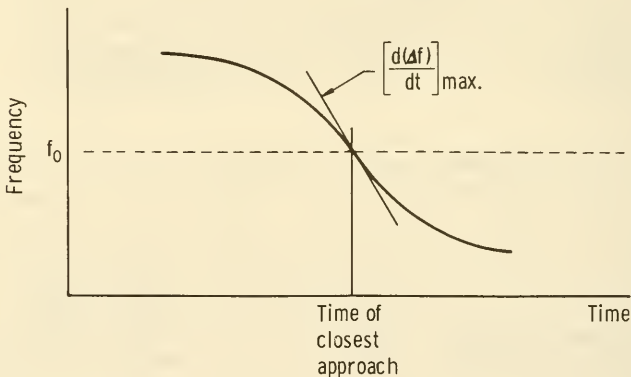
FIGURE 6–5.—Qualitative illustration of a typical Doppler record.

zero instantaneous radial velocity relative to the station, and the received frequency is precisely the transmitted frequency. The data of figure 6–5 can be turned into orbital elements in the following manner. The geometry of the problem is illustrated in figure 6–6.[2] At any moment the range rate, $\dot{\rho}$, is

---

[2] The Doppler technique described here should not be confused with that used with Doppler radar or the STADAN range-rate equipment.
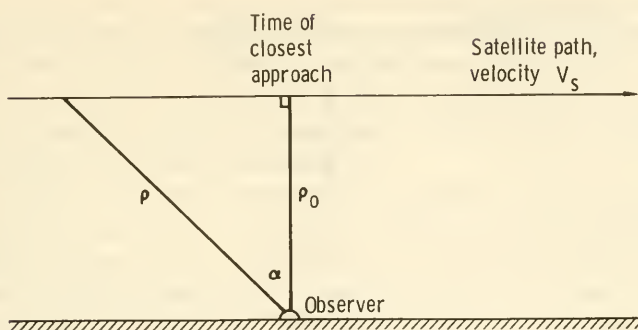
FIGURE 6-6.—Geometry for the derivation of Doppler-
tracking equations.

$$\dot{\rho} = c \frac{\Delta f}{f_0} \qquad (6\text{-}2)$$

where

  c = the velocity of light
  f_0 = the transmitted frequency
  Δf = the instantaneous Doppler shift.

In terms of the satellite velocity, V_s

$$\Delta f = \frac{f_0 V_s \sin \alpha}{c} \qquad (6\text{-}3)$$

Differentiating equation (6-3) with respect to time

$$\frac{d(\Delta f)}{dt} = \frac{f_0 V_s}{c} \cos \alpha \frac{d\alpha}{dt}$$

At the point of closest approach, ρ_0

$$\frac{d(\Delta f)}{dt} = \max, \qquad \cos \alpha = 1, \qquad \text{and} \qquad \frac{\Delta \alpha}{\Delta t} \cong \frac{V_s}{\rho_0}$$

So that

$$\left[\frac{d(\Delta f)}{dt} \right]_{\max} \cong \frac{f_0 V_s^2}{c \rho_0} \qquad (6\text{-}4)$$

By recording Δf as a function of time, the ratio V_s^2/ρ_0 can be
found (fig. 6-7) (ref. 1). Theoretically, the complete analysis
of the Doppler record obtained from a single satellite pass can
fix all six orbital elements (ref. 2). DOPLOC stations, which
have three separate antenna arrays and the capability of locking
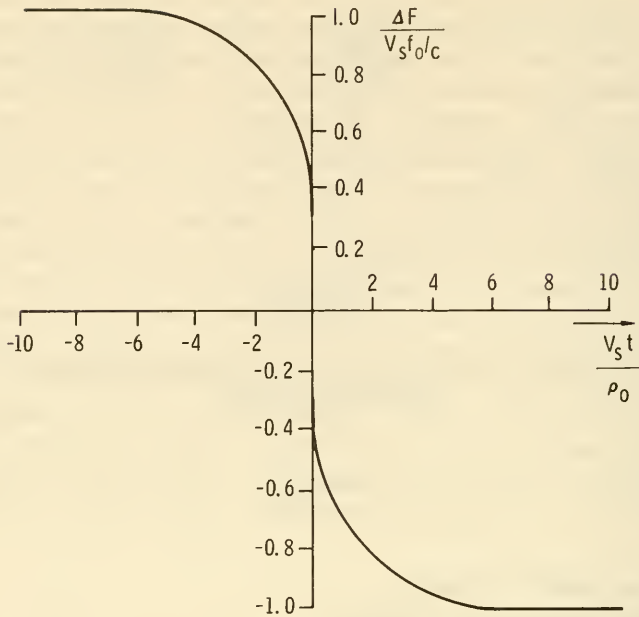
FIGURE 6–7.—Universal Doppler-shift curve ($t = 0$ at the closest approach) (ref. 1).

onto the signal, can do this with high accuracy. The Johns Hopkins University, for example, has used a DOPLOC station to pinpoint localized orbital distortions a few hundred feet in magnitude occurring over gravitational anomalies. The calculation of orbital elements from Doppler data is the inverse of the Transit navigation-satellite concept, where terrestrial position fixes are made by analyzing the Doppler data obtained from satellites in precisely known orbits. Doppler tracking, as described above, is not employed in any worldwide scientific-satellite networks, although the Navy TRANET (Transit network) is occasionally pressed into the service of science. Doppler tracking is a convenient and economical technique for geodetic and aeronomy research from a geographically limited number of sites, and it is presumed that Russia tracks its scientific satellites by means of this technique.

Tracking by Highly Directional Antennas.—The large, steerable, paraboloid antennas (or dishes) built for radio astronomy are occasionally enlisted in tracking beacon-carrying deep-space probes and, more rarely, Earth satellites. The Jodrell Bank, Millstone Hill, and DSIF (Deep Space Instrumentation Facility)

dishes tracked satellites in the early phases of the space program. Satellites, however, move across the sky so rapidly that these big antennas, which have extremely narrow receiving lobes, cannot acquire and track them easily. With STADAN and radar networks in operation, big-dish tracking is primarily of historical interest, except for deep-space probes.

Optical Tracking.—Sun-illuminated satellites can be followed visually with instruments, such as telescopes and theodolites, or their track images can be recorded on film against the known background of the fixed stars. Only angular data evolve from optical observations, but the resolution of optical instruments is so far superior to that of microwave equipment that use of the optical devices makes it possible to calculate the most precise orbits of all. Photographs taken by the Smithsonian Astrophysical Observatory's Baker-Nunn camera network are particularly noted for the precise orbital data they produce. Unfortunately, observations can be made only in clear weather at dusk and dawn (ref. 3).

The Moonwatch program, originated and activated by the Smithsonian Astrophysical Observatory (SAO) for the International Geophysical Year (IGY), is of historical interest [3] (ref. 4). The purposes of Moonwatch were:

(1) To provide data for determining the orbits of new IGY satellites

(2) To track the satellites just prior to and during orbital decay, when they might be out of Minitrack range

(3) To locate lost satellites, especially those without a functioning beacon

Moonwatch went into operation with the launchings of the first Sputniks and Explorers.

Amateurs made up most Moonwatch teams. Armed with six-power monocular telescopes with 12° fields, they could observe satellites up to magnitude 6.5. A few teams were equipped with 20-power, "apogee" telescopes with 2.5° fields for following the more eccentric satellites. Moonwatch accuracy varied between 0.1° and 1.0° in angle and 0.1 to 1.0 second in time. Time was measured by stopwatches calibrated against WWV signals. The Moonwatch teams were eventually supplanted by STADAN and Baker-Nunn stations.

---

[3] The Russians have reported a similar amateur program, employing simple instruments.

Astronomical telescopes and theodolites (transitlike instruments) have also obtained good angular measurements of satellites. As in the case of Doppler tracking, theodolites are quite effective for use by individuals and small research teams who wish to study independently orbits and their perturbations. There are no worldwide networks of these instruments.

By substituting photographic film for the eye in these instruments, the track of a satellite can be permanently recorded against a stellar background. Time can be inserted on the record by shutter action or, in the case of the ANNA and Geos geodetic satellites, by a flashing light on the satellite itself.

Two varieties of cameras are installed in networks: ballistic cameras and the Baker-Nunn cameras, which were specially designed for satellite work.

The U.S. Coast and Geodetic Survey and the U.S.S.R. have deployed ballistic cameras for precision satellite work. The U.S. network, set up mainly for geodetic purposes, has baselines hundreds of kilometers long that are known to accuracies of 10^{-6}. The Wild BC–4 ballistic camera has been adopted for the Coast and Geodetic Survey network (ref. 5). With this instrument, images of ninth-magnitude stars are easily discerned on glass plates. Shutters at various stations are synchronized to within 1 millisecond by reference to the vlf time signals from the Navy Canal Zone station of the National Bureau of Standards (NBA). Angular accuracy is about 10^{-5}, thus enabling the distance across the United States to be determined to better than 10 meters by satellite triangulation from several sites.

During the IGY, the Smithsonian Astrophysical Observatory (SAO) constructed 12 Baker-Nunn satellite-tracking stations. The two belts of stations are centered around latitudes 30° N. and 30° S. Each IGY station was equipped with the Baker-Nunn camera, a Normann crystal clock, and auxiliary equipment for film processing, film reading, etc. The camera itself is a modified Schmidt design with a three-element corrector system (fig. 6–8). The wide field of 30° is specially designed for tracking fast-moving satellites. The camera is mounted on a triaxial pedestal and can be driven at speeds matching those of the satellites (ref. 4). Four important operational modes exist:

(1) *Stationary Camera Mode*.—The tracks of bright satellites are recorded with exposure times so short that the fixed stars move only a diameter or two

(2) *Uniform Tracking Mode*.—The camera is driven at the rate anticipated for the satellite. The satellite image is intensified
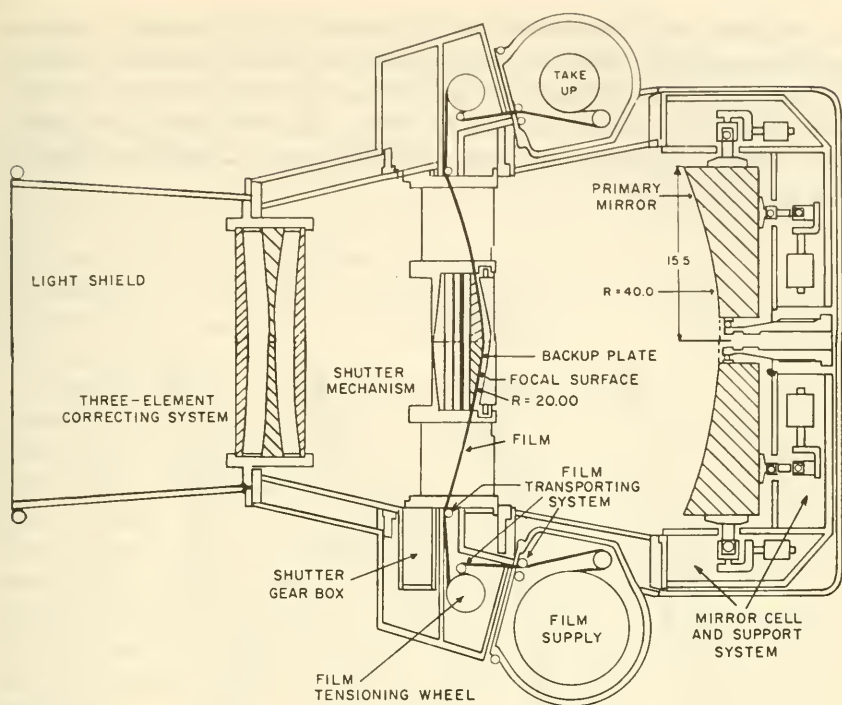
FIGURE 6–8.—Cross section of the Baker-Nunn camera.

in this way, permitting 13.5-magnitude satellites to be photographed. Satellites to magnitude 17 can be photographed if the camera can be manually guided on the satellite.

(3) *Oscillating Motion Mode.*—Two exposures are made: one while tracking the satellite, the other with the camera stationary

(4) *Time Exposure Mode.*—The shutter is held open for about 20 seconds while the camera follows the satellite. This mode is used to help identify the satellite and analyze light variations due to tumbling.

Rough plate measurements are made at the station. Precise measurement and data reduction are made at the Smithsonian Astrophysical Observatory, Cambridge, Mass. Angular accuracy is about 2 seconds of arc. The Smithsonian camera network is now part of the NASA worldwide tracking complex, though it is still operated by SAO.

The USAF has also set up an independent network of Baker-Nunn cameras as part of the Department of Defense Spacetrack program.

Tracking of Illuminated and Triggered Satellites.—By illuminating a satellite with an electromagnetic beam (radar or laser) or triggering an onboard transponder, range and range-rate data can be added to angular measurements. A large family of tracking systems is founded on such artificial target stimulation (table 6–2 and fig. 6–9).
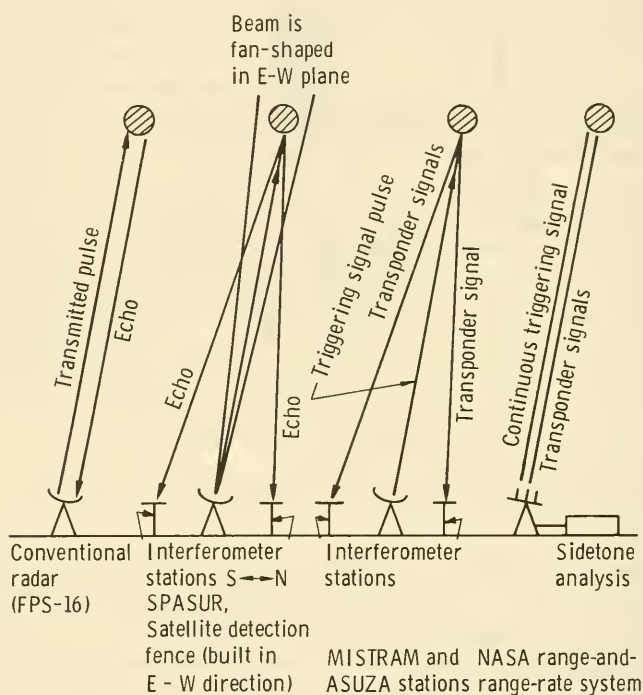
FIGURE 6–9.—Tracking systems based on radar and satellite transponders.

Conventional radars direct a narrow, pulsed beam of electromagnetic energy at the target satellite. A small fraction of the energy striking the illuminated satellite will be reflected and intercepted by the ground antenna. Measurements of echo times and Doppler-frequency shifts yield ranges and range rates, parameters that cannot be directly measured by passive observation alone. Radar beams are too broad to permit precise angular measurements, but range and range-rate data are adequate for orbit determination in themselves (ch. 4). Conventional radars, however, are rarely used in tracking for scientific purposes.

Rather than rely on weak echoes, scientific satellites almost inevitably carry beacons or transponders. There is no alternative to the use of radar echoes when the satellite is intentionally "dark" for military reasons or is not transmitting by virtue of equipment failure. Several big radars can skin-track small, high satellites; viz, BMEWS (Ballistic Missile Early Warning System) radars, the Stanford radar, and the Millstone Hill radar. The last one can detect Explorer-class satellites at several thousand kilometers and fix their bearings to within 1 minute of arc. Reflections of laser beams from satellites can, of course, be used in lieu of radar.

Another kind of radar illuminates the satellite in the conventional fashion, but the echoes are picked up by other stations. The Department of Defense Space Surveillance System (SPASUR), also called the Satellite Detection Fence, employs this principle to keep track of all satellites crossing the United States. The "fence" of transmitting and receiving stations crosses the continent in an east-west direction, stretching from Brown Field, Calif., to Fort Stewart, Fla. A few high-powered transmitters continuously illuminate the sky. Any object entering these fan-shaped beams will reflect some energy into the waiting receiving antennas. There, interferometer measurements determine the orbit of the object.

The reflected signals reaching ground receivers from small, scientific satellites vary as the inverse fourth power of the range. If transponders are installed, however, the received signal varies only as the inverse square of the range—a power-saving stratagem. A satellite transponder sends out a signal only when it is triggered. The transmitted signal may or may not be at the same frequency as the received signal. Time delays are incorporated on occasion. If the time delay and transponder frequency are known, tracking equipment can measure range and range rate after the fashion of conventional radar.

Radars frequently used with transponding targets are the FPS–16 and FPQ–6 (table 6–3). Launch vehicles and manned satellites are generally tracked by such radars, but NASA tracks its scientific satellites with a portable Range-and-Range-Rate System, developed by Goddard Space Flight Center and deployed at some STADAN stations (ref. 6). The NASA approach involves a principle termed "sidetone" tracking. Here, a continuous-wave carrier is modulated by eight mathematically related tones; viz, 8, 32, 160, and 800 cps; 4, 20, 100, and 500 kilocycles. Instead of measuring echo times to fix the range, the Range-and-Range-Rate System

TABLE 6–3.—*Typical Tracking Radars*

Parameter	Modified FPS–16 [a]	FPQ–6 [a]	Tradex [a]	Verlort [b]
Band_____	C	C	uhf	S
Frequency, Mc_____	5600	5600	425	2700–2900
Peak power, MW_____	3.0	3.0	4.0	0.25
Pulse width, μsec_____	1.7	2.4	50	800
Repetition vote, pps_____	855	640	1500	410–1707
Antenna size, m_____	5	9.5	25	3
Beamwidth, mils_____	14	8	35	2.5
Accuracy:				
Angular, mils_____	0.15	0.1	0.3	1.7
Range, m_____	2.4	4.6	4.6	11

[a] From ref. 7.
[b] From ref. 8.
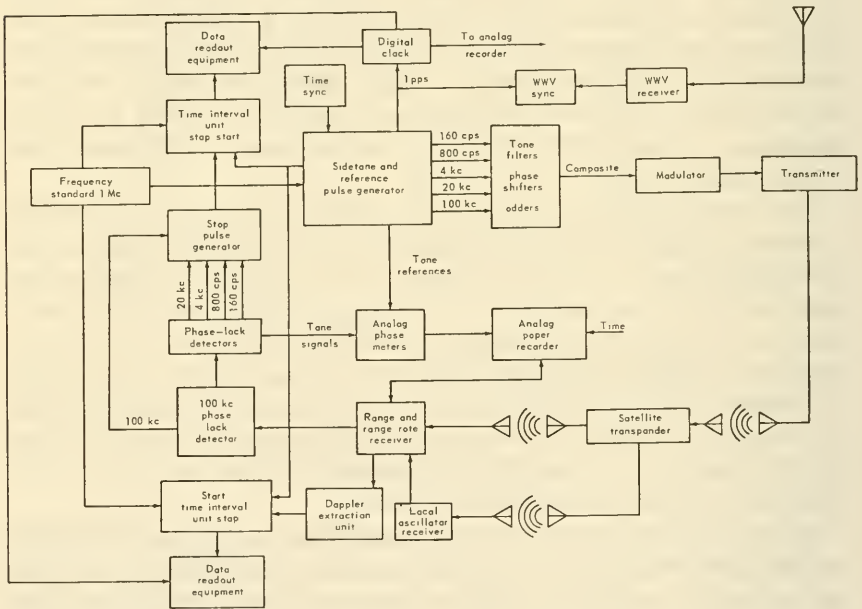
FIGURE 6–10.—Block diagram of the NASA Goddard Range-and-Range-Rate tracking system (GRARR) (ref. 6).

determines the relative phases of the sidetones received from a transponder on the satellite (fig. 6–10). The sidetone wavelengths vary from 0.6 to 37 500 kilometers, bracketing the usual satellite altitudes. A ground-station carrier is at one of three frequencies

in the 2771-megacycle range (S band). The triggered transponder replies at 1705 megacycles. A vhf ground signal at 148 megacycles is also sent, and the response is at the Minitrack frequency of 136 megacycles. Range rate is found by Doppler analysis of the transponder signals. The addition of the Range-and-Range-Rate System to STADAN allows NASA to track eccentric and synchronous satellites more accurately. Nominal accuracies for the NASA system are 15 meters in range and 0.1 m/sec in range rate over distances from 150 to 400 000 kilometers.

The final type of radar considered here triggers a space vehicle's transponder and analyzes the response with antennas arranged in an interferometer pattern. The precision radars of the Department of Defense MISTRAM (missile trajectory measurement) tracking stations are of this type. MISTRAM receivers are arranged on extremely long baselines, so that excellent precision is possible; i.e., 10^{-5} to 10^{-6} in angle (ref. 9). The mission of MISTRAM is primarily military in character.

In summary, radar-type tracking equipment is most often used with launch vehicles and missiles and in military networks. The NASA and foreign scientific satellites almost always carry beacons so they can be tracked by Minitrack interferometers deployed in STADAN, DIANE, and ESTRACK. Transponders are incorporated, particularly on eccentric satellites, to permit tracking by the Goddard Range-and-Range-Rate System, which is also part of STADAN. Department of Defense scientific satellites are sometimes tracked by STADAN, sometimes by the other systems described above. All satellites, regardless of their origin or purpose, are followed by the military networks.

Satellite Tracking Networks.—Independent, uncoordinated tracking stations cannot support a large space-science program. Stations must be linked together, but still be spread out over a large geographical area. The big U.S. networks, such as STADAN, TRANET, NORAD, and their foreign equivalents, are tied together in four ways:

(1) Common time standards: WWV, NBA, etc.
(2) Accurate geodetic positioning
(3) Communication lines: radio, teletype, mail, etc.
(4) Data analysis and processing:
        (*a*) Central network processing
        (*b*) Intercomparison of data from different networks

The first two items—time and position—are the most critical.[4]

---

[4] See sec. 7–4 for descriptions of tracking-network facilities.

Obvious redundancy exists in the various NASA, military, and foreign networks. NASA also maintains separate tracking networks for the manned-spaceflight program and deep-space probes, which have different requirements. For example, manned missions cannot wait through several orbits for orbital elements. Satellites are also constantly watched and tracked by many scientific and amateur organizations throughout the world. There has been little effort to integrate tracking data on a worldwide basis. The best, readily available syntheses of tracking data for scientific satellites are the NASA Goddard Space Flight Center ephemerides and Satellite Situation Reports.

6–3.   Onboard Satellite Navigation

No unmanned scientific satellites use self-contained navigation instruments for orbit determination. Gyros, star trackers, horizon sensors, and other such instruments are incorporated in the attitude-control subsystem (sec. 6–5), but they are concerned with orientation rather than orbit fixing. Ground-based tracking, now and in the foreseeable future, will provide scientific satellites with all the navigational information they require.

Scientific satellites with onboard propulsion subsystems have the capability to change the orbital elements, maintain an orbit in the presence of environmental forces, and deorbit the satellite. The commands to carry out such propulsive functions invariably originate on the Earth and, as just mentioned, are based on Earth-measured navigational data. This exclusive assignment of the first two orbit-control functions (navigation and command formulation) to Earth facilities emphasizes three important facts:

(1) Earth-based tracking facilities can determine the orbital elements of an unmanned satellite more accurately and conveniently (in terms of satellite weight and power) than satellite-based gyros, accelerometers, radar, loran-type devices, or star trackers

(2) The extensive computations needed to determine quantitative commands are carried out more easily and reliably in ground computers

(3) Unmanned scientific satellites have little need for in-orbit maneuvers, reentry and station keeping of synchronous satellites being the major satellite-based propulsive functions. Consequently, there has been little impetus to develop satellite-based orbital-guidance equipment.

Valid as these observations are for unmanned scientific satellites, there is intense development activity in spacecraft-based

guidance for the manned-spaceflight program and the planetary-probe program. Both efforts include complicated maneuvers, such as orbital rendezvous and planetary soft landings, which cannot be properly controlled from Earth. The most common application of onboard guidance equipment to unmanned scientific satellites will probably be in the internal, closed-loop control of the deorbiting propulsive function.

6–4.   Satellite Orbital Guidance and Command

Once ground-based tracking networks have fixed the orbit of a satellite, what use is made of the orbital elements and ephemeris? We always want to know where any specific satellite is for purposes of data readout and military accounting. Geodeticists and aeronomists also wish to study how the orbit changes with time. There is one other purpose of tracking, however, and that is orbital guidance, the subject of this section.

Only two aspects of satellite guidance are basic to the satellite itself: orbit modification and controlled reentry. The guidance of the launch vehicle during ascent and injection is the province of the launch vehicle.

Before dismissing ascent guidance, it is instructive to see how it is accomplished from a qualitative viewpoint. Navigation during ascent is accomplished by tracking stations and/or internal sensors (gyros, accelerometers, etc.). Each launch mission has a carefully calculated ascent program that specifies the desired position, velocity, acceleration, and attitude of the launch vehicle as a function of time after launch. In guidance, the desired program is compared, parameter for parameter, with measured data. If deviations exist, corrections are computed and the engines are commanded to change the thrust magnitude and direction accordingly. On occasion, the launch vehicle is "steered" into orbit by ground commands; i.e., radio guidance. Or, all corrective commands may be given by internal circuitry, as in modern ICBM's. Injection velocity and angle strongly affect the final orbit (sec. 4–4). They must be controlled with precision (refs. 1, 10).

Guidance During Orbit Correction and Modification.—Orbit correction and modification are prime features of synchronous communication satellites, manned rendezvous, and some military satellites, but not for unmanned scientific satellites. Eventually, someone may wish to vary the orbital elements of a scientific satellite or prolong its life by offsetting drag. Such satellite maneuvers are contrary to present philosophy, which strips the satellite of as many functions as possible and leaves them behind on Earth; viz,

tracking and data processing. In essence, this philosophy says: Launch the satellite as precisely as possible into the desired orbit and (except for attitude control) let it go its own way. Reliability and simplicity go hand in hand. Why burden a satellite with maneuvering equipment when dozens of scientific satellites are being launched each year and targets of opportunity can be investigated with new satellites? Nevertheless, progress in equipment reliability may ultimately take us far beyond present complexity limits (OGO and OAO) to maneuvering scientific satellites.

Assuming that orbit control can be justified, how would it be carried out? Most likely, the orbit-correcting or orbit-sustaining commands would be formulated on Earth, where the tracking and computing are done, and sent to the satellite's onboard propulsion subsystem. A block diagram of this approach is illustrated in figure 6–11 (ref. 11).

In a practical case, the magnitude and direction of the velocity increment needed for the maneuver would be sent to the satellite as a series of commands. First, the attitude-control subsystem would be commanded to turn the thrust axis in the proper direc-
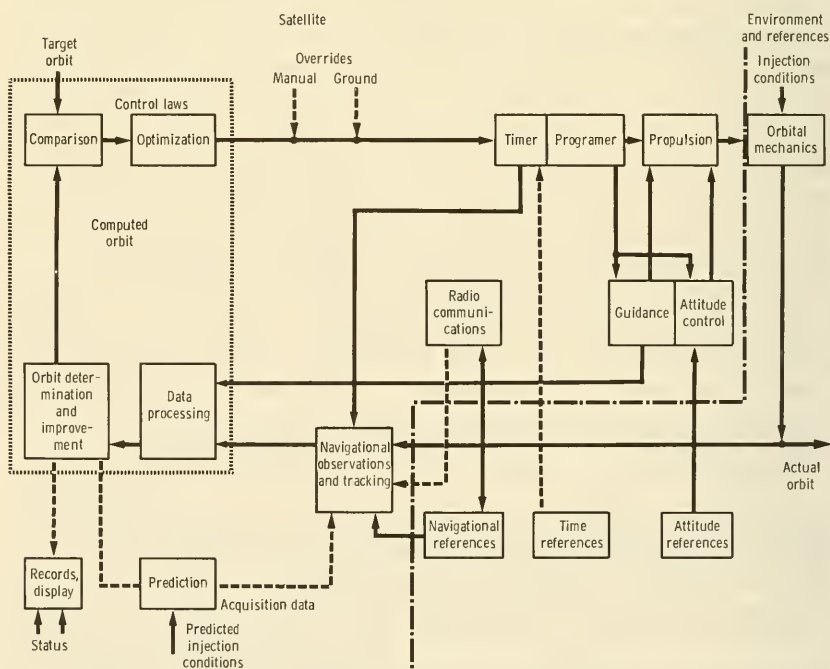
FIGURE 6–11.—Block diagram of an onboard orbit-control system (ref. 11).

tion.   Then, the propulsion subsystem would be commanded to fire a specified length of time.   This use of commands illustrates external control.   If no further attempts at correction are made, the loop is an open one. If subsequent tracking shows that the new orbit needs further correction, and new commands are dispatched, the loop is closed.

The parameters of the maneuvers needed to attain the corrected orbit are analogous to the error signals generated, say, by a misalined star tracker.   Guidance is the computation of these errors and their translation into the appropriate commands for the satellite subsystems (ref. 12).

Orbital guidance may be surveyed from a different level of abstraction.   The required velocity increment may be viewed as the controllable item rather than the orbit itself.   In this instance, an onboard integrating accelerometer would measure the actual velocity increment delivered by the engine, while sensors in the attitude-control subsystem would monitor the orientation of the thrust axis.   Detected errors would be immediately rectified in closed-loop fashion.   The thrust duration, for example, might be controlled by a closed, internal circuit, set by Earth command at a particular velocity increment.

Reentry Guidance.—Reentry guidance is very similar to orbital guidance.   Deorbiting is, in a broad sense, just another orbit modification, resulting in an ellipse that follows the reentry corridor (fig. 4–24). Again, the thrust initiation, timing, and vectoring are calculated and commanded from the ground in practical cases; viz, Biosatellite.   The effects of thrust magnitude and direction have been summarized in figures 4–25 and 4–26.

Errors in timing and the magnitude and direction of the deorbiting thrust will cause dispersion of the reentry trajectories. These can be easily estimated from the graphs and the satellite velocity.

The salient fact about orbital guidance of scientific satellites is that it is primarily external and open loop in character.   The desire for satellite simplicity has relegated the functions of navigation (tracking) and guidance to Earth-based facilities.   Since orbital maneuvering, even controlled reentry, is rare with scientific satellites, there appears to be no reason to alter this division of labor.

6–5.   Attitude Control

Satellite designers always single out attitude control as a most critical area of satellite technology.   This attention is deserved

for the satellites themselves, and the environments they measure are far from isotropic. Attitude control has the same major ingredients as other spacecraft-control problems—namely, error sensing, the generation of corrective commands, and actuation. Attitude control differs in detail, however, in the types of sensors and actuators employed. The generalized control schematic (fig. 6–1) still suffices.

Typical components of attitude-control subsystems are: [5]

(1) *Attitude and Attitude-Change Sensors.*—Horizon sensors, star trackers, star-field trackers, gyroscopes, radar, pendulums, magnetometers, solar-aspect sensors, Sun trackers, television

(2) *Error Detectors and Command Generators.*—Voltage-subtraction circuits, digital computers, analog computers

(3) *Attitude-Change and Stabilization Actuators.*—Yo-yo despin devices, magnetic torquers, solar-pressure vanes, aerodynamic vanes, gravity-gradient devices, gas jets, subliming rockets, electric-propulsion engines, gyroscopes, inertia wheels, ball-in-tube wobble dampers

Attitude control is consummated through electrical analog and/ or digital signals. In the simplest cases, attitude sensors deliver voltage levels that can be subtracted from reference signals to generate the error signal needed by the actuators. The stark simplicity of this sequence is shattered in practice by the need for precision stabilization and complicated experiment-pointing programs on the larger satellites; e.g., the OAO's. The communication and manipulation of information becomes so involved that analog signals are converted to digital form, so that digital computers can be enlisted to perform coordinate transformations and construct command words. Sensors with direct digital outputs have been developed with such applications in mind. Actuators, such as inertia wheels, are addressed and commanded by digital words, even though they may be basically unquantized (fig. 5–4(b)).

Examples of Satellite Attitude-Control Problems.—Satellite attitude-control and stabilization requirements vary greatly from mission to mission and even during a single mission (table 6–4). Brief descriptions of the attitude-control philosophies of a simple Explorer and an OAO will highlight the differences.

Explorer XII represents the class of spin-stabilized satellites to which taxonomy assigns most scientific satellites. Here, the final stage of the launch vehicle is spun prior to orbital injection. After

---

[5] The hardware of the sensors and actuators listed above are discussed in Sec. 9–7.

TABLE 6–4.—*Some Typical Attitude-Control Requirements* [a]

Attitude-control function	Typical requirement
Despin (most satellites)_____	Reduce spin by 0–100 rpm to zero or design level.
Stop tumbling and wobbling (all satellites).	Reduce unwanted motion to tolerance level dictated by experiments.
Acquire Sun, Earth, or reference stars (OSO, OGO, OAO).	Search, lock, and stabilize to about 1°.
Stabilize on Sun (OSO)_____	Stabilize to less than 1 sec.
Stabilize on Earth (OGO)_____	Stabilize to between 0.1° and several degrees.
Stabilize on target star (OAO)___	Stabilize to about 0.1 sec. for 150 min.
Aline thrust vector for reentry (Biosatellite).	Aline to between 0.3° and 1°.

[a] See also table 4–2.

separation, the satellite is still spinning. Environmental torques will very slowly reduce this spin, but for many months the spin will be adequate to stabilize the spin axis against small environmental perturbations. Frequently, the initial spin rate is too great for experimental purposes. In such cases, the satellite is despun
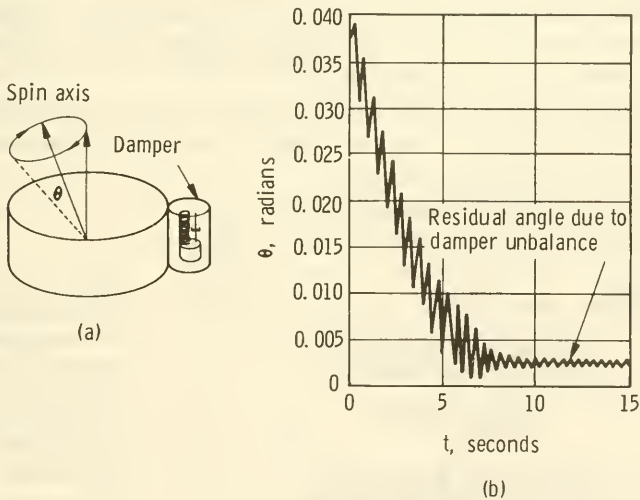
FIGURE 6–12.—(*a*) Spin-stabilized satellite with a damping device to reduce wobble. (*b*) Wobble reduction as energy in spin-axis wobble is absorbed as heat in damping mechanism (ref. 13).

by the release of weights (yo-yo's) on long wires or the erection of antennas and solar paddles. Mechanical precession, or "wobble," dampers (sec. 9–8) dissipate energy tied up in spin-vector precession in internal friction (fig. 6–12). Magnetic coils and bars are being used more and more to remove unwanted motion from the injected satellite. Generally, spin-stabilized satellites depend upon gravity gradients, radiation pressure, and other environmental forces for attitude control. After spinup and postinjection despin, no further attempts are made to influence the satellite attitude by command or feedback attitude from sensors. Directional scientific experiments will sweep the heavens with each rotation—a frequently desirable feature—and solar-aspect or other attitude sensors will inform the experimenter on the ground of the attitude of his equipment.

To the OAO's must be assigned the dubious distinction of possessing the most difficult attitude-control requirements among the scientific satellites. This type of satellite must search for, acquire, and stabilize instruments on a long series of stars. There are four modes of operation (refs. 14, 15):

(1) *Initial Stabilization Mode.*—This begins after orbital injection and ends when the star trackers have locked onto their guide stars. Random tumbling is reduced to below a preset threshold (fig. 6–13). The Sun is acquired and the roll axis is stabilized on it (fig. 6–14). A "roll search" then commences as the high-thrust roll jets accelerate the roll rate to 0.2°/sec (fig. 6–15). Ultimately the star trackers will pick up preselected guide stars and attitude control is transferred to celestial coordinates.

(2) *Coarse Pointing Mode.*—The OAO's optical axis is pointed to the selected star with an accuracy of about 1 minute of arc.
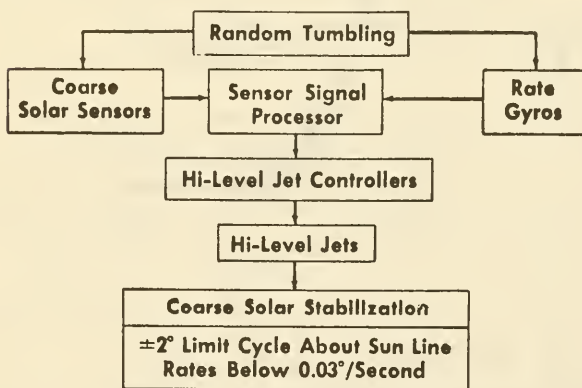
FIGURE 6–13.— Block diagram showing the sensors and actuators used in the OAO initial stabilization mode (ref. 15).

```
                    ┌──────────────────────────────────┐
                    │   Coarse Solar Stabilization     │
                    └──────────────────────────────────┘
         ┌──────────────┐   ┌──────────────┐   ┌──────────────┐
         │ Fine Sensors │   │ Disable Eye  │   │ Rate Gyros   │
         └──────────────┘   └──────────────┘   └──────────────┘
              ┌────────────────────────────────┐
              │    Sensor Signal Processor     │
              └────────────────────────────────┘
              ┌────────────────────────────────┐
              │  Fine Wheel & Jet Controllers  │
              └────────────────────────────────┘
              ┌────────────────────────────────┐
              │  Hi-Thrust Jets & Fine Wheels  │
              └────────────────────────────────┘
              ┌────────────────────────────────┐
              │     Fine Solar Stabilization   │
              │  Stabilized on Sun Line within │
              │   ±0.25° with Minimum Rates    │
              └────────────────────────────────┘
```

FIGURE 6–14.— Block diagram showing the sensors and actuators used in the OAO fine solar-stabilization mode (ref. 15).

```
              ┌────────────────────────────────┐
              │    Fine Solar Stabilization    │
              └────────────────────────────────┘
   ┌──────────┐   ┌──────────────┐   ┌──────────────┐
   │ Roll Rate│   │ Roll Signal  │   │  Programer   │
   │   Gyro   │   │  Processor   │   │              │
   └──────────┘   └──────────────┘   └──────────────┘
              ┌────────────────────────────────┐
              │       Roll Controller          │
              └────────────────────────────────┘
              ┌────────────────────────────────┐
              │      Roll Hi-Thrust Jet        │
              └────────────────────────────────┘
         ┌────────────────────────────────────────┐
         │           Roll Search Mode             │
         │ Rolling About Sun Line at 0.2°/Second  │
         │  Pitch & Yaw Stabilized within ±0.25°  │
         └────────────────────────────────────────┘
```
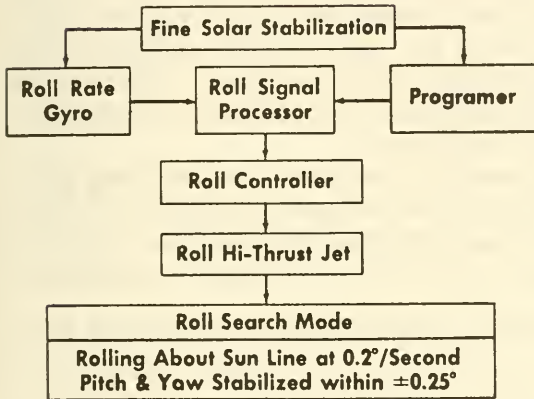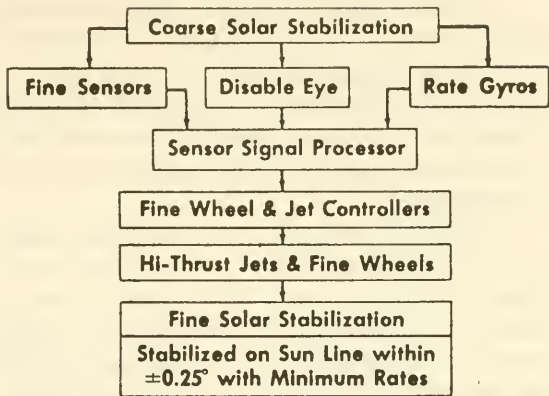
FIGURE 6–15.— Block diagram showing the sensors and actuators used in the OAO roll-search mode (ref. 15).

Experiments that do not need extreme pointing accuracy can be carried out during this mode.

(3) *Fine-Pointing Mode.*—Here the optical axis is pointed with an accuracy of about 0.1 second for the more demanding experiments. The optics of the prime experiment can be used to detect pointing errors.

(4) *Reorientation and Acquisition Mode.*—New stellar targets are acquired as commanded by a stored program. The satellite axes are slewed to the desired orientation in the celestial sphere by addressing specific inertia wheels and commanding them to turn a certain number of times.

Table 6–5 shows that the OAO requirements are extreme. In comparison, the OGO's require only relatively coarse Earth pointing by one face. The OSO's, on the other hand, are articulated hybrids—half spin-stabilized (the "wheel" section) and half Sun-stabilized (the "sail" section).

Attitude-Control Theory.—Attitude control involves error detection, feedback, and actuation. Conventional control theory (i.e., using linear approximations) is usually quite adequate.[6] Rather than developing these well-known relationships here, emphasis is placed on two representative types of attitude control: (1) spin stabilization and (2) three-axis orientation and stabilization in inertial space.

The kinetic behavior of a satellite under applied torques is described by its equations of motion (sec. 4–7). Attitude-control theory concerns itself with orienting and stabilizing the satellite under the influence of perturbing torques and within the constraints of the equations of motion. Stability, for example, must be charted during all phases of operation. Certain combinations of mechanical and signal-feedback parameters can lead to divergent oscillations and other instabilities, as we shall see below.

First, the important case of the spin-stabilized satellite, where no attitude-control circuits exist, will be examined. Stability here means that environmental torques cannot reorient the satellite or stimulate it into unwanted oscillations.

A simple but practical example illustrates the stabilizing effect of spin. Consider a satellite with moments of inertia I_x, $I_y = I_z$ (fig. 6–16). Successful experimentation depends upon maintaining the spin vector normal to the orbital plane under the influence

---

[6] Where attitude perturbations are large, viz, the OAO, nonlinear theory must be used.
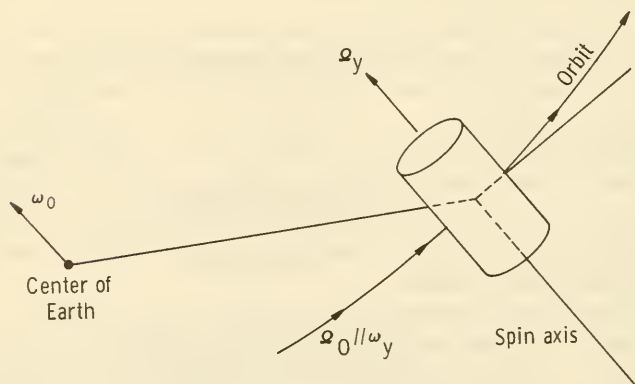
FIGURE 6–16.—Geometry for derivation of spin-stabilization equations.
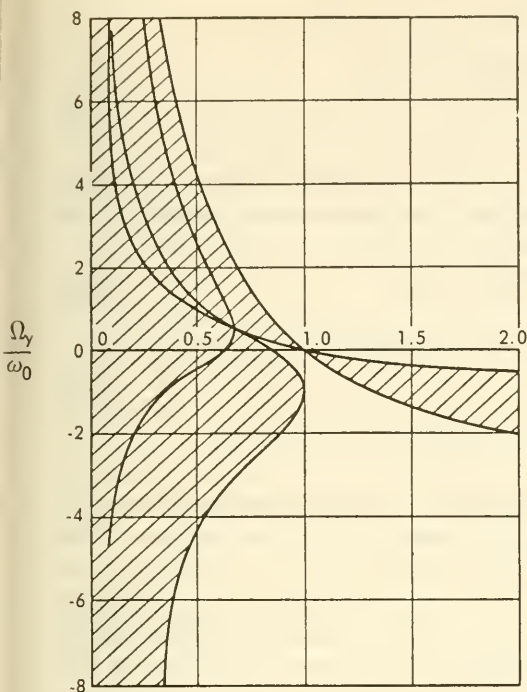
FIGURE 6–17.—Spin required to spin-stabilize a satellite against gravity-gradient perturbations (ref. 16. Used by permission of the McGraw-Hill Book Co.).

of gravity-gradient torques, which tend to pull the long axis into a vertical position (sec. 4–7). When $I_y/I_z < 1$, small gravity-gradient torques will immediately disorient an unspun satellite. The introduction of spin about the symmetric axis generates the stable areas plotted in figure 6–17.

Assuming an Earth-pointed satellite coordinate system and perturbations θ_x, θ_y, θ_z, the angular velocities of the satellite axes are

$$\begin{aligned}
\Omega_x &= \dot{\theta}_x - \omega_0\theta_z \\
\Omega_y &= \dot{\theta}_y - \omega_0 \\
\Omega_z &= \dot{\theta}_z + \omega_0\theta_x
\end{aligned}$$
(6–5)

where products of θ have been ignored and Ω_x, Ω_y, Ω_z = the angular velocities of the satellite (sec. 4–7). If an artificial spin Ω_s is introduced, the components of the angular momentum vector are

$$\begin{aligned}
H_x &= I_z(\dot{\theta}_x - \omega_0\theta_z) \\
H_y &= I_y(\dot{\theta}_y - \omega_0 - \Omega_s) \\
H_z &= I_z(\dot{\theta}_z + \omega_0\theta_x)
\end{aligned}$$
(6–6)

The gravity-gradient torques are approximately

$$L_x = 3\omega_0^2(I_z - I_y)\theta_x$$
$$L_y = 0 \hspace{4cm} (6\text{-}7)$$
$$L_z = 0$$

where $I_x = I_z$ and where the gravity-gradient torque equation (eq. 4–18) has been replaced by the more general form shown above. Substituting into equation (4–19)

$$\mathbf{L} = \dot{\mathbf{H}} + \omega \times \mathbf{H} \hspace{3cm} (4\text{-}20)$$

$$I_x\ddot{\theta}_x - \omega_0\dot{\theta}_z(2I_z - I_y) - \omega_0^2\theta_x(I_z - I_y) + I_y\Omega_s(\dot{\theta}_z + \theta_x\omega_0) = 3\omega_0^2(I_z - I_y)\theta_x$$

$$I_y\ddot{\theta}_y = 0 \hspace{6cm} (6\text{-}8)$$

$$I_x\ddot{\theta}_z + \omega_0\dot{\theta}_x(2I_z - I_y) + \omega_0^2\theta_z(I_y - I_z) - I_y\Omega_s(\dot{\theta}_x - \omega_0\theta_z) = 0$$

By taking the Laplace transformation of these equations, areas of stability can be determined by the usual analytic techniques. The result is figure 6–17. Inherent in figure 6–17 is the instability of a nonspinning satellite $(\Omega_y/\omega_0 = -1)$ under gravity gradients when $I_y < I_x$. The effect of spin is to increase the stable region for $I_y < I_x$; the smaller the ratio I_y/I_x, the more spin needed for stability. Stability does not infer complete lack of spin-axis motion. The complete solution to the equation (6–8) would show satellite oscillations similar to the librations described for a dumbbell satellite in section 4–7.

Spin also stabilizes satellites against aerodynamic, radiation, and other torques. Spin stabilization is effective, easy to accomplish, and conservative of weight and power. The fuel employed in spinning the last stage of the launch vehicle, as well as the weight of yo-yo despin devices and wobble dampers and despin devices, must be charged against this technique, however. The major disadvantage of spin stabilization is the spin itself, which hampers some experiments but aids others.

In contrast to the small, relatively simple, spin-stabilized scientific satellites, the fully stabilized OAO is at the complex end of the spectrum of satellite attitude-control subsystems. During the sequence of operations by which the injected OAO stabilizes itself, acquires the Sun, the guide stars, and finally its first targets, two actions occur that illustrate some key features of satellite attitude control. Some topics are left untouched by this concentration of attention, particularly the Earth-pointing satellites. The bibliography, however, contains many references to these subjects. (See also refs. 17, 18.)

By describing how an OAO points its optical axis from star to star, two facts emphasize the complexity of the OAO attitude-control subsystem: (1) the complexity and extent of the computations necessary to generate a slewing (attitude-change) command, and (2) the operational constraints—typical of satellite missions—that preclude free operation of the attitude-control subsystem.

If the OAO has an initial attitude in inertial space specified by the three angles α, δ, and β, and slewing commands must be generated that will reorient the satellite to a new target attitude α_2, δ_2, and β_2, there are $3 \times 2 \times 2$, or 12, possible slewing sequences: yaw-pitch-roll, yaw-roll-pitch, yaw-pitch-yaw, yaw-roll-yaw, etc. (ref. 19). If negative slewing angles are included, the number of potential sequences is doubled.

If $\mathbf{v}$ is any vector with coordinates known in attitude No. 1 (before slewing), the new coordinates in attitude No. 2 (after slewing) can be found by multiplying six 3 x 3 matrices together

$$T_{\beta_2} T_{\delta_2} T_{\alpha_2} \qquad T_{\alpha_1}{}^{-1} T_{\delta_1}{}^{-1} T_{\beta_1}{}^{-1}$$

where the T's are defined below

$$T_\alpha = \begin{bmatrix} \cos\alpha & \sin\alpha & 0 \\ -\sin\alpha & \cos\alpha & 0 \\ 0 & 0 & 1 \end{bmatrix} \qquad T_\delta = \begin{bmatrix} \cos\delta & 0 & \sin\delta \\ 0 & 1 & 0 \\ -\sin\delta & 0 & \cos\delta \end{bmatrix}$$

$$T_\beta = \begin{bmatrix} 1 & 0 & 0 \\ 0 & \cos\beta & \sin\beta \\ 0 & -\sin\beta & \cos\beta \end{bmatrix}$$

where again the angles α, δ, and ρ define the directions of the satellite axes relative to a satellite-fixed coordinate system. Each slewing command therefore requires the onboard multiplication of many matrices containing trigonometric terms. The point being made here is one of calculational complexity. To compound the problem, the star-tracker gimbal angles depend upon their physical mounting. And since star-tracker data are the sole source of precision attitude information, additional matrices must be multiplied to translate their readings into the vector coordinates that fix the satellite attitude before the slewing command. Needless to say, the matrix multiplications are burdensome for an onboard computer.

A logical question asks which of the 24 sequences of slewing

commands is best.   Two constraints eliminate some of the sequences:

(1) The optical axes of the experiments should not come within, say, 45° of the Sun to preclude damage to the experiments if their sunshades fail to work.   Slewing sequences must be examined mathematically to find one meeting this condition for all experiments.   In addition, star trackers must not exceed their gimbal limits during the slewing operation.   If no acceptable sequence can be found, intermediate star assignments must be made.

(2) The satellite attitude after slewing has ceased should leave the solar paddles in positions where they will receive the maximum amount of sunlight.   For this reason, the last slewing command might well be a roll command, once the optical axis has been alined with the target star.

The final topic in attitude-control theory investigates the fine (precision) solar-orientation phase of the OAO initial solar-stabilization mode of operation (ref. 20).   Solar stabilization for the OAO requires that:

(1) The satellite negative roll-control axis shall be alined to within ±0.5° of the Sun-satellite line regardless of the initial condition following launch-vehicle separation

(2) Satellite angular velocities about the yaw, roll, and pitch axes shall be reduced to ±0.03°/sec or less

(3) Solar stabilization shall not require more than 26 minutes.

OAO solar stabilization is divided into coarse- and fine-control loops, with the changeover occurring at about 10° from the Sun. The fine-solar-orientation control loop is pictured in figure 6–18. The pitch and yaw axes are controlled by inertia wheels that respond to angular errors generated by the fine-control solar sensors.[7]   The error signals are converted to driving signals that are fed back to the wheel motors.   Linear control is obtained for small angular excursions in the proportional range of the sensor around the null point. A lead-lag network creates stability compensation for the loop.   Limiter circuits prevent signal levels from exceeding the motor-voltage ratings. The precessional cross-coupling torques that are inevitably caused by rotation of the yaw and pitch inertia wheels have to be included in the overall torques.

6–6.   Satellite Status Control

Satellite status is defined as a combination of two things:

(1) The collective positions of all switches and steplike opera-

---

[7] More complete discussion of the sensors and actuators will be found in ch. 9.
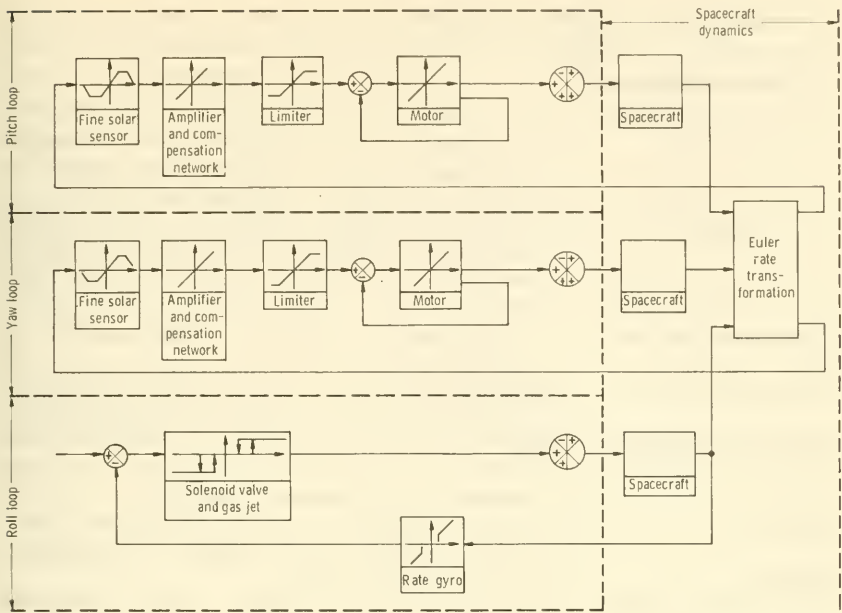
FIGURE 6-18.—Block diagram of the OAO fine solar-stabilization loops (ref. 20).

tional modes (i.e., experiment "on," "off," or "calibrate") of all satellite subsystems, except the attitude-control and environments-control subsystems (table 6-5)

(2) The aggregation of all currents, voltages, and other satellite parameters reported by the engineering-instrument subsystem

In mathematical terms, the dependent variables through which satellite status is controlled are almost invariably quantized or discrete, while the independent variables are continuous, even though they may be digitized for transmission to Earth.

Seven of the 10 satellite subsystems may be placed in various operational modes by ground-based or internally generated commands (table 6-5). In a satellite as complex as OGO, there will be thousands of different combinations of subsystem modes. OGO, for example, can accept 254 separate external commands, 150 for experiments alone. Even if the command is only two valued (i.e., on and off), an astronomical number of combinations exists. Because continuous (analog) control is difficult by radio, external commands are quantized in terms of relays and stepping switches. Many stored internal commands are also quantized, such as those timer-thrown switches that start the unfolding of satellite append-

TABLE 6–5.—*Typical Satellite Status-Control Functions*

Satellite subsystem	Status-control functions
Communication_____	Extend antennas. Turn off high-power transmitter to conserve power. Automatic gain control of receiver. Switch to different data rate.
Power supply_____	Extend solar paddles. Disconnect a shorted solar-cell paddle. Disconnect solar cells from battery to "kill" satellite at end of life. Voltage regulation.
Onboard propulsion____	Fire for specified period to deorbit satellite or modify orbit.
Attitude control a_____	Begin roll-search mode. Orient thrust axis in specified direction. Lock on Sun. Lock on vertical.
Environment control a__	Maintain satellite temperature within preset limits.
Guidance and control___	Detect performance errors and issue corrective commands. No actuators present.
Computer_____	Read out memory over STADAN station. Compute slewing data for attitude-control subsystem.
Structural_____	Separate reentry capsule.
Engineering instrument_	None. No actuators present. Status indicators only.
Scientific instrument____	Extend experiment boom. Turn off defunct experiment. Reverse or alter orientation of sensor.

a Not included as part of "status" control in this book.

ages after orbit is attained. Many other internal controls are steplike or quantized, however, such as voltage regulation and temperature control. Commands may be further categorized as open or closed loop,[8] and internally or externally generated. The decision to make a particular control function quantized open-loop/external or to use one of the five other possibilities depends upon the satellite, its mission, the state of the art, and who designs it.

The sum total of all commandable operational modes is a measure of satellite flexibility. The more flexible it is, the more things an Earth-based operator can make it do. Flexibility is especially important in cases of component failures (sec. 6–1). But it is an attribute purchased with complexity.

Errors or unwanted deviations in satellite status are communicated by engineering-instrument subsystem sensors. Some will be corrected on board by closed-loop circuits. Thermostatically controlled louvers in the environmental-control subsystem are excellent examples. On the other hand, overheating of an isolated component might indicate a failure to an Earth-based operator,

[8] I.e., without or with feedback, respectively.

who would then switch it off by command. Some changes in satellite status are the results of normal operation—the commanded data readout over a data-acquisition station, for example. Other changes are preprogramed and may be stored as switches to be triggered in a satellite timer.

Assume that a change in satellite status is necessary. How is the command formulated and transmitted to the proper actuator? Quantized commands depend upon electrical pulses to trip a relay or step a switch. Since a large satellite will possess thousands of relays and switches, some way of addressing the right circuit must be found. Simple addressing might involve no more than the sending of a certain frequency signal to the satellite which, through filter action, will admit it to the correct switch. Using a more modern approach, OGO and OAO have adopted computer-type addressing. Command words are tagged with numerical addresses, enabling computer logic circuits to sort them out (fig. 5–4(b). Ultimately, the command ends up as an electrical signal that triggers a switch that, in turn, switches something on or off or steps it into a new mode of operation. The command has then been executed and the satellite status is duly changed.

References

1. Stearns, E. V. B.: Navigation and Guidance in Space. Prentice-Hall, Inc., 1963.
2. Mass, J.; and Vassy, E.: Doppler Effect of Artificial Satellites. *In* Advances in Space Science and Technology, vol. 4, F. I. Ordway, ed., Academic Press, 1962.
3. Veis, G.: Optical Tracking of Artificial Satellites. Space Sci. Rev., vol. 2, 1963, p. 250.
4. Henize, K. G.: Tracking Artificial Satellites and Space Vehicles. *In* Advances in Space Science, vol. 2, F. I. Ordway, ed., Academic Press, 1960.
5. Taylor, E. A.: Optical Tracking System for Space Geodesy. *In* The Use of Artificial Satellites for Geodesy, G. Veis, ed., John Wiley & Sons, Inc., 1963.
6. Habib, E. J., et al.: Development of a Range and Range Rate Spacecraft Tracking System. NASA TN D–2093, 1964.
7. Barton, D. K.: Recent Developments in Radar Instrumentation. Astronaut. Aerospace Eng., vol. 1, July 1963, p. 54.
8. Truszynski, G. M.: Radio Tracking of Earth Satellites. *In* Space Research II, H. C. van de Hulst, C. de Jager, and A. F. Moore, eds., Interscience Publishers, 1961.
9. Mullen, E. B.; and Woods, C. R.: Precision Radio Tracking of Space Vehicles. *In* Space Research II, H. C. de Hulst, C. de Jager, and A. F. Moore, eds., Interscience Publishers, 1961.
10. Braham, H. S.: Trajectory Aspects of Guidance. *In* Guidance and Control of Aerospace Vehicles, C. T. Leondes, ed., McGraw-Hill Book Co., Inc., 1963.

11. UNGER, J. H. W.: Orbit Control of Satellites. *In* Handbook of Astronautical Engineering, H. H. Koelle, ed., McGraw-Hill Book Co., Inc., 1961.

12. STEFFAN, K. F.: Orbital Guidance. *In* Guidance and Control of Aerospace Vehicles, C. T. Leondes, ed., McGraw-Hill Book Co., Inc., 1963.

13. REITER, G. S.; AND THOMSON, W. T.: Rotational Motion of Passive Space Vehicles. *In* Torques and Attitude Sensing in Earth Satellites, S. F. Singer, ed., Academic Press, 1964.

14. PAPSCO, R. E.: The Stabilization and Control System for the Orbiting Astronomical Observatory. Navigation, vol. 11, 1964, p. 3.

15. IMGRAM, D. A.; ZIEMER, R. R.; AND STERN, E.: Design and Dynamic Testing of an Ultrahigh Accuracy Satellite Stabilization and Control System for the Orbiting Astronomical Observatory. *In* Proc. of the XIIIth International Astronautical Congress, N. Boneff and I. Hersey, eds., Springer-Verlag, 1964.

16. THOMSON, W. T.: Passive Attitude Control of Satellite Vehicles. *In* Guidance and Control of Aerospace Vehicles, C. T. Leondes, ed., McGraw-Hill Book Co., Inc., 1963.

17. MERRICK, V. K.: Some Control Problems Associated With Earth-Oriented Satellites. NASA TN D–1771, 1963.

18. PAIKEN, M.; AND FLEIZIG, R.: Momentum Control of the OAO Spacecraft Using the Earth's Magnetic Field. Paper presented at the XIVth International Astronautical Congress, 1965.

19. DAVENPORT, P. B.: Mathematical Analysis for the Orientation and Control of the Orbiting Astronomical Observatory Satellite. NASA TN D–1668, 1963.

20. COOK, J. M.; AND FLEISIG, R: OAO Initial Stabilization and Control. Astronaut. Aerospace Eng., vol. 1, Sept. 1963, p. 88.

Chapter 7

EARTH-BASED FACILITIES AND OPERATIONS

7-1. Prolog

From a systemwide perspective, the scientific satellite is merely the sensor end of a huge, radio-connected machine. Reminiscent of an iceberg, the largest part of the total satellite system remains out of the limelight, down on Earth. In scientific-satellite programs, a large fraction of the money and engineering labor goes into three Earth-based activities and the facilities that support them. These activities are:

(1) The prelaunch testing of the satellite, when the satellite and its components are shaken, heated, put in vacuum chambers, radiated, and bombarded with micrometeoroid-like particles prior to shipment to the launch site

(2) Satellite checkout at the launch site, where the satellite and its interfaces are checked several times for compatibility. The scientific instruments are calibrated and their responses to simulated forces are checked

(3) Postlaunch satellite tracking, command, data acquisition, data processing, and data archiving

Test facilities are activated many months before the satellite actually leaves the launch pad. Reliability is such a critical figure of merit that each satellite component, as well as the completely assembled satellite, is comprehensively [1] tested in simulated operating modes and environments. In the most general sense, environmental testing includes simulating all environments created during shipping, handling, and launch, in addition to orbital operation. The total testing program therefore expands to encompass the smallest satellite part and the entire satellite system, including the ground-tracking and data-acquisition sta-

---

[1] Another adverb might be "exhaustively," but the section that follows will demonstrate that this is not and cannot be the correct word for satellite testing.

tions.   Along the time dimension, it stretches from the moment of mission conception until the satellite has died a natural or commanded death in orbit.   Time in orbit must be included in the testing panorama because engineering data telemetered back from a satellite are actually the most valid test data.   The successful satellite is at the apex of a pyramid whose base dimensions are time (several years) and money (several millions). Grand as this metaphor is, failure of a 10-cent part can reduce the pyramid to a shambles.

No satellite design begins with a completely clean slate.   Many of the supporting facilities are already in place.   Extant tracking systems, telemetry facilities, and launch vehicles are likely to dictate parameters such as maximum weight and dimensions, telemetry approach, and frequency.   "Economy" and "compatibility" are important words here.   Who would duplicate or even significantly modify STADAN [2] for a new satellite or even a series of satellites?   The sizes of existing environmental test chambers may even conspire to fix the maximum size of a satellite.   Such design inertia is a key feature but not necessarily a negative feature of space research.

Once a satellite is in orbit, only the electromagnetic interface connects it with the Earth-based facilities (fig. 7–1).   Before launch, however, it is taken for granted that a good testing program will lay bare all sensitive interfaces and assess their effect on mission success.   The formal satellite model introduced in chapter 4 again becomes a good skeleton upon which to hang the Earth-based-facility story.

The purpose of this chapter is not only the description of the major Earth-based facilities and the satellite-support operations performed by them but also the way in which they are welded into a meaningful whole.   Some space will be devoted to the management objectives, plans, and specifications that are used in marshaling the widespread resources.   Good program management is just as critical to satellite success as experimental insight.

7–2.   Testing Scientific Satellites and Their Components

Before a costly launch vehicle is committed to a satellite launch, some assurance that the satellite will work properly for a stipulated length of time is desirable.   Ideally, a new machine, whether refrigerator or satellite, is repeatedly tested under actual operating conditions until a sound underpinning of statistical success

---

[2] STADAN is NASA's Satellite Tracking and Data Acquisition Network.

FIGURE 7–1.—Interface diagram showing the more important relationships between the Earth-based facilities and the rest of the satellite system.   The dotted lines represent prelaunch testing and checkout relationships; the solid lines show postlaunch interfaces.

(or failure) data have accumulated.   Only when performance can be guaranteed—in the way, for instance, that an automobile is guaranteed—is the commercial machine released for consumption.   These utopian thoughts are shattered by three facts of satellite life:

(1) The design lifetimes of most scientific satellites ($\frac{1}{2}$ to 1 year) are too long to permit the demonstration of high system reliability in reasonable test times.   To illustrate, a demonstration that a satellite will survive without failure for 1 year with a probability of 0.96 would require an experimentally demonstrated MTBF (mean time before failure) of 25 years, a clearly

unreasonable period of time in the fast-paced space program.

(2) Scientific satellites, unlike automobiles and refrigerators, are not manufactured by the millions. They are several-of-a-kind machines. Usually, there will be only a structural model, a prototype, and one flight machine.[a] The limited edition, combined with limited time for testing, militates further against any experimental proof of reliability. Sometimes statistical reliability data will be available on the component level, but this is meager and often unsatisfactory. Accentuating the problem is the fact that many satellite failures result from human carelessness—an untestable factor.

(3) The satellite space and launch environments cannot be simulated in all their complexity and intensity here on Earth. In particular, the radiation and micrometeoroid facets are simulated neither well nor simultaneously with the other environmental factors. Although the complete space environment is expected to be more severe than the superposition of its parts, there is little experimental evidence that this is so. In fact, in many satellite series the first spacecraft launched are essentially test vehicles; viz, San Marco 1.

To summarize the situation: the satellite environment from the moment it is shipped from its point of manufacture until its end of life in orbit is known fairly well. Most of the diverse environments encountered can be simulated, but no reasonable test program can guarantee anything about satellite performance in the usual statistical sense. With this fact recognized and accepted, the objectives of the satellite test program must be modified until they are meaningful in terms of time, money, and enhancement of the probability of satellite success. As current terminology goes, a test philosophy must be formulated—a practical, meaningful test philosophy.

Scientific satellites are enough alike so that a rather widely accepted and applied test philosophy has had time to take root and grow since 1957. NASA's approach has been iterated several times in the literature (refs. 1, 2). It is a philosophy frequently applied to complicated, few-of-a-kind machines. The cornerstone of the NASA test philosophy is the subjection of the entire satellite to a comprehensive series of simulated environmental stresses for a period of time much less than length of the planned mission in order to identify and eliminate failures due to: (1) major design weaknesses, (2) defects in workmanship, and (3) defects

---

[a] The prototype is subjected to the highest level of testing and is essentially identical to the flight article. On occasion, prototypes have been flown.
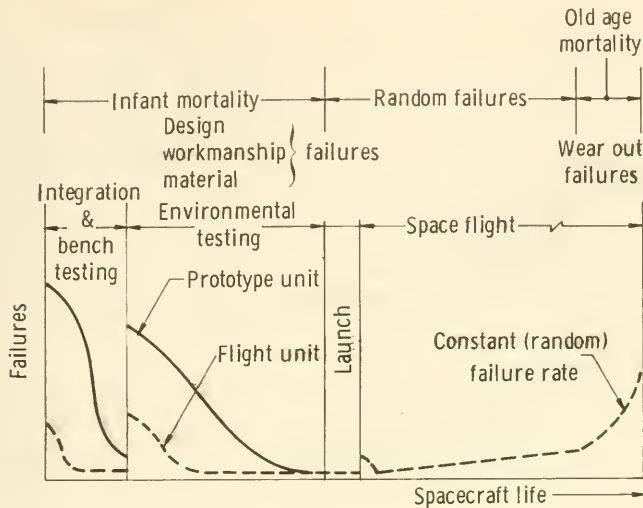
FIGURE 7–2.—Failure patterns for prototype and flight-
model scientific satellites. The objective of testing is
to identify and fix those failures occurring during the
infant-mortality stage.

in materials. The graph in figure 7–2 portrays this approach
very nicely. Satellite assembly and bench testing prior to en-
vironmental tests will eliminate some incipient failures; the
environmental tests themselves will point out even more weak-
nesses. In these tests, there is no attempt to guarantee any level
of future performance.[4] The prime purpose is the systematic
elimination of causes of infant mortality. While this approach
may seem unsophisticated amid today's huge environmental test
chambers and lengthy tracts on reliability theory, NASA's suc-
cess with scientific satellites shows that it is nevertheless effec-
tive. It is in actuality a philosophy based on experience and
therefore "sophisticated." Besides, there is no reasonable alter-
native.

Test Specifications and Requirements.—Test specifications are
formal (usually contractual) statements of those tests that a
purchaser believes will insure him a successful product. Specifi-
cations are management tools based upon knowledge of the satel-
lite environment from factory door to end of life. They are in-
fluenced, on one hand, by the practical limitations of test facilities,
and, on the other, by the buyer's understandable conservatism.

_____

[4] That is, although the tests must be passed with 100 percent success, they
themselves guarantee no specific level of future performance.

Radiation sources		Variable monoergic	Selected monoergic	Constant spectrum	Selected spectra	Variable spectrum	Variable polyergic
Electrons or beta particles (β)	Electron guns	β					
	Special x-ray machines	β					
	Isotopes				β		
	Direct accelerators	β			β		
	Indirect accelerators	β			β		
X-rays or gamma rays (γ, X-ray)	X-ray machines					X-ray	
	Isotopes/reactors		γ ray	γ ray	X-ray		
	Direct accelerators			γ ray		X-ray	
	Indirect accelerators			γ ray		X-ray	
Protons (P)	Ion source	P					
	Direct accelerators	P					
	Indirect accelerators	P					
Heavy ions (Hi)	Ion sources	Hi					
	Direct accelerators	Hi					
	Indirect accelerators	Hi					
Neutrons (N)	Isotopes				N		
	Reactors			N			
	Direct accelerators	N				N	
	Indirect accelerators	N				N	

Radiation energy (eV): 10^2 10^4 10^6 10^8 10^{10}

FIGURE 7–3.—Techniques employed in simulating the space-radiation environment. (Adapted from ref. 3.)

Really satisfactory test specifications do not exist in the scientific-satellite business, because no one can predict or properly quantify the incipient failures that the tests are supposed to discover. In other words, test specifications can be called successful only after the satellite has proven itself successful in orbit.

Before maligning specifications further, let us take a look at the environment we try to simulate on Earth by machines and express verbally in our contracts. Tests are first classified as either environmental or functional. The latter class includes tests of
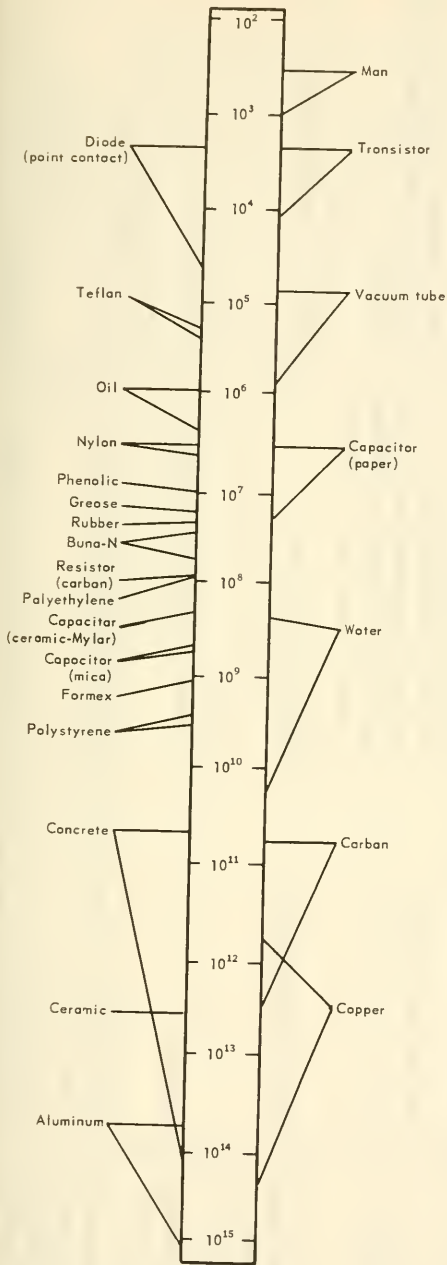
FIGURE 7–4.—Radiation doses required to initiate damage in various structural and insulating materials. Threshold scale is in rads, where 1 rad = 100 ergs/g (ref. 3).

TABLE 7-1.—*Potentially Damaging Aspects of the Space Environment* [a]

Type of force	Typical magnitude used for component qualification	Consequences to satellite	Methods of simulation
Thermal:			
Aerodynamic heating.	Varies widely.	Protective shroud required at launch. Ablating nose cone during reentry.	Wind tunnels, plasma jets, reentry test vehicles.
Insolation	1400 W/m² at Earth's orbit.	Heat load on satellite, solar-cell and battery performance degradation with temperature, dimensional changes.	Lamps.
Sterilization by heat.	135° C for 24 hours or more	Degradation of components on life-detection satellites.	Ovens.
Internal heat loads.	Varies with satellite design	Heat loads may compromise component performance, especially in electronic assemblies. Dimensional changes, battery degradation.	Electrical heaters, prototype tests with actual components, "hot soaking."
Low temperature in Earth's shadow.	~10° C for several hours	Performance degradation	Refrigerators, "cold soaking."
Mechanical:			
Launch-vehicle vibration and noise.	See table 7-2	Physical damage, metal fatigue	Shake tables.
Launch-vehicle and transportation shocks.	22.5-g half sine wave for 11 msec (Explorer XII).	Physical damage, metal fatigue	Drop and impact tests.

		Physical damage, metal fatigue	Centrifuges.
Launch-vehicle, transportation, and spin accelerations.	28 g for 1 min, 180 rpm for 1 min (Explorer XII).	Physical damage, metal fatigue	Centrifuges.
Micrometeoroid impact.	See fig. 1-13	Abrasion and puncture	Light-gas guns, exploding metal shapes, electrostatic accelerators.
Radiative:			
Space particulate radiation.	See fig. 7-3	Component degradation. (See fig. 7-4.)	Research reactors, radioisotopes, particle accelerators.
Solar ultraviolet radiation.		Degradation of surfaces and optical equipment.	Lamps.
Nuclear powerplants.	Varies with powerplant.	See fig. 7-4	Research reactors, radioisotopes, particle accelerators.
Magnetic:			
Space fields.	See fig. 1-9	Minor influences on attitude control	Generally not simulated.
Internal fields.	1 γ for a magnetically "clean" satellite.	Interfaces with experiments, but no physically damaging effects.	Not simulated. Effects checked in prototype functional tests.
Other:			
Vacuum.	Space goes down to 10^{-15} torr, but most tests occur at 10^{-8} torr or more. (See fig. 7-5.)	Sublimation and cold welding	Space chamber.
Prelaunch humidity.	95 percent at 40° C for 50 hr (Explorer XII).	Moisture may degrade electronic equipment.	Humidity chamber.
Time.	Actual lifetimes, 6 to 12 mo. Test time, 2 mo.	Random and wearout failures. (See fig. 7-2.)	No life tests applied to satellite as a whole.

[a] Other interface forces, such as those caused by electromagnetic signals, are nondamaging (at least physically). They are duplicated during functional tests on the prototypes and flight models.
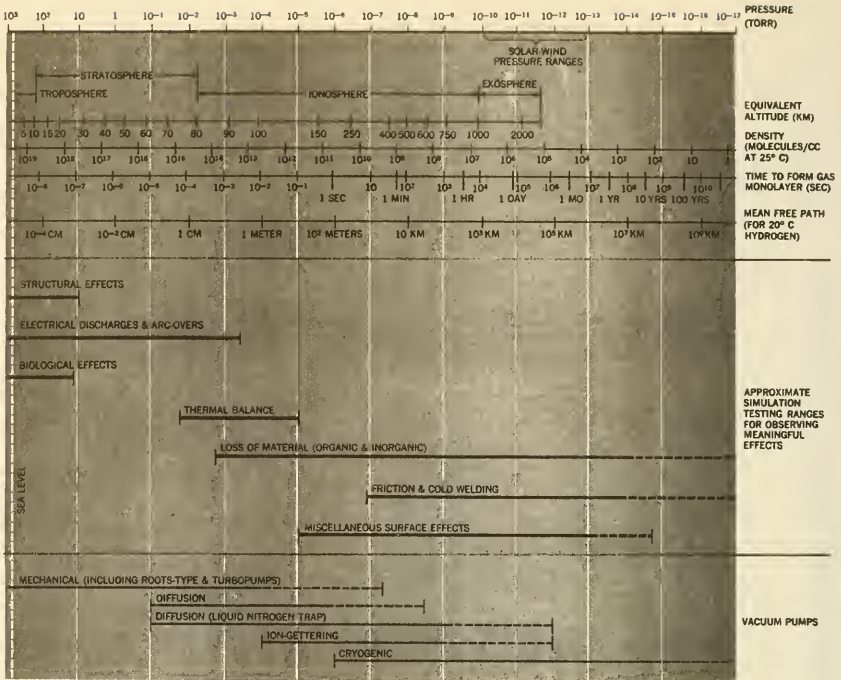
FIGURE 7–5.—Effects of vacuum on space components and types of vacuum pumps used in simulators to duplicate the space environment (ref. 4).

boom extension, attitude stabilization, switch throwing, and the like. The environmental tests receive the most attention and require the largest facility investments. The space and launch-vehicle environments are so radically different from anything encountered on Earth that a great deal of money has had to be spent in simulating them. And even now they are not simulated completely. In fact, only the obviously damaging aspects of the environment are simulated at all. Furthermore, only occasionally can they be simulated simultaneously.

The description of the space environment in chapter 1 was organized according to the classical scientific disciplines of aeronomy, astronomy, etc. This traditional categorization does not mesh with the "functional" satellite model introduced in chapter 3. In table 7–1, the damaging factors of the space environment are rearranged according to the type of satellite interface they bridge, except, of course, for the dimension of time, which pervades everything.

TABLE 7-2.—*Typical Vibration Test Requirements*

[From ref. 5]

Type of vibration	Satellite		Components and experiments	
	Design qualification	Flight acceptance	Design qualification	Flight acceptance
Sinusoidal	10–2000 cps, 21-g peak in thrust axis, 2 octaves/min.	10–2000 cps, 14-g peak in thrust axis, 4 octaves/min.	10–2000 cps, 32-g peak in thrust axis, 2 octaves/min.	Not required.
Random	20–2000 cps, 0.07 g²/cps, 11.8-g rms acceleration, 4 min per axis.	20–2000 cps, 0.03 g²/cps, 7.7-g rms acceleration, 2 min per axis.	20–2000 cps, 0.07 g²/cps, 11.8-g rms acceleration, 4 min per axis.	20–2000 cps, 0.03 g²/cps, 7.7-g rms acceleration, 2 min per axis.
Combustion resonance dwell.	550–650 cps, ½ octave/min, ±2.67×10⁸ dynes in thrust axis or 50-g peak.	550–650 cps, 1 octave/min, ±1.78×10⁸ dynes in thrust axis.	550–650 cps, ½ octave/min, 40-g peak.	Not required.

Tables 7–1 and 7–2 are crude indicators of what a satellite must endure during environmental testing. Test specifications actually·go much further than the tables indicate. They stipulate not only the levels of the applied forces but also the way in which they will be simulated, the method to be used in installing the equipment on the testing fixtures, and just what deviations from perfect performance are tolerable.

Test Planning and Consummation.—Test plans convert the test philosophy into a series of action steps. The first steps consist of a series of conventional inspection and quality-control checks that begin with the raw materials, follow them through fabrication, and continue right up to the point where the satellite manufacturer (Government or industry) accepts the products, be they entire subsystems, resistors, or just reflecting paint. For example, only certain materials and "preferred parts" are approved for satellite applications. Every manufacturer must meet quality standards and test specifications that come into play long before the completed satellite is subjected to environmental and functional tests.

Taking NASA's satellite test programs as representative, the first two hurdles for all major subsystems and complete satellites are the design-qualification tests and flight-acceptance tests. The design-qualification tests are the more difficult. A prevailing rule of thumb states that they should be about $1\frac{1}{2}$ times more severe than the later flight-acceptance tests, which are run approximately at flight levels. The intent of the design qualifications, consistent with NASA's test philosophy, is the pinpointing of weak spots in the satellite design as early as possible. When part failures occur under the strain of testing or when engineering errors become obvious, design fixes are made until a prototype of the test article has finally been qualified. Qualified components and subsystems are assembled to make the prototype satellite, which, of course, must be qualified as a system through further testing. Experience with space hardware has shown repeatedly that components and subsystems that work well in isolation may not perform well when immersed in the complete system—perhaps because there is so little room for safety factors and operating tolerances under the exacting specifications set for satellite equipment. Structural resonances under vibration forces and electronic crosstalk are common system-induced problems.

The less-demanding flight-acceptance tests come next. They are performed on subsystems, including experiments, and the entire satellite. NASA usually builds a minimum of one proto-

type and one flight model for each mission.   Both satellites are tested and sent to the launch site, where one serves as a backup.

One school of thought in satellite testing leans strongly toward concentrating testing at the satellite level rather than at the subsystem and component levels.   Justification for this approach stems, first, from the sheer cost of trying to test at all levels. More significant is the fact that system-level tests are always needed, in any case, because of subsystem interactions.   In other words, the whole is greater than the sum of its parts in testing. Practical testing programs, however, will always do considerable testing at the component and subsystem levels because cause and effect and failure mechanisms are much easier to spot in simpler pieces of equipment and there is more time to correct them.
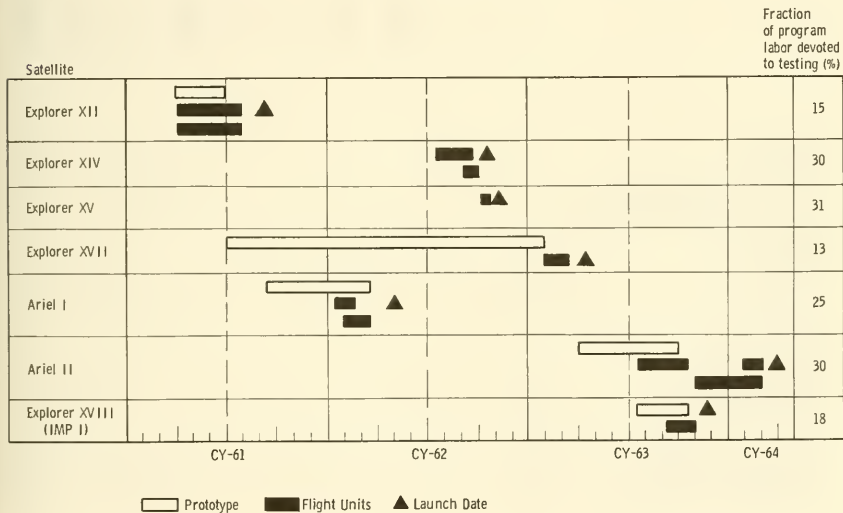
FIGURE 7–6.—Representative test schedules for several Explorer-class satellites.   (Adapted from ref. 6.)

Full-scale tests of prototype and flight models of a satellite usually run for at least several months (fig. 7–6).   A sizable fraction of the total satellite engineering effort is consumed in the process.   Test results fall into two categories:

(1) Failures resulting in immediate design changes that improve the probability that the satellite will perform as planned (table 7–3)

(2) Failure data that are added to a general fund of satellite know-how that will help design better satellites in the future (figs. 7–7 and 7–8)

TABLE 7–3.—*Performance Review of a Typical Scientific Satellite (Ariel 1)*

Space

Ariel 1 FLIGHT NO. 1 SPACECRAFT Spacecraft Subsystems		Test condition Operating mode Date	Incoming inspection Operational checkout 7/19/63	Ozone experiment calibration Ozone experiment only 7/22/63– 7/24/63	Static and dynamic balance Nonoperating 7/25/63– 7/27/63	Operational spin Operational 7/27/63	Moment of inertia Nonoperating 8/9/63	Vibration Launch operational 8/12/63– 8/16/63	Ozone experiment calibration Ozone experiment only 8/17/63	Thermal vacuum Operational 8/22/63– 9/5/63	Sunshine check Operational 9/7/63– 9/9/63
			1	2	3	4	5	6	7	8	9
Power supply:											
Solar paddles	A		N				N		N	N	
Batteries	B										
Power supply electronics	C							C			
Undervoltage det. and recycle timer	D									1	
Battery control and protect. circuit	E						M				
Communications:											
Tape recorder	F										
Programmers	G						M				
Data storage control	H										
Transmitter	I										
Receiver	J										
Encoders	K		C 2			R					
Scientific instrument:											
Ozone electronics	L										
Spectrometers	M										
Broadband ozone detector	N										
Galactic noise receiver	O										
Structure:											
Batteries (galactic noise)	P										
Galactic-noise antenna reel	Q										
Micrometeorite detectors	R										
Micrometeorite electronics	S					D	M	R		2	2
Spacecraft	T		1		S	S	S	2		2	

CODE

1—Special problem	C—Subsystem changed
2—Questionable operation	D—Subsystem redesigned
3—Failure	E—Facility-induced problem

Environmental tests, with their large, expensive facilities, divert attention from the more routine functional tests. Yet, perhaps one-third to one-half of all major satellite problems are uncovered when engineers try to make subsystems work singly or in harmony with the rest of the satellite while still in an Earth environment. Solar paddles get stuck during erection, structures are stressed to failure during despin tests, and, on too many occasions, parts just do not fit together. Some of the more common functional tests are listed in table 7–4.

After Completion of Some Environment and Functional Tests at the Goddard Flight Center

Magnetic check	Antenna pattern	Center of gravity balance	Ozone experiment calibration	Thermal vacuum retest	Sunshine check	Special temp. test for MM experiment	Vibration retest	Ozone experiment calibration	Final balance	Sunshine check	Quasi-storage	Ozone-experiment calibration	Vibration retest	Thermal vacuum retest	Final ozone-experiment calibration
Nonoperating, also operational	Operational	Nonoperating	Ozone experiment only	Operational	Operational	Operational	Launch oper., 1 min. random thrust axis	Ozone experiment only	Nonoperating	Operational	Operate 6 hr/wk	Ozone experiment only	Launch operational	Operational	Ozone experiment only
9/11/63–9/13/63	9/13/63	9/23/63	9/26/63 9/27/63	10/2/63–10/4/63	10/5/63	10/7/63	10/8/63	10/9/63	10/10/63 10/11/63	10/15/63	Oct., Nov., Dec., Jan.	2/17/64	2/18/64	2/17/64	2/24/64–2/26/64
10	11	12	13	14	15	16	17	18	19	20	21	22	23	24	25
	N		N	N	S	N	N	N	N		N	N	N	N	N
											M				
				C	C						2				
			C								C				
				C											
S			R	2		M					C 3				

CODE—Continued

M—Subsystem modified   R—Subsystem repaired
N—Subsystem not under test   S—Special operating condition for test

Summarizing, the sequence of tests in a scientific-satellite program is:

(1) Inspection and quality-control tests performed by the satellite manufacturer. These include the selection of materials and components suitable for space use through the application of preferred-parts lists, standards, and specifications. Similar tests are performed on procured parts.

(2) Design-qualification tests performed on the structural model, prototype satellite, and prototype subsystems. Both environmental and functional tests are included.

TABLE 7–4.—*Some Common Functional Tests*

Name of test	Purpose
Center-of-gravity test__	To insure that attitude-control and orbit-modification thrusts are properly computed and applied.
Moment-of-inertia test__	To measure an experimental moment of inertia for attitude-control and despin operations.
Dynamic-balance test___	To assure balance in spin-stabilized satellites.
Scientific-instrument-excitation tests.	Calibration and confirmation of operational readiness.
Aspect-sensor test_____	To check aspect-sensor readings with an artificial "Sun-gun."
Stabilization test_____	To check satellite's ability to stabilize itself in presence of artificial light source (air-bearing tables used).
Despin test_____	Despin weights and devices are deployed to check their readiness and response of satellite.
Appendage test_____	Antennas, solar paddles, and instrument booms are erected to test their operability.
Electrical test_____	Connections are tested for mechanical soundness, voltages and currents checked for correct values.
Antenna test_____	Satellite antenna patterns checked.
Launch-vehicle fit test__	Satellite is mated to dummy final stage.

TABLE 7–5.—*Some Large Environmental Test Chambers*

Location	Size	Characteristics
Goddard Space Flight Center (Space Environment Simulator).	10 ٦ dia, 18 m high__	−65° to 100° C. 10^{-9} torr, artificial Sun.
Goddard Space Flight Center (Dynamic Test Chamber).	10 m dia, 18 m high__	10^{-3} torr, vibration source (fig. 7–9).
Langley Research Center_____	18 m dia, sphere_____	0.1 torr.
	18 m dia, sphere_____	2×10^{-4} torr.
General Electric (Valley Forge)__	10 m dia, 16 m high__	Vacuum, artificial Sun.
TRW Systems_____	9 m dia, sphere_____	Vacuum, artificial Sun.
Hughes Aircraft_____	4 m dia, 9 m high___	Vacuum, artificial Sun.
Bendix_____	6 m dia, 8 m high___	Vacuum, artificial Sun.

(3) Flight-qualification tests performed on the flight hardware. Both environmental and functional tests are included.

(4) Prelaunch checkout tests at the launch site (described in next section).

Test Facilities.—Almost all manufacturers of space equipment, in both industry and Government, offer impressive arrays of
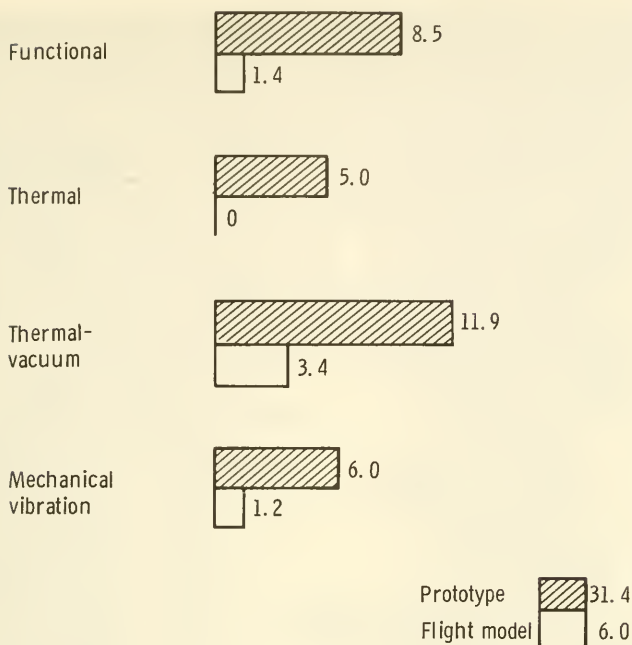
FIGURE 7–7.—Average numbers of problems encountered during the tests of several Explorer-class satellites at Goddard Space Flight Center. A problem here means a malfunction or fault serious enough to abort the mission. Note the value of the prototype tests (ref. 6).

shake tables, space chambers, centrifuges, and similar test equipment. They could not compete for space programs without them. Such facilities are so numerous and well publicized that only two major items are described here.

A symbol of Space-Age testing is the large, evacuated environmental test chamber, with liquid-nitrogen-cooled walls and an artificial Sun. The larger chambers, from a total of nearly 100, are listed in table 7–5. The two large NASA chambers at Goddard Space Flight Center are particularly pertinent because many of NASA's scientific satellites pass through them. The Goddard chamber in figure 7–9 is a "dynamic" chamber in which Observatory-class satellites are vibrated in a vacuum of approximately 1×10^{-3} torr. The elimination of air damping makes vibration tests more realistic. The use of liquid nitrogen or steam in the walls of environmental test chambers can expose satellites to radiative heat sinks over a wide range of temperatures; viz, $-65°$

Scientific-
instrument
subsystem
11.9
2.4

Power-
supply
subsystem
5.4
0.5

Communication
subsystem
4.4
0.9

Structural
subsystem
2.6
0.2

Other
subsystems
7.4
2.4

Prototype   31.7
Flight model   6.4
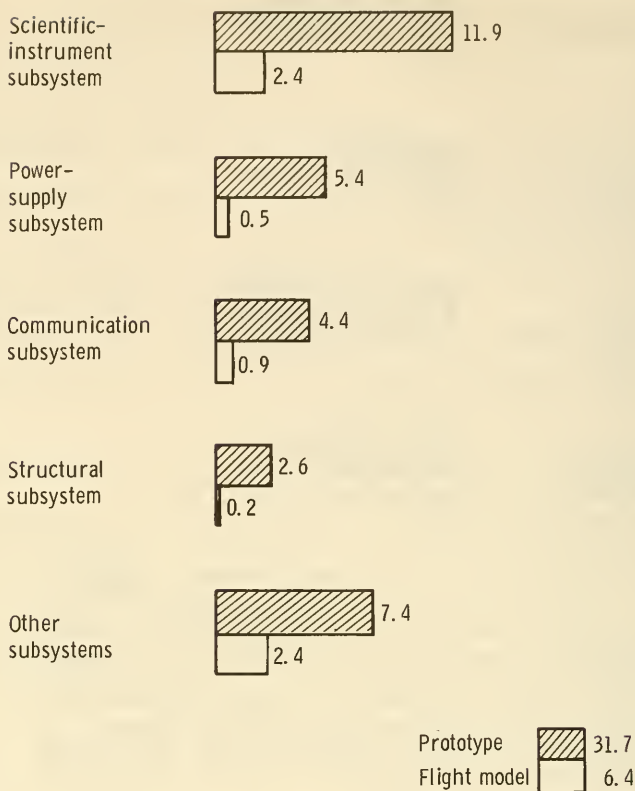
FIGURE 7-8.—Average numbers of problems encoun-
tered during the tests of several Explorer-class
satellites at Goddard Space Flight Center. In con-
trast to the generic categories of figure 7-7,
division here is on a subsystem basis (ref. 6).

to 100° C in the Goddard Space Environment Simulator. Simula-
tion of the Sun with collimated lamps bathes the satellite in ap-
proximately 1400 W/m² of radiation with the solar spectral
distribution.

The full spectrum of environmental test equipment in a well-
equipped facility is rather impressive. Figures 7-10 through
7-13 are included at this point to illustrate the sizes and variety
of equipment used by Goddard Space Flight Center for testing
their scientific satellites.

Even amid this abundance of test facilities, nowhere is outer
space simulated in all its complexity. Nor is time completely
simulated, save through intensifying the applied forces over and
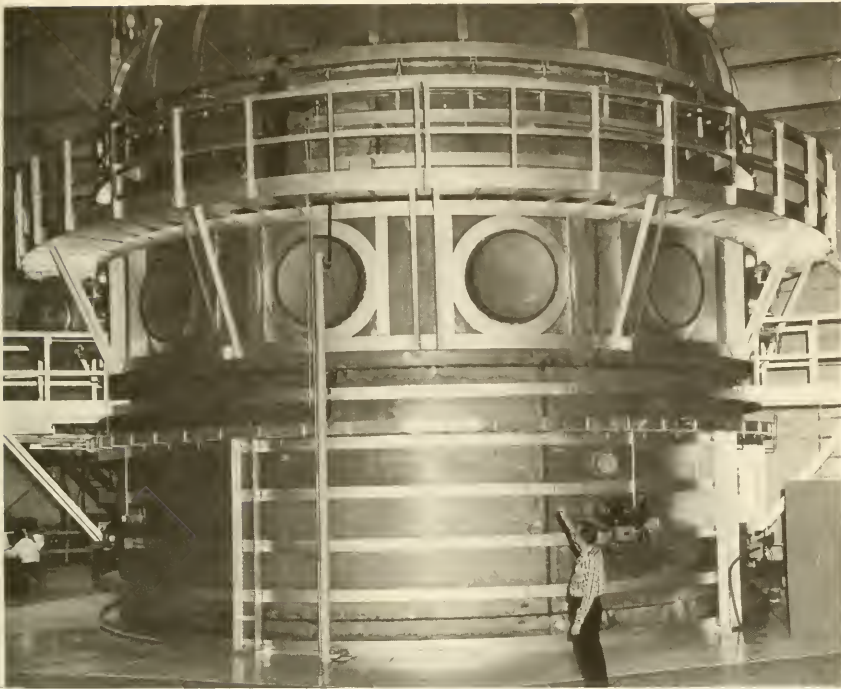
FIGURE 7–9.—The Dynamic Test Chamber at Goddard Space Flight Center used for conducting dynamic tests, such as solar-paddle erection, in a high vacuum.

above those actually expected. Despite such shortcomings, testing programs have helped give us a highly successful space-science program for a reasonable cost.

7–3.   Prelaunch Operations and Facilities

Scientific satellites are carried to their launch sites in specially built, sealed containers, usually by aircraft. When they arrive at the test range, they begin a new regimen of tests that continue right to the moment of liftoff. The major steps in the new test sequence are—

(1) Payload inspection for transportation damage and completeness of shipment

(2) Payload checkout

(3) Spin test and dynamic balance

(4) Mating to launch-vehicle final stage

(5) Installation of pyrotechnics

(6) Final checkout on the launch pad
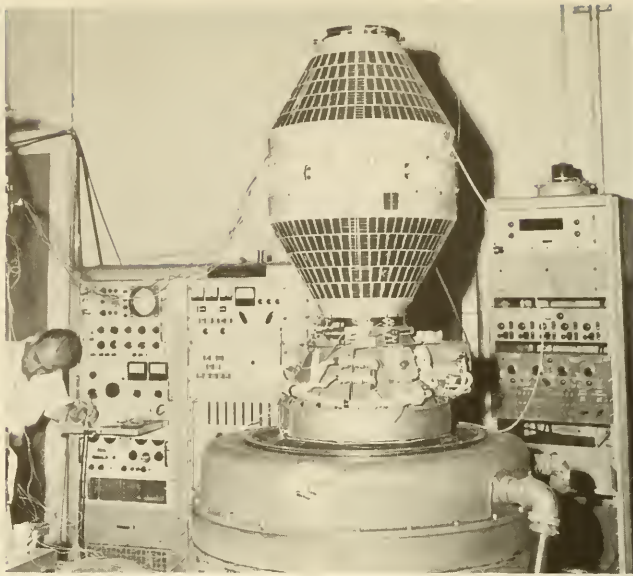
FIGURE 7–10.—Explorer XX undergoing vibration-table tests at Goddard Space Flight Center.
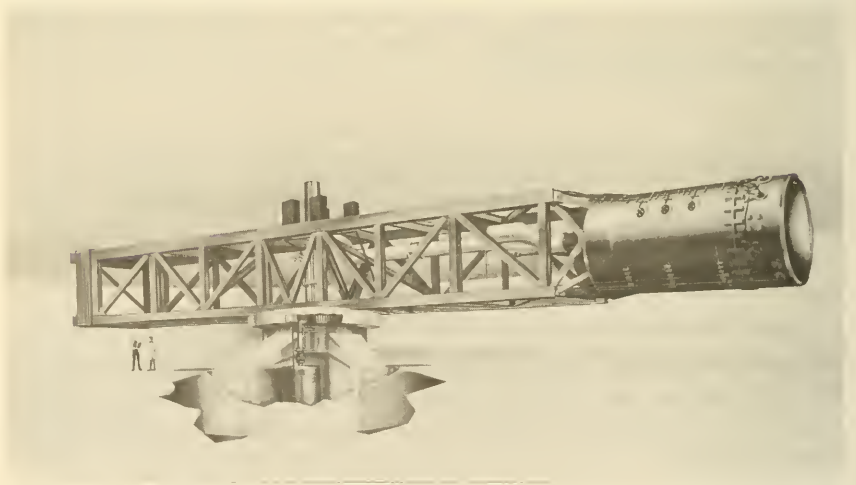
FIGURE 7–11.—The Launch Phase Simulator at Goddard Space Flight Center. This facility is capable of simulating simultaneously the acceleration, vibration, noise, and variable levels of vacuum for Observatory-class satellites.

FIGURE 7–12.—The Vertical Antenna Test Range at Goddard Space Flight Center. The radiation pattern of the satellite under test can be measured under conditions that are almost echo-free.

FIGURE 7–13.—The Magnetic Field Component Test Facility at Goddard Space Flight Center. The large external coils can null out the Earth's field, which, at sea level, is many times larger than the fields to be measured in space. Residual spacecraft fields can be mapped and instruments calibrated.

The term "checkout" is reserved for a special brand of testing carried out at the launch site. Some checkout tests are simple functional tests, but most are accomplished with the aid of electrical measurements and interrogating electronic signals. Launch-pad checkout is always automated to some extent. The implication for satellite design is that special electrical leads have to be brought out to test jacks so that the internal status of the satellite can be measured by computer-aided ground-support equipment. In some cases, the internal "status" measurements will be identical to those telemetered back to Earth during the mission.

All operations at the launch site are subjected to rigorous scheduling because the facilities, including downrange tracking stations as well as the launch pads, are heavily committed to military and nonmilitary space programs. Management controls are therefore more in evidence at the launch site than at other facilities.

Prelaunch Operations.—The objectives of prelaunch testing and checkout are:

(1) The identification and repair of faults that may have occurred since the flight-acceptance tests or that may have gone undetected until mating with the launch vehicle [5]

(2) Final checking and calibration of all satellite and Earth-based instrumentation

(3) Final verification and doublechecking of system operational readiness, including the Earth-based facilities themselves

A good (and interesting) way to describe prelaunch operations and the problems encountered during them is to list the highlights for a specific satellite. IMP II, which was launched from the ETR on October 3, 1964, is the satellite used as the example. In the following chronology, IMP's B and C are the two flight models. (IMP A was orbited as IMP I on November 26, 1963.)

Aug. 13 _____IMP B [6] arrives at ETR in a USAF C–118 aircraft and is placed in storage at GLO (Goddard Launch Operations) Hangar AE (fig. 7–14). Included in shipment were checkout racks, solar paddles, and radioactive sources for calibration.

Aug. 15 _____IMP checkout trailer leaves Goddard for ETR

Aug. 18 _____IMP checkout trailer arrives at ETR and setup operations begin

Aug. 26 _____Hurricane Cleo arrives. All operations suspended.

Aug. 28 _____IMP C, the backup flight model, is shipped to the ETR via commercial aircraft

---

[5] Launch operations are guided by formal Launch Operations Manuals and Payload Description Documents.

[6] Became IMP II or Explorer XXI after launch.
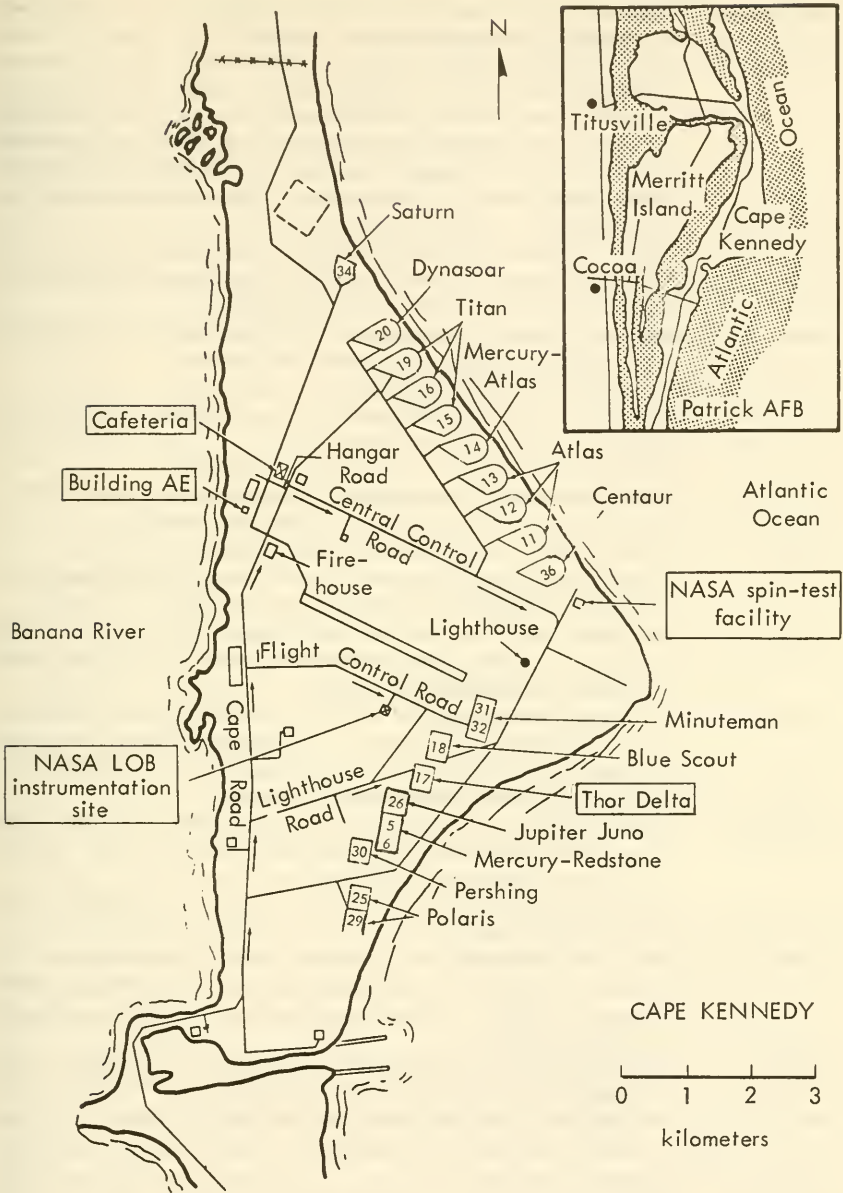
FIGURE 7–14.—Map of Cape Kennedy, showing the sites presently used by NASA for scientific-satellite programs.

Aug. 31 _____ Prelaunch operations begin with the checkout of both satellites. Defective battery cell found in IMP B, R versus dE/dx experiments in IMP's B and C interchanged. IMP-B magnetometer boom did not fully extend. Boom rough spot discovered and sanded. Coordination meeting disclosed that safety considerations required a 10-foot minimum separation between ground-support equipment on gantry and the X–258 final-stage, solid-propellant motor. IMP checkout cables permitted only an 8-foot separation.

Sept. 1 _____ IMP-C[7] antenna pattern, Range-and-Range-Rate System, and Rb magnetometer checked out at NASA Antenna Trailer Site

Sept. 2 _____ IMP-B checkout at Antenna Trailer Site

Sept. 3 _____ Further checkout of satellites. IMP-C programer card IG2–04 returned to Goddard for repair and retest.

Sept. 4 _____ Further checkout of satellites

Sept. 5 _____ IMP-C R versus dE/dx experiment removed and flown to University of Chicago for repairs

Sept. 8 _____ Hurricane Dora nearby. Equipment secured.

Sept. 14 _____ IMP B removed from storage. Checkout continues. IMP C now minus several components and experiments.

Sept. 15 ____ First stage of Delta launch vehicle erected on Pad 17A

Sept. 16 _____ Thermal ion-electron experiment calibrated; experimenter requested permission to install a new ion trap

Sept. 17 _____ No waiver could be obtained for short checkout cables. New cables, with the attendant risk of error, had to be made. Further checkout of spacecraft.

Sept. 18 _____ Final mechanical checkout of IMP B, including detailed inspection, vacuuming of interior, cleaning of mating surfaces. Nuts and screws were tightened and sealed, photographs taken, top cover "permanently" secured.

Sept. 21 _____ Complete dry run of IMP-B launch-pad checkout routine using countdown procedure. IMP-C checkout continues. Newly flight-qualified parts installed.

Sept. 22 _____ Newly qualified ion trap installed on IMP B. Thermal coatings touched up.

Sept. 23 _____ IMP-B R versus dE/dx experiment not functioning well. It was interchanged with IMP-C experiment. Wiring error found in IMP C. (Top cover had to be removed during all these changes.)

Sept. 24 _____ Spin-balance test for IMP B with dummy solar paddles. Rebalance after installation of flight paddles.

Sept. 25 _____ RF Systems and Acceptance Test on IMP C. Satellite could not be turned on from blockhouse owing to error in umbilical wiring.

Sept. 26 _____ IMP B mated to launch vehicle on launch pad. The E versus dE/dx experiment was not functioning properly and had to be removed.

Sept. 27 _____ E versus dE/dx experiment reinstalled on IMP B

Sept. 28 _____ An IMP-B All Systems Test was delayed 4 hours because of connecter problem in booster ground-support equipment

---

[7] Became IMP III or Explorer XXVIII after launch.

Sept. 29 _____Pyrotechnics installed on IMP B. An Oct. 1 launch window was received from Goddard. Foreign material found in launch-vehicle liquid-oxygen system. Launch date moved from Oct. 1 to Oct. 3.

Sept. 30 _____Dry run of spacecraft checkout

Oct.   3 _____IMP-B operations listed below:

0100_____Strip coat removal

0530_____Satellite checkout (for the 10th time). MIT plasma probe showed anomalous operation. Experimenter called in to troubleshoot.

0745_____Satellite Tracking Station reported spacecraft frequency and signal strength.

1447_____Protective covers removed from experiment sensors.

1453_____Solar-paddle installation begins. Hand-held Sun gun used to check out operation. Fairing installed. (See fig. 2–5.)

1748_____Vehicle destruct tests (simulated)

1813_____Data from all experiments recorded with no calibrating sources present

1825_____Satellite was deenergized, visually inspected for last time, ground-support equipment secured, all personnel cleared from the tower

2040_____Tower removed. Start of 90-min built-in hold.

2210_____T–35 min. Terminal count begins.

2214_____T–31 min. Satellite Tracking Station reported frequency to be 136.144955 Mc.

2221_____T–24 min. Range-and-Range-Rate System interrogated.

2235_____T–10 min. All 16 performance parameters measured as normal.

2236_____Magnetometer lamp temperature changed abruptly. Experimenter agrees to go ahead with launch despite abnormality.

2240_____T–5 min. Blockhouse power to satellite cutoff. Satellite operates on battery alone.

2245_____T–0 min. Engine start and liftoff.

The facilities that followed the satellite downrange and in orbit will be covered in the next section. Meanwhile, the portable checkout equipment, special ground-support equipment, and the backup satellite (assuming a successful launch of the first) must be packed up and shipped back to their points of origin. The launch pad must be cleaned and readied for the next shot on the agenda.

The preceding discussion has centered on the checkout of the satellite itself. While the satellite is undergoing these probing, diagnostic examinations in auxiliary buildings around the launch pad and, during the final stages, on top of the launch vehicle, it is surrounded by a host of other prelaunch operations concerned with the rest of the total system. The satellite, after all, is small in weight, volume, and complexity in comparison to the launch vehicle and Earth-based facilities. The booster rocket and each downrange tracking station must also be checked out and readied

for the mission. By way of illustration, a large launch vehicle may have thousands of electrical, pneumatic, fuel, coolant, and signal connections tying it by umbilicals to the blockhouse and its checkout equipment. In contrast, the number of connections for IMP B, whose launch was described above, is two orders of magnitude smaller. Checkout of the system-minus-satellite is so large a task that a computer is ordinarily enlisted to automate the process. (The acronym ''ACE,'' for automatic checkout equipment, is applied here.)

Launch-Site Facilities.—The most obvious endowments of a launch site are the launch pad, with its associated gantries and towers, and the nearby blockhouse.[8]

The United States uses only the following three sites for launching its scientific satellites:

(1) The ETR (Eastern Test Range), at Cape Kennedy, Fla.[9] Most scientific satellites are launched here.

(2) The WTR (Western Test Range), at Point Arguello, Calif. Polar-orbit scientific satellites are usually launched here, although they can be ''doglegged'' into polar orbit from the ETR by upper stage maneuvers.

(3) The Wallops Island, Va., site, where smaller satellites are launched by Scout and other solid-propellant rockets

The pertinent NASA facilities at the ETR, which is operated by the U.S. Air Force, include the LOB (Goddard Launch Operations Branch)[10] AE Hangar, or Spacecraft Assembly Building (fig. 7-14). This building holds the LOB offices, the Mission Control Center, and the telemetry and rf laboratories. Here, the satellites are assembled and checked out, using the satellite's special ground-support equipment. Launch complex 17 (fig. 7-14) has two pads with the necessary supporting gantries, a blockhouse, and an administrative and engineering building. NASA launches scientific satellites from complex 17 with Thor and Delta launch vehicles. Figure 7-14 also shows the location of the Spin Test Facility at the Cape, where NASA payloads are statically and dynamically balanced, alined, and accurately weighed prior to flight. NASA, in addition, operates a Satellite Tracking Station (STS) at the ETR, which provides prelaunch measurements of transmitter frequency and power level. The transmission and

---

[8] For a comprehensive description of all launch facilities, the reader is referred to the review articles by Sharpe (ref. 7).

[9] Collectively, the ETR and WTR are called the National Range Division by DOD.

[10] Also called GLO (Goddard Launch Operations).
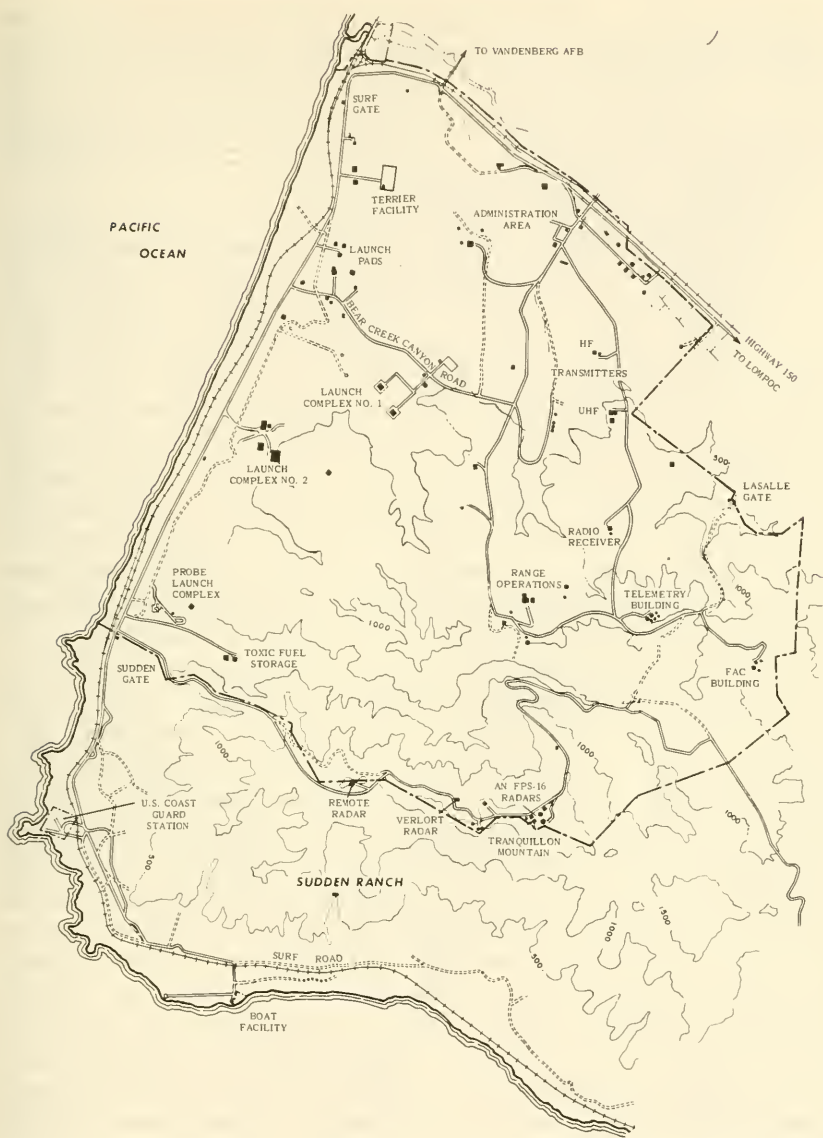
FIGURE 7–15.—Map of the Point Arguello, Calif., launch complex on the Pacific Missile Range.

reception of commands and data are also checked out by the STS. During launch, the STS produces real-time tracking and telemetry data for experimenters.

The Department of Defense also launches scientific satellites

from the ETR. Similar checkout equipment and facilities are available, but they are all connected with classified military programs. Most DOD scientific satellites ride piggyback into orbit on missile tests or alongside military satellites. Of course, the downrange and numerous on-site facilities are shared between the military and civilian agencies.

The primary mission of the USAF-run WTR is also military. Four different ranges are delineated: (1) The Sea Test Range, (2) the Ballistic Missile Range, (3) the Antimissile Range, and (4) the Polar Satellite Range. The last range, which is the only one of interest here, commences at Point Arguello, Calif. (fig. 7–15). NASA orbits polar satellites, such as POGO [11] and Explorers XXIV and XXV from the Point Arguello Complex, using Scouts and Atlas–Agena B's. This is the only convenient spot in the continental United States where a launch vehicle ascending directly to polar orbit will pass mainly over water—an important safety factor. Prelaunch and launch facilities at Point Arguello are analogous to those at the ETR (ref. 7). Altogether there are four launch pads, with associated blockhouses, gantries, and support buildings, at this particular WTR launch complex.

The Wallops Island facility is entirely NASA run (fig. 7–16). While its mission is predominantly one of research and development, DOD satellite launches and programs are occasionally undertaken there. Of the five launch sites located along the Virginia beach, only Launch Area 3 is equipped to launch the Scout rocket. Satellites such as San Marco 1 and Explorer XXIII have been placed in orbit from the Wallops site. Generally speaking, the Wallops-site prelaunch activities follow the lines of those at the ETR. Payloads are inspected, assembled, and checked out in one or more of several assembly shops located at the Wallops Main Base, which is several miles from the launch areas proper: A Dynamic Balance Facility (fig. 7–17), located on the shore just north of the launch areas, is used for spin-and-balance tests. When checkout is complete, the satellite is mated with the final stage of the launch vehicle and moved to Launch Area 3 (fig. 7–18).

7–4.   Postlaunch Facilities

Just prior to the moment of launch, the umbilical connections with the launch vehicle and satellite are severed. From that instant, the rocket and its payload are independent of Earth-based power, coolants, fuels, and other services. As the launch

---

[11] Polar Orbiting Geophysical Observatory.

FIGURE 7-16.—Map of NASA's Wallops Island, Va., facility.

FIGURE 7–17.—San Marco 1 and the Scout fourth stage undergoing a spin test at Wallops Island.

FIGURE 7–18.—Scout launch vehicle on pad in Launch Area 3 at Wallops Island.

vehicle ascends and pitches over toward the downrange sites, it is tracked by many optical and radar instruments located at the launch site and by the tracking stations as they appear over the horizon. Other tracking facilities will pick up the space vehicle as it moves downrange until it passes beyond Ascension Island (on the ETR) and the last tracking ship and approaches the African Continent. Once the satellite has been injected into orbit and separated from the last stage of the launch vehicle, the tracking and data-acquisition functions are assigned to one or more of

the worldwide tracking networks introduced in chapter 6. The operating principles of the various types of tracking equipment were explained in that chapter. Data-acquisition techniques were covered in chapter 5. In the present chapter, the geographical dispositions of the several networks and their major items of equipment are described.

Launch-Range Tracking and Data-Acquisition Facilities.—Some of the pertinent major equipment of the launch-range stations are tabulated below:

Eastern Test Range (ETR)

List of stations_____Cape Kennedy, Fla.; Jupiter Inlet, Fla.; Grand Bahama Island; Eleuthera Island; San Salvador; Mayaguana; Grand Turk Island; the Dominican Republic; Puerto Rico; Antigua; Fernando de Noronha; Ascension Island; and the mobile ARIS (Advanced Range Instrumentation Ships) (fig 7–19)

Major equipment_____Many types of tracking radars, including FPS–16, FPQ–6, MPS–25, FPS–43, FPS–44; continuous-wave tracking systems, such as MISTRAM (see ch. 6), AZUSA, GLOTRAC (Global Tracking Network, which was actually never installed on a worldwide basis), and UDOP (uhf Doppler); optical equipment includes ballistic cameras, cinetheodolites, and tracking telescopes; many varieties of telemetry receivers and antennas; and, finally, computers

Western Test Range (WTR)

List of stations_____Point Arguello, Calif.; Point Mugu, Calif.; San Nicolas Island, Calif. There are no fixed downrange stations for the Polar Satellite Range.
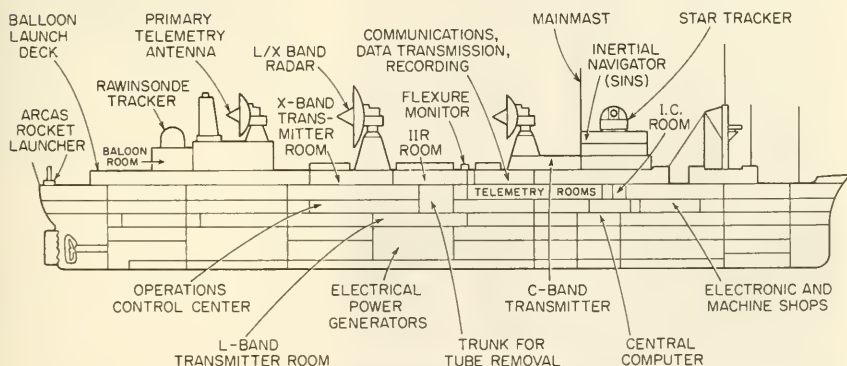
FIGURE 7–19.—Cross section of an ARIS ship.

Major equipment_____Many types of tracking radars, including FPS–16,
                    SCR–584/615, M33, and VERLORT. COTAR and
                    GERTS are continuous-wave precision tracking
                    radars similar to AZUSA and MISTRAM. There
                    are also the usual cinetheodolites, tracking tele-
                    scopes, telemetry receiving equipment, and com-
                    puters.

Wallops Island

List of stations_____None, except the launch facility itself.
Major equipment_____Tracking radars include FPS–16, FPQ–6, MSQ–1A
                    and SPANDAR. There is a DOVAP (Doppler ve-
                    locity and position) system installed at Wallops.
                    Fig. 7–20 shows a photograph of the Wallops 33-
                    element, high-gain telemetry antenna. Many types
                    of optical tracking apparatus and telemetry receiv-
                    ing equipment are also located at Wallops.
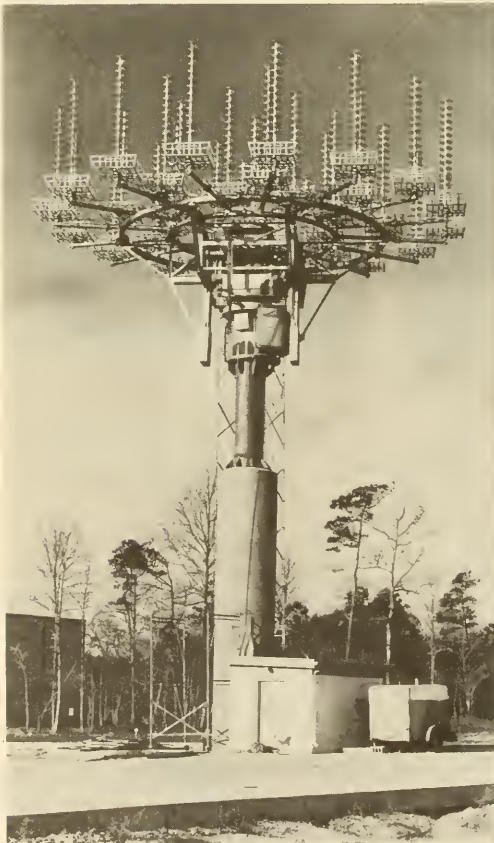
FIGURE 7–20.—The Wal-
lops Island 33-element
tracking and telem-
etry antenna.

Foreign Ranges

Russian satellites are launched from pads at either Kapustin Yar, about 50 kilometers from Volgograd; or Tyuratam, Kazakhstan, near the Aral Sea (lat. 45°38′ N, long. 63°15′ E). Sharpe has pieced together a surprising store of information about the Soviet sites (ref. 7). Little is known, however, about the types of equipment employed at these locations.

France launched the A–1 test satellite from its launch complex in Hammaguir, Algeria, in 1966. This base is being vacated for a new launch range, which commences in the northwest part of French Guiana, about 50 kilometers from Cayenne. Future French satellites will be launched from this spot.

Italy has built a well-publicized, towable launch platform, which is stationed in the Indian Ocean, for its San Marco program.

Japan plans to launch its MS–1 scientific satellite from a site within the country.

Few additional details are available about any of the foreign sites mentioned above.

Facilities for Tracking Satellites and Acquiring Data.—The United States tracked the first Sputniks, Explorers, and Vanguards with a complex of a dozen Minitrack interferometer stations arranged in a north-south "fence" in North and South America. Since then, satellite-tracking and data-acquisition networks have proliferated. There are, in fact, so many networks now in operation that it is best to adopt a tabular approach in describing them.

STADAN (Satellite Tracking and Data Acquisition Network)

STADAN is NASA's primary tracking network. It grew from the original Minitrack net as new equipment and stations were added to handle second- and third-generation satellites. The launching of synchronous, polar, and high-data-rate satellites did much to stimulate the evolution of the present STADAN network.

List of stations_____Blossom Point, Md.; College, Alaska; East Grand Forks, Minn.; Fort Myers, Fla.; Fairbanks, Alaska (Alaska and Gilmore sites); Johannesburg, Republic of South Africa; Lima, Peru; Mojave, Calif.; Quito, Ecuador; Rosman, N.C.; St. Johns, Newfoundland; Santiago, Chile; Winkfield, England; Woomera, Australia; Orroral Valley, Australia; Tananarive, Malagasy Republic; Carnarvon, Australia (fig. 7–21)[12]

---

[12] In all the older networks, there have been numerous changes of location and of equipment assignment.
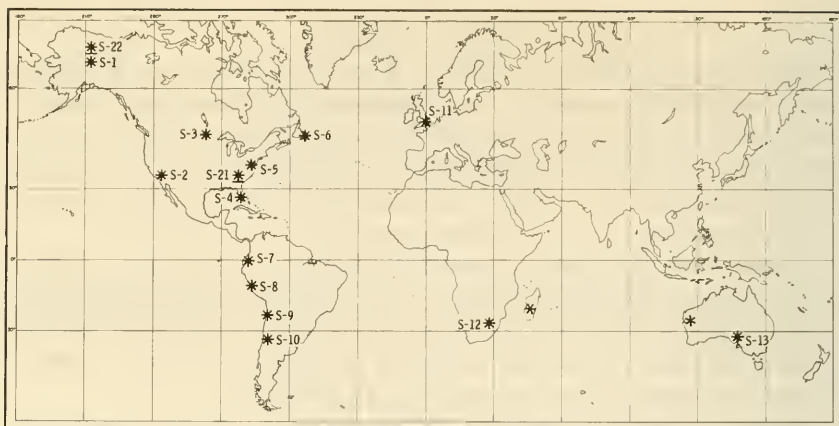
Station	Minitrack inter- ferometer	12-m dish	26-m dish	SATAN	R&RR[a]	Station	Minitrack inter- ferometer	12-m dish	26-m dish	SATAN	R&RR[a]
S-1 College, Alaska	x					S-10 Santiago, Chile	x	x		x	x
S-2 Mojave, Calif.	x					S-11 Winkfield, Great Britain	x				
S-3 East Grand Forks, Minn.[b]	x					S-12 Johannesburg, Rep. S.A.	x	x		x	
S-4 Ft. Myers, Fla.	x					S-13 Woomera, Australia[b]	x			x	
S-5 Blossom Point, Md.[b]	x			x		S-21 Rosman, N.C.			xx	x	x
S-6 St. Johns, Newfoundland	x					S-22 Fairbanks, Alaska			xx		x
S-7 Quito, Ecuador	x	x		x		Orroral, Australia	+		x	x	
S-8 Lima, Peru	x					Tananarive, Malagasy Rep.	+	+		+	x
S-9 Antofagasta (phased out)						Carnarvon, Australia[c]					x

[a]Range and Range Rate System.

[b]Will be phased out.

[c]Planned.

FIGURE 7–21.—NASA's STADAN network.

Major equipment_____Minitrack interferometers (fig. 7–22), 12- and 26-meter dish antennas (figs. 7–23 and 7–24), SATAN command and telemetry antennas, Range-and-Range-Rate equipment. For details on what stations have which equipment, consult Goddard Report X–530–66–33 and figure 7–21.

SAO Optical Network

Set up simultaneously with Minitrack, the Baker-Nunn cameras of the Smithsonian Astrophysical Observatory can track bright satellites with great precision at dawn and dusk. NASA funds the SAO.

List of stations_____Organ Pass, N. Mex.; Olifantsfontein, South Africa; Woomera, Australia; San Fernando, Spain; Tokyo, Japan; Naini Tal, India; Arequipa, Peru; Shiraz, Iran; Curaçao, N.W.I.; Jupiter, Fla.; Villa Dolores, Argentina; Maui, Hawaii (fig. 7–25)
Major equipment_____Baker-Nunn cameras (fig. 7–26 and fig. 6–8)

FIGURE 7–22.—Aerial view of the Minitrack station at Fort Myers, Florida. The interferometer arrays shown were moved from the Havana Minitrack station when it was dismantled, in 1959.
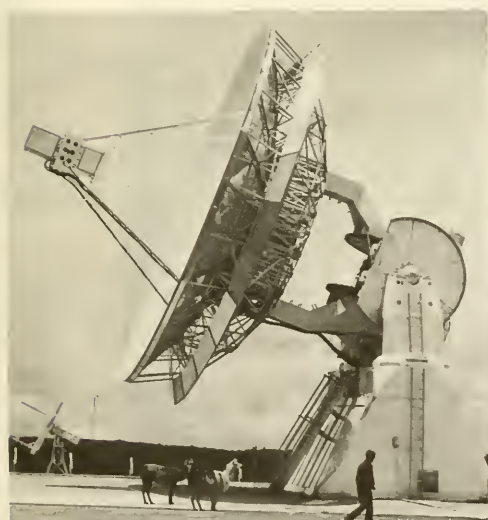
FIGURE 7–23.—The STADAN 12-meter (40-ft) telemetry receiving antenna at Quito, Ecuador.

TRANET (Transit Network)

TRANET is maintained by the U.S. Navy to support the Transit navigational-satellite program. Many scientific satellites with suitable Doppler beacons are also tracked; viz, Geos.

List of stations_____Howard County, Md.; Austin, Tex.; Las Cruces, N. Mex.; Lasham, England; San Jose dos Campos, Brazil; South Point, Hawaii; San Miguel, Philip-

pines; Smithfield, Australia; Misawa, Japan; An-
chorage, Alaska; Pretoria, Republic of South
Africa; Tafuna; Samoa; Thule, Greenland; Mahe,
Seychelles; Wahiawa, Hawaii; Point Mugu, Calif.;
Minneapolis, Minn.; Winter Harbor, Maine; Mc-
Murdo Sound, Antarctica (fig. 7–27)

Major equipment_____Doppler receivers
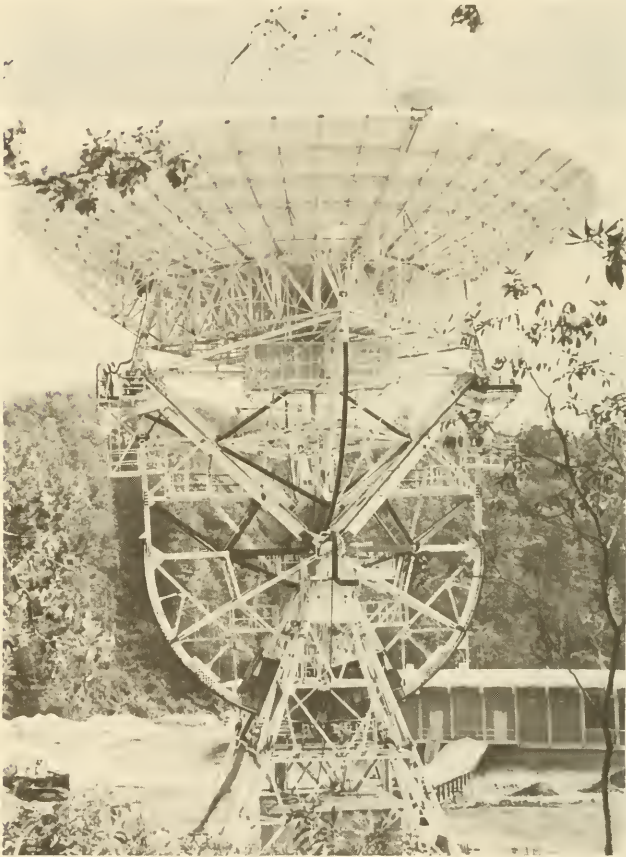
FIGURE 7–24.—One of the two 26-meter (85-ft)
STADAN telemetry antennas at Rosman, N.C.

SPASUR (Space Surveillance System)

This network consists of an east-west fence of active interfer-
ometer stations across the southern United States. SPASUR is
maintained by the U.S. Navy to keep track of all satellites and
pieces of debris.

List of stations_____Jordan Lake, Ala.; Fort Stewart, Ga.; Silver Lake,
Miss.; Gila River, Ariz.; Brown Field, Calif.; Ele-
phant Butte, N. Mex.; Lake Kickapoo, Tex.
Major equipment_____Transmitters to illuminate satellites, interferometers
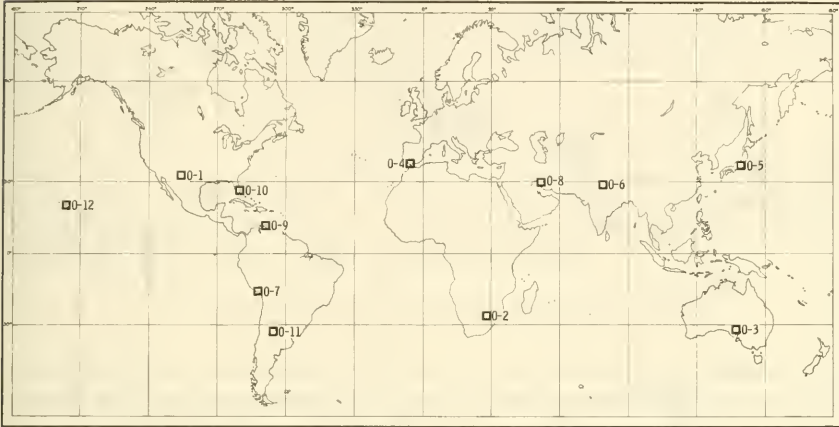
O-1 Organ Pass, New Mexico
O-2 Olifantsfontein, Rep. S. A.
O-3 Woomera, Australia
O-4 San Fernando, Spain
O-5 Tokyo, Japan
O-6 Naini Tal, India

O-7 Arequipa, Peru
O-8 Shiraz, Iran
O-9 Curaçao, Neth. W. I.
O-10 Jupiter, Florida
O-11 Villa Oolores, Argentina
O-12 Maui, Hawaii

FIGURE 7–25.—Map of the Baker-Nunn camera network run for NASA
by the Smithsonian Astrophysical Observatory.

FIGURE 7–26.—Baker-Nunn tracking camera in opera-
tion at the SAO site in Iran.

1. Anchorage, Alaska
2. Pretoria, South Africa
3. Tafuna, American Samoa
4. Thule, Greenland
5. Mahe, Seychelles
6. Wahiawa, Hawaii
7. Pt. Mugu, California
8. Minneapolis, Minnesota
9. Winter Harbor, Maine
10. McMurdo Sound, Antartica
11. A. P. L. (J. H. U.), Howard County, Md.
12. Austin, Texas
13. Las Cruces, New Mexico
14. Lasham, England
15. São Jose´ Dos Campos, Brazil
16. South Point, Hawaii
17. San Miguel, Philippines
18. Smithfield, Australia
19. Misawa, Japan

FIGURE 7–27.—Map of the U.S. Navy TRANET Doppler network.

U.S. Department of Defense (DOD) Complex

DOD maintains hundreds of radars, Baker-Nunn cameras, interferometers, and other equipment all over the world. The locations and capabilities of these instruments are classified. However, it is possible to identify here some of their major features. The National Range Division operates the ETR and WTR, which collectively possess enough sensors to track and acquire data from DOD scientific satellites. The National Range Division also operates the Satellite Control Facility (SCF) at Sunnyvale, Calif., which is sometimes referred to as SATNET. SATNET commands and controls military satellites, but does not track them. SPADATS is the acronym for the Air Force's Space Detection and Tracking System (formerly called Project Space Track). SPADATS is primarily a data processing and cataloging operation. SPADATS passes its information on to NORAD

(North American Air Defense Command) and, where pertinent, to NASA. Space Track is now the research arm of SPADATS.

SECOR Network

The U.S. Army presently has a system of 10 stations equipped with receivers and electronics capable of analyzing signals from SECOR (Sequential Collation of Range) transmitters in satellites. These stations are mobile.

Coast and Geodetic Survey Optical Network

For the purpose of acquiring better geodetic data, the U.S. Coast and Geodetic Survey maintains a number of stations equipped with Wild BC–4 tracking cameras.

French IRIS and DIANE Networks

France has independently set up the DIANE interferometer tracking network and the IRIS command-and-telemetry network. The primary purpose of these stations is to track and acquire data from French satellites, such as D–1.

List of stations_____Bretigny, France; Hammaguir, Algeria (to be transferred to Gran Canaria in 1967); Ouagadougou, Upper Volta; Brazzaville, Congo; Pretoria, South Africa

ESTRACK Network

ESRO (European Space Research Organization) is establishing an interferometer network to track their satellites; viz, ESRO 1, etc.

List of stations_____Netherlands, Alaska, Spitsbergen, Falkland Islands, Belgium

Other Networks

Italy is establishing a tracking and data-acquisition network to handle the satellites it launches from its platform in the Indian Ocean. Russia, of course, must have a relatively sophisticated complex of tracking and data-acquisition stations. The bulk of these must be on the Eurasian landmass, though tracking ships frequently supplement these fixed stations. Probably Russia relies heavily on Doppler tracking, since it does not possess the worldwide network of stations desirable for interferometry. Russia undoubtedly also tracks satellites and space debris with the equivalents of the U.S. SPASUR and BMEWS radars.

Data-Archiving Facilities.—The scientific data received from NASA satellites alone now fill several thousand rolls of magnetic tape each week. In chapter 6, the techniques for processing these tapes and turning their data into manageable records for the experimenters were discussed. Such data-processing facilities consist primarily of computer production lines, such as NASA's STARS. In the remainder of this chapter, the problems of archiving and retrieving these data upon command are discussed.

Early in the days of the IGY, scientists had to face the problems of handling and integrating disparate data from all points of the compass. To facilitate the handling of IGY data, World Data Centers were established at the U.S. National Academy of Sciences, in Washington, D.C., and the Akademia Nauk, Moscow. These two centers were labeled "World Data Centers A and B" (WDC-A and WDC-B). A third data center has recently been set up in Japan. This early apparatus has been overwhelmed by satellite and sounding-rocket activities far greater than that foreseen in 1956. Today, there is no international, comprehensive mechanism for collecting, cataloging, and disseminating space data. To be sure, scientific results from satellite research reach the scientific community through the open literature and informal channels between specialists. Some supranational agency is still needed, however, to collect, store, catalog, and loan all raw space data (not reduced or interpreted data) on a systematic basis. It is hard enough for an individual to keep track of all the satellites in orbit, much less the kinds of data they telemeter to Earth.

NASA has taken a step toward systematic data collection and archiving through its formation of the NASA Space Science Data Center at Goddard Space Flight Center, in April 1964. The Center is responsible for the collection, organization, indexing, storage, retrieval, and dissemination of all scientific data resulting from NASA-sponsored experiments in space and the upper atmosphere. Data from DOD and foreign scientific satellites are included when made available.

The most significant policies of the Space Science Data Center are:

(1) Experimenters on NASA spacecraft have exclusive rights to their data for the limited period of time specified in their contracts. Data then become part of the public domain. Experimenters also have an obligation to analyze their data and publish the results. (See ch. 10.)

(2) All reasonable requests to obtain data will be met at mini-

mum cost; data will usually be in tabular form, on graphs, or, most probably, on magnetic tape

(3) Data will be listed in semiannual catalogs with indication of its availability

(4) The Center will *not* archive report literature—an assigned function of NASA's Scientific and Technical Information Facility

(5) Working facilities will be provided at the Center to encourage use of the data by the scientific community

(6) Center data will not be made available to foreign scientists, except those with experiments on American spacecraft, in accord with international agreements. The World Data Centers perform this function.

References

1. BOECKEL, J. H.: The Purposes of Environmental Testing for Scientific Satellites. NASA TN D–1900, 1963.
2. TIMMINS, A. R.; AND ROSETTE, K. L.: Experience in Thermal-Vacuum Testing Earth Satellites at Goddard Space Flight Center. NASA TN D–1748, 1963.
3. BURRILL, E. A.: Simulating Space Radiation. Space/Aero., vol. 40, May 1964, p. 78.
4. NESWALD, R. G.: Space Simulation—How Far To Go. Space/Aero., vol. 45, Mar. 1966, p. 65.
5. GERTEL, M.: Vibration and Shock Testing. Space/Aero., vol. 42, Sept. 1964, p. 191.
6. NEW, J. C.: Experiences in Simulating the Space Environment for Scientific Satellites. NASA TM X–55120, 1964.
7. SHARPE, M. R.; AND LOWTHER, M.: Progress in Rocket, Missile, and Space Carrier Vehicle Testing, Launching, and Tracking Technology. *In* Advances in Space Science and Technology, vols. 6–7, F. I. Ordway, ed., Academic Press, 1964 and 1965.

Chapter 8

SATELLITE LAUNCH VEHICLES

8-1. Prolog

One cornerstone of any satellite research program is a reliable, low-cost launch vehicle, or, even better, a family of such vehicles, with a range of payload capabilities tailored to the planned missions. The "stable" of U.S. satellite launch vehicles extends from the relatively small, solid-propellant Scout rocket, with orbital payloads of 50–150 kilograms, to the immense, liquid-fuel Saturn-class rockets, which can orbit 100 times the Scout payload. Russia presumably possesses a similar array of launch vehicles. France has developed the Diamant satellite launcher, and the ELDO satellite launch vehicle (Europa 1) will soon be available to the countries that make up the European Launcher Development Organization.[1] In section 8–6, the "workhorses" in these "stables"—to use the rocket vernacular—are described in more detail.

The anatomy of a typical launch vehicle is outlined in figure 8–1. The first stage is properly called the "booster," although the term is frequently applied to the entire launch vehicle. The term "launch vehicle" does not include the spacecraft (the satellite, in this case), even though the final stage of the launch vehicle occasionally goes into orbit as an integral part of the spacecraft; viz, Explorer XVI and OV–1.

A rocket for attitude control may be no bigger than one's hand, while launch vehicles in the Apollo program stand several stories high on the launch pad. Regardless of their size, all present-day launch vehicles have these elements in common:

---

[1] The ELDO countries are: Great Britain, Germany, France, the Netherlands, Italy, and Belgium.
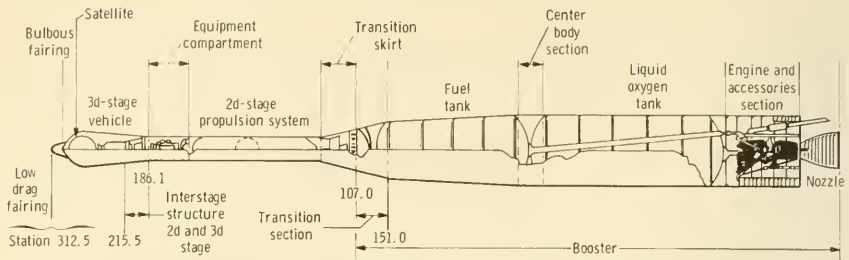
FIGURE 8–1.—Inboard profile of the Delta launch vehicle. The first stage consists of a modified Thor booster, using LOX and RP–1 (kerosene). The second stage uses unsymmetrical dimethylhydrazine (UDMH) and inhibited red fuming nitric acid (IRFNA). The third stage uses a solid-fuel motor.

(1) A chemical rocket engine, which burns a fuel and an oxidizer to generate large volumes of hot gases that produce, in turn, a thrust when expanded through a nozzle

(2) The fuel and oxidizers, stored either in tanks connected to the engine by pumps or a pressurized feed system (liquid rockets), or as integral solid-propellant grains (solid rockets)

(3) A structure that supports the engine and reservoirs on the launch pad and during flight

(4) A guidance-and-control system that stabilizes the launch vehicle and keeps it on the calculated trajectory

Even though the launch vehicle has a transitory existence, lasting but a few minutes, it exerts several powerful influences on satellite design. First, there is the fact that launch vehicles are quantized in size and payload-carrying capability. Scientific payloads are almost always molded to fit one of the extant launch vehicles. Economics rarely permit an alternative course.

Other launch-vehicle constraints exist, too. The launch environment is a tough one, which challenges both experimenter and satellite designer. Shock, vibration, and thermal forces are imposed on the satellite across the many interfaces it temporarily shares with the launch vehicle. The interface diagram (fig. 8–2) illustrates the most important of these interfaces. The mechanical interfaces are the most sensitive; ruggedness in satellite design is a virtue and a necessity.

Launch vehicles constitute quantized building blocks that are calculated to handle a wide spectrum of payloads. The building blocks are not rigid, though. The basic launch vehicles are continually being uprated by improvements to the various stages, better engine design, and the use of more energetic fuel-oxidizer

FIGURE 8–2.—Interface diagram showing the more important relationships between the launch vehicle and the rest of the satellite system.

combinations. A technique that helps fill in the blank spots that occur in the payload spectrum between the basic launch vehicles is that of "stage shuffling." That is, launch-vehicle stages are interchangeable to some degree. Various combinations of second, third, and fourth stages can be made with the help of adapters and transition stages.

History shows that solid-fuel rockets, which held sway from antiquity until the V–2, succumbed at first to the higher specific impulses of the liquid-chemical fuels used in the V–2, Atlas, and Titan. However, today's inventory of satellite launch vehicles illustrates a resurgence of solid-fuel rockets in the Scout, the Titan-3 strap-ons, and the upper stages of most launch vehicles,

as exemplified by the ubiquitous X–258. The solid-liquid con-
troversy has been with us for many years now, with both sides
claiming legitimate advantages. At the moment, liquid-fuel
rockets are the best developed, and they are readily available for
launching large satellites, though some design studies show them
to be more complicated and costly than comparable solid-fuel
rockets. Liquid fuels are undeniably more energetic than solid
fuels, yielding more payload for a given gross weight on the
launch pad. For the next decade or two, it appears that our satel-
lite launch-vehicle stable will boast both breeds, as well as hybrids
of the two (ref. 1).

8–2.   Launch-Vehicle Performance

The launch vehicle's role as the prime mover in the overall satel-
lite system makes it all the more susceptible to the figures of merit
discussed in chapter 3. The launch vehicle must not unduly
compromise system reliability or cost—factors that are relatively
easy to relate to launch-vehicle performance.

Launch-vehicle reliability can be found empirically by dividing
the number of launch successes by the total number of attempts.
This factor, plotted in figure 8–3, is a good indicator of the state
of the art for space-vehicle launching, at least in the United
States. Similar plots could be constructed for each of the 20-odd
launch vehicles employed to orbit scientific satellites; generally
they show the same shape as the composite graph, reaching a
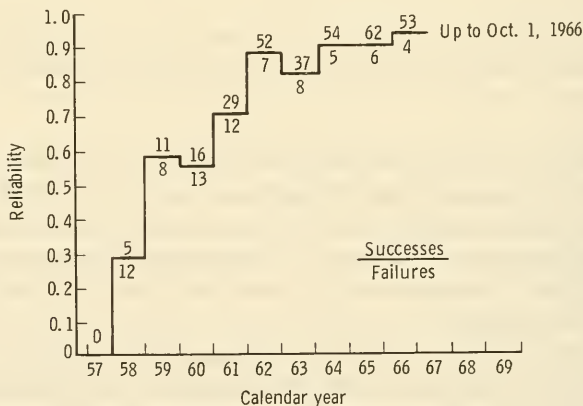
Figure 8–3.—Reliability of launch vehicles in the
U.S. space program. Military launch vehicles
are included only when used for space vehicles.
(Data source: TRW Systems' *Spacelog*.)

reliability plateau in about 5 years. The reliability improvements shown since 1957 have brought launch-vehicle technology the highest level of reliability that is attainable without undue development and launch-vehicle costs. In other words, additional launch-vehicle reliability would cost more than the benefits it would bring are worth.

Launch-vehicle costs can be projected from assumptions about materials, fabrication methods, and, most important of all, the number of launch vehicles to be constructed. The estimated cost per kilogram in a 500-kilometer orbit plotted in figure 8-4 shows
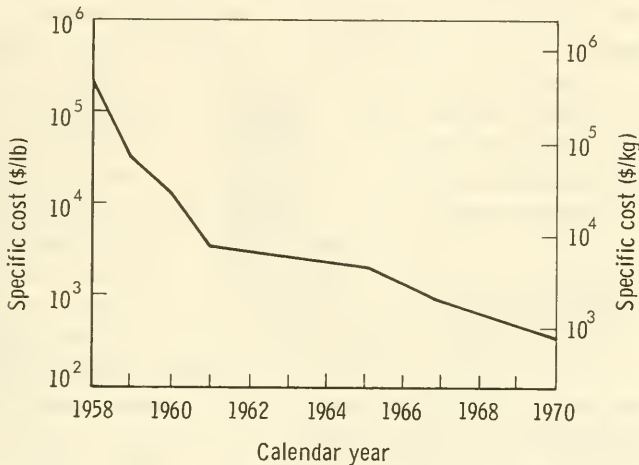
FIGURE 8-4.—Approximate cost of placing payloads into 500-kilometer orbits. Costs have decreased three orders of magnitude since the Juno-I launches of 1958 (ref. 2).

a downward cost trend. In one sense, this curve is misleading for scientific satellites, because it incorporates data for big launch vehicles like the Saturn V, which will probably never be regularly used for unmanned scientific satellites.[2] Present Scout and Delta costs are $8 000–$10 000/kg for low orbits. The trend shown in figure 8-4 amounts to an order-of-magnitude reduction of costs between 1960 and 1970. The big launch vehicles reduce costs by putting more payload into orbit per shot. Small launch vehicles have reduced manufacturing costs with their higher production rates. There is also the possibility that scientific satellites may

[2] Fifty-ton experiments are conceivable, e.g., bubble chambers; and they might be orbited in lieu of ballast on test shots.

be launched at reduced cost by using ICBM's that are retired from service.

Two popular subjects should be discussed in the cost context: booster recovery and nuclear energy. Scientific satellites will only rarely employ the very large boosters, such as the Saturns I, I–B, and V, where many claim it makes sense economically to recover and refurbish the first stages. In other words, if recoverable boosters are ever built, the resulting cost savings will not help small, unmanned satellite costs much. Scientific-satellite sizes are also generally incompatible with the capabilities of nuclear-fuel launch vehicles, which must be made relatively large if they are to compete in cost with chemical-fuel stages.

Summarizing the cost picture: scientific-satellite costs will gradually decrease from roughly $8000/kg today to perhaps $1000/kg in the middle 1970's. Booster recovery and nuclear rocket stages are not likely to affect this picture greatly.

In rocketry, there has always been intense pressure to shave the last bits of excess weight off the launch vehicle and its payload. In 1958 and 1959, when U.S. launch vehicles could barely struggle into orbit with a few kilograms of payload, this was understandable. Lightweight design was unequivocally essential to mission success. With the large, reliable rockets now in our inventory, lightweight design is associated with the degree, rather than the fact, of success. A kilogram saved on the payload means another kilogram available for experiments. A kilogram saved on the launch vehicle means perhaps 10 grams in extra payload. But even 10 grams are useful on a payload where a redundant resistor or transistor increases the probability of success.

It is, in fact, impossible to measure the real worth of an extra kilogram of payload. The worth conundrum was discussed in chapter 3, where the lack of, and even the impossibility of, an agreed-upon overall figure of merit was pointed out. There is no meaningful measure of the scientific worth of a kilogram of additional instrumentation. It might, in a specific case, be better to incorporate an extra kilogram of housekeeping instrumentation to tell designers how to construct better satellites in the future.

Good design of a specific launch vehicle-satellite combination demands insight and intuition at best. The optimization of an entire scientific-satellite program, involving hundreds of launch vehicles and large-scale, esoteric tradeoffs between costs, weights, staging, and reliabilities, requires even more perspicacity, with perhaps a touch of the occult.

8–3.   Types of Launch-Vehicle Propulsion Systems

Most of the volume of any launch vehicle is occupied by large fuel and oxidizer tanks.   Turbine-driven pumps expel the tanks' contents into the comparatively small appendage at the bottom of the rocket stage called the rocket engine. Here, the chemicals are burned in a combustion chamber to create large volumes of hot gases (figs. 8–5 and 8–6).   The hot gases are then expanded
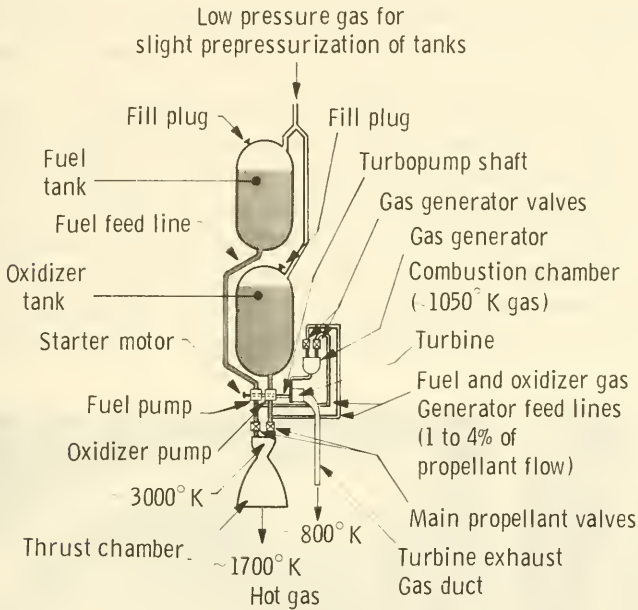
FIGURE 8–5.—Schematic of a pump-fed liquid-chemical rocket engine.   In many liquid-fuel engines, the nozzle is cooled by LOX before combustion takes place.

through a nozzle, producing a thrust on the flared sides of the nozzle and doing mechanical work on the launch vehicle.

A good rocket engine generates a large amount of thrust for each kilogram of mass consumed.   The performance parameter measuring this essential factor is specific impulse, defined by

$$I_{sp} \equiv F/g_0 \dot{m}$$

where

$F =$ thrust (newtons)
$I_{sp} =$ specific impulse (sec)

g_0 = the acceleration due to gravity at the Earth's surface (9.8 m/sec^2)

$\dot{m}$ = the mass flow rate of the rocket fluids (fuel plus oxidizer, in the case of the chemical rocket) (kg/sec)

Since the thrust of the rocket engine in empty space is simply $\dot{m}v$, where v = the exhaust velocity

$$I_{sp} = v/g_0.$$

The value of the high specific impulse is that the rocket's fuel and oxidizer tanks are not drained as rapidly at a given thrust level as they are at lower specific impulse.

For the so-called heat engine, a class including all liquid- and solid-chemical engines and the heat-transfer nuclear rocket as well, specific impulse is proportional to $\sqrt{T/M}$, where T = the combustion-chamber temperature and M = the mean molecular weight of the exhaust gases. Most liquid rocket engines use kerosene or the closely related RP–1 and RJ–1 fuels. When burnt with oxygen, these fuels produce a sea-level specific impulse of about 300 seconds. Better fuels (hydrogen) and better oxidizers (fluorine)
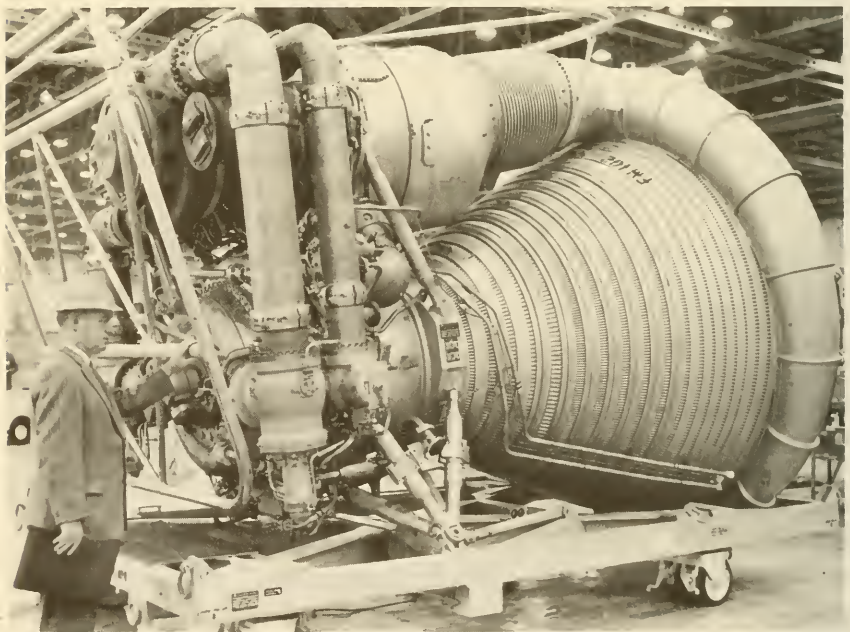
FIGURE 8–6.—Side view of an F–1 engine mockup. The F–1 is used on the Saturn S–IC stage. Note the size and the complex plumbing.

are now reaching development status (table 8–1). These chemicals not only evolve more heat per kilogram consumed but also produce exhaust gases with lower average molecular weights.

TABLE 8–1.—*Characteristics of Some Rocket Engines* [a]

Engine designation	Thrust, kg (lb)	Fuel	Oxidizer	Sea-level I_{sp}, sec [b]	Typical launch vehicle [c]
V–2 engine	25 000 (56 000)	Alcohol	LOX	279	V–2.
MA–3	82 000 (180 000)	RP–1	LOX	300	Atlas.
H–1	85 000 (188 000)	RP–1	LOX	300	Saturn I.
RL–10	6 800 (15 000)	LH	LOX	391	Centaur.
HF engine	------------	LH	LOX	410	
Titan–3 strap-on.	454 000 (1 000 000)	Synthetic rubber polymer.	Ammonium perchlorate.	----------	Titan 3
X–258	2 810 (6 180)	--------------	---------------	----------	Scout, Delta.

[a] The numbers in this table may change during an engine's development and will vary with engine model number.

[b] Actual specific impulses vary with altitude and engine type. Values shown were computed for a chamber pressure of 70 atmospheres, shifting equilibrium, and optimum sea-level expansion.

[c] See table 8–4 for details.

The engines listed in table 8–1 illustrate the progressive improvements in specific impulse attained by changing from alcohol fuel (in the V–2) to RP–1 (kerosene), and, finally, to liquid hydrogen (LH) in the RL–10. Eventually fluorine may replace oxygen as the oxidizer in chemical engines, but a great deal of development work remains before fluorine sees operational use. The concept of "floxing," or adding liquid fluorine to liquid oxygen (LOX), will see operational use before pure HF engines. The payloads of Atlas-based launch vehicles could, for example, be increased 10–30 percent through floxing. Tripropellants also offer significant increases in performance (table 8–2).

Despite the attractiveness of new propellant combinations, at least 5 and as many as 10 years must be assigned to research, development, and testing before a new engine can be incorporated in operational launch vehicles.

TABLE 8–2.—*Specific Impulses of Advanced Propellants*

Propellant	Sea-level specific impulse, sec
Tripropellants:	
F_2-H_2-Li	435
O_2-H_2-Be	457
O_3-H_2-Be	473
Cryogenic propellants:	
F_2-N_2H_4	364
OF_2-B_2H_6	365
O_2-H_2	391
F_2-H_2	411
Metallized storable propellants:	
N_2O_4-N_2H_4+Al	303
H_2O_2-N_4H_4+Be	335

Liquid-Chemical-Fuel Engines.—Liquid-chemical fuels supply much higher specific impulses than solid fuels, but at a price of greater engine complexity, higher costs, and more difficult ground-handling problems. The higher specific impulses have been well worth the price until recently, when large production runs of small rockets (Scouts) and the sheer size of boosters in the Apollo program have forced a reexamination of the cost and reliability tradeoffs.

The liquid engine proper consists of a forest of pipes and valves, turbine-driven pumps for the fuel and oxidizer, a combustion chamber, and a convergent-divergent nozzle (fig. 8–6). Usually, small portions of fuel and oxidizer are bled off from the main streams to energize a small gas turbine that drives the fuel and oxidizer pumps.[3] In essence, there are two combustion chambers —the smaller one powering the pumps for the bigger one (fig. 8–5). After passing through the pumps, the fluids are often directed through cooling passages that line the engine nozzle. This is called regenerative cooling. The fuel and oxidizer finally enter the combustion chamber through injector nozzles that spray the streams in a pattern that promotes steady burning. The hot combustion products are compressed in the convergent section of the nozzle, become supersonic in the throat area, and expand isentropically in the divergent section of the nozzle. The engine thrust is produced by the reaction force of the gases leaving the engine.

Some aspects of liquid-engine design are really more of an art

---

[3] This procedure is called "bootstrapping."

than a science. Combustion instability, for example, is most often cured by exhaustive testing and manipulation of chamber and injector design through trial and error. Experience gained in working the bugs out of one engine will not necessarily be applicable to another. Engine combustion is a far from exact science in both liquid and solid rockets (ref. 3).

Solid-Fuel Rocket Engines.—The venerable history of solid-fuel rockets began centuries ago with the Chinese toy and war rockets. A huge technological gap separates their simple powder-filled tube from the many-ton "grains," 3 meters in diameter, that are strapped on the Titan-3 booster.

Like their liquid allies, solid rockets terminate with a convergent-divergent nozzle, where the thrust is generated by the force of expanding hot gases. The hot gases, in this case, are now produced at the burning wall of a huge solid-propellant grain (fig. 8–7). No pumps and associated plumbing are necessary.
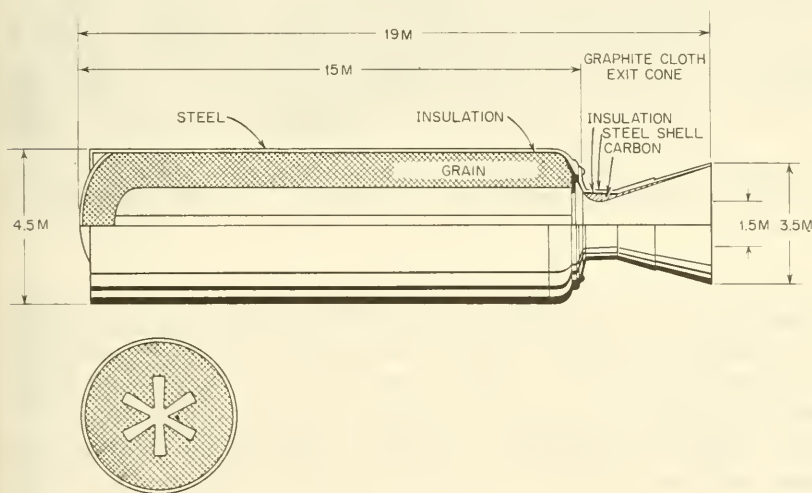
FIGURE 8–7.—Drawing of a large solid-chemical rocket motor. The thrust of a motor of this size would be about 500 000 kilograms.

The relatively flimsy fuel tanks and oxidizer tanks of the liquid rocket are replaced by a strong casing that must contain the high pressures stemming from the fiercely burning fuel grain.

One of the major accomplishments of solid-rocket technology has been the design and manufacture of large, strong, lightweight

FIGURE 8–8.—A solid-propellant rocket-motor case segment being wound with glass-fiber filament. (Courtesy of United Technology Center.)

pressure shells. Filament-wound casings (fig. 8–8) have proven to be stronger per unit weight than massive metal shells. Another design problem of solid rocketry was created by the erosion of the nozzle throat by the hot, reactive, particle-laden combustion products. Ablative materials, like those installed on missile nose cones, now line the throat areas of most solid rockets.

Originally, solid-fuel rockets burned inward along the rocket axis from the exposed end. Modern rocket-propellant grains have a central hole made in the shape of a star or some other reentrant pattern (fig. 8–9). By shrewd design of the grain's transverse cross section, thrusts can be made constant in time, or time-increasing, or varied in almost any desired way.

While liquid engines can conveniently control the direction of the thrust vector by gimbaling the combustion chamber and nozzle, the solid rockets must rely upon vanes or tabs in the gas stream, or the injection of peripheral gas streams that deflect the
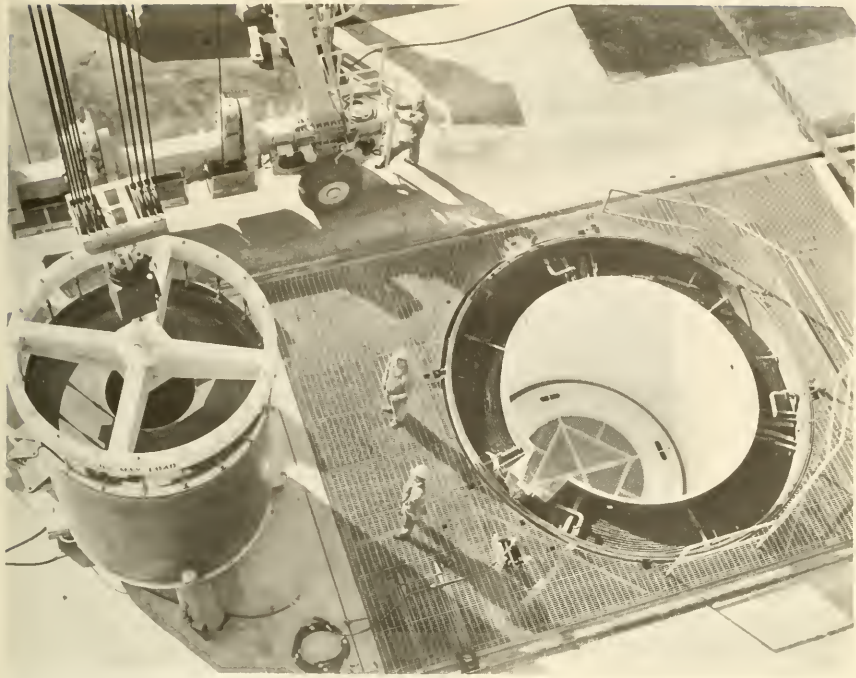
FIGURE 8–9.—A large solid-propellant grain is shown at the left. Several of these stacked together in a casing could make a launch vehicle of impressive size. (Courtesy of United Technology Center.)

stream of combustion gases in the proper direction, or, as on Scout, external control rockets. Extinguishing and restarting solid rockets also turn out to be tough problems. There are no fuel and oxidizer valves to close and open on the solid rocket.

Solid fuels are continually being improved through the discovery of more energetic chemical reactions. The incorporation of metal additives, such as beryllium and lithium, has been notably successful.

Perhaps the most intriguing frontier in propulsion research concerns the so-called hybrid engine, in which the fuel is retained in solid form and the oxidizer is stored separately as a liquid (ref. 4). In equilibrium operation, the oxidizer (LOX, in most research programs) is pumped into the chamber where combustion occurs, as portrayed in figure 8–10. The hybrid engine possesses much of the simplicity of the solid rocket, and better combinations of fuel and oxidizer can be selected to enable it to reach higher specific impulses. Separation of the fuel and oxidizer is an important safety feature.
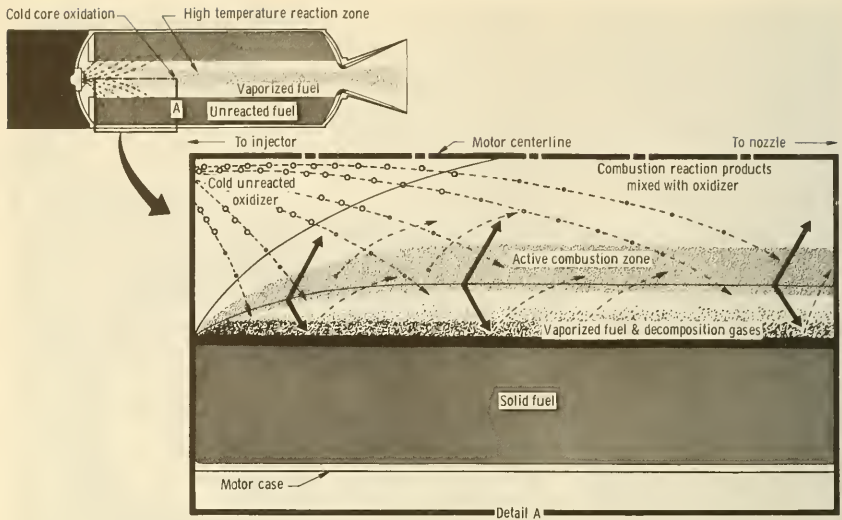
FIGURE 8–10.—Combustion process in a hybrid rocket. Once combustion is triggered, the heat of reaction decomposes and vaporizes the solid fuel, which then reacts with the incoming oxidizer. Heavy arrows show the heat flow (ref. 4).

Solid and liquid rockets are always in competition with one another for space missions. The contest has been somewhat one-sided until a few years ago. Liquid engines, because they were applied to space missions first, now do some jobs that solids might do better. At present, solid rockets seem dominant in the following areas:

(1) Launch-vehicle upper stages smaller than 2000–3000 kilograms where solids, by virtue of their better mass ratios—i.e., a higher weight percentage of fuel—are more efficient

(2) In small, long-production-run launch vehicles, where solids are sometimes—but not always—cheaper than their liquid counterparts

(3) As strap-on stages that uprate or, in the case of Titan-3, substantially increase the first-stage thrust

(4) In military rockets, where storability and fast reaction time are essential

Note that solid rockets are not necessarily more reliable than liquid rockets, nor are the impulses they deliver any easier to predict and control.

Gun Launchers.—For several years, the United States and

Canadian Governments have been jointly funding a program investigating the capabilities of large guns for launching high-altitude probes and satellites. The High Altitude Research Project (HARP) is the major effort. HARP is conducted by McGill University and the U.S. Army Ballistic Research Laboratories.

FIGURE 8–11.—A rebored, 16-inch Navy cannon used for firing high-altitude research probes from Barbados Island, B.W.I. Small satellites could also be launched with such a gun.

Under HARP, many small Martlet probes have been fired to altitudes above 200 kilometers with 5- and 7-inch guns. The guns, in essence, serve as the (reusable) first stage of the launch vehicle. Small solid rockets within the projectile accelerate the probe and its contained instruments to its final velocity.
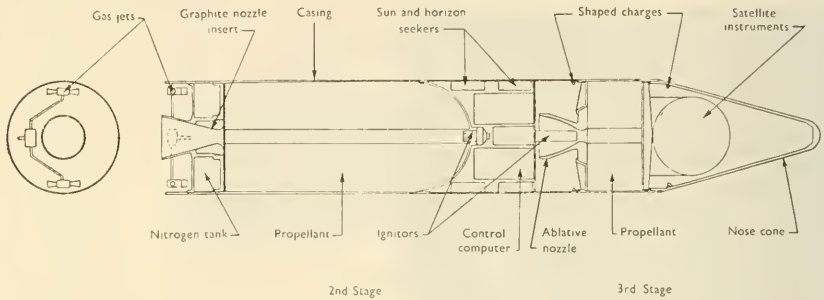
FIGURE 8–12.—Second and third stages of a gun-launched satellite-carrying projectile. The first stage (not shown) consists of a solid rocket and fins that deploy once the projectile is clear of the gun. Diameter is roughly 40 centimeters (16 in.) (ref. 6).

While guns were considered for satellite launching early in the Space Age (ref. 5), they never attracted much serious attention until the obvious successes of the HARP program came along. Now, satellite launchings are being planned using a rebored 16-inch, World War I Navy cannon, presently set up on the island of Barbados (fig. 8–11). A possible projectile design is presented in figure 8–12 (ref. 6). If satellite components are found capable of withstanding the 150-g acceleration of a gun launch, a new, economical way of propelling small satellites into orbit may be in the offing. The upper limit to the size of such satellites would be about 50 kilograms, unless larger-bore cannons can be acquired.

8–4. Launch-Vehicle Technology

A launch vehicle is, of course, more than just the engines and their fuel reservoirs. There are also a supporting structure and a guidance-and-control system. Furthermore, underneath the monolithic, cylindrical exterior of the launch vehicle are miles of pipes and wiring, a multitude of valves and transducers, and large complements of gyros and servos. The design of the launch vehicle is obviously a major technological undertaking (ref. 7).

TABLE 8–3.—*Launch-Vehicle Design Problems*

Basic effect	Description	Implications
Base heating_____	Hot air reflected from trailing engine shock waves heat booster base.	Thermal insulation and booster skirts needed.
Aerodynamic heating.	Aerodynamic heating reaches its maximum around 10-km altitude. Maximum temperature lags slightly.	Internal stresses from differential thermal expansion. Material strengths are reduced.
Ground-wind loads.	Steady winds cause oscillations of vertical cylinder.	Guidance alinement affected. Structures must be stiffened.
Buffeting_____	Caused by shock boundary-layer interactions, blunt-body separation, and wake buffeting.	Structural damage; viz, first Mercury-Atlas shot. Requires structural stiffening.
Longitudinal bending moments.	High-altitude winds cause vehicle to fly at an angle of attack near point of maximum dynamic pressure (10-km altitude). Pressure on rocket nose produces a vehicle torque. Maneuvers also generate bending moments.	Autopilot must compensate for pitch forces, increasing bending moment. Structure must be stiffened.
Shock and vibration.	Ground transportation can cause shocks up to several g (50 g for railroad humping). Rocket engine generates vibration. Shocks produced by stage-separation pyrotechnics may be 50 to 200 g for 10 μsec.	Air transport preferred. Sustained vibration causes structural fatigue. Absorbers and damping devices needed.
Propellant sloshing.	Lateral oscillations may cause resonant oscillations in partially filled tanks.	Structural damage may occur. Guidance system may be affected if its resonant frequency is near that of sloshing frequency. Tank baffles needed.

Rather than divert the reader from the book's theme of satellite technology, the major launch-vehicle design tasks are abbreviated and presented in table 8–3.

8–5.   Launch-Vehicle-Satellite Integration

The interface diagram (fig. 8–2) shows that the launch vehicle mechanically influences the satellite, but it does not specify just how. The first and most obvious requirement is that the final
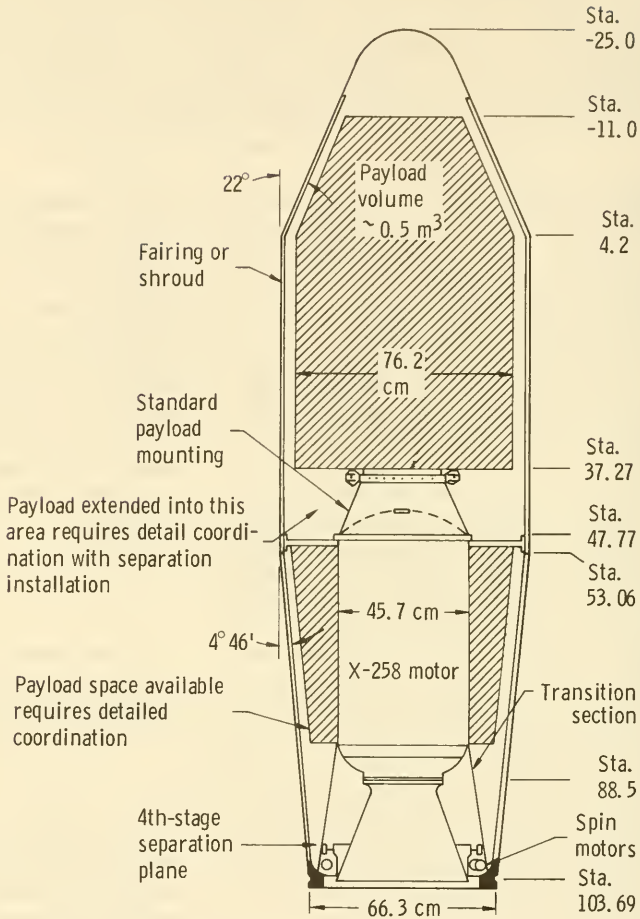
FIGURE 8–13.—Upper portion of the Scout launch vehicle, showing the X–258 solid-fuel motor, the payload volume, the payload adapter, and the launch shroud.

launch-vehicle stage and the satellite fit together properly. One would expect this to be the easiest of all conditions to meet, but it is not. There have been many misfits discovered when all the parts finally meet at the launch site. One solution is the provision of standard payload mountings or adapters, such as that shown for Scout in figure 8–13. The adapter can be provided by the launch-vehicle manufacturer to the satellite prime contractor

to insure proper fits long before the satellite is shipped to the launch site.

Vibration, shock, and acoustic noise have been frequently mentioned as effects of the launch vehicle. These factors can be summarized in launch profiles, such as that shown in figure 8–14 for
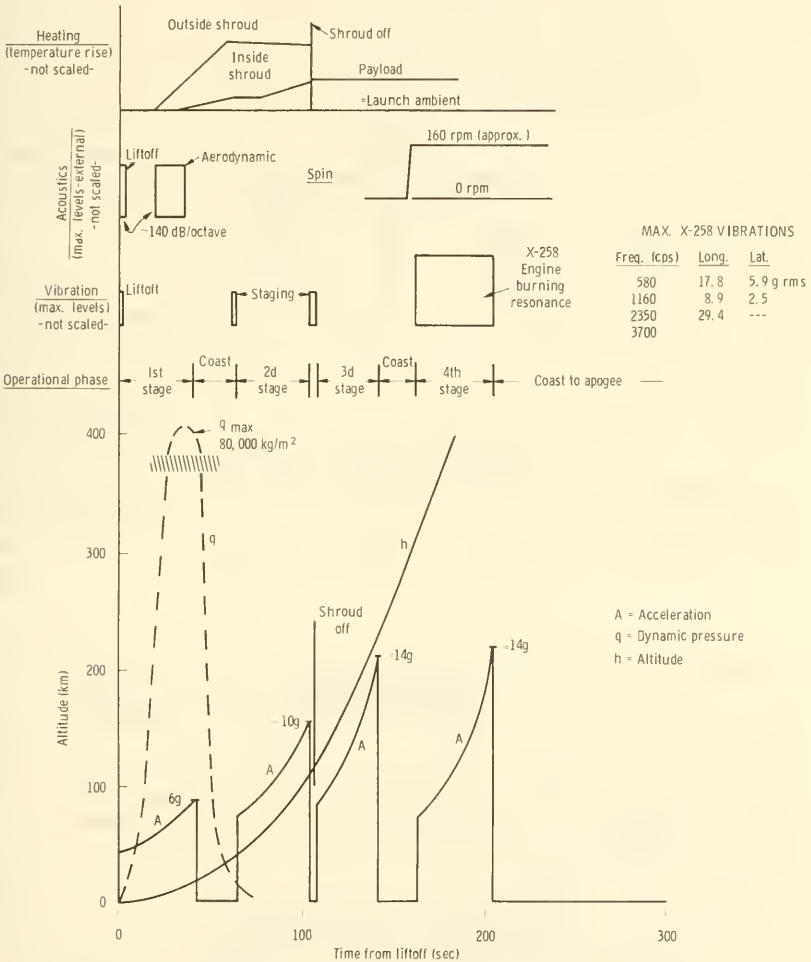
FIGURE 8–14.—Representative Scout launch profile (ref. 8).

Scout. Integration here implies proper satellite mechanical design, keeping in mind the possible resonance of satellite structures at the frequencies generated by the launch vehicle. It was pointed
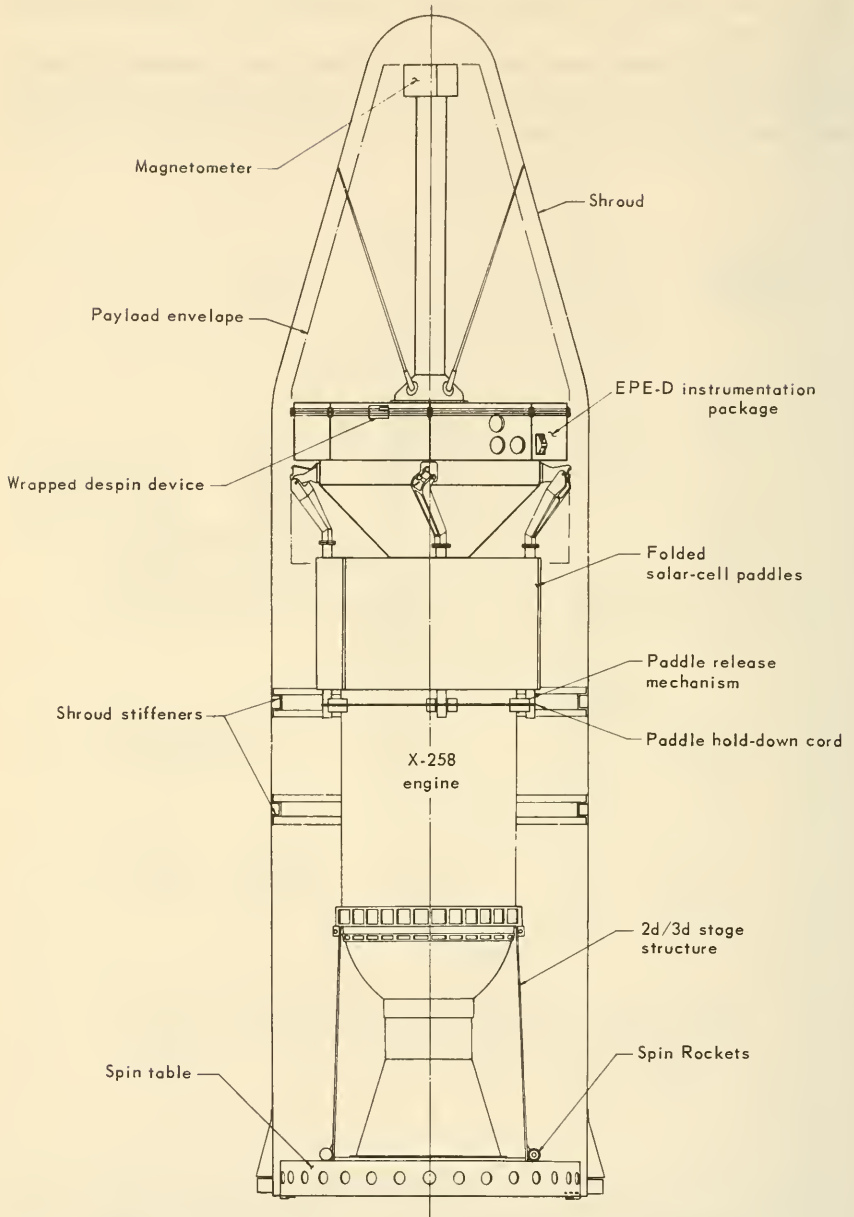
FIGURE 8–15.—An Energetic Particles Explorer (EPE) with all its appendages folded in and mounted on a Delta launch vehicle.

out in chapter 7 that only thorough testing under simulated launch conditions will result in satisfactory satellite designs.

Figure 8–14 introduces the subject of thermal and acoustic forces that arise from high speeds through the atmosphere. The payload proper is partially protected from these influences by a shroud or fairing (fig. 8–13). Occasionally, outsized shrouds will be built for special payloads, but the standard size is preferred. Before the satellite booms and solar panels can be erected, the shroud, which is built in several sections, is blown off by pyrotechnics or pushed away by springs that are freed pyrotechnically.

Prior to orbital injection, spin rockets will spin up the final stage-satellite combination. The centrifugal forces exerted during spinup may be severe.

Satellite separation from the launch vehicle also must occur before the satellite metamorphoses from its compact, stowed configuration (fig. 8–15) to its operational, extended shape. Pyrotechnics, such as explosive bolts, are also used to sever all mechanical connections with the final stage of the launch vehicle. The shocks of these explosions impose additional forces on the payload. Compressed springs, compressed gas, or small rocket engines complete the separation phase by imparting a relative velocity difference to the satellite and launch vehicle.

Additional and sometimes difficult steps in the integration process occur at the launch site, where the satellite is mated to a dummy final stage and balanced statically and dynamically before flight.

8–6.   Characteristics of Major Satellite Launch Vehicles

Scientific satellites have been launched by just about every combination of rocket stages that could be conveniently assembled into a launch vehicle. Most of the launch vehicles listed in table 8–4 were not built specifically for satellite launching, though Vanguard and Diamant might be considered exceptions. Launch vehicles, in other words, are general-purpose machines. Missing from table 8–4 are the very large launch vehicles, such as Saturn V, which have capabilities far beyond the requirements of most scientific satellites.[4]

---

[4] As mentioned earlier in this book, there are a few experiments that might justify 10 000-kilogram payloads—viz, bubble chambers and artificial comets —but generally payloads carrying more than a few hundred kilograms of instruments are very difficult to integrate properly.

TABLE 8-4.—*Characteristics of Satellite Launch Vehicles* [a]

Launch vehicle	Engines [b]	Thrust, kg (lbs) [c]		Approximate mass in 500-km orbit, kg	Successful scientific satellites orbited
Atlas-Agena B [d]				2720	Explorer XXXI, OGO I, OGO III.
Stage 1 (Atlas)	2 MA-3 (L)	167 000	(367 000)		
Stage 2 (Agena B)	1 8018 (L)	7 300	(16 000)		
Atlas-Agena D [d]					ERS 12, ERS 13, ERS 17, Hitchhiker 2, OAO I, Secor 4, Secor 6, Secor 7.
Stage 1	2 MA-5 (L)	177 000	(390 000)		
Stage 2 (Agena D)	1 8096 (L)	7 300	(16 000)		
Atlas-Centaur [d]				3900	
Atlas D	2 MA-3 (L)	167 000	(367 000)		
Centaur	2 RL-10 (L)	14 000	(30 000)		
Delta (Thor-Delta)				360	Ariel 1, Explorers X, XII, XIV, XV, XVII, XVIII, XXI, XXVIII, XXXII, OSO II.
Stage 1 (DM-21)	1 MB-3 (L)	77 000	(170 000)		
Stage 2	1 AJ 10 (L)	3 440	(7 575)		
Stage 3 (Altair) [e]	1 X-258 (S)	2 730	(6 000)		
Diamant 1				~60	D-1A.
Stage 1 (Emeraude)	(L)	28 500	(62 700)		
Stage 2 (Topaze)	(S)	14 800	(32 500)		
Stage 3 (Saphir)	(S)	5 320	(11 700)		
ELDO Launcher A (Europa 1):					
Stage 1 (Blue Streak)	2 RR RZ2 (L)	136 000	(300 000)		
Stage 2	(L)	28 100	(61 700)		
Stage 3	(L)	2 320	(5 100)		

Juno I (Jupiter-C)				20	Explorers I, III, IV.
Stage 1 (Redstone)	1 A-7 (L)	37 700	(83 000)		
Stage 2	11 solids f (S)	7 510	(16 500)		
Stage 3	3 solids f (S)	2 180	(4 800)		
Stage 4	1 solid f (S)	728	(1 600)		
Juno II				40	Explorers VII, VIII, XI.
Stage 1 (Jupiter)	1 S-3 D (L)	68 200	(150 000)		
Stage 2	11 solids f (S)	7 510	(16 500)		
Stage 3	3 solids f (S)	2 450	(5 400)		
Stage 4	1 solid f (S)	818	(1 800)		
Myu	(S)	100 000	(220 000)	9100	Pegasus I, II, III.
Saturn IB					
Stage S-I	8 H-1 (L)	680 000	(1 500 000)		
Stage S-IV	6 RL-10 (L)	41 000	(90 000)		
Stage S-V g	2 RL-10 (L)	14 000	(30 000)		
Scout				120	Ariel 2, Explorers IX, XIII, XVI, XIX, XX, XXII, XXIII, XXIV, XXV, XXVI, XXVII, XXX FR-1, Geophysical Research Satellite, OV-3-1, OV-3-3, OV-3-4, San Marco 1, Secor 5.
Stage 1 (Algol)	XM-68 (S)	45 400	(100 000)		
Stage 2 (Castor)	XM-33 (S)	28 000	(62 000)		
Stage 3 (Antares)	X-259 (S)	10 000	(22 000)		
Stage 4 (Altair)	X-258 (S)	2 700	(6 000)		
Scout (uprated)				150	
Stage 1 (Algol)	XM-68 (S)	45 400	(100 000)		
Stage 2 (Castor)	XM-33 (S)	28 200	(62 000)		
Stage 3 (Antares)	X-259 (S)	10 000	(22 000)		
Stage 4	FW4-5 (S)	2 840	(6 250)		
Thor-Able				160	Explorer VI.
Stage 1	1 MB-1 (L)	68 000	(150 000)		
Stage 2	1 AJ-10 (L)	3 500	(7 700)		
Stage 3	1 X-248 (S)	1 400	(3 100)		

See footnotes at end of table.

TABLE 8-4.—*Characteristics of Satellite Launch Vehicles*—Continued

Launch vehicle	Engines[b]	Thrust, kg (lbs)[c]		Approximate mass in 500-km orbit, kg	Successful scientific satellites orbited
Thor-Able Star (Thor Epsilon)	---	---		150	Anna 1B; Injun 1; Lofti 1; Secor 2; Solrad 1; Solrad 3; Traac, 1963 3SC.
Stage 1 (DM-21)	1 MB-3 (L)	77 000	(170 000)		
Stage 2 (Able Star)	AJ-10 (L)	3 590	(7 900)		
Thor-Agena B	---	---		730	Alouette 1, Alouette 2, Oscar 1, Oscar 2.
Stage 1 (DM-21)	1 MB-3 (L)	77 000	(170 000)		
Stage 2 (Agena B)	1 8018 (L)	7 300	(16 000)		
Thor-Agena D	---	---		---	Injun 3, Lofti 2A, Oscar 3, Radose, Secor 3, Solrad 6, Solrad 7B, Starad.
Stage 1 (DM-21)	1 MB-3 (L)	77 000	(170 000)		
Stage 2 (Agena D)	1 8096 (L)	7 300	(16 000)		
Thrust-Augmented Thor (TAT) Agena B					OGO II.
Stage 1 (DM-21 and Castor)	1 MB-3 and 3 TX-33 (L/S)	151 000	(332 000)		
Stage 2 (Agena B)	1 8018 (L)	7 300	(16 000)		
Thrust-Augmented Thor (TAT) Agena D				820	Hitchhiker 1, Pageos, Secor 1, Solrad 7A.
Stage 1 (DM-21 and Castor)	1 MB-3 and 3-TX-33 (L/S)	151 000	(332 000)		
Stage 2 (Agena D)	1 8096 (L)	7 300	(16 000)		
Thrust Augmented Delta (TAD) (Improved Delta).				520	Explorer XXXIII.
Stage 1 (DM-21 and Castor)	1 MB-3 and 3 TX-33 (L/S)	151 000	(332 000)		
Stage 2	1 AJ-10 (L)	3 400	(7 500)		
Stage 3	1 X-258 (S)	1 270	(2 800)		

Thrust-Augmented Improved Delta (TAID).					
Stage 1 (DM-21 and Castor)	1 MB-3 and 3 TX-33 (L/S).	151 000	(332 000)	550	Explorer XXIX.
Stage 2					
Stage 3	1 AJ-10 (L)	3 400	(7 500)		
Titan 3C				11 500	Oscar 4.
Stage 0	2 solid (S)	910 000	(2 000 000)		
Stage 1	2 XLR-87 (L)	195 000	(430 000)		
Stage 2	2 XLR-91 (L)	45 000	(100 000)		
Transtage	2 AJ-10 (L)	7 300	(16 000)		
Vanguard				45	Vanguards I, II, III.
Stage 1	1 X-405 (L)	12 700	(23 000)		
Stage 2	1 AJ-10 (L)	3 400	(7 600)		
Stage 3	1 X-243 (S)	1 400	(3 100)		
Atlas plus SATAR	(L+S)				OV-1 series.

[a] Launch-vehicle characteristics vary with manufacturing lot (block) number and during the development cycle.

[b] L=liquid engine, S=solid motor. The RL-10 is a LH-LOX engine.

[c] Payloads vary with orbit inclination and launch site. Those listed are for easterly launches from the ETR.

[d] The Atlas-D has a 36 400-kg (80 000-lb) sustainer engine. Atlas-D, without an Agena stage, orbited OV-1-4, OV-1-5, and OV-1-8.

[e] Early Deltas used an X-248, 1410 kg (3100 lb).

[f] These small solid rockets were scaled-down versions of the Sergeant missile.

[g] The S-V stage has been eliminated from the Apollo Program vehicles.

References

1. MUELLER, G. E.: Launch Vehicle Technology. AIAA paper 64–527, 1964.
2. KOELLE, H. H.: Trends in Earth-to-Orbit Transportation Systems. Astronaut. Aerospace Eng., vol. 1, Oct. 1963, p. 25.
3. BEICHEL, R.: Liquid Rockets. Space/Aero., vol. 42, Sept. 1964, p. 39.
4. ORDAHL, D. D.: Hybrid Propulsion. Space/Aero., vol. 41, Apr. 1964, p. 108.
5. STOIKO, M.; AND DORSEY, J. W.: Rocket Catapult Facts and Fables. Astronautics, vol. 5, July 1960, p. 30.
6. BRUCKNER, A. P.: A Gun-Launched Satellite. McGill Engineer, Dec. 1964. (Also in Spaceflight, vol. 7, July 1965, p. 118.)
7. LANGE, O. H.; AND STEIN, R. J.: Space Carrier Vehicles. Academic Press, 1963.
8. NEFF, W. J.; AND MONTES DE OCA, R. A.: Launch Environment Profiles for Sounding Rockets and Spacecraft. NASA TN D–1916, 1964.

Chapter 9

DESIGN OF SCIENTIFIC SATELLITES

9–1. Prolog

In satellite research, it is not always easy to say which comes first, the idea for an experiment or the concept of the experiment carrier (satellite). Regardless of how the concept of any particular scientific satellite originates, someone eventually makes a feasibility study to determine the soundness of the idea, whether the satellite can be built, and whether significant data can be returned for a reasonable amount of money. Once feasibility is assured, a fairly standard sequence of events follows: the launch vehicle is selected, experiments chosen, design objectives established, and so on, as illustrated by the chain of events portrayed in figure 9–1.

The subject of this chapter is "satellite design," a process that begins with the rough shaping of the design during the feasibility study and really ends only when the satellite has left its place of birth for the launch site. In essence, satellite design is the conversion of an idea—experimental or vehicular—into a smoothly functioning, objective-meeting machine.

There is no typical scientific satellite. The ERS satellites weigh only a kilogram or two apiece, while an OAO grosses almost 2 tons.[1] Scientific satellites may be spherical, cylindrical, boxlike, or polyhedral. The only common element is the singleminded dedication to the measurement of space phenomena and the relay of these data back to Earth. Despite such obvious variety, the design process always seems to give birth to one of three major species of satellite. The genetics are controlled by a factor called design philosophy.

First, though, what is design philosophy? It is different from, but not independent of, the satellite's scientific objectives.

---

[1] See appendix for short descriptions of all scientific satellites.
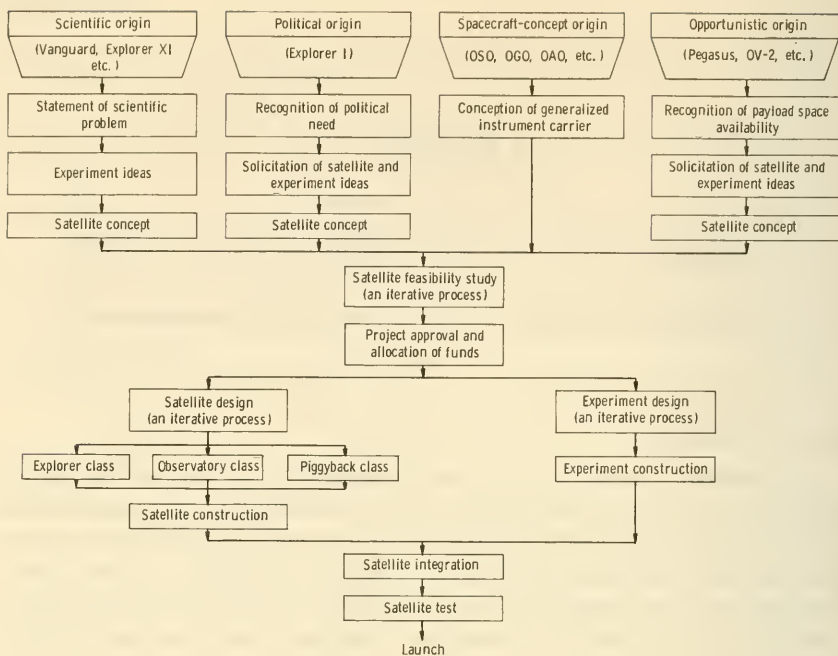
FIGURE 9–1.—Four evolutionary paths of scientific satellites.

Neither is design philosophy the sum of the design and engineering objectives, which merely set targets and say nothing on how to attain them. A design philosophy is a set of heuristic rules—generally the result of experience rather than revelation—that guide engineers in expeditiously meeting the design objectives. The clue to understanding design philosophy is in the word "expeditiously," because a good design philosophy makes satellite engineering easier, quicker, and more efficient. Some design guidelines that make up the philosophy (design philosophy is always informal) merely state the obvious; viz, satellite components should be located symmetrically about the spin axis in spin-stabilized satellites. Other rules of thumb are just as general but not so obvious; for example, magnetic materials and uncompensated current loops must be rigorously avoided to insure magnetic cleanliness. Such are the ingredients of a design philosophy.

Superficially, one might expect that one design philosophy would be sufficient, but three major approaches have in fact emerged, each associated with a particular class of scientific satellites. In the broadest sense, each of the three design philosophies is defined by the "attitude" taken toward space experimenta-

tion: specialized, generalized, or secondary. Lest these adjectives confuse the picture, elaborations follow:

(1) The Explorer class of scientific satellites consists of small, highly integrated spacecraft that carry a few specialized, closely related experiments. Each satellite is tailored to the special needs of the experiments. The number of experiments per kilogram of satellite is high. Examples: the Energetic Particles Explorers and the Injuns.

(2) The Observatory class of scientific satellites generally includes larger and more complex spacecraft than the Explorers. The spacecraft interfaces are more tolerant, and many diverse experiments can be accommodated without excessive interference. Observatory research is more generalized and is likely to be oriented toward an entire discipline, such as geophysics, solar physics, or astronomy. The defining features, however, are the generalization and standardization of experiment space. Examples: the OGO's, the OAO's, and possibly the SSS's now under study.

(3) The Piggyback class of scientific satellites is characterized not by size or degree of experiment specialization but rather by the secondary importance and opportunistic nature of scientific research. Piggyback satellites (or subsatellites) ride into orbit alongside military satellites or on launch-vehicle test shots on a noninterference basis, a fact that causes many aspects of satellite design to be controlled by the primary mission; e.g., the impossibility of spin stabilization in some instances. The piggyback satellite is usually not highly integrated and its experiments may be varied in nature, so long as they do not interfere with the primary mission.[2] Piggyback satellites tend to be either very small, when they are orbited in multiple launches (Oscar, ERS 7), or large, if instruments replace ballast on launch-vehicle tests (OV-2, Pegasus).

Any fragmentation of design philosophy, like that above, is artificial. The semantic boundaries in the Piggyback class are particularly fuzzy. Still, this chapter will repeatedly show that many design features stem from three rather distinct collections of design philosophies, or ground rules.

Satellite design is aided by a variety of management techniques. Plans, schedules, specifications, and design reviews are essential to integrating a satellite, testing it, and getting it to the launch

---

[2] The ERS satellites built by Space Technology Laboratories (STL) carry only closely related experiments, such as space radiation detectors, in order to simplify experiment integration.

Aspects of Design Philosophy	Satellite Design Process	Management Aids

Heuristic guidelines for shape selection, materials choice, telemetry type, component location, status sensors, number of commands, attitude-control scheme, packaging, interface matching	Feasibility study	Mission objectives
	Satellite design	Preferred-parts lists, interface specifications, design reviews, design objectives, parts specifications, codes, standards, PERT[a]
	Satellite construction	PERT[a], quality control, zero defects programs, inspection, training programs, codes, standards
	Satellite integration	Interface documents
	Satellite test	Test plans, test specifications
	Launch	Operations plans, payload-description documents, PERT[a]

[a] PERT = Program Evaluation and Review Technique, one of several management approaches to program control.

FIGURE 9–2.—Influences of design philosophy and management aids on the design of scientific satellites.

pad at the appointed time (fig. 9–2). While many of the great discoveries in science, including the Van Allen Belts, were made with a minimum of fuss and rigmarole, farflung contractors, experimenters, networks, and test facilities cannot be coordinated without paperwork. Space research cannot be consummated in a backroom.

Are there any general trends of importance in satellite design? The advent of large launch vehicles, such as Saturn I–B and Titan 3, might presage a shift toward the large, general-purpose Observatory-class satellites, such as the OAO. Or, the availability of retired ICBM rockets, such as the Minuteman, might suggest an emphasis on the small, Explorer-class satellites (table 9–1). The fact is that satellite research is both opportunistic and flexible; it will put instruments on any launch vehicles that are available—and the cheaper, the better. There are no marked trends toward the Explorers or Observatories. If an advancing frontier exists, it is probably in the engineering of simple, reliable, easy-to-integrate, inexpensive, experiment packages that can be placed on the shelf until launch-vehicle space becomes available. The more formal and orderly Explorer and Observatory programs will continue to provide most of the research space, but the low cost, informality, and simplicity of the secondary piggyback satellites are attracting more and more interest.

TABLE 9–1.—*Comparison of the Capabilities of the 3 Major Classes of Satellites*

[Partially adapted from ref. 1]

Property	Explorer class	Observatory class	Piggyback class
Ability to carry very large experiments or many related experiments.	Low	High	High [a]
Information rate	Medium	High	Low
Experiment interference	Low	High	Low
Ease of experiment integration (interface standardization).	Low	High	Low
Ease of experiment design	Medium	High	High
Ability to meet orbital requirements of all experiments (orbit "tailoring").	High	Low	High
Reflex time: ability to investigate "targets of opportunity."	High	Low	High
Utilization of ground-based facilities	Medium	High	Low
Utilization of payload space ("experiments/kg").	High	Medium	Low
Reliability (including reprograming in presence of failures).	High	High	Low
Cost	Medium	High	Low
Ease of satellite-subsystem integration.	Low	Low	High
Constraints due to launch vehicle and other payloads.	Low	Low	High
Ability to study space phenomena simultaneously from different locations.	High	Low	Low
Pointing capabilities	Low	High	Low
Ease of program management	Medium	Low	High
Typical satellites	Explorers, Vanguard, Injun, Traac, Ariel, San Marco.	OGO, OAO, OSO, AOSO.	TRS, ERS, Pegasus, OV–2

[a] For launch-vehicle tests, low otherwise.

9–2. The Feasibility Study

Many satellite concepts do not survive close technical scrutiny. Weak ideas are customarily eliminated by what are termed "feasibility studies"; feasibility being defined in this case as a high probability that the mission can be accomplished, despite all constraints, with the concept at hand. Feasibility studies make rather fine-meshed sieves that pass only the soundest satellite

concepts. Such studies are customarily carried out by a handful of highly experienced engineers over a period of a few weeks. A good feasibility study is the best insurance against committing large blocks of resources to weak satellite concepts.

The feasibility study begins with the satellite concept, which may be in verbal form and not completely thought out, but which possesses no obvious faults, at least at this stage of the analysis. Someone might suggest, for example, that the theory of general relativity be checked with a satellite-borne clock. Good clocks and good satellite platforms both exist, but can they be made to work well together? Occasionally, the feasibility study will commence with a proposal or study buttressed by calculations and other evidences of feasibility. Such analyses must be repeated to insure that proper assumptions were made and the correct constraints applied. The most viable satellite concepts, as one might expect, are those derived from successful satellites in orbit.

What is the product of a feasibility study? It is much more than a "yes, it is feasible" or "no, it isn't." First, many critical design decisions are made during this stage, such as those listed in table 9–2. In effect, the major features of the satellite are fixed. The resulting satellite may look quite different from that originally proposed. Second, if the satellite appears feasible, the feasibility study will generate design specifications that will control the later detailed design, should the project be approved and funded. Finally, a good feasibility study estimates the program cost, schedule, and probability of success.

TABLE 9–2.—*Typical Design Decisions Made During a Feasibility Study*

General
Identity of launch vehicle
Range of orbits that can be achieved versus payload weight
Identity of tracking and data-acquisition stations
Number of prototype and flight models to be built
Test philosophy and plan
Satellite recovery technique

Communications Subsystem
Type of telemetry (e.g., PFM, PCM)
Telemetry format
Bit rate
Real-time transmission or memory device
Numbers of telemetry transmitters, command receivers, tracking beacons
Power required
Antenna type plus pointing and stabilization requirements

Power-Supply Subsystem

Energy source (Sun, radioisotopes, or batteries)
Average power level (from composite power profile)
Power-regulation requirements
Pointing and stabilization requirements
Solar-cell radiation protection scheme

Onboard Propulsion Subsystem

Velocity increment required
Pointing and stabilization requirements
Type of propulsion system

Attitude-Control Subsystem

Method of stabilization (spin, gravity-gradient, magnetic, or others)
Attitude-control requirements (from totality of pointing and slewing requirements)
Method of attitude change (e.g., gyros, gas jets)
Despin technique

Environmental Control Subsystem

Types of temperature controls (passive or active)
Magnetic shielding requirements
rf shielding requirements
Micrometeoroid protection scheme
Provision of air, food, and other essentials for living specimens
Hermetic-sealing requirements
Method of protection during reentry (if needed)

Guidance-and-Control Subsystem

Identities of aspect and attitude sensors
Number and character of external and internal commands
Need for killer timer

Computer Subsystem

Need for centralized computer
Type of computer (if needed)

Structural Subsystem

Satellite shape (from such factors as: strength under applied loads, convenience in installing and removing components, spin stability, experiment requirements, thermal-control needs, compatibility with launch vehicle, ease of appendage attachment)
Need for and types of appendages
Packaging and harness approach
Pyrotechnics needed for separation and release of appendages

Engineering-Instrument Subsystem

Number and identity of satellite status points to be telemetered

Scientific-Instrument Subsystem

Experiment selection
Power, pointing, stabilization, orbital and environmental-control requirements

Feasibility studies and detailed designs of satellites are not simple sequences of steps leading logically from start to finish. Design is an iterative process, with many false starts and assumptions that must be corrected. Design begins with experienced guesses about the major features of the satellite. The consequences of these guesses are then calculated. In this first iteration, the pieces (the subsystems or even smaller items) will probably not fit together well (fig. 9–3). More refined parameters are tried during the second iteration. And so on, until interfaces are matched and compatibility attained, or, perhaps, an entirely new approach seems desirable.
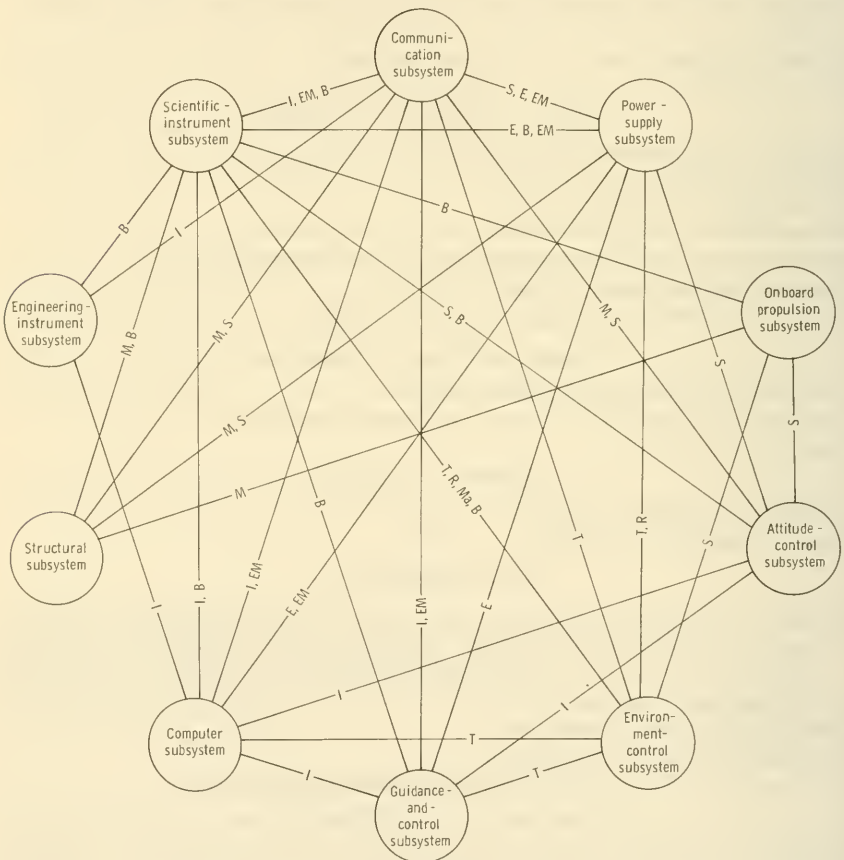
FIGURE 9–3.—Spacecraft-interface diagram. Only the major interfaces are shown: T = thermal, S = spatial, E = electrical, R = radiative, Ma = magnetic, I = information, B = biological, EM = electromagnetic, M = mechanical.

The failure of all reasonable approaches to achieve a satisfactory satellite design is, of course, an admission of technical unfeasibility. Political unfeasibility results if costs are too high, the probability of success too low, or some international complication seems likely; viz, the release of radioactivity.

All design decisions are made in the face of constraints; those limitations, ground rules, and restrictions set by technical and political facts of life. Constraints should not be confused with objectives, which specify desirables that the designer tries to reach by manipulating his dependent design variables (table 9–3). Constraints, in contrast, are relatively immutable entities, typified by those listed in table 9–4.

TABLE 9–3.—*Representative Design Objectives*

Specific payload mass, including specific fraction for scientific instrumentation
Specific orbital parameters
Specific launch date
Specific satellite lifetime (*not* necessarily maximized)
Minimum program cost
Various experimental objectives affecting overall design, such as:
    Provision of antennas hundreds of meters long (RAE, Radio Astronomy Explorer)
    Provision of high bit rate (OGO)
    Precise stabilization and pointing (OAO)
    Magnetic cleanliness (Explorer XVIII)
    Scanning platform for instruments (OSO)

TABLE 9–4.—*Representative Design Constraints*

Existing launch-vehicle spectrum
Existing networks of tracking and data-acquisition stations
Cost limitations
Engineering state of the art
Physical laws
Public safety (affects launch trajectories and use of nuclear energy)
Space environment (solar flux, vacuum, micrometeoroids, plasma, etc.)

To summarize the terminology, satellite designers, in both the feasibility study and detailed design stages, attempt to attain the design objectives, despite the design constraints, by varying the dependent design variables, using some design philosophy as an empirical guide.

9-3.   Common Elements in Satellite Design

Before proceeding to the details of subsystem design, the discussion of several design factors, which have roots common to all subsystems, seems appropriate.   The most obvious, and certainly the most widely discussed of these factors, is reliability.   A second common element is materials selection, for all subsystems are designed with an eye to the unique behavior of materials in the space environment.   Not so obvious is the specialized field of component packaging, an engineering area devoted to compactly and astutely arranging satellite components for minimum weight and maximum reliability.

Other design techniques, such as value analysis and quality control, are not covered here because the reader is assumed to be familiar with them.   The reader is assumed also to be aware of the fundamentals of basic engineering fields, such as electronics, structural analysis, heat transfer, etc., all of which are obviously common elements in satellite design.

Reliability.—Reliability is defined as the probability that a system will perform satisfactorily for a specified period of time under a given set of operating conditions; i.e., the space environment.

A solar observatory, for example, might have a probability of 0.50 of telemetering 10 000 bits/sec of meaningful scientific data from 10 experiments for 10 000 hours.   The probability and time ingredients of reliability are well understood.   More difficult are the specification of "meaningful scientific data" and "satisfactory."   Reliability is a frequently abused parameter.   It cannot be employed blindly, because some failures may be due to operational errors rather than chance alone.   Such failures would not be properly described by the probabilistic formulas that follow.

The simplest and most easily described reliability theory occurs when system failures are purely random in time.   In this case

$$R(t) = \exp\left(-\rho t\right) \tag{9-1}$$

where

R = the system reliability
ρ = the chance failure rate (1/hr)
t = time (hr)

This simple equation is applicable only to systems that have been adequately debugged (no manufacturing defects), burned-in (incipient failures eliminated), and have not yet reached that point in time where parts begin to wear out.   This region of ap-
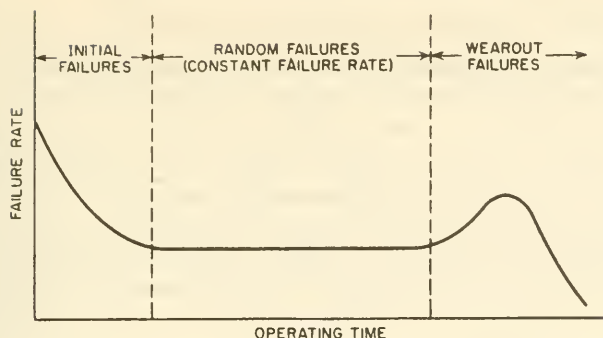
FIGURE 9–4.—Typical component mortality curve. "Burned in" satellite components operate in the central flat region, where the equations of this chapter apply.

plication is illustrated in figure 9–4, where the mortality curve has flattened out in the middle, yielding a constant failure rate.

The reciprocal of ρ is the mean time between failures (MTBF), another often-used reliability term. If a system must have a reliability of 0.999999 for 1 hour, the mean time between failures has to be 1 000 000 hours (over 100 years), according to equation (9–1). Such a MTBF would be hard to demonstrate experimentally, but it gives a feeling for the magnitudes involved.

If the system is made up of four devices arranged in series, so that the failure of any one of them fails the whole system, the system reliability, $R(t)$, is given by the product rule

$$R(t) = R_1 R_2 R_3 R_4 \qquad (9\text{--}2)$$

Referring to figure 9–5, a considerable improvement may be achieved by paralleling the weakest component. The equation for parallel or redundant components is

$$R_p(t) = 1 - (1 - R_3)^n \qquad (9\text{--}3)$$

where

R_p = the combined reliability of the redundant components
R_3 = the reliability of the individual paralleled components
n = the number of redundant components

In figure 9–5, the addition of one redundant component increases the system reliability to 0.968, a great improvement.

Reliability figures are frequently quoted with confidence levels attached, because it is not a play on words to say that reliability
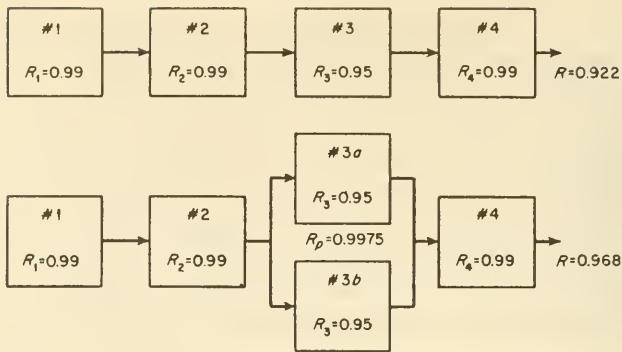
FIGURE 9–5.—Reliability models of series- and parallel-connected components. Paralleling of component No. 3 markedly improves overall reliability. See discussion in text.

levels themselves are not 100 percent reliable. To take an example, if a reliability calculation says that a spacecraft has a reliability of 0.90 for specified conditions over a given period of time, actual measurements on a series of spacecraft will show a spread of values between 0.00 and 1.00. If the original reliability calculation was based on good component data, most of the experimental reliability points would be clustered in a normal distribution around 0.90. Suppose that half the observed points fall between plus and minus one standard deviation around 0.90, then there is an experimentally observed confidence level of 0.50. Good component reliability data will also give confidence levels. Mathematical techniques are available to handle reliability calculations with attached confidence levels. For the rest of this discussion, only the point values, the peaks of the normal distributions, will be used.

It is worth reemphasizing that the preceding theory assumes a constant failure rate in time (fig. 9–4). Furthermore, since reliability is a statistical concept, it is necessarily based upon many observations, or, as the phrase goes, "statistically significant data." The point is this: most missiles and spacecraft are classified as "one-shot" systems, which means that there is no recovery, no reuse, and no opportunity for maintenance. The burden on the reliability engineer is magnified by the scarcity of system- and subsystem-reliability data and the extreme scientific, financial, and political pressure for a long active life for the spacecraft.

Scientific satellites are complex machines. The presence of tens of thousands of parts can reduce overall reliabilities drastically. Even redundancy, preferred-parts lists, the enforcement of tough military standards (MIL specs), extreme care in manufacture, and the "burning in" of components to eliminate incipient failures do not boost overall satellite reliabilities to much higher than 0.70. In fact, many successfully launched satellites have experienced some degree of failure, although sometimes just one experiment has been lost or the telemetry has failed, only to return mysteriously later. Satellite success is a matter of degree, with perfection a most rare occurrence. Because reliabilities are rather low, backup flight-model satellites and some subsystems are frequently constructed, tested, and readied simultaneously with the regular flight model.

Materials.—Save for a few special bearings, pins, and other critical items, satellites are made mostly from aluminum, magnesium, and plastics. The so-called "exotic" structural materials, such as graphite and tungsten, are rare. Ordinary materials succeed because not only are mechanical stresses low after launch but service temperatures are on the cool side, usually between 0° and 50° C. Materials are selected for their abilities to save weight and resist the baleful effects of the space environment. Stability in a vacuum and under bombardment by space radiation and plasma are especially important for lubricants, semiconductors, lenses, and many other nonstructural materials.

Looking at structural materials first, table 9–5 lists the properties of some of the most popular substances. Table 9–6 elaborates, but in a more qualitative fashion. In general, the satellite designer has few problems with structural materials; there are many stable, lightweight, strong, nonmagnetic materials to choose from. Very light structures, such as solar-cell panels and instrument platforms, are fabricated in honeycomb form from aluminum, magnesium, fiber glass, and plastics. Aluminum or magnesium cylinders, spheres, and tubular struts usually carry the mechanical loads in satellites.

A wealth of materials is also available for use in gears, yo-yo despin wires, radiation shields, and other special applications. If it were not for the inimical space environment, one might be tempted to say that there are no solid-materials problems in satellite construction.

More specifically, the vacuum and radiation levels encountered by scientific satellites complicate design immensely. The most important effects are tabulated in table 9–7. Sunlight, including

Table 9-5.—*Properties of Typical Satellite Structural Materials*

[From ref. 2]

Material	Tensile strength, ultimate, F, kg/cm² (psi)	Tensile strength, yield, kg/cm² (psi)	Young's modulus, Y, kg/cm² (psi)	Density, ρ, g/cm³ (lb/in.³)	Thermal conductivity, watts/cm²°C (Btu/hr-ft²°F)	Y/ρ	F/ρ
Alloy steel (4130, 4140)	440 000 (150 000)	390 000 (132 000)	85×10^6 (29×10^6)	7.8 (0.283)	0.38 (22)	11×10^6 (102×10^6)	56×10^3 (530×10^3)
Stainless steel (A-286)	410 000 (140 000)	280 000 (95 000)	85×10^6 (29×10^6)	7.9 (0.286)	0.15 (8.7)	11×10^6 (102×10^6)	52×10^3 (495×10^3)
Aluminum (6061-T6)	120 000 (42 000)	100 000 (35 000)	29×10^6 (10×10^6)	2.7 (0.098)	1.6 (96)	11×10^6 (100×10^6)	52×10^3 (430×10^3)
Magnesium (AZ 80A-T5)	140 000 (48 000)	97 000 (33 000)	19×10^6 (6.5×10^6)	1.8 (0.065)	0.76 (44)	11×10^6 (100×10^6)	78×10^3 (738×10^3)
Titanium (6 Al-4V)	380 000 (130 000)	350 000 (120 000)	47×10^6 (16×10^6)	4.4 (0.160)	0.065 (3.8)	11×10^6 (100×10^6)	86×10^3 (810×10^3)
Beryllium-copper (BeCu AT)	530 000 (180 000)	380 000 (130 000)	47×10^6 (16×10^6)	8.2 (0.297)	0.83 (48)	5.7×10^6 (54×10^6)	65×10^3 (605×10^3)
Beryllium	180-290 000 (60-100 000)	120-160 000 (40-55 000)	130×10^6 (45×10^6)	1.85 (0.067)	1.7 (100)	70×10^6 (670×10^6)	155×10^3 (1500×10^3)
Fiber-glass laminate	200 000 (70 000)		9×10^6 (3×10^6)	1.85 (0.067)	0.027 (0.16)	5.4×10^6 (45×10^6)	108×10^3 (1050×10^3)

TABLE 9-6.—*Usage of Satellite Structural Materials*

[Adapted from ref. 2]

Class of materials	Usage
Steels_____	Carbon steels are magnetic and rarely used, except where high strength is important; e.g., springs and pins. Stainless steels are less magnetic and therefore more common, particularly where high strength is important.
Aluminums_____	Comparable to steel in terms of strength per unit weight, aluminum can save significant weight where a given volume of metal must be installed regardless of load. Aluminum also saves weight where structural elements are sized by buckling criteria. Aluminum is widely used in most satellites.
Magnesiums_____	Less dense than aluminum, which it replaces as the major structural material in some satellites. Easy to machine. Some alloys are hard to weld.
Titanium_____	High strength at high temperatures, but few satellite applications need such properties.
Beryllium-copper_____	Used where toughness, high-strength, and non-magnetic properties are essential (e.g., springs and high-strength electrical conductors).
Beryllium_____	High strength-to-weight and stiffness-to-weight ratios make it a superior structural material. Its brittleness and forming problems have restricted its use in satellites.
Fiber glass_____	This mixture of glass fibers and epoxy is used for many structures where low weight is important (i.e., instrument shelves). Fiber glass is transparent to rf.

ultraviolet radiation, and the micrometeoroid fluxes are relatively easy to deal with. Cold welding of surfaces, however, particularly deployable booms and antennas, and radiation damage to semiconductors seriously constrain satellite designers. Space radiation, to mention the most notable instance, degrades the performance of solar cells, which are made from semiconductors. Designers have had to add glass or quartz covers to protect the cells.

Packaging.—Most scientific satellites are weight and volume limited. In these connections, the term "packaging" applies to the art (and it is most definitely an "art") of stuffing many parts into small volumes. It is not merely a question of squeezing, because compression has some undesirable consequences:

TABLE 9–7.—*Effects of the Space Environment on Materials*

Environment component	Qualitative effects
Vacuum	Most metals and alloys are quite stable. Magnesium sublimes appreciably above 175° C. Polished optical surfaces may roughen through selective sublimation. Seizing of sliding surfaces and cold welding are serious problems. Some semiconductors (selenium, phosphides, and arsenides, and many polymers (nylon, neoprene, acrylics)) decompose or sublime at moderate temperatures. Oils and greases do not lubricate properly. Plastics (silicone resins, polyethylene) and natural rubber behave well, however.
Sunlight	No important effects on metals and crystalline inorganics. Sunlight may darken insulators, polymers, and glasses.
Radiation (including solar plasma).	No important effects on metals. Semiconductors (solar cells, transistors) will be damaged. Glasses, greases, and oils will suffer radiation damage. Flexibility, strength, and electrical properties of nylon, acrylics, butyl rubber, and similar materials are degraded.
Micrometeoroids	Walls, lenses, and other external surfaces may be punctured or pitted. Spalling of inner surfaces may occur.

(1) Heat evolved from components must be dissipated. The magnitude of this problem increases as part density increases and cooling area decreases

(2) Inertial and moment-of-inertia properties of the satellite cannot be compromised

(3) Structural resonances at the frequencies applied by the launch vehicle must be avoided

(4) Packaging should not make the satellite more difficult to fabricate

(5) Packaging should permit easy access to components for testing and repair

(6) Satellite reliability should not be impaired

It is customary to discuss packaging at several levels. First, there is satellite packaging; that is, fitting the satellite and its appendages into the launch-vehicle shroud. This process frequently entails the installation of extendable booms, antennas, and

solar-cell paddles. Second, one speaks of subsystem packaging or the placement of subsystem packages within the satellite shell. At the lowest level, there is component packaging, where transistors, resistors, and other electronic parts are crammed into minuscule volumes.

The metamorphosing, erectable structures of satellites and the placement of subsystem packages within the satellite proper will be treated in section 9–11, which deals with structural design. Component packaging, however, transcends any one subsystem. Satellite part counts often top 10 000 in Observatory-class satellites, and most of these parts are electronic in nature. It is in electronic packaging that engineers are making the advances that will affect satellite design the most.

Over a period of 40 years, electronic equipment has shrunk from bulky home receivers to radios smaller than a cigarette lighter. Simple miniaturization came first as tubes, coils, and other parts were made smaller and smaller. Parts were then subminiaturized. When cheap, reliable interconnection of subminiaturized parts was needed, printed circuits were invented, in which conducting patterns of paint are deposited on circuit boards. Printed circuits not only brought tiny, integral modules of many parts but also enhanced reliability, because better interconnections resulted. (The soldering process has proven a recalcitrant and persistent threat to reliable satellite electronics.) Electronic shrinkage is continuing with two recent innovations: integrated circuits and thin-film circuits.

In the integrated circuits, functional circuits elements (flip-flops, gates, amplifiers) are formed on a single "chip" of active substrate. Transistors, for example, are made by successive masking, etching, and diffusion on a single piece of germanium semiconductor. Resistors, capacitors, and the interconnecting leads are formed in the same way.

"Thin film," or "deposited," circuits are placed on inactive substrates, such as glass, by successive vacuum depositions through masks and by means of photoetching. Active components (transistors, diodes) are added as discrete components. Thin-film circuits give the circuit designer more latitude than integrated circuits in choosing circuit parameters, because the deposition process cannot come close to duplicating the performance ranges of the separately made discrete active components.

Some electronics engineers estimate that eventually hundreds of thousands of electronic parts can be packaged within a few cubic centimeters. In the meantime, component packaging has
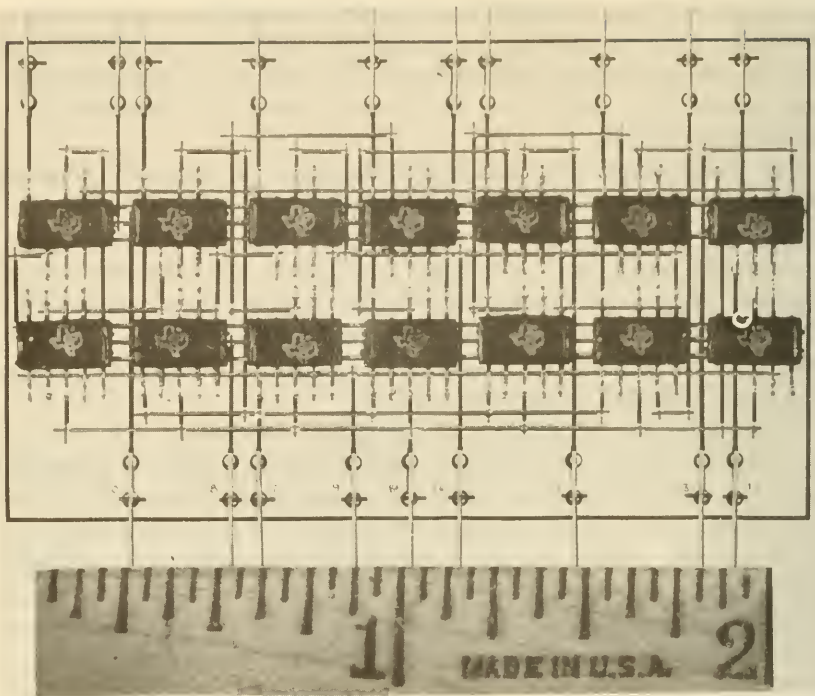
FIGURE 9–6.—A satellite counter module containing 14 separate integrated circuits. Scale is in inches.

compressed satellite circuitry to an impressive degree (fig. 9–6) and substantially contributed to the high bit rates now possible with relatively small scientific satellites.

A rather ironic problem arises as electronic equipment approaches the microscopic: the bundles of wires connecting satellite subsystems and packages become proportionally larger. Wires cannot be too thin or their electrical resistance rises to unacceptable levels. The consequence is that the interior of a satellite is traversed by ubiquitous, thick, heavy bundles of wires (called "harnesses") that connect marvelously small electronic packages (fig. 9–7). Cabling is a problem, not only because it is heavy and occupies valuable volume but also because it carries heat and vibration throughout the satellite. Satellite designers must plan in advance where their signal conduits are going and leave room for them. Cabling does not seem to be susceptible to the same magic that made electronic parts small. Wire harnesses seem crude and archaic inside today's sophisticated satellites.

9–4. The Communication Subsystem

All scientific data, satellite-status data, tracking signals, and ground-originated commands funnel through the satellite communication subsystem. Applying an overworked biological analogy, it is the "nerve center" of the satellite, with information-carrying wires linking all satellite and Earth-based equipment. The primary functions performed are:

Function	*Typical equipment*
(1) Telemetry: the transmission of experimental and status data to the Earth.	Transmitter(s), antenna(s).
(2) The receipt of commands from Earth.	Command receiver(s), antenna(s).
(3) The transmission of signals to enhance satellite tracking and identification.	Beacon(s) (radio or optical), transponder(s), antenna(s).
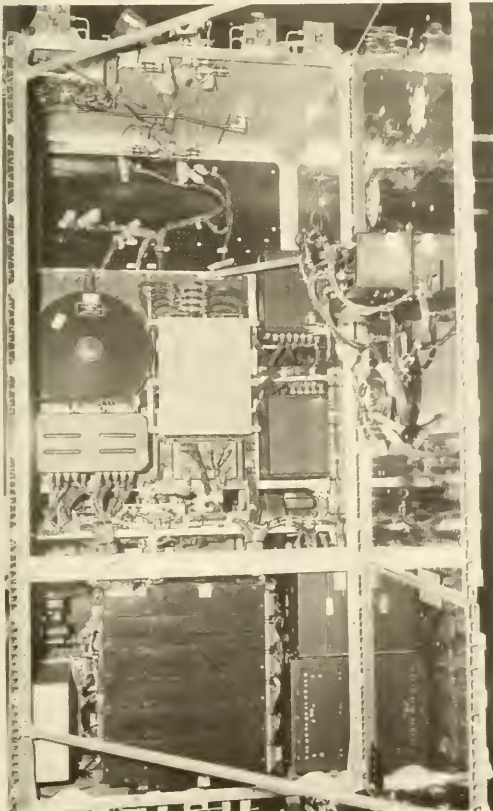
FIGURE 9–7.—Interior of the OGO "box," showing the multitude of components and the thick cabling connecting them. (Courtesy of TRW Systems.)

Function	*Typical equipment*
(4) Signal conditioning and the translation of instrument outputs into the proper language and telemetry format (encoding).	Encoders, commutators, analog-digital (AD) converters, voltage-frequency converters.
(5) Data storage for later burst transmission over data-acquisition stations.	Tape recorder(s), magnetic-core memories.

These communication functions are clear cut except for the fuzzy frontier between the communication and scientific-instrument subsystems. In the highly integrated Explorer-class satellites, much of the signal conditioning, including analog-digital conversion and signal amplification, falls on the communication-subsystem side of the line. The more standardized Observatory-class spacecraft usually require the experimenter to manipulate his signals to fit the established format.

Not all satellites perform all five listed functions. Explorers IX and XIX, for example, carried only tracking beacons; there were no onboard experiments per se. Explorer I and some piggyback satellites have telemetered in real time, and dispensed with tape recorders. And, of course, the command receiver is not essential to the simpler satellites.

The importance of the communication subsystem is underscored by the observation that its failure demotes the satellite from the "active" list to the category of "space debris." Attitude and environment-control subsystems may sometimes fail without seriously compromising scientific value, but telemetry and power are imperative.

Communication-Subsystem Interfaces.—The designer of satellite communication equipment cannot have a completely free hand. His apparatus is but a link in a chain stretching from the experiment sensors, through the data-acquisition stations, to the experimenter. He is constrained further by the space environment, physical laws (obviously), and the host of interfaces portrayed in figure 5–2, page 136. Let us review the interfaces systematically, for much that is said here also applies to the other subsystems.

Communication usually consumes a substantial fraction of the total satellite electrical power; if densely packed electronic modules are to remain at operable temperatures, all degraded electrical power, now appearing as heat, must be transported to the satellite surface and radiated away. In most instances, this thermal interface is bridged by installing high-conductivity paths

to the satellite skin. In extreme cases, thermoelectric cooling may be attractive. The problem is reversed, however, when the satellite passes into the Earth's cold shadow. Here, heat may be welcome, because electronic components are compromised by low as well as high temperatures (sec. 9–8).

The mechanical interface with the satellite launch vehicle was mentioned earlier (sec. 8–1). Shock and vibration absorbers decouple the electronic chassis from the impressed forces. A second technique employs printed and integrated circuits to desensitize this interface. Any construction approach that reduces the number of soldered connections and lead-supported parts enhances the probability that the equipment will survive the launch process. Potting of electronic assemblies also helps to make the structure more rugged. Occasionally, the entire satellite interior, as in the case of Telstar, will be potted in plastic foam.

In all scientific satellites, there is intense competition for every steradian of solid angle. The communication subsystem feels this when likely spots for mounting antennas are found to block
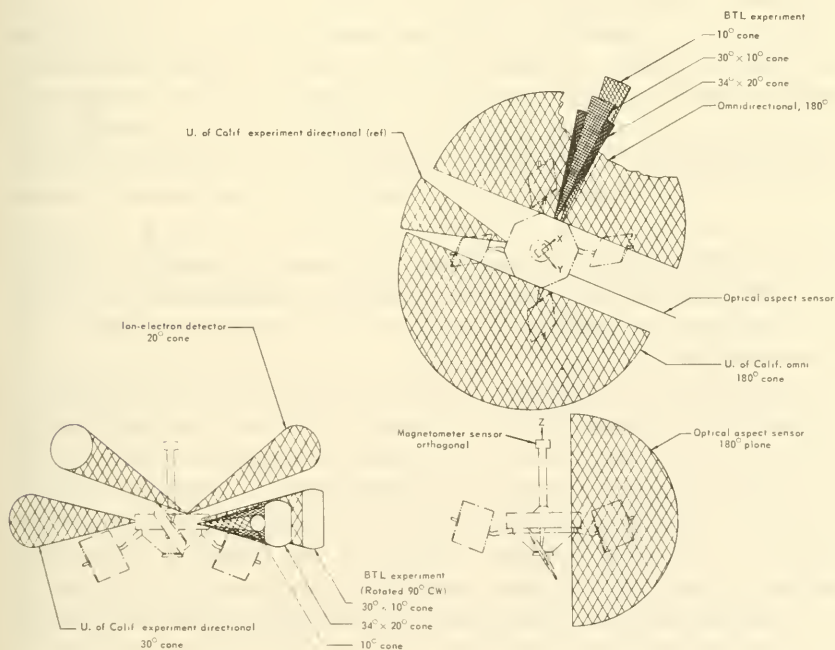
FIGURE 9–8.—The spatial interface problem on satellites is illustrated by the competing look angles on Explorer XXVI.

instrument-view cones or interfere with solar-cell paddles (fig. 9-8). This kind of interface problem is solved partially by the use of booms, but more significant are the delicate tradeoffs and negotiations between subsystem design groups.

An electrical interface separates the communication and power-supply subsystems. The power provided must be well filtered and regulated. Power-supply transients and instabilities caused by low voltages could insert errors into the telemetry.

Nuclear-radiation interfaces might originate with radioisotopic power generators. The major consequence would be radiation damage to the electronic components, an effect that could be reduced with radiation shielding, providing the extra weight did not offset any advantages of the nuclear fuel.

Magnetic interference with satellite-scientific instruments is reduced by using nonmagnetic materials, requiring the installation of shielded, twisted leads, and wiring layouts that preclude uncompensated current loops. Residual magnetic fields inevitably survive the best planned magnetic-cleanliness campaigns. Magnetic mapping of the satellite during the final stages of satellite integration may suggest rewiring, material replacement, or installment of instrument booms.

Electronic crosstalk or radiofrequency interference is a two-way affair, where transients and signals in other subsystems interject disturbing signals into the communication subsystem, and vice versa. Every lead that threads its way through the satellite harness is a potential originator and recipient of crosstalk. An obvious solution is the elimination of unnecessary wires through good electronic design; say, the insistence on a single-point ground. Electromagnetic shielding and component isolation are other possibilities. As with magnetic cleanliness, many crosstalk problems are not identified until final integration tests with actual hardware.

The biological interface is rather academic for most satellites, though it is a critical one for planetary probes. One satellite experiment has been proposed in which instruments will search for indigenous life in the high atmosphere. In this instance, satellite sterilization will preclude contamination of the instrument with micro-organisms carried by the other satellite components. Even potting compounds, fuel, and electrical insulation can be contaminated. Component sterilization exacts a high price; few conventional electronic parts can withstand heat soaking at 135° C for 24 hours or more.

Signal conditioners and data encoders in the communication

and connecting subsystems bridge the so-called "information" interface. Data formats, flow rates, reference voltages, and synchronization signals typify the parameters that must be matched.

Communication-Subsystem Design.—The interplay of the major communication parameters—range, power, frequency, bandwidth, bit rate, signal-to-noise ratio, telemetry type—was examined in section 5–5. Pertinent now is the translation of theory into hardware.

It is tempting to generalize about each functional component in the satellite: transmitter, encoder, transponder, etc. The diversity of satellite telemetry systems reduces generalization to either triteness or statements hedged with abundant exceptions. The approach adopted here describes representative communication subsystems, in which the solutions of typical problems are implicit. The selected satellites are:

Explorer I_____Illustrating FM/FM and FM/PM telemetry and historically interesting aspects of the first U.S. satellite

Explorer XIII_____Illustrating PDM/FM/AM telemetry and the use of redundant transmitters

Explorer XVIII   Illustrating a typical Goddard Space Flight Center
   (IMP I).   satellite using PFM telemetry

OV–3–1_____Illustrating PAM telemetry, as employed by many small satellites, and the extensive use of off-the-shelf components

OGO I_____Illustrating the flexibility and redundancy typical of Observatory Class satellites and the use of PCM/PM telemetry

The Explorer-I Communication Subsystem.—Explorer I was built on a crash basis (sec. 2–2). Simplicity was essential. Except for scaling circuits, no data processing was done before transmission to Earth. Examination of the block diagram (fig. 9–9) shows two separate telemetry subsystems: a long-life, low-power, FM/PM unit, transmitting data at 108.00 megacycles (also used for Microlock tracking); and a short-life, high-power, FM/FM telemeter at 108.03 Mc, keyed to the Minitrack tracking network. The Geiger counter was the only scientific instrument shared between the two telemeters. Dual-telemetry transmitters are rather common on scientific satellites, for they materially increase the probability of successful data acquisition and tracking.

In each Explorer-I transmitter, information from the scientific and spacecraft-status instruments was fed into FM oscillators,
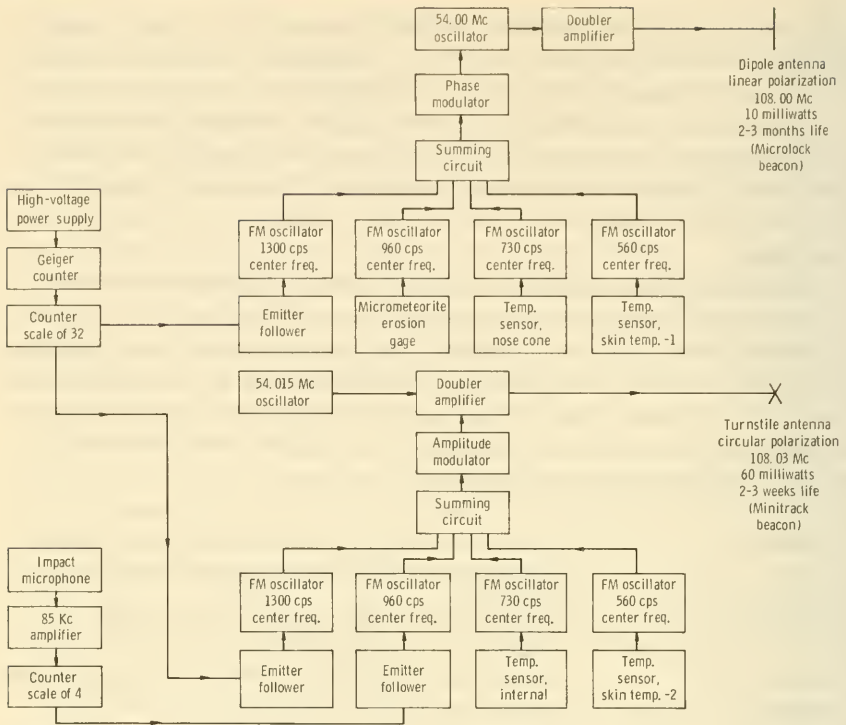
FIGURE 9–9.—The Explorer-I communications-subsystem block diagram. This is a particularly simple approach, with minimum data conditioning, no data storage, and no command receiver.

operating at center frequencies in the audio range. The oscillator frequencies were either resistance or current controlled, depending upon the type of sensor. Summing circuits added the oscillator outputs and fed the resultant into the transmitter carrier modulator. Unlike later, more sophisticated telemeters, data commutation and tape recording were absent. All eight measured parameters were transmitted in real time. There was no command receiver.

Turnstile and whip antennas transmitted Explorer-I signals to Minitrack and Microlock ground stations. The turnstile radiation pattern, nominally isotropic (fig. 9–10), was skewed by the satellite structure. Measurement of signal fluctuations on the ground was useful in determining the satellite spin rate.

The Explorer-XIII Communication Subsystem.—Explorer-XIII, a micrometeoroid satellite, needed a reliable telemetry subsystem that could transmit microphone impacts, pressure-cell punctures,
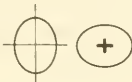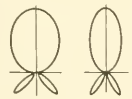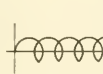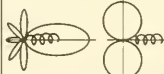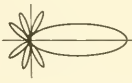
Type	Propagation pattern	Typical performance values				Typical applications
		Polarization	Gain over isotropic	Frequency range	Bandwidth	
Whip, stub		Linear	3-4 dB	1 Mc-6 Gc	Up to 40%	Many satellites, such as Oscar I, Pegasus I, TRS I
Half-wave dipole		Linear	2.15 dB	1 Mc-6 Gc	Up to 40%	Many satellites, such as Explorer XX RAE
Canted turnstile		Circular off ends; linear in plane	1.3 dB	50 Mc-3 Gc	Up to 10%	Many satellites, such as Alouette I, Ariel I, Explorer I, Greb 5, etc.
Half-wave slot (cavity)		Linear	5 dB	100 Mc-35 Gc	<10%	Launch vehicles, Syncom
Helix		Circular	Axial, 4-5 dB; broadside, 2-3 dB	50 Mc-6 Gc	Axial, up to 60%; broadside, up to 20%	Telstar, LEM
Cavity-backed spiral		Axial, circular; broadside, elliptical	3-5 dB	200 Mc-10 Gc	10-1	Launch vehicles, Gemini, Transit
Paraboloidal reflector		Determined by feed	20-50 dB	Determined by feed	Determined by feed	Ranger, Mariner
Horn		Linear	2-25 dB	1-75 Gc	1.6-1	Feeds for paraboloidal reflectors
Phased array		Depends on elements, dipoles, slots, etc.	10-30 dB	2-70 Gc	Depends on elements	Future communications satellites

FIGURE 9–10.—Summary of spacecraft antenna characteristics. Propagation patterns shown with crosses are made looking straight down on the antenna. Turnstile antennas are very common on scientific satellites because of their isotropic pattern. (Adapted from ref. 3.)

satellite temperature, and several other analog and event-type data. The telemetry approach finally selected combined FM and PDM modulation on the same carrier. The telemetry signal consisted of a train of FM bursts, the durations of which were con-
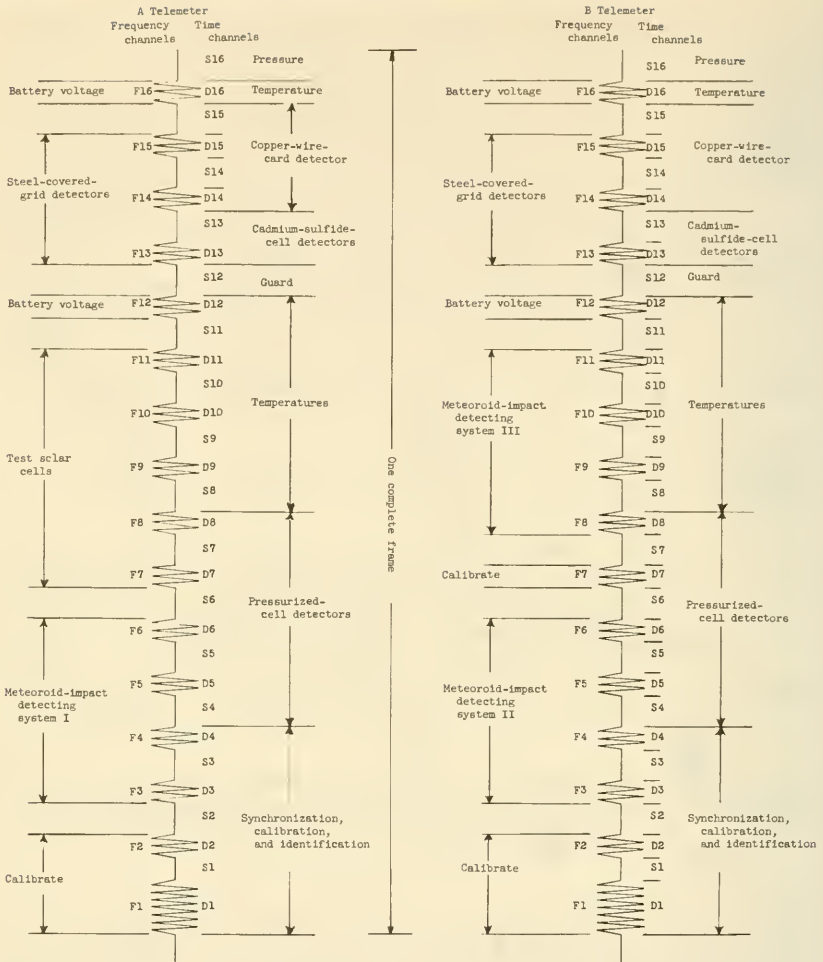
FIGURE 9–11.—Explorer-XIII telemetry format. Information is carried by both pulse duration and signal frequency (ref. 4).

trolled by the outputs of some of the scientific instruments (fig. 9–11). Both the carrier frequency and burst duration carried information to experimenters on the ground. The communication-subsystem block diagram (fig. 9–12) shows some of the sensor signals going to an encoder, which gated 16 subcarrier oscillators on and off in sequence. The gate width depended upon the magnitude of the sensor data point received by the encoder. The frequency of the subcarrier, however, was controlled by a dif-
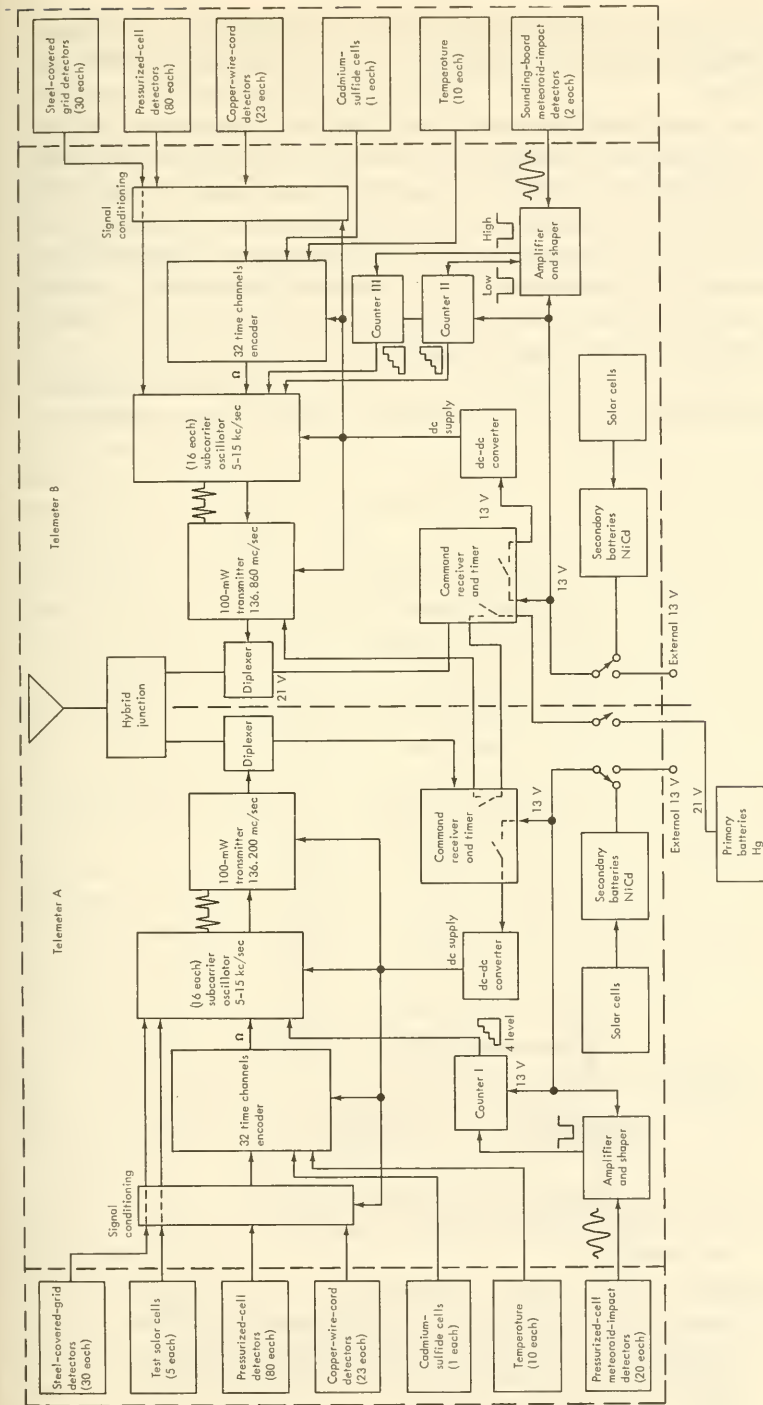
FIGURE 9–12.—The Explorer-XIII dual-telemeter approach. Experiments are divided between the two independent but very similar telemeters, so that the failure of one will only reduce by half the area actively measuring micrometeoroids (ref. 4).

ferent data point, which arrived at the subcarrier oscillator directly from the signal-conditioning unit without passing through the encoder.

The two separate, but essentially identical, telemeters served roughly half of the instruments in each category; i.e., half the pressurized cells, etc. The loss of one transmitter would only have halved the effective area of each experiment rather than knocked out whole experiments. All telemetry modules (fig. 9–13) except the transmitter itself were constructed on printed circuit boards and potted in place with polyurethane foam. Solid-state components were used throughout.

The Explorer-XIII transmitters were of the master-oscillator, power-amplifier type, with a crystal-stabilized oscillator and base-
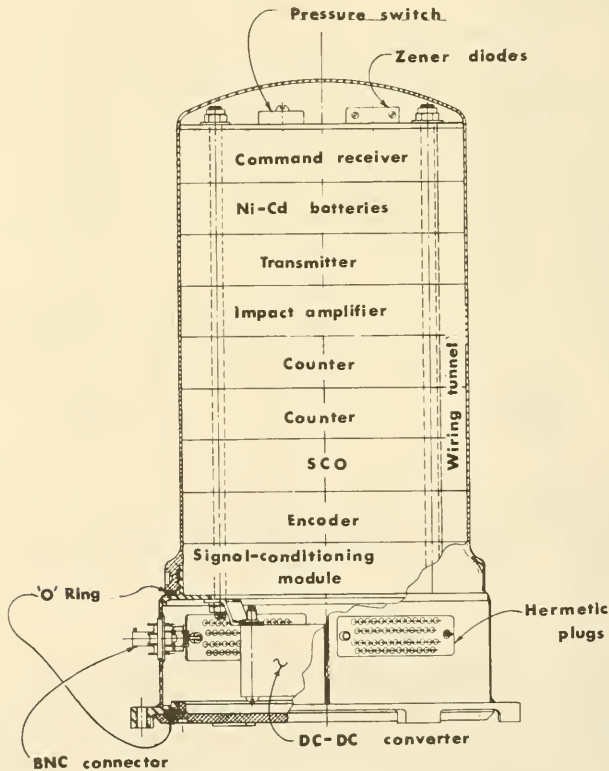
FIGURE 9–13.—Cutaway view showing the arrangement of the Explorer-XIII Telemeter B. The components were foamed in place with polyurethane, and the container was hermetically sealed. Height: about 25 centimeters (ref. 4).

modulated final amplifier. The transmitter power input was 750 milliwatts. The modulated output power was 150 milliwatts, for an overall efficiency of 20 percent.

The command receiver, like most satellite receivers, was a superheterodyne tuned to the single command frequency. The circuitry derived directly from the Vanguard program, except that an automatic turnoff timer was added.

Telemeter B on Explorer XIII also served as the Minitrack beacon. Interlocks silenced it whenever the satellite was interrogated from the ground. A more recent trend is toward beacons that are completely divorced from the rest of the communication subsystem.

Analysis predicted that Explorer XIII would eventually shift from its initial stabilizing spin motion to tumbling. An antenna with an isotropic pattern was therefore selected. The choice was a turnstile with four erectable whips, spaced 90° apart around the satellite body (fig. A–15). The same antenna was used for telemeters A and B and reception of ground commands. A frequency-selective diplexer separated the transmitter and receiver, while a hybrid junction isolated the two transmitters.

The Explorer-XVIII Communication Subsystem.—A PFM telemetry system was selected for Explorer-XVIII (IMP I), because of its relatively low power requirements. Analog and digital data were electronically commutated by an encoder into a series of time-multiplexed PFM bursts and blanks (fig. 5–6). The frequency of the signal in a burst from an analog channel varied directly from 5 to 10 kilocycles in response to the analog input, ranging from 5 to 0 volts dc. The signal frequency for digital channels varied from 5 to 15 kilocycles in eight discrete steps, depending upon three-bit words being telemetered. The basic format consisted of 256 channels in 16 frames (ref. 5).

The output of the encoder drove the IMP transmitter modulator. The carrier was phased-modulated with an output rf power of 4 watts. A turnstile antenna completed the spacecraft portion of the communication link.

The OV–3–1 Communication Subsystem.—The OV–3 communication subsystem differs from the preceding examples in three important ways:

(1) The decision to incorporate flight-qualified, off-the-shelf components wherever possible—a departure from the usual custom-built equipment, which also points out a difference in DOD and NASA philosophy

(2) The decision to rely upon the tracking and data-acquisition facilities of the Department of Defense National Range System instead of NASA's STADAN. (See sec. 7–4.) The more limited data-acquisition equipment and geographical coverage are reflected in telemetry design

(3) The choice of PAM/FM/FM telemetry, a distinct change from most NASA satellites
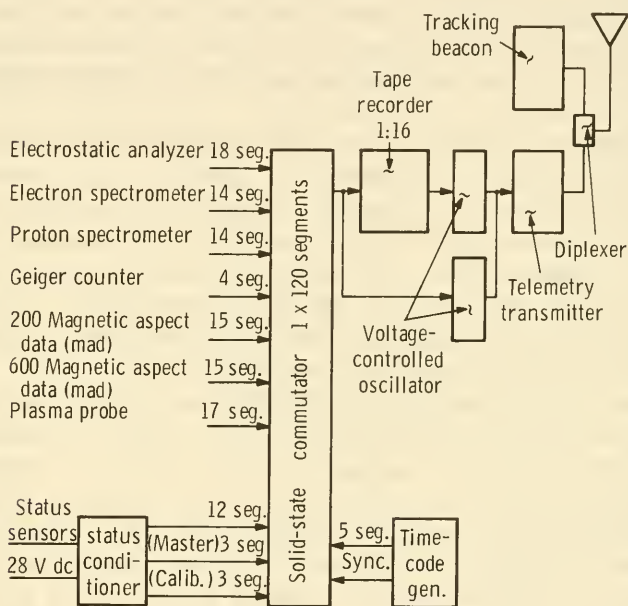
FIGURE 9–14.—Block diagram of the OV–3–1 telemetry system. (Courtesy of Space General Corp.)

The telemetry block diagram (fig. 9–14) is relatively straightforward. In selecting an off-the-shelf transmitter, 18 different commercial units were evaluated, thus showing the ready availability of such equipment. The vendors of three telemetry units were finally chosen and asked to respond with quotations based upon a detailed set of specifications drawn up by the Space General Corp., the OV–3 prime contractor. Some pertinent excerpts, illustrating typical modern satellite requirements:

Frequency range: 215–260 Mc, with stability better than 0.01 percent
Output power: 2 W
Power requirement: 26.5 V dc±3.5 volts at 650-mA maximum

Weight: less than 655 grams (23 oz)
Volume: less than 410 cm³ (25 in.³)
Operating temperature range: $-20°$ to $+85°$ C
No potentiometers or varactors
Extensive and detailed test specifications

The final choice was a Conic Corp. CTM–301 telemetry transmitter (figs. 9–15 and 9–16). The rating procedure leading to the final selection heavily weighted prior successful performance in satellites, sounding rockets, and aircraft.

The OV–3–1 data requirements demanded a 1 x 120 commutator. No suitable, off-the-shelf, solid-state items were available, so vendors were asked to quote a price for a custom-built unit on
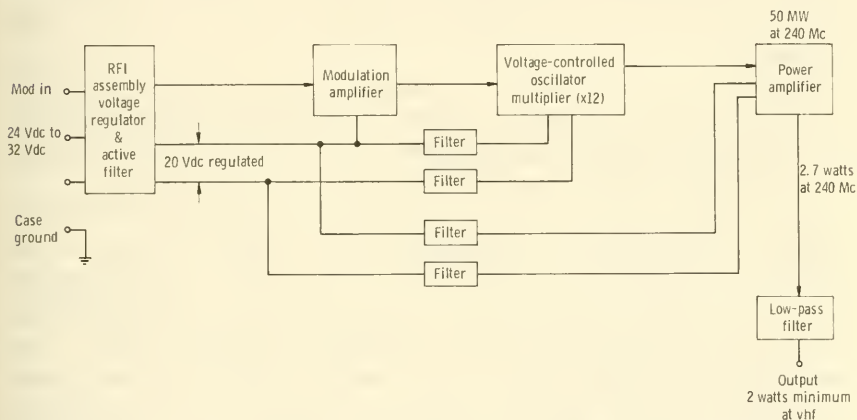
FIGURE 9–15.—Block diagram of the Conic CTM–301 telemetry transmitter used on OV–3–1. (Courtesy of Conic Corp.)
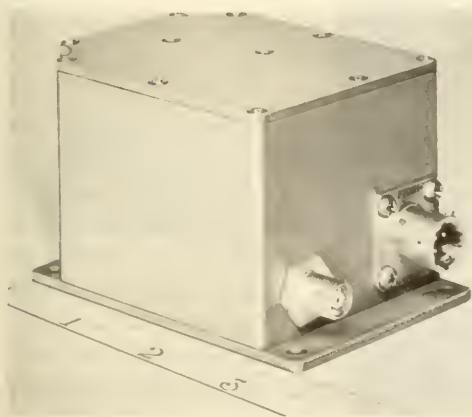
FIGURE 9–16.—Telemetry transmitter from figure 9–16 illustrating the small size of satellite electronic equipment; scale is in inches. (Courtesy of Conic Corp.)

the basis of detailed specifications. In this case, a Stellarmetrics bid was accepted.

The same sort of selection procedure resulted in the choice of an off-the-shelf Conic Corp. CTB–202–03 beacon. This was a crystal-controlled, continuous-wave unit with an output power of 150 milliwatts at 215–260 megacycles; weight, less than 85 g; volume, less than 37 cm³.

Several space-qualified tape recorders capable of the required 16:1 record:playback ratio were also available off the shelf for OV–3–1. One manufactured by the R. M. Parsons Electronics Co. was selected (fig. 9–17). The tape recorder was the only communication-subsystem component that contained moving parts —dual electric motors drove the tape reels through a clutch and negator switch. The tape recorder weighed less than 4 kilograms, and consumed 3.5 watts while recording and 9.3 watts during playback.

The OV–3–1 telemetry transmitter and beacon fed a canted turnstile through a diplexer, which isolated the two transmitters. The command receiver—a small uhf, FM unit—received its signals through two dipoles attached to the body of the satellite.

The OGO-I Communication Subsystem.—The OGO's were designed to transmit up to 128 000 bits/sec from as many as 50 different experiments. In addition, OGO's status could be modified by up to 254 different ground-originated command words. In short, the OGO communication subsystem is large, complex, and sophisticated, displaying all five communication functions: data telemetry, command receipt, beacon transmission, data encoding, and data storage. These capabilities had to be provided in a
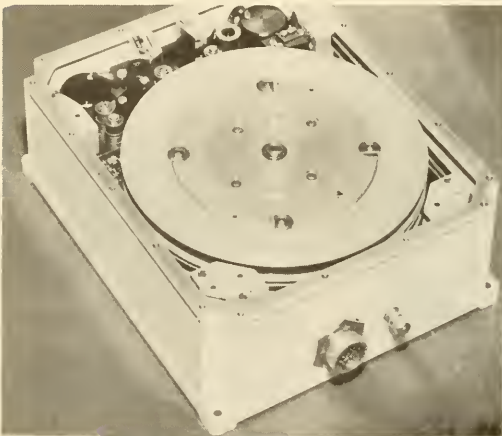
FIGURE 9–17.—Photograph of the OV–3–1 tape recorder. (Courtesy of R. M. Parsons Co.)

standardized, yet flexible form. In other words, the interface between the communication subsystem and the experiments had to be simple in order to fulfill the Observatory role as a "bus" for scientific "passengers," who were not particularly concerned with the workings of the satellite. Thus, in OGO, we see a communication subsystem well along one of the main paths of satellite evolution, with very high bit rates, frequent redundancy, many commanded modes of operation, and electronic nerve fibers in every subsystem.

Three digital, wideband telemetry transmitters handle the bulk of OGO's data. Data may be analog or digital in character and originate in experimental or satellite-status sensors. The two redundant digital units, shown in figure 9–18, operate either in
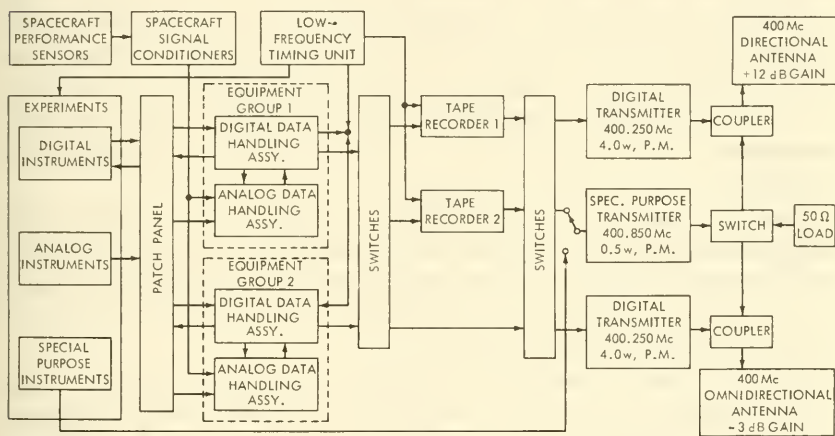
FIGURE 9–18.—Block diagram of the OGO data-handling and telemetry system. Note the redundant transmitters (ref. 1).

real time or through redundant tape recorders. The main frame of the telemetry format consists of 128 nine-bit words. Three 128-word subcommutators are also available, 1 for experiments and 2 for status sensors. One of the latter commutators can be operated at the main frame rate upon command, when operational problems arise—a good example of OGO flexibility. Several bit rates can be commanded from the ground: 64 000, 8000, or 1000 bits/sec when the tape recorder operates with an input of 1000 bits/sec. When the tape-recorder input is 4000 bits/sec, data readout can be consummated at 128 000 bits/sec.

In addition to the digital, wideband telemetry, a special-purpose FM transmitter can handle up to five subcarriers from experiments with outputs unsuited to digital telemetry.

Raw data from the OGO experiments are fed through a patch panel, which is a flexible yet standard way to route signals from the many different experiments that are installed on the various OGO's. From the patch panel, experimental data are fed into the redundant data-handling assemblies (fig. 9–18). Status data, in contrast, may bypass the patch panel, because they vary little from OGO to OGO. The data-handling assembly consists of five multiplexers, all basically arrays of solid-state electronic gates that either pass or block signals at prescribed times in such a way that each bit is inserted into its proper spot in the telemetry format. There is a main multiplexer, assigned to the main frame, the 3 subcommutators mentioned above, and a flexible-format multiplexer, which permits selection, from the ground, of any 32 combinations of 32 experiment parameters to be inserted into the telemetry frame. Behind "flexible formating" is the desire to sample selected experiments more rapidly when physical phenomena, such as solar flares, change the focal point of scientific interest.

Analog data are also converted into digital data in the data-handling assembly. The OGO AD converters, using a successive-approximation technique, accept analog-input signals between 0 and 5 volts. These are then quantized (or "chopped") into 250 0.02-volt levels at 128 bits/sec.

Each of OGO's two tape recorders can store 43 200 000 bits. When recording at 1000 bits/sec, the two can accumulate 24 hours of data. Total readout time is 22.5 minutes for the two recorders.

Two redundant AM receivers detect digital ground commands at approximately 120 megacycles. The digital decoders have the capability to process and route as many as 254 independent commands: 104 for satellite-status modification and 150 for experimental adjustments. Digital command words are 24 bits long and contain a sync bit, satellite and decoder addresses, decoder mode, the command itself, and an address that will select the proper relay in the command-distribution unit. The command word, like a telephone number, chooses the right satellite and combination of circuits and actuators within it. The command word itself, plus two mode bits, is also transmitted in complement form as a check.

An independent tone-command system, through which a few of the most important status commands can be transmitted, is an

excellent example of the functional redundancy found in the larger satellites. Tone-command systems are common in satellite technology, and experience has made them simple and very reliable. The OGO tone-command decoder recognizes a command as three specific tones in the proper sequence. The first tone addresses a particular OGO, while the 2 others can provide a total of 12 different commands. Tone control permits limited operation of an OGO in the event the digital decoders fail.

Beacons and transponders in the OGO communication subsystem aid in the tracking of the OGO's (fig. 9–19). Two redundant,
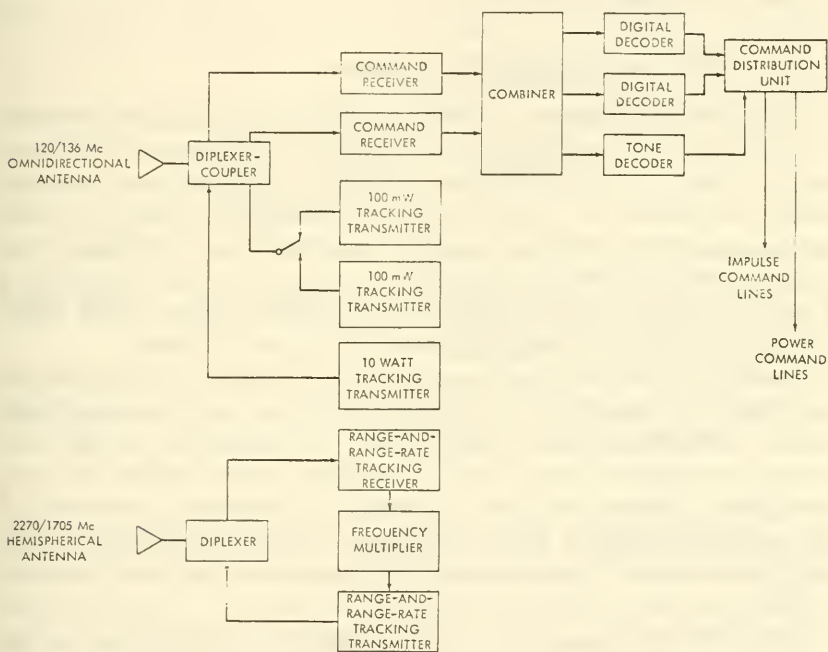
FIGURE 9–19.—Block diagram of the OGO beacon transmitters and command receivers (ref. 1).

100-milliwatt STADAN beacons at 136 megacycles suffice for close orbits. A 10-watt, 136-megacycle beacon is used when the satellite is over two Earth radii away, as it is on EGO (Eccentric Geophysical Observatory) missions. OGO also carries a Goddard Range-and-Range-Rate (R and RR) tracking transponder, enabling faster and more accurate fixing of eccentric orbits. Triggering signals at about 2270 megacycles are received from

one or more ground stations. A transponder signal is returned at 1705 megacycles. Details on the operation of the Range-and-Range-Rate system are given in section 6–2.

Reference to figure A–33 shows OGO's four antennas:

(1) a 400-megacycle omnidirectional turnstile for wideband telemetry (two are provided for polar missions)

(2) a 400-megacycle directional antenna, consisting of driven elements, plus a reflecting screen (for the EGO mission only)

(3) a 120/136-megacycle crossed-dipole, omnidirectional antenna for the beacon transmitters and command receivers

(4) a hemispherical, pointable antenna for the Range-and-Range-Rate tracking system

9–5. The Power-Supply Subsystem

A few watts of electrical power enable a small satellite to measure directly the features of outer space and transmit the data back to Earth. A few hundred watts, on the other hand, are sufficient to operate an Observatory-class satellite, which is a veritable laboratory with dozens of instruments. Although the sciences of aeronomy and geodesy can profit from observing a silent satellite, scientific utility is multiplied many times when a reliable source of electrical power is placed on board.

Sunlight is the obvious source of power in outer space, and the overwhelming majority of scientific satellites have captured this energy with solar cells. The handful of exceptions carried batteries for primary power, but only when short active life was acceptable. Solar cells have seemingly unassailable command of the scientific-satellite power market, a position of superiority achieved through demonstrated performance and ready availability.

Just what makes up good space powerplant performance? The major factors, as always, are weight, reliability (lifetime), and cost. The powerplant also must deliver the power needed, at the right moment, and at the right voltages and degrees of regulation (table 9–8). In other words, raw power must be refined, or "conditioned," and made to match the satellite power "profile." It takes power, weight, and many additional, fallible parts to condition, switch, and otherwise make raw power palatable to satellite equipment.

The dominance of solar cells in satellite power ties the hands of satellite designers in several respects. As indicated in table 9–8, solar cells cost fixed numbers of dollars and kilograms for each

TABLE 9–8.—*Satellite-Powerplant Performance Factors*

Performance Factor	Typical requirements	Design implications and observations
Weight_____	Minimum_____	Lightweight construction—honeycomb solar panels, etc. Weight proportional to average power level.
Reliability_____	~0.95 for 6–12 months.	Solid-state circuitry virtually mandatory. Solar-cell covers necessary to prevent excessive radiation damage and help thermal control. Series-parallel solar-cell arrays are common.
Cost_____	Minimum_____	Only solar cells and radioisotopic power generators are qualified for long-life use. Costs are about $250–$800/watt and $19 000–$50 000/watt, respectively.
Power level_____	1–100 W for Explorer class, 100–500 W for Observatories. Highly variable.	Solar paddles needed above 50–100 watts. Radioisotopic fuel not available for large generators.
Power profile_____	Highly variable_____	Energy accumulators (batteries) and switching circuits required.
Voltage levels____	5–50 volts dc on bus bars.	Power-conditioning equipment with attendant weight, power losses, and reliability burden necessary.
Degree of regulation.	Voltages ±1 percent_	Power-conditioning equipment with attendant weight, power losses, and reliability burden necessary.

watt. Furthermore, each watt will require a relatively inflexible number of square centimeters of exposed area, the precise quantity depending, of course, upon satellite attitude control and orbit, estimated power-supply degradation with time, etc. The point is that one cannot do much except take solar cells as they are. There is little room for major tradeoffs.

Since weight, cost, and exposed area are proportional to the power level needed, low power is a favorable attribute. Power, though, is roughly synonymous with scientific capability. The small, Explorer-class satellites consume less than 100 watts, while Observatory-class spacecraft need between 100 and 500 watts to handle their more complex missions. In the context of Apollo manned spacecraft, scientific satellites are low-powered craft. Indeed, 500 watts is probably the upper power limit for the unmanned scientific satellites discussed in this book. Larger scien-

tific spacecraft will undoubtedly be manned space laboratories, such as the USAF MOL (Manned Orbital Laboratory).

Possible Powerplants for Satellite Use.—The size and power limits of scientific satellites also severely limit the spectrum of applicable power supplies. Before examining various types of space powerplants now under development, let us look at the internal anatomy of the generalized space powerplant.

First, there must be an energy source, either the environment itself or an onboard reservoir, such as chemical or nuclear fuel (fig. 9–20). Next, an energy converter is provided—to change, for instance, photonic energy into electricity. Since no energy converter is perfectly efficient, the waste energy, usually in the form of heat, must be disposed of. In heat engines, such as the
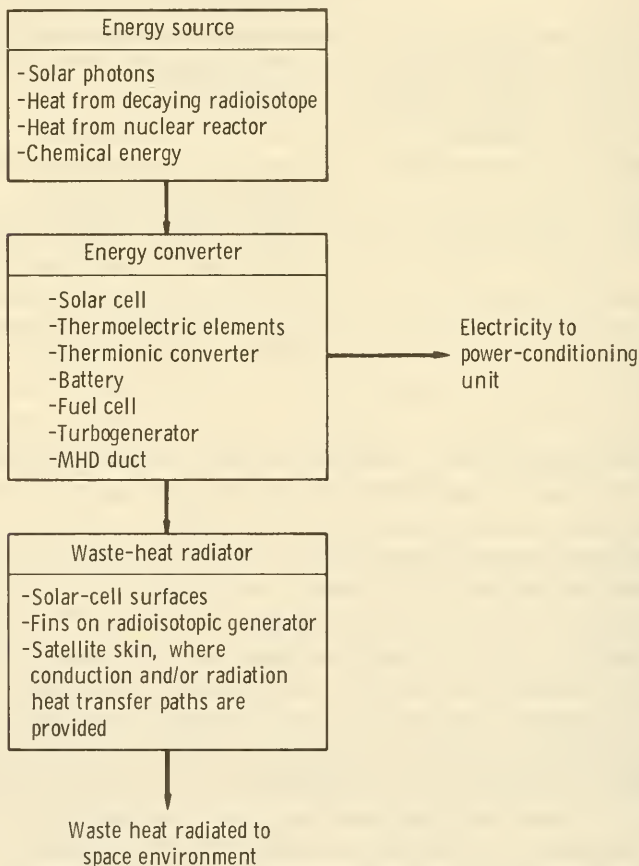
FIGURE 9–20.—Block diagram of a space powerplant, showing typical components.

radioisotopic power generator, 95 percent of the fuel's energy may be radiated uselessly away to empty space. Completing the picture is the power-conditioning equipment, which feeds regulated power, at the correct voltages, to the satellite equipment.

TABLE 9–9.—*Comparison of Space Powerplants* [a]

Type of powerplant	Status, advantages, and disadvantages
Solar cell	Used on almost all scientific satellites. Rugged, relatively reliable, and, most important, available and flight proven. Solar cells are heavy, costly, and require a great deal of area. Must be pointed toward Sun for optimum power generation.
Solar-thermoelectric	Potentially rugged and reliable, but not yet operational. Heavy and relatively inefficient.
Solar-thermionic	Potentially rugged and reliable. Requires high pointing accuracy. Still in R&D stage.
Solar-dynamic	Under development for multikilowatt applications. Still in R&D stage. Too big and too heavy for unmanned scientific-satellite applications.
Radioisotopic-thermoelectric	Proven for satellite use in Transit program (Snap 9A). Competitive in weight with solar cells, but generally more costly. Nuclear radiation hinders use on satellites with radiation instrumentation.
Radioisotopic-thermionic	Under development (Snap 13), but still several years away from operational status. Potentially very lightweight.
Radioisotopic-dynamic	In study stage. Potentially lightweight at the several-kilowatt level. Probably not applicable to unmanned scientific satellites.
Chemical battery	Widely used for energy storage. Chemical-energy density too low for all except missions shorter than a few months.
Chemical fuel cell	Unsuited to most scientific satellites because chemical energy density is too low. Biosatellite is an exception. Good for short missions (Gemini, Apollo).
Chemical-dynamic	Do.

[a] Nuclear-reactor powerplants are omitted from this table because they are weight-competitive only at powers above several kilowatts.

Space powerplants are characterized by their energy source and conversion scheme. Thus, we have the solar family, consisting of solar cells, solar-thermoelectric generators, solar-thermionic generators, and solar-dynamic; i.e., turbogenerator powerplants. Nuclear and chemical energy sources are allied with the same energy converters (table 9–9). The functional descriptions of the many combinations of power source and converter that have been under development since the beginning of the Space Age make a fascinating story, but it is a tale that is out of place here. Of all the combinations listed in table 9–9, only three have reached operational status in satellites: solar cells, batteries, and radioisotopic-thermoelectric power generators. Actually, there is little likelihood that any other types of power supplies in table 9–9 will find use on scientific satellites before 1975. They are either unsuited to long-life satellites or too far from operational status. Because of these facts, only solar cells, batteries, and radioisotopic generators will be covered in the following descriptions.

Batteries.—Explorer I, the first U.S. satellite, relied solely upon batteries for its power. It is fitting, therefore, to begin with this very common component.

TABLE 9–10.—*Characteristics of Satellite Batteries*

Type	Reaction [a]	Practical storage capacity, whr/kg	Remarks
Nickel-cadmium (NiCd).	$2NiOOH + Cd + 2H_2O \rightarrow$ $2Ni(OH)_2 + Cd(OH)_2$	20–40	High cycling life, negligible gassing, can be overcharged.
Silver-cadmium (AgCd).	$Ag_2O + Cd + H_2O \rightarrow$ $2Ag + Cd(OH)_2$ also $AgO + Cd + H_2O \rightarrow$ $Ag + Cd(OH)_2$	50–60	Durable, nonmagnetic, lower cycle life.
Mercuric-oxide (HgO).	$HgO + H_2O + 2e^- \rightarrow$ $Hg + 2OH^-$	60–70	Good for high-temperature operation. Always used as a primary battery.
Silver-zinc (AgZn).	$Ag_2O + Zn + 2OH^- \rightarrow$ $2Ag + ZnO_2^= + H_2O$ also $AgO + Zn + 2OH^- \rightarrow$ $Ag + ZnO_2^= + H_2O$	60–100	High capacity, reliable, high discharge rate, but temperature-sensitive. Gas evolved on standing or charging.

[a] These reactions are rather idealized; cell chemistry is not nearly so clear cut.

Secondary batteries, which may be discharged and recharged and thus serve as energy accumulators, almost inevitably accompany solar cells on satellites because of the Earth-shadow and power-profile problems. Even satellites with radioisotopic power generators find secondary batteries useful in handling uneven power profiles. Primary batteries, on the other hand, are not rechargeable and find application only on those satellites with short design lifetimes; i.e., Explorer I, the Oscar series, the early Sputniks, and others. Statistically speaking, fully 75 percent of all scientific satellites have carried secondary batteries.

Batteries are chemical-energy accumulators. They are common household items, and it seems superfluous to describe their operation in detail. Typical chemical reactions occurring in space batteries are presented in table 9–10.

The silver-zinc (AgZn) cell [3] (table 9–10) is frequently put to use as a primary battery because of its high storage capacity of 180–200 watt-hr/kg. Mercury batteries have also seen some use as primary batteries.[4] By far the most popular battery in space, however, is the nickel-cadmium (NiCd) secondary battery, which has proven to be stalwart and capable of withstanding the many charge-discharge cycles typical of scientific-satellite missions (fig. 9–21). Silver-zinc and silver-cadmium batteries, as they become more reliable, are replacing nickel-cadmium secondary batteries on some satellites.

Speaking generally, batteries have been the source of many frustrations in space-power-plant design, despite a venerable history stretching back to Volta. Problems have included the failure of seals and separators, the narrow useful temperature range, evolved gases, and the need to protect them from overcharging. Ceramic seals have conquered some of these problems. Also, a three-electrode battery has been designed that increases the recombination rate of evolved oxygen and signals the onset of overcharging. The prosaic battery is finally becoming adequately tailored to satellite use.

Solar Cells.—Of the many devices that can tap the Sun's energy, only solar cells have reached operational status.

Briefly, the solar cell is a sandwich of n- and p-type semiconductors. Silicon is usually the basic material, with phosphorus-doped silicon forming the n-layer and boron-doped silicon the p-layer. When photons are absorbed in the vicinity of the p–n

[3] More accurately, the silver-oxide zinc cell.
[4] The appendix lists all scientific satellites and briefly describes their power supplies.
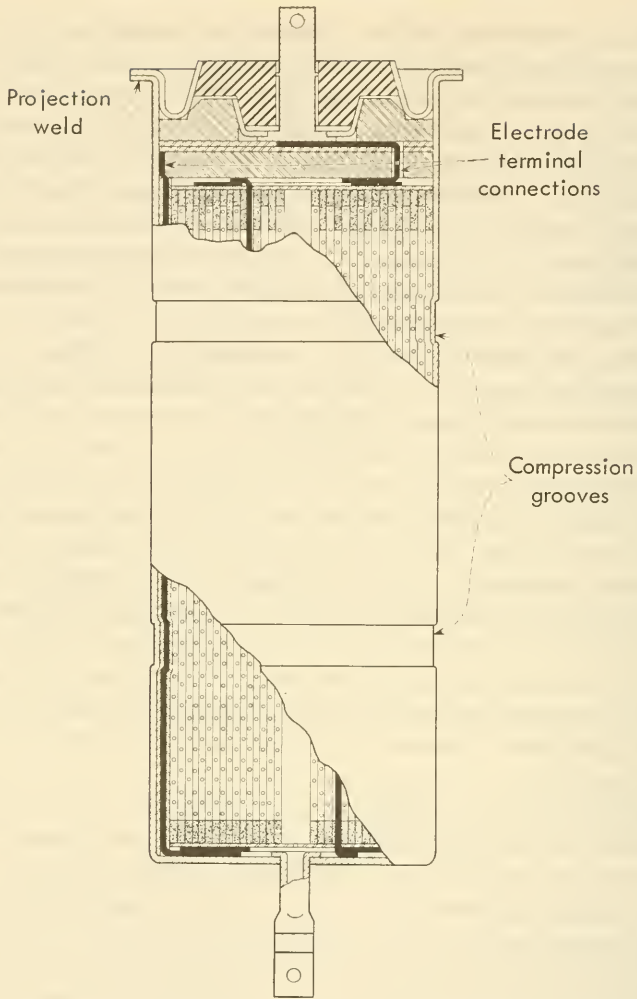
FIGURE 9–21.—Cross section of a nickel-cadmium battery designed expressly for space use. Length: 8.2 centimeters (ref. 6).

junction (fig. 9–22), electron-hole pairs are created and an electromotive force is established across the junction. Current will flow through an external circuit connected across the junction. Nonproductive heat from absorbed photons flows to the cell surfaces, where it is radiated to empty space or to portions of the satellite that may be in view. Silicon solar-cell response peaks at about 8000 Å, but the spectrum extending from 4000 to 11 000 Å is effective. Conducting grid lines are often added to the solar-cell
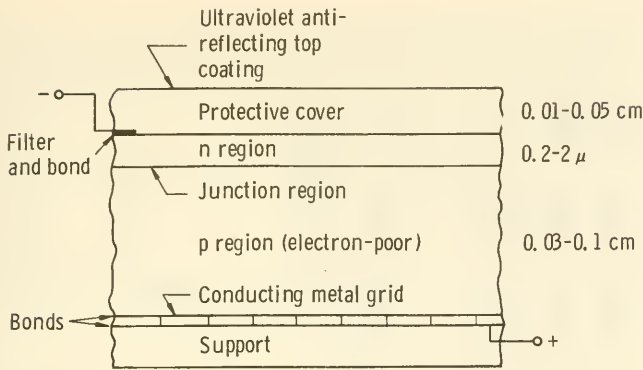
FIGURE 9–22.—Schematic of a conventional, rigid, n–p solar cell.

surface to decrease the resistance of the thin, diffused layer on top of the cell.

Solar-cell design problems are many—notwithstanding the enviable success of this energy converter. It is pertinent to list a few troublesome areas and the engineering approaches to their solutions:

(1) Solar-cell response falls off as the cosine of the angle with the Sun. Since unilluminated cells make open circuits, cells connected in series should be in the same plane; that is, the same satellite facet or paddle. Obviously, a spin-stabilized satellite must have several facets, or paddle faces, oriented in different directions to generate continuous power. Series strings can then be paralleled for reliability, with blocking diodes added to prevent current from circulating uselessly through dark cells (fig. 9–23).

(2) Solar power fluctuates as the satellite spins or tumbles in space—another consequence of the cosine law. The question here is one of attitude prediction. Saint-Jean has computed two generalized curves that are pertinent to spin-stabilized satellites with body-mounted or paddle-mounted solar cells, categories including most scientific satellites (figs. 9–24 and 9–25).

(3) Solar cells generate no power at all in the Earth's shadow (fig. 9–26). Assessing the magnitude of this all-but-unavoidable problem depends on geometry and orbital dynamics. Low satellites in near-equatorial orbits are shadowed nearly half the time. Eccentric satellites with distant apogees, such as the IMP's, will be in the Sun most of the time. At the sunny extreme are retrograde polar orbits, like the orbits once planned for AOSO, which remain in full sunlight for many months. There are too many
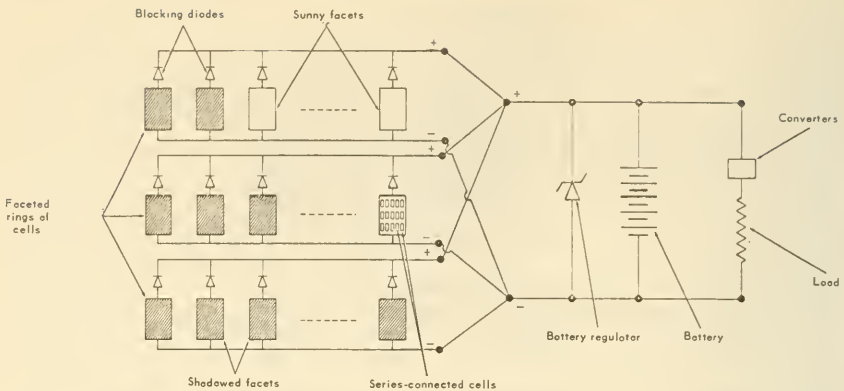
FIGURE 9–23.—Generalized schematic of a solar-cell power supply. Several satellite faces (or facets) are shown, but only a few are sunlit. Regulator protects battery from overcharging. (Adapted from ref. 7.)

variables and different orbits to express the eclipse problem in a general way. During the preliminary design of a satellite, the orbit will be predicted as a function of time by computer programs. Eclipse factors can be derived from these computations. One is illustrated later in this section for the OV–3–1 satellite. Each case is different. Knowledge of eclipse factors must be combined with satellite solar-aspect information to estimate the number of solar cells and batteries that will be needed to meet the power profile.

(4) Solar-cell efficiency decreases with increasing temperature (fig. 9–27) (ref. 8). To maintain solar cells at low (and efficient) temperatures, the ratio of solar absorptivity to blackbody emissivity (α/ϵ) is made as low as possible. Thin glass, quartz, or artificial-sapphire covers reduce the α/ϵ ratio considerably. A top antireflecting coating and bottom filter on the covers (fig. 9–22) to reduce: (a) cell heating by unproductive ultraviolet rays, and (b) degradation of the adhesive that bonds the glass to the cell. Actual thermal design of the solar-cell array involves heat inputs from the absorbed photons and heat intercepted from the body of the satellite. Heat is conducted to the cell surfaces and radiated to space. If high temperatures are unavoidable, gallium-arsenide cells (still under development) perform better than silicon cells at high temperatures.

(5) By far the most publicized solar-cell problem is that of radiation damage in the Earth's Van Allen Belts. Some satellite-power levels have decreased 22 percent in less than a month under
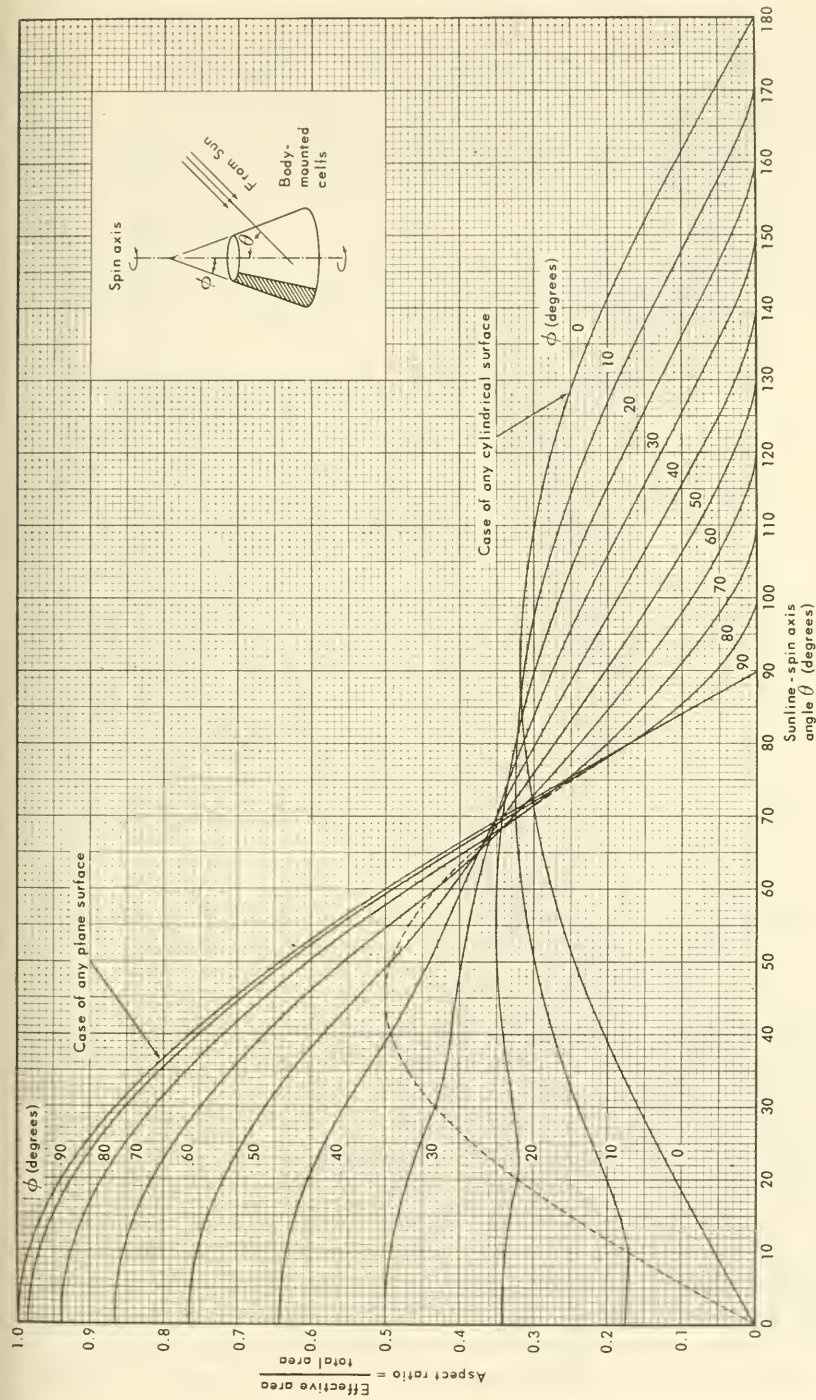
FIGURE 9–24.—Aspect ratio for a spinning satellite with a conical external surface (ref. 7).
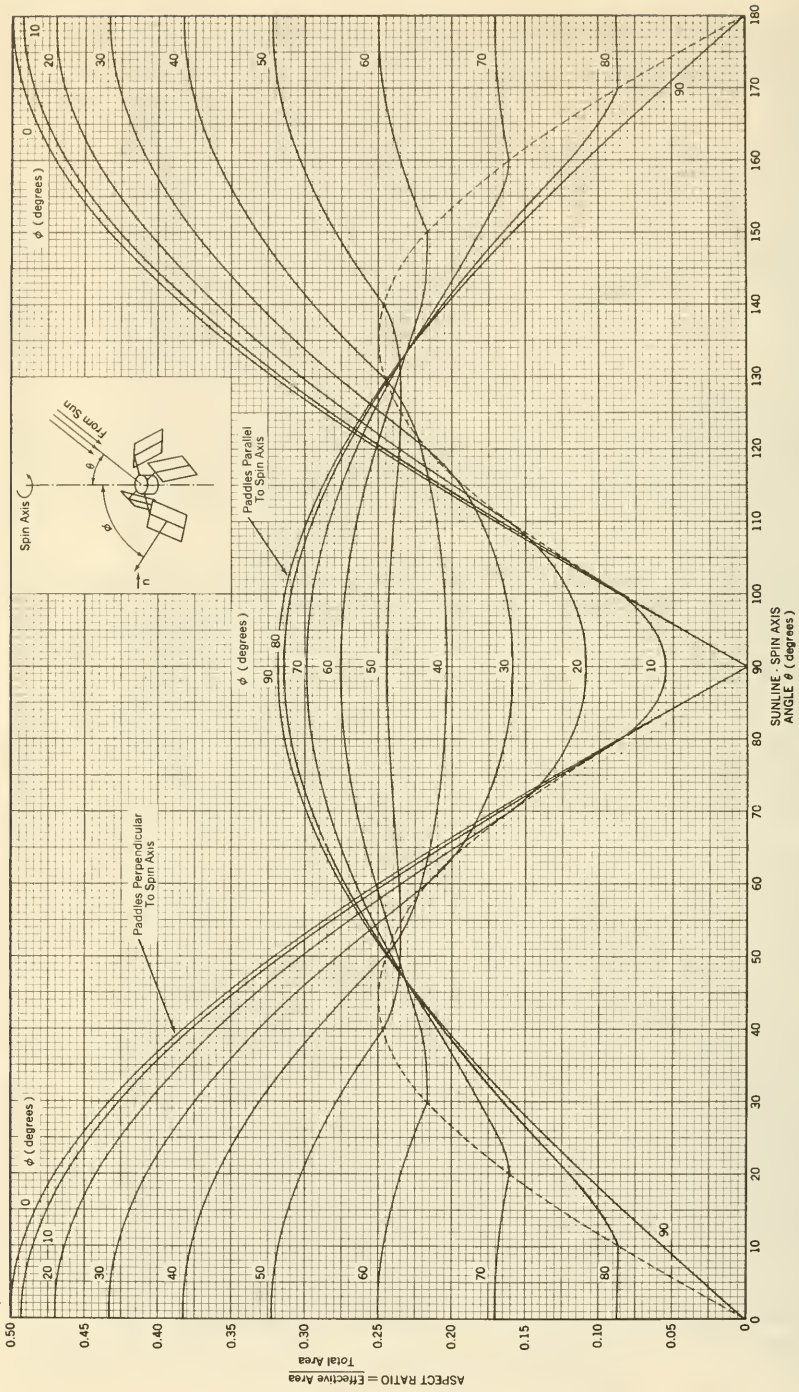
FIGURE 9–25.—Aspect ratio for a spinning satellite with solar-cell paddles (ref. 7).
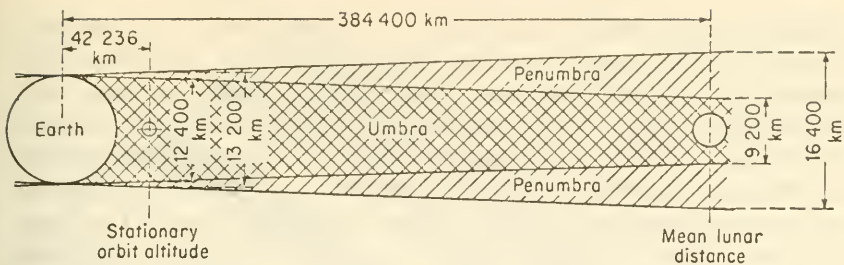
FIGURE 9–26.—Earth's umbra and penumbra. The penumbra is almost negligible at most satellite orbits.
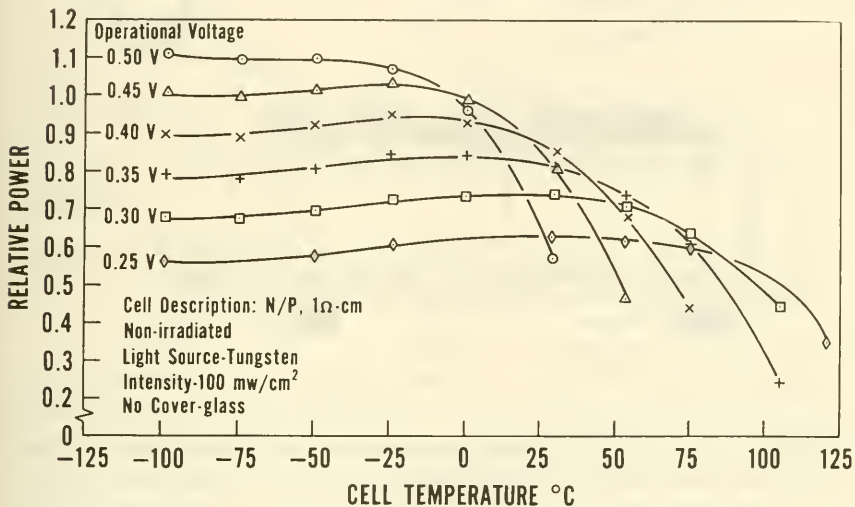
FIGURE 9–27.—Solar-cell power versus temperature, showing performance deterioration at high temperatures (ref. 8).

intense bombardment (ref. 9). Solar-cell covers made of glass or quartz a few tenths of a millimeter thick are effective in reducing degradation. In addition, the now nearly universal adoption of n–p cells over p–n cells has improved long-term performance of solar cells by at least a factor of 10. Some degradation still occurs —perhaps only 10 percent a year—but extra cells can be added to compensate for this loss of power (ref. 8).

(6) Solar-cell efficiency is also degraded by the surface abrasion of micrometeoroids. Again, the use of solar-cell covers reduces the inimical effects of this facet of the space environment.

The basic solar-cell sandwich—transparent cover, n-layer, n–p junction region, p-layer, 1- x 2-centimeter area (fig. 9–22)—is

rather useless until it and hundreds more like it are ruggedly
fastened onto some structure and electrically interconnected.
Solar cells are first fabricated into modules, which are then com-
bined into arrays. There are two important module-construction
techniques: shingling and flat mounting. In shingling, solar cells
are series connected in stairstep fashion (fig. 9–28), until enough
are strung together to make up the design voltage or the series
number desired for reliability purposes. Shingling is now going
out of style, principally because defective solar cells cannot be
replaced easily during the manufacturing process. Flat-mounted
cells do not overlap and can be removed simply. In flat mounting,
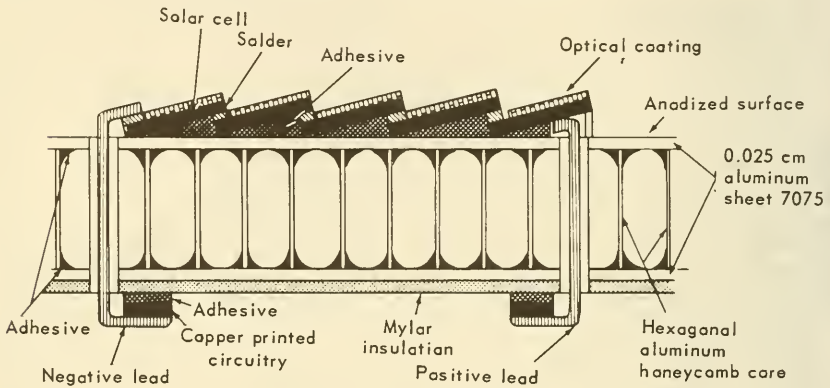
FIGURE 9–28.—Shingled solar cells, showing series connections. Note
how cells are bonded to the aluminum-honeycomb support (ref. 10).

adjacent cells are generally connected in parallel with bus bars
along their edges. Groups of shingled or flat-mounted cells con-
nected in a series-parallel combination make up the basic module.

In attaching solar-cell modules to the satellite, three approaches
are in vogue today: body mounting, paddle mounting, and panel
mounting. Body-mounted cells are cemented either directly to the
satellite skin or to light metallic sheets that are then attached to
the satellite. Small, spin-stabilized satellites tend to favor body
mounting. Several patches of solar cells are mounted on various
facets or distributed symmetrically around the spin axis to pro-
vide relatively constant power. Since some cells will always be
shaded, even cells that are 10 percent efficient yield an overall
efficiency of only 1–2 percent in body-mounted arrays. Medium-
sized satellites, such as the IMP's, cannot obtain enough power
with body-mounted arrays, and resort to the familiar paddle
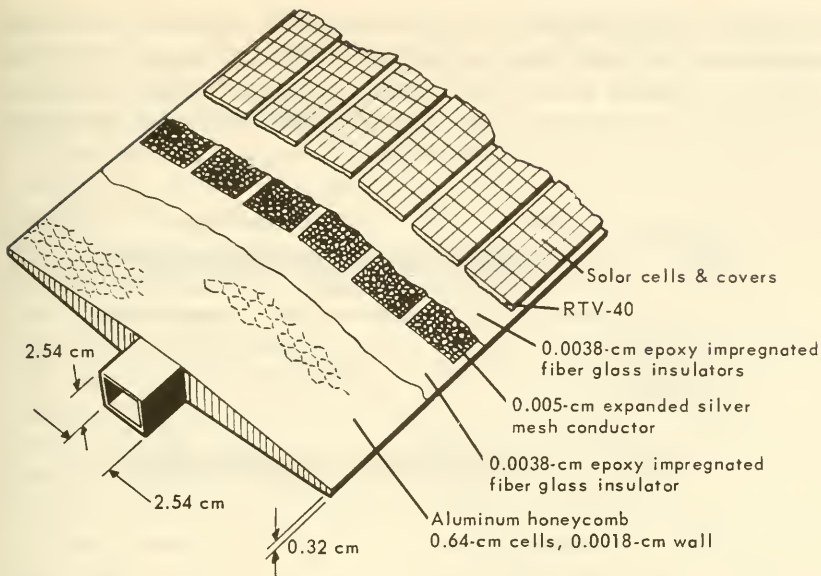
FIGURE 9–29.—Construction of the IMP–D solar paddles (ref. 11, copyright Aviation Week and Space Technology).

arrays (fig. A–17). Paddles are usually lightweight, honeycomb structures with cells bonded to the external faces (fig. 9–29). Since a large fraction of the paddle cells are always in the shadow, overall powerplant efficiency again falls between 1 and 2 percent. Paddles serve only to increase the satellite's total exposed area and add nothing to the solid angle available.

The most efficient solar-cell array is the oriented panel, as used on OSO and OGO, which is kept pointed toward the Sun by drive motors and attitude-control devices that are controlled by solar sensors. The production-line solar-cell efficiency of about 11 percent is not obtainable even with oriented panels, because the prolonged exposure to the direct rays of the Sun heats the cells up to as high as 50°–60° C. Overall efficiency is reduced to 6–8 percent.[5] Intense thermal stresses are also encountered with oriented panels as they plunge into the Earth's shadow zone and drop to as low as −100° C.

In terms of the ultimate performance parameters—weight, cost, and reliability—solar cells have attained the following: 1000 kg/kW for small, unoriented satellites (including the necessary

---

[5] Laboratory-measured efficiencies of advanced cells using tungsten light are around 15 percent.

batteries); large satellites in high orbits with oriented panels can achieve 150 kg/kW, but the weight of the necessary attitude-control equipment is excluded from this figure. Costs for solar-cell/battery powerplants run between $250/watt for favorable
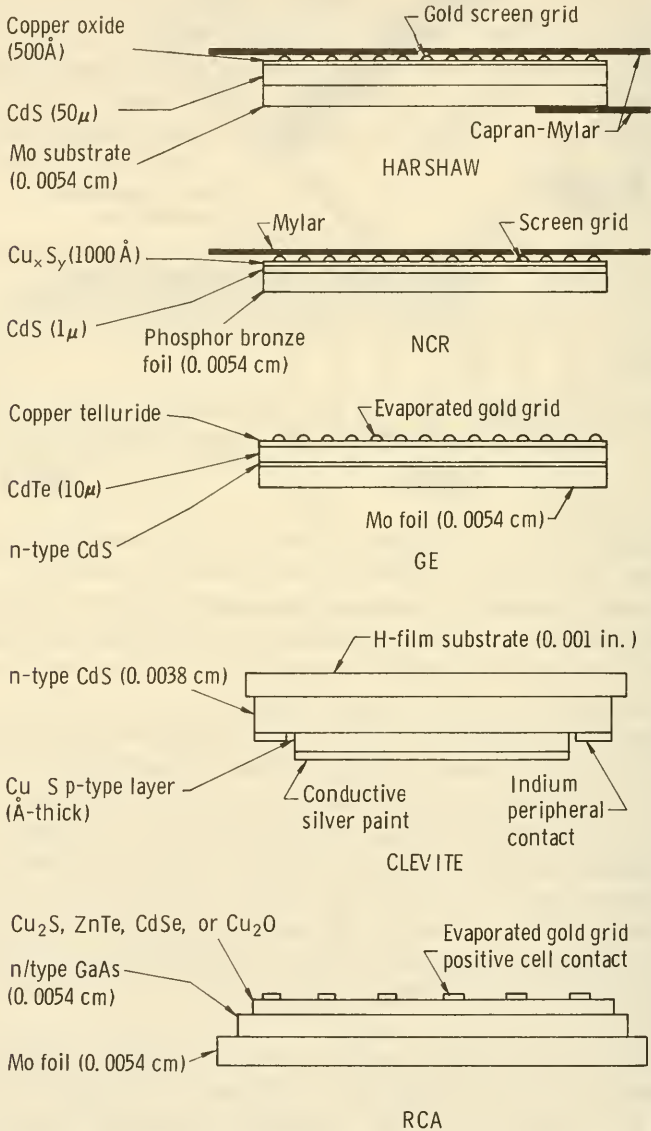
FIGURE 9–30.—Several approaches in the construction of thin-film solar cells. Not to scale (ref. 12).

orbits to as much as $800/watt in the radiation belts. The reliability of the solar cells themselves has been good; most power-supply failures have been attributed to the power conditioning and distribution equipment.

The conventional, rigid, single-crystal solar cell seems to have reached a performance plateau in terms of efficiency. The high costs may drop if production volume increases. Advances are still being made in adhesives, filters, and semiconductor materials, but, at the best, cost and weight will probably be only halved during the next decade. On another research front, thin-film poly-crystalline semiconductor cells (cadmium sulfide is a common material) can be made lightweight and flexible with laboratory efficiencies of 2–3 percent (fig. 9–30) (ref. 12). Thin-film cells may be useful in the future on space vehicles with spare external surface area, but scientific satellites will probably always be denied this luxury.

There seems little likelihood that the conventional solar cell will be deprived within the next decade of its preeminent position on scientific satellites by either exotic photovoltaic developments, solar-thermionic converters, or nuclear-power plants.

Radioisotopic-Thermoelectric Generators.—The radioisotopic power generator is the only other power source that has been operationally flown on satellites. In operational versions, such as Snap 9A, the Transit generator, heat from decaying radioisotopes is converted into electricity by thermoelectric couples. The fuel, usually plutonium-238, is located in a heavy fuel capsule placed along the centerline of the cylindrical generator (fig. 9–31). Radial thermoelectric elements, surrounded by thermal insulation, convert 5–7 percent of the heat into electricity. The remaining 93–95 percent of the heat must be radiated to outer space (ref. 13).

Experience with radioisotopic generators in space has been meager. Several modified Snap–3B and Snap–9A generators have been launched on the Transit series of satellites, but the total accumulated time in space is less than 1 percent of that experienced by solar cells. Nevertheless, radioisotopic generators have performed well and should be considered wherever they appear competitive with solar-cell/battery combinations.

The question of competitive performance is a ticklish one, because radioisotopic fuel costs, in particular, are deceptive. As yet, there is no abundant, reliable supply of the long-half-life fuels needed for scientific-satellite missions. Cost estimates for plutonium-238 and curium-244 generators run between $10 000
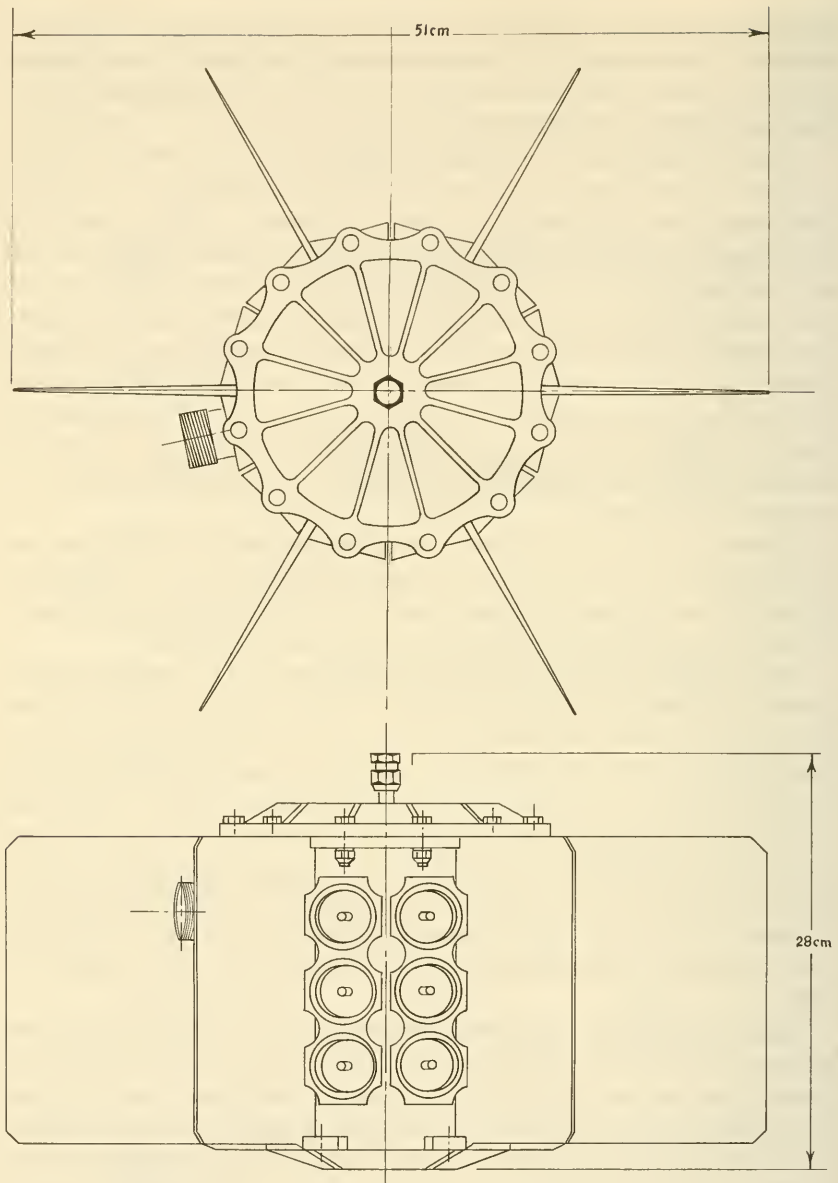
FIGURE 9–31.—Drawing of the Snap–9A, 25-watt radioisotopic generator installed on some of the Transit satellites.

and $50 000/electrical watt—much higher than equivalent solar cells. Radioisotopic power generators would have to offer critical and unique advantages to compete with solar-cell powerplants costing one or two orders of magnitude less. In the matter of

weight, radioisotopic generators can achieve 300 to 500 kg/kW—figures that compare well with all except oriented solar panels. A further disadvantage of radioisotopes on scientific missions is their radiation field, which may interfere with magnetometers and radiation detectors. In summary, it appears that radio-isotopic power generators will be used on only those scientific satellites where solar cells find the going difficult—perhaps in long-shadow-period orbits or the heart of the Van Allen Belts. At the moment, none of the scientific satellites scheduled up to 1970 is expected to use a radioisotopic power generator.

Power-Conditioning Equipment.—Estimates place 90 percent of the space powerplant failures and malfunctions at the doorstep of the power-conditioning equipment. Most of the malfunctions, though, have been minor and have not seriously compromised mission objectives. The impact of power-conditioning equipment on overall performance is underscored by the observation that about 30 percent of the total powerplant weight and 10–20 percent of its cost are tied up in this often-ignored component.

Power conditioning has four purposes:

(1) Inversion, where dc is converted into ac, or vice versa. On scientific satellites, dc is almost always applied to the bus bars, and since the powerplant generates dc directly, inversion is relatively unimportant.

(2) Conversion, where dc at the power-supply voltage is converted into one or more lower or higher bus-bar voltages

(3) Regulation, where powerplant transients and ripple are suppressed below some acceptable minimum

(4) Protection, where circuits are protected from high voltages and currents. Battery-overcharge protection is a familiar example.

The above functions are also common in terrestrial and aircraft electronic equipment. They will not be discussed further here, except in the context of complete powerplant systems.

Voltage conversion, a very common power-conditioning function on satellites, can be largely eliminated, along with its weight, cost, and reliability burdens, if satellite power buses could be standardized. A trend toward standard 28-volt dc power supplies is evident, but most power-conditioning equipment is still custom-built for each satellite. The trouble with custom-made electronic equipment is that it must be specially debugged and flight qualified. It is not possible to build up lengthy records of experience and reliability data. Ultimately, satellites will probably

standardize their operating conditions, just as aircraft manufacturers long ago fixed on 400-cycle ac power. Until then, power-conditioning equipment will continue to produce many headaches.

Powerplant Interfaces.—The solar-cell power supply is constructed from components similar to those in the communication
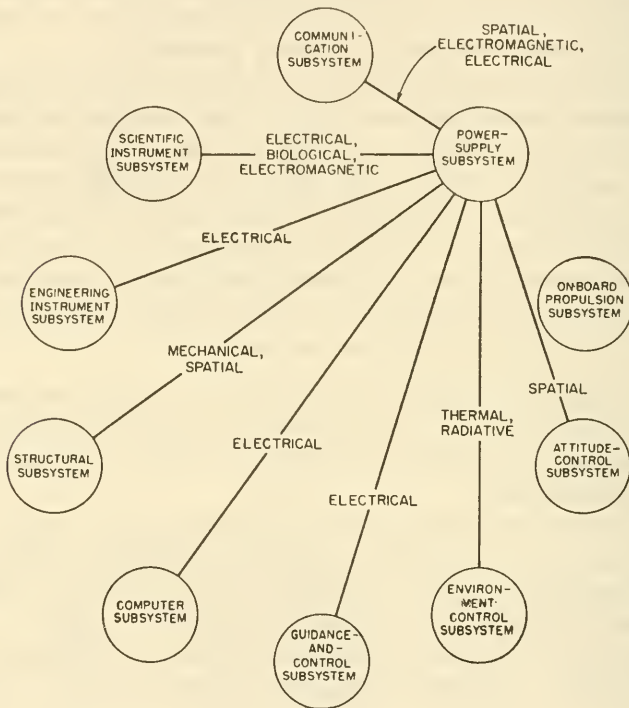
FIGURE 9–32.—Portion of the satellite-interface diagram showing the relationship of the power-supply subsystem to the remainder of the spacecraft.

subsystem. Most of the interfaces, therefore, are similar in nature, as indicated on the interface diagram (fig. 9–32). The electrical interface is handled by the power-conditioning equipment. The thermal interface, as mentioned earlier, can be serious because of the heavy loads of waste heat disposed of by the powerplant, particularly radioisotopic generators. On large satellites, the spatial interface may be a problem when solar-cell panels crowd the solid angle desired by the scientific instruments.

Power-Supply Subsystem Design.—The sequence of events in the preliminary design of a space powerplant is:

(1) Summation of all satellite subsystem and experimental power requirements. The plot of these requirements versus time is termed the "power profile" (fig. 9–33).
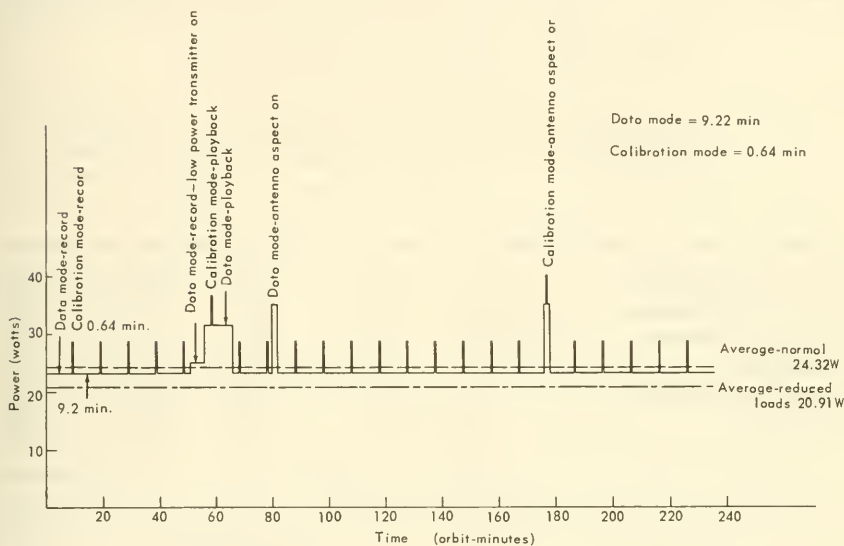
FIGURE 9–33.—Typical power profile for a scientific satellite. The power supply must provide these requirements despite its own variable solar input.

(2) The satellite orbit and associated eclipse factors are computed as functions of time to determine the solar flux impinging on the satellite. Satellite-attitude history is also predicted.

(3) Power losses due to radiation effects, temperature effects, and power conditioning are estimated

(4) The above factors are combined to estimate the solar-cell or radioisotopic fuel requirements. Of course, the type of solar-cell array must be selected before the total cell area can be projected.

(5) Preliminary computation of powerplant weight, cost, reliability, and delineation of the major interface problems

Before the design is completed, there will be several iterations through the list, as well as calculational refinements.

To illustrate the basic types of satellite powerplants, three specific systems will be discussed:

(1) The body-mounted solar-cell power supply of OV–3–1
(2) The paddle-mounted solar-cell power supply of Explorer XVIII
(3) The oriented-panel solar-cell power supply of OGO I

The Power-Supply Subsystem of OV–3–1.—The power requirements for OV–3–1 (table 9–11) illustrate how electrical loads are

TABLE 9–11.—*OV–3–1 Power Requirements*

Experiments	Voltage			Active power, W [a]
	Max, V	Min, V	Reg. percent	
Electrostatic analyzer_____	30	22	0.02	4.21
Electron spectrometer_____	30	22	.02	.68
Proton spectrometer_____	30	22	.02	.90
Geiger counter_____	30	22	.02	.59
Magnetic-aspect sensors_____	30	22	.02	2.64
Plasma probe_____	32	24	.02	5.00
Total_____				14.02

Spacecraft	Operating mode		
	Record	Transmit	Passive
Tape recorder_____	3.5	9.3	_____
Transmitter_____	_____	17.0	_____
Voltage-controlled oscillators_____	_____	.6	_____
Command receiver_____	3.5	3.5	3.5
Commutators_____	3.4	3.4	_____
Time-code generator_____	.6	.6	.6
Tracking beacon [b]_____	(1.0)	(1.0)	(1.0)
Status instruments_____	3.3	3.3	_____
	14.3	37.7	4.1
Experiments_____	14.0	14.0	_____
Total_____	28.3	51.7	4.1

[a] Zero passive power.
[b] Tracking beacon operates only for first few days.
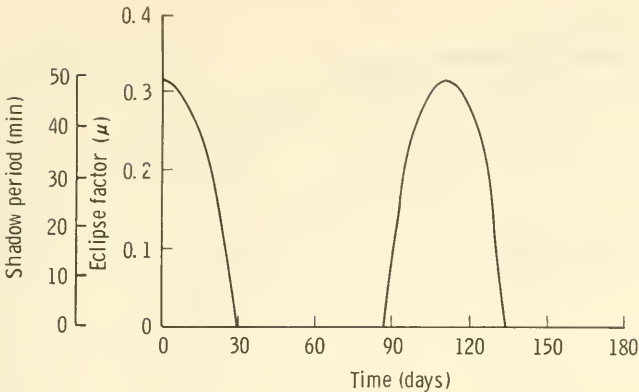
FIGURE 9–34.—Orbital shadow periods computed for the OV–3–1 satellite. (See also fig. 9–63.)

estimated and categorized during a typical preliminary design. These estimates were combined with the projected eclipse factor (fig. 9–34) to figure solar-cell requirements. Radiation and temperature effects on solar-cell performance were summarized in voltage-current plots (fig. 9–35). $n-p$ solar cells with 10-ohm-cm resistivity, topped by 0.051–centimeter quartz covers coated with an ultraviolet reflector, were selected. Two sizes, 1 x 2 centimeters and 2 x 2 centimeters, were body mounted, as shown in figure 9–36. Up to 72 cells were connected in series. Cells were insulated from their aluminum support by a 0.01-centimeter layer of epoxy-impregnated fiber-glass cloth bonded to the aluminum. Nickel-cadmium batteries, the old standbys, were chosen as the energy accumulators. Figure 9–37 shows the block diagram of the complete power supply. Note that an information interface exists with the guidance-and-control subsystem, and that power conditioning is carried out on both sides of the satellite-experiment interface. The total mass of the entire OV–3–1 power supply was 13 kilograms.

The Explorer-XVIII Power-Supply Subsystem.—Explorer-XVIII (IMP I) derived an average of 38 watts from four solar-cell paddles (fig. A–17) and a silver-cadmium battery pack containing thirteen 5-amp-hr cells (fig. 9–38). The primary system voltage was regulated at 19.6 volts, the maximum safe potential that could be continuously applied to the batteries without causing excessive gassing and pressure buildup (ref. 5). When the power output of the solar paddles was greater than that needed by the spacecraft, the surplus power was "dumped" as heat in
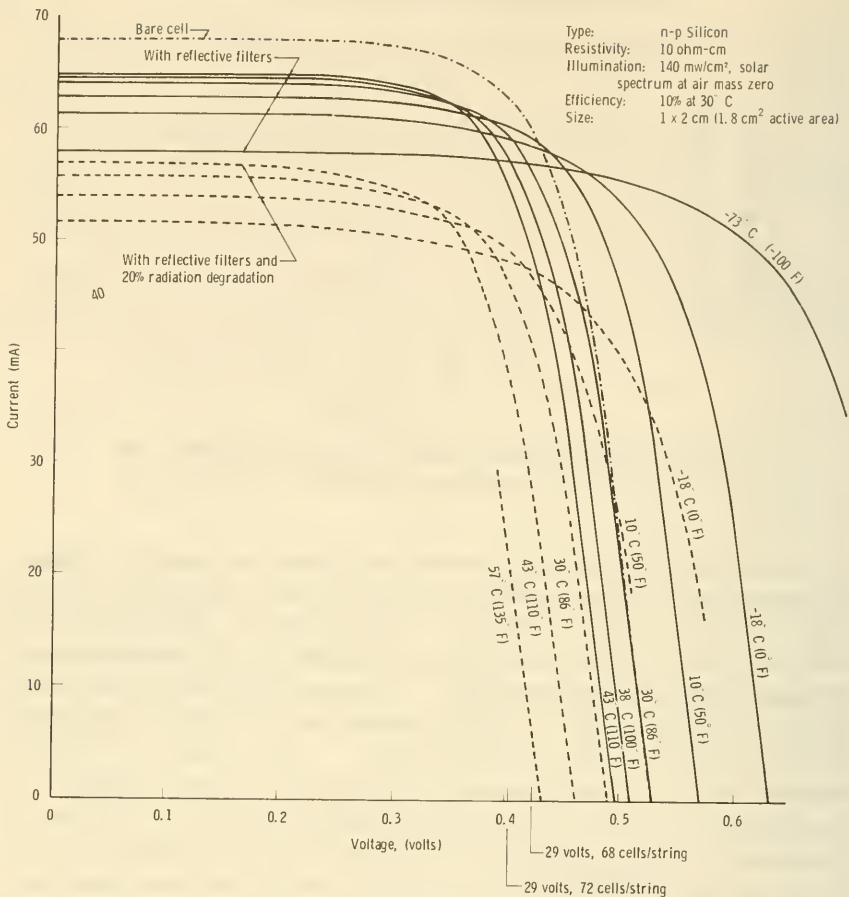
FIGURE 9–35.—Solar-cell performance curves calculated for the OV–3–1. (See also figure 9–27.) Note the many design parameters that must be considered.

resistors and transistors located on the paddle support arms. If the primary voltage fell below 12 volts, the spacecraft was turned off and recycle timers allowed an 8-hour battery-recharge period.

The prime converter shown in the block diagram conditioned the power for the rest of the spacecraft. It operated at an efficiency of about 70 percent over the 12–19.6-volt input range. A special connection to the MIT experiment (a Faraday-cup plasma probe) supplied a high-power transient.

On Explorer XVIII, great care was taken to avoid current loops and twist all high-power leads so that spacecraft-generated mag-
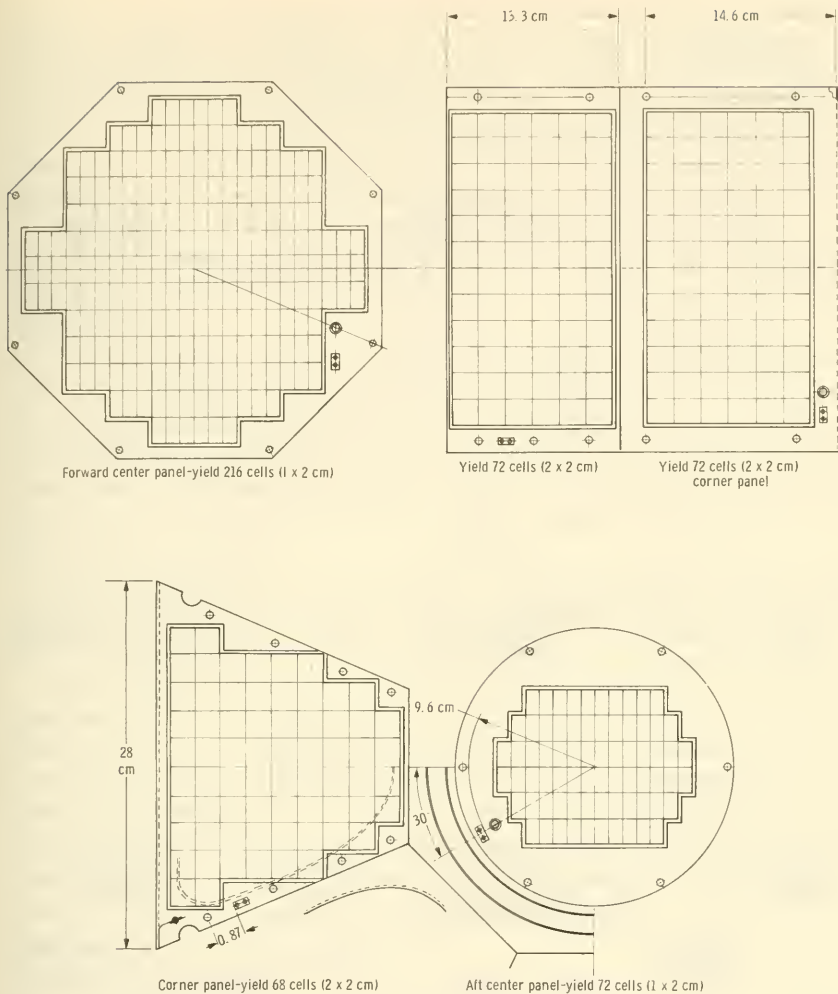
FIGURE 9–36.—Solar-cell layout for the OV–3–1. (Courtesy of Space General Corp.)

netic fields would not interfere with the magnetometers. In some cases, compensating current loops had to be added to cancel offending fields.

The OGO-I Power-Supply Subsystem.—The OGO-I power supply, designed under the Observatory-design philosophy, aimed not at providing specific quantities of power at particular voltages for specific experiments but, rather, a block of so many watts at a standardized bus voltage for whatever experiments might be carried by the various OGO satellites. The design power level pre-
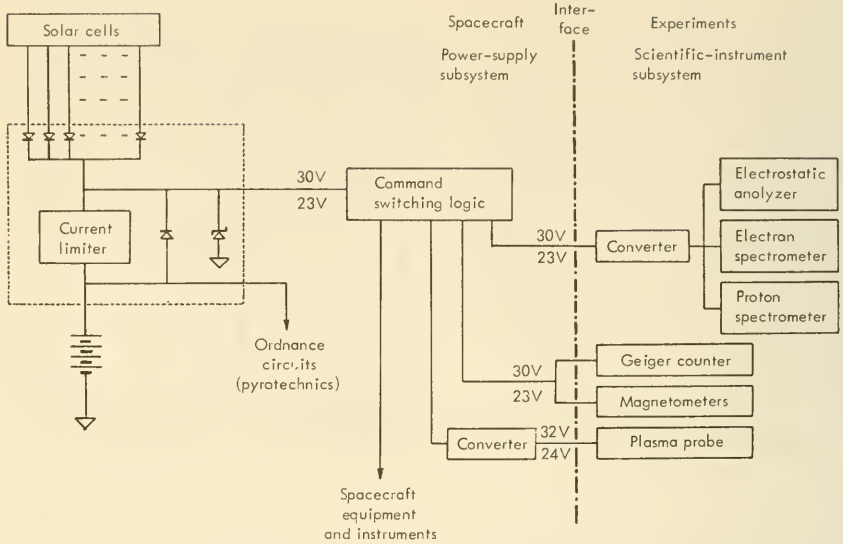
FIGURE 9–37.—Block diagram of the OV–3–1 power-supply subsystem. This is typical for Explorer-class satellites. (Courtesy of Space General Corp.)
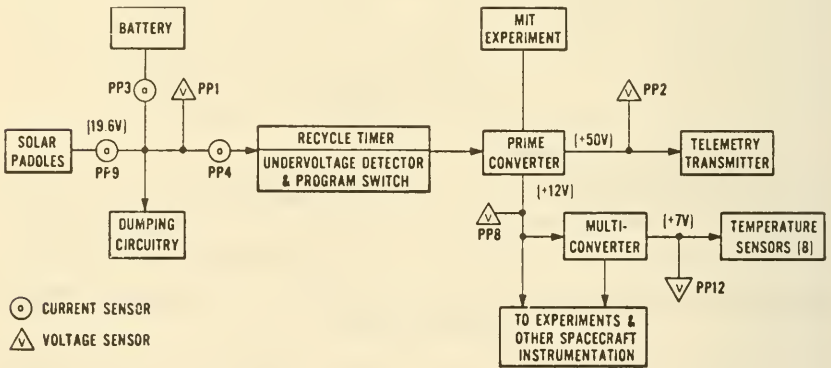
FIGURE 9–38.—Simplified block diagram for IMP I (Explorer XVIII). Measurement points for housekeeping telemetry are also indicated.

dicted for OGO I immediately after launch was 490 watts at 29.5 volts. During a year's operation, radiation and micrometeoroid bombardment on the EGO mission were estimated to reduce the total power to possibly 300 watts. Of this quantity, 50 watts were reserved for experiments, while the remainder went to the various satellite subsystems, especially the communication and

attitude-control subsystems (over 60 watts apiece, more than the experiments). Comparison with the OV–3–1 power allocations (table 9–11) shows that Observatories consume a larger fraction of the total power to keep their more complex subsystems operating. Of course, the Observatories do much more for the experimenter, such as stabilizing and pointing his experiments.

The high OGO power requirements made it obvious from the start that body-mounted cells would not suffice. Since complete attitude control was contemplated, solar-cell panels were the manifest choice.

The OGO power-supply subsystem received its energy from two large panels (fig. 9–39). A total of 32 256 gridded, 1 x 2 centimeters, p–n [6] cells with 0.15-centimeter glass covers were mounted in modules of 112 each on beryllium plates (fig. 9–40), and 140 modules were attached to each panel. The modules were interwired in a fashion that reduced the magnetic moment of the circulating currents.

Two nonmagnetic silver-cadmium battery packs, each of 12-amp-hr capacity, were used. Each battery consisted of 24 cells and weighed approximately 11 kilograms.

The complete OGO-I powerplant block diagram (fig. 9–41) indicates that, relative to OV–3–1 and Explorer XVIII, an OGO carries out more power conditioning, provides ground operators with more powerplant status data, and possesses many more commandable modes of operation. The main voltage bus carried approximately 28 volts throughout the satellite and to the experiments. The total OGO power-supply weight was about 79 kilograms, excluding power-conditioning equipment.

9–6. The Onboard Propulsion Subsystem

Onboard propulsion equipment first should be distinguished from launch-vehicle propulsion systems, which terminate thrust at orbital injection, and from propulsion for attitude control, which modifies the satellite orientation but not its orbit. Onboard propulsive functions are limited to: (1) station keeping, (2) orbital maneuvering, (3) deorbiting, and (4) descent braking. Interestingly enough, only the Biosatellite and Anchored IMP series have carried onboard propulsion systems, as just defined. Manned satellites (Gemini), some military satellites (Discoverers), and deep-space probes (Mariners) employ onboard propul-

---

[6] OGO-I mission only; n–p cells were used on all subsequent OGO's.

FIGURE 9–39.—The OGO solar panels shown in folded position. The OGO is shown undergoing tests. (Courtesy of TRW Systems.)
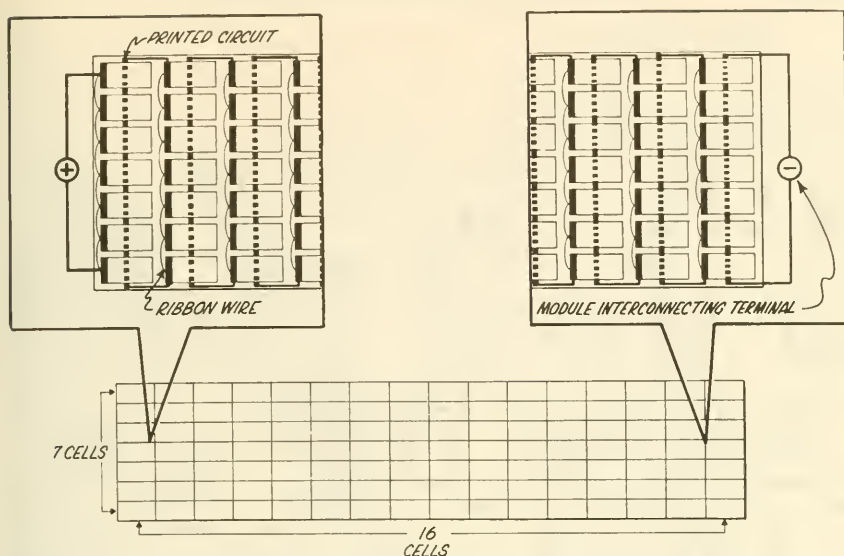
FIGURE 9–40.—Interconnections among OGO solar-cell groups. An OGO module consists of a 7-x 16-cell block of solar cells.

sion, but scientific satellites usually find propulsion either unnecessary or not worth its price in weight and reliability.

Are the functions of station keeping and orbital maneuvering essential to satellite science? Very succinctly, these capabilities would be nice to have on only a few isolated missions. An experimenter, for example, might wish to conduct instrumental surveys over all orbit inclinations or possibly maintain a particular perigee or inclination in the presence of perturbing forces. Both inclination changing and orbit keeping are expensive in terms of velocity increments and the reliability burden of the added guidance-and-control equipment. So high is the price that no scientific satellites now in the planning stage contemplate these functions. The trend, in fact, seems toward simpler satellites, such as the SSS,[7] in which the luxury of orbital adjustment or maintenance is even less probable.

Detailed velocity requirements for orbital modifications, especially deorbiting, are presented in section 4–6. Beyond the simple momentum requirements are tougher propulsion-system necessities, such as restart, throttleability, and the storage of propellants in space (fig. 9–42). These and the interface problems help shape the design of the onboard propulsion equipment.

---

[7] Small Scientific Satellite. See appendix.
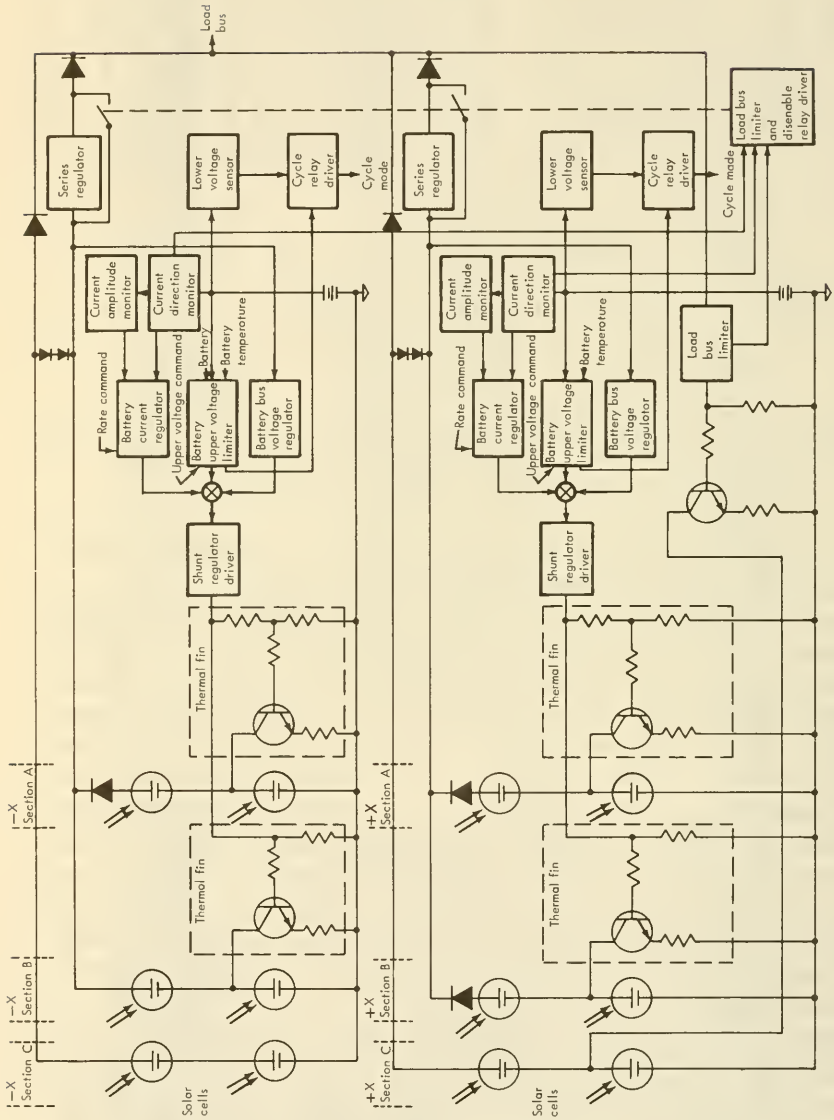
FIGURE 9-41.—Overall block diagram for the OGO-I power-supply subsystem.

	Thrust range (kg) 10^0–10^7	Critical operational requirements					
		High-level thrust	Continuous throttleability	Long life in space	Multiple restarts	High ratio, total-to-single impulse	Vernier thrust capability
Spacecraft propulsion — Stationkeeping				●	●	●	●
Attitude control				●	●	●	●
Orbit injection				●			
Midcourse maneuver				●	●		
Limited maneuver			●	●	●	●	●
Retrothrust				●			
Planetary or lunar landing		●	●	●	●		●
Planetary or lunar ascent		●		●			
Other aerospace engines — Tactical missiles		●	●				
Ballistic missiles		●					
Booster first stages		●					

FIGURE 9–42.—Thrust ranges of onboard satellite engines compared with other space engines. Not only are the thrust levels lower, but the operational requirements shown at the right are more severe (ref. 14).

Satellite interfaces with the onboard propulsion subsystem are relatively unimportant when the discussion is limited to deorbiting engines, the only ones likely to be used on scientific satellites in the near future. Deorbiting engines are dormant until the moment of ignition; there is little interaction with the remainder of the spacecraft during this interlude. The most critical moment occurs when the attitude-control subsystem swings the engine around into firing position (assuming it is fixed to the satellite structure) and the guidance-and-control subsystem starts and stops the precisely metered impulse. The pertinent interfaces at this critical moment pass electrical signals carrying information among the mentioned subsystems. The engine, of course, must have a clear field for its exhaust jets and be properly supported by the structure.

Satellite rocket engines can be very small (microrockets), at least when compared with launch-vehicle motors. The term ''secondary rocket'' applies to onboard engines. In the next section, the profusion of small-momentum expellers, such as gas jets, cap pistols, and electrical propulsion units which have been developed primarily for attitude control will be described. Here, the focus
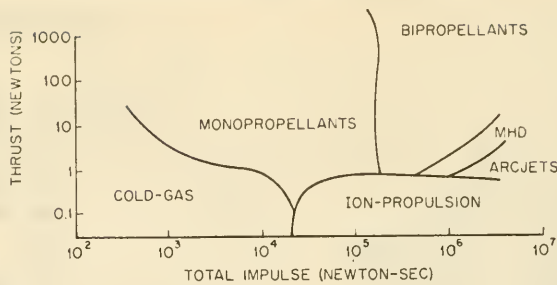
FIGURE 9–43.—Areas of onboard propulsion
    superiority on a total-weight basis. Elec-
    trical propulsion schemes still lack proven
    power supplies for high-power missions (ref.
    15).

is on engines for gross maneuvers, but the distinction is one of
size only, and smaller units can be ganged together to carry out
orbital changes (fig. 9–43).

The story of onboard engines is similar to that of their launch-
vehicle counterparts—both types depend upon solid- and liquid-
chemical fuels.

Mercury, Gemini, and some military satellites have used solid
rockets for deorbiting. These solid rockets are not very different
from those on Scout or Titan-3, except for size. Solid rockets
have been notably successful where carefully controlled impulses
are needed; viz, in orbital injection. Rocket research has even
found ways to snuff out and restart solid motors. Indeed, a stack
of "wafers," consisting of solid fuel, igniters, and restrictors,
can provide dozens of precision bursts of thrust upon command.
Solid-rocket throttling (vernier-thrusting) is more difficult to
achieve, however. One line of attack varies the throat area, but
this idea is still in the research stage.

The top solid-rocket specific impulse is about 260 seconds.
Liquid-fuel rockets can attain much higher values (ch. 8). Spe-
cific impulses over 400 seconds, attainable with cryogenic fuels and
oxidizers, are unfortunately not applicable to onboard propulsion,
because such fluids cannot be stored conveniently for long periods
in space. Designers must resort to storable bipropellants and
monopropellants, with much lower specific impulses (table 9–12).
While liquid engines are easy to start, stop, and throttle, two
major modifications must be made to adapt them for space use:
(1) Because there is no gravity field to pull liquids into pump
intakes, a positive liquid-expulsion scheme, using, say, bladders

TABLE 9–12.—*Propellants for Secondary Rockets*

[Adapted from ref. 15]

Oxidizer and fuel	Theoretical specific impulse,[a] sec
Storable bipropellants:	
N_2O_4-Hydrazine_____	292
N_2O_4-Aerozine 50_____	289
Monopropellant: 90 percent hydrogen	
peroxide_____	147
Typical solid propellant_____	255
Cryogenic propellants: Oxygen-hydrogen___	391

[a] At pressure ratio of 70:1, with shifting equilibrium.

or pistons, must be incorporated; (2) because the flow of liquids in small engines is small and possibly discontinuous, the usual regenerative engine-cooling is inadequate. Radiation and ablative cooling have been adopted instead, with considerable success.

Summarizing: In the restricted (but realistic) context of deorbiting and major orbit modifications, solid- and liquid-chemical engines have been universally adopted for onboard propulsion. Should the need ever arise for station-keeping and other minor propulsion functions, the chemical and electrical propulsion units being designed for attitude control should suffice. These are described in the next section. The only contemporary scientific satellites requiring large orbital modifications are Biosatellite and the Anchored IMP's (IMP's D/E). The Anchored IMP onboard solid-chemical motor is typical of the propulsion units used for such functions (fig. 9–44).

9–7. The Attitude-Control Subsystem

Satellite scientific instruments, antennas, and solar cells must be pointed, because they, like the phenomena they sense and utilize, are often strongly anisotropic. Pointing, in the case of spin-stabilized satellites, simply means alining the spin axis in inertial space. In other kinds of pointing, a satellite axis may be directed toward a star, the Earth, the Sun, or some other target. To accomplish these feats in airless, weightless space, the satellite's attitude-control subsystem expels mass, couples the satellite to natural force fields, alters its internal angular momenta, dissipates unwanted rotational energy, or accomplishes some combination of these things.
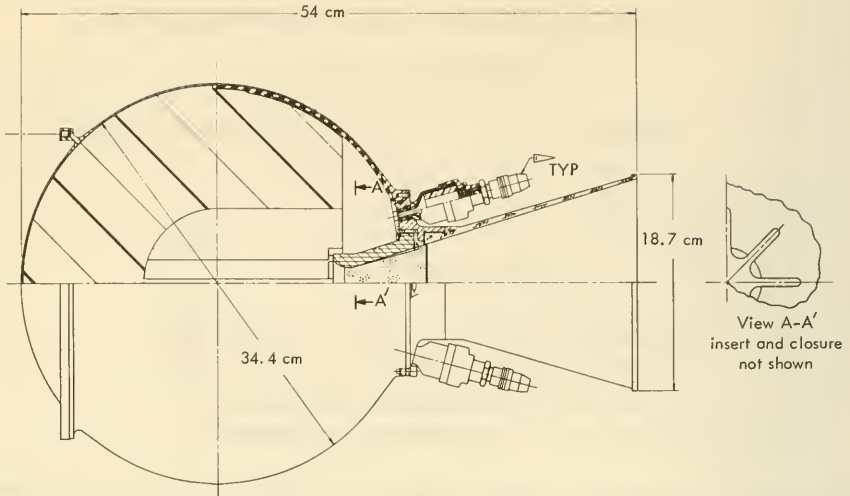
FIGURE 9–44.—The Anchored IMP (IMP's D/E) retromotor. It is a
solid-fuel rocket with a star-shaped cavity in the grain.

More specifically, the attitude-control functions are:

(1) *Despin.*—Almost all satellites are spun up prior to orbital
injection for purposes of stability. The subsequent injected spin
rate is often too high for proper functioning of the scientific in-
struments on spin-stabilized satellites. Machinery, therefore, is
often added that increases the satellite moment of inertia, con-
sequently reducing its spin rate. Obviously, satellites that are
pointed at some astronomical target must be completely despun.

(2) *Search and Acquisition.*—In this function, the attitude-con-
trol subsystem may be commanded to: (a) slew the satellite
through a specified discrete angle; (b) lock onto a "target," say,
the Earth's magnetic field, the local vertical, or the Sun ("hunt-
ing" motion transpires as, with the aid of feedback, the system
zeros in on the target); or (c) roll the satellite at a specified rate
while the guidance-and-control subsystem searches for a target.

(3) *Stabilization.*—Not only must the satellite be alined with
the target within certain limits, but fluctuations in attitude
(jitter) must be damped despite the presence of perturbing
torques (sec. 4–7). If the target is a star, limits for angular dis-
placement and rate of angular displacement will be prescribed.

Typical attitude-control subsystem requirements were delin-
eated in section 4–7. In a spin-stabilized satellite, for instance,
the precession angle might be limited to 5°. An OSO, for exam-

ple, is a suitable instrument platform if directed to within ±1 minute of arc of the Sun, while an OAO might require ±0.1 second of arc pointing accuracy.

In section 6–1, it was pointed out that any control system could be classified in one of four categories:

Active/open-loop   Passive/open-loop
Active/closed-loop   Passive/closed-loop

"Passive" means that no power or sensor signals are needed after the component is deployed. "Open loop" means that feedback is absent. In assigning satellite attitude-control subsystems to these categories, one is struck by the fact that attitude control in Explorer-class satellites is open-loop and passive wherever possible. Gravity-gradient stabilization, which is both passive and open-loop, is common, for example. Observatory-class satellites, on the other hand, usually want precision pointing and have active, closed-loop attitude-control subsystems. One expects such a morphological division because Explorer-class satellites, by definition, are simple and specific when contrasted with Observatory satellites, which are generically complex, flexible, and sophisticated instrument platforms.

An attitude-control subsystem may perform one or all of the functions just listed. Requirements vary radically across the spectrum of several hundred scientific satellites. Two- or three-axis precision attitude control, however, is rare (the OAO's), and so is the complete lack of attitude control (the ERS's). In fact, more than 90 percent of all scientific satellites have been spin stabilized. They carry only simple despin devices and, perhaps, precession and nutation dampers.

An attitude-control subsystem depends upon the guidance-and-control subsystem for open-loop commands, such as the signal that fires the squib releasing yo-yo despin weights. Closed-loop feedback comes from star trackers, horizon sensors, and the like in the guidance-and-control subsystem (fig. 6–14). Other satellite subsystems also enter the picture; an onboard computer might be installed if its added weight is preferred to performing attitude-control computations on the ground via the communication subsystem. There are also the usual interfaces with the communication and power-supply subsystems (fig. 9–45). The always intense competition for solid angle is evident in the interface diagram. Other interfaces involve the magnetic fields of magnetic attitude actuators and the possible damage of solar cells and sensors by the efflux of gas jets and electrical propulsion equipment.

FIGURE 9-45.—Portion of the satellite-interface diagram showing the relationship of the attitude-control subsystem to the rest of the satellite.

Attitude-Control Actuators.—All of the attitude-control functions listed above require the adding to, subtracting from, or changing the direction of the satellite angular-momentum vector. Despin is simple subtraction. Slewing from one orientation to another necessitates addition, then subtraction. Stabilization implies damping, or momentum subtraction, as well as torque generation to compensate for perturbing forces. Torques and angular-momentum changes can be generated by actuators comprising five clear-cut categories. All depend for their operation on the laws of conservation of momentum and conservation of energy.

(1) *Mass Expulsors, Which Add or Subtract Angular Momentum by Directed Application of Thrust via the Rocket Principle.*—Mass-expulsion devices are all active devices and need modulation controls and their associated reliability burden. They also need heavy propellant reservoirs, whose weight limits restrict the total deliverable angular impulse. Mass expulsors are rich in variety (table 9–13). They are found on the heavier satellites.

(2) *Angular-Momentum Reservoirs.*—The category heading is unusual, but apt for inertia wheels, inertia spheres, etc. Conservation of momentum insists that the satellite structure itself acquire angular-momentum changes equal and opposite to those forced upon inertia wheels or spheres. Such inertial equipment is "saturable"; that is, limited in ability to absorb momentum. This is due to their finite top speed of rotation. Mass expulsors usually complement inertial equipment for the purpose of desaturation, or "dumping." The large scientific satellites, such as the OAO's, employ angular-momentum reservoirs, backed by cold-gas jets, for precision slewing.

(3) *Moment-of-Inertia Changers.*—By increasing a satellite's moment of inertia, its spin rate is decreased. In practice, this is accomplished by deploying masses radially outward from the satellite spin axis; viz, the de Havilland erectable boom and the ubiquitous yo-yo despin mechanism.

(4) *Environmental-Force Couplers.*—Satellites can exchange angular momentum with the environment in four ways: magnetic-field couplers, gravity-gradient devices, solar-pressure vanes, and aerodynamic surfaces. Most attitude-control equipment falling into this category is passive. The quest for reliability has made gravity-gradient and magnetic actuators very popular.

(5) *Energy Absorbers.*—Precession (wobble), nutation, and libration dampers are typical of this class. By properly positioning energy dampers, such as springs, viscous fluids, and eddy-current brakes, the energy tied up in undesired motion can be transferred to a dissipative component, which eventually radiates it away as heat. Artificial energy dampers find their way onto satellites because natural dissipative forces, such as aerodynamic forces, are too weak in satellite orbits.

A complete attitude-control subsystem often needs more than one type of actuator. A gravity-gradient device may, on the average, point a satellite axis toward the Earth, but the swinging motion about this direction, the librations, must be damped out with springs, magnetic hysteresis, or some other nonconservative force.

TABLE 9-13.—*Descriptions of Some Attitude-Control Actuators*

Category	Type	Principle of operation	Remarks [a]
Mass expulsors	Cold-gas jets	Gas, usually nitrogen, stored under pressure is released by electrically controlled valves through nozzles. Active.	$I_{sp} \sim 80$, $0.001 < L < 25$. Accurate, no power required. Used on most large satellites. Heavy but well proven (fig. 9-46).
	Solid rockets	Solid propellant, possibly in "wafer" form, is ignited electrically. Hot gases pass through nozzles to produce thrust. Active.	$200 < I_{sp} < 270$, $0.01 < L < 80$. Good for large thrust bursts. Not used for attitude control on scientific satellites, except for spinup, as on Scout.
	Liquid rockets (hot-gas jets).	Storable bipropellants or monopropellants are ignited to generate hot gases, which are expanded through nozzles. Active (fig. 9-47).	$150 < I_{sp} < 250$, $0.01 < L < 80$. Can be modulated relatively easily. Rarely used on scientific satellites for attitude control.
	Vapor-pressure devices	Vapor (viz, ammonium hydrosulfide) evolved (sublimed) from a solid or liquid at ambient temperatures is released through nozzles by electrically controlled valves. Active (fig. 9-48).	$I_{sp} \sim 800 < L < 0.1$. High-pressure tanks not needed. More compact than cold-gas devices. Used occasionally to overcome environmental forces.
	Radioisotopic thrusters	Stored gas is heated by decaying radioisotopes and expanded through nozzles. Active (fig. 9-49) (Project Poodle).	$500 < I_{sp} < 1000$, $0.01 < L < 10$. Radiation field limits use on scientific satellites; not yet operational.
	Electrothermal thrusters	Stored gas is heated by electrical resistors or arcs and expanded through nozzles. Active. (Resistojet, plasma jet.)	$500 < I_{sp} < 2000$, $10^{-5} < L < 10^{-4}$. High power drain and low thrust, but high I_{sp}. Complex. Unattractive for scientific-satellite attitude control, though possible for station-keeping.
	Electromagnetic and electrostatic thrusters.	Plasma or ions are accelerated by electromagnetic or electrostatic fields and expelled from satellite (ion engine). Active (fig. 9-50).	$5000 < I_{sp} < 20\,000$, $10^{-6} < L < 10^{-5}$. High power drain and low thrust but high I_{sp}.
	Pyrotechnic devices	Caps, squibs, or cartridges are ignited. The	$80 < I_{sp} < 120$. Small impulses. Shocks

		expelled gases create quantized thrust bursts. Active.	sometimes undesirable. Mechanical feed devices usually needed. Rare on scientific satellites.
Angular-momentum reservoirs.	Inertia wheels	Wheels are accelerated and decelerated by electric motors. Orthogonal set of 3 needed for full attitude control. Active.	For precision slewing and stabilization. Can saturate. Multiple wheels create cross-coupling. Used on large, pointable satellites (fig. 9–51).
	Inertia spheres	Sphere is suspended by aerodynamic, electrostatic, or electromagnetic forces. Torques are coupled electromagnetically. Replaces 3 inertia wheels. Active. No cross-coupling.	For precision stabilization. Can saturate. Not as well developed as inertia wheels. Development programs have run into serious suspension problems.
	Liquid loops	Liquid metal circulated in large loop by electromagnetic pump. No moving parts except fluid. Large radii possible. Active.	Same as inertia wheel, except not as well developed. Consumes considerable power even when not accelerating fluid.
Moment-of-inertia changers.	Booms	Telescoping and hinged booms are popular. De Havilland despin booms are formed when prestressed metal tape is unrolled and assumes tubular shape. Passive once erected (fig. 9–52).	Rigid booms, tens of meters long, are possible. Rather expensive, but operationally successful. Used for gravity-gradient devices and large antennas.
	Despin weights	Small weights on ends of long wires or springs are released when orbit is attained. Added moment of inertia despins satellite (yo-yo). Passive once erected (fig. 9–53).	Simple and reliable for small spin-stabilized satellites. Used on many Explorer-class craft. Variable yo-yo's now developed to adjust for variable spinup procedure.
	Erection of appendages	Routine erection of antennas, instrument booms, and solar-cell paddles increases satellite moment of inertia. Passive once erected.	Most scientific satellites possess appendages and are consequently partially despun by these routine events.
Environmental-force couplers.	Magnetic	Permanent magnets or coils interact with Earth's field to create torques. Passive or active.	Now commonly used on close Earth satellites, especially those making radiation studies.

See footnotes at end of table.

TABLE 9–13.—*Descriptions of Some Attitude-Control Actuators*—Continued

Category	Type	Principle of operation	Remarks [a]
Environmental-force couplers—Con.	Gravity-gradient	Variation of force of gravity with distance will create torques on asymmetric satellites (see sec. 4–7). Extended masses accentuate effect. Passive (fig. 9–54).	Used extensively on Earth-pointing scientific satellites. Circular orbit desirable.
	Solar	Pressure of sunlight on asymmetric satellite appendages torques craft. Passive or active.	Force~10^{-5} newton/m². Not intentionally used to date, but under consideration for some scientific satellites used in solar research.
	Aerodynamic	Aerodynamic forces on satellite vanes and extended surfaces will orient craft—like an arrow. Added drag can reduce satellite lifetime. Passive.	Possible for satellites under 500 km. Rarely used intentionally on scientific satellites.
Energy absorbers	Springs	Internal friction in high-hysteresis spring removes energy from system and radiates it away.	Has been used to damp out librations of gravity-gradient-controlled satellites.
	Fluid	Viscous fluid is sheared and energy consequently absorbed. Vertistat damper consists of small steel balls in curved, fluid-filled tube. Spheres separated by fluid and other configurations also possible (fig. 9–55).	Also used with gravity-gradient-controlled satellites.
	Electromagnetic	Eddy-current damping uses conducting surface and permanent magnet; current induced generates heat. . Magnetic hysteresis in permanent magnets interacting with Earth's field also evolves heat.	Also used with gravity-gradient-controlled satellites.

[a] Specific impulse (I_{sp}) measured in seconds; torque measured in newton-meters (approximately equal to pound-feet).
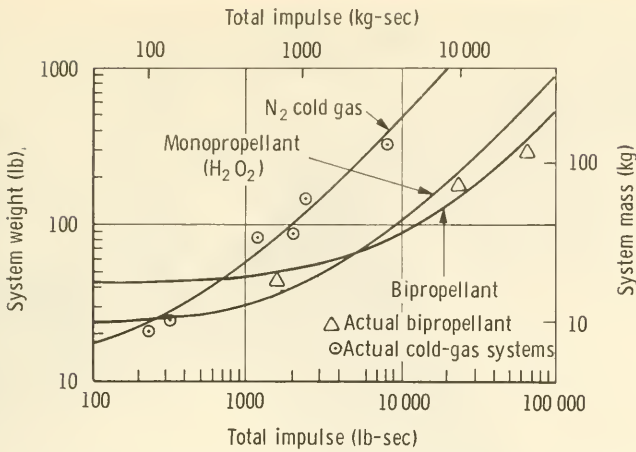
FIGURE 9–46.—Attitude-control   subsystem   weights
versus total impulse (ref. 16).
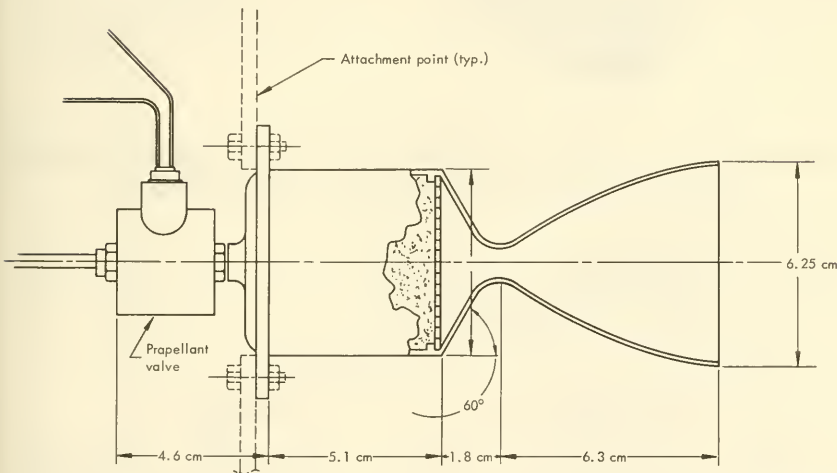
FIGURE 9–47.—A small, 10-kilogram-thrust, N_2H_4 rocket engine suitable
for onboard propulsion and attitude control.   (Courtesy of Rocket
Research Corp.)

Having described the five broad classes of actuators, let us
examine some specific equipment.   Since the devices proposed
and in use are legion, a tabular approach is indicated (table
9–13).

Specific Attitude-Control Subsystems.—In this book, the atti-
tude-control subsystem is defined so that it comprises only the
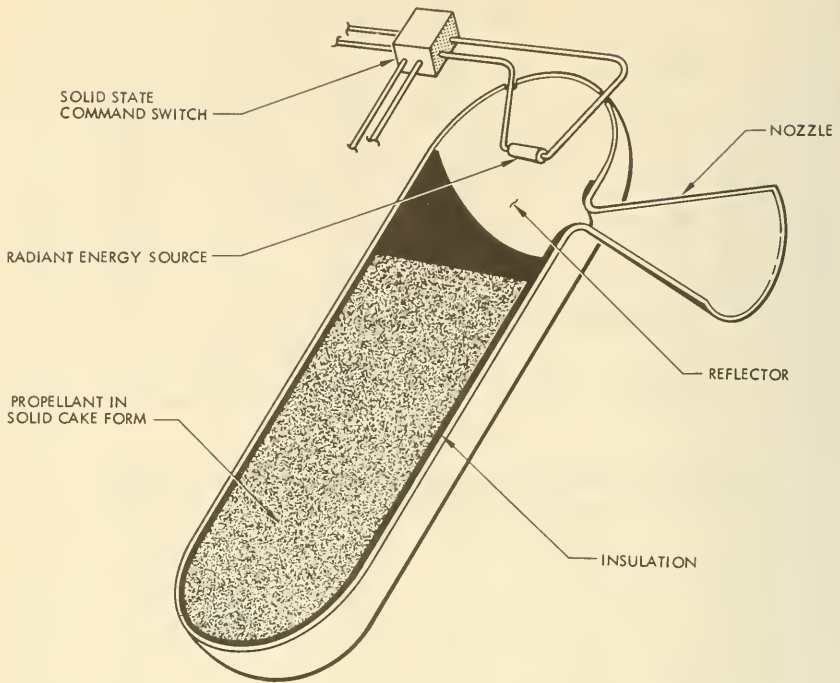
FIGURE 9–48.—A valveless, subliming-solid-fuel microrocket for attitude control. Activation of heater generates thrust (ref. 17).
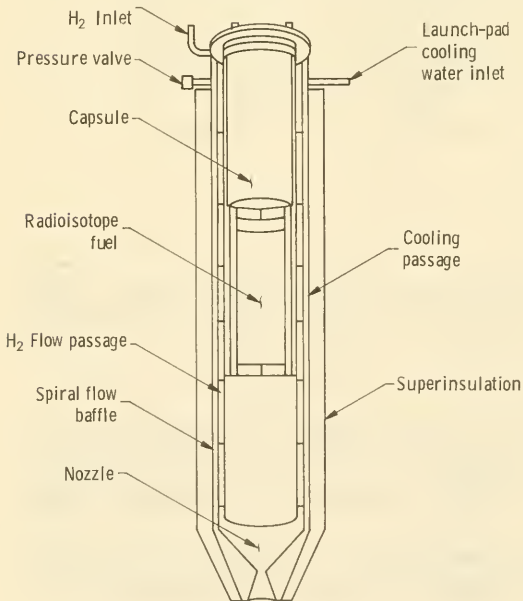
FIGURE 9–49.—Sketch of a Poodle radioisotopic rocket. Hydrogen gas is heated by a decaying, alpha-emitting radioisotope as it passes the fuel capsule (ref. 18).
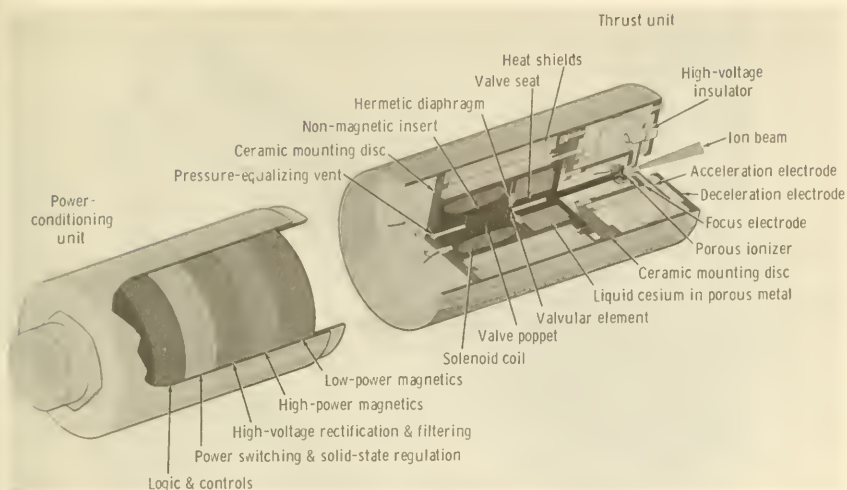
FIGURE 9–50.—Conceptual drawing of a 5-milligram ion rocket suitable for attitude control and station keeping. Completely contained within a 5-x 20-centimeter cylinder, the unit draws 10 watts. (Courtesy of Hughes Research Labs.)
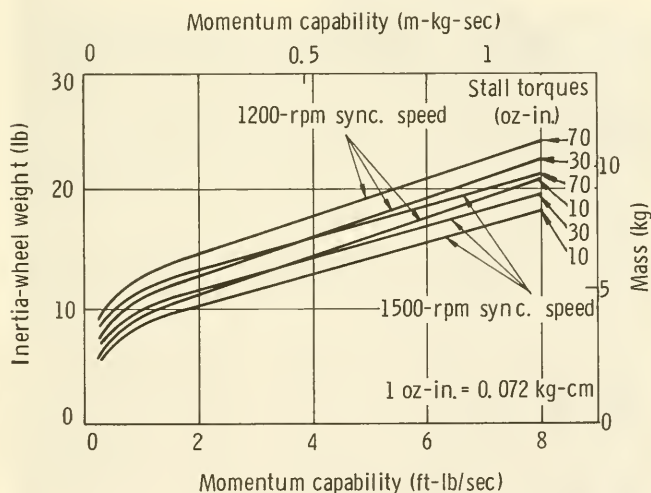
FIGURE 9–51.—Inertia-wheel weight versus momentum capability for various stall torques. (After ref. 16.)

actuators and their associated circuitry. The attitude sensors are relegated to the guidance-and-control subsystem, with the position-finding and command-handling equipment. In picturing the attitude-control equipment for specific satellites, it will be con-
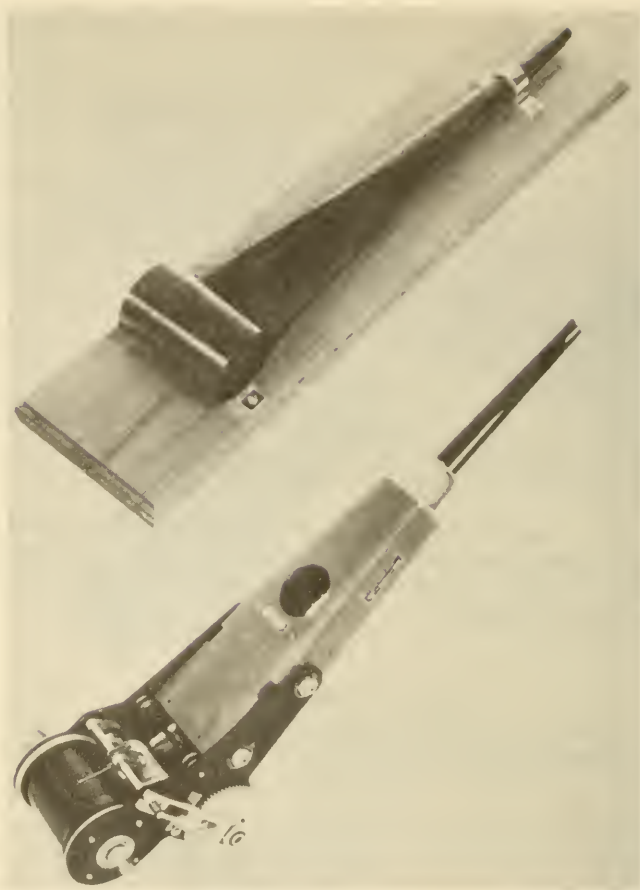
FIGURE 9–52.—The extendable Alouette antenna; in
actuality, a small de Havilland boom.

venient to bridge the interface between these two closely associ-
ated subsystems and indicate the attitude sensors, at least in
block-diagram form.

Among the hundreds of scientific satellites, three have been
selected for detailed description:

(1) The Atmosphere Explorer B (AE–B), which illustrates
magnetic attitude and spin-rate control

(2) The OSO, chosen because it combines spin stabilization
with Sun pointing and Sun scanning

(3) OGO, which utilizes cold-gas jets and inertia wheels, and
has articulated components pointed in various directions
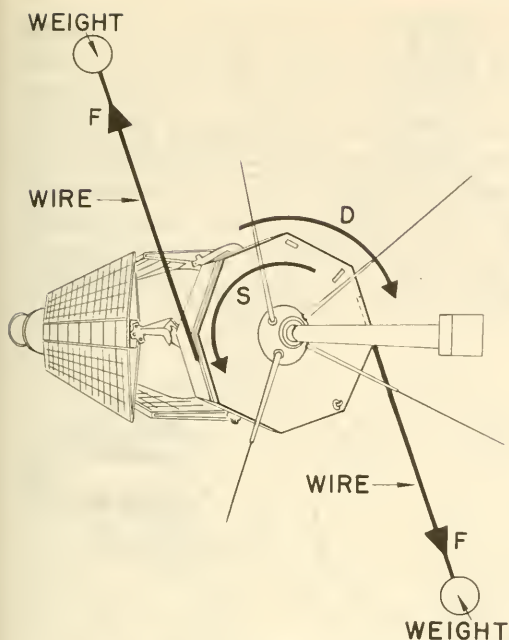
FIGURE 9–53.—Drawing showing how yo-yo despin weights are flung off a spinning satellite after they have been released by pyrotechnic actuators.
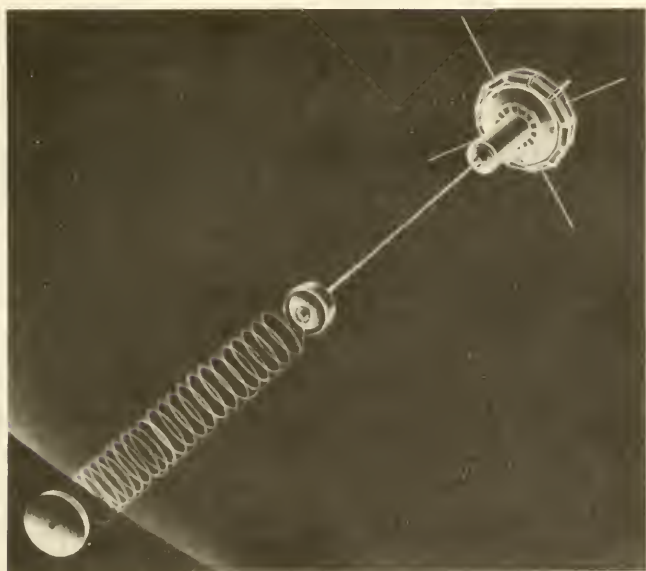
FIGURE 9–54.—Gravity-gradient stabilization system used on the Traac satellite. Boom length: about 20 meters; extended spring length: about 12 meters. Energy in unwanted oscillations is dissipated as heat in the damping spring.
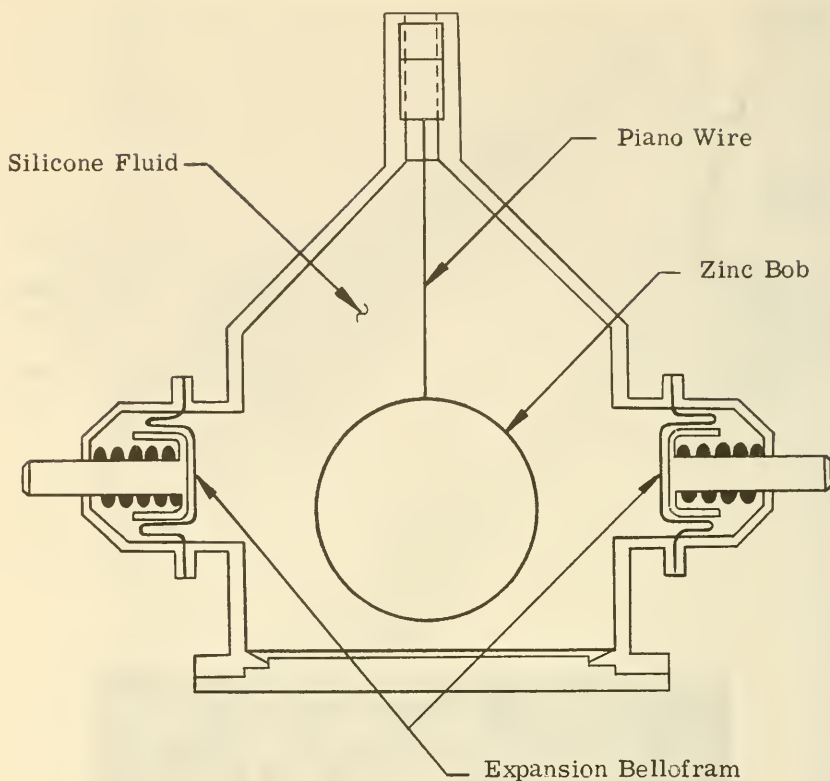
FIGURE 9–55.—Drawing of the OSO nutation damper. Motion of bob
in fluid converts energy of satellite nutation into heat.

Missing from the list are the simplest spin-stabilized satellites
and the most sophisticated attitude-control subsystem of all, that
of the OAO. Spin stabilization has been discussed from the
theoretical point of view in section 4–7; typical spinup rockets are
illustrated in figure 8–13; and a representative wobble damper is
portrayed in figure 9–55. OSO also illustrates spin stabilization.
Attitude control of the OAO was presented in some detail in sec-
tion 6–5. With this apology for not detailing the entire panorama
of attitude control, let us focus on AE–B, OSO, and OGO.

   The AE–B Attitude-Control Subsystem.—The AE–B (Explorer
XXXII) is a spherical satellite (fig. A–26), spin stabilized at 30
rpm. The forerunner of AE–B (Explorer XXXII), the AE–A
(Explorer XVII), experienced large variations in spin-axis orien-
tation during its mission (ref. 19). This unwanted precession

apparently originated from the interaction of the Earth's magnetic field with the natural satellite dipole moment. The AE–B attitude-control subsystem included: (1) magnetic actuators to control the precession observed on the AE–A; and (2) another set of magnetic actuators to control satellite spin rate.

Spin-axis orientation was controlled by artificially creating a dipole moments of M, $M/2$, or 0. The AE–B variable magnet was a permanent one, with a dipole moment $M/2$, and a variable magnet, with a dipole-moment range $\pm M/2$ (fig. 9–56). Upon ground
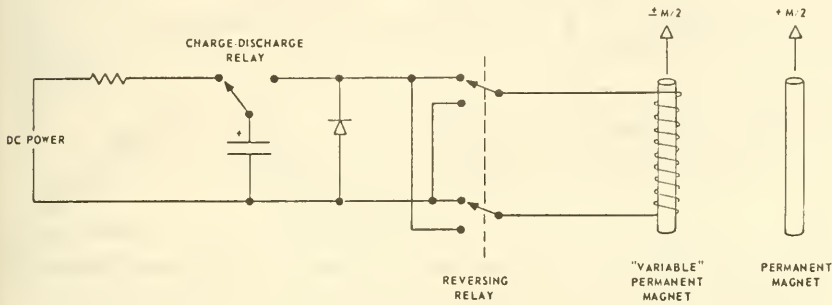
FIGURE 9–56.—Schematic of the pulsed magnetic actuators on the AE–B attitude-control subsystem (ref. 19).

command, a capacitor bank was discharged through the windings of the variable magnet, in one direction or the other, to produce dipole moments of M, $M/2$, or 0. The AE–B variable magnet was built from a vanadium-permendur alloy.

The AE–B can be spun up or down by ground command. Two electromagnets, shown in figure 9–57, are alined with the two satellite axes perpendicular to the spin axis. Torque about the spin axis is generated, after the fashion of a dc motor, by interaction between the Earth's field and the fields of the electromagnets. The vector magnetometers in figure 9–57 generate signals proportional to the Earth's field. These are amplified and activate the electromagnets. To obtain dc motor action, the X-axis magnetometer drives the Y-axis electromagnet with a 180° phase change, and the Y-axis magnetometer drives the X-axis electromagnet. The change in AE–B spin rate, using this approach, can be as high as 15 rpm/day.

The OSO Attitude-Control Subsystem.—The OSO's were the first scientific satellites to combine spin stabilization and experiment pointing. The heavy wheel section of OSO (fig. 9–58) spins
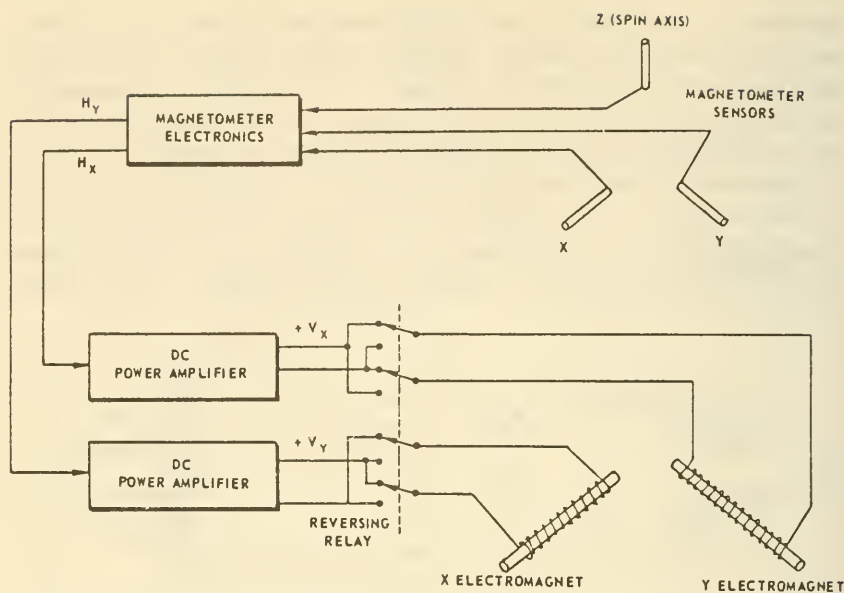
FIGURE 9–57.—The AE–B magnetic torquer. Application of current to the electromagnets can increase or decrease satellite spin (ref. 19).

at 30 rpm to stabilize the craft; at the same time, the sail portion is motor driven to point toward the Sun to within ±1 minute of arc. OSO also carried the fluid-filled nutation damper illustrated in figure 9–55.

During the OSO launch phase, the third stage of the Delta launch vehicle is spun up to 120 rpm. After third-stage burnout and orbital injection, the three OSO "arms" are extended, providing some despin. Then, third-stage separation occurs and the satellite is despun to the nominal 30 rpm by cold-gas jets (fig. 9–59). Deviations from design spin rate are detected by solar sensors, and the cold-gas jets will fire to bring the spin rate back to within design limits. Any nutation is removed when the damper is uncaged.

The Sun is acquired by the guidance-and-control subsystem's coarse and fine "eyes" following launch and at every "Observatory dawn" thereafter. Error signals from these eyes drive azimuth servomotors that rotate the sail so that it points steadily at the Sun despite the spining-wheel section under it. Fine Sun sensors also drive an elevation servo that raises or lowers the pointable instruments so that they point at the Sun. The instruments, however, may be elevated only ±5°. Pitch-axis gas jets
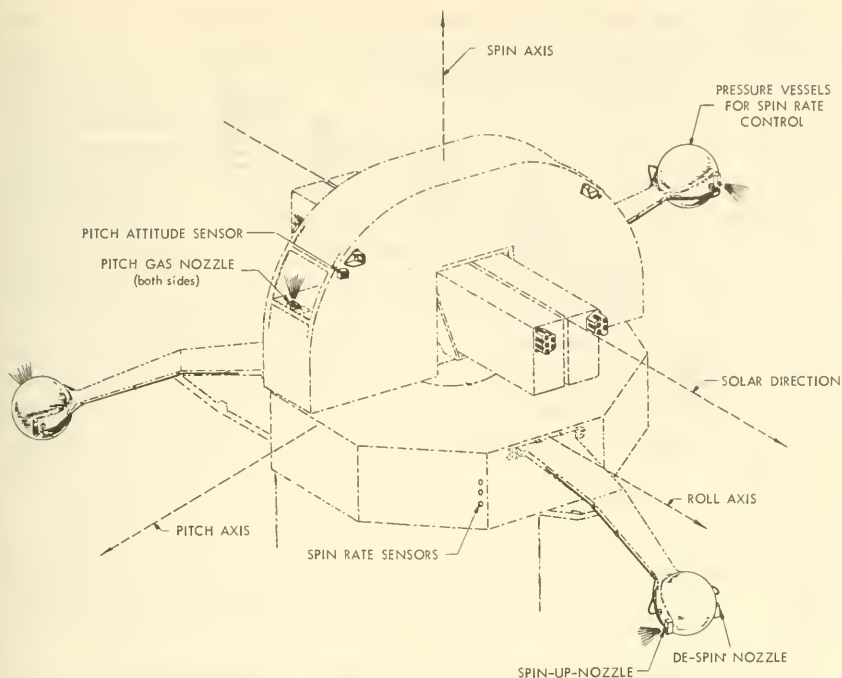
FIGURE 9–58.—Elements of the OSO attitude-control subsystem.

are turned on whenever the pitch axis deviates more than 3.5°. The pitch jets can also be turned on from the ground.

During its swing through the Earth's shadow, the OSO loses the Sun and must reacquire it when it again moves into sunlight at ''Observatory dawn.'' This is accomplished in about 20 satellite axial revolutions.

Note that the satellite roll axis is not controlled at all. Magnetic effects, solar-radiation pressure, gravitational gradients, and other perturbations will cause a slight roll, but this does not adversely affect experimentation.

OSO can also drive the instruments on the sail in a scanning mode that sweeps through a 40×40 minute-square raster centered on the spot of maximum intensity on the solar disk. Motors drive the instruments in a 40-step pattern, with a 1-minute of arc elevation step and scan reversal occurring at the end of each trace.

In a sense, OSO represents an intermediate step between the Explorer and Observatory classes of satellites. (In fact, some people refer to OSO as a big Explorer.) It is both spin stabi-

+1495, Nutation damper unlock (+800)

+1295, Power on for systems, de–spin, azimuth
acquisition and pitch presession (+600)

+1895, Elevation unlock and
acquisition (+1200)

+822, Payload separation (+127)

+1945, Sequence following
timer start repeated (+1250)

+785 Arms out (+90)

First flight recorder
playback (+95 minutes)

+725, Third stage burnout (+30)

+702, Third stage ignition (+7)

(Spacecraft acquires Sun
each satellite morning)

+698, Separation (+3)

+695, Spin–up,
spacecraft timer starts (0)

SUN

Coast and positioning

+300, Second stage burnout

+180, Jettison shroud

+150, Second stage ignition, separation

+146, First stage burnout

NOTE

0, First stage firing

Time at left of each event is measured from T–0, in seconds.
Time in parentheses at right of events is measured from start
of spacecraft timer. (Times are approximate.)

FIGURE 9–59.—Launch and injection events for OSO.

lized and pointable. It uses reaction jets and requires feedback
from several sets of "eyes," much like the OAO and OGO.

The OGO Attitude-Control Subsystem.—The OGO's have five
degrees of freedom: rotation of the main body about its three
axes, rotation of the solar panels, and rotation of the OPEP
(Orbital-Plane Experiment Package). (See fig. A–33.) These
joints or articulations are needed to meet the demands of the
following components:

(1) The solar panels, which obviously should be perpendicular
to the Sun's rays

(2) The thermally radiating surfaces of the environmental-
control subsystem, which should *not* face the Sun

(3) The directional antenna, which should point at the Earth

(4) Experiments, which must be pointed at the Earth, Sun,
or along the orbital plane

These objectives are met by controlling the pitch-and-roll axes so
that the yaw axis, and the face of OGO supporting the directional
antenna and the Earth-pointing experiments, are pointed toward
the Earth with an accuracy of ±2°. Rotation about this yaw
axis and the rotation of the solar panels on their shafts are then

controlled so that the panels and the two SOEP's (Solar-Oriented Experiment Packages) mounted on them are normal to the Sun line within ±5°. A separate OPEP is directed in the orbital plane to an accuracy of ±5°.

In its normal mode of operation, signals from infrared horizon sensors drive roll-and-pitch inertia wheels whenever the errors exceed 0.4° (fig. 9–60). Cold argon jets are activated whenever errors are large or the inertia wheels saturate. Ordinarily, the gas jets would not be called upon more than once per orbit.

The Sun is sensed by coarse and fine silicon p–n junction sensors. Error signals from the yaw Sun sensor drive the yaw-axis inertia wheel and cold-gas jets. A drive motor rotates the solar panels to keep the solar-array's Sun-sensor error signals within prescribed limits. As in the case of OSO, OGO must reacquire the Sun at each Observatory dawn.

An independent control loop positions the OPEP's. It employs a single-degree-of-freedom position gyroscope. The gyro's angular-momentum vector is perpendicular to the local vertical and
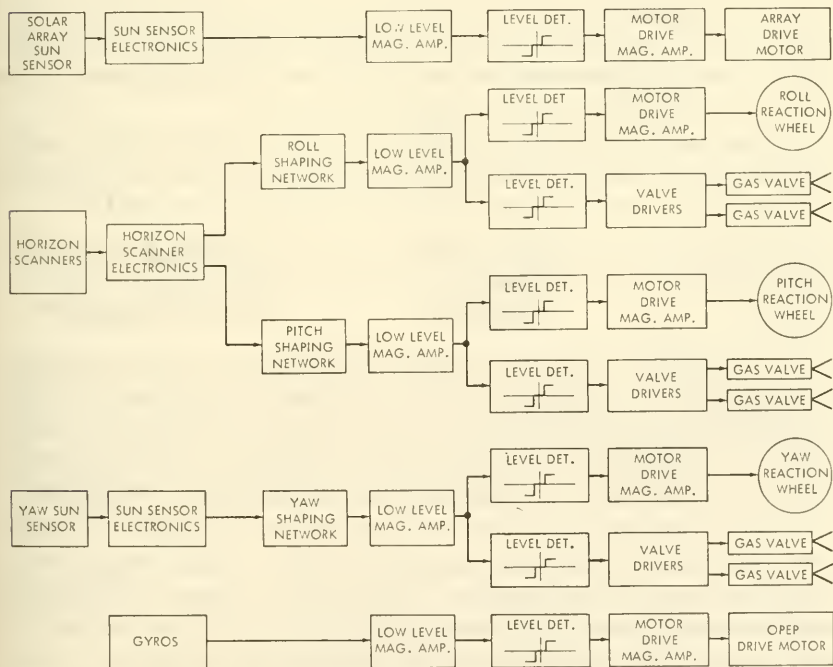
FIGURE 9–60.—Simplified block diagram of the OGO attitude-control subsystem. Subsystem is shown in the "normal" control mode (ref. 1).

also the OPEP axis of rotation. As OGO makes each revolution around the Earth, it makes a complete rotation about a line perpendicular to the orbital plane. If the gyro angular-momentum vector is also alined normal to the orbital plane, no rotation of this vector occurs. The OPEP's are then properly positioned, and there is no error signal. When error signals do occur, a motor repositions the OPEP, so that the angular-momentum vector is again normal to the orbital plane.

The OGO attitude-control subsystem has three separate modes of operation: launch, Sun-and-Earth acquisition, and normal. In the second of these modes, the OGO rotates about its yaw-and-roll axes until the Sun is acquired. In Earth search, the OGO is rotated first about its pitch axis and then about its roll axis until the horizon scanner is locked on the Earth. The subsystem then switches to the normal mode of operation.

9-8. The Environment-Control Subsystem

By definition, the scientific satellites described here do not carry fragile man into orbit. Yet, electronic circuitry and scientific experiments are in some ways more sensitive than man to the forces and fluxes that pervade satellites. The task of the environment-control subsystem is one of protection—protection of equipment from the space environment and from self-generated forces that constitute the internal environment.

Taking the most general view, all forces imposed upon a satellite subsystem may be categorized according to the nine types of interfaces in our conceptual model of a satellite (fig. 9–61):

Thermal	Electrical	Information
Mechanical	Radiative	Biological
Spatial	Magnetic	Electromagnetic

"Environment control" implies shielding the satellite subsystems against extreme values of the parameters that measure these nine forces; viz, high and low temperatures. It would be conceptually helpful if a satellite's environment-control subsystem could be packaged in a blackbox, like the drawers of transistors and wires that make up the communication subsystem. Unhappily, the environment-control subsystem cannot be severed easily from the rest of the satellite. Custom has made environment control synonymous with thermal control, while protection against the eight other, just-as-pervasive environmental factors is considered only part of good design practice. That is, all except thermal and perhaps magnetic forces are controlled on a narrow
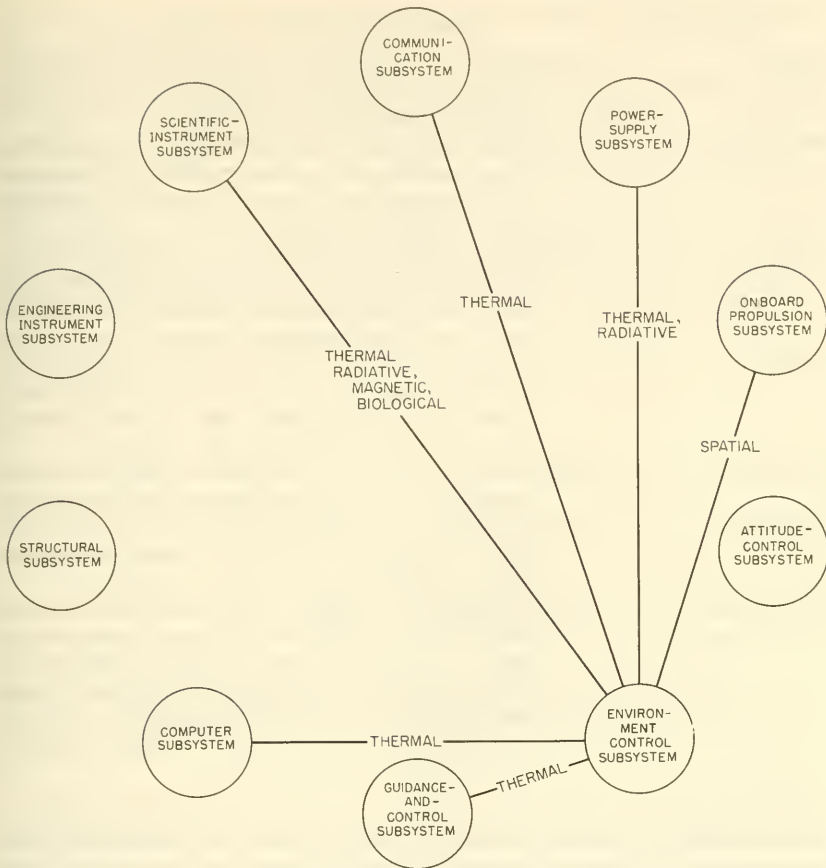
FIGURE 9–61.—Portion of the satellite-interface diagram showing the relationship of the environment-control subsystem to the rest of the satellite.

subsystem basis instead of a systemwide basis, even though the forces themselves are truly environmental and satellitewide. The following tabulation illustrates how the eight other forces are handled. Thermal control warrants separate and more extensive treatment.

Type of force	*How handled during satellite design*
Mechanical_____	Forces applied are calculated from definition of the vibration, shock, and load environment. "Protection" entails installation of shock and vibration absorbers and proper sizing of structural members. Control of mechanical forces is a normal part of good structural design (sec. 9–11).

Type of force	How handled during satellite design
Spatial_____	Allocation of equipment and experiment view cones decided by arbitration. Control, here, means managing and budgeting of solid angle.
Electrical_____	Satellite components are customarily protected from power surges, and the like, by fuses, circuit breakers, regulators, etc. Again, protection is inherent in good design practice.
Radiative_____	Radiation shields are installed where protection is needed against nuclear-power plants and/or space radiation. Solar-cell covers exemplify control of the radiation environment.
Magnetic_____	Good design practice requires using a minimum of magnetic materials, shielded and twisted leads, current-loop compensation, and isolation of sensitive components on booms.
Information_____	Good management of data formats standardizes this aspect of the environment throughout the satellite.
Biological_____	On life-detection missions, parts that cannot be heat sterilized must be "canned" to protect instruments from contamination.
Electromagnetic_____	The reduction of radio-frequency interference and crosstalk is accomplished by good circuit design, shrewd component arrangement, and electromagnetic shielding. Again, this is only good design practice and is not usually handled on a satellite-wide basis, at least not until a complete satellite is assembled.

Pertinent at this juncture is the fact that some experiments require very special environments. Biological satellites may carry live animals, for example. Some instruments operate well only at cryogenic temperatures. The control of specialized instrument environments will be covered in Part III in connection with the experiments themselves.

Thermal Control.—Classically, thermal control has always been recognized as a major feature of overall satellite design. Perhaps this special emphasis is due to these facts: (1) Just about all spacecraft components are temperature sensitive; and (2) temperature control is a well-established engineering discipline, in contrast to, say, magnetic-cleanliness control. It has been obvious from Vanguard days that temperatures must be controlled on a satellitewide basis and that uncoordinated toying with thermal control on isolated components is completely inadequate.

Thermal control, like attitude control or any other kind of control, may be passive or active, open-loop or closed-loop. Simplicity and reliability favor passive means, but in some satellites the heat

inputs may be so large and variable that designers have to resort to moving parts and feedback.

Each satellite component—solar cell, electronic package, instrument—has a temperature range where it operates best. The range −40° to +60° C brackets the cumulative ranges on most satellites (fig. 9–62). Frequently, a satellite cannot escape carrying components with very narrow temperature ranges; these may have to be separately controlled with special heaters and coolers. Some spacecraft run rather hot, near the upper limit of the range given above; others, such as the OAO, run at average temperatures well below the freezing point of water.
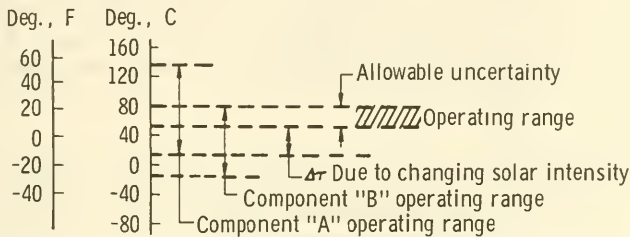
FIGURE 9–62.—The acceptable operating temperature range of a satellite depends upon component ranges and variations in solar-heat input (ref. 2).

The heat loads generated within a satellite are not large by terrestrial standards. Rarely does the heat load from degraded electrical power exceed 100 watts. But the thermal inertia (heat capacity) of satellites is not large either. Regardless of the magnitudes involved, heat inflow must equal heat outflow. Even a watt of heat-budget unbalance will rapidly raise a satellite's temperature. On the other side of the coin, satellites also cool rapidly to points where instruments and electronic parts cease functioning.

Externally, 1400 W/m² reach the satellite surface from the Sun, plus a smaller contribution from the Earth. Solar heating is obviously directional, and periodically blocked by eclipses in a most complex way (fig. 9–63).

The conceptual picture that emerges is that of a satellite structure that probably possesses some geometrical symmetry, but is covered with paints and finishes of various absorptivities and emissivities. The satellite contains time-varying, asymmetric heat sources and is bombarded by a time-varying, spatially asymmetric flux of electromagnetic radiation, peaking at 5500 Å.
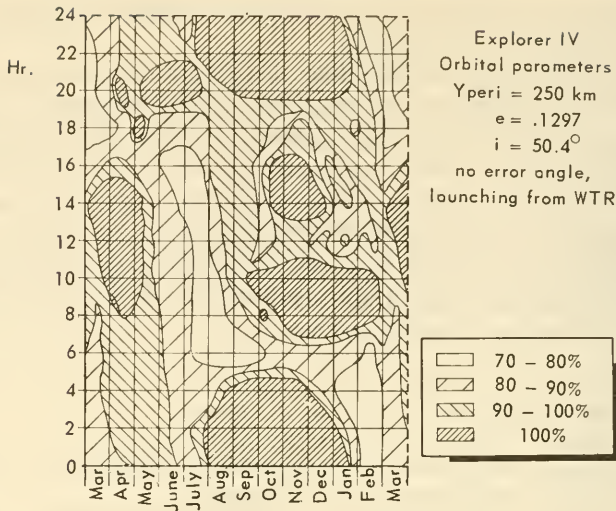
FIGURE 9–63.—Time in sunlight for Explorer IV as a function of day and hour of launch. The complexity of the thermal-control problem stems, in part, from this variable input (ref. 20).

It is small wonder that satellite thermal analysis is not noted for its precision and that full-scale thermal models are almost invariably built and tested in space simulators (sec. 7–2). Thermal analysis, even with computer assistance, finds it difficult to predict a satellite's temperature distribution to within $\pm 10°$ C. If analysis suffers from the asymmetry and time variability of the situation, so does the physical implementation of thermal control.

Before seeing how satellite thermal analysis proceeds, consider how a satellite component might be cooled if analysis were to indicate it was running too hot. The following potential modifications give some insight to thermal-control techniques:

(1) Add conduction and radiation paths leading to cold sinks

(2) Move the component to a cooler part of the satellite, say, a facet facing away from the Sun

(3) Reduce the conduction and radiation paths leading to the component from the major heat sources, such as the sunlit side of a solar-oriented satellite

(4) Lower the electrical power dissipation in the component

(5) Install thermoelectric cooling (implying a power drain and reliability burden)

(6) Use convective cooling (implying power drain and reliability burden)

(7) Find a replacement part with a wider temperature range

(8) Modify the orbit and/or attitude history

For parts that run too cold, the above actions would be reversed. Some practical ways of implementing thermal control are listed in table 9–14.

The preliminary design of a satellite is carried out, of course, with thermal control in mind, mainly in the form of rules of thumb, which are elements of the design philosophy described in section 9–1. If the design philosophy dictates conduction cooling, ample conduction paths will be provided during the preliminary design. Or, if thermal insulation of the main structure from the Sun may be specified, as in the OAO, provisions will be made in the conceptual design to incorporate the necessary insulation. The point here is that detailed thermal analysis does not and cannot begin until the major elements of the satellite geometry and structure have been established. Subsequent thermal analysis may dictate major changes in configuration and structure, but a "first-iteration" configuration must be available prior to analysis.

One of the first steps in thermal analysis is the construction of the "thermal model." Heat sources and sinks are specified. Thermal resistances—both conductive and radiative—are detailed. The heat sources, of course, comprise internal loads and solar inputs. The latter are especially difficult to describe analytically, since they vary with orbit, attitude, and spectral character of the satellite surfaces. Figure 9–64 presents a solar input curve as a function of time in orbit and a specific direction of the spin axis of OV-3, an octagonal cylinder.

Continuing with the OV-3 example, the thermal model is divided into nodes, each having a finite thermal capacity and connected to other nodes or empty space (a node, in a sense) by thermal resistances, which represent conductive or radiative heat-transfer paths (figs. 9–65 and 9–66). Using the well-known laws of conductive and radiative heat transfer (ref. 22), the nodal model can be rapidly analyzed on a digital computer using finite-difference techniques. Computers also make it simple to try out different nodes, sources, sinks, and thermal resistances. Various surface paints and finishes may be applied by computer, for example. Components can also be rearranged analytically. The output of such analysis is a series of temperature-history curves, such as that illustrated in figure 9–67, plotted for various conditions and arrangements.

TABLE 9–14.—*Thermal-Control Techniques for Scientific Satellites*

[After ref. 21]

	Technique	Materials	Advantage	Disadvantage	Examples of use
Surface paints and coatings (passive).	Stripes, patches, polka dots.	Polished or evaporated metals; black, white, aluminum paint.	Simplicity of application, control of tolerances by using materials with well-known properties, flexibility.	Nonuniform surface temperatures, difficult to apply to large spacecraft.	Many Explorer satellites, Tiros, Syncom, Ariel 1, 2.
Surface property control (passive).	(1) Mirror finish plus controlled thickness of transparent coating; (2) Surface treatment by chemical baths; (3) Sandblasting.	(1) Opaque coating of aluminum plus controlled thickness of evaporated silicon or aluminum oxide, or barrier layer anodized aluminum;	(1) Uniform coating can control absorptance-to-emittance ratio over wide range; (2) Uniform coating, suitable for application to large spacecraft;	(1) Precision technique, limited to small satellites; (2) Quality control; (3) Quality control.	(1) All Vanguards, Explorer XVII, NRL satellites (Lofti, Solrad); (2) Echo II, OAO; (3) Used in combination with paints on early Explorers and Pioneers.

		(2) Aluminum conversion coatings; (3) Stainless steel, aluminum.	(3) High temperature, stable.		
Electric heaters, coolers (active).	Heaters, coolers, temperature sensing, power switching.	Insulation to minimize power requirements.	Simplicity, flexibility of control.	Poses reliability problem, limited power available for temperature control.	OGO experiments on booms, IMP Rb magnetometer.
Movable external surfaces (active).	Louvers, Maltese cross (movable surface) actuated by bimetal elements or bellows.	Insulation, polished aluminum, white paint.	Controls temperature over wide range of inputs, requires no heater power.	Incident sunlight on louvers may pose problems, bearing failure, vibration during launch.	Mariner II, Mariner IV, OGO I, Nimbus.
Variable internal heat paths (active).	Actuators vary radiation from internal areas to outer surface by bimetal elements, bellows or louvers.	Insulation, polished surfaces, paints.	Makes efficient use of satellite's waste heat, requires no heater power.	Requires compartments insulated from shell.	Telstar, Relay.
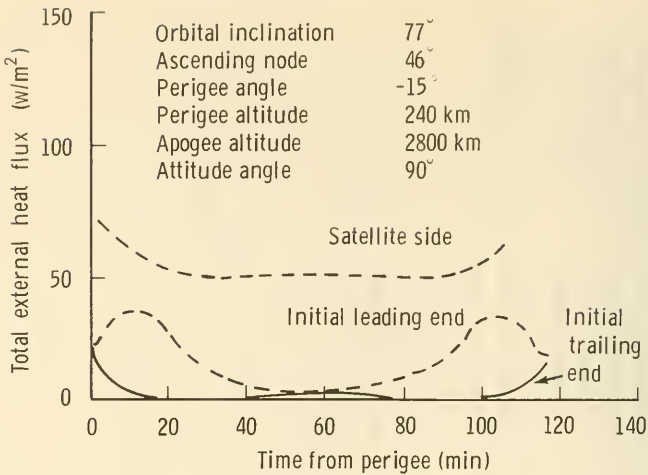
FIGURE 9–64.—An orbital heat-flux curve used during the design of OV–3–1.

When satellites are of simple geometry, analytical solutions are often possible. Spherical balloon satellites (Explorer IX) and the cylindrical micrometeoroid satellite (Explorer XIII) yielded to pure analysis (refs. 23, 24). Solar panels, which are thermally isolated from the rest of the satellite, can be satisfactorily handled without resorting to nodal analysis. Rarely is such simplicity encountered; most thermal analysis resorts to approximate methods and digital computers. Occasionally, satellite thermal problems will be modeled with electrolytic tanks and conducting-paper analogs.

So far, steady-state analysis has been implied. When a spacecraft abruptly plunges from sunlight into shadow, thermal transients invade the satellite interior. Such fluctuations may generate thermal forces much greater than those calculated from steady-state conditions. Transient solutions can also be obtained from nodal models as well as the physical analogs mentioned above.

Eventually, thermal analysis reaches a point of diminishing returns, and a thermal mockup of the satellite must be built. The main structure is constructed—almost always to full scale. Components are thermally simulated, perhaps using electrical heat sources. Sometimes, the prototype itself will be used as the thermal mockup. In any event, a physical simulation of the satellite is installed in an environmental test chamber. Tempera-
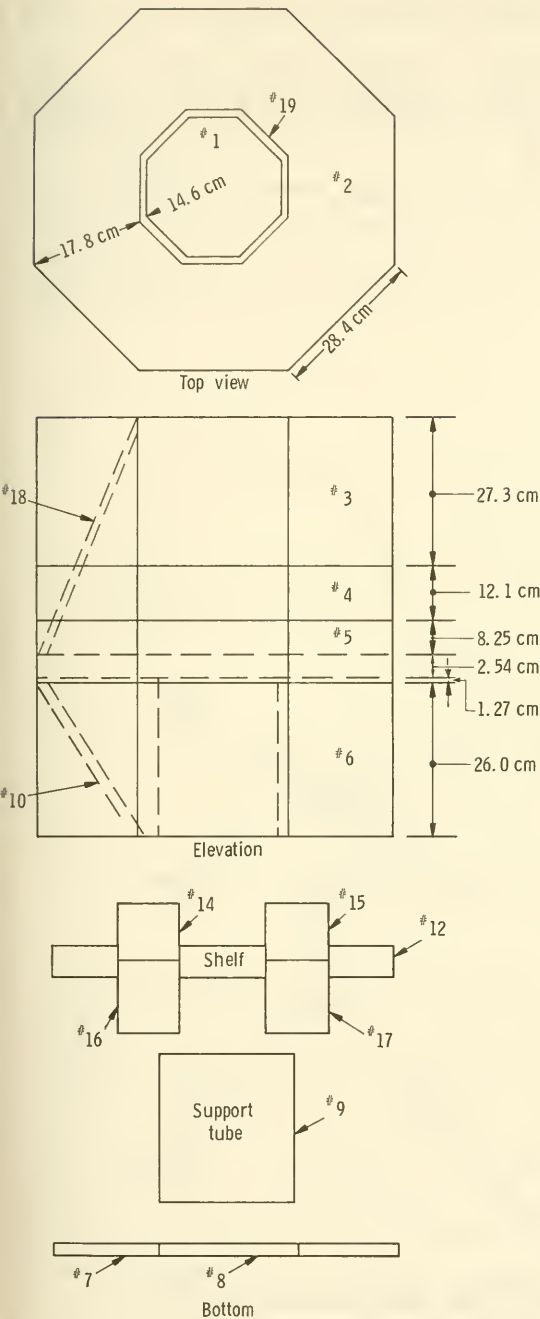
FIGURE 9–65.—One of the nodal models employed in the OV–3–1 design. Numbered nodes are also shown on figure 9–66. (Courtesy of Space General Corp.)

tures are measured as the artificial Sun is turned on and off, and at various satellite attitudes. Hopefully, simulation will confirm analysis.

Two other points relevant to thermal design should be mentioned before we look at specific satellites. One feature of thermal

(N) = Node number
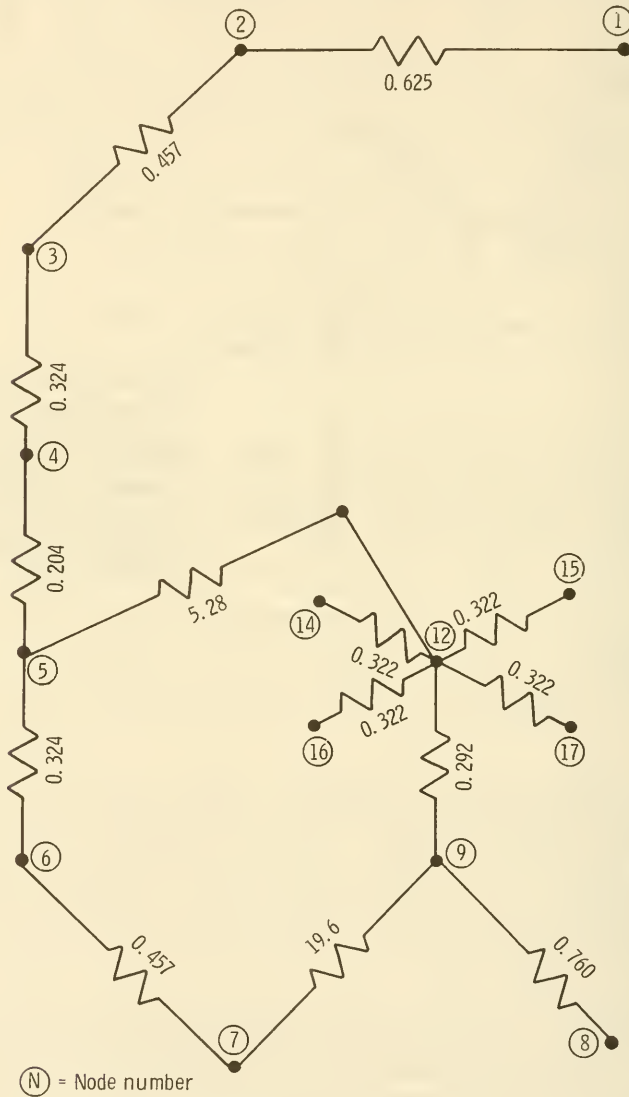
FIGURE 9–66.—Conduction paths for the thermal model portrayed in figure 9–65. Numbers in circles refer to nodes from model. Radiative heat paths also exist. (Courtesy of Space General Corp.)

conduction in the vacuum of space is the high thermal resistance of unwelded joints. Not only is the resistance high, but it is difficult to predict with confidence. The hardware solution to this problem is the application of stable, thermally conducting grease between the joints. The second point is the great variability of the absorptivity-emissivity (α/ϵ) ratio that figures so prominently in thermal computations (table 9–15). This variability is actually a boon to design, because surfaces with various paints and finishes can represent passive heat valves. Most smaller satellites have their temperatures controlled by paint and finish patterns.
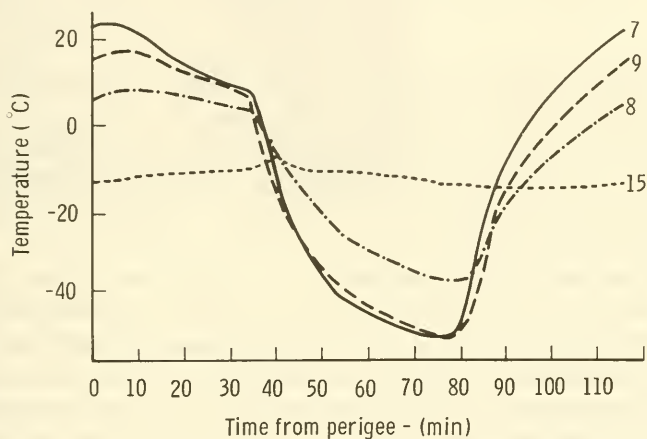
FIGURE 9–67.—Typical temperature curves plotted for the various OV–3–1 nodes.

Thermal Control of Specific Satellites.—Over 90 percent of all scientific satellites have been passively thermally controlled. They have been painted with stripes, spots, and other patterns to control the flow of heat into and out of the satellite. In looking at specific instances of thermal control, the OV-3 thermal model described earlier typifies the passively controlled satellite and illustrates one common analytical technique. The OV-3 structure and its mockup (figs. 9–65 and 9–66) show how heat is channeled outward to the satellite skin, where it is radiated to empty space.

Large satellites, particularly the Observatories, depend upon different thermal-control philosophies. Two examples are significant to this section:

TABLE 9–15.—*Typical Values of* α/ϵ *for Satellite Surface Materials*

Material	α	ϵ	α/ϵ
Polished aluminum	0.35	0.04	8.8
Aluminum oxide	.24	.75	.32
Polished beryllium	.4	.05	8.0
Polished gold	.3	.03	10.0
Stainless steel	.5	.13	3.8
Titanium dioxide	.15	.90	.17
Black paint	.94	.90	1.0
White paint	.76	.23	3.3
Aluminum paint	.30	.25	1.2

(1) OGO, which illustrates active thermal control and separate thermal control of external packages

(2) OAO, which illustrates passive control of a large satellite through fragmentation of its subsystem into many small, thermally isolated compartments

The OGO Environment-Control Subsystem.—Normally, OGO's attitude-control subsystem keeps two sides of its boxlike structure (the sides pierced by the solar-panel shafts) pointed away from the Sun's rays. This fortunate circumstance permits a thermal-control philosophy radically different from that described above. Four sides of the satellite are carefully insulated against solar-heat input by multiple layers of aluminized Mylar, an excellent barrier to radiative heat transfer. The two dark sides expose the satellite interior, where several hundred watts of electrical power are dissipated, to cold space. The thermal resistance of these two sides is automatically controlled by the satellite temperature. Shutters, or louvers, controlled by bimetal strips, open and close as the satellite heat load varies (fig. 9–68). Action of these heat valves keeps the internal temperatures within the limits 5°–35° C. It is interesting to note that during OGO's conceptual design, passive thermal control was shown to be unfeasible.

OGO's external experimental packages and solar-cell panels have separate thermal controls. They are isolated on booms or shafts, so that conduction and radiation to and from the main satellite body are minimized. Depending upon the contained experiments, passive paint patterns or louvers are installed.

The OAO Environment-Control Subsystem.—The OAO struc-
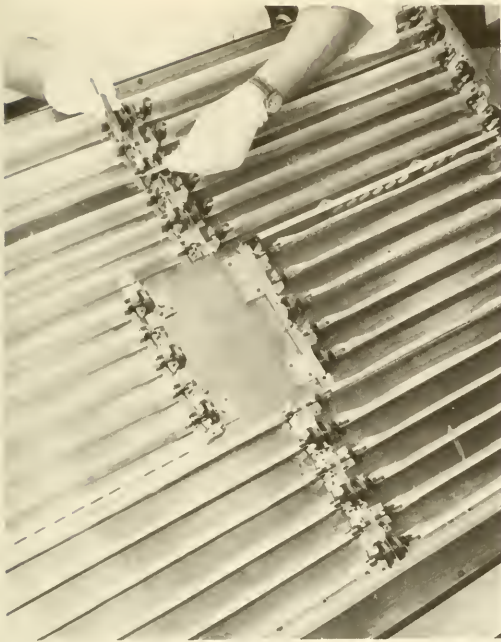
FIGURE 9–68.—The thermal louvers on OGO. (Courtesy of TRW Systems.)

ture is basically a tube, 122 centimeters in diameter and 300 centimeters long. It is surrounded by 48 truncated equipment bays, arranged in an octagonal pattern. The sequestering of OAO equipment into small bays insulated from the main satellite structure is the key to successful passive thermal control (ref. 25). (See figs. 9–69 and 9–70.) Superinsulation made of aluminized Mylar covers all but one side of each bay (fig. 9–71). The bulk of the heat flowing out of (or into) each bay follows the path between the honeycomb mount and the aluminum satellite skin. Thus, the bay skins can be painted or finished in a manner appropriate to the enclosed equipment. The small equipment packages in the bays are each handled separately, as if they were small, passively controlled satellites.

The major heat input to the main OAO structure and the contained telescope is leakage through the superinsulation of the equipment bays. By careful insulation and design, heat inputs to the structure through fittings and supports are minimized. Heat leaves the structure through radiation escaping via the open tube ends and heat transfer to nonequipment bays and end skin sections. Since the heat sinks are difficult to control, the heat flow into the structure is varied by changing the amount of superinsulation around the bay walls. The design temperature of the
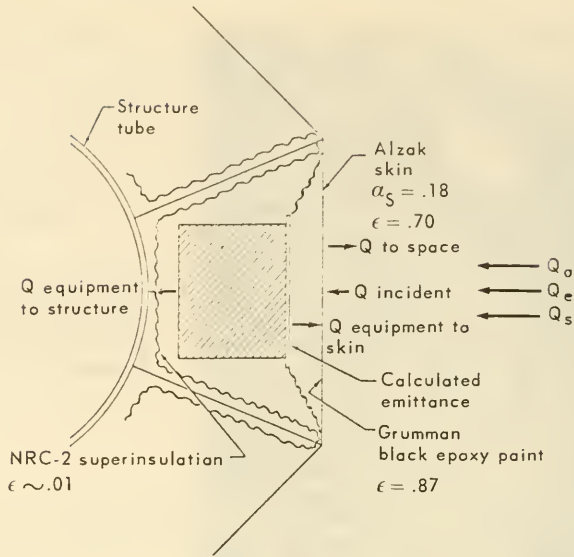
FIGURE 9–69.—Plan view of an OAO equipment bay, showing an instrument package surrounded by superinsulation on all sides except the one facing the outer skin (ref. 25).
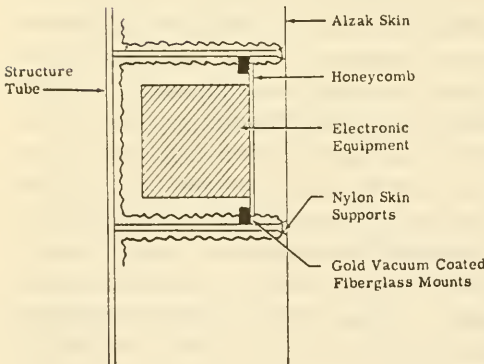
FIGURE 9–70.—Side view of the OAO equipment bay shown in figure 69 (ref. 25).

cylinder and contained telescope in the OAO is about $-30°$ $\pm15°$ C.

9–9.   The Guidance-and-Control Subsystem

Satellite simplicity is frequently commended in this book, and the trends toward passive attitude and thermal control support this position.   In the matter of overall satellite control, however, satellites are becoming more complex as more commandable functions are added to their repertoire.   Yet, these more intricate

FIGURE 9–71.—Photograph of the OAO bay structure. (Courtesy of Grumman Aircraft Engineering Corp.)

scientific satellites can perform better—despite any loss of reliability—because they are more flexible and present their operators and experimenters on Earth with many alternate modes of operation.

Guidance and control were defined in chapter 6. Briefly, the main functions to be carried out by this satellite subsystem are:

(1) The measurement of satellite position and attitude (the navigation function) with onboard sensors. The formulation of commands based upon this information (the guidance function) and their dispatch to the proper spacecraft actuators.

(2) Satellite-status control, whereby satellite switches are thrown and components turned on and off upon receipt of commands from the ground or an internally stored program

The dividing lines between the two other "control" subsystems—the attitude- and environment-control subsystems—are purely arbitrary. Closed-loop, environment-control circuits—e.g., thermostats—are not included in the guidance-and-control subsystem. Neither are the actuators that reside in the attitude-control subsystem. In other words, across the nine information interfaces that the guidance-and-control subsystem shares with the rest of the satellite flow all externally and internally generated commands—except for intrasubsystem feedback loops, such as automatic-gain controls, temperature-controlled louvers, and voltage regulators. Because of these definitions, it might be more appropriate to call the attitude-control subsystem the attitude-actuation subsystem. See figure 6–2 for the guidance-and-control subsystem interface diagram showing other subsystem interrelationships.

A potentially important information interface exists with the computer subsystem. A general-purpose onboard computer might receive considerable traffic from the guidance-and-control subsystem, because much difficult computation often intervenes between the receipt of navigational information and the forwarding of responsive commands to the actuators. Coordinate transformations typify such calculations. Centralized, general-purpose computing is not yet a feature of scientific satellites. When computations are needed, they are carried out by small, specialized onboard computers—viz, AD converters—or on the ground via the communication subsystem.

The guidance-and-control subsystem may be characterized, then, as an action center that receives sensor signals, interprets them, transforms them into appropriate commands, and directs them to the proper actuators. Internally stored and Earth-generated commands are also dispatched to the actuators from here, giving the subsystem the trappings of a telephone exchange.

Sensors for Measuring Satellite Position and Attitude.—Satellites, in principle, can fix their own position and compute orbital

parameters. In practice, though, simpler and more reliable satellite operation results when Earth-based tracking stations are the sole determiners of position. Satellites carry transponders and laser-beam reflectors to enhance tracking, but there is no onboard orbital navigation. Exclusive concentration on attitude sensors is therefore reasonable.

Attitude sensing, on the contrary, is solely satellite based; although, in principle, it could be consummated from Earth, say, by observing signals from directional antennas aboard a satellite. Attitude sensors exist in profusion. A descriptive table is the most compact method of presentation. Table 9–16 lists the gyro—an inertial device—as well as those instruments relying upon directional radiation fluxes (sunlight) and force fields for reference. Inertial equipment, so vital to launch vehicles and deep-space probes, has little application on scientific satellites.[8] First, few scientific satellites need inertial references—the gyro that guides OGO's OPEP experiments along the orbital plane is the exception that proves the rule. Second, the drift of gyros is too high for the precise attitude control of long-lived scientific satellites.

Specific Guidance-and-Control/Attitude-Control Subsystems.— The attitude-control subsystems of AE–B, OSO, and OGO (delineated in sec. 9–7) and OAO (sec. 6–5) could not function without pointing-error inputs from attitude sensors chosen from table 9–16. Reference should be made to these sections for the synthesis of the guidance-and-control and attitude-control subsystems. (See fig. 9–60, in particular.)

Satellite Command.—The ''command'' function has been touched upon lightly (secs. 6–6 and 9–4). Here, reference is to satellite-status control—or, as it turns out in practice, switch throwing. The elements of the function are: a ground-based transmitter, a satellite-based command receiver, and the existence of a code with which the satellite operator selects the desired satellite and the proper switches with his electromagnetic signals. An adjunct to any command system is a set of internally stored commands, constituting a ''program,'' that are dispatched automatically to appropriate subsystems at times measured by a clock of some sort. Timed commands are almost always reserved for erecting antennas, stimulating the initial acquisitions of Sun, Earth, or star, and eventually turning the satellite off at a fixed time after launch, when its mission is deemed complete.

---

[8] Strictly speaking, the spin-stabilized satellite could be considered a gyro in the sense that its spin axis provides an inertial reference.

TABLE 9-16.—*Descriptions of Some Attitude Sensors*

Category	Type	Principle of operation	Remarks
Inertial	Gyroscopes	Conventional gyros consist of high-speed rotating wheels on low-friction bearings. One-degree-of-freedom rate gyros (fig. 9–72) are used on spacecraft. Torque about input axis causes gyro to precess about output axis, where displacement against spring generates signal proportional to angular acceleration. "Unconventional" gyros use electrostatic or magnetic fields for suspension. Nuclear-spin gyros, laser gyros, vibrating gyros, and fluid gyros are under development (ref. 26).	Rarely used on scientific satellites for attitude sensing—drift rates are too high. OGO, however, directs its OPEP with a gyro.
Optical (detectors of directional electromagnetic radiation).	Solar-aspect sensors	Aspect (relative bearing of the Sun) is determined by the output amplitudes of one or more photosensitive devices; viz, solar cells, CdS cells (fig. 9–73). Digital aspect sensors are common on NASA satellites (fig. 9–74).	Aspect sensors are mounted on most small scientific satellites to give experimenters attitude information. *Not used for guidance.* Measures attitude to ±5°.
	Sun trackers	Image of Sun (an extended source) is either split (fig. 9–75) or focused through a slit. Photosensitive devices yield error signals if tracker is not pointing accurately.	OSO, OGO, and other solar-research satellites need Sun trackers to stabilize spacecraft. Accuracy: ± a few minutes of arc (fig. 9–76).

Star trackers	Image of star (a point source) is focused on array of photosensitive devices (fig. 9–77). Error signals are generated when target drifts off axis. Trackers do not identify stars per se, but can provide angular coordinates with respect to reference sources.	Essential to OAO series for stabilization. Accuracy: ± a few seconds.
Horizon-sensors	Infrared detectors scan space and detect the temperature discontinuity between warm Earth and cold space (fig. 9–78). Two conical scanners or 1 limb scanner will produce symmetric signals when desired axis is perpendicular to Earth.	Earth-oriented satellites generally boast horizon scanners. OGO is one of the few scientific satellites so oriented. Accuracy: ± a few tenths of a degree (fig. 9–79).
TV	Photosensitive surface is scanned by electron beams. Signals proportional to image intensity produced. Image could be matched, say, to star fields, to yield guidance information.	Not planned at present for scientific satellites.
Radar	Electromagnetic signals bounced off target gives range, range-rate, and directional information. Could, in principle, be used for Earth tracking.	Not contemplated at present for scientific satellites.
Magnetometer	Direction of Earth's magnetic field is sensed by one of the vector magnetometers described in detail in sec. 11–2. Signals proportional to field components sometimes drive magnetic attitude actuators (sec. 9–7, figs. 9–56 and 9–57).	Used in fields-and-particles satellites for both field-aspect information and attitude control.

Field (detectors of directional fields).
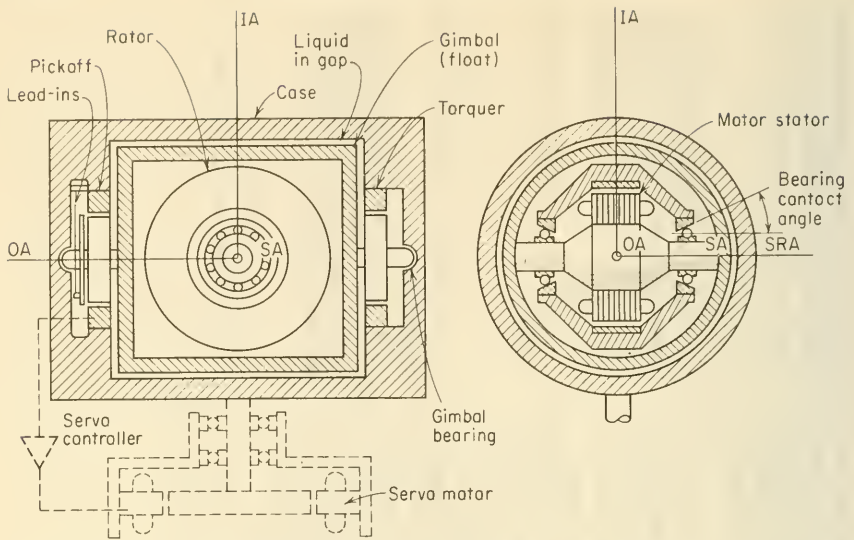
FIGURE 9–72.—Elements of a single-axis gyro. IA = input axis, OA = output axis, SA = spacecraft axis (ref. 26).

Ground-command systems are critical, for herein lies potential flexibility of operation, particularly modification of satellite operation in the presence of component failure(s). Redundant command receivers and the associated distribution circuits are almost always installed in duplicate (sec. 9–4). Command codes are simple and redundant to preclude misinterpretation. Tone commands have found great favor in the smaller U.S. scientific satellites. A series of four tone pulses, using four different tones or four pulsewidths, accommodate $4^4 = 256$ satellite-command combinations. The large observatories, such as OGO and OAO, which have adopted PCM telemetry, find it convenient to send binary command words with addresses and instructions coded like digital-computer words (fig. 5–4). Binary command words are customarily transmitted along with the binary complements of the most critical portions of the word, to enhance the probability that only undistorted commands will be taken seriously by the satellite.

To illustrate a representative command system, consider the approach used on OSO—a spacecraft which may be considered a small Observatory or large Explorer.

The OSO Command Equipment.—When an operator wishes to command an OSO to change its status, he punches the command
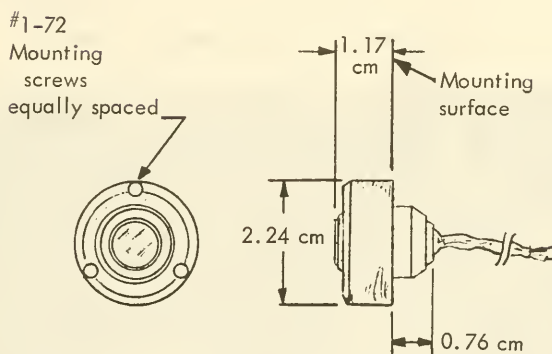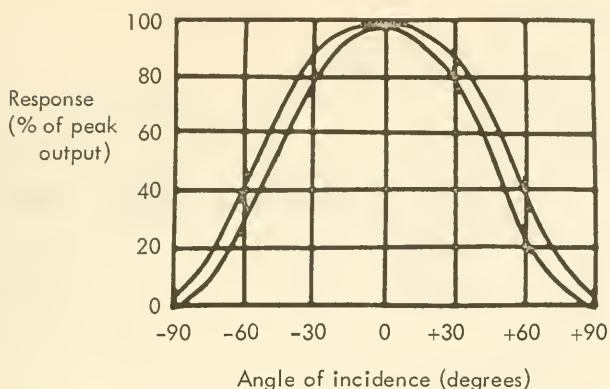
FIGURE 9–73.—The OV–3–1 solar-aspect sensor and a typical response curve. (Courtesy of Space General Corp.)

on a paper tape. The tape is then fed through a STADAN command encoder that modulates a vhf AM transmitter. The rf output is a series of tone-modulated pulses of different widths. An OSO passing over the STADAN station will pick up these signals on its command receivers (fig. 9–80). All three decoders shown in the block diagram will receive the same pulses, but only the addressed decoder will respond by relaying signals to the waiting satellite equipment.

First, how is a specific decoder addressed and how can it tell one command from another? Answering this question means revealing the pulsewidth binary code used by OSO. In the code, a binary "0" is a tone pulse 2.58 milliseconds long; a "1" is 5.15 milliseconds long. A decoder address consists of a series of two
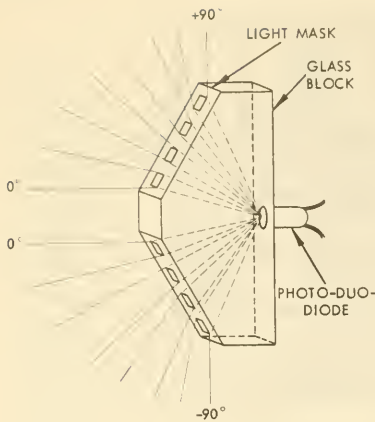
FIGURE 9–74.—Binary light sensor (ref. 27).
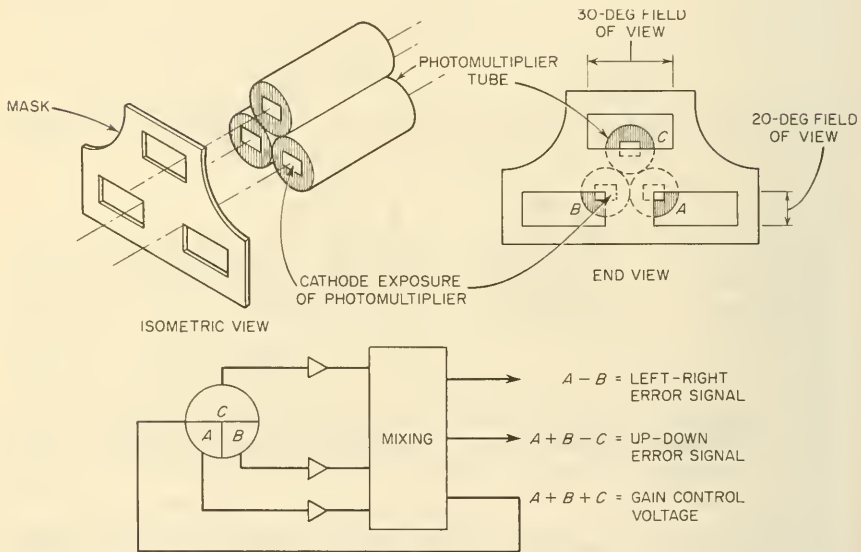
FIGURE 9–75.—One approach to image splitting used in tracking extended sources (ref. 28).

1-bits and six 0-bits, or six 1-bits and two 0-bits. A command comprises a mixture of four 1-bits and four 0-bits. A full code word consists of eight bits, plus one blank and one sync bit. A full command frame has five words: two repeated addresses and three repeated command words, followed by blank and sync bits. The selected decoder will respond by relaying pulses of 9–20 volts amplitude and 35-millisecond duration to one of 47 [9] satellite cir-

---

[9] 70 in OSO D and thereafter.
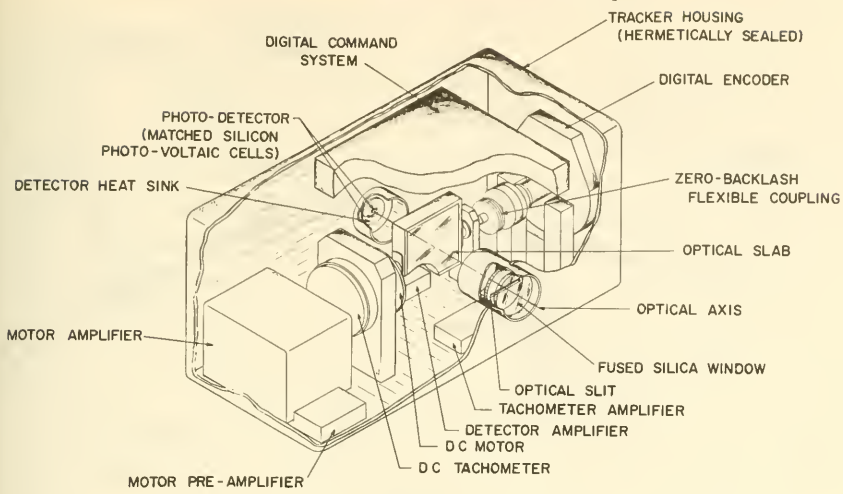
FIGURE 9–76.—One type of Sun sensor.
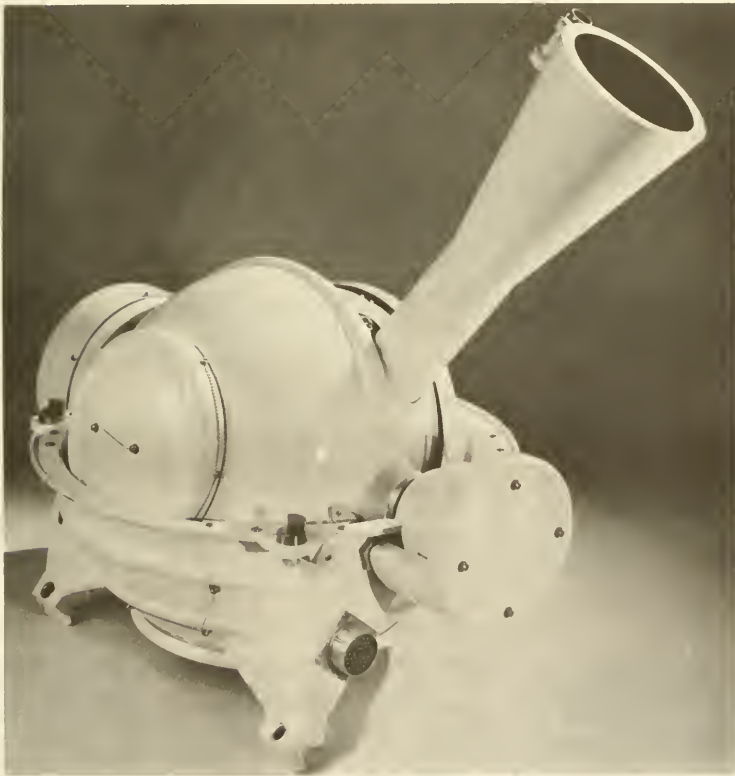
FIGURE 9–77.—An OAO star tracker.   (Courtesy of Bendix Corp.)

(a)

(b)
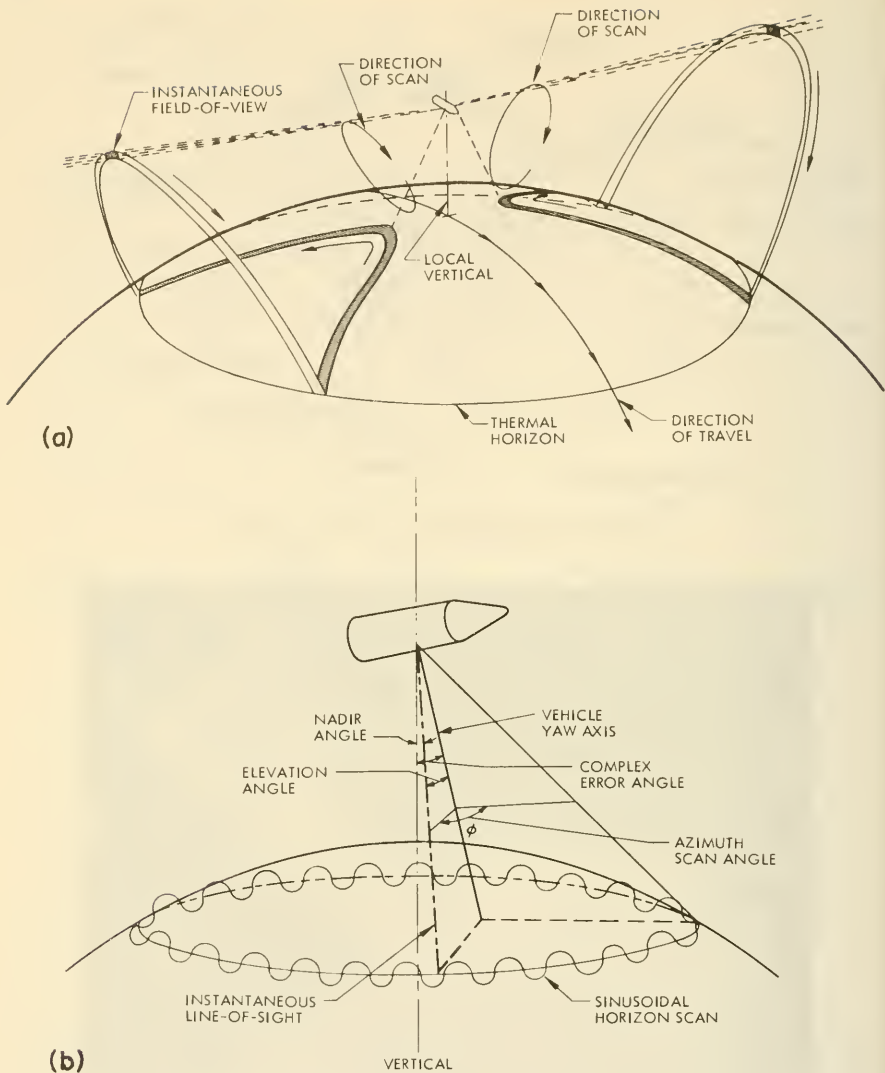
FIGURE 9–78.—Two horizon-scanning techniques: (a) conical scanning using two scanners; (b) limb scanning with one scanner (ref. 29).

cuits or components, which, of course, are keyed to a specific combination of eight command bits. The selected circuits respond by closing or opening relays. A typical list of OSO commands is presented in table 9–17. One notes immediately from the list that decoders 1 and 2 address the same 47 wheel circuits, though they
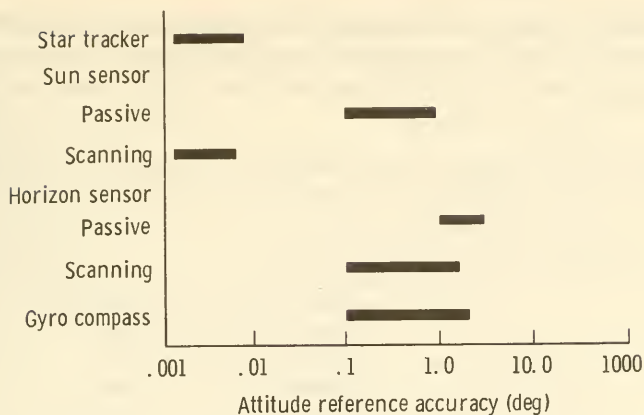
FIGURE 9-79.—Attitude accuracy of several sensors (ref. 16).
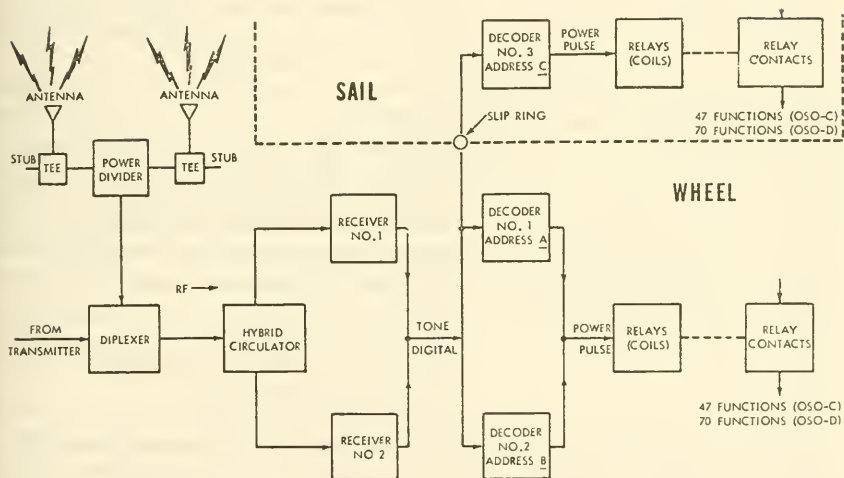
FIGURE 9-80.—Block diagram of the OSO PCM/AM/AM digital tone-command system.   OGO D handles 40 commands.

have different addresses, while decoder 3 addresses 47 circuits in the sail.   Redundancy is essential in these vital circuits.

The first and last commands received by OSO equipment originate on the satellite itself.   During the period following orbital injection and prior to Sun lock, a satellite timer dispatches electrical signals to the various pieces of equipment that enact the sequence illustrated in figure 9-59.

Mechanical timers are valuable during the beginning of a mission, but they are not considered reliable enough to shut satellites down after the elapse of a year or some other specified mission

TABLE 9–17.—*Typical Command-Word Allocation, OSO's A–C*

Command-word number	Wheel-decoder system [a]
1	Tape Recorder Playback On
2	Tape Recorder Playback Off
3	Multiplexer No. 1 Select
4	Multiplexer No. 2 Select
5	Tape Recorder No. 1 Select
6	Tape Recorder No. 2 Select
7	Transmitter No. 1 Select
8	Transmitter No. 2 Select
9	MIT Experiment Power Off
10	Rochester Experiment Power Off
11	MIT Experiment Power On
12	Rochester Experiment Power On
13	Day Power—Sail On
14	Day Power—Sail Off
15	rf Power On
16	rf Power Off
17	Michigan Experiment Power On
18	California Experiment Power On
19	Ames Albedo Experiment Power Off
20	Ames Albedo Experiment Power On
21	Spin Control—Ground Select
22	Spinup Actuation
23	Spindown Actuation
24	Spin Control—Automatic Select
25	Day-Night Bypass Closed
26	Day-Night Bypass Open
27	Undervoltage Switch Bypass Closed
28	Undervoltage Switch Bypass Open
29	One-Year Timer Bypass Closed
30	One-Year Timer Bypass Open
31	Tape Recorder Playback On (Redundant)
32	MIT Command No. 1
33	Spare
34	Ames Emissivity Experiment Power Off
35	Ames Emissivity Experiment Power On
36	California Experiment Power Off
37	Michigan Experiment Power Off
38	Undervoltage Security Closed
39	Undervoltage Security Open
40	Tape Recorder Power On
41	Tape Recorder Power Off
42–47	Spares

TABLE 9–17.—*Typical Command-Word Allocation, OSO's A–C*—Continued

Command-word number	Sail-decoder system
48–64	GSFC Commands Nos. 1-17
65–81	AFCRL Commands Nos. 1-17
82	Pitch Control—Ground Selected
83	Pitchup Actuation
84	Pitchdown Actuation
85	Pitch Control—Automatic Select
86	GSFC Experiment Power On
87	AFCRL Experiment Power On
88	GSFC Experiment Power Off
89	AFCRL Experiment Power Off
90–91	AFCRL Commands Nos. 18-19
92–94	GSFC Commands Nos. 18-20

[a] GSFC = Goddard Space Flight Center; AFCRL = Air Force Cambridge Research Laboratory.

length. The satellite must be removed from the air—that is, all transmission must cease—if bandwidth for space research is to be conserved. Electrochemical "killer"-timers [10] have been selected as more reliable than electronic or mechanical types. Like most of this breed, the OSO killer-timer irrevocably breaks the satellite power circuit. The quest for reliability in killer-timers has not been completely successful. Explorer VII, for example, launched on October 13, 1959, carrying a 1-year killer-timer, transmitted until August 24, 1961.

9–10. The Computer Subsystem

When the word "computer" is used in this book, a general-purpose computer is implied; in all probability, a digital computer. The functions of such an onboard computer would be:

(1) Centralized computing for all spacecraft subsystems, replacing the specialized computers now prevalent on the larger scientific satellites—viz, analog-digital converters. Data processing, including compression and selection, falls in this category. No contemporary satellites enjoy this function.

(2) A storage unit for spacecraft data, programed commands, information for fault finding and repair, and internal checking routines. The omnipresent tape recorder now serves many satellites as a repository for scientific data. Satellites such as the

---

[10] Also called "guillotine" timers.

OAO and Geos (Explorer XXIX) replace the tape recorder with magnetic-core memories. The OAO memory, for example, has a storage capacity of 204 800 bits, equivalent to 8192 data words of 25 bits each. Scientific data, as well as commands, are stored in this way, so that we can say that this particular computer function is already achieved.

(3) A computer can also serve as a clock and as an event timer. Many satellites already possess crystal clocks to synchronize their activities; Geos, for instance, times its light flashes with the clock blocked out in figure 9–81.
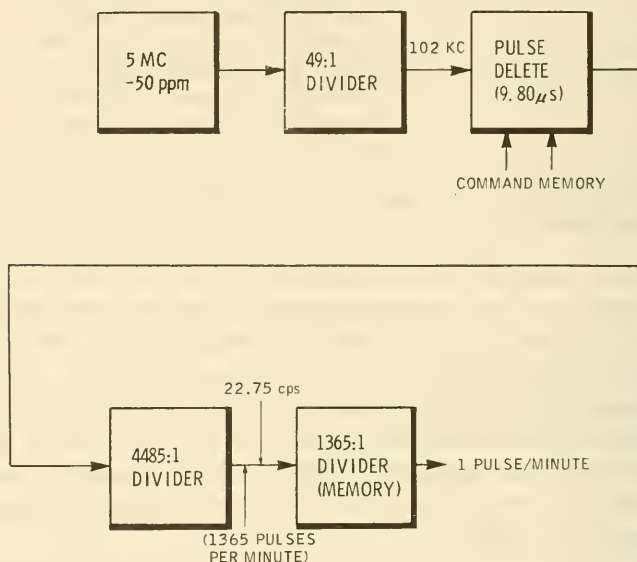
FIGURE 9–81.—Functional block diagram for the Geos clock. Like most satellite clocks, this is basically just a frequency divider or counter.

Reviewing these functions, one discovers that the only general-purpose-computer function not already in vogue on scientific satellites is centralized satellite computing.

Centralized computers might save weight and power over dispersed, special-purpose computers on the Observatory class of satellite, but this is only surmise. The engineering discipline of electronics packaging aims at packing tens of millions of parts into a cubic meter; there is no concern about the size of digital computers. There is, however, a question concerning the reliability of a computer with tens of thousands of fallible parts,

particularly when almost all of the satellite subsystems would depend upon it absolutely for 6 to 12 months in space. Computers could be paralleled to solve this problem. At the present time, it is unlikely that centralized, general-purpose computers can be justified for those satellites now in the planning stages. With the Observatories, we seem to have reached a temporary plateau in complexity, a plateau still short of centralized computers.

9–11. The Structural Subsystem

The satellite structure forms the backbone of the spacecraft. It supports, unites, and protects the nine other subsystems. More than just a framework on which to hang electronics and instrument packages, the structure establishes the satellite geometry, isolates equipment on booms, and shields vital equipment from the impact of micrometeoroids and the heat of reentry.

By leafing through the illustrations of scientific satellites presented in the appendix, the reader can assure himself that satellite shapes are a geometer's delight: spheres, cylinders, winged polyhedrons, simple cubes. Why have designers chosen particular shapes, and why the great variety? The important factors molding satellite shape are listed below:

(1) *Spacecraft Mission.*—The absence of weight and air in orbit permits arbitrariness in shape, but some missions dictate specific shapes. Recoverable satellites, for example, are contoured to survive reentry. Aeronomy satellites should be spherical to simplify drag computations. Balloon satellites have little choice except the sphere.

(2) *Strength and Weight.*—The loads, shocks, and vibration spectra of launch and reentry demand that the satellite structure maintain its integrity under severe conditions. Resonances under vibration loads obviously must be avoided. Spheres, cylinders, polygonal trussed frames are typical of the shapes that meet these requirements. All these things must be accomplished while attempting to minimize weight.

(3) *Attitude-Control Scheme.*—The bulk of the scientific satellites are spin stabilized and therefore have symmetry around their spin axes. Cylinders and cylindrical polygons are very common.

(4) *Ease of Fabrication.*—The structure should be designed so that it can be constructed without resorting to special jigs, fixtures, and the like. Since simplicity is a virtue in fabrication, boxes and polygons often appear. Perfect spheres are unusual,

though one finds many-faceted polygons that approach spheres (fig. A–20).

(5) *Accessibility of Equipment.*—The countdown sequence presented in section 7–3 revealed that engineers and experimenters are adjusting instruments and replacing faulty equipment right down to $t = 0$. Many satellites thus use the modular approach, in which equipment is mounted in bays and packages, where it is
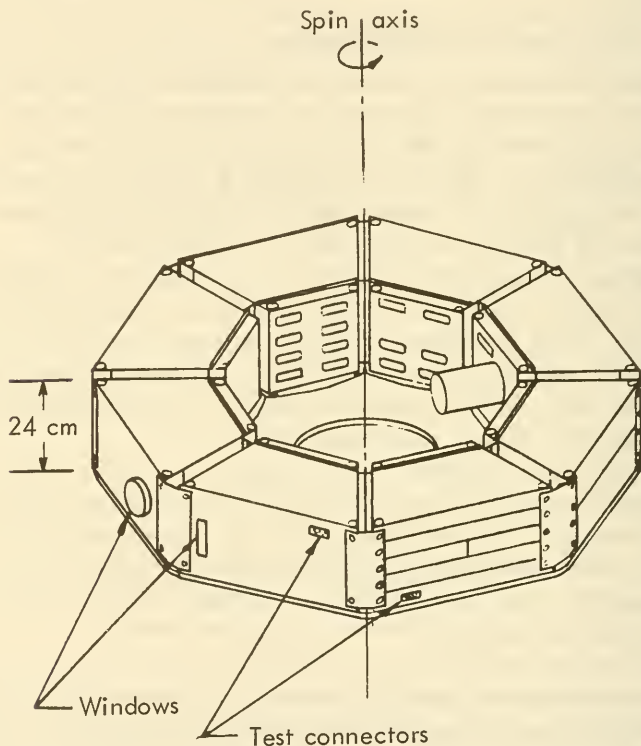
FIGURE 9–82.—The IMP F/G bays, showing the drawer-type modules.

easy to reach and, if necessary, replace with a plug-in unit (fig. 9–82). Equipment is frequently mounted on doors or in drawers that can be swung or pulled out (fig. A–33). Another common occurrence is the instrument shelf attached directly to the main support structure (fig. 9–83).

(6) *Instrument Layout.*—Most satellite instruments sample the space environment and must be mounted where they have a view of the target phenomena. Magnetometers and a few other
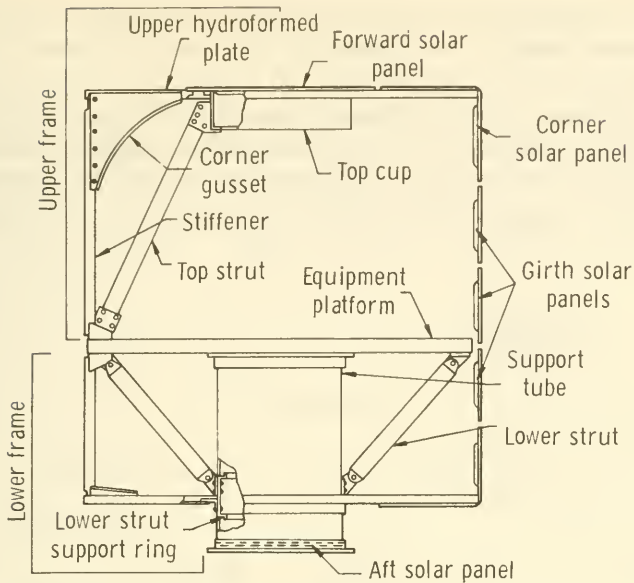
FIGURE 9–83.—The OV–3–1 structure, showing the equipment shelf and upper frame supported by the central thrust or support tube. The external geometry is octagonal. (Courtesy of Space General Corp.)

instruments are often isolated from the satellite by long booms or superstructures. The conical superstructures of Explorers X, XVIII, and XXI are dictated by their magnetometers.

(7) *Need for Surface Area and Solid Angle.*—While each satellite can have only 4π steradians of solid angle, the surface area available to solar cells, attitude-control jets, instruments, etc., can be increased markedly by the use of appendages, such as booms and panels. The powerful urge to gain surface area and solid angle leads to the insectlike appearance of many satellites.

(8) *Launch-Vehicle Compatibility.*—The satellite, first of all, must fit within the launch-vehicle shroud (fig. 8–13). It may metamorphose and extend its appendages later. Almost all launch vehicles spin-stabilize their final stage. Satellites, regardless of their final geometry, should have mass symmetry about the spin axis of the injection stage.

(9) *Thermal-Control Considerations.*—All internally generated heat must be radiated eventually from the satellite surface. Thermal control may impose the requirement for either high- or low-resistance heat paths to the outer skin and structures. Metals are

good heat conductors and the location of metallic structures should be contemplated with heat-flow paths as well as mechanical strength in mind.

The interfaces the structural subsystem shares with other subsystems are summarized in the interface diagram (fig. 9–3). The discussion of the major structural interfaces is inherent in the preceding listing of factors that shape satellite structure.
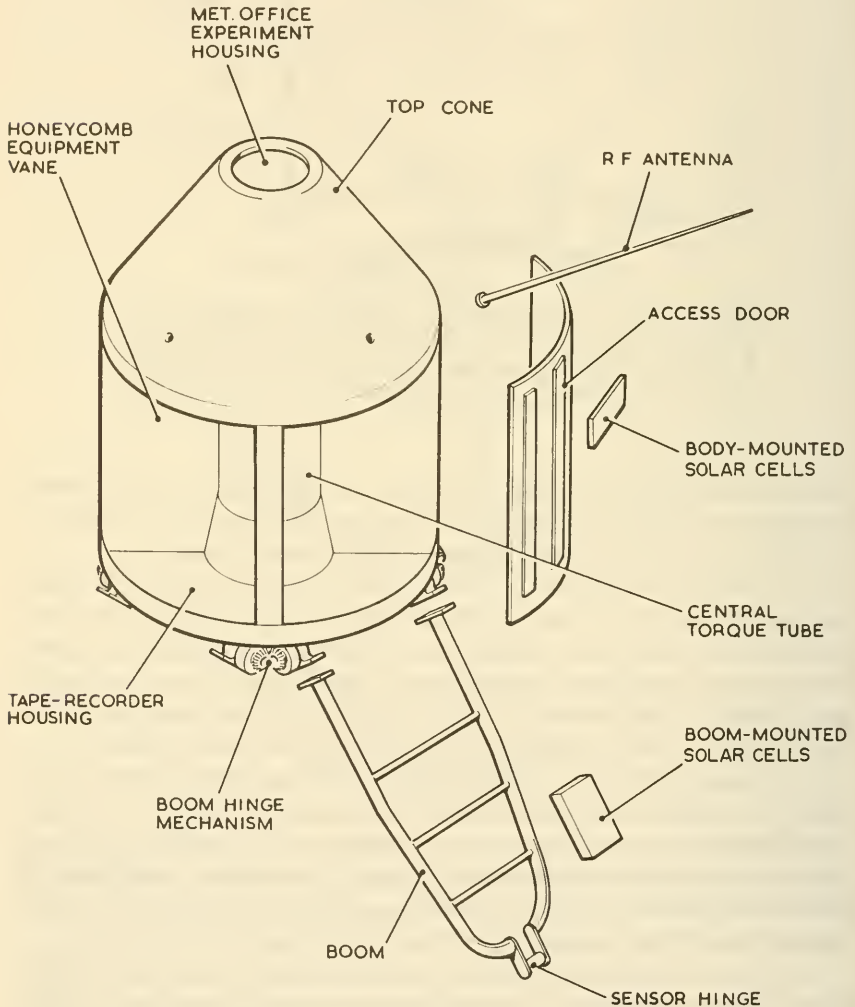
FIGURE 9–84.—The UK-3 structure, illustrating a central thrust tube and hinged booms (ref. 31).

Structural Analysis.—Once a basic structure has been selected, based upon the above considerations, it must be proven mechanically feasible. Structural analysis, like thermal analysis, involves defining the imposed loads—steady state and time varying —and calculating the response of the subsystem. In the case of structures, this means determining whether any portions of the structure will fail under the imposed loads during the design life of the spacecraft. The analytical techniques involved are thoroughly described in the literature and will be bypassed here (refs. 2, 30).

Satellite Appendages.—The satellite metamorphosis from its tightly constrained configuration within the launch-vehicle shroud cannot take place without extensible devices, such as hinges and telescoping booms, plus source of energy to do the work of extension, and, finally, a timer-controlled or commandable release mechanism. Extension is movement, and moving parts frequently give rise to reliability problems. Booms and unfolding solar paddles have not been perfect performers in space, as exemplified by the incompletely extended boom on OGO I.

The most frequently used extensible structure is the hinged boom, paddle, and antenna. In figure 9–84, we see a hinged boom on the UK-3 satellite, which deploys the satellite's solar paddles and several sensors. Booms such as this one are usually restrained by pins during launch. At the moment of deployment, an explosive pin puller or cord cutter is fired by the electrical "deploy" signal, releasing the boom. If the satellite is spin stabilized, centrifugal force will unfold the booms without the aid of springs or other energy sources. In the case of the UK-3, the booms would deploy violently if the yo-yo despin device failed —possibly damaging equipment by shock—therefore, boom deployment is regulated by an escapement mechanism that pays out a tension cord that runs to the boom tips (ref. 31). Hinged booms can become quite complex, as illustrated by the OGO boom portrayed in figure 9–85. Hinged structures reach their zenith with the Pegasus "wings," which unfold the satellite's 200 m² of micrometeoroid detectors (fig. 9–86). The detector panels are hinged together, and deployment is controlled by a series of scissor links pivoted at the center of each frame. The links are geared to a torque shaft that receives its energy from a torsion spring.

Telescoping booms are also put to use on satellites. Gas pressure commonly forces extension of the boom, which then locks itself into its final position. The de Havilland extensible boom (fig. 9–52) is made from a strip of beryllium copper that is heat
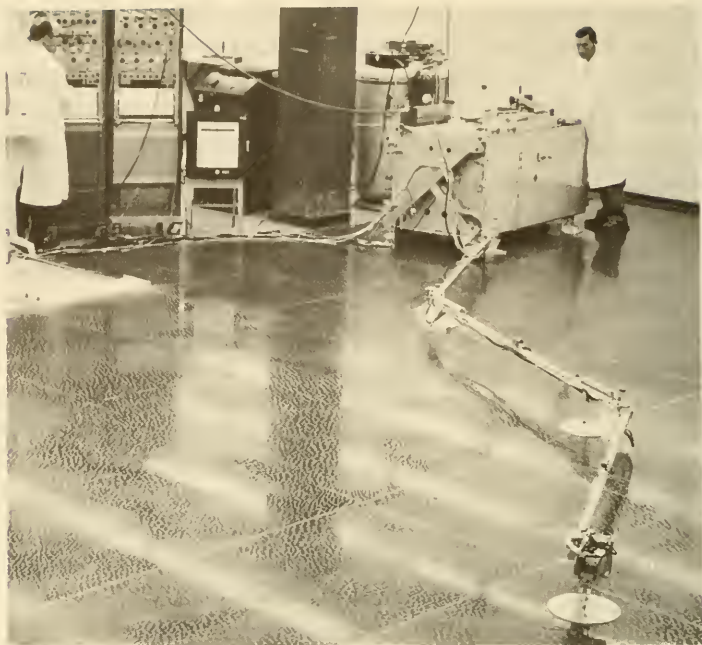
FIGURE 9–85.—The OGO/EP–5 extendable boom dur-
ing test.   Note the mechanical complexity and
wiring.   (Courtesy of TRW Systems.)

treated while in tubular form.   The strip is then flattened and
rolled up into a coil.   When the deploy signal is received, the strip
is unwound through a flat-to-tubular guide.   The original tubular
shape is recovered, and a fairly rigid sensor support, antenna, or
despin rod is formed in space.

Summarizing, satellite appendages are rods, panels, and pad-
dles that are unlatched from their folded positions by relays or
pyrotechnic release.   The energy needed for extension may reside
in springs, gas stored under pressure, electric motors, or the
energy of the spinning satellite itself.

Major Types of Satellite Structures.—Earlier in this section,
the question of satellite shape was discussed.   One of the factors
affecting the choice of external shape was structural strength.   It
is important to recognize, however, that the external shape may
not parallel the shape of the structural skeleton, just as flesh con-
ceals the true nature of animal skeletons.   The skeleton is the
satellite's load-bearing foundation, upon which equipment and
sensors are mounted.   It must be rigid and strong.   There are
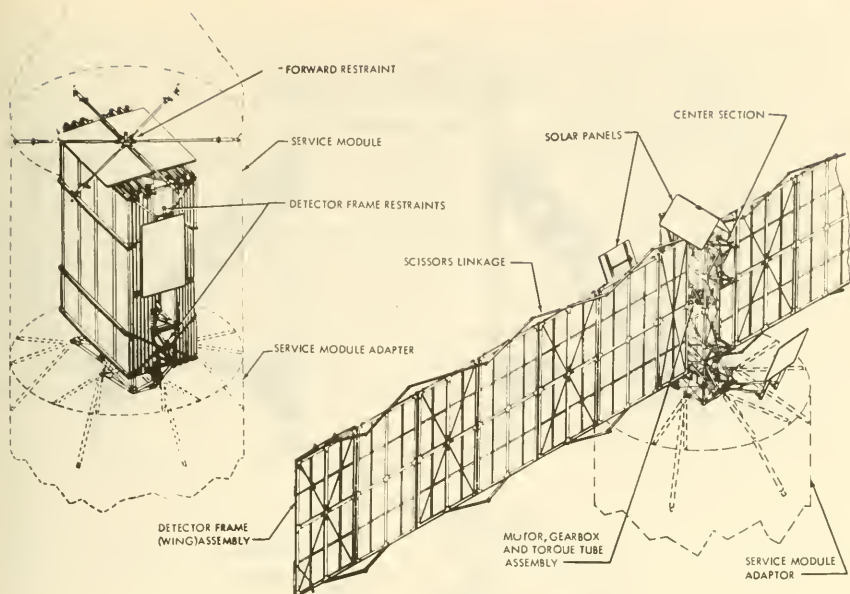
FIGURE 9–86.—The Pegasus satellite with its unfolding "wings" bearing micrometeoroid detectors.

only four basic structures used in scientific satellites: spheres, cylinders, polygonal frames, and cones. These are discussed below.

Though many satellites may look like true spheres, few really use perfect spheres as load-bearing structures. Most are polygonal frames or shells. The balloon satellites, Explorer IX and XIX, were true spheres, of course. In these, layers of aluminized Mylar skin were pressurized after orbital injection (fig. A–38). After they attained their spherical shape, and the pressurizing gas leaked away, they were deformed very gradually by the various forces present in space. It is perhaps stretching the definition of the word "structure" to apply it to an unpressurized balloon, which is sensitive to the least incident force; yet, the spherical configuration of these satellites was preserved for many months, despite the skin's weakness. A few scientific satellites have used rigid, pressurized spherical shells; viz, Vanguard I, Explorer XVII, and San Marco 1 (figs. A–16, A–42). True spheres are difficult to fabricate, but aeronomy experiments demand spherical symmetry for calculational purposes.
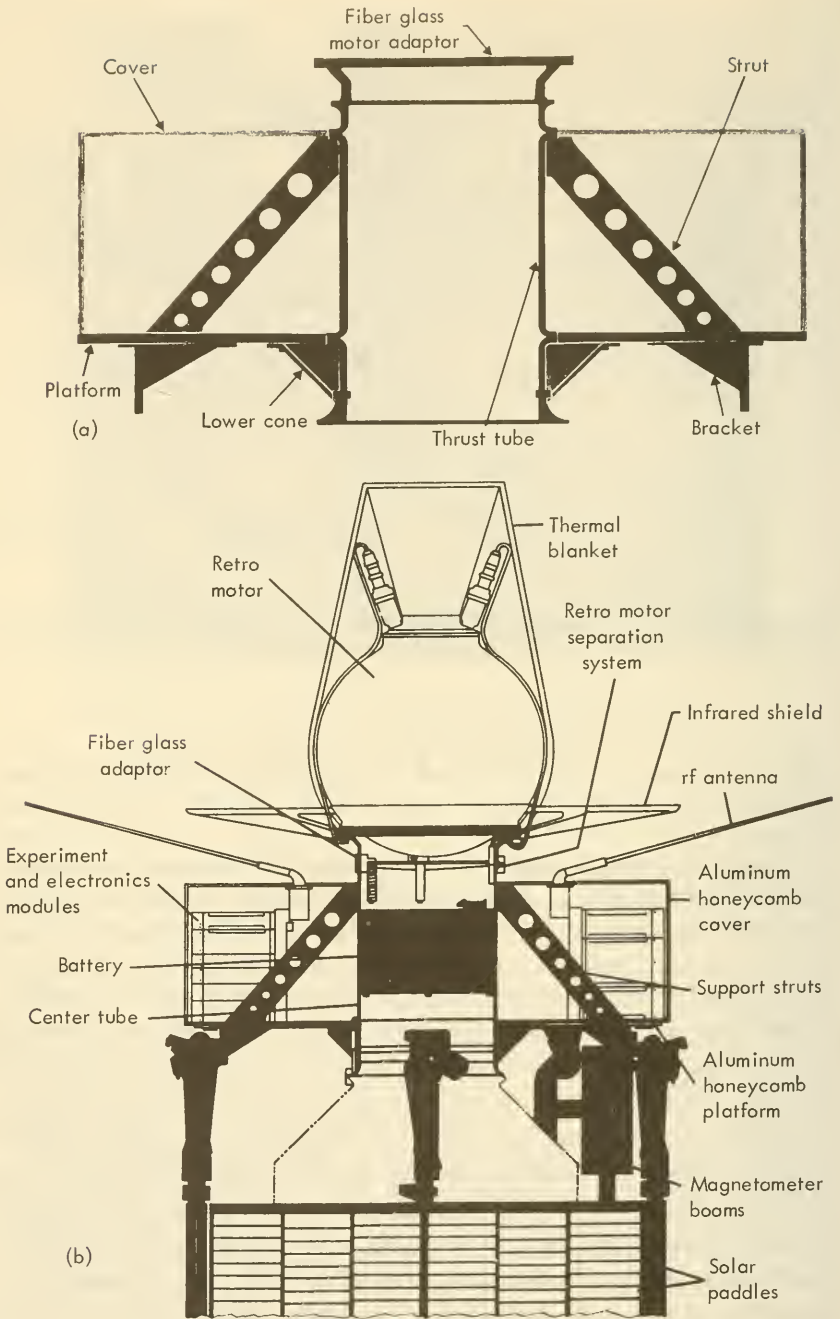
FIGURE 9–87.—The Anchored IMP structure: (a) thrust tube, platform, and struts; (b) the complete structure (ref. 32).

A good many satellites that appear to be polygonal cylinders, truncated cones, and the like really hide load-bearing cylinders under their external skins and facets. Cylinders are simple to manufacture and make admirable skeletons for spin-stabilized satellites. OV 3, for example, has a cylindrical thrust tube, upon which are mounted an instrument platform and the skins that give the external octagonal appearance (fig. 9–83). UK 3 has a similar internal structure, though its external appearance is quite different from OV 3 (fig. 9–84). The Anchored IMP, too, depends upon a cylinder for its basic strength (fig. 9–87).

Another popular skeleton is the polygonal-cylinder framework or shell illustrated in figure 9–88 for OSO. Polygonal cylinders
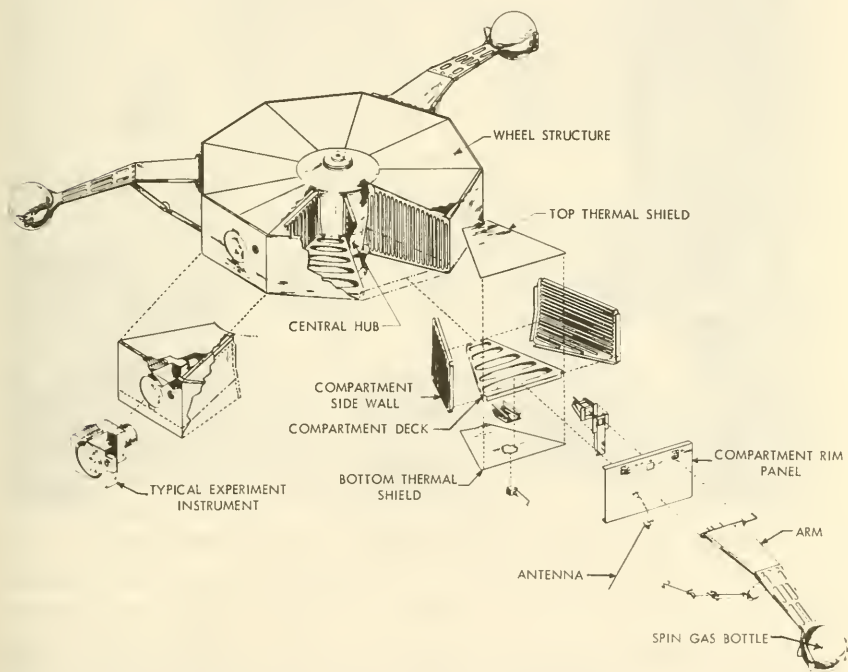
FIGURE 9–88.—Major features of the OSO wheel structure.

are convenient structures for spin-stabilized satellites: there is an obvious spin axis, surrounded by symmetrical equipment bays. Explorer XVIII illustrates the rather common practice of mounting permanent magnetometer superstructures along the spin axis (fig. A–17).
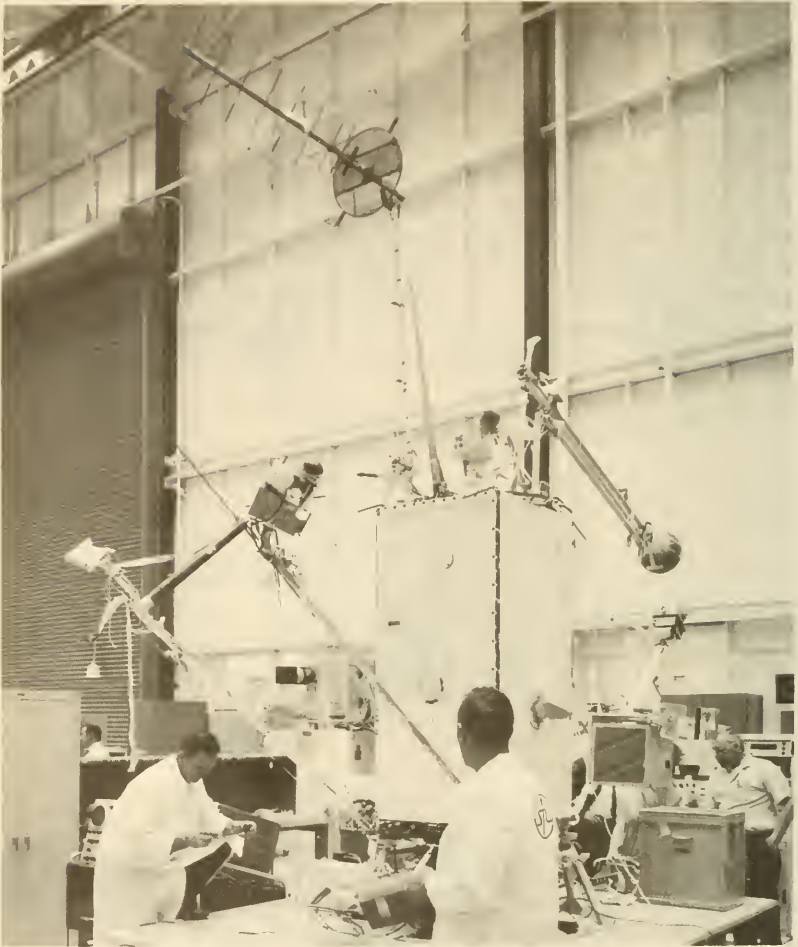
FIGURE 9–89.—The OGO's have a boxlike structure.
(Courtesy of TRW Systems.)

Some piggyback satellites, which do not depend upon spin stabilization, have adopted frameworks whose struts form the edges of tetrahedrons, cubes, octahedrons, and so on. Examples are: the TRS, Oscar, Secor, and ORS series. Solar cells are mounted on all of the faces of the polyhedral satellites, for they can assume any orientation with respect to the Sun.[11] Internal equipment is mounted on the struts. OGO is also a polyhedron— more specifically, a rectangular parallelepiped (fig. 9–89). OGO's

[11] Oscar, a cubic structure, was battery powered.

structural strength is not in a framework of struts, as it is in the small polyhedrons, but rather in skins that are fastened together to make the boxlike main body of the satellite.

Biosatellite and all recoverable scientific satellites boast a unique structure: the reentry capsule (fig. 2–7). The structure that must bear the mechanical and thermal loads during reentry is blunt shaped, with a conical cast. Ablative reentry structures are now fairly standard in space technology. Made from materials like phenolic nylon, they char upon heating and in the process evolve gases that protect the spacecraft and carry away aerodynamic heat.

9–12. The Engineering-Instrument Subsystem

Part of the telemetry data received from scientific satellites is diagnostic in character; that is, it monitors the status of the spacecraft. The fraction of telemetry time devoted to engineering data varies widely from satellite to satellite. On well-proven spacecraft, less than 10 percent of the telemetry will be devoted to status. New satellite designs and satellites in the Observatory class may transmit several times this amount. One of the features of the larger satellites is a variable telemetry format, which permits the ground operator to call for a higher proportion of status data when operational difficulties arise. In other words, more status data allow the operator to "drive" the satellite better and diagnose malfunctions.

What status data should be telemetered? Generally, temperatures, voltages, currents, and switch positions are indicative of spacecraft health. These quantities are simple to measure, usually ending up as a voltage level, probably in digital form, that is telemetered to Earth. Pressure, frequency, angle, light intensity, and similar parameters are sometimes telemetered. Specific examples seem appropriate here. Table 9–18 lists the engineering parameters telemetered from Explorer XVIII and OV–3–1. Note below that Explorer XVIII telemetered no switch positions, while OV–3–1 telemetry was heavy with switch data.
In Explorer XVIII, one telemetry word out of 16 conveyed status information.

Engineering instruments (and scientific instruments as well) are generally asked to provide signals that carry information in terms of voltage level. Battery voltages and reference voltages pose no problem. The positions of switches can be easily telemetered by telemetering a reference voltage if they are closed and nothing if open. Temperature is a more difficult parameter. Con-

TABLE 9–18.—*Typical Engineering Data Points From Scientific Satellites*

Explorer XVIII (IMP I)	OV–3–1
Battery voltage	Command-receiver case temperature.
+50-volt regulated voltage	Battery temperature.
Battery-charge current	Plasma-probe boom switch.
Satellite-load current	Magnetometer-boom switch.
Top-cover skin temperature	Solar-panel temperature.
Rb-gas-cell temperature	Structure temperature.
Battery temperature	Yo-yo deployment switch.
+12-volt regulated voltage	Power-bus voltage.
Solar-paddle current	Solar-panel current.
Solar-paddle temperature	Battery current.
Skin temperature at side of top cover.	Command-receiver automatic-gain-control voltage.
Skin temperature at spring seat	Satellite low-voltage monitor.
Rb-lamp temperature	Command-logic status.
Prime-converter temperature	Master-pulse reference voltage.
Transmitter temperature	Ground-reference voltage.
Frame identification	100 percent reference voltage.

ventional thermocouple probes require amplifiers and a reference junction. Wire probes, thermistors, and semiconductor probes are more suitable. The semiconductor temperature probes are popular and yield a voltage proportional to temperature. The magnitude of an electrical current can be converted into a voltage level by inserting a resistor in the line or running the line through a magnetically coupled current sensor. The latter sensors do not introduce components into the measured circuit but are relatively complex, requiring magnetic amplifiers and an inverter. As Part III of this book will show, almost any physical parameter can be measured with a sensor that yields a voltage proportional to the parameter.

The final satellite subsystem, the scientific instrumentation, is described in detail in Part III of this book.

References

1. LUDWIG, G. H.: Relative Advantages of Small and Observatory-Type Satellites. NASA TM X–55243, 1965. (Also paper at the 6th COSPAR meeting, 1965.)
2. ADAMS, J. L.: Space Technology, vol. 2, Spacecraft Mechanical Engineering. NASA SP–66, 1965.

3. KORVIN, W.; AND JACKSON, R. B.: Antennas for Space Vehicles. Space/Aero., vol. 42, Nov. 1964, p. 60.

4. D'AIUTOLO, C. T., ED.: The Micrometeoroid Satellite Explorer XIII (1961 Chi). NASA TN D–2468, 1964.

5. BUTLER, P.: The IMP–I (Explorer XVIII) Satellite. Record of the 1964 International Space Electronics Symposium, IEEE, New York, 1964.

6. BOMBERGER, D. C., ET AL.: The Spacecraft Power Supply System. Bell System Tech. J., vol. 42, July 1963, p. 943.

7. SAINT-JEAN, B. J.: Theoretical Considerations for Preliminary Design of a Solar Cell Generator on a Satellite. NASA TN D–1904, 1963.

8. CHERRY, W. R.; AND ZOUTENDYK, J. A.: The State of the Art in Solar Cell Arrays for Space Electrical Power. AIAA paper 64–738, 1964.

9. FISCHELL, R. E.: Solar Cell Performance in the Artificial Radiation Belt. AIAA J., vol. 1, Jan. 1963, p. 242.

10. OSGOOD, C. C.; AND WINKLER, S. H.: Optimizing the Design of a Solar Power Supply System. Adv. Astronaut. Sci., vol. 6, 1960, p. 607.

11. HIBBEN, R. D.: Improved Solar Cells Planned for IMP–D. Av. Wk., July 26, 1965, p. 53.

12. MASSIE, L. D.: Advanced Solar Cells. Space/Aero., vol. 42, Sept. 1964, p. 60.

13. CORLISS, W. R.; AND HARVEY, D. J.: Radioisotopic Power Generation. Prentice-Hall, Inc., 1964.

14. SERAFINI, V. R.; FRIEDMAN, J.; AND KUHLMANN, E. J.: Engines for Spacecraft. Space/Aero., vol. 42, Dec. 1964, p. 56.

15. ROMAINE, O.: Secondary Rockets. Space/Aero., vol. 39, May 1963, p. 83.

16. WOESTEMEYER, F. B.: General Considerations in the Selection of Attitude Control Systems. In Proc. of the Aerospace Vehicle Flight Control Conf., 1965.

17. SUTHERLAND, G. S.; AND MAES, M. E.: A Review of Micro-Rocket Technology: 10^{-6} to 1-lb Thrust. AIAA paper 65–620, 1965. (Also published in J. Spacecraft and Rockets, vol. 3, Aug. 1966, p. 1153.)

18. MARTINEZ, J. S.: Isotopic Propulsion. Space/Aero., vol. 42, Nov. 1964, p. 77.

19. MOBLEY, F. F.: Attitude Control System for the Atmosphere Explorer B Satellite. AIAA paper 65–432, 1965.

20. HELLER, G.: Problems Concerning the Thermal Design of Explorer Satellites. IRE Trans., MIL–4, 1960, p. 98.

21. SCHACH, M.; AND KIDWELL, R.: Thermal Control of Spacecraft. Space/Aero., vol. 44, July 1965, p. 55.

22. MCADAMS, W. H.: Heat Transmission. McGraw-Hill Book Co., Inc., 1954.

23. WOERNER, C. V.; AND KEATING, G. M.: Temperature Control of the Explorer IX Satellite. NASA TN D–1369, 1962.

24. HASTINGS, E. C.; TURNER, R. E.; AND SPEEGLE, K. C.: Thermal Design of Explorer XIII Micrometeoroid Satellite. NASA TN D–1001, 1962.

25. HEMMERDINGER, L. H.: Thermal Design of the Orbiting Astronomical Observatory. J. Spacecraft Rockets, vol. 1, Sept.–Oct. 1964, p. 477.

26. SLATER, J. M.; AND AUSMAN, J. S.: Inertial and Optical Sensors. In Guidance and Control of Aerospace Vehicles, C. T. Leondes, ed., McGraw-Hill Book Co., Inc., 1963.

27. ALBUS, J. S.: Digital Solar-Aspect Sensors. Astronautics, vol. 7, Jan. 1962, p. 30. (Also NASA TN D–1062, 1961.)

28. SCULL, J. R.: The Application of Optical Sensors for Lunar and Planetary Space Vehicles. JPL TR 32-274, 1962.

29. BURN, J. W.: Electro-Optical Design of Horizon Sensors. *In* Technical Papers, 11th Annual East Coast Conference on Aerospace and Navigational Electronics. Western Periodicals (North Hollywood), 1964.

30. KOELLE, H. H., ED.: Handbook of Astronautical Engineering. McGraw-Hill Book Co., Inc., 1961.

31. BLONSTEIN, J. L.: Engineering and Test Problems on the UK 3 Satellite. Raumfahrtforschung, vol. 8, Oct.–Dec. 1964, p. 170.

32. MADEY, J. M.; AND BAUMANN, R. C.: Structures for Small Scientific Satellites. NASA X–670–65–279, 1965.

Part III

SCIENTIFIC INSTRUMENTS

Chapter 10

SATELLITE SCIENCE—AN OVERALL VIEW

10-1. Scope and Organization of Part III: Scientific Instrumentation

In chapter 1, the scientific satellite was extolled as an instrument platform par excellence, carrying sensors beyond the Earth's atmosphere into space. The advantages gained by transporting scientific sensors into orbit have had profound effects upon the disciplines of geophysics, solar physics, astronomy, biology, and cosmology. Part III of this book focuses on the thousands of satellite-borne instruments that have stimulated interest and growth in these fields.

Geophysics has been the main beneficiary of satellite science. Fully three-quarters of all satellite instruments probe the radiation belts, the geomagnetic field, and other "local" phenomena. Chapter 11 describes the operating principles of the major satellite geophysical instruments; it is necessarily a very long chapter. Solar physics, by virtue of the strong interaction between the Sun's emanations and the Earth's mantle of gases, plasmas, and force fields, is the second-most-active research area. (See ch. 12.) Satellite experiments in astronomy, cosmology, and biology are covered in chapters 13 and 14.

As scientists become overwhelmed by thousands of magnetic tapes filled with geophysical data, a shift of experimental effort away from geophysics might be anticipated. Two facts impede such a trend. First, many of the desired astronomical and biological experiments are complex and will have to wait until manned-orbiting laboratories are operational. Geophysics, in contrast, does not have to wait for such developments. Second, the geophysical environment is endlessly varying and far from understood in detail. Small, unmanned scientific satellites will

be launched in increasing numbers—like weather balloons and sounding rockets—to sample the Earth's environment on a synoptic basis. In short, unmanned satellites will probably tend to concentrate on near-Earth phenomena, while manned-space laboratories study the Sun, the stars, and the behavior of life in space.

Chapter 1 emphasized the fact that almost all satellites carry scientific instruments, regardless of their main mission. Military satellites (Discoverers, Transits), applications satellites (Syncoms, the Tiros series), and technology satellites have all added to our fund of scientific data. Although this book does not cover satellites in these categories, the instruments and techniques described in the following chapters are universal. A Tiros photometer, for example, does not differ substantially from a Solrad photometer.

So many instruments have been flown on scientific satellites— more than 1500 to date—that the remaining chapters might easily turn into a mere recapitulation of more than 1500 experiments. Actually, such a summation has already been completed under a NASA contract (ref. 1). The approach here is to describe operating principles and the problems of spacecraft integration, giving specific instrument examples as needed.

10-2.   The Sensors, Instruments, and Experiments

Three similar terms must be defined at the outset:

(1) The "sensor" is a detector of some physical phenomenon. A Geiger tube senses the passage of a charged particle. A cadmium-sulfide cell senses light through holes made by micrometeoroids. Sensors convert natural stimuli into signals (usually electrical) that can be transmitted to the scientist by the spacecraft communications subsystem.

(2) The "instrument" includes one or more sensors, possibly even different sensors, as well as such devices as lenses, supports, radiation shields, scanning platforms, pulse-height analyzers, and auxiliary equipment needed to match interfaces with the rest of the satellite. Sensors detect phenomena, while instruments convert sensor signals into meaningful data words at the proper rate and in the correct format.

(3) The total "experiment" involves such things as instrument calibration; experiment synchronization with other experiments; experiment flexibility and dynamic range; data reduction and interpretation (most important); and the final publication of results. The experiment thus transcends hardware and encom-

passes responsibilities to the scientific community and the organization supplying the funds.

In the light of these definitions, the instrument is the specific, identifiable piece of hardware. Sensors, in contrast, are less specific; for instance, cadmium-sulfide cells can be used in both radiation and micrometeoroid instrumentation. On the other hand, experiments possess all the extra dimensions cited above. In the hardware stage, discussion converges on instruments; whereas one talks of experiments when satellites are being planned. Since this book is hardware oriented, instruments will be highlighted.

Satellite instruments generally resemble terrestrial instruments, where terrestrial counterparts exist, except for weight, volume, power consumption, ruggedness, the enhancement of reliability through redundancy and superior construction practices. Many instruments originally designed for terrestrial applications have been gradually modified during the ever-more-demanding succession of high-altitude balloons; sounding rockets; and, finally, satellites. The transformation of cosmic-ray telescopes into flight hardware, for example, has transpired over a period of 30 years. The evolution of micrometeoroid detectors and plasma electrostatic analyzers has been much more rapid, but the terrestrial roots of the family trees are easily recognized.

Space instruments must meet an imposing list of special requirements and limitations:

(1) Remote calibration is desirable

(2) The capacity for internal storage of data is limited

(3) Magnetic materials must be minimized

(4) Weight, volume, and electric power are in short supply

(5) Instruments must operate in a vacuum, or, rarely, in a hermetically sealed container

(6) The operating temperature range must be compatible with the range predicted for the satellite

(7) The instrument must be rugged enough to withstand the vibration and shock of launch

(8) Signals must be conditioned and delivered to the communications subsystem at the right moment and in the proper format

(9) Instruments must operate reliably with a minimum of manipulation and no maintenance at all

(10) Life-detection payloads must survive sterilization procedures

Specialized papers on instrument design and development are relatively rare, in contrast to the abundance of literature referred

to in parts I and II. The written word emphasizes the spacecraft and the scientific results, not the instruments that make the measurements. Surveys of satellite instruments are uncommon (refs. 2, 3).

The scientific literature is neither precise nor consistent in naming satellite instruments and sensors. A Geiger-Müller counter may be readily recognized when called a GM tube or a Geiger counter, but it is frequently hidden under more general appellations, such as "trapped-radiation detector" and "cosmic-ray telescope," in cases where it serves as a sensor in a larger instrument. Comparatively new instruments may be given seemingly unrelated names. The curved-surface electrostatic analyzer, for example, is sometimes called a plasma probe or plasma spectrometer. A photometer passing 1216 Å becomes a Lyman-α detector. In other words, instrument names often depend upon the application and the range of the phenomenon being investigated; viz, infrared, ultraviolet, and X-ray.

Table 10–1 represents an effort to organize instrument terminology and, at the same time, impress the reader with the great variety of instruments used in satellite research. The organization of table 10–1 parallels the organization of chapters 11 through 14. (One notes in table 10–1 that the satellite itself and its beacon signals are essential to many experiments in aeronomy and geodesy.)

TABLE 10–1.—*List of Instruments and Experiments in Satellite Science*

Geophysical Instruments and Experiments (See Ch. 11)

Aeronomy instruments and experiments (see table 11–1):

Satellites plus Earth-based observers	Neutral mass spectrometers
Accelerometers	Radiometers and photometers
Ram-pressure gages	Spectrometers (dispersive)
Ionization gages	Star trackers and measurement of stellar refraction

Instruments and experiments for ionospheric physics (see table 11–5):

Satellite transmitters plus Earth-based observers	Standing-wave impedance probes
Satellite-to-satellite propagation experiments	rf impedance probes
Topside-sounder experiments	Langmuir probes
Passive radio-receiver experiments	Planar ion traps
Electric-field meters	Spherical ion traps
	Ion mass spectrometers

Instruments and experiments in the trapped radiation zone (see table 11–8):

Geiger counters	Ionization chambers
Proportional counters	Channel multipliers

TABLE 10–1.—*List of Instruments and Experiments in Satellite Science*—Continued

Instruments and experiments in the trapped radiation zone (see table 11–8) — Continued

Scintillators	Faraday-cup probes
Cerenkov detectors	Electrostatic analyzers
Cadmium-sulfide cells	Ionization chambers, plus Geiger
Solid-state detectors	counters
Current collectors	Emulsions
Telescopes (various types)	Spark chambers
Magnetic spectrometers	Scintillation chambers

Satellite magnetometers (see table 11–11):

Search-coil magnetometers	Alkali-vapor magnetometers
Fluxgate magnetometers	Helium magnetometers
Proton-precession magnetometers	

Instruments and experiments for measuring micrometeoroids (see table 11–14):

Piezoelectric detectors	Wire-grid detectors
Capacitor detectors	Light-transmission-erosion detectors
Light-flash detectors	Time-of-flight experiments
Pressurized cells	

Solar Physics Instruments and Experiments (See Ch. 12)

Instruments and experiments for the analysis of the solar electromagnetic flux (see table 12–3):

Filter photometers	Spectroheliographs
Spectrophotometers (nondispersive)	Coronagraphs
Dispersive spectrometers and spectrophotometers	Radiation counters

Instruments and experiments for the analysis of the solar wind (see table 12–7):

Faraday-cup plasma probes	Curved-surface electrostatic analyzers

Instruments and Experiments for Satellite Astronomy (See Ch. 13)

Instruments and experiments used in observational astronomy (see table 13–1):

Spectrometers and spectrophotometers	OAO experiment packages and astronomical satellites
Radio-astronomy experiments	

Cosmic-ray instruments and experiments (see table 13–4):

Basic detectors (e.g., ionization chambers)	Solid-state telescopes
Geiger-counter telescopes	Scintillator E-versus-dE/dx telescopes
Proportional-counter telescopes	Spark chambers
Cerenkov-scintillator telescopes	

Biological Experiments for Scientific Satellites (See Ch. 14)

Weightlessness and zero-g experiments (see table 14–1)
Weightlessness-radiation experiments (see table 14–2)
Biological-rhythm experiments
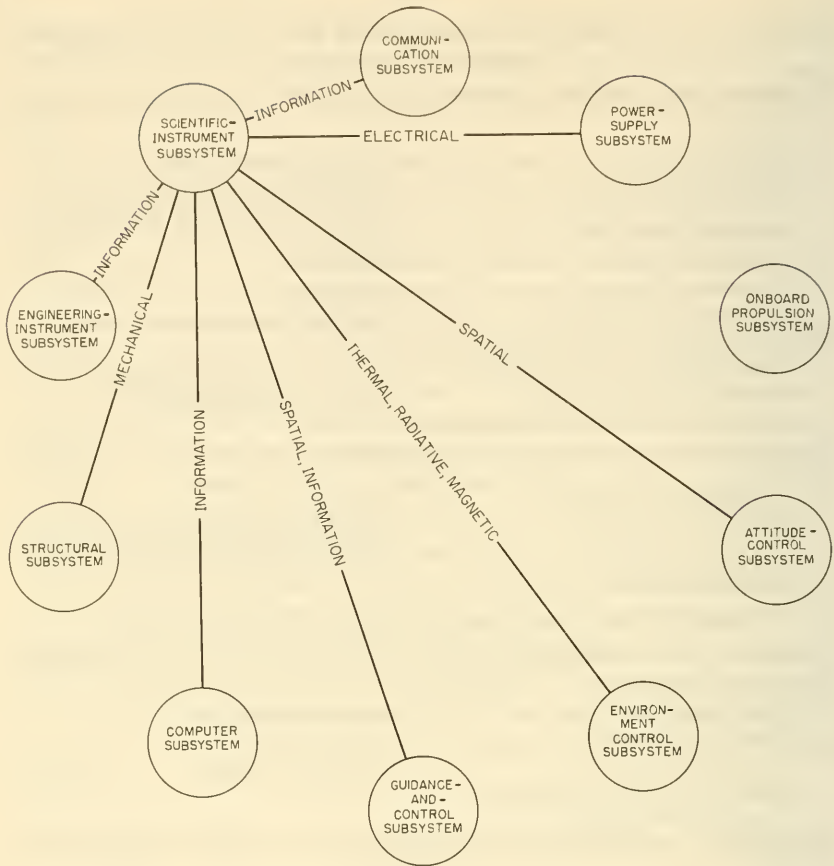
FIGURE 10–1.—Portion of the spacecraft-interface diagram showing the relationship of the scientific instrumentation to the rest of the subsystems.

10–3. Experiment Design and Integration

In this book, the scientific instruments are treated collectively as a satellite subsystem. The interface diagram showing the major links with the rest of the spacecraft subsystems is presented in figure 10–1. Scientific instruments "see" the nine other subsystems across the nine different kinds of interfaces introduced in parts I and II:

Mechanical	Electrical	Information
Thermal	Radiative	Electromagnetic
Spatial	Magnetic	Biological

The subsystem and interface definitions in chapter 3 should be reviewed at this point. As before, the discussion will be molded by the formal satellite model built from the 10 subsystems and their interlocking interfaces.

A properly designed experiment should result in a properly integrated experiment, because the experiment's interfaces should shape the design philosophy. First, let us examine the technical and management features of experiment design.

Experiment Design Philosophy.—An instrument design is manifestly "good" if it successfully passes the qualification and flight-acceptance tests described in chapter 7 and obtains valid data in orbit. Good instrument design is difficult to codify, however, and is even more of an art than satellite design. Nevertheless, an instrument design philosophy can be set down rather crudely as a set of guidelines, a list of do's and don'ts that deal with such practical problems as bad solder connections.[1] The guidelines that follow were established by NASA for IMP experimenters, and are presented here to illustrate the kinds of instrument design problems encountered in satellite research.

(1) All low-level signals should be run coaxially into the experiment to reduce stray fields

(2) Power leads should be twisted and, if they are adjacent to sensitive lines, shielded as well

(3) Power converters or oscillators should not be placed near sensors or sensitive electronics

(4) Parasitic oscillations should be eliminated up to 200 megacycles

(5) Conductors above 350 volts should be insulated or potted so that air cannot come in contact with the conductors

(6) Insulations must minimize outgassing, weight, and sensitivity to space radiation

(7) Magnetic materials should be avoided

(8) All wires entering the experiment must be filtered at the interface to eliminate rf crosstalk

(9) All wire connections should be made in a way that does not create strains in the wires

(10) Wire insulation should terminate as close as possible to the solder pot

(11) Solder pots should be filled and wire pretinned before soldering to insure strong joints

(12) Only thermal wire strippers should be used

(13) Wires should be redundant in critical functions

---

[1] See section 9–3 for overall spacecraft design philosophy.

The IMP's are highly integrated Explorer-class satellites. Many of the interface problems implied above shrink or vanish in the standardized environment of larger, Observatory-class satellites. Instrument design philosophy then becomes simpler. On a piggyback satellite, by way of comparison, the main concern may be noninterference with the primary mission—a fact leading to an altogether different design philosophy.

Dynamic range and flexibility enter an experimenter's thinking early and help shape design philosophy. A wide dynamic range may be desirable to insure bracketing the phenomenon being studied and encompass unexpected but possible events, such as the eruption of a very large solar flare. On the other hand, a wide dynamic range means long data words. To illustrate, a magnetometer with a dynamic range of 10^4 (0.1 γ to 1000 γ) may be limited by a word length of only 8 bits to an overall dynamic range of 256. This illustration shows vividly the intimate relationship between instrument design and satellite design. It also leads to the problem of coordinating the instrument designer with the satellite designer.

Experiment Management.—When an experimenter and experiment are selected for a satellite, the award carries responsibilities. The duties of an ''experimenter'' are:

(1) Defining the experiment and the functional requirements of the instrument(s)

(2) Assuring that an adequate research program minimizes the possibility of ambiguous interpretation of the data

(3) Organizing the efforts of, assigning tasks to, and guiding the other members of his team

(4) Timely processing, analysis, and publication of experimental results

In addition, an investigator is responsible for—

(1) Assuring that the design and construction of the instrumentation, its development, and its test program are appropriate to the experiment objectives, and reflect properly the environmental and interface constraints under which the instrumentation must operate

(2) Assuring that adequate calibrations are made through the entire period of data acquisition

(3) Participating in the operational phase of the mission as may be required

A satellite experiment is only one cog in a complex system stretching from the sensors back to Earth and, eventually, to those scientists who read about it in the scientific literature.

In addition, experiment design usually proceeds in accordance with the following kinds of management documents:

Functional specifications	Test specifications
Design specifications	Flight schedules
Interface specifications	Cost allocations

TABLE 10–2.—*Typical Schedule of Experiment Commitments* [a]

Event	Approximate time, months	Remarks
Electrical-interface information.	0	Interface documents for all electrical connections and electronic signals to and from the spacecraft and to and from experiment instrumentation physically separated from the main unit.
Mechanical-interface information.	2	Includes interface requirements for all structural connections between the instrument and the spacecraft, with an overall layout of the external configuration of the instrument.
Checkout and test procedures and equipment information.	9	Includes requirements and procedures for checkout on instrument on the bench and in the spacecraft.
Bench tests and structural fit in the spacecraft.	12–13	Includes bench tests with the spacecraft telemetry subsystem and structural fit of the instrument in the spacecraft.
Delivery of the instrument.	18	All flight instruments and all checkout equipment delivered.
Launch_____	24	

[a] For an OSO, a highly integrated satellite. Small satellites, such as the SSS, may have faster reaction times—say, a few months—a great advantage where rapid feedback is needed for advancing instrument design and where natural phenomena call for a quick reaction time. Abstracted from *Experimenter's Manual for the OSO.*

A few of these essential controls are illustrated by table 10–2 and the following slightly edited excerpts from the *Experimenter's Manual for the OSO.*

All experiment-spacecraft interfaces are negotiated with the OSO Project Office and are documented with engineering drawings exchanged between the experimenter, the Project Office, and the spacecraft contractor. Note carefully: Any change desired by experimenters in the objectives of their experiments must have prior approval by NASA.

GSFC [2] requires that each experimenter provide a certification to GSFC at

[2] Goddard Space Flight Center, Greenbelt, Md.

the time of delivery of experiments to the spacecraft contractor to the effect that flight model and flight spare experiments are qualified for flight on the spacecraft as specified in this manual. A similar certification of prototype experiment is required prior to delivery of flight experiments to document that the experiment has passed specified prototype qualification tests as detailed in this manual.

The OSO experiment test specifications included the following categories of information:

Experiment description (e.g., drawings)
Data format (e.g., word length)
Experiment handling and safety precautions
Ground-support equipment
Experiment operation and checkout

These samplings further illustrate that experiment design for satellite flight is an exacting task. The great value of data taken in orbit are usually well worth the effort.

10–4.   Experiment Selection

Satellites can accommodate only a limited number of experiments on any particular flight. The selection of those that are finally propelled into space is beset with technical and logical problems. If it is hard to agree upon a single, overall figure of merit for an entire spacecraft, it is more difficult to rank scientific experiments in order of desirability. Nevertheless, decisions must be made, and, lacking universally accepted measures of excellence, scientific and engineering judgment must be applied to the task.

The philosophy that has guided NASA payload assignments has been that of open competition for payload space. Choice of payloads has followed one of two paths. One is competition by individual experiments for a position on a spacecraft. In general, NASA has used this method. The other is competition between (or among) groups for the entire payload of a spacecraft. This calls for "block allocation" of the payload space to a group that has successfully competed for an entire satellite. Following this procedure NASA has, for instance, assigned the entire Owl satellite to Rice University. Either method of selecting experiments has employed the same review processes in NASA for evaluation of the experiments. Selection of individual experiments by open competition gives everyone with a good idea a chance for payload space for his experiment. Selection of groups of experiments to fill an entire satellite, or block allocation, permits a group of investigators to study a phenomenon in depth with several instru-

ments. The Owl, for example, is aimed at a better understanding of the auroras.

Since an instrument's flight performance is critical to the success of the entire mission, new instruments are frequently tested out on sounding rockets before they are assigned satellite space. In this way, an experiment can be checked out realistically and economically.

When a scientific satellite program has been approved, NASA solicits the scientific community for experiment proposals. Once proposals have been received, the following factors enter the selection process:

(1) *Scientific Merit.*—The scientific contributions likely to be made and the appropriateness of the experiment to the mission at hand are important.

(2) *Experiment Design.*—Here are considered technical feasibility, reliability, weight, cost, instrument availability, and ease of satellite integration. A vital question is whether the experiment, as designed, will answer the scientific questions that have been posed.

(3) *Experimenter's Qualifications.*—The competence already shown by the proposed principal investigator is reviewed. His experience in terrestrial and space research is examined.

(4) *The Experimenter's Institution.*—The organization employing the experimenter is scrutinized. What is its attitude toward research; does it support its researchers?

The evaluation of experiment proposals is carried out with the assistance of the various subcommittees of outstanding scientists of the NASA Space Science Steering Committee. For any given satellite, as many as 50 proposals of widely varying character may be under consideration. The proposed experiments naturally fall into several groups:

(1) Those with good science

(2) Those with good science but needing further instrument development before flight

(3) Those not acceptable

Study and evaluation reduce the number of proposals under consideration to those that can be accommodated on the satellite. The time is roughly 2 years before flight. Each of the remaining experiments usually needs further research and development, often up to the point where all components can be assembled for testing; i.e., the "breadboard" stage.

After about a year of development, the originally selected experiments will need to be reconsidered. It is now about 1 year

before flight, and the satellite itself and the surviving experiments are better defined and understood. The final experimental payload is chosen at about this time. Provision for further eliminations may be made in case unexpected spacecraft design problems arise. One or two backup experiments may also be carried along to replace experiments that run into trouble on this final lap.

The subcommittees assisting in the selection are appointed from scientists in NASA, other Government agencies, the universities, and not-for-profit organizations. The subcommittees are discipline oriented:

Astronomy	Particles and Fields
Solar Physics	Planetology
Planetary Atmospheres	Bioscience
Ionospheres and Radio Physics	

In summary, a well-defined procedure for judging spacecraft experiment proposals exists within NASA. Excellence is always sought, and opportunity is there for good experimental ideas.

In addition to NASA, the Department of Defense supports some satellite research. The Air Force, through its Office of Aerospace Research (OAR), provides launch vehicles, funds, and ground-based equipment for investigating phenomena pertinent to Air Force objectives. Experiment choice is influenced by:

(1) The experiment's importance to Air Force missions
(2) The availability of a suitable launch vehicle

In general, the selection criteria parallel those used by NASA. In connnection with the first item, however, one would not expect the Air Force to be as interested in astronomy as in geophysics; i.e., the environment in which it must operate its vehicles. The second item is also revealing, because most Air Force research is carried out with piggyback satellites, where science is secondary to military objectives.

References

1. RICHTER, H. L., JR., ED.: Space Measurements Survey, Instruments and Spacecraft. NASA SP–3028, 1966.
2. LINDNER, J. W.: Experimental Techniques Employed in Space Physics. *In* Space Physics, D. P. LeGalley and A. Rosen, eds., John Wiley & Sons, Inc., 1964.
3. SONETT, C. P.: Experimental Physics Using Space Vehicles. *In* Advances in Space Science, vol. 2, F. I. Ordway, ed., Academic Press, 1960.

Chapter 11

GEOPHYSICAL INSTRUMENTS AND EXPERIMENTS

11-1. Prolog

The discipline of geophysics embraces all of the natural and artificially stimulated phenomena that transpire in the region stretching from the center of the Earth's core to the outer boundary of the magnetosphere. Geophysics seeks to quantify scientific subdisciplines that are as diverse as seismology, oceanography, and atmospheric physics. Patently, scientific satellites cannot contribute data to all of geophysics, though their range of utility is striking. Six areas of satellite geophysical instrumentation have been selected for description in this book:

Aeronomy (sec. 11–2)	Geomagnetism (sec. 11–5)
Ionospheric Physics (sec. 11–3)	Geodesy (sec. 11–6)
Trapped Radiation (sec. 11–4)	Meteoritics (sec. 11–7)

Even with the remarkable span of phenomena included within the above disciplines, several well-known areas of satellite science are omitted:

(1) Satellite meteorology, which arbitrarily has been assigned to the so-called applications satellites defined in chapter 1. Included here are infrared heat-budget studies and the French EOLE experiment, which employs a satellite to relay data from balloons in the atmosphere.

(2) Satellite geology, where satellites help distinguish large-scale terrestrial formations, such as huge, heavily weathered meteor craters, and identify mineral deposits through spectroscopy of reflected sunlight.

(3) Satellite oceanography, in which satellite-borne thermal-radiation sensors can chart the flow of warm and cold currents. Satellite relay of data from oceanographic buoys is also omitted.

Both satellite geology and oceanography are still in the speculative stage. Weather satellites are, of course, an integral part of our global array of meteorological sensors.

The instruments and experiments employed in satellite geophysics are as varied as the subdisciplines: viz, ionization gages, mass spectrometers, Geiger counters, photometers, and microphones. For complete lists of the instruments and experiments covered in this chapter, see the summary tables near the beginning of each section.

Balloons and sounding rockets have long penetrated the lower edges of the region now being explored by satellites. Satellite instrumentation therefore had a substantial foundation to build upon. Most satellite instruments, in fact, have been proven out first in balloons and rockets. This instrumental foundation has also been bolstered by many flights on military and applications satellites (particularly the Tiros series) and Air Force satellites. Geophysical instrumentation, consequently, is relatively well developed compared to the instruments introduced in the other chapters in part III.

11–2. Aeronomy Instruments and Experiments

The first Earth satellites decayed far more rapidly than scientists expected on the basis of rocket and balloon soundings of the upper atmosphere. Careful observations of satellites soon demonstrated that the Earth's upper atmosphere is denser, more extensive, and more variable than predicted—a discovery as crucial to geophysics as the surprise of the great radiation belts. A few years after Explorer I, satellites had also demonstrated the existence of a layer of helium in the upper atmosphere (ref. 1) and the presence of a Sun-heated atmospheric bulge rotating about the Earth each day. This revolution in aeronomy is still going on.

Any satellite with a perigee below 200 kilometers is useful to aeronomy, because the progressive distortion of its orbit by atmospheric friction is indicative of average atmospheric density. The large balloon satellites, such as Explorers IX, XIX, XXIV (now called Air Density Explorers), are designed to accentuate these frictional effects. Also important to aeronomy are the direct, instantaneous measurements of the neutral [1] components of the atmosphere by accelerometers, ionization gages, and mass spec-

---

[1] Generally speaking, the word "aeronomy" refers only to the neutral portion of the upper atmosphere. The next section deals with the coexisting populations of ions and electrons that constitute the ionosphere.

trometers. The Atmosphere Explorers carry such instruments into orbit. Furthermore, the unrivaled visual vantage point of an Earth satellite permits unique observation of the airglow, the aurora, Sun-stimulated emission processes, and other optical phenomena of the upper atmosphere. The full range of satellite aeronomy instrumentation is presented in table 11–1.

A.   Observations of Earth Satellites From Earth

Satellites and Earth-Based Observers.—When a satellite intersects the upper atmosphere during its passage through perigee, friction with the atmosphere reduces the vehicle's kinetic energy. As a result, the satellite does not swing as far out on its next apogee. The height of perigee, in contrast, is affected but little. The total effect is one of orbit circularization, with a corresponding reduction in period. Since both orbit eccentricity and period are readily measured from Earth (see sec. 4–4), a basis exists for measuring frictional forces and thence density. In a sense, the satellite itself is an instrument, like a pendulum bob.

To discover how atmospheric density is related to the observed orbit parameters, the drag force, F_d, is first set down

$$F_d = \tfrac{1}{2}\rho A V_s^2 C_D$$

where

ρ = density of the atmosphere
A = satellite cross-sectional area perpendicular to V_s
V_s = satellite velocity
C_D = drag coefficient, which is about 2.2 for altitudes between 200 and 600 kilometers

At this point, it is customary to introduce an assumption about how density varies with height

$$\rho = \rho_p e^{-(R-R_p)/H} \tag{11-1}$$

where

ρ_p = the density at perigee
R = satellite height above the Earth's surface
R_p = the height of perigee above the Earth's surface
H = the *density scale height,* which is assumed to vary linearly with height

The drag force and its effects are then integrated over the perigee section of the orbit, where most of the deceleration takes place. King-Hele gives the following equation for the density, ρ_A, at a height $\tfrac{1}{2}H_p$ above the perigee height (ref. 2):

TABLE 11-1.—*Aeronomy Instruments, Experimenters, and Experiments*

Observations of Earth Satellites From the Earth [a]

OV-3-6	Narcisi, R./AFCRL	Air Force latitudinal-structure satellite.

Direct Measurements From Satellites

Accelerometers:		
San Marco 1	Broglio, L./U. Rome	Transducers measure drag-induced displacement between inner and outer spherical shells.
Ram-pressure gages:		
USAF satellite	Sharp, G. W./Lockheed	Ram air distorts ribbon, indicating ram pressure.
Ionization gages:		
AE-B	Newton, G. P./GSFC	Redhead gages.
Explorer XVII	Newton, G. P./GSFC	Bayard-Alpert and Redhead gages.
OGO II, D	Newton, G. P./GSFC	Bayard-Alpert gages.
OV-3-6	Narcisi, R./AFCRL	Redhead gages.
Sputnik 3	—/—	Bayard-Alpert gages and "magnetic manometer."
Neutral mass spectrometers:		
AE-B	Reber, C./GSFC	Magnetic. For neutral density and temperature.
Explorer XVII	Reber, C./GSFC	Two double-focusing magnetic spectrometers.
Geophysical Research Satellite	—/AFCRL	Magnetic spectrometer. H through O_2.
Michael	—/U. Mich	Quadrupole.
OGO II, D	Schaefer, E. J./U. Mich	Quadrupole; neutral and ion modes; 0-6 amu.
OV-3-6	Narcisi, R./AFCRL	Quadrupole; 1-50 amu, ions over 40 amu.
Sputnik 3	—/—	Rf mass spectrometer.
TD-2	Priester, W./U. Bonn	Density of neutral atmosphere.

[a] All visible satellites are useful, particularly the Air Density Explorer series, including Explorers IX, XIX, and XXIV.

Satellite Optical Experiments

Radiometers and photometers:

Ariel 2	Frith, R./Air Ministry	Two broadband ozone filter photometers; 2650 Å.
ESRO 1	Omholt, A./U. Oslo	Two Earth-pointing auroral filter photometers.
Injun 1, 3	O'Brien, B. J./S. U. Iowa	Airglow and auroral interference-filter photometers; 5577 Å.
OGO I, B	Mange, P. W./NRL	Ultraviolet ionization-chamber photometer to study Lyman-α scattering in geocorona and interplanetary gas.
OGO II, D	Mange, P. W./NRL	Like OGO I, C, except used to compare airglow and albedo.
OGO II, D	Blamont, J. E./U. Paris	Airglow and auroral filter photometer; 2630, 6300, 6225, 5892, 5577, 3914 Å.
OGO E	Blamont, J. E./U. Paris	Hydrogen-absorption cell for geocoronal hydrogen.
OGO E	Barth, C. A./U. Colo	Ultraviolet-filter photometer for airglow hydrogen and oxygen; 1304, 1216 Å.
OSO D	Mange, P. W./NRL	Wheel. Lyman-α ionization chamber for geocoronal hydrogen.
OV-1-5	Lovett, J. J./AFCRL	Photometers for Earth and planetary radiance; ultraviolet to millimeter region.
OV-1-10	Elliott, D./Aerospace	Nightglow filter-wheel photometer; 3914, 5577, 5735, 6300 Å, plus continuum channel.
OV-1-11	Elliott, D./Aerospace	Nadir-directed filter photometer for nightglow; 6300, 3577, 5735, 3914 Å.
Owl	O'Brien, B. J./Rice	TV to observe auroras from orbit. Various photometers.
TD-2	Blamont, J./CNRS Aeronomy Service	Photometers for O and N emissions.
UK-3	Frith, R./Meteor. Office	PM tube and scanning mirror for O_2 distribution in atmosphere.
USAF satellite	Friedman, R. M./—	Two filter photometers for Earth's ultraviolet radiance; 2500–2800 Å and 2550 Å.

TABLE 11–1.—*Aeronomy Instruments, Experimenters, and Experiments*—Continued

Satellite Optical Experiments—Continued

Dispersive spectrometers:

Ariel 2	Frith, R./Air Ministry	Ozone prism spectrometer; scanning 2500–4000 Å.
OGO II, D	Barth, C. A./U. Colo	Ultraviolet airglow spectrometer; 1100–3400 Å.
OV–1–5	Lovett, J. J./AFCRL	Spectrometers for Earth and planetary radiance.
OV–1–10	Clark, M./Aerospace	Grating spectrometer for all-sky Lyman-α survey.
OV–1–10	Hudson, R./Aerospace	Dayglow grating spectrometer; 1600–3100 Å.
OV–1–11	Pragg, A. B./Aerospace	Solar-pointed grating spectrometer with magnetic-strip photomultipliers for O_2 and O_3.
OV–1–11	Elliott, D./Aerospace	Grating spectrometer to measure Earth's ultraviolet radiance; scanning 1600–3000 Å.
USAF satellite	Block, L. C./AFCRL	Infrared interference spectrometer for Earth's radiance.

$$\rho_A = \frac{0.157\dot{T}}{\delta}\sqrt{\frac{e}{aH_p}}\left[1-2e+\tfrac{5}{2}e^2-\frac{H_p}{8ae}\left(1-10e+\frac{7H_p}{16ae}\right)\right] \quad (11\text{--}2)$$

where

$\delta = FAC_D/M$
$\dot{T}$ = the rate at which the period, T, is reduced
M = satellite mass
F = a factor between 0.9 and 1.1, which takes into account the rotation of the atmosphere
a = the semimajor axis
e = eccentricity of orbit

Equation (11–2) is intended to be used when $0.02 < e < 0.2$. Similar equations are available for other ranges of eccentricity and for an oblate atmosphere.

From equation (11–2), three undesirable features of this method may be discerned:

(1) The procedure depends upon the assumption of an exponential atmosphere.

(2) It leads to time-averaged values of density rather than instantaneous values, since $\dot{T}$, the measured variable, is determined from several successive orbits or, at the best, a large segment of a single orbit. Diurnal and long-term variations can be resolved from this technique, but fine time structure, such as transients arising from solar-flare interactions, would be averaged out.

(3) Satellite acceleration by other forces, such as solar pressure, can distort these density computations, although it is usually possible to subtract out these perturbations.

Despite these problems, much of our knowledge of upper atmosphere density has come from terrestrial observations of satellites.

King-Hele has carried the technique described above a step farther. By studying the changes of orbit inclination with time, he has computed the speed of rotation of the upper atmosphere near perigee. One can think of the satellite being carried "off course" by the moving air mass. The results from these calculations were rather startling: the upper atmosphere seems to rotate faster than the Earth itself. This departure from commonsense makes the technique suspect, but there are no obvious faults in the approach.

A practical point in favor of atmosphere sounding by orbit study is that any scientist—even an amateur—can, with simple instrumentation, study the variations of the upper atmosphere.

Explorers IX, XIX, and XXIV have been particularly useful in this work because of their large sizes (see appendix).

B.   Direct Measurements From Satellites

Accelerometers.—Atmospheric drag can be measured directly and instantaneously by an onboard satellite accelerometer. Once the effects of solar pressure have been subtracted out, the measurement of deceleration leads immediately to the drag force and density. The question is: How can the very small decelerations caused by a rarefied medium, which is a good vacuum by terrestrial standards, be measured in practice? Conventional rocket and aircraft accelerometers do not have the requisite sensitivities. An unusual approach was adopted in the design of the San Marco satellite: the whole satellite, a 70-centimeter sphere, was made into an accelerometer in order to increase cross-sectional area and sensitivity (ref. 3). The satellite exterior is formed by a
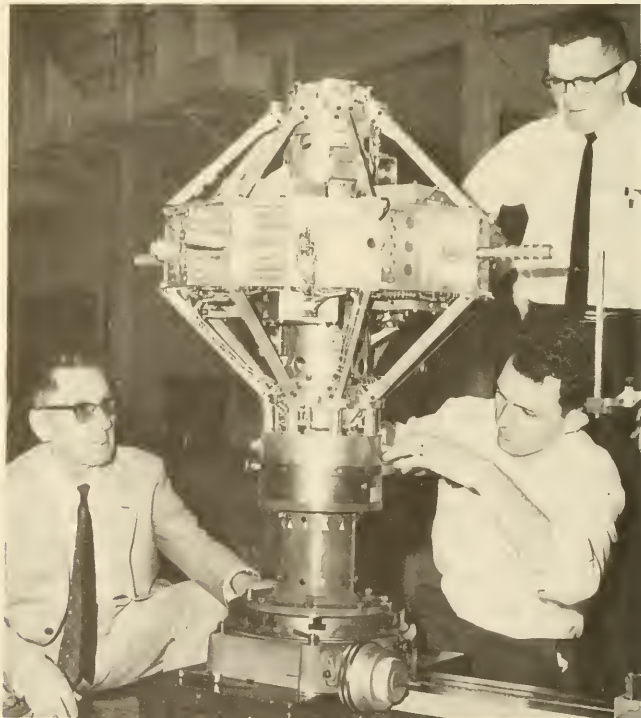
FIGURE 11–1.—The San Marco prototype, showing the accelerometer transducers jutting out radially. A spherical outer shell fits over the whole assembly.

large, lightweight, spherical shell that can move with respect to an inner, massive body, consisting of the main San Marco structure, power supply, telemetry, and so on. A set of three perpendicular pairs of springs separates the shell and inner mass (fig. 11–1). Since the rigidity of the springs is well known, any displacement due to air drag can be converted into drag force directly. The results from San Marco 1 have confirmed the validity of this technique.

Ram-Pressure Gages.—A satellite traveling at a velocity, V_s, through the tenuous upper atmosphere will encounter a ram pressure, P, over its exposed area. The equation for P must be similar in form to that written for drag force above

$$P = K\rho V_s^2 \qquad (11-3)$$

where

$K=$ an accommodation coefficient equal to $\frac{1}{2}C_D$. $K=0.5$, if the gas particles stick to the satellite surface; $K=1$, for specular reflection. Above 200 km, molecular flow is assumed, and K is taken as approximately 1.1.

If the ram pressure can be sensed, density can be determined immediately. In the ram-pressure gage, a stream of the gas is admitted to the instrument as the satellite plows through the atmosphere. Sharp flew the ram-pressure gage diagramed in
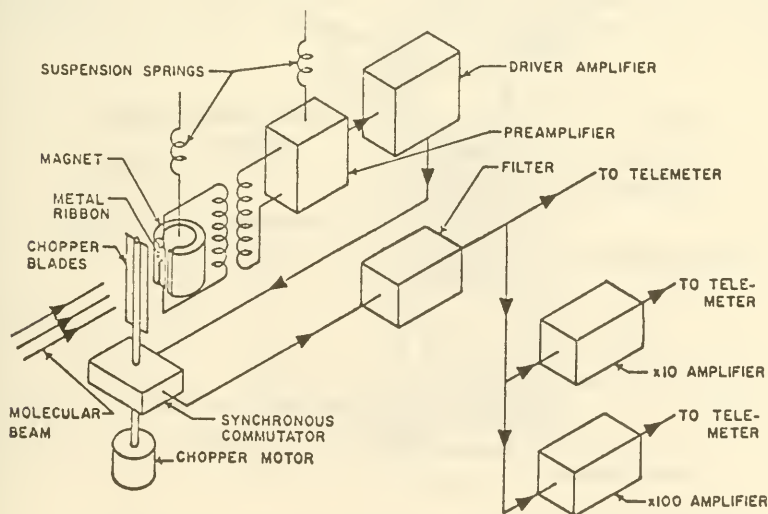
FIGURE 11–2.—Schematic representation of the ram-pressure gage. This type of instrument was flown on an Air Force satellite (ref. 4).

figure 11–2 on a military satellite in 1961 (ref. 4). Ionized particles were first electrostatically extracted from the entering stream of gas. The stream was then chopped at 200 cps by blades before encountering a ribbon microphone. The aluminum ribbon (0.0005 centimeter thick) vibrated at the chopper frequency with an amplitude proportional to the ram pressure. The electromotive force induced as the conducting ribbon cut the impressed magnetic field was amplified and telemetered to Earth. Periodically, the instrument was calibrated by admitting a beam of anthracene molecules from a heated box. The entire experiment weighed about 2.5 kilograms.

Ionization Gages.—The density of the neutral gas in the atmosphere can be measured directly if a known volume of gas is collected, ionized, and attracted to a charged electrode, where the total current is recorded and subsequently telemetered. The ionization gages employed in satellite aeronomy operate in just this fashion. The operating principle is intrinsic in the Bayard-Alpert, hot-cathode ionization gage pictured in figure 11–3. In a sense, the Bayard-Alpert gage is an inside-out triode, with the
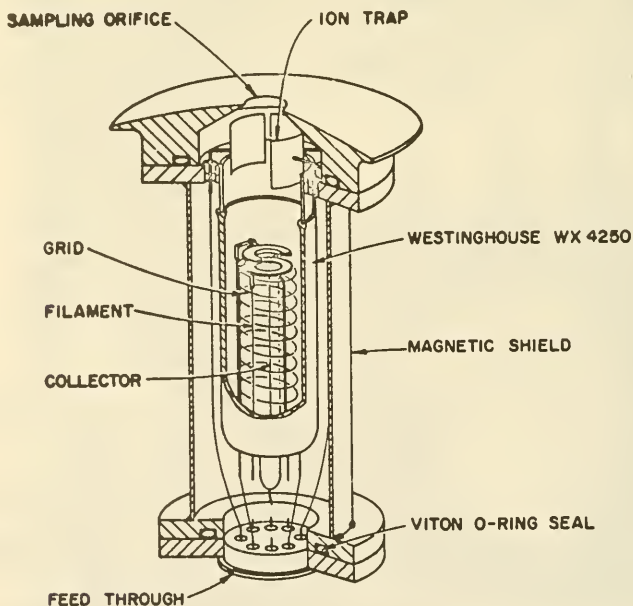
FIGURE 11–3.—Sketch of a Bayard-Alpert ionization gage. Air admitted through the orifice is ionized by filament-emitted electrons. Collected current is a measure of neutral density.

filament on the outside and a central, axial wire "plate" that collects ions. The atmosphere enters through the top orifice and is swept clean of indigenous ions by the electrostatic ion traps. The neutral gas enters the space between the filament and collector, where it is ionized by collisions with electrons that are boiled off the filament and accelerated into the active volume by the positively charged grid. Most of the electrons make repeated oscillations through the grid into the active volume. Ionized gas atoms and molecules are attracted to and collected by the negatively charged central grid. The magnitude of the collector current can be related directly to the density (and pressure) of the neutral gas in the active volume.

In addition to the Bayard-Alpert ionization gage, three other gages are used in space research: They are:

(1) The Redhead ionization gage, which employs a cold cathode in place of the Bayard-Alpert filament: Though fewer ionizing electrons are emitted in the Redhead gage, they are more efficiently trapped and used. An axial magnetic field forces the electrons to travel in circles (radial trapping) through magnetron action and negatively charged end plates trap them axially.

(2) The Alphatron, which replaces hot and cold cathodes with an alpha-emitting radioisotope: The alpha particles substitute for the electrons in the ionization process.

(3) The Omegatron (fig. 11–4), in which the active volume is bombarded by thermionically emitted electrons that are accelerated by the positive anode: A magnetic field is applied parallel
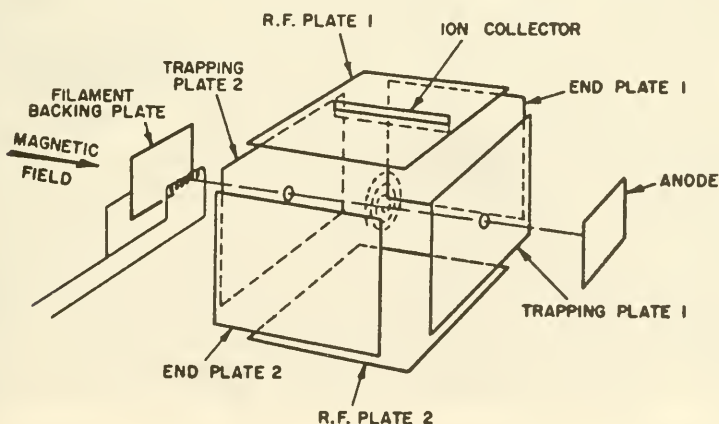
FIGURE 11–4.—Schematic of the Omegatron ionization gage, showing magnetic and electrostatic trapping of the ionizing electrons.

to the direction of flight to provide the magnetron action, which results in radial trapping. Plates on opposite sides of the active volume superimpose a radiofrequency field perpendicular to the magnetic field, B. Ions having a specific charge-to-mass ratio, e/m, given by $e/m = \omega/B$, where $\omega = 2\pi$ (frequency), will be resonant and travel radially outward in an Archimedes spiral until they are intercepted by a collector. Nonresonant ions form a space charge around the electron beam. The Omegatron is really a form of mass spectrometer, since it can be tuned to various mass components in the sample, such as N_2.

All ionization gages have outgassing problems. The first satellite ionization gage on Sputnik 3 indicated that satellite outgassing distorted density measurements for several days. In practice, ionization gages are evacuated, outgassed, and sealed before launch. Once orbit has been attained, an orifice is opened remotely. With such admonishments taken into account, ionization gages are roughly linear over the pressure range 10^{-11} to 10^{-4} torr. They are also responsive to rapid changes in density and pressure.

Several satellites have carried ionization gages into orbit. (See table 11–1.) The Bayard-Alpert and Redhead gages installed on Explorer XVII are illustrated in figure 11–5 (ref. 5). Figure
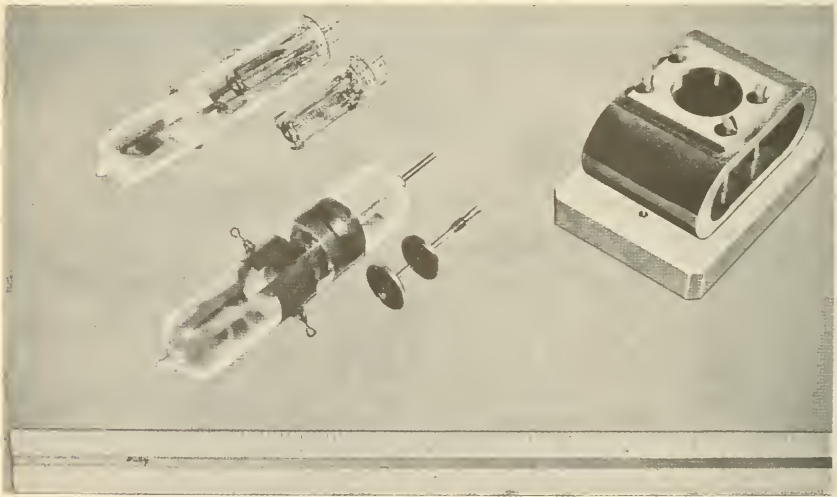
FIGURE 11–5.—The Explorer-XVII ionization gages. Bayard-Alpert gage, top left; Redhead gage, bottom. At the right is the permanent magnet that traps the ionizing electrons in the Redhead gage (ref. 5). Scale is in inches.

A–16, in the appendix, should be consulted for the gages' locations on the satellite.

Temperature Measurements.—Direct temperature measurements of the neutral component of the upper atmosphere are never made from satellites. The mean free paths of the atoms and molecules are many times longer than the dimensions of any thermometer. Thermal equilibrium cannot be attained and temperature has no operational meaning. Kinetic temperature, which is really a measure of velocity, can be inferred from the broadening of spectral lines and bands and from pressure measurements with the help of the hydrostatic equation. In section 11–3, satellite instruments will be described that measure "electron temperature" directly. The instruments usually depend, however, upon particle velocity rather than any measurement of temperature per se.

Neutral Mass Spectrometers.—The density-determining instruments just presented, except for the Omegatron, cannot separate out and identify the various constituent species in the neutral atmosphere. The atmosphere's species vary in mass and chemical affinity, suggesting the possibilities of putting mass spectrometers and gas chromatographs to work in determining composition. Mass spectrometers are far simpler, and more appropriate for a mixture of very light—and, on occasion, chemically inert—atoms and molecules. They are the dominant instrument in the *in situ* analysis of the atmosphere.

Mass spectrometers separate atoms and molecules possessing differing masses by applying an equal accelerating force to all. As a consequence, the lighter particles acquire more speed in a given time and draw away from their heavier companions. The accelerating force may either be applied perpendicular to the particles' direction of motion, so that the different masses fan out in a spectrum, or it may be parallel, causing like particles to clump together but not altering their direction of flight (fig. 11–6). In all mass spectrometers there is a mass scale, which is usually made directly proportional to mass. Distance and time of arrival are the mass scales in the simple situations shown in figure 11–6.

The application of equal accelerating forces to the different atoms in the sample is easily accomplished by singly ionizing the particles. The presence of electrical charge also provides a means of particle-flux measurement. Both electrostatic and magnetic forces, $\mathbf{F}_e = q\mathbf{E}$ and $\mathbf{F}_m = q\mathbf{v} \times \mathbf{B}$, are linear in the charge, q, and the applied fields, E and B. Electrostatic and magnetic mass
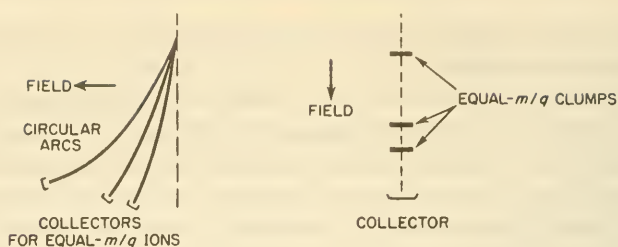
FIGURE 11–6.—Transverse electrostatic and magnetic
forces cause spatial dispersion of ions. Longitudinal
electrostatic forces cause clumping by mass number.

analysis both imply precollimated beams of ions, while magnetic separation has the added condition of equal ion velocity.

From these simple considerations, the major components of a mass spectrometer must be:

(1) An ionization mechanism, if the population being sampled is not already ionized. In this case, we have a neutral gas spectrometer.

(2) Collimators, focusing devices, and velocity filters, as needed by the mass-dispersion scheme adopted.

(3) A mass-dispersion mechanism, such as the magnetic and electrostatic fields just mentioned. More complicated combinations of static and time-varying fields are presented later.

(4) An electric-current detector to measure the flow of charged particles meeting the mass-separation criteria.

(5) Logic circuitry to make time-of-flight measurements, electrically scan spatially separated detectors, and synchronize the various parts of the instrument.

(6) An analog-digital (AD) converter to feed the data words in the proper format to the communication subsystem.

All instruments disturb the parameters they measure, and mass spectrometers are no exception. Instrument surfaces, for example, encourage ion recombination. A hot filament emitting ionizing electrons may cause hot-surface chemical reactions. Filaments are usually located away from the main gas stream for this reason. Electrostatic and aerodynamic distortions, such as those discussed in section 12–3, apply to the m/q mass spectrometers.

Five different types of mass spectrometers have been used in satellites and sounding rockets:

Type	Mass-dispersion mechanism
Simple mass spectrometer_____	Magnetic field
Double-focusing mass spectrometer__	Electrostatic energy filter, plus magnetic field
Quadrupole mass spectrometer_____	Radiofrequency field superimposed on static field (see discussion)
Time-of-flight mass spectrometer___	Time of flight
Radiofrequency mass spectrometer__	Resonant grid structure (see discussion)

The first two spectrometers listed require the use of magnetic fields for ion separation. The strong fields set up through the spacecraft by magnetic-dispersion instruments usually preclude their use on spacecraft carrying magnetometers, a fact explaining why they are seldom used on scientific satellites.
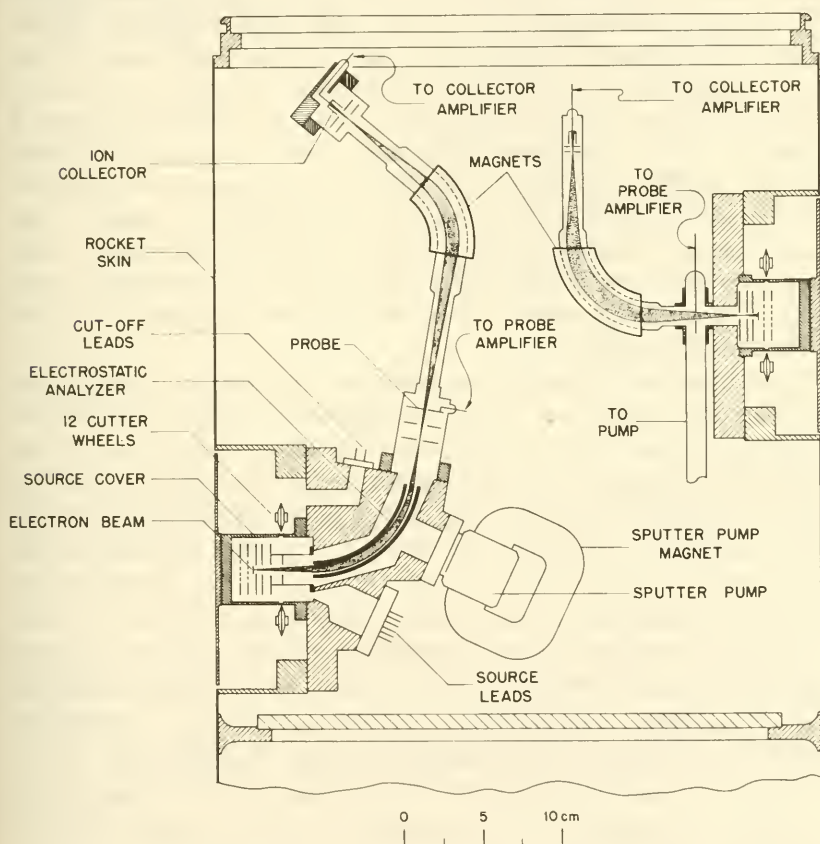
FIGURE 11-7.—These single- and double-focusing magnetic mass spectrometers were flown on Aerobee sounding rockets. They are representative of satellite neutral mass spectrometers (ref. 6).

Two instruments designed by the University of Minnesota group for the Aerobee series of sounding rockets are typical of the single- and double-focusing mass spectrometers that have been used near the Earth (ref. 6). Shown mounted together for redundancy purposes in the Aerobee structure (fig. 11–7), both employ permanent magnets to disperse ions of different masses laterally into a spectrum. At the same time, the magnetic field focuses ions in equal m/q groups through the correct exit slits. In both of the spectrometers shown, the neutral gas is ionized by electron bombardment and accelerated by grids through the entrance slits into the analyzer sections. The analyzer sections are evacuated by a single sputter pump to insure long mean free paths. After the rocket attains an altitude of about 100 kilometers, cutter wheels remove the caps covering the recessed ion sources, exposing them directly to the space environment. Figure 11–7 shows a single ion collector and amplifier for each instrument. Spectrum scanning is accomplished by sweeping the ion-accelerator grid voltage from 1000 down to 200 volts every 2 seconds. This corresponds to a mass sweep from 10 to 50 amu. The major difference between the two units is seen in the electrostatic analyzer used before the magnetic-dispersion stage in the double-focusing spectrometer. A curved-plate electrostatic analyzer provides both energy filtering and spatial focusing. As a result, the double-focusing instrument is more precise; i.e., it has better mass resolution.

A double-focusing mass spectrometer for satellite application has been designed at the NASA Goddard Space Flight Center and flown on Explorer XVII (refs. 7, 8). One difference between the two double-focusing spectrometers shown in figures 11–7 and 11–8 is in the latter's use of an exposed rather than a recessed ion source. More significant, however, is the fixed tuning of the second instrument to masses of 4, 14, 16, 18, 28, and 32, corresponding to major components of the Earth's atmosphere, He, N, O, H_2O, N_2, and O_2. Six separate collectors are connected to a single electrometer tube, which is switched from one collector to another every 8 seconds. The detector circuits can measure currents as low as 10^{-15} amp or, equivalently, partial pressures as low as 10^{-11} torr. Fixed tuning provides more precision than swept tuning, but it is inflexible and presumes prior knowledge of the atmosphere being studied. The mass of the instrument shown in figure 11–8 is approximately 7 kilograms, and it consumes an average of 26 watts. Most satellites would find the magnetic
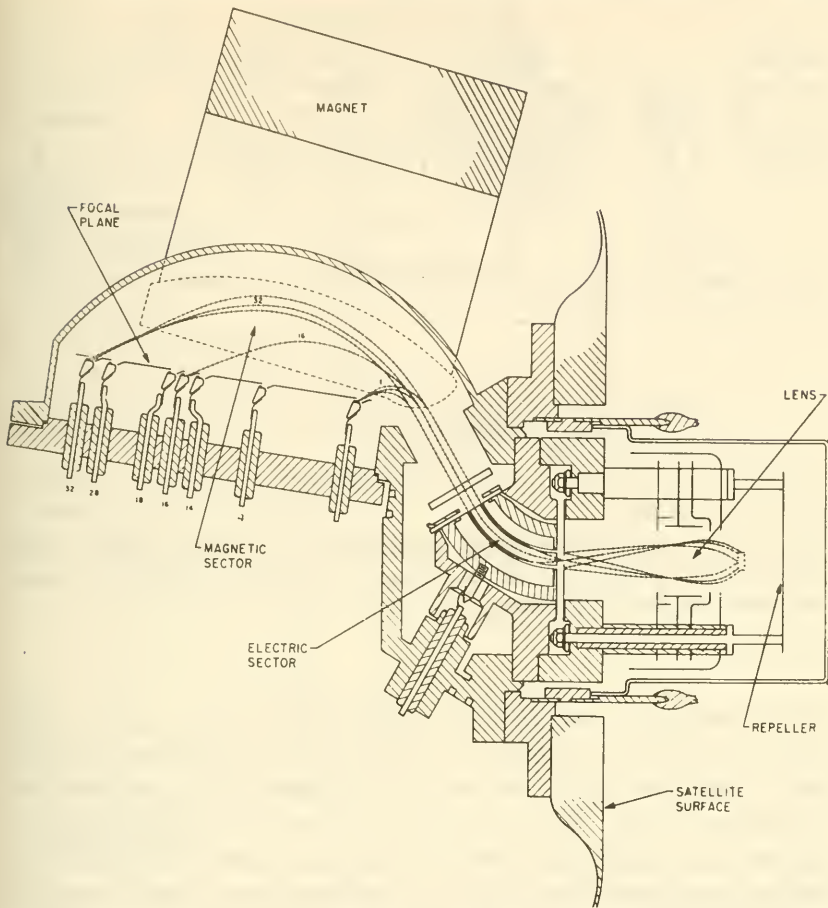
FIGURE 11–8.—The Explorer XVII double-focusing mass spectrometer. This instrument is tuned to six mass components common in the upper atmosphere (ref. 8).

field objectionable and the weight and power requirements high, but double-focusing mass spectrometers are hard to surpass for precision.

Much interest has shifted to lighter, nonmagnetic instruments, like the quadrupole, time-of-flight, and radiofrequency mass spectrometers.

The quadrupole mass spectrometer, or Paul Massenfilter (after W. Paul), has flown frequently on sounding rockets and has proven to be an accurate, sensitive, rugged, lightweight piece of equipment (ref. 9). In essence, it consists of four parallel, cylin-
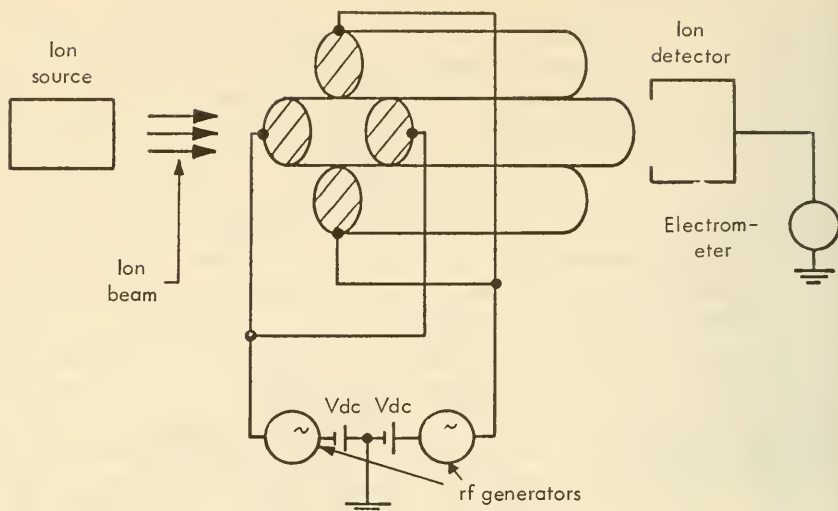
FIGURE 11–9.—Schematic of the quadrupole mass spectrometer. Only ions with a specific m/q ratio will pass all the way through the space between the four cylinders.

drical electrodes arranged on a square pitch (fig. 11–9). The usual ion source is followed by a grid, which accelerates the mixture of ions into the space running lengthwise between the four cylinder surfaces. The secret of mass separation is the superposition of a radiofrequency (rf) field on a steady direct-current field between electrodes. Such a combination of fields forces all except a select group of ions with a specific m/q ratio into unstable transverse trajectories, so that they eventually collide with the electrodes and are removed from the ion stream. The desired m/q group travels the full length of the spectrometer to become the detector current. By varying the dc and rf fields, the mass spectrum can be swept.

An accurate description of the m/q filtering action calls upon potential theory. The potential between the four electrodes, assuming electrodes of hyperbolic cross section is

$$\phi(x,y,z,t) = (A + B \cos \omega t)\frac{x^2 - y^2}{R^2} \tag{11–4}$$

The differential equations of motion for an ion in this space are

$$m\ddot{x}+2q(A+B\ \cos\ \omega t)\frac{x}{R^2}=0$$

$$m\ddot{y}-2q(A+B\ \cos\ \omega t)\frac{y}{R^2}=0 \qquad (11\text{--}5)$$

$$m\ddot{z}=0$$

where

ϕ = potential

x, y, z = cartesian coordinates, z-axis parallel to the cylinder axes

t = time

$\omega = 2\pi \times$ frequency

A = the applied dc voltage

B = the amplitude of the superimposed rf voltage

R = one-half the distance between electrode surfaces

The approximation of hyperbolic electrodes by circular cylinders is acceptable for this instrument. The above equations of motion can be transformed into Mathieu differential equations

$$\frac{d^2x}{dp^2}+(a+2b\ \cos\ 2p)x=0$$

$$\frac{d^2y}{dp^2}-(a+2b\ \cos\ 2p)y=0 \qquad (11\text{--}6)$$

where

$p=\omega t/2$

$a=8qA/mR^2\omega^2$

$b=4qB/mR^2\omega^2$

Only for certain small ranges of a and b do the equations predict stable transverse ion trajectories. For a fixed a/b (note $a/b = 2A/B$), only a narrow m/q group can pass down the instrument's axis without experiencing unstable transverse oscillations and electrode collision.

In a time-of-flight mass spectrometer, neutral gas atoms are first ionized and then accelerated in discrete groups by a grid structure such as that shown in figure 11–10. Each ion receives the same kinetic-energy increment regardless of mass, so that its time of flight, t, down a drift tube of length S is

$$t=\frac{S}{[2qV/m]^{1/2}}$$

The grid structure also helps to focus the ion beam. In the illustrated Bendix Corp. instrument, the ions impinge on an electron-multiplier detector. (See sec. 11–4.) The amplitudes and timing of the signals yield the environmental ion densities and identities.
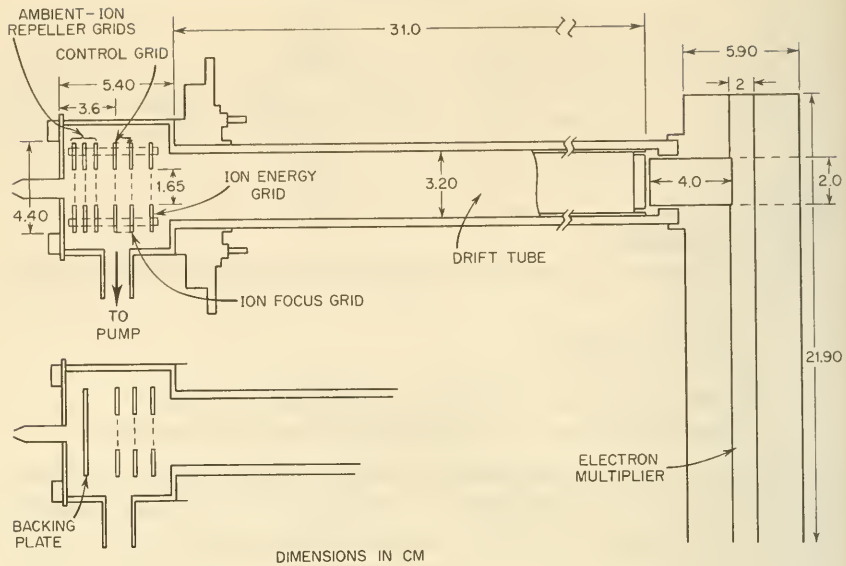
FIGURE 11–10.—A time-of-flight mass spectrometer designed for space use (ref. 10).

Superficially, the rf mass spectrometer, or Bennet tube, resembles the time-of-flight instrument. Ions of different masses are again separated by grid-produced, axial electrostatic fields (fig. 11–11). The important difference is the resonant condition set up in the rf spectrometer for ion groups with the desired m/q. Ions are drawn in from the environment or the ion source by a charged grid. A negative, low-frequency sawtooth voltage applied to grid no. 2 in figure 11–11 pulls bunches of these ions into the first rf stage. An rf field of several megacycles applied to grid no. 3 imparts kinetic energy to those ions that receive maximum acceleration between grids nos. 2 and 3 and that pass grid no. 3 at the instant of field reversal. Those ions that pass between grids nos. 3 and 4 at the proper moment are accelerated
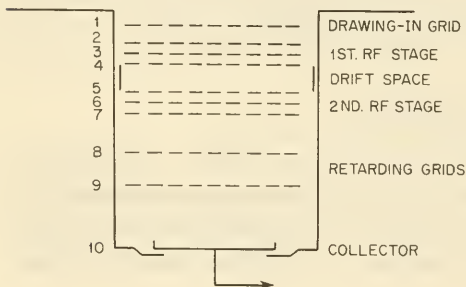
FIGURE 11–11.—Diagram of an rf mass spectrometer. See text for details of operation.

down the drift tube.   Ion sorting depends upon dynamic effects
resulting from mass differences.   Further filtering occurs farther
down the tube.   Ions are accepted by the second rf stage only if
they take an integral number of cycles to clear the drift tube.
The retarding grids, nos. 8 and 9, act as another sieve, passing
only those ions having a fixed m/q. Rf mass spectrometers easily
separate ions from 1 to 5 amu and can probably separate the
spectrum from 1 to 45 amu.   Instruments like the one just de-
scribed have flown on the Eccentric Geophysical Observatory
(EGO I/OGO I). (See fig. 11–12.)
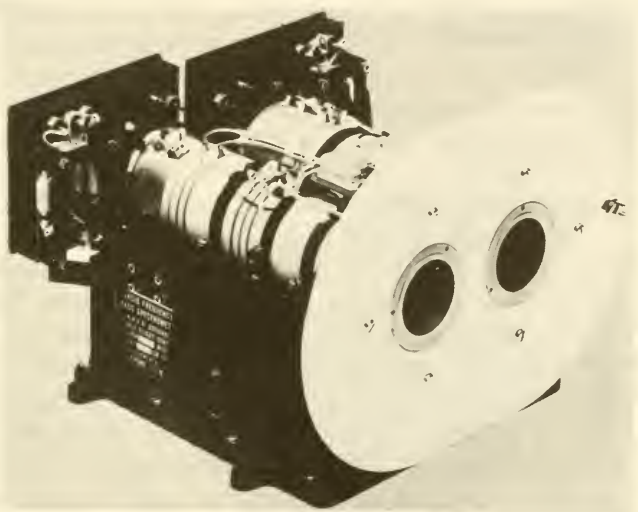
FIGURE 11–12.—The OGO-I rf mass spectrometer.
(Courtesy of H. A. Taylor.)

Atmospheric-Sample Collection by Satellites.—Sounding rockets
and balloons have carried evacuated vessels for the remote collec-
tion of atmospheric samples.   Compositional analysis then follows
in terrestrial laboratories.   Such an approach is never used in
satellite research, for several reasons:

(1) Densities at satellite altitudes are so low that significant
quantities of gas cannot be conveniently collected.

(2) Any ionized constituents collected would be quickly neutral-
ized in a container.

(3) Some species, particularly components like NO, would be
altered by reactions within a closed container.

C.   Satellite Optical Instruments

Atmospheric Studies by Analysis of Electromagnetic Radiation.—
Scientific satellites are well placed to analyze the electromag-
netic radiations emitted by, reflected from, and transmitted
through the Earth's envelope of gases.   The diagnostic utility of
scientific satellites stems from several experimental possibilities:

(1) Starlight passing through the atmosphere is refracted by
the different layers.   By measuring the occultation of stars by
the Earth from a satellite, atmospheric structure can be divined.

(2) Sunlight is reflected from the Earth's surface and low-
lying clouds, passing through the atmosphere twice before reach-
ing the satellite's sensors (fig. 11–13).   Absorption spectra are
indicative of atmospheric composition.
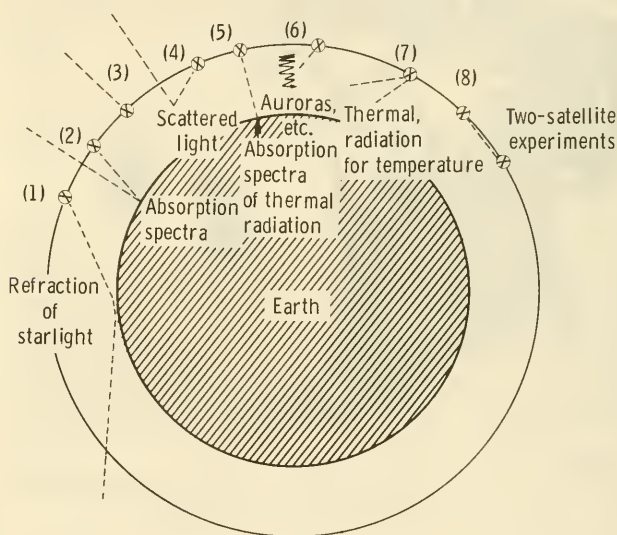
FIGURE 11–13.—Sketch showing some situations where
satellite optical measurements might aid aeronomy.
The numbers are keyed to the discussions in the text.

(3) The absorption spectrum of sunlight seen through the
atmosphere above the satellite reveals density and composition.

(4) The spectrum, intensity, and polarization of sunlight, as
scattered by the upper atmosphere into a satellite's instruments,
are indicative of composition and density.

(5) The atmospheric absorption spectrum of the radiation
emitted by the warm Earth can lead to determination of composi-
tion.

(6) Emission spectra from various physical processes occurring in the upper atmosphere—particularly those stimulated by solar-particulate and electromagnetic bombardment—are useful in composition and density studies. Even more important is the elucidation of the physical processes themselves; i.e., the nature and origin of the airglows and auroras.

(7) Thermal radiation from various portions of the upper atmosphere indicates temperatures.

(8) Two satellites, one carrying an artificial light source and the other analysis equipment, can measure directly the composition and density of the upper atmosphere through absorption spectra.

Satellite optical instruments measure the intensity of received electromagnetic radiation as a function of wavelength and polarization. Spectral dispersion or filtering of the received radiation is a key feature of the radiometers and spectrometers described below. The instrument-pointing coordinates, of course, are critical in interpreting the measurements. For the moment, consider just the optical instrumentation. The instruments may be divided into the three classes listed below and in table 11–2.

(1) Radiometers and photometers, which measure electromagnetic-flux intensity over a few broad spectral areas and/or at several narrow lines in the spectrum. There is no physical dispersion of the spectrum with radiometers. Spectral resolution is accomplished by filters and other methods of tuning (table 11–3).

(2) Spectrometers and spectrophotometers, which disperse electromagnetic radiation into a spectrum and then scan it with high resolution. The properties of dispersion, spectrum-scanning, and high resolution distinguish spectrometers from photometers. Interferometric techniques are sometimes used with spectrometers.

(3) Polarimeters, which measure the amount of polarization that has been introduced into a beam of radiation in its passage from source to detector.

Most probe electromagnetic instruments begin with a lens, mirror, or some other flux concentrator that gathers and focuses electromagnetic energy. They all end with a radiation detector that converts the electromagnetic radiation into electrical signals essential for telemetering. In between may lie prisms, analyzers, filters, and other optical devices. Such "optical" instruments may change their character radically with wavelength. Glass, for example, passes only a narrow portion of the spectrum, and the

TABLE 11–2.—*Types of Optical Instruments for Atmospheric Research*

Instrument type	Principle of operation	Phenomena observed
Radiometer/photometer.	Electromagnetic radiation is focused on a detector that gives a signal proportional to intensity. Filters and antennas restrict the spectrum observed to a few specific lines or spectral regions.	Emission: Aurora, permanent airglows, synchrotron radiation, twilight flashes, sferics, fluorescence, resonance radiation.
Spectrometer/spectrophotometer.	Electromagnetic radiation is collected, collimated, dispersed, and focused on a detector that scans broad spectrum with high resolution.	Scattering: Aerosol and micrometeoroid scattering, night airglow, halo structures. Absorption: Extinction of portions of solar spectrum with atmospheric depth, absorption spectra of planet-emitted thermal radiation, limb studies, atmospheric reflection at angles not observable from Earth.
Polarimeter.	Electromagnetic radiation is passed through an analyzer to determine amount of polarization.	Polarization: Scattering properties of small suspended particles in atmosphere.

Table 11–3.—*Radiometer and Photometer Components*

Spectral region	Collectors	Common selectors	Detectors
Microwave_____	Dish antenna____	Tuned dish and circuits.	Antenna diode, thermistor, or bolometer.
Infrared_____	Dish mirror, lens.	Filter, grating, prism, interferometer.	Thermopiles, PbS, PbSe, and other materials.
Visible_____	Lens, mirror____	Filter, grating, prism, interferometer.	Photomultiplier, photocell, CdS.
Ultraviolet_____	Lens, mirror____	Filter, grating, prism.	Photomultiplier, ionization chamber.
X-rays and gamma rays.	None_____	Shields, radiation telescopes.	Ionization chamber, solid-state detector, etc. (see sec. 11–4).

sensitivity of detectors varies greatly from one part of the spectrum to another. Most optical instruments are static, but others are burdened with vibrating reeds and scanning motors. Obviously, there is no typical instrument.

The major interface between the optical instrument and the remainder of the spacecraft is spatial in character. Optical instruments must be able to see their target and gather enough of its light to make good measurements. The field of view needed may vary from a small fraction to several steradians. Electromagnetic observations are often, but not always, directional, which means that the links between the attitude-control and guidance-and-control subsystems are also important.

Radiometers and Photometers in Satellite Aeronomy.—When integrated flux measurements are desired over one or more broad portions of the spectrum, or perhaps a few spectral lines, a radiometer, or photometer, is the appropriate instrument. The term "radiometer" is generally applied at the microwave and infrared ends of the spectrum, while "photometer" is reserved for the shorter wavelengths. Usage is not firm, however. Radiometers and photometers perform the same functions. They both collect radiation, select spectral lines and bandpasses, and detect the transmitted fluxes. But they generally employ different components, as shown in table 11–3.

Radiometers—that is, photometers in the radio region of the spectrum—have little diagnostic value in studying the Earth's

atmosphere. It is too thin and cold. Microwave and infrared radiometers on Mariner II have helped in the understanding of the hot, dense Venusian atmosphere, but they are of little use to earthly aeronomy. Radiometers have been orbited on Earth satellites, such as the Tiros series and Explorer VII, for the temperature mapping of the Earth's surface and its cloud cover. These radiometers deal mainly with surface phenomena and meteorology; they are not covered here. Photometers in the visible and ultraviolet do, however, have value in aeronomy.

In the optical region, the simplest photometers separate out the different wavelength regions of interest with filters. A detector,
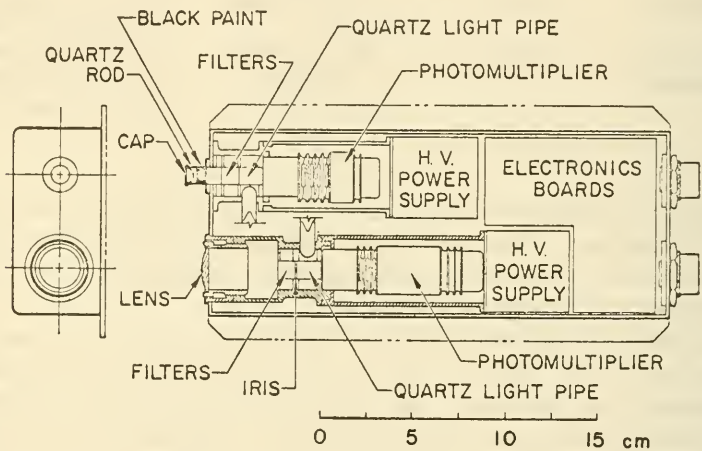
FIGURE 11-14.—Double-photometer instrument package flown on an Air Force satellite. Top photometer measured ozone distribution; bottom instrument measured the Earth's ultraviolet radiance (ref. 11).

such as a photomultiplier tube, then measures the intensity of the light passed as a function of time and pointing angle.

Two simple filter photometers have been reported by Friedman and Rawcliffe. Both were mounted in a single package (fig. 11-14) and pointed toward the Earth from an attitude-controlled Air Force satellite launched in 1962. The upper instrument admitted light to the filters through a quartz rod, which had a polished hemisphere ground into one end. Light was thus directed into the light pipe from all azimuths and from elevations 10° above and below the local horizontal. The filters transmitted only the light within the ozone-absorption band at 2500 Å to 2800 Å.

The photomultiplier tube recorded the extinction of light at satellite sunset (and the reverse at sunrise) as the layers of atmospheric ozone absorbed the light normally passed by the filter. The vertical distribution of ozone could be determined from the telemetered signals.

The second instrument, in contrast, looked straight down into the Earth's atmosphere through a lens and a filter combination that passed light in the 2550 Å±140 Å range. A photomultiplier tube recorded the intensity of the transmitted light. The Earth's ultraviolet albedo, due to Rayleigh scattering of the incident solar flux, was measured in this way. This simple photometer is typical of many photometers employed in space research.

A more sophisticated and complex photometric experiment was constructed for OGO II by Blamont and Reed. One of the experiment's two photometers was installed in the OGO's OPEP (Orbital Plane Experimental Package) and looked forward along the orbital plane to measure the 6300-Å, red atomic-oxygen line. A second instrument was mounted on the main body of the OGO, so that it could look both straight down ($Z+$ direction) and straight up ($Z-$ direction) from the Earth-stabilized spacecraft. Light admitted along the $Z-$ optical axis was passed through a 6300-Å filter. The $Z+$ optics comprised a synchronized pair of rotating mirrors that sequentially directed the $Z+$ light through eight filter positions located on the periphery of a circle (fig. 11–15). It is this second photometer, with its stepping motor and
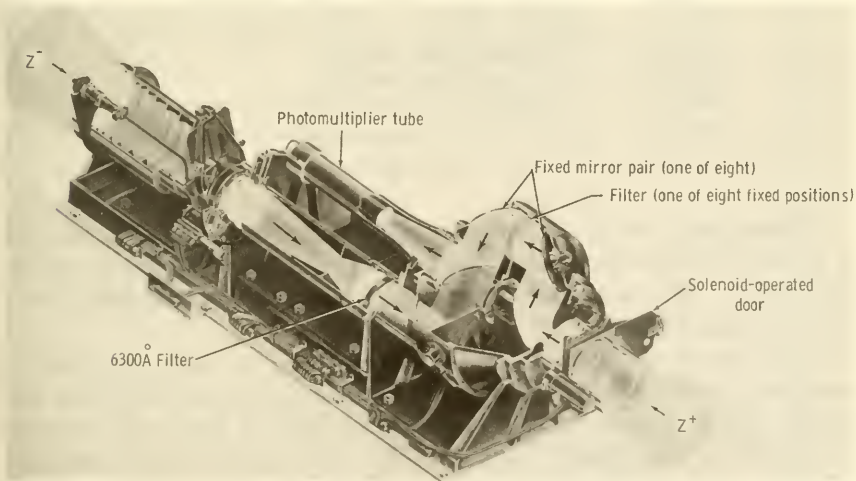
FIGURE 11–15.—The OGO-II airglow photometer package.   (Courtesy of E. Reed.)

several fixed filters, that holds more interest for instrument technology.

The $Z-$ axis optics are straightforward. Once the spacecraft is in orbit and stabilized, a solenoid-operated door is opened and admits light through a quartz lens, past a shutter, through a 6300-Å filter, onto two mirrors, and into a photomultiplier tube. Figure 11–15 shows the components schematically. The $Z+$ axis has a similar door, shutter, and lens. The experimenters wished to measure light intensity at several wavelengths from the down direction, so they built eight fixed filter positions and scanned them mechanically with mirrors driven by a stepping motor. This scanning approach contrasts with the rotating filter wheel employed on some military-satellite photometers. When a series of filters is mechanically scanned, the instrument is usually called a spectrophotometer.

In the OGO-II experiment, the eight positions scanned were fitted with the filters shown in table 11–4.

TABLE 11–4.—*Light Filters in OGO–II Spectrophotometer*

Position	Filter	Significance
0	Opaque_____	Calibration and measurement of photomultiplier dark current.
1	2630 Å_____	Ultraviolet airglow.
2	Opaque_____	6300-Å light from $Z-$ axis admitted.
3	6300 Å_____	Red atomic-oxygen line in airglow.
4	6225 Å_____	Red hydroxyl radiation.
5	5892_____	Yellow sodium airglow.
6	5577 Å_____	Green atomic oxygen in airglow and aurora.
7	3914 Å_____	Molecular nitrogen in visible aurora.

Experiments with commandable moving parts always require a great deal of supporting electronic circuitry. Figure 11–16 is included to illustrate the extent of the control-and-command supporting equipment.

Spectrometers.—The interferometer principle can be applied to satellite spectrometers. Block and Zachor designed and flew an infrared interferometer-spectrometer on an Air Force satellite in 1962. This instrument used the Michelson optical arrangement of interferometer components shown in figure 11–17. The mirror M_1 in the sketch is moved at a constant velocity in the direction of the source by a sawtooth drive. For an instantaneous displace-
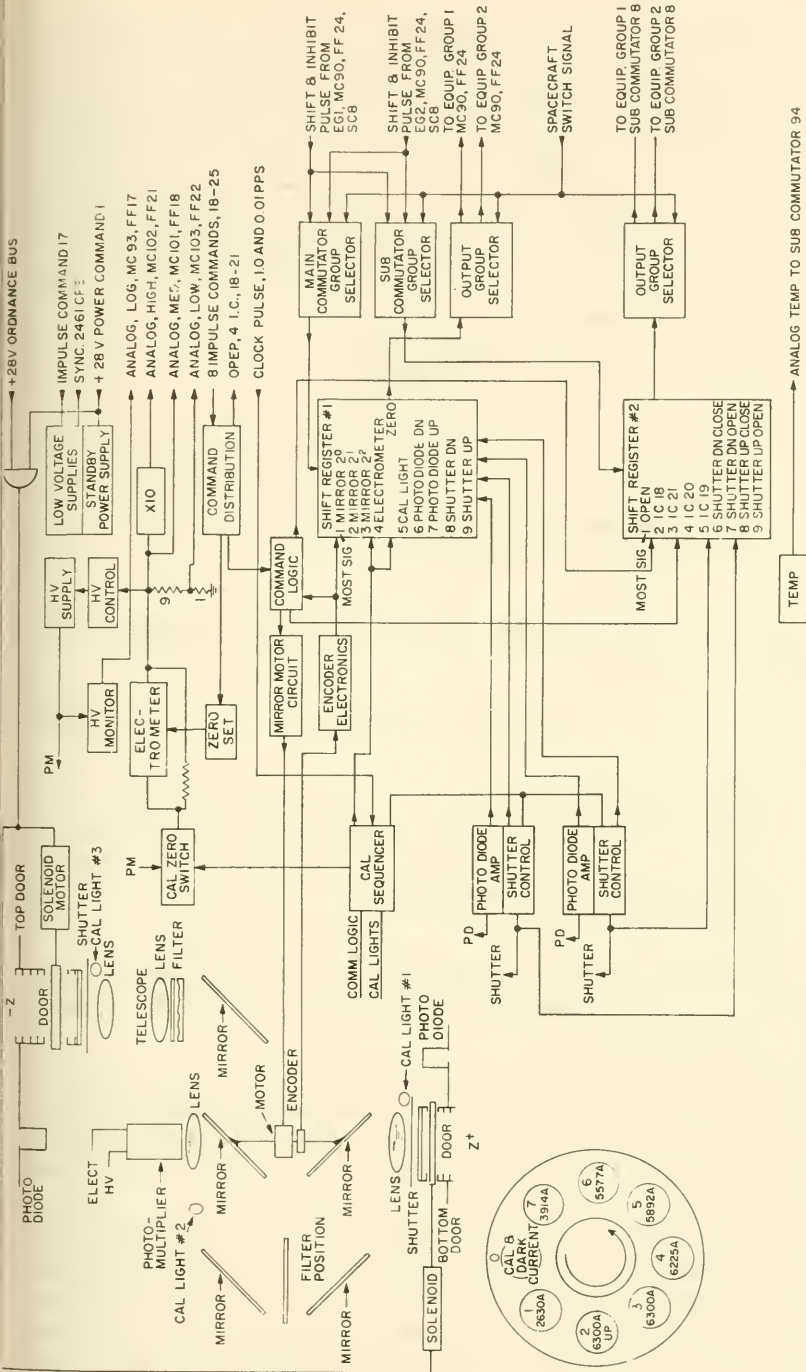
FIGURE 11-16.—Block diagram of the OGO-II airglow photometer electronics. Supporting circuitry is sometimes a major problem in experiment design. (Courtesy of E. Reed.)
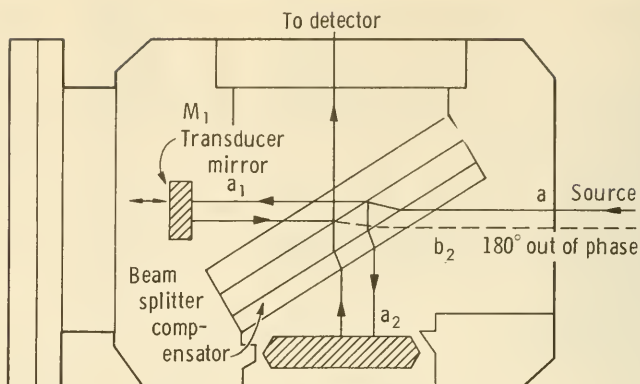
FIGURE 11–17.—An infrared interferometer spectrom-
eter flown on an Air Force satellite. Mirror M_1
moves back and forth to generate interferometer
action, as described in the text (ref. 12. Copyright
Optical Society of America).

ment of mirror M_1 of $Bt/2T$, the intensity of the spectrum ob-
served by the detector is

$$I_\nu = 0.5 I_{0\nu}(1 + \cos 2\pi Bt/2) \tag{11-7}$$

where

$I_{0\nu}$ = the intensity of the spectrum at the entrance aperture

ν = the wave number (the wave number is the number of wave-
lengths occupying 1 centimeter of distance; it is equal to
the reciprocal of the wavelength)

t = time

The instrument of Block and Zachor scanned the infrared radiance
of the Earth's surface and atmosphere in the 1.8- to 15-μ range
with a resolution of 40 cm^{-1}.

Infrared radiation penetrates the atmosphere so well that its
analysis is more useful to meteorology and geology than to aeron-
omy of the upper atmosphere. The Tiros meteorological-satellite
program, in particular, has developed a wide array of infrared
instrumentation.

To illustrate further the use of spectrometers in atmospheric
research, a grating instrument developed by D. D. Elliott, of the
Aerospace Corp., is now described. The purpose of Air Force
Experiment CRLU–737 is the determination, on a global basis,
the concentrations of O_2, O_2^+, N_2, and NO as a function of alti-
tude between 30 and 120 kilometers. To accomplish this, the

spectrometer scans the ultraviolet radiance of the Earth versus altitude at the local horizon between 1600 Å and 3100 Å. The Air Force planned to orbit this experiment on one of its piggyback satellites, the OV–1–11, in 1967. The experiment arrangement, shown in figure 11–18, collects light and defines an altitude interval at the local horizon with a small Cassegrain telescope. The satellite must be Earth stabilized. Light from the telescope is admitted to the spectrometer through an entrance slit. Reflected by a spherical mirror, the light encounters a diffraction grating,
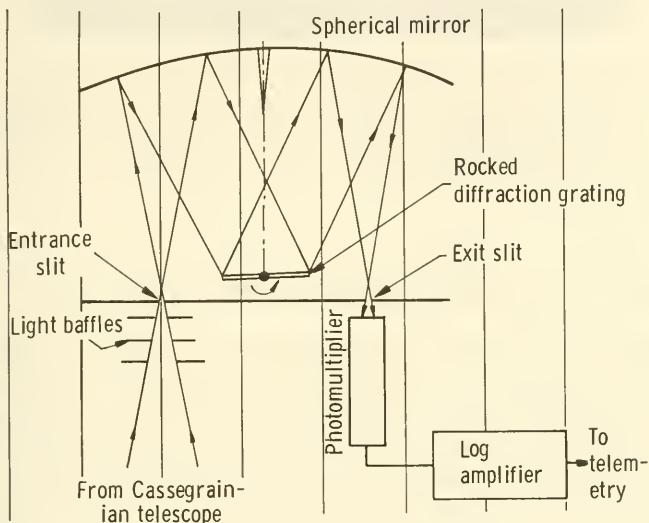
FIGURE 11–18.—Optical sketch of Air Force Experiment CRLU 737. This grating spectrometer will scan the Earth's ultraviolet radiance as a function of altitude. The spectrometer is of the Ebert-Fastie type. (Courtesy of D. D. Elliott.)

which is driven by a motor-and-cam arrangement (fig. 11–19) so that the spectrum is scanned from 1600 Å to 3100 Å in 20 seconds. After each spectral scan, the secondary mirror in the telescope is tilted a step so that a new 10-kilometer altitude interval is scanned during the next grating cycle. Dispersed light from the grating reflects off the spherical mirror and, after passing through an exit slit, is converted into an electrical signal by a photomultiplier tube. In this instrument, the slits are set for 5–Å resolution, and the minimum detectable signal is 500 rayleighs. The double-scanning action (in both wavelength and altitude) permits
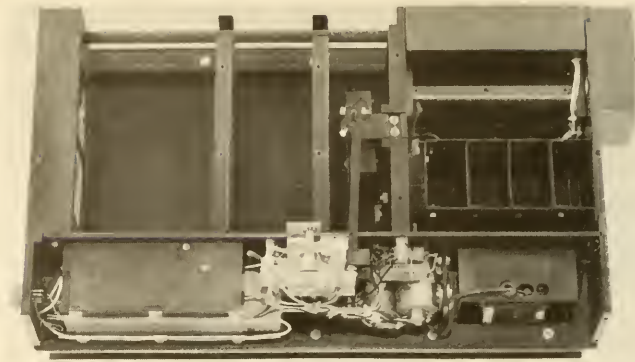
FIGURE 11–19.—Photograph of the grating spectrometer sketched in figure 11–18. Far left, spherical mirror; center, grating and rocking arm; and upper right, photomultiplier tube. (Courtesy of D. D. Elliott.)

the experimenter to build up worldwide maps of O_2, O_2^+ N_2, and NO.

Star Trackers and the Measurement of Stellar Refraction.—An unusual experiment for studying the structure of the atmosphere has been suggested by the High Altitude Engineering Laboratory of the University of Michigan (ref. 13). In essence, a satellite-borne star tracker would measure the angular position of a star as it sets into the Earth's atmosphere and is finally occulted. A single stellar scan would produce stellar refraction angle as a function of time. Since the index of refraction depends upon density, a density profile can be computed, which, in turn, leads to a pressure profile and estimates of temperature. Stellar refraction by the Earth's atmosphere would probably be measurable from a satellite from a height of about 40 kilometers down to the Earth's surface or the cloud level. Perhaps 100 to 150 density profiles could be taken per orbit.

In this instance, as with infrared instrumentation, we see how satellite sensors can explore the lower regions of the atmosphere through the analysis of radiation reaching them through the atmospheric windows.

A few words about satellite instrumentation for auroral studies are pertinent here. Several of the photometers and spectrometers described above are designed specifically to detect the auroral electromagnetic radiations. Electromagnetic radiation tells only

part of the story, however. The auroras are apparently stimulated by charged particles precipitating from the radiation belts and other sources. For this reason, auroral payloads usually include low-energy particle detectors, such as those introduced in section 11–4. Typically, several particle detectors and optical instruments are mounted on the same satellite but with different view angles. As satellites with such instrumentation pass through the polar regions, their observations are coordinated with those made simultaneously from aircraft, balloons, and sounding rockets. One of the USAF/Lockheed auroral payloads is described in section 11–4.

11–3. Instruments and Experiments for Ionospheric Physics

Coexisting with the neutral atoms and molecules in the upper atmosphere is a population consisting of electrons and various species of ions. Collectively, these charged species form the ionosphere, which was described in section 1–2. Experimentally, these charged particles are easy to distinguish from their neutral neighbors, which are not affected by applied electrostatic and magnetic fields. There is still a third intermingling population that must be resolved by satellite instruments; this is the portion of the solar plasma that invades the upper atmosphere. (See sec. 12–3.) Though electrically charged, the solar-plasma particles can be recognized by their much higher average energies, as illustrated in figure 11–20. All three populations constantly exchange energy and members among themselves.

Scientists wish to know the densities, species, and energies of the ionospheric particles as functions of time and position. The presence of electrical charge introduces a wide variety of instruments not applicable to neutral populations. A comparison of tables 11–1 and 11–5 accentuates the differences in experimental approaches. Missing from the list of ionospheric instruments and experiments are those depending upon frictional effects on the satellite orbit. The drag due to the ionosphere cannot be conveniently separated from the generally much larger forces due to the neutral atmosphere. Neither are there satellite optical experiments specifically designed to record the spectra of ions, although this may be done eventually in order to study the distributions of heavy ions at high altitudes. As a matter of fact, electrons and protons, which make up the bulk of the ionosphere, emit no optical spectra at all unless they combine. Replacing the Earth-based observation of orbital drag distortion is a class of experiments based upon the observation of the distorting effects
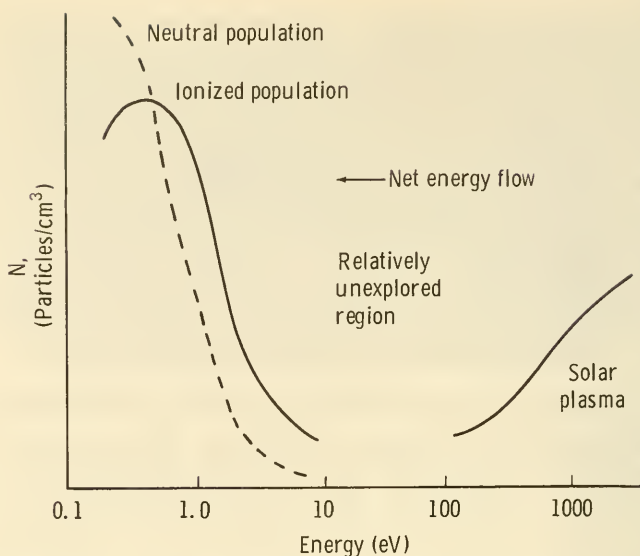
FIGURE 11-20.—Three particle populations existing in the ionosphere. These populations constantly exchange energy and members. The distributions change with place and time.

of the ionosphere upon the propagation of radio waves. Instead of optical experiments, plasma probes and ion traps electrostatically analyze the velocities of ions and electrons. Despite the fact that the ionosphere is considerably less dense than the neutral atmosphere, the presence of electrical charge opens up so many opportunities for instrumentation that the ionosphere stands out vividly against the background of neutral species.[2]

A. Radio-Propagation Experiments

Satellite Transmitters and Earth-Based Observers.—The bulk of the Earth's ionosphere lies between a transmitting satellite and the Earth-based antennas that pick up its signals. The free electrons in this dilute layer refract, absorb, polarize, and otherwise distort the signals that reach the ground. From the analysis of the received signals, scientists can deduce the integrated electron density along the signal's path and infer the existence and

---

[2] In the case of the ionosphere, one can also conceive of active experiments employing nuclear explosions or particle accelerators. Artificial auroras and controlled enhancement of the ionosphere are among the possibilities that have been suggested (refs. 14, 15).

sizes of ionospheric irregularities.[3] The overall experimental picture is summarized in table 11–5.

One notes an obvious parallel between the Earth-based visual observation of satellite orbits and the analysis of satellite radio signals. Both yield integrated values of upper atmosphere parameters instead of instantaneous point values derivable from in-situ measurements. Variations in time and position are thus blurred in radio-signal analyses. Both kinds of experiments, however, can be carried out on the ground with a minimum of apparatus. Both optical and radio observations have added much to our knowledge about the upper atmosphere.

Before launching into a more detailed discussion of ionospheric effects on satellite radio signals, it is worthwhile noting that these effects are strongly frequency dependent. The lower the transmitted frequency, the more marked the effect. (See sec. 5–5.) The ionosphere is generally opaque to radio waves below the maximum plasma frequency of the ionosphere, which is usually between 5 and 15 megacycles. Above 1000 megacycles, the ionosphere is so transparent it might as well not exist. Many Russian satellites have used 20- and 40-megacycle telemetery, while most U.S. satellites have transmitted data at 108 and 136 megacycles, (the Minitrack frequencies), which are less affected by the ionosphere. The United States, however, has provided special low-frequency beacons on many satellites to aid the scientists engaged in ionospheric studies.

First, consider the Faraday effect. When a linearly polarized radio wave enters the ionosphere, electrons in the ionosphere are forced to vibrate in concert with the electric-field vector. If no magnetic field were present, the presence of the electrons would only increase the phase velocity of the wave, causing the usual refraction. A magnetic field, however, will exert a force at right angles to both the direction of electron motion and the magnetic-field vector. The radio wave reemitted by the accelerated electrons will be slightly distorted, because the electrons have deviated from plane of polarization of the incident wave. The net result is a rotation of the plane of polarization. This phenomenon is termed the ''Faraday effect.''

The amount of rotation depends, in part, upon the total number of electrons along the path of transmission. Consequently, as a satellite passes over a ground station and the slant transmission path changes, a simple dipole antenna will record a signal with

---

[3] Two excellent survey articles have been written, by Garriott and Bracewell (ref. 16) and Mass (ref. 17).

TABLE 11–5.—*Instruments, Experimenters, and Experiments for Ionospheric Physics*

Radio Propagation Experiments

Satellite transmitters and Earth-based receivers: [a]

OV–2–5	Mullen, J. P./AFCRL	ORBIS beacons at 10, 30, 31 Mc. High orbit.
USAF satellites	Mullen, J. P./AFCRL	ORBIS beacons carried by many classified satellites.

Satellite-to-satellite propagation experiments:

OV–4–1, 2	Barker, J. L./USAF	Study of ionospheric ducts by satellite-to-satellite transmission in range 20–50 Mc.

Topside-sounder experiments:

Alouette 1	Warren, E. S./DRTE	Swept-frequency type; 0.5–11.5 Mc at 1 Mc/sec.
Alouette 2	Chapman, J. H./DRTE	Swept-frequency type; 0.2–14.8 Mc.
Alouette C	Chapman, J. H./DRTE	Swept-frequency type; 0.1–16 Mc.
Alouette C	Chapman, J. H./DRTE	Fixed-frequency type.
Explorer XX	Knecht, R. W./Central Radio Prop. Lab	Fixed-frequency type; 2.85, 3.72, 4.60, 5.47, 6.82, 8.57 Mc.
TD–2	Dieminger/Max Planck Iono. Phys. Inst.	Swept-frequency type; 0.5–18 Mc.

Passive radio-receiver experiments:

Alouette 1	Belrose, J. S./DRTE	vlf receiver for whistlers, choruses, hiss bands.
Alouette 2	Belrose, J. S./DRTE	vlf receiver for whistlers, choruses, hiss bands.
Alouette C	Belrose, J. S./DRTE	vlf receiver; 0.05–30 kc; same purpose as above.
Explorer VI	Helliwell, R. A./Stanford	vlf receiver.
FR–1A	Storey, L. R. O./CNES	vlf receiver to study propagation from natural and manmade noise sources.
Hitchhiker 2	White, S./Aerospace	vlf receiver.
Injun 3	Gurnett/S. U. Iowa	vlf receiver; 1–10 kc.
Injun follow-ons	Van Allen, J. A./S. U. Iowa	Receiver using two balanced dipoles.
Lofti 1, 2A	—/USN	Two vlf receivers each; 10.2 and 18 kc.
OGO I, B, II, D	Helliwell, R. A./Stanford	vlf receiver for noise-propagation studies; 0.2–100 kc.
OGO II, D	Morgan, M. G./Dartmouth College	vlf receiver to study terrestrial noise; 0.5–10 kc.
OGO E	Crook, G. M./TRW Systems	Electric- and magnetic-field antenna to study low-frequency waves.

OV-1	McPherson, D. A./Aerospace	vlf receiver; 2–1000 cps.
OV-2-5	McPherson, D. A./Aerospace	vlf receivers; 8 bands, 10 cps to 20 kc.
UK 3	Kaiser, T. R./U. Sheffield	vlf receiver; less than 20 kc.
UK 3	Ratcliffe, J. A./Radio Res. Sta.	Intensity, distribution, propagation of terrestrial noise; 5, 7.5, 10 Mc.
USAF satellites	—/	Over 40 military satellites have carried vlf receivers.

Direct Measurements From Satellites

Electric-field meters:		
Explorer VIII	Donley, J./GSFC	Shutter type. See text.
OV-1-7	Heppner, J. P./GSFC	
Sputnik 3	—/	
Standing-wave impedance probes:		
OV-2-3	Ulwick, J. C./AFCRL	
OV-3-5	Ulwick, J. C./AFCRL	
USAF satellites	—/	Several classified satellites have carried this type of instrument.
rf impedance probes:		
Ariel 1	Sayers, J./U. Birmingham	rf-capacitance probe for dielectric current.
Explorer VIII	Kane, J. A./GSFC	6-m dipole sensor.
FR-1A	Sayers, J./U. Birmingham	39-Mc capacitance probe, wire-mesh plates.
OV-3-5	Ulwick, J. C./AFCRL	
RAE A, B	Stone, R. G./GSFC	
Starad	Haycock, O. C./U. Utah	
UK 3	Sayers, J./U. Birmingham	rf-capacitance probe, wire-mesh plates.
USAF satellites	—/	Several classified satellites have carried this type of instrument.
Langmuir probes:		
Ariel 1	Boyd, R. L. F./University College	Electron-temperature gage.

[a] All transmitting satellites are useful here, particularly those carrying low-frequency beacons. Special beacons were installed on Alouette C, Explorer XXII, Explorer XXVII, IMP D, IMP E, Lofti 1, Lofti 2A, OGO I, all Oscars, and San Marco 1.

TABLE 11–5.—*Instruments, Experimenters, and Experiments for Ionospheric Physics*—Continued

Radio Propagation Experiments—Continued

Langmuir probes—Continued

DME–B	Brace, L./GSFC	Two probes for temperature/density variations.
ESRO 1	Willmore, A. P./University College	
Explorer VIII	Bourdeau, R. E./GSFC	
Explorer XVII	Spencer, N./GSFC	
Explorer XX, XXVII, XXXI	Brace, L./GSFC	
OV–1	Sandock, J. A./AFCRL	
OV–3–5	Ulwick, J. C./AFCRL	

Planar ion traps:

AE–B	Brace, I. H./GSFC	Thermal electron density.
Explorer VIII	Bourdeau, R. E./GSFC	Five traps with various electrode arrangements.
Explorer XVIII, XXI, XXVIII.	Serbu, G. P./GSFC	Two grids, plus collector for thermal-ion and electron experiments.
Explorer XXXI	Willmore, A. P./University College	Three traps for thermal ions and electrons and energetic electrons.
	Donley, J./GSFC	Energetic electron-current monitor.
	Maier, E./GSFC	Planar retarding-potential analyzer.
Geophysical Research Satellite	—/AFCRL	Electrons and protons: 0.1–50 keV.
IMP F/G	Van Allen, J. A./SUI	Gridded traps for ion and electron densities.
OGO I, B	Whipple, E. C./GSFC	Retarding-potential analyzer.
OGO II, D	Bourdeau, R. E./GSFC	Ions and electrons <100 eV.
OGO E	Serbu, G. P./GSFC	Electron trap.
RAE A/B	Stone, R. G./GSFC	

Spherical ion traps:

Ariel 1	Boyd, R. L. F./University College	9-cm sphere with 10-cm grid for ion mass, composition temperature.
DME–B	Sagalyn, R. C./AFCRL	Ion temperature and density.
Elektron 2, 4	—/—	Ion temperature and density.

ESRO 1	Willmore, A. P./University College	Ion temperature and density.
Explorer XX, XXXI	Boyd, R. L. F./University College	Ion temperature and density.
Explorer XXV	Sagalyn, R. C./AFCRL	Two traps; electrons and ions; 0–1.5 keV.
Injun follow-ons	Sagalyn, R. C./AFCRL	Ions, 0–1.3 keV.
OGO I, B	Sagalyn, R. C./AFCRL	Ion density and energy; 0–1 keV.
OGO E	Sagalyn, R. C./AFCRL	Thermal and epithermal plasma; 0–2 keV.
	Boyd, R. L. F./University College	Electron temperature and density.
OV–2–5	Smiddy, M./AFCRL	Study of ionosphere storms.
Sputnik 3	Gringauz, K./—	
Ion mass spectrometers:		
AE–B	Taylor, H. A./GSFC	rf type.
DME–B	Narcisi, R./AFCRL	Quadrupole type; 1–20 amu.
Elektron 1, 2, 3, 4	—/—	Probably rf type; 1–34 amu.
Explorer XXXI	Hoffman, J./NRL	Magnetic type; 1–32 amu.
Michael	—/U. Mich.	Quadrupole type.
OGO I, B	Taylor, H. A./GSFC	rf type; 1–50 amu.
OGO II, D	Taylor, H. A./GSFC	rf type; 1–6, 7–45 amu.
	Schaefer, E. J./U. Mich.	Quadrupole type; ion and neutral modes; 0–6, 0–40 amu
OGO E	Sharp, G. W./Lockheed	Magnetic type; H^+, H_2^+, He^+, and heavy ions.
OV–3–6	Narcisi, R./AFCRL	Quadrupole type; ionospheric irregularities.
Sputnik 3	—/—	rf type.
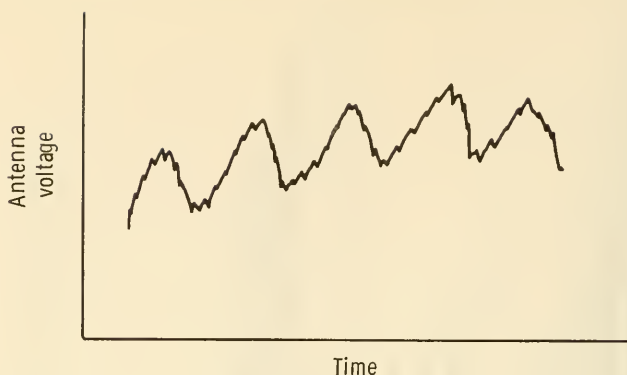
FIGURE 11–21.—Satellite signal strength received by a
ground station, showing noise superimposed on
Faraday fading. Minima occur when signal's plane
of polarization is perpendicular to ground antenna.

deep minima (fig. 11–21), caused as the angle of polarization
rotates with respect to the antenna. This effect is superimposed
upon signal maxima and minima due to satellite spin. The dis-
tance between adjacent minima represents one complete revolu-
tion of the plane of polarization.

Garriott gives the following equation for the number of total
revolutions of the plane of polarization

$$\Omega = \frac{K}{f^2} \int_0^{h_s} H_L N \sec \chi \, dh \qquad (11\text{–}8)$$

where

Ω = the number of revolutions of the angle of polarization
f = frequency
h_s = the height of the satellite above the receiving station
N = the electron density, which depends upon both time and
position
H_L = the component of the magnetic field in the direction of
propagation
χ = the angle the ray makes with the vertical. Since the propa-
gation path is not straight, this is also a variable
h = height above the receiving station
K = a collection of constants = 4.72×10^{-3} (mks)

It is apparent that a ground-based observer can count the number
of complete revolutions of the plane of polarization as the satellite
passes overhead, but he cannot find the total number of revolu-
tions at any one time without additional knowledge. A "zero"

from which counting may begin occurs when the direction of propagation is transverse to the Earth's magnetic field. At this instant, no magnetic force is exerted on the ionospheric electrons accelerated by the radio-wave's force, and there is no rotation at all of the plane of polarization. If the satellite can be received at this point, the observer can count each subsequent fading minimum and obtain the total rotation, and, hence, the product $H_L N$ at each point along the satellite orbit.

An alternate way of adding a reference scale to the experiment involves placing two or more transmitters on a satellite. The transmitters would have close frequencies; say, 40 and 41 megacycles. Because the total angle of rotation of the plane of polarization is inversely proportional to the square of the frequency, simultaneous recordings of the signals will show a clear-cut difference in the frequency of the minima arising from polarization fading. For 40 and 41 megacycles the minima would coincide every 20 cycles. In other words, the rates of rotation differ by 5 percent. Assuming constant rates of rotation, extrapolation backward (or forward) of the two rates in time will permit an estimate of when $\Omega = 0$ and, thence, a count of the total number of revolutions. Satellites, such as Explorer XV, carry multiple beacons for just this purpose.

A second important technique employed in estimating the total number of electrons in the path of the electromagnetic waves moving between satellite and ground-based observer utilizes the distorting effect of the free electrons of the normal Doppler shift. In section 6–2, it was shown how the satellite's position can be determined by making a record of the apparent satellite transmitter frequency as a function of time. Imagine first a Doppler record, such as that shown in figure 6–5, made at a high frequency, where the effects of the ionosphere are nearly nil. Next, consider a lower frequency signal, between 20 and 200 megacycles, from a second transmitter, traversing the same space. The presence of the electrons in the ionosphere will first increase the low-frequency signal's phase velocity. Second, refraction changes the ray path more than it does for the high-frequency signal. Both effects combine to create the dispersive Doppler effect, or Doppler-shift offset, a change in the frequency change seen as the satellite passes over a station. The shift in the Doppler shift depends upon the total electron content of the ray path. This second-order shift is easily measured when high- and low-frequency transmitters are present on the same satellite. It leads to estimates of total electron content of the ray path. The mathematical rela-

tionships are rather complex, and the reader is referred to Garriott and Mass for details. It is significant that the Faraday effect yields the integral of $H_L N$, while the dispersive Doppler effect gives the integral of N alone. Simultaneous application of the two techniques and subsequent separation of H_L can be useful in geomagnetic studies.

So far, the ionospheric experimental techniques presented have depended upon measurements of the satellite signal's polarization and frequency. The first measurement led to calculations of changes in polarization angle and the second to changes in Doppler shift. A ground-based observer can also attempt to measure absolute amplitude and direction of arrival. In the latter instance, the difference between the angles of arrival of radio and optical signals (visual sightings) is a function of the total electron content of the ray path, which determines the refraction of the radio waves. Some studies have been made of angles of arrival, but they have generally been less successful in establishing the electron content of the ionosphere than the Faraday and Doppler measurements described above. The comparison of received signal amplitudes with those expected without an absorbing and scattering ionosphere lead to insights regarding the fine structure of the ionosphere, as described below.

The ionosphere is often described as "layered," but this adjective incorrectly describes the overall morphology, which actually consists of a smooth variation of electron density with height with a varying fine structure of pockets and troughs of high and low electron density. When the radio signal from a moving satellite impinges on this fine structure, it is scattered and refracted in the same way that the turbulent neutral atmosphere causes visible stars to twinkle. The net result is an amplitude record at the receiving station like those portrayed in figure 11-22 (ref. 18). The sharp variations, or scintillations, occurring within time periods on the order of seconds can be easily distinguished from the longer period, regular fadings due to satellite spin and polarization changes. Scintillations indicate ionospheric fine structure and give the observer some clues about the sizes and shapes of the scattering regions. Analyses, such as those of Yeh and Swenson, show that scintillations vary systematically with geomagnetic latitude, season, time of day, and phase of the sunspot cycle. Strong scintillations have been observed simultaneously with red auroral arcs, illustrating a probable common source.
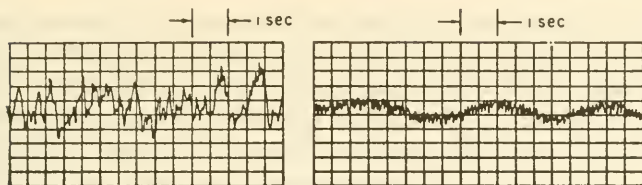
(a) URBANA, 2343 CST, JAN 23, 1960. (LEFT TRACE SHOWED SCINTILLATION, RIGHT TRACE NO SCINTILLATION, NOTE THE SPIN AND FARADAY FADINGS.)
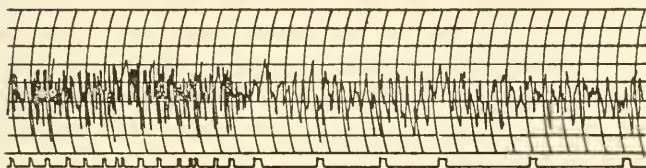
(b) BAKER LAKE, 1015 CST. JAN. 10, 1960. (SECOND MARKS ON THE LOWER SCALE.)

FIGURE 11–22.—Some typical scintillation records (ref. 18).
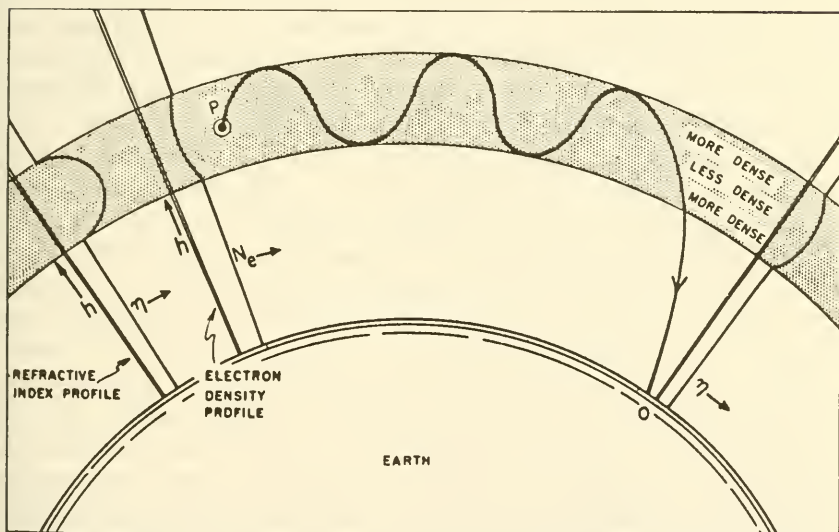
FIGURE 11–23.—Signal ducting due to a "trough" in the electron-density profile (ref. 19).

A fascinating ionospheric structure is the propagation duct that can be created when there is a minimum in electron density occurring between two maxima, as shown in figure 11–23. Satellite signals emitted and "trapped" within the highly refractive

sides of the duct may propagate thousands of kilometers.[4] It is possible that stable propagation ducts for frequencies between 20 and 50 megacycles may exist around the entire Earth. The low-frequency signals of the early Sputniks, for example, were frequently heard when the satellites were on the opposite side of the Earth. The Air Force has sponsored the Orbis (Orbiting Radio Beacon Ionospheric Satellite) experiments, which are intended to explore propagation ducts in a more systematic fashion and which are carried on Air Force piggyback satellites. An Orbis beacon transmits continuously on two frequencies; one will usually be above the daytime plasma frequency and the other below it. Signals are monitored by a dozen or more ground stations. The satellite position is well known, and the presence of ducting would be indicated when signals were picked up far from the source, where "windows" in the duct are present (ref. 19). Similar beacon experiments, under the code name "Nora Alice," were built by the University of Illinois and carried on Discoverers 32 and 36 in 1961 and 1962.

Satellite-to-Satellite Propagation Experiments.—Two scientific satellites operating together can give the researcher more control over the experiment than a single satellite with fixed ground stations. One class of satellite-to-satellite propagation experiments removes much of the ambiguity and confusion inherent in transmissions that must pass through hundreds of kilometers of uncertain atmosphere and ionosphere. Visualize two satellites in roughly the same orbit but separated by a few kilometers, armed with transmitters and receivers. Carefully controlled experiments involving ionospheric absorption, the Faraday effect, and the dispersive Doppler effect could be carried out free from the distortions caused by portions of the ionosphere below the satellites. A second class of experiments that naturally falls to coordinated pairs of satellites is the controlled study of long-distance ducting. Satellites, perhaps located at conjugate points but still within the postulated ionospheric duct, could transmit signals to one another to study the stability, extent, information-carrying capability, and general geometry of the duct. There would be no need to rely upon fortuitous duct windows that permit ground stations to get a glimpse of ducted transmissions. The Air Force has built such an experiment to investigate long-range propagation beyond satellite-to-satellite line of sight. In the Air Force concept, two 100-kilogram, battery-powered satellites would be

---

[4] A good analogy is the sound duct in the ocean, in which distress signals may be transmitted several thousand kilometers.

launched by the same rocket into an orbit between 230 and 320 kilometers. Once in orbit, springs and/or a small rocket would separate and propel the pair of spacecraft into diverging orbits, so that the duct could be studied as a function of satellite-separation distance. Such an experiment may also be carried out using the MOL (Manned Orbiting Laboratory) as the mother vehicle and the OV 4 scientific satellite as an ejected transmitter.

Topside-Sounder Experiments.—Directed radio beams with frequencies below 20 megacycles are usually reflected by the Earth's ionosphere, the precise reflecting conditions being dependent upon electron density and therefore highly variable. The phenomenon of radio-wave reflection can be put to scientific use if one pulses the radio beams and times the echoes. Ionosphere "sounders" made their appearance in the 1930's and laid the foundations for the subsequent development of radar. The timing of the echoes and the sweeping of the transmitter frequency leads to the construction of an ionogram, a plot of apparent height of reflection above the Earth's surface versus transmitter frequency (fig.

Frequency (Mc)
1601 hours l.s.t., 13 June 1962, Maui, Hawaii
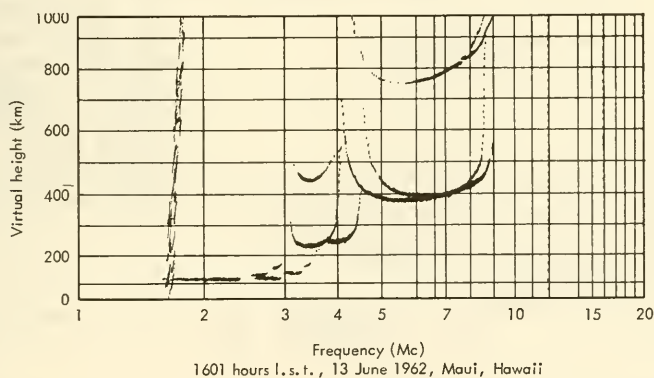
FIGURE 11–24.—A representative bottomside ionogram
(ref. 20).

11–24). From an ionogram comes the computation of electron density as a function of true height. Unfortunately, as figure 11–24 (ref. 20) implies, "bottomside sounding" can only give electron density as a function of altitude below the highest reflections. In other words, the upper regions of the ionosphere beyond the level of maximum electron density are inaccessible to bottomside sounding. The obvious solution to this dilemma is "topside sounding," by a rocket or satellite above the region of peak density. The United States and Canada have cooperated in the

development and launch of several topside sounders: Explorer XX, the Alouettes, and the ISIS (International Satellites for Ionospheric Studies) (table 11–5). The reader should refer to the appendix for descriptions of the listed satellites. Two different but complementary philosophies have been followed in the topside-sounder program:

(1) The United States has concentrated on simultaneous sounding at several fixed frequencies. Only a few points on the ionogram are measured, but soundings are made very quickly, since there is no need to sweep a transmitter. Fixed-frequency soundings reveal fine structure well but are not as successful in obtaining electron-density profiles (fig. 11–25).
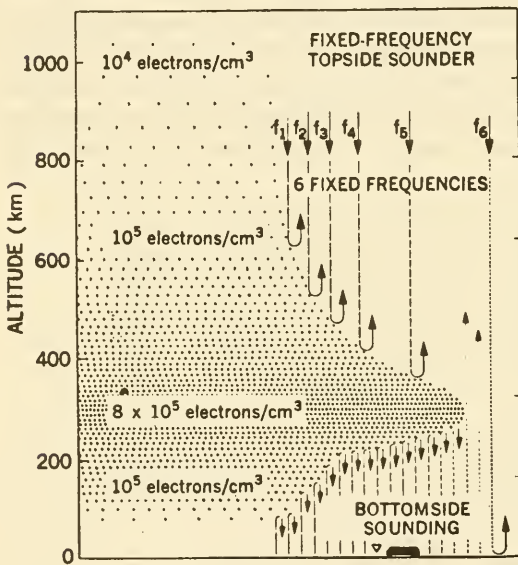
FIGURE 11–25.—Conceptual sketch comparing bottomside sounding with fixed-frequency topside sounding. Note that electron-density minima between maxima would not be seen.

(2) Canada employs swept-frequency sounders, analogous to those used in bottomside sounding. Frequency resolution is good (ionograms are complete), but during the frequency sweep, which takes several seconds, the satellite moves perhaps 50 kilometers horizontally, so that the fine structure of the ionosphere is blurred.

A topside-sounder experiment requires a pulsed transmitter and a listening receiver on the satellite. The antennas must be directed downward into the ionosphere, necessitating either Earth-pointing stabilization or the loss of data when the antennas are not pointing downward. The Canadian satellite, Alouette 1, is taken as representative. The sounder specifications were (ref. 21):

Frequency range_____ 0.5 to 13 Mc
Transmitter power output_____ 100 W
Frequency sweep rate_____ 1 Mc/sec
Transmitter pulse length_____ 100 μsec
Pulse repetition rate_____ 67 pulses/sec
Receiver bandwidth_____ 30 kc
Telemetry frequency (to Earth)_____ 136 Mc
Antenna type_____ Dipole

A block diagram of the Alouette-1 sounder is presented in figure 11–26.
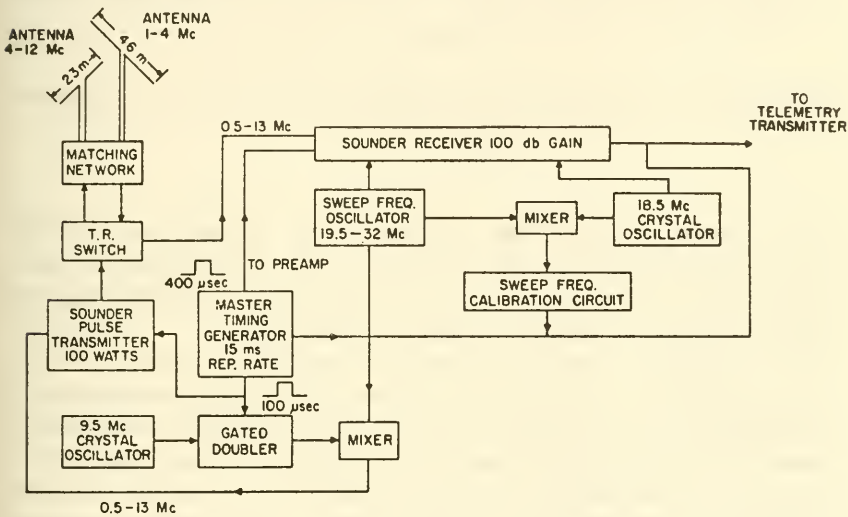
FIGURE 11–26.—Block diagram of the Alouette-1 topside sounder (ref. 21).

The diagnostic capability of the topside-sounder satellite is apparent in the typical ionogram shown in figure 11–27. Here is a good illustration of the value of a satellite's unique vantage point, where it can gather data inaccessible to earthbound equipment. Sounding satellites can also carry vlf receivers, beacons, and instruments for in-situ measurements of ionosphere phenomena. Simultaneous measurements from such an array of instruments are useful in unraveling ionosphere structure.

Passive Radio-Receiver Experiments.—A radio receiver located on a satellite can listen for electromagnetic signals generated by a surprising variety of natural and artificial phenomena. The experimental apparatus is so simple—an antenna plus a receiver—

Satellite height —1023 km
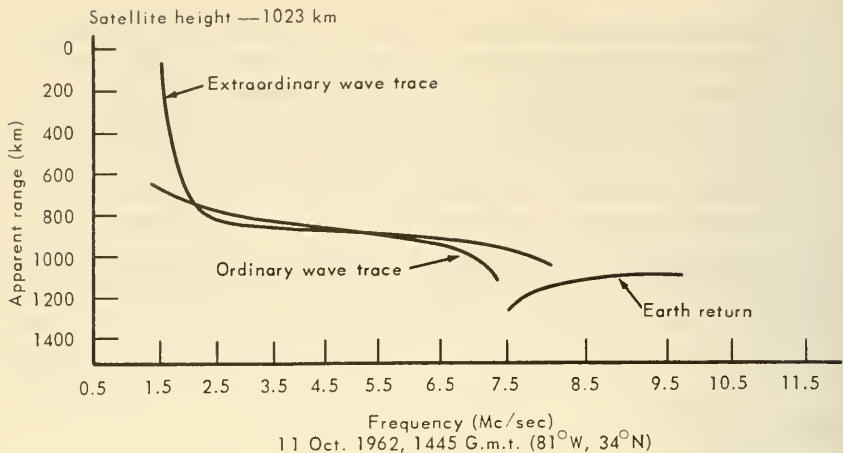
FIGURE 11–27.—A representative topside ionogram taken by a satellite at medium latitudes.

that military and scientific satellites have carried well over 50 such experiments into orbit (table 11–5). The following sampling of some of the experimental possibilities demonstrates the high diagnostic value of this passive approach:

(1) Analysis of vlf radio signals transmitted from Earth stations. (The Navy station NBA, in the Canal Zone, transmitting at 18 kilocycles, is a favorite signal source.) Echoes, propagation losses, and time delays caused by ionospheric phenomena can be studied. Vlf propagation in the ionosphere, for example, is up to 30 times slower than it is in free space. On occasion, repeated echoes of signals bouncing back and forth from pole to pole in whistler ducts can be heard for more than a second after the receipt of the primary signal.

(2) Analysis of natural vlf signals. The possible sources are many: sferics (or whistlers) from lightning, synchrotron radiation from planetary atmospheres (viz, that of Jupiter), synchrotron radiation from cosmic-ray electrons in the interstellar magnetic field, vlf noise from solar plasma interacting with the Earth's magnetosphere, radiation at the local proton gyrofrequency, and the passage of magnetohydrodynamic waves.

(3) Analysis of radio noise from missile launches for purpose of detection.

(4) Measurement of radiofrequency interference (rfi) at orbital altitudes to assess communication problems.

(5) Analysis of propagation modes of cosmic noise in the ionosphere above the satellite.

In the foregoing list, the first two categories involve primarily vlf signals in the frequency range from 1 cps to about 20 kilocycles. The last three categories concern radio noise over the entire radio spectrum. The receivers and antennas employed naturally vary with the frequencies being studied. In addition to the differences caused by frequency, the radio spectrum may either be swept by the receiver (as it is on the UK-3 cosmic-noise receiver) or multiple, fixed-tuned receivers can be used. The latter approach is common in vlf experiments. Conventional radio techniques are used both in receiver design and the transmission of the received analog signals back to Earth (fig. 11–28). The an-
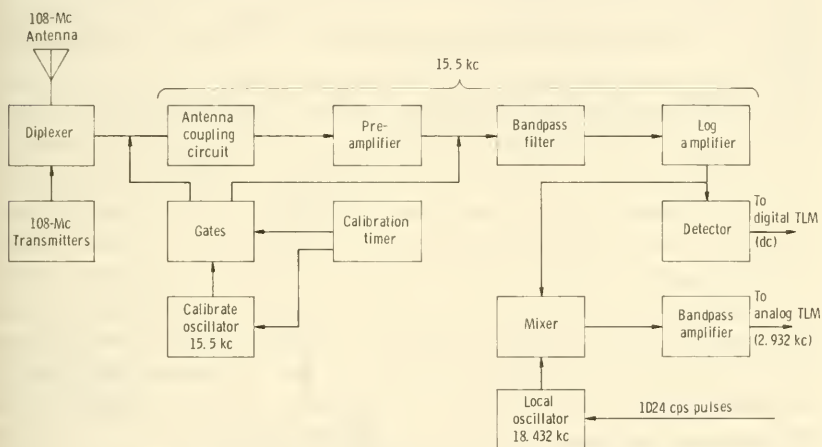
FIGURE 11–28.—Block diagram of the Explorer-VI receiver.

tennas at very low frequencies, however, differ from their high-frequency counterparts. Loop antennas with ferrite cores make their appearance in the low-kilocycle range. Satellite magnetometers, in fact, are also sensitive to low-frequency oscillations in the local field and can be used as vlf receivers.[5]

The OGO–C/D experiment, prepared by R. A. Helliwell at Stanford University, will serve to illustrate a sophisticated version of this kind of instrument (ref. 22). Part of the instrumentation—the inflatable-loop antenna and preamplifier—is located on one of the OGO's extendable booms (EP–5), while a main-body package

---

[5] Search coils are sometimes used. (See table 11–11.)

contains three sweeping receivers, a broadband receiver, and a phase-tracking receiver. Six impulse commands are employed to place the experiment in its different operating modes and tune its receivers to the desired signals. One command inflates the antenna—2.8 inches in diameter—out on the boom. The Stanford instrument is sensitive to magnetic-flux densities on the order of 10^{-5} γ at 0.2 kilocycle to 10^{-6} γ between 10 and 100 kilocycles. Six kinds of measurements are made in this experiment:

(1) Amplitude spectral analysis of signals in the bands: 0.2–1.6, 1.6–12.5, and 12.5–100 kilocycles.

(2) Signal amplitude at single frequencies with the above bands.

(3) Signal amplitudes (with 0.5-kilocycle bandwidth) and relative phase of coherent signals anywhere in the 12.5–100-kilocycle band.

(4) Broadband spectrum of signals in the 0.3–12.5-kilocycle range.

(5) Signal-envelope amplitude in the 0.3–12.5-kilocycle range.
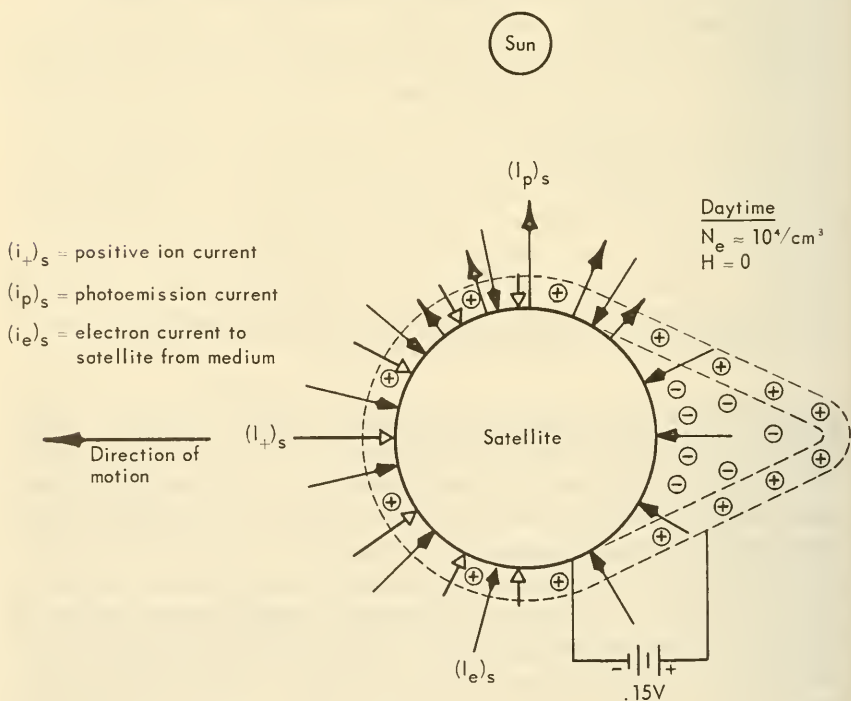
FIGURE 11–29.—The Explorer-VIII ion-sheath model as postulated from experimental data (ref. 1).

(6) Amplitude and phase, relative to the spacecraft clock, of signals between 14.4 and 26.3 kilocycles in 100-cycle increments.

Obviously, radio-signal analysis can become rather involved, but it is such sophistication that extracts the most useful information about the ionosphere.

B.   Direct Measurements from Satellites

Electric-Field Meters.—The purpose of a satellite electric-field meter is the measurement of the strength of the electric field built up between the satellite and the plasma sheath created by interaction of the satellite with the space environment (fig. 11–29). The electric-field strength is directly proportional to the satellite potential relative to the medium and inversely proportional to the thickness of the plasma sheath. An electric-field meter is also sensitive to the net current flowing between the medium and the satellite, as indicated in figure 11–29 for the Explorer-VIII satellite. The meter, which was placed at the forward end of the Explorer-VIII spin axis, consisted of a motor-driven, four-bladed shutter (fig. 11–30). As the shutter turns, and ac signal, V_E, proportional to the product of the electric-field strength and the stator area is generated; i.e., the meter functions as an electrostatic generator. Another signal, V_J, 90° out of phase with V_E and proportional to the net current flow between medium and satellite, is also generated. The two currents can be separated by phase discrimination. As indicated on figure 11–29, the total daytime potential difference between Explorer VIII and environment was only about 0.15 volt when the medium's electron density was about $10^4/cm^3$. At apogee, where the electron density was about $10^3/cm^3$, the potential reversed and became a few tenths of a volt positive. Still, these differences are enough to distort electron-temperature measurements unless care is taken. Vehicle potential and net current flow will be taken up again later in this section when ion traps are discussed.

A few particulars about the Explorer-VIII electric-field meter are: The rotor driven at approximately 7500 rpm was grounded to the satellite skin by brushes. The stator was connected to ground through a resistive load. Exposed surfaces on the meter were gold plated. Rotor-stator spacing was 3 millimeters. The experiment consumed 3 watts, a relatively large quantity of power.

Standing-Wave Impedance Probes.—A possible way to measure the local electron density in the ionosphere is to study how the
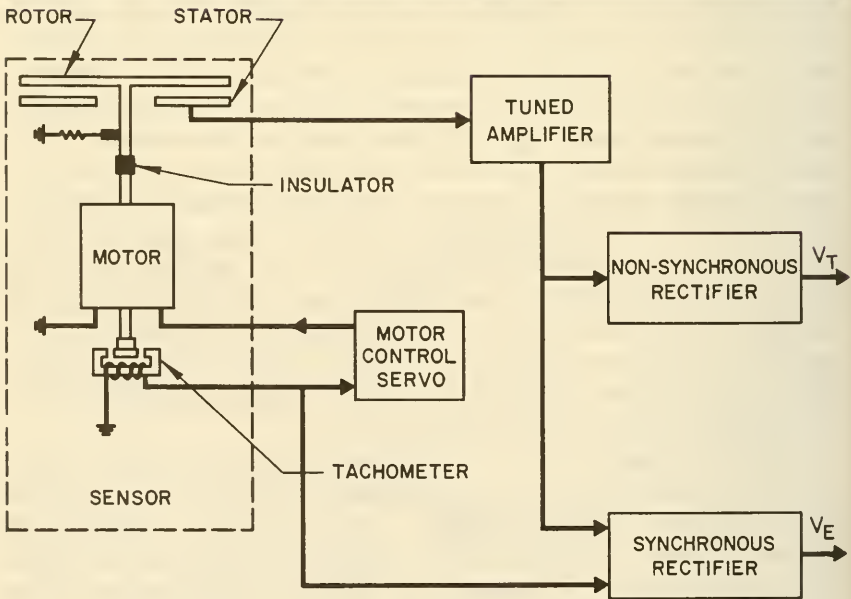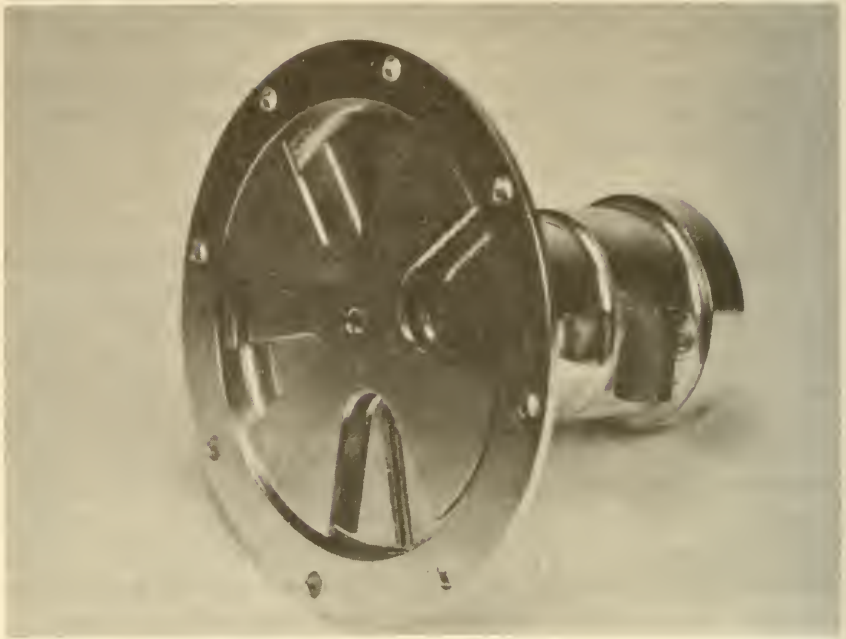
FIGURE 11–30.—The Explorer-VIII electric-field meter (ref. 23).

electrons affect the impedance of a satellite antenna (refs. 24, 25).
Above the local plasma frequency, the presence of free electrons
makes an antenna appear electrically shorter than it would in a
vacuum, thus increasing its capacitive reactance. Below the
plasma frequency, the antenna will appear inductive. At plasma
resonance, resonance occurs. A standing-wave impedance probe
(SWIP) determines the satellite antenna impedance by measuring
the voltages existing on an artificial transmission line, such as
that illustrated in figure 11–31. Haycock gives the following
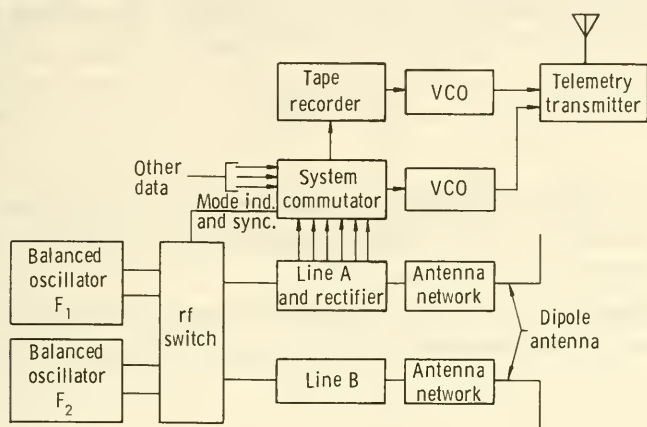
FIGURE 11–31.—Block diagram of a standing-wave-
impedance probe flown on an Air Force satellite
(ref. 24).

equations for the determination of electron density from the
change in antenna reactance, which is computed from the shift
in the standing-wave pattern when the satellite is in the iono-
sphere

$$N = \left[\frac{f^2}{80.6}\right]\left[\frac{C_a + C_{sh}}{C_a}\right]\left[\frac{\Delta X}{X_0 + \Delta X}\right] \times 10^6 \qquad (11\text{–}9)$$

where

    N = electron density (1/cm³)
    f = oscillator frequency (Mc)

    C_a = antenna capacitance
    C_{sh} = shunt capacitance in antenna base (preflight measurement)
    $X_0 = 1/\omega\,(C_a + C_{sh})$ = free-space antenna reactance (preflight
       measurement)

    ΔX = change in antenna reactance

The shift in the standing-wave pattern is measured at tap points along the artificial transmission line. In practice, several different oscillator frequencies are applied and a second artificial line is added for electrical balance. The standing-wave impedance probe has flown frequently on sounding rockets and on military satellites, such as Discoverer 34.

Rf Impedance Probes.—The physical basis of the rf impedance probe is identical to that of the standing-wave impedance probe— the change in antenna impedance due to the presence of free electrons in the ionosphere. Instead of measuring the shift in a standing-wave pattern, however, the change of antenna capacitance is measured. The appropriate equation is

$$\frac{C}{C_a} = 1 - \frac{80.6N}{f^2} \tag{11–10}$$

where

C = the antenna capacitance measured in the ionosphere
C_a = the antenna capacitance measured in a vacuum
f = frequency (kc)

The change in capacitance is easily measured by using the antenna capacitance to control the frequency of an oscillator. Such
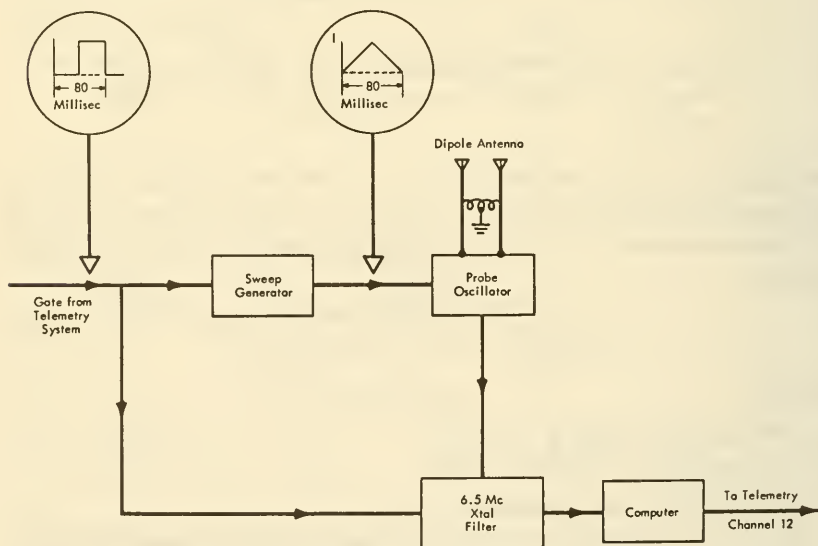
FIGURE 11–32.—The Explorer-VIII rf-impedance probe. The timing of the pulses passing the 6.5-megacycle filter determines the electron density (ref. 1).

a scheme was employed on Explorer VIII, as illustrated in figure 11-32. In this case, a sweep generator started the probe oscillator on a 80-msec up-and-down sweep in frequency. Every time the probe oscillator swept past 6.5 megacycles, a signal would pass the crystal filter shown in the block diagram. There obviously would be two pulses occurring during each 80-msec sweep, but the times at which the pulses occurred, in relation to the start of the sweep, were modified by the capacitance of the antenna, which was an integral part of the oscillator tuned circuit. A small computer associated with the experiment calculated the time intervals between the pulses and the start of the sweep and relayed this data to the telemetry system. On Explorer VIII, the electron density was measured every 40 msec, so that the experiment, considering the satellite velocity, could detect ionospheric inhomogeneities as small as 300 meters. Similar experiments have been included on FR-1, UK 3, and several military satellites (table 11-5). Capacitance bridges are used on some of these satellites to measure antenna impedance changes.

Langmuir Probes.—The Langmuir probe is used extensively to measure electron temperature in the ionosphere. A simple form of this kind of probe exposes a single electrode to the environment, as on Explorer XVII (fig. 11-33). A sweep voltage is then applied between the probe and the other electrode—in this case, the satellite skin itself. At some negative voltage, the probe will
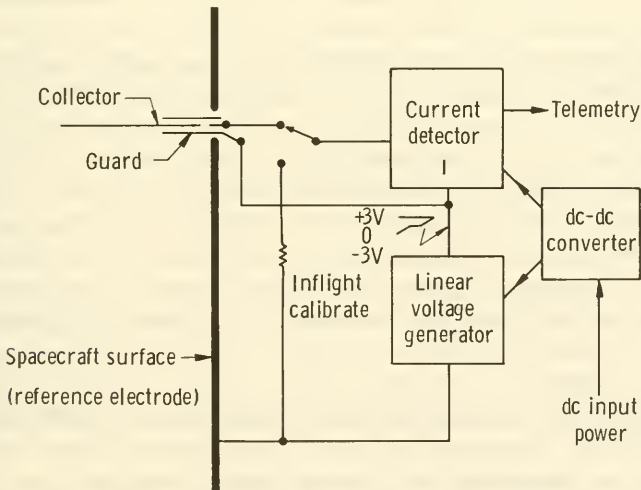
FIGURE 11-33.—Block diagram of the Explorer-XVII Langmuir probe.

draw in and collect a space-charge-limited ion current; at some positive voltage, the current collected will be the space-charge-limited electron current. In between these two extremes, as the probe voltage is swept, the volt-ampere plot will show a region where the electron current collected can be approximated by

$$I_e = I_{e0} \exp\left(\frac{-eV}{kT_e}\right) \tag{11-11}$$

where

I_e = electron current collected
I_{e0} = the undisturbed electron-diffusion current
V = the probe potential
e = the charge on the electron
k = the Boltzmann constant

T_e = the electron temperature

This region is seen on figure 11–34, on the curve marked A. The total probe current is the sum of the electron and ion currents. If the ion current can be subtracted out and I_e is plotted versus probe voltage on a log scale, the slope of the straight-line region will, in theory, yield the electron temperature.

The theoretical curve A in figure 11–34 is based upon assumptions of thermodynamic equilibrium, Maxwellian distributions of ions and electrons, and plane geometry. Actual experimental curves (B in fig. 11–34) vary somewhat from the theoretical plot expected (ref. 26). Simultaneous independent measurements of such parameters as satellite potential and electron-diffusion current help interpret the measurements of a Langmuir probe.

The Langmuir probe has been orbited on many scientific satellites (table 11–5), usually in the company of other instruments, which measure other characteristics of the ionosphere. The physical geometry of the Langmuir probe varies considerably. Besides the simple cylinder of Explorer XVII, flush disk probes are common (Ariel 1). Here again, the satellite skin forms the second electrode. Langmuir probes made from concentric spheres with a perforated outer surface have also made their appearance.

Planar Ion Traps.—In the studies of the Earth's ionosphere, sounding rockets and satellites have carried a large variety of flush-mounted plasma probes with plane, parallel grids and collectors. With few modifications, these probes have also been employed in interplanetary plasma measurements (sec. 12–3). The gridded planar probes reject or accept charged particles in various energy ranges by stepping the voltages impressed on their
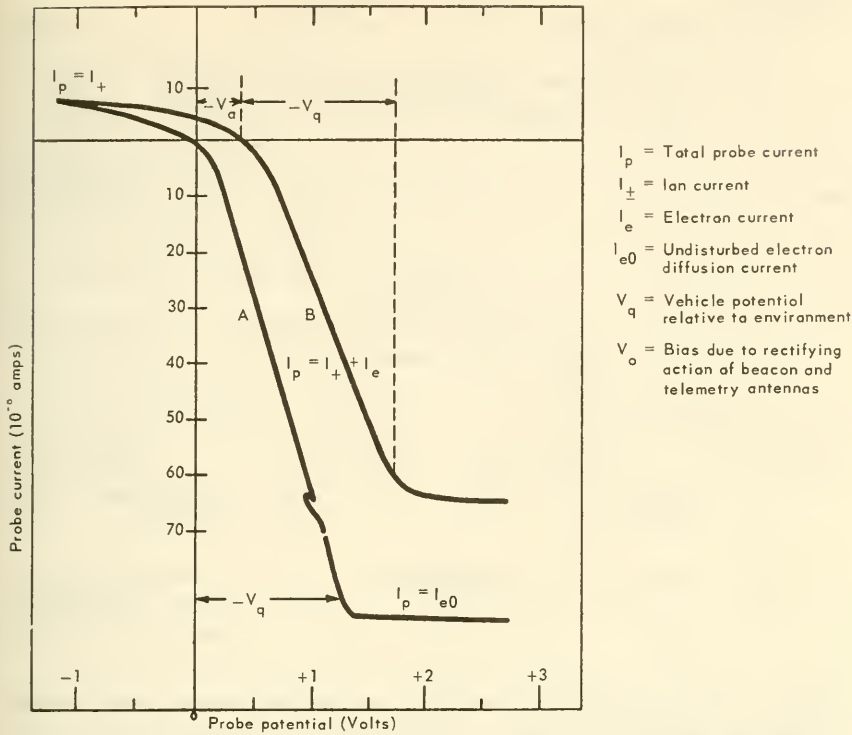
FIGURE 11–34.—Langmuir-probe *I–V* curves.   *A:* theoretical; *B:* experimental (ref. 26).

grids.   This method of particle-energy selection has led to the use of the term "retarding-potential probes" in describing these devices.   The planar probes constitute a large class.   There exist many variations in geometry, number of grids, grid-modulation techniques, and number of collectors.

Explorer VIII carried a series of planar probes that merits description.   The exposition logically begins with a simple, bare collector mounted flush with and electrically insulated from the Explorer-VIII satellite skin (fig. 11–35*a*).   A collector exposed like this measures the total current of incident protons, electrons, other charged particles, and photoelectrons emitted from the collector.

The addition of a single grounded grid and a positively biased collector (fig. 11–35*b*) permits the measurement of electron current as a function of satellite attitude.   Ambient positive ions are repelled and photoelectrons are pulled back to the collector surface.   The recessing of the collector defines a conical acceptance
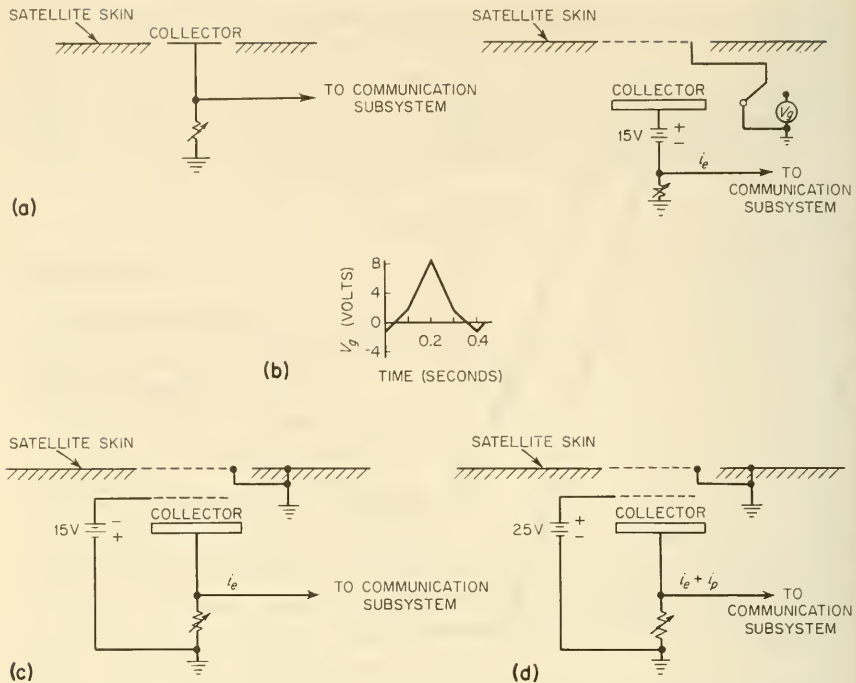
FIGURE 11-35.—Electrical connections for the four planar plasma probes flown on Explorer VIII. (*a*) Total-current monitor, which uses Langmuir-probe geometry but lacks the swept voltage. (*b*) Electron-temperature probe. (*c*) Ion-current probe. (*d*) Electron-current probe (ref. 1).

angle. The Explorer-VIII experiment sketched in figure 11–35(*b*) also allows the grid to be swept from −1.2 to +8 volts in order to measure the spacecraft equilibrium potential and the external electron temperature (ref. 26).

The addition of a second grid between the grounded outer grid and the collector enables a probe to measure positive ion and electron currents. Explorer VIII carried two of these three-element probes. One, with the inner grid at −15 volts, collected incoming positive ions while repelling external electrons and suppressing internal photoelectrons. The second probe, with an inner grid bias at +25 volts, measured the incident electron flux and the now unsuppressed photoemission current (figs. 11–35*c* and 11–35*d*). Bourdeau et al., at the Goddard Space Flight Center, have approximated the positive-ion current obtained with a three-element planar probe by

$$i = \alpha A N e V \cos \theta \qquad (11\text{--}12)$$

where

i = the positive-ion current
α = the outer-grid transparency to positive ions
A = the probe area
N = the ambient positive-ion density
e = the charge on the electron
V = the satellite velocity
θ = the angle with the probe axis

This equation is accurate only when $\theta = 45°$.
Summarizing the four Explorer-VIII probes:

Probe construction	Figure	Currents measured
Bare collector	(11–35(a))	electron + positive ion + photoelectron
Two elements	(11–35(b))	electron
Three elements, +bias	(11–35(c))	electron + photoelectron
Three elements, −bias	(11–35(d))	positive ion

The operation of the various Explorer VIII planar probes is representative of the many similar probes, listed in table 11–5, that have already flown or are about to fly.

Spherical Ion Traps.—The operating principles of spherical ion traps are essentially identical to those of the planar traps. The spherical geometry, of course, makes the experiment insensitive to the satellite attitude in space. On the other hand, experimenters sometimes wish to provide directionality to their apparatus.

In table 11–5, one notes the widespread use of spherical ion traps. Gringauz was the first to place this kind of instrument on a satellite; Sputnik 3, in this instance (ref. 27). Boyd and Wilmore, at University College, London, have applied this instrument extensively.[6] Sagalyn, at the Air Force Cambridge Research Laboratories, has built spherical probes for several USAF and NASA satellites. Her OGO-E equipment is used here to illustrate this type of instrument.

The objective of the OGO-E experiment is the measurement of the spatial and temporal variations in the concentration and energy distribution of changed particles in the region from 200 kilometers to 15–50 Earth radii. The experiment employs two multielectrode spherical analyzers, which are shown attached to their folded booms in figure 11–36. By suitably varying the sweep

---

[6] Boyd and Wilmore apply the term "mass spectrometer" to the spherical ion trap, whereas American usage reserves this name for instruments where there is a dispersion or filtering of ions of different mass.
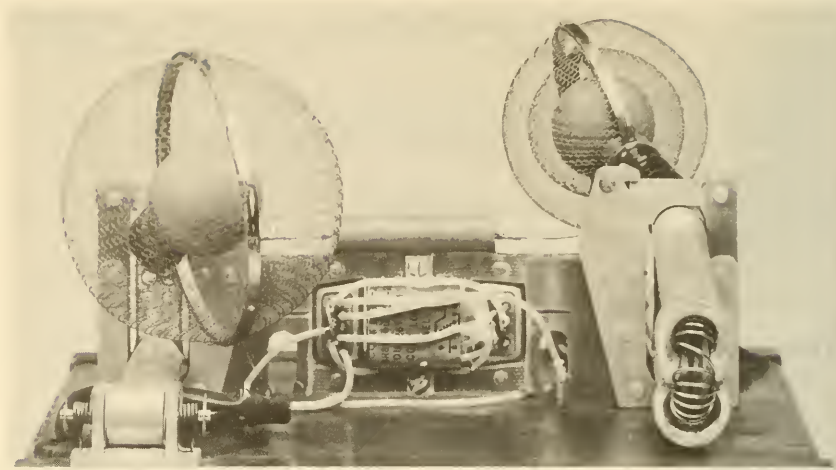
FIGURE 11–36.—Spherical plasma probes of the type used on OGO E. One sensor is for electrons, the other for ions. The outside tungsten spherical meshes are about 7.5 centimeters in diameter. In space, the booms (about 1 m long) will be unlocked. (Courtesy of R. Sagalyn.)

and step voltage applied to the concentric mesh-type grids, the following parameters can be measured.

(1) Densities of positive and negative particles.

(2) Kinetic temperatures of thermal ions and electrons in the 700°–4000° K range.

(3) Flux and energy spectrum of protons and electrons in the range 0–2 keV.

(4) The potential of the satellite relative to the undisturbed plasma.

Each of the two sensors is made of tungsten mesh with a transparency of 80–90 percent. One sensor measures electrons, the other protons. To obtain all the information listed above, the experiment operates in five distinct modes, each mode consisting of different potentials, sweeps, and stepped voltages applied to the various grids.

Faraday-Cup Plasma Probes.—Faraday-cup probes are in reality planar, retarding-potential probes, like those described earlier. The current-collecting electrode of the Faraday-cup probes are generally cuplike rather than flat, and this electrode is sometimes segmented in order to measure plasma-velocity vectors. Probe operation, though, is essentially the same as that of the gridded probes. For more details concerning Faraday-cup probes and discussion of their use in plasma measurements, see section 12–4.

Ion Mass Spectrometers.—The only difference between ion and neutral mass spectrometers is the presence of an ionizing element and an ion trap in the latter. The ionizing element or ion source is needed in the neutral mass spectrometer to add the necessary charge to the particles being analyzed, while the ion trap excludes the unwanted ion population. In ionospheric research, however, only the ionized population is desired. A drawing-in grid often precedes the spectrometer proper. Neutral particles that invade the spectrometer will not be analyzed. Since the two types of spectrometers are otherwise identical, only representative ion mass spectrometers from table 11–5 will be covered here. The reader should refer to section 11–2 for a presentation of operating principles.

G. W. Sharp, at Lockheed Missiles & Space Co., has built a magnetic mass spectrometer for OGO E that can resolve H^+, H_2^+, and He^+ at the upper edges of the atmosphere. Ions enter the instrument (fig. 11–37) with a velocity determined by the satellite velocity and charge. The entrance grids collimate the ions and accelerate them to velocities much greater than that due to
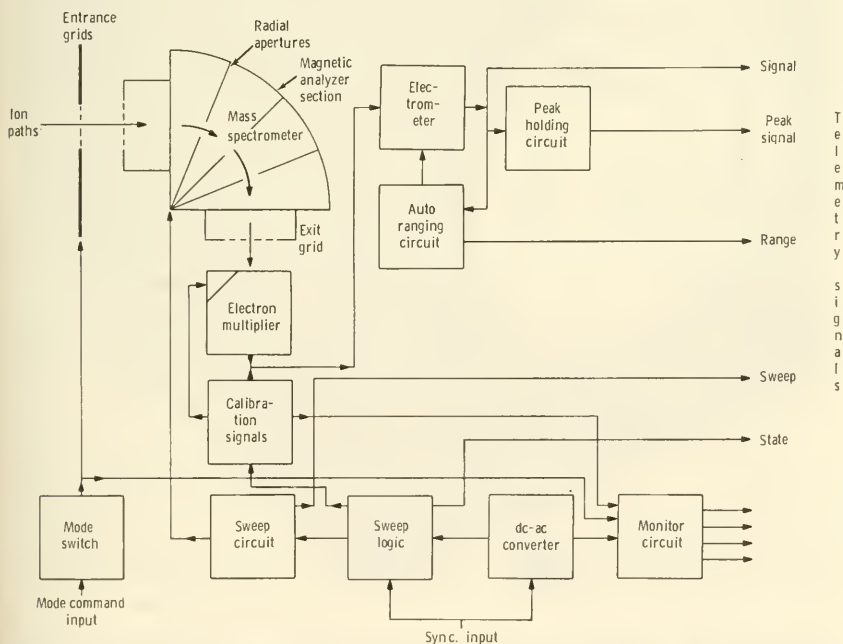
FIGURE 11–37.—Block diagram of the OGO-E light-ion magnetic mass spectrometer. Four components are measured: H^+, H_2^+, He^+, and all heavier ions. (Courtesy of G. W. Sharp.)

vehicle velocity and charge. The ions now enter the magnetic analyzer section, which is formed from two 90°-sector ceramic magnets. The ions traverse a uniform field of about 600 gauss with radii of curvature that depend upon their masses and velocities. The three light ions, H^+, H_2^+, and He^+, will be dispersed into three separate arcs. Depending upon the voltage applied to the entrance grids, only one of these mass components will have the right radius of curvature to follow the tunnel formed by radial apertures inside the analyzer section. The selected ionic component then passes through an exit grid and impinges upon a bare copper-beryllium multiplier, which feeds a signal to an electrometer and the telemetry circuits. The concentrations of other light-ion components can be measured by changing the voltages on the entrance grids. In actuality, the accelerating voltage is swept periodically to provide spectrometer action. Besides isolating the three light ions mentioned above, the spectrometer measures the relative concentration of N^+ and all heavier ions, but cannot resolve them separately.

The quadrupole mass spectrometer is also used frequently for measurements in the ionosphere. A schematic of the OGO–C/D Massenfilter built for NASA by L. M. Jones, at the University of Michigan, is presented in figure 11–38. The reader will note the presence of filaments at the spectrometer's input. This instrument
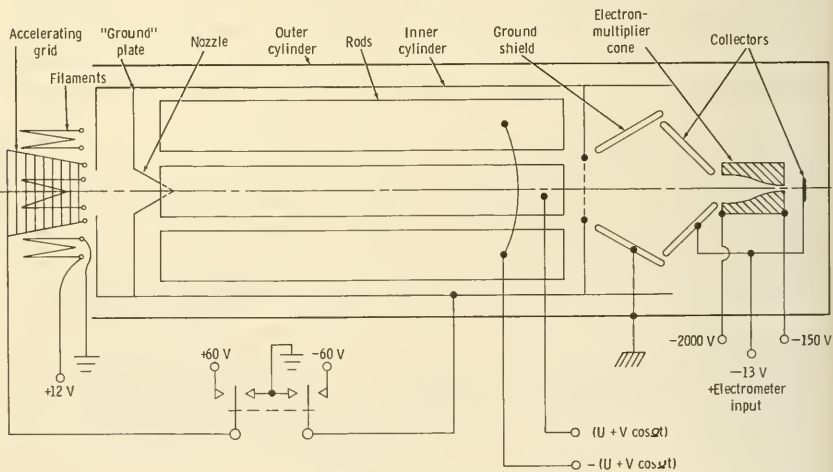
FIGURE 11–38.—The OGO–C/D quadrupole mass spectrometer. This instrument operates in both neutral and ionic modes. (Courtesy of E. J. Schaefer.)

operates in both neutral and ionic modes.   An electrometer is connected to the ion-current collectors to generate an electrical-signal input for the telemetry circuits.   The instrument, plus its supporting electronics, is housed in a cube 20 centimeters on a side (fig. 11–39).   A similar quadrupole spectrometer, designed by R. Narcisi at the Air Force Cambridge Research Laboratories, for the Direct Measurements Explorer A (DME–A), is pictured in
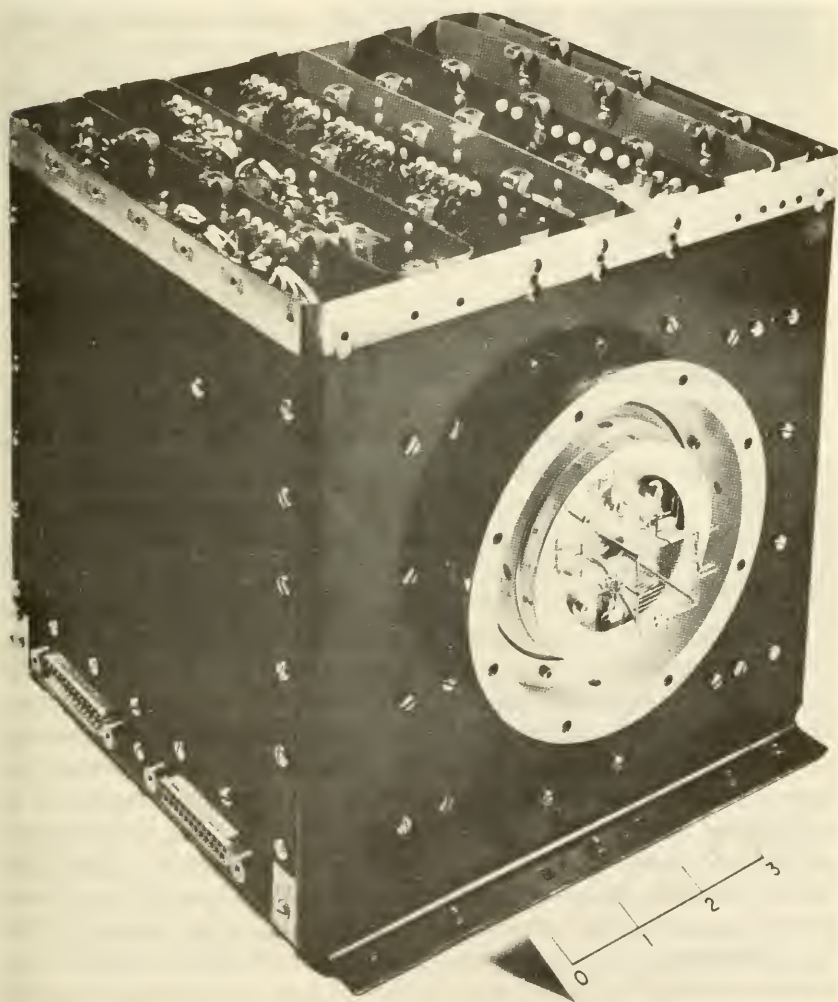
FIGURE 11–39.—The OGO–C/D mass spectrometer package.   The analyzer section lies behind the filaments and grids shown on the side. Scale is in inches.   (Courtesy of E. J. Schaefer.)

FIGURE 11–40.—The
DME–A quadrupole
mass spectrometer with
cover removed. The
analyzer section is
located within the per-
forated cone. Scale is in
inches. (Courtesy of
R. Narcisi.)

figure 11–40. The physical operation of the quadrupole mass
spectrometer was described in section 11–2.

11–4. Instruments and Experiments in the Trapped-Radiation Zone

The first great discovery of the scientific satellite was, of course,
the great radiation zone that enshrouds the Earth. A discovery
per se, however, fully satisfies no scientist. The radiation zone,
or Van Allen Belts, must be measured quantitatively as functions
of time and position. Furthermore, the interfaces between the
belts and the Earth's auroras and the Sun's plasma flux must be
established in detail. To accomplish these purposes, hundreds of
radiation experiments have been flown on scientific satellites.
Many more are planned, for the radiation belts have proven to be
a complicated welter of changing populations and blurred, shift-
ing geometries. No longer does one speak of distinct "belts," but
rather of a zone of trapped radiation. The purpose of this section
is to describe the many and varied orbital instruments used to
probe this zone.

A satellite intersecting the zone of trapped radiation encounters
not only the electrons and protons temporarily captured by the

Earth's magnetic field but also solar and galactic cosmic rays and the particles in the solar-plasma flux. Experiments must distinguish the trapped-particle populations from the solar and galactic invaders. The characteristics of these coexisting populations, listed in table 11–6, indicate that there are several physical parameters of concern. First is the scalar flux, the number of particles or photons crossing a square centimeter of surface each second, regardless of direction. Next, particle energy is of great interest in untangling the origin of the radiation. The directional or vector properties of the particles may also be indicative of their source. Scalar flux, energy, and direction can all be linked together in the definition of the differential flux

$$F = \int_E \int_\Omega F(E,\Omega) d\Omega \ dE$$

where

F = the scalar flux or omnidirectional flux
$F(E,\Omega)$ = the differential flux
E = energy
Ω = solid angle

Space-radiation studies have continually attempted to increase the resolution of energy and directional measurements. The variation of each flux component with time may also help in deciphering its significance. Last, but not least, is the identification of particle species. In mapping the fluxes of space, therefore, the properties of the ideal radiation instrument should include the capabilities for measuring scalar flux, direction, energy, and species as functions of time and position.

Radiation is detected primarily by its interactions with matter, especially those interactions that yield electrical and photonic signals. The chief reaction is bond disruption—an effect including ionization, the creation of lattice defects, and the production of electron-hole pairs. All of the basic detectors described here, except the current collectors, depend upon some bond disruption for signal generation. Since the ultimate signal on a spacecraft must be electrical, if information is to be telemetered back to Earth, all nonelectrical signals (light flashes) must be converted into electrical information, usually digitally coded electrical signals. Furthermore, the signals should be capable of carrying information beyond the fact that a particle has passed through the detector. In other words, the instrument's dynamic range and the bandwidth of its information channels must be consistent with the aims of the experiment.

TABLE 11-6.—*Characteristics of Radiation Encountered in Orbit of the Earth* [a]

Phenomenon	Particles	Energies, eV	References for instrument descriptions
Galactic cosmic rays	p, d, α, γ, and heavier nuclei up to Fe	10^4 to 10^{20}	Section 13-3.
Solar cosmic rays	p, d, α, γ, X-rays, and heavier nuclei	10^4 to 10^9	Section 13-3.
Trapped radiation (Van Allen belts)	p, e	10^3 to 10^8	This section.
Solar wind (plasma)	p, e, perhaps a few heavier ions	Up to 2×10^3	Section 12-3.

[a] See sec. 1-2, for further descriptions.

To illustrate the taxonomy of radiation detectors, they have been divided into three groups in table 11–7.   Intrinsic in the table is the admission that the simple, basic detectors of radiation actually reveal little information when used singly.   Auxiliary equipment is needed to help sort out the energies, species, and directions of the radiation.   Telescope configurations, collimators, different shielding arrangements, pulse-height analyzers, and magnetic dispersion are typical of the stratagems used to turn simple event recorders into sophisticated instruments capable of sorting out the confusion of particles and photons encountered by satellites.

The ensuing discussion of specific radiation instruments follows the organization presented in table 11–7.   Much of the description will be applicable in later chapters that cover cosmic rays and solar plasma.

A.   Basic Detectors

Geiger-Müller Counters.—The Geiger-Müller counter is a ubiquitous space-research tool.   Not only have Geiger-Müller tubes flown on almost every satellite and space probe since Explorer I, but they have been employed widely in arrays to form cosmic-ray telescopes (table 11–8).   Used with magnets, they make spectrometers; combined with other particle detectors, like the ionization chamber, they help to resolve the fluxes, energies, and species of the particles that make up space radiation (table 11–6).

A Geiger-Müller tube usually takes the form of a cylindrical glass or metal tube filled with a gas, like neon or argon (fig. 11–41).   A central wire, positively charged at several hundred to
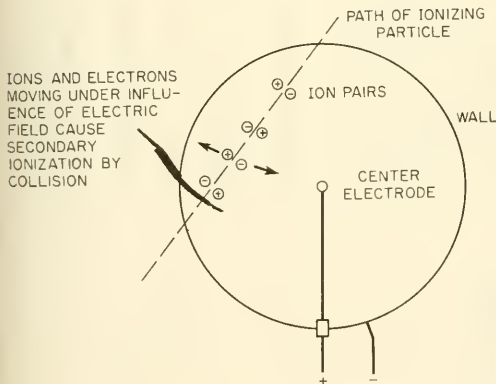
FIGURE 11–41.—Sketch for radiation detectors that depend upon ionization in a gas.   In the Geiger-Müller tube, the high impressed voltage causes electron avalanches to fill the whole tube.   In the proportional counter, the number of ion pairs created by the ionizing particle is multiplied by secondary ionization, but no discharge occurs.   In the ionization chamber, there is no secondary ionization at all.

TABLE 11-7.—*Types of Radiation Instrumentation Used in Satellite Research* [a]

Class	Instrument	Principle of operation	Remarks
Basic detector	Geiger-Müller counter	Particle ionizes gas. Electric field causes avalanche. Counter tube discharges.	Event counter. Used in telescopes, etc. Little discrimination of particles. No energy resolution.
	Proportional counter	Particle ionizes gas. Electric field causes charge multiplication. No discharge.	Weak analog output signal proportional to the amount of ionization.
	Ionization chamber	Particle ionizes gas. Ions and electrons collected without multiplication.	Used with other detectors. Currents low. Integrating chambers used in space. Measures total ionization.
	Channel multiplier	Particle ejects secondary electrons, which then multiply by creating more secondaries.	Used in particle spectrometers. In development stage.
	Scintillators	Particle excites crystal lattice. Recombination causes light flash.	Used in telescopes, etc. Requires photomultiplier tube.
	Cerenkov detector	Particle traveling faster than light in medium emits Cerenkov radiation.	Used in telescopes, etc. Requires photomultiplier tube.
	Cadmium-sulfide cell	Particle creates current carriers in cell, reducing its conductivity.	Analog signal. Requires continuous current supply.
	Solid-state detector	Particle creates hole-electron pairs, which flow as current under influence of junction emf.	Used in telescopes. Generates own signal power. Small active volume often used as a dE/dx detector.

	Current collector	Charged particles in the primary flux are collected directly and a current is measured on an electrometer.	Used in Faraday-cup probes and other plasma analyzers. Applied where there is a large current of charged particles, particularly the solar plasma.
Detector combination.	Telescopes	Geometry and electrical circuitry resolve energy and direction.	Gives energy and direction. Uses almost any basic detector. Primarily a cosmic-ray instrument.
	Magnetic spectrometers	Magnetic field disperses particles into array of basic detectors.	Trapped-radiation spectrometry. Its magnetic fields are often incompatible with magnetometer experiments.
	Electrostatic analyzer	Retarding electrostatic fields sort out charged particles according to energy. Current collectors measure flux.	Used to analyze high fluxes of low-energy particles, particularly the solar plasma, the low-energy components of the trapped-radiation zone, and the particles causing auroras.
	Ionization chamber and Geiger counters.	GM tube counts events. Chamber integrates their energies.	General radiation measurements.
Track imager	Spark chamber	Ionized track in gas causes sparking between foils.	Track-imaging or microphone pickup. In development for satellite use.
	Scintillation chamber	Same as scintillation detector	Track-imaging. In development stage.
	Sensitized emulsions	Ionized trails of particles initiate track forming.	Widely used on recoverable satellites.
	Cloud and bubble chambers.	Ionized trails of particles initiate track forming.	Track-imaging. Generally inferior to above imaging devices in satellite usage.

a Table 11–8 lists the instruments and investigators connected with specific scientific satellites.

TABLE 11–8.—*Trapped Radiation Zone Instruments, Experimenters, and Experiments* [a]

Basic Detectors

Geiger-Müller counters:

Satellite	Experimenter/Institution	Description
Alouette 1	Rose, D. C./DRTE	Three, variously shielded.
Alouette 2	—/Nat. Res. Council	Four, with electron thresholds of 3.9 MeV, 40 keV, 250 keV, 40 keV. Proton thresholds of 40 MeV, 500 keV, 500 keV, 500 keV, 500 keV.
Alouette C	McDiarmid, I. B./Nat. Res. Council	Similar to Alouette 2.
Ariel 1	Elliot, H./Imperial College	Two, in conjunction with cosmic-ray experiment.
Elektron 1, 2, 3, 4	—/—	
ERS 17	—/Aerospace	
ESRO 1	Rybner, J./Tech. U. of Denmark	Four, for angular-distribution studies.
Explorer I, III	Van Allen, J. A./S. U. Iowa	Original intent was to measure cosmic rays.
Explorer IV, VII	Van Allen, J. A./S. U. Iowa	Two, variously shielded.
Explorer XII	O'Brien, B. J./S. U. Iowa	Three. Electrons over 10, 90–100, 2 MeV. Protons over 20, 50 MeV.
Explorer XIV	Van Allen, J. A./S. U. Iowa	One omnidirectional; three directional.
Explorer XXV	Van Allen, J. A./S. U. Iowa	Four directional; two for monitoring; one heavily shielded to measure Starfish decay.
Hitchhiker 1, 2	—/AFCRL	Electrons over 4 MeV, protons over 40 MeV.
IMP D/E	Van Allen, J. A./S. U. Iowa	Two, associated with p-n detector.
Injun 1	Van Allen, J. A./S. U. Iowa	Electrons over 40 keV, protons over 500 keV.
Injun 3	Van Allen, J. A./S. U. Iowa	Five.
Injun follow-ons	Van Allen, J. A./S. U. Iowa	
OGO I	Van Allen, J. A./S. U. Iowa	Three; electrons over 40, 120, 1500 keV.
OGO II, D	Van Allen, J. A./S. U. Iowa	Auroral zone electrons over 40, 100, 250 keV.
OGO E	Frank, L. A./S. U. Iowa	
OSO I	Hess, W./U. Calif.	$B^{10}F_3$ counters for Earth's albedo neutrons.
OV-1	Smart, D. F./AFCRL	Electrons over 4, 40 MeV.
OV-5	Vette, J./Aerospace	Three orthogonal tubes, electrons over 40 keV.
Traac	—/—	Two.
Vanguard I	—/NRL	

Proportional counters:
  None; used only in telescopes so far.
Ionization chambers:[b]

Geophysical Research Satellite	—/USAF	Tissue-equivalent ionization chamber.
Injun 3	Van Allen, J. A./S. U. Iowa	Electron multiplier.

Channel and electron multipliers:
Scintillators:

Alouette 2	—/Nat. Res. Council	Protons 100–600 keV.
Elektron 1, 2, 3, 4	—/—	
ERS 12, 13	—/—	Plastic, omnidirectional.
ERS 17	—/Aerospace	Two. Electrons over 0.7, 5 MeV. Proton ranges 40–80 and 10–30 MeV.
ESRO 1	Dalziel, R./DSIR	Two. Electrons 40–400 keV, protons 1–30 Mev.
Explorer IV	Van Allen, J. A./S. U. Iowa	Two. One plastic, 1 CsI(Tl).
Explorer VI	Farley, T. A./STL	Electrons over 200 keV, protons over 2 MeV.
Explorer XII	Davis, L. R./GSFC	Electrons 10–100 keV, protons 0.1–4.5 MeV.
Explorer XIV, XV, XXVI	Davis, L. R./GSFC	Stepped absorbing wheel. Photomultiplier tube coated with ZnS(Ag).
Explorer XV, XXXVI	McIlwain, C./U. Calif	Two. Spherical omnidirectional plastic, plus directional shielded cylinder.
Explorer XXV	Van Allen, J. A./S. U. Iowa	Two. Electrons over 1.6 keV, protons over 10 keV.
Hitchhiker 1	—/AFCRL	Electrons 0.3–4 MeV.
Injun 3	O'Brien, B. J./S. U. Iowa	Protons over 40 MeV.
OGO I, B, II, D	Konradi, A./GSFC	Trapped and auroral particles. Electrons 10–100 keV, protons 0.12–4.5 MeV.
OSO D	Waggoner, J. A./U. Calif	Electrons over 60 keV, protons over 2 MeV.
OV–1–9	Trafton, L. M./USAF	Shielded, plastic. Protons 20–40 MeV.
OV–1–13	Smart, D. F./AFCRL	Electrons 1–10 MeV.
OV–2–5	White, R. S./Aerospace	Two, CsI.
		See table 13–4.

[a] See table 13–4 for radiation instruments used in cosmic-ray research.
[b] Most ionization chambers are used in conjunction with other detectors.

TABLE 11-8.—*Trapped Radiation Zone Instruments, Experimenters, and Experiments*—Continued

Basic Detectors—Continued

Scintillators—Continued

Sputnik 3	White, R. S./Aerospace	Two.
Starad	—/AFCRL	Five.
	Smith, R./Lockheed	Threshold sensors.
	Paolini, F. R./Amer. Sci. and Eng.	Two in beta-beta-gamma detector.

Cerenkov detectors:

This type of detector is found in cosmic-ray telescopes. See table 13-4.

Cadmium-sulfide cells:

Explorer XII	O'Brien, B. J./S. U. Iowa	Three; 1 with magnetic broom, 1 for total energy, 1 as an optical monitor.
Explorer XXV	Van Allen, J. A./S. U. Iowa	Three; protons over 0.5 keV, electrons over 0.4 keV. One other; electrons over 250 keV.
Injun 1	Van Allen, J. A./S. U. Iowa	Five; 2 with magnetic brooms, 1 as optical monitor.

Solid-state detectors:

Alouette 1, 2	Rose, D. C./Nat. Res. Council	p–n junctions.
Alouette C	McDiarmid, I. B./Nat. Res. Council	Four; protons 0.1–6.3 MeV.
Elektron 1, 2, 3, 4	—/—	
ERS 12, 13, 17	—/Aerospace	p–n junctions.
ESRO 1	Rybner, J./Tech. U. Denmark	Auroral protons 0.1–1 MeV.
Explorer XV, XXVI	Brown, W./Bell Labs	Four for electron spectra, 2 for angular distribution.
Explorer XXV	Van Allen, J. A./S. U. Iowa	One p–n type with 4 energy channels.
IMP D/E	Van Allen, J. A./S. U. Iowa	p–n type; allied with Geiger counters.
IMP F/G	Bostrom, C./J. Hopkins U. APL	
Injun 1	Pieper, G./J. Hopkins U. APL	Four p–n junctions. Protons 1–17, 1–11 MeV.
Injun 3	O'Brien, B. J./S. U. Iowa	Four p–n. Protons 1–2, 2–8, 8–26, 26–100 MeV.
Injun follow-ons	Van Allen, J. A./S. U. Iowa	
OGO E	Coleman, P. J./U. Calif	Used with magnetometers to study magnetohydrodynamic waves.
OV-1-9	Trafton, L. M./USAF	Thick, Li-drift detectors.

OV-1-13	Smart, D. F./AFCRL	Two.
OV-1-14	Blake, J. B./Aerospace	Five, variously shielded.
OV-2-5	Blake, J. B./Aerospace	Five, variously shielded.
	Paulikas, G. A./Aerospace	Five, variously shielded.
OV-5-2	Vette, J./Aerospace	Five, Li-drifted, variously shielded.
Starad	Dyal, P./USAF	Total energy detectors.
Traac	—/—	Six $p-n$ junctions for charged particles; 1 for neutrons.

Current collectors:

Used primarily as detectors in various radiation instruments.

Detector Combinations

Telescopes:

Alouette 2	—Nat. Res. Council	Geiger telescope, protons over 100 MeV.
ERS 17	—/Aerospace	Phoswich.
ESRO 2	Elliot, H./Imperial College	4-element solid-state telescope. Protons 1–100 MeV.
Hitchhiker 1	—/AFCRL	Phoswich.
IMP F/G	Brown, W./Bell Labs	Three-element solid-state telescope; electrons 0.3–3 MeV, protons 0.5–18 MeV.
OGO I, B	Cline, T. L./GSFC	Double gamma-ray spectrometer for positrons.
OV-1-9	Trafton, L. M./USAF	Phoswich for "flare-activated radiobiological observatory."
OV-1-14	Freden, S. C./Aerospace	E vs. dE/dx telescope.
OV-2-5	Mihalov, J. D./Aerospace	
Starad	Paolini, F./Amer. Sci. and Eng	Phoswich with magnetic broom.

Magnetic spectrometers:

Explorer XII	O'Brien, B. J./S. U. Iowa	With Geiger counters, electrons 40–55 keV.
Injun 1	Van Allen, J. A./S. U. Iowa	With Geiger counters, electrons 45–60, 80–100 keV.
Injun 3	O'Brien, B. J./S. U. Iowa	With Geiger counters, electrons 40–60, 80–110 keV. Plus integral magnetic spectrometer.
OGO I, B	Winckler, J. R./U. Minn	With ionization chamber and Geiger counter.
OGO E	D'Arcy/U. Calif	Electrons 50 keV–3 MeV; protons 0.1–50 MeV.
OV-1	Vampola, A. L./Aerospace	Electrons 40–3000 MeV.
OV-1-13	Smart, D. F./AFCRL	Electrons 0.1–1 MeV.

TABLE 11-8.—*Trapped Radiation Zone Instruments, Experimenters, and Experiments*—Continued

Detector Combinations—Continued

Magnetic spectrometers—Continued

OV-5-6	Knecht, D. J./AFCRL	Magnetospheric boundary study.
Pegasus I, II, III	—/—	Electrons 0.5-2 MeV.
Starad	Bloom, S./U. Calif	

Faraday-cup probes:

OV-1-7	Katz, L./AFCRL	
OV-1-14	Stevens, J. R./Aerospace	
OV-2-5	Stevens, J. R./Aerospace	Electrons and protons 1-20 keV.
OV-5-6	Knecht, D. J./AFCRL	

Electrostatic analyzers:

DME-B	Heikkila, W. J./Grad. Res. Center SW	For energy anisotropy and time variations. Electrons 10 eV-10 keV.
ESRO 1	Riedler, W./Kiruna Geophys. Obs	Electron and proton flux vs pitch angle at 1.5, 10, 15, and 20 keV.
IMP F/G	Van Allen, J. A./S. U. Iowa	Cylindrical.
Injun follow-ons	Van Allen, J. A./S. U. Iowa	Cylindrical. Electrons and protons 0.1-50 keV.
OGO B, E	Frank, L. A./S. U. Iowa	
OGO E	Ogilvie, K. W./GSFC	Triaxial electron analyzer, 0-15 keV.
OV-1-13	Smart, D./AFCRL	
OV-1-14	Stevens, J. R./Aerospace	Protons 40-400 keV.
OV-3-1	Smart, D./AFCRL	Two, with spherical quadrants.

Ionization chamber plus Geiger counter:

Explorer VI	Winckler, J. R./U. Minn	
Explorer XVIII, XXI, XXVIII	Anderson, K. A./U. Calif	
IMP D/E, F/G	Anderson, K. A./U. Calif	
OGO I, B	Winckler, J. R./U. Minn	

Track-Imaging Instruments

These instruments are used primarily for cosmic-ray research. See table 13-4.

a few thousand volts with respect to the wall, runs along the length of the cylinder. Sometimes a halogen quenching gas [7] is added to reduce resolution times by shortening the length of the tube discharge. The passage of ionizing radiation leaves a trail of electrons and ions, which are accelerated toward the wire and wall, respectively. The high-voltage gradients soon accelerate the electrons to speeds at which they cause additional ionization. An electrical discharge quickly forms along the length of the tube. The passage of the ionizing particle is thus signaled by a voltage pulse at the tube's output. The simplicity, reliability, and low-power requirements of the Geiger-Müller counter are balanced by several disadvantages:

(1) There is no particle-species discrimination. Even gamma rays and X-rays are counted—though with low efficiencies—since they produce secondary electrons in the counter walls, which trigger the tube.

(2) Even the thinnest tube walls (about 1 mg/cm²) are too thick to pass any but the most energetic alpha particles and protons.

(3) The output pulse gives no information concerning the ionizing particle's energy.

(4) The resolving times are long, over 40 μsec. To some degree, these disadvantages can be overcome by telescoping counters and allying them with other detectors. (See the later treatment of the combination of ionization chamber and Geiger-Müller counter.)

Historically speaking, the earliest Earth satellites carried simple Geiger-Müller tubes surrounded by various quantities of shielding material, which provided some energy discrimination. When the complexity of space radiation became apparent—particularly in the vicinity of the Earth—a single Geiger-Müller tube by itself did not have the versatility to sort out the profusion of particle fluxes as functions of energy and species. It has long been commonplace to combine several Geiger-Müller tubes, with different characteristics, apertures, and shielding in a single experimental package called a "trapped-radiation detector." Most of the Geiger-Müller tube experiments listed in table 11–8 have, in fact, carried two, three, and sometimes four tubes.

The ESRO-2 Geiger-Müller trapped-radiation experiment typifies modern satellite practice. Two off-the-shelf Geiger-Müller

---

[7] Halogens are used for quenching in space; alcohol is more common in terrestrial work.

tubes, Anton types 302 and 112, feed separate telemetry channels on this satellite. The low-energy thresholds are:

	MeV
Anton 302:	
Electrons -------------------------	3
Protons -------------------------	20
Anton 112:	
Electrons -------------------------	1
Protons -------------------------	15

Maximum count rates are 10 000 and 2 000 per second, respectively. On the satellite, the tubes are shielded so they are responsive only to radiation entering within a solid angle 90° wide in elevation and azimuth. The tube apertures scan large segments of the trapped-radiation zone as the satellite spins on its axis and orbits the Earth. The intent of the ESRO-2 experiment is the correlation of changes in atmospheric density and radiation levels in the lower edge of the radiation zone. It is interesting to note that Explorer VII, launched on October 13, 1959, carried the same-type Geiger-Müller tubes, but with different shields and apertures, illustrating the long and successful use of this simple radiation detector, despite its inability to discriminate energy and species by itself.

Although the simplicity of the Geiger-Müller tube is manifest, the quantity of auxiliary circuitry needed to feed data into the telemetry system can be impressive. This fact is illustrated by figure 11–42 for ESRO 2, which employs PCM telemetry. Most satellite radiation experiments require such complements of subsidiary equipment.

Proportional Counters.—Like Geiger-Müller counters, proportional counters have long held an honored place in nuclear intrumentation. Their principle of operation is also similar to that of the Geiger-Müller tubes (table 11–7). An ionizing particle penetrates a gas-filled cylindrical tube and creates n ion pairs (fig. 11–41). Under the influence of the electrical field impressed between the central wire and the wall, the ions and electrons accelerate in opposite directions. Upon colliding with neutral atoms, the electrons and ions create m new ion pairs, but because the voltage gradients are smaller than they are in the Geiger-Müller tube, the charge avalanches are small and localized. No tube discharge occurs. Instead, the amplitude of the output pulse is proportional to the product nm, where the quantity m is called the tube's multiplication factor.

Proportional counters have much shorter resolving times (<1 μsec) than the Geiger-Müller tubes and since they do not
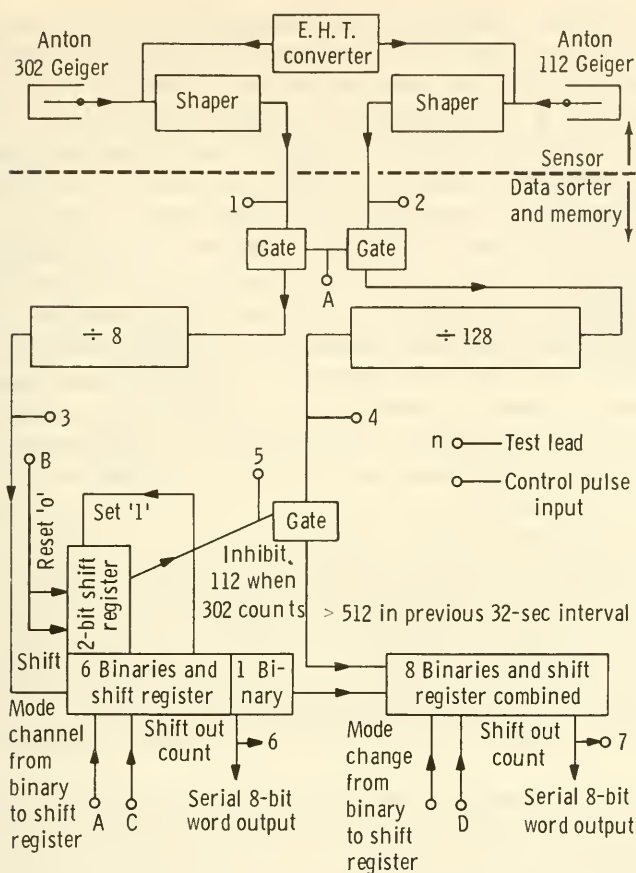
FIGURE 11–42.—Block diagram of the ESRO-2 trapped-radiation experiment.

discharge, they do not need to be quenched. Because the quantity n is related to the passing particle's species, charge, and energy, the proportional counter provides the experimenter with more information than the Geiger-Müller counter, in which the pulse amplitude is independent of the properties of the triggering particle.

Despite all these advantages, proportional counters are not often used on scientific spacecraft. Their output pulses are so low that very-high-gain amplifiers are required. Even more telling is the need for ultrastable, high-voltage, power supplies.

Of historical interest is the fact that a triple-coincidence pro-

portional-counter telescope was employed by the University of
Chicago group on Pioneer V to measure the cosmic-ray flux. Such
telescopes have also been used on Ranger I, Explorer VI, ESRO 2,
and Discoverer 25 for cosmic-ray studies (table 13–4). In gen-
eral, however, proportional counters are being displaced by solid-
state and scintillation counters, which also provide signals propor-
tional to the energy deposited by the triggering particle.

Ionization Chambers.—The third member of the family of de-
vices in which particle detection is based upon ionization in a gas
is the progenitor of them all, the ionization chamber. In its
simplest form, the ionization chamber is a volley-ball-sized sphere,
or possibly a cylinder, containing an inert gas under relatively
high pressure (usually several atmospheres). The potential dif-
ference between the central electrode and the outside wall (fig.
11–43) is only a few hundred volts, too low for the ion pairs
created by the passage of ionizing radiation to cause secondary-
charge production through collisions. The ions and electrons col-
lected by the electrodes thus constitute a current directly related
to the total energy deposited in the chamber per unit time. The
currents drawn from an ionization chamber (on the order of 10^{-11}
amp in space) give the experimenter an integrated energy rate,
which, when correlated with particle-count data from Geiger-
Müller tubes, helps to determine individual particle energies and
species.

The extremely small current output of the conventional ioniza-
tion chamber is unhandy in space probes, because it is analog in
character and must be amplified many orders of magnitude. The
Neher integrating ionization chamber (fig. 11–43) produces pulses
with healthy amplitudes. This type of chamber begins each cycle
fully charged by the spacecraft power supply. Ionizing radiation
will slowly discharge the chamber, causing the central quartz rod
to return to its discharged position in the manner of an electro-
scope leaf. The moving quartz rod, acting as a switch, ultimately
completes an electrical circuit, thus producing an output pulse
and also recharging the chamber. The number of pulses counted
per unit time is obviously a measure of the rate at which energy
has been deposited in the chamber.

An ionization chamber can be made simple, rugged, and reliable,
although their manufacture seems more of an art than a science.
Like the Geiger-Müller counter and the proportional counter, it is
easily calibrated by exposure to a known source of radiation.
Ionization chambers have been carried on several satellites (Ex-
plorer VI and the IMP series), but usually in conjunction with

PLATINUM-COATED QUARTZ
COLLECTOR ROD

ARGON GAS

TUNGSTEN
FIBER

0.076 CM ALUMINUM

ELECTROSTATIC
SHIELD
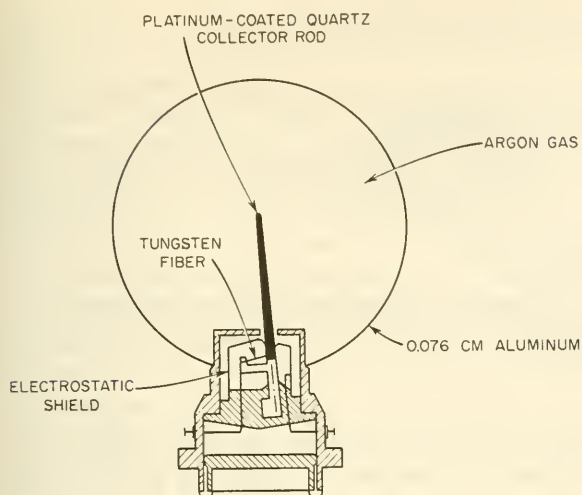
FIGURE 11–43.—
The Neher inte-
grating ionization
chamber flown on
Explorer XVIII.
(Courtesy of K.
A. Anderson.)

particle counters. Actually, a lone ionization chamber is a rarity on a spacecraft, because it is an integrating instrument that yields little useful data unless coupled to a detector that can differentiate individual particles. Explorer VI used an ionization chamber by itself to measure the total amount of ionizing radiation in space, and the Naval Research Laboratory has employed thin-walled ionization chambers on satellites like Vanguard III and Solrad 1 to measure the total solar X-ray flux.

Channel Multipliers.—The channel multipliers [8] is a relatively new type of radiation detector. It is similar to the Geiger-Müller tube in that it depends upon the avalanching of the secondary electrons to produce an output pulse. It is also closely related to the photomultiplier tube, as the following description will show.

Take a long, thin glass tube with a high-resistance coating on its inside surface (fig. 11–44). Charged particles or energetic photons passing through the tube eject one or more secondary electrons from the inside surface into the central void. The secondary electrons usually possess enough kinetic energy to carry them across the narrow diameter of the tube. There would be no electron-avalanching unless energy were somehow added to these electrons. In the channel multiplier, a longitudinal electrostatic field of a few thousand volts, applied across the metalized ends of the tube, accelerates the electrons along the axis. The secondary electrons pick up enough kinetic energy to eject more

---

[8] Not to be confused with the electron multiplier, which is just a window-less photomultiplier tube used to detect electrons. (One was flown on Injun 3.)
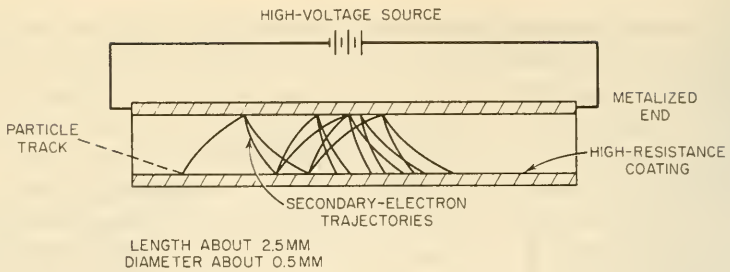
FIGURE 11–44.—The channel multiplier discharges when an incoming particle photon creates secondary electrons and causes an avalance.

than one tertiary electron upon impact with the tube's inner surface. Multiplication down the channel is rapid, as figure 11–44 indicates.

Tests at Goddard Space Flight Center have indicated that channel multipliers are useful in detecting auroral electrons in the range 250 eV to 10 keV (ref. 28). Count rates of at least 100 000 per second are possible in practice. Besides this potential satellite application, the channel multiplier is also sensitive to ultraviolet and other short-wavelength electromagnetic radiation and can serve as a detector in photometers, replacing ionization chambers and photomultipliers. Electron spectrometers, such as those on OGO II and OGO E, utilize channel multipliers to detect energy-analyzed electrons.

Scintillators.—The passage of a high-velocity charged particle or energetic photon through a crystal lattice leaves behind a trail of disrupted bonds and excited atoms. In a number of materials— for example, polystyrene and cesium iodide—some of the energy imparted to the crystal by the ionizing radiation is suddenly re-emitted as a light pulse by the atoms returning to their normal states. In other words, the crystal fluoresces, or scintillates, when triggered by radiation. Tens of thousands of photons may be generated by the passage of a single energetic particle. The photon flux rises sharply to a peak and then trails off to zero, in times ranging from 10^{-9} to 10^{-4} seconds, depending on the material used.

To make a practical particle detector out of this physical phenomenon, the emitted light must ultimately be converted into an electrical signal. The scintillation counter thus requires the double conversion of energy. The photomultiplier tube, or, less frequently, the photodiode is an essential component of the scintilla-

tion counter. Photons impinging on the photomultiplier's cathode cause the photoemission of electrons from its surface. These electrons are accelerated down the tube by a series of dynodes. Electron impacts at these dynodes cause the ejection of several secondary electrons per incident electron from their surfaces. Through this electron multiplication at the successive dynodes, a large electrical signal can be produced at the output of the photomultiplier tube in response to the input of just a few photons.

A most important property of the scintillation counter is the proportionality of the photomultiplier's output pulse to the amount of energy deposited in the crystal by the triggering radiation. It turns out that the light emitted along the particle's track and the response of the photomultiplier tube are both nearly linear. The addition of a pulse-height analyzer permits particle counts to be sorted according to energy range. A little reflection, however, shows that the light-pulse intensity coming from the scintillator must be a double-valued function when plotted against particle energy (fig. 11–45). This is because the ionizing ability of a particle increases as its velocity in the crystal decreases. High-velocity particles (B in fig. 11–45) may whisk right through the crystal and deposit even less energy than a much slower particle.
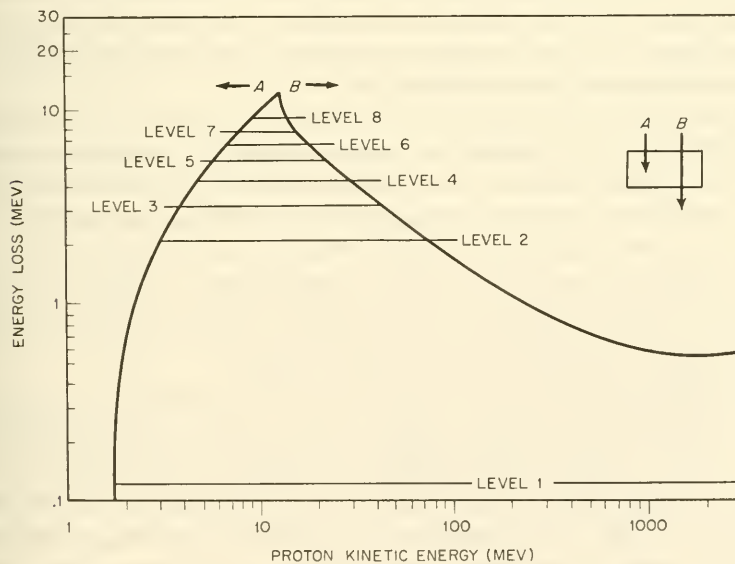
FIGURE 11–45.—Scintillator response to energetic protons. Protons to the right of the peak completely penetrate the crystal; those to the left do not (ref. 29).

At very high particle energies, pair production again increases the particles' ionizing power (A in fig. 11–45). The shape of the response curve dictates the use of additional scintillators or other companion detectors to remove the energy ambiguity. This is one of the reasons why scintillators are rarely used singly, but rather in groups or as the basic sensitive elements in the more sophisticated and versatile telescopes and spectrometers described later.

Scintillator crystals must obviously be transparent to the light they emit. This means that the accompanying photomultiplier tube may see the external environment through the crystal, unless a thin, optically opaque barrier is provided. With this precaution, the scintillation counter is responsive to all energetic charged particles and, to a lesser extent, X-rays and gamma rays.

There are two classes of scintillator materials:

(1) Inorganic scintillators, like sodium iodide (NaI) and cesium iodide (CsI), that are doped with an element like thallium (Tl) or europium (Eu). The heavy thallium converts the energy of gamma rays into detectable electrons and positrons by the pair-production reaction.

(2) Organic scintillators, such as anthracene, naphthalene, and polystyrene. These materials are not nearly as sensitive to energetic photons as their inorganic analogs. In addition, their response times (10^{-9} to 10^{-8} sec) are several orders of magnitude shorter than those of the inorganics.

The scintillators themselves are simple and rugged. To flight-qualify the whole scintillation counter, however, the photomultipliers, with their vibration- and shock-sensitive dynode structures, had to be redesigned and strengthened. Acceptable photomultipliers are now readily available. The dynode accelerators also require the availability of a high-voltage power supply on the spacecraft. The popularity of scintillation counters on spacecraft testifies to their successful adaptation to space.

Scintillator installations in satellites are physically and electronically similar to those of other event counters. The drawing of a scintillator flown on the ERS-17 satellite (fig. 11–46) shows a photomultiplier tube with a Pilot-B scintillator crystal mounted on its end. The conical opening in the aluminum housing defines the solid angle of radiation seen by the scintillator. Two thin aluminum windows shield the detector from very-low-energy protons and electrons. As with the Geiger-Müller tubes, gross shielding provides crude geometric and energy discrimination. Later,
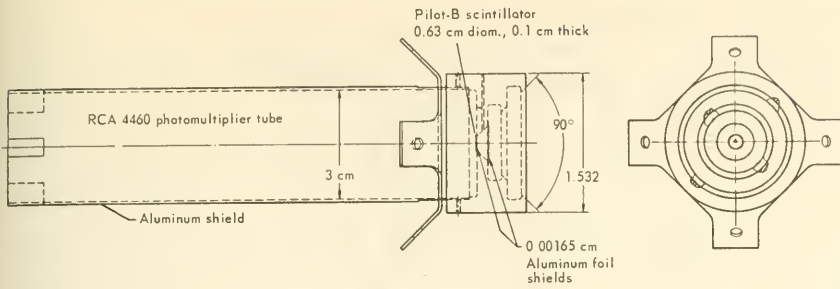
FIGURE 11–46.—The ERS-17 scintillator experiment.   This sensor counted low-energy protons and electrons.

scintillator arrays (i.e., telescopes) will be described in which energy discrimination is much more precise.

Sharp et al., at Lockheed, have constructed scintillators covered with thin aluminum and plastic sheets, which they call "threshold detectors." The name comes from the fact that the thin shielding layers create energy barriers that particles must overcome if the scintillator and accompanying photomultiplier tube are to be triggered. In function, there is no difference between the foils covering the threshold detectors and those covering the ERS-17 scintillator (fig. 11–46). Threshold detectors are commonly employed in groups, each scintillator being covered with a slightly different thickness or shielding. In this way, crude energy spectra can be obtained. Sharp and his coworkers have used this approach to measure auroral electrons from 180 eV to 31 keV.

Reagan et al., also at Lockheed, have flown a scintillation spectrometer on a low, polar Air Force satellite to study trapped electrons. The experimental configuration (fig. 11–47) is much like that used on ERS 17 and is typical of most scintillator instruments. Energy spectrometry was accomplished in this instance by a pulse-height analyzer (fig. 11–48). Two energy ranges were analyzed alternately; 0.28–2.61 MeV and 0.28–10.02 MeV. The large aperture and minimum collimation gave the instrument a high detection efficiency over nearly 2π steradians.

Cerenkov Detectors.—When a charged particle moves through a transparent medium at a velocity greater than that of light in the same medium, a cone of light, somewhat analogous to a shock wave in supersonic aerodynamics, is thrown aside. This is the Cerenkov effect, which accounts for the blue glow around the core
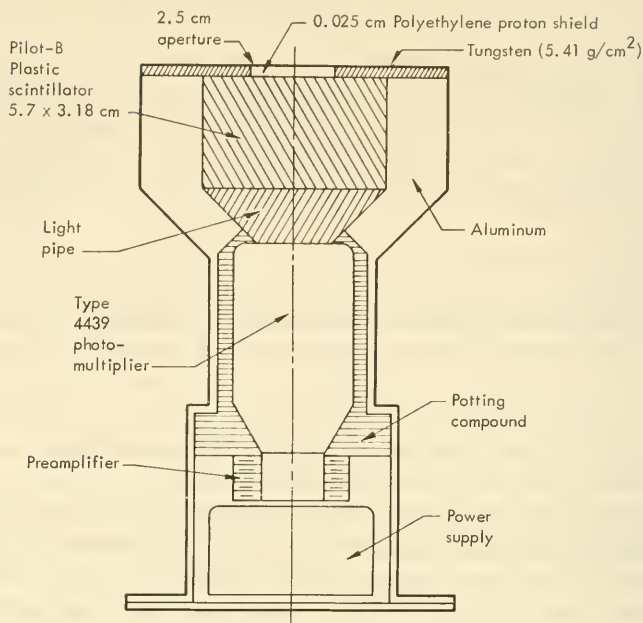
FIGURE 11-47.—Cross section of an electron scintillator spectrometer flown on an Air Force polar satellite (ref. 30).

of swimming-pool nuclear reactors and also serves in radiation detection. The angle of the cone of light is given by

$$\sin \theta = c/nv$$

where

$\theta =$ the cone's half angle with the particle track (fig. 11-49)
$c =$ the velocity of light in a vacuum (2.99×10^8 m/sec)
$n =$ the index of refraction of the medium
$v =$ the velocity of the particle (m/sec).

The quantity c/n represents the velocity of light in the medium and obviously may be less than v.

The pulse of light from the Cerenkov detector is roughly proportional to the energy of the stimulating particle. The directional characteristics of the emitted light flash can be of use in defining the geometry of radiation telescopes. Gammas and other energetic photons are not counted by the Cerenkov detector unless a heavy element is introduced into the detector. Lead gamma converters, for example, are used in Cerenkov gamma-ray telescopes to convert incident gammas into positron-electron pairs,
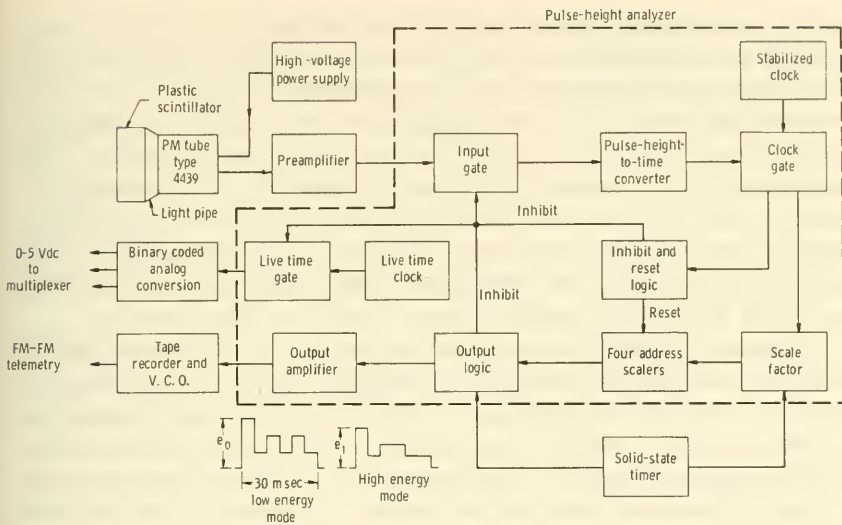
FIGURE 11–48.—Block diagram of the supporting circuitry for the scintillation spectrometer shown in figure 11–47 (ref. 30).

which will then trigger the detector. The rapid decay of the Cerenkov light pulse (about 10^{-9} sec) makes it possible, by using two Cerenkov detectors, to measure the velocities of charged particles by time-of-flight techniques.

Cerenkov detectors may be made from almost any transparent material: liquid, solid, or gas. Typical materials used in space research are Plexiglas, Lucite, and lead glass (for gamma conversion). In a practical detector, a cylinder of the chosen material is connected to the photomultiplier tube through a light pipe, or optically bonded directly.

As a basic detector, like the scintillators and Geiger-Müller tubes, the Cerenkov counter is used most frequently in telescopes
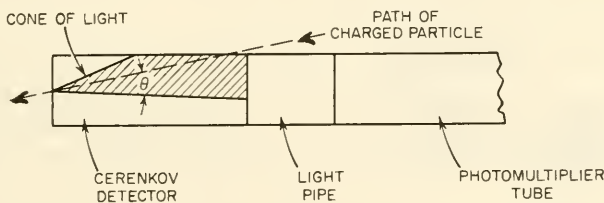
FIGURE 11–49.—Elements of a Cerenkov counter. Light spreads out from the particle's path much like the shock wave created by a projectile.

and in conjunction with other kinds of detectors. The fact that a particle, to be detected, must travel faster than light within the Cerenkov counter means that these counters have little utility in measuring the relatively low-energy trapped radiation. Cerenkov detectors are most often found in cosmic-ray experiments. The response of the Cerenkov detector to radiation is somewhat different from that of the scintillator and has made desirable a combination of the two types into an instrument with more energy and species discrimination than either type alone. (See sec. 13–3 for typical applications of Cerenkov detectors.)

Cadmium Sulfide Cells.—Cadmium sulfide (CdS) is best known as a photoconductive detector of infrared light. The passage of ionizing radiation through a crystal of CdS reduces its electrical resistance in the same way photons do, making it also a detector of particulate radiation. The change in the current flowing across a CdS cell is proportional to the energy deposited by the radiation (fig. 11–50). In other words, the cell conductivity is proportional to the rate of energy deposition. Some scientists term the cadmium-sulfide detector a solid-state ionization chamber, because of the similarity in properties.

In space, the CdS detector must obviously be protected from the influence of the Sun's rays—say, by baffles and/or a thin, opaque shield placed around the crystal. Even charged particles reaching the crystal with just a few electron volts of energy have a strong effect on its conductivity. This sensitivity to slow particles should not be surprising, since the crystal is affected by infrared photons with far less energy. The common CdS detectors used in space research are sensitive to electrons >100 eV and to protons >5 keV. Unless steps are taken to shield or deflect these abundant low-energy particles, the detector will be saturated by them. On several Earth satellites, a "magnetic broom" has been installed to sweep aside the low-energy fluxes of charged particles that were not germane to the experiments and also provide crude
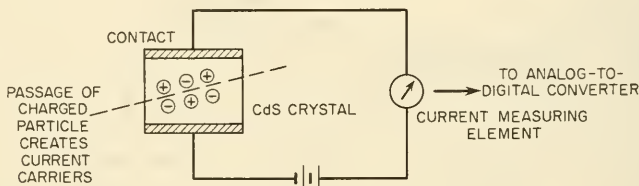
FIGURE 11–50.—A cadmium-sulfide cell. The passage of ionizing radiation creates current carriers in the crystal, lowering its electrical conductivity.

energy measurements through the broom's magnetic spectrometer action. A field of just a few hundred gauss is enough to deflect all electrons under a few hundred keV. Magnetic brooms are usually incompatible with the magnetometer experiments present on satellites.

Cadmium-sulfide detectors have been carried on satellites like Injun 1, Explorer XII, and Explorer XXV (table 11–8). Their use is restricted to some extent by their small active volumes and their long recovery time from saturation. Where radiation fluxes are much lower than they are in the Van Allen Belts, the CdS cell is supplanted by the integrating ionization chamber described earlier. The ionization chamber weighs less per unit volume and still can provide the large active volumes needed.

The cadmium-sulfide cells on Explorer XXV (Injun 4) are typical. Three of the four cells measure the total energy flux of electrons over 400 eV and protons over 500 eV. A fourth detector retains the same sensitivity to protons, but its electron threshold is increased to 250 keV by means of a magnetic electron "broom." The dynamic ranges of all cells are identical: 1 to 10 ergs/cm²-sec-steradian.

Solid-State Detectors.—The same physical process that generates power in solar cells can be used to measure space radiation. Particles and photons passing through solids leave trails of electron-hole pairs that may be drawn off as current by an impressed voltage, as in the CdS detector, or forced through an external load by the electromotive force that exists naturally across a $p-n$ junction. Since the number of electron-hole pairs created in the neighborhood of a $p-n$ junction is proportional to the energy deposited in the region by the bombarding particles, the $p-n$ junction can serve as a very efficient solid-state ionization chamber, at least within the thin, active volume around the junction. This volume is so small that the $p-n$ junction cannot make total energy measurements, but acts instead as a dE/dx device. It is in this role that solid-state detectors perform on scientific satellites, particularly in cosmic-ray telescopes and experiments measuring dE/dx versus total energy or range. (See discussions of cosmic-ray instrumentation in secs. 12–5 and 13–3.)

Although the above paragraph centers around the $p-n$ junction, there are actually three distinct species of solid-state detectors employed in satellite research:

(1) The diffused $p-n$ junction, consisting of a wafer of silicon or some other semiconductor, diffusion-doped on one face by an element such as phosphorus. This is the familiar solar cell.

(2) The surface-barrier solid-state detector, which functions just like the $p–n$ junction, is made by evaporating a thin film ($\sim$75 μg/cm²) of gold on a wafer of n-type silicon. The $p–n$ junction exists between the gold and silicon. These detectors are common in cosmic-ray telescopes; viz, on the IMP's.

(3) The lithium-drift solid-state detector, in which lithium (a donor) is drifted into a wafer of p-type silicon under reverse electrical bias at temperatures on the order of 100° to 150° C. The concentration of drifted lithium automatically adjusts to compensate the acceptors. The result is a detector with a much larger active volume than the silicon $p–n$ junction. Lithium-drift detectors are frequently call $n–i–p$ detectors.

All three types of solid-state detectors are lightweight and reliable. They have short resolution times and are relatively insensitive to gamma rays and neutrons.

All three also find applications on satellites (table 11–8). The surface-barrier type is widely used in telescopes. The diffused $p–n$ junctions, or solar cells, have seen a great deal of service on satellites, such as the Alouette and Injun series. Lithium-drift detectors are, in contrast, a more recent development, and have not yet had widespread application.

Current Collectors.—If the space radiation being sampled is intense enough, sensitive electrometers can measure the current collected by a charged electrode. This approach is, of course, the same as that found in the electron-temperature gages covered in the preceding section. Current collectors are also basic to the Faraday-cup probe in studies of the solar plasma. In the trapped-radiation zone, the mere collection of electrons or protons reveals little about energy, species, and direction of arrival. Current collectors are found therefore only as basic detectors in instruments such as the electron spectrometers described later.

B. Detector Combinations

The instruments that follow have evolved from the desire to learn more about the trapped radiation than is possible with just basic detectors allied with various collimators and shield thicknesses. Included below are radiation instruments such as telescopes and magnetic spectrometers. The common distinction is the manner of electrical or geometric arraying of basic detectors and, in some instances, the application of electrostatic and magnetic fields to analyze the incident radiations.

Telescopes.—Different types of radiation telescopes exist in profusion. The key feature of any telescope is the special geometrical

and/or electrical arrangement of two or more detectors. A radiation telescope will resolve particle energies and directions of arrival, but it does not magnify anything. The energies of charged particles can be measured either by a detector whose output is proportional to the energy lost in passage by the ionizing particles or by linear stacks of detectors that signal the depth of penetration of a particle into the stack. Depth of penetration is, of course, related to energy. To measure total particle energy by the pulse-height-analysis method, the particle has to be completely stopped in one of the detectors. Assurance that this occurs must be provided by a guard detector in anticoincidence, which discards particles that completely penetrate the internal detectors. Detector anisotropy can obviously be used to measure direction by
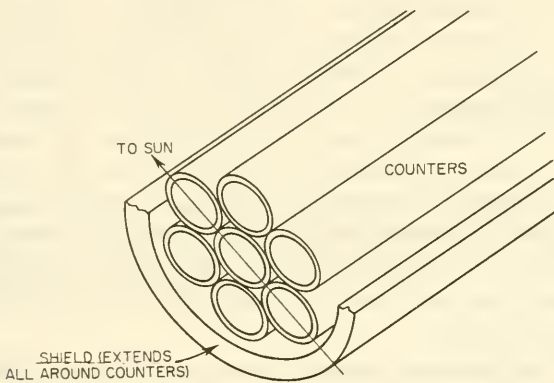
FIGURE 11–51.—A proportional-counter telescope. The counters are connected so that a count will be recorded only when three counters in a row are triggered.

scanning space with its open, or sensitive, area if attitude data are available. It is important to realize that a telescope's anisotropy, in both energy and direction, may be due to either the geometrical stacking of detectors or the electrical selectivity of coincidence and anticoincidence circuitry of an otherwise isotropic group of detectors; e.g., the triple-coincidence proportional-counter telescope of figure 11–51. Besides the many arrangements of detectors that are possible, the number of telescope varieties is further multiplied by the incorporation in telescopes of most of the basic radiation detectors: solid-state detectors, Geiger-Müller tubes, proportional counters, scintillators, and Cerenkov detectors Some of these detectors are intermixed in the same instrument.

Rather than delineate all possible telescope types and their widely varying properties, this book concentrates on telescopes that have already flown or are planned for flight on satellites. The types that will be covered are:

(1) The solid-state, or surface-barrier, detector telescopes
(2) The scintillator telescope
(3) The proportional-counter telescope
(4) The scintillation-Cerenkov detector telescope
(5) The phoswich
(6) The gamma-ray telescope
(7) The nuclear-abundance detector
(8) The positron detector
(9) Neutron detectors

Most often, the telescopes just listed are put to use in measuring solar and galactic cosmic rays.[9] Item (1), however, has been applied to the energy analysis of electrons and protons in the zone of trapped radiation. Satellites flying in the radiation zone have to distinguish between the cosmic rays and indigenous trapped radiations that overlap for several decades of energy (table 11–6). A particle's direction of flight is an aid in identifying its source. Trapped electrons and protons spiral along the Earth magnetic lines of force; solar cosmic rays are obviously directional; and galactic cosmic rays are isotropic. The telescope described below can analyze both energy and direction of arrival of all three populations.

A typical solid-state telescope was built for the ESRO-2 satellite by H. Elliot and his group at Imperial College, London. Figure 11–52 illustrates how four separate surface-barrier counters are arranged along a vertical axis and separated by various amounts of shielding. The absorber thicknesses are so chosen that counters B, C, and D respond to protons of energies 10, 50, and 100 MeV, respectively. Each of the four counters, however, generates a pulse with a height proportional to the amount of energy lost by the particle in passing through the counter; i.e., dE/dx. Counters A and B each feed a separate trio of pulse-height discriminators, as portrayed in figure 11–53; but counters C and D lead to only one discriminator apiece. The "logical" circuitry following the discriminators is for the electronic analysis of detector signals for the purpose of particle-energy analysis. Of course, the telescope is also made directional by the axial alinement of the counters and their surrounding shielding.

---

[9] See sec. 13–3 for descriptions of cosmic-ray instruments; i.e., items (2)–(9).
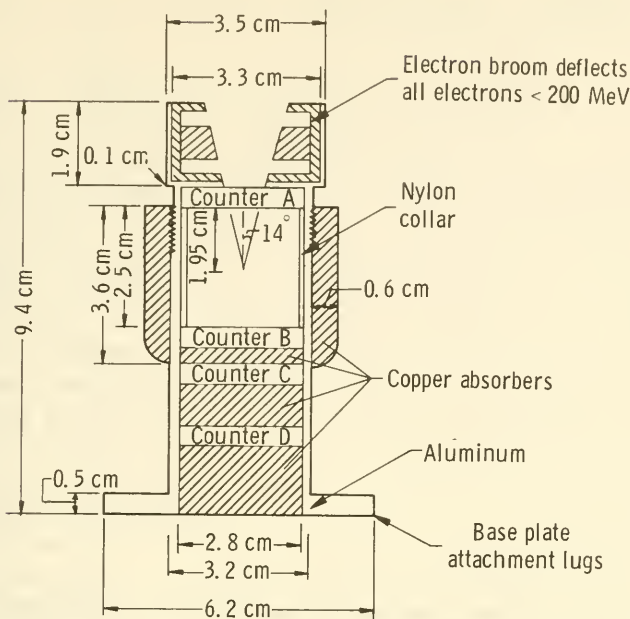
FIGURE 11–52.—The ESRO-2 solid-state telescope for measuring protons and alpha particles. Trapped protons above 1 MeV were recorded as well as solar and galactic cosmic rays.

The electronic logic of the ESRO-2 experiment goes like this: A proton between 1 and 10 MeV will generate a pulse in detector A that is high enough to pass discriminator $A1$ (fig. 11–53), but it will not produce a large enough pulse in counter B to pass discriminator $B1$. The experiment is also set up to measure alpha particles, which, by virtue of their greater charge and mass, lose more energy in passing through a counter than a proton. A proton between 1 and 10 MeV will not produce a pulse large enough to pass discriminator $A\alpha$. Discriminator $A2$ is set lower than $A1$, so that a proton in the desired range will send a pulse through the delay network shown to the Channel-I logic box. Four conditions, then, must be fulfilled before Channel I will relay an output pulse to the telemetry system. They are summarized by the following:

$$\text{Protons} \cdots \text{1–10 MeV} \cdots A1, \overline{B1}, \overline{A\alpha}, dA$$

Where the null indicates *no* pulse received, and the d in dA symbolizes a delayed pulse from discriminator $A2$. The reasoning
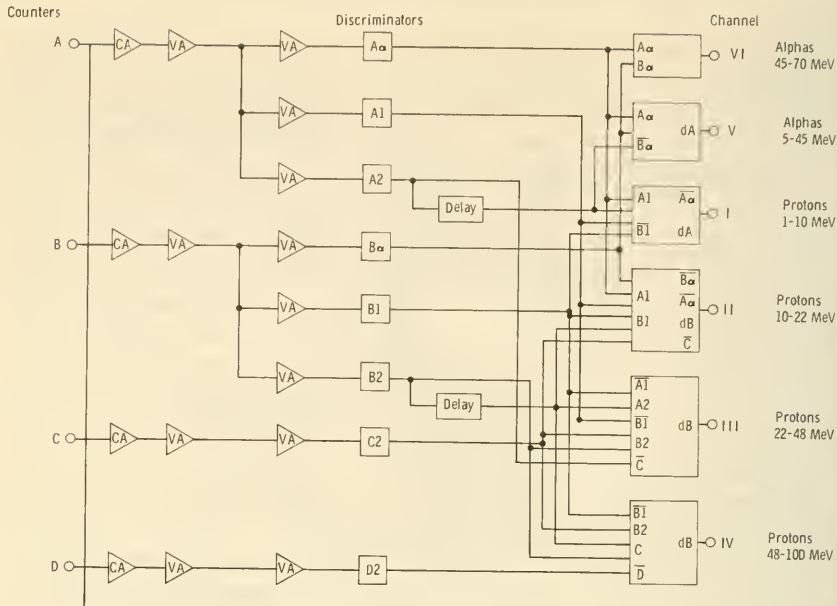
FIGURE 11–53.—Block diagram for the ESRO-2 solid-state telescope, showing the logical circuits that provide particle and energy discrimination.

is similar for the five other channels, and the requisite conditions for output pulses are indicated in figure 11–53. The description is involved, but the electronic sorting of particles and energies is effective in practice. More such telescopes are described in section 13–3, under the heading of "Cosmic-Ray Instrumentation."

Magnetic Spectrometers.—In attempting to map the energy spectra of the charged particles in space, the use of telescoped detectors with pulse-height counting and discrimination has already been described. Separate detectors surrounded by different amounts of shielding material can serve the same purpose, although the spectral measurements here are rather coarse, owing to the limited number of shielded detectors that can be carried. The classical way to disperse the energy spectrum of charged particles is through the use of a magnetic field. When a collimated beam of particles with mixed energies enters a magnetic field, particles are deflected by an amount dependent upon their charge-to-mass ratios. An array of detectors, precisely positioned, can intercept and read off the fluxes in different spectral regions. This approach is, of course, limited by the number of

detectors that can be carried and the tolerance of other experiments to the strong magnetic fields required for particle dispersion.   The latter constraint has prohibited the use of magnetic spectrometers on magnetometer-carrying satellites.

Electrostatic Analyzers.—When radiation counters, telescopes, and other "event" analyzers were discussed above, it was mentioned that the cosmic-ray flux overlapped that of the trapped radiation in both energy spectrum and composition.   Instrumentation for measuring these distinctly different phenomena is therefore similar where species and energy ranges are common.   A similar situation occurs again when the energy range of particles in the solar plasma is compared to that of the particles comprising the trapped radiation (table 11–6).   In fact, the problem of overlapping spectra and common instrumentation is so involved that figure 11–54 is introduced here to clarify the situation.   The graph shows several places where phenomena are different but instruments are the same.

The instruments of interest here are the curved-surface and planar electrostatic analyzers, which are commonly employed in analyzing the upper end of the energy spectrum of the solar wind.
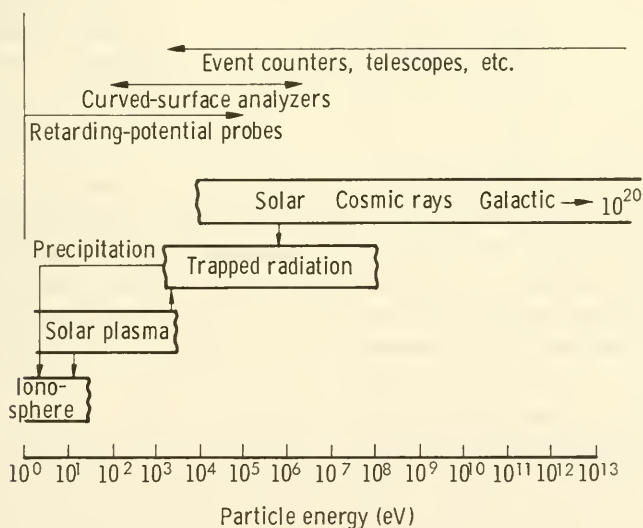
FIGURE 11–54.—Comparison of the energy spectra of three populations of charged particles found in space and the various instruments used to measure them. Populations are much larger at low-energy levels, leading to saturation of event counters.

This energy range overlaps the lower end of the energy spectrum of the trapped radiation. The theory of the curved-surface electrostatic analyzer is introduced at this point, and a specific instrument used in trapped-radiation work is described. For comparison, the reader can refer to section 12–3, where a typical planar plasma analyzer used to measure solar plasma is presented. One should not lose sight of the fact, however, that either instrument can do either job. The ESRO-1 instrument (table 11–8), for example, analyzes trapped radiation when the satellite is swinging through the belts, and solar plasma when it is outside them.

The physical parameters of solar plasma and trapped radiation are the same: scalar flux, direction, energy, and species. Instead of detecting individual, penetrating particles, as is done with more energetic radiation, the curved-surface plasma analyzer employs electron multipliers or charge-collecting surfaces (plates and cups) connected to sensitive electrometers. There is a superficial resemblance between this instrument and the better known mass
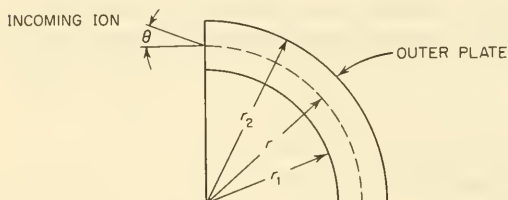
FIGURE 11–55.—Definitions of symbols used in deriving the energy equation for the curved-surface electrostatic analyzer.

spectrometer. While the mass spectrometer separates a monoenergetic beam of charged particles into groups with different mass-to-charge ratios by means of a magnetic field, the electrostatic analyzer splits a flux of charged particles into equal energy-to-charge-ratio groups with an electric field. The functions of the two instruments are actually complementary. The use of both together would provide both mass and energy discrimination, leading to unequivocal analysis of plasma fluxes.

To see how the electrostatic analyzer works, consider the two curved plates shown in figure 11–55. The plates may be either spherical or cylindrical. A positively charged particle entering the space between the plates at $\theta = 0$ will be pulled downward by a negative voltage on the lower plate. If the plates were flat, the particle would quickly impact and be neutralized. Their curvature, however, permits particles with a certain energy-to-charge ratio to travel circular trajectories and reach a detector located at the other ends of the plates. By balancing the centrifugal and

electrostatic forces, the radius of the particle's trajectory can be derived

$$\left. \begin{array}{c} \dfrac{1}{\ln\,(r_2/r_1)}\cdot\dfrac{qV}{r}=\dfrac{mv^2}{r}=\dfrac{2E}{r} \\[2mm] \dfrac{2E}{q}=\dfrac{V}{\ln\,(r_2/r_1)} \end{array}\right\} \text{(for cylinders)}$$

$$\left. \begin{array}{c} \dfrac{r_1r_2}{r_2-r_1}\cdot\dfrac{qV}{r^2}=\dfrac{mv^2}{r}=\dfrac{2E}{r} \\[2mm] \dfrac{2E}{q}=\dfrac{Vr_1r_2}{r\,(r_2-r_1)} \end{array}\right\} \text{(for spheres)}$$

where

$E=$ particle energy (joules)
$m=$ particle mass (kg)
$v=$ particle velocity (m/sec)
$q=$ particle charge (coulombs)
$V=$ voltage applied between the plates (volts)
r, r_1, and r_2 are defined in figure 11–55

Particles entering the space between the plates with energy-charge ratios substantially different from that dictated by the dimensions and applied voltage of the analyzer will collide with the walls and not be detected. There is, of course, a small energy range of particles, $E\pm\Delta E$, which will just clear the rims of the plates and be detected. The same is true for the elevation angle, θ. There is actually a fan of flux that will be accepted and detected. The acceptance angle in the azimuthal plane is small for cylindrical analyzers, but may be nearly 180° for quadrispherical analyzers (fig. 11–56). In fact, instruments developed at Ames Research Center use arrays of detectors around the sphere rim to resolve different segments of the azimuthal flux.

At a fixed voltage, the analyzer acts like a narrow energy-to-charge-ratio filter. Voltage stepping allows it to sample different portions of the energy spectrum with time. By synchronizing the detector readings with the voltage steps, energy groups can be distinguished by electrostatic analyzers. Charges of both signs can be analyzed by reversing the polarity of the plates during the stepping process. If alpha particles are present, in addition to electrons and protons, they will be indistinguishable from protons with the same E/q, or, equivalently, $\sqrt{2}$ times the proton velocity.
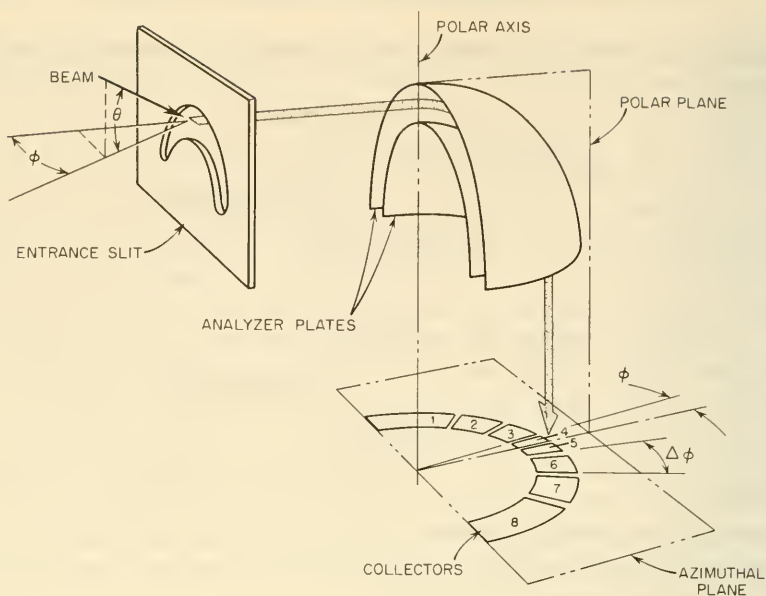
FIGURE 11–56.—The spherical electrostatic analyzer can measure
flux azimuth using segmented collectors. Spectral analysis is
accomplished by stepping the voltage applied across the con-
centric surfaces.

This ambiguity must be resolved only with further separation by
a magnetic field, except possibly with the solar wind, where all ion
species travel at the same convective velocity.

Once a flux of charged particles reaches the detector, a usable
signal must be generated. Commonly, a Faraday cup collects the
charge and feeds an electrometer tube, which, in turn, is followed
by several stages of amplification. Recently, Bendix Corp. chan-
neltrons (electron multipliers) have been used as detectors, re-
sulting in much greater sensitivity. Commercially available elec-
trometer tubes can handle the currents of 10^{-14} to 10^{-7} amperes
that typify interplanetary plasma measurements. The weak cur-
rents, though, are difficult to amplify.

All instruments affect to some extent the phenomena they
measure. Satellites and probes carrying plasma instruments are
no exception. Several effects have to be compensated for in the
instrument-spacecraft design or during the reduction of data:

(1) Distorting, fringe electrostatic fields between instrument
electrodes and the spacecraft skin

(2) Ram-pressure effects (especially in satellites)

(3) Spacecraft magnetic fields, which may modify the flow of nearby plasma

(4) Photoemission of electrons from spacecraft surfaces

The electrostatic analyzers built by Frank and his associates at the State University of Iowa are representative of the electrostatic analyzers employed in the trapped-radiation zone. The particular instrument described below is assigned to OGO's B and E, but similar equipment will also fly on Injun 5 (AD/I C). The mechanical arrangement of the analyzer is illustrated in figure 11–57. Three concentric segments of cylinders—P1, P2, and P3— form two parallel analyzing channels. P1 and P3 are held at ground potential, while P2 is stepped between 5 volts and 6000

A: +150 V
B: -3 000 V
C: +2 950 V
D: -50 V
X: 0 V., TO AMPLIFIER
Y: +3 000 V, ⫴ TO AMPLIFIER

SI: ENERGETIC PROTON SHIELD FOR ELECTRON CHANNEL

P1: 0 V

P2: STEPPED VOLTAGE 5 V TO 6 000 V

P3: 0 V

TWO 270° BENDIX CONTINUOUS CHANNEL MULTIPLIERS

R: SAWTOOTH SERRATIONS ¦ 1mm DEPTH
C1: PROTON CHANNEL
C2: ELECTRON CHANNEL
T: COLLIMATOR TRIM

COLLIMATOR AND LIGHT BAFFLES

INTERIORS OF COLLIMATOR AND CYLINDRICAL ANALYZER ARE PLATINUM-BLACKENED

FIGURE 11–57.—Mechanical arrangement of the electron-and-proton electrostatic analyzer constructed for OGO B and OGO E. The serrations and platinum black on the interiors suppress the scattering of spurious electrons and ultraviolet photons into the channel multipliers.

volts. The inner channel, *C*1, analyzes protons, while the outer channel, *C*2, because of the opposite polarity of its plates, analyzes electrons. The spectra of both electrons and protons are scanned in 14 steps from 90 eV to 70 000 eV. A normal scan of the spectrum is completed in a cycle time of 300 seconds, but a fast scan mode is included, in which the scan is accomplished in 25 seconds. The only electrons and protons that pass all the way through to the detectors fall within the solid angle indicated on figure 11–57 and
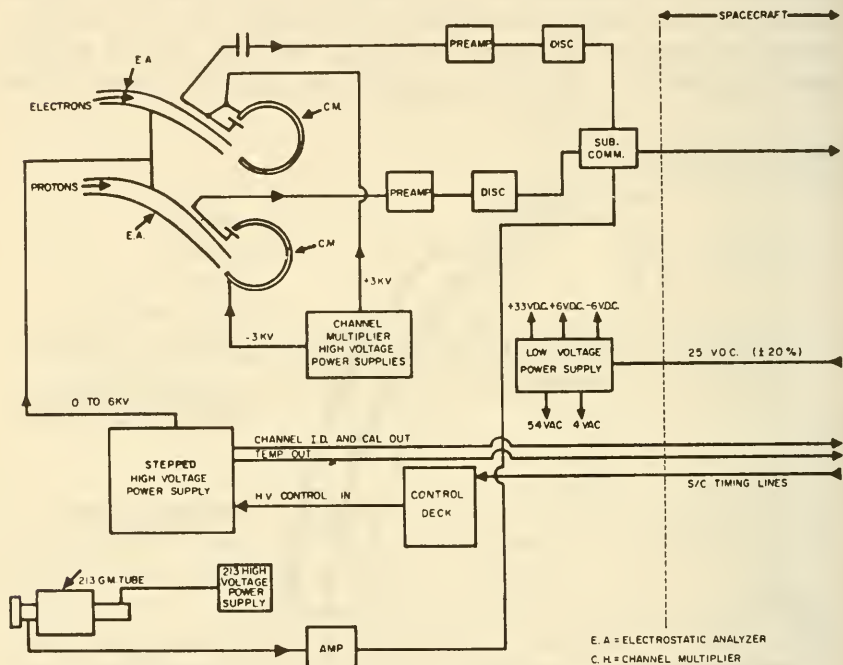
FIGURE 11–58.—Schematic of the OGO–B and OGO–E electrostatic analyzer shown in figure 11–57 (ref. 31).

within the energy range selected by the applied voltage step. Charged particles that succeed in making the transit are detected by a curved Bendix channel multiplier (channeltron). The resulting stepped analog signal is dispatched to the satellite communication subsystem, as indicated in figure 11–58. The dynamic range of the experiment is 10^4 to 10^{10} particles/cm²-sec-steradian at 1 kilobit/sec. The experiment weighs about 3 kilograms and consumes roughly 2 watts.

Ionization Chamber and Geiger Counters.—Following the various kinds of telescopes, the most frequent type of radiation instru-

mentation aboard space probes is a combination of an ionization chamber and one or more Geiger counters.   Geiger tubes, variously shielded, can measure the fluxes of ionizing particles in terms of different ranges of penetrating ability.   There are several species of penetrating particles in space, however, and the Geiger data alone are frequently ambiguous.   The addition of an ionization chamber tells the experimenters the total energy being deposited per unit time by the ionizing radiation.   With the two kinds of instruments working in unison, unequivocal particle species and energy identifications can often be made.
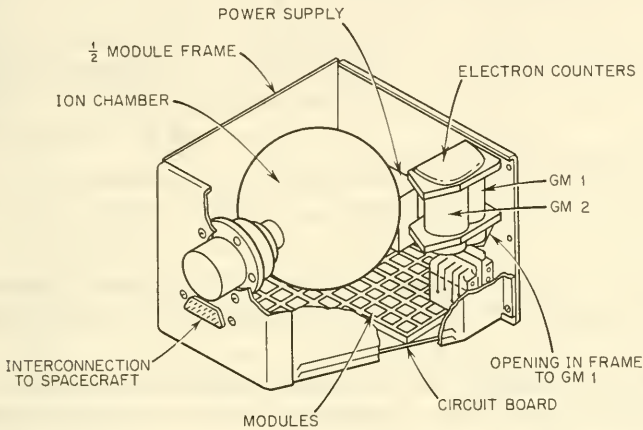
FIGURE 11–59.—The IMP ionization chamber and Geiger-Müller tube arrangement.   Dimensions: 12.4 x 12.4 x 10.0 centimeters.   Mass: 0.87 kilogram, after potting.   (Courtesy of K. A. Anderson.)

One of the IMP radiation experiments used two Geiger counters, one of which had directional properties, and an ionization chamber. The ionization chamber (fig. 11–59) is a 7.6-centimeter aluminum sphere pressurized with argon to 7 atmospheres.   It was designed and built at the Space Sciences Laboratory at the University of California at Berkeley.   Like most, it is of the Neher, integrating variety.   The chamber's output pulse occurs after approximately 3×10^{-10} coulombs of charge have been collected.   The chamber's dynamic range is from 10^{-3} pulses/sec (2 mR/hr) to 7 pulses/sec (100 R/hr).   The first Geiger tube, GM–1 in the drawing of the experiment (fig. 11–60), is accessible to low-energy electrons in the outside environment through 0.02-centimeter gold foil.   The foil scatters electrons into the tube.
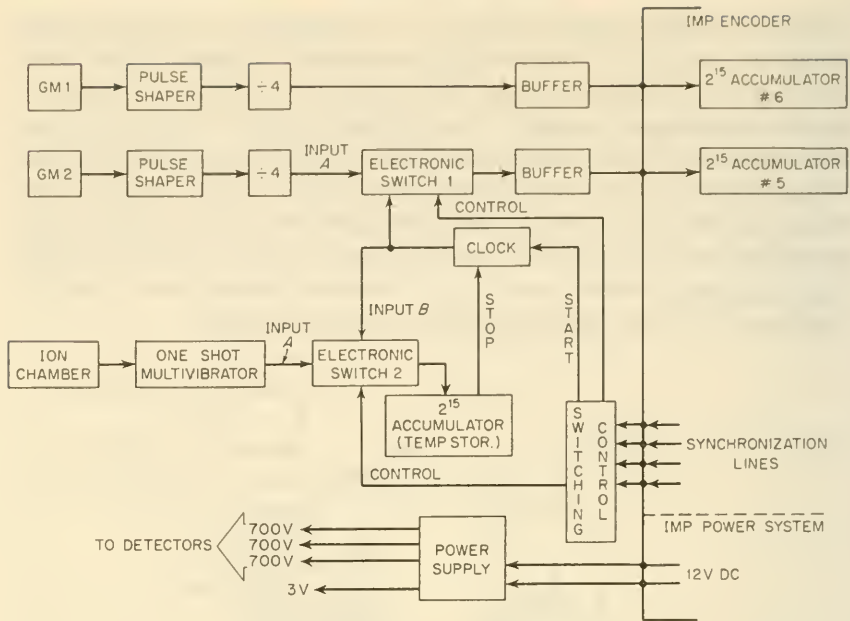
FIGURE 11–60.—Block diagram of the IMP ionization chamber and Geiger-Müller tube combination. (Courtesy of K. A. Anderson.)

The second tube (GM–2) does not possess this window. Both tubes are of the halogen-quenched type with mica end windows. The ionization chamber and Geiger tubes are shielded to provide the detection capabilities shown in table 11–9.

TABLE 11–9.—*Detection Capabilities of Radiation Detectors*

Detector	Shielding	Proton range, MeV	Electron range
GM–1 (omnidirectional)_____	3.09 g/cm^2	>52	>6 MeV
GM–1 (window)_____	1.7 mg/cm^2	_____	>45 keV
GM–2_____	3.09 g/cm^2	>52	>6 MeV
Ion chamber_____	0.43 g/cm^2	>17	>1 MeV

C. Track-Imaging Instruments

Emulsions.—In 1896, Becquerel discovered the presence of radioactivity by using photographic film as a detector. Sensitized emulsions still find extensive application as radiation detectors on

Earth.   In space, thick emulsions can record the tracks of ener-
getic particles and the consequences of nuclear reactions transpiring
within the emulsion.   Being able to see particle tracks gives the
experimenter much more information than a counter signal that
tells only that the particle has passed.   Particle species, energy,
and direction can be computed from track measurements.   Sec-
ondary particles resulting from nuclear reactions can also be fol-
lowed and identified (ref. 32).   Besides their scientific value as a
track imager, film packs are frequently used on satellites as
dosimeters;[10] that is, records of the integrated radiation dose
received during a satellite's flight.   Emulsions are compact,
rugged, of variable geometry, and draw no electrical power.   A
key application is on biosatellites and manned space vehicles,
where one wishes to know the biological impact of space radiation.

   Before emulsions can be used as radiation detectors on satellites,
one of two conditions must prevail:

   (1) The satellite or the film packs must be recoverable, so that
development and studies can be made in terrestrial laboratories

   (2) Development and transmission of the resulting images
must be accomplished on the satellite

Although the second alternative is technically feasible, all radia-
tion work to date has been done using recoverable satellites.   Of
the 150 scientific satellites listed in the appendix, only those in
the Biosatellite series are recoverable.   The Air Force, however,
has recovered many of its military satellites.   Many have carried
film packs of various descriptions, as typified by figure 11–61.

   The typical nuclear emulsion is a dispersion of approximately
equal volumes of silver bromide and gelatin, with minor additions
of plasticizers and sensitizing agents.   The emulsions flown on
recoverable satellites are inevitably of the unsupported type; that
is, they are not backed by the fragile glass plate common in
terrestrial work.   Unsupported emulsions shrink during the de-
veloping process and have to be moistened and restored to their
original sizes before finally being mounted on a glass plate prior
to measuring tracks.   It is common to stack several thick (600 μ)
emulsions (called pellicles) together so that the particle tracks
can be followed through several sheets of emulsions as well as
across the area of the film.

   The photograph presented in figure 11–62 shows an emulsion
recovered from the radiation belt.   The contrast between the

---

[10] Nonphotographic dosimeters, such as the thermoluminescent dosimeter,
have also flown on recoverable satellites.

FIGURE 11–61.—Circular film packs are frequently mounted on the rear ballast plates of recoverable Air Force satellites. The film packs shown in the photograph consist of 600-μ emulsions mounted in watertight steel and aluminum cassettes about 5 centimeters in diameter. (Courtesy of Air Force Cambridge Research Laboratories.)

heavy primary cosmic-ray track and the trapped-proton tracks is strong. Particle discrimination, in fact, is one of the strong points of emulsion technique. Proton tracks can be distinguished against a background of electron-flux orders of magnitude higher. A deficiency is also inherent in the nuclear emulsion method (fig. 11–62); the experimenter cannot say precisely what occurred when. Emulsions on spinning satellites are time-integrating, direction-integrating, and position-integrating detectors. Some idea of particle direction can be gained by shielding the emulsion, in effect collimating the incident radiation. Since some emulsions are flown on stabilized military satellites, they can be mounted to
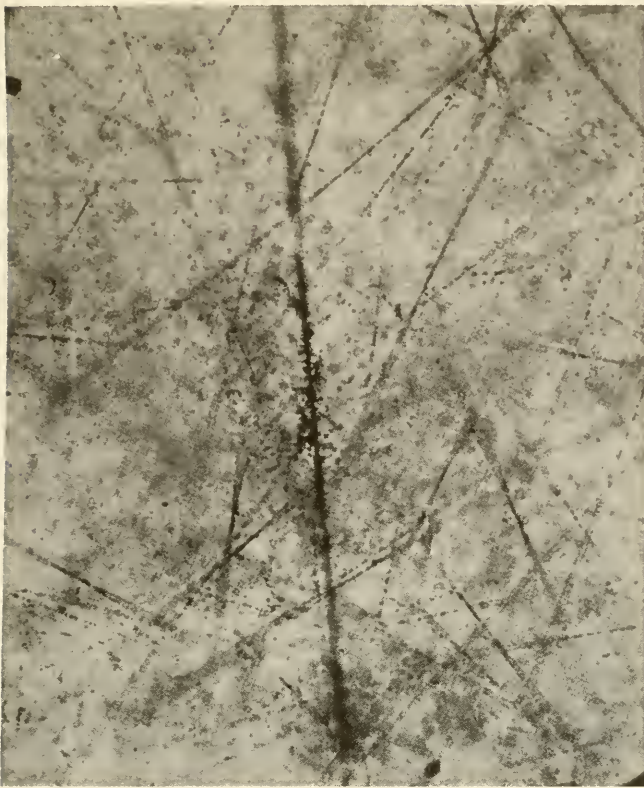
FIGURE 11–62.—Photomicrograph of an emulsion exposed to trapped radiation and cosmic rays. The heavy primary cosmic-ray track contrasts strongly with the tracks of trapped protons in the background.

look downward, upward, or backward along the direction of satellite motion.

In summary, emulsions are useful in diagnosing the precise nature of space radiation and in measuring integrated doses, but the mapping of radiation fluxes as a function of time and position is difficult and better left to instruments that can measure instantaneous properties.

Spark Chambers.—The desire to see the paths traced by charged particles has led to the development of two other track-imaging devices better suited to data-telemetry requirements.

One of the more recent track-imaging instruments is the versatile spark chamber, now a common appurtenance to terrestrial high-energy-physics laboratories. The spark chamber consists

basically of a series of parallel, thin metal foils separated by gas-filled gaps of perhaps a millimeter or two. Three-dimensional arrays of wires are also being developed. When voltages on the order of a kilovolt are applied between adjacent plates, or wires, the ionized trails left by charged particles passing through the array of foils reduce the local resistance enough to cause sparks to jump between plates. When the foils are viewed edgewise, each spark forms a segment of the charged particle's track (fig.
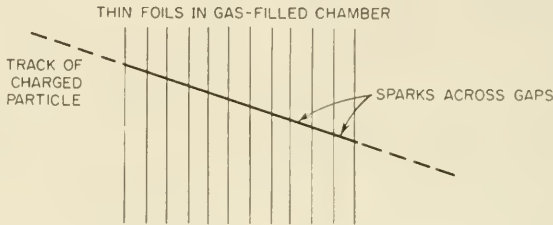
FIGURE 11–63.—A spark chamber uses an array
of wires or foils.

11–63). Of course, in order to view such an event occurring on an unmanned spacecraft, a television circuit must be installed.[11] The increase in information content is reflected in the much larger bandwidth needed by the television equipment.

Spark chambers usually contain a discharge-quenching gas, such as argon or xylene. Even though the spark itself may last only 10^{-9} seconds, the quenching time is much longer, just as it is in the Geiger tube. An experimental disadvantage of the spark chamber is its lack of isotropy and homogeneity; that is, particles see different masses of absorbing material in different directions. As if in compensation, spark chambers are fairly easy to build, even with volumes of several cubic meters. Furthermore, they are reliable, and can be designed to trigger the viewing apparatus only when a particle has passed through.

The spark chamber used in terrestrial laboratories are heavy and cumbersome. Several groups are working at lightening and miniaturizing these instruments for space use. The high-energy nuclear reactions that experimenters wish to view in space with spark chambers are rather rare, however, and large-volume chambers will be required. This volume problem will probably relegate imaging chambers to large satellites for some time to

[11] In a three-dimensional wire chamber developed at the Jet Propulsion Laboratory (JPL), signals from the activated wires give the coordinates of the sparks.

come. A spark chamber designed for cosmic-ray studies on OGO E is described in section 13–3.

Scintillation Chambers.—The crystals used in scintillation counters can be grown to sizes appropriate to small imaging chambers. The inherent sensitivity, reliability, and ruggedness of a solid-state chamber has encouraged the development of scintillation chambers for space research. One advantage of the scintillation chamber over the spark chamber is derived from the higher density of the chamber and the resulting smaller active volume needed for a given experiment. It is also homogeneous throughout its active volume. Like the spark chamber, the scintillation chamber can easily be triggered and can give accurate information on particles species, energy, and direction. On the negative side, scintillation chambers are relatively expensive and will probably require the use of image-intensifier tubes (fig. 11–64). The
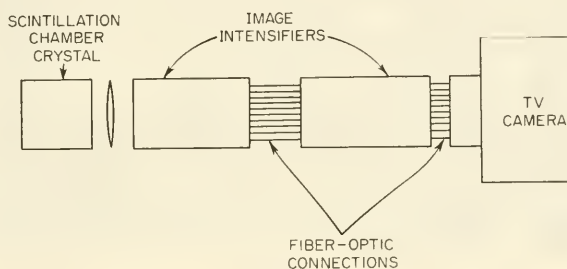
FIGURE 11–64.—Schematic of a scintillation chamber. Three-dimensional viewing is also possible.

scintillation chamber will also probably be limited to Earth-orbital missions for reasons of weight and bandwidth.

Other Track-Imaging Instruments.—Two other kinds of imaging devices are frequently employed in terrestrial nuclear physics: the cloud chamber and the bubble chamber. Both give good energy, direction, and species discrimination. The cloud chamber and the bubble chamber can provide direct views of nuclear tracks. Accompanied by a television camera, these two chambers might be applied to the same purposes as the spark and scintillation chambers. Unfortunately, the cloud and bubble chambers are heavy, possess moving parts, and cannot be rapidly triggered electrically. For these reasons, development efforts have concentrated on the handier spark and scintillation chambers for space research.

D.   Integrated Payloads

In closing this section on trapped-radiation experiments, it should be emphasized that single radiation detectors are rarities on Earth satellites. It is customary to mount several instruments, some identical, some different, on the same vehicle. Some reasons behind the integrated payload philosophy follow:

(1) To explore a wide energy spectrum, several instruments with overlapping ranges are desirable

(2) To study radiation arriving at all angles, instruments with different cones of acceptance are employed

(3) Different instruments with different dynamic ranges may be necessary to measure the different flux levels encountered

(4) When different particle species must be detected, different instruments may be useful

(5) It is always desirable to measure the same phenomenon with different instruments for purposes of cross-checking

(6) Sometimes, identical instruments are included for purposes of redundancy

Stemming directly from such considerations have been two satellite series: the Energetic Particle Explorers (Explorers XII, XIV, XV, and XXVI) and the Injun series. (See appendix.) Radose and Starad were also devoted to radiation research. The integrated auroral payloads (fig. 11–65) constructed by Lockheed and flown on Agena shots also illustrate the integrated payload philosophy.

11–5.   Satellite Magnetometers

Earth satellites frequently carry magnetometers to investigate four important magnetic phenomena[12] in nearby space:

(1) The geomagnetic field inside the magnetosphere

(2) The interplanetary (solar) magnetic field outside the magnetosphere

(3) The structure of the transition zone between the geomagnetic and interplanetary fields; viz, the Earth's magnetic "wake" and the magnetopause (fig. 1–9)

(4) The fluctuations of the fields just listed arising from interactions with the solar wind and from magnetohydrodynamic activity

Satellite magnetometers must be capable of measuring magnetic fields over a range of several orders of magnitude. At the Earth's

---

[12] Satellites often employ fluxgate magnetometers to sense the satellite's orientation (aspect) with respect to the magnetic field (sec. 9–9).
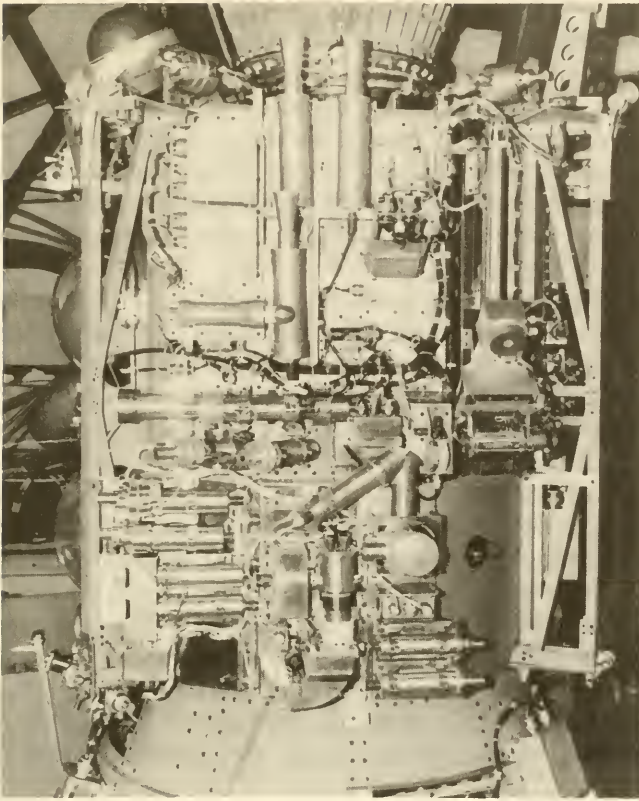
FIGURE 11–65.—A Lockheed auroral payload mounted on an Agena vehicle. The many coordinated instruments include threshold detectors, scintillators, spectrometers, and electrostatic analyzers. (Courtesy of USAF.)

surface, the total field is about 50 000 γ (0.5 gauss). It drops off as the inverse cube of the distance from the Earth's center (sec. 1–2). Outside the magnetosphere, where the Sun's field is dominant, the field to be measured drops well below 100 γ and usually below 10 γ. Such low fields can easily be overwhelmed by the spacecraft's own magnetic field unless strict attention is paid to magnetic cleanliness. Magnetometer calibration is also critical, since a drift of a few γ's can grossly distort measurements. Still another problem area arises when attempts are made to detect the magnetohydrodynamic waves that propagate through nearby space; here, the velocity and rotation of the satellite impress spurious modulations and other distortions upon the magnetometer

readings (ref. 33). Obviously, the design of satellite magnetometers and the interpretation of their signals is a complicated business.

What sensitive, dependable, physical phenomena are both easily measurable and simply related to the ambient magnetic field? [13] Magnetic induction and the Zeeman effect immediately come to mind. These and some less obvious phenomena are listed in table 11-10, along with the five kinds of space magnetometers to be discussed in this section.

The magnetometers in table 11-10 may be further classified by their ability to distinguish the direction of the ambient field. Only the fluxgate magnetometer is a vector instrument. The search coil response is direction sensitive. The others, the so-called *scalar* magnetometers, depend on physical processes that yield no information about the ambient field's direction. The limitations of scalar magnetometers are sometimes offset by the absolute character of the scalar measurements. That is, the output of scalar magnetometers is often related to the ambient magnetic field only by well-known physical constants, so that calibration against a known field is not needed. The complementary properties of the vector and scalar magnetometers may be put to advantage by using the two types together. Explorer X and the IMP's, for example, used an absolute rubidium-vapor instrument alongside two fluxgates, which provided the vector information.

Weight and power consumption are problems for magnetometers as they are for most space instruments. The search coil manages to generate its own signal power—it is in fact a dynamo— but the rubidium-vapor and helium magnetometers demand considerable power for thermal control and the relatively inefficient process of "optical pumping."

From the viewpoint of the magnetometer designer, the most sensitive spacecraft interface is undeniably magnetic in character. "Magnetic cleanliness" has long been a major spacecraft-design objective. The intrinsic fields on complex spacecraft may be tens, even hundreds, of gammas, enough to make the use of absolute magnetometers questionable, unless the satellite field can be measured with precision before flight and subtracted out of the computations. This strategy is most successful when the ambient

---

[13] In sec. 11-3, it was pointed out that simultaneous Faraday and Doppler measurements could lead to the integrated magnetic-field vector over the path of a radio wave. Similarly, plasma resonances observed by topside sounders (sec. 11-3) can measure the local magnetic field.

TABLE 11–10.—*Types of Magnetometers Used in Satellite Research*

Magnetometer type	Principle of operation	Remarks
Search coil	Coil spinning with spacecraft cuts lines of force. Generates emf proportional to dH/dt.	Direction-sensitive, not absolute. Used to detect magnetohydrodynamic waves and vlf signals. Accurate to 0.1 γ.
Fluxgate	Ambient field gated in a saturable core. Even harmonics in secondary winding proportional to H.	Vector instrument, not absolute. Most common satellite magnetometer. Accurate to about 0.1 γ.
Proton precession	Polarized field excites protons. When field is removed, protons emit signal proportional to field.	Scalar, absolute. Rarely used. Good for $>10\,000\,\gamma$ only.
Alkali vapor (Rb, Cs)	Optically pumped Rb atoms are deexcited by electromagnetic field, whose frequency is proportional to magnetic field.	Scalar, absolute. Often used with fluxgates which add vector data. Measures to 1 gauss.
Helium	Similar to alkali vapor, but not self-resonant for low-field applications.	Vector or scalar. Can be absolute. Development lags that of Rb-vapor.

field is large and the spacecraft field constant. To avoid distorting the ambient field with that of the spacecraft, nonmagnetic materials must be used in spacecraft construction, and current-generated fields should be canceled by opposing currents. Careful design can push the spacecraft fields down below 1 γ, as it did on the IMP's. Extendable booms must still be employed, however, to isolate the magnetometer from the spacecraft. The length of the boom will depend upon the success of the spacecraft magnetic-cleanliness program.

Search-Coil Magnetometers.—The simplest (and most limited) space magnetometer is the search coil (or spin coil). Used on early probes, the Pioneers I, II, and V, and on such satellites as Explorer VI and the OGO's (table 11–11), it is simply a coil of wire that generates an electromotive force as it spins and cuts the lines of the ambient field (fig. 11–66). The emf generated can be calculated from Faraday's law. It is proportional to

$$\frac{dH}{dt} \sin \theta$$

where

H = the ambient magnetic field strength
θ = the angle between the coil spin axis and H
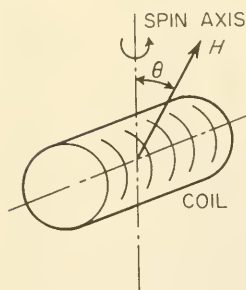
FIGURE 11–66.—Sketch of the search-coil geometry. The coil is usually fixed to the spacecraft and spins with it.

When the search coil is fixed on a spacecraft and spins with it (Explorer VI), only the component of the magnetic field perpendicular to the spin axis will be measured. If the satellite's spin axis is known—say, from a solar-aspect sensor—such measurements are useful. The search coil can also be spun relative to the spacecraft by a motor. The spacecraft-fixed coil, however, measures the true ambient field only, and is unaffected by the spacecraft intrinsic field, which, of course, spins with it—unless the spacecraft's field varies in time, causing induction effects.

TABLE 11–11.—*Satellite Magnetometer Experiments and Experimenters*

Search-coil magnetometers:

Explorer VI	Smith, E. J./STL	
OGO I, B, II, D, E	Smith, E. J./JPL	For field fluctuations. Triaxial, 0.01–1000 cps.

Fluxgate magnetometers (those used for attitude sensing not included):

Elektron 2, 4	—/—	Two triaxial. ±120 γ, ±1200 γ.
Explorer VI	Coleman, P. J./STL	
Explorer X	Heppner, J. P./GSFC	Allied with Rb-vapor magnetometer. 1000 γ±10 γ.
Explorer XII	Cahill, L./U. N. H	Triaxial. <1000 γ±10 γ.
Explorer XIV, XV, XXVI	Cahill, L./U. N. H	Triaxial. <500 γ±5 γ.
Explorer XVIII, XXI, XXVIII	Ness, N. F./GSFC	Two. <30 γ.
IMP D/E	Sonett, C. P./Ames	0–200 γ.
IMP D/E	Ness, N. F./GSFC	Triaxial. 0–64 γ.
IMP F/G	Ness, N. F./GSFC	Triaxial. 0–64 γ.
OGO I, B, II, D, E	Heppner, J. P./GSFC	Allied with Rb-vapor magnetometer.
OGO E	Coleman, P. J./U. Calif	Triaxial. Associated with solid-state detectors for study of magnetohydrodynamic waves and trapped particles.
OV-2-5	Shuman, B. M./AFCRL	Triaxial. Magnetic-storm study.
OV-5-6	Knecht, D. J./AFCRL	With flipper.
Sputnik 3	—/—	0–48 000 γ.

Proton-precession magnetometers:

Vanguard I, III	Heppner, J. P./NRL, GSFC	

Alkali-vapor magnetometers:

Explorer X	Heppner, J. P./GSFC	Rb-vapor with fluxgates. 0.1–7000 γ.
Explorer XVIII, XXI, XXVIII	Ness, N. F./GSFC	Rb-vapor with fluxgates. 0.1–1000 γ.
IMP F/G	Ness, N. F./GSFC	Rb-vapor with fluxgates. 0–2000 γ.
OGO I, B, II, D, E	Heppner, J. P./GSFC	Rb-vapor with fluxgates. 1–14 000 γ, except OGO C/D 1–50 000 γ and OGO E 1–30 000 γ.
OV-1-10	Hutchinson, R. O./AFCRL	Cs-vapor.

Helium magnetometers: Not used on satellites to date.

The output of the search coil is proportional to dH/dt rather than H. Integration of the usually sinusoidal signal is electronically easy, resulting only in a 90° change of phase. Magnetic-field transients, however, will be distorted. Another electronic problem arises because the signal is at a very low frequency—just the spin frequency of the spacecraft, a few cycles per second. Since the search coil is not an absolute instrument, it has to be calibrated in a known field before flight.

Despite its simplicity, the search coil has been supplanted in most scientific satellites by the fluxgate and alkali-vapor magnetometers. The search coils on the first OGO's are exceptions (table 11–11). The intent of the OGO instruments, however, was not the measurement of the ambient field, but rather the detection of fluctuations in the field due to magnetohydrodynamic waves and other transients (ref. 34). Such analysis is made simpler on the OGO's, which are designed to be stabilized in orbit, with one axis pointing toward the Earth.

The search coil from Explorer VI will serve as a typical example of early instruments of this type. It was simply a long, thin cylindrical coil with 30 000 turns of No. 40 copper wire wound on a nickel-iron alloy core. Overall, the core was about 25 centimeters long, but only 5 centimeters was wound. The length-to-diameter ratio of the core was 40:1. The coil was rigidly mounted, so that only that component of the magnetic field perpendicular to the spin axis was measured as the satellite rotated. In contrast to the single-axis Explorer-VI search coil, those mounted on the OGO's are triaxial instruments.

The OGO-I satellite carries a triaxial search-coil magnetometer consisting of three mutually orthogonal coils wound on highly permeable cores. The sensors and their preamplifiers are mounted at the end of a 6-meter boom (EP–5) to minimize magnetic interference from the spacecraft. Signals from the preamplifiers are divided into a low-frequency, "waveform" channel and a high-frequency, "spectral" channel (fig. 11–67). The waveform channel permits the experimenter to see the shape of very slow changes in the magnetic field, while the spectral channel amplifies field fluctuations at 10, 30, 100, 300, and 1000 cycles/sec.

Fluxgate Magnetometers.—The adjective "fluxgate" is derived from a key physical feature of this magnetometer: the "gating" of the ambient field being measured. Consider the two long, ferromagnetic cylinders shown in figure 11–68. Two external fields are applied to each: H_1, the field being measured; and $H_0 \sin \omega t$,

(ONLY ONE AXIS IS SHOWN)
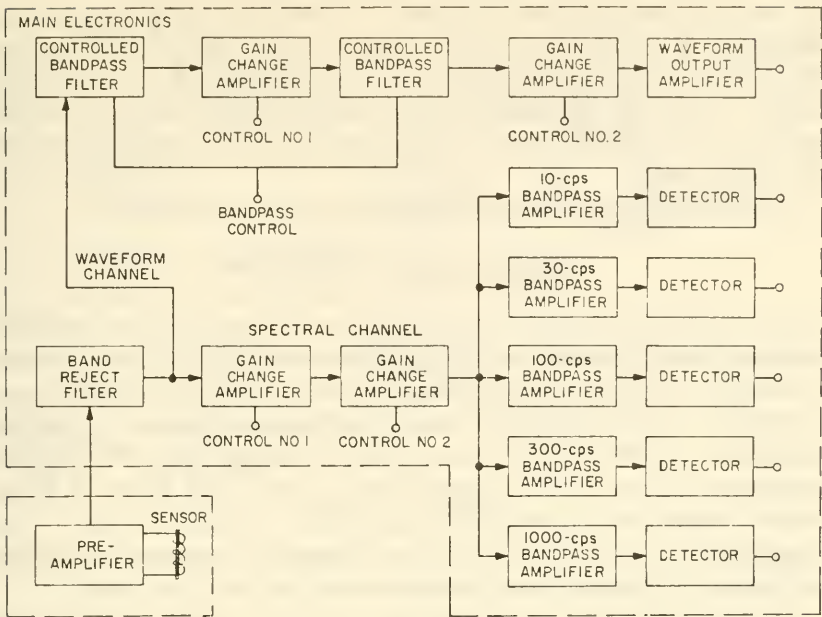
FIGURE 11–67.—Block diagram of the OGO–I triaxial search-coil magnetometer designed for recording field fluctuations and the passage of magnetohydrodynamic waves. (Courtesy of E. J. Smith.)
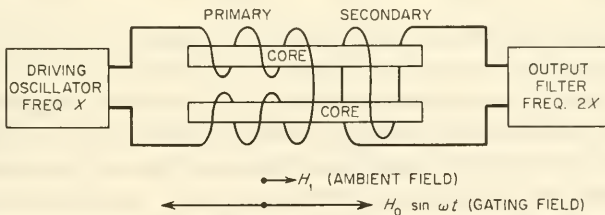
FIGURE 11–68.—Arrangement of a typical fluxgate magnetometer. Single toroidal coils can also be used.

an ac gating field impressed by the primary winding around the cylinders. Inside the cylinders, the total impressed field is $H = H_0 \sin \omega t + H_1$. The magnetic induction, found from $B = \mu\mu_0 H$, is modified by the saturability of the ferromagnetic core. During the peaks of the gating field, the cylinder cores are saturated at

B_0, and the ambient field is gated. In between the peaks, the induction is $B = \mu\mu_0 (H \pm H_1)$ (fig. 11–69). The presence of the ambient field, H_1, thus introduces an asymmetry into the induction cycle. It is this asymmetry that provides the measure of the ambient field, and the asymmetry appears only in the presence of the gating field.

If the total induction is expanded in a Fourier series,

$$B = a_0 + \Sigma a_n \cos n\omega t + \Sigma b_n \sin n\omega t$$

it can be shown that the source of the asymmetry, the ambient field, is also the source of the even harmonics in the expansion. The logic of the coil arrangement shown in figure 11–68 is now apparent. The oppositely wound primaries impress a gating signal at a frequency X (usually about 10 kilocycles). The output secondary coil is wound around both cores and feeds a filter, which passes only the second harmonic, frequency $2X$. The fundamental, X, and all its odd harmonics are canceled out by the stratagem of winding the primaries in opposite directions.

The magnetometer circuit shown in figure 11–68 is of the open-loop type; that is, there is no feedback of the output signal. Its output is an analog signal whose amplitude is proportional to the ambient field. A null-type instrument is sometimes used, in which a bucking coil supplies a field in digital steps. This field is adjusted until the ambient field is nulled and all even harmonics disappear.

A fluxgate is sensitive to a tenth of a gamma and can span the range from zero up to thousands of gammas. It is direction sensitive, and is sometimes teamed with absolute magnetometers because of this property alone. The first three IMP's (Explorers XVIII, XXI, XXVIII) used two fluxgates in conjunction with a rubidium-vapor magnetometer for this very purpose. The functional block diagram of one of the fluxgates is illustrated in figure 11–70. (See fig. 11–73 for the corresponding diagram for the Rb-vapor magnetometer.)
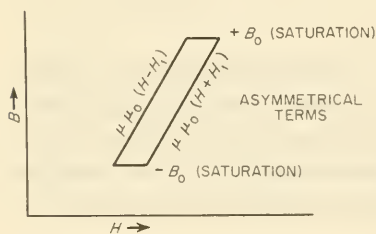
FIGURE 11–69.—Hysteresis loop for the fluxgate magnetometer.
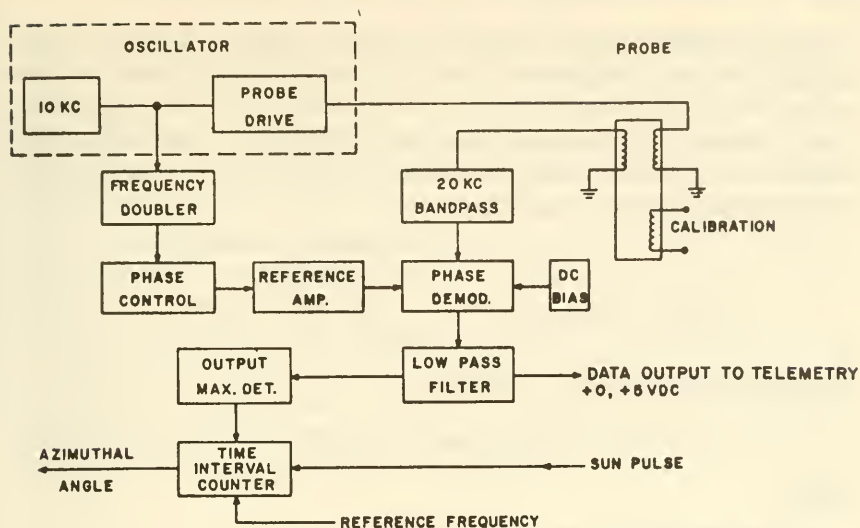
FIGURE 11–70.—Block diagram of one of the IMP fluxgate magnetometers (ref. 35).

Since the fluxgate cores (probes) are only pencil sized, it is possible to flip them back and forth by 180° in order to calibrate them for accuracy. Ness, at Goddard Space Flight Center, has constructed such probe flippers. The first one was flown successfully on Pioneer VI in December 1965. It operated from spring power and gave the experimenter several dozen calibration fixes during flight. IMP's D, E, F, and G will employ flippers driven by the expansion and contraction of an electrically heated element.

The Proton-Precession Magnetometer.—The proton-precession magnetometer is in common use on the Earth's surface—geophysical prospecting, etc. It is also suitable for field measurements from low satellite orbits. Beyond the magnetosphere, though, the fields are much too weak to be accurately measured by this type of magnetometer, which is generally applied only above 10 000 γ. In fact, Vanguard III and some early Russian spacecraft have been the only satellites to carry proton-precession magnetometers. The proton-precession magnetometer, however, was the first of the absolute, scalar magnetometers that depend for their operation upon atomic, or nuclear-energy, states that have been split by the ambient field. It thus has historical as well as instructive value.

Consider a small bottle filled with water or a hydrogen-rich liquid hydrocarbon, such as hexane. If an artificial magnetic field

—always much stronger than the ambient field—is applied to the bottle, some of the protons (N_1 of them) in the liquid will be polarized so that their spin axes are alined with the impressed field. Others (N_2) will be alined in opposition to the field. The creation of two new energy states is analogous to the Zeeman splitting of atomic-energy states.

$$\text{Unsplit population } N \mathrel{-\!\!\!<} \begin{array}{l} \text{Spin population } N_1 \\ \quad -+\tfrac{1}{2} \\ \text{—Spin population } N_2 \\ \quad --\tfrac{1}{2} \end{array}$$
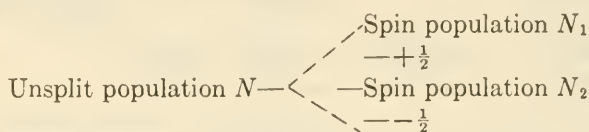
The split populations are related by

$$N_1/N_2 \sim \exp\,(-\mu H/kT)$$

where

H = the polarizing magnetic-field strength
k = Boltzmann's constant (1.38×10^{-23} joules/°K)
T = the ambient temperature
μ = the nuclear magnetic moment

When the impressed field is removed, leaving only the much weaker ambient field, the Zeeman splitting decreases accordingly, and the population ratio changes in response. As protons shift from population N_2 to N_1, they radiate electromagnetic energy at a frequency proportional in the first order to the ambient magnetic field. The frequency of the radiation is a function only of the magnetic field and physical constants. No calibration is usually needed for this absolute instrument.

The name of this magnetometer comes from the classical mechanistic portrait of protons in a magnetic field, which are pictured as precessing like tops around the ambient magnetic-field vector, with a precession frequency proportional to the ambient field. The quantum-mechanical interpretation, given earlier, is preferred and is also more convenient in describing the more complex rubidium-vapor and helium magnetometers.

In actual space operation, a large, power-consuming current must be applied every few seconds to generate the magnetometer's strong polarizing field. After the current is switched off, the electromagnetic energy from the switching proton populations can be picked up as a very weak, exponentially decaying signal. The signal frequency is 4.26 kc/gauss, corresponding to only 0.0426 cycle/gamma. In an ambient field of 10 γ, the frequency is still so low that it is difficult to amplify electronically. For this reason,

the working range of the proton-precession magnetometer is approximately 10^4–10^5 γ, not very useful for general satellite research.

Alkali-Vapor Magnetometers.—Like the proton-precession magnetometer, this instrument is an absolute, scalar device whose operation depends upon magnetically split atomic-energy states (Zeeman effect). Instead of using a strong artificial magnetic field to shift populations of excited atoms, the alkali-vapor magnetometer employs circularly polarized, monochromatic light to "pump" rubidium- or cesium-vapor atoms into long-lived—i.e., "metastable"—energy states. These energized atoms can subsequently be stimulated to leave the metastable state by applying an artificial electromagnetic field with a frequency equal to the Larmor frequency, which, in the classical view, is the electron's
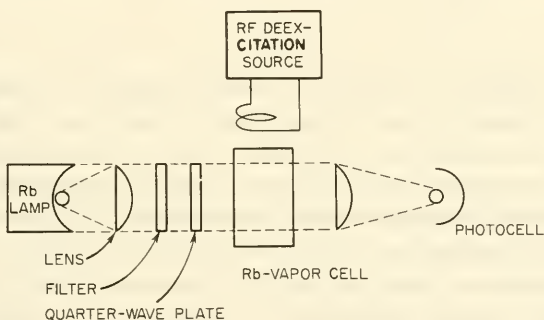
FIGURE 11–71.—Schematic of a rubidium-vapor magnetometer with no feedback.

precessional frequency around the ambient magnetic-field vector. As we shall see, the Larmor frequency and the energy gaps between the magnetically split energy levels are both proportional to the ambient magnetic-field strength. The scheme is complicated. In essence, a population of excited atoms is artificially created by optical pumping. The population is then destroyed by a signal whose frequency is proportional to the ambient field.

The optical-pumping process so basic to lasers, masers, and rubidium and helium magnetometers has an abstract description. Imagine the experiment pictured in figure 11–71. The light from a rubidium lamp is collimated, passed through a filter to remove all wavelengths except the D_1 line at 7947.6 Å, and then circularly polarized by a quarter-wave plate. When these monoenergetic photons bombard a rubidium-vapor cell, they have just the right amount of energy to raise some of the atoms from the $^2S_{1/2}$ state
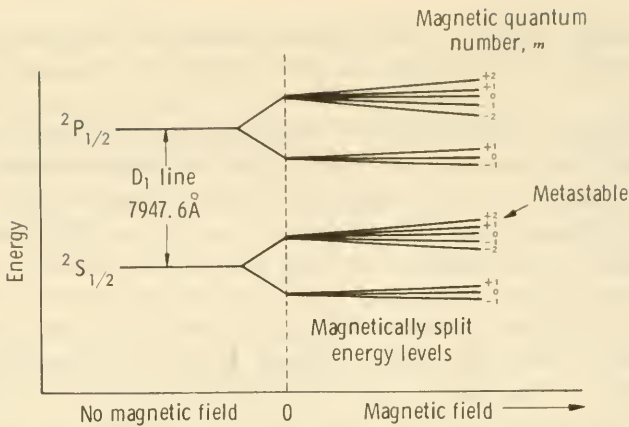
FIGURE 11–72.—Energy-level diagram for rubidium 87.

to the $^2P_{1/2}$ state, as shown in the energy level diagram (fig. 11–72). If these states are split by an applied magnetic field, quantum-mechanical laws dictate that the magnetic quantum number, m, can increase only by 1. Energized atoms in the $^2P_{1/2}$ state, no matter what the value of m, return to the $^2S_{1/2}$ state by emitting a photon within about 10^{-8} seconds. Clearly, there is no metastable state at the $^2P_{1/2}$ level. The deenergized atoms, however, return in equal proportions to all eight of the split levels in the $^2S_{1/2}$ state. The level with $m = +2$ receives its fair share, but once an atom enters this level it cannot be stimulated to leave again by absorbing one of the incident photons from the rubidium lamp. Why? Because the change in m must be $+1$, and there are no levels in the $^2P_{1/2}$ state where $m = +3$. The $^2S_{1/2}$, $m = +2$ state is thus a dead end. Eventually many of the rubidium atoms are pumped into this metastable state. The experimenter can tell when this occurs because the rubidium-vapor cell becomes transparent to the light from the rubidium lamp. There are no longer any atoms that can absorb the light, so the photons pass right through. The secret of pumping, then, is the discovery of a dead-end or near-dead-end state that can be used to shift the normal populations of atoms in a sample.

Measuring the magnetic field seems rather remotely connected with this complicated procedure. The keys to measuring the ambient field are, first, the observation that the separation of the magnetically split line is proportional to the ambient field; and, second, the application of an electromagnetic wave with just the

right frequency perpendicular to the ambient field. The wave with the right frequency is represented in quantum mechanics by a photon whose energy is equal to one of the gaps between the metastable state and the other energy levels. The electromagnetic wave has the effect of ejecting the rubidium atoms from the metastable state. When this occurs, the rubidium-vapor cell can again absorb radiation. A photocell on the opposite side of the vapor cell signals the sharp resonance when electromagnetic waves have just the right frequency to depopulate the metastable state. Since the resonant frequency can be measured with precision, the ambient field can be found from the Larmor-frequency equation, which specifies about 7 cycles/gamma for an Rb^{87} magnetometer.

In practice, rubidium-vapor magnetometers are made to oscillate at the Larmor frequency; that is, the transparency of the vapor cell varies at the Larmor frequency, and this signal is detected and fed back. In this type of arrangement, the ambient field must be inclined to the axis of the pumping light.

Rubidium-vapor magnetometers using Rb^{85} and Rb^{87} have been built. Satellites such as Explorers X, XVIII, XXI, XXVIII, and OGO's I, B, II, D, and E have used Rb^{87} with good success (table 11–11). Schuman, at the Air Force Cambridge Research Laboratories, has used Varian Associates cesium magnetometers in space applications. Usually fluxgates are flown alongside scalar instruments to provide directional data. Offsetting this requirement for directional data is the absolute character of the rubidium-vapor magnetometer. This eliminates the calibration step. Rubidium lamps draw a relatively large amount of electrical power, which can be a disadvantage on space probes. The accurate range of the rubidium-vapor magnetometer is excellent, roughly 10γ–1 gauss. It is an important research tool in mapping magnetic fields in deep space.

The rubidium-vapor magnetometer on Explorer XVIII (IMP I) is representative of this type of instrument. A functional block diagram of the instrument is presented in figure 11–73, and the illustration of the IMP satellite in the appendix (fig. A–27) shows how the sensor was contained within a 33-centimeter-diameter sphere at the end of a fixed boom. Data from the rubidium-vapor instrument was combined with that from two monoaxial fluxgates (fig. 11–70) to yield both magnitude and direction of the ambient field. One of the major problems associated with the IMP magnetometer was the maintenance of the lamp and gas-cell temperatures. Three separate temperature-control circuits were neces-
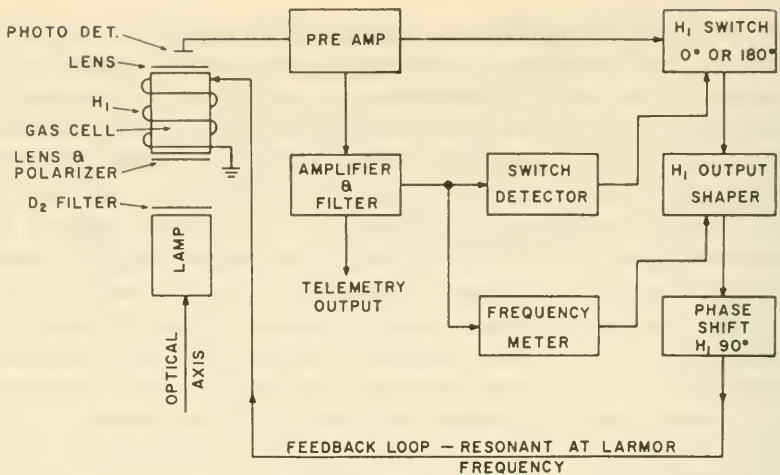
FIGURE 11–73.—Block diagram of the IMP resonant rubidium-vapor magnetometer (ref. 35).

sary. In general, the combination of fluxgates and alkali-vapor magnetometers has proven very successful in satellite work.

The Helium Magnetometer.—The great variety of lasers and masers testifies that atoms other than rubidium can be pumped and therefore can serve in magnetometers. The metastable, $^3S_1$ state of helium has been selected for space-magnetometer work. The pumping process, the deexcitation of the metastable state, and the measurement of the ambient magnetic field through the frequency of the deexcitation field are all similar to those of the rubidium-vapor magnetometer. Some differences are worth noting, though, particularly where low fields are to be measured.

First, the energy-level diagram is quite different (fig. 11–74). Helium exists in two distinct states, termed "orthohelium" and "parahelium." The optical pumping described here occurs in orthohelium, which is created by exciting parahelium with a radio-frequency field. Since transitions back to parahelium are statistically unlikely, the orthohelium energy-level diagram of figure 11–74 is essentially independent of the parahelium, which may be thought of as a buffer gas. The term "metastable" is applied to the entire $^3S_1$ orthohelium population, because all orthohelium energy levels are metastable (long-lived) with respect to para-helium.

Orthohelium is pumped by a helium-discharge lamp where transitions from the P_0, P_1, and P_2 levels to S_1 provide three closely
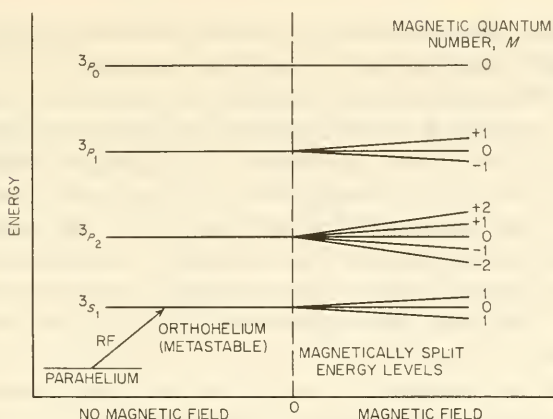
FIGURE 11–74.—Energy-level diagram for helium.
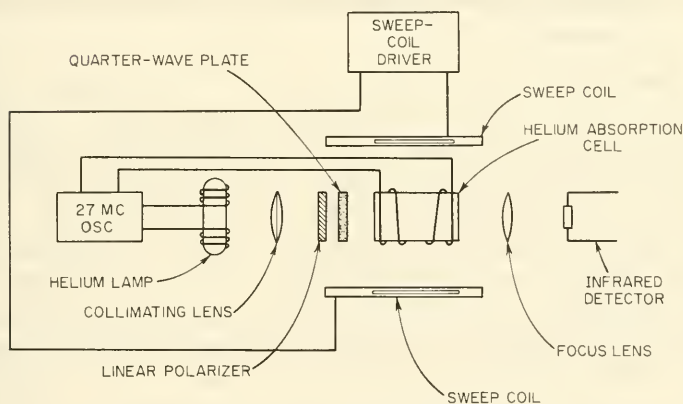
FIGURE 11–75.—Schematic of a helium magnetometer.

spaced spectral lines. Referring to the magnetometer schematic (fig. 11–75), the interposition of a quarter-wave plate generates circularly polarized light. The $^3S_1$ atoms, regardless of the value of m, are excited to the three P-states with the stipulation that $m = +1$. The excited P-states quickly decay back to the three $^3S_1$ states with equal probability. The helium pumping is different from rubidium pumping in that the $^3S_1$, $m = +1$ state is not a completely dead-end road. With the stipulation that $m = +1$, the $^3S_1$, $m = +1$ atoms can still be excited back to a P-state. The population in the S-state becomes highly skewed, however, because there is only one excitation route open for escaping the $m = +1$ level; namely, $^3S_1$, $m = +1$ to $^3P_2$, $m = +2$. There are many more transi-

tions open for the other levels. The result is a population shift strong enough to be detected by a light detector.

Another difference existing between helium and rubidium magnetometers is that the helium-pumping light is in the infrared region, 1.08 μ, instead of the visible. An infrared detector, such as lead-sulfide or cadmium-sulfide cell, must replace the photocell. In addition, the Larmor frequency is higher—23 cycles/gamma versus the 7 cycles/gamma for rubidium. This factor gives the experimenter higher frequencies, which are easier to handle electronically. This is an advantage in deep space, where the fields are very low.

So far, helium magnetometers have not been carried aboard scientific satellites, although the probe Mariner IV transported one to Mars on its historic flight.

11-6. Instruments and Experiments for Measuring Micrometeoroids

The preceding sections have dealt with the mutually interacting fields and particles that occupy nearby space. Another important component of this regime is the micrometeoroid flux, composed of those minuscule bits of matter that the Earth intercepts at relative velocities between 10 and 70 km/sec. These particles have essentially no interaction with the coexisting space radiation, plasma, and magnetic fields. No one yet knows how many of the micrometeoroids owe their origin to comet tails, the asteroid belt, or ejection by collision from satellite and planetary surfaces. Maps of the meteoroid distribution and their chemical analysis will tell science much about the origin and evolution of the solar system. In addition, micrometeoroids, with their capacity for spacecraft damage, present a potential hazard to manned space exploration. From this standpoint alone, it is desirable to understand them better.

The micrometeoroid properties of importance to the scientist differ substantially from those that interest the engineer. The former is concerned with a description of nature, the latter with the effects of nature. The following list of parameters illustrates this division of interest:

Scientific parameters		*Engineering parameters*
Scalar flux	Composition	Scalar flux
Direction	Structure	Direction
Velocity	Charge	Penetrating ability
Size	Radioactivity	Hole size
	Momentum	

What micrometeoroid interactions with sensors might measure the scientific parameters just listed? A meteoroid will impact the spacecraft sensor at such a high velocity that heat evolution, ionization, shock waves, sound, light, and vaporization will result. These physical phenomena form the basis for the surprising variety of micrometeoroid detectors listed in tables 11–12 and 11–13. Note that none employ magnetic or electrostatic fields to maneuver the meteoroids; the effects are too slight. The abundance of instruments on the lists comes from the diversity of different interactions between micrometeoroids and matter. In contrast, the profusion of different radiation instruments stems from combinations of a few basic detectors. Most of the micrometeoroid interactions, instead of revealing fundamental properties like mass and velocity, yield the derived quantities of momentum and energy. This is a serious deficiency when it comes to interpreting data. As with most fluxes, where the number of events recorded depends upon the detector area presented, telescopic arrangements of detectors and baffles can produce the directional information desired.

The first micrometeoroid detectors listened to the sound waves generated from impacts with spacecraft skins, and they measured the damaging effects on the pressurized vessels and wire-wound grids. As we shall see, many ingenious schemes have followed, but the mainstay of space research is still the piezoelectric microphone (table 11–14). The most scientifically significant instrument developments today deal with the direct measurement of velocity through time-of-flight detectors and large-area capacitor detectors.

Besides being sensitive over a large area, the micrometeoroid detector must, like all space instruments, be rugged, reliable, lightweight, and draw little power. The most serious interface of the sound-sensitive detectors is with spacecraft internal noise (e.g., relays). Detectors using scintillators and photosensitive elements may also be triggered by space radiation and sunlight. Shields and covers are required if discrimination is not feasible. All micrometeoroid sensors compete with other scientific instrumentation for solid angle.

Calibration of micrometeoroid sensors has proven to be a major problem, because terrestrial facilities cannot duplicate the extreme micrometeoroid velocities. Light-gas guns and explosive devices can produce fragments of matter in the lower end of the velocity spectrum. Electrostatic accelerators of charged dust particles

TABLE 11–12.—*Major Types of Micrometeoroid Detectors Used in Space Research* [a]

Instrument	Principle of operation	Remarks
Piezoelectric microphones.	Impact generates elastic waves in plate. Piezoelectric crystal transforms them into electrical signal.	Measures some unresolved function of mass and velocity. Most common micrometeoroid experiment.
Piezoelectric ballistic pendulums.	Impact moves ballistic pendulum. Piezoelectric crystals are flexed, generating electric signal.	Measures momentum.
Capacitor detectors.	Passage of particle through metal foil and dielectric causes temporary short and capacitor discharge.	Usually records events only. Goddard capacitors also measure energy. Large areas possible. Used in time-of-flight experiments and as direction indicator.
Light-flash detectors.	Impact causes light flash, which triggers a photo-multiplier tube.	Flash proportional to energy. Very sensitive. Can be used with momentum detector to separate mass and velocity.
Pressurized can.	Impact punctures can, releasing gas inside. Pressure-sensitive switch relays signal.	Records single event. Relation to mass, diameter, and velocity vague. Engineering experiment.
Wire grid.	Impact breaks wire opening an electrical circuit.	Records single event. Relation to mass, diameter, and velocity vague. Engineering experiment.
Light-transmission erosion experiments.	Impact removes bit of opaque layer covering a light-sensitive detector. Sunlight generates signal.	Records events. Relation to mass, diameter, and velocity vague. Very sensitive.
Time-of-flight experiments.	Time of flight over fixed length measured by 2 "event" recorders.	Measures velocity directly. Complex.

[a] See table 11–13 for micrometeoroid detectors of lesser importance.

TABLE 11–13.—*Miscellaneous Micrometeoroid Detectors*

Name	Physical principles	Status
Plasma detector	Trail of plasma left in gas is detected by charged electrodes, in the fashion of ionization chambers.	Idea.
Strain-gage detector	Thin foil transmits impact distortions to strain gages bonded to rear surface.	In development.
Foil-strip erosion detector	Micrometeoroids abrade foil strip, increasing its electrical resistance. Experiments showed punctures instead of erosion.	Discarded (used on Vanguard III).
Radioactive-coating erosion detector	Thin surface layer of radioactive material is eroded away, reducing signal to radiation detector.	Idea.
Rotating drum or vane detector	Slotted drum or vane rotates at high speed. When particle passes through 2 drum slots, time of flight can be calculated.	Discarded.
Crystal-erosion detector	Surface of crystal in crystal-controlled oscillator is eroded, changing its characteristic frequency.	In development.
Charge-flow detector	Most micrometeoroids are photoelectrically charged. Their passage can be detected by grids and electrodes.	On OGO.
Scattered-light detector	Photons scattered off micrometeoroids are detected by photomultiplier tube.	Suggested for time-of-flight instruments.
Beta-backscattering detector	Backscattered portion of beta beam is function of thin target thickness. Erosion rate measured.	Discarded.

TABLE 11–14.—*Instruments, Experimenters, and Experiments for Measuring Micrometeoroids*

Piezoelectric detectors:

Elektron 1, 3	Manring, E./AFCRL	0.03 m², >10⁻⁸ g.
Explorer I, VI		Two microphones. Also microphone on PM tube.
Explorer VIII	Alexander, W. M./GSFC	Two sounding boards, 20 pressurized cells with impact detectors.
Explorer XIII, XVI	Beswick, A. G./Langley	
Explorer XXIII	Beswick, A. G./Langley	24 triangular sounding boards, total 1500 cm².
IMP D/E	Bohn, J. L./Temple U	
OGO I, B, II, D	Alexander, W. M./GSFC	
Sputnik I, 3		
Vanguard III	LaGow, H. E./GSFC	>10⁻² dyne-sec.

Capacitor detectors:

Explorer XXIII	Siviter, J. H./Langley	Two, each 16.8 x 20.0 cm.
IMP D/E	Bohn, J. L./Temple U	Thin-film charge detector.
OGO I, B, II, D	Alexander, W. M./GSFC	
Pegasus I, II, III		426, each 50 x 100 cm.

Light-flash detector:

Explorer VIII	Alexander, W. M./GSFC	

Pressurized cells:
Explorer XIII, XVI, XXIII-- ----- ----- LaGow, H. E./GSFC----- 160 cells.   Total area 2.1 m².
Vanguard III----------- -----

Wire-grid detectors:
Explorer I, III----------- Manring, E./AFCRL----- 12 erosion gages.
Explorer XIII----- Secretan, L./GSFC----- 46 wire grids.
Explorer XIII, XVI----- Davison, E./Lewis----- Triangular foils with deposited conducting grids.
Vanguard III----- LaGow, H. E./GSFC----- Two resistive strips.

Light-transmission erosion detectors:
Ariel 2----- Jennison, R. C./U. Manchester----- Moving Al and Mylar foils.   Solar-cell detectors.
Explorer VII----- LaGow, H. E./GSFC----- Three CdS cells.
Explorer XIII, XVI, XXIII----- Secretan, L./GSFC----- The CdS cells with aluminized Mylar covers, each 24 cm².
Vanguard III----- LaGow, H. E./GSFC----- Detected particles over 1.2×10^{-9} g.

Time-of-flight experiments:
IMP D/E----- Bohn, J. L./Temple U-----
OGO I, B, II----- Alexander, W. M./GSFC-----
OGO D----- McCracken, C./------
OGO B----- Nilsson, C./------

can now attain 15 km/sec with micron-sized particles and up to 80 km/sec with submicron particles.

As things stand now, we do not know precisely what our micrometeoroid detectors actually measure in space. The historical calibration technique of dropping glass beads on piezoelectric microphones was necessary and reassuring, but possibly misleading. Happily, the calibration problem promises to be solved within the next few years.

Piezoelectric Microphones.—Many scientific satellites and most space probes have included a micrometeoroid microphone in their inventories of instruments. A thin metal plate with a small piezoelectric crystal bonded to it makes a simple, rugged, and esthetically appealing space instrument (fig. 11–76). Some questions,
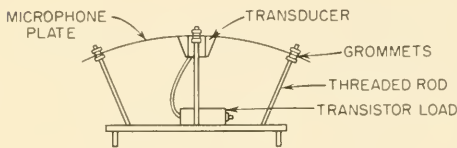
FIGURE 11–76.—Early type of microphone micrometeoroid detector.

however, must be asked about such an instrument. What properties of the meteoroid are actually measured? How is the detection of internal spacecraft mechanical noise avoided? How can the microphone be calibrated?

Consider what happens when a minute bit of matter weighing perhaps 10^{-12} g impacts a metal sheet at 50 km/sec. Some of the micrometeoroid's kinetic energy obviously goes into physically damaging the plate (pitting). This destructive effect has spawned a whole series of other detectors, described later in this section. Another part of the energy is transformed into elastic vibrations, or sound waves, in the plate. The waves propagate outward from the impact point and are distorted by and reflected from plate mountings and edges. The sonic energy of the waves can be coupled to a piezoelectric crystal (made, say, of barium titanate or lead zirconate), which will produce an electrical "ringing" signal, an exponentially damped wave train at the characteristic frequency of the plate-crystal assembly. By shaping and bending the plate, perhaps even serrating its edges, wave distortion can be minimized and the entire plate made of relatively uniform impact sensitivity. By decoupling the plate from the spacecraft proper with absorber mountings, internal noise due to such things as solenoids, relays, and servomotors can be attenuated by as much as 80–100 dB.

Noise interference can also be reduced considerably by using sensor characteristic frequencies well above the interfering frequencies. It is customary, for example, to tune the stages amplifying the sensor signals to 100 kilocycles.

Early sounding rockets and satellites often attached a piezoelectric crystal transducer directly to the vehicle skin and counted the signals received. This procedure had the advantages of simplicity and large detector areas, but the elastic waves were considerably distorted by the skin structure and internal noise. Understandably, sensor sensitivity varied with impact location. Today, the separate impact plate is the accepted approach.

The voltage peaks produced by the piezoelectric crystals are roughly proportional to the perpendicular component of the impacting particle's momentum at velocities below 10 km/sec when the crystal is compressed along one of its axes. At actual meteoroid velocities, 10 to 70 km/sec relative to the Earth, the relationship is confused. Some results show that the signal amplitude is proportional to the particle's energy rather than momentum. Other data indicate proportionality to (momentum)[1,5]. Until electrostatic accelerators of charged dust (similar to those used in nuclear research) thoroughly explore the high-velocity part of the spectrum, microphone momentum data will be questionable, though impact-frequency data are not affected.

Piezoelectric microphones are commonly calibrated by dropping small glass beads a few hundred microns in diameter onto a plate from a height of a few centimeters. Signal amplitudes can then be related to the known momenta of the dropped beads. Spacecraft instruments sometimes employ piezoelectric transducers in reverse for in-flight calibration. That is, an electrical calibrating signal will stimulate a separate piezoelectric crystal to produce a known mechanical impulse to the plate, which is then picked up by the regular crystal sensor.

The microphone detectors installed on the Micrometeoroid Satellite series (Explorer XIII, XVI, and XXIII) are fairly typical. Stainless-steel curved plates (fig. 11–77), each with two piezoelectric transducers, were fixed to the satellites' forward shells by raised acoustic-isolator standoffs (ref. 36). A lead-zirconate-titanate piezoelectric disk was mounted in the transducer, as shown in figure 11–78. Trains of decaying oscillations were generated by the crystal every time a micrometeoroid of sufficient size struck the sounding board. The wave train was fed into the signal-conditioning circuits illustrated in figure 11–79 and then into storage to await transmission to Earth.
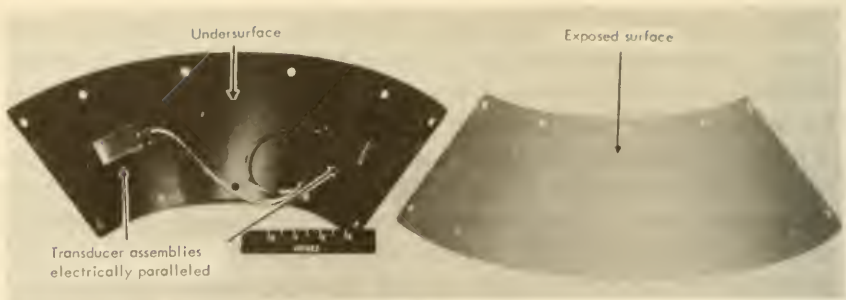
FIGURE 11–77.—Explorer-XIII microphone sounding boards. Two piezoelectric transducers were mounted on each stainless-steel plate.
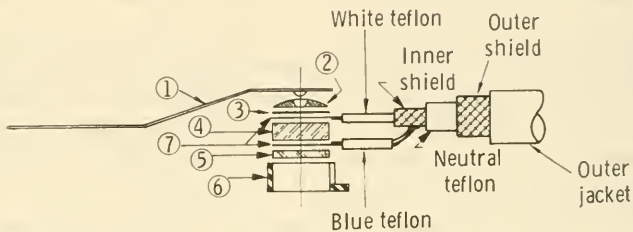
Part description

1. Holding clamp   4. Piezoelectric element
2. Dome   5. Transfer disc
3. Insulator spacer, mica   6. Holding collar
            7. Contact electrodes

FIGURE 11–78.—Construction details of the Explorer-XIII piezoelectric transducer (ref. 36).

Microphone-type detectors have been part of the instrument complement on a number of other scientific satellites; these detectors are listed in table 11–14.

Piezoelectric Ballistic Pendulums.—The piezoelectric microphone just described uses the crystal detector in its acoustic mode (ref. 37). The piezoelectric effect is also observed when crystals are suddenly flexed or bent by shear forces. An impact plate, mounted as shown in figure 11–80, will transmit shear forces to the crystal when struck by a meteoroid. In effect, we have a ballistic pendulum. Experiments have shown that such a mounting produces electrical signals that are more nearly proportional to the momentum of the impacting particle. Furthermore, the signals are proportional to that component of momentum perpendicular to
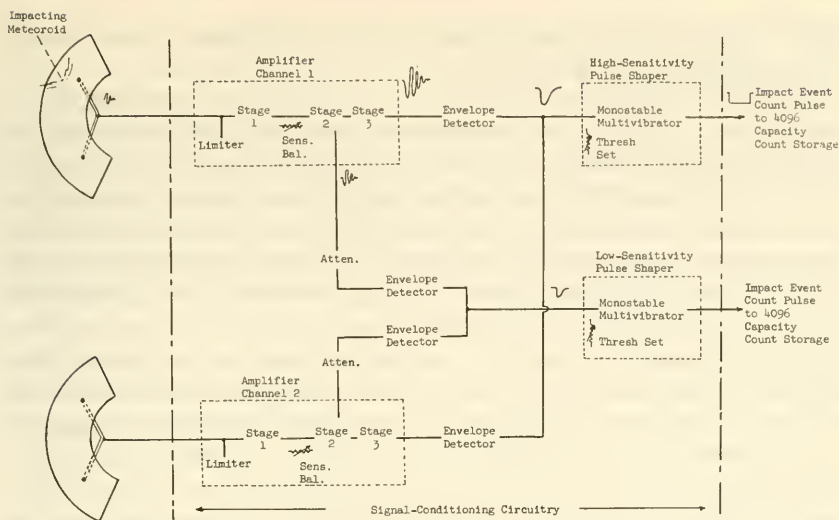
FIGURE 11–79.—Block diagram of the Explorer-XIII microphone micro-meteoroid detector (ref. 36).
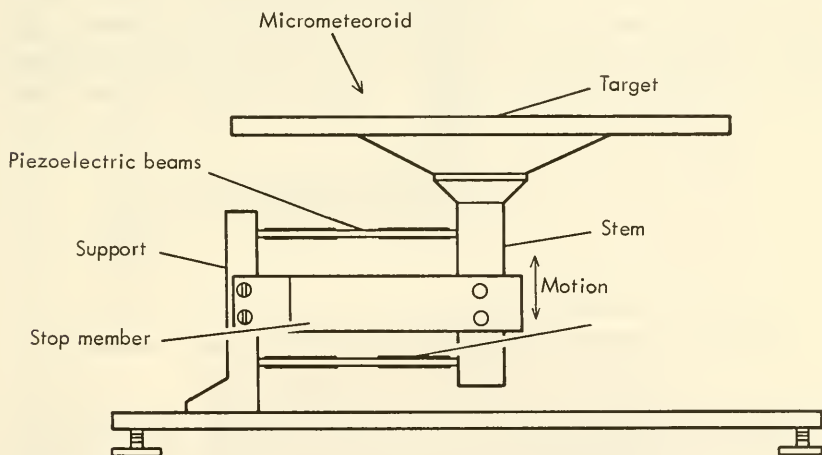
FIGURE 11–80.—One arrangement of the piezoelectric ballistic-pendulum micrometeoroid detector (ref. 37).

the plane of the impact plate. The sensitivity threshold of the ballistic pendulum is estimated to be as low as 10^{-5} dyne-sec, so low that spacecraft noise and solar-pressure fluctuations due to the spacecraft's spin are limiting conditions. Such characteristics, high sensitivity and momentum proportionality, make the

piezoelectric ballistic pendulum a welcome addition to the family of micrometeoroid detectors.

Thin-Film Capacitor Detectors.—If a thin layer of dielectric is pierced by a high-velocity micrometeoroid, the trail of ionization and disruption creates a temporary conduction path. By evaporating a thin metallic coat on the side of the dielectric facing the environment, and bonding the other side to a metal plate or perhaps another evaporated metal film, a capacitor detector can be built. This detector will discharge the condenser and generate a signal every time the dielectric is breached. After the event, the ions will recombine and the condenser can be recharged for another event. Capacitor detectors can be made by evaporating a layer of alumina (Al_2O_3) on a metal plate and then coating it with aluminum. Or a detector relatively transparent to micrometeoroids can be made by aluminizing both sides of a thin Mylar plastic film. Two such filmlike detectors can then be used to signal the flight of a micrometeoroid over a fixed course in time-of-flight experiments discussed later. A "transparent" capacitor detector, of course, provides event information only and says nothing about the micrometeoroid properties themselves. It is possible, however, to prepare double capacitor arrangement, like that illustrated in figure 11–81, with a metallic sheet of known thickness sandwiched in between. Capacitor signals would then
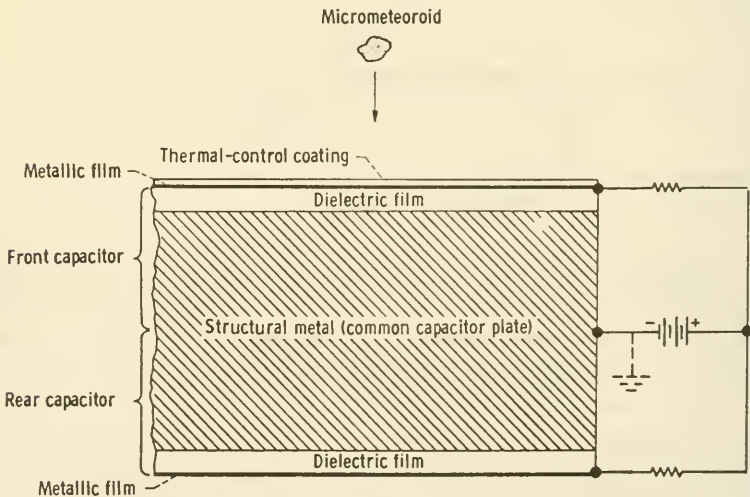
FIGURE 11–81.—Schematic of a double-capacitor micrometeoroid-penetration detector (ref. 38).

reveal the numbers of micrometeoroids above and below a fixed level of penetrating ability. Another possible arrangement is described below.

The simplicity of the capacitor detector has led to its installation on a number of recent satellites (table 11–14). The most impressive experiments made use of the huge, winglike sections of the three Pegasus satellites [14] (fig. 11–82). Each Pegasus satellite exposed roughly 213 m² (2300 ft²) of detectors to the micrometeoroid environment. Each of the satellite's two wings was made from seven hinged frames that unfolded accordion fashion, once orbit was achieved. On the frames were mounted panels, 208 in all, that were constructed of sheet aluminum, called the "target," to which was bonded a sheet of Mylar plastic coated with a thin layer of copper (fig. 11–82). Each panel was approx-
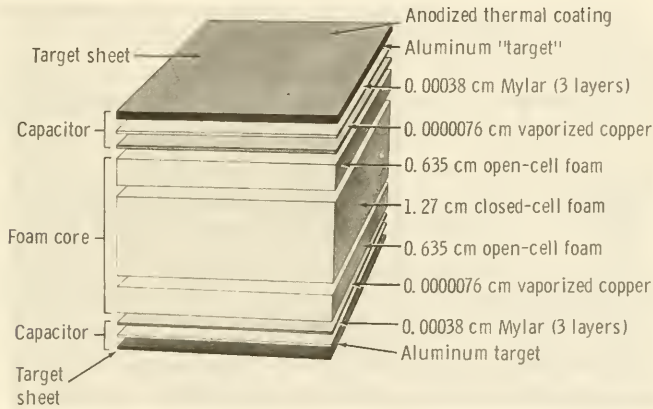
FIGURE 11–82.—Cross section of the Pegasus back-to-back capacitor detectors.

imately 51 x 102 centimeters. Two capacitor detectors were mounted back to back on each panel on a foam core about 2.5 centimeters thick. Target sheets varied in thickness: on 8 panels they were 0.0038 centimeter thick; on 17 panels they were 0.0203 centimeter thick; on the remaining 183 panels they were 0.0406 centimeter thick. Back-to-back capacitors were identical. On the first Pegasus satellite, some of the capacitor detectors shorted. To prevent a power drain, whole groups of detectors had to be

---

[14] On Pegasus III, 48 aluminum coupons were attached for possible recovery by astronauts.

switched out of operation by ground command.   On the sub-
sequent two Pegasus satellites, fuses were added so that defective
capacitors could be removed singly.   Thirty-six were removed
during the first 4 weeks on Pegasus II.   The overall block dia-
gram showing data flow on Pegasus I is presented in figure 11–83.

Light-Flash Detectors.—When a high-velocity micrometeoroid
hits a substance, such as cadmium sulfide, a great deal of energy
is released in the small volume around the point of impact.   The
heat, shock waves, and ionization cause the crystal to emit a flash
of light, just as it does when penetrated by ionizing radiation
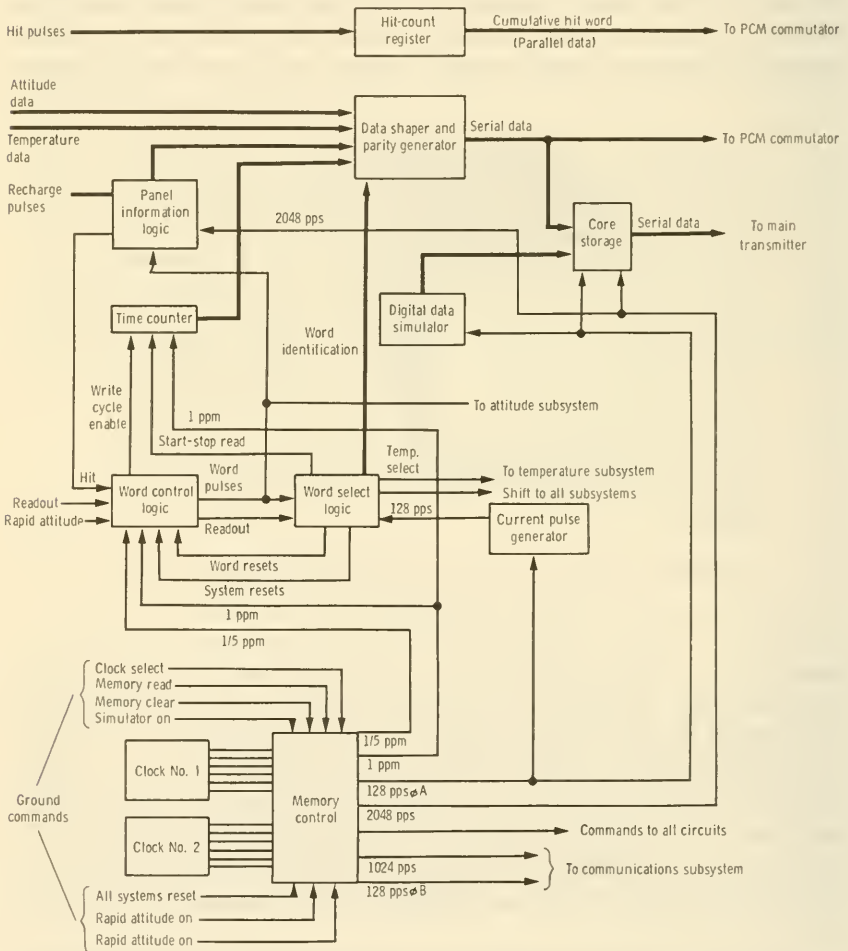
FIGURE 11–83.—Block   diagram   of   the   Pegasus-I   capacitor-detector
experiment (ref. 39).

(sec. 11–4). The amplitude of the light pulse is proportional to the amount of energy imparted to the crystal. The photons from the event are converted into an electrical signal by a photomultiplier tube adjacent to the scintillator. A pulse-height analyzer following the photomultiplier tube will sort the impacts out according to the amplitudes of the light flashes, which in turn can be related to the particle energy through preflight calibration. The light-flash detector is also sensitive to penetrating radiation, but such signals can be discriminated against by guard counters, like those used in radiation detectors. Some crystals, notably cadmium sulfide, are also photoconductive, necessitating an opaque covering. As a family, light-flash detectors are extremely sensitive, probably the most sensitive of all micrometeoroid detectors. Thresholds are as low as 10^{-14} g at 2 km/sec or, equivalently, 2×10^{-12} dyne-sec. The sensor signal is proportional to energy rather than momentum, which brings forward an interesting possibility. A combination instrument using a momentum-sensitive microphone and an energy-sensitive light-flash detector can, through simultaneous measurements, separate the mass and velocity parameters. Light-flash detectors were used on Explorer VIII (table 11–14). Unfortunately, these detectors were also triggered by protons >40 MeV, and the data had to be discarded.

Pressurized Cells.—Here is a very straightforward micrometeoroid detector. A particle penetrates a pressurized vessel, usually a cylinder; the gas inside escapes; and a pressure switch sends an electrical signal to the communication subsystem. The cell is useless after one puncture, and information about the meteoroid itself is limited to the knowledge that a certain thickness of metal has been penetrated. Pressurized-cell data are therefore of primary interest to spacecraft designers. Cells with different wall thicknesses can, of course, provide crude size-and-velocity data if reliable terrestrial calibration is available. It has also been proposed that the rate at which gas escapes from a punctured cell measures the hole size and, indirectly, the micrometeoroid size. Here, again, calibration is difficult, because hole size is a complex function of particle energy, mass, size, and possibly shape. Furthermore, the rate of pressure loss would be a hard parameter to measure and telemeter. Finally, the walls of the pressure cells that are commonly used are very thin (25–100 μ), and they must be well protected during the spacecraft launching.

Vanguard III carried 0.162 m² of exposed pressure-cell surface in the form of two cylinders with 0.066-centimeter magnesium walls. The major use of pressure cells to date was on Explorers

XIII, XVI, and XXIII, the Micrometeoroid Satellite series. Here, 160 beryllium-copper cylinders were mounted around the final-stage rockets. Each cell was filled with helium and included a pressure-sensitive switch (fig. 11–84). Three different wall thicknesses—25, 51, and 127 μ (0.001, 0.002, 0.005 inch)—were used. Altogether, the cylinders exposed 0.156 m² of area to the environment (ref. 36).
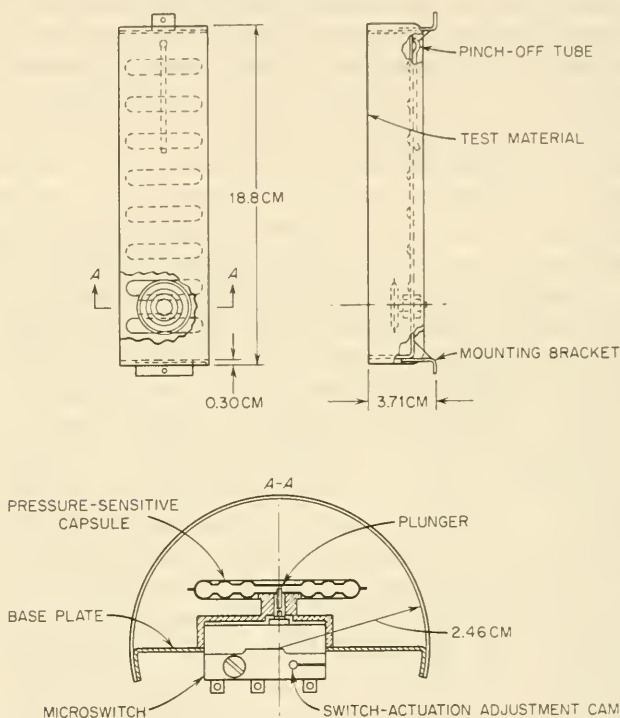
FIGURE 11–84.—Pressure-cell micrometeoroid detectors from the Micrometeoroid Satellite series (ref. 36).

Wire-Grid Detectors.—The destructive properties of micrometeoroids are put to good use in the wire-grid sensors. The usual form taken is that of enamel-wire-wound cards electrically connected in parallel (fig. 11–85). A micrometeoroid large enough to sever a wire removes the struck card from the circuit and changes the overall electrical resistance. This kind of event is convenient to telemeter. But just what does a severed wire mean in terms of micrometeoroid properties? The effect depends upon the particle's size and energy as well as the diameter and composition of the broken wire. Low-velocity calibration experiments
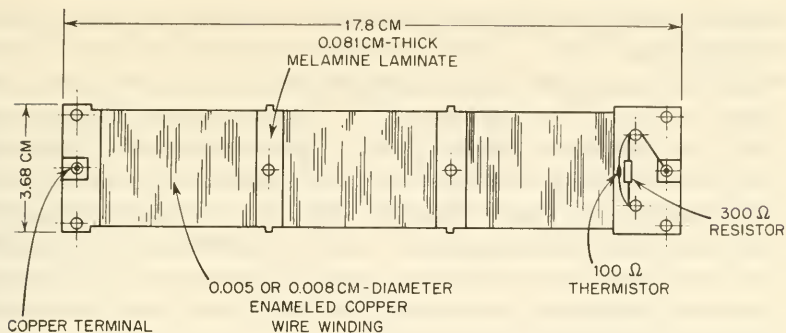
FIGURE 11–85.—Copper-wire cards from Explorers XIII and XVI (ref. 36).

have indicated that micrometeoroids may break wires twice their own diameter, but the effects of velocity and wire composition are still vague. At the least, a severed wire signals an event; at the best, there is a crude measure of the micrometeoroid's destructive properties. Although wire-wound cards are light and simple, they are limited to one event apiece, and even that event yields little information about mass, velocity, and direction. The cards also draw electrical power until a wire is broken.

The first Explorer satellites carried wire grids. The Micrometeoroid Satellite series used 46 cards, like those sketched in figure 11–85. Explorer XVI also carried a more refined detector, based on the same principles of operation. Thin grids of conducting gold were deposited on the bottoms of stainless-steel sheets of different thicknesses. A particle penetrating the steel sheet would almost invariably break one of the current channels underneath. Much better engineering penetration data can be recorded in this way (as was the intent), but little is revealed about the intrinsic properties of the bombarding particle.

Light-Transmission Erosion Detector.—The destructive properties of micrometeoroids are used for measurements in still another way. Holes made by impacts on an opaque film will transmit light in proportion to the collective area of the holes. Hole area can be related empirically to micrometeoroid diameter on a hypervelocity-particle range, but, as usual, the adequacy of velocity simulation is a problem. Either a photomultiplier tube or a photoconductive cell (CdS) can be used as the light detector, the latter being simpler and more rugged but not as sensitive. Holes as small as 1 and 2 microns in diameter can be detected. Like most sensors depending upon destructive effects, this type pro-

vides only meager information about the meteoroid mass, velocity, and direction.

Light-transmission experiments have flown on several satellites (table 11–14). The Explorer-XVI cadmium-cell detector (fig. 11–86) is perhaps typical of the light-transmission approach. Two such cells, with a total effective area of 48 cm², were deployed on the satellite surface. Explorer VIII, in contrast, adopted the photomultiplier-tube approach. Approximately 1000 Å of aluminum were evaporated onto the face of a commercial photomultiplier tube. Terrestrial calibration indicated that particles as small as 10^{-13} g generated usable signals.
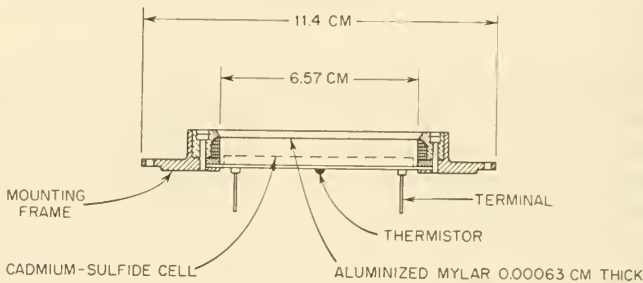
FIGURE 11–86.—The light-transmission micrometeoroid detector from the Micrometeoroid Satellite series (ref. 36).

Jennison has described a more complicated light-transmission experiment flown on Ariel 2. The fundamental differences were the use of moving opaque strips and solar-cell-type light detectors. Two types of instruments were constructed: IROD's (Instantaneous Readout Detectors) and DROD's (Delayed Readout Detectors). Ariel 2 carried two of each type. Since the basic principles are the same, only the IROD will be described. In the IROD's, 10-centimeter-wide aluminum-foil strips (12 μ and 15 μ thick) were fitted into lighttight, slotted guides located at the tops of the wedge-shaped slots. At the bottoms of the slots, which were 5×27.3 centimeters in size (long dimension parallel to satellite spin axis), were strips of solar cells that detected any sunlight transmitted by micrometeoroid holes in the foils above them. A molded-epoxy cylindrical lens was inserted between the foil and solar-cell strip. The foil strips, which were wound on spools, were advanced 0.16 centimeter by a solenoid actuator every other time the satellite passed into the Earth shadow.

Miscellaneous Detectors.—Micrometeoroid-detector concepts are legion. Some of the lesser concepts listed in table 11–13 are only ideas; some are in the development stage; some have been tried only to be discarded.

Time-of-Flight Measurements.—Since the micrometeoroid velocity is not directly related to the parameters actually measured by most detectors, there has been considerable thinking done about time-of-flight experiments. The average micrometeoroid travels at about 30 km/sec. If there is a distance of 10 centimeters between two event counters, the associated electrical circuits will have to measure times on the order of 2 microseconds, an easy feat for today's electronics. The first event detector must be "transparent" and capable of repeated use. Included in this category are the capacitor detector, the plasma detector, the charge-flow detector, and the scattered-light detector. Several combinations of sensors are now being tested in the laboratory. One using scattered light has been conceived by Neuman (fig. 11–87).

11–7.   Satellite Geodesy

Geodesists have long needed the unique information attained by observational unmanned Earth satellites. Until the advent of
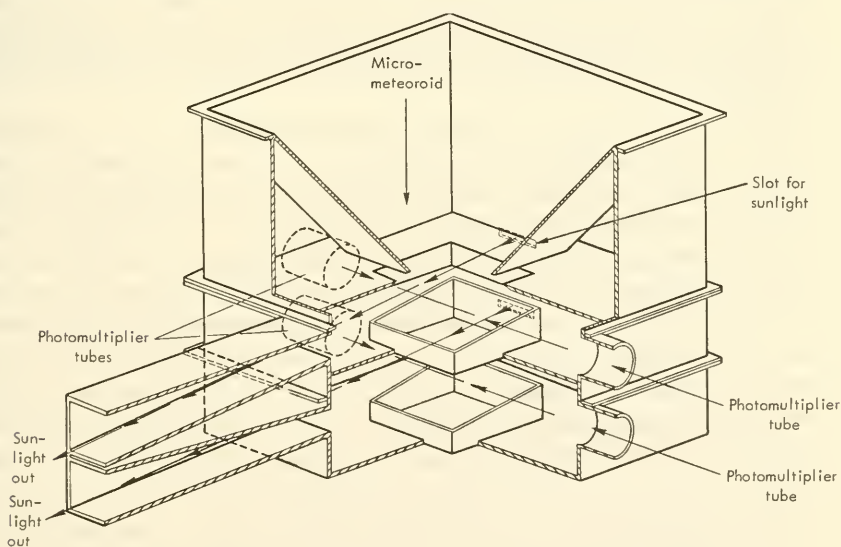
FIGURE 11–87.—A time-of-flight micrometeoroid velocity experiment. Sunlight scattered off entering micrometeoroids activates photomultiplier tubes (ref. 40).

scientific satellites, man's knowledge of the Earth's shape and size was inferred—not very precisely—from geodetic and gravimetric observations on the surface. The gravitational perturbations of local, small-scale inhomogeneities in the Earth and the inability to make accurate visual observations when distances exceed a few tens of kilometers have made Earth-based geodesy quantitatively unsatisfying when describing the planet as a whole. In a sense, earthbound man is too close to his subject; he cannot see directly large-scale distortions of the Earth's spheroid. Of course, we have a natural satellite to observe, but the Moon is too far away to be significantly affected by the Earth's equatorial bulge and triaxiality. Several solar-system planets are fortunate enough to have close-in satellites that respond to their planets' irregularities; viz, Phobos and Deimos for Mars. Not being so blessed, we have had to create close-in artificial satellites in order to accurately chart where the Earth departs from a perfect sphere.

The objectives of geodesy are often stated as follows:

(1) Accurately measure the size and shape (figure) of the Earth

(2) Accurately locate points on the Earth's surface

(3) Accurately describe the gravitational field at all points on the surface of the Earth

It is significant that the adverb ''accurately'' appears in all three objectives. Surface geodesy makes progress toward each objective; Earth satellites aid substantially in making the results more accurate.

Theory of Satellite Geodesy.—Satellite geodesy, in its simplest form, works as follows: Satellites, as many as possible, are tracked from the Earth's surface with the utmost accuracy. From these observations, deviations of the satellites' orbits from the ideal Keplerian ellipse are computed (refs. 41, 42). Next, perturbations due to solar pressure, atmospheric drag, the attractions of the Sun and Moon, and other forces are estimated and subtracted out. Two crucial steps come next. Observed changes in orbital elements are translated into coefficients in a series expansion of the Earth's gravitational potential. The terms in the series expansion are then interpreted as irregularities in the figure of the Earth. Objective (1) has then been partially attained; viz, the degree of flattening of the Earth. Much remains to be done, however. Objective (2) can be achieved by observing the same satellites from widely separated points and trying these points together by triangulation. Objective (3), on the other hand, does

not benefit so much from satellite geodesy.   Large-scale features of the Earth's field can be inferred from the methods that led to objective (1), but the fine structure of the gravitational field at the surface is best mapped with gravimeters and other conventional surface instruments.   Here, the emphasis will be on the attainment of objective (1), the accurate measure of the figure of the Earth.

The first step consists of setting down the expansion of the Earth's gravitational potential in Legendre spherical harmonics

$$V(r,\phi,\lambda) = \frac{K}{r}\left[1 + \sum_{n=2}^{\infty} J_n\left(\frac{R_0}{r}\right)^n P_n \sin\lambda \right.$$
$$\left. + \sum_{n=2}^{\infty}\left(\frac{R_0}{r}\right)^n \sum_{m=1}^{n} J_n{}^m P_n{}^m \sin\phi \cos m(\lambda - \lambda_n{}^m)\right]$$

where

V = the gravitational potential (the geopotential)
r = the geocentric radius
ϕ = the geocentric, Earth-fixed latitude
λ = the geocentric, Earth-fixed longitude
R_0 = the mean equatorial radius of the Earth
J_n = zonal harmonics coefficients on degree n
$J_n{}^m, \lambda_n{}^m$ = nonzonal harmonic coefficients of degree n and order m

This generalized mathematical ''model'' of the Earth's potential does not include the ''centrifugal'' potential due to the Earth's spin in inertial space.   Since the expansion takes the Earth's
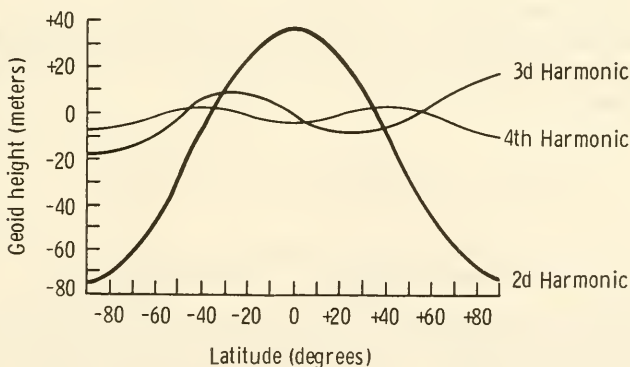
FIGURE 11–88.—Effects of the second, third, and fourth zonal harmonics on the height of the geoid above and below a perfect sphere. (*Space Log*, Spring 1965.)

center of mass as its origin, the term $n=1$ is missing. The first summation includes only terms that are rotationally symmetric about the Earth's spin axis. These are the zonal harmonics. The second summation contains those asymmetric terms that depend upon longitude. Where $m=n$, these are called tesseral harmonics.

Now, the transition from observables [15] to coefficients in the mathematical model must be made. Physically, the zonal harmonics are the most important, particularly the even ones, for they are interpreted in terms of the Earth's bulge (fig. 11–88). The perturbations in the observable orbital elements that lead to nonzero, even zonal harmonics are the westward precession of the orbit and the rotation of perigee within the orbital plane. Mathematically, the observable effects and harmonic coefficients are related by

$$\frac{d\Omega}{dt} = -\frac{3}{2} J_2 \left(\frac{R_0}{a}\right)^2 b \cos i + 0(J_2{}^2) + 0(J_4)$$

$$\frac{d\omega}{dt} = \frac{3}{4} J_2 \left(\frac{R_0}{a}\right)(4 - 5 \sin^2 i)b + 0(J_2{}^2) + 0(J_4)$$

where

Ω = the ascending node
ω = the argument of perigee
a = the semimajor axis of the orbit
i = the inclination of the orbit
b = the mean motion (2π/satellite period)

(These effects are also discussed in ch. 4.) The computed value of J_2 is so large—larger by almost 1000 than other even zonals—that even its second-order effects are important.

The orbital perturbations that are represented by the odd zonal harmonics are oscillations in the eccentricity, e, and the argument of perigee:

$$e = e_0 - \frac{1}{2} \frac{J_3}{J_2}\left(\frac{R_0}{a}\right) \sin i \sin \omega + 0\left(\frac{J_5}{J_2}\right)$$

$$\omega = \omega_0 - \frac{1}{2} \frac{J_3}{J_2}\left(\frac{R_0}{a}\right) \frac{\sin i}{e} \cos \omega + 0\left(\frac{J_5}{eJ_2}\right)$$

Summarizing, the even and odd zonal harmonics lead to a better description of the figure of the Earth, but only in terms of axially symmetric departures from a perfect sphere; viz, the Earth's bulge (fig. 11–88)

---

[15] See sec. 4–4 for description of orbital elements.

The nonzonal harmonics in the series expansion arise from irregularities in the Earth that are longitude dependent, like the deep negative gravitational anomaly in the area of the Indian Ocean. Each time a satellite swings by such anomalies, its orbit is slightly changed. The resulting orbital perturbations must have the same period as the satellite. Furthermore, the satellite passes over the perturbing area so fast that the irregularities in the gravitational force field have little chance to alter the orbit before the satellite is out of their range, and probably over a different anomaly, possibly one with a different sign. The satellite path thus has a fine structure of undulations superimposed upon it. The amplitudes of these deviations are typically on the order of a kilometer or less. They are best observed by making precise measurements of the satellite path for each orbit rather than collecting data on perturbations of the orbital elements over long periods of time. Doppler tracking, particularly by the Navy's TRANET (sec. 7–4), is most often used for following these small variations in the satellite path (ref. 43). Figure 11–89 illustrates these large-scale gravitational anomalies that are measured with the aid of satellites. Pendulums and gravimeters, of course, do a similar job, but on a much finer scale. While figure 11–89 shows linear departures from a standardized oblate spheroid (described by zonal harmonics), corresponding hills and valleys on the Earth's surface do not necessarily exist, for the map really describes only gravitational anomalies which can be created by inhomogeneities well below the Earth's surface.

Facilities and Tracking Techniques.—Satellite geodesy can be effective only when worldwide tracking networks with instruments of great accuracy are available. For more detail, the reader should consult section 6–2 for the various tracking techniques and section 7–4 for descriptions of the several global tracking networks that now exist.

Geodetic Satellites.—All satellite geodetic experiments involve terrestrial observers who track satellites, preferably more than one, with varied and complementary instruments. In this sense, satellite geodesy is related to observational satellite aeronomy and ionospheric study by radio-wave propagation analysis (sec. 11–3). The observer and the observed, though separated by hundreds of kilometers, are integral parts of the experiment. In other words, it is the vantage point of the satellite that makes it important rather than its capacity to measure the environment directly.
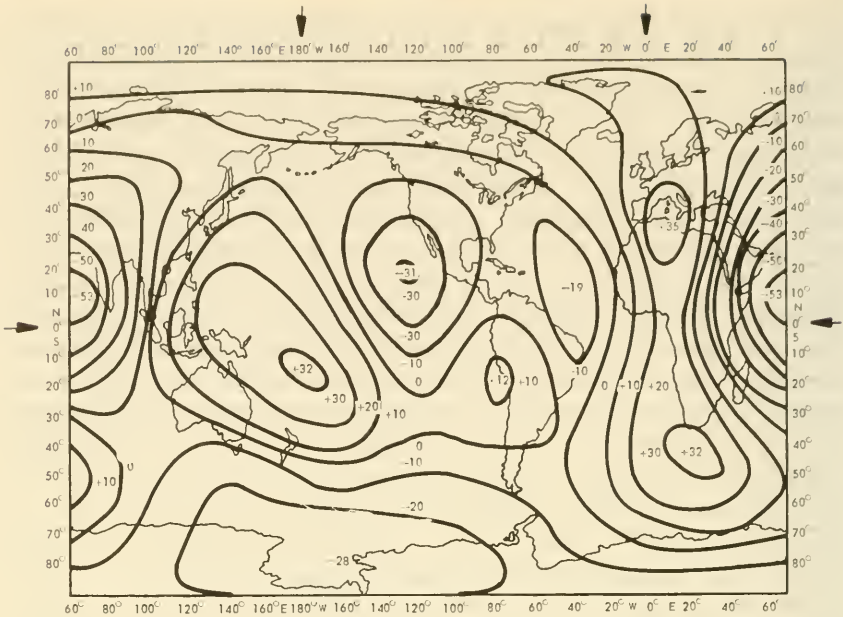
FIGURE 11–89.—Isopotential contours of the Earth above and below a reference oblate spheroid. Contours are in meters. (*Space Log,* Spring 1965.)

The many approaches to satellite tracking were discussed in section 6–2. Of these, the following techniques have enough inherent precision to be used in geodesy:

(1) Optical tracking of solar-illuminated, self-illuminated, and laser-illuminated satellites. Note that radar illumination is not widely applied to geodesy.

(2) Doppler tracking, especially for nonzonal harmonics. An active satellite is required here, preferably one with a special Doppler beacon.

(3) Special transponders, such as the Goddard Range-and-Range-Rate and Secor equipment, can also pinpoint orbital parameters.

Any satellite, if it is large enough or boasts a flashing light, can be optically tracked. Much of the early work in satellite geodesy perforce came from passive or silent satellites, and from active satellites with radio beacons that were not designed with geodesy in mind. The manifest value of satellites to geodesy and missile-targeting programs soon generated several series of satellites

TABLE 11-15.—*Geodetic Experiments*

Satellite	Onboard equipment	Tracking network(s)	Remarks
Anna 1B	Flashing light	DOD, SAO cameras	DOD program. Secor transponder did not function.
	Doppler beacon	TRANET	
	Secor transponder	Army Secor stations	
Secor series	Secor transponder	Army Secor stations	Piggyback satellites. Army program.
Beacon Explorers A and B (Explorers XXII and XXVII).	Laser reflectors	Wallops, AFCRL	NASA program.
	Doppler beacon	TRANET	
Geos A and B (Geos A = Explorer XXIX)	Laser reflectors	Wallops, AFCRL	NASA has overall responsibility with DOD and Department of Commerce participating. Part of national program.
	Flashing light	DOD, SAO cameras	
	Doppler beacon	TRANET	
	Secor transponder	Army Secor stations	
	Range-and-Range-Rate transponder.	STADAN	
Pageos	None	DOD, SAO cameras	Balloon satellite. Part of national program.
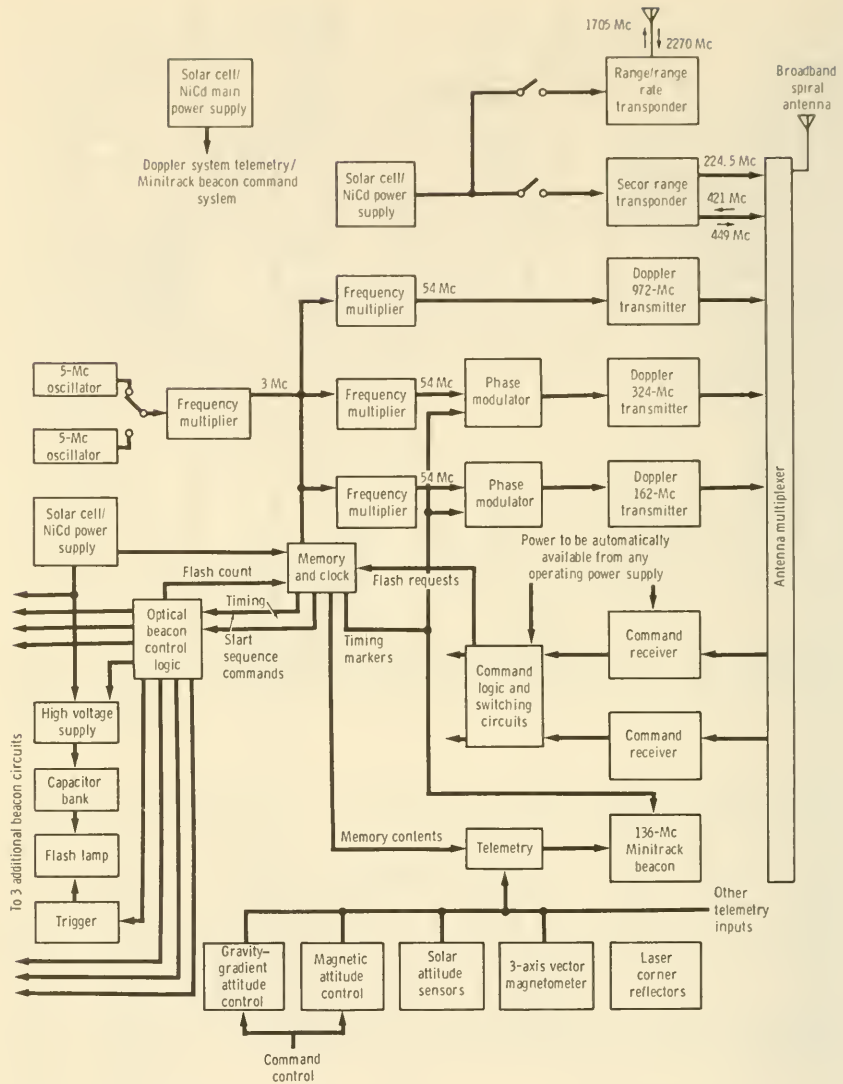
FIGURE 11–90.—Block diagram showing the Geos geodetic aids. Flash commands are transmitted to the satellite and stored in its memory. The Range-and-Range-Rate and Secor transponders transmit only when interrogated. The Doppler beacon transmits continuously. The laser corner reflectors are passive.

whose primary purpose was geodesy. These programs are listed in table 11–15, along with the tracking methods employed. All U.S. geodetic work with satellites has now been combined into the National Geodetic Satellite Program, in which NASA has overall responsibility, with the Departments of Defense and Commerce participating (ref. 44). The total experiment, of course, is the sum of the satellite(s) and all ground observers. The instruments in the experiment are the satellites themselves, their transponders and beacons, and the ground tracking-station equipment.

The basic elements of all previous geodetic satellites (table 11–15) are included in the new Geos series. In fact, one of the primary objectives of the Geos satellites is the comparison of results from the five different tracking aids included in the payload. (One hesitates to call a beacon an instrument, since in itself it cannot measure anything.) Other objectives of Geos are:

(1) The production of a worldwide system of control points accurate to 10 meters, on the surface of the Earth, but tied to the Earth's center of mass. This represents an order-of-magnitude improvement over the present system of control points.

(2) The linking of the dozen-or-so major geodetic systems, which are usually tied very accurately to separate central control points. The central control points themselves, unfortunately, are not tied together accurately, mainly because of intervening bodies of water.

(3) The definition of the Earth's gravitational field to better than 5 parts in 10^8, an improvement of 10 to 100 over present information [16]

(4) The improvement of the accuracy of the coefficients of the terms in the expansion of the Earth's gravitational potential

The appendix contains a capsule description of the Geos series of satellites. The principles behind each of the five tracking aids on board Geos have already been described in section 6–2. An overall block diagram of the Geos instrumentation is presented in figure 11–90.

References

1. Bourdeau, R. E., et al.: Experimental Evidence for the Presence of Helium Ions Based on Explorer VIII Satellite Data. J. Geophys. Res., vol. 67, Feb. 1962, p. 467. (Also NASA TN D–1346, 1962.)
2. King-Hele, D. G.: Upper-Atmosphere Densities. J. Brit. Interplanetary Soc., vol. 19, 1964, p. 374.

---

[16] Note that Geos alone cannot accomplish this, but it will complement other geodetic techniques in the attainment of this goal.

3. BROGLIO, L.: First Density Experiment With San Marco Instrumentation. *In* Space Research V, D. G. King-Hele, P. Muller, and G. Righini, eds., John Wiley & Sons, Inc., 1965.

4. SHARP, G. W.; HANSON, W. B.; AND MCKIBBIN, D. D.: Atmospheric Measurement With a Satellite-Borne Microphone Gage. J. Geophys. Res., vol. 67, Apr. 1962, p. 1375.

5. NEWTON, G. P., ET AL.: Response of Modified Redhead Magnetron and Bayard-Alpert Vacuum Gauges Aboard Explorer XVII. NASA TN D–2146, 1964.

6. NIER, A. O., ET AL.: Neutral Composition of the Atmosphere in the 100-to-200-kilometer Range. J. Geophys. Res., vol. 69, Mar. 1, 1964, p. 979.

7. SPENCER, N. W.; AND REBER, C. A.: A Mass Spectrometer for an Aeronomy Satellite. *In* Space Research III, W. Priester, ed., Interscience Publishers, 1963.

8. REBER, C. A.; AND HALL, L. G.: A Double-Focusing Magnetic Mass Spectrometer for Satellite Use. NASA TN D–3211, 1966.

9. SCHAEFER, E. J.; AND NICHOLS, M. H.: Mass Spectrometer for Upper Air Measurements. ARS J., vol. 31, Dec. 1961, p. 1773.

10. NARCISI, R. S., ET AL.: Calibration of a Flyable Mass Spectrometer for N and O Atom Sensitivity. *In* Space Research III, W. Priester, ed., John Wiley & Sons, Inc., 1963.

11. FRIEDMAN, R. M.; RAWCLIFFE, R. D.; AND MELOY, G. E.: Radiance of the Upper Atmosphere in the Middle Ultraviolet. J. Geophys. Res., vol. 68, Dec. 15, 1963, p. 6419.

12. BLOCK, L. C.; AND ZACHOR, A. S.: Inflight Satellite Measurements of the Infrared Spectral Radiance of the Earth. Appl. Optics, vol. 3, Feb. 1964, p. 209.

13. FISCHBACH, F. F.: A Satellite Method for Pressure and Temperature Below 24 KM. Am. Meteor. Soc. Bull., vol. 46, Sept. 1965, p. 528. (See also NASA CR–64045, 1965.)

14. ARGO, H., ET AL.: Nuclear Explosions in Space for Scientific Purposes. Univ. of Calif., UCRL–5679, 1959.

15. COOK, T. B.: The Use of Upper Atmosphere Nuclear Explosions as a Research Tool. Livermore Radiation Lab. UCRL–5679, 1959.

16. GARRIOTT, O. K.; AND BRACEWELL, R. N.: Satellite Studies of the Ionization in Space by Radio. *In* Advances in Geophysics, H. E. Landsberg and J. Van Mieghem, eds., Academic Press, 1961.

17. MASS, J.: Survey of Satellite Techniques for Studying Propagation. *In* Radio Astronomical and Satellite Studies of the Atmosphere, J. Aarons, ed., Interscience Publishers, 1963.

18. YEH, K. C.; AND SWENSON, G. W.: F-Region Irregularities Studies by Scintillation of Signals From Satellites. J. Res. Nat. Bur. Std., vol. 68, Aug. 1964, p. 881.

19. MULLEN, J. P.; DANIELS, G.; AND ALLEN, R.: Investigating Ionospheric Ducting With the ORBIS Beacon. AD 430420, 1964.

20. BLUMLE, L. J.; FRITZENREITER, R. J.; AND JACKSON, J. E.: The National Aeronautics and Space Administration Topside Sounder Program. NASA TN D–1913, 1963.

21. MOLOZZI, A. R.: Instrumentation of the Ionospheric Sounder Contained in the Satellite 1962 Beta Alpha (Alouette). *In* Space Research IV, P. Muller, ed., John Wiley & Sons, Inc., 1964.

22. FICKLIN, B. P.: Description and Operation of the Instruments for the Stanford University/Stanford Research Institute Experiment (5002) to Be Flown on the POGO Satellite. Stanford Res. Inst. Rept., Tech. Memo. 2, Menlo Park, 1965.

23. FLATLEY, T. W.; AND EVANS, H. E.: The Development of the Electric Field Meter for the Explorer VIII Satellite. NASA TN D–1044, 1962.

24. HAYCOCK, O. C.; AND BAKER, K. D.: New Ionosphere Measurement Technique: Plasma Frequency Probe. Electronics, vol. 35, Nov. 30, 1962, p. 81.

25. ULWICK, J. C., ET AL.: Description of Standing Wave Impedance Probe. COSPAR Info. Bull., no. 17, Feb. 1964.

26. BOURDEAU, R. E., ET AL.: The Ionosphere Direct Measurements Satellite Instrumentation (Explorer VIII). ARS paper 61–173–1867, 1961. (See also NASA TN D–414, 1962.)

27. GRINGAUZ, K. I.: Some Results of Experiments in Interplanetary Space by Means of Charged Particle Traps on Soviet Space Probes. *In* Space Research II, H. C. van de Hulst, C. de Jager, and A. F. Moore, eds., Interscience Publishers, 1961.

28. EVANS, D. S.: Low Energy Charged Particle Detection Using the Continuous Channel Electron Multiplier. IEEE Trans., NS–12, Feb. 1965, p. 34.

29. LUDWIG, G. H.; AND MCDONALD, F. B.: Cosmic Ray Experiments for Explorer XII and the OGO. *In* Space Research III, W. Priester, ed., John Wiley & Sons, Inc., 1963.

30. REAGAN, J. B., ET AL.: Multichannel Spectrometer for the Measurement of Trapped Particles. IEEE Trans., NS–12, Feb. 1965, p. 83.

31. FRANK, L. A.: Low-Energy Proton and Electron Experiment for the Orbiting Geophysical Observatories B and E. AD 466738, 1965.

32. YAGODA, H.: Radiation Studies in Space with Nuclear Emulsion Detectors. Space Sci. Rev., vol. 1, 1962, p. 224.

33. SONETT, C. P.: Modulation and Sampling of Hydromagnetic Radiation. NASA TN D–2950, 1965.

34. PATEL, V. L.: Low Frequency Hydromagnetic Waves in the Magnetosphere. Planetary and Space Sci., vol. 13, June 1965, p. 485.

35. NESS, N. F.; SCEARCE, C. S.; AND SEEK, J. B.: Initial Results of the IMP I Magnetic Field Experiment. J. Geophys. Res., vol. 69, Sept. 1, 1964, p. 3531.

36. D'AIUTOLO, C. T.: The Micrometeoroid Satellite, Explorer XIII (1961 Chi). NASA TN D–2468, 1964.

37. ROGALLO, V. L.; AND NEUMAN, F.: A Wide-Range Piezoelectric Momentum Transducer for Measuring Micrometeoroid Impacts. NASA TN D–2938, 1965.

38. POLLACK, F. G.; WINSLOW, P. C.; AND DAVISON, E. H.: Preliminary Experimental Investigation of a Double Capacitor Coincidence Discharge-Type Micrometeoroid Penetration Sensor. NASA TM X–1037, 1964.

39. ROSENTHAL, R. D.: The Pegasus Meteoroid Technology Satellite. Paper presented at Unmanned Spacecraft Meeting. AIAA Pub. CP–12, 1965.

40. NEUMAN, F.: A Micrometeoroid Velocity Detector. NASA TN D–1977, 1963.

41. COOK, A. H.: The Contribution of Observations of Satellites to the Determination of the Earth's Gravitational Potential. Space Sci. Rev., vol. 2, 1963, p. 355.
42. KAULA, W. M.: Theory of Satellite Geodesy. Blaisdell Pub. Co., 1965.
43. GUIER, W. H.: Recent Progress in Satellite Geodesy. AD 462616, 1965.
44. DULBERGER, L. H.: Geodetic Measurements From Space. Space/Aero., vol. 44, June 1965, p. 34.

Chapter 12

SOLAR-PHYSICS INSTRUMENTS AND EXPERIMENTS

12-1. Prolog

When rockets and spacecraft carry instruments above the Earth's absorbing and distorting atmospheric blanket, the observable spectrum of the Sun is extended at short and long wavelengths. With atmospheric ozone and other absorbers far below their instruments, solar physicists can finally see the rich spectral details of the Sun that lie below 3000 Å in the X-ray and ultraviolet regions. In orbit, the atmosphere's water vapor no longer blocks the infrared spectrum. Neither is there an ionosphere to turn back low-frequency radio waves that help diagnose solar activity. If a satellite possesses an elongated orbit, it can also pierce the magnetosphere and measure the solar plasma (solar wind) directly, so that these particulate emissions can be correlated with the foregoing electromagnetic observations. Finally, once the atmosphere is out of the way, the solar cosmic rays can be observed free from the scattering, absorption, and transmutations that occur in the 100 kilometers of atmosphere before they reach the Earth's surface. For these reasons, experiments in solar physics were conducted from high-flying balloons and rockets a decade before the advent of satellite platforms. The major advantage of the scientific satellite is that instruments can be kept pointed at the Sun with greater stability and for longer periods of time. It is not surprising, then, to find many solar experiments common on scientific satellites.

A major difference between geophysical and solar experimentation is the requirement for instrument (or satellite) pointing; that is, the use of highly directional instruments and aiming them at the Sun. The Sun subtends an angle of only 31 minutes, and instruments fixed on spin-stabilized satellites will rarely pick up the Sun as they rotate in outer space unless they have wide fields of

view. As we have seen in chapter 11, this scanning of the entire space environment is desirable in many geophysical experiments, but it is manifest that the study of the Sun's emissions demands precision pointing in many, though not all, experiments. Furthermore, some instruments—especially optical instruments—can image small portions of the Sun, so that a satellite scanning platform that sweeps the Sun's disk periodically in a geometric pattern (raster) is a desirable experimental tool.

Besides these changes in general satellite-design philosophy, the instruments themselves must change to adjust to the new ranges of phenomena. The optical instruments of chapter 11, which viewed the Earth's low-temperature, low-energy atmospheric emission and absorption spectra, must find new optical devices and different photon detectors to measure the short wavelengths characteristic of the hot Sun. The detectors of particulate radiation must also adjust to the much more energetic emissions of the Sun. Solar cosmic radiation is much harder than the trapped radiation, and, of course, is directional. Solar cosmic rays also include neutrons, gamma rays, and heavy particles that are not native to the radiation belts. As always in solar research, there is intense interest in detecting changes in solar activity, such as the sudden onset of storms and the long-term variations associated with the 11-year solar cycle.

Several dozen solar experiments are listed in the summary tables of this chapter. Despite the desirability of accurate instrument pointing, most solar instruments to date have flown on small spin-stabilized satellites. The solar-radiation satellites instrumented by the Naval Research Laboratory are typical of the specialized spacecraft in this category. NASA's highly successful OSO (Orbiting Solar Observatories) series of satellites has carried the great bulk of all pointed solar experiments. Many other satellites have aided solar research by transporting plasma probes out beyond the magnetopause and by recording solar cosmic rays as they scanned outer space. The influence of the Sun on geophysical phenomena is so strong that an event such as a large solar flare is recorded by magnetometers, plasma probes, radiation detectors, auroral photometers, and other geophysical instruments all over the Earth.

This chapter covers four classes of solar phenomena: solar electromagnetic emissions, solar plasma, the solar magnetic field, and solar cosmic rays. Many of the instruments described here are merely extensions or modifications of basic instruments used in satellite geophysics and described in chapter 11. Rather than

repeat the fundamentals, there will be frequent references to the previous discussions.

12–2.   Instruments   and   Experiments   for   Analyzing   the Solar Electromagnetic Flux

The satellite in orbit intercepts electromagnetic radiation that covers the entire spectrum from radio waves to X-rays.[1] Yet, satellites and sounding rockets have concentrated almost exclusively on the analysis of the very short wavelengths: the ultraviolet and X-ray regions marked on table 12–1. History shows rocket and satellite payloads of increasingly sophisticated ultraviolet and X-ray instruments. Infrared and microwave equipment is conspicuously absent. The reasons for the concentration of effort are two: (1) The Sun is so hot that the short wavelengths give many more clues about the physical processes taking place, from the 6000° C photosphere to the million-degree corona. (2) Much infrared research can be done more conveniently from the Earth's surface through the several infrared windows and from high-flying balloons above the bulk of the atmosphere's water vapor. Satellites again become vital instrument platforms when one is interested in the radio noise of the Sun below 15 megacycles or so, the point where the ionosphere prevents radio waves from reaching balloon levels or the surface. Infrared and microwave radiometers are found, of course, on space probes, such as Mariner II, where relatively cold planetary atmospheres are the subjects of experimentation.

The sunlight intercepted by a satellite instrument possesses the property of flux or intensity, which is usually measured as a function of wavelength. Elaborating upon the definitions tendered earlier in tables 11–2 and 11–3, an instrument that disperses the light and scans the resulting spectrum is called a spectrograph or spectrometer, and its resulting record of intensity vs. wavelength, a *spectrogram* (table 12–2). When only a single narrow region of the spectrum is measured, the instrument is termed a "photometer." Spectrophotometers measure the intensities of several spectral lines or narrow spectral regions.

---

[1] Gamma rays from solar nuclear reactions are considered part of the solar cosmic-ray flux (sec. 13–3), even though they are electromagnetic in nature. It is also pertinent to point out that X-rays, by definition, originate in the quantum jumps of the inner electrons of atoms. When the same emission lines result from the transitions of outer electrons of the same—but multiply ionized —atoms, the radiation is considered by many to be part of the ultraviolet spectrum rather than X-rays. Others say simply: X-rays<100 Å< X-ultra violet (XUV).

TABLE 12-1.—*Table Showing How Solar Instruments and the Associated Terminology Change With Wavelength*

[Use this table in conjunction with table 12-2]

	Spectral terminology			
	Sea-level ultraviolet (~4000–2900 Å)	Near ultraviolet (~2900–1500 Å)	Far ultraviolet (~1500–500 Å)	Extreme ultraviolet (EUV, XUV) (~500–1 Å)
Solar phenomena		Chromospheric emission, continuum and Fraunhofer lines.	Chromospheric emission (1216 Å, Lyman-α).	Coronal emission.
Detectors		Films, photoelectric detectors		Photon counters.
Wavelength discriminators	Prisms	Filters, gratings	Filters, gratings	Detector response, crystals, pulse-height analysis.
Spatial discriminators	Lenses, slits	Reflective optics, slits	Reflective optics, slits	Grazing-incidence optics, pinholes.

TABLE 12–2.—*Chart of Components Used in Solar-Physics Optical Instrumentation*

Spatial discrimination	Wavelength discrimination	Detectors (amplitude discrimination)

Spatial dissection:
    Field stops
    Slits
    Masks (in corona-
        graphs)
Imaging:
    Lenses
    Reflective optics
    Grazing-incidence optics
    Pinholes
    Fresnel-zone plates
	Nondispersive:
	    Filters
	    Detector response:
	        Proportional
	          counters
	        Pulse-height
	          analysis
	        Photoelectron
	          energy
	        Emulsion, etc.
	    Combinations of
	        above
	Dispersive:
	    Gratings
	    Crystals
	    Prisms
		Continuous detectors:
		    Photocells
		    Photomultipliers
		    Emulsions
		    Ionization chambers
		    Channel multipliers
		Photon counters:
		    Geiger counters
		    Scintillators
		    Proportional counters

Unlike the other stars, the Sun is close enough so that instruments can produce images of small portions of it at various wavelengths and scan its surface in a rasterlike fashion. An instrument that maps the Sun in a single wavelength is a spectroheliograph. In solar instrumentation, the term "telescope" is extended to include ultraviolet and X-ray imaging devices employing reflection and grazing-incidence optics. Completing the glossary, a coronagraph images only the Sun's corona, while blocking out the bright photosphere.

Another physically important measurable parameter of sunlight involves the dimension of time. Ideally, scientists would like to record the Sun's image at all wavelengths over long periods of time with sufficient resolution to discern transient phenomena.

In sum, there are four critical measurable quantities: intensity, energy (wavelength), ray angle (in imaging), and time. To resolve sunlight along these four dimensions, an instrument utilizes some combination of the three elements shown in table 12–2, plus supporting electronic circuitry.[2] A simple Lyman-α photometer,

---

[2] Actually, the characteristics of the satellite communication and attitude-control subsystems help determine maximum data rates and experiment accuracy.

for example, might have its field of view limited only by a circular aperture (spatial discrimination). Wavelength discrimination might come from a filter that passes only the Lyman-α line and a small region of the spectrum around it. The third element of the instrument, the detector, could be an ionization chamber. The detector provides amplitude discrimination. Instruments like this have been flown frequently and will be described in more detail later. A more complex instrument is the ultraviolet spectroheliograph. Mounted on a satellite scanning platform, its curved reflecting mirrors might image small sections of the Sun on a photocell detector. A grating between the optics and detector would produce the spectrum by dispersion. Spectral scanning (in addition to spatial scanning) might be accomplished by mechanically moving the detector along the line of dispersed images (Rowland circle). In both illustrations, discrimination along the time dimension depends upon the instrument, the data-sampling rate and the response of electronic equipment on the satellite and back on Earth.

Several excellent reviews of experimental techniques employed in the ultraviolet and X-ray regions exist (refs. 1, 2, 3, 4). Here, a few general remarks about the major instrument components listed in table 12–2 seem sufficient. They will be buttressed later by hardware examples from satellite research.

Most satellite instruments flown so far have not attempted to image the Sun or even dissect its image. The early instruments were predominantly simple photometers with wide fields of view that caught the Sun's rays as the satellite spun. The entrance apertures were usually just holes that admitted light to the filter and detector. Slit spectrographs did not appear on satellites until OSO I, though many were flown much earlier on sounding rockets. Imaging in the ultraviolet and X-ray portions of the spectrum cannot be achieved conveniently with reflective optics; absorption is too high. Reflection and diffraction are utilized instead. The first X-ray image of the Sun, for example, was acquired with a pinhole camera and filter from a sounding rocket, in 1960, by Chubb and his colleagues at the Naval Research Laboratory (NRL). X-ray "telescopes" are made from several slightly curved mirrors positioned almost parallel to the incoming radiation (fig. 12–1). Only at such angles will reflectivity be high enough at these wavelengths. More than one mirror is used to help correct astigmatism inherent in reflective optics. Advanced imaging instruments of this type are planned for future, more precisely pointed solar observatories.
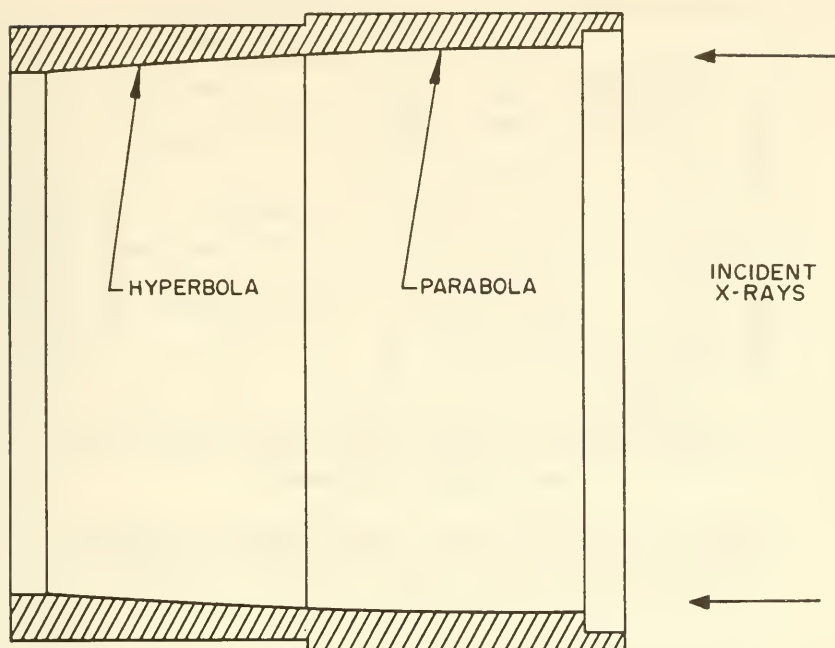
FIGURE 12–1.—Reflecting optics of an X-ray telescope. Incident, nearly parallel rays will be reflected once from each of the two sections and ultimately come to a focus (ref. 5).

The different wavelengths present in sunlight can be resolved in several ways. One usually distinguishes the so-called dispersive methods, which spatially separate the spectrum, from the nondispersive filters and spectrally sensitive detectors. Historically, simple techniques generally come first, and the early satellite photometers used filters to separate out different segments of the solar spectrum, particularly the crucial Lyman-α line of hydrogen at 1216 Å. It is possible to isolate the Lyman-α region by passing sunlight through LiF and CaF_2 filters mounted on separate photometers, as their transmission properties (fig. 12–2) demonstrate. Or, a narrow portion of the hard X-ray spectrum can be isolated by use of a beryllium window (fig. 12–3). The various detectors used in X-ray research (table 12–2) are often spectrally selective. The photoelectric yields of different cathode materials, for example, vary markedly with wavelength. The window materials and filling gases in proportional counters can be varied to select the desired portion of the incident spectrum (fig. 12–4). At very short wavelengths, the quanta are so penetrating that scintillators and pulse-height counting are feasible. Different combinations of
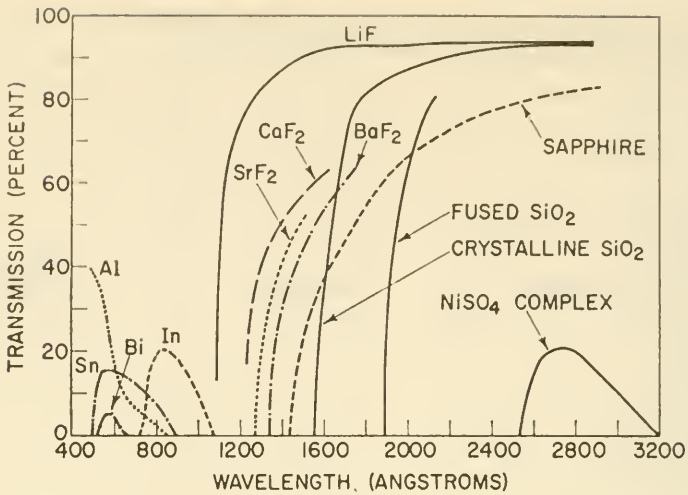
FIGURE 12–2.—Transmission characteristics of various
ultraviolet filters. Metal films are 1000 Å thick; other
materials are 1 millimeter thick (ref. 2).
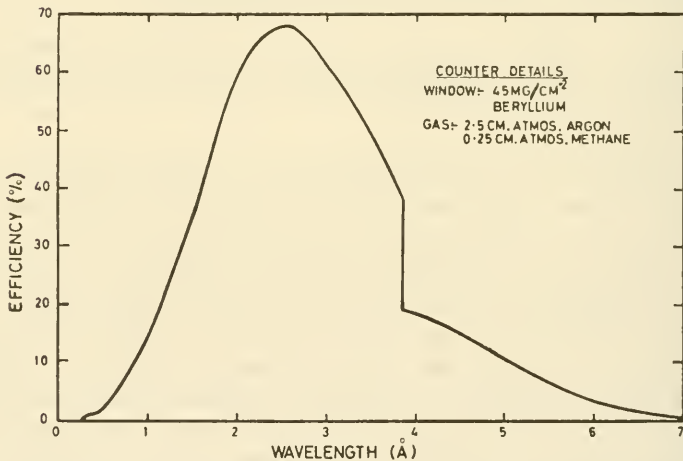
FIGURE 12–3.—Beryllium-window counter with long-
wavelength response modified by argon K-edge (ref. 1).

detectors and filters can isolate just about any desired region of
the solar ultraviolet and X-ray spectra. The approach is simple,
but inflexible in the sense that each instrument sees only a single,
narrow portion of the available spectrum. Multiple photometers
or rotating filter wheels make nondispersive instruments more
versatile.
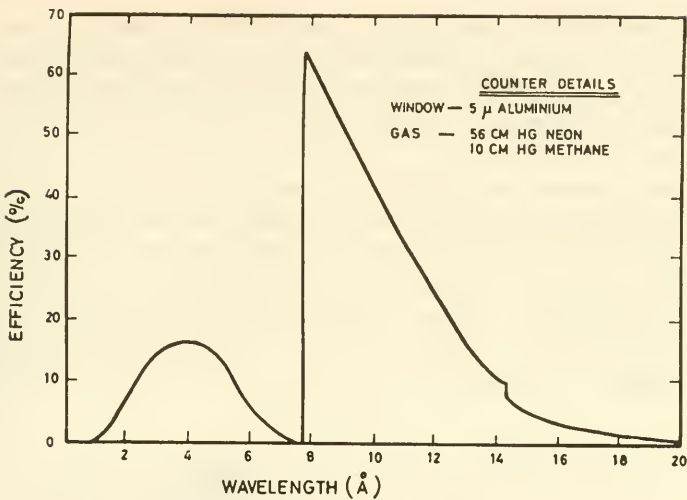
FIGURE 12–4.—Computed photon efficiency of a neon-filled proportional counter with an aluminum window (ref. 1).

Dispersive instruments, like imaging instruments, are at the apex of the development cycle. They are more complicated but, as if in compensation, generate a great deal more information. Prisms are the common dispersive elements in the visible region of the spectrum, but they cannot be used for X-rays and ultraviolet light, for the same reasons that lenses cannot be incorporated in short-wavelength telescopes. Reflecting devices, such as ruled gratings, again replace refractive components. Crystal spectrometers are common at the X-ray end of the solar spectrum. Since dispersive elements spatially separate the different wavelengths, some mechanical method of scanning the spectrum must be devised.[3] The detector, the dispersive element (grating or crystal), or the entrance slit can be moved to accomplish this scanning. Examples of these scanning methods will be presented in this section.

The final element of the optical instrument to be considered here is the detector—the device that converts photons into electrical signals (excepting, of course, recoverable emulsions). Once again, there are two classes of elements: those that produce an analog signal proportional to the intensity of the incident flux and those that count individual photons. The photon counters are gen-

---

[3] An instrument that disperses the spectrum and records only a narrow region of it is called a monochromator.

erally reserved for the "hard" end of the spectrum, where the quanta are energetic (penetrating) and their particle-like properties are accentuated. Table 12–2 lists examples of both classes of detectors. Most have already been described in detail in section 11–4.

Filter Photometers.—The Navy satellite Solrad 1 carried two simple filter photometers, one in the Lyman-α region and one measuring hard X-rays. These instruments were designed and built by NRL, and typify this basic instrument, which has been used on subsequent Solrad satellites, Explorer XXX, and many others (refs. 6, 7). (See table 12–3.) Photographs showing the basic design are presented in figure 12–5. The geometry of the
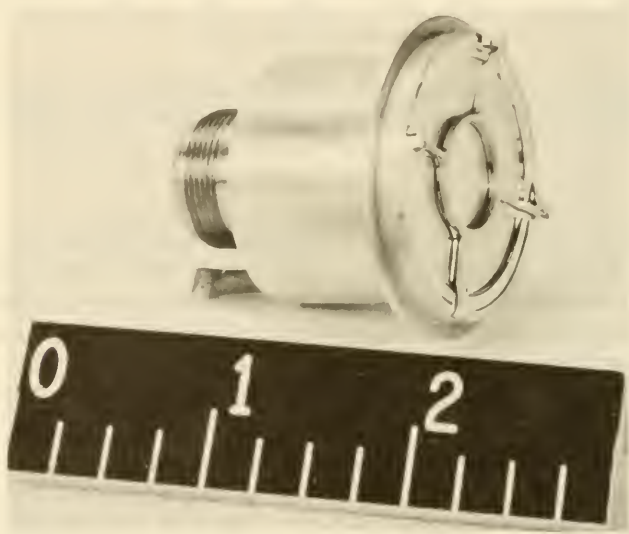
Figure 12–5.—The NRL X-ray photometer flown on Solrad 1. (U.S. Navy photograph.) Scale is in inches.

aperture and ionization chamber define the instrument's view angle. In Solrad 1 a solar-aspect sensor was mounted on the satellite so that it looked along the same axis as the X-ray photometer. An Alnico magnetic broom preceded the filter and shielded the detector from most of the trapped electrons. The magnet, however, also affected the satellite's attitude stability once it was placed in orbit—a rather unusual example of a sensitive satellite-instrument interface. Spectral selectivity was provided by the combined characteristics of the filters and the ionization-chamber responses.

Table 12–4 lists the characteristics of both photometers. The range of the X-ray photometer, 2–8 Å, was limited by the transmission characteristics of the beryllium filter, as modified by the K-edge of the argon gas filling the ionization chamber. The response curve of the Solrad-1 X-ray photometer was similar to that portrayed in figure 12–3. The bandpass of the Lyman-α photometer again depended upon the combination response of filter and ionization chamber. Figure 12–2 indicates the short-wavelength cutoff of lithium fluoride filters. This is confirmed by the composite response of the total photometer shown in figure 12–6. The long-
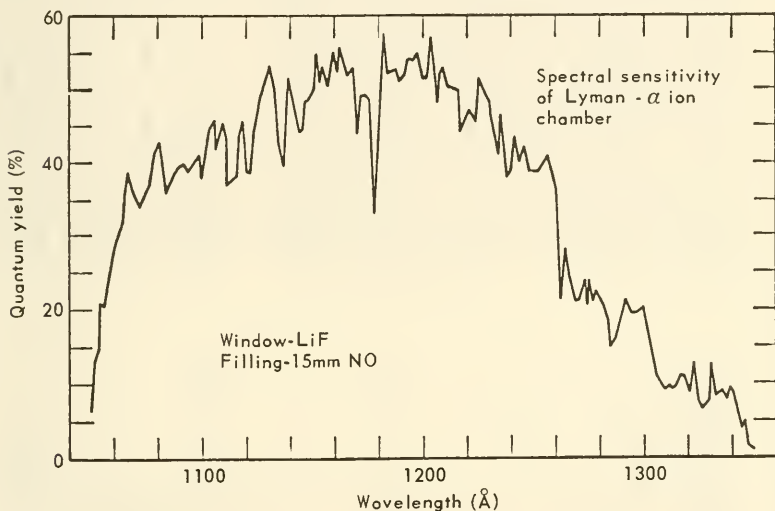
FIGURE 12–6.—Spectral sensitivity of the Lyman-α filter photometer carried on Solrad 1 (ref. 6).

wavelength cutoff is provided by the declining response of the ionization chamber. These simple instruments have performed well in orbit and are still widely used. Frequently, as on Sputnik 3 and Explorer XXX, the photometer ionization chambers are replaced by Geiger counters or proportional counters.

Spectrophotometers.—Boyd and Stewardson and their coworkers at University College, London, and the University of Leicester have designed two similar X-ray spectrophotometers for ESRO 2 and the wheel section of OSO D. By combining appropriate filters and filler gases for their proportional counters (table 12–5), their ESRO-2 instrument spans the range from 1 Å to 20 Å. The OSO D experiment contains two additional photometers that cover the wavelengths from 44 Å to 70 Å (ref. 1). Both experiments will

Table 12-3.—*Instruments, Experimenters, and Experiments for the Study of Solar Radiation*

Photometers (nondispersive):

Ariel 1	Bowles, J. A./University College	Three Lyman-α ionization chambers.
	Boyd, R. L. F./University College	Two X-ray proportional counters, 3–12 Å.
Elektron 2, 4	—/—	Two X-ray counters, 2–8 Å, 8–18 Å.
ESRO 2	Stewardson, E. A./U. Leicester	Five proportional counters, 1–20 Å.
Explorer VII	Friedman, H./NRL	Two X-ray ionization chambers, 2–8 Å; 2 Lyman-α ionization chambers, LiF windows, 1050–1350 Å.
Explorer XXX	Friedman, H./NRL	Ionization chambers: Mylar window, 0–20 Å; Be window, 1–8 Å; Mylar window, 44–60 Å; Be window plus magnet, 1–8 Å; Al window, 8–16 Å; LiF window, 1080–1350 Å; CaF₂ window, 1225–1350 Å.
		Geiger detectors: pair with Be windows, 1–8 Å; pair with mica windows and Be filter, 0.5–3 Å.
OGO II, D	Kreplin, R. W./NRL	Ionization chambers, 0.5–3 Å, 2–8 Å, 8–16 Å, 44–60 Å.
OGO E	Kreplin, R. W./NRL	X-ray proportional counters.
OSO I	Frost, K./GSFC	Two Be-window ionization chambers, 1–8 Å, pointed.
	Hallam, K./GSFC	Ultraviolet filter photometer, 3800–4800 Å, wheel.
		LiF-window ionization chamber, 1100–1250 Å, wheel.
OSO II	Chubb, T. A./NRL	X-ray telescope, 2–8 Å, 8–20 Å, 44–60 Å, pointed.
OSO D, F	Kreplin, R. W./NRL	Ionization chambers, 0.1–1.6 Å, 0.5–3 Å, 2–8 Å, 8–16 Å.
OSO D	Boyd, R. L. F./University College	Seven proportional counters, 1.2–70 Å.
OSO E	Teske, R. G./U. Mich	X-ray ionization chambers, 8–20 Å, wheel.
OSO F	Blamont, J./U. Paris	Lyman-α telescope using hydrogen-absorption cell, wheel.
OSO G	Argo, H. V./Los Alamos	Solar X-ray monitor, 16–40 Å, wheel.
	Brini, D./U. Bologna	Solar X-ray monitor, 20–200 keV, wheel.
	Kreplin, R. W./NRL	Three filtered Geiger tubes, 1–8 Å, 8–16 Å, 44–60 Å, pointed.
OV–1–11	Friedman, R. M./Aerospace	Be-window proportional counter, 2–14 Å.
OV–5–1	DeGiacomo, G. M./AFCRL	Be-window proportional counter, 0.5–14 Å.

Solrad 1	Friedman, H./NRL	Two Be-window ionization chambers, 2–8 Å; 2 with LiF windows, 1040–1340 Å.
Solrad 3	Friedman, H./NRL	Ionization chambers, 2–8 Å, 8–20 Å.
Solrad 4A	Friedman, H./NRL	Four ionization chambers, 0.5–3 Å, 2–8 Å, 8–16 Å. Four Lyman-α ionization chambers.
Solrad 7A	Kreplin, R. W./NRL	Ionization chambers, 2–8 Å, 8–14 Å, 8–16 Å, 44–55 Å, 44–60 Å, 1225–1350 Å.
TD–2	Blamont, J./U. Paris	Lyman-α, hydrogen absorption cell.
Vanguard III	Friedman, H./NRL	Ionization chambers, Be windows, 2–8 Å; LiF windows, 1050–1350 Å.

Dispersive spectrometers and spectrophotometers:

OGO II, E	Hinteregger, H. E./AFCRL	Monochromator, 250–1300 Å.
OSO I	Behring, W./GSFC	Scanning grating spectrometer, 10–400 Å, pointed.
OSO II, D	Goldberg, L./Harvard U	Grating stepped over range, 300–1400 Å, pointed.
OSO D	Chubb, T. A./NRL	Bragg crystal spectrometer, 1–8 Å, pointed.
OSO D	Boyd, R. L. F./University College	Grating monochromator, 304 and 1216 Å, wheel.
OSO F	Rense, W./U. Colo	Grating, 760–1030 Å, 465–630 Å, 280–370 Å, pointed.
OSO G	Kreplin, R. W./NRL	Bragg crystal spectrometer, 0.6–25 Å, pointed.
OV–1–10	Rugge, H./Aerospace	Bragg crystal spectrometer.
OV–1–11	Rugge, H./Aerospace	Two crystal spectrometers, one scanning.
TD 2	Stewardson, E. A./U. Leicester	Bragg crystal spectrometer, 1–25 Å.

Spectroheliographs:

OSO II, D, G	Goldberg, L./Harvard U	Monochromatic image in range 300–1400 Å, pointed.
OSO II	Tousey, R./NRL	Scans Sun at 304 Å, 584 Å, 1216 Å, pointed.
	Chubb, T. A./NRL	Filters and Geiger-Müller tubes, 8–20 Å, 44–60 Å, pointed.
OSO D	Paolini, F./Amer. Sci. and Eng	Scans at 18–37 Å, 3–38 Å, 44–75 Å, 3–13 Å, 3–50 Å, 3–14 Å, pointed.
OSO F	Stewardson, E. A./U. Leicester	Scans at 3–9 Å, 8–18 Å, pointed.
	White, W. A./GSFC	Scans at 1–2.5 Å, 2.5–6 Å, 6–25 Å, 25–400 Å, pointed.
	Purcell, J. D./NRL	Scans at 284, 304, 335, 584, 1216 Å, pointed.
TD 2	Boyd, R. L. F./University College	Far ultraviolet.

TABLE 12–3.—*Instruments, Experimenters, and Experiments for the Study of Solar Radiation*—Continued

Coronagraphs:

    OSO II _____ Tousey, R./NRL _____ Lyot-type, white light, pointed.

Scintillators and solid-state detectors:

    ESRO 2 _____ de Jager, C./U. Utrecht _____ Soft solar X-rays between 44 and 70 Å.

    OSO I _____ Frost, K./GSFC _____ NaI crystal, 20–100 keV, pointed.

TABLE 12–4.—*Characteristics of the Solrad-1 Photometers*

[From ref. 6]

Wavelength	2–8 Å	1050–1350 Å
Window material	Beryllium	Lithium fluoride
Window thickness	0.013 cm	Approx. 1 mm
ρX (window)	0.025 gm/cm²	
Window area	2.33 cm²	$2 \times 9.4 \times 10^{-5}$ cm²
Absorbing gas	Argon	Nitric oxide
Gas pressure	760 mm Hg	15 mm Hg
Ion-chamber depth at normal incidence.	2.54 cm	2.4 cm
ρX (gas)	0.0045 gm/cm²	
Ion pairs/erg	2.2×10^{10}	

be launched between 1966 and 1968 to measure the X-ray emissions of the Sun during a relatively quiescent period.

The major difference between the present instruments and the Solrad photometers, in addition to the collective spectrophotometer action, is the substitution of proportional counters for ionization chambers. In the proportional counter, each photon produces a count with an amplitude proportional to the photon's energy. Pulse-height analyzers, shown in the ESRO-2 schematic (fig. 12–7), then provide an additional means of resolving the energy spectrum. In comparison, the ionization chamber yields an analog signal with an amplitude proportional to the integrated energy of photons passing through the chamber. Two modes of operation are possible for the ESRO-2 experiment: the normal, high-sensitivity mode, with counters A, B, and D monitoring a quiet Sun; and a low-sensitivity mode, when counters A, C, and E are automatically switched in during flareups on the Sun. With the two modes, six orders of magnitude of solar X-ray flux can be telemetered to Earth. The schematic also shows a guard counter in coincidence with counter D. The purpose is to reduce the background noise in the 1–3-Å region, where the X-rays from the quiet Sun have hithertofore been lost in noise and thus have yet to be measured. The ESRO-2 experiment is calibrated by the 2.1-Å radiation from an Fe[55] radioactive source, which can be admitted by shutters to those counters sensitive to this wavelength upon command from the ground. Figure 12–8 illustrates the arrangement of the counters and their look angles.

Dispersive Spectrometers.—As early as June 28, 1946, a group at the Naval Research Laboratory flew a spectrograph on a captured V–2 rocket. Exposures during the tumbling flight were too

TABLE 12–5.—*Characteristics of the ESRO-2 Proportional Counters*

Counter identification	Wavelength band	Counter geometry and dimensions	Filler gas	Window material
A	8–20 Å	Cylindrical, 22.2-mm dia, 139.3-mm length.	Neon/methane	Aluminum.
B	3–9 Å (high sensitivity)	Cylindrical, 31.75-mm dia, 175-mm length.	Neon/methane	Beryllium.
C	3–9 Å (low sensitivity)	Cylindrical, 31.75-mm dia, 167.2-mm length.	Neon/methane	Beryllium.
D	1–3 Å (high sensitivity)	End window (disk-shaped), 60-mm dia, 24-mm thick.	Argon/methane	Beryllium.
D (guard)		Within D	Same as D	No X-ray window.
E	1–3 Å (high sensitivity)	Cylindrical, 22.2-mm dia, 116.4-mm length.	Argon/methane	Beryllium.
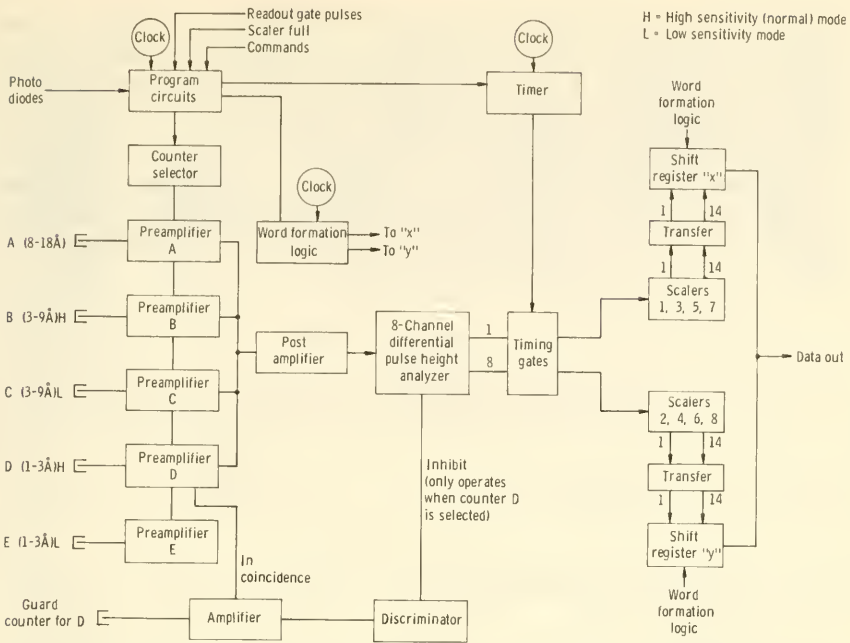
FIGURE 12-7.—Block diagram of the ESRO-2 proportional-counter spectrophotometer for analyzing hard solar X-rays.
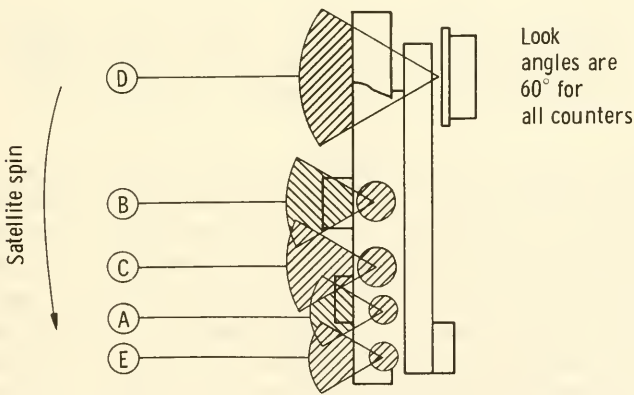
FIGURE 12-8.—Arrangement and look angles of the ESRO-2 proportional counters.

short for successful recording of solar radiation below about 2000 Å. These experiments made it obvious that pointed instrument platforms were a necessity to solar spectroscopy in the far ultraviolet.

The first pointed spectrographs with dispersive optics to be launched into outer space were mounted on Aerobee rockets, fired from White Sands in the early 1950's. These instruments were aimed by the University of Colorado Sunfollower, mentioned in chapter 2. The first satellite spectrograph to study the far ultraviolet was orbited on OSO I, in 1962, on the satellite's pointed section (sail). This instrument, built by Behring and his associates at the Goddard Space Flight Center, will now be described.
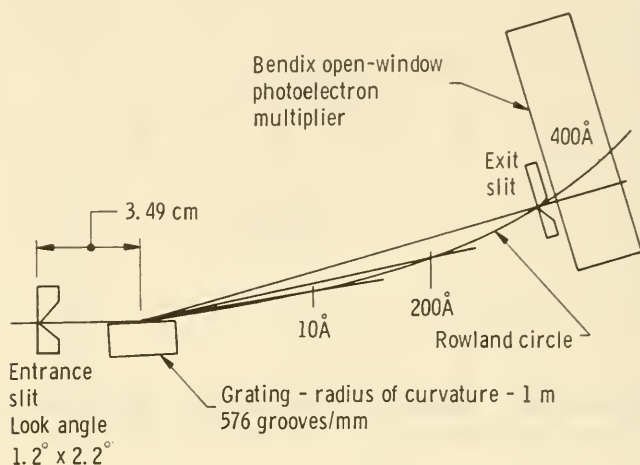
FIGURE 12–9.—The OSO-I XUV spectrograph. It is of the grazing-incidence type. Exit slit and detector are moved along the Rowland circle to scan the dispersed spectrum mechanically. See figure 12–10.

Referring to the instrument schematic (fig. 12–9) and the photograph (fig. 12–10), one sees how sunlight enters through the slit and falls on the curved, ruled glass grating at grazing incidence. The spectrum is imaged along the Rowland circle, where it is mechanically scanned by a detector moving on a carriage along curved rails. Approximately 1 watt of spacecraft power was consumed by an oscillator that drove the three-phase, 137-cps synchronous motor that moved the scanning carriage. The detector is also of more than passing interest. The detection of ultraviolet waves depended upon the emission of photoelectrons from a tungsten surface. The photoelectrons under the influence of crossed electric and magnetic fields moved between two coated-glass strips that emitted secondary electrons upon electron impact. This type of detector is obviously a close relative of the electron multiplier described in section 11–4. The OSO-I spectrograph per-
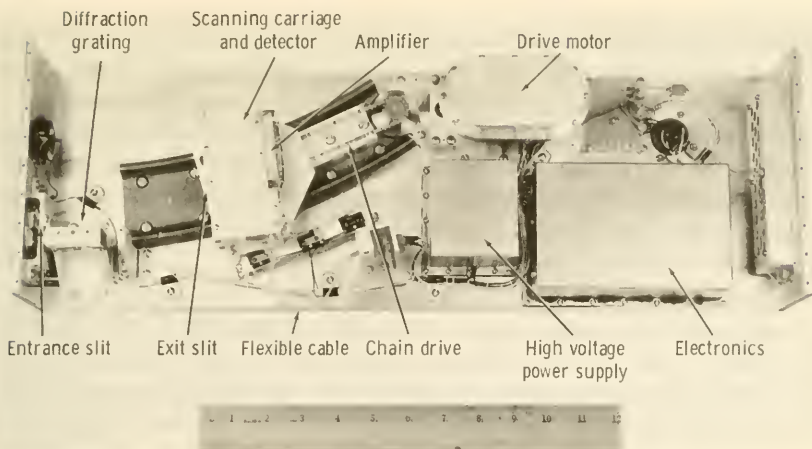
FIGURE 12–10.—Photograph of the OSO-I spectrograph.   See also figure 12–9.   (Courtesy of W. Behring.)

formed well in space and provided good spectrograms from 400 Å down to 171 Å, in extreme ultraviolet.

OGO's C and D carry a scanning ultraviolet spectrograph that employs a different scanning technique (ref. 8). This instrument was designed by Hinteregger, at the Air Force Cambridge Research Laboratories (AFCRL). In this approach, six separate
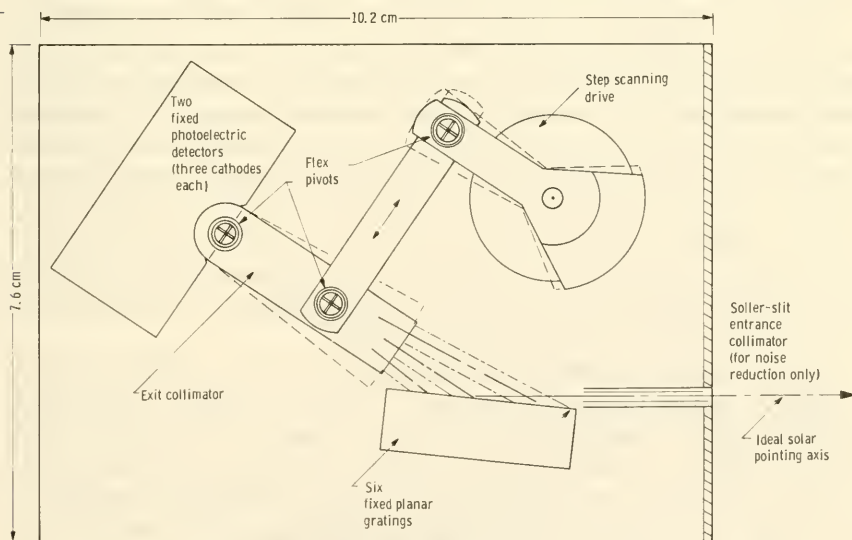
FIGURE 12–11.—Schematic of the OGO-C/D scanning ultraviolet spectrograph. Six stacked gratings plus 512 stepped positions of the exit collimator provide 3072 output readings in six overlapping ranges.

gratings are illuminated simultaneously (fig. 12–11). The six fans of dispersed light fall on six exit collimators, which pass six very narrow portions of the spectrum on to six photocathodes, located in two photomultiplier tubes (three to a tube). Mechanical scanning, here, rotates the collimator a total of 12° in 512 discrete steps. There are, therefore, 3072 wavelength intervals measured in a full spectral scan. There is intentional overlap of the six channels, particularly where important solar-emission lines occur; viz, the Lyman-α and He II lines, at 1216 Å and 584 Å, respectively. The ranges of the gratings are: 170–430 Å, 280–700 Å, 350–850 Å, 400–1000 Å, 500–1250 Å, and 660–1680 Å. The overlaps also permit internal checks and data comparisons. One should observe that exit-slit stepping and resulting discrete nature of the output signals meld well with the digital character of the OGO communication subsystem (sec. 9–4). The observation is all the more interesting because, historically, space-spectrograph technology seems to move from "coarse" photometers, to less-coarse spectrophotometers, to continuous-spectrum-dispersion spectrographs, and, finally, in what might seem a backward step, to stepped spectrographs. In some experimental situations, the ease of telemetry coding and data analysis is more important than continuous spectral analysis. As always, however, one designs an instrument that can do the job at hand; time histories of solar transients, for example, are more conveniently monitored by simple photometers.

Spectroheliographs.—All of the photometers and spectrographs mentioned so far have had wide-look angles. Even the entrance slits on the OSO and OGO spectrographs were installed to reduce background light rather than dissect the Sun's image. By insuring that the image of the entire Sun was being recorded, even in the presence of small attitude perturbations (jitters), the experimenter would be confident that amplitude changes originated on the Sun rather than from the temporary loss of a portion of the Sun's disk. With better attitude-control equipment and raster-scanning instrument platforms, it became possible to map the face of the Sun spatially as well as spectrally.

X-ray and ultraviolet spectroheliographs were proposed by the Goddard Space Flight Center and NRL for AOSO (Advanced Orbiting Solar Observatory), a program that was canceled in December 1965. (In addition, NRL flew an XUV spectroheliograph on OSO II.) The principles behind these instruments remain interesting and valid, however, and instruments like those in the description that follows will undoubtedly be flown eventually. Knowing exactly what portions of the spectrum come from the corona, the Sun's limb, and the various surface features is critical

to understanding the physics of the Sun and the many stars it typifies.

To begin with, we know that reflection optics must be employed at these short wavelengths and that the mirrors must be positioned so that the incoming light is almost parallel to their surfaces (grazing incidence). Figure 12–12 emphasizes this point. Fur-
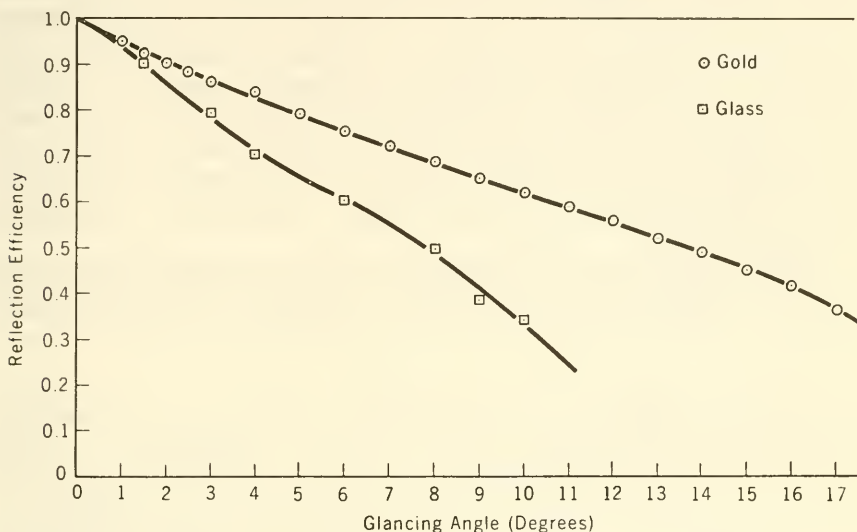
FIGURE 12–12.—Reflection efficiency of gold and glass at 113 Å.

thermore, we realize that when two reflecting surfaces form the imaging optics, astigmatism is often reduced. The extreme-ultraviolet spectroheliograph portrayed in figure 12–13 makes use of these observations. After two successive reflections from parabo-
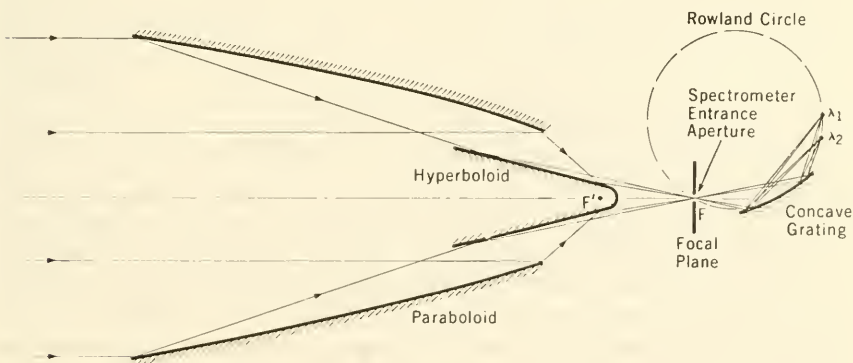
FIGURE 12–13.—Schematic of an ultraviolet spectroheliograph proposed for AOSO.

loid and hyperboloid mirrors, light from an infinite, on-axis source is imaged at the focal plane, as shown. A concave grating, mounted along the Rowland circle, disperses the spectrum into detectors also positioned along the circle. It should be emphasized here that the pictured instrument does not image the whole Sun, like a camera, but images small elements of the Sun's surface, building the complete image as the instrument platform scans the Sun, after the fashion of a TV camera. The ultraviolet spectroheliograph proposed by Goddard is intended to scan between 170 Å and 400 Å. The detector suggested is a Bendix magnetic electron multiplier mounted on a carriage that moves along the Rowland circle (like the detector on the OSO-I spectrograph). The entire instrument would probably weigh about 25 kilograms and would be 3 meters long—the length being a consequence of grazing-incidence optics.

The design of the corresponding X-ray spectroheliograph (fig. 12–14), though based on the same principles, is rather different
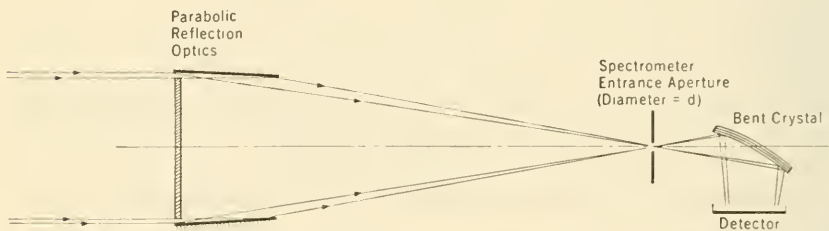
FIGURE 12–14.—Schematic of an X-ray spectroheliograph proposed for AOSO.

(ref. 5). First, only one imaging reflecting surface is seen. It turns out that at the shorter wavelengths characteristic of X-rays, the glancing angles must be much smaller for good reflection (fig. 12–12). At these smaller angles of incidence, the astigmatism problem is much less severe; so much so that the hyperboloid mirror can be eliminated. Another change is the substitution of a bent crystal for the curved grating; crystals are more effective dispersive elements at the short X-ray wavelengths. The last major change proposed is the replacement with a proportional counter of the electron multiplier used on the ultraviolet spectroheliograph. Pulse-height analysis could then be put to work in discriminating against spurious radiation. The Goddard group estimated that the X-ray spectroheliograph would weigh about the same as the ultraviolet instrument and have about the same

length.[4] The instrument would generate heliograms at two fixed wavelengths: 7 Å and 25 Å. This instrument should be contrasted with the NRL instrument flown on OSO II, which relies on a grating for dispersion of the spectrum (fig. 12–15).
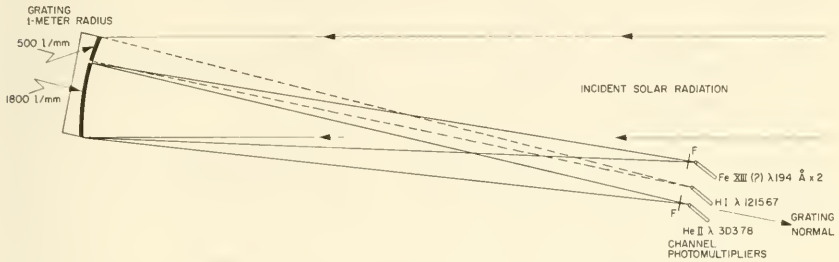
FIGURE 12–15.—Diagram of the NRL extreme-ultraviolet spectroheliograph flown on OSO II.   (Courtesy of R. Tousey.)

Solar Radio Astronomy.—Moving now from the very short wavelengths to the radio-wave portion of the electromagnetic spectrum, there are two spectral regions where Earth-based radio telescopes are foiled by absorption in the atmosphere:

(1) At wavelengths shorter than 4 millimeters, where water vapor is the dominant absorber.

(2) At wavelengths longer than about 30 meters (10 megacycles), where the ionosphere prevents extraterrestrial signals from reaching the Earth.

The longer wavelengths are of greater interest to solar physics, for the spectral analysis of noise bursts from the Sun can help elucidate the genesis and structure of solar flares and other large-scale movements of plasma. The millimeter region of the radio spectrum, which merges into the infrared, is more useful in the study of planetary atmospheres, as already mentioned.

So far, the radio-astronomy experiments flown and those planned for future satellites have scientific objectives broader than solar physics alone. The RAE (Radio Astronomy Explorer) and the University of Michigan experiments on OGO II and OGO E are galactic in scope, although they are used for solar research, too. Because of this larger purpose and scope, these experiments are covered in section 13–3 rather than here.

---

[4] Even though one mirror is eliminated in the X-ray version, the focal length is longer, because the angle of incidence is lower.

12-3.   Instruments and Experiments for Analysis of the Solar Wind

A scientific satellite in a very eccentric orbit encounters plasma at four places. As it dips into the ionosphere at perigee, there are plasma particles created by the photoionization of the upper atmosphere. Farther out, as it passes through the region of trapped radiation, the satellite's instruments can detect protons and electrons that were born on the Sun but subsequently trapped and thermalized in the Earth's magnetic field. As the satellite passes through the magnetopause (fig. 1-9), it encounters the third type of plasma—the turbulent plasma generated in the interaction region where the solar wind collides with the Earth's magnetic field. Finally, as the satellite penetrates the shock layer, it sees (instrumentally) the unmodified interplanetary solar wind. Figure 11-20 portrayed the energetics of three of the four populations.

Several kinds of satellite instruments commonly employed in analyzing the plasma-energy spectrum, the species, and angle of arrival have already been described. Table 12-6, which follows, summarizes the types of analyzers in use and gives references to where they are described in this book.

To amplify the theory and examples of typical plasma instrumentation presented earlier, two additional cases are covered below. The distinction between these examples and those in sections 11-3 and 11-4 are minor—primarily a matter of the portion of the energy spectrum being analyzed. Both examples below are from highly eccentric satellites that penetrated far out into interplanetary space, where the energies of the particles in the solar wind have not been modified by interaction with the Earth's atmosphere and magnetic field.

Faraday-Cup Plasma Probes.—The plasma probe sketched in figure 12-16 shows typical Faraday-cup geometry. In operation, it is the same as other planar probes and those retarding-potential probes constructed with spherical geometry that also measure the energy-to-charge (E/q) ratio of plasma (sec. 11-3).

The Faraday-cup probes flown on Explorer X and the first three IMP's (Explorers XVIII, XXI, and XXVIII) were like that illustrated in figure 12-16. One exception was the use of a split collector on the IMP's to gain angular information on solar-wind protons as the spacecraft spun on its axis. The outer grid of the Explorer-X probe and the collector(s) were kept at vehicle potential. A stepped square wave, varying between 5 and 3000 volts in amplitude on the IMP's, was applied to the second grid. When

TABLE 12-6.—*Types of Plasma Analyzers Used in Satellite Research*

Instrument	Principle of operation	Reference to theory	Satellite-usage summaries
Curved-surface analyzers	Electrostatic fields separate out particles of equal energy-to-charge ratios. Applied fields nearly normal to trajectories. Best at upper end of energy spectrum.	Sec. 11-4, p. 474	Tables 11-8 and 12-7.
Planar probes and Faraday-cup probes.	Retarding electrostatic fields repel particles in different energy ranges. Applied fields nearly parallel to trajectories. Best at lower end of energy spectrum.	Sec. 11-3, p. 443	Tables 11-5 and 12-7.
Spherical ion traps	Same as planar probes	Sec. 11-3, p. 443	Tables 11-5 and 12-7.
Plasma-species probes	(a)	Sec. 11-2, p. 412	Table 11-5.

[a] See mass spectrometers.
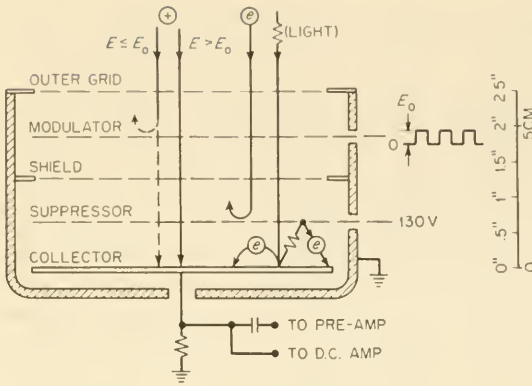
FIGURE 12–16.—The Explorer-X Faraday-cup plasma probe. The IMP instruments were similar in geometry (ref. 9).

$E = 0$, at the bottom of the square wave, all intercepted protons reach the collector; when $E = E_0$, the top of the square wave, only those protons whose energies exceed E_0 are detected by the dc amplifiers connected to the collector(s) (fig. 12–17). Incident
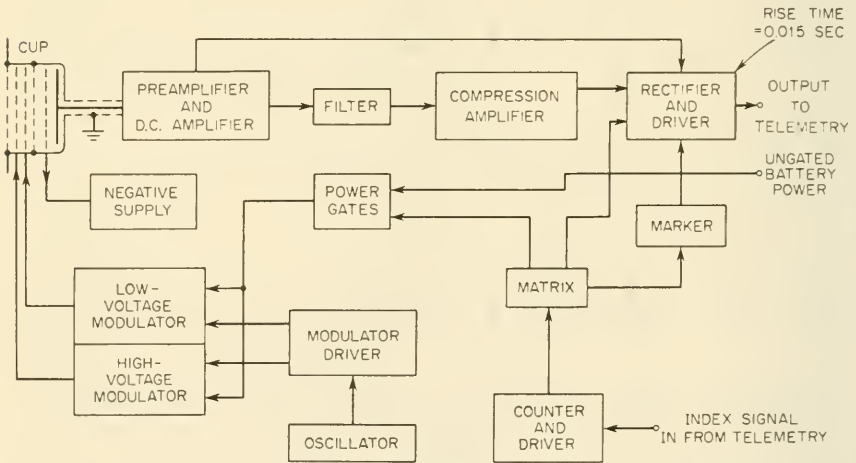
FIGURE 12–17.—Block diagram of the Explorer-X Faraday-cup plasma probe (ref. 9).

electrons are turned back by the negative voltage on the suppressor grid, and so are any photoelectrons emitted by the collector surface. The resulting data telemetered from such a probe permit the experimenter to plot a histogram of proton energies as $E_0 \pm \Delta E_0$ is varied stepwise. Knowledge of the probe's look angle and satellite aspect yields rough directional information. Table 12–7 indicates that Faraday-cup probes and other probes of the

TABLE 12–7.—*Instruments, Experimenters, and Experiments for Solar-Wind Analysis*

Faraday-cup plasma probes:		
Explorer X, XVIII, XXI, XXVIII.	Bridge, H./MIT	—/—
Hitchhiker 2		—/—
IMP D/E	Bridge, H./MIT	100–10 000 eV.
OGO I, B	Bridge, H./MIT	10–10 000 eV.
OGO E	Snyder, C. W./JPL	3–16 000 eV. Allied with 2 electrostatic analyzers.
Curved-surface electrostatic analyzers:		
Elektron 2, 4		Spherical, 100, 200, 400 eV; 1, 2, 4, 10 keV.
Explorer XII, XIV	Bader, M./Ames	Spherical, 200 eV–20 keV.
Explorer XVIII, XXI, XXVIII	Wolfe, J. H./Ames	Spherical, 200 eV–20 keV.
Hitchhiker 2	—/AFCRL	Proton unit, 4–100 keV; electron unit, 4–100 keV.
IMP F/G	Harrison, F. B./TRW Systems	Spherical. Proton range, 100–10 000 eV; electron range, 5–100 keV.
	Ogilvie, K. W./GSFC	Cylindrical, with velocity selector. Measures proton-alpha ratio up to 10 keV.
OGO I, B	Wolfe, J. H./Ames	Spherical. Proton range, 0.2–20 keV.
OGO E	Snyder, C. W./JPL	Two spherical units, 3 eV–16 keV.

retarding-potential type have had many satellite flights. It is important to note, however, that planar probe is more often employed at the low-energy end of the solar-wind energy spectrum.

Curved-Surface Electrostatic Analyzers.—The reader will recall from the discussion in section 11–4 that the curved-plate plasma analyzers are in reality E/q (energy/charge) filters that are electrostatically stepped over the energy range being explored (fig. 12–18). By reversing the polarities of the analyzing plates, elec-
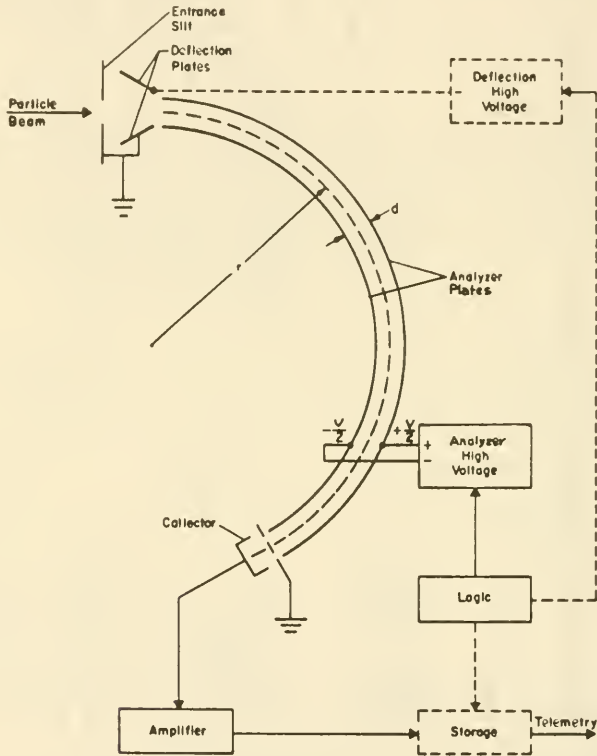
FIGURE 12–18.—Geometry of the Ames curved-plate plasma analyzer flown on OGO I and Explorers XVIII, XXI, and XXVIII (ref. 10).

trons can be analyzed as well as protons. Charged particles moving along the instrument axis are deflected at right angles to their direction by the curved-plate probes, but parallel to the instrument axis, by retarding-potential probes. Cup-probe response is therefore hard to interpret when the plasma angular distribution is unknown. The curved-plate analyzers are more commonly used

at the upper end of the energy spectrum, and generally their look angles are narrower, so that there is better flux resolution in elevation and azimuth. On OGO I and OGO B, the analyzers on the SOEP (Solar-Oriented Experimental Package), designed by the Ames Research Center, used four separate sets of plates and electronic elevation scanning to refine the picture of the angular dependence of the solar wind.

The schematic of figure 12–18 is representative of the Ames analyzers flown on the OGO's and first three IMP's. The block diagram of the experiment is given in figure 12–19. Physically,
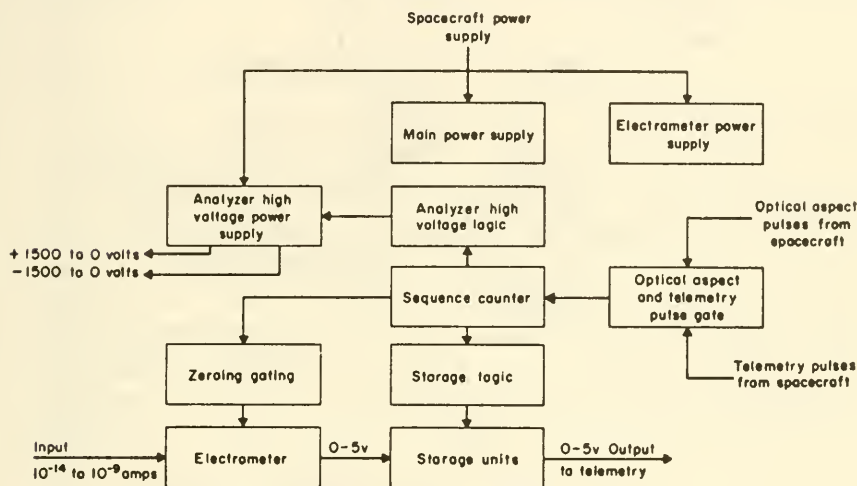
FIGURE 12–19.—Block diagram of the Ames plasma analyzer used on Explorers XVIII, XXI, and XXVIII (ref. 10).

the IMP probes were rather small, weighing only 0.727 kilogram apiece and consuming an average of 0.3 watt. The narrow cylindrical strips used 14 voltage steps to analyze protons in the range 450–18 000 eV. The entrance slit presented a capture area of 0.5 cm² to the solar plasma, and the angular resolution was 12° in azimuth and 60° in elevation, with an angular resolution better than 4°. The output of the collector and associated electrometer is, of course, analog in character and slowly varying. This kind of signal is difficult to amplify. Other versions of the curved-plate analyzer modulate the ion beam before it reaches the detector to overcome this problem.[5]

---

[5] This approach was abandoned on Pioneer VI because of problems with capacitive coupling.

Two deficiencies of the conventional curved-plate plasma analyzer are its inability to distinguish different ions possessing the same value of E/q and the problem of handling the extremely low dc collector currents (10^{-14} amperes and lower). Ogilvie et al., at Goddard Space Flight Center, have proposed an experimental approach that gets at both of these difficulties. In figure 12–20,
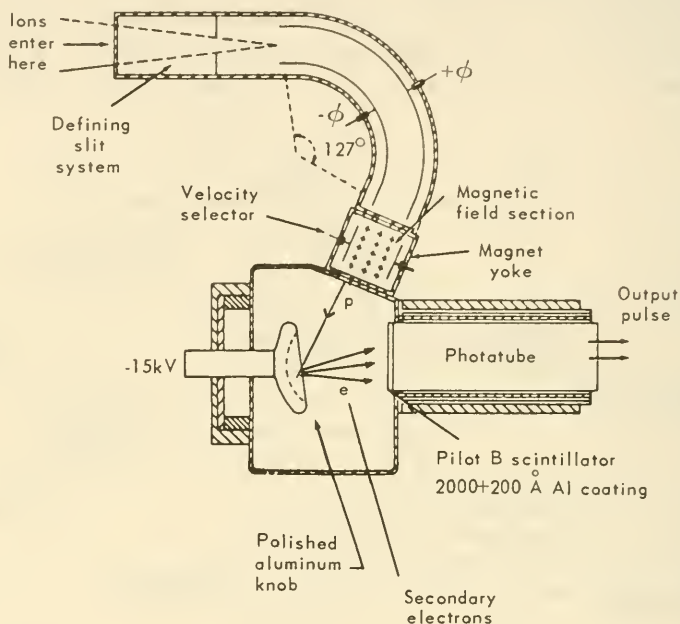
FIGURE 12–20.—A curved-plate plasma analyzer with an added magnetic stage for velocity selection. (Courtesy of K. W. Ogilvie.)

we see how the usual curved-plate E/q filter is followed by a velocity filter of the type used on the inputs to mass spectrographs (sec. 11–2). This filter is simply a volume with crossed magnetic and electrostatic fields. By varying the strength of the electrostatic field, different ions with the same E/q ratio can now be separated. The addition of the magnetic section makes this a plasma-species probe.

The low-current problem is attacked by counting each ion that passes successfully through both sections of the analyzer rather than measuring the net current. Ions are accelerated onto an emission knob of highly polished aluminum, which emits several secondary electrons. These electrons are accelerated, in turn, onto a scintillator crystal mounted on the face of a photomultiplier tube.

The secondary electrons from each proton produce sufficient light nearly simultaneously to generate one light pulse of intensity sufficient to trigger the photomultiplier tube.

A Deuterium Detector.—A highly specific instrument has been suggested by Floyd for the detection of deuterium ions in the solar wind. Solar-wind particles are accelerated by roughly 100 kilovolts onto a target containing tritium. The pertinent nuclear reaction is

$$D+T \rightarrow He^4+n+17.6 \text{ MeV}$$
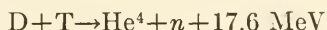
The neutron and He^4 nucleus have known energies and are easily detectable.

12–4. Measuring the Sun's Magnetic Field

With one exception, the satellite magnetometers used to measure the geomagnetic field can be used directly for studying the Sun's field engulfing the Earth beyond the magnetopause. That exception is the proton-precession magnetometer, which is suitable only for measuring relatively high fields; fields much higher than the 10 γ and less encountered in interplanetary space. The reader should refer to section 11–5 for descriptions of the various magnetometers. Table 11–11 summarizes the usage of magnetometers on scientific satellites. Of course, the only satellites that actually measure the interplanetary field are those that have apogees well beyond the magnetopause.

12–5. Measurements of Solar Cosmic Rays

The adjective "cosmic" in cosmic rays presumes that this type of space radiation originates outside the solar system in the reaches of interstellar space. In 1942, however, a general increase in cosmic-ray flux was observed soon after the appearance of a solar flare. Subsequently, scientists have discovered that many large solar flares, particularly those accompanied by radio bursts, bombard the Earth with cosmic rays of solar origin. Some of the high-energy particles born in solar eruptions travel to the Earth trapped in plasma tongues by magnetic fields. These cosmic rays appear isotropic to Earth-centered instruments; their energies are generally low: 10 MeV–1 BeV. A second general class of solar cosmic rays is comprised of the more energetic particles—over 1 BeV—that travel directly to Earth at close to the velocity of light. Solar cosmic rays are distinguishable from galactic cosmic rays by their lower energies, transient nature, and, in the case of the most energetic particles, anisotropy.

How does an experimenter discover the source of observed cosmic rays? Since solar cosmic rays are sporadic, satellite instruments measuring the steady galactic cosmic-ray background from the galaxy will signal the presence of solar cosmic rays as transients. Directional instruments, such as the particle telescopes that sweep most of outer space as the satellite spins on its axis and swings around the Earth, will record any solar anisotropies in the cosmic-ray flux. The energy spectra of galactic and solar cosmic rays overlap (table 11–6). An instrument surveying the entire energy spectrum would record an increase in solar activity as a skewing of the spectrum toward the low-energy end. One common element of all three approaches to measuring solar cosmic rays is the use of the galactic background as a point of reference in terms of energy and flux level. Satellite cosmic-ray experiments [6] have dual purposes: the study of galactic cosmic rays and—should they appear during the flight—solar cosmic rays. On none of the OSO's, for example, does one find Sun-pointed cosmic-ray experiments. Cosmic-ray instrumentation is really a single topic and, for this reason, descriptions of typical instruments are deferred to section 13–3.

References

1. BOYD, R. L. F.: Techniques for the Measurement of Extraterrestrial Soft X-Radiation. Space Sci. Rev., vol. 4, Feb. 1965, p. 35.
2. FRIEDMAN, H.: Rocket Spectroscopy. In Space Science, D. P. LeGalley, ed., John Wiley & Sons, Inc., 1963.
3. HINTEREGGER, H. E.: Absolute Intensity Measurements in the Extreme Ultraviolet Spectrum of Solar Radiation. Space Sci. Rev., vol. 4, June 1965, p. 461.
4. TOUSEY, R.: Techniques and Results of Extraterrestrial Radiation Studies From the Ultraviolet to X-Rays. In Space Age Astronomy, A. J. Deutsch and W. B. Klemperer, eds., Academic Press, 1962.
5. GIACCONI, R., ET AL.: An X-Ray Telescope. NASA CR–41, 1965.
6. KREPLIN, R. W.; CHUBB, T. A.; AND FRIEDMAN, H.: X-Ray and Lyman-Alpha Emission From the Sun as Measured From the NRL SR–1 Satellite. J. Geophys. Res., vol. 67, June 1962, p. 2231.
7. ACTON, L. W., ET AL.: Observations of Solar X-Ray Emission in the 8-to-20 Å Band. J. Geophys. Res., vol. 68, June 1, 1963, p. 3335.
8. SULLIVAN, J. D.; McGRATH, J. F.; AND THORBURN, W. J.: Investigation of the Ultraviolet Solar Radiation and Its Influence on the Aerospace Environment. AD 608680, 1965.
9. BRIDGE, H. S., ET AL.: Plasma Probe Instrumentation on Explorer X. In Space Research III, W. Priester, ed., John Wiley & Sons, Inc., 1963.
10. BECK, C. W., ET AL.: Solar Wind Measurement Techniques, Part II. Solar Plasma Energy Spectrometers. In Proceedings of the National Aerospace Electronics Conference, IEEE (New York), 1965.

---

[6] Including gamma-ray experiments.

Chapter 13

INSTRUMENTS AND EXPERIMENTS FOR
SATELLITE ASTRONOMY

13–1. Prolog

The value of satellite stellar astronomy lies not in more magnification but in better "seeing." Interpretation of this truism is hardly necessary. Better seeing means freedom from atmospheric absorption, atmospheric distortions, and manmade radiations. The advantages of extraterrestrial astronomical measurements are so obvious that scientists proclaimed the virtues of a lunar telescope long before the Space Age began. With no large rockets to boost instruments out of the perturbing and deadening atmospheric blanket, astronomers had to settle for mountaintop observatories far from civilization. Balloons and sounding rockets carried the first spectrographs and cosmic-ray instruments to high altitudes, just as they aided the discipline of solar physics before satellites became available. In fact, balloons and sounding rockets still do appreciable astronomical research, but where lengthy surveys of the skies are desired, satellites should prove most effective.

"Astronomy" is broadened in this chapter to include the study of galactic cosmic rays and cosmology, as well as the more conventional stellar and planetary observations. In short, satellite astronomy here embraces all natural phenomena of the heavens except those centered on the Earth and Sun, which were covered in the preceding two chapters. Four groups of phenomena and associated instrumentation evolve:

(1) *Observational astronomy,* which employs telescopes, photometers, and spectrographs to analyze the electromagnetic spectrum from γ-rays to radio waves.

(2) *Cosmic-ray astronomy,* using particle counters and counter telescopes to measure the gamma rays and high-energy particulate radiation that engulf the Earth from all directions.

(3) *"Active" astronomical experiments,* which include arti-
ficial-comet experiments and, ultimately, direct measurements of
interplanetary gas, cometary materials, and the asteroid belt.

(4) *Cosmology,* where scientists endeavor to check the predic-
tions of the general theory of relativity against experiments with
gyroscopes, clocks, and perturbations of satellite orbits. Observa-
tions that yield insight into the history and future of the universe
also fall into this category.

Most satellite experiments to date have fallen into the first two
categories, save for those implications that observational astron-
omy and cosmic-ray physics may have for cosmology. The scien-
tific instruments found on astronomical satellites are much the
same as those introduced for solar physics and the study of the
trapped-radiation zone. There are, however, significant differ-
ences in the way one conducts an observational program involving
thousands of stars rather than one (the Sun).

The pattern of this chapter follows that of the previous two.
Where instrument-operating principles are new, they will be de-
scribed. A pertinent example or two will follow. In each section,
a table summarizes the astronomical instruments, experimenters,
and experiments that have flown or are in the process of being
prepared for flight on scientific satellites.

13-2. Instruments and Experiments Used in Observational Astronomy From Satellites

Observational astronomy is passive in character; that is, it
analyzes the electromagnetic radiations received from stars,
planets, comets, and other astronomical objects. It studies the
absorption and scattering of these radiations as they pass through
interstellar space and the solar system. "Passive" should not be
construed as derogatory, because for objects outside the solar
system, there is little hope for "active" experiments for decades
to come.

Electromagnetic radiation is characterized by the parameters of
intensity, wavelength, and direction of arrival. A scientist uses
photometers (including radio-noise receivers), spectrophotom-
eters, and, spectrographs to plot intensity versus wavelength for
any particular source, such as a star. So far, these statements are
reminiscent of those in the chapter on solar physics. Instrument
terminology and hardware actuality, as a matter of fact, are the
same, with one exception: the astronomical counterparts of the
spectroheliograph are star-field scanners and ultraviolet television
photometers. The stars are too far away to permit us to build up

magnified images of single stars at various wavelengths as we do for the Sun. (See sec. 12–2.) A necessary corollary is that satellite telescopes are needed, not for star magnification but rather to collect more light from a point source and, in addition, to aid in resolving stars that are close together.

Stellar observation also requires much more precision in instrument pointing and satellite attitude control. In the case of the Sun, radiation at all wavelengths is much more intense than that of the background. Except for fine detail, coarse instrument pointing, plus simple collimation, is sufficient. In contrast, in stellar astronomy from a satellite, an optical system is necessary to detect the targets and separate them from their neighbors. Stellar instruments must stay on targets for many minutes with minimum jitter if enough energy is to be gathered for accurate measurements.

Astronomical instrumentation on satellites tends to be more complex than that used for solar physics.[1] One reason, of course, is the general need for a telescope, which adds complexity and physical size. But, in addition, satellite astronomy has arrived on the scientific scene later than satellite geophysics and solar physics. It therefore has a less broad and firm instrumental foundation to build upon. Astronomical instruments often employ multichannel spectrophotometers and scanning spectrographs rather than the simple photometers characteristic of early satellite studies of the upper atmosphere and the Sun. One reason, obviously, is that one should try and extract as much information as possible from the intercepted starlight as long as one has decided to put up a big, pointable, high-data-capacity satellite like an OAO.

Before launching into descriptions of specific instruments, it should be pointed out that satellite astronomical instruments are used in two ways. High-resolution telescopes, spanning the spectrum from the X-ray region to radio wavelengths, can search out and measure specific radiating objects. The planned surveys of selected hot stars in the ultraviolet are good examples. In such research, the satellite is usually a specialized one, such as an OAO, and the satellite is directed by ground command and internally stored programs to slew from one star to another in a planned sequence. Less selective are the all-sky surveys with low-resolution instruments. Such surveys are exploratory in nature. Broadband, low-resolution X-ray photometers, for example, are used to locate X-ray sources for more precise study by X-ray tele-

---

[1] Target acquisition and satellite stabilization are also much more difficult in satellite astronomy. These factors were discussed in ch. 6.

scopes that are orbited later. In practice, sounding rockets instrumented by the Naval Research Laboratory, Lockheed, and other institutions have already roughly mapped much of the sky in the X-ray region. Satellite telescopes will refine such data.

In both satellite astronomy and solar physics, the early research emphasis has been on the short wavelengths: the ultraviolet and X-ray regions of the spectrum. The reasoning is the same in both instances: the physical processes occurring on stars naturally generate the shorter wavelengths. It has been the astronomer's misfortune that these wavelengths have been blocked by the Earth's atmosphere until now.

In the instrument descriptions that follow, the reader should make frequent reference to chapters 11 and 12, where the basic principles of photometers, spectrographs, and other optical instruments are set down.

A. Short-Wavelength, Nontelescopic Photometry

Zodiacal-Light Photometry.—While most objects of interest in satellite astronomy are either point sources (stars) or close to it (planets), one astronomical phenomenon that remains susceptible to simple, low-resolution photometry is the zodiacal light, or gegenschein (counterglow). The faint, elusive tongue of light seen in the west just after sunset and in the east before sunrise comprises the visible zodiacal light. Present evidence favors the supposition that the zodiacal light is sunlight scattered by dust particles out in space. Satellite instruments can map the intensity and polarization of the zodiacal light better than Earth observers, who are hampered by the perturbations of the atmosphere and extraneous light sources.

In table 13–1, two zodiacal-light experiments are listed. The first was constructed by E. P. Ney, at the University of Minnesota, and flew on OSO II, in 1965. In this experiment, two pairs of photomultiplier tubes monitored the light between 4750 Å and 8500 Å. Each pair consisted of one tube sensitive in the visible and one in the infrared. Polaroid filters enabled the instruments to measure the angle of polarization. Since this experiment was mounted in the OSO-II wheel section, it constantly scanned the sky as the wheel section spun.

The second experiment, designed by C. L. Wolff and S. P. Wyatt, at Goddard Space Flight Center and the University of Illinois, respectively, was in effect a "photoelectric camera." The instrument, which is shown schematically in figure 13–1, forms images of the sky at 3000 Å, 5000 Å, and 7000 Å with the help of a filter wheel. Each image encompasses about 100 square degrees of the

TABLE 13-1.—*Instruments, Experimenters, and Experiments Used in Observational Astronomy*

Photometers and spectrophotometers:

OAO A1	Fisher, P./Lockheed	Proportional-counter array for night-sky X-ray survey.
OGO I, B	Wolff, C. L./GSFC	Gegenschein photometry in ultraviolet, green, infrared.
OSO II, F	Ney, E. P./U. Minn.	Five telescopes with filters and polaroids, wheel.
OSO II	Hallam, K./GSFC	Spectrophotometry of stars and nebulae, 1300–2600 Å, wheel.
OSO D	Gursky, H./Amer. Sci. and Eng.	Scintillator telescope for celestial X-ray survey, 0.1–10 Å, wheel.
OSO G	Rony, A. L./Rutgers U	Study of the gegenschein brightness and polarization.

OAO experiment packages and other astronomical satellites:

LAS	—/ESRO	No details.
OAO A1, A2	Code, A. D./U. Wisc.	Two filter photometers; 2 grating spectrometers.
OAO A2	Whipple, F./SAO	Uvicon photometry, 1200–2900 Å. See text.
OAO B	Bogess, A./GSFC	Telescope and grating. See text.
OAO C	Spitzer, L./Princeton U	Telescope and grating, 800–3000 Å. See text.
TD 1	—/ESRO	No details.

Radio-astronomy experiments:

Alouette 1, 2	Hartz, T. R./DRTE	Cosmic-noise receiver, 0.5–13 Mc, 0.2–14.8 Mc, respectively.
Ariel 2	Smith, F. G./U. Cambridge	Cosmic-noise receiver, 0.75–3.0 Mc.
Elektron 1, 2, 3, 4		Cosmic-noise receiver, 200 and 400 m.
Explorer XX, IE–B		Cosmic-noise receiver.
OGO I, B, II, D, E	Haddock, F. T./U. Mich	Cosmic-noise receiver, various ranges, 2 kc–4 Mc.
RAE A/B	Stone, R. G./GSFC	Cosmic-noise survey. Study of long-wavelength solar and planetary emissions vs. frequency and time.
UK 3	Smith, F. G./U. Manchester	Cosmic-noise receiver, 2–5 Mc.
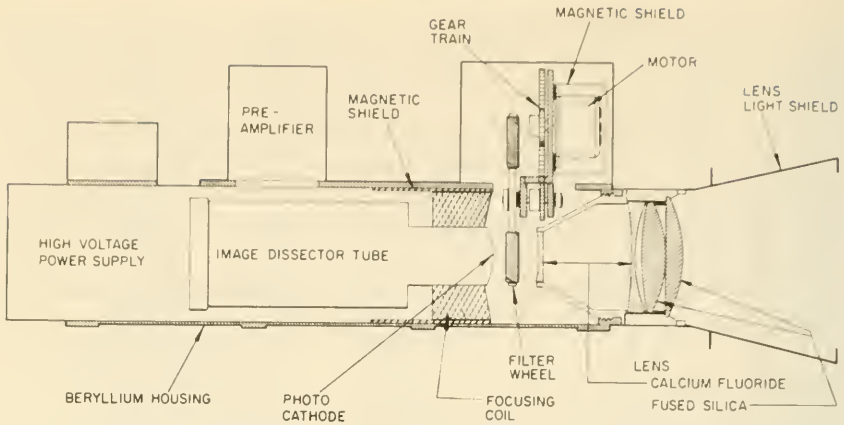
FIGURE 13–1.—The OGO-I "photoelectric camera" used in gegenschein studies. Length is approximately 35.3 centimeters. (Courtesy of C. L. Wolff.)

sky, with a resolution of about one-half of a degree. The lens system forms the desired image on the surface of an image-dissector-tube cathode. The number of photoelectrons leaving a point on the inside surface of the tube's cathode is proportional to the intensity of the light focused at that spot. The image-dissector tube periodically scans the cathode, and the photoelectrons are accelerated to a photomultiplier tube that generates the output signal. In this way, images of sky can be taken at different wavelengths.

The perceptive reader will note that the two zodiacal-light experiments described above are unusual not only in that they deal with the mapping of an extended source of light but also in the fact that they are exceptions to the previous generalization made about astronomical research being concentrated at the short wavelengths. The probable origin of the zodiacal light—scattering of sunlight by micron-sized particles—is responsible for this invasion of the infrared region.

X-ray Photometers.—Several X-ray astronomy experiments are planned for the OAO series. On OAO A1,[2] P. Fisher, at Lockheed, flew an array of about 20 proportional counters, preceded by an aluminum collimator. The purpose of this experiment was the mapping of X-ray sources in the night sky. Another mapping experiment that extends into the gamma-ray region is that of W. Kraushaar, at MIT. This experiment, also launched on OAO A1, was a duplicate of that flown on Explorer XI, back in 1961.

---

[2] OAO A1 was successfully launched on Apr. 8, 1966, but its power supply failed after 3 days.

It is described more completely in section 13–3, along with cosmic-ray instrumentation. A third X-ray photometer experiment is planned for OAO C. R. L. F. Boyd, at University College, London, is constructing a three-channel X-ray photometer experiment, using detectors sensitive to the bands 3–12 Å, 8–18 Å, and 44–60 Å. Since the purpose of Boyd's experiment is the measurement of the X-ray emissions of a wide assortment of stars and nebulae, an optical system is called for in order to resolve the sources and gather enough quanta to provide adequate counting rates. Boyd has chosen paraboloidal reflectors to focus the energy on the detectors. The design of this experiment is not complete at this writing.

B.   The OAO Primary Experiments

The four primary OAO experiment packages planned for OAO's A1, A2, B, and C contain instruments that can be classed as multichannel-filter photometers, spectrophotometers, and scanning spectrographs. These experiments, described below, are termed "primary" because they occupy the central cylindrical well of the OAO spacecraft (fig. 9–71) rather than equipment-bay compartments.[3] All depend upon large reflecting telescopes to collect light and resolve stars in the ultraviolet region of the spectrum.

The knowledge of the ultraviolet spectra of stars that we have gained from rockets and balloons is particularly perplexing—a fact accounting for the extensive surveys in the ultraviolet planned with the OAO primary experiments. For example, stars do not seem to radiate nearly as much energy in the ultraviolet spectrum as our stellar theories lead us to expect. Furthermore, stars that appear identical in visible light unexpectedly turn out to look radically different in the ultraviolet.

The Wisconsin OAO Experiment Package.—The first OAO primary experiment package to be launched will be that prepared by A. Code and his collaborators at the University of Wisconsin. The primary objectives of this experiment are:

(1) To measure the energy spectra of several hundred stars of all types in the range 900 Å to 3000 Å.

(2) To make multiple—possibly up to three—observations on selected stars to check observational consistency and (it is hoped) to establish that stellar-energy spectra are not intrinsically variable.

---

[3] The adjective "piggyback" has been applied to these experiments riding in the OAO equipment bays; viz, the OAO photometers just described. They should not be confused with experiments on the "piggyback class" of satellites.

(3) To measure the emission spectra of diffuse nebulae in the range 1800 Å to 2800 Å.

The Wisconsin package consists of three separate instruments: a stellar photometer, a nebular photometer, and a scanning spectrograph. Figure 13–2 indicates how the three separate optical systems are arranged within the basic dimensions dictated by the OAO satellite.

Dust cover

Nebular-photometer module (center tube)   Pitch

Insulating cover plate

Primary structure

Yaw

Scanning-spectrometer module

Stellar-photometer module
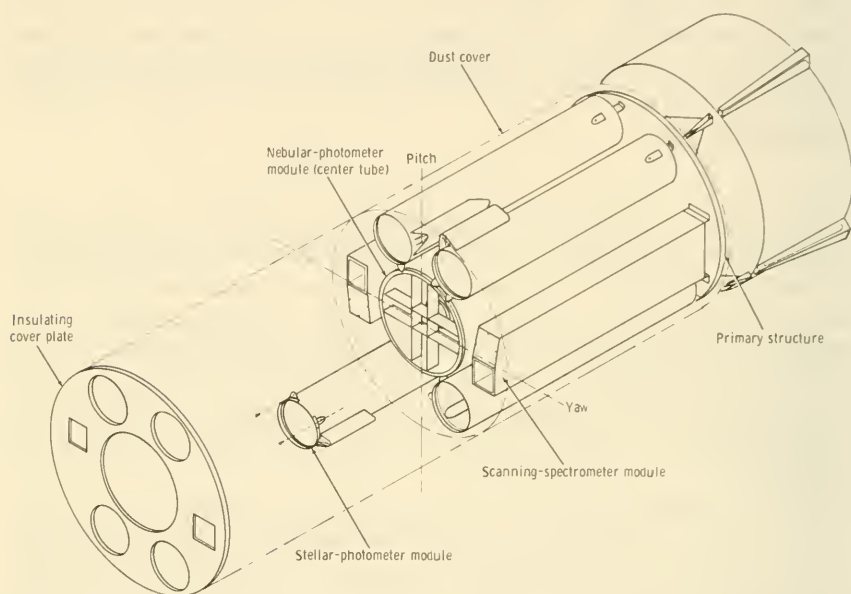
FIGURE 13–2.—Optical arrangement of the University of Wisconsin OAO Experiment Package.

The stellar photometer consists of four 20-centimeter-diameter paraboloidal mirrors with focal lengths of 80 centimeters each. These are off-axis mirrors; the image is focused on the photomultiplier detectors located off the axis of the incoming light, where they will not interfere (fig. 13–3(a)). Each of the four photometer systems has a five-color filter wheel prior to the photomultiplier tube. One position in each wheel is opaque and allows dark measurements. Another exposes the photometer to a Cerenkov ultraviolet calibration source. Filters with selected bandpasses occupy the three other wheel positions—a total of 12 bandpasses, when all 4 wheels are considered. The bandpasses duplicate and overlap to permit intercomparison of data, and if one photometer is incapacitated, another can partially fill the data gap. Such redundancy is possible only because all four photom-

(a)

(b)

(c)
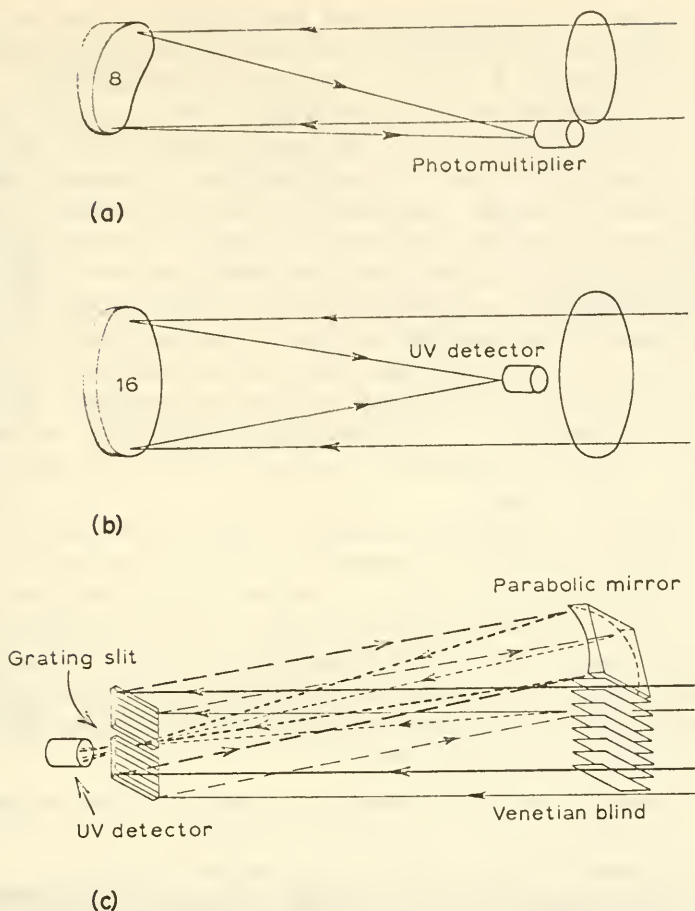
FIGURE 13–3.—Optical layouts in the University of Wisconsin OAO Experiment Package. (*a*) off-axis telescope; (*b*) nebular photometer; (*c*) ultraviolet spectrometer.

eters are independent and under separate control. One of the 12 bandpasses is in that region of the ultraviolet visible on the Earth's surface. Comparison of ground and satellite observations will thus be possible. The normal fields of view of the four telescopes is 2 minutes of arc each, with search fields of 10 minutes. Alinement of the optical axis with a specific star is, of course, the function of the spacecraft, since all experiments are rigidly mounted to the satellite structure.

The nebular photometer uses a 40-centimeter-diameter paraboloid mirror and an (on-axis) phototube (fig. 13–3(*b*)). This, too, is a filter photometer, with a six-position wheel. One position is

dark, another for calibration, and four for ultraviolet measurements. The field of view is only one-half degree. Otherwise, the nebular photometer is similar to the stellar photometers.

The third type of Wisconsin instrument, the scanning spectrograph, is to be used for more thorough studies of the brightest stars. Actually, there are two spectrographs, on opposite sides of the experiment package. Starlight is admitted to the instruments through venetian-blind collimators (fig. 13–3(c)). Gratings ruled with 300 lines/mm and 600 lines/mm reflect dispersed spectra to 17.5 x 20-centimeter paraboloidal mirrors, which focus very narrow regions of the spectrum on slits in the gratings themselves. Phototubes behind the gratings record the intensities of the spectra. Each grating can be rotated to scan the spectrum. The 300-lines/mm grating can be rotated in 20-$\mathring{A}$ steps over the region 2000 $\mathring{A}$ to 4000 $\mathring{A}$. The other grating covers the region 1000 $\mathring{A}$ to 2000 $\mathring{A}$ in 10-$\mathring{A}$ steps.

The Goddard Experiment Package (*GEP*).—The sole experiment planned for OAO B consists of a large telescope combined with a grating spectrograph. A. Boggess III, at Goddard Space Flight Center, is the principal investigator. This instrument, like the other primary OAO experiments, should be regarded as a general scientific tool. Like terrestrial telescopes, it will be available to scientists with sound research programs. The major objectives of the Goddard experiment are:

(1) Precision ultraviolet spectrophotometry of normal stars to determine their energy distributions in the continuum and identify and measure the intensities of strong emission lines.

(2) To measure energy spectra as a function of time for unusual stars, such as those of the Wolf-Rayet type.

(3) To study the reddening law and the spectra of nebulae.

(4) Spectrophotometry of nearby galaxies.

The initial research programs, as confirmed by the above objectives, are quite general, much like those of a terrestrial telescope, save for the fact that this instrument will explore parts of the ultraviolet spectrum that cannot be seen on Earth.

The Goddard optical system (figs. 13–4 and 13–5) employ a 91-centimeter, $f/5$ primary mirror constructed by Kollsman from beryllium. Beryllium was selected over the usual quartz because of its high strength, high thermal conductivity, and low density—a choice that saved over 100 kilograms. The secondary mirror, convex and made from quartz, reflects the ultraviolet light into an entrance slit and thence through a hole in the grating to the spectrometer mirror. Reflection of the spectrometer mirror car-
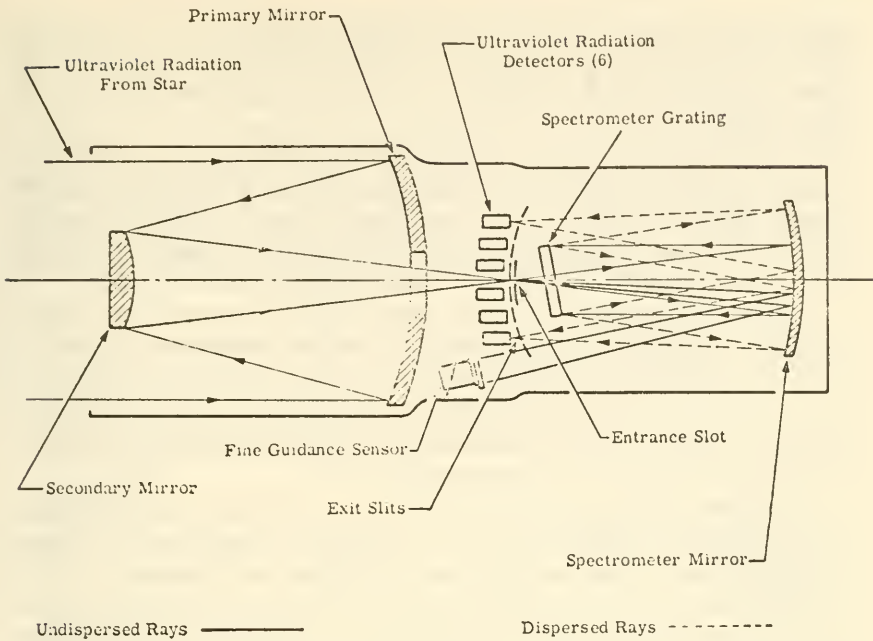
FIGURE 13–4.—Optical diagram for the OAO Goddard Experiment Package. In this Cassegrainian configuration, the distance between the primary and secondary mirrors, is roughly 107 centimeters.

FIGURE 13–5.—Conceptual drawing showing the light paths in the Goddard Experiment Package.

ries the light rays to a 20-centimeter-square beryllium grating ruled with 1219.5 lines/mm. The dispersed spectrum is reflected from the spectrometer mirror onto an array of six slits and six phototubes.

Spectral scanning is accomplished by rotating the grating by command over 512 steps. The six photocell detectors cover the range 1050 Å to 4000 Å in six overlapping bands. Spectral resolution is expected to be about 2 Å, which is rather coarse compared to the high-resolution Princeton spectrograph described later.

The remote operation of such a complex instrument from Earth requires a sophisticated guidance-and-control subsystem. Some of the OAO control philosophy has already been presented in section 6–5. Not only can the grating be commanded to scan but other signals can alter exit-slit widths and disable portions of the experiment in the event of malfunctions.

The sheer size of the OAO primary experiments dwarfs most other satellite experiments. The Goddard Experiment Package illustrates why Observatory-class satellites are necessary. It is approximately 284 centimeters long and 104 centimeters in diameter; its weight is roughly 420 kilograms, more than any Explorer-class scientific satellite. An interesting observation is that the OAO B, which will carry the Goddard instrument, will be a one-instrument satellite, similar to Explorer XI. Most Observatories carry many related experiments. The OAO's are exceptions, in that they carry one primary experiment and perhaps one or two piggyback instruments. It is the requirement for a large telescope and high data-transmission rates, of course, that put the OAO into the Observatory class.

The SAO OAO Experiment Package.—The SAO (Smithsonian Astrophysical Observatory) experiment goes back to the beginnings of the American space program. In 1958, the SAO proposed ultraviolet television studies to NASA (ref. 1). From this proposal evolved Project Celescope, a nickname for the SAO experiment destined for an unspecified OAO. F. Whipple is the principal investigator at SAO. Celescope is a survey-type experiment, as the following objectives demonstrate:

(1) Survey the entire sky between 1200 Å and 2900 Å, with the expectation of recording the ultraviolet brightnesses of 50 000-or-more hot stars.

(2) Map the brightness characteristics of faint nebulae over the entire sky.

Celescope contemplates area mapping of the sky, segment by segment, rather than star by star. In contrast to all the other

astronomical instruments presented so far, the SAO instrument will actually image star fields—several stars at a time—rather than measure the intensities of individual stars in sequence. By transmitting star-field images, in the fashion of television, a map of ultraviolet-bright objects can be reconstructed on Earth. There will be little spectral detail in the maps, but Project Celescope dovetails neatly with other OAO primary experiments by providing them with targets for more precise measurements.
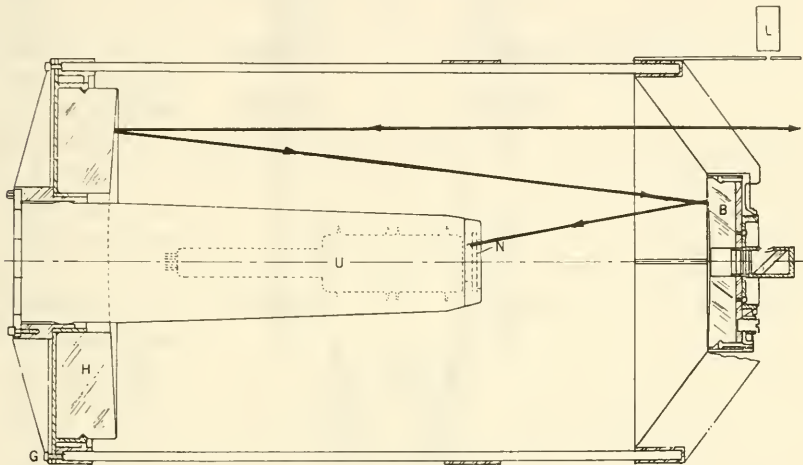
FIGURE 13–6.—Optical diagram of the SAO Schwartzschild telescope used in the Celescope. *H* is the primary mirror; *B* is the secondary mirror; *N* is an ultraviolet filter; *U* is the Uvicon imaging tube (see also fig. 13–7); and *L* is a calibration lamp.

Four high-resolution telescopes (fig. 13–6), four filters, and four image-forming Uvicon tubes will image sections of the sky about 2.8° in diameter in four spectral ranges. The primary, ring-shaped mirror is 32 centimeters in diameter and made of quartz. The central hole, which is occupied by the Uvicon assembly, is about 12.7 centimeters in diameter. Light reflected from the primary mirror impinges on the 16-centimeter quartz secondary mirror and is reflected onto the Uvicon photocathode, passing through an ultraviolet filter on the way. The optics are similar to those of the Schwartzschild camera.

The Uvicon imaging device is central to the Celescope concept and worthy of further mention. Developed by Westinghouse, the Uvicon in the SAO telescopes combines the SEC (Secondary Emission and Conduction) Vidicon concept with an ultraviolet cathode. The conventional Vidicon is not sufficiently sensitive, so one first
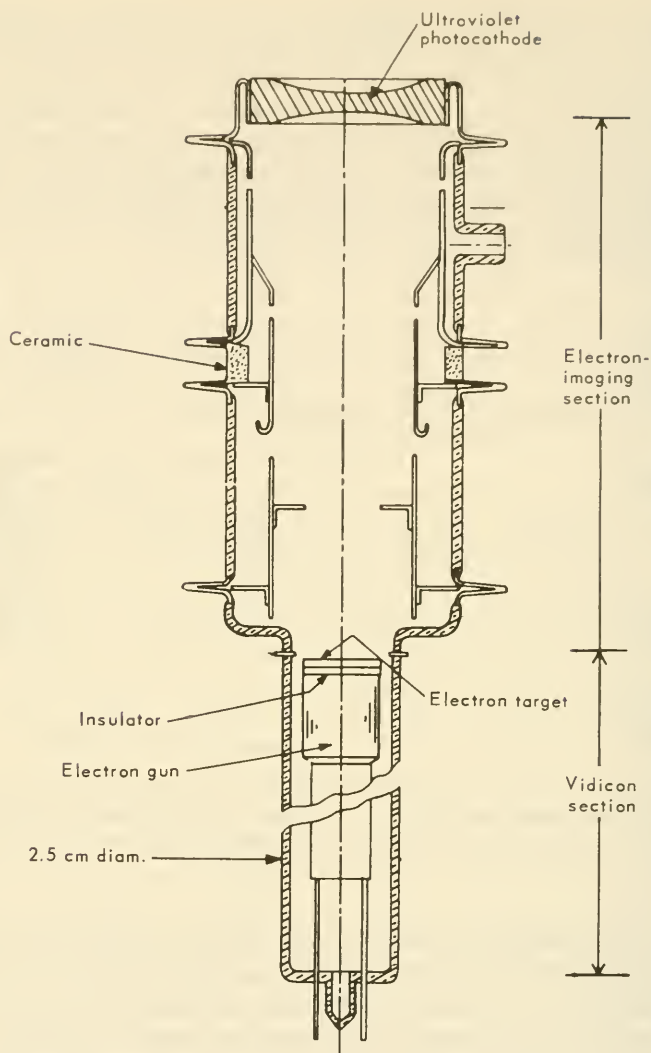
FIGURE 13–7.—A Uvicon imaging tube. A detector of this type converts images of star fields in the ultraviolet into electrical signals for subsequent telemetering.

transforms the ultraviolet image into an electron image, which is amplified by secondary emission at the SEC target (fig. 13–7). Stage No. 1 of the Uvicon consists of a photocathode, which emits electrons where it has been activated by the images of ultraviolet-emitting stars. These photoelectrons are then accelerated through

about 12 kilovolts and focused electrostatically on the target of an SEC-Vidicon. The electrical-charge pattern created on the SEC-Vidicon target corresponds to the ultraviolet image on the photocathode. An electron beam then scans the SEC-Vidicon target and converts the image into an analog signal that can be digitized and transmitted to Earth, where a replica of the original ultraviolet image is reconstituted. The SAO imaging system is expected to record stars of the eighth magnitude. The Uvicon signals will be quantized into 128 levels, providing an accuracy of about 0.1 magnitude. A complete image requires the transmission of about a half-million bits of information. Normally, exposure times will be about 1 minute.

The Princeton Experiment Package.—An ultraviolet telescope-spectrograph is being prepared under the direction of L. Spitzer at Princeton University, for launching on OAO C. The Princeton instrument utilizes a high-dispersion grating to spread the ultraviolet spectrum out so that the very narrow lines due to the absorption of interstellar gas and dust may be observed. The Goddard Experiment Package, discussed earlier, also scanned the ultraviolet spectrum, but in a stepwise fashion and with relatively low dispersion. These narrow absorption lines, whose interpretation is critical to cosmology, cannot be accurately measured under such conditions. A secondary objective of the Princeton instrument would be spectral analysis of hot stars in the ultraviolet at high dispersion.

The optical diagram of the experiment (fig. 13–8) shows a Cassegrain arrangement of primary and secondary quartz mirrors. Light passing through the slit is dispersed by a fused-silica grating ruled with 2400 lines/mm. Two carriages carrying photocells move along the Rowland circle, in a manner similar to that of the OSO-I spectrometer (sec. 12–2). Each carriage has two spectrally sensitive photomultiplier tubes mounted upon it; one measures the intensity of the first-order, long-wavelength spectrum; the second is sensitive to the second-order, short wavelengths. Together the carriages scan the regions 750 Å to 1500 Å and 1500 Å to 3000 Å. Resolving power is about 0.1 Å. Stars of the sixth magnitude should be observable.

The positions of the carriages must be accurately known and commandable from the Earth, if the inherent precision of the instrument is to be realized. Figure 13–9 shows the block diagram of the supporting circuitry. The overall physical arrangement of components is illustrated in figure 13–10.
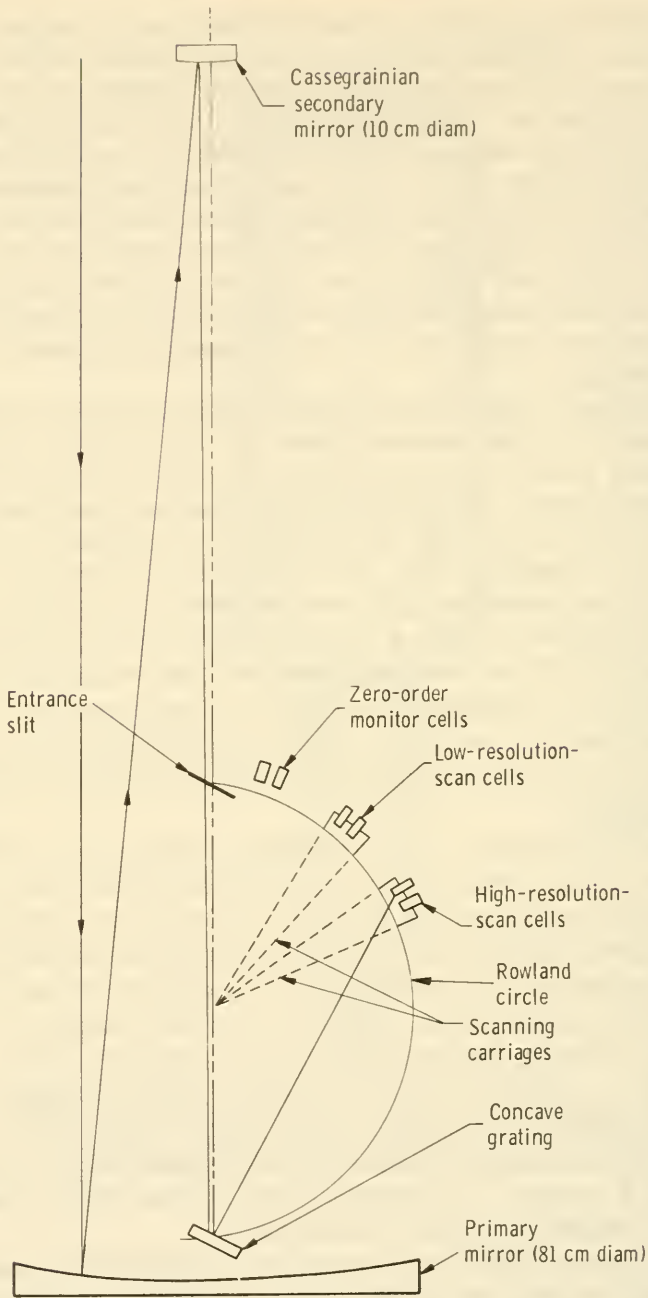
FIGURE 13–8.—Optical layout of the telescope and spectrograph in the Princeton OAO Experiment Package.
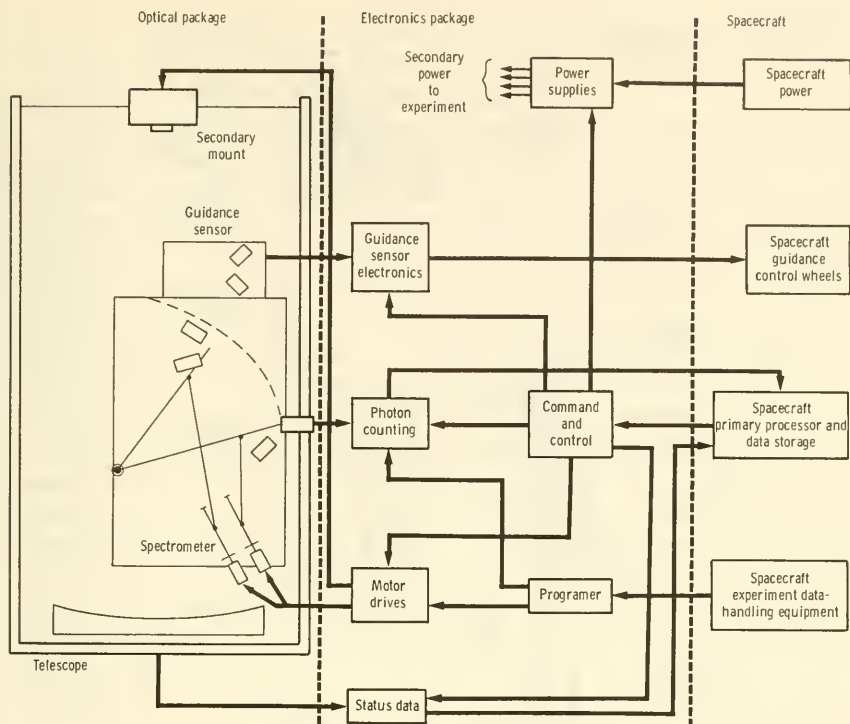
FIGURE 13–9.—Block diagram of the supporting components for the Princeton Experiment Package (ref. 2).

C. Radio-Astronomy Experiments

In the early 1930's, when Reber and Jansky first turned directional receiving antennas toward the skies, the scientific world was somewhat startled by the discovery of numerous intense radio sources superimposed upon a general cosmic-noise background. Many scientists subsequently built instruments to study this unexplored region of the electromagnetic spectrum. Radio astronomy has proved very fruitful; not only are there radio stars and a radio continuum, but the Sun, Moon, and planets (especially Jupiter) emit diagnostic radio waves (sec. 1–2). Unfortunately, though, the Earth's atmosphere begins to abridge our view of the radio universe at wavelengths longer than about 30 meters, and again when wavelengths are shorter than a few millimeters. Ionospheric and water-vapor absorption processes, respectively, are the main causes of this blindness. Thus we place radio-receiver experiments on satellites for the same basic reason we want to transport ultraviolet spectrographs beyond the atmosphere.
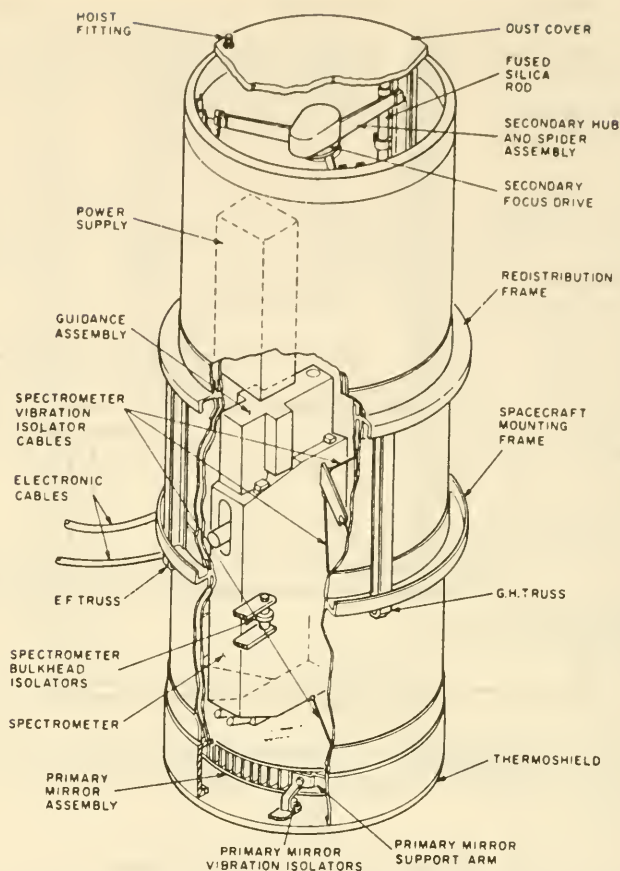
FIGURE 13–10.—Mechanical arrangement of com-
ponents in the Princeton Experiment Package.
The whole assembly fits into the central well of
the OAO. (See figure 9–69.)

The simplest type of satellite experiment in radio astronomy
involves nondirectional listening, usually at several frequencies.
The ultraviolet parallel would be the broadband, wide-field pho-
tometers described earlier. Or, one can sweep the frequency range
being explored. F. G. Smith's experiment on Ariel 2 (table 13–1),
for example, listened to cosmic noise over the range 0.75 to 3
megacycles. The solar radio-noise experiments presented in sec-
tion 12–2 were also of the nondirectional listening type; so were
the vlf receivers of section 11–3. The next obvious step beyond
such surveys is the construction of satellites with large directional-
antenna arrays that can pinpoint galactic and planetary sources

of long wavelengths. The RAE (Radio Astronomy Explorer) satellite series of NASA takes this step. Some of the RAE instrumentation will be described shortly.

The previous paragraph really deals only with the long wavelengths (those greater than 30 m[1]) that do not penetrate the ionosphere. The millimeter and centimeter region of the spectrum has not been explored at all by satellite instruments, though the space probe Mariner II carried microwave and infrared radiometers to Venus in 1962. Satellite instruments could not, of course, examine planet surfaces in detail across interplanetary distances, but emission spectroscopy of thermal sources on the Moon is a possibility. Primary emphasis in satellite radio astronomy, however, is at the long-wavelength end of the spectrum.

The RAE Instrumentation.—The RAE spacecraft (fig. A–41) seems relatively insignificant in size when the four 238-meter-long antennas are deployed. The antennas are, of course, only the sensors for the onboard instruments, and the instruments themselves depend upon telemetry transmitters, clocks, and power supplies for getting the information from the signals they intercept back to Earth. The RAE instrumentation consists of the following elements (fig. 13–11):

(1) Four 238-meter antennas arranged in an acute double-V. A short dipole, 61 meters tip to tip, mounted 60° to the plane of the double-V and normal to the local vertical.

(2) Three Ryle-Vonberg radiometers; two connected to the double-V antennas and one to the dipole.

(3) A rapid-burst radio receiver.

(4) Two antenna impedance probes and one capacitance probe, connected, as shown in figure 13–11, for the purpose of determining antenna characteristics as they vary with antenna distortion and ambient conditions.

Six varieties of experiments can be carried out with such instruments:

(1) Observation of galactic radiation from ionized hydrogen (H II) and interstellar synchrotron radiation.

(2) Observation of sporadic low-frequency radio bursts from the Sun.

(3) Observation of sporadic radio bursts from Jupiter.

(4) Observation of sporadic radio bursts from the Earth's ionosphere.

---

[1] Even satellites have their low-frequency cutoff, owing to the far-reaching halo of electrons surrounding the Earth. At a few thousand kilometers, satellites will be blind (or deaf) to radiation below about 300 kc.
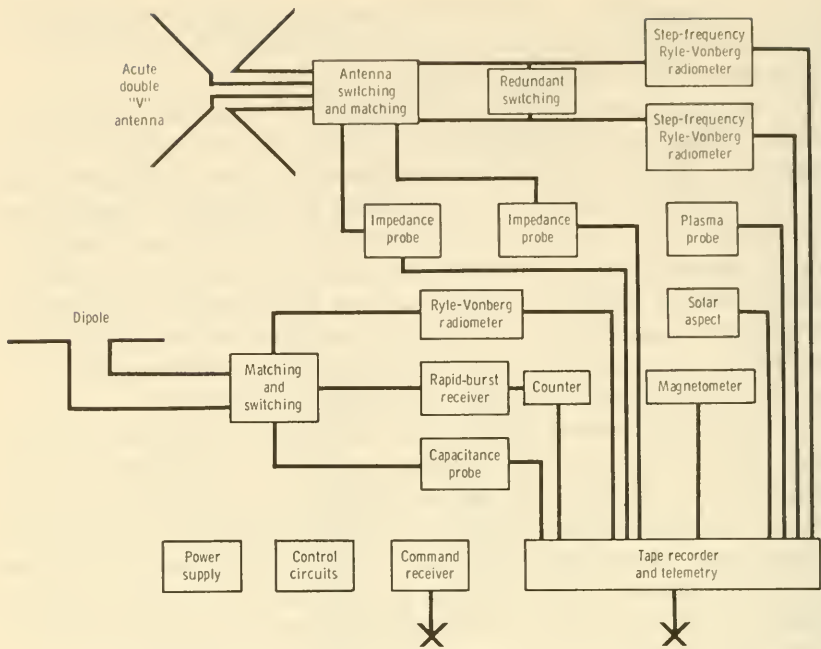
FIGURE 13–11.—Block diagram of RAE instrumentation.

(5) Mapping of discrete cosmic-noise sources at low frequencies.

(6) Observation of low-frequency radio waves induced by plasma oscillations.

The RAE objectives manifestly have important implications for geophysics and solar physics as well as astronomy.

Taking the antennas first, some of the considerations leading to the choice of the V-configuration for the main RAE antennas were: (1) good directional pattern over the frequency band to be investigated; (2) simple, reliable mechanical deployment; and (3) insensitivity to the space environment; viz, radiation pressure (ref. 3). Dish antennas, such as those customarily used in ground-based radio astronomy, would weigh far too much for space use, even if made from thin metallic foil. Some arrangement of linear antenna elements would seem to be the easiest to deploy. The V-type antenna was selected for the RAE for this reason and because it has a solid main lobe and good side-lobe suppression (table 13–2). The RAE double-V consists of four 238-meter elements made of highly polished, silver-plated, beryllium-copper tape. Each tape, which is 0.005 centimeter thick and 5 centimeters

TABLE 13–2.—*Comparison of the Directivity of RAE Acute-Angle V-Antenna With RAE Short Dipole*

	Half-power beamwidth		Front-to-back ratio	Maximum side-lobe level	Exploring frequency, Mc
	In antenna plane, deg	Perpendicular to antenna plane, deg			
Short dipole	120	360	None	None.	
V-type: [a]					
$L/\lambda = 1$	40	90	Average 18 dB	Maximum side-lobe level down 7 dB on the average.	1.35
$L/\lambda = 1.5$	30	40			2.02
$L/\lambda = 3$	30	40			4.05
$L/\lambda = 4$	20	30			5.40
$L/\lambda = 5.5$	15	30			7.42
$L/\lambda = 6$	10	20			8.10
$L/\lambda = 8$	10	15			10.80

[a] L/λ = Antenna leg-length-to-wavelength ratio.

wide, is rolled on a reel about 15 centimeters in diameter. A motor deploys the tape, which then curls to form a cylinder about 1.25 centimeters in diameter, in the same way that de Havilland spacecraft booms (fig. 9–52) are extended. By inserting terminating resistances one-quarter wavelength from the ends of the antenna legs, the pattern can be made unidirectional, with a front-to-back ratio of about 18 dB. Antenna distortions due to gravitational and thermal forces are not serious.

The RAE dipole antenna is made of the same material as the double-V antenna and is deployed in the same fashion. Its purpose is the observation of intense solar and Jovian noise bursts of short duration when the V-antennas are not pointed in the proper directions.

The other instrument components are relatively straightforward. The Ryle-Vonberg closed-loop, stepped radiometer was selected for the RAE because of its accuracy and stability over long periods of time. A block diagram of the basic radiometer is shown in figure 13–12. It covers the frequency range 0.3 to 20 mega-
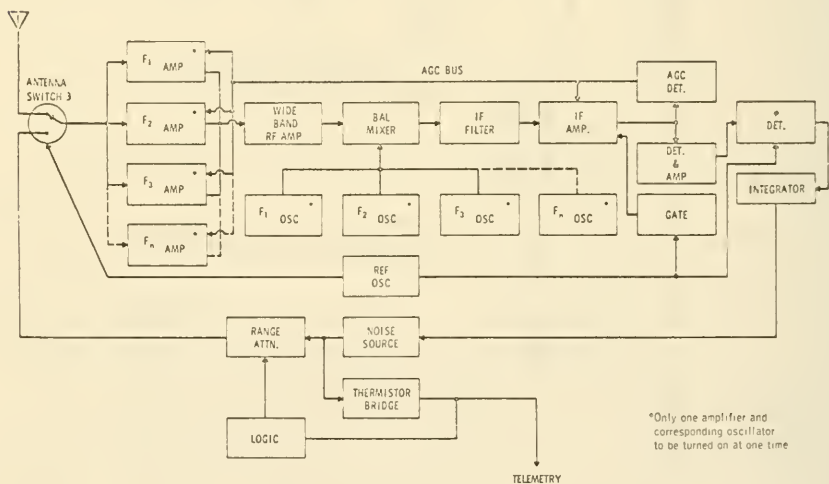
FIGURE 13–12.—Block diagram of the RAE Ryle-Vonberg stepped radiometer. Range 0.3–10 megacycles.

cycles in 10 steps. The other major component, the burst receiver, is presented in figure 13–13. Two features of interest here are the use of a calibrating noise source and a provision for automatically signaling the observer whenever the noise signal level exceeds 10 times the normal background.
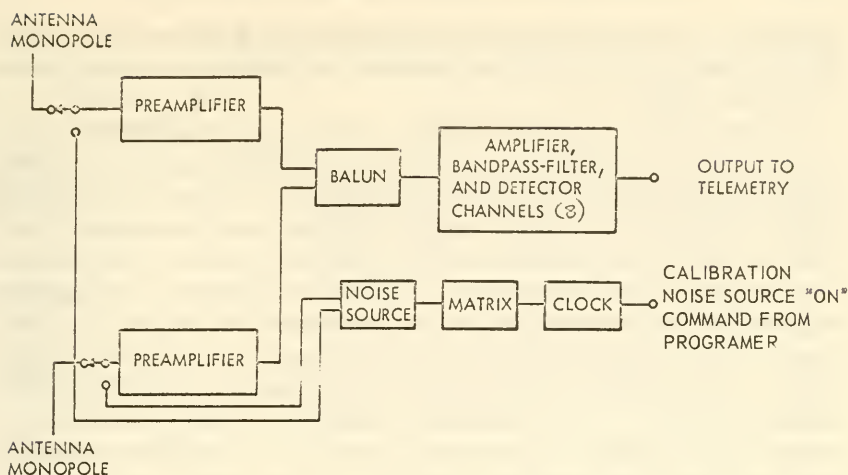
FIGURE 13–13.—Block diagram of the rapid-burst, radio-noise receiver carried on the RAE for observing solar and planetary phenomena.

The RAE itself, which is described in the appendix, is a gravity-gradient-stabilized spacecraft. The most sensitive lobe of the double-V antenna will then sweep the sky as the satellite circles the Earth. The satellite is not "pointable" like the OAO series. It is planned to place the RAE in a 6000-kilometer, retrograde orbit, well above most of the Earth's ionized halo. Orbit inclination will be about 58°, so that the instruments will frequently sweep out that portion of the sky containing the Sun, the planets, and the plane of the galaxy. Orbital precession will enable mapping of the entire celestial sphere over the period of a year.

13–3. Cosmic-Ray Instruments and Experiments

The cosmic rays that bombard the Earth are divided by custom into solar and galactic components. Solar cosmic rays are the less energetic and their composition is different from those of galactic origin (table 1–3). Solar cosmic rays, since they stem from solar storms, are sporadic and directional. In comparison, galactic cosmic rays are omnidirectional, and modulated only when a tongue of solar plasma diverts them away from the Earth (Forbush decrease). Instrumentation is very similar for both types of cosmic rays, and solar cosmic-ray instrumentation was referred to this section from chapter 12. It should also be pointed out that gamma rays, though they are electromagnetic in character, are included here with cosmic rays. The very-short-wavelength X-rays discussed in section 12–2 overlap the gamma-ray portion of the

spectrum. Some of the instruments used to measure hard solar X-rays (sec. 12–2) therefore resemble the gamma-ray experiments described below.

Scientists instrument satellites to measure the following cosmic-ray parameters: intensity, direction of arrival, energy, and species; all determined, of course, as functions of time. The flux of cosmic rays is so low that charge collection and subsequent current collection are almost never used (table 13–3). Particle or "event" counting is standard. The basic detectors, such as the Geiger and scintillation counters introduced in chapter 11 perform this function. Cosmic-ray energies are so high that electrostatic and magnetic dispersion are usually impractical. To measure energy, an investigator conducts E vs. dE/dx and R vs. dE/dx experiments. Pulse-height analysis of scintillator flashes can also yield total energy. The point is that cosmic-ray energies are measured by stopping the particles in matter and somehow converting their kinetic energies into measurable quantities, such as distance traveled in a known material or scintillation intensity. Cosmic-ray species can be recognized, not by mass dispersion but rather by comparing their penetrating abilities and energy-loss factors when they collide with instrument materials. One can also cause cosmic rays to induce nuclear reactions, which produce easily recognized secondary particles. The final factor in the list of parameters to be measured as functions of time is direction of arrival. Since one cannot conveniently focus or divert cosmic rays with mirrors, lenses, or electromagnetic fields and still have an instrument that will fit on a satellite,[5] collimators and arrays of interconnected detectors are commonly applied to this task. In fact, all of the stratagems proposed above and those in table 13–3, too, depend upon arrays of basic detectors to determine energy, species, direction of arrival, and so on. Such arrays and combinations of basic detectors are called telescopes, presumably because a cosmic ray must pass through two or more linearly arranged elements in order to be counted, just as light is "analyzed" by linear optical telescopes. Cosmic-ray telescopes obviously do not magnify, but if the experimenter is ingenious, he can use them to determine all the cosmic-ray parameters needed for understanding this phenomenon.

Cosmic-ray instrumentation is diverse and frequent cargo on satellite flights, as table 13–4 well demonstrates. The following

---

[5] Charged cosmic-ray particles are affected by electromagnetic fields; and gamma rays, in principle, can be focused by total reflection; but the effects are too small to lend themselves to satellite instrumentation.

TABLE 13–3.—*Physical Effects Used in Analyzing Cosmic Rays*

Parameter to be measured	Applicable physical effects
Intensity_____	Particle or quantum counting by any of the many basic detectors described in sec. 11–4. Current collection, as in ionization chambers, is seldom used.
Energy_____	Kinetic energies are converted into measurable scintillator flashes, proportional-counter pulse heights, ranges in known materials.
Species_____	Penetrating power and energy-loss factors in known materials. Secondary particles generated by nuclear reactions.
Direction of arrival____	Collimators. Arrays of detectors. Directions taken by secondary particles from nuclear reactions. Track images.

descriptions of typical cosmic-ray instruments adhere to the classification scheme introduced in section 11–3. Although basic detectors are almost never applied singly, the Explorer-VII ionization chamber is pertinent. The cosmic-ray telescopes, classed as detector combinations, form by far the largest group. Finally, the spark chamber, a track-imaging instrument, is now finding its way into satellite payloads. The reader will find that occasional reference to section 11–3 and the detector operating principles described there may be helpful.

A.   Basic Detectors [6]

Ionization Chambers.—In chapter 11, it was remarked that ionization chambers are seldom used alone, but rather in conjunction with other basic detectors, typically Geiger counters. Table 13–4 confirms that this is the case for cosmic-ray research, too. The reason for this experimental prejudice is that ionization chambers, as they are usually employed, merely integrate all energy increments deposited within the chamber by all particles passing through, and tell nothing about single-particle flux, direction of arrival, or energy. The ionization chamber, however, can be put to work on the problem of discriminating particle species. The Explorer-VII ionization chamber, also called a "heavy-nuclei chamber," was built to identify heavy nuclei in cosmic rays.

[6] See ch. 11 for descriptions of operating principles.

TABLE 13-4.—*Cosmic-Ray Instruments, Experiments, and Experimenters* [a]

Basic Detectors

Ariel 1	Elliot, H./Imperial College	Cerenkov counter, Perspex sphere, plus 2 Geiger counters.
ESRO 2	Elliot, H./Imperial College	Two proportional counters, 2 scintillators, 2 Cerenkov counters, 0.4–0.8 GeV.
	Marsden, P. L./U. Leeds	CO_2 Cerenkov counter, >20 GeV.
	Elliott, H./Imperial College	Two Geiger counters, electrons over 1 and 3 MeV, protons over 15 and 20 MeV.
Explorer VII	Groetsinger, G./RIAS	Argon-filled ionization chamber.
Explorer XII, XIV	McDonald, F. B./GSFC	Two Geiger counters; electrons over 8 MeV, protons over 70 MeV.
		CsI scintillator.
OAO A1	Frost, K./GSFC	NaI scintillator.
OAO C	Boyd, R. L. F./University College	Three photon detectors and 3 gas counters for stellar X-rays; 3–12 Å, 8–18 Å, 44–60 Å.
OGO II, D	Anderson, H. R./Rice U.	Ionization chambers, 10 MeV–15 BeV.
OGO E	Anderson, K. A./U. Calif	Scintillator allied with proportional-counter telescope.
OSO I, II, E	Frost, K./GSFC	NaI(Tl), for e-p annihilation line, wheel.
OSO E	Peterson, L. E./U. Calif	NaI scintillator, 15–600 keV.

Detector Combinations

Geiger telescopes:		
Explorer XII, XIV	McDonald, F. B./GSFC	
Explorer XVIII, XXI, XXVIII	McDonald, F. B./GSFC	Orthogonal telescope.
Proportional-counter telescopes:		
Explorer VI	Simpson, J. A./U. Chicago	Two triple-coincidence telescopes.
OGO E	Anderson, K. A./U. Calif	Telescope with scintillators; X-ray range, 1–90 keV; proton range, 8–300 MeV.

Scintillator telescopes:

Explorer XII, XIV	McDonald, F. B./GSFC	Two plastic scintillators, 100–600 MeV and over 600 MeV.
Explorer XVIII, XXI, XXVIII	McDonald, F. B./GSFC	E vs. dE/dx telescope, 10–100 MeV/nucleon.
IMP F/G	McCracken, K. G./GRCSW	For cosmic-ray anisotropy; protons, 10–100 MeV; alphas, 200–400 MeV.
OGO I, B	Anderson, K. A./U. Calif	Solar cosmic rays, proton range, 10–90 MeV.
	McDonald, F. B./GSFC	Nuclear-abundance detector. See text.
OGO II, D	Simpson, J. A./U. Chicago	0.3–30 MeV.
OGO E	Cline, T. L./GSFC	Protons, 20–70 MeV; electrons, 0.1–8 MeV; positrons, 0.5–8 MeV; gammas, 50–700 MeV.
	McDonald, F. B./GSFC	Allied with solid-state telescope. Protons, 0.4–1200 MeV; electrons, 1–10 MeV; alphas, 2–1200 MeV.
	Wapstra, A. H./Netherlands Inst. Nuc. Phys. Res.	Electrons, 0.5–10 BeV; protons, 20–100 BeV; gammas over 500 MeV.
OSO I	White, W./GSFC	Two NaI(Tl). 0.2–1.5 MeV, wheel.
	Winckler, J. R./U. Minn.	Compton coincidence telescope. 0.05–3 MeV, wheel.

Cerenkov-scintillator telescopes:

Elektron 2, 4		Over 600 MeV/nucleon.
Explorer XI	Kraushaar, W./MIT	Phoswich-Cerenkov telescope, 100–400 MeV.
OAO A1	Kraushaar, W./MIT	Same as Explorer XI.
OGO E	Meyer, P./U. Chicago	Cosmic-ray electrons, 20–100 MeV.
OSO I	Fazio, G./U. Rochester	Lead converter, solar gammas, 100–500 MeV.
OSO II	Leavitt, C./U. N. Mex.	Lead-glass type. Gammas, 50–1200 MeV.
OSO E	Kaplon, M. F./U. Rochester	Over 3.3 MeV/nucleon.
	Kraushaar, W./MIT	Nonsolar gammas over 100 MeV.
Sputnik 3		
OV–1–10	Ely, J. T. A./AFCRL	Two thin Cerenkov detectors.

Solid-state telescopes:

ESRO 2	de Jager, C./U. Utrecht	Soft solar X-rays, 2 bands between 44 and 70 Å.
	Labeyrie, J./Centre d'Etudes Nucleaires de Saclay.	Three-element telescope.

a See also table 11–8.

TABLE 13-4.—*Cosmic-Ray Instruments, Experiments, and Experimenters*—Continued

Detector Combinations—Continued

Solid-state telescopes—Continued

Explorer XVIII, XXI, XXVIII.	Simpson, J. A./U. Chicago	25–40 elements. R vs. dE/dx telescope. Protons, 100 keV–200 MeV.
IMP F/G	Simpson, J. A./U. Chicago	Three solid-state detectors plus scintillator. Protons, 0.5–85 MeV; alphas, 6 MeV and up.
	McDonald, F. B./GSFC	Three elements; 2 in dE/dx arrangement. Electrons, 1–20 MeV; H, D, T, He range 12–80 MeV/nucleon.
		Solid-state scintillator telescope. Protons, 0.4–8 MeV; alphas, 2–8 MeV/nucleon.
OGO I, B	Simpson, J. A./U. Chicago	Protons over 0.2 MeV.
OGO E	McDonald, F. B./GSFC	Allied with scintillator telescope. Protons, 0.4–1200 MeV; electrons, 1–10 MeV; alphas, 2–1200 MeV.
OV–1–14	Gram, P. A. M./Aerospace	Twenty-element dE/dx telescope.
	Freden, S. C./Aerospace	Two dE/dx telescopes.
OV–2–5	Gram, P. A. M./Aerospace	Same as OV–1–14.
Sputnik 3		35 keV to several MeV.

Track-Imaging Instruments

OGO E	Hutchinson, G. W./U. Southampton	Acoustic-type spark chamber. See text.

The Explorer-VII chamber, shown in figure 13–14, was constructed of Dow metal and filled with nine atmospheres of argon (ref. 4). The central wire collected all electrons produced by passages of charged particles. A polonium alpha source was provided for calibration, and a pressure gage indicated, via telemetry, if the pressure was below a preset value. The species discrimination of heavy cosmic-ray nuclei depended upon three facts and assumptions:

(1) All heavy cosmic rays are energetic enough to pass completely through the chamber. By inference, the cosmic rays detected are relativistic.

(2) The amount of ionization they leave behind is proportional to the square of the particle's atomic number.

(3) No other incident particles or particles created in secondary reactions in the walls will produce as much ionization as relativistic particles with an atomic number of 6, the experiment's mass threshhold.
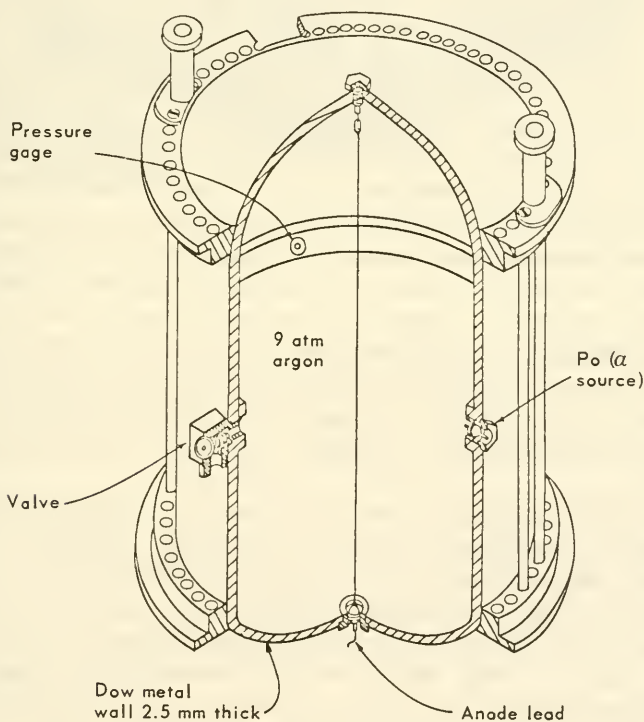
FIGURE 13–14.—Cutaway view of the Explorer-VII ionization chamber. Height: about 22 centimeters (ref. 4).

With this information available, one merely has to measure the numbers and amplitudes of the pulses caused by threshold particles and heavier components. In the Explorer-VII experiment, an amplifier pulse output of 0.42 volt represented a relativistic particle with an atomic number of 6; 0.95 volt corresponded to 9; and 3.0 volts corresponded to 16. Discriminator circuits sorted out particles in these three categories and the count rates were telemetered to Earth.

The Explorer-VII ionization chamber, because it counted only particles passing completely through it, functioned as a dE/dx device; that is, it measured only deposited-energy increments. Later, in connection with E vs. dE/dx solid-state telescopes, we shall see how scintillators and solid-state detectors operate as if they were thin ionization chambers.

B. Detector Combinations (Telescopes)

Geiger Telescopes.—The Explorer-XII cosmic-ray package included a simple two-counter Geiger telescope (ref. 5). The counters were of the pancake type and filled with a halogen. Protons with energies greater than 27 MeV were adequate to trigger either counter alone, but 70 MeV were required to trigger both in coincidence. The counters were connected so that both single and coincident events were telemetered. In this way, crude directional and energy data were obtained. It should be mentioned, however, that the Explorer-XII cosmic-ray package also included a double scintillator telescope and a single crystal detector that analyzed other portions of the proton energy spectrum (fig. 13–15). A meaningful picture of cosmic-ray protons depended, in this case, upon the integration and correlation of data from all three instruments. A perusal of table 13–4 will show that Geiger telescopes are used sparingly in cosmic-ray research, primarily because they give no direct measurement of energy (E) or energy increments (dE/dx).

Proportional-Counter Telescopes.—The first radiation telescopes to be used in satellites were the two hexagonal packages of seven cylindrical proportional counters flown on Explorer VI in 1959 (fig. 13–16). The two packages differed only in the amounts of shielding placed around them, making them separately responsive to high- and low-energy particles. The high-energy counters were 7.5 centimeters long and were formed from 1.27-centimeter-diameter brass tubing with walls 0.071 centimeter thick. A lead shield of 5 g/cm² surrounded the entire assembly. The low-energy counters had steel walls and were shielded only halfway around.
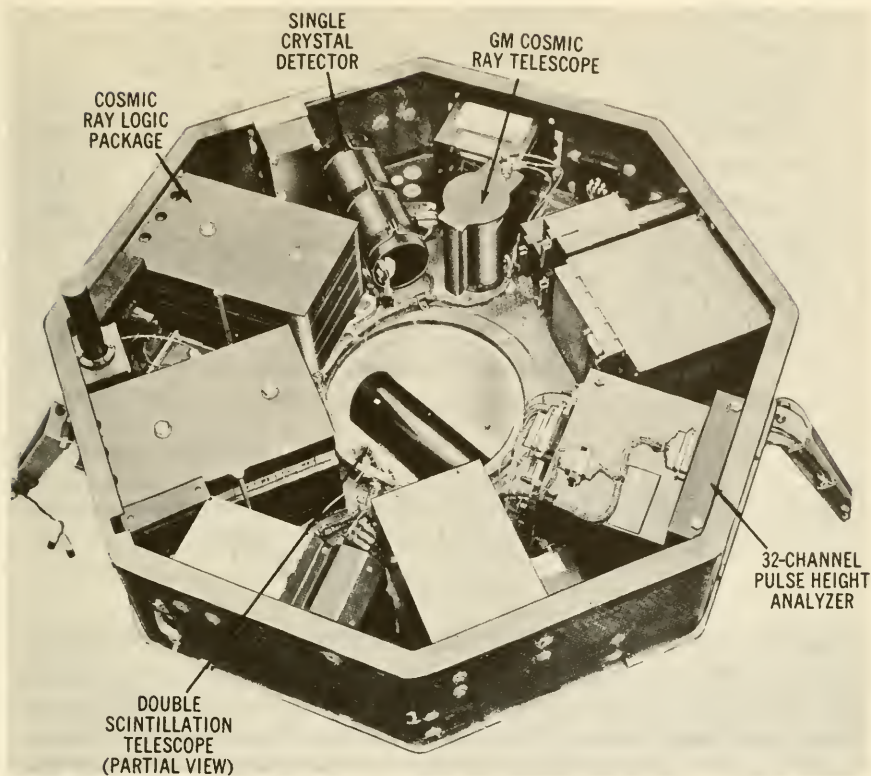
FIGURE 13–15.—The Explorer-XII instrument package, showing the locations of the three cosmic-ray experiments. The octagon is about 69 centimeters across the flats.

Both instrument packages had their counters connected in triple coincidence, so a particle would have to penetrate three in a line before a signal would be telemetered. This gave the experiment crude directional sensitivity. Comparison of data from the low- and high-energy counters (they have overlapping energy ranges) made it possible to determine the average energy per particle. From this, some insight into particle energy and species was gained. Because of their ability to measure energy, proportional counters are used extensively in satellite research, but mainly in the very-low-energy-loss region appropriate for measuring X-rays and gamma rays.

Scintillator Telescopes.—The type of scintillator telescope presented here was flown on OSO E and OAO A1. Its purpose was to measure the flux and direction of arrival of low-energy gamma rays in the range 2 to 150 keV (ref. 6). The OAO version, shown
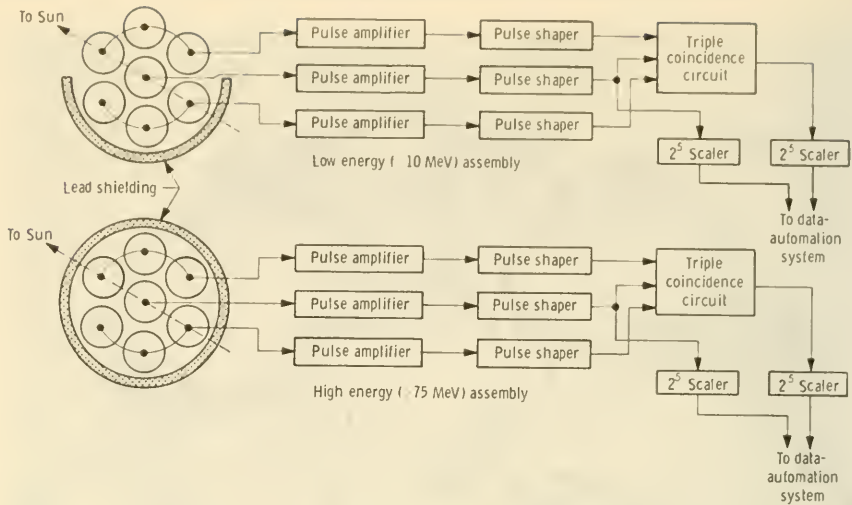
FIGURE 13–16.—Block diagram of the Explorer-VI proportional-counter telescope built by the University of Chicago.

in figure 13–17, uses two thallium-activated, inorganic scintillator crystals. The heavy thallium atoms convert incident gamma rays into detectable positron-electron pairs by the pair-production reaction and also produce Compton electrons. Directionality is conferred on the pictured arrangement by the shielding effect of the bucket-shaped anticoincidence crystal and the areal exposure of the pancake-shaped central crystal. An acceptance cone of 20° half-angle results. The outer crystal, or "guard," counter inhibits counts by the central crystal whenever it detects a gamma ray more energetic than 50 keV. This feature suppresses noise and secondary particles. The central crystal and its nine-channel pulse-height analyzer count only those events in the 2- to 150-keV range that survive the anticoincidence feature. The three photomultiplier tubes monitoring the central crystal are connected in coincidence; i.e., all must be triggered simultaneously; this arrangement also suppresses noise. The very low energies being measured make noise suppression more critical here than on experiments in the MeV range. A block diagram of this experiment is presented in figure 13–18 to illustrate typical supporting circuitry.

The scintillator telescope described above represents only one of the many scintillator arrangements that have been flown on satellites. The OGO-E E vs. dE/dx detector and the position detector presented later are also scintillator telescopes, of a more specialized variety. The above example, however, illustrates how
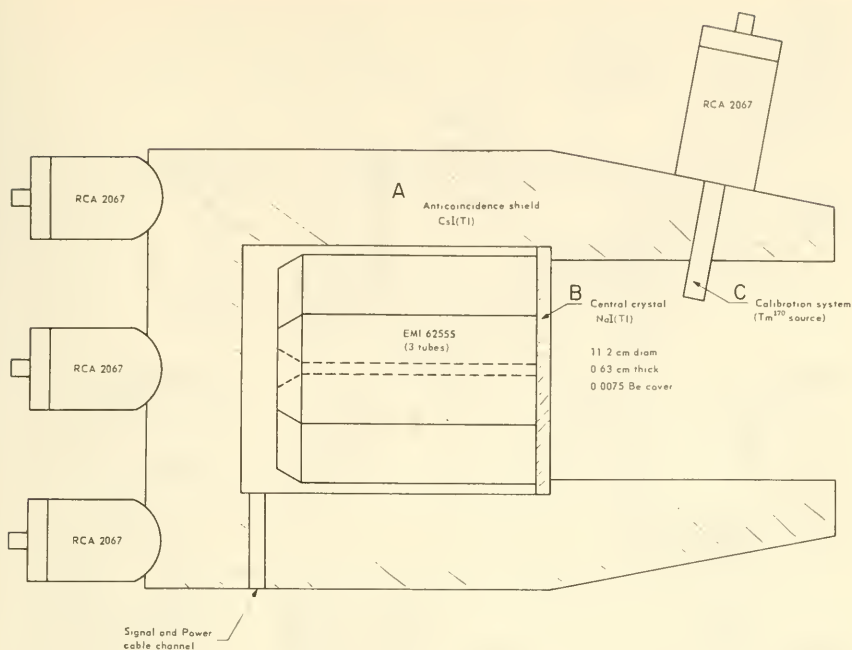
FIGURE 13–17.—Sketch of the OAO low-energy gamma-ray scintillation telescope. Three RCA 2067 photomultiplier tubes monitoring the anticoincidence shield at the forward end have been omitted for simplicity. The noise-supression features enable measurements of fluxes as low as 10^{-2} or 10^{-3} gammas/cm²-sec (ref. 6).

a combination of scintillators can reject unwanted particles and provide directionality.

Cerenkov-Scintillator Telescopes.—Cerenkov counters are most often used in conjunction with some other kind of detector. Here, an experiment proposed for ESRO 2 is presented as an example of the Cerenkov telescope.[7] The purpose of the ESRO-2 experiment is the measurement of the flux and energy distribution of cosmic-ray electrons in the GeV range (10^9 eV). The actual instrument (fig. 13–19) is rather unusual in satellite work because the Cerenkov counter employs a gas (CO_2 at 3 atm) to produce the Cerenkov effect, rather than the more common glass or Lucite. Cerenkov flashes produced by charged particles in the filler gas are seen by a photomultiplier tube at the top of the instrument, with the help of a mirror at the bottom of the gas chamber. A scintillator (S1) is optically bonded to the face of the top photomultiplier in order to shift the

---

[7] The principal investigators are P. L. Marsden and R. Jakeways, University of Leeds.
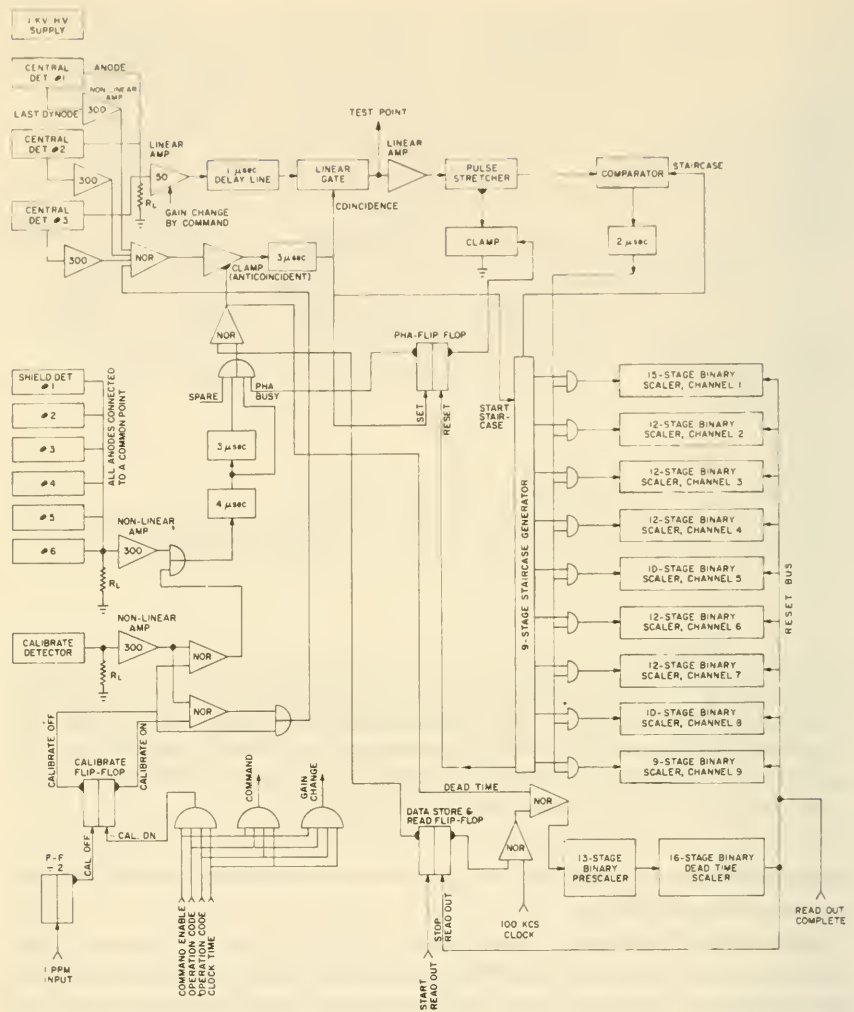
FIGURE 13–18.—Block diagram of the OAO low-energy gamma-ray experiment (ref. 6).

wavelength of the Cerenkov ultraviolet light, making it more easily detected by the photomultiplier, and also to discriminate against particles passing through the photomultiplier cathode that would otherwise create spurious signals. Telescopic action is provided by the addition of two more scintillators separated from the gas chamber by lead shields. Electrons can be distinguished from protons because secondary-particle cascades created by the cosmic rays in the lead will show different counting rates at scintillators
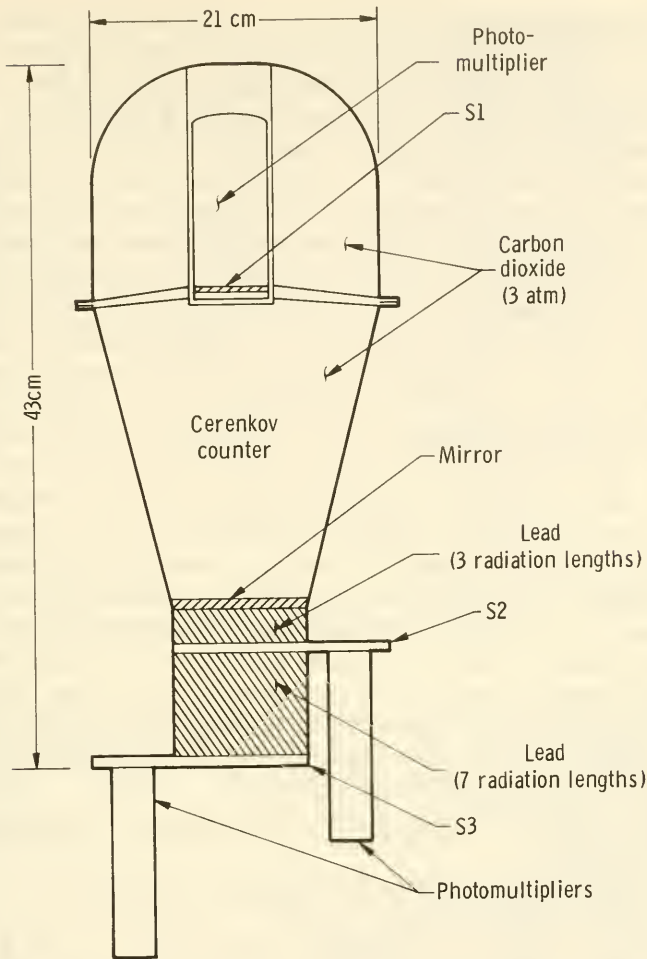
FIGURE 13–19.—Sketch of a Cerenkov scintillator tele-
scope proposed for ESRO 2 by P. L. Marsden and R.
Jakeways, University of Leeds.

S2 and S3. Electrons between 1 and 5 GeV, for example, will show
significant decreases in counting rates at S3 when compared with
those at S2. Protons would produce cascades still increasing in
intensity at S3. In addition to this species selectivity, the linear
arrangement of the counters provides some directionality. De-
tectors S1, S2, and S3 will also be used in coincidence to measure
the flux of protons with energies greater than 300 MeV. Only
protons of these energies can penetrate both lead shields.

An elaborate but more conventional Cerenkov-scintillator tele-
scope was flown on the satellite Explorer XI to measure gamma

rays with energies over 100 MeV as a function of direction (ref. 7). The scientific objective here was to test various cosmological hypotheses, which predict different high-energy gamma fluxes from interstellar space. A gamma telescope depends upon a secondary reaction to create charged particles that can be counted by the instrument's detectors. In a gamma-ray telescope, the pair-production reaction is employed. In this sense, the instrument reverses the approach used in the positron detector described later in this section of the book. The gamma-ray telescope consists of a sandwich of sodium-iodide and cesium-iodide scintillators viewed by a single photomultiplier tube, and, in addition, a Lucite Cerenkov detector seen by two photomultipliers. This detector assembly is surrounded by a shield of scintillating plastic, which is monitored by five photomultiplier tubes. The sandwich provides high-Z material for the pair-production process.[8] The electrons and positrons thus generated enter the Cerenkov detector, which, because of the directional property of Cerenkov light emission, detects only the charged particles moving toward the photomultiplier. Signals from high-energy charged particles in the space environment are eliminated by the outside plastic scintillator used in anticoincidence. Pulses from both the internal scintillator sandwich and Cerenkov counter, in the absence of a signal from the surrounding plastic, indicates that a high-energy gamma ray has passed through the effective aperture of the instrument. Summarizing, the instrument's capabilities are:

(1) The detection of gammas in the presence of high-energy charged particles.

(2) Gamma-energy sensitivity only above 100 MeV.

(3) Crude directional information.

Solid-State Telescopes.—Solid-state detectors, as mentioned in section 11–4, are basically dE/dx devices; that is, they generate a pulse proportional to the amount of energy (dE) deposited by the particle in passing through the thin counter (dx). Typical dE curves are presented in figure 13–20. Single solid-state detectors manifestly yield ambiguous energy information unless the particle species is known unequivocally. By adding other solid-state detectors and intervening shields to degrade particle energies, discrimination in direction of arrival, energy, and species can be achieved. These techniques will be seen more clearly in the E vs. dE/dx telescope, described shortly. Meanwhile, let us examine a simpler telescope.

---

[8] Frequently, lead sheets are introduced to promote the pair-production reaction. High-Z pieces of material are termed "gamma-ray converters."
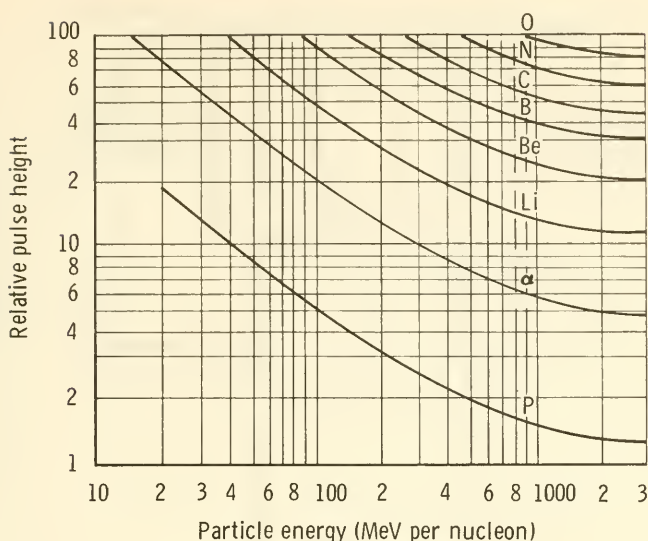
FIGURE 13–20.—Relative pulse heights produced by cosmic rays penetrating the solid-state detector of the instrument pictured in figure 13–19.

The solid-state telescope illustrated in figure 13–21 was proposed for the ESRO-2 satellite by J. Labeyrie and his collaborators at the Centre d'Etudes Nucleaires de Saclay, France. Two linear solid-state detectors provided directional discrimination, while a third, boxlike (without ends), solid-state detector, connected in anticoincidence with the two others, allowed the discard of shower-type events. The main purpose of the experiment is the measurement of the flux and energy distribution of cosmic-ray protons between 35 MeV and 1 GeV. Alphas between 140 MeV and 1200 MeV as well as relativistic heavier nuclei are also measured. There are, of course, ambiguities in this experiment because alpha particles above 240 MeV cannot be distinguished from protons between 35 and 120 MeV (fig. 13–20). The experiments assume that the alpha flux is small and may be determined by extrapolation.

Scintillator E *vs.* dE/dx *Telescope.*—Scientists at NASA's Goddard Space Flight Center designed a scintillation telescope of special configuration (also called a "nuclear-abundance detector") which can measure cosmic-ray energy spectra in the energy range from 15 to 90 MeV/nucleon for protons through oxygen nuclei. In addition, the instrument can measure the electron spectrum from 2.3 to 20 MeV (ref. 8). A smaller version of the nuclear-
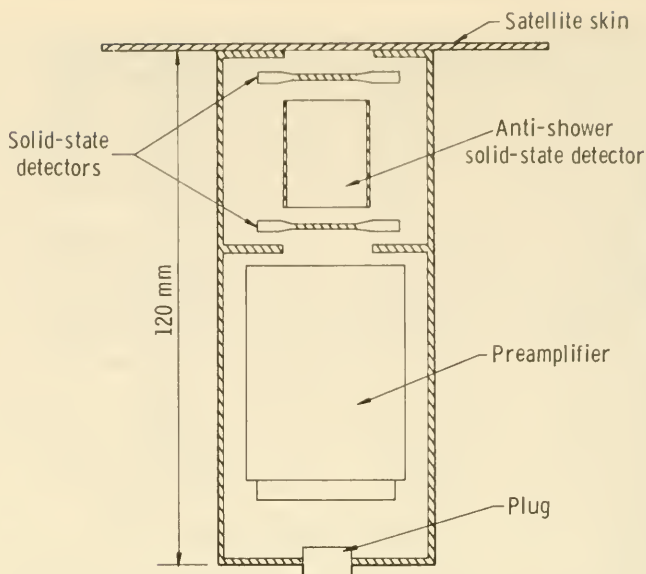
FIGURE 13–21.—Arrangement of solid-state detectors in the ESRO-2 cosmic-ray experiment of Labeyrie et al.

abundance detector, capable of analyzing nuclei where $Z < 3$, was flown on IMP's I and II (Explorers XVIII and XXI). The full-scale experiment was orbited on OGO's I and II.

The telescope consists of two thallium-doped cesium-iodide (CsI) crystal scintillators plus a plastic guard scintillator (fig. 13–22). The two CsI crystals measure the total energies of the incident charged particles as well as their differential energy losses, dE/dx. Charged particles entering from the left first pass through a 1-millimeter crystal that yields a pulse proportional to the energy lost in passage, ΔE. (Note that a thin scintillator is employed rather than a solid-state detector.) The second crystal is 2 centimeters thick, thick enough to stop particles in the energy range given above. The pulse emitted by the scintillator when the Particle is completely stopped is proportional to $E - \Delta E$. A Pilot-B plastic guard scintillator is in anticoincidence with the thick crystal to discard events where the particles are not completely stopped. The calibration curves in figure 13–23 show how the measurement of both E and $E - \Delta E$ can uniquely determine the species of charged particle. The scintillator geometry shown in figure 13–23 accepts particles within a cone of half-angle of 25°.
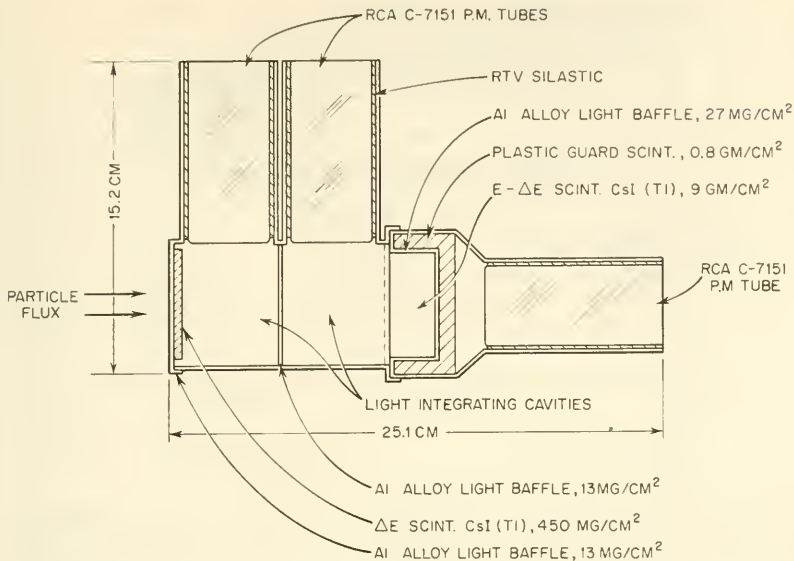
FIGURE 13–22.—Geometry of the OGO/IMP E versus dE/dx scintillator telescope (ref. 8).

Output pulses are fed to a pair of 256-channel pulse-height analyzers.

In connection with E vs. dE/dx telescopes, it is worthwhile noting that R vs. dE/dx experiments can also be designed in which the particle range, R, is determined by a multiple sandwich of solid-state detectors and shielding layers. The more energetic a particle, the greater its range, and the more layers of the sandwich it penetrates. A number of telescopes of this type have been built and flown on satellites by Simpson and his associates at the University of Chicago (table 13–4).

Phoswiches.—The phoswich is a unique kind of scintillation telescope used to differentiate between photons and charged particles. One type uses two scintillators with different rates of light-pulse decay, so that particle coincidences can be distinguished electronically with only one photomultiplier tube. The physical event is sketched in figure 13–24. The neutron phoswich counter designed by Reagan and Smith is typical of this class of instruments. It uses four lithium-iodide scintillators, surrounded by a plastic guard scintillator, which eliminates charged-particle counts by anticoincidence logic (fig. 13–25) (ref. 9). The lithium-iodide crystals are made neutron-sensitive by using lithium enriched with the Li[6] isotope, which has a high cross section for the neu-
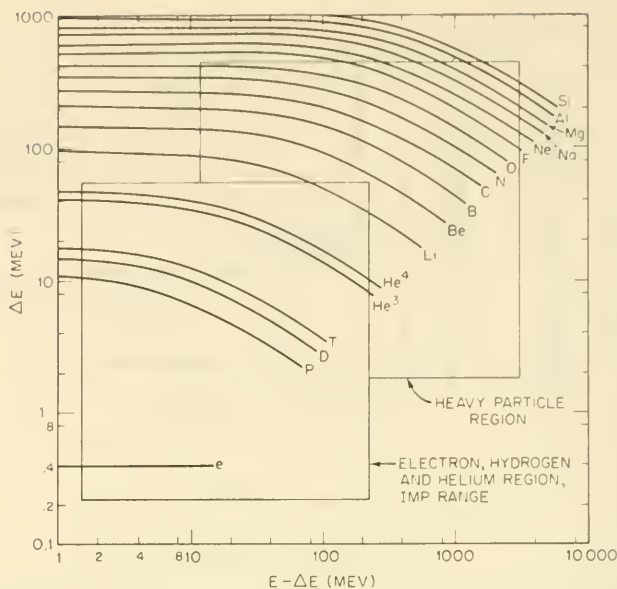
FIGURE 13-23.—Plot of energy loss in the E-scintillator versus the energy loss in the $E - \Delta E$-scintillator for various constituents in the cosmic-ray flux. The end points of the curves correspond to particles barely penetrating the $E - \Delta E$ scintillator (ref. 8).
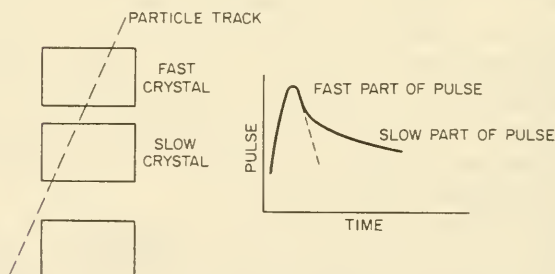
FIGURE 13-24.—In the phoswich counter, coincidences can be detected by a single photomultiplier through pulse-shape analysis.

tron-alpha reaction. The alphas generated actually trigger the phoswich crystals. (See the discussion of neutron detectors below.)

Neutron Detectors.—The neutron's lack of electrical charge and consequently extremely low ionizing power force a modification of
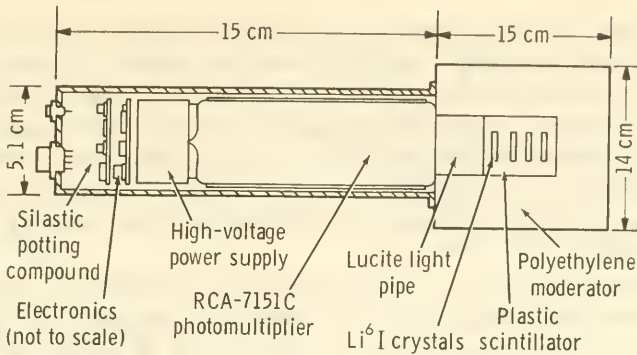
FIGURE 13–25.—A typical phoswich neutron counter
(ref. 9).

the basic charged-particle detectors that were described earlier.
In one such modification, Li^6, an isotope with a high cross section
for alpha-particle production, is incorporated in a scintillator ma-
terial (ref. 10). The secondary alphas produced by the Li^6 trigger
the scintillator. The use of neutron-alpha (n, α) reactions is typi-
cal in neutron detection. A very common terrestrial counter, for
example, is a proportional-counter tube filled with boron trifluoride
gas (BF_3). (See fig. 13–26 (ref. 11).) The B^{10} isotope, like Li^6,
has a high cross section for alpha production. Without the BF_3
gas, proportional counters detect neutrons only with very low
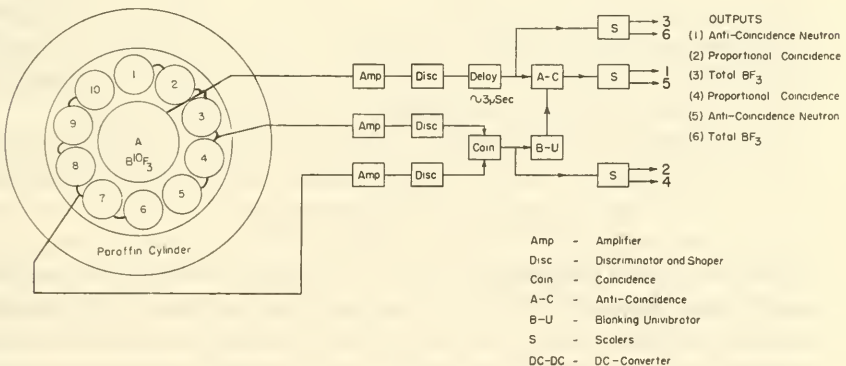
FIGURE 13–26.—End view of a $B^{10}F_3$ neutron detector surrounded by
guard proportional counters. The paraffin cylinder slows the neutron
down, promoting their reaction with B^{10}. The neutron-sensitive coun-
ter, A, is 2.54 centimeters in diameter and 7.6 centimeters long. It is
filled with 96 percent enriched BF_3 at 60 cm Hg (ref. 11).

efficiencies. Detectors that have been made neutron sensitive may also be surrounded by a second detector—usually a guard scintillator in anticoincidence—which produces a pulse every time a charged particle penetrates its active volume. By discarding all pulses from the guard detector and all coincident pulses from both detectors, only neutron counts remain. Neutron detectors have been orbited on several Air Force satellites (ref. 11) as well as on OSO I.

Positron Detectors.—Several physical processes in interplanetary space can create positrons. Among these are the beta decay of cosmic-ray-excited nuclei and the double decay of pi mesons. The detection and measurement of the positron flux may therefore tell us something about the types and frequencies of high-energy interactions in space. There is also the possibility of directly measuring the low-energy tail of the galactic positron flux that penetrates inward from the boundaries of the solar system.

A positron detector was developed by the Goddard Space Flight Center for OGO's I and B (ref. 12). This instrument actually detects positron-electron annihilation events rather than positrons directly. The mutual annihilation of a positron-electron pair yields two 0.51-MeV gammas 180° apart. These gammas are diagnostic for the positron-electron reaction, because of their unique energies and directional relationship.

The positron detector shown in figure 13–27 consists of two cylindrical, thallium-doped, cesium-iodide (CsI) crystals, each completely embedded in a plastic scintillator. The two "phoswiches" are optically separated. A third CsI crystal is located in a conical well machined in the joined plastic scintillator blocks. Two photomultiplier tubes separately view the bottom surfaces of the outer scintillators. Another photomultiplier tube sees the crystal in the well through a plastic scintillator light pipe.

The incident positron flux is in effect collimated and focused on the well crystal by the encasing plastic scintillators, which are connected in anticoincidence. Positron-electron annihilations occur in the well crystal as the positrons are slowed down. The thickness of the well crystal limits the kinetic energy of reacting positrons to about 2.5 MeV. Small ionizing particles with greater energies will penetrate to the anticoincidence case. Discrimination against particles entering any of the outside plastic is accomplished by circuits sensitive to the light-pulse shape. (See the previous phoswich discussion.)

Positron events may be signaled in three ways. First, two 0.51-MeV gammas, 180° apart, can emerge from the crystal in the well and be recorded by the two side-crystal scintillators in co-

Well

CsI(Tl)

RCA 7151 phototube

Plastic scintillator

Optical separation

Mass: 3.4 kg

Plastic scintillator

Pu^{239} α source

RCA 7151 phototube
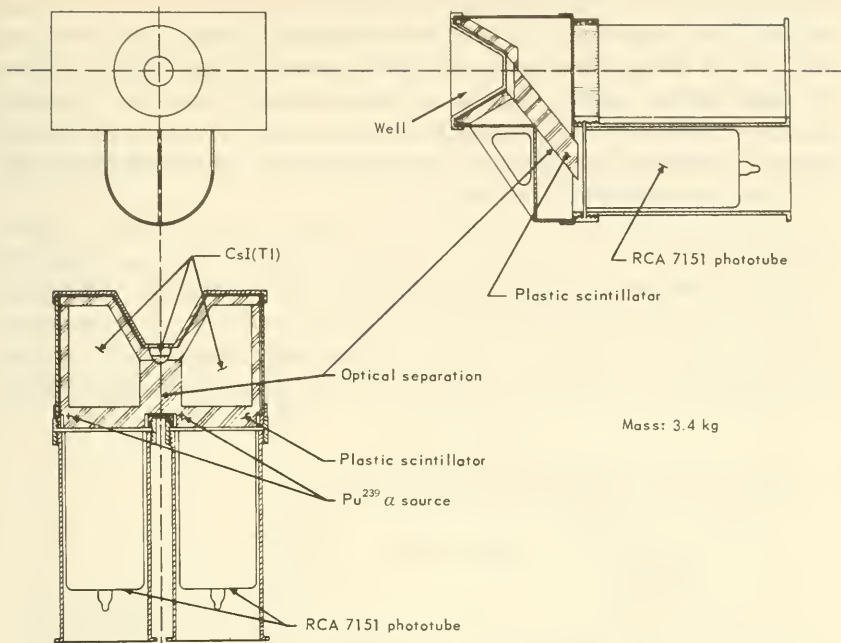
FIGURE 13–27.—The OGO double gamma-ray spectrometer was used to detect positron flux in outer space (ref. 12).

incidence with themselves and the well crystal. Or, less specifically, coincidences between the well crystal and just one of the outer crystal scintillators can also indicate an annihilation reaction. A third method is used to identify nonpenetrating positrons. Two coincident gammas may be detected emerging from annihilations in inert portions of the detector. In the OGO positron detector, all three of these detection modes were employed to search for a positron flux and determine background corrections.

C. Track-Imaging Instruments

Spark Chambers.—The only tracking-imaging satellite instrument presently being applied to the analysis of cosmic rays is the spark chamber (table 13–4). The first type to be flown is a microphone instrument designed by G. W. Hutchinson, at the University of Southampton, for OGO E. This instrument, which is about the size of a coffee mug, consists of a stack of thin, parallel metal foils separated by gas-filled gaps. The passage of an ionizing particle will create a series of sparks between the foils. Sparks at various levels in the chamber will be recorded by several triads of

microphones, one triad to each foil. Each spark will be recorded by all three microphones in the triad, the precise order being a function of where the spark occurred on the circular foil. In effect, the microphone triad forms a sound-ranging system, for, by timing the pulses, the experimenter can trace the track of the particle through the stack of foils, assuming, of course, only one particle has triggered the device.

T. L. Cline and C. E. Fichtel, at Goddard Space Flight Center, have proposed a wire spark chamber for flight on one of the SSS (Small Scientific Satellite) series planned by NASA. The proposed instrument, shown in figure 13–28, consists of 2 adjacent chambers, each containing 32 trays of orthogonal X–Y wires, 128 X and 128 Y wires to a tray, all insulated from one another
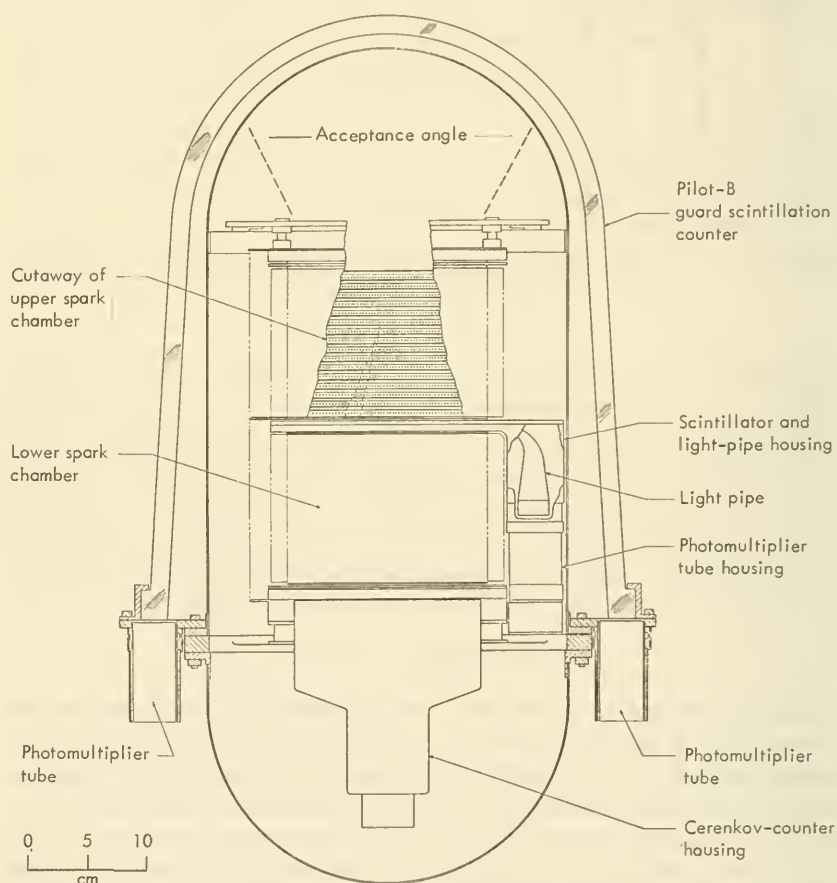
FIGURE 13–28.—Cross section of the Goddard double spark chamber. (Courtesy of T. L. Cline.)

by a gas-filled gap (fig. 13–29). An ionizing particle will cause the formation of sparks between adjacent trays of wire. Instead of employing microphones to locate the positions of the spark at each level, the $X–Y$ coordinates of the spark can be fixed by knowledge of the $X–Y$ wire pairs stimulated by the spark in each tray. Sense wires and ferrite-core memories, similar to those
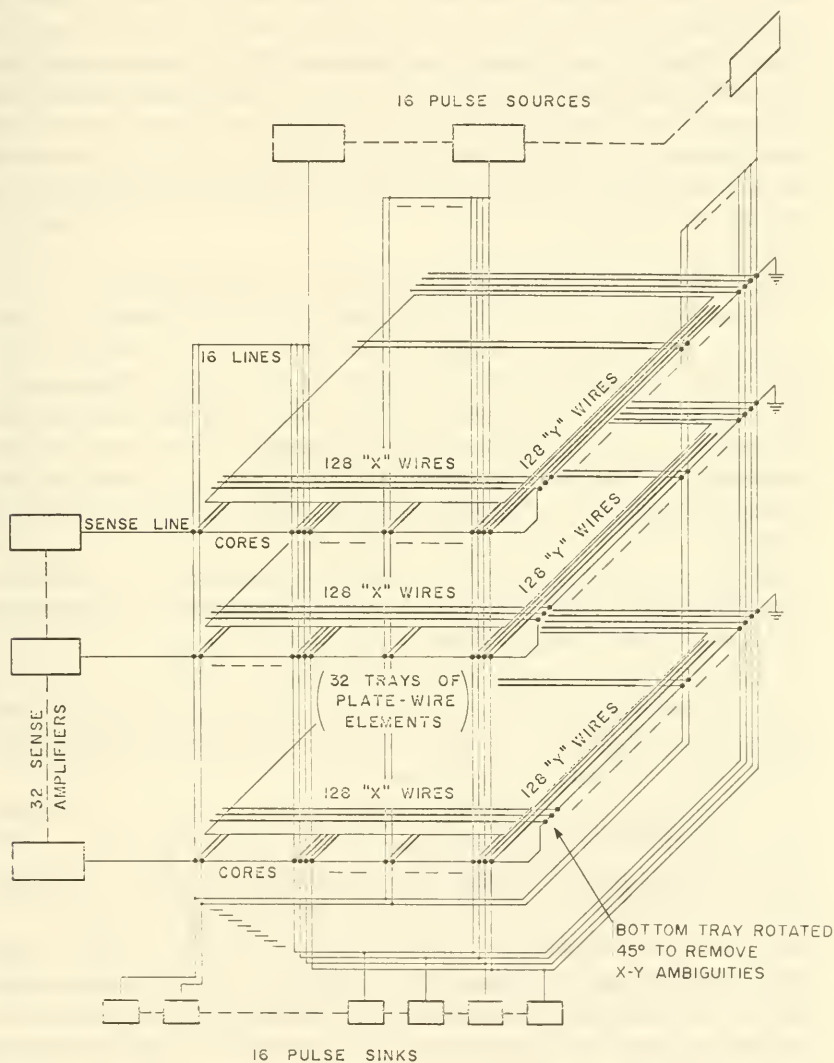
FIGURE 13–29.—Arrangement of wires and wire trays in the Goddard double spark chamber. The beryllium-copper wires are 0.015 centimeter in diameter. The active area of each tray is about 15 x 15 centimeters. (Courtesy of T. L. Cline.)

found in digital computers, record these coordinates and can be read out to the communication subsystem. In addition to the wire arrays, three other counters can be seen in figure 13–28; a dome-shaped guard scintillator, at the top; a thin, central scintillator, center; and the Cerenkov counter, bottom. Two modes can be used to trigger the chamber; i.e., apply high voltages to the wires to stimulate spark production. These modes are termed the CA and $\overline{BCA}$ modes, where the bar indicates anticoincidence. The actual operation and supporting logical circuitry are too complex to describe here, but the essence of the concept—electronic readout of spark coordinates—should be evident from the figures and above discussion. The pulsed output of this type of spark chamber meshes well with PCM telemetry and computer analysis of the results on the ground.

13–4. Active Satellite Experiments in Astronomy

Astronomy is an observational science that depends, almost without exception, upon nature to provide clues about the underlying laws that govern her behavior. Now that the Space Age is here, however, we may assist nature by simulating natural phenomena at times and places of our choosing. Two such "active" experiments that have been proposed involve the creation of artificial meteors and artificial comets with the help of satellite vehicles.

Adelman and Hochstim have suggested the use of satellites as meteor-launching platforms (ref. 13). The great advantages over the observation of natural meteors include:

(1) Selection of time and place of meteor entry into the atmosphere through the use of ground commands to the satellite. Earth-based observers could then make simultaneous measurements with a variety of equipment.

(2) The meteor material, density, mass, and reentry parameters, especially velocity, would be known.

(3) The experiment could be repeated under identical conditions or with variations in the parameters mentioned in (2).

The study performed by Adelman and Hochstim indicates that entry velocities up to 20 km/sec for gram-sized pellets are reasonable, while kilogram masses could be projected at 10 km/sec. A near-polar orbit with a perigee of about 250 kilometers is proposed. So far, no satellites have been assigned to this scientific mission.

In 1961, B. Donn suggested the orbiting of a large mass of ices to simulate an artificial comet (ref. 14). In 1962, P. Swings

elaborated on this suggestion (ref. 15). Ices of water, ammonia, and carbon dioxide, which are postulated to make up much of a comet's mass, could probably survive the vacuum and solar heating in orbit for several days, providing the initial payload orbited weighed about a ton. The artificial comet head would presumably release enough gases so that Earth-based spectrographs and photometers could analyze the radiation received from Sun-stimulated molecules, free radicals, and ionized atoms. Comparisons could then be made with the spectra obtained from natural comets.

Several releases of comet-type materials have already been made at orbital altitudes. Liquid ammonia and water, for example, have been released by high-altitude rockets.[9] The results have been generally disappointing, because the liquids quickly vaporized and formed frozen particles that scattered so much sunlight that the hoped-for reactions could not be observed. Recent proposals, such as the one described in the following paragraph, depend upon the use of ices or gases adsorbed on solids rather than liquids.

One artificial comet experiment is moving toward reality. This experiment, which is directed by N. W. Rosenberg, at the Air Force Cambridge Research Laboratories, anticipates using a Titan 3 to carry about 700 kilograms of material into a 160-kilometer orbit. The payload section of the rocket will be divided into three longitudinal sections, each filled with highly adsorbing granules, such as zeolite, silica, or activated alumina. Adsorbed ammonia, acetylene, and cyanogen will each be segregated in separate compartments. At some point in the orbit, the granules would be jettisoned by command. Sunlight would bake the gases out of the adsorbing materials and stimulate cometlike spectra from them. Ground observers with spectroscopes, filter photometers, etc., would observe the results. No firm launch date has been set for this experiment at this writing.

13–5. Experiments in Relativity and Cosmology

As early as 1956, before the first satellite was even launched, S. F. Singer suggested that satellites could carry superaccurate atomic clocks to check the effect of gravitational potential upon clock speed. If the satellite clock could be compared with an identical Earth-based clock to an accuracy of one part in 10^{11}, the red shift (slowing down) of the satellite clock predicted by the general theory of relativity could be verified or contradicted. This "clock," or "red-shift," experiment was a strong candidate for

---

[9] The well-publicized sodium releases in the upper atmosphere are similar in principle but have no value in cometary research.

satellite payloads prior to 1961. In the early 1960's, several experiments utilizing the Mossbauer effect verified the red shift terrestrially without the need for satellites. Consequently, there is much less urgency for clock experiments today.

This isolated victory of Earth-based research over space research did not noticeably stem the flow of suggestions for satellite relativity experiments. In fact, this area of satellite research is notable for the number of experiment ideas. Some of the more important proposals will be listed in the following paragraphs. It should be emphasized, though, that none of these proposals has yet made much headway in getting satellite-payload space assigned. Undoubtedly, some will eventually be orbited, but priority is a controversial issue.

(1) A satellite-borne gyroscope to measure relativistic precession effects has received considerable attention (refs. 16, 17, 18). In the case of Mercury's orbit, the general theory of relativity predicts a difference in precession of 40 arcseconds per century over Newtonian theory. The various experiments proposed to measure this minute difference depend upon electrostatic or superconducting magnetic gyroscopes to obtain the desired precision. Another feature of interest connected with the gyroscope experiment is the possibility of designing an orbiting payload that is shielded from drag and radiation pressures by a protective orbiting shell. The outer shell keeps the inner satellite centered through a system of transducers and external gas jets (ref. 17).[10] With such shielding from the environment, the inner satellite would be subjected only to gravitational and electromagnetic fields. Presumably, the latter could be shielded out and the gravitational attraction of the outer satellite made symmetrical. Only the Earth's gravitational field would remain, and we would have an ideal environment for the gyroscope experiment.

(2) One of the classic relativity experiments is the measurement of the deflection of starlight by the Sun during an eclipse. Eclipse observations are unfortunately brief and subject to atmospheric distortions. Lillestrand has proposed a special satellite to carry out the same type of experiment in orbit, where distortions are minimized (ref. 19). In this concept, several stars would be tracked simultaneously during an eclipse. While this concept is probably feasible, most scientists are fairly well satisfied that terrestrial observations of this relativistic phenomenon satisfactorily support Einstein's theory.

---

[10] Apparently, this idea was originally suggested by M. Schwartzschild.

(3) If the universal constant of gravitation varies with time in a secular fashion, artificial satellites may help detect such an effect (refs. 20, 21). Two satellites, identical except for their masses, would exhibit different orbital changes if the constant of gravitation did change with time. The satellite-within-a-satellite idea suggested above might be put to good use here to shield out many of the perturbing effects on satellite orbits.

(4) The universal constant of gravitation may also vary with velocity (ref. 21). If it does, the precision tracking of an artificial satellite might detect it.

(5) The relativistic advance of the line of apsides of a satellite might be measured to support (or contradict) the relativity theory. As mentioned in section 4–5, this effect amounts to only a few seconds per year and is virtually submerged in other perturbations. Still, it is a possibility, particularly if applied to an artificial planet, such as a solar satellite.

(6) It is possible that the velocity of light may vary with frequency. Satellites, as distant sources of controlled electromagnetic radiation, could check out this possibility.

(7) Since a scientific satellite is well divorced from earthly perturbations, such as seismic waves, several scientists have proposed that it might serve to detect gravitational waves (ref. 22). Such experiments involve the minute relative displacement of large masses as hypothesized gravitational waves pass by.

(8) Einstein's theories predict that a test body should not fall directly toward the center of a rotating massive body, but rather be deflected to one side in the direction of rotation. Ultimately, satellite-based active experiments might prove or disprove this supposition.

There are many other experiments that have been suggested for checking out Einstein's theories and supporting one or another theory of cosmology. In the latter instance, probably the most important advantage of the satellite is its position of vantage high above the perturbing and absorbing atmosphere. Several of the more conventional astronomical experiments described in sections 13–2 and 13–3 may be more important to cosmology than the relativity experiments just cited. The universal problem with relativity experiments is the almost immeasurably small effects that are predicted. Such small effects are very likely submerged among the many other perturbations that a satellite is subject to. Despite the fact that the substantiation or demise of the various theories of relativity and cosmology is vital to our concept of the universe, satellite experiments in this realm are marked "Low

Priority." The experiments are either too difficult or can be carried out better on the Earth.

References

1. DAVIS, R. J.: Project Celescope. Smithsonian Astrophys. Observ. Special Rept. 110, 1962.

2. GUNDERSEN, N. A.: The Princeton Experiment Package for OAO–C. Unmanned Spacecraft Meeting. AIAA Pub. CP–12, 1965.

3. ALEXANDER, J. K.; AND STONE, R. H.: A Satellite System for Radio-Astronomical Measurements at Low Frequencies. Ann. Astrophys., vol. 27, Nov. 1964, p. 837. (Also NASA TM X–55089, 1964.)

4. SCHWED, P., ET AL.: Satellite-Borne Instrumentation for Observing Flux of Heavy Primary Cosmic Radiation. J. Franklin Inst., vol. 271, Apr. 1961, p. 275. (Also NASA CR–58203, 1963.)

5. DESAI, U. D.; VAN ALLEN, R. L.; AND PORRECA, G.: Explorer XII Satellite Instrumentation for the Study of the Energy Spectrum of Cosmic Rays. NASA TN D–1698, 1963.

6. FROST, K. J.; AND ROTHE, E. D.: A Detector for Low Energy Gamma-Ray Astronomy Experiments. NASA TN D–1693, 1963.

7. KRAUSHAAR, W., ET AL.: Explorer XI Experiment on Cosmic Rays. Astrophys. J., vol. 141, Apr. 1, 1965, p. 845.

8. LUDWIG, G. H.; AND MCDONALD, F. B.: Cosmic Ray Experiments for Explorer XII and the Orbiting Geophysical Observatory. In Space Research III, W. Priester, ed., John Wiley & Sons, Inc., 1963.

9. SMITH, R. V.; REAGAN, J. B.; AND ALBER, R. A.: Use of Scintillation Counters for Space Radiation. IRE Trans., NS–9, June 1962, p. 386.

10. LOCKWOOD, J. A.; AND FRILING, L. A.: Design of a Neutron Monitor for Measurements in Space. NASA CR–59403, 1964.

11. TRAINOR, J. H.; AND LOCKWOOD, J. A.: Neutron Albedo Measurements on Polar Orbiting Satellites. J. Geophys. Res., vol. 69, Aug. 1, 1964, p. 3115.

12. CLINE, T. L.; AND SERLEMITSOS, P.: A Double Gamma-Ray Spectrometer to Search for Positrons in Space. NASA TN D–1464, 1962.

13. ADELMAN, F. L.; AND HOCHSTIM, A. R.: Satellite-Launched Artificial Meteors. Paper presented at the 16th Int. Astronaut. Cong., 1965.

14. DONN, B.: Coma Formation and an Artificial Comet Experiment. Astron. J., vol. 66, Sept. 1961, p. 282.

15. SWINGS, P.: Possible Contributions of Space Experiments to Cometary Physics. Smithsonian Astrophys. Observ. Special Rept. 111, 1962.

16. CANNON, R. H.: Requirements and Design for a Special Gyro for Measuring General Relativity Effects From an Astronomical Satellite. Paper presented at the Symposium on Gyrodynamics (Celerina, Switzerland), 1962.

17. LANGE, B.: Feasibility Study for a Purely Gravitational Orbit Satellite. IAS paper 62–111, 1962.

18. PALAMARA, R. D.: Synthesis of a Simplified Orbiting General-Relativity Experiment. AIAA paper 65–36, 1965.

19. LILLESTRAND, R. L.: Test of Theory of Relativity by Measurement of Gravitational Light Deflection. Adv. Astronaut. Sci., vol. 6, 1960, p. 871.

20. CLEMENCE, G. M.: Controlled Experiments in Celestial Mechanics. Astronom. J., vol. 65, June 1960, p. 272.
21. DICKE, R. H.; AND PEEBLES, P. J.: Gravitation and Space Science. Space Sci. Rev., vol. 4, June 1965, p. 419.
22. DEWITT, B. S.: Gravity. *In* Advances in Space Science and Technology, vol. 6, F. I. Ordway, ed., Academic Press, 1964.

Chapter 14

BIOLOGICAL EXPERIMENTS ON
SCIENTIFIC SATELLITES

14-1. Prolog

Most of the satellite experiments we send out into space measure physical phenomena, such as cosmic rays, starlight, magnetic fields, and micrometeoroids. In this chapter, a major change of direction occurs with the introduction of biological experiments, where living objects (specimens) are deliberately propelled into space to assess the effects of this "unnatural" environment and to employ the space environment as a unique research tool. In the language of this book, these are "active" experiments, in that we intentionally vary experimental parameters, such as the force of gravity, radiation levels, and stimuli that affect an organism's rhythm, and watch what happens. In contrast, most physical space experiments are "passive." As the material that follows will demonstrate, experiment philosophy and instrumentation are quite different from those employed in the physical sciences.

Actually, we deal here with a very restricted portion of satellite biology. The Gemini, Mercury, and Apollo programs have been excluded in this book as the emphasis is on the unmanned scientific satellite, although manned satellites *do* carry biological experiments. Therefore, "space medicine," a term used almost exclusively in connection with manned spaceflight, is not a part of this discussion. The discipline of bioastronautics, which according to common usage deals mainly with life support and the pertinent engineering aspects of spacecraft systems, is included in part in this chapter because an experiment's organisms must be kept alive. The subject of exobiology, which relates primarily to the discovery and study of extraterrestrial life, is not dealt with in this chapter. With several major segments of space biology thus eliminated, there still remains much stimulating and scientifically productive

grist for this chapter, specifically, the study of the effects of the space environments on living cells, plants, primates—the entire spectrum of Earth life.

From the phenomenological standpoint, satellite biological experiments are classified as:

(1) Weightlessness, or zero-g, experiments

(2) Radiation-weightlessness experiments

(3) Biological- or circadian-rhythm experiments

The sections of this chapter that survey satellite experiments are organized in this fashion; so are the summary tables that list the various experiments.

What properties of cells, plants, animals, and other organisms can be easily measured remotely and still have biological significance? A survey of the satellite biological experiments already performed and those planned for NASA's Biosatellite program reveals that most require visual observation or measurements of the shapes and sizes of the specimens, either during the flight itself or after recovery. Sometimes, prolonged observation after flight is needed to assess possible delayed reactions. Typical biological parameters are growth rate; change in shape (as in plants); color changes; the appearance of abnormalities, cell counts; and, in the case of animals, activity and problem-solving ability. Added to these parameters, which are so radically different from those of the previous chapters, are the more easily handled output signals from electrodes embedded in animals and automated chemical-analysis (urinalysis) equipment. Obviously, a great deal of ingenuity must be exercised if biological measurements are to be made in space and conveyed to the experimenter on the ground.

How will these things be accomplished? The microscopes, behavior-testing equipment, and other sophisticated accouterments of the terrestrial biological laboratory cannot be conveniently carried into orbit. Weight, volume, and bit rates are limited. The relatively small spacecraft in the Biosatellite series preclude even one television camera to make the visual observations so typical of biology. There are several ways out, however.

(1) Observations may be made on specimens after recovery. Microscopic studies and the tracing of mutations induced by radiation under zero-g conditions fall in this category. So do chemical analyses of storable animal wastes.

(2) Specimens may be killed upon command and preserved. In this way, one could obtain a series of "snapshots" of plant growth

and cell development in time, for example. This procedure is termed "fixation."

(3) The specimens can be photographed in flight and the film developed upon recovery. Tremendous amounts of information (in terms of bits) can be recorded in this way without taxing the communication subsystem.

(4) Physiological data, such as blood pressure, respiration rate, and brain waves from primates and lower animals, can be transmitted to the ground in real time, either in analog or digital form.

Considering the frequent desire for visual observations in satellite biology, one might wonder whether experiments might be carried out more conveniently on the manned orbiting laboratories planned for the future. There seems little question that the more complex experiments, especially those requiring much equipment manipulation and calibration, will be better done on manned craft (see chapter 1). Unmanned satellites, however, retain several advantages: they are available now; they can stay up for much longer periods of time than manned satellites; they can carry radiation sources without endangering man; and biological experiments can enjoy top priority and full use of the data link. Intuitively, one might expect experiments on unmanned satellites to be cheaper per experiment. This may be so, but there are no thorough studies that conclusively prove this point at the present time.

One of the major satellite-design problems discussed in chapter 9 was environment control. Since biological satellites carry cargo more sensitive than, say, magnetometers or proportional counters, the spacecraft designer finds the limits of operating temperature more restricted. In another example, g-levels must be kept below 10^{-5} 95 percent of the time on the Biosatellite series. Shock levels during launch and recovery should not damage specimens or prejudice the experiment. Finally, the term "environment control" must be expanded to include life support—that is, the provision of a breathable atmosphere, sanitary facilities, food, and water. These extra dimensions of the environment-control problem will be treated briefly in the specific experiment descriptions that follow.

As a conclusion to this introduction, let us put a historical perspective on satellite biological experimentation. The first biological satellite was, of course, Sputnik 2, launched in 1957 (ref. 1). The dog orbited on this flight caused quite a sensation at the time. The first American biological experimentation in satellites came with the U.S. Air Force Discoverer program, which commenced in

1959.[1] Although the primary purpose of the Discoverers was proving out satellite technology for military purposes, several biological experiments were carried out, mainly by scientists at the USAF Aerospace Medical Center, Brooks Air Force Base, Tex. (ref. 2). The first biological specimens recovered from orbit (by any country) were those in the Discoverer-13 capsule, which returned to Earth on August 11, 1960. Since completion of the Discoverer program in 1962, there have been many manned space flights in the Mercury and Gemini programs, but only a few other biological experiments; viz, Bios I in 1961. The three-orbit flight of the chimpanzee Enos, in November 1961, on Mercury-Atlas 5, was a prelude to the manned Mercury missions, though we can also consider it a primate experiment similar to that intended for Biosatellite D.[2] Undoubtedly, other biological experiments were flown on military satellites and ICBM's during the 4-year lull in U.S. satellite biology. Of course, Russia has also orbited many biological experiments; viz, Cosmos 110, with two dogs, in 1966. The tempo is now increasing rapidly. The first NASA Biosatellite was launched in December 1966. It presages a systematic program of satellite research that emphasizes not the solution of engineering problems connected with manned flights but, rather, basic biological research; in other words, how weightlessness, weightlessness plus radiation, and different rhythms affect life processes.

14–2.   Weightlessness and Zero-g Experiments

Several biological phenomena are thought to be affected by changes in gravity—embryonic development, plant development, and metabolic activity in mammals, to cite a few examples. The scientific satellite offers an excellent laboratory for gravity experiments, providing, of course, meaningful experimental results can be conveyed to the experimenter. In this section, one or more representative experiments from each of the three categories cited above will be described. The experiments selected are also representative of three of the four major techniques employed in getting biological data back to Earth: namely, fixation and postrecovery analysis, photography, and biotelemetry.

Biosatellite Experiment, Development of Frog Eggs.—A longrecognized biological phenomenon is the inducement of abnormal embryonic development in frogs by changing the embryo's orien-

---

[1] There were many rocket experiments before this date.
[2] See appendix for Biosatellite descriptions. NASA's Biosatellite Program is managed by Ames Research Center. Ames provided all photographs in this chapter.

tation during early stages of development. Inversion of the embryo during the first cell division, for example, produces twins or abnormal frogs with, say, two tails. What would the near-zero-g environment of a satellite do? To find out, fertilized frog eggs, which are kept cold after launch, will be allowed to develop on Biosatellite A/B. As the embryos develop, they will be automatically fixed (killed and preserved) with formalin at programed intervals. The killed embryos will show the sequence of development when studied after recovery.

The frog-egg experiment package consists of an assembly of 16 Lucite blocks, each containing a cylindrical chamber. Each chamber is divided into two parts by a Lucite piston and an O-ring. One side contains the fertilized frog eggs; the other, the formalin. The operation of the pistons is controlled by a motor-driven cam that forces formalin into the frog-egg chambers in sequence. Several of the Lucite blocks contain thermistors, which relay temperature reading to the experimenter via the telemetry link. No separate heating or cooling system is provided. The location of this experiment within the satellite is shown in figure 14–1.

Biosatellite Experiment, Liminal Angle in the Pepper Plant.— The goal of this experiment is the photography of the liminal angle
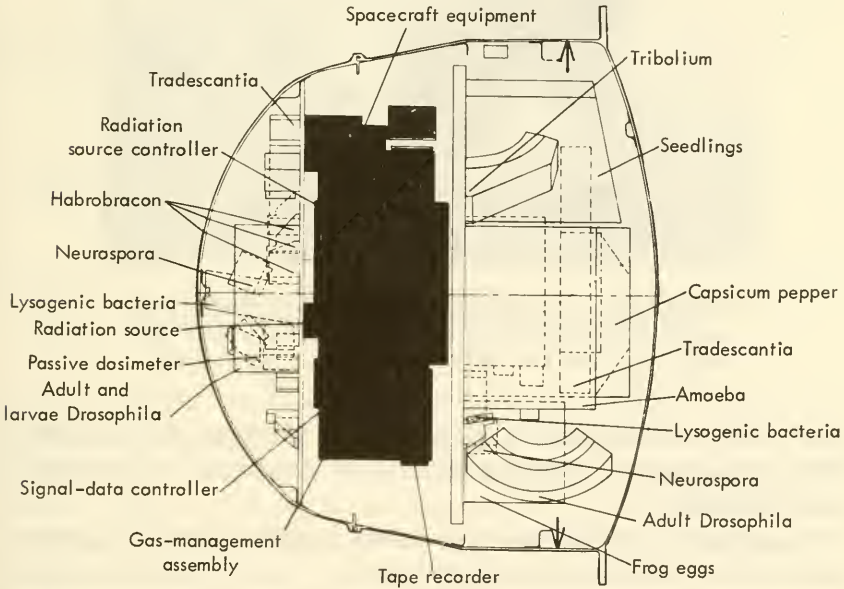
Figure 14–1.—Diagram of the Biosatellite-A/B experiment capsule, showing the radiation experiments (forward) and the nonradiation experiments (aft).

(the angle between stalk and leaf) of a higher-order plant under weightless condition. Normally, this angle is controlled by geotropic response, as modified by several physiological conditions. In this experiment, the cotyledons and shoots will be removed from pepper plants that are about 5½ weeks old; only the first two leaves will be retained. Four plants will be orbited, each in a separate container (fig. 14–2). Through the use of mirrors, the
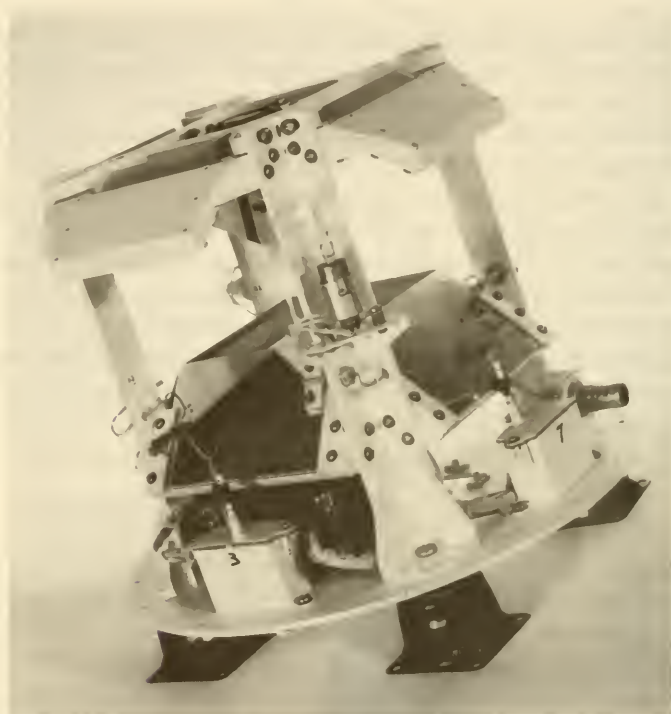
FIGURE 14–2.—Prototype pepper-plant package. Camera is in the center. mirrors are at the top and sides, and one of the two lights is on the corner support.

front and top views of the plant will be photographed by time-lapse photography. Photographs will be developed and analyzed upon recovery.

The pepper-plant package (fig. 14–2) is built around the special camera shown in the center. Top and side views of all four plants are recorded simultaneously on one piece of film. Pictures will be taken every 10 minutes. The two lights are turned on only during actual picture taking. The package is open to the spacecraft in-

terior environment. Thermistors provide the experimenter with telemetered temperature data.

Biosatellite Experiment, Primate Studies.—While some primates have flown in satellites, viz, Enos, on Mercury MA–5, and undoubtedly some Russian counterparts, satellite studies of mammals have so far been largely confined to dogs. The Russian Sputnik series contained many flights with dogs (table 14–1). But, like most previous biological experiments in space, these were usually proof-of-principle tests in manned flight programs [3] (ref. 3). The first primate experiments of a primarily scientific nature are scheduled for Biosatellite D/F (fig. 14–3).

Blood pressure sensor

Gas–management assembly

Heparin pump

Heparin tank

Urine actuator
Urine solenoid valve

Feces container
Disinfectant reservoir

Urine collector

Psychomotor tester

Psychometer logic/controller

Spacecraft equipment

Pellet dispenser assembly

Feces solenoid valve

Primate life–support controller

Camera controller
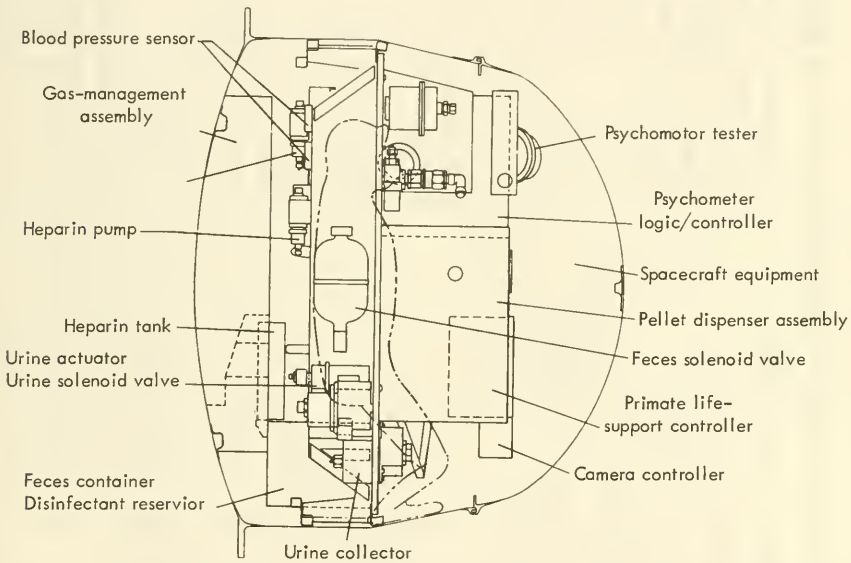
FIGURE 14–3.—Diagram of the Biosatellite-D/F experiment capsule, showing an outline of the primate and couch.

The principal objective of Biosatellite, Experiment P–1001 is the monitoring of the brain functions, primate performance, and cardiovascular and metabolic functions of a single pigtailed monkey under prolonged weightlessness. Biosatellite D/F is scheduled for 30 days in orbit, considerably longer than any manned flight to date, so that results may be useful to the manned programs as well as to general biology.

---

[3] The recent Cosmos 110 flight included a great deal of purely biological instrumentation.

Table 14–1.—*Weightlessness and Zero-g Experiments and Experimenters*

Biosatellite A/B	Finn, J. C./N. Amer. Aviation	Liminal angle in the pepper plant. In-flight photography in 3 dimensions. Three plants.
	Gray, S. W./Emory U	Orientation of roots and shoots in wheat seedlings. Growth progress recorded by fixation.
	Price, R. W./U. Colorado	Nutrition and growth in amoeba (*Pelomyxa*). Terrestrial analysis only. Fixation in orbit.
	Young, R. S./Ames	Development of frog eggs. Eggs fertilized and fixed on command. Analysis made after recovery.
	Lyon, C. J./Dartmouth College	Emergence of wheat seedlings. Fixation in flight and postrecovery analysis.
	Conrad, H. M./N. Amer. Aviation	Orientation of root and shoot of corn. Growth of seedlings photographed in flight. Postrecovery analysis.
Biosatellite C/E	Brown, A. H./U. Pa	Plant morphogenesis in a leafy plant. Stereo and time-lapse camera. Postrecovery analysis.
	Montgomery, P. O'B./U. Tex	Human liver cells in tissue culture. Time-lapse photography of cell mitotic cycles.
	Pitts, G. C./U. Va	Gross body composition and metabolism in rats. Activity, food, and oxygen consumption recorded.
Biosatellite D/F	Adey, W. R./U. Calif	Central nervous system, cardiovascular, and metabolic studies of primates. (See text.)
	Mack, P. B./Tex. Women's College	Loss of calcium in primates. Postrecovery bone densitometry, biochemical studies, excreta analysis.
Discoverer series	/USAF	Various specimens on a noninterference basis.
Mercury MA–5	/NASA	Primate flight.
Cosmos series	/	Dogs, primates, and many other specimens have been flown on Russian spacecraft. Few details are available.
Sputnik series		
Vostok series		
Voskhod series		

Numerous physiological functions will be telemetered during this flight. They include electromyographs, electrocardiographs, blood pressure at various points, electroencephalographs, psychomotor testing, brain temperature, and galvanic skin resistance, which will be used to study the sleep-wakefulness cycles, the cardiovascular function, the depth of sleep, and the altered states of consciousness likely to be associated with diminished attention span. Surface and deep electrodes will be implanted in the brain of the monkey to make the brain measurements. The animal will also be trained in such a way that simple behavioral tests (discrimination and motor coordination) can be carried out in flight. Experiment P–1062, consisting of an investigation of bone-density changes in various parts of the monkey skeleton because of weightlessness, will be carried out with the same animal. These measurements will be performed before and after flight, using bone X-ray densitometry.

The monkey will be strapped to a couch similar to those used by the astronauts (fig. 14–4). The pressurized capsule and the abundance of supporting equipments are illustrated in figure 14–3. The environment-control system (fig. 14–5) will provide sea-level atmosphere of 80 percent nitrogen and 20 percent oxygen. A heat exchanger will keep the air temperature at about $24° \pm 3°$ C, and through its control of the dewpoint will keep the relative humidity in the 40- to 70-percent range. Lithium-hydroxide absorbers will keep the CO_2 level below 1 percent. Power for the satellite is generated by a hydrogen-oxygen fuel cell, which also provides drinking water as a byproduct.

14–3.   Weightlessness-Radiation Experiments

In the prolog to this chapter, it was mentioned that the Air Force satellites in the Discoverer series and other military vehicles carried many biological specimens into space to assess the effects of radiation on life processes (refs. 2, 5). Much of the interest in these flights centered around the hazards of space radiation to manned flight. The Biosatellite experiments listed in table 14–2, on the other hand, are oriented toward finding out just what happens when organisms are exposed simultaneously to weightlessness and a strong radiation field. Both weightlessness and radiation environments can be created separately, making it possible to discern cross-coupling between the effects, if it exists.

Only Biosatellite A/B will be employed for radiation experiments. Since the orbit of this satellite will be below the Van Allen radiation zone, the experiments normally would receive doses of
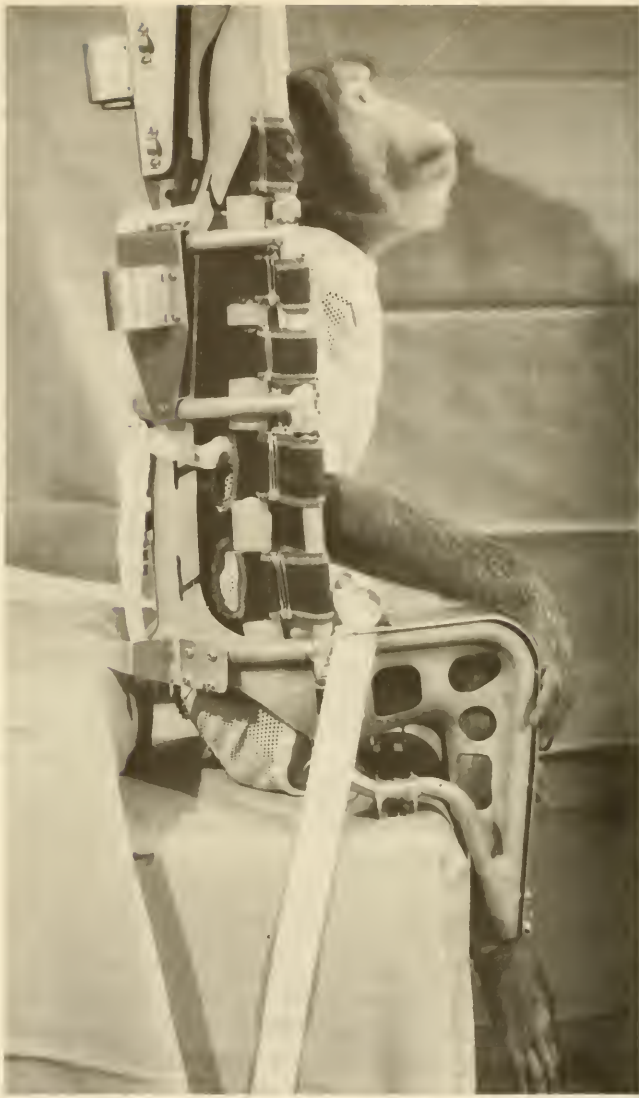
FIGURE 14–4.—Side view of the primate couch and restraint for experiments on Biosatellite D/F.

less than 1.0 rad, considerably less than that needed. To provide a larger known amount of radiation, Sr^{85} (providing a 1.33-curie source of radioactivity) will be mounted in the forward portion of the satellite capsule (figs. 14–1 and 14–6). Depending on the location of the experiments within the capsule, the radioactive
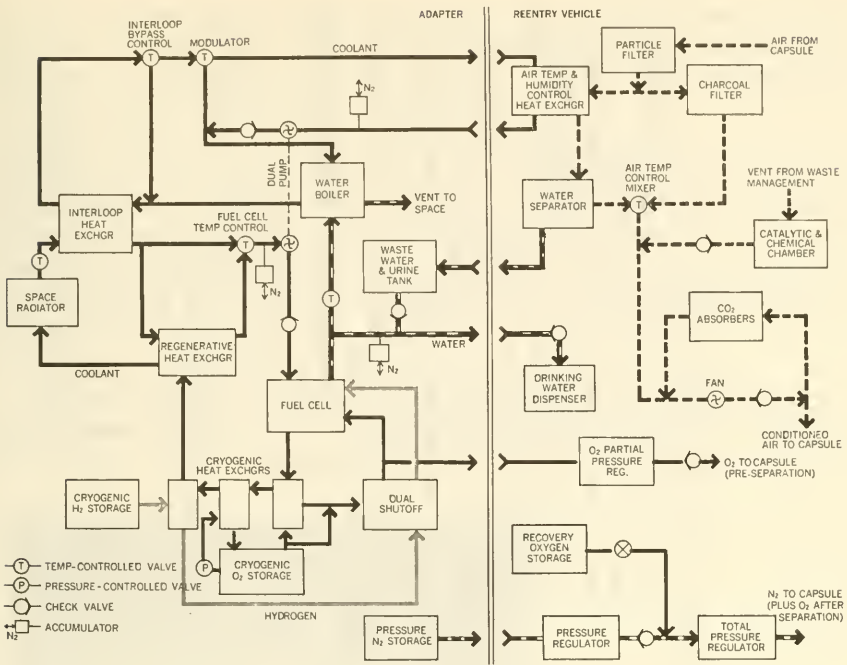
FIGURE 14–5.—Preliminary block diagram of the capsule environment-control subsystem for Biosatellite D/F (ref. 4).
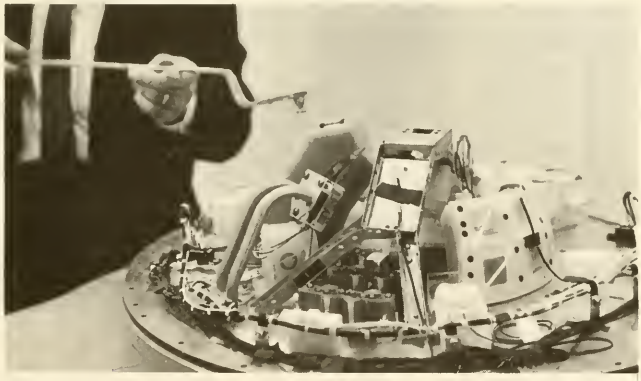
FIGURE 14–6.—Inserting the Sr[85] gamma source into holder on mockup of Biosatellite A/B.

source will provide them with doses of 0.513-MeV gammas between 200 and 5000 rads.

One thing that all the weightlessness-radiation experiments listed in table 14–2 have in common is the requirement for post-

TABLE 14-2.—*Weightlessness-Plus-Radiation Experiments and Experimenters*

Biosatellite A/B	De Serres, F. J./Oak Ridge Nat. Lab	Cellular inactivation and mutation in mold spores (*Neurospora*). Sr85 source. Postrecovery analysis.
	Slater, J. V./U. Calif	Effects on embryonic development of flour beetles (*Tribolium*). Postrecovery study of adults from irradiated pupae.
	Von Borstel, R. C./Oak Ridge Nat. Lab	Chromosome translocations in wasps (*Habrobracon*). Postflight mating and studies of offspring.
	Sparrow, A. H./Brookhaven Nat. Lab	Somatic mutations in blue-flowering plant (*Tradescantia*). Postflight observation of color changes.
	Mattoni, R./N. Amer. Aviation	Effects on proliferation of viruses in slow-growing bacteria (*E. coli*). Postrecovery analysis.
	Altenburg, E./Tex. Medical Center	Genetic changes in mature germ cells of adult *Drosophila*. Postrecovery analysis only.
	Oster, I./Cancer Res. Inst	Somatic damage to *Drosophila* larvae. Postrecovery study of chromosome damage.
Discoverer series	—/USAF	Various specimens on a noninterference basis.
Cosmos series		
Sputnik series	—/	Probably as many as 50 different species have been orbited in the ambitious Russian programs.
Vostok series		
Voskhod series		

recovery analysis. Generally, the experiments are concerned with genetic damage that either cannot be assessed easily in space or will not be evident until after recovery. Two typical experiments in this category are sketched briefly below.

Biosatellite Experiment, Embryonic Development of Flour Beetles.—In this experiment, approximately 2000 larvae of the flour beetle *Tribolium* will be exposed to 1200 rads and, of course, to zero gravity, for 3 days on Biosatellite A/B. After recovery, the larvae will be allowed to change into adults, which will then be examined for wing abnormalities. Two experiment packages will be flown in the same spacecraft; one of these will not be irradiated, for purposes of control.

Each flour-beetle experiment package consists of a polypropylene frame, a thermostatically controlled strip heater, and foam-type insulating materials (fig. 14–7). Three compartments in

FIGURE 14–7.—Loading flour-beetle larvae (*Tribolium*) into Biosatellite-A/B experiment package. Wires are for strip heaters.

each frame are loaded with larvae and flour. Front and back covers are made of Millipore filter material to permit the satellite atmosphere to diffuse to the larvae. A thermistor measures the internal package temperature. Lithium-fluoride crystals and a film badge will be included to measure the actual radiation doses received by the beetle larvae.

Biosatellite Experiment, Genetic Changes in Drosophila.—The fruit fly *Drosophila* has a long and distinguished record in genetic

research. In Biosatellite A/B, approximately 1000 recently mated
adult females will be placed in each of two experiment packages,
one of which will be exposed to about 2000 rads and weightlessness
during the 3-day flight. For purposes of control, the second pack-
age will not be irradiated. Postflight generations will be studied
for genetic damage to both maternal and paternal reproductive
cells.

Each of the two experiment packages holds eight cubical, poly-
propylene modules which contain the flies and agar nutrient (fig.
14–8). The modules are opened to the satellite atmosphere just

FIGURE 14–8.—Assembling
one of the two *Drosoph-
ila* packages to be
flown on Biosatellite
A/B.   Each package
has eight cubical
modules holding flies
and agar nutrient.

enough to provide sufficient air for the flies but not enough to dry
out the agar. Each experiment package is instrumented with a
thermistor for temperature data and a film badge and lithium-
fluoride crystals for radiation dosimetry.

14–4.   Biological-Rhythm Experiments

Outside of the observations on the astronauts, little satellite
data have been acquired concerning biological rhythms in animals
that have been isolated from the 24-hour cycle that normally molds
biological functions on the Earth's surface. The following Bio-
satellite experiment is the only one planned in this category.

Biosatellite Experiment, Metabolic Rhythms in Mammals.—In
this experiment (by F. Halberg, Univ. of Minn.) eight adult fe-
male rats will be instrumented to provide body-temperature and
gross-body-activity data to the telemetry system. Flight will be
on Biosatellite C/E, with a planned time in orbit of 21 days. Upon

recovery, six of the rats will be sacrificed for gross-body-composition studies, in connection with the Biosatellite experiment with rats by G. C. Pitts. The remaining two rats will be studied for about a month to see what effects the flight had upon their biological rhythms.

During the flight, the lighting in the satellite will be varied in intensity and period in an attempt to alter rhythms in the rats. Another interesting feature of the experiment is the implantation of a miniature transmitter and battery on each rat. The changes in the signal picked up by sensors on the satellite itself are indicative of gross body activity and body temperature.

The rat "house" is pie-shaped and about 66 centimeters in diameter and 30 centimeters high, as illustrated in figure 14–9. The
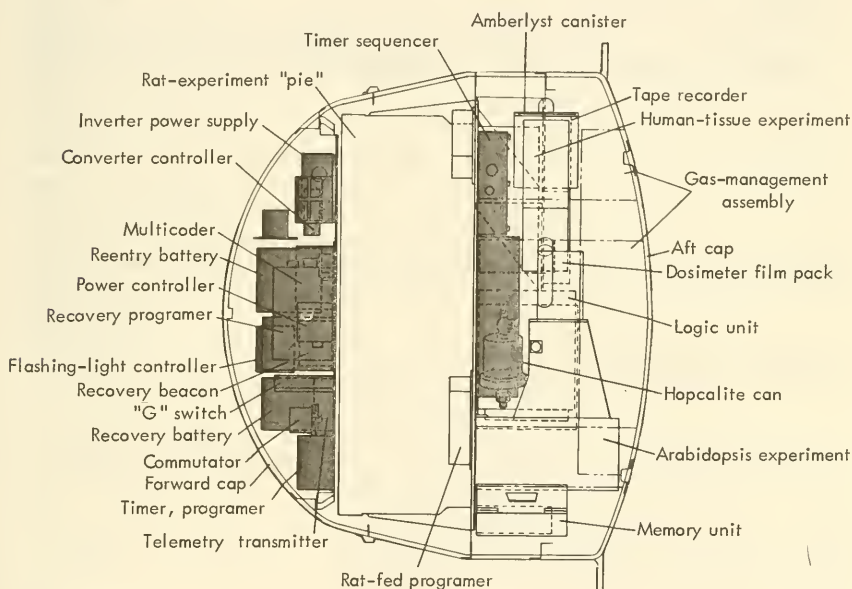
FIGURE 14–9.—Diagram of the Biosatellite-C/E experiment capsule. The rat experiments are located in the central "pie."

center of the assembly is reserved for the feeding mechanism and canisters containing liquid food. Each rat has a separate section of the remainder of the "pie." A total of 35 measurements is obtained every 5 minutes. These include:

(1) Body temperature of each rat via the implanted transmitter
(2) Gross activity over a 5-minute period
(3) Amount of food dispensed to each rat over a 5-minute period

    (4)　Light status in each cage

    (5)　Three representative rat-cage air temperatures

These data are stored in the satellite's memory core and then read out when over a STADAN station.

References

1.　ANTIPOV, V. V., ET AL.: Some Results of Medical and Biological Investigations in the Second and Third Satellites. *In* Problems of Space Biology, vol. 1, N. M. Sisakyan, ed., NASA TT F–174, 1963.

2.　PRINCE, J. E., ED.: Biologic Systems of Discoverer Satellites. USAF School of Aerospace Med., Rep. 62–62, 1962.

3.　GAZENKO, O. G.; YAZDOVSKIY, V. I.; AND CHERNIGOVSKIY, V. N.: Medical and Biological Investigations Carried Out on Soviet Artificial Satellites. *In* Problems of Space Biology, vol. 1, N. M. Sisakyan, ed., NASA TT F–174, 1963.

4.　STAMBLER, I.: Bioscience in Orbit. Space/Aero., vol. 44, July 1965, p. 46.

5.　CRAWFORD, G. W., ET AL.: Radiological Experiments in Discoverer Satellites. *In* Lectures in Aerospace Medicine, USAF, Brooks AF Base, 1961.

GENERAL BIBLIOGRAPHY

The lengthy scientific-satellite bibliography that follows lists most of the key engineering reports, through mid-1966, that have not already been cited in the chapter and appendix references of this book. Reports not accessible to the general public in the open literature or through the U.S. Government have been excluded. Furthermore, except for major review articles and reports featuring satellite and instrument descriptions, the large body of literature dealing with scientific results has also been excluded.

Entries are arranged according to the chapter to which they most specifically pertain, except that the bibliographic listings for chapter 1 contain, in addition, background material generally pertinent to the entire book. The references are arranged alphabetically by personal author or, if no author is cited, following the designation "Anon." A final section cites the major sources used in compiling the descriptions of scientific satellites in the appendix—sources not already listed in the appendix references.

Many of the pertinent reports were generated by U.S. Government agencies and their contractors. Understandably, those produced by NASA are particularly important. They are published in several series, as indicated by the following key:

NASA TR R–000	Technical reports considered important, complete, and a lasting contribution to existing knowledge.
NASA TN D–0000	Technical notes, less broad in scope.
NASA TM X–00000	Technical memorandums, receiving limited distribution because of their preliminary nature and various other reasons.
NASA CR–00000	Contractor reports generated under a NASA contract or grant and released under NASA auspices.
NASA TT F–000	Technical translations of important foreign literature.
NASA SP–000	Special publications, such as conference proceedings, data compilations, etc.
X–000–00–000	A series of internal technical reports generated at NASA's Goddard Space Flight Center. Many of these ultimately reach the open literature, but until they do, they are available only from the author. These are referenced only where they are vital to the book.

NASA reports, except for those in the last category, are available to NASA contractors, grantees, subcontractors, and consultants through the NASA

Scientific and Technical Information Facility, Post Office Box 33, College Park, Md., 20740. Others may obtain them through the Clearinghouse for Federal Scientific and Technical Information, Port Royal Road, Springfield, Va., 22151.

Reports generated by the Department of Defense (DOD) and its contractors are handled by the Defense Documentation Center (DDC), Cameron Station, Alexandria, Va., 22314. Such reports are identified by AD numbers; viz, AD–00000. (AD stands for ASTIA Document. ASTIA, the Armed Services Technical Information Agency, was the predecessor of DDC.) AD reports are available to DOD contractors through DDC and the Federal Clearinghouse.

Three series of abstracts were particularly valuable in writing this book:

> STAR (Scientific and Technical Aerospace Reports), a semimonthly abstract journal published by NASA.
>
> International Aerospace Abstracts, published semimonthly by the American Institute of Aeronautics & Astronautics, 750 Third Ave., New York, N.Y., 10017.
>
> Technical Abstract Bulletin, published semimonthly by DDC.

Chapter 1

AIKIN, A. C.; AND BAUER, S. J.: The Ionosphere. *In* Introduction to Space Science, W. S. Hess, ed., Gordon & Breach, 1965.

AL'PERT, YA. L.; GUREVICH, A. V.; AND PITAEVSKII, L. P.: Space Physics with Artificial Satellites. Consultants Bureau (New York), 1965.

ANON.: AIAA Unmanned Spacecraft Meeting. Pub. CP–12, Am. Inst. of Aeronaut. & Astronaut., 1965.

ANON.: Conference on Artificial Satellites. Virginia Polytechnic Inst., NASA CR–60131, 1963.

ANON.: The Observatory Generation of Satellites. NASA SP–30, 1963.

ANON.: Opportunities for Participation in Space Flight Investigations. Semiannual pub., Office of Space Science and Applications, NASA, 1965.

ANON.: Proceedings of the NASA-University Conference on the Science and Technology of Space Exploration. Vols. 1 and 2. NASA SP–11, 1962.

ANON.: A Review of Space Research. Pub. No. 1079, National Academy of Sciences—National Research Council, 1962.

ANON.: Space Research, Directions for the Future. National Academy of Sciences—National Research Council, 1966.

ANON.: United States Space Science Program. An annual report to COSPAR. National Academy of Sciences—National Research Council, 1965.

ATHAY, R. G.: Astronautical Investigations of the Sun. *In* Advances in Space Science and Technology, vol. 5, F. I. Ordway, ed., Academic Press, 1963.

AUBINIERE, R.: The French National Space Programme. Spaceflight, vol. 6, 1964, p. 146.

BAKER, M. B.: Geomagnetically Trapped Radiation. AIAA J., vol. 3, Sept. 1965, p. 1569.

BELTON, M. J. S.: Dynamics of Interplanetary Dust. Science, vol. 151, Jan. 7, 1966, p. 35.

BERKNER, L. V.; AND ODISHAW, H.: Science in Space. McGraw-Hill Book Co., Inc., 1961.

BERMAN, A. I.: The Physical Principles of Astronautics. John Wiley & Sons, Inc., 1961.

BJORGE, S.: Scientific Satellites. ASTIA Bibliography, AD 290800, 1962.

BLANCO, V. M.; AND MCCUSKEY, S. W.: Basic Physics of the Solar System. Addison-Wesley Publishing Co., 1961.

BLASINGAME, B. P.: Astronautics. McGraw-Hill Book Co., Inc., 1964.

BOURDEAU, R. E., ET AL.: Experimental Evidence for the Presence of Helium Ions Based on Explorer VIII Satellite Data. J. Geophys. Res., vol. 67, Feb. 1962, p. 467. (Also: NASA TN D–1346, 1962.)

BOWHILL, S. A.: The Ionosphere. Astronautics, vol. 7, Oct. 1962, p. 80.

BOYD, R. L. F.: Space Research by Rocket and Satellite. Harper & Bros., 1960.

BRADFORD, D. C.; AND DYCUS, R. D.: A Review of the Meteoroid Environment in Cis-Lunar Space and on the Lunar Surface. AIAA Preprint 64–63, 1964.

BRANDT, J. C.; AND HODGE, P. W.: Solar System Astrophysics. McGraw-Hill Book Co., Inc., 1964.

BURBANK, P. B.; COUR-PALAIS, B. G.; AND MCALLUM, W. E.: A Meteoroid Environment for Near-Earth, Cis-Lunar, and Near-Lunar Operations. NASA TN D–2747, 1965.

CAHILL, L. J.: The Geomagnetic Field. In Space Physics, D. P. LeGalley and A. Rosen, eds., John Wiley & Sons, Inc., 1964.

CHAMBERLAIN, J. W.: Motion of Charged Particles in the Earth's Magnetic Field. Gordon & Breach, 1964.

CHUBB, T. A.: Solar and Stellar Radiations Above the Earth's Atmosphere. In Conference on Artificial Satellites. Virginia Polytechnic Inst. NASA CR–60132, 1963.

COLEMAN, P. J.: Interaction of the Solar Wind With the Planets. AIAA J., vol. 4, Jan. 1966, p. 4.

CORLISS, W. R.: Space Probes and Planetary Exploration. D. Van Nostrand Co., 1965.

D'AIUTOLO, C. T.: Satellite Measurements of the Meteoroid Environment. Ann. N.Y. Acad. Sci., vol. 119, Nov. 11, 1964, p. 82.

DAUVILLIER, A.: Cosmic Dust. Philosophical Library, 1964.

DAVIS, T. N.: The Aurora. In Introduction to Space Science, W. N. Hess, ed., Gordon & Breach, 1965.

EHRICKE, K.: Space Flight, I. Environment and Celestial Mechanics. D. Van Nostrand Co., 1960.

FRIEDMAN, H.: The Next 20 Years of Space Science. Astronaut. Aeron., vol. 3, Nov. 1965, p. 40.

FRY, B. M.; AND MOHRHARDT, F. E.: A Guide to Information Sources in Space Science and Technology. Interscience Publishers, 1963.

GARMIRE, G.; AND KRAUSHAAR, W. L.: High Energy Cosmic Gamma Rays. Space Sci. Rev., vol. 4, Feb. 1965, p. 123.

GATLAND, K. W.: Space Technology in Western Europe. Astronaut. Aerospace Eng., vol. 1, Sept. 1963, p. 80.

GIACCONI, R.; AND GURSKY, H.: Observation of X-Ray Sources Outside the Solar System. Space Sci. Rev., vol. 4, Mar. 1965, p. 151.

GREENSTEIN, J. L.: Quasi-stellar Radio Sources. McGraw-Hill Yearbook of Science and Technology, 1965, p. 19.

HARRIS, I.; AND SPENCER, N. W.: The Earth's Atmosphere. In Introduction to Space Science, Gordon & Breach, 1965.

HAVILAND, R. P.; AND HOUSE, C. M.: Handbook of Satellites and Space Vehicles. D. Van Nostrand Co., 1965.

HEPPNER, J. P.: The World Magnetic Survey. Space Sci. Rev., vol. 2, 1963, p. 315.

HESS, W. N.; AND MEAD, G. D.: The Boundary of the Magnetopause. *In* Introduction to Space Science, W. N. Hess, ed., Gordon & Breach, 1965.

HESS, W. N.: The Earth's Radiation Belt. *In* Introduction to Space Science, W. N. Hess, ed., Gordon & Breach, 1965.

HESS, W. N.; MEAD, G. D.; AND NAKODA, M. P.: Bibliography of Particles and Fields Research. NASA X–640–65–37, 1965.

HESS, W. N.; MEAD, G. D.; AND NAKODA, M. P.: Advances in Particles and Field Research in the Satellite Era. Rev. Geophys., vol. 3, Nov. 1965, p. 521.

HESS, W. N.: The Radiation Environment Near the Earth. NASA TM X–54730, 1965.

HESS, W. N.: Energetic Particles in the Inner Van Allen Belt. Space Sci. Rev., vol. 1, 1962, p. 278.

HINES, C. O., ET AL., EDS.: Physics of the Earth's Upper Atmosphere. Prentice-Hall, Inc., 1965.

HINES, C. O.: The Magnetopause: A New Frontier in Space. Science, vol. 141, July 12, 1963, p. 128.

JASTROW, R., ED.: The Exploration of Space. The Macmillan Co., 1960.

JASTROW, R.; AND CAMERON, A. G. W.: Space: Highlights of Recent Research. Science, vol. 145, Sept. 11, 1964, p. 1129.

JETER, I. E., ED.: Scientific Satellites, Mission and Design. Vol. 12 of Advances in the Astronautical Sciences, Western Periodicals (North Hollywood), 1963.

KATZOFF, S.; AND MODISETTE, J. L.: The Electromagnetic Environment of a Satellite. NASA TN D–1360 and –1361, 1962.

KAULA, W. M.: The Shape of the Earth. *In* Introduction to Space Science, W. N. Hess, ed., Gordon & Breach, 1965.

KERN, J. W.; AND VESTINE, E. H.: Magnetic Field of the Earth and Planets. Space Sci. Rev., vol. 2, 1963, p. 136.

KING-HELE, D. G.: The Shape of the Earth. Inst. Navig. J., vol. 17, Jan. 1964, p. 1.

KOELLE, H. H., ED.: Handbook of Astronautical Engineering. McGraw-Hill Book Co., Inc., 1961.

KOELLE, H. H.; AND VOSS, R. G., EDS.: A Procedure to Analyze and Evaluate Alternative Space Program Plans. NASA TM X–53212, 1965.

KRASOVSKIJ, V. I.; AND SEFOV, N. N.: Airglow. Space Sci. Rev., vol. 4, Mar. 1965, p. 176.

LEGALLEY, D. P., ED.: Space Science. John Wiley & Sons, Inc., 1963.

LEGALLEY, D. P.; AND ROSEN, A.: Space Physics. John Wiley & Sons, Inc., 1964.

LEGALLEY, D. P.; AND MCKEE, J.: Space Exploration. McGraw-Hill Book Co., Inc., 1964.

LEGALLEY, D. P.: Scientific and Technical Results of U.S. and U.S.S.R. Satellites and Space Probes. *In* Space Exploration, D. P. LeGalley, ed., McGraw-Hill Book Co., Inc., 1964.

LIBBY, W. F.: Science and Manned Spacecraft. Astronaut. Aeron., vol. 3, Apr. 1965, p. 70.

LINDSAY, J. C.: The Solar Extreme Ultraviolet Radiation (1–400Å). Planet. Space Sci., vol. 12, May 1964, p. 379.

LINDSAY, J. C.: The Mission of the Advanced Orbiting Solar Observatory. *In* Scientific Satellites, I. E. Jeter, ed., Western Periodicals Co., 1963. (Also in The Observatory Generation of Satellites, NASA SP–30, 1963.)

LUST, R.: Interplanetary Plasma. Space Sci. Rev., vol. 1, 1962, p. 522.

MACHOL, R. E.; TANNER, W. P.; AND ALEXANDER, S. N., EDS.: System Engineering Handbook. McGraw-Hill Book Co., Inc., 1965.

MAEHLUM, B.: High Latitude Particles and the Ionosphere. Academic Press, 1965.

MANDEL'STAM, S. L.: X-ray Emission of the Sun. Space Sci. Rev., vol. 4, Sept. 1965, p. 587.

MANRING, E.: Interplanetary Matter. In Advances in Space Science and Technology, vol. 3, F. I. Ordway, ed., Academic Press, 1961.

MAYO, A. M.: Space Exploration by Remote Control. International Astronautical Congress paper, 1964.

McCRACKEN, C. W.; AND ALEXANDER, W. M.: Interplanetary Dust Particles. In Introduction to Space Science, W. N. Hess, ed., Gordon & Breach, 1965.

McDONALD, F. B.: Solar Proton Manual. NASA TR R–169, 1963.

McILWAIN, C. E.: The Radiation Belts, Natural and Artificial. Science, vol. 142, Oct. 18, 1963, p. 355.

McMAHON, S. N.: Astrophysics and Space Science: An Integration of Sciences. Prentice-Hall, Inc., 1965.

MILFORD, A. J.: Cosmic Ray Hazards in the Solar System. AIAA J., vol. 3, Feb. 1965, p. 193.

MORRISON, A.; AND BIRD, J. B.: Photography of the Earth From Space and Its Non-Meteorological Applications. In Michigan University Proceedings of the 3d Symposium on Remote Sensing of Environment, 1965. STAR acquisition no. N65–33573.

MOUREU, H.; AND BERNARD, N. Y.: Astronautique et Récherche Spatiale. Dunod Editeur (Paris), 1964.

NAUGLE, J. E.: Unmanned Space Flight. Holt, Rinehart & Winston, 1965.

NAUMANN, R. J.: Pegasus Satellite Measurements of Meteoroid Penetration (Feb. 16–July 20, 1965). NASA TM X–1192, 1965.

NESS, N. F.: The Interplanetary Medium. In Introduction to Space Science, W. N. Hess, ed., Gordon & Breach, 1965.

NESS, N. F.: The Earth's Magnetic Tail. J. Geophys. Res., vol. 70, July 1, 1965, p. 2989.

NEWELL, H. E.: Space Science. Science, vol. 139, Feb. 8, 1963, p. 464.

NOMURA, T., ET AL., EDS.: Proceedings of the Fourth International Symposium on Space Technology and Science. Japan Publications Trading Co. (Rutland), 1962.

ODISHAW, H., ED.: Research in Geophysics, Vol. 1: Sun, Upper Atmosphere and Space. MIT Press (Cambridge), 1964.

ORDWAY, F. I., ET AL.: Applied Astronautics. Prentice-Hall, Inc., 1963.

ORDWAY, F. I.; GARDNER, J. P.; AND SHARPE, M. R.: Basic Astronautics. Prentice-Hall, Inc., 1962.

PIERCE, J. R.: Satellite Science and Technology. Science, vol. 141, July 19, 1963, p. 237.

POMERANTZ, M. A.: International Years of the Quiet Sun, 1964–1965. Science, vol. 142, Nov. 29, 1963, p. 1136.

RILEY, F. E.; AND SAILOR, J. D.: Space Systems Engineering. McGraw-Hill Book Co., Inc., 1962.

ROSSI, B., ED.: Space Exploration and the Solar System. Academic Press, 1964.

SCULL, W. E.: The Mission of the Orbiting Geophysical Observatories. *In* Scientific Satellites, I. E. Jeter, ed., Western Periodicals, 1963. (Also in The Observatory Generation of Satellites, NASA SP–30, 1963.)

SEIFERT, H. S., ED.: Space Technology. John Wiley & Sons, Inc., 1959.

SHTERNFELD, A.: Soviet Space Science. Basic Books (New York), 1959.

SMITH-ROSE, R. L., ED.: Space Research VI. Spartan Books (Washington), 1966.

SONETT, C. P.: Magnetic Fields in Space. Astronautics, vol. 7, Aug. 1962, p. 34.

STARKEY, D. G.: The Space Vehicle—Manned Versus Unmanned. IAS Paper 62–153, 1962.

STEINBUCH, K.: Man or Automaton in Space? *In* Basic Environment Problems of Man in Space Symposium. Springer-Verlag (Vienna), 1964.

STUHLINGER, E., ET AL., EDS.: Astronautical Engineering and Science. McGraw-Hill Book Co., Inc., 1963.

SUGIURA, M.; AND HEPPNER, J. P.: The Earth's Magnetic Field. *In* Introduction to Space Science, W. N. Hess, ed., Gordon & Breach, 1965.

TOUSEY, R.: The Extreme Ultraviolet Spectrum of the Sun. Space Sci. Rev., vol. 2, 1963, p. 3.

VALLEY, S. L., ED.: Handbook of Geophysics and Space Environments. USAF Office of Aerospace Research (Hanscom Field), 1965.

VERTREGT, M.: Principles of Astronautics. Revised ed., Elsevier Publishing Co., 1965.

VETTE, J. I.: Models of the Trapped Radiation Environment. Vol. I: Inner Zone Protons and Electrons. NASA SP–3024, Aerospace Corp., 1966.

WHIPPLE, H. E., ED.: Civilian and Military Uses of Aerospace. Ann. N.Y. Acad. Sci., vol. 134, art. 1, Nov. 22, 1965.

WOLFF, E. A.: Spacecraft Technology. Spartan Books (Washington), 1962.

Chapter 2

ANANOFF, A.: L'Astronautique. Libraire Artheme Fayard (Paris), 1950.

ANON.: Astronautics and Aeronautics: Chronology on Science, Technology, and Policy. An Annual Summary. NASA SP–4004, 1963; NASA SP–4005, 1964.

ANON.: The Early Years. NASA Goddard Space Flight Center, 1963.

ANON.: Earth Satellites as Research Vehicles. Monograph 2, Franklin Institute, 1956.

ANON.: Explorer I. Ext. Pub. 461, Jet Propulsion Lab., 1958.

ANON.: From the History of Rocket Technology. Izdatel'stro Nauka, Moscow, 1964.

ANON.: On the Utility of an Artificial Unmanned Earth Satellite. Jet Propulsion, vol. 25, Feb. 1955, p. 71.

ANON.: Project Feedback Summary Report. Rand–262, Rand Corp., Santa Monica, Mar. 1954.

ANON.: Proposed United States Program for the International Geophysical Year. National Academy of Sciences—National Research Council, 1956.

ANON.: Space Handbook: Astronautics and Its Applications. Select Committee on Astronautics and Space Exploration, 1959.

ANON.: The Station in Space. J. Am. Rocket Soc., no. 63, 1945, p. 8.

ANON.: Ten Steps Into Space. Monograph 6, Franklin Institute, 1958.

AUGENSTEIN, B. W.: Scientific Satellite—Payload Considerations. RM–1459, Rand Corp., 1955.

BERKNER, L. V., ED.: Manual on Rockets and Satellites. Pergamon Press, 1958.

BLAGONRAVOV, A. A.: Collected Works of K. E. Tsiolkovskiy, Vol. II: Reactive Flying Machines. NASA TT F–237, 1965.

BOEHM, J.; FICHTNER, H. J.; AND HOBERG, O. A.: Explorer Satellites Launched by Juno 1 and Juno 2 Space Carrier Vehicles. *In* Astronautical Engineering and Science, E. Stuhlinger et al., eds., McGraw-Hill Book Co., Inc., 1963.

BURGESS, E.: Into Space. Aeronaut., vol. 18, Nov. 1946.

CANBY, C.: A History of Rockets and Space. Hawthorn Books, 1963.

CANNEY, H. E.; AND ORDWAY, F. I.: The Uses of Artificial Satellite Vehicles. Astronaut. Acta, vol. 2, 1956, p. 147; vol. 3, 1957, p. 1.

CHAZY, J.: Sur les Satellites Artificiels de la Terre. Compt. Rend., vol. 225, Sept. 22, 1947, p. 469.

CLARKE, A. C.: Stationary Orbits. J. Brit. Astron. Assoc., vol. 57, 1947, p. 232.

CLARKE, A. C.: Electronics and Spaceflight. J. Brit. Interplanetary Soc., vol. 7, 1948, p. 49.

CROSS, C. A.: The Fundamental Basis of Power Generation in a Satellite Vehicle. J. Brit. Interplanetary Soc., vol. 11, 1952, p. 117.

CROSS, C. A.: Orbits for an Extra-Terrestrial Observatory. J. Brit. Interplanetary Soc., vol. 13, 1954, p. 204.

CROSS, C. A.: Extra-Terrestrial Observatories—Their Purpose and Location. J. Brit. Interplanetary Soc., vol. 14, 1955, p. 137.

DEBUS, K. H.: The Evolution of Launch Concepts and Space Flight Operations. *In* Astronautical Engineering and Science, E. Stuhlinger et al., eds., McGraw-Hill Book Co., Inc., 1963.

DORNBERGER, W. R.: The German V–2. Technology and Culture, vol. 4, Fall 1963, p. 393.

EHRICKE, K. A.: Astronautical and Space-Medical Research With Automatic Satellites. *In* Earth Satellites as Research Vehicles. Franklin Institute, 1956.

EMME, E. M.: Aeronautics and Astronautics, 1915–1960. Government Printing Office, 1961.

GARDENHIRE, L. W.: Evolution of PCM Telemetry. Instruments and Control Systems, vol. 38, Apr. 1965, p. 87.

GATLAND, K. W.; DIXON, A. E.; AND KUNESCH, A. M.: Initial Objectives in Astronautics. J. Brit. Interplanetary Soc., vol. 9, 1950, p. 155.

GATLAND, K. W.: Project Satellite. Allan Wingate (London), 1958.

GAZLEY, C.; AND MASSON, D. J.: A Recoverable Scientific Satellite. RM–1844 and P–958, Rand Corp., Santa Monica, 1956 and 1957.

GLUSHKO, V. P.: Stansiia vne Zemli. (Station beyond the Earth.) Nauka. i Teknika, vol. 4, Oct. 8, 1926, p. 3.

GODDARD, R. H.: Rocket Development: Liquid-Fuel Rocket Research, 1929–1941. Prentice-Hall, Inc., 1961.

GOLDMAN, D. T.; AND SINGER, S. F.: Studies of a Minimum Orbital Unmanned Satellite of the Earth (MOUSE). Part III. Astronaut. Acta, vol. 3, 1957, p. 110.

HABER, H.: Space Satellites, Tools of Earth Research. Nat. Geog. Mag., vol. 109, Apr. 1956, p. 487.

HAGEN, J. P.: The Viking and the Vanguard. Technology and Culture, vol. 4, Fall 1963, p. 435.

HAGEN, J. P.: The Exploration of Outer Space With an Earth Satellite. Proc. IRE, vol. 44, 1956, p. 744.

HAVILAND, R. P.: On Applications of the Satellite Vehicle. Jet Propulsion, vol. 26, 1956, p. 360.

HAVILAND, R. P.: The Geodetic Satellite. ARS Paper 711–58, 1958.

HAYES, E. N.: The Smithsonian's Satellite-Tracking Program: Its History and Organization. *In* Annual Report, Smithsonian Institution, 1962.

HOOVER, G. W.: Instrumentation for Space Vehicles. ARS Paper 157–54, 1954.

JARRETT, F. E., JR.: Historical Origins of the George C. Marshall Space Flight Center. *In* Historical Origins of NASA's Launch Operations Center to July 1, 1962. NASA TM X–54991, 1964.

JOQUEL, A. L.: The Space-Station as an Astronomical Observatory Site. *In* The Artificial Satellite, L. J. Carter, ed., Brit. Interplanetary Soc., London, 1951.

KALLMANN, H. K.; AND KELLOGG, W. W.: Scientific Use of an Earth Satellite. RM–1500, Rand Corp., Santa Monica, 1955.

KRIEGER, F. J.: Soviet Astronautics; 1957–1962. RM–395–PR, Rand Corp., Santa Monica, 1963.

KRIEGER, F. J.: Behind the Sputniks: A Survey of Soviet Space Science. Public Affairs Press (Washington), 1958.

KURNOSOVA, L. V., ED.: Artificial Satellites. Vols. 1–6. Plenum Press (New York), 1960–1961.

LAGOW, H. E.; SECRETAN, L.; AND GURLIANI, J.: Experiments for Satellite Environmental Measurements. *In* Annals of the IGY, Pergamon Press, 1958.

LAGOW, H. E.: Instrumenting Unmanned Satellites. ARS Paper 281–55, 1955.

LASSER, D.: The Conquest of Space. Penguin Press, 1931.

LEVITT, I. M.: Geodetic Significance of a Minimum Satellite Vehicle. J. Astronaut., vol. 2, 1955, p. 1.

LEY, W.: The Satellite Rocket. The Technology Review, vol. 52, Dec. 1949, p. 93.

LEY, W.: A Station in Space. *In* Across the Space Frontier, C. Ryan, ed., Viking Press, 1952.

LEY, W.: The Long History of Space Travel. *In* Ten Steps into Space, Franklin Institute, 1958.

LUDWIG, G. H.; AND VAN ALLEN, J. A.: Instrumentation for a Cosmic Ray Experiment for the Minimal Earth Satellite. J. Astronaut., vol. 3, 1956, p. 59.

LUST, R.: The European Space Research Organization. Science, vol. 149, July 23, 1965, p. 394.

MATTHEWS, W.: Earth Satellite Instrumentation. Elect. Eng., vol. 76, July 1957, p. 562.

MAXWELL, W. R.: Some Aspects of the Origins and Early Development of Astronautics. J. Brit. Interplanetary Soc., vol. 18, 1962, p. 415.

MOORE, P.: Earth Satellites. W. W. Norton & Co., 1956.

MUEHLNER, J. W.: Trends in Missile and Space Radio Telemetry. Rpt. 5–10–62–28, Lockheed Missiles & Space Co., 1962.

NEWELL, H. E.: Scientific Uses of an Artificial Earth Satellite. Jet Propulsion, vol. 25, Dec. 1955, p. 712.

NEWELL, H. E.: The Satellite Project. Sci. Am., vol. 193, Dec. 1955, p. 29.

NEWELL, H. E.: The International Geophysical Year Satellite Program. *In* Earth Satellites as Research Vehicles, Monograph 2, Franklin Institute, 1956.

NYLANDER, H. E.; AND HOPPER, F. W.: The Development of Multiple Staging in Military and Space Carrier Vehicles. *In* Advances in Space Science and Technology, vol. 4, F. I. Ordway, ed., Academic Press, 1962.

O'BRIEN, B. J.: Review of Studies of Trapped Radiation With Satellite-Borne Apparatus. Space Sci. Rev., vol 1, 1962, p. 415.

ODISHAW, H.; AND RUTTENBERG, S., EDS.: Geophysics and the IGY. Monograph 2, American Geophysical Union, Washington, 1958.

ORDWAY, F. I.: The U.S. Satellite Vehicle Program. Astronaut. Acta, vol. 2, 1956, p. 115.

ORDWAY, F. I.: Project Vanguard—Earth Satellite Vehicle Program. Astronaut. Acta, vol. 3, 1957, p. 67.

OVENDEN, M. W.: Astronomy and Astronautics. J. Brit. Interplanetary Soc., vol. 8, 1949, p. 180.

PATTERSON, W.: From Sputnik 1 to Cosmos 16. Space/Aero., vol. 41, June 1963, p. 84.

PENDRAY, G. E.: Pioneer Rocket Development in the United States. Technology and Culture, vol. 4, Fall 1963, p. 384.

PERRY, R. L.: The Atlas, Thor, and Titan. Technology and Culture, vol. 4, Fall 1963, p. 466.

PETERSEN, N. V.: General Characteristics of Satellite Vehicles. J. Astronaut., vol. 2, 1955, p. 41.

PICKERING, W. H.: The United States Satellite Tracking Program. *In* Geophysics and the IGY, Monograph 2, American Geophysical Union, Washington, 1958.

PORTER, R. W.: Recovery of Data in Physical Form. *In* Earth Satellites as Research Vehicles, Monograph 2, Franklin Institute, 1956.

ROBILLARD, G.: Explorer Rocket Research Program. ARS J., vol. 29, July 1959, p. 492.

ROSS, H. E.: Orbital Bases. J. Brit. Interplanetary Soc., vol. 8, 1949, p. 1.

RYAN, C., ED.: Across the Space Frontier. Viking Press, 1952.

SAMPSON, W. F.: A Feasibility Study for Minimum-Weight Radio Instrumentation of a Satellite. JPL Rpt. 28, Pasadena, 1955.

SANDORFF, P. E.; AND PRIGGE, J. S.: Thermal Control of a Space Vehicle. J. Astronaut., vol. 3, 1956, p. 4.

SANGER, E.: Rocket Flight Engineering. NASA TT F–223, 1965.

SHTERNFELD, A.: Artificial Satellites. Office of Technical Services, Washington, 1958.

SINGER, S. F.: Research in the Upper Atmosphere With Sounding Rockets and Earth Satellite Vehicles. J. Brit. Interplanetary Soc., vol. 11, 1952, p. 61.

SINGER, S. F.: Studies of a Minimum Orbital Unmanned Satellite of the Earth (MOUSE). Astronaut. Acta, vol. 1, 1955, p. 171, and vol. 2, 1956, p. 125.

SINGER, S. F.: The Mouse, a Minimum Orbital Unmanned Satellite of the Earth for Astrophysical Research. J. Astronaut., vol. 2, 1955, p. 91.

SINGER, S. F.: Geophysical Research With Artificial Earth Satellites. *In* Advances in Geophysics, vol. 3, H. E. Landsberg, ed., Academic Press, 1956.

SINGER, S. F.: Scientific Problems in Cis-Lunar Space and Their Exploration With Rocket Vehicles. Astronaut. Acta, vol. 5, 1959, p. 116.

SMELT, R.; AND ODER, F. C. E.: Some Experimental Results From the Agena Satellite Program. Aerospace Eng., vol. 20, Feb. 1961, p. 10.

SMITH, F. A.: The Satellite Telescope. J. Brit. Interplanetary Soc., vol. 16, 1958, p. 361.

SMITH, G. O.: Radio Communication Across Space Ship-to-Ship and Ship-to-Planet. J. Brit. Interplanetary Soc., vol. 12, 1953, p. 13.

STEHLING, K. R.: Project Vanguard. Doubleday & Co., 1961.

STUHLINGER, E.: Army Activities in Space—A History. Trans. IRE, MIL–4, 1960, p. 64.

TOKATY, G. A.: Soviet Rocket Technology. Technology and Culture, vol. 4, Fall 1963, p. 515.

TSIOLKOVSKY, K. E.: Issledovanie Mirovikh Prostranstv Reaktivi'mi Priborami. Nauchnoye Obozrenie, 1963. (Also: Collected Works of K. E. Tsiolkovsky, A. A. Blagonravov, ed., NASA TT F–237, 1965.)

VAN ALLEN, J. A., ED.: Scientific Uses of Earth Satellites. U. Mich. Press, 1956 and 1958.

VAN ALLEN, J. A.: The Artificial Satellite as a Research Instrument. Sci. Am., vol. 195, Nov. 1956, p. 41.

VAN ALLEN, J. A.: Scientific Instrumentation of the Satellite. *In* Geophysics and the IGY, H. Odishaw and S. Ruttenberg, eds., Monograph 2, American Geophysical Union, Washington, 1958.

VON BRAUN, W.: Multistage Rockets and Artificial Satellites. *In* Space Medicine, J. P. Marbacher, ed., U. Ill. Press (Urbana), 1951.

VON BRAUN, W.: Firing of Explorer 1. ARS Paper 610–58, 1958.

VON BRAUN, W.: The Explorers. Astronaut. Acta, vol. 5, 1959, p. 126.

VON BRAUN, W.: The Redstone, Jupiter, and Juno. Technology and Culture, vol. 4, Fall 1963, p. 452.

VON PIRQUET, G.: Fahrtrouten. Die Rakete, vol. 2, 1928, p. 117.

WHIPPLE, F. L.; AND HYNEK, J. A.: Optical and Visual Tracking of Artificial Satellites. *In* Proceedings of the VIIIth International Astronautical Congress, F. Hecht, ed., Springer-Verlag (Vienna), 1958.

WHIPPLE, F. L.: Astronomy From the Space Station. Second Symposium on Space Travel (Hayden Planetarium), Oct. 1952.

WHIPPLE, F. L.: Scientific Value of Artificial Satellites. J. Franklin Inst., vol. 262, Aug. 1956, p. 95.

WINTERNITZ, P. F.: The Physical and Chemical Fundamentals of Satellite Flight. J. Astronaut., vol. 3, 1956, p. 43.

ZAEHRINGER, A. J.: Soviet Space Technology. Harper & Bros., 1961.

Chapter 3

AFFEL, H. A.: Systems Engineering. Inter. Sci. and Tech., no. 35, Nov. 1964.

ANON.: Systems Engineering in Space Exploration. Proceedings of a conference at Jet Propulsion Laboratory. NASA CR–68801, 1963.

ELLIS, D. O.; AND LUDWIG, F. J.: Systems Philosophy. Prentice-Hall, Inc., 1962.

FRANTA, A. L.: Integrating Spacecraft Systems. NASA TN D–3049, 1966.

GOODE, H. H.; AND MACHOL, R. E.: Systems Engineering. McGraw-Hill Book Co., Inc., 1957.

HALL, A. P.: A Methodology for Systems Engineering. D. Van Nostrand Co., 1962.

MACHOL, R. E., ED.: Systems Engineering Handbook. McGraw-Hill Book Co., Inc., 1965.

TURKIEWICZ, J. M., ET AL.: Electronic Integration of the UK–1 International Ionosphere Satellite. NASA TN D–3001, 1965.

WHITAKER, A. B.; AND SCHUHLEIN, C.: Integrating Spacecraft Electronics. Space/Aero., vol. 42, Aug. 1964, p. 53.

Chapter 4

ABZUG, M. J.: Active Satellite Attitude Control. *In* Guidance and Control of Aerospace Vehicles, C. T. Leondes, ed., McGraw-Hill Book Co., Inc., 1963.

ADAMS, W. M.; AND HODGE, W. F.: Influence of Solar Radiation Pressure on Orbital Eccentricity of a Gravity-Gradient-Oriented Lenticular Satellite. NASA TN D–2715, 1965.

ALPER, J. R.: Analysis of Pendulum Damper for Satellite Wobble Damping. J. Spacecraft and Rockets, vol. 2, Jan. 1965, p. 50.

ANON.: Orbital Flight Handbook. The Martin Co. (Baltimore), 1963.

BAKER, R. M. L.: Astrodynamics. *In* Space Exploration, D. P. LeGalley, ed., McGraw-Hill Book Co., Inc., 1964.

BILLIK, B.: Survey of Current Literature on Satellite Lifetimes. ARS J., vol. 32, Nov. 1962, p. 1641.

BRUCE, R. W.: Dynamic Atmospheric Effects Upon Satellite Motion and Satellite Lifetime. *In* Space Research V, D. G. King-Hele, P. Muller, G. Righini, eds., John Wiley & Sons, Inc., 1965.

CHAPMAN, D. R.: An Approximate Method for Studying Entry Into Planetary Atmospheres. NASA TR R–11, 1959.

CITON, S. J.: Satellite Lifetimes Under the Influence of Continuous Thrust, Atmospheric Drag, and Planet Oblateness. AIAA J., vol. 1, June 1963, p. 1355.

CLANCY, T. F.; AND MITCHELL, T. D.: Effects of Radiation Forces on the Attitude of an Artificial Satellite. AIAA J., vol. 2, Mar. 1964, p. 517.

CONTE, S. D.: The Computation of Satellite Orbit Trajectories. *In* Advances in Computers, vol. III, Academic Press, 1962.

COOK, G. E.: The Effect of Aerodynamic Lift on Satellite Orbits. Planetary and Space Science, vol. 12, Nov. 1964, p. 1009.

DAVIS, A. H.; AND HARRIS, I.: Interaction of a Charged Satellite With the Ionosphere. NASA TN D–704, 1961.

DENHAM, D.: Satellite Orbit Determination, a Bibliography. AD 468532, Army Missile Command, Huntsville, 1965.

DUNCAN, R. C.: Dynamics of Atmospheric Entry. McGraw-Hill Book Co., Inc., 1962.

DUNCOMB, R. L.; AND SZEBEHELY, V. G.: Methods in Astrodynamics and Celestial Mechanics, Academic Press, 1966.

EHRICKE, K. A.: Space Flight, II. Dynamics. D. Van Nostrand Co., 1962.

ESCOBAL, P. R.: Methods of Orbit Determination. John Wiley & Sons, Inc., 1965.

EVANS, W. J.: Aerodynamic and Radiation Disturbance Torques on Satellites Having Complex Geometry. *In* Torques and Attitude Sensing in Earth Satellites, S. F. Singer, ed., Academic Press, 1964.

FEDOR, F. V.: The Effect of Solar Radiation Pressure on the Spin of Explorer XII. NASA TN D–1855, 1963.

GROVES, G. V., ED.: Dynamics of Rockets and Satellites. North Holland Publishing Co. (Amsterdam), 1965.

HAVILAND, R. P.; AND HOUSE, C. M.: Nonequatorial Launching to Equatorial Orbits and General Nonplanar Launching. AIAA J., vol. 1, June 1963, p. 1336.

HELVEY, T. C., ED.: Space Trajectories. Academic Press, 1960.

HERRICK, S.: Earth Satellites and Related Orbit and Perturbation Theory. In Space Technology, H. S. Seifert, ed., John Wiley & Sons, Inc., 1959.

JACCHIA, L. G.; AND SLOWEY, J.: Formulae and Tables for the Computation of Lifetimes of Artificial Satellites. Special Rept. 135, Smithsonian Astrophysical Observatory, Cambridge, 1963.

KERSHNER, R. B.; AND NEWTON, R. R.: Attitude Control of Artificial Satellites. In Space Astrophysics, W. Liller, ed., McGraw-Hill Book Co., Inc., 1961.

KING-HELE, D.: Theory of Satellite Orbits in an Atmosphere. Butterworth (London), 1964.

LEWIS, D. E.; AND SHUBERT, G. H.: Efficiency in Space-Rocket Launching Operations: Recent Advances and Future Opportunities. Rept. RM–3913–PR, Rand Corp., Santa Monica, 1963.

LUIDENS, R. W.: Approximate Analysis of Atmospheric Entry Corridors and Angles. NASA TN D–590, 1961.

McELVAIN, R. J.: Effects of Solar Radiation Pressure on Satellite Attitude Control. In Guidance and Control, R. E. Roberson and J. S. Farrior, eds., Academic Press, 1962.

MOE, K.: The Orbit of Explorer VI—A Test of the Dynamic Model Atmospheres. In Scientific Findings from Explorer VI. NASA SP–54, 1965.

MURPHEY, J. P.; AND FELSTENTREGER, T. L.: Analysis of Lunar and Solar Effects on the Motion of Close Earth Satellites. NASA TN D–3559, 1966.

MUSEN, P.: On the Long-Period Lunisolar Effect in the Motion of the Artificial Satellite. In Scientific Findings from Explorer VI. NASA SP–54, 1965.

MUSEN, P.; BAILIE, A.; AND UPTON, E.: Development of the Lunar and Solar Perturbations in the Motion of an Artificial Satellite. In Scientific Findings from Explorer VI. NASA SP–54, 1965.

NAUMANN, R. J.: Observed Torque-Producing Forces Acting on Satellites. NASA TR R–183, 1963.

NELSON, W. C.; AND LOFT, E. E.: Space Mechanics. Prentice-Hall, Inc., 1962.

NEWFIELD, M. J.: Orbit Correction. Space/Aero., vol. 43, Feb. 1965, p. 48.

OTTERMAN, J.; AND LICHTENFELD, K.: The Effects of Air Drag on Near-Circular Satellite Orbits. J. Spacecraft, vol. 1, Sept. 1964, p. 513.

PHELAN, H. T.: Computation of Satellite Orbits by the Hansen Method as Modified by Musen. NASA TR R–147, 1962.

PILKINGTON, J. A.: Unusual Satellite Orbits. Spaceflight, vol. 6, 1964, p. 165.

POGORELOV, D. A.: Fundamentals of Orbital Mechanics. Holden-Day (San Francisco), 1964.

POLIAKHOVA, E. N.: Solar Radiation Pressure and the Motion of Earth Satellites. AIAA J., vol. 1, Dec. 1963, p. 2893.

REITER, G. S.; AND THOMSON, W. T.: Rotational Motion of Passive Space Vehicles. In Torques and Attitude Sensing in Earth Satellites, S. F. Singer, ed., Academic Press, 1964.

ROBERSON, R. E.: Generalized Gravity-Gradient Torques. In Torques and Attitude Sensing in Earth Satellites, S. F. Singer, ed., Academic Press, 1964.

ROBERSON, R. E.: Torques on a Satellite Vehicle From Internal Moving Parts. J. Appl. Mech., vol. 25, 1958, p. 196.

ROBERSON, R. E., ED.: Methods for the Control of Satellites and Space Vehicles. AD 254052, Systems Corp. of Am., 1960.

ROWELL, L. N.; SMITH, M. C.; AND SIBLEY, W. L.: On the Motion of Echo I-Type Earth Satellites. *In* Proceedings of the XIIIth International Astronautical Congress, N. Boneff and I. Hersey, eds., Springer-Verlag (Vienna), 1964.

ROY, A. E.: The Foundations of Astrodynamics. Macmillan Co., 1965.

ROY, M., ED.: Dynamics of Satellites. Academic Press, 1963.

SAVET, P. H.: Attitude Control of Orbiting Satellites at High Eccentricity. ARS J., vol. 32, Oct. 1962, p. 1577.

SCHRELLO, D. M.: Passive Aerodynamic Attitude Stabilization of Near Earth Satellites. AD 267521, 1961.

SEIFERT, H. S.: Dynamics of Long Range Rockets. Am. J. Phys., vol. 15, 1947, p. 265.

SHAPIRO, I. I.: Sunlight Pressure Perturbations on Satellite Orbits. Adv. Astronaut. Sci., vol. 11, 1962, p. 35.

SINGER, S. F.: Forces and Torques Due to Coulomb Interaction With the Magnetosphere. *In* Torques and Attitude Sensing in Earth Satellites, S. F. Singer, ed., Academic Press, 1964.

SIRY, J. W.: The Vanguard IGY Earth Satellite Launching Trajectories and Orbits. *In* Space Technology, H. S. Seifert, ed., John Wiley & Sons, Inc., 1959.

SUDDATH, J. H.: Theoretical Study of the Angular Motions of Spinning Bodies in Space. NASA TR R–83, 1961.

SUMMERFIELD, M.: Problems of Launching an Earth Satellite. Astronautics, vol. 2, Nov. 1957, p. 18.

SZEBEHELY, V. G., ED.: Celestial Mechanics and Astrodynamics. Academic Press, 1964.

THOMAS, L. C.; AND CAPPELLARI, J. D.: Attitude Determination and Prediction of Spin-Stabilized Satellites. Bell Sys. Tech. J., vol. 43, July 1964, p. 1657.

THOMPSON, W. T.: Introduction to Space Dynamics. John Wiley & Sons, Inc., 1961.

WOLVERTON, R. W., ED.: Flight Performance Handbook for Orbital Operations. John Wiley & Sons, Inc., 1963.

WOOD, G. P.: The Electric Drag Forces on a Satellite in the Earth's Upper Atmosphere. *In* Proceedings of the NASA-University Conference on the Science and Technology of Space Exploration, vol. 2. NASA SP–11, 1962, p. 337.

ZEE, C.: Trajectories of Satellites Under the Influence of Air Drag. *In* Celestial Mechanics and Astrodynamics, V. G. Szebehely, ed., Academic Press, 1964.

Chapter 5

BAILEY, J. S., ET AL.: Computer Operational Systems Engineering for an Orbiting Satellite and Its Command and Telemetry Data Acquisition Station. IEEE Trans., AS–2, Apr. 1964, p. 193.

BALAKRISHNAN, A. V., ED.: Space Communications. McGraw-Hill Book Co., Inc., 1963.

CORRY, J. D.: Data Handling Equipment for the OAO Satellite. Proceedings National Telemetering Conference, IRE, New York, 1962.

CREVELING, C. J.: Telemetry and Data Processing Systems for Scientific Satellites. NASA TM X–54808, 1965.

CREVELING, C. J.: Comparison of the Performance of PCM and PFM Telemetry Systems. *In* Record of the 1965 International Symposium on Space Electronics, IEEE, New York, 1965.

FERRIS, A. G.: Data Acquisition and Processing From Scientific Satellites. *In* Proceedings of the NASA-University Conference on the Science and Technology of Space Exploration, Vol. 1. NASA SP–11, 1962, p. 293.

FILIPOWSKY, F.; AND MUEHLDORF, E. I.: Space Communication Systems. Prentice-Hall, Inc., 1965.

FOSTER, L. E.: Telemetry Systems. John Wiley & Sons, Inc., 1965.

GODWIN, F.: A Unified Approach to Data Processing. J. Brit. Interplanetary Soc., vol. 19, 1963, p. 212.

GOETT, H. J.; AND HABIB, E. J.: Methods of Processing Satellite Data. Paper presented at the 16th International Astronautical Congress, 1965.

GRUEN, H.; AND OLERSKY, B.: Increasing Information Transfer. Space/Aero., vol. 43, Feb. 1965, p. 40.

HOFF, H. L.: Tracking, Command, Control and Data Acquisition of NASA Flight Programs. Ann. N.Y. Acad. Sci., vol. 134, Nov. 22, 1965, p. 475.

JAMISON, D. E.: Integrated Telemetry-Computer System. NASA TN D–3396, 1966.

KLEIGER, L. B.: Design of the Orbiting Geophysical Observatory Data Handling System. *In* Proceedings of the Spaceborne Computer Engineering Conference, IRE, New York, 1962.

LOWE, M. L.: Design Study for Telemetry and Instrumentation Systems for University Satellites. Paper presented at the 1965 Nat. Telemetering Conf., 1965.

LYNCH, T. J.: Space Data Handling at Goddard Space Flight Center. NASA TM X–55180, 1965.

MATTHEWS, W.: Telemetering in Earth Satellites. Elect. Eng., vol. 76, Nov. 1957, p. 976.

MUELLER, G. E.: Telebit—An Integrated Space Navigation and Communication System. Astronautics, vol. 5, May 1960, p. 26.

RICHTER, H.: Data Processing. *In* Space Communications, A. V. Balakrishnan, ed., McGraw-Hill Book Co., Inc., 1963.

SANDERS, R. W.: Communication Efficiency Comparison of Several Communication Systems. Proc. IRE, vol. 48, Apr. 1960, p. 575.

SCHWARTZ, L. S.: Telemetry. Space/Aero., vol. 42, Sept. 1964, p. 231.

STILTZ, H. L.: Aerospace Telemetry. Prentice-Hall, Inc., 1961.

STOCKWELL, E. J.: Spacecraft Tracking and Data Acquisition. Trans. Amer. Geophys. Union, vol. 44, June 1963, p. 685.

STOLLER, M. J.: Satellite Telemetry and Data Recovery Systems. *In* Space Research II, H. C. van de Hulst, C. de Jager, and A. F. Moore, eds., Interscience Publishers, 1961.

TISCHER, F. J.: Basic Theory of Space Communications. D. Van Nostrand Co., 1965.

WILLIAMS, W. E.: Space Telemetry Systems. Proc. IRE, vol. 48, Apr. 1960.

Chapter 6

BAGHDADY, E. J.; AND KRUSE, K. W.: The Design of Signals for Space Communications and Tracking. IEEE Conv. Rec., vol. 12, pt. 7, 1964, p. 152.

BARRON, R. L., ET AL.: Self-Organizing Spacecraft Attitude Control. AD 475167, Adaptronics, Inc., 1965.

BARTON, D. K.: Satellite Tracking. In Modern Radar—Analysis, Evaluation, and System Design, R. S. Berkowitz, ed., John Wiley & Sons, Inc., 1965.

BATTIN, R. H.: Astronautical Guidance. McGraw-Hill Book Co., Inc., 1964.

BIVAS, R., ET AL.: Satellite Orbit Determination by Laser Tracking. Paper presented at 6th COSPAR Meeting, 1965.

BRANDENBERGER, A. J.: The Use of Baker-Nunn Cameras for the Tracking of Artificial Earth Satellites. Photogram. Eng., vol. 28, Nov. 1962, p. 727.

CAHILL, W. F.; AND HARRIS, I.: Determination of Satellite Orbits From Radar Data. NASA TN D–489, 1960.

CANNON, R. H.: Some Basic Response Relations for Reaction-Wheel Attitude Control. ARS J., vol. 32, Jan. 1962, p. 61.

DECANIO, F.: Attitude Control for a Radio Telescope Satellite. In Proceedings of the Aerospace Vehicle Flight Control Conference, Soc. Auto. Eng., New York, 1965.

DEGRAFF, W.; AND DE JAGER, C.: The Optical Tracking of Satellites. COSPAR Bull., no. 25, Oct. 1965.

EASTON, R. L.: Radio Tracking of IGY Satellite: The Mark II Minitrack System. J. Astronaut., vol. 4, 1957, p. 31.

FERNANDEZ, M.; AND MACOMBER, G. R.: Inertial Guidance Engineering. Prentice-Hall, Inc., 1962.

FISCHELL, R. E.: Passive Gravity-Gradient Stabilization for Earth Satellites. In Torques and Attitude Sensing in Earth Satellites, S. F. Singer, ed., Academic Press, 1964.

FRAZIER, M.; KRIEGSMAN, B.; AND NESLINE, F. W.: Self-Contained Satellite Navigation Systems. AIAA J., vol. 1, Oct. 1963, p. 2310.

GLUCK, R.; AND GALE, E. H.: Motion of a Spinning Body During the Deployment of N Asymmetrical Appendages. AIAA Paper 66–100, 1966.

HENRIKSEN, S. W.: Electronic Tracking of Artificial Satellites. In The Use of Artificial Satellites for Geodesy, G. Veis, ed., Interscience Publishers, 1963.

KANE, T. R.: Attitude Stability of Earth-Pointing Satellites. AIAA J., vol. 3, Apr. 1965, p. 726.

KRONMILLER, G. C.; AND BAGHDADY, E. J.: The Goddard Range and Range Rate Tracking System: Concept, Design, and Performance. Space Sci. Rev., vol. 5, Mar. 1966, p. 265.

LANGFORD, R. C.; AND MUNDO, C. J., EDS.: Guidance and Control—II. Academic Press, 1964.

LEONDES, C. T., ED.: Guidance and Control of Aerospace Vehicles. McGraw-Hill Book Co., Inc., 1963.

LUDWIG, G. H.: The Orbiting Geophysical Observatories. Space Sci. Rev., vol. 2, 1963, p. 175.

MACKO, S. J.: Satellite Tracking. John F. Rider, Publisher (New York), 1962.

MASSEVITCH, A. G.: Optical Tracking of Satellites. In Space Research II, H. V. van de Hulst, C. de Jager, and A. F. Moore, eds., Interscience Publishers, 1961.

MENGEL, J. T.: Tracking the Earth Satellite, and Data Transmission by Radio. Proc. IRE, vol. 44, June 1956, p. 755.

NEWTON, R. R.: Method of Stabilizing an Astronomical Satellite. ARS J., vol. 29, Sept. 1959, p. 665.

PADDACK, S. J.; DEVANEY, R. A.; AND MONTGOMERY, H. E.: OGO Earth Acquisition. NASA TM X–55002, 1964.

PRINGLE, R., JR.: On the Capture, Stability, and Passive Damping of Artificial Satellites. NASA CR–139, 1964.

RICHTER, H. L.; SAMPSON, W. F.; AND STEVENS, R.: Microlock: A Minimum Weight Radio Instrumentation System for a Satellite. Jet Propulsion, vol. 28, Aug. 1958, p. 532.

ROBERSON, R. E.; AND FARRIOR, J. S., EDS.: Guidance and Control. Academic Press, 1962.

ROBERSON, R. E.: Stability and Control of Satellite Vehicles. In Handbook of Astronautical Engineering, H. H. Koelle, ed., McGraw-Hill Book Co., Inc., 1961.

ROBERSON, R. E.: Space Navigation, Guidance, and Control. In Space Exploration, D. P. LeGalley, ed., McGraw-Hill Book Co., Inc., 1964.

SINGER, S. F., ED.: Torques and Attitude Sensing in Earth Satellites. Academic Press, 1964.

SIRY, J. W.: Goddard Orbit Information Systems. NASA TM X–55044, 1964.

STOCKWELL, E. J.: Spacecraft Tracking and Data Acquisition. Nat. Acad. Sci. Bull., no. 72, June 1963, p. 1.

STONE, A. M.; AND WEIFFENBACH, G. C.: Radio Doppler Method of Using Satellites for Geodesy, Navigation and Geophysics. In Progress in the Astronautical Sciences, S. F. Singer, ed., Interscience Publishers, 1962.

VONBUN, F. O.: Analysis of the "Range and Range Rate" Tracking System. NASA TN D–1178, 1962.

VON HANDEL, P. F.; AND HOEHNDORF, F.: Accuracy Limits in Electronic Tracking of Space Vehicles. In Proceedings of the Xth International Astronautical Congress, F. Hecht, ed., Springer-Verlag (Vienna), 1960.

WHITE, J. B.: Meteoric Effects on Attitude Control of Space Vehicles. ARS J., vol. 32, Jan. 1962, p. 75.

WHITE, J. S.; SHIGEMOTO, F. H.; AND BOURQUIN, K.: Satellite Attitude Control Utilizing the Earth's Magnetic Field. NASA TN D–1068, 1961.

Chapter 7

ALELYUNAS, P.: Checkout: Man's Changing Role. Space/Aero., vol. 44, Dec. 1965, p. 66.

ALFONSI, P. J.: A Simulation of the Response of the OAO Spacecraft Structure to the Launch Acoustic Environment. AIAA Pub. CP–12, Unmanned Spacecraft Meeting, AIAA, New York, 1965.

ANDERSON, D. E.; AND STEPHENSON, W. B.: The Role of Ground Testing in Space Flight. AIAA paper 65–207, 1965.

ANDERSON, J. W.; LABLANC, E. A.; AND COHAN, H.: Experimental and Analytical Assessment of Space Thermal and Vacuum Simulation Requirements. AIAA paper 64–201, 1964.

ANDERSON, K. R.; AND CRUMLEY, T. D.: Mistram—A "State of the Art" Tracking System. In Proceedings of the IAS National Symposium on Tracking and Command of Aerospace Vehicles, IAS, New York, 1962.

ANON.: A Study of Spacecraft Testing Philosophies and Techniques. NASA CR–60410, Gen. Electric Co., 1964.

ANON.: Proceedings of the International Symposium on Solar Radiation Simulation. Institute for the Environmental Sciences, Mt. Prospect, Ill., 1965.

ANON.: Space Tracking and Data Acquisition Network Facilities Report (STADAN). NASA X–530–66–33, 1966.

BABECKI, A. J.: Quality Control and Nondestructive Testing for the Prevention of Failures in Scientific Satellites. *In* Record of the International Space Electronics Symposium, IEEE, New York, 1964.

BACHOFER, B. T.; AND SEAMAN, L. T.: One-Arc-Second Simulator for Orbiting Astronomical Observatory. J. Spacecraft and Rockets, vol. 2, Mar. 1965, p. 260.

BAILEY, J. S., ET AL.: Computer Operational Systems Engineering for an Orbiting Satellite and Its Command and Data Acquisition Station. IEEE Trans., AS–2, Apr. 1964, p. 143.

BEACHLEY, N. H.; MARTIN, L. B.; AND OTTEN, D. D.: Testing OGO's Attitude Controls. Control Eng., vol. 11, Oct. 1964, p. 93.

BERKNER, L. V., ED.: Manual on Rockets and Satellites. Pergamon Press, 1958.

BERNIER, R. E., ET AL.: Solar Simulation Testing of an Earth Satellite at Goddard Space Flight Center. NASA TN D–2614, 1965.

BLASSEL, P.; AND CHIQUET, P.: The CNES/ESRO Network for Tracking and Monitoring of Satellites. Sciences et Industries Spatiales, vol. 1, 1965, p. 23.

BRISKMAN, R. D.: NASA Ground Support Instrumentation. *In* Proceedings of the IAS National Symposium on Tracking and Command of Aerospace Vehicles, IAS, New York, 1962.

BROWN, W. G.: Development of Magnetic Test Facilities at Goddard Space Flight Center. Tech. Memo. 33–216, Jet Propulsion Laboratory, 1965.

CARR, F. A.: The Environmental Test Program and Systems Evaluation of the S–3 Energetic Particles Satellite. NASA TM X–50853, 1963.

CLEVENSON, S. A.; AND MACCONOCHIE, I. O.: Characteristics of Environmental Test Equipment at the Langley Research Center. NASA TM X–1129, 1965.

COOPER, H. W., ET AL.: Ground Operation Equipment for the Orbiting Astronomical Observatory. *In* Proceedings of the IAS National Symposium on Tracking and Command of Aerospace Vehicles, IAS, New York, 1962.

COX, R. N.: Laboratory Simulation of the Perturbations of the Ionosphere by Space Vehicles. Astronaut. Acta, vol. 11, 1965, p. 183.

DAVIS, R. B.; AND WIGGINS, E. T.: Automation for Spacecraft Ground Support Equipment. ISA Proc., vol. 8, 1962, p. 33.

DEBUS, K.; AND GRUEN, H. F., EDS.: Launching Sites and Space Ports. *In* Handbook of Astronautical Engineering, H. H. Koelle, ed., McGraw-Hill Book Co., Inc., 1961.

DRAKE, R. M. L.: Ground Support Equipment for the UK–2/S–52 International Satellite. IEEE Trans., AS–1, Aug. 1963, p. 375.

DUNCAN, C. H., ET AL.: Solar Simulation Research. NASA TM X–55364, 1965.

FURSTENAU, B. W.: The Next Generation of Automated Checkout Equipment. AIAA paper 65–517, 1965.

GAUMER, R. E.; AND PLASKETT, V. A.: Environmental Simulation. Space/ Aero., vol. 42, Sept. 1964, p. 187.

GOLLOMP, B.; LAWTON, J.; AND VAN RENNES, A. B.: Evolution of Automatic Check-Out Equipment. J. Brit. Interplanetary Soc., vol. 19, 1963, p. 223.

GRANT, M. M.; STEPHANIDES, C. C.; AND STEWART, W. N.: Explorer XVII (1963 9A) Real Time PCM Telemetry Data Processing and Display Test Stand. NASA TN D–2318, 1964.

HABIB, E. J.; KEIPERT, F. A.; AND LEE, R. C.: Telemetry Processing for NASA Scientific Satellites. ISA preprint 7.2–2–65, 1965.

HABIB, E. J., ET AL.: Ground Operation Equipment for the Orbiting Astronomical Observatory. NASA TN D–1856, 1963.

HANSON, N. L.; AND WARD, A. B.: Advanced Range Instrumentation Ships. AD 429095, 1963.

HARRIS, D. W., ET AL.: MOTS—The Minitrack Optical Tracking System. Phot. Sci. and Eng., vol. 7, Mar. 1963, p. 73.

HERCULES, F.; AND BUTLER, R.: Orbital Testing Requirements for Guidance and Control Devices. McDonnell Aircraft Corp. NASA CR–355, 1965.

HNILICKA, M. P.; AND GEIGER, K. A.: Simulating Interplanetary Space. Astronaut. Aerospace Eng., vol. 1, July 1963, p. 31.

HOGGARD, W. D.: Final Report on Environmental Testing of Ionospheric Explorer Spacecraft. NASA TM X–55109, 1964.

HORD, W. H., JR.: Environmental Test Program for Ariel I. NASA TN D–2099, 1964.

IMGRAM, D. A.; AND MUENCH, W. K.: Dynamic Testing of the OAO Stabilization and Control Subsystem. AIAA paper 63–176, 1963.

KIRKMAN, R. A.: The Use of Automation in the Checkout of Aircraft, Spacecraft, and Missile Systems. AIAA paper 64–250, 1964.

KLASS, P. J.: Navy Improves Accuracy, Detection Range of Space Surveillance Chain. Av. Wk., vol. 56, Aug. 16, 1965.

KLEIN, E., ED.: Final Report of the Goddard Summer Workshop Program in Measurement and Simulation of Space Environments. NASA X–320–64–341, 1964.

KLEIN, G. H.; AND PIERSOL, A. G.: The Development of Vibration Test Specifications for Spacecraft Applications. NASA CR–234, 1965.

LANTZ, P. A.: Handbook of Antennas at NASA Satellite Tracking and Space Data Acquisition (STADAN) Facilities. NASA TM X–55031, 1964.

LEMKE, L. C.: Thermal Simulation of a Satellite. AIAA paper 65–475, 1965.

LEVERONE, H.; MANDELL, N.; AND YAFFEE, P.: Instrumentation for the GSFC Space Environment Simulator. In MILECON/9, Conference on Military Electronics, IEEE, New York, 1965.

MACFARLANE, G.: Solar Simulation: Requirements for Large Aerospace Environmental Chambers. AD 469008, 1965.

MARTENS, L. E.; AND TABELING, R. H.: Tracking Instrumentation and Accuracy on the Eastern Test Range. IEEE Trans., SET–11, Mar. 1965, p. 14.

MASON, J. F.: Modernizing the Missile Range. Electronics, vol. 38, Feb. 22, 1965, p. 94, and vol. 38, Mar. 8, 1965, p. 108.

MAST, L. T.: Automatic Test and Checkout in Missile and Space Systems. Astronaut. Aerospace Eng., vol. 1, Mar. 1963, p. 41.

MENGEL, J. T.; AND HERGET, P.: Tracking Satellites by Radio. Sci. Am., vol. 198, Jan. 1958, p. 23.

MERCY, K. R.; AND TIMMINS, A. R.: Upgrading Unmanned Spacecraft Quality and Reliability Through Environmental Testing. *In* Proceedings of the 11th Annual Technical Meeting, Institute for the Environmental Sciences, Mt. Prospect, Ill., 1965.

MICHAUD, C.: DIANE—A European Satellite Tracking Network. Sciences et Industries Spatiales, vol. 1, 1965, p. 28.

NESS, N. F.: Magnetic Fields—Reasons for Simulation and Methods Available. *In* Proceedings of the Conference on the Role of Simulation in Space Technology, Virginia Polytechnic Institute, 1965.

PARSONS, C. L.; AND HARRIS, C. A.: IMP–1 Spacecraft Magnetic Test Program. NASA TN D–3376, 1966.

PARSONS, C. L.: Magnetic Testing of Spacecraft. *In* Proceedings of the Magnetic Workshop, Jet Propulsion Lab., 1965.

PETERSON, M. C.: The Orbiting Geophysical Observatory Test Program. IEEE Trans., AS–1, 1963, p. 362.

PIAZZA, F.: Computer Analysis of Interplanetary Monitoring Platform (IMP) Spacecraft Performance. NASA TN D–3340, 1966.

PLOTKIN, H. H.: The S–66 Laser Satellite Tracking Experiment. NASA TM X–52075, 1963.

PLOTTIN, G.: Telemetry Reception and Remote Control Transmission Stations of the CNES Network. Sciences et Industries Spatiales, vol. 1, 1965, p. 33.

POEHLS, V. J.: The Atlantic Missile Range Global Tracking System. *In* Proceedings of the International Conference on Military Electronics, B. J. Goldfarb, ed., Western Periodicals, 1964.

POWELL, H. R.: Reliability and Developmental Testing. *In* Space Logistics Engineering, K. Brown and L. D. Ely, eds., John Wiley & Sons, Inc., 1962.

PRENTICE, H. A. J.; AND PORTER, J.: Environmental Testing in Support of Satellite Design at the Royal Aircraft Establishment. *In* Proceedings of the 11th Annual Technical Meeting, Institute of Environmental Sciences, Mt. Prospect, Ill., 1965.

PRICE, W. E.: The Simulation of Space Radiation Damage to Spacecraft Systems. IEEE Trans., NS–12, Dec. 1965, p. 2.

RELF, K. E.: MISTRAM. AD 429095, 1963.

SCAVUILO, J. J.; AND PAUL, F. J.: Aerospace Ranges: Instrumentation. D. Van Nostrand Co., 1965.

SCHANBACHER, W. A.; AND SCHORKEN, C. A.: The Orbiting Geophysical Observatory Test and Support Program. AIAA paper 63065, 1963.

SMITH, F.: Biosatellite System Qualification Test Plan for the Radiation and General Biology Spacecraft. 65SD749, General Electric Co., 1965.

SOULE, H. A.: NASA Worldwide Tracking Systems. *In* Reentry Dynamics, Virginia Polytechnic Institute, 1962.

SPEER, F. A.: Trends in Space-Vehicle Test Ranges. Astronaut. Aerospace Eng., vol. 2, July 1964, p. 50.

STEPHENSON, J. W.; AND WELLER, R. K.: The GLOTRAC System. AD 429095, 1963.

STOCKWELL, B.: The Use of a Space Chamber in Satellite Design. Paper at the British Interplanetary Society Symposium on Space Environment Simulators, 1964.

THOMAS, S.: Satellite Tracking Facilities. Holt, Rinehart & Winston, 1963.

VEIS, G.: The Precision Optical Satellite Tracking Net of the Smithsonian Astrophysical Observatory. *In* The Uses of Artificial Satellites for Geodesy, G. Veis, ed., John Wiley & Sons, Inc., 1963.

VEIS, G.; AND WHIPPLE, F. L.: Experience in Precision Optical Tracking of Satellites for Geodesy. *In* Space Research II, H. C. van de Hulst, C. de Jager, and A. F. Moore, eds., Interscience Publishers, 1961.

WOERNER, C. V.; AND COFFEE, C. W., JR.: Comparison of Ground Tests and Orbital Launch Results for the Explorer IX and Explorer XIX Satellites. NASA TN D–2466, 1964.

Chapter 8

ALBERI, A.; AND ROSENKRANZ, C.: Structures of Carrier and Space Vehicles. *In* Advances in Space Science and Technology, vol. 3, F. I. Ordway, ed., Academic Press, 1961.

ANON.: Shells Into Orbit. Machine Design, vol. 37, Jan. 7, 1965, p. 115.

ANON.: Launch Vehicles of the National Launch Vehicle Program. NASA SP–10, 1962.

ATTALI, C.: The Diamant Satellite Launcher. Paper at the 5th European Space Flight Symposium, 1965.

BULL, G. V.: Development of Gun Launched Vertical Probes for Upper Atmosphere Studies. Can. Aero. Space J., vol. 10, Oct. 1964.

BULL, G. V.; AND MURPHY, C. H.: Gun-Launched Missiles for Upper Atmosphere Research. AIAA paper 64–18, 1964.

BURLAGE, H.: Liquid Propulsion. Space/Aero., vol. 41, Feb. 1964, p. 60.

CHRISTMAS, A. N.: The ELDO Initial Launcher System: Design Objectives and Development Programme. J. Brit. Interplanetary Soc., vol. 20, Sept.–Oct. 1965, p. 129.

GATLAND, K. W.: Spacecraft and Boosters. Aero Publishers (Los Angeles), 1964.

HOOPER, W. H.: Thor Delta Description and Payload Capability. NASA CR–56312, Douglas Aircraft Co., 1962.

ISAACS, J. D., ET AL.: Satellite Elongation Into a True "Sky Hook." Science, vol. 151, Feb. 11, 1966, p. 682.

KOVIT, B.: The Coming Kick Stage. Space/Aero., vol. 44, Aug. 1965, p. 55.

MORRISON, R. B.; AND BOS, W. F.: The Economics of Launch Vehicles. AIAA paper 64–276, 1964.

PARDOE, G. K. C.: Integration of Payload and Stages of Space Carrier Vehicles. *In* Advances in Space Science and Technology, vol. 6, F. I. Ordway, ed., Academic Press, 1964.

PETERS, R. L.: Design of Liquid, Solid, and Hybrid Rockets. Hayden Book Co. (New York), 1965.

ROMAN, P.: The Booster Crossroads. Space/Aero., vol. 43, Mar. 1965, p. 58.

STAMBLER, I.: Centaur. Space/Aero., vol. 40, Oct. 1963, p. 70.

STAMBLER, I.: Titan III. Space/Aero., vol. 40, Aug. 1963, p. 72.

STONER, G. H.: Launch-Vehicle Systems. *In* Lunar Missions and Exploration, C. T. Leondes and R. W. Vance, eds., John Wiley & Sons, Inc., 1964.

SUTTON, G. P.: Rocket Propulsion Elements. John Wiley & Sons, Inc., 1963.

THACKWELL, H. L.: Solid Rockets—A Maturing Technology. Astronaut. Aero., vol. 3, Sept. 1965, p. 74.

THACKWELL, H. L.: Status of United States Large Solid Rocket Programs. AIAA paper 65–422, 1965.

WILKINS, C. T., ET AL.: Europa I. Flight International, vol. 85, June 11, 1964, p. 967.

Chapter 9

ADOLPHSEN, J. W.; AND MALINOWSKI, A. B.: Telemetry Encoder for International Satellite UK–C. IEEE Conv. Rec., vol. 12, pt. 7, 1964, p. 192.

ALBUS, J. S.; AND SCHAEFER, D. H.: Satellite Attitude Determination: Digital Sensing and On-Board Processing. NASA X–631–63–133, 1963.

ALEXANDER, A. L.: Thermal Control in Space Vehicles. Science, vol. 143, Feb. 14, 1964, p. 654.

ALEYUNAS, P.: Reliability. Space/Aero., vol. 42, Oct. 1964, p. 48.

ANDERSON, J. R.: Performance of Ion Thrustors and Systems for Satellite Control. AIAA paper 65–417, 1965. (Also published in: J. Spacecraft and Rockets, vol. 3, July 1966, p. 1086.)

ANGULO, E. D.; AND BROWNING, R. K.: The Structure of the Explorer X Magnetometer Space Probe. NASA TN D–1175, 1962.

ANON.: Electrical Power Generation Systems for Space Applications. NASA SP–79, 1965.

ANON.: Electromagnetic Attitude Control System Study. NASA CR–24, Westinghouse Electric Corp., 1964.

ARNOWITZ, A.: The Vanguard Control System. Astronautics, vol. 2, Oct. 1957, p. 34.

BANNISTER, T. C.: Pegasus Thermal Design. NASA TM X–53300, 1965.

BARNEY, R. A.: Space Vehicle Power Sources Handbook. AD 441574, 1964.

BARTOE, O. E., ET AL.: Design and Development of the Orbiting Solar Observatory. Ann. N.Y. Acad. Sci., vol. 134, Nov. 22, 1965, p. 194.

BAUER, H. A.; AND MONGOLD, G. E.: The Telecommand/Telemetry System for the France-1 Satellite. Paper at the 1965 National Telemetering Conference, 1965.

BOEHM, J.: Considerations to the Development of Explorer VII Satellite. IRE Trans., MIL–4, 1960, p. 86.

BOUCHER, R. A.: Electrical Propulsion for the Control of Stationary Satellites. J. Spacecraft and Rockets, vol. 1, Mar. 1964, p. 164.

BRANDHORST, H. W., JR.; AND HART, R. E., JR.: Radiation Damage to Cadmium Sulfide Solar Cells. NASA TN D–2932, 1965.

BRISCOE, H. M.: The Choice of Propellent for a Cold Gas Propulsion System for a Satellite. J. Brit. Interplanetary Soc., vol. 20, May 1965, p. 72.

BROOKS, G. W.: Research, Design Considerations, and Technological Problems of Structures for Spacecraft. In Proceedings of the NASA-University Conference on the Science and Technology of Space Exploration, NASA SP–11, vol. 2, 1962.

BROWN, S. C.: An Analytical Comparison of Some Electromagnetic Systems for Removing Momentum Stored by a Satellite Attitude Control System. NASA TN D–2693, 1965.

BUSH, E. G.: The Use of Solid Circuits in Satellite Instrumentation. NASA TN D–1758, 1964.

CANTOR, C.: Fine Sun Tracker for Advanced Orbiting Solar Observatory. In Proceedings of the Annual East Coast Conference on Aerospace and Navigation Electronics, Western Periodicals, 1963.

CARR, F. A.: Flight Report, Interplanetary Monitoring Platform, IMP–1—Explorer XVIII. NASA TN D–3352, 1966.

CASHMORE, D. J.: Earth Pointing Satellites: A Method of Attitude Control To Maximize Power From Solar Cell Arrays. J. Brit. Interplanetary Soc., vol. 20, May 1965, p. 63.

CERVENKA, A. J.: One Approach to the Engineering Design of the Advanced Orbiting Solar Observatory. *In* The Observatory Generation of Satellites, NASA SP–30, 1963.

CHERRY, W. R.: Status of Photovoltaic Solar Energy Converters. IEEE Trans, AES–1, Aug. 1965, p. 10.

CHIARAPPA, D. J.; AND NELSON, K. F.: An Analysis of the Vertistat Gravity Gradient Satellite Orientation. J. Spacecraft and Rockets, vol. 2, Mar. 1965, p. 167.

CHUTE, F. S.; AND WALKER, G. B.: The Possibility of Stabilizing a Space Vehicle Using Electromagnetic Angular Momentum. Can. Aero. Space J., vol. 11, Sept. 1965, p. 219.

CLAUSEN, O. W.; AND NEU, J. T.: The Use of Directionally Dependent Radiation Properties for Spacecraft Thermal Control. Astronaut. Acta, vol. 11, Sept.–Oct. 1965, p. 328.

COFFEE, C. W., JR.; BRESSETTE, W. E.; AND KEATING, G. M.: Design of the NASA Lightweight Inflatable Satellites for the Determination of Atmospheric Density at Extreme Altitudes. NASA TN D–1243, 1962.

COOLEY, W. C.; AND JANDA, R. J.: Handbook of Space-Radiation Effects on Solar-Cell Power Systems. NASA SP–3003, 1963.

COOPERMAN, R. S.: Geos A Optical Memory and Control Unit. AD 476291, 1965.

CORNILLE, H. J., JR.: A Method of Accurately Reducing the Spin Rate of a Rotating Spacecraft. NASA TN D–1420, 1962.

COSBY, W. A.; AND LYLE, R. G.: The Meteoroid Environment and Its Effect on Materials and Equipment. NASA SP–78, 1965.

CRAIG, B. D.: Nutation Damper for OSO. Astronaut. Aerospace Eng., vol. 1, Dec. 1963, p. 50.

DELIBERATO, V. C.: Design of the Biosatellite Spacecraft. Ann. N.Y. Acad. Sci., vol. 134, Nov. 22, 1965, p. 385.

DELISLE, J. E.; OGLETREE, E. G.; AND HILDEBRANT, B. M.: The Application of Gyrostabilizers to Orbiting Vehicles. *In* Torques and Attitude Sensing in Earth Satellites, S. F. Singer, ed., Academic Press, 1964.

DENNIS, P. R.; AND SESHU, S.: Reliability and Redundant Circuitry. NASA CR–128, 1964.

DOMITZ, S., ET AL.: Survey of Electromagnetic Accelerators for Space Propulsion. NASA TN D–3332, 1966.

DUNBAR, A. S.: Spacecraft Antennas. *In* Electromagnetics in Space, K. R. Spangenberg, ed., McGraw-Hill Book Co., Inc., 1965.

DZILVELIS, A. A.: Satellite Attitude Control Systems. Astronaut. Aerospace Eng., vol. 1, Mar. 1963, p. 78.

ERGIN, E. I.; AND WHEELER, P. C.: Magnetic Attitude Control of a Spinning Satellite. J. Spacecraft and Rockets, vol. 2, Nov. 1965, p. 846.

EVANS, W. B.: Development Approach for an Advanced Orbiting Solar Observatory Spacecraft. J. Spacecraft and Rockets, vol. 3, Jan. 1966, p. 84.

FEDOR, J. V.: Analytical Theory of the Stretch Yo-Yo for De-Spin of Satellites. NASA TN D–1676, 1963.

FEDOR, J. V.: Theory and Design Curves for a Yo-Yo De-Spin Mechanism for Satellites. NASA TN D–708, 1961.

FINCH, H. L., ET AL.: Orbiting Satellite Surface Temperature Prediction and Analysis. NASA CR–56277, 1964.

FISCHELL, R. E.: Effects of Passive Attitude Control on Solar Power Systems. AD 622483, Applied Physics Laboratory, 1964.

FISCHELL, R. E.: Spin Control for Earth Satellites. APL Tech. Digest, vol. 5, Sept.–Oct. 1965, p. 8.

FISCHELL, R. E.: Passive Gravity-Gradient Stabilization for Earth Satellites. *In* Torques and Attitude Sensing in Earth Satellites, S. F. Singer, ed., Academic Press, 1964.

FISCHELL, R. E.: Magnetic and Gravity Attitude Stabilization of Earth Satellites. *In* Space Research II, H. C. van de Hulst, C. de Jager, and A. F. Moore, eds., Interscience Publishers, 1961.

FITZ, C. D., ET AL.: Albedo and Planet Radiation Intercepted by an Earth Satellite. AD 404175, 1963.

FIXLER, S. Z.: Passive Thermal Control by Phase-Change Materials. Space/Aero., vol. 45, Feb. 1966, p. 104.

FIXLER, S. Z.: Umbra and Penumbra Eclipse Factors for Satellite Orbits. AIAA J., vol. 2, Aug. 1964, p. 1455.

FRANCIS, H. T.: Space Batteries. NASA SP–5004, 1964.

FRANKLIN, C. A., ET AL.: Electronic and System Design of the Canadian Ionospheric Satellite. AD 627209, 1965.

FRANKLIN, C. A.; BIBBY, R. J.; AND STURROCK, R. F.: Telemetry and Command Systems for the Canadian Ionospheric Satellite. AD 627208, 1965.

FRANTA, A. L.; AND DAVIDSON, A. C.: Achieving Ariel II Compatibility Design. NASA X–672–64–381, 1964.

FRIED, E.; AND COSTELLO, F. A.: Interface Thermal Contact Resistance Problem in Space Vehicles. ARS J., vol. 32, Feb. 1962, p. 237.

FUSCA, J. A.: Advanced Guidance Concepts. Space/Aero., vol. 42, Dec. 1964, p. 46.

GANSSLE, E. R.: Structural Design of the Meteoroid Technology Satellite. Unmanned Spacecraft Meeting. AIAA publ. CP–12, 1965.

GEHRING, J. W.; CHRISTMAN, D. R.; AND McMILLAN, A. R.: Experimental Studies Concerning the Meteoroid Hazard to Aerospace Materials and Structures. J. Spacecraft and Rockets, vol. 2, Sept. 1965, p. 731.

GERLACH, O. H.: Attitude Stabilization and Control of Earth Satellites. Space Sci. Rev., vol. 4, June 1965, p. 541.

GLASER, P. F.: The Orbiting Geophysical Observatory Communications and Data Handling Subsystems. Proceedings of the 1962 National Telemetering Conference, vol. 2, 1962.

GLEGHORN, G. J.: The Engineering Design of the Orbiting Geophysical Observatories. *In* The Observatory Generation of Satellites, NASA SP–30, 1963.

GLEGHORN, G. J.; AND LINDNER, J. W.: Magnetic Considerations in the Design and Testing of the OGO and Pioneer Spacecraft. Paper presented at the 16th International Astronautical Congress, 1965.

GLEGHORN, G. J.; AND WIGGINS, E. T.: Design and Development of the Orbiting Geophysical Observatories. Ann. N.Y. Acad. Sci., vol. 134, Nov. 22, 1965, p. 205.

GUNDERSON, N. A.: Fine Guidance Sensor for High-Precision Control of the OAO. J. Spacecraft and Rockets, vol. 1, Jan.–Feb. 1964, p. 91.

HALL, K. L., ET AL.: Data Handling Equipment (OAO) Redundant Design: Its Tradeoffs and Performance Analysis. *In* PGSET Record of the 1962 National Symposium on Space Electronics and Telemetry, IRE, New York, 1962.

HALPERN, G.; AND ZIMMER, F. C.: The Ionospheric Explorer XX Communications System—Description and Performance. IEEE Conv. Rec., vol. 13, pt. 4, 1965, p. 25.

HENNING, I.; AND OLESEN, H. L.: Designing Against Space Radiation. Electronics, vol. 37, Dec. 28, 1964, p. 61.

HERING, K. W.; AND HUFNAGEL, R. E.: Inertial Sphere System for Complete Attitude Control of Earth Satellites. ARS J., vol. 31, Aug. 1961, p. 1074.

HERRON, D. P.: Optimizing Trade-Offs of Reliability vs. Weight. IEEE Trans., R–12, Dec. 1963, p. 50.

HOLAHAN, J.: Attitude Control for Unmanned Spacecraft. Space/Aero., vol. 39, Feb. 1963, p. 78.

HUSSON, C.: Bringing Microelectronics to Spacecraft. Astronaut. Aerospace Eng., vol. 2, Apr. 1964, p. 29.

IMGRAM, D. A.: Design and Development of the Orbiting Astronomical Observatory. Ann. N.Y. Acad. Sci., vol. 134, Nov. 22, 1965, p. 184.

IMGRAM, D. A.; ZIEMER, R. R.; AND STERN, E.: Design and Dynamic Testing of an Ultrahigh Accuracy Satellite Stabilization and Control System for the Orbiting Astronomical Observatory. In Proceedings of the XIIIth International Astronautical Congress, N. Boneff and I. Hersey, eds., Springer-Verlag (Vienna), 1964.

JAFFE, L. D.; AND RITTENHOUSE, J. B.: Behavior of Materials in Space Environments. ARS J., vol. 32, Mar. 1962, p. 320.

JAMISON, S. S.: Satellite Systems Reliability. In 7th National Convention on Military Electronics IEEE, New York, 1963.

JASIK, H., ED.: Antenna Engineering Handbook. McGraw-Hill Book Co., Inc., 1961.

JOHNS, R. H.; COCHRAN, R. P.; AND SPERA, D. A.: Some Design Considerations for Spin-Stabilized Satellites with Rigid Expandable Structures. NASA TM X–1061, 1965.

KAMM, L. J.: "Vertistat": An Improved Satellite Orientation Device. ARS J., vol. 32, June 1962, p. 911.

KATUCKI, R. J.: Gravity-Gradient Stabilization. Space/Aero., vol. 42, Oct. 1964, p. 42.

KEENEY, R. L.: Environmental Effects on Space Structures. AD 618030, 1964.

KERSHNER, R. B.: Gravity-Gradient Stabilization of Satellites. Astronaut. Aerospace Eng., vol. 1, Sept. 1963, p. 18.

KIEFER, P. J.; AND BULL, H. I.: Effects of Radiation on the Weight Requirements of a Satellite Solar Power Supply. In 11th Annual East Coast Conference on Aerospace and Navigational Electronics, Western Periodicals, 1964.

KIERNER, F. A., JR.: A Digital Command System for Satellites. NASA TN D–1076, 1962.

KLASS, P. J.: Thin-Film Solar Cells Boost Output Ratio. Av. Wk., Nov. 29, 1965, p. 67.

KOERNER, T. W.: Static Power Conversion for Spacecraft. Astronaut. Aerospace Eng., vol. 1, May 1963, p. 89.

KRAUSZ, A.; AND ROBINSON, R. L.: The Electric Power Supply of the Orbiting Geophysical Observatory. Unmanned Spacecraft Meeting. AIAA publ. CP–12, 1965.

KREITH, F.: Radiation Heat Transfer for Spacecraft and Solar Powerplant Design. International Textbook Co. (Scranton), 1962.

LaVan, J. T.: Unconventional Inertial Sensors. Space/Aero., vol. 41, Dec. 1963, p. 73.

LeCompte, G. W.; and Bland, J. G.: Simply Mechanized Attitude Control for Spinning Vehicles. J. Spacecraft and Rockets, vol. 1, Nov.–Dec. 1964, p. 593.

Lemke, L. C.: Thermal Simulation of a Satellite. AIAA paper 65–475, 1965.

Lemke, L. C.; and Tatro, R. E.: Analytical Techniques for Temperature Predictions for the SATAR I Scientific Satellite. AIAA paper 65–436, 1965.

Lines, A. W.: Design of Spacecraft for Experiments in the ESRO Scientific Program. J. Roy. Astro. Soc., vol. 69, Nov. 1965, p. 759.

Lingle, J. T.: Reliable Energy Conversion Power Systems for Space Flight. IEEE Trans., AS–3, June 1965, p. 543.

Lipkis, R. P.: Temperature Control of Spacecraft. In Materials for Missiles and Spacecraft, E. R. Parker, ed., McGraw-Hill Book Co., Inc., 1963.

Lloyd, W. W.: The Theory and Application of Solar Cells. J. Brit. Interplanetary Soc., vol. 19, 1963, p. 110.

Lokerson, D. C.: Synchronization and Control of the IMP Information Processing System. In Record of the International Space Electronics Symposium, IEEE, New York, 1964.

Ludwig, G. H.: The Orbiting Geophysical Observatories. NASA TN D–2646, 1965. (Also Space Sci. Rev., vol. 2, 1963, p. 175.)

Lunde, B. K.: A Reliable Earth Sensor for Attitude Sensing. In Proceedings of the 10th Annual East Coast Conference on Aerospace and Navigational Electronics, Western Periodicals, 1963.

Lunde, B. K.: Horizon Sensing for Attitude Determination. In Torques and Attitude Sensing in Earth Satellites, S. F. Singer, ed., Academic Press, 1964. (Also NASA TM X–956, 1964.)

Mar, J.: Earth Satellite Design, Materials and Environmental Testing. AD 256835, 1961.

Marcotte, P. G.: IMP D&E Feasibility Study. NASA TM X–55166, 1964.

McElvain, R. F.: Satellite Angular Momentum Removal Utilizing the Earth's Magnetic Field. In Torques and Attitude Sensing in Earth Satellites, S. F. Singer, ed., Academic Press, 1964.

McKellar, L. A.: Effects of the Spacecraft Environment on Thermal Control Materials Characteristics. AD 274162, 1962.

McKeown, D.; Fox, M. G.; and Schmidt, J. J.: Effects of Atomic and Molecular Impacts on Spacecraft. AIAA J., vol. 3, Apr. 1965, p. 710.

Merritt, S. Y.: Interface Problems in the Use of Aerospace Static Power Conversion Equipment. IEEE Trans., AS–3, June 1965, p. 436.

Molitor, J. H.; and Kaplan, M. H.: Design and Performance of Ion Engine Systems for the Control of Earth Satellites. J. Spacecraft and Rockets, vol. 2, Sept. 1965, p. 712.

Moyer, R. G.; Katucki, R. J., and Davis, L. K.: A System for Passive Control of Satellites through the Viscous Coupling of Gravity Gradient and Magnetic Fields. AIAA paper 64–659, 1964.

Mueller, G. E.: Practical Aspects of Data Processing and Encoding for Space Communications. NASA CR–55017, 1963.

Newkirk, H. L.: Pendulum-Type Nutation Damper Used in the NASA Atmospheric Structure Satellite, S–6. AD 616118, 1965.

Nichol, K. C.: Research and Investigation on Satellite Attitude Control. AD 468354, 1965.

OSTHOFF, R. C.: Batteries. International Sci. Tech., Nov. 1964, p. 48.

OTTEN, D. D.: Attitude Control for an Orbiting Observatory—OGO. Control Eng., vol. 10, Dec. 1963, p. 81.

PARKER, E. R., ED.: Materials for Missiles and Spacecraft. McGraw-Hill Book Co., Inc., 1963.

PAULKOVICH, J.: Dynamic Solar Cell Power System Simulation. NASA TM X–55308, 1965.

PECK, D. S.; AND SHENNUM, R. H.: Long-Life Electronics. Space/Aero., vol. 45, Mar. 1966, p. 81.

PHENIX, J. E.: Structural Design Analysis and Testing of the Geos Satellite. AD 476286, 1965.

PHILLIPS, G. G.; MAR, J.; AND JACQUES, P.: Payload Packaging Design— Alouette Satellite. AD 422758, 1963.

PLAMONDON, J. A.: Analysis of Movable Louvers for Temperature Control. J. Spacecraft and Rockets, vol. 1, Sept. 1964, p. 492.

PORTER, R. N.; AND EVANS, D. D.: Advanced Propulsion Systems for Unmanned Spacecraft. Astronaut. Aeron., vol. 6, June 1965, p. 75.

QUASIUS, G.; AND MCCANLESS, F.: Star Trackers and Systems Design. Spartan Books (Washington), 1966.

RADANY, E. W.: Pegasus Spacecraft Attitude Sensing System. AIAA paper 65–382, 1965.

RAY, K. A.; AND WINICUR, D. H.: A Large Area Solar Cell Array. AIAA paper 64–739, 1964.

RAYMOND, H. A.: Orbit Injection Control for Harp. Can. Aero. Space J., vol. 11, May 1965, p. 153.

ROBERSON, R. E.: Methods for the Control of Satellites and Space Vehicles. AD 250270 and AD 254052, 1960.

ROGERS, S. C.: Radiation Damage to Satellite Electronic Systems. IEEE Trans., NS–10, Jan. 1963, p. 97.

ROTH, C. E.: Reliability in Space Vehicles. Engineering Publishers (Elizabeth), 1965.

SAVET, P. H.: Gyroscopes. International Sci. and Tech., Jan. 1966, p. 50.

SAWYER, R. H.: Secondary Propulsion System Capabilities as Compared With Flight Control Requirements. Unmanned Spacecraft Meeting. AIAA pub. CP–12, 1965.

SCHEELE, P. F.; AND SEWELL, B. L.: S–17 OSO Communications System. In Proceedings of the 1963 National Telemetering Conference, IEEE, New York, 1963.

SCOTT, W. H.: The Engineering Design of the Orbiting Astronomical Observatory. In The Observatory Generation of Satellites, NASA SP–30, 1963.

SEIGER, H. N.: Large Size Sealed Nickel-Cadmium Cells. IEEE Trans., AS–3, June 1965, p. 533.

SEYLAR, G. R.: Telemetry System Functions and Calibrations for Beacon Explorer Satellite BE–C. AD 472048, 1965.

SHATZ, B.; AND BERNSTEIN, M.: Development of Vibration Design Procedures for the Orbiting Astronomical Observatory. Paper at the 31st Symposium on Shock, Vibration, and Associated Environments, 1962.

SHEIR, R. C.: Sealed Secondary Cells for Space Power Systems. J. Spacecraft and Rockets, vol. 3, Jan.–Feb. 1966, p. 68.

SHURE, L. I.; AND SCHWARTZ, H. J.: Survey of Electric Power Plants for Space Applications. NASA TM X–52158, 1965.

SMITH, A. H.: Progress in Photovoltaic Energy Conversion. NASA TM X–57120, 1966.

SMITH, R. E., ED.: Space Environment Criteria Guidelines for Use in Space Vehicle Development (1965 revision). NASA TM X–53273, 1965.

STAMBLER, I.: Surface Effects in Space. Space/Aero., vol. 45, Feb. 1966, p. 95.

STERNBERG, S.; AND LANDON, V. D.: Satellite Systems. *In* System Engineering Handbook, R. E. Machol, ed., McGraw-Hill Book Co., Inc., 1965.

STEVENSON, J. A.; AND GRAFTON, J. C.: Radiation Heat Transfer Analysis for Space Vehicles. AD 271917, 1961.

STURGEON, C. W.: On-Board Storage and Processing of Spacecraft Commands. ISA Proc., vol. 8, 1962, p. 43.

SZEGO, G. C.; AND TAYLOR, J. E., EDS.: Space Power Systems Engineering. Academic Press, 1966.

SZEGO, G. C.: Space Power Systems State of the Art. J. Spacecraft and Rockets, vol. 2, Sept. 1965, p. 641.

THOMSON, J. D.; AND MASON, A. E.: The Communication and Data Handling Subsystem for the Advanced Orbiting Solar Observatory. IEEE Trans., AS–3, June 1965, p. 345.

TOOLEY, J. R.; AND SERRAFIAN, G. P.: A Programmable Spacecraft Data Handling System. *In* Record of the International Space Electronics Symposium, IEEE, New York, 1964.

TOSSMAN, B. E.: Eddy Current Ball-in-Ball Damper. AIAA paper 65–404, 1965.

ULE, L. A.: Orientation of Spinning Satellites by Radiation Pressure. AIAA J., vol. 1, July 1963, p. 1575.

VAN VLIET, R. M.: Passive Temperature Control in the Space Environment. Macmillan Co., 1964.

VICKERS, J. M. F.: Thermal Scale Modeling. Astronaut. Aeron., vol. 3, May 1965, p. 34.

VICTOR, W. K.; RICHTER, H. L.; AND EYRAUD, J. P.: Explorer Satellite Electronics. IRE Trans., MIL–4, 1960, p. 78.

VOLKOFF, J. J.: System Protection Requirements for the Resistance of Meteoroid Penetration Damage. J. Spacecraft and Rockets, vol. 3, Jan. 1966, p. 26.

WAGNER, C. L., JR.: Ariel I—Evolution of Its Structure. NASA TN D–1903, 1963.

WARREN, H. R.; AND MAR, J.: Structural and Thermal Design of the Topside Sounder Satellite. Can. Aero. Sp. J., vol. 8, Sept. 1962, p. 161.

WARREN, H. R.; AND MACNAUGHTON, J. D.: The Use of Extendable Booms for Space Aerials and for Satellite Attitude Control. Paper at the 14th International Astronautical Congress, 1963.

WENZINGER, C. J.; AND CARLETON, H.: The Solar Power Supply System for Orbiting Astronomical Observatories. AIAA paper 63–217, 1963.

WHITE, H. D.: Evolution of Satellite PFM Encoding Systems. NASA X–631–65–114, 1965.

WHITE, J. S.; SHIGEMOTO, F. H.; AND BOURQUIN, K.: Satellite Attitude Control Utilizing the Earth's Magnetic Field. NASA TN D–1068, 1961.

WHITE, J. S.; AND HANSEN, Q. M.: Study of a Satellite Attitude Control System Using Integrating Gyros as Torque Sources. NASA TN D–1073, 1961.

WIEBELT, J. A.; PARMER, J. F.; AND KNEISSL, G. J.: Spacecraft Temperature Control by Thermostatic Fins-Analysis. NASA CR–155, 1965.

WILSON, T. G.; AND MOORE, E. T.: Power Conditioning—Inversion, Conversion, and Regulation. NASA CR–59538, 1964.

WINTANEN, T.: Evolution of the ANNA–1 Satellite Optical Beacon. AF-CRL–63–56, Air Force Cambridge Research Laboratories, 1963.

WOLFGANG, J. L.: Design Philosophy of the IMP Information Processing System. *In* Record of the 1964 International Space Electronics Symposium, IEEE, New York, 1964.

WOLMAN, W.: Reliability Program Elements for Satellite Systems. NASA TM X–51608, 1964.

WOLMAN, W.: The Status of Reliability Assessment for Unmanned Satellites. *In* Proceedings of the 11th National Symposium on Reliability and Quality Control, IEEE, New York, 1965.

WORK, G. A., ET AL.: Design and Performance of Ion Engine Systems for Control of Earth Satellites. AIAA paper 64–501, 1964.

WORMSER, E. M.; AND ARCK, M. H.: Infrared Navigation Sensors for Space Vehicles. *In* Guidance and Control, R. E. Roberson and J. S. Farrior, eds., Academic Press, 1962.

XYDIS, F. E.: Designing Long-Life Satellites. Aerospace Eng., vol. 21, Sept. 1962, p. 84.

YAGERHOFER, F. C.: The Design of the United Kingdom Scientific Satellite Solar Power System. ARS paper 2498–62, 1962.

ZIPKIN, M. A.; AND EDWARDS, R. N., EDS.: Power Systems for Space Flight. Academic Press, 1963.

Chapter 10

ANON.: Opportunities for Participation in Space Flight Investigations. (Semiannual.) NASA, 1965.

ANON.: Space Measurements Survey. Electro-Optical Systems. AD 415161, 1962, and AD 465914, 1965.

GOLOMB, S.: Influence of Data Processing on the Design and Communication of Experiments. J. Res. NBS, Sec. D, Radio Science, vol. 68D, Sept. 1964, p. 1021.

HEACOCK, R. L.: Scientific Instruments in Space Exploration. Science, vol. 142, Oct. 11, 1963, p. 188.

KING-HELE, D.: Satellites and Scientific Research. Dover Publications (New York), 1965.

RICHTER, H. L., ED.: Instruments and Spacecraft, October 1957–March 1965. NASA SP–3028, 1966.

WILLMORE, A. P.: On Board Data Processing in Spacecraft as an Aid to Optimising the Design of Experiments. Paper at the 6th COSPAR Meeting, 1965.

Chapter 11

AARONS, J., ED.: Radio Astronomical and Satellite Studies of the Atmosphere. Interscience Publishers (New York), 1963.

ANON.: Manual for Fluxgate Ferrite Magnetometer. NASA CR–58342, 1964.

ANON.: Advances in Scintillation and Semiconductor Radiation Detection. Atomics, July/Aug. 1965, p. 11.

ANON.: Experiments on Explorer XV, Project SERB, Study on the Enhanced Radiation Belts. (Final report.)   NASA CR–67106, Bell Laboratories, 1964.

ANON.: Proceedings of the Contemporary Geodesy Conference.   Geophysical Monograph No. 4, Smithsonian Institution, 1962.

ANON.: Project Able-3, Final Mission Report. (Explorer VI Instrumentation.)   AD 245934, Space Technology Laboratories, 1960.

ANON.: Micrometeoroid Satellite (Explorer XIII) Stainless-Steel Penetration Rate Experiment.   NASA TN D–1986, 1963.

ARENDT, P. R.; PAPAYOANOU, A.; AND SOICHER, H.: Determination of the Ionospheric Electron Content Utilizing Satellite Signals.   Proc. IEEE, vol. 53, Mar. 1965, p. 268.

ARNOLD, J. T.: Spin Precession Magnetometers for Applications in Space. *In* ISA Proceedings of the National Aerospace Instrument Symposium, ISA, Philadelphia, 1962.

BAKER, K. D.; HAYCOCK, O. C.; AND ULWICK, J. C.: Experiences With the Impedance Probe on Satellites.   IEEE Proc., vol. 52, Sept. 1964, p. 1029.

BAKER, K. D.; DESPAIN, A. M.; AND ULWICK, J. C.: Simultaneous Comparison of RF Probe Techniques for Determination of Ionospheric Electron Density. IEEE Int. Conv. Rec., vol. 13, pt. 4, 1965, p. 16.

BAUERNSCHUB, J. P.: Mechanisms for Spacecraft Optical Instrumentation. NASA TN D–3008, 1965.

BECK, C. W., ET AL.: Solar Wind Measurement Technique II—Solar Plasma Energy Spectrometers. *In* Proceedings 17th National Aerospace Electronics Conference, IEEE, New York, 1965.

BETTINGER, R. T.: A Thermal Equalization Probe Experiment for a Satellite. AD 457239, 1964.

BETTS, J. F.; AND O'HALLORAN, G. J.: Miniaturized Bendix Time-of-Flight Mass Spectrometers.   Paper presented at the 11th Annual Conference on Mass Spectroscopy and Allied Topics, 1963.

BLOOM, A. L.: Principles of Operation of the Rubidium Vapor Magnetometer. Appl. Optics, vol. 1, 1962, p. 61.

BOWEN, P. J., ET AL.: Measurement of Electron Temperature and Concentration from a Spacecraft.   Proc. Roy. Soc., London, Series A, vol. 281, Oct. 6, 1964, p. 514.

BOWHILL, S. A.: Electron Density Measurements by the Radio Propagation Technique.   COSPAR Info. Bull., no. 17, 1964.

BOYD, R. L. F.; AND WILLMORE, A. P.: A Method of Studying the Energy Distributions of Ionospheric Ions and Electrons. *In* Space Research III, W. Priester, ed., John Wiley & Sons, Inc., 1963.

BRACE, L. H.; AND REDDY, B. M.: Latitudinal Variations of Electron Temperature and Concentration from Satellite Probes.   NASA TM X–55262, 1965.

CAHILL, L. J.: Magnetic Field Measurements in Space.   Space Sci. Rev., vol. 1, 1962, p. 399.

CLARK, J. F.: The Role of Rockets, Satellites and Space Probes in Atmospheric Electricity Research. *In* Problems of Atmospheric and Space Electricity, S. C. Coroniti, ed., Elsevier Publishing Co. (Amsterdam), 1965.

CLINE, T. L.; AND SERLEMITSOS, P.: A Double Gamma-Ray Spectrometer to Search for Positrons in Space.   NASA TN D–1464, 1962.

CRAIG, S. E.: Satellite-to-Satellite Radio Propagation Experiment.   AD 628222, 1965.

CRAWFORD, F. W.; AND HARP, R. S.: The Resonance Probe—A Tool for Ionospheric and Space Research.   J. Geophys. Res., vol. 70, Feb. 1, 1965, p. 587.

DAVISON, E. H.; AND WINSLOW, P. C., JR.: Micrometeoroid Satellite (Explorer XVI) Stainless-Steel Penetration Rate Experiment. NASA TN D–2445, 1964.

DIETER, C. L.: Instrumentation for Satellite Studies of the Ionosphere. *In* Radio Astronomical and Satellite Studies of the Atmosphere, J. Aarons, ed., Interscience Publishers, 1963.

DOLGINOV, S. S.; ZUGGOV, L. N.; AND SELYUTIN, V. A.: Magnetometers in the Third Soviet Earth Satellite. *In* Artificial Earth Satellites, vol. 4. Plenum Press, 1961.

DOOLITTLE, R. F.; AND GRAVES, C. D.: The Application of Scintillation Chambers to Space Research. Paper at the Second Symposium on Photo-Electric Image Devices, London, 1961.

FILLIUS, R. W.: Satellite Instruments Using Solid State Detectors. NASA CR–53510, 1963.

FILLIUS, R. W.; AND MCILWAIN, C. E.: Solid-State Detectors for Inner Zone Protons. *In* Space Research III, W. Priester, ed., John Wiley & Sons., Inc., 1963.

FISHER, P. C., ET AL.: Soft Particle Detectors. IEEE Trans., NS–10, Jan. 1963, p. 211.

FLOWERDAY, T. W.: An Instrument for Measuring Ion Composition of the Upper Atmosphere. IEEE Trans., IM–13, Mar. 1964, p. 14.

FRIEDMAN, H.: The Vanguard Instrument Package. Astronautics, vol. 2, Aug. 1957, p. 66.

FRIICHTENICHT, J. F.: Response of Microphone Meteorite Detectors to the Impact of High Velocity Particles. NASA CR–63126, 1965.

GARRIOTT, O. K.; AND DE MENDONCA, F.: A Comparison of Methods Used for Obtaining Electron Content From Satellite Observations. J. Geophys. Res., vol. 68, Sept. 1, 1963, p. 4917.

GILMOUR, A. S.: Radio-Frequency Mass Spectrometers and Their Applications in Space. IEEE Trans., AS–1, 1963, p. 1404.

GOETTELMAN, R. C., ET AL.: The Meteoroid and Cosmic-Ray Environment of Space Vehicles and Techniques for Measuring Parameters Affecting Them. AD 262013, 1961.

GREENFIELD, R. J.; ROSSONI, J. P.; AND SCONZO, P.: Atmospheric Density Determination from Satellite Observations. AD 606698, 1964.

GRYCAN, J.: Certain Untypical Effects Noticed in Radio Observations of Artificial Earth Satellites. COSPAR Info. Bull., no. 26, Oct. 1965.

HEPPNER, J. P., ET AL.: Explorer 10 Magnetic Field Measurements. J. Geophys. Res., vol. 68, Jan. 1, 1963, p. 1.

HEPPNER, J. P., ET AL.: Project Vanguard Magnetic-Field Instrumentation and Measurements. *In* Space Research, H. Kallmann-Bilj, ed., Interscience Publishers, 1960. (Also NASA TN D–486, 1960.)

HOUSTON, R. C.: Ionospheric Studies Utilizing Artificial Earth Satellite Radio Signals. AD 615585, 1964.

HUBBARD, E. L.: Nuclear Particle Spectrometers for Satellites and Space Probes. IRE Trans., NS–9, June 1962, p. 357.

HUNDLEY, R. O.: Ultraviolet Spectroscopy of the Upper Atmosphere. NASA CR–53508, 1963.

HUNTER, W. R.: Extreme Ultraviolet Detection With the Bendix Channel Multiplier. *In* Space Research III, W. Priester, ed., Interscience Publishers, 1963.

JACCHIA, L. G.: Variations in the Earth's Upper Atmosphere as Revealed by Satellite Drag. Rev. Mod. Phys., vol. 35, 1963, p. 973.

JENNISON, R. C.; AND MCDONNELL, J. A. M.: A Technique for the Detection and Determination of the Velocity, Mass, Radiant, Charge, and Flux of Micrometeorite Particles in Space. Planet. Space Sci., vol. 12, June 1964, p. 627.

JUDGE, D. L.; MCLEOD, M. G.; AND SIMS, A. R.: The Pioneer 1, Explorer 6, and Pioneer 5 High Sensitivity Transistorized Search Coil Magnetometer. IRE Trans., SET–6, Sept. 1960, p. 114.

KATZENSTEIN, H. S.; AND ZIEMBA, F. P.: A High Energy Proton Spectrometer Utilizing Semiconductor Detectors for Space Physics Experimentation. AD 600156, 1964.

KAULA, W. M.: The Use of Artificial Satellites for Geodesy. AAS paper, 1965.

KAULA, W. M.: International Dictionary of Geophysics, Dynamic Satellite Geodesy. NASA TM X–51584, 1964.

KEATING, G. M., ET AL.: Determination of Mean Atmospheric Densities from the Explorer IX Satellite. NASA TN D–2895, 1965.

KERWIN, W. J.; MUNOZ, R. M.; AND PRUCHA, M. J.: Solar Wind Measurement Techniques I—An Improved Magnetometer for Deep Space Use. In Proceedings of the 17th National Aerospace Electronics Conference, IEEE, Dayton, 1965.

KING-HELE, D. G.: Properties of the Atmosphere Revealed by Satellite Orbits. In Progress in the Astronautical Sciences, S. F. Singer, ed., Interscience Publishers, 1962.

KING-HELE, D. G.: The Rotational Speed of the Upper Atmosphere Determined from Changes in Satellite Orbits. Planetary and Space Sci., vol. 12, Sept. 1964, p. 835.

KREISMAN, W. S.: Development of Cold Cathode Ionization Gauges for Space Vehicles. NASA CR–57594, 1964.

LANGE, B.: The Drag-Free Satellite. AIAA J., vol. 2, Sept. 1964, p. 1590.

LING, S. C.: Fluxgate Magnetometer for Space Applications. J. Spacecraft and Rockets, vol. 1, 1964, p. 175.

LUDWIG, G. H.: Cosmic-Ray Instrumentation in the First U.S. Earth Satellite. Rev. Sci. Inst., vol. 30, Apr. 1959, p. 223.

LUDWIG, G. H.; AND WHELPLEY, W. A.: Corpuscular Radiation Experiment of Satellite, 1959 Iota (Explorer VII). J. Geophys. Res., vol. 65, Apr. 1960, p. 1119.

MAY, E. C.; AND KAHLE, A. B.: On the Satellite Determination of High-Altitude Water Vapor. J. Geophys. Res., vol. 69, Oct. 1, 1964, p. 4141.

MUELLER, I. I.; AND RACKIE, J. D.: Gronimetric and Celestial Geodesy. Frederick Ungar Pub. Co., 1966.

MUELLER, I. I.: The Geodetic Applications of Satellites. AD 605657, 1964.

NAGY, A. F.; AND FARUI, A. Z.: Ionospheric Electron Density and Body Potential Measurements by a Cylindrical Probe. NASA CR–59158, 1964.

NARCISI, R. S.; AND BAILEY, A. D.: Mass Spectrometric Measurements of Positive Ions at Altitudes from 64 to 112 Kilometers. J. Geophys. Res., vol. 70, Aug. 1, 1965, p. 3687.

NARDONE, L. J.; AND STUART, R. D.: Design, Construction, and Testing of Instrumentation for the Investigation of the Electrical Structure of the Upper Atmosphere. AD 436588, 1963.

NEWTON, G. P.; HOROWITZ, R.; AND PRIESTER, W.: Atmospheric Density and Temperature Variations From the Explorer XVII Satellite and a Further Comparison With Satellite Drag. Planetary and Space Sci., vol. 13, July 1965, p. 599.

NEWTON, R. R.: Geodesy by Satellite. Science, vol. 144, May 15, 1964, p. 803.

OGILVIE, K. W.; LIND, D. L.; AND WILKERSON, T. D.: A Triaxial Electron Detector. Paper at the Sixth COSPAR Meeting, 1965.

ORTNER, J.; AND MASELAND, H., EDS.: Introduction to Solar Terrestrial Relations. D. Reidel Publishing Co. (Dordrecht), 1965.

O'SULLIVAN, W. J.; COFFEE, C. W.; AND KEATING, G. M.: Air Density Measurements From the Explorer IX Satellite. In Space Research III, W. Priester, ed., John Wiley & Sons, Inc., 1963.

PAOLINI, F. R., ET AL.: Measurements in the Radiation Belts from Hitchhiker I. In Space Research V, D. G. King-Hélé, P. Muller, and G. Righini, eds., John Wiley & Sons, Inc., 1965.

PETERS, B., ED.: Cosmic Rays, Solar Particles, and Space Research. Academic Press, 1963.

RAWCLIFFE, R. D., ET AL.: Measurement of Vertical Distribution of Ozone From a Polar Orbiting Satellite. J. Geophys. Res., vol. 68, Dec. 15, 1963, p. 6245.

REAGAN, J. B., ET AL.: Satellite Instrumentation for the Measurement of Auroral Phenomenon. IEEE Trans., NS–11, June 1964, p. 441.

REAGAN, J. B.; AND SMITH, R. V.: Instrumentation for Space Radiation Measurements, I. IEEE Trans., NS–9, Jan. 1962, p. 172.

ROSEN, A.; AND FARLEY, T. A.: Character of the Van Allen Radiation Zones as Measured by the Scintillation Counter on Explorer VI. J. Geophys. Res., vol. 66, July 1961, p. 2013.

ROSSONI, J. P., ET AL.: Atmospheric Density Determination From Satellite Observations. In Celestial Mechanics and Astrodynamics, V. G. Szebehely, ed., Academic Press, 1964.

ROWLAND, J. H., ET AL.: Instrumentation for Space Radiation Measurements. IEEE Trans., NS–10, Jan. 1963, p. 178.

RUDDOCK, K. A.: Optically Pumped Rubidium Vapor Magnetometer for Space Experiments. In Space Research II, H. C. van de Hulst, C. de Jager, and A. F. Moore, eds., Interscience Publishers, 1961.

SAGALYN, R. C.: Space Electricity—Physical Problems and Experimental Techniques. In Problems of Atmospheric and Space Electricity, S. C. Coroniti, ed., Elsevier Publishing Co. (Amsterdam), 1965.

SAGALYN, R. C.; SMIDDY, M.; AND BHARGAVA, Y. N.: Satellite Measurements of the Diurnal Variation of Electron Temperatures in the F Region. In Space Research V, D. G. King-Hele, P. Muller, and G. Righini, eds., John Wiley & Sons, Inc., 1965.

SERBU, G. P.; BOURDEAU, R. E.; AND DONLEY, J. L.: Electron Temperature Measurements on the Explorer VIII Satellite. J. Geophys. Res., vol. 66, Dec. 1961, p. 4313.

SHAPIRO, I. I.: New Method for Investigating Micrometeoroid Fluxes. J. Geophys. Res., vol. 68, Aug. 15, 1963, p. 4697.

SHARP, R. D., ET AL.: Satellite Measurements of Low-Energy Electrons in the Northern Auroral Zone. J. Geophys. Res., vol. 69, July 1, 1964, p. 2721.

SINGER, S. F.: Artificial Modification of the Earth's Radiation Belt. Adv. Astronautical Sci., vol. 4, 1959, p. 335.

SINGER, S. F.: Satellite Instrumentation—Results for the IGY. *In* Ten Steps Into Space. Franklin Institute, 1958.

SMITH, L. G.: Langmuir Probes for Measurements in the Ionosphere. COSPAR Info. Bull., no. 17, 1964.

SMITH, R. A.: Detectors for Ultraviolet, Visible, and Infrared Radiation. Applied Optics, vol. 4, June 1965, p. 631.

SWENSON, J.: The Utilization of Ionosphere Beacon Satellites. COSPAR Info. Bull., no. 15, May 1960.

TAYLOR, H. A.; BRINTON, H. C.; AND SMITH, C. R.: Positive Ion Composition in the Magnetoionosphere Obtained From the OGO-A Satellite. J. Geophys. Res., vol. 70, Dec. 1, 1965, p. 5769.

TAYLOR, H. A.; BRINTON, H. C.; AND SMITH, C. R.: Instrumentation for Atmospheric Composition. Proceedings of the 1962 National Aerospace Instrumentation Symposium. Instrument Society of America, 1962.

TITHERIDGE, J. E.: The Refraction of Satellite Signals—II. J. Atm. Terr. Phys., vol. 26, 1964, p. 177.

TITHERIDGE, J. E.: The Calculation of the Electron Density in the Ionosphere From Elevation-Angle Measurements on Artificial Satellites. J. Geophys. Res., vol. 66, Oct. 1961, p. 3103.

TIURI, M.: Observations of Worldwide Ionospheric Disturbances Associated With Satellites. Paper at the Sixth COSPAR Meeting, 1965.

TWOMEY, S.: On the Deduction of the Vertical Distribution of Ozone by Ultraviolet Spectral Measurements From a Satellite. J. Geophys. Res., vol. 66, July 1961, p. 2153.

ULWICK, J. C.; PFISTER, W.; AND MCINERNEY, R. E.: Direct Satellite Probe Measurements of Ionosphere Irregularities. *In* Space Research V, D. G. King-Hele, P. Muller, and G. Righini, eds., John Wiley & Sons, Inc., 1965.

VEIS, G., ED.: The Use of Artificial Satellites for Geodesy. Interscience Publishers, 1963.

VENKATESWARAN, S. V.; MOORE, J. G.; AND KRUEGER, A. J.: Determination of the Vertical Distribution of Ozone by Satellite Photometry. J. Geophys. Res., vol. 66, June 1961, p. 1751.

WAGNER, C. A.: Determination of the Ellipticity of the Earth's Equator From Observations of the Drift of the Syncom II Satellite. NASA TN D-2759, 1965.

WEST, H. I.; MANN, L. G.; AND BLOOM, S. D.: Some Electron Spectra in the Radiation Belts in the Fall of 1962. *In* Space Research V, D. G. King-Hele, P. Muller, and G. Righini, eds., Interscience Publishers, 1965.

WETMORE, W. C.: Soviets Describe Equipment for Elektron. Av. Wk., June 8, 1964, p. 49.

WILLMORE, A. P.: Instrumentation for the First Anglo-American Scout Satellite. *In* Space Research and Technology, G. V. E. Thompson, ed., Gordon & Breach, 1962.

WIRTANEN, T.: Evolution of the ANNA-1 Satellite Beacon. AD 402213, 1963.

WOLFE, J. H.; SILVA, R. W.; AND MYERS, M. A.: Preliminary Results from the Ames Research Center Plasma Probe Observations of the Solar-Wind-Geomagnetic Field Interaction Region on IMP-II and OGO-1. Paper at the Sixth COSPAR Meeting, 1965.

ZACHARY, W. W., ET AL.: Determination of Ionosphere Parameters by Means of a Satellite Antenna-Type Probe. AD 270723, 1961.

ZARKHIN, B. I., ET AL.: RF Mass Spectrometer for the "Elektron" Satellites. Kosmicheskie Issledovaniia, vol. 3, Sept.–Oct. 1965, p. 768.

Chapter 12

BADER, M.: Preliminary Explorer XII Data on Protons Below 20 keV. *In* Space Research III, W. Priester, ed., Interscience Publishers, 1963. (Also, J. Geophys. Res., vol. 67, Dec. 1962, p. 5007.)

BADER, M.; FRYER, T. B.; AND WITTEBORN, F. C.: Two Instruments for Measuring Distributions of Low-Energy Charged Particles in Space. NASA TN D–1035, 1961.

BEHRING, W. E.; NEUPERT, W. M.; AND LINDSAY, J. C.: Preliminary Solar Flare Observations with a Soft X-Ray Spectrometer on the Orbiting Solar Observatory. *In* Space Research III, W. Priester, ed., John Wiley & Sons, Inc., 1963.

BRIDGE, H., ET AL.: Preliminary Results of Plasma Measurements on IMP–A. *In* Space Research V, D. G. King-Hele, P. Muller, and G. Righini, eds., John Wiley & Sons, Inc., 1965.

BRYANT, D. A.; LUDWIG, G. H.; AND McDONALD, F. B.: A Scintillation Counter Telescope for Charge and Mass Identification of Primary Cosmic Rays. NASA TN D–1757, 1963.

CHUBB, T. A., ET AL.: Results From the NRL Solar Radiation Satellite. *In* Space Research II, H. C. van de Hulst, C. de Jager, and A. F. Moore, eds., Interscience Publishers, 1962.

DUNKELMAN, L.; HENNES, J. P.; AND FOWLER, W. B.: Middle Ultraviolet Photoelectric Detection Techniques. *In* Space Research III, W. Priester, ed., John Wiley & Sons, Inc., 1963.

FLOYD, F. W., JR.: A Solar Wind Deuterium Detector and Charge-Spectrum Analyzer. NASA CR–59788, 1964.

GOLDBERG, L.: Solar Experiments. Astron. J., vol. 65, June 1960, p. 274.

HICKS, D. B.; REID, L.; AND PETERSON, L. E.: X-Ray Telescope for an Orbiting Solar Observatory. IEEE Trans., NS–12, Feb. 1965, p. 54.

HILLS, R. S.: Electronic Instrumentation for Ionospheric and Extreme Ultraviolet Radiation Measurements. NASA CR–64074, 1965.

KREPLIN, R. W.: NRL Solar Radiation Monitoring Satellite: Description of Instrumentation and Preliminary Results. *In* Space Research V, D. G. King-Hele, P. Muller, and G. Righini, eds., John Wiley & Sons, Inc., 1965.

LAMPORT, J. E.: Instrumentation for the Measurement of Energetic Particles in Space. *In* ISA Proceedings of the National Aerospace Instrument Symposium, ISA, Philadelphia, 1962.

LILLER, W.: The Harvard Solar Satellite Project. J. Quant. Spectrosc. Rad. Trans., vol. 2, 1962, p. 519.

LINDSAY, J. C.: Solar Radiation Monitoring. IAS paper 63–2, 1963.

LINDSAY, J. C.; AND GIACCONI, R.: High Resolution (5 arc sec) X-Ray Telescope for Advanced Orbiting Solar Observatory. NASA X–614–63–112, 1963.

LOCKWOOD, J. A.; AND FRILING, L. A.: Design of a Neutron Monitor for Measurements in Space. NASA CR–59403, 1964.

MANDEL'STAM, S. L., ET AL.: Investigations of the Sun's X-Radiation—II. Planetary and Space Sci., vol. 11, Jan. 1963, p. 61.

MEL'NIKOV, V. V., ET AL.: Experimental Application of an Electrostatic Analyzer Aboard "Cosmos-12." NASA TT F–9672, 1965.

NEUPERT, W. M.; UNDERWOOD, J. H.; AND LINDSAY, J. C.: An Extreme Ultraviolet Spectroheliograph for Advanced Orbiting Solar Observatory. NASA X–614–65–310, 1965.

OGILVIE, K. W.: Solar Proton Experiments. *In* Proceedings of the Plasma Space Science Symposium, C. C. Chang and S. S. Huang, eds., D. Reidel Publishing Co. (Dordrecht), 1965.

OGILVIE, K. W., ET AL.: A Detector-Analyzer for Studying the Interplanetary Plasma. NASA TN D–2111, 1964.

POUNDS, K. A.: Instrumentation of Satellite UK1 for Obtaining Low Resolution Solar X-Ray Spectra. *In* Space Research III, W. Priester, ed., John Wiley & Sons, Inc., 1963.

RENSE, W. A.: Techniques for Rocket Solar UV and for UV Spectroscopy. Space Sci. Rev., vol. 5, Mar. 1966, p. 234.

RENSE, W. A.: Recent Advances in Space Solar Observatory Instrumentation. ARS J., vol. 30, Apr. 1960, p. 313.

RUDY, A. L.; AND ALLER, L. H.: A Feasibility Study of a Radiation Analyzer for the Zodiacal Light. NASA CR–56313, 1964.

SERBU, G. P.: Results From the IMP–I Retarding Potential Analyzer. *In* Space Research V, D. G. King-Hele, P. Muller, G. Righini, eds., John Wiley & Sons., Inc., 1965.

TOUSEY, R.: Observations of the White-Light Corona by Rocket. Annales d'Astrophysique, vol. 28, 1965, p. 600.

UNDERWOOD, J.; AND WHITE, W.: A Dual Telescope for Spectroheliography in the Extreme Ultra-violet. NASA X–641–65–470, 1965.

VASIL'EV, B. N., ET AL.: Study of the Sun's X-Radiation—III. Planetary and Space Sci., vol. 11, Dec. 1963, p. 1493.

YOUNG, R. M.; AND STOBER, A. K.: A Soft X-ray Photoionization Detector. NASA TN D–3169, 1966.

ZIOCK, K.: A Proposed Orbiting X-Ray Telescope. NASA CR–56815, 1964.

Chapter 13

BENJAMIN, H., ET AL.: Satellite-Borne Instrumentation for Observing Flux of Heavy Primary Cosmic Radiation. J. Franklin Inst., vol. 271, Apr. 1961, p. 275.

BERMAN, A. I.: Observatories in Space. Sci. Am., vol. 209, Aug. 1963, p. 29.

BURNS, J.: OAO Image Converter Research. NASA CR–55425, 1963.

CHOMET, M.; GROSS, S.; AND STONE, R.: A Cosmic Noise Radio Astronomy Experiment for the Ionospheric Explorer. IEEE Conv. Rec., vol. 12, pt. 8, 1964, p. 156.

CODE, A. D.: Stellar Astronomy From a Space Vehicle. Astron. J., vol. 65, June 1960, p. 278.

DICKE, R. H.: The Nature of Gravitation. *In* Science in Space, L. V. Berkner and H. Odishaw, eds., McGraw-Hill Book Co., Inc., 1961.

ELLITO, H.: Cosmic Ray Measurements in the U.S./U.K. Satellite S–51. *In* Cosmic Rays, Solar Particles, and Space Research, B. Peters, ed., Academic Press, 1963.

FAIRBANKS, W. M.; AND BOL, M.: Proposed General Relativity Experiment Using a Cryogenic Gyroscope. ARS paper 1950–61, 1961.

FAN, C. Y., ET AL.: Cosmic Radiation Helium Spectrum Below 90 Mev per Nucleon Measured on Imp 1 Satellite. J. Geophys. Res., vol. 70, Aug. 1, 1965, p. 3515.

FLORMAN, E. F.: Proposed Use of Earth Satellite Signals to Measure Propagation Velocity of Electromagnetic Waves. Appl. Phys. Ltrs., vol. 3, Dec. 1, 1963, p. 193.

GOLDBERG, L.: Astronomy From Satellites and Space Vehicles. J. Geophys. Res., vol. 64, Nov. 1959, p. 1765.

HADDOCK, F. T.: Radio Astronomy Observations From Space. ARS J., vol. 30, July 1960, p. 598.

HALLAM, K.; AND MANGUS, J.: An Ultraviolet Spectrophotometer for Satellite Astronomy. NASA X–610–64–188, 1964.

HIBBEN, R. D.: OAO–B Telescope Will Scan Stars Mapped by First OAO. Av. Wk., July 19, 1965, p. 74.

HIBBEN, R. D.: Prototype Telescope for OAO–C Tested. Av. Wk., Mar. 22, 1965, p. 71.

HUGILL, J.; AND SMITH, F. G.: Cosmic Radio Noise Measurements From Satellite Ariel II. I. Receiving System and Preliminary Results. Roy. Astron. Soc., Monthly Notices, vol. 131, 1965, p. 137.

KRAUSHAAR, W. L.; AND CLARK, G. W.: Search for Primary Cosmic Gamma Rays With the Satellite Explorer XI. Phys. Rev. Ltrs., vol. 8, 1962, p. 106.

KUPPERIAN, J. E.; AND ZEIMER, R. R.: Satellite Astronomy. International Sci. and Tech., Mar. 1962, p. 48.

LEAVITT, C. P.: High Energy Gamma Ray Satellite Experiment. IRE Trans., NS–9, June 1962, p. 400.

LILLEY, A. E.: Satellite Measurements of Cosmic and Planetary Radio Noise. In Space Age Astronomy, A. J. Deutsch and W. B. Klemperer, eds., Academic Press, 1962.

MEINEL, A. B.: High Resolution Optical Space Telescopes. In Space Age Astronomy, A. J. Deutsch and W. B. Klemperer, eds., Academic Press, 1962.

ROBINSON, A. D.; PAXTON, R. K.; AND WAGGENER, W. N.: Project Celescope— An Astronomical Data Processing System. Paper at the 1965 National Telemetering Conference, 1965.

SCHIFF, L. I.: On Experimental Tests of the General Theory of Relativity. J. Physics, vol. 28, 1960, p. 340.

SCHWED, P., ET AL.: The Heavy Primary Cosmic Ray Experiment. In NASA TN D–608, 1961.

SHERMAN, W. L.: Conversion of a Spacecraft Designed for Manned Space Flight to a Recoverable Orbiting Astronomical Observatory. NASA TN D–2535, 1964.

SINGER, S. F.: Application of an Artificial Satellite to the Measurement of the General Relativistic "Red Shift." Phys. Rev., vol. 104, Oct. 1, 1956, p. 11.

SPITZER, L., ET AL.: Research Into the Design Features of a High-Resolution Ultraviolet Spectroscopic Satellite. AD 623587, 1965.

SPITZER, L.: The Beginnings and Future of Space Astronomy. Amer. Sci., vol. 50, Sept. 1962, p. 473.

SPITZER, L.: Space Telescopes and Components. Astron. J., vol. 65, June 1960, p. 242.

STECHER, T. P.; AND MILLIGAN, J. E.: Stellar Spectrophotometry From Above the Atmosphere. Astrophys. J., vol. 136, July 1962, p. 1.

SUBOTOWICZ, M.: Test of the General Theory of Relativity. Nature, vol. 196, Nov. 17, 1962, p. 628.

SWINGS, P.: Current Objectives of Astronomical Space Research. *In* Space Age Astronomy, A. J. Deutsch and W. B. Klemperer, eds., Academic Press, 1962.

WILLIAMS, D. J.; AND BOSTROM, C. O.: Albedo Neutrons in Space. J. Geophys. Res., vol. 69, Feb. 1, 1964, p. 377.

WITTEN, L.: Experimental Aspects of General Relativity Theory. J. Astronaut., vol. 4, 1957, p. 46.

ZIEMER, R. R.; AND KUPPERIAN, J. E.: The Mission of the Orbiting Astronomical Observatory. *In* The Observatory Generation of Satellites. NASA SP–30, 1963.

Chapter 14

ADEY, W. R.: Biosatellite Performance Simulations. *In* Symposium on the Analyses of Central Nervous System and Cardiovascular Data Using Computer Methods. NASA SP–72, 1964.

BAKHRAMOV, A. M.; AND YAZDOVSKIY, V. I.: Pressurized Capsule for an Animal. *In* Problems of Space Biology, vol. 1, N. M. Sisakyan, ed., NASA TT F–174, 1963.

BERSCHER, D. E.; AND FREGLY, A. R.: Animals and Man in Space. Rept. ACR–64, Office of Naval Research, 1961.

BUYLOV, B. G.; AND GRYUNTAL, R. G.: Research Apparatus. *In* Problems of Space Biology, vol. 1, N. M. Sisakyan, ed., NASA TT F–174, 1963.

CARPENTER, D. L.; FAIRWEATHER, S. H.; AND MORTIMER, J. E.: A Longlife Biosatellite for Exploratory Television Viewing of Physiologic Development. Ann. N.Y. Acad. Sci., vol. 134, Nov. 22, 1965, p. 423.

GRAY, S.; AND EDWARDS, B. F.: Effect of Weightlessness and Radiation on the Growth of the Wheat Coleoptile for the Purpose of Defining and Verifying an Experiment Suitable for Use in a Biosatellite. NASA CR–303, 1965.

HENRY, J. P.; AND MOSELY, J. D., EDS.: Results of the Project Mercury Ballistic and Orbital Chimpanzee Flights. NASA SP–39, 1963.

KATZBERG, A. A.; AND MORI, L. H.: Biologic Systems of Discoverer Satellites XXIX and XXX: Organ and Tissue Cultures. USAF SAM rept. 62–62, 1962.

KATZBERG, A. A.: The Effect of Space Flight on Living Human Cells Aboard Discoverer XVIII. USAF SAM rept. 62–67, 1962.

LINDBERG, R. G.; DEBUONO, G. J.; AND ANDERSON, M. M.: Animal Temperature Sensing for Studying the Effect of Prolonged Orbital Flight on the Circadian Rhythms of Pocket Mice. Unmanned Spacecraft Meeting. AIAA rept. CP–12, New York, 1965.

SAUNDERS, J. F.; JENKINS, D. W.; AND DALLOW, T. P.: The NASA Biosatellite Program. Astronaut. Aeron., vol. 4, Jan. 1966, p. 48.

SISAKYAN, N. M., ED.: Problems of Space Biology. NASA TT F–174, 1963.

WALTER, D. O.: Biosatellite Program. *In* Symposium on the Analysis of Central Nervous System and Cardiovascular Data Using Computer Methods, NASA SP–72, 1964.

YAZDOVSKIY, V. I.: Biological Experiments on Rockets and the Artificial Earth Satellite. Annals IGY, vol. 12, 1961, p. 771.

Appendix

ANON.: Proton 1 Details. Flight International, vol. 88, Aug. 19, 1965, p. 286.

ANON.: International Satellite Ariel II. COSPAR Info. Bull., no. 21, Dec. 1964, p. 56.

ANON.: The Elektron Cosmic Station. NASA TT F–9040, 1965.

ANON.: IGY Bull.; many issues from 1958 to date contain summary descriptions of various scientific satellites.

ANON.: Juno II Summary Project Report, vol. I; Explorer VII Satellite, vol. II. The S–46 Satellite. NASA TN D–608, 1961.

ANON.: Ariel I: the First International Satellite. NASA SP–43, 1963.

ANON.: Polar Ionosphere Beacon Satellite (S–66). NASA TM X–55009, 1963.

AUCREMANNE, M. J., ED.: The Ionosphere Beacon Satellite, S–45. NASA TN D–695, 1961.

BOEHM, J.: Considerations to the Development of Explorer VII Satellite. IRE Trans., MIL–4, Apr. 1960, p. 86.

BRANIGAN, T. L., ED.: Space Log, a quarterly. TRW Systems, Redondo Beach, Calif.

CAUSSE, J.: The D–1 Satellite. Sciences et Industries Spatiales, vol. 1, 1965, p. 27.

CORTRIGHT, E. M.: Unmanned Spacecraft of the United States. Government Printing Office, 1964.

GLASER, P. F.: Project Able-3. (Explorer 6.) AD 245934, 1960.

GODDARD SPACE FLIGHT CENTER: Orbiting Solar Observatory. NASA SP–57, 1965.

HIBBEN, R. D.: Michigan Satellite Design Near Completion. Av. Wk., Nov. 22, 1965, p. 75.

ORDWAY, F. I.; AND WAKEFORD, R. C.: International Missile and Spacecraft Guide. McGraw-Hill Book Co., Inc., 1960.

SCULL, W. E.; AND LUDWIG, G. H.: The Orbiting Geophysical Observatories. Proc. IRE, vol. 50, 1962, p. 2287.

STAFFORD, W. H.; AND CROFT, R. M.: Artificial Earth Satellites and Successful Solar Probes, 1957–1960. NASA TN D–601, 1961.

STAMBLER, I.: The Explorers. Space/Aero., vol. 41, Feb. 1964, p. 38.

STAMBLER, I.: The Orbiting Observatories. Space/Aero., vol. 42, Sept. 1964, p. 34.

STAMBLER, I.: The OGO. Space/Aero., vol. 39, Feb. 1963, p. 70.

THOMAS, J. O.: Canadian Satellite: The Topside Sounder Alouette. Science, vol. 139, Jan. 18, 1963, p. 229.

TRUSZYNSKI, G. M.: The NASA Geodetic Satellite Program. In Space Research V, D. G. King-Hele, P. Muller, and G. Righini, eds., John Wiley & Sons, Inc., 1965.

WARREN, H. R.; AND MAR, J.: Canada's First Satellite. Spaceflight, vol. 4, 1962, p. 70.

Appendix

DESCRIPTIONS OF SCIENTIFIC SATELLITES

This appendix lists all the unclassified scientific satellites known to the author. Included are satellites already launched as well as those planned for launch during the next 5 years. Data on satellites still in the development stage are, of course, subject to change, and the reader should update information on satellites launched after mid-1966.

Satellites are listed alphabetically by common name rather than by launch date. Thus, the reader will find all the Explorers, Solrads, and other genera together. The listing problem is complicated, however, by synonyms. It is not uncommon to find a half-dozen-or-more different names for the same satellite in the literature. To help unravel the synonyms, a list of all known synonyms is included in each satellite description. Each synonym is also listed in the index at the back of the book. This will lead the reader to the proper description in the appendix regardless of the name he uses for the satellite under consideration.

Each scientific satellite possesses a minimum of two names: the common name and the international designation. At present, NASA also gives a letter designation to each satellite model before launch; viz, Geos A or OAO A. If the satellite is successfully orbited, it will be given a number to replace the letter; i.e., OAO I. If the satellite is in the Explorer class, it will be given an Explorer number regardless of its previous name. In this way, Geos A became Explorer XXIX. The unsuccessful Explorers II and V are exceptions to this rule. NASA has also assigned S and P designations (for Satellite and Probe) to many satellites in the past; viz, S–27 for Alouette 1. These designations are included in the lists of synonyms where known. On the other hand, the Department of Defense (DOD) has orbited many scientific satellites in classified launches. Their common names and engineering data were not included in this book. The satellite 1963 38C is an excellent example.

Data in each satellite vignette are arranged in the following pattern:

Satellite common name		*International designation*
Synonym list		
Launch date	*Launch vehicle*	*Launch site/tracking net*
Satellite mass	*Initial period*	*Initial inclination*
Initial perigee/apogee	*Silent date*	*Reentry date*
Project information		
Descriptions of subsystems		
Experiments/instruments	*Experimenter*	*Institution*

AIR-DENSITY EXPLORER FOLLOW-ONS

Air Density/Injun Follow-ons, AD/I Follow-ons

Balloon-type satellites similar to Explorer XXIV, which was designated AD–B and launched with Injun 4 as AD/I–B on November 21, 1964. AD–C will probably be launched in 1966 with Injun 5 as AD/I–C. Like all other balloon-type Explorers, this is a project of NASA's Langley Research Center.

Descriptions of subsystems

See Explorer XXIV

ALOUETTE 1   1962 BA 1

Alouette A, S–27, S–27A, Swept Frequency Topside Sounder, Topside Sounder, Ionosphere Monitor, Topsi (an acronym more commonly associated with Explorer XX).

Sept. 28, 1962	Thor-Agena B	WTR/Minitrack
145 kg	105.4 min	80.5°
998/1027 km	—	—

First of the International Satellite projects. Project managed by GSFC. Built by Canadian Defence Research Telecommunications Establishment (DRTE). Launched and tracked by NASA. Primary objective: topside sounding of the ionosphere. Complemented by NASA's Fixed Frequency Topside Sounder, Explorer XX.

Descriptions of subsystems

Communication:	Wideband FM telemetry transmitter at 136.080 Mc; narrowband PM transmitter at 136.590 Mc. Telemetry commanded "on" from ground, but turned off automatically. Command receiver. Tape recorder. Turnstile telemetry antenna.
Power supply:	Glass-covered p–n solar cells plus sealed NiCd batteries supplied an average of 18 W
Onboard propulsion:	None
Attitude control:	Spin stabilization
Environment control:	Wholly passive, using external surfaces and internal insulation blankets
Guidance and control:	Fluxgate magnetometers; Minitrack beacon
Onboard computer:	None
Structure:	Central thrust tube, equipment decks, and spun-aluminum shell in shape of oblate spheroid 86 cm high and 110 cm in diameter (fig. A–1)

Experiments/instruments	*Experimenter*	*Institution*
Topside sounder (table 11–5) _____	Warren, E. S.	DRTE
Cosmic-noise receiver (table 13–1) __	Hartz, T. R.	DRTE
vlf receiver (table 11–5) _____	Belrose, J. S.	DRTE
Six particle detectors (table 11–8) __	McDiarmid, I.	Canadian National Research Council

Selected reference: Reference 1.
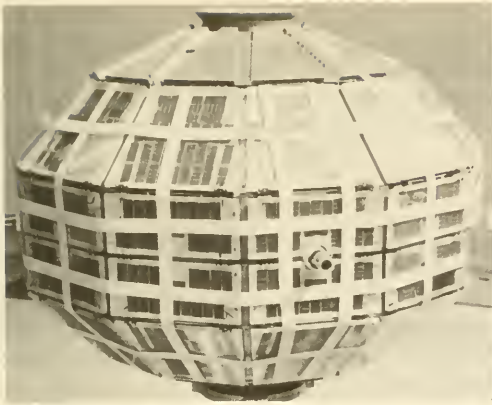
FIGURE A–1.—Alouette 1.

ALOUETTE 2   1965 98A

See Alouette-1 synonyms. Launched with DME–A as ISIS X. S–27B Alouette B.

Nov. 28, 1965	Thor-Agena B	WTR/STADAN
145 kg	121.4 min.	79.8°
489/2990 km	—	—

Launched by NASA along with DME–A as ISIS X. ISIS = International Satellites for Ionospheric Study. See Alouette 1.

Descriptions of subsystems

Wideband FM/FM telemetry at 136.086 Mc, narrowband PAM/FM/PM telemetry at 136.590 Mc. Otherwise, Alouette 2 is essentially identical to Alouette 1.

ALOUETTE C

See Alouette-1 synonyms. To be launched with DME–B as ISIS A.

1967	TA Thor-Delta	WTR/STADAN
—	—	80°
750/3500 km	—	—

Second of the ISIS series of International Satellites. See Alouettes 1 and 2.

Descriptions of subsystems

No firm data except instrument list below

Experiments	*Experimenter*	*Institution*
Topside sounder, swept-frequency type (table 11–5).	Chapman, J. H.	DRTE
Topside sounder, fixed-frequency type (table 11–5).	Chapman, J. H.	DRTE
Cosmic-noise receiver (table 13–1) __	Hartz, T. R.	DRTE
elf/vlf receiver (table 11–5) _____	Belrose, J. S.	DRTE
Special beacons (table 11–5) _____	Chapman, J. H.	DRTE
Particle detectors (8 geiger counters, 4 solid-state counters) (table 11–8).	McDiarmid, I. B.	Canadian National Research Council

ANNA 1A

(See Anna 1B synonyms)
May 10, 1962   Thor-Able Star   ETR
Owing to a second-stage ignition malfunction, this geodetic satellite did not
  reach orbit. See Anna 1B for details of construction.

ANNA 1B   1962 BM 1

ANNA = Army, Navy, NASA, Air Force
Oct. 31, 1962   Thor-Able Star   ETR/TRANET, etc.
159 kg   107.8 min   50.1°
1076/1170 km   —   —

A geodetic satellite sponsored jointly by the Army, Navy, Air Force, and
  NASA. The first Anna, Anna 1A, was not launched successfully. Prime
  contractor: Applied Physics Laboratory.

Descriptions of subsystems
Communication: No telemetry of scientific data. Command re-
                              ceiver.
Power supply: Solar cells and NiCd batteries provided an aver-
                              age of 22 W
Onboard propulsion: None
Attitude control: Permanently stabilized the field to within 3° of
                              Earth's magnetic-field vector
Environment control: Passive
Guidance and control: Clock for timing xenon lamps. Navigation aids
                              discussed under experiments below.
Onboard computer: None
Structure: Diffusively reflecting sphere, 107 cm in diameter.
                              Basic structure made from aluminum and
                              fiber glass (fig. A-2).
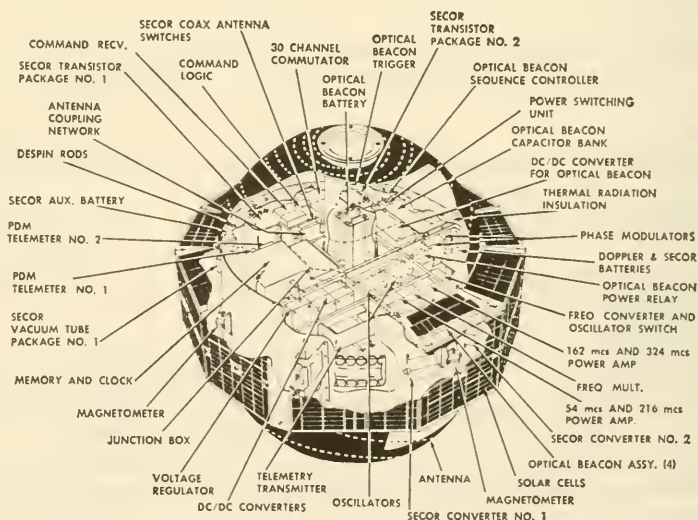
FIGURE A-2.—Anna 1B.

Experiments

Pair of xenon flash lamps on each side of satellite, 1100 joules/flash. Sequence of five flashes at 5.6-sec intervals. Smithsonian optical net tracked flashes. Doppler beacons at 162 and 324 Mc were tracked by TRANET
Army Secor navigation equipment failed on launch
Selected reference: Reference 2

AOSO

Advanced Orbiting Solar Observatory, Helios
This advanced version of the basic OSO satellite was to have provided greater pointing accuracy, more control flexibility, and better data-handling capability. The AOSO program was managed by Goddard Space Flight Center, and Republic Aviation was the prime contractor. Before the program was canceled, in 1965, plans called for launching AOSO in 1969 into a polar-retrograde orbit using a thrust-augmented Thor-Agena D launch vehicle.

ARIEL 1   1962 O 1

S–51, UK–1, UK–A, International Ionosphere Explorer, International Satellite, Direct Measurements Explorer (not a NASA DME) (UK–B not launched).

Apr. 26, 1962	Delta	ETR/Minitrack
60 kg	100.9 min	53.9°
390/1210 km	Nov. 1964	—

First British satellite; first NASA International Satellite. Named after the "airy" spirit in "The Tempest." Built by NASA. Instruments provided by several English universities and coordinated by the Royal Society's British National Committee on Space Research.

Descriptions of subsystems

Communication:	PFM telemetry at 136.410 Mc. Telemetered 69 parameters; 66 from scientific experiments. Tape recorder. Command receiver. Canted turnstile telemetry antenna.
Power supply:	p–n solar cells and NiCd batteries provided between 7.5 and 30 W, depending upon orientation.
Onboard propulsion:	None
Attitude control:	Spin stabilization. Despin through boom erection and yo-yo mechanism. Final spin rate about 12 rpm.
Environment control:	Passive thermal control, using various paints
Guidance and control:	Solar-aspect sensor. One-year electrochemical killer time (failed).
Onboard computer:	None
Structure:	Cylinder with rounded ends. 27.2 cm high, 58.5 cm in diameter, exclusive of rounded ends. Epoxy-bonded fiber-glass construction.

Experiments/instruments	*Experimenter*	*Institution*
Langmuir probe (table 11–5) _____	Boyd, R. L. F.	University College
Spherical plasma probe (table 11–5)	Boyd, R. L. F.	University College

Experiments/instruments	Experimenter	Institution
rf capacitance probe (table 11–5) __	Sayers, J.	U. Birmingham
Spherical Cerenkov counter and 2 Geiger counters (table 11–8).	Elliot, H.	Imperial College
Three ionization-chamber Lyman-α detectors (table 12–3).	Bowles, J. A.	University College
Two solar X-ray proportional counters (table 12–3).	Boyd, R. L. F.	University College

Selected reference: NASA SP–43, 1963

ARIEL 2   1964 15A

S–52, S–52A, UK–2, UK–C, International Satellite (UK–D not flown)
Mar. 27, 1964   Scout   Wallops/STADAN
68 kg   101.3 min   51.6°
290/1355 km   Nov. 1964   —

Ariel 2, like Ariel 1, was launched for Great Britain by NASA. Experiment management was by the British National Committee on Space Research. Westinghouse built the spacecraft itself. Payload and launch vehicle differed from Ariel 1.

Descriptions of subsystems

Communication: PFM telemetry at 136.557 Mc. Tape recorder. Command receiver. Canted turnstile plus 40-m dipole antennas.

Power supply: Four paddles with n–p solar cells. NiCd batteries. Power required: 6.3 W in shadow, 8.1 W in sunlight.

Onboard propulsion: None
Attitude control: Spin stabilization. Yo-yo despin device
Environment control: Paint patterns for thermal control
Guidance and control: Solar-aspect sensor
Onboard computer: None
Structure: Fiber-glass cylinder with rounded ends. 58 cm diameter, 89 cm long (fig. A–3).

Experiments/instruments	Experimenter	Institution
Galactic-noise receiver (table 13–1) _	Smith, F. G.	U. Cambridge
Two light-transmission micro-meteoroid detectors (table 11–14).	Jennison, R. C.	Jodrell Bank
Two broadband ozone photometers (table 11–1).	Frith, R.	Meteorology Office
Ozone prism spectrometer (table 11–1).	Frith, R.	Meteorology Office

Selected reference: Reference 3

ARIEL 3. (See UK–3.)

ATMOSPHERE EXPLORERS. (See Explorers XVII and XXXII.)

BEACON EXPLORER A

S–66A, BE–A. (See Explorer XXII-synonyms.)
Mar. 19, 1964   Delta   ETR
This satellite was the first in NASA's Beacon Explorer series. It did not attain orbit because of insufficient third-stage thrust.
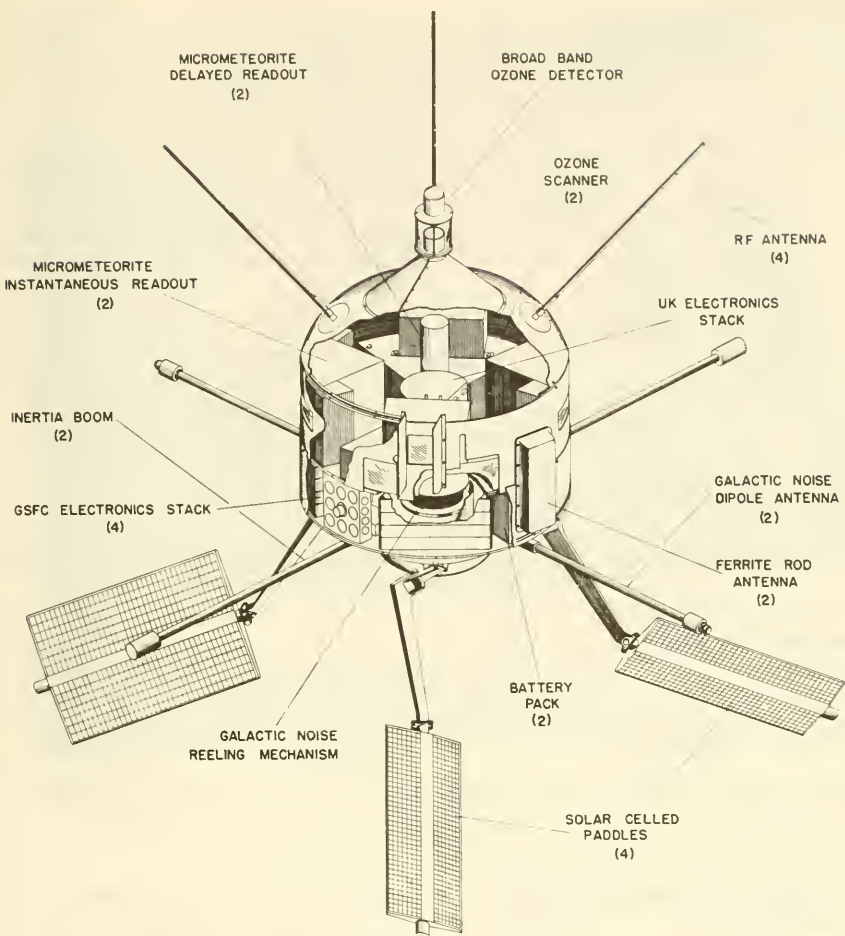
FIGURE A–3.—Ariel 2.

BEACON I

(Occasionally called Explorer VI in error)

Oct. 23, 1958	Jupiter C	ETR
4 kg	—	
—	—	

This small radio beacon was intended for ionospheric research, but orbit was not attained because of premature separation of the upper stages.

BEACON II

Aug. 14, 1959	Juno II	ETR

Slightly larger than Beacon I, Beacon II did not reach orbit because of upper-stage malfunctions.

BIOSATELLITE I   1966 114A

Bios, Biosatellite A, Biosatellite B is a backup satellite

Dec. 14, 1966	Thrust-Augmented Delta	ETR/STADAN
427 kg	90.7 min	33.5°
308/317 km	—	Dec. 17, 1966

Recoverable satellite designed to test the effects on living organisms of weightlessness alone and weightlessness combined with radiation. Biosatellite A/B flights were planned to last 3 days. Recovery will be by helicopter or aircraft over the ocean. Project management by NASA's Ames Research Center. General Electric built the spacecraft. Retrorockets did not fire and recovery was impossible.

Descriptions of subsystems

Communication:	PCM telemetry at 136.68 Mc, 16 channels with 8 samples/frame, 114 channels with 1 sample/frame. Tape recorder. Command receiver. Omnidirectional antenna.
Power supply:	Ag-Zn batteries
Onboard propulsion:	Small solid rocket for deorbiting
Attitude control:	Cold nitrogen gas jets
Environment control:	Electric temperature control in capsule. Heating during deorbit and recovery also needed.
Guidance and control:	
Onboard computer:	None
Structure:	206 cm long, adapter base 145 cm. Phenolic-nylon heat shield with fiber-glass liner (fig. A–4).

Experiments	*Experimenter*	*Institution*
Liminal angle in the pepper plant (table 14–1)	Finn, J. C.	North American Aviation
Orientation of roots and shoots in wheat seedlings (table 14–1)	Gray, S. W.	Emory U.
Nutrition and growth in amoeba (table 14–1)	Price, R. W.	U. Colorado
Development of frog eggs (table 14–1)	Young, R. S.	Ames Research Center
Emergence of wheat seedlings (table 14–1)	Lyon, C. J.	Dartmouth College
Orientation of root and shoot of corn (table 14–1)	Conrad, H. M.	North American Aviation
Cellular inactivation and mutation in mold spores (table 14–2)	De Serres, F. J.	Oak Ridge National Lab.
Effects on embryonic development of flour beetles (table 14–2)	Slater, J. V.	U. California
Chromosome translocations in wasps (table 14–2)	Von Borstel, R. C.	Oak Ridge National Lab.
Somatic mutations in blue-flowering plant (table 14–2)	Sparrow, A. H.	Brookhaven National Lab.
Effects on proliferation of viruses in slow-growing bacteria (table 14–2)	Mattoni, R.	North American Aviation
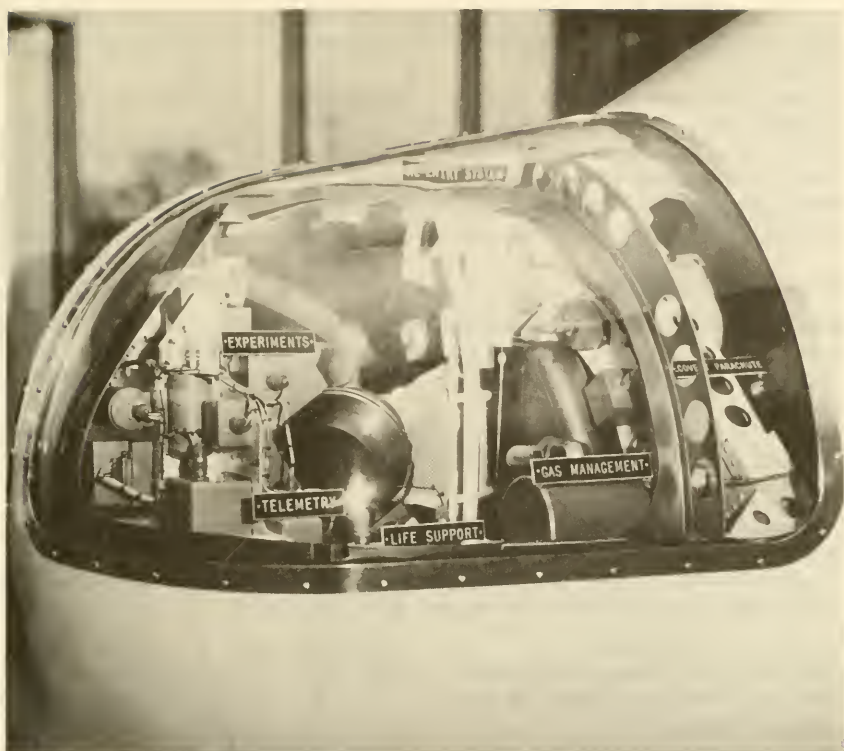
FIGURE A–4.—Model of the Biosatellite reentry capsule with the primate experiment.

Experiments	Experimenter	Institution
Genetic changes in mature germ cells of adult *Drosophila* (table 14–2)	Altenburg, E.	Texas Medical Center
Somatic damage to *Drosophila* larvae (table 14–2)	Oster, I.	Cancer Research Institute

Selected references: References 4, 5, 6

BIOSATELLITE C/E

Bios, Biosatellite E is a backup satellite

—	Thrust-Augmented Delta	ETR/—
—	—	33.5°
—/—	—	—

Biosatellite C/E is designed for a 21-day mission. All experiments are of the zero-g type.

Descriptions of subsystems

Essentially the same as Biosatellite A/B, except for the replacement of the A/B batteries by H–O ion membrane fuel cells (fig. 14–9).

Experiments	Experimenter	Institution
Plant morphogenesis in a leafy plant (table 14–1)	Brown, A. H.	U. Pennsylvania
Human liver cells in tissue culture (table 14–1)	Montgomery, P. O'B.	U. Texas
Gross body composition and metabolism in mammals (table 14–1)	Pitts, G. C.	U. Virginia
Metabolic rhythms in mammals (table 14–1)	Halberg, F.	U. Minnesota

BIOSATELLITE D/F

Bios, Biosatellite F is a backup satellite

1968	Thrust-Augmented Delta	ETR/—
—	—	33.5°
—/—	—	—

Biosatellite D/F is designed for a 30-day mission. All experiments are developed around a primate passenger. See Biosatellite A/B for more background.

Descriptions of subsystems

Essentially the same as Biosatellite A/B, except for the replacement of the A/B batteries by H–O ion membrane fuel cells. A sea-level atmosphere is provided for the experimental subject (figs. 14–3, 14–5).

Experiments	Experimenter	Institution
Central nervous system, cardiovascular and metabolic study of primates (table 14–1)	Adey, W. R.	U. California (L.A.)
Loss of calcium in primates (table 14–1)	Mack, P. B.	Texas Women's U.

COMPOSITE 1

Jan. 24, 1962	Thor-Able Star	ETR

Five satellites formed this payload, including Solrad 4A and Injun 2. Orbit was not attained because of low second-stage thrust.

COSMOS SERIES

Well over 100 satellites in this series have been launched by Russia, which certainly contains many scientific satellites in addition to military spacecraft and defunct space probes. Since few details have been released on the satellites and no one can say for sure which are scientific satellites, Cosmos listings have been omitted.

DIRECT-MEASUREMENTS EXPLORER FOLLOW-ONS

DME–B through DME–D

—	—	—/—
—	—	—
—/—	—	—

The DME's are part of the ISIS program. (ISIS = International Satellites for Ionospheric Studies.) Each ISIS consists of a U.S. DME and a Canadian Alouette.

ISIS–X = DME–A + Alouette B = Explorer XXXI + Alouette 2.
ISIS–A = DME–B + Alouette C = —
ISIS–B = DME–C + Alouette D = —
ISIS–C = DME–D + Alouette E = —

Descriptions of subsystems
See Explorer XXXI

Experiments/instruments (DME–B)	*Experimenter*	*Institution*
Spherical retarding potential analyzer (table 11–5)	Sagalyn, R.	AFCRL
Langmuir probes (table 11–5)	Brace, L. H.	GSFC
Quadrupole mass spectrometer (table 11–5)	Narcisi, R. S.	AFCRL
Electrostatic analyzer (table 11–8) _	Heikkila, W. J.	Graduate Research Center of the SW.
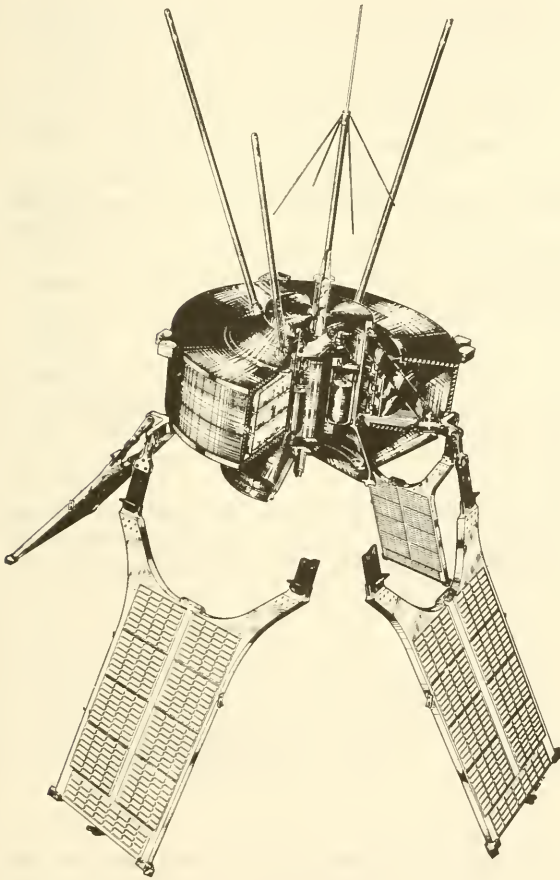
FIGURE A–5.—The D–1A.

D–1A   1966 13A
Diamant Satellite, FR–2 (initially), Diapason
Feb. 17, 1966   Diamant   Hammaguir/DIANE,
                                                       IRIS
18.6 kg   118.7 min   34.11°
503/2747 km   —   —

A series of French scientific satellites. D–1A was launched primarily to test
   the Diamant launch vehicle and the French tracking and data acquisition
   network. Geodetic experiments were also included. D–1B, a backup satellite,
   was not launched.

Descriptions of subsystems

Communication: PFM telemetry at 136.980 Mc. Command re-
                                ceiver with dipole antenna. Turnstile antenna
                                for telemetry. Tape recorder.
Power supply: Four solar paddles with n–p cells, plus AgZn
                                batteries provided an average of 2.8 W
Onboard propulsion: None
Attitude control: Spin-stabilized. Yo-yo despin device.
Environment control: Passive thermal control
Guidance and control:
Onboard computer: None
Structure: Aluminum and magnesium cylinder, 47 cm in
                                diameter and 28 cm high (fig. A–5)

Experiments/instruments

Beacons for Faraday-rotation experiment (table 11–5) (149.970 and 399.920
   Mc)
Solar-cell degradation experiment

Selected references: References 7, 8

D–1 FOLLOW-ONS
Diamant Satellite
—   —   Hammaguir/DIANE,
                                                       IRIS
—   —   —
—/—   —   —

Continuation of the D–1 series of French satellites. D–1C and D–1D are
   geodetic satellites. D–1B not launched. D–1C and D–1D were launched on
   Feb. 8 and Feb. 15, 1967, respectively, and are called Diademe 1 and 2.

Descriptions of subsystems
See D–1A

D–2
Diamant Satellite
1968   Diamant   French Guiana/
                                                       DIANE, IRIS
80 kg   —   —
450/900 km   —   —

The second Diamant series of scientific satellites. Built by Nord Aviation, the
   D–2 series will study the distribution of monoatomic hydrogen around the
   Earth.

Descriptions of subsystems
Communication:
Power supply:
Onboard propulsion: None
Attitude control: Oriented toward Sun; yo-yo despin device
Environment control:
Guidance and control:
Onboard computer:
Structure:

Experiment
Lyman-α experiment

D–3

Diamant Satellite, EOLE
—   Diamant   French Guiana/—
—   —   —
—/—   —   —

The third Diamant series of French scientific satellites. The purpose of the
   D–3 series is to study the movements of lower layers of the atmosphere in
   conjunction with balloons carrying beacons.

ELEKTRON 1   1964 6A

Jan. 30, 1964   —   —/—
—   169 min   61°
406/7110 km   —   —

A Russian satellite launched with Elektron 2 to make simultaneous measure-
   ments of the inner and outer radiation zones. Ejected during final-stage
   ignition. Onboard rocket injected satellite into orbit. First Soviet dual
   launch.

Descriptions of subsystems
Communication: Four antennas
Power supply: Six solar-cell paddles, total area of 20 m^2
Onboard propulsion: Small rocket for orbit injection
Attitude control:
Environment control: Thermal louvers
Guidance and control:
Onboard computer: None
Structure: Cylinder (fig. A–6)

Experiments/instruments
rf mass spectrometer (table 11–5)
Geiger counters, scintillators, semiconductor detectors (table 11–8)
Piezoelectric micrometeoroid detector (table 11–14)
Galactic radio-noise receiver (table 13–1)
Mayak beacon for ionosphere studies

ELEKTRON 2   1964 6B

Jan. 30, 1964   —   —/—
—   1360 min   61°
460/68 000 km   —   —
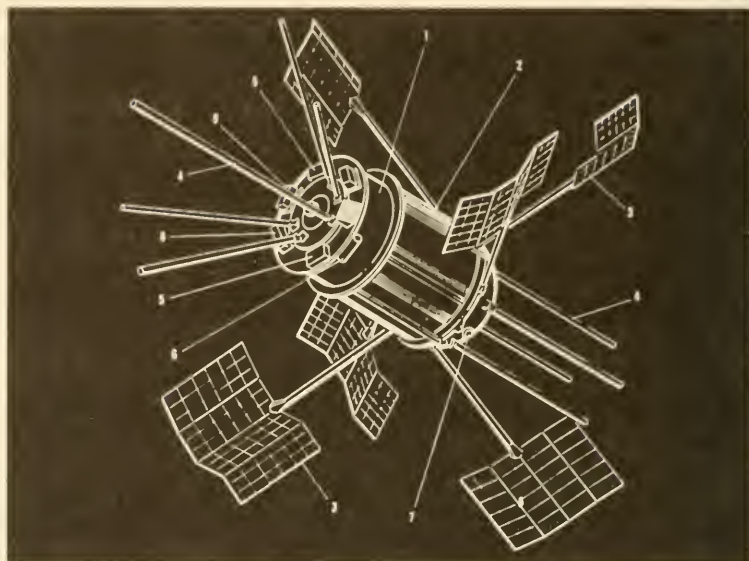
FIGURE A–6.—Elektron 1: (1) spacecraft shell, (2) thermal louvers, (3) solar paddles, (4) antennas, (5) micrometeoroid detectors, (6) corpuscular radiation detectors, (7) mass spectrometer, (8) proton detector, (9) electron detector.

A Russian satellite launched with Elektron 1 to make simultaneous measurements of the inner and outer radiation zones. Injected into orbit by final stage of launch vehicle. First Soviet dual launch.

Descriptions of subsystems

Communication:	Four antennas
Power supply:	Cylindrical body and skirt covered with 20 m² of solar cells
Onboard propulsion:	None
Attitude control:	
Environment control:	Thermal louvers
Guidance and control:	Sun sensor
Onboard computer:	None
Structure:	Cylinder with flared skirt (fig. A–7)

Experiments/instruments

rf mass spectrometer (table 11–5)
Geiger counters, scintillators, semiconductor detectors (table 11–8)
Spherical ion trap (table 11–5)
Two three-axis fluxgate magnetometers (table 11–11)
Galactic radio-noise receiver (table 13–1)
Solar X-ray photometers (table 12–3)
Cerenkov-scintillator cosmic-ray telescope (table 13–1)
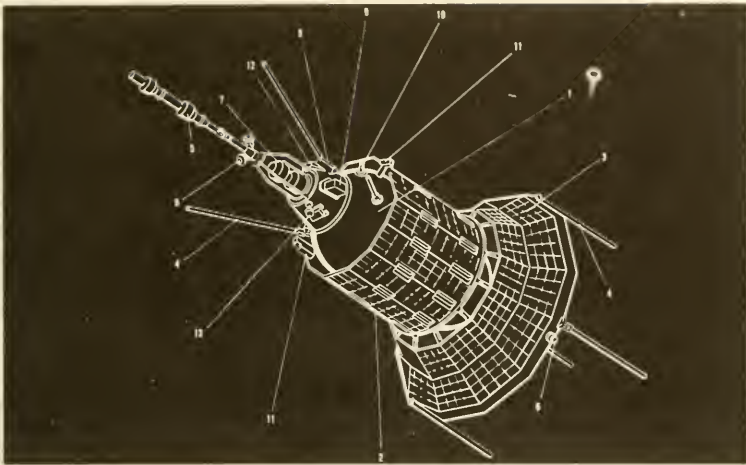
FIGURE A–7.—Elektron 2: (1) spacecraft shell, (2) thermal louvers, (3) solar cells, (4) antennas, (5) magnetometer, (6) Sun sensor, (7) low energy particle spherical analyzer, (8) cosmic-ray detector, (9) electron detector, (10) mass spectrometer, (11) solar X-ray detector, (12) low energy proton detector, (13) charged particle trap.

ELEKTRON 3   1964 38A

July 11, 1964	—	—/—
—	168 min	61°
408/7030 km	—	—

One of the second pair of Soviet Elektron satellites. Identical to Elektron 1.

ELEKTRON 4   1964 38B

July 11, 1964	—	—/—
—	1314 min	61°
459/66 100 km	—	—

One of the second pair of Soviet Elektron satellites. Identical to Elektron 2.

ENVIRONMENTAL SCIENCES RESEARCH SATELLITE

June 25, 1964	Scout	WTR

This Air Force scientific satellite carried radiation and micrometeoroid experiments. It failed to orbit when the second stage exploded.

EROS

Earth Resources Observation Satellite		
1969	Thor-Delta	WTR/STADAN
150 kg	Sun-synchronous	Polar
—/—	—	—

A scientific satellite series proposed by the U.S. Department of the Interior. EROS would survey global resources for the U.S. Geological Survey.

ERS 12   1963 39B

TRS 5, TRS IIa, Tetrahedral Research Satellite, Environmental Research
    Satellite

Oct. 16, 1963	Atlas-Agena D	ETR/STADAN, others
2 kg	39 hr	36.7°
208/103 000 km	Oct. 30, 1963	—

The ERS series of piggyback satellites is built by TRW Systems for the
    Department of Defense. Within the series are the tetrahedral types (in
    three different sizes) and the octahedral types (also in three different sizes).
    Many of these spacecraft were employed on classified projects and cannot
    be described here. Several that were formerly known as TRS 1 through
    TRS 4—now ERS 2, ERS 5, ERS 6, and ERS 9—carried solar-cell radia-
    tion-damage experiments.

Descriptions of subsystems

Communication:	PAM/FM/PM telemetry at 136.771 Mc. Dipole antenna
Power supply:	Solar cells (no batteries) generated approximately 1.2 W
Onboard propulsion:	None
Attitude control:	None; unstabilized
Environment control:	Passive thermal control
Guidance and control:	1-year killer timer
Onboard computer:	None
Structure:	Aluminum tetrahedral from 23 cm on an edge (fig. A–8)

Experiments/instruments
Plastic scintillator (table 11–8)
Solid-state detectors (table 11–8)
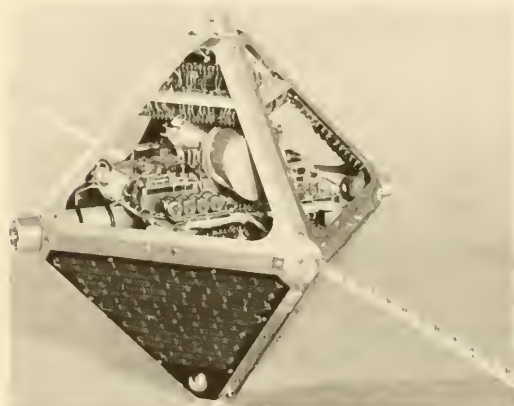
FIGURE A–8.—ERS 12, a
tetrahedral research
satellite. (Courtesy of
TRW Systems.)

ERS 13   1964 40C

(See ERS-12 synonyms.)	TRS 6	
July 17, 1964	Atlas-Agena D	ETR/STADAN
2 kg	39.2 hr	36.7°
193/104 000 km	Jan. 25, 1965	—

Descriptions of subsystems
See ERS 12

Experiments/instruments
See ERS 12

ERS 17   1965 58C

Octahedral Research Satellite, ORS 1, ORS IIIa, Environmental Research
    Satellite
July 20, 1965   Atlas-Agena D   ETR/—
5.5 kg   2595 min   35°
207/112 000 km   —   —
An Air Force piggyback satellite built by TRW Systems. The ORS series
    is a follow-on to the TRS (Tetrahedral Research Satellite) series. Col-
    lectively, the ORS and ERS series make up the ERS (Environmental
    Research Satellite) series. Many of these small satellites are classified.
    (See also TRS and OV–5.)

Descriptions of subsystems
Communication: Analog telemetry at 136 Mc
Power supply: Solar cells provide an average of 5 W
Onboard propulsion: None
Attitude control: None; satellite is not stabilized
Environment control: Passive thermal control
Guidance and control: None
Onboard computer: None
Structure: Octahedral frame

Experiments/instruments	*Experimenter*	*Institution*
Solid-state detector (table 11–8) ___	—	Aerospace Corp.
Scintillation counters (table 11–8) __	—	Aerospace Corp.
Phoswich counter (table 11–8) _____	—	Aerospace Corp.
Geiger counter (table 11–8) _____	—	—

ESRO 1

Polar Ionospheric Satellite. ESRO = European Space Research Organization.
1967   Scout   WTR/STADAN,
                                                  ESTRACK
80 kg   103 min   90°
280/1500 km   —   —
First ESRO-built satellite. Actually, plans call for ESRO 2 to be launched
    first. Primary mission of ESRO 1 is the study of the physics of the polar
    ionosphere. Will be launched by NASA.

Descriptions of subsystems
Communication: Two separate PCM telemetry systems. Low-
                            power system at 136.170 Mc; high-power sys-
                            tem at 136.950 Mc. Command receiver. Tape
                            recorder. Turnstile antenna.
Power supply: Solar cells (*n–p*) plus NiCd batteries generate
                            an average of 15 W
Onboard propulsion: None
Attitude control: Magnetic stabilization and damping. Yo-yo de-
                            spin.

Environment control: Passive thermal control
Guidance and control:
Onboard computer: None
Structure: Magnesium thrust cone. Exterior cylinder 76 cm
      diameter, 153 cm long (fig. A–9).
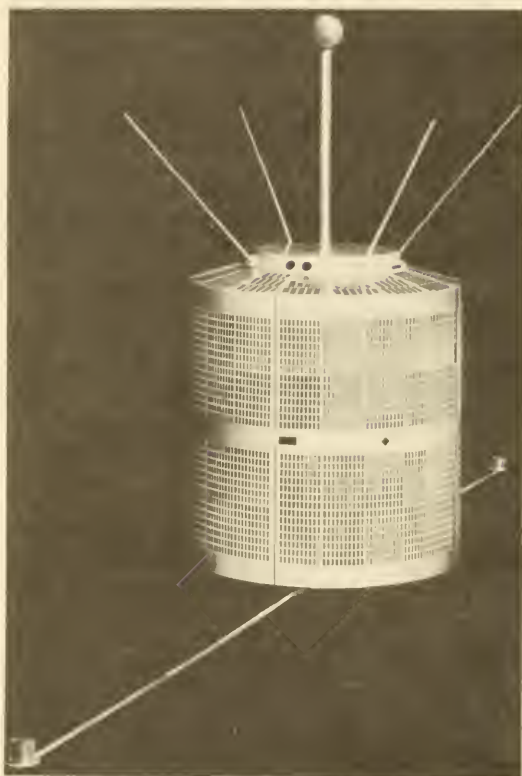
FIGURE A–9.—Model of ESRO 1.

Experiments/instruments	Experimenter	Institution
Langmuir probes (table 11–5) ____	Willmore, A. P.	University College
Spherical retarding potential analyzer (table 11–5)	Willmore, A. P.	University College
Two auroral photometers (table 11–1)	Omholt, A.	U. Oslo
Scintillator detector (table 11–8) __	Dalziel, R.	DSIR, Slough
Electrostatic analyzer (table 11–8)_	Riedler, W.	Kiruna Geophysical Observatory
Solid-state detectors (table 11–8) __	Rybner, J.	Technical U. Denmark
Four Geiger counters (table 11–8) _	Rybner, J.	Technical U. Denmark
Plastic scintillator (table 11–8) ___	Dalziel, R.	DSIR, Slough

ESRO 2

Cosmic Ray and Solar Astronomy Satellite
May 29, 1967   Scout   WTR/STADAN,
                                      ESTRACK

85 kg   —   —
—   —   —

Second ESRO-built satellite. Launched before ESRO 1. Primary mission of ESRO 2 is the study of cosmic rays and the Sun. Launch failure.

Descriptions of subsystems

Communication:	PCM/FM/PM telemetry for low-speed channels on 136.89 Mc. PCM/PM high-speed channels at 136.05 Mc. Tone digital command receiver. Tape recorder.
Power supply:	Solar cells (n–p) plus NiCd battery
Onboard propulsion:	None
Attitude control:	Magnetic nutation damper and torquer. Yo-yo despin mechanism. Spin stabilized.
Environment control:	Passive thermal control
Guidance and control:	Horizon scanners, fluxgate magnetometers, solar aspect sensors
Onboard computer:	None
Structure:	Magnesium cylinder with honeycomb experiment shelves. Twelve-sided external surface around magnesium thrust tube. 85 cm long, 76 cm maximum diameter.

Experiments/instruments	*Experimenter*	*Institution*
Solid-state detectors (table 11–8) __	Elliot, H.	Imperial College
Solar X-ray proportional counters (table 12–3)	Stewardson, E. A.	U. Leicester
Cosmic-ray package, proportional counters, scintillators, Cerenkov counters (table 13–4).	Elliot, H.	Imperial College
Cosmic-ray Cerenkov counter (table 13–4)	Marsden, P. L.	U. Leeds
Cosmic-ray Geiger counters (table 13–4)	Elliot, H.	Imperial College
Solar X-ray solid-state telescope (table 13–4)	de Jager, C.	U. Utrecht
Cosmic-ray solid-state telescope (table 13–4)	Labeyrie, J.	Centre d'Etudes Nucleaires de Saclay

EXPLORER S–1

See Explorer-VI synonyms
July 16, 1959   Juno II   ETR
Failed to orbit. See Explorer VI for details.

EXPLORER S–45

Feb. 24, 1961   Juno II   ETR
Failed to orbit because of third- and fourth-stage ignition malfunctions

EXPLORER S–45A

May 24, 1961   Juno II   ETR
Failed to orbit because of second-stage ignition malfunction

EXPLORER S–46

Mar. 23, 1960   Juno II   ETR
Failed to orbit because of upper-stage ignition malfunction

EXPLORER S–55

See Explorer-XIII synonyms
June 30, 1961   Scout   Wallops
First in the NASA Micrometeoroid Explorer series. Failed to orbit because
   of third-stage ignition malfunction. See Explorer XIII for details.

EXPLORER S–56

See Explorer-IX synonyms
Dec. 4, 1960   Scout   Wallops
Failed to orbit because of second-stage ignition malfunction. See Explorer IX
   for details.

EXPLORER I   1958 A 1

Jan. 31, 1958   Jupiter C   AMR/Minitrack,
                                                    Microlock
14 kg   114.7 min   33.3°
361/2550 km   May 23, 1958
                        —

First U.S. satellite. Explorer I was built by the Jet Propulsion Laboratory
   in a crash project directed by the U.S. Army Ballistic Missile Agency.

Descriptions of subsystems
Communication: 10-mW PM transmitter using dipole antenna at
                                  108.00 Mc. 60-mW AM transmitter using
                                  turnstile antenna at 108.03 Mc. Transmitters
                                  were beacons for Microlock and Minitrack
                                  tracking nets, respectively. Real-time telem-
                                  etry. No command receiver.
Power supply: Hg batteries
Onboard propulsion: None
Attitude control: Spin stabilized
Environment control: Eight white, Al_2O_3 strips for passive thermal
                                  control
Guidance and control: None
Onboard computer: None
Structure: Stainless-steel cylinder 15.2-cm diameter and
                                  203 cm long (fig. A–10)

Experiments/instruments	*Experimenter*	*Institution*
Geiger counter (table 11–8) _____	Van Allen, J. A.	State U. of Iowa
Microphone piezoelectric micro-meteoroid detector (table 11–14)	Manring, E.	AFCRL
Wire-grid micrometeoroid detector table 11–14)	Manring, E.	AFCRL

15.2 cm

Sub-carrier oscillators
External temp. gage
Low-power transmitter
Geiger tube
Internal temp. gage
Cosmic-ray experiment

Instrumentation section
Forward antenna gap (low-power transmitter)

Aft antenna gap
(int. receiver)
(high-power transmitter)

2m

Last stage motor case

Micrometeorite erosion gages (12 each)
Launching surfaces

FIGURE A–10.—Drawing of Explorer III.

EXPLORER II

| Mar. 5, 1958 | Jupiter C | ETR |

Failed to orbit because of unsuccessful fourth-stage ignition. See Explorer III for details.

EXPLORER III   1958 Γ 1

Mar. 26, 1958	Jupiter C	AMR/Minitrack, Microlock
14 kg	115.87 min	33.5°
188/2800 km	June 16, 1958	June 28, 1958

Second success in the Army satellite program. (Explorer II failed to orbit.)

Descriptions of subsystems
Except for the addition of a tape recorder, Explorers I and III were identical (fig. A–10).

Experiments/instruments	*Experimenter*	*Institution*
Geiger counter (table 11–8) _____	Van Allen, J. A.	State U. of Iowa
Wire-grid micrometeoroid detector (table 11–14)	Manring, E.	AFCRL

EXPLORER IV   1958 E 1
July 26, 1958   Jupiter C   AMR/Minitrack,
                                                 Microlock
17 kg   110.27 min   50.3°
262/2210 km   Oct. 6, 1958   Oct. 23, 1959
See Explorers I and III

Descriptions of subsystems
Communication: Five-channel FM/PM telemetry. 10-mW trans-
                                   mitter at 108.00 Mc; 30-mW transmitter at
                                   108.03 Mc. Both transmitters used dipole an-
                                   tennas.
Rest of subsystems similar to Explorer I

Experiments/instruments	*Experimenter*	*Institution*
Geiger counters (table 11–8) _____	Van Allen, J. A.	State U. of Iowa
Scintillator detector (table 11–8) __	Van Allen, J. A.	State U. of Iowa

EXPLORER V

Aug. 24, 1958   Jupiter C   ETR
Failed to orbit because the upper stages fired in the wrong direction. See
    Explorer IV for details.

EXPLORER VI   1959 Δ 1

S–2, Paddlewheel Satellite (the name "Explorer VI" was also applied to Bea-
    con I, a launch failure)
Aug. 7, 1959   Thor-Able   AMR/Minitrack
65 kg   768 min   47.0°
253/42 400 km   Oct. 6, 1959   July 1961
First Explorer launched by NASA. Primary objective was the study of the
    magnetosphere with a variety of instruments.

Descriptions of subsystems
Communication: PCM (Digilock) telemetry at 378.21 Mc. Bea-
                                   cons at 108.09 and 108.06 Mc. Digital mem-
                                   ory. Command receiver. Two dipole antennas.
Power supply: First use of solar-cell paddles. Four paddles
                                   each 51 cm square. NiCd batteries. One
                                   paddle failed to extend fully and lock.
Onboard propulsion: None
Attitude control: Spin stabilized
Environment control: Passive thermal control
Guidance and control: Solar aspect sensor and single-axis fluxgate
                                   magnetometer
Onboard computer: None
Structure: (fig. A–11)

Experiments/instruments	*Experimenter*	*Institution*
Scintillation counter (table 11–8) _	Farley, T. A.	STL
Ionization chamber and Geiger counter (table 11–8)	Winckler, J.	U. Minnesota
Search-coil magnetometer (table 11–11)	Smith, E. J.	STL
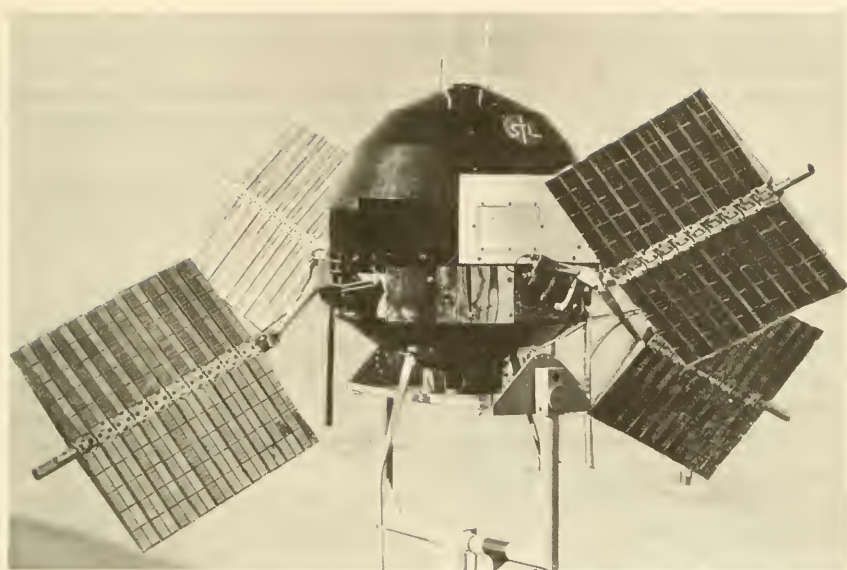
FIGURE A–11.—Explorer VI.

Experiments/instruments	Experimenter	Institution
Fluxgate magnetometer (table 11–11)	Coleman, P. J.	STL
Piezoelectric micrometeoroid detector (table 11–14)	Manring, E.	AFCRL
Proportional-counter telescope (table 13–4)	Simpson, J. A.	U. Chicago
vlf receiver (table 11–5) ----------	Helliwell, R.	Stanford

EXPLORER VII   1959 I 1

S–1A
Oct. 13, 1959   Juno II   AMR/Minitrack
42 kg   101.2 min   50.3°
557/1085 km   Aug. 24, 1961   —
A NASA satellite carrying a variety of instruments

Descriptions of subsystems

Communication:	Two separate telemetry systems. PAM telemetry at 19.99 Mc with turnstile antenna for housekeeping and Wisconsin experiment data. PM telemetry at 108.00 Mc with turnstile antenna for remainder of experiments. Tape recorder.
Power supply:	Solar cells for 19.99-Mc telemetry and Hg batteries for other spacecraft power requirements.
Onboard propulsion:	None
Attitude control:	Spin stabilized; antenna nutation damping

Environment control: Passive thermal control
Guidance and control: Solar-aspect sensor; killer-timer (failed)
Onboard computer: None
Structure: Double-cone structure with central cylindrical
                            connecting section. Fiber-glass and aluminum-
                            foil structure.

Experiments/instruments	*Experimenter*	*Institution*
Solar X-ray ion chambers (table 12–3)	Friedman, H.	NRL
Lyman-α ion chambers (table 12–3)	Friedman, H.	NRL
Cosmic-ray ion chamber (table 13–4)	Groetzinger, G.	RIAS
Geiger counters (table 11–8) _____	Van Allen, J. A.	State U. of Iowa
Light-transmission-erosion micro-meteoroid detectors (table 11–14)	LaGow, H.	GSFC
Suomi radiometer _____	Suomi, V.	U. Wisconsin

Selected reference: NASA TN D–608

EXPLORER VIII   1960 Ξ 1

S–30A, Direct Measurements Satellite
Nov. 3, 1960   Juno II   AMR/Minitrack
41 kg   112.7 min   50.0°
431/2290 km   Dec. 28, 1960   —
First of NASA's "direct measurements" satellites. Compare with Explorer
XX and Ionosphere Explorers.
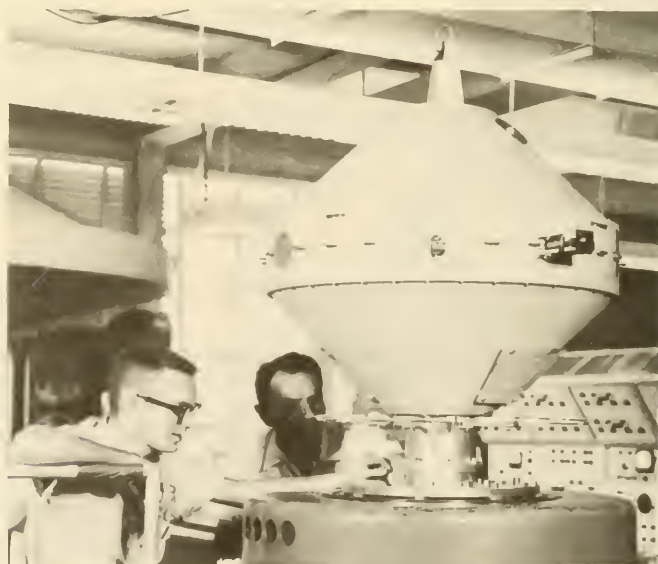
FIGURE A–12.—Explorer VIII being vibration tested.
(NASA photograph.)

Descriptions of subsystems

Communication:	Telemetry at 108.00 Mc. Dipole antenna.
Power supply:	Hg batteries
Onboard propulsion:	None
Attitude control:	Spin stabilized
Environment control:	Passive thermal control
Guidance and control:	Solar-aspect sensor
Onboard computer:	None
Structure:	Aluminum double-cone structure, 46 cm long and 46-cm diameter (fig. A–12)

Experiments/instruments	*Experimenter*	*Institution*
rf impedance probe (table 11–5) __	Kane, J. A.	GSFC
Five planar ion traps with various grid arrangements (table 11–5)	Bourdeau, R.	GSFC
Langmuir probe (table 11–5) _____	Bourdeau, R.	GSFC
Electric-field meter (table 11–5) __	Donley, J.	GSFC
Light-flash micrometeoroid detector (table 11–14)	Alexander, W. M.	GSFC
Piezoelectric micrometeoroid detector (table 11–14)	Alexander, W. M.	GSFC

EXPLORER IX   1961 Δ 1

S–56A

Feb. 16, 1961	Scout	Wallops/Minitrack
7 kg	118.3 min	38.6°
636/2580 km	Feb. 16, 1961	Apr. 9, 1964

NASA's first balloon and first Scout-launched satellite. See later Atmospheric Density Explorers. Optical instruments all over the world were used to track this bright satellite.

Descriptions of subsystems

Communication:	No telemetry. Minitrack 136-Mc beacon failed. Two halves of sphere were used as antenna.
Power supply:	NiCd batteries for beacon
Onboard propulsion:	None
Attitude control:	None
Environment control:	Passive thermal control using white-paint patterns on balloon
Guidance and control:	None
Onboard computer:	None
Structure:	3.65-m-diameter balloon. Fabric consisted of 4 layers each of aluminum foil and Mylar, with aluminum on the outside. Total fabric thickness: 0.005 cm. Balloon was inflated by gas pressure.
Experiments:	None

Selected reference: Reference 9

EXPLORER X   1961 K 1

P–14

Mar. 25, 1961	Delta	AMR/Minitrack
36 kg	112 hr	33.0°
161/233 000 km	Mar. 27, 1961	—

A NASA satellite with an extremely high perigee to measure interplanetary phenomena and the interaction of the solar wind with the magnetosphere. Similar to later IMP's.

Descriptions of subsystems

Communication: PFM telemetry at 108.06 Mc. Turnstile antenna. Real-time telemetry for 60 hr.

Power supply: AgZn batteries

Onboard propulsion: None

Attitude control: Spin stabilization

Environment control: Passive thermal control

Guidance and control: Digital solar-aspect sensor. Slit aspect sensor for Earth and Moon.

Onboard computer: None

Structure: Cylinder 48-cm diameter, with tubular magnetometer boom mounted on axis. Length, including spherical magnetometer housing: 132 cm (fig. A–13).

Experiments/instruments	Experimenter	Institution
Rb-vapor magnetometer (table 11–11)	Heppner, J. P.	GSFC
Two fluxgate magnetometers (table 11–11)	Heppner, J. P.	GSFC
Faraday-cup plasma probe (table 11–5)	Bridge, H.	MIT
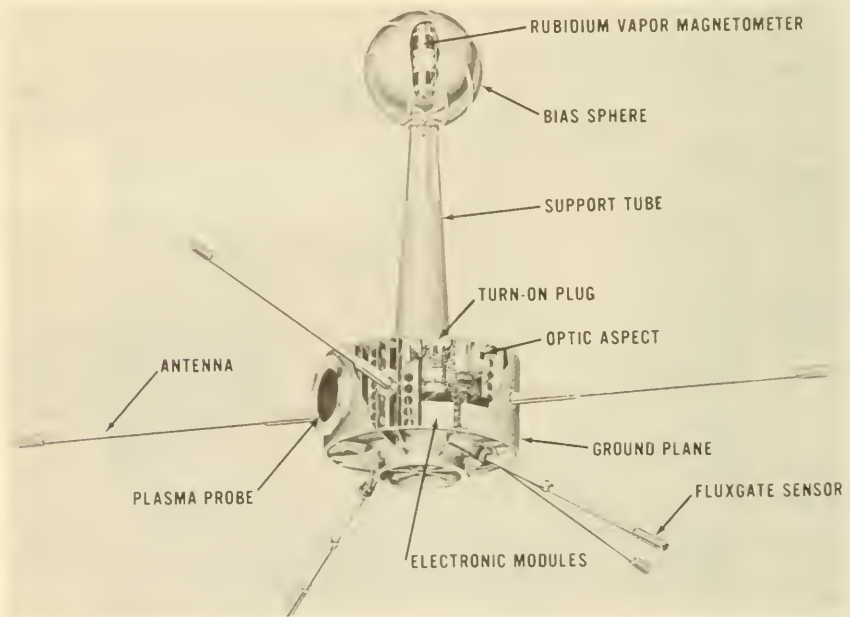
FIGURE A–13.—Explorer X.

EXPLORER XI

S–15, Gamma-Ray Astronomy Satellite

Apr. 27, 1961	Juno II	AMR/Minitrack
37 kg	108.1 min	28.8°
489/1790 km	Dec. 6, 1961	—

NASA launched Explorer XI for the purpose of mapping the sources of high-energy gamma rays. In this sense, it was the first astronomical satellite.

Descriptions of subsystems

Communication:	2 PM transmitters at 107.97 and 108.06 Mc. Command receiver. Cloverleaf antenna. Tape recorder (failed).
Power supply:	Solar cells and NiCd batteries
Onboard propulsion:	None
Attitude control:	Spin stabilization. Mercury-filled cylinder used as nutation damper.
Environment control:	Passive thermal control
Guidance and control:	Photodiode Sun and Earth sensors
Onboard computer:	None
Structure:	Octagonal aluminum box (30.5 cm square, 58.5 cm long) on cylinder (15.2-cm diameter, 52.2 cm long)

Experiments/instruments	*Experimenter*	*Institution*
Phoswich-Cerenkov counter telescope (table 13–4)	Kraushaar, W.	MIT

EXPLORER XII

S–3, EPE–A, Energetic Particles Explorer

Aug. 15, 1961	Delta	AMR/Minitrack
37 kg	1585 min	33.3°
293/77 300 km	Dec. 6, 1961	—

First of the NASA EPE series. See Explorers XIV, XV, and XXVI. Major objectives of series were to study the solar wind, the interplanetary field, trapped radiation, and cosmic rays.

Descriptions of subsystems

Communication:	PFM telemetry at 136.02 Mc. No tape recorder or command receiver. Turnstile antenna.
Power supply:	Four solar-cell paddles, plus AgCd batteries provided average of 16 W.
Onboard propulsion:	None
Attitude control:	Spin stabilization
Environment control:	Passive thermal control
Guidance and control:	Digital solar-aspect sensor
Onboard computer:	None
Structure:	Aluminum octagon 66 cm across flats, 48 cm high, with truncated cone. Entire assembly 129 cm high (fig. A–14). Magnetometer on end of superstructure.
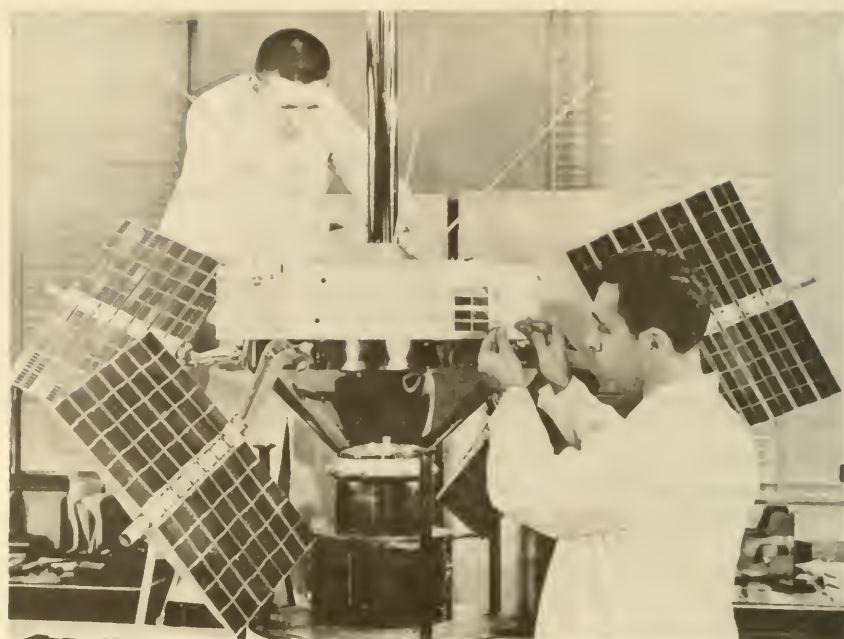
FIGURE A–14.—Explorer XII.

Experiments/instruments	Experimenter	Institution
Curved-surface electrostatic plasma analyzer (table 12–7)	Bader, M.	Ames Research Center
Cosmic-ray scintillation telescope (table 13–4)	McDonald, F. B.	GSFC
Geiger telescope (table 13–4) _____	McDonald, F. B.	GSFC
Scintillation counter (table 13–4) __	McDonald, F. B.	GSFC
Triaxial fluxgate magnetometer (table 11–11)	Cahill, L.	U. N.H.
Trapped radiation Geiger counters (table 11–8)	O'Brien, B. J.	State U. of Iowa
Magnetic particle spectrometer (table 11–8)	O'Brien, B. J.	State U. of Iowa
Cadmium-sulfide cell-radiation detectors (table 11–8)	O'Brien, B. J.	State U. of Iowa
Geiger trapped-radiation detector (table 11–8)	O'Brien, B. J.	State U. of Iowa
Scintillation counter (table 11–8) __	Davis, L. R.	GSFC

Selected reference: Reference 10

EXPLORER XIII   1961 X 1

S–55A, Micrometeoroid Satellite, Micrometeoroid Explorer

Aug. 25, 1961	Scout	Wallops/Minitrack
85 kg	97.3 min	36.4°
282/976 km	Aug. 28, 1961	Aug. 28, 1961

Explorer XIII was the first of the Langley micrometeoroid satellites. (See Explorers XVI and XXIII.) The orbit of Explorer XIII was too low, and reentry occurred before significant data were returned.

Descriptions of subsystems

Communication:	PDM/FM/AM telemetry. Two separate telemetry systems at 136.20 and 136.86 Mc. Command receiver. Four whip antennas. Real time.
Power supply:	Two separate power supplies; 1 for each telemeter. Solar cells and NiCd batteries constituted main supply with Hg batteries for Minitrack beacon.
Onboard propulsion:	None
Attitude control:	Spin stabilization
Environment control:	Passive thermal control
Guidance and control:	None
Onboard computer:	None
Structure:	Instrument payload and solar cells were wrapped around the Scout fourth stage. Cylindrical shape: 63-cm diameter, 193 cm long (fig. A–15).

Experiments/instruments	*Experimenter*	*Institution*
Pressurized-cell micrometeoroid detectors (table 11–14)	Gurtler, C. A.	Langley Research Center
Wire-grid micrometeoroid detectors (table 11–14)	Secretan, L.	GSFC
Light-transmission-erosion micrometeoroid detectors (table 11–14)	Secretan, L.	GSFC
Piezoelectric micrometeoroid detectors (table 11–14)	Beswick, A. G.	Langley Research Center
Foil-type gridded micrometeoroid detectors (table 11–14)	Davison, E.	Lewis Research Center

Selected reference: Reference 11

EXPLORER XIV
1962 BΓ 1

S–3A, EPE–B, Energetic Particles Explorer-B, Energetic Particles Satellite

Oct. 2, 1962	Delta	AMR/Minitrack
40 kg	2184 min	32.9°
280/98 500 km	Oct. 8, 1963	—

The second NASA EPE. See Explorers XII, XV, and XXVI.

Descriptions of subsystems

Communication:	PFM telemetry at 136.440 Mc. No tape recorder or command receiver. Turnstile antenna.
Power supply:	Four paddles with p–n solar cells, plus AgCd batteries provided an average of 35 W
Onboard propulsion:	None
Attitude control:	Spin stabilization; despin weights. Erection of appendages also used for despin.
Environment control:	Passive thermal control

Guidance and control: Six digital photodiodes as solar-aspect sensors; killer-timer

Onboard computer: None

Structure: Aluminum octagon 66 cm across flats, 48 cm high, with truncated cone for superstructure. Entire assembly 129 cm high. Magnetometer on end of superstructure (fig. A–14).

Experiments/instruments	Experimenter	Institution
Curved-surface electrostatic plasma analyzer (table 12–7)	Bader, M.	Ames Research Center
Same as Explorer XII		

EXPLORER XV   1962 BΛ 1

S–3B, EPE–C, Energetic Particles Explorer C; Radiation Detection Satellite; Project SERB (Study of the Enhanced Radiation Belt).

Oct. 27, 1962	Delta	AMR/Minitrack
45 kg	312.0 min	18.0°
312/17 300 km	Feb. 9, 1963	—

The third NASA EPE was launched to study the location, composition, and decay rate of the artificial radiation belt created July 9, 1962, by the Starfish high-altitude nuclear explosion.

Descriptions of subsystems
Essentially identical to Explorer XIV. Despin device failed, leaving satellite spinning at 60 rpm, too high for optimum radiation measurements. Telemetry at 136.100 Mc.

Experiments/instruments	Experimenter	Institution
p–n junction electron detectors (table 11–8)	Brown, W.	Bell Labs.
Scintillation detectors (table 11–8) _	McIlwain, C.	U. Calif. (SD)
Scintillation counter (table 11–8) __	Davis, L. R.	GSFC
Triaxial fluxgate magnetometer (table 11–11)	Cahill, L.	U. N.H.

EXPLORER XVI   1962 BX 1

S–55B, Micrometeoroid Satellite, Micrometeoroid Explorer

Dec. 16, 1962	Scout	Wallops/Minitrack
100 kg	104.4 min	52.0°
750/1180 km	July 22, 1963	—

Second NASA Micrometeoroid Explorer. See Explorers XIII and XXIII.

Descriptions of subsystems
Same as Explorer XIII, except for addition of command receiver and tape recorder. Two telemeters at 136.20 and 136.86 Mc (fig. A–15).

Experiments/instruments
See Explorer XIII

Selected reference: Reference 12
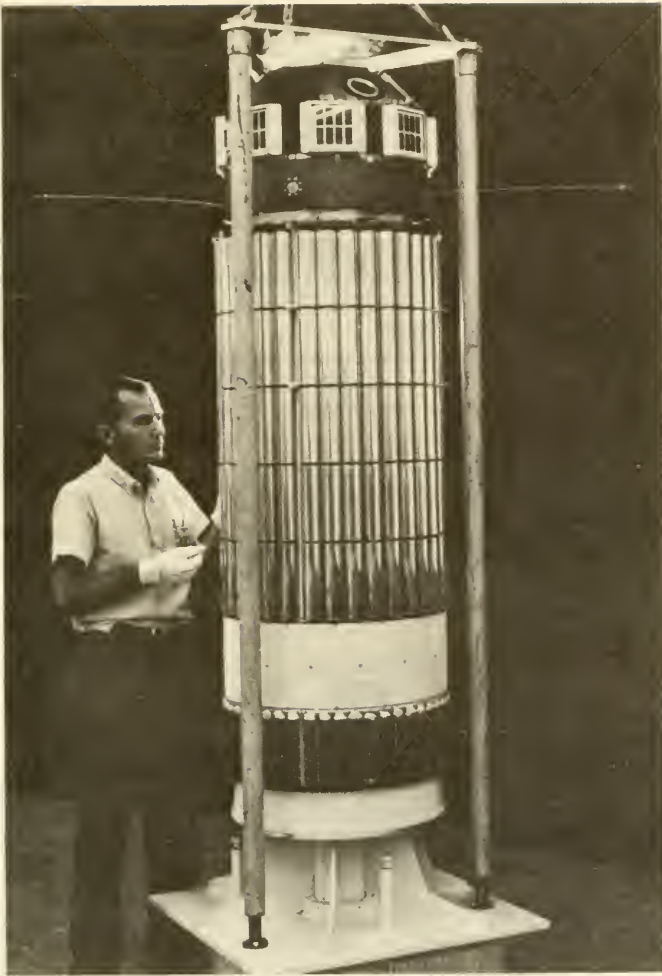
FIGURE A–15.—Explorer XVI.

EXPLORER XVII   1963 9A

S–6A, AE–A, Atmosphere Explorer A, Aeronomy Satellite, Atmospheric
Structure Satellite, Direct Measurements Explorer (Explorer XVII was
not a NASA DME).

Apr. 2, 1963	Delta	AMR/STADAN
184 kg	96.4 min	57.6°
254/915 km	July 10, 1963	—

NASA's first satellite in the AE series. See also Explorer XXXII. The pur-
pose of this series is to measure directly atmospheric composition, density,
pressure, and temperature.

Descriptions of subsystems

Communication:
PCM/PM telemetry at 136.320 Mc. Beacon at 136.560 Mc. Two command receivers, but no tape recorder. Canted turnstile antenna.

Power supply:
68 kg of AgZn batteries provided enough energy for about 800 experiment turn-ons, or 70 hours of data

Onboard propulsion:
None

Attitude control:
Spin stabilization at 90 rpm; nutation damper

Environment control:
Passive thermal control

Guidance and control:
Infrared and visible horizon sensors, slit detector for Moon, digital solar-aspect sensor

Onboard computer:
None

Structure:
Hermetically sealed, stainless-steel spherical shell 0.063 cm thick and 89 cm in diameter (fig. A–16)
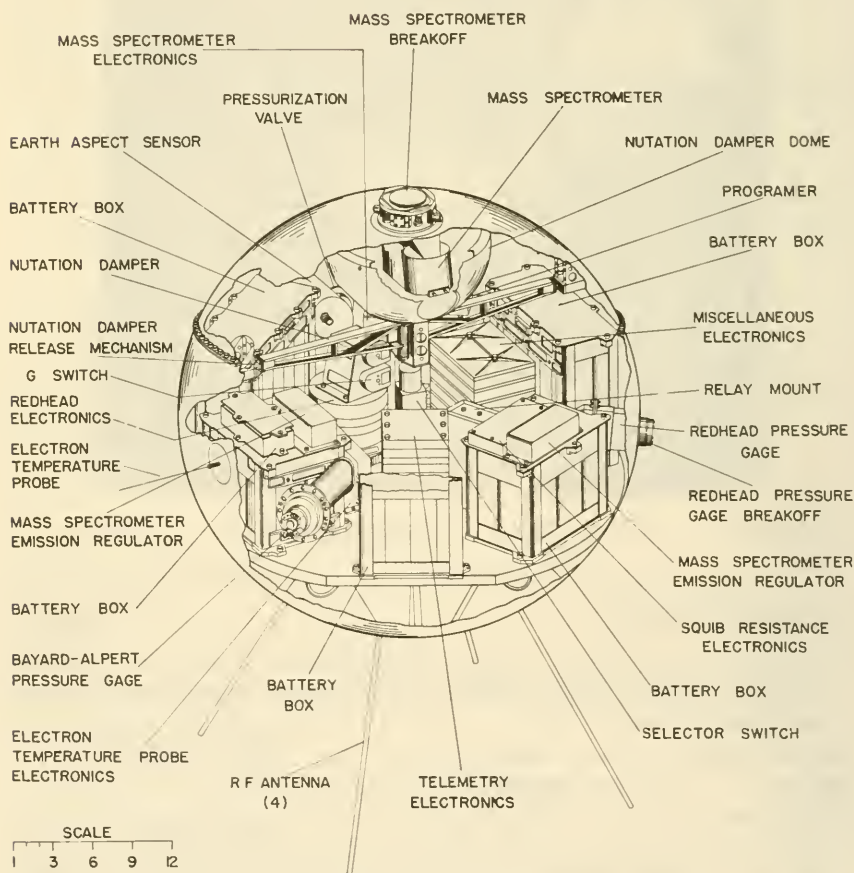
FIGURE A–16.—Explorer XVII. Scale is in inches.

Experiments/instruments	*Experimenter*	*Institution*
Two neutral mass spectrometers (table 11–1)	Reber, C.	GSFC
Two Redhead and 2 Bayard-Alpert pressure gages (table 11–1)	Horowitz, R.	GSFC
Two Langmuir probes (table 11–5)	Spencer, N.	GSFC

Selected references: References 13, 14

EXPLORER XVIII   1963 46A

S–74, IMP I, Interplanetary Monitoring Platform, Interplanetary Monitoring
   Probe; IMP–A, Interplanetary Explorer; IMS, Interplanetary Monitoring
   Satellite

Nov. 26, 1963	Delta	ETR/STADAN
63 kg	96.3 hr	33.3°
192/197 000 km	—	—

First of the IMP series. See also Explorers XXI and XXVIII. The IMP
   scientific objectives include the probing of the magnetosphere and the inter-
   planetary space beyond it by use of a wide variety of instruments.

Descriptions of subsystems

Communication:	PFM telemetry at 136.110 Mc. No tape recorder.
Power supply:	Four paddles with p–n solar cells plus AgCd batteries provide an average of 38 W
Onboard propulsion:	None
Attitude control:	Spin stabilized at 20 rpm
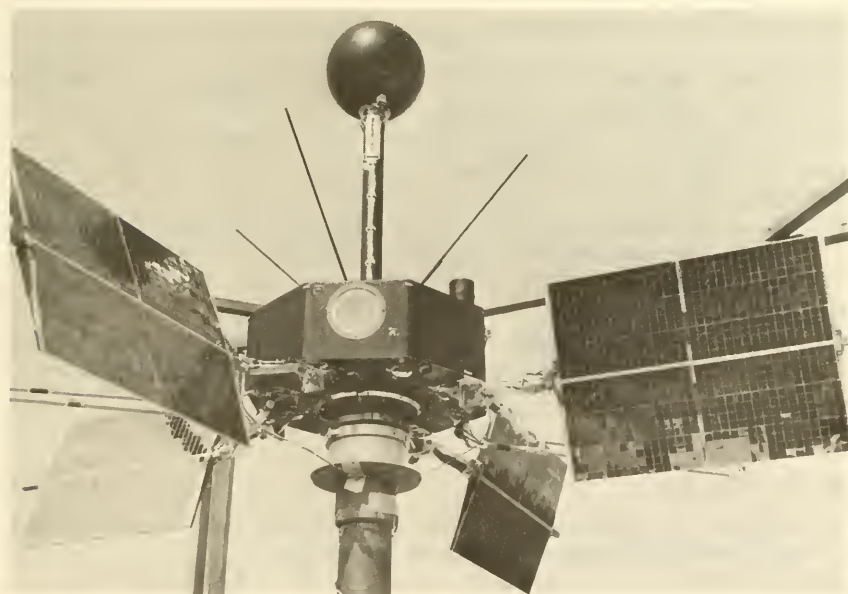
FIGURE A–17.—Explorer XVIII (IMP A).

Environment control:	Passive thermal control using black and white paints and evaporated aluminum coatings
Guidance and control:	Digital solar-aspect sensor. Transponder.
Onboard computer:	None
Structure:	Octagonal exterior with central thrust tube. Magnesium and epoxy fiber-glass construction. Magnetometer boom on top 1.8 m from base. Octagon 30.5 cm deep and 71 cm across flats (fig. A–17)

Experiments/instruments	Experimenter	Institution
Cosmic-ray solid-state telescope (table 13–4)	Simpson, J. A.	U. Chicago
Cosmic-ray scintillation telescope (table 13–4)	McDonald, F. B.	GSFC
Cosmic-ray Geiger telescope (table 13–4)	McDonald, F. B.	GSFC
Curved-plate electrostatic plasma analyzer (table 12–7)	Wolfe, J.	Ames Research Center
Faraday-cup plasma probe (table 12–7)	Bridge, H.	MIT
Planar ion and electron probes (table 11–5)	Bourdeau, R.	GSFC
Rb-vapor magnetometer (table 11–11)	Ness, N.	GSFC
Two fluxgate magnetometers (table 11–11)	Ness, N.	GSFC
Ionization chamber and Geiger counter (table 11–5)	Anderson, K. A.	U. Calif.

Selected reference: Reference 15

EXPLORER XIX   1963 53A

AD–A, ·Air Density Explorer A, ADE
Dec. 19, 1963   Scout   WTR/STADAN
8 kg   115.9 min   78.6°
589/2390 km   —

NASA's second balloon satellite for air-density measurements. First satellite in AD series. See also Explorer XXIV. Explorer XIX STADAN beacon stopped transmitting shortly after launch.

Descriptions of subsystems
Essentially identical to Explorer IX except for the addition of a few solar cells to aid NiCd batteries in powering beacon. Beacon was at 136.62 Mc.

Experiments/instruments
None

EXPLORER XX   1964 51A

S–48, IE–A, IE–I, Ionosphere Explorer I, Fixed Frequency Topside Sounder, Topsi, Ionosphere Satellite, Ionosphere Explorer A
Aug. 25, 1964   Scout   WTR/STADAN
44 kg   103.9 min   79.9°
869/1020 km   —   —

NASA's topside sounder was similar in purpose to Canada's Alouette, but instead of sweeping a band of frequencies, Explorer XX employed 6 fixed frequencies.

Descriptions of subsystems

Communication:	FM telemetry for experiments, PM for status data; transmitted on 136.680 and 136.350 Mc, respectively. Two command receivers, but no tape recorder. Turnstile antennas.
Power supply:	Solar cells $(p-n)$ with NiCd batteries provided 30 W while sounding and 1.7 W on standby.
Onboard propulsion:	None
Attitude control:	Spin stabilized at 2.2 rpm
Environment control:	Passive thermal control
Guidance and control:	1-yr killer timer
Onboard computer:	None
Structure:	Truncated cone 51 cm in diameter at base. Central thrust tube (fig. A–18)

Experiments/instruments	Experimenter	Institution
Spherical plasma probe (table 11–5)	Boyd, R. L. F.	University College
Galactic radio-noise receiver (table 13–1)	Stone, R.	GSFC
Six transmitters for topside sounding (table 11–5)	Knecht, R. W.	NBS Central Radio Propagation Lab.

Selected reference: Reference 16
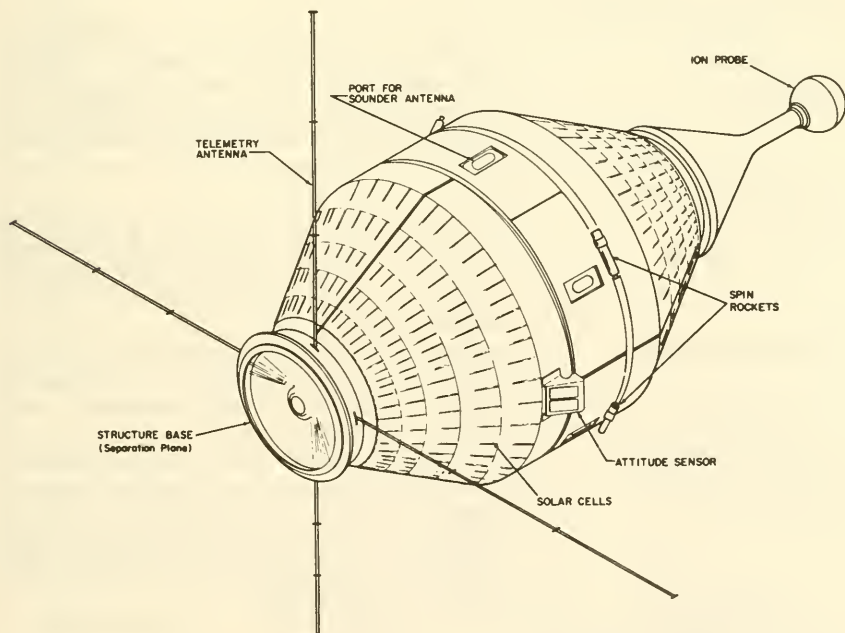
FIGURE A–18.—Explorer XX.

EXPLORER XXI   1964 60A

S–74A, IMP, IMP–B, IMP II, Interplanetary Monitoring Platform, Inter-
planetary Monitoring Probe, Interplanetary Explorer
Oct. 3, 1964   Delta   ETR/STADAN
62 kg   35 hr   33.5°
196/95 500 km   —   —
Second NASA IMP. See also Explorers XVIII and XXVIII. Apogee much
lower than planned 200 000 km.

Descriptions of subsystems
See Explorer XVIII. Transmitted on 136.145 Mc.

Experiments/instruments
See Explorer XVIII

EXPLORER XXII   1964 64A

S–66B, BE–B, Beacon Explorer B; PIBS, Polar Ionospheric Beacon Satellite;
Orbiting Radio Ionospheric Satellite
Oct. 9, 1964   Scout   WTR/STADAN,
                                            TRANET
53 kg   104.7 min   79.7°
885/1075 km   —   —

Launched by NASA to study the ionosphere and shape of the Earth. Built
for NASA's Langley Research Center by the Johns Hopkins Applied
Physics Laboratory. BE–A was a failure; BE–C was launched as Explorer
XXVII.

Descriptions of subsystems

Communication: PAM, PDM, and PCM telemetry. Transmitted
                            at 136.170 Mc. Command receiver. Two di-
                            pole and 2 61-cm whip antennas.
Power supply: Four solar-cell panels plus NiCd batteries pro-
                            vided an average of 10 W. Special banks of
                            solar cells for thermal control.
Onboard propulsion: None
Attitude control: Initial spin stabilization. Yo-yo despin from 200
                            to 40 rpm. Panel deployment reduced spin
                            from 40 to 3 rpm. Magnetic bars eliminated
                            rest of spin and alined satellite with Earth's
                            magnetic field.
Environment control: Vacuum insulation between instrument package
                            and satellite shell. Instruments warmed by
                            electric heater-thermostat arrangement con-
                            suming 4–6 W.
Guidance and control: Four solar-cell aspect sensors. Three-axis flux-
                            gate magnetometer. Laser tracking. Beacons.
Structure: Octagonal exterior 30 cm high and 46 cm in
                            diameter. Nylon honeycomb and fiber-glass
                            construction with metal box as load-bearing
                            structure (fig. A–19).

Experiments/instruments	*Experimenter*	*Institution*
Langmuir probe (table 11–5) _____	Brace, L. H.	SFC

Selected reference: Reference 17
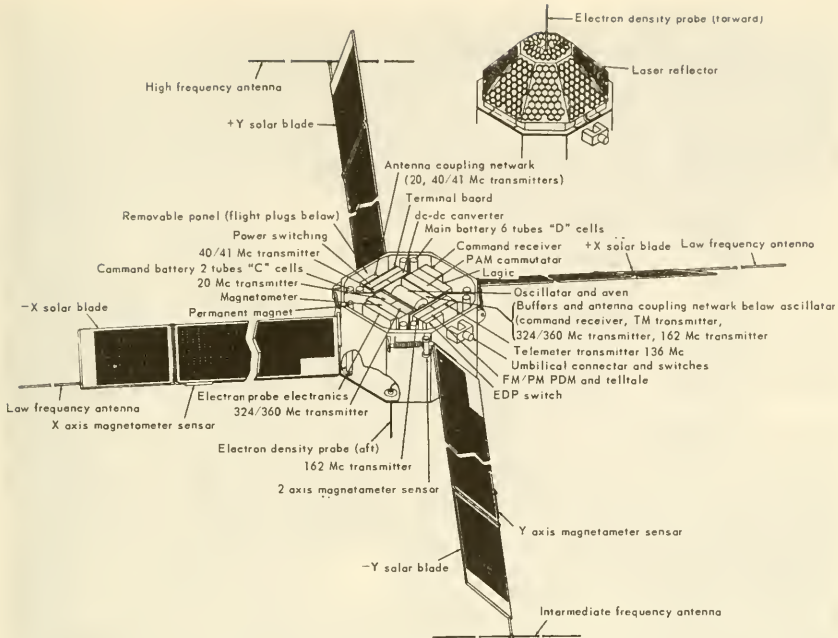
FIGURE A–19.—Explorer XXII.

EXPLORER XXIII 1964 74A

S–55C, Micrometeoroid Explorer, Meteoroid Detection Satellite

Nov. 6, 1964	Scout	Wallops/STADAN
134 kg	99.2 min	51.9°
463/982 km	—	—·

Third and last of NASA's S–55 series of micrometeoroid satellites. See also Explorers XIII and XVI.

Descriptions of subsystems
See Explorer XVI. Transmitted on 136.080 and 136.857 Mc.

Experiments/instruments	Experimenter	Institution
Pressurized-cell micrometeoroid detectors (table 11–14)	Gurtler, C. A.	Langley Research Center
Piezoelectric micrometeoroid detectors (table 11–14)	Beswick, A. G.	Langley Research Center
Light-transmission-erosion micrometeoroid detectors (table 11–14)	Secretan, L.	GSFC
Capacitor micrometeoroid detectors (table 11–14)	Siviter, J. H.	Langley Research Center

Selected reference: Reference 18

EXPLORER XXIV   1964 76A

Air Density Explorer B, AD–B, AD/I–B, Air Density/Injun Explorer B
Nov. 21, 1964   Scout   WTR/STADAN
9 kg   116.3 min   81.4°
553/2500 km   —   —
Explorer XXIV was a NASA balloon satellite carrying only a beacon to aid
    tracking and atmospheric-density measurements

Descriptions of subsystems

Communication:	No telemetry. Beacon at 136.710 Mc. Insulated halves of sphere served as antenna.
Power supply:	280 solar cells plus NiCd batteries for beacon
Onboard propulsion:	None
Attitude control:	None
Environment control:	White dots of epoxy paint for passive thermal control
Guidance and control:	None
Onboard computer:	None
Structure:	Balloon 3.66 m in diameter. Skin: 4 alternating layers of Mylar and aluminum foil.

Experiments/instruments: None

EXPLORER XXV   1964 76B

Injun 4, AD/I–B, Air-Density/Injun-B, University Explorer
Nov. 21, 1964   Scout   WTR/STADAN
41 kg   116.3 min   81.4°
554/2490 km   —   —
The first NASA-launched Injun—the previous satellites in the series were
    launched by the U.S. Navy. All of the Injuns are designed to study the
    radiation belts. All have been designed by the State University of Iowa.

Descriptions of subsystems

Communication:	PCM telemetry. Two transmitters at 136.860 and 136.292 Mc. Command receiver and tape recorder.
Power supply:	Solar cells and NiCd batteries
Onboard propulsion:	None
Attitude control:	Magnetic despin rod. Permanent magnet alines satellite with Earth's field. Electromagnet.
Environment control:	Passive thermal control
Guidance and control:	Two solar-aspect sensors. Fluxgate magnetometer.
Onboard computer:	None
Structure:	Aluminum shell with 40 sides, 63.5 cm in diameter. Three booms (fig. A–20).

Experiments/instruments	Experimenter	Institution
Two spherical retarding-potential analyzers (table 11–5)	Sagalyn, R.	AFCRL
Four directional Geiger counters, 2 for general monitoring, 1 for Starfish decay. Total of 7 (table 11–8)	Van Allen, J. A.	State U. of Iowa
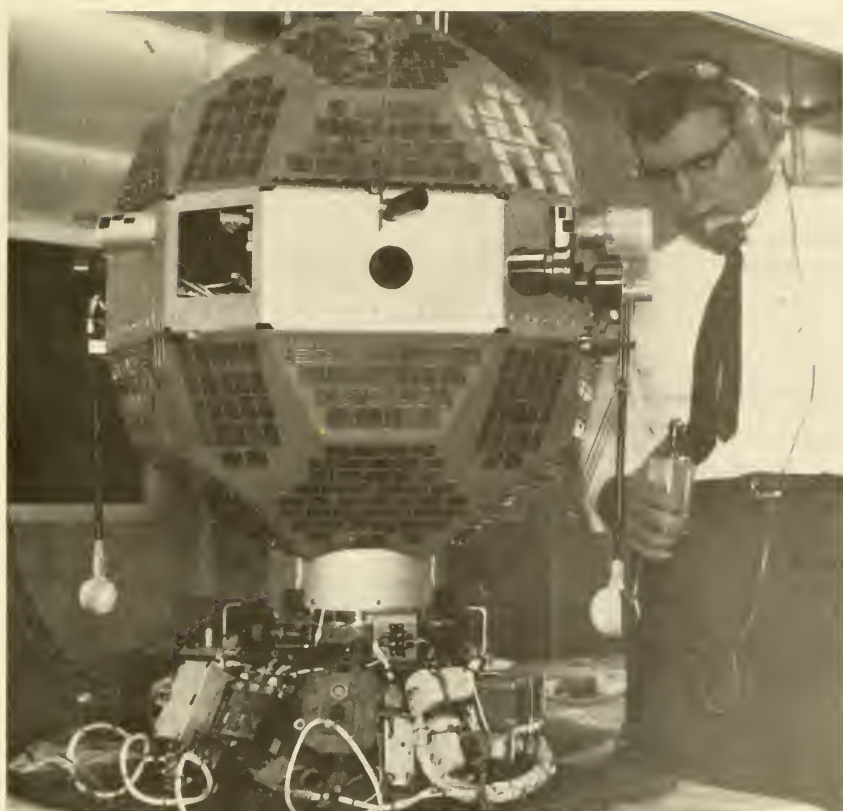
FIGURE A–20.—Explorer XXV (Injun 4).

Experiments/instruments	Experimenter	Institution
Two scintillator counters (table 11–8)	Van Allen, J. A.	State U. of Iowa
One *p–n* junction detector (table 11–8)	Van Allen, J. A.	State U. of Iowa
Four CdS cells (table 11–8) _____	Van Allen, J. A.	State U. of Iowa

EXPLORER XXVI
1964 86A

S–3C, EPE–D, Energetic Particles Explorer D, Radiation Detection Satellite

Dec. 21, 1964	Scout	WTR/STADAN
46 kg	456 min	20.2°
360/26 200 km	—	—

The fourth and last satellite in NASA's EPE series. See also Explorers XII, XIV, and XV. The EPE primary mission was to study how energetic particles are trapped and lost in the radiation belts.

Descriptions of subsystems

Communication: PCM telemetry at 136.275 Mc. No command receiver or tape recorder. Turnstile antenna.

Power supply:	Four solar-cell paddles covered with p–n cells, combined with AgCd batteries, produced an average of 15 W
Onboard propulsion:	None
Attitude control:	Spin stabilized at 25 rpm. Nutation damper. Despin device plus effect of paddle erection.
Environment control:	Passive thermal control
Guidance and control:	Digital solar-aspect sensor; electronic killer-timer
Onboard computer:	None
Structure:	Octagon with truncated conical superstructure. Octagon was 43 cm high and 70 cm in diameter. Aluminum cover with fiber-glass-honeycomb interior structure (fig. A–21).

Experiments/instruments: See Explorer XV

BTL BIAS
OPTICAL ASPECT COMPUTER
ENCODER-CONVERTER
TELEMETRY ENCODER
SOLAR DOOR
REGULATOR CONVERTER
UNIVERSITY OF CAL DIRECTIONAL
SOLAR PADDLE NO 2
IV
BTL
OPTICAL ASPECT CONVERTER
COSMIC RAY LOGIC BOX CONVERTER
MAGNETOMETER ELECTRONICS
BATTERY PACK "A"
SOLAR PADDLE NO 3
SOLAR PADDLE NO 1
ION-ELECTRON DETECTOR
UNIVERSITY OF CAL. OMNI
COSMIC-RAY LOGIC BOX
III
BATTERY PACK "B"
OPTICAL ASPECT SENSOR
DATA ENCODER
24°
28°
SOLAR PADDLE NO 4

FIGURE A–21.—Explorer XXVI. See also figure A–14.

EXPLORER XXVII   1965 32A

BE–C, Beacon Explorer C

Apr. 29, 1965	Scout	Wallops/STADAN, TRANET
60 kg	107.8 min	41.2°
940/1315 km	—	—

Second successful Beacon Explorer (fig. A–22). See Explorer XXII.

Descriptions of subsystems
See Explorer XXII

Experiments/instruments
See Explorer XXII
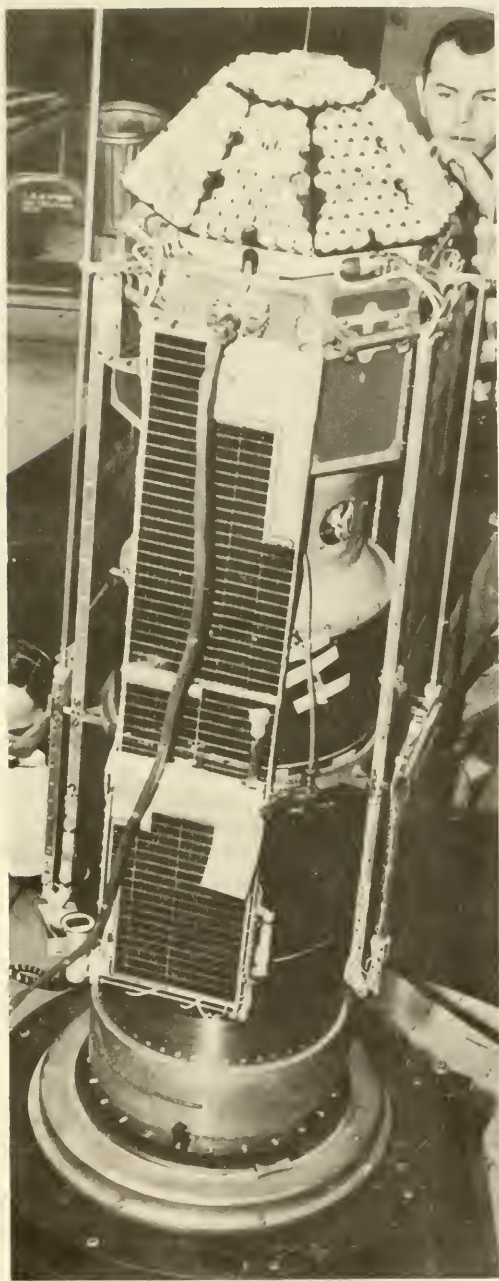
FIGURE A-22.—Explorer XXVII (BE-C).

EXPLORER XXVIII   1965 42A

IMP–C, IMP III, Interplanetary Monitoring Platform, Interplanetary Explorer

May 29, 1965   Delta   ETR/STADAN
59 kg   8558 min   33.9°
195/264 000 km   —   —

Third NASA IMP. See Explorers XVIII and XXI. IMP–C was the last in the first block of 3 IMP's. IMP D/E and IMP F/G constitute 2 other blocks.

Descriptions of subsystems
See Explorer XVIII. Transmitter at 136.125 Mc.

Experiments/instruments
See Explorer XVIII

EXPLORER XXIX   1965 89A

Geos-A, Geos I, Geodetic Explorer A

Nov. 6, 1965   Thrust-Augmented   ETR/STADAN,
                       Improved Delta   TRANET
175 kg   120.3 min   59.4°
1110/2280 km   —   —

NASA's first geodetic satellite (NASA cooperated in the ANNA program, but ANNA 1 B was launched by DOD). Geos carried equipment developed by NASA, DOD, and the Department of Commerce. Built by Johns Hopkins Applied Physics Laboratory.

Descriptions of subsystems

Communication:	Two PAM commutators, 2 PDM subcommutators, 3 telltale registers and a telemetry time marker. Telemetry at 136.830 Mc. Command receiver. Conical and spiral antennas. Turnstile. Status telemetry only.
Power supply:	Three independent power supplies using n–p solar cells and NiCd batteries. Main power supply, 16–20 W; light, 9–12 W; transponder, 9–12 W.
Onboard propulsion:	None
Attitude control:	Yo-yo and eddy-current despin devices. Gravity-gradient stabilization with extendable 20-m boom with eddy-current damper on end.
Environment control:	Passive thermal control.
Guidance and control:	Three fluxgate magnetometers and 6 solar cells for aspect sensing. See geodetic measurement aids below.
Onboard computer:	None
Structure:	Octagonal aluminum cylinder, 123 cm across flats, 81 cm high, including truncated pyramidal superstructure (fig. A–23).

Experiments/instruments

Geodetic measurement aids: Optical beacon, radio Doppler beacon, range transponder (Secor), range and range-rate transponder, laser corner reflectors

Selected reference: Reference 19
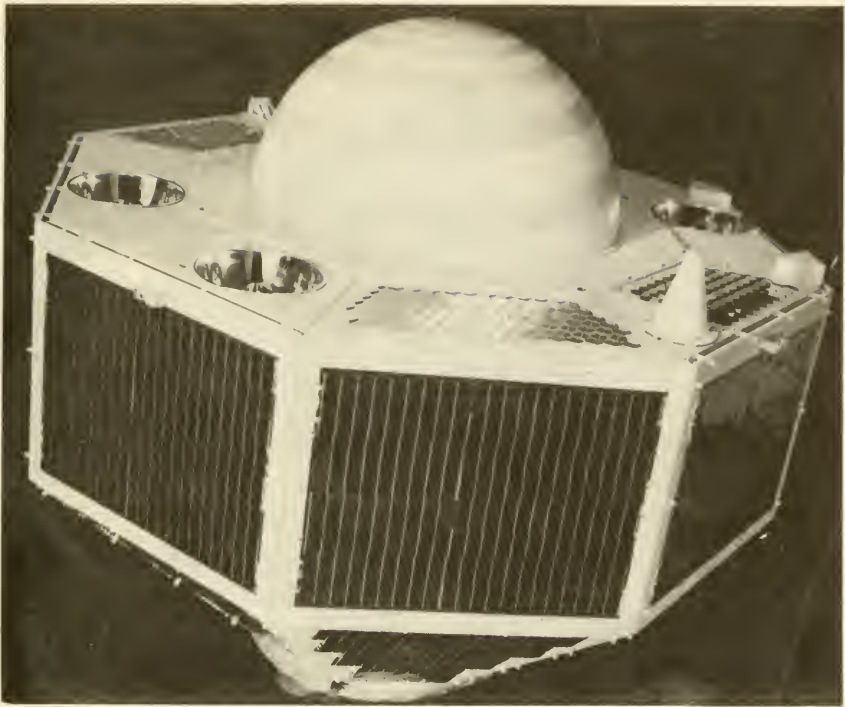
FIGURE A-23.—Explorer XXIX (Geos A).

EXPLORER XXX 1965 93A

IQSY Solar Explorer, Solar Explorer, Solrad 8, SR 8

Nov. 18, 1965	Scout	Wallops/STADAN
57 kg ·	102.8 min	59.7°
709/882 km	—	—

Explorer XXX is a continuation of the NRL Solrad series, designed to monitor the Sun's X-rays and the spectra of solar flares. Explorer XXX was launched by NASA, while all previous Solrads were launched by DOD.

Descriptions of subsystems

Communication:	FM/AM telemetry at 136.530 Mc. PAM/FM/AM telemetry at 137 Mc. Command receiver. Turnstile telemetry antenna.
Power supply:	Solar cells and batteries
Onboard propulsion:	None
Attitude control:	Spin stabilized. Vapor jet to increase spin rate. Nutation damper. Pulsed vapor jet to precess spin axis.
Environment control:	Passive thermal control
Guidance and control:	Two Sun sensors control pulsed vapor jets
Onboard computer:	None
Structure:	Two hemispheres, 61 cm in diameter, separated by cylindrical equatorial section (fig. A-24)
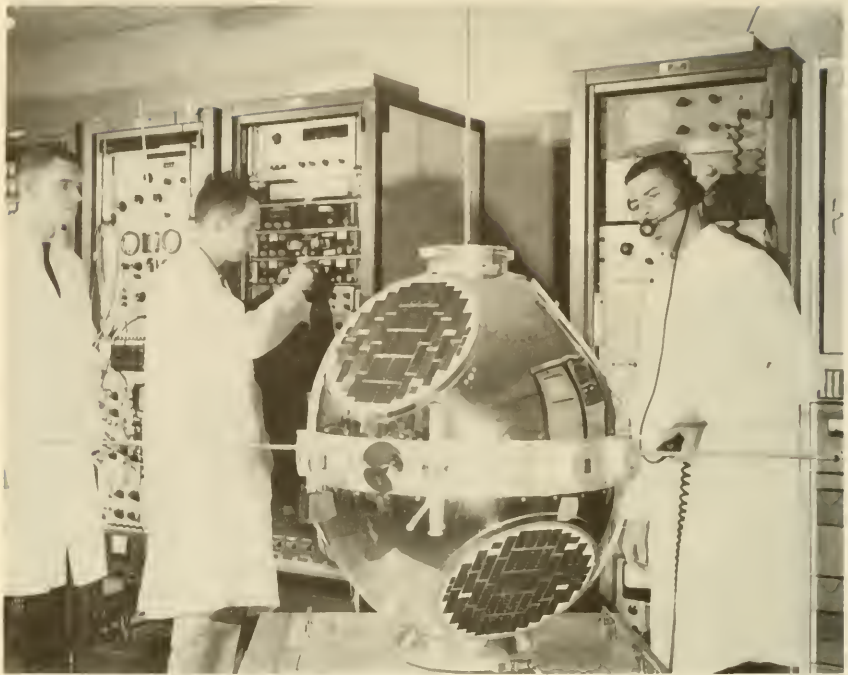
FIGURE A–24.—Explorer XXX (IQSY Solar Explorer).

Experiments/instruments	Experimenter	Institution
Five ionization-chamber X-ray photometers (table 12–3)	—	NRL
Two pairs of Geiger X-ray counters (table 12–3)	—	NRL
Two pairs of Lyman-α ionization chambers (table 12–3)	—	NRL

EXPLORER XXXI
1965 98B

S–30A, DME–A, Direct Measurements Explorer A, ISIS–X (actually, this term refers to both Explorer XXXI and Alouette 2).

Nov. 28, 1965	Thor-Agena B	WTR/STADAN
99 kg	121.3 min	79.8°
489/2980 km	—	—

Launched with Alouette 2 as ISIS–X (ISIS = International Satellites for Ionospheric Studies). See Direct Measurements Explorer Follow-ons for terminology.

Descriptions of subsystems

Communication: PCM/PM and PAM/FM/PM telemetry modes, both at 136.380 Mc. Command receiver. Tape recorder.

Power supply:	n–p solar cells plus NiCd batteries
Onboard propulsion:	None
Attitude control:	Spin stabilized. Magnetic torquer for spin up and despin.
Environment control:	Passive thermal control
Guidance and control:	Solar-aspect sensors and 3-axis fluxgate
Onboard computer:	None
Structure:	76 cm in diameter, 64 cm high (fig. A–25)

FIGURE A–25.—Explorer XXXI (DME–A).

Experiments/instruments	Experimenter	Institution
Planar ion and electron probes (table 11–5)	Donley, J.	GSFC
Electrostatic probe (table 11–5) ___	Brace, L. H.	GSFC
Spherical retarding-potential analyzer (table 11–5)	Boyd, R. L. F.	University College
Planar electron probe (table 11–5) _	Wilmore, A. P.	University College

Experiments/instruments	Experimenter	Institution
Magnetic-ion mass spectrometer (table 11–5)	Hoffman, J.	NRL
Energetic-electron current probe (table 11–5)	Maier, E.	GSFC

EXPLORER XXXII   1966 44A

S–6A, AE–B. (See Explorer-XVII synonyms.)
May 25, 1966	Delta	ETR/STADAN
225 kg	6.0 min	64.7°
279/2620 km	—	—

Descriptions of subsystems

Like Explorer XVII except for the following additions: tape recorder, solar cells for limited battery recharging, magnetic torquer to modify spin axis, and 3-axis fluxgate magnetometer for aspect sensing (fig. A–26).

Experiments/instruments	·Experimenter	Institution
Three Redhead ionization gages (table 11–1)	Newton, G.	GSFC
Neutral magnetic mass spectrometer (table 11–1)	Reber, C.	GSFC
Two planar ion traps (table 11–5) _	Brace, L.	GSFC
rf ion mass spectrometer (table 11–5)	Taylor, H.	GSFC

EXPLORER XXXIII   1966 58A

IMP D/E, AIMP, Anchored IMP. (See Explorer-XVIII synonyms.)
July 1, 1966	Thrust-augmented Delta	ETR/STADAN
96 kg	8540.0 min	28.7°
15 900/435 000 km	—	—

A small lunar satellite designed to measure fields and particles in the vicinity of the Moon. Uses IMP technology. IMP E was a backup spacecraft. Explorer XXXIII did not attain lunar orbit because of its excessive velocity.

Descriptions of subsystems

Communication:	PFM/PM telemetry at 136.020 Mc. Command receiver. No tape recorder. Modified turnstile antenna.
Power supply:	Solar cells (*p–n*) and AgCd batteries generate an average of 45 W. Four paddles.
Onboard propulsion:	Retromotor Thiokol TE–M–458 solid
Attitude control:	Spin stabilized at 25 rpm; yo-yo despin
Environment control:	Passive thermal control
Guidance and control:	Optical aspect sensors. GSFC Range-and-Range-Rate transponder used for navigation during critical lunar-orbit injection.
Onboard computer:	None
Structure:	Configuration similar to Explorer XVIII. Diameter, 71 cm; body height, 88 cm. Magnesium central thrust tube with retromotor attached. Two magnetometer booms (fig. A–27).

FIGURE A-26.—Atmosphere Explorer B (AE-B), Explorer XXXII.
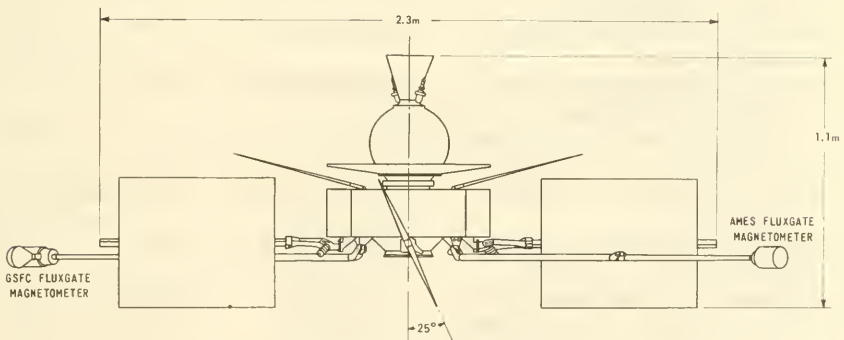
FIGURE A-27.—Explorer XXXIII (IMP D/E).

Experiments/instruments	Experimenter	Institution
Fluxgate magnetometers (table 11–11)	Sonett, C. P.	Ames Research Center
Triaxial fluxgate magnetometer (table 11–11)	Ness, N.	GSFC
Ionization chamber plus 2 Geiger counters (table 11–8)	Anderson, K. A.	U. Calif.
Solid-state detector and 2 Geiger counters (table 11–8)	Van Allen, J. A.	State U. of Iowa
Thin-film micrometeoroid charge detector and microphones (table 11–14)	Bohn, J. L.	Temple U.
Faraday-cup plasma probe (table 12–7)	Bridge, H. S.	MIT
Radio propagation experiment _____	Peterson, A. M.	Stanford U.

EXPLORER XXXIV

IMP F, Super IMP. (See Explorer-XVIII synonyms.)

May 24, 1967	TA Delta	WTR/STADAN
74.2 kg	106 hr	67°
245/214 000 km	—	—

Larger versions of the first three IMP's: Explorers XVIII, XXI, and XXVIII.

Descriptions of subsystems

See Explorer XVIII for basic design philosophy

Experiments/instruments	Experimenter	Institution
Ionization chamber and geiger tubes (table 11–8)	Anderson, K. A.	U. Calif.
Single-axis fluxgates plus Rb-vapor magnetometers (table 11–11)	Ness, N. F.	GSFC
Cosmic-ray scintillation telescope (table 13–4)	McCracken, K. G.	Graduate Research Center of the S.W.
Solid-state-scintillator cosmic-ray telescope (table 13–4)	Simpson, J. A.	U. Chicago
Cosmic-ray scintillator telescope (table 13–4)	McDonald, F. B.	GSFC
Large-area solid-state-scintillator telescope (table 13–4)	McDonald, F. B.	GSFC
Cylindrical electrostatic analyzer (table 13–4)	Van Allen, J. A.	State U. of Iowa
Spherical electrostatic analyzer (table 12–7)	Harrison, F. B.	TRW Systems
Cylindrical electrostatic analyzer (table 12–7)	Ogilvie, K. W.	GSFC
Solid-state telescope (table 11–8) __	Brown, W.	Bell Labs.
Solid-state detectors (table 11–8) __	Bostrom, C.	Applied Physics Lab.

FR–1

FR–1A, International Satellite		1965 101A
Dec. 6, 1965	Scout	WTR/STADAN, DIANE, IRIS
60 kg	99.9 min	75.9°
739/779 km	—	—

A French satellite in NASA's International Satellite series. Launched by NASA, built by Nord Aviation, managed by Centre National d'Etudes Spatiales. Primary objective was ionospheric research. FR–2 is connected with the EOLE meteorology program and is not covered here.

Descriptions of subsystems

Communication:	PAM/FM/PM telemetry at 136.800 Mc and FM/PM telemetry at 136.350 Mc. Command receiver. Tape recorder. Turnstile antenna.
Power supply:	Solar cells (n–p) plus AgCd batteries provide a nominal 9 W
Onboard propulsion:	None
Attitude control:	Spin stabilized. Yo-yo despin. Precession damper.
Environment control:	Passive thermal control
Guidance and control:	Solar-aspect sensor plus 3-axis fluxgate magnetometer
Onboard computer:	None
Structure:	Two truncated octagonal prisms with octagonal center section. Height 70 cm, minus appendages. Central magnesium thrust tube (fig. A–28).

Experiments/instruments	*Experimenter*	*Institution*
Electron density probe (table 11–5)	Sayers, J.	U. Birmingham
vlf experiment (table 11–5) _____	Storey, L. R. O.	CNES

Selected reference: Reference 7

GEOPHYSICAL RESEARCH SATELLITE   1963 26A

June 28, 1963	Scout	Wallops/STADAN
100 kg	102.1 min	49.8°
410/1312 km	June 29, 1963	—

U.S. Air Force geophysical satellite designed to measure atmospheric composition. Power supply failed owing to excessive heating. AFCRL was spacecraft contractor. Second satellite in series was a launch failure.

Descriptions of subsystems

Communication:	PAM/FM/PM telemetry at 136.740 Mc. Beacon at 136.530 Mc. Command receiver. No tape recorder. Four-loop antenna.
Power supply:	AgZn and Hg batteries
Onboard propulsion:	None
Attitude control:	Spin stabilized
Environment control:	
Guidance and control:	Magnetic and solar-aspect sensors
Onboard computer:	None
Structure:	Magnesium (fig. A–29)

Experiments/instruments	*Experimenter*	*Institution*
Magnetic mass spectrometer (table 11–1)	—	AFCRL
Planar ion trap (table 11–5) _____	—	AFCRL
Tissue-equivalent ionization chamber (table 11–8)	—	AFCRL
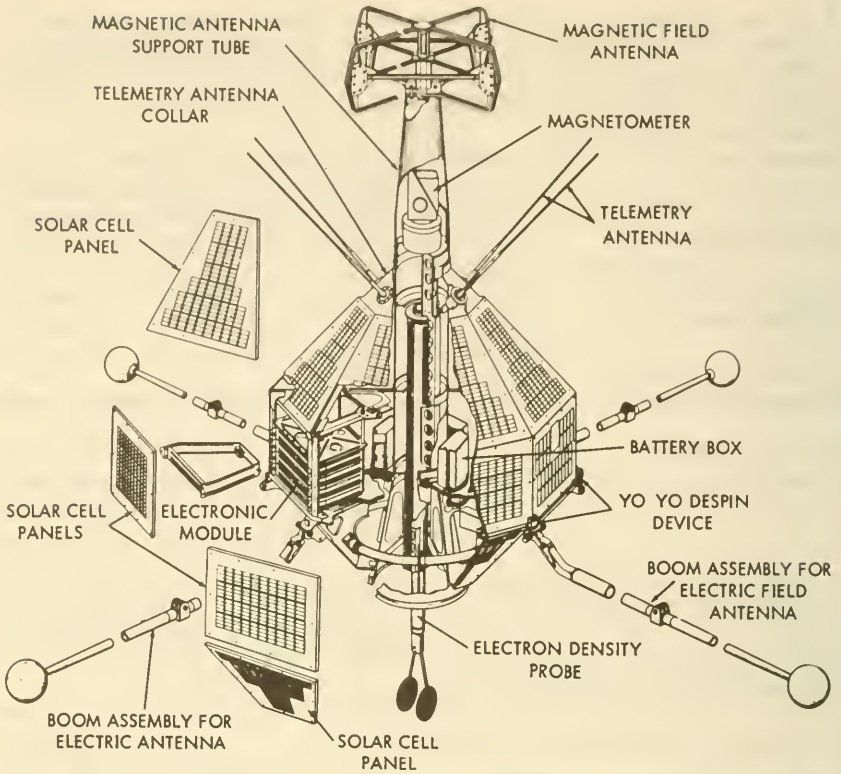
FIGURE A–28.—FR–1.

GEOS B

Geos B planned for launch in 1967. See Explorer XXIX (Geos A) for details. Additional Geos follow-ons planned for 1969 and 1970.

GRS–A

German Research Satellite, 625A–1, International Satellite

1968	Scout	WTR/STADAN
60–70 kg	—	—
300/2400 km	—	—

A German satellite to be launched by NASA. Objectives: study of the radiation environment around the Earth. German agency is the Federal German Ministry of Scientific Research (BMwF).

Descriptions of subsystems

Satellite in development phase. The GRS–A will be similar to NASA's Explorer-class satellites. Magnetic stabilization is planned.
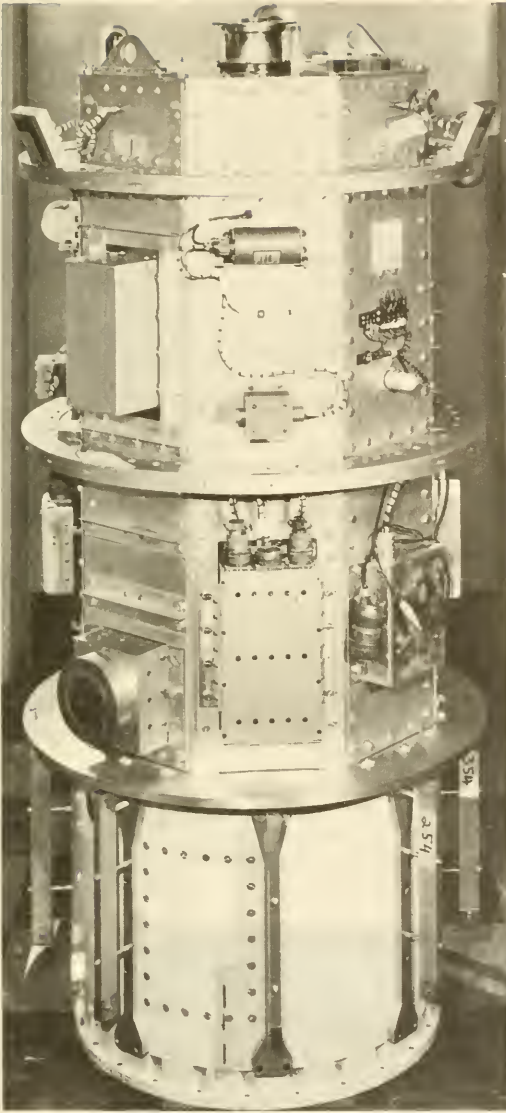
FIGURE A–29.—The Geophysical Research Satellite. (Courtesy of AFCRL.)

HEOS

Highly Eccentric Orbit Satellite

1968	Thrust-Augmented Improved Delta	ETR/—
100 kg	—	33°
193/ > 200 000 km	—	—

An ESRO project. Models A and B planned. Generally, Heos is patterned after the NASA IMP in design and purpose. Development team headed by Junkers Flugzeugund Motorwerke A.G.

Descriptions of subsystems

Communication: PCM telemetry. Command receiver.
Power supply: Solar cells plus batteries
Onboard propulsion: None
Attitude control: Spin stabilized
Environment control:
Guidance and control:
Onboard computer: None
Structure.

Experiments/instruments	*Experimenter*	*Institution*
Ion-cloud experiment _____	—	Max Planck Institut fur Extraterrestrische Physik
Interplanetary magnetic-field experiment	—	Imperial College
Cosmic-ray proton experiments ____	—	Imperial College
Solar-wind experiment _____	—	U. Brussels
Cosmic-ray protons, electrons, and alphas	—	C.E.A. Laboratoire
Solar-wind experiment _____	—	U. Bari, U. Rome
Electrons in primary cosmic rays __	—	U. de Milano, C.E.A. Laboratoire

HITCHHIKER 1   1963 25B

P–11

June 26, 1963	Thrust-Augmented Thor Agena B	WTR/—
80 kg	132.6 min	82.1°
326/4150 km	Oct. 1963	—

USAF piggyback satellite launched from an orbiting Agena. Purpose was to explore Van Allen Belts. Spacecraft built by Lockheed. Experiments managed by AFCRL.

FIGURE A–30.—Hitchhiker 1. (Courtesy of AFCRL.)

Descriptions of subsystems

Communication:	PAM/FM/FM telemetry. Tape recorder.
Power supply:	Solar cells $(p-n)$ plus NiCd batteries
Onboard propulsion:	Injection solid rocket for injection from orbiting Agena
Attitude control:	Spinup rockets. Spin-stabilized at 60 rpm
Environment control:	Sliding shutters for thermal control
Guidance and control:	Solar-cell aspect sensor. Two 3-axis fluxgate magnetometers.
Onboard computer:	None
Structure:	Irregular octagonal cylinder 1 m by 30 cm (fig. A–30)

Experiments/instruments	*Experimenter*	*Institution*
Proton scintillation spectrometer (table 11–8)	—	Amer. Sci. and Engineering
Planar retarding-potential analyzer (table 12–7)	Bridge, H.	MIT
Electron-scintillation spectrometer (table 11–8)	—	Amer. Sci. and Engineering
Spherical electrostatic analyzers for protons and electrons (table 12–5)	—	Amer. Sci. and Engineering
Geiger counter (table 11–8) _____	—	Amer. Sci. and Engineering

HITCHHIKER 2   1964 45B

P-11, Radiation Belt Monitoring Satellite

Aug. 14, 1964	Atlas-Agena D	WTR/—
—	127.4 min	95.6°
262/3750 km	—	—

A USAF piggyback satellite designed to measure trapped radiation

Descriptions of subsystems
See Hitchhiker 1

Experiments/instruments	*Experimenter*	*Institution*
vlf experiment (table 11–5) _____	White, S.	Aerospace Corp.
Faraday-cup plasma probe (table 12–7)		
Four particle spectrometers _____		
Geiger counter (table 11–8) _____		

INJUN 1   1961 O 2

June 29, 1961	Thor-Able Star	ETR/Minitrack
25 kg	103.8 min	67.0°
860/1020 km	Mar. 6, 1963	—

The first of a series of radiation-measuring satellites developed by the State University of Iowa. Injun 1 was launched by the Navy with Solrad 3 and Transit 4A. After Injun 3, the Injuns were launched by NASA and classified as Explorers; viz, Injun 4 = Explorer XXV.

Descriptions of subsystems

Communication:	PCM/FSK/AM telemetry at 136.500 Mc. Tape recorder. Command receiver.
Power supply:	Solar cells and NiCd batteries
Onboard propulsion:	None
Attitude control:	Magnetic stabilization
Environment control:	Passive thermal control. Designed to run cold: $-5°$ to $-20°$ C.
Guidance and control:	Single-axis fluxgate magnetometer
Onboard computer:	None
Structure:	Cylinder, 41-cm diameter, 33 cm high

Experiments/instruments	*Experimenter*	*Institution*
Five CdS detectors (table 11–8) __	Van Allen, J. A.	State U. of Iowa
Four *p–n* junction detectors (table 11–8)	Pieper, G.	Applied Physics Lab.
Geiger counter (table 11–8) _____	Van Allen, J. A.	State U. of Iowa
Magnetic electron spectrometer (table 11–8)	Van Allen, J. A.	State U. of Iowa
Auroral-airglow photometer (table 11–1)	O'Brien, B. J.	State U. of Iowa

Selected reference: Spacelog, Dec. 1961

INJUN 2

Jan. 24, 1962   Thor-Able Star   ETR

One of the five satellites included in the unsuccessful Composite 1 launch. See Composite 1.

INJUN 3   1962 ΒΓ 2

Dec. 12, 1962	Thor-Agena D	WTR/Minitrack
52 kg	116.3 min	70.3°
246/2780 km	Nov. 3, 1963	—

The second successful Injun (Injun 2 was not orbited). Injun 3 was launched with 4 classified military satellites. Injun 3 was particularly useful in the study of the Starfish artificial-radiation belt.

Descriptions of subsystems

Communication:	PCM/FSK/PM and PCM/FSK/AM telemetry at 136.860 Mc. Two independent telemetry and command systems. Tape recorder. Turnstile telemetry antenna.
Power supply:	Solar cells and NiCd batteries
Onboard propulsion:	None
Attitude control:	Magnetic stabilization
Environment control:	Passive thermal control. Designed to run cold: $-5°$ to $-20°$ C.
Guidance and control:	Five solar-aspect sensors. Fluxgate magnetometers.
Onboard computer:	None
Structure:	61-cm aluminum sphere with 9-cm bellyband

Experiments/instruments
Magnetic particle spectrometer (table 11–8)
vlf receiver (table 11–5)
Three auroral-airglow photometers (table 11–1)
Four p–n junction detectors (table 11–8)
Electron-multiplier detector (table 11–8)
Scintillators (table 11–8)
Geiger counters (table 11–8)

Selected reference: Reference 20

INJUN FOLLOW-ON, AD/I–C

University Explorer. (See Explorer-XXV synonyms.)
This Injun will be launched in the company of an Air Density Explorer, after the fashion of Explorers XXIV and XXV.

Descriptions of subsystems
See Explorer XXV

Experiments/instruments	*Experimenter*	*Institution*
Geiger counter (table 11–8) _____	Van Allen, J. A.	State U. of Iowa
Solid-state detectors (table 11–8) __	Van Allen, J. A.	State U. of Iowa
Spherical retarding-potential analyzer (table 11–5)	Sagalyn, R. C.	AFCRL
vlf receiver (table 11–5) _____	Van Allen, J. A.	State U. of Iowa
Curved-plate electrostatic analyzer (table 11–8)	Van Allen, J. A.	State U. of Iowa
Retarding-potential analyzer (table 11–8)	Van Allen, J. A.	State U. of Iowa

IONOSPHERE EXPLORER B

S–46A, IE–B

1967	—	—/—
—	—	—
—/—	—	—

The second satellite in NASA's IE series. Explorer XX was IE–A.

Descriptions of subsystems
See Explorer XX

Experiments/instruments
See Explorer XX

ISIS SERIES

ISIS launches actually consist of 2 separate satellites: a DME (Direct Measurements Explorer) and an Alouette. See the specific satellites for details. ISIS = International Satellites for Ionospheric Studies. For example:

    ISIS X = DME–A + Alouette B
          = Explorer XXXI + Alouette 2
    ISIS A = DME–B + Alouette C
    ISIS B = DME–C + Alouette D

LAMBDA 4S 1

L 4S 1

Sept. 26, 1966	Lambda 4S	Kagoshima
26 kg	—	—

Lambda 4S 1 represented Japan's first attempt to launch a satellite. Orbit was not attained.

LAMBDA 4S 2

L 4S 2

Dec. 20, 1966	Lambda 4S	Kagoshima
26 kg	—	—

Failed to orbit when fourth stage did not ignite

LAS

Large Astronomical Satellite

1970	Eldo A	—/—
820 kg	—	—
500 km/—	—	—

An ESRO project similar in purpose to NASA's OAO series. The LAS program is in the conceptual development stage. The main objective is to obtain spectra of stars in the range 900–3000 Å with a resolution of 1 Å or better.

LOFTI 1   1961 H 1

Low-Frequency Trans-Ionospheric Satellite

Feb. 21, 1961	Thor-Able Star	ETR/Minitrack
26 kg	94.5 min	28.4°
188/823 km	Mar. 30, 1961	Mar. 30, 1961

The Lofti satellites were designed by the U.S. Navy to study the transmission of vlf signals through the ionosphere. This piggyback satellite was launched with Transit 3B, but the pair failed to separate in orbit.

Descriptions of subsystems

Communication:	FM/AM telemetry at 136.17 Mc. Command receiver. Turnstile telemetry antenna.
Power supply:	Solar cells and NiCd batteries
Onboard propulsion:	None
Attitude control:	None
Environment control:	
Guidance and control:	Four photovoltaic cells each for Earth- and solar-aspect measurements
Onboard computer:	None
Structure:	51-cm-diameter aluminum sphere (fig. A–31)

Experiments/instruments	*Experimenter*	*Institution*
Two vlf receivers (table 11–5) ____	Leiphart, J. P.	NRL

LOFTI 2A   1963 21B

Low-Frequency Trans-Ionospheric Satellite

June 15, 1963	Thor-Agena D	WTR/STADAN
—	95.2 min	69.9°
176/886 km	July 18, 1963	July 18, 1963

FIGURE A–31.—Lofti 2A.   (Navy photograph.)

Lofti 2A was the last in the Navy Lofti series. Lofti 2 was not orbited.
Lofti 2A was launched with 4 other satellites, including Solrad 6 and
Radose.

Descriptions of subsystems
See Lofti 1

Experiments/instruments
See Lofti 1

MICHAEL

University Explorer
1967   —   WTR/STADAN
68 kg   —   polar
—/—   —   —

Michael is being designed by the University of Michigan High-Altitude Engi-
neering Laboratory (accounting for the acronym). It will be an aeronomy
satellite investigating variations in temperature and composition between
300 and 1000 km.

Descriptions of subsystems
Communication:
Power supply:
Onboard propulsion: None
Attitude control: Gravity-gradient rods and damper

Environment control:
Guidance and control: Three fluxgate magnetometers
Onboard computer: None
Structure:

Experiments/instruments	Experimenter	Institution
Quadrupole mass spectrometer (table 11–5)	—	U. Minn.
Proton and electron electrostatic analyzer		

MS 1

1967	Myu	Uchinoura/—
80 kg	90 min	—
300/400 km	—	—

A Japanese satellite designed for ionospheric research. This satellite is still in the development stage and the information presented here is subject to change.

Descriptions of subsystems
Communication: Seven antennas
Power supply: Solar cells and batteries
Onboard propulsion: None
Attitude control:
Environment control: Passive thermal control
Guidance and control:
Onboard computer: None
Structure: Nearly spherical with 26 sides. Octagonal cross
                           section on spin axis. 75 cm in diameter, 69 cm
                           high. Honeycomb panels.

Experiments/instruments
vlf experiment, various particle detectors

OAO I   1966 31A

OAO A1, S-18, Orbiting Astronomical Observatory

Apr. 8, 1966	Atlas-Agena D	ETR/STADAN
1770 kg	100.9 min	35.0°
790/804 km	Apr. 10, 1966	—

Our largest scientific satellite to date. The OAO's are standardized instrument platforms for stellar observation. The OAO program is managed by Goddard Space Flight Center. The spacecraft prime contractor was Grumman Aircraft. The OAO-I batteries failed 3 days after launch.

Descriptions of subsystems
Communication: PMC telemetry. Narrowband transmitter at
                           136.260 Mc; wideband (50 000 bits/sec) trans-
                           mitter at 400.55 Mc. Ferrite core memory of
                           204 000 bits. Command receiver.
Power supply: Solar cells and NiCd batteries provide about
                           1000 W. Oriented solar panels.
Onboard propulsion: None
Attitude control: Nitrogen cold-gas jets. Coarse and fine inertia
                           wheels. Magnetic torquers. Axis stabilized to
                           within 0.1 arcsec of target.

Environment control: Sun trackers, star-trackers, gyros

Onboard computer: Ferrite core memory, digital command system, and data-handling equipment possess many features of a centralized computer

Structure: Octagonal cylinder, 2.9 m long and 2.0 m across flats. Aluminum is primary structural material (fig. A–32).

Experiments/instruments	Experimenter	Institution
X-ray proportional counters (table 13–4)	Fisher, P.	Lockheed
Gamma-ray telescope (table 13–4)	Frost, K. J.	GSFC
Gamma-X-ray telescope (table 13–4)	Kraushaar, W.	MIT
Wisconsin Experiment: broadband ultraviolet photometry (table 13–1)	Code, A. D.	U. Wis.

Selected reference: Reference 21
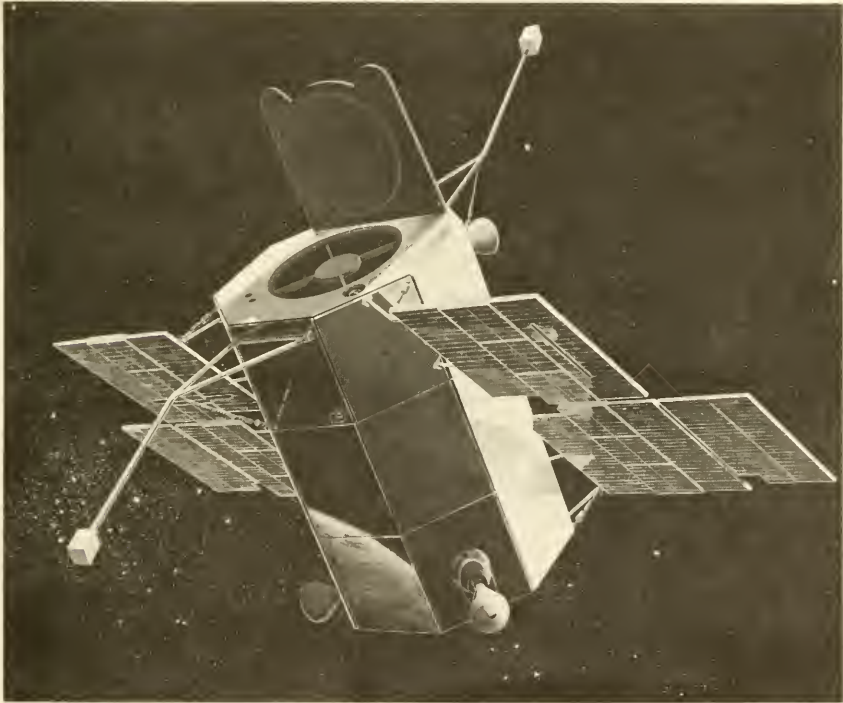
FIGURE A–32.—The OAO.

OAO A2
See OAO-I synonyms

1967	Atlas-Agena D	ETR/STADAN
—	—	—
—/—	—	—

Descriptions of subsystems
See OAO-I synonyms

Experiments/instruments	*Experimenter*	*Institution*
Ultraviolet TV photometry (table 13–2)	Whipple, F.	Smithsonian Astrophys. Obs.
Broadband ultraviolet photometry (table 13–2)	Code, A. D.	U. Wis.

OAO B

See OAO-I synonyms

1966	Atlas-Agena D	ETR/STADAN
—	—	—
—/—	—	—

Descriptions of subsystems
See OAO I

Experiments/instruments	*Experimenter*	*Institution*
Goddard Experiment Package (GEP), absolute spectrophotometry (table 13–1)	Boggess, A.	GSFC

OAO C

See OAO-I synonyms

1967	Atlas-Agena D	ETR/STADAN
—	—	—
—/—	—	—

Descriptions of subsystems
See OAO I

Experiments/instruments	*Experimenter*	*Institution*
Ultraviolet spectrometry with high resolution (table 13–1)	Spitzer, L.	Princeton
X-ray emission of stars and nebulas in ranges 3–12 Å, 8–18 Å, 44–60 Å with photometers (table 13–1)	Boyd, R. L. F.	University College

OGO I   1964 54A

Orbiting Geophysical Observatory, OGO A, S–49, EGO I, EGO A, EOGO, Eccentric Orbiting Geophysical Observatory

Sept. 4, 1964	Atlas-Agena B	ETR/STADAN
488 kg	64.0 hr	31.1°
282/149 000 km	—	—

The first of a series of large, standardized instrument platforms for geophysical research. Program is managed by NASA's Goddard Space Flight Center, while TRW Systems is the spacecraft prime contractor. After launch, OGO I did not deploy 2 of its booms properly. One boom obscured a horizon sensor, preventing Earthlock. OGO I was then spin-stabilized rather than Earth oriented.

Descriptions of subsystems

Communication:	PCM/PM telemetry with wide- and narrow-band transmitters at 400 Mc. Special-purpose FM/PM telemetry transmitter. Minitrack beacon. Two PCM/FM/AM command receivers. Two tape recorders. Directional and omnidirectional antennas.
Power supply:	Sun-oriented panels of p–n solar cells plus NiCd batteries were designed to generate an average of 560 W at the beginning of the mission
Onboard propulsion:	None
Attitude control:	Inertia wheels, argon-gas jets intended for Earth stabilization
Environment control:	Designed so that sides facing Sun (under proper stabilization) would be protected by super-insulation, while 2 sides facing away from the Sun would radiate excess heat through bi-metal-actuated louvers.
Guidance and control:	Horizon scanners, fine and coarse Sun sensors. Complex repertoire of status and experiment commands.
Onboard computer:	None
Structure:	Aluminum box 1.73-m long, 84 cm square. Six booms of various lengths (fig. A–33). Two special experiment packages are extended after orbit is attained: the SOEP (Solar-Oriented Experiment Package) and the OPEP (Orbital Plane Experiment Package).

Experiments/instruments	*Experimenter*	*Institution*
Cosmic-ray scintillation counters (table 13–4)	Anderson, K. A.	U. Calif.
Curved-surface electrostatic plasma analyzer (table 12–7)	Wolfe, J. H.	Ames Research Center
Faraday-cup plasma probes (table 12–7)	Bridge, H.	MIT
Positron detector (table 11–8) ____	Cline, T. L.	GSFC
Trapped-radiation scintillation counter (table 11–8)	Konradi, A.	GSFC
Cosmic-ray nuclear-abundance detector (table 13–4)	McDonald, F. B.	GSFC
Cosmic-ray solid-state telescope (table 13–4)	Simpson, J. A.	U. Chicago
Geiger counters (table 11–8) _____	Van Allen, J. A.	State U. of Iowa
Ionization chamber and Geiger counters (table 11–8), magnetic spectrometer	Winckler, J. R.	U. Minn.
Search-coil magnetometer (table 11–1)	Smith, E. J.	JPL
Fluxgate and Rb-vapor magnetometer (table 11–11)	Heppner, J. P.	GSFC
Spherical ion trap (table 11–5) ____	Sagalyn, R. C.	AFCRL

Experiments/instruments	Experimenter	Institution
Gridded planar ion and electron trap (table 11-5)	Whipple, E. C.	GSFC
Transponder for Faraday rotation measurements (table 11-5)	Lawrence, R. S.	NBS
rf ion mass spectrometer (table 11-5)	Taylor, H. A.	GSFC
Microphone micrometeoroid detector plus plasma detector and velocity discriminator (table 11-14)	Alexander, W. M.	GSFC
vlf receiver (table 11-5) _____	Helliwell, R. A.	Stanford U.
Radio-noise receiver (table 13-1) __	Haddock, F. T.	U. Michigan
Lyman-α ionization chambers (table 11-1)	Mange, P. M.	NRL
Gegenschein photometer (table 13-1)	Wolff, C. L.	GSFC

Selected reference: Reference 22
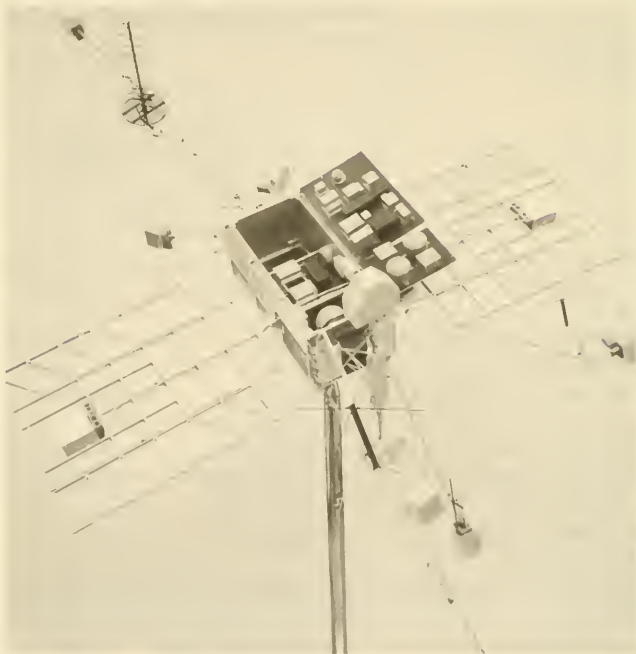
FIGURE A-33.—Model of OGO. (Courtesy of TRW Systems.)

OGO II   1965 81A

Orbiting Geophysical Observatory, OGO C, S-50, POGO I, POGO A, Polar Orbiting Geophysical Observatory

Oct. 14, 1965	Thrust-augmented	WTR/STADAN
	Thor-Agena D	
508 kg	104.3 min	87.4°
418/1510 km	—	—

Second OGO. See OGO I for program details. On OGO II, oversensitive horizon scanners picked up false horizons and caused attitude-control subsystem to exhaust gas supply in correction attempts.

Descriptions of subsystems
Similar to OGO I

Experiments/instruments	Experimenter	Institution
Galactic radio-noise receiver (table 13–1)	Haddock, F. T.	U. Michigan
vlf receiver (table 11–5) _____	Helliwell, R. A.	Stanford U.
	Morgan, M. G.	Dartmouth College
Search-coil magnetometer (table 11–11)	Smith, E. J.	JPL
Rb-vapor magnetometer (table 11–11)	Heppner, J. P.	GSFC
Ionization chamber (table 13–4) ___	Anderson, H. R.	Rice Inst.
Cosmic-ray scintillator telescopes (table 13–4)	Simpson, J. A.	U. Chicago
Cosmic-ray Cerenkov-scintillator telescope (table 13–4)	Webber, W. R.	U. Minn.
Geiger counters (table 11–8) _____	Van Allen, J. A.	State U. of Iowa
Scintillator detectors (table 11–8) _	Hoffman, R. A.	GSFC
Airglow photometer (table 11–1) __	Blamont, J.	U. Paris
Ultraviolet ionization chambers (table 11–1)	Mange, P. W.	NRL
Airglow ultraviolet spectrometer (table 11–1)	Barth, C. A.	U. Colo.
Quadrupole mass spectrometer (tables 11–1, 11–5)	Jones, L. M.	U. Michigan
rf ion mass spectrometer (table 11–5)	Taylor, H. A.	GSFC
Bayard-Alpert ionization gage (table 11–1)	Newton, G. P.	GSFC
Micrometeoroid detectors (table 11–14)	Alexander, W. M.	GSFC
Retarding-potential analyzer (table 11–5)	Bourdeau, R. E.	GSFC
X-ray ionization chamber (table 12–3)	Kreplin, R. W.	NRL
Solar-ultraviolet grating spectrometer (table 12–3)	Hinteregger, H. E.	AFCRL

OGO III
1966 49A

OGO B, S–49A. (See OGO-I synonyms.)

June 6, 1966	Atlas-Agena B	ETR/STADAN
516 kg	48.6 hr	30.9°
274/128 000 km	—	—

OGO III maintained Earth stabilization for more than 6 weeks and was then placed in a spin-stabilized mode

Descriptions of subsystems
Essentially identical to OGO A (OGO I)

Experiments/instruments	*Experimenter*	*Institution*
[See OGO I and the following changes:]		
Cylindrical electrostatic analyzer (table 11–8)	Van Allen, J. A.	State U. of Iowa
Proton electrostatic and electromagnetic analyzers (table 11–8)	Evans, D. S.	GSFC

OGO D

S–50A. (See OGO-II synonyms.)

1967	—	—/—
—	—	—
—/—	—	—

Descriptions of subsystems
Essentially identical to OGO C (OGO II)

Experiments/instruments
See OGO-II. Micrometeoroid detector added by C. S. Nilsson, Smithsonian Astrophysical Observatory

OGO E

S–59. (See OGO-I synonyms.)

1967	—	—/—
—	—	—
—/—	—	—

Descriptions of subsystems
See OGO II

Experiments/instruments	*Experimenter*	*Institution*
Spherical retarding-potential plasma analyzers (table 11–5)	Boyd, R. L. F.	University College
Spherical retarding-potential plasma analyzers (table 11–5)	Sagalyn, R. C.	AFCRL
Planar retarding-potential analyzer (table 11–5)	Serbu, G. P.	GSFC
Scintillator and proportional-counter telescope (table 13–4)	Anderson, K. A.	U. Calif.
Scintillator telescope (table 13–4)	Cline, T. L.	GSFC
Electron/proton magnetic spectrometer (table 11–8)	D'Arcy, R.	U. Calif.
Cylindrical electrostatic analyzer plus Geiger tube (table 11–8)	Frank, L. A.	State U. of Iowa
Cosmic-ray spark chamber (table 13–4)	Hutchinson, G. W.	U. Southampton
Cerenkov-scintillator telescope (table 13–4)	Meyer, P.	U. Chicago
Scintillator-solid-state telescopes (table 13–4)	McDonald, F. B.	GSFC
Triaxial electron electrostatic analyzer (table 11–8)	Ogilvie, K. W.	GSFC

Experiments/instruments	Experimenter	Institution
Cosmic-ray telescope (table 13–4) __	Wapstra, A. H.	Netherlands Inst. Nuclear Phys. Res.
Triaxial fluxgate magnetometers and 6 solid-state detectors (tables 11–8, 11–11)	Coleman, P. J.	U. Calif. (L.A.)
Triaxial fluxgate and Rb-vapor magnetometers (table 11–11)	Heppner, J. P.	GSFC
Triaxial search-coil magnetometers (table 11–11)	Smith, E. J.	JPL
Curved-surface electrostatic analyzer and Faraday-cup analyzer (table 12–7)	Snyder, C. W.	JPL
Magnetic ion mass spectrometer (table 11–5)	Sharp, G. W.	Lockheed
Micrometeoroid detectors (table 11–14)	Alexander, W. M.	GSFC
Cosmic-noise receiver (table 13–2) _	Haddock, F. T.	U. Michigan
Airglow ultraviolet photometer (table 11–1)	Barth, C. A.	U. Colo.
Geocoronal H–D cell (table 11–1) __	Blamont, J. E.	U. Paris
Solar X-ray proportional-counter spectrometer (table 12–3)	Kreplin, R. W.	NRL
Study of plasma oscillations using antennas (table 11–5)	Crook, G. M.	TRW Systems

OGO F

S–60. (See OGO-II acronyms.)

1968	—	—/—
—	—	—
—/—	—	—

Descriptions of subsystems
See OGO II

Experiments/instruments	Experimenter	Institution
Microphone density gage _____	Sharp, G. W.	Lockheed
Langmuir probe _____	Nagy, A. F.	U. of Mich.
Ion energy analyzer _____	Hanson, W. B.	GRCS/W
Neutral mass spectrometer _____	Reber, C. A.	GSFC
Ion mass spectrometer _____	Pickett, P.	GSFC
Ion mass spectrometer _____	Hanson, W. B.	GRCS/W
Energy-transfer probe _____	McKeown, D.	General Dynamics/ Convair
Solar X-ray experiment, spectrometer		
Solar UV survey _____	Kreplin, R. W.	NRL
Solar Lyman-α experiment, H–D cell	Regenu, V. H.	U. of N. M.
Celestial Lyman-α hydrogen cell ___	Blamont, J. E.	U. of Paris
UV photometer _____	Clark, M. A.	Aerospace
Aurora and airglow experiment, photometer and interferometer.	Barth, C. A. Blamont, J. E.	U. of Colo. U. of Paris
Low-energy auroral particles experiment, channeltron detector.	Evans, D. S.	GSFC

Experiments/instruments	*Experimenter*	*Institution*
Trapped and precipitating electrons experiment, plastic scintillators.	Farley, T. A.	UCLA
Trapped and precipitating electrons experiment.	Williams, D. J.	GSFC
Neutron monitor _____	Lockwood, J. A.	U. of N. H.
Low-energy solar cosmic rays experiment.	Masky, A. J.	Douglas Aircraft Co.
Solar and galactic cosmic rays experiment.	Stone, E. C.	CIT
Rb vapor magnetometer _____	Cain, J. C.	GSFC
Triaxial search coil magnetometer __	Smith, E. J.	JPL
Electric field antenna _____	Aggson, T. L.	GSFC
vlf experiment, electric and magnetic field antenna.	Helliwell, R. A.	Stanford U.
Whistler-mode waves experiment, antenna.	Laaspere, T.	Dartmouth College

ORBIS

Orbiting Radio Beacon Ionospheric Satellite

The term "Orbis" is applied to satellite experiments conducted by the Air Force in which subsatellites carrying beacons are ejected from the primary satellite. Propagation in the high ionosphere can be studied by examining the signals received by the primary satellite.

While the Orbis experiments do involve the creation of additional satellite bodies, these bodies can hardly be classified as new scientific satellites. Such experiments are described under primary satellite entries. See OV–3–4 and OV–4.

OSCAR 1   1961 AK 2

Radio Amateur Satellite, Oscar = Orbiting Satellite Carrying Amateur Radio
Dec. 12, 1961   Thor-Agena B   WTR/—
4.5 kg   91.1 min   81.2°
235/415 km   Dec. 30, 1961   Jan. 31, 1962

A piggyback satellite launched by the Air Force in cooperation with the American Radio Relay League for the purpose of studying propagation phenomena. Radio amateurs have filed many thousands of reports after receiving Oscar signals.

Descriptions of subsystems
Communication:	Beacon at 145 Mc. Whip antenna.
Power supply:	Mercury battery
Onboard propulsion:	None
Attitude control:	None
Environment control:	Passive thermal control
Guidance and control:	None
Onboard computer:	None
Structure:	Wedge-shaped magnesium box, 15.2 x 25.4 x 30.5 cm

Experiments/instruments: Transmitter sent letters "HI" continuously

OSCAR 2 1962 X 2

See Oscar-1 synonyms
June 1, 1962	Thor-Agena B	WTR/—
4.5 kg	90.5 min	74.3°
208/386 km	June 20, 1962	June 21, 1962

Second radio amateur satellite

Descriptions of subsystems
Essentially identical to Oscar 1. Transmitted at 144.992 Mc.

OSCAR 3 1965 16F

See Oscar-1 synonyms
Mar. 9, 1965	Thor-Agena D	WTR/—
15 kg	103.5 min	70.1°
906/942 km	Mar. 25, 1965	

Substantially larger than Oscars 1 and 2, this satellite was launched in co-operation with the Army and Navy. A battery failure limited the active life to 16 days. See Oscar 1.

Descriptions of subsystems
Communication:	Beacon. Transponder that received at 144.1 Mc and retransmitted instantaneously at 145.9 Mc.
Power supply:	Solar cells plus AgZn batteries
Onboard propulsion:	None
Attitude control:	None
Environment control:	Passive thermal control
Guidance and control:	None
Onboard computer:	None
Structure:	Boxlike, 17.8 x 30.5 x 43.2 cm

Experiments/instruments: Transponder described above

OSCAR 4 1965 108C

See Oscar-1 synonyms
Dec. 21, 1965	Titan 3–C	ETR/—
13 kg	—	—
—/—	—	—

Oscar 4 was a radio amateur communications satellite transmitting on 431.962 and 431.972 Mc

OSO I 1962 Z 1

S–16, OSO A, Orbiting Solar Observatory
Mar. 7, 1962	Delta	ETR/Minitrack
208 kg	96.2 min	32.8°
554/596 km	Aug. 6, 1966	—

A relatively small Observatory-class satellite, built by Ball Bros. for NASA GSFC. The satellites in the OSO series are designed primarily for solar research.

Descriptions of subsystems

Communication:	FM/FM telemetry. Tape readout and real-time transmitter at 136.744 Mc. Command receiver. Tape recorder (failed after 3 months). Satellite arms act as antenna.
Power supply:	$p-n$ solar cells and NiCd batteries produced an average of 16 W
Onboard propulsion:	None
Attitude control:	Wheel section rotates at about 30 rpm to spin-stabilize satellite. Sail section points at Sun as it is driven by a motor. Cold-gas jets and inertia wheels control attitude and spin rate. Nutation damper.
Environment control:	Passive thermal control
Guidance and control:	Sun sensor and gyros. Ten status commands.
Onboard computer:	None
Structure:	Wheel section is nonagonal cylinder 112 cm across. Sail section is fan shaped. Aluminum was primary structural material (fig. A–34).
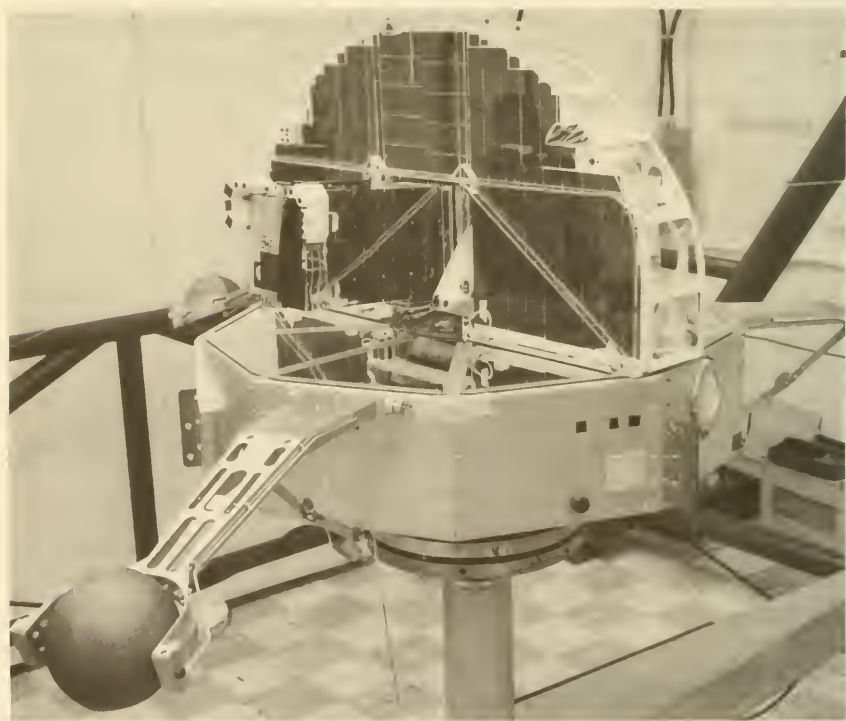
FIGURE A–34.—OSO II.

Experiments/instruments	Experimenter	Institution
Grating spectrometer (table 12–3) _	Behring, W.	GSFC
X-ray scintillator (table 12–3) (wheel)	Frost, K.	GSFC
Two X-ray ionization chambers (table 12–3)	Frost, K.	GSFC
Photomultiplier and microphone micrometeoroid detectors (table 11–14)	Alexander, W. M.	GSFC
$B^{10}F_3$ neutron counters (table 11–8)	Hess, W.	U. Calif.
Gamma-ray Cerenkov-scintillator telescope (table 13–4)	Fazio, G.	U. Rochester
Gamma-ray scintillators (table 13–4)	White, W.	GSFC
X-ray Compton telescope and scintillator (table 13–4)	Winckler, J. R.	U. Minnesota
Scintillator telescope (table 11–8) _	Bloom, S.	U. California
X-ray scintillators (sail) (table 13–4)	Frost, K.	GSFC
Ultraviolet photodiode monitor (table 12–3)	Hallam, K.	GSFC
Lyman-α ionization chamber (table 12–3)	Hallam, K.	GSFC

Selected reference: Reference 23

OSO II
<div style="text-align: right">1965 7A</div>

S–17, OSO B, OSO B2, Orbiting Solar Observatory

Feb. 3, 1965	Delta	ETR/STADAN
247 kg	96.5 min	32.9°
552/632 km	—	—

Second successful OGO. Experiments were pieced together from OSO B1 that was damaged in an explosion at ETR in 1964. (See OSO I.)

Descriptions of subsystems

Similar to OSO I except PCM telemetry at 136.712 Mc, digital command receiver, 36-W power supply, magnetometer attitude sensors, and 4 photodetectors for Sun pointing, new tape recorder, and change to *n–p* solar cells.

Experiments/instruments	Experimenter	Institution
Ultraviolet spectroheliograph and grating spectrometer (table 12–3)	Goldberg, L.	Harvard U.
White-light coronagraph (table 12–3)	Tousey, R.	NRL
Ultraviolet spectroheliograph (table 12-3)	Tousey, R.	NRL
X-ray telescope (table 12–3) _____	Chubb, T. A.	NRL
X-ray spectroheliograph (table 12–3)	Chubb, T. A.	NRL
Zodiacal-light telescopes (table 13–1)	Ney, E. P.	U. Minnesota
Gamma-ray Cerenkov telescope (table 13–4)	Leavitt, C.	U. New Mexico

Experiments/instruments	Experimenter	Institution
Gamma-ray scintillator (table 13–4)	Frost, K. J.	GSFC
Ultraviolet spectrophotometer (table 13–2)	Hallam, K.	GSFC

OSO III   1967 20A

OSO E. See OSO-I synonyms

Mar. 8, 1967	Delta	ETR/STADAN
285 kg	96 min	33°
540/570 km	—	—

Descriptions of subsystems
Similar to OSO II

Experiments/instruments	Experimenter	Institution
Solar-ultraviolet monochromator (table 12–3)	Hinteregger, H. E.	AFCRL
Cerenkov-scintillator cosmic-ray telescope (table 13–4)	Kaplon, M. F.	U. Rochester
Solar X-ray ionization chambers (table 12–3)	Teske, R. G.	U. Mich.
Earth's albedo photometer (table 11–1)	Neel, C. B.	Ames
X-ray scintillation telescope (table 13–4)	Peterson, L. E.	U. Calif.
Gamma-ray telescope (table 13–4) _	Kraushaar, W. L.	MIT
Solar spectrometer _____	Neupert, W. M.	GSFC
Directional radiometer telescopes ___	Neel, C. B.	Ames

OSO D

See OSO-I synonyms

1967	Delta	ETR/Minitrack
—	—	—
—/—	—	—

Descriptions of subsystems
Similar to OSO II

Experiments/instruments	Experimenter	Institution
Ultraviolet grating spectrometer (table 12–3)	Goldberg, L.	Harvard U.
X-ray crystal spectrometer (table 12–3)	Friedman, H.	NRL
X-ray spectroheliograph (table 12–3)	Paolini, F.	Amer. Sci. and Eng.
Grating monochromators (table 12–3)	Boyd, R. L. F.	University College
X-ray proportional-counter and Geiger spectrophotometer (table 12–3)	Boyd, R. L. F.	University College
Four X-ray ionization chambers (table 12–3)	Chubb, T. A.	NRL

Experiments/instruments	*Experimenter*	*Institution*
Lyman-α ionization chambers (table 11–1)	Mange, P.	NRL
Scintillator telescope (table 11–8) __	Waggoner, J.	U. California
X-ray scintillator telescope (table 13–1)	Giacconi, R.	Amer. Sci. and Eng.

OSO F

See OSO-I synonyms

Descriptions of subsystems
Similar to OSO I

Experiments/instruments	*Experimenter*	*Institution*
Solar X-ray spectroheliograph (table 12–3)	Stewardson, E. A.	University College
Solar ultraviolet spectroheliograph (table 12–3)	Purcell, J. D.	NRL
Solar X-ray spectrometers and ion chambers (table 12–3)	White, W. A.	GSFC
Solar X-ray photometers (table 12–3)	Chubb, T. A.	NRL
Gamma-ray scintillator (table 13–4)	Frost, K.	GSFC
Lyman-α photometer (table 12–3) __	Blamont, J.	U. Paris
Gegenschein photometers (table 13–1)	Ney, E. P.	U. Minn.
Solar ultraviolet grating spectrometer (table 12–3)	Rense, W. A.	U. Colo.

OSO G

See OSO-I synonyms

Descriptions of subsystems
Similar to OSO I

Experiments/instruments	*Experimenter*	*Institution*
Ultraviolet spectrometer-spectroheliometer (table 12–3)	Goldberg, L.	Harvard
Bragg crystal spectrometer (table 12–3)	Kreplin, R. W.	NRL
Gegenschein study (table 13–1) ____	Rouy, A. L.	Rutgers
Solar X-ray monitor (table 12–3) __	Argo, H. V.	Los Alamos
Solar X-ray monitor (table 12–3) __	Brini, D.	U. Bologna
He-I and He-II resonance radiation study and correlation (table 12–3)	Boyd, R. L. F.	University College
Space neutron study (table 13–4) __	Leavitt, C. P.	U. N. Mex.

OV–1–1

Orbital Vehicle 1, SATAR, Satellite for Aerospace Research; ARS, Aerospace Research Vehicle

Jan. 21, 1965	Atlas D	WTR/—
86kg	—	—
—/—	—	—

First of a series of 14 or more Air Force piggyback scientific satellites. Early satellites in this series were to be ejected from pods attached to the side of

the Atlas booster and inject themselves into orbit with an onboard propulsion unit. Later models were nose mounted. The OV 1's are built by General Dynamics.

OV–1–1 did not orbit because of the failure of the onboard thruster.

Descriptions of subsystems

Communication:	PAM/FM/FM telemetry. C-band beacon. Command receiver. Tape recorder. Turnstile antenna.
Power supply:	$n–p$ solar cells and AgCd batteries generate approximately an average of 22 W
Onboard propulsion:	Solid-rocket engine for orbital injection
Attitude control:	None
Environment control:	Passive thermal control
Guidance and control:	
Onboard computer:	None
Structure:	Aluminum cylinder with hemispherical ends, ∼ 70 cm in diameter, ∼ 180 cm long, constitutes payload structure. Entire vehicle including propulsion unit is orbited (fig. A–35).
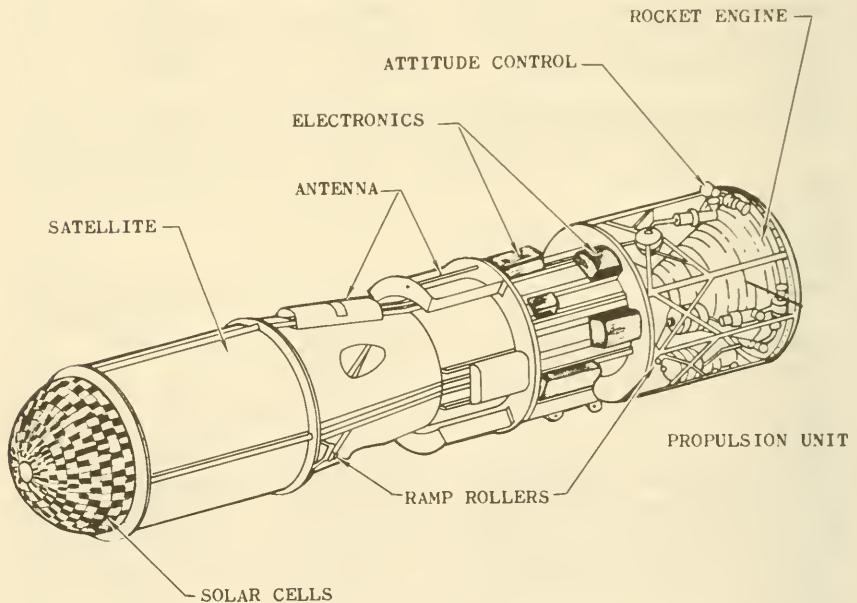
FIGURE A–35.—An OV–1.

OV–1–2		1965 78A
See OV–1–1 synonyms		
Oct. 5, 1965	Atlas D	WTR/National Range Div.
86 kg	125.7 min	144.3°
412/3460 km	—	—
First successful OV–1		

Descriptions of subsystems
See OV–1–1

Experiments/instruments
Radiation-measuring instruments

OV–1–3

See OV–1–1 synonyms

May 27, 1965	Atlas D	WTR/—
92 kg	—	—
—/—	—	—

OV–1–3 was not orbited because of a booster failure

Descriptions of subsystems
See OV–1–1

OV–1–4   1966 25A

See OV–1–1 synonyms

Atlas D	Mar. 30, 1966	WTR/National Range Div. (NRD)
103.9 min	88 kg	144.5°
—	885/1010 km	—

Second OV-1 success

Descriptions of subsystems
See OV–1–1
Experiments/instruments
Two zero-g biological experiments using photosynthetic organisms and small vascular plants. Thermal-coating experiment.

OV–1–5   1966 25B

See OV–1–1 synonyms

Mar. 30, 1966	Atlas D	WTR/National Range Div.
114 kg	104.4 min	144.7°
985/1060 km	—	—

Third OV-1 success. Launched with OV–1–4.

Descriptions of subsystems
See OV–1–1

Experiments/instruments
Optical radiation experiment. Five optical sensors in range 0.5–30 μ measured Earth's radiance.

OV–1–6   1966 99C

See OV–1–1 synonyms

Nov. 3, 1966	Titan 3C	ETR/NRD
—	—	—
—	—	—

Classified payload

OV–1–7

See OV–1–1. This satellite was launched on July 14, 1966, but failed to reach orbit when its injection motor failed.

OV–1–8   1966 63A

See OV–1–1 synonyms
July 12, 1966   Atlas D   WTR/National Range
                                                    Div.
34 kg   105.2 min   95.5°
985/10 200 km   —   —

OV–1–9   1966 111A

Dec. 11, 1966   Atlas D   WTR/NRD
104 kg   142.3 min   99.4°
478/4840 km   —   —

OV–1–10   1966 111B

Dec. 11, 1966   Atlas D   WTR/NRD
130 kg   98.9 min   93.5°
648/755 km   —   —

OV–1 FOLLOW-ONS

At least 14 satellites constitute the OV–1 series. Those not previously de-
   scribed are in the construction or planning phases and will be launched as
   boosters become available.

OV–2–1   1965 82A

Orbital Vehicle 2, MARENTS, Modified ARENTS (in error)
Oct. 15, 1965   Titan 3C   ETR/SCF
170 kg   99.7 min   32.6°
707/791 km   Oct. 15, 1965   —
The OV–2's constitute a series of Air Force satellites that were designed for
   launch by Titan 3C test vehicles. These satellites were built from on-the-
   shelf components as far as possible; viz, components from the ARENTS
   Program. Northrop Space Laboratories was the prime contractor.
OV–2–1 was launched with LCS 2, but the Titan 3C transtage broke up,
   presumably destroying the satellites. Orbital data are for the pieces.

Descriptions of subsystems
Communication: PAM/FM/FM telemetry.   Command receiver.
                                   Tape recorder. Two turnstile antennas.
Power supply: Four solar-cell paddles plus NiCd batteries pro-
                                   vided an average of 60 W
Onboard propulsion: None
Attitude control: Spin stabilized. Precession damper. Small solid
                                   rockets on tips of solar paddles for spinup.
                                   Cold-gas jets and subliming solid motor.
Environment control: Passive thermal control using surface coatings
                                   and finishes and internal insulation blankets.
Guidance and control: Solar-aspect sensor. Two fluxgate magnetom-
                                   eters.

Onboard computer: None
Structure: Aluminum honeycomb box, 58 x 58 x 61 cm
                           (fig. A–36)

Selected reference: Reference 24
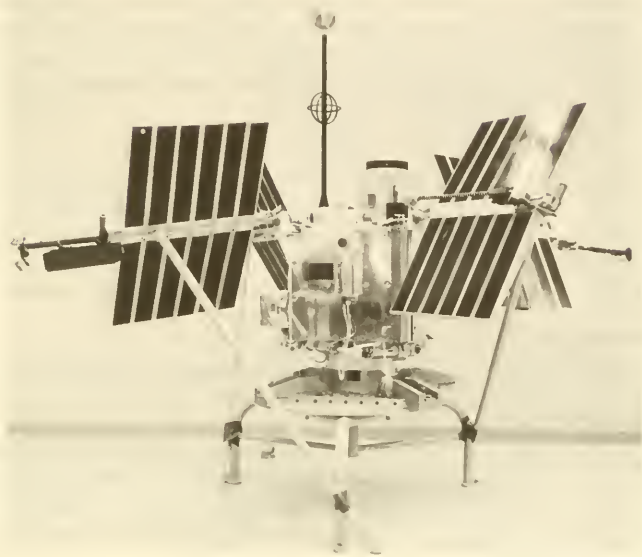
FIGURE A–36.—An OV–2. (Courtesy of Northrop
Corp.)

OV–2–2

See OV–2–1 synonyms
This satellite was never built

OV–2–3   1965 108A

See OV–2–1 synonyms
Dec. 21, 1965   Titan 3C   ETR/NRD
194 kg   589.7 min   26.4°
177/33 700 km   Dec. 21, 1965   —
OV–2–3 was not ejected from the Titan 3C transtage. No data were received.

OV–2–4

See OV–2–1 synonyms
This satellite was never built

OV–2 FOLLOW-ONS

See OV–2–1 synonyms
At least one additional OV–2 satellite (OV–2–5) is planned

OV–3–1   1966 34A

Orbital Vehicle 3
Apr. 22, 1966   Scout   WTR/NRD
69 kg   151.7 min   82.5°
354/5730 km   —   —

The OV–3 series of Air Force satellites differs from the other OV's in the
  sense that science is the primary purpose of the launch. In the terminology
  of this book, the OV–3's are Explorer-class satellites rather than piggyback
  satellites. The first four OV–3's are built by Space General Corp.; OV–3–5
  and OV–3–6 are constructed by AFCRL.

Descriptions of subsystems
Communication: PAM/FM/FM telemetry. Command receiver.
                              Tape recorder. Turnstile antenna.
Power supply: *n–p* solar cells and NiCd batteries
Onboard propulsion: None
Attitude control: Spin stabilization. Precession damper. Yo-yo
                              despin mechanism.
Environment control: Passive thermal control
Guidance and control: Sun sensors and fluxgate magnetometers for as-
                              pect measurement
Onboard computer: None
Structure: Internal aluminum thrust tube with magnesium-
                              aluminum honeycomb instrument platform.
                              External octagonal cylinder 74-cm long and
                              74 cm across the points (fig. A–37).

Experiments/instruments

Proton and electron spectrometer
Electrostatic analyzer
Plasma probes
Geiger counter
Two magnetometers

OV–3–2   1966 97A

Oct. 28, 1966   Scout   WTR/NRD
81 kg   104.2 min   82.0°
318/1598 km   —   —

OV–3–3   1966 70A

Aug. 4, 1966   Scout   WTR/NRD
75 kg   136.6 min   81.6°
354/4480 km   —   —

OV–3–4   1966 52A

June 10, 1966   Scout   Wallops/NRD
77 kg   143.2 min   40.8°
642/4732 km   —   —
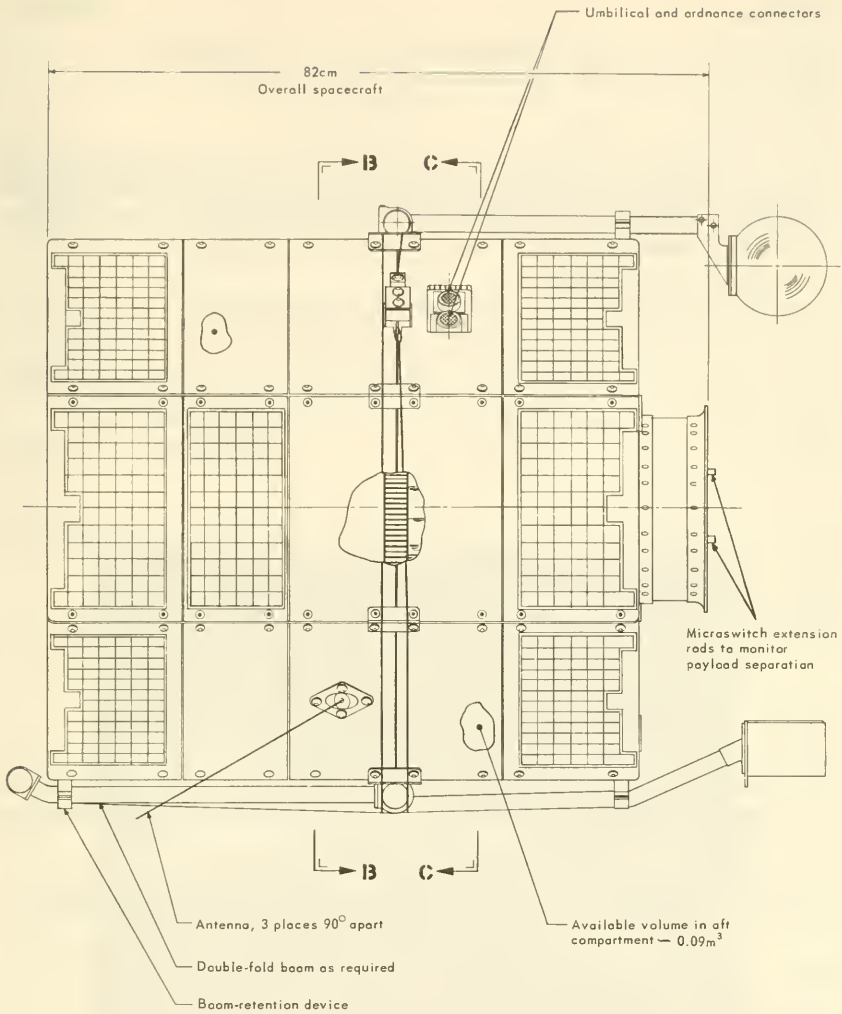
Figure A–37.—An OV–3. (Courtesy of Space General Corp.)

OV–3 FOLLOW-ONS

OV–3–2, OV–3–3, and OV–3–4 are built by Space General Corp. OV–3–4 is also termed "PHASR" (Personnel Hazards Associated with Space Radiation). OV–3–5 and OV–3–6, built by AFCRL, are called ATCOS 1 and ATCOS 2 (Atmospheric Composition Satellite). These last two will only be 50.8 cm long. An electrically heated battery is planned for OV–3–5.

Descriptions of subsystems
See OV–3–1

OV–4–1R   1966 99B

Nov. 3, 1966	Titan 3C	ETR/NRD
136 kg	90.4 min	32.8°
291/291 km	—	—

Orbital Vehicle 4

OV–4–1 was built by Raytheon Corp. for the Air Force. This satellite will carry out satellite-to-satellite communication experiments by ejecting a sub-satellite containing radio equipment. The transmitting and receiving satellites are designated OV–4–1T and OV–4–1R, respectively.

Descriptions of subsystems
The primary satellite is a cylinder with hemispherical ends

OV–4–1T   1966 99D

Nov. 3, 1966	Titan 3C	ETR/NRD
109 kg	90.7 min	32.8°
291/319 km	—	—

OV–4–3   1966 99A

Nov. 3, 1966	Titan 3C	ETR/NRD
9680 kg	90.6 min	32.8°
305/313 km	—	—

Nine experiments on Titan-2 tank.

OV–5

Orbital Vehicle 5; ORS, Octahedral Research Satellite

This series of Air Force satellites constitutes several ORS-type satellites purchased from TRW Systems. The satellites will be the 28-cm size and will be tracked by STADAN.

Descriptions of subsystems
See ORS 1. PCM telemetry and a command receiver will be incorporated.

OWL   L

University Explorer, Owl A and Owl B

1968	—	—/—
64 kg	—	—
—/—	—	—

The Owl satellites are built by Rice University and named after the school's mascot. A pair of satellites will be launched and injected into orbits so that they are in the same orbital plane but on opposite sides of the Earth. Trapped radiation, auroral displays, and interaction between the trapped radiation and auroras can thus be studied simultaneously at conjugate points.

Descriptions of subsystems
Magnetic orientation planned

Experiments/instruments
TV viewing of auroral displays (table 11–1)

PAGEOS   1966 56A

Passive Geodetic Earth-Orbiting Satellite; Passive Geos

June 23, 1966	Thrust-Augmented Thor-Agena D	WTR/net of optical stas.
57 kg	181.4 min	87.1°
4198/4286 km	—	—

Pageos satellites are of the balloon type. Optical observations of these passive satellites are expected to complement radio observations of the active Geos satellites. The Pageos satellite is built for NASA's Langley Research Center by G. T. Schjeldahl Co.

Descriptions of subsystems

The 30-m-diam. balloon is made from aluminized Mylar. An external paint pattern controls the internal temperature. The balloon is folded in a spherical magnesium canister during launch. Gas pressure inflates it. There are no other subsystems (fig. A–38).

Experiments/instruments
None

FIGURE A–38.—Pageos inflation test.

PEGASUS I   1965 9A

Pegasus A; MTS, Meteoroid Technology Satellite; MDS, Meteoroid Detection
    Satellite; Meteoroid Explorer, Saturn Explorer

Feb. 16, 1965	Saturn I	ETR/STADAN
10 400 kg	97.0 min	31.7°
496/744 km	—	—

The Pegasus series of satellites was built for NASA's Marshall Space Flight
    Center by Fairchild-Hiller. Since they are carried into orbit as a byproduct
    of launch tests of the Saturn I-B, the Pegasus satellites are classified as
    piggyback satellites. There are three in the series.

Descriptions of subsystems

Communication:	PCM telemetry at 136.44 and 136.89 Mc. Command receivers. Tape recorders. Two bent-stub antennas.
Power supply:	n–p solar cells and NiCd batteries
Onboard propulsion:	None
Attitude control:	None; allowed to tumble
Environment control:	Passive thermal control on extended panels; louvers on aft section of electronic canister
Guidance and control:	Solar-aspect sensors and infrared horizon sensors
Onboard computer:	None
Structure:	Two large (4.3 x 14.7 m), flat aluminum wings deployed by scissors-like linkage and electric motors. Electronics canister (fig. A–39).

Experiments/instruments

Capacitor micrometeoroid detectors (table 11–14)
Electron spectrometer (table 11–8)

Selected reference: Reference 25
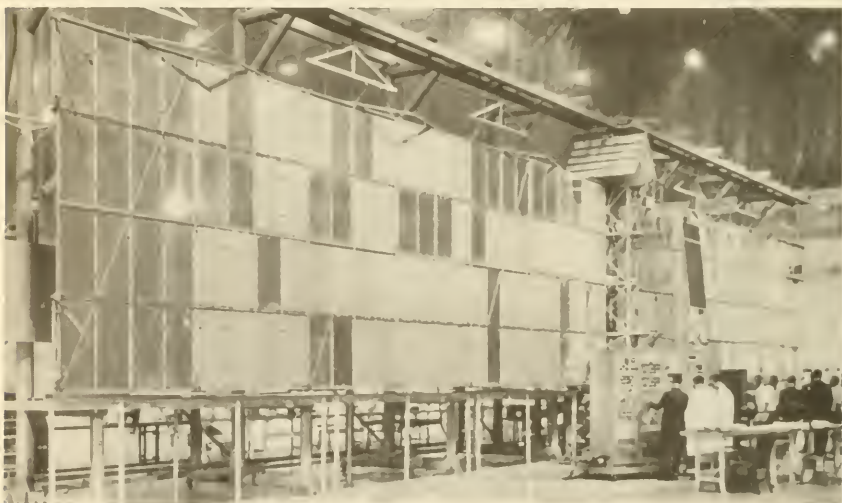
FIGURE A–39.—Pegasus dynamic test.

PEGASUS II

Pegasus B. (See Pegasus-I synonyms.)

May 25, 1965	Saturn I	ETR/STADAN
10 500 kg	97.3 min	31.7°
505/750 km	—	—

Descriptions of subsystems
See Pegasus I. New logical arrangement for detector panels added to overcome short-circuit problems encountered with Pegasus I. Transmitted on 135.41 and 136.89 Mc.

Experiments/instruments
See Pegasus I

PEGASUS III

Pegasus C. (See Pegasus-I synonyms.)

July 30, 1965	Saturn I	ETR/STADAN
10 500 kg	95.3 min	28.9°
520/541 km	—	—

Descriptions of subsystems
See Pegasus II

Experiments/instruments
See Pegasus I

PILGRIM

A University Explorer under study at Harvard University

PROTON 1

July 16, 1965	—	—/—
12 200 kg	92.5 min	63.5°
190/627 km	—	Oct. 11, 1965

A large Soviet satellite carrying a number of heavy cosmic-ray experiments. The Proton satellites are widely thought to be unmanned test vehicles for eventual manned orbital laboratories.

Descriptions of subsystems

Communication:	Beacon at 19.910 Mc
Power supply:	Solar cells on 4 panels plus batteries
Onboard propulsion:	None
Attitude control:	Spin stabilized. Gas jets plus a "power damping device."
Environment control:	Heat exchanger
Guidance and control:	
Onboard computer:	Yes, but no details known
Structure:	Hermetically sealed cylinder with convex ends (fig. A–40).

Experiments/instruments
Gamma-ray telescope
Scintillator telescope
Proportional counters
Gas-Cerenkov-scintillator telescope

Selected reference: Spacelog, Winter, 1965
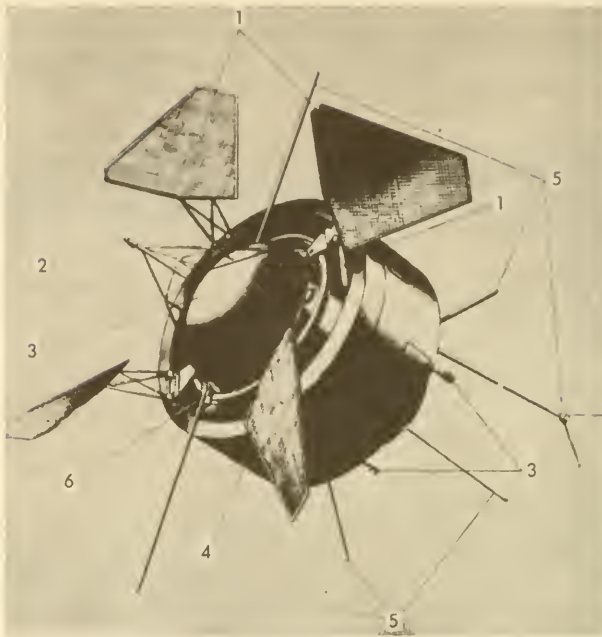
(1) Solar panels
(2) Pickups for axis-orientation system
(3) Hermetic sealer
(4) Outer cover
(5) Antennas
(6) Chemical fuel cells

FIGURE A–40.—Proton 1.

PROTON 2			1965 87A
Nov. 2, 1965	—	—/—	
12 200 kg	92.6 min	63.5°	
191/638 km	—	—	
See Proton 1			

PROTON 3			1966 60A
July 6, 1966	—	—/—	
12 200 kg	92.5 min	63.5°	
190/630 km	—	—	
See Proton 1			

RADOSE			1963 21D
Radiation Dosimeter Satellite			
June 15, 1963	Thor-Agena D	WTR/—	
—	95.2 min	69.9°	
174/884 km	July 30, 1963	July 30, 1963	

A USAF–USN piggyback satellite designed to measure radiation levels in space. No details available.

RAE

RAE A, RAE B, Radio Astronomy Explorer; OREO, Orbiting Radio Emission Observatory

1967	Thrust-Augmented Improved Delta	WTR/STADAN
125 kg	—	58° retrograde
6000 km	—	—

A series of Explorers with extremely long antennas to measure the directions and intensities of radio-noise sources at frequencies below ionospheric cutoff. Built for Goddard Space Flight Center by the Applied Physics Laboratory of Johns Hopkins University. Two spacecraft approved.

Descriptions of subsystems

Communication:	PFM telemetry between 136 and 137 Mc. Real-time telemetry or tape-recorder playback. Command receiver. Turnstile antenna.
Power supply:	$n-p$ solar cells and NiCd batteries generate an average of 25 W
Onboard propulsion:	Solid apogee kick motor to circularize initial orbit; 20 000 kg-sec impulse
Attitude control:	Yo-yo despin device, libration dampers, magnetic stabilization. Booms provide for gravity-gradient stabilization.
Environment control:	Passive thermal control. Sunlit side heavily insulated. Cold side radiates excess heat.
Guidance and control:	Two solar-aspect sensors. Two fluxgate magnetometers.
Onboard computer:	None
Structure:	Cylinder, 92 x 74 cm long, capped by two truncated cones. Structural material mainly aluminum and aluminum honeycomb (fig. A–41). Four 250-m BeCu antennas.

Experiments/instruments	*Experimenter*	*Institution*
Antenna impedance measurements using capacity probe, analog impedance probe, electron trap (table 11–5)	Stone, R. G.	GSFC
Cosmic-noise survey with "fast burst" radiometer (table 13–1)	Stone, R. G.	GSFC
Cosmic-noise survey below ionospheric cutoff (table 13–1)	Stone, R. G.	GSFC

Selected references: References 26, 27

SAN MARCO 1   1964 84A

SM 1, SM–A, International Satellite

Dec. 15, 1964	Scout	Wallops/STADAN
115 kg	94.9 min	37.8°
206/821 km	—	Sept. 13, 1965

An Italian-built satellite launched by NASA for atmospheric and ionospheric research. San Marco 1 was primarily a test vehicle to qualify the satellite and train the Italian crew. Later launches planned from Italian sites.
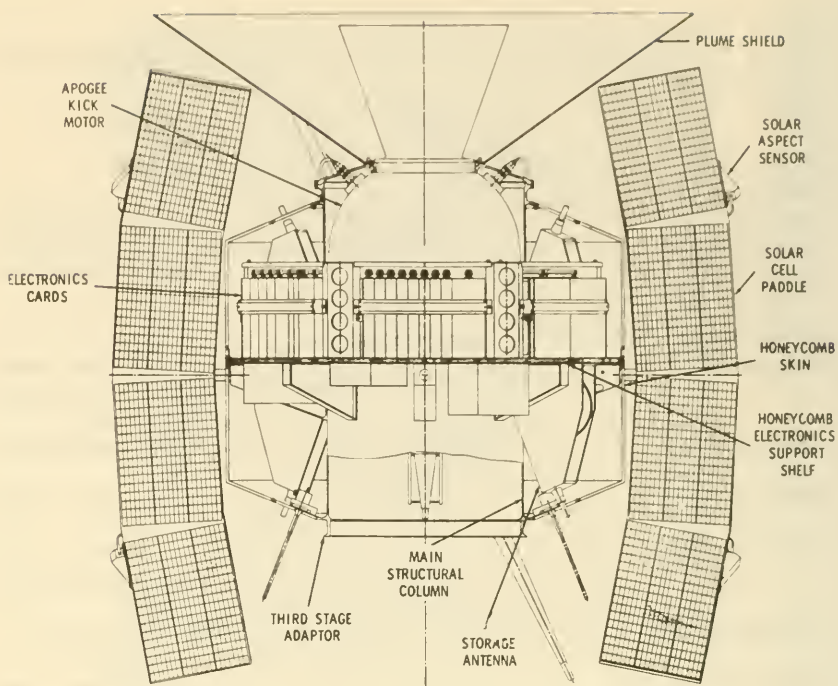
FIGURE A–41.—Radio Astronomy Explorer (RAE).

Descriptions of subsystems

Communication: FM/PM telemetry at 20.005 Mc and 136.536 Mc.
                              Beacon at 136.738 Mc. Command receiver.
                              Four monopole antennas.
Power supply: Mercury batteries
Onboard propulsion: None
Attitude control: Spin stabilization
Environment control: Passive thermal control
Guidance and control:
Onboard computer: None
Structure: Spherical external aluminum shell 66 cm in
                              diameter. Internal instrument package sepa-
                              rated from shell by transducers installed to
                              measure atmospheric drag (fig. A–42).

Experiments/instruments	*Experimenter*	*Institution*
Accelerometer (table 11–1) _____	Broglio, L.	U. Rome
Ionospheric electron content using beacon signals	Carrara, N.	Microwave Center, Florence

Selected reference: Reference 28
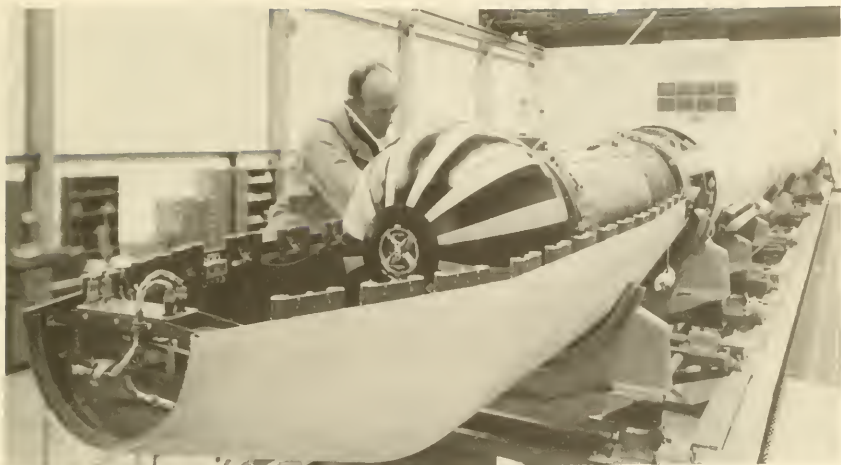
FIGURE A–42.—San Marco 1 being mated to Scout.

SAN MARCO 2

San Marco B
Apr. 26, 1967   Scout   Platform/—
129 kg   —   3°
177/700 km   —   —

San Marco follow-ons are scheduled to be launched from a towable platform
  in the Indian Ocean. San Marco 2 was essentially the same as San Marco 1.

SECOR 1   1964 1C

Sequential Collation of Range Satellite, ERGS 1
Jan. 11, 1964   Thrust-augmented   WTR/STADAN
                          Thor-Agena D
18.2 kg   103.5 min   69.9°
906/930 km   —   —

Secors are piggyback geodetic satellites built for the Army by ITT Federal
  Laboratories. Tracking is done by NASA and special Secor stations.

Descriptions of subsystems
Communication: Telemetry at 136.804 Mc. Secor transponder.
                            Whip antennas.
Power supply: Solar cells and batteries
Onboard propulsion: None
Attitude control:
Environment control:
Guidance and control:
Onboard computer: None
Structure: Box, 22.8 x 27.9 x 35.6 cm (fig. A–43)

Experiments/instruments
Secor transponder only

FIGURE A–43.—Secor 1.

SECOR 2   1965 17B

Sequential Collation of Range Satellite, ERGS 2
Mar. 11, 1965   Thor-Able Star   WTR/STADAN
18 kg   98.0 min   89.9°
331/1000 km   —   —
Second Secor geodetic satellite. See Secor 1 for details. Secor 2 did not
    function as planned.

Descriptions of subsystems
See Secor 1

SECOR 3   1965 16E

Sequential Collation of Range Satellite, ERGS 3
Mar. 9, 1965   Thor-Agena D   WTR/STADAN
18 kg   103.4 min   70.1°
905/940 km   —   —

Descriptions of subsystems
See Secor 1. Housekeeping telemetry on 136.84 Mc.

SECOR 4   1965 27B

Sequential Collation of Range Satellite, ERGS 4
Apr. 3, 1965   Atlas-Agena D   WTR/STADAN
18 kg   111.6 min   90.2°
1280/1310 km   —   —

Descriptions of subsystems
See Secor 1. Failed to operate as planned.

SECOR 5   1965 63A

Sequential Collation of Range Satellite
Aug. 10, 1965   Scout   Wallops/STADAN
20 kg   122.1 min   69.2°
1130/2420 km   —   —

Descriptions of subsystems
Instead of a boxlike structure, this Secor was a polished 51-cm aluminum
   sphere. It also included a magnetic despin device.

SECOR 6   1966 51B

June 9, 1966   Atlas-Agena D   WTR/STADAN
17 kg   125.1 min   90.1°
167/3648 km   —   —

SECOR 7   1966 77B

Aug. 19, 1966   Atlas-Agena D   WTR/STADAN
20 kg   167.6 min   90.1°
3682/3701 km   —   —

SECOR 8   1966 89B

Oct. 5, 1966   Atlas-Agena D   WTR/STADAN
17 kg   167.6 min   90.2°
3680/3710 km   —   —

SLEP

Second Large ESRO Project. Possibly a comet fly-by.
No details known yet

SOLRAD 1   1960 H 2

Greb 1, SR 1, Solar Radiation Satellite 1, Solar Monitoring Satellite, Sunray
   (Greb = Galactic Radiation Energy Background)
June 22, 1960   Thor-Able Star   ETR/Minitrack
19 kg   101.6 min   66.8°
615/1055 km   Nov. 1960   —
First piggyback satellite; launched with Transit 2A. Solrad 1 was the first
   in a long series of satellites built by the Naval Research Laboratory (NRL)
   to monitor solar radiation.

Descriptions of subsystems

Communication: FM/AM telemetry at 108.000 Mc. Command receiver. Tape recorder. Turnstile antenna.
Power supply: Solar cells and NiCd batteries
Attitude control: Spin stabilized; spinup device
Environment control: Passive thermal control
Guidance and control: Photodiode solar-aspect sensor
Onboard computer: None
Structure: 51-cm aluminum sphere (fig. A–44)

Experiments/instruments	*Experimenter*	*Institution*
X-ray ionization chamber (table 12–3)	Friedman, H.	NRL
Two Lyman-α ionization chambers (table 12–3)	Friedman, H.	NRL
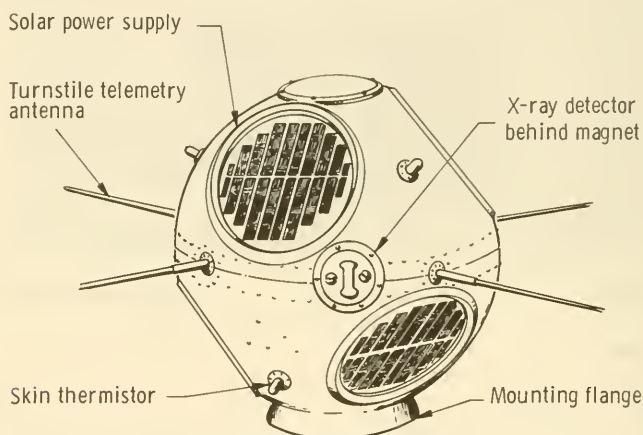
FIGURE A–44.—Solrad 1.

SOLRAD 2

Greb 2. (See Solrad-1 synonyms.)
Nov. 30, 1960   Thor-Able Star   ETR
18 kg
Failed to orbit

SOLRAD 3   1961 O 2

Greb 3. (See Solrad-1 synonyms.)
June 29, 1961   Thor-Able Star   ETR/Minitrack
18 kg   103.8 min   67.0°
860/1020 km   Late 1961   —
Second successful Solrad; launched with Transit 4A and Injun 1. Failed to separate from Injun 1.

Descriptions of subsystems
See Solrad 1.

Experiments/instruments	Experimenter	Institution
Two X-ray ionization chambers (table 12–3)	Friedman, H.	NRL

SOLRAD 4A

Greb 4. (See Solrad-1 synonyms.)
Jan. 24, 1962   Thor-Able Star   ETR
Failed to orbit. Part of Composite 1 five-satellite payload.

SOLRAD 4B

Greb 4B. (See Solrad-1 synonyms.)
Apr. 26, 1962   Scout   WTR
Failed to orbit

SOLRAD 5

Never launched

SOLRAD 6   1963 21C

See Solrad-1 synonyms
June 15, 1963   Thor-Agena D   WTR/STADAN
26 kg   95.1 min   69.9°
176/878 km   Aug. 1, 1963   Aug. 1, 1963

Descriptions of subsystems
Telemetry transmitter at 136.890 Mc. No other details available.

Experiments/instruments	Experimenter	Institution
Four X-ray ionization chambers (table 12–3)	Friedman, H.	NRL
Four Lyman-α ionization chambers (table 12–3)	Friedman, H.	NRL

SOLRAD 7A   1964 1D

Greb 5. (See Solrad-1 synonyms.)
Jan. 11, 1964   Thrust-augmented   WTR/STADAN
                        Thor-Agena D
45 kg   103.5 min   69.9°
906/930 km   —   —

Fourth Solrad success. First in a group of Solrads intended for continuous monitoring of the Sun during the IQSY. These larger Solrads were also constructed by the Naval Research Laboratory and launched piggyback.

Descriptions of subsystems

Communications:	FM/FM telemetry. STADAN beacon. Turnstile antenna.
Power supply:	Six solar-cell patches. Batteries.
Onboard propulsion:	None
Attitude control:	Spin stabilized at 120 rpm
Environment control:	Passive thermal control
Guidance and control:	
Onboard computer:	None
Structure:	

Experiments/instruments	*Experimenter*	*Institution*
Five X-ray ionization chambers (table 12–3)	Friedman, H.	NRL
Lyman-α ionization chamber (table 13–3)	Friedman, H.	NRL

SOLRAD 7B   1965 16D

Solar Radiation, Greb 6. (See Solrad-1 synonyms.)

Mar. 9, 1965	Thor-Agena D	WTR/STADAN
—	103.4 min	70.1°
905/937 km	—	—

Second satellite in NRL IQSY series. Launched with seven other piggyback satellites.

Descriptions of subsystems
Transmitting on 136.801 Mc. No other details available.

Experiments/instruments
No details available

SPUTNIK 1   1957 A 2

Oct. 4, 1957	—	—/—
84 kg	96.2 min	65.1°
227/946 km	Oct. 25, 1957	Jan. 4, 1958

This first satellite was placed in orbit along with the launch-vehicle upper stage. Total mass in orbit was about 2 tons.

Descriptions of subsystems

Communications:	Telemetry at 20.005 and 40.002 Mc. Four whip antennas.
Power supply:	Batteries
Onboard propulsion:	None
Attitude control:	None; unstabilized
Environment control:	Circulation of nitrogen gas in sphere by natural convection
Guidance and control:	None
Onboard computer:	None
Structure:	Polished, hermetically sealed aluminum sphere 58 cm in diameter

Experiments/instruments
Cosmic-ray and micrometeoroid instrumentation

SPUTNIK 2   1957 B 1

Nov. 3, 1957	—	—/—
509 kg	103.7 min	65.3°
225/1670 km	Nov. 10, 1957	Apr. 14, 1958

Sputnik 2, like Sputnik 1, was orbited along with the final stage of the launch vehicle. No figure for payload mass available.

Descriptions of subsystems

Communication:	Telemetry at 20.005 and 40.002 Mc
Power supply:	Batteries
Onboard propulsion:	None

Attitude control:
Environment control: Pressurized cabin with regenerative air conditioning
Guidance and control:
Onboard computer: None
Structure: Two spheres and a cylinder within a tubular structure. Major structural material: aluminum.

Experiments/instruments
Instruments to measure solar X-rays, cosmic rays, solar ultraviolet. Major experiment concerned dog "Laika."

SPUTNIK 3   1958 Δ 2

May 15, 1958	—	—/—
1330 kg	105.8 min	65.2°
225/1880 km	Apr. 6, 1958	Apr. 6, 1960

Sputnik 3 was orbited along with the final stage of the launch vehicle. Total mass in orbit about 3500 kg.

Descriptions of subsystems
Communications: PAM telemetry at 66 Mc. Beacons at 20.004 and 40.008 Mc. Folded dipole antennas.
Power supply: Solar cells and AgZn batteries
Onboard propulsion: None
Attitude control:
Environment control:
Guidance and control:
Onboard computer: None
Structure: Aluminum cone, 3.56 m long, 1.1-m diameter at base (fig. A–45)
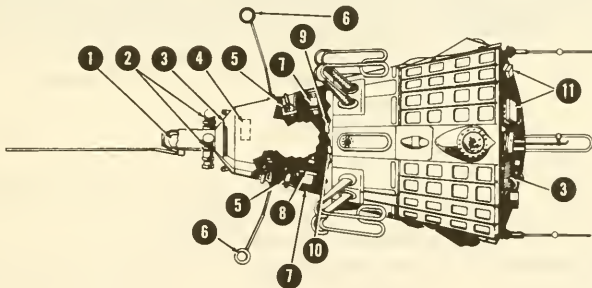
1 Magnetometer
2 Photomultipliers for registration of Sun's corpuscular radiation
3 Solar batteries
4 Device for registration of photons in cosmic rays
5 Magnetic and ionization manometers
6 Ion catchers
7 Electrostatic fluxmeter
8 Mass spectrometric tube
9 Device for registration of heavy nuclei in cosmic rays
10 Device for measuring intensity of primary cosmic radiation
11 Pickups for registration of micrometeoroids

FIGURE A–45.—Sputnik 3.

Experiments/instruments	Experimenter	Institution
Cosmic-ray scintillator (table 13–4)		
Fluxgate magnetometer (table 11–11)		
rf mass spectrometer (table 11–1) _		
Electrostatic fluxmeter (table 11–5)		
Spherical ion trap (table 11–5) ___	Gringauz, K.	USSR
Two scintillation counters (table 11–8)		
Cosmic-ray Cerenkov detector (table 13–4)		
Micrometeoroid microphone (table 11–14)		

SSS

Small Scientific Satellite; SMO, Small Magnetospheric Observatory; SMS, Small Magnetospheric Satellite, Small Solar Satellite, S-cube.

A small, standardized satellite under development at NASA. The SSS will provide inexpensive payload space for experimenters from universities and other research institutions. One objective of the SSS is the continuation of the experiments begun by the EPE (Energetic Particles Explorer) series.

STARAD   1962 BK 1

Starfish Radiation Satellite

Oct. 26, 1962	Thor-Agena D	WTR/—
340 kg	147.8 min	71.4°
193/5560 km	Jan. 18, 1963	—

Starad was launched by the Air Force to chart the decay of the Starfish artificial-radiation belt

Descriptions of subsystems

Communications:	PAM/FM/FM telemetry. Two tape recorders. Command receiver. Quarter-wave stub antennas.
Power supply:	AgZn batteries
Onboard propulsion:	None
Attitude control:	Spin stabilized. Starad actually spun end over end as well as rolled.
Environment control:	Passive thermal control
Guidance and control:	Solar-aspect sensors. Fluxgate magnetometer.
Onboard computer:	None
Structure:	Magnesium frame for instruments and subsystems on standard Agena (fig. A–46)

Experiments/instruments	Experimenter	Institution
Five scintillation counters (table 11–8)	—	AFCRL
Electron spectrometer (table 11–8) _	Bloom, S.	Lawrence Rad. Lab.
Threshold scintillators (table 11–8)_	Smith, R.	Lockheed
Solid-state detectors (table 11–8) __	Dyal, P.	USAF
Scintillator beta-beta-gamma detector (table 11–8)	Paolini, F.	Amer. Sci. and Eng.

Experiments/instruments	Experimenter	Institution
Phoswich proton-alpha spectrometer (table 11–8)	Paolini, F.	Amer. Sci. and Eng.
Scintillator spectrometer (table 11–8)	Paolini, F.	Amer. Sci. and Eng.
Impedance probe (table 11–8) _____	Haycock, O. C.	U. Utah
Tissue-equivalent ionization chamber	Clark, B.	USAF
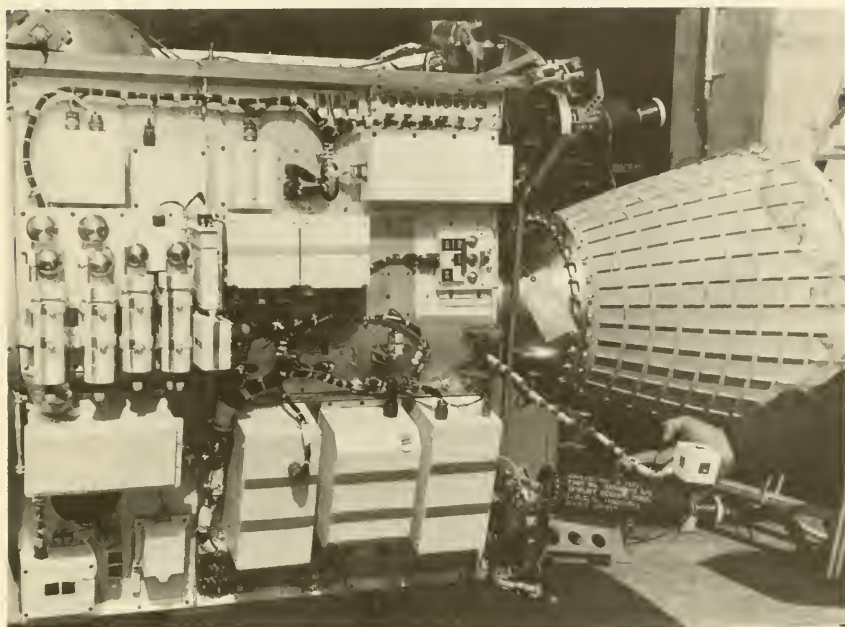
FIGURE A–46.—Starad. (Courtesy of AFCRL.)

TD SERIES

Thor-Delta Satellites

A series of four general-purpose satellites planned by ESRO. Satellite masses will be between 200 and 400 kg; they will be launched by Thor-Deltas. TD 1 is assigned to stellar astronomy and will be launched in 1969. TD 2 is planned for the same year; its experiments will focus on the solar ionosphere.

The instruments for TD 2 have been announced and are listed as follows:

Experiments/instruments	Experimenter	Institution
Topside sounder (table 11–5) _____	Dieminger	Max Planck Iono. Phys. Inst.
Solar Lyman-α hydrogen absorption cell (table 12–3)	Blamont, J.	Aeronomy Lab., Natl. Sci. Res. Center
Ultraviolet spectroheliograph (table 12–3)	Boyd, R. L. F.	University College

Experiments/instruments	Experimenter	Institution
Crystal X-ray spectrometer (table 12–3)	Stewardson, E. A.	U. Leicester
Solar particle experiment (table 13–4)	—	—
Electron flux experiment (table 11–5)	Ratcliffe, J. A.	Slough Res. Sta.
Energy and pitch angle of iono-spheric particles (table 11–5)	Hulqvist	Kiruna Geophys. Obs.
O and N light emissions (table 11–1)	Blamont, J.	CNRS Aeronomy Service
Ion mass spectrometer (table 11–1) _	Priester, W.	U. Bonn Phys. Inst.

TRAAC   1961 AH 2

Transit Research and Attitude Control Satellite

Nov. 15, 1961	Thor-Able Star	ETR/—
109 kg	105.6 min	32.4°
905/1160 km	Aug. 1962	—

Traac was intended to be a test vehicle for a Transit gravity-gradient experiment. Although this engineering experiment failed, Traac returned considerable radiation data.

Descriptions of subsystems
No details available

Experiments/instruments
Six p–n junction detectors (table 11–8)
Two Geiger counters (table 11–8)
p–n neutron detector (table 13–4)

UK-3

UK–E, UK–F, S-53, Ariel 3, International Ionospheric Satellite

May 5, 1967	Scout	WTR/STADAN
80 kg	95.6 min	80°
295/359 km	—	—

The third British satellite. UK–3 was built in Britain by the British Aircraft Corp., while Ariel 1 and Ariel 2 were built in the United States, with Britain supplying the experiments. NASA launched UK-3.

Descriptions of subsystems

Communications:	PFM/PM telemetry at 136 Mc. Tape recorder. Command receiver. Canted turnstile antenna.
Power supply:	n–p solar cells plus NiCd batteries produce 5 W in the Earth's shadow and 12 W in sunlight
Onboard propulsion:	None
Attitude control:	Spin stabilized. Yo-yo despin plus despin through boom erection.
Environment control:	Passive thermal control
Guidance and control:	
Onboard computer:	None
Structure:	75-cm diameter, 109 cm long (fig. A–47)

FIGURE A–47.—UK-3.

Experiments/instruments	Experimenter	Institution
rf capacitance bridge (table 11–5) _	Sayers, J.	U. Birmingham
Galactic-noise receiver (table 13–1) _	Smith, F. G.	U. Manchester
vlf receiver (table 11–5) _____	Kaiser, T. R.	U. Sheffield
O₂-scanning photometer (table 11–1)	Frith, R.	Meteorological Office
Natural terrestrial radio-noise experiment (table 11–5)	Ratcliffe, J. A.	Radio and Space Research Station, Slough

VANGUARD TV SERIES

Three Vanguard Test Vehicles had the potentiality of launching satellites in late 1957 and early 1958, although their main purpose was system testing. Unfortunately, these three failures were widely publicized as satellite-launch failures, rather than tests. These vehicles were:

Vanguard TV III, Dec. 6, 1957
Vanguard TV III backup, Feb. 5, 1958
Vanguard TV V, Apr. 28, 1958

VANGUARD SLV SERIES

A number of shots in the Vanguard Satellite Launch Vehicle series were failures. These are listed as follows:

    Vanguard SLV I, May 27, 1958
    Vanguard SLV II, June 26, 1958
    Vanguard SLV III, Sept. 26, 1958
    Vanguard SLV V, Apr. 13, 1959
    Vanguard SLV VI, June 22, 1959

VANGUARD I   1958 B 2

Mar. 17, 1958	Vanguard	ETR/Minitrack
1.5 kg	134.3 min	34.3°
652/3960 km	May 1964	—

The Vanguard IGY satellite program was directed by the Naval Research Laboratory. Martin Co. was the prime contractor. The intent was to orbit at least one satellite during the IGY.

Descriptions of subsystems

Communications:	Battery-powered transmitter at 108.00 Mc. Solar-cell-powered transmitter at 108.03 Mc. Turnstile and dipole antennas.
Power supply:	Solar cells and mercury batteries
Onboard propulsion:	None
Attitude control:	None, unstabilized
Environment control:	Passive thermal control
Guidance and control:	None
Onboard computer:	None
Structure:	Aluminum sphere 16.5 cm in diameter (fig. 2–4)

Experiments/instruments	*Experimenter*	*Institution*
Geiger counter (table 11–8) _____	—	—
Micrometeoroid gage (table 11–14) _	—	—
Proton-precession magnetometer (table 11–11)	Heppner, J. P.	NRL

VANGUARD II   1959 A 1

Feb. 17, 1959	Vanguard	ETR/Minitrack
10 kg	125.9 min	32.9°
559/3320 km	Mar. 6, 1959	—

By the time Vanguard II was launched, NASA had been created and the whole program had been transferred out of NRL. The prime purpose of Vanguard II was study of the Earth's cloud cover. Satellite wobble degraded the data. According to the definitions employed in this book, Vanguard II was an Applications Satellite.

Descriptions of subsystems

Communications:	Telemetry transmitter at 108.03 Mc. Minitrack beacon at 108.00 Mc. Command receiver. Tape recorder. Turnstile antenna.
Power supply:	Mercury batteries
Onboard propulsion:	None
Attitude control:	Spin stabilized at 50 rpm
Environment control:	Passive thermal control

Guidance and control:
Onboard computer: None
Structure: Magnesium sphere 50.8 cm in diameter

Experiments/instruments
Four photocells, two optical telescopes provided by the Army Signal R&D
    Laboratory

VANGUARD III   1959 E 1

Magne-Ray Satellite

Sept. 18, 1959	Vanguard	ETR/Minitrack
45 kg	130.2 min	33.3°
511/3750 km	Dec. 11, 1959	—

The third successful Vanguard satellite was orbited with the final stage of
    the launch vehicle, accounting for the high in-orbit mass

Descriptions of subsystems
Communications: Beacon and real-time telemetry at 108.00 Mc.
                        Burst telemetry at 108.03 Mc. Command re-
                        ceiver. Tape recorder.
Power supply: AgZn batteries
Onboard propulsion: None
Attitude control: Spin stabilized
Environment control: Passive thermal control
Guidance and control:
Onboard computer: None
Structure: Magnesium sphere 50.8 cm in diameter. 66-cm
                        magnetometer boom (fig. A–48)

Experiments/instruments	*Experimenter*	*Institution*
Proton-precession magnetometer (table 11–14)	Heppner, J. P.	GSFC
Microphone micrometeoroid detector (table 11–14)	LaGow, H. E.	GSFC
Resistive-strip micrometeoroid detectors (table 11–14)	LaGow, H. E.	GSFC
Light-transmission micrometeoroid detector (table 11–14)	LaGow, H. E.	GSFC
Pressurized-cell micrometeoroid detector (table 11–14)	LaGow, H. E.	GSFC
Two solar X-ray ionization chambers (table 12–3)	Friedman, H.	NRL

X-RAY EXPLORER

A relatively new NASA satellite program. Presently in the study phase, the
    objective is to provide a series of satellites carrying X-ray detectors that
    can survey the sky in a more complete and systematic fashion than is now
    possible with sounding rockets.

NONE   1963 38C

Sept. 28, 1963	Thor-Able Star	WTR/STADAN, TRANET
55 kg	107.4 min	89.9°
1070/1130 km	—	—
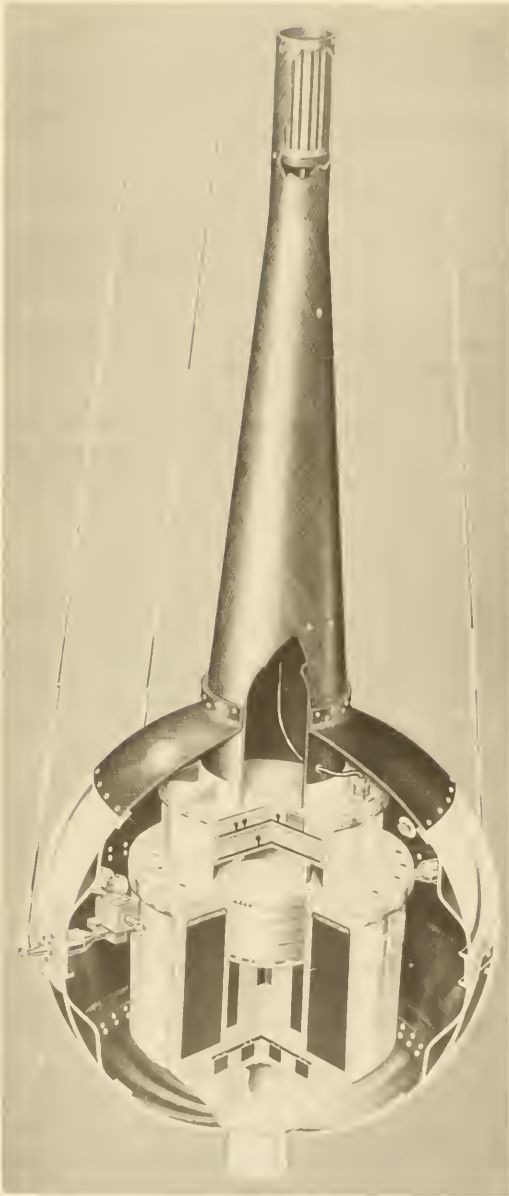
FIGURE A–48.—Vanguard III.

This satellite typifies the numerous scientific satellites that have been launched
under military auspices and rarely are found in the literature. This satellite
was built by the Johns Hopkins Applied Physics Laboratory for the Navy.

Descriptions of subsystems

Communications: Telemetry at 136.650 Mc. Doppler beacons at
162 and 324 Mc.

Power supply:	Four solar-cell paddles and NiCd batteries
Onboard propulsion:	None
Attitude control:	Magnetically stabilized by bar magnet. Four magnetic hysteresis rods provide spin and oscillation damping.
Environment control:	
Guidance and control:	Three-axis fluxgate magnetometer
Onboard computer:	None
Structure:	Octagonal cylinder with 4 solar paddles (fig. A–49)

Experiments/instruments

Solid-state electron spectrometer

Solid-state proton spectrometer

Three omnidirectional solid-state detectors
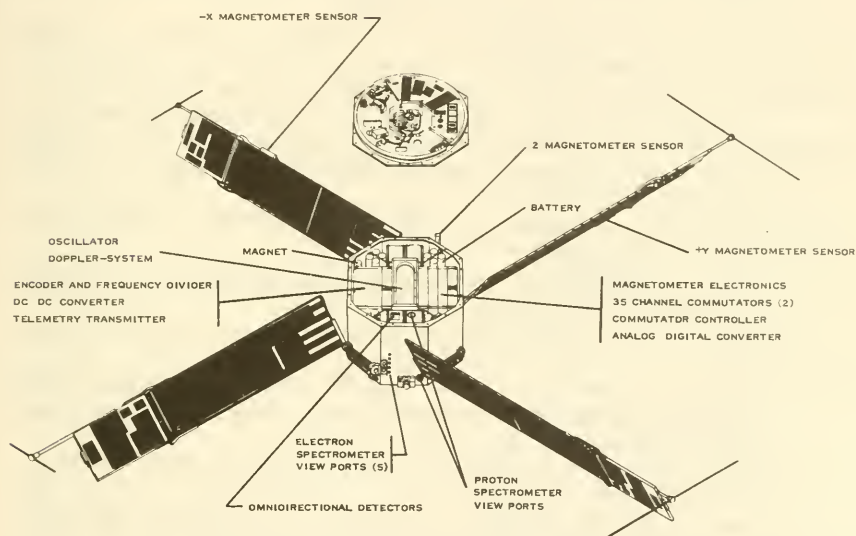
FIGURE A–49.—The 1963 38C.

References

1. MOLOZZI, A. R.: Instrumentation of the Ionospheric Sounder Contained in the Satellite 1962 Beta Alpha (Alouette). *In* Space Research IV, P. Muller, ed., John Wiley & Sons, 1964.
2. NEWTON, R. R.: Geodesy by Satellite. Science, vol. 144, May 15, 1964, p. 803.
3. HYMOWITZ, E. W.; AND WATSON, H. M.: The UK–2/S–52 International Satellite. *In* Proceedings of the 10th Annual East Coast Conference on Aerospace and Navigational Electronics. Western Periodicals Co. (North Hollywood), 1963.
4. STAMBLER, I.: Bioscience in Orbit. Space/Aero., vol. 44, July 1965, p. 46.
5. SAUNDERS, J. F.; JENKINS, D. W.; AND DALLOW, T. P.: The NASA Biosatellite Program. Astronaut. Aeron., vol. 4, Jan. 1966, p. 48.

6. WALTER, D. O.: Biosatellite Program. *In* NASA SP–72, 1964.
7. WETMORE, W. C.: FR–1 Bolsters French Civil Space Ambition. Av. Wk., Jan. 10, 1966, p. 54.
8. WETMORE, W. C.: D–1A Bolsters French Space Aspirations. Av. Wk., Apr. 18, 1966, p. 111.
9. COFFEE, C. W.; BRESSETTE, W. E.; AND KEATING, G. M.: Design of the NASA Lightweight Inflatable Satellite for the Determination of Atmospheric Density at Extreme Altitudes. NASA TN D–1243, 1962.
10. EHRLICH, E.: NASA Particles and Fields Spacecraft. AIAA paper 64–337, 1964.
11. D'AIUTOLO, C. T., coordinator: The Micrometeoroid Satellite Explorer XIII (1961 Chi). NASA TN D–2468, 1964.
12. HASTINGS, E. C.: The Explorer XVI Micrometeoroid Satellite. NASA TM X–810, 1963.
13. HOROWITZ, R.: S–6, an Aeronomy Satellite. *In* Scientific Satellites, I. E. Jeter, ed., Western Periodicals Co., 1963.
14. SPENCER, N. W.: The Explorer XVII Satellite. Planetary and Space Sci., vol. 13, July 1965, p. 593.
15. BUTLER, P.: The IMP–I (Explorer XVIII) Satellite. *In* Record of the 1964 International Space Electronics Symposium. IEEE, 1964.
16. BLUMLE, J. J.; FITZENREITER, R. J.; AND JACKSON, J. E.: The National Aeronautics and Space Administration Topside Sounder Program. NASA TN D–1913, 1963.
17. BOURDEAU, R. E.: Description of the S–66 Spacecraft. COSPAR Info. Bull., no. 15, May 1963.
18. O'NEAL, R. L., compiler: The Explorer XXIII Micrometeoroid Satellite. NASA TM X–1123, 1965.
19. NEWTON, R. R.: Characteristics of the Geos A Spacecraft. AD 463141, 1964.
20. O'BRIEN, B. J.; LAUGHLIN, C. D.; AND GURNETT, D. A.: High Latitude Geophysical Studies With Satellite Injun 3—Description of the Satellite. J. Geophys. Res., vol. 69, Jan. 1, 1964, p. 1.
21. ROGERSON, J. B.: The Orbiting Astronomical Observatories. Space Sci. Rev., vol. 2, 1963, p. 621.
22. LUDWIG, G. H.: The Orbiting Astronomical Observatories. Space Sci. Rev., vol. 2, 1963, p. 175. (Also available in NASA TN D–2646, 1965.)
23. DOLDER, F. P., ET AL.: The Orbiting Solar Observatory Spacecraft. *In* Space Research III, W. Priester, ed., John Wiley & Sons, 1963. (Also available in NASA TM X–55038, 1964.)
24. MUINCH, G.; AND ARMSTRONG, W. C.: Development and Management of a Low Cost Satellite. Unmanned Spacecraft Meeting. AIAA pub. CP–12, 1965.
25. ROSENTHAL, R. D.: The Pegasus Meteoroid Technology Satellite. Unmanned Spacecraft Meeting. AIAA pub. CP–12, 1965.
26. FINK, D. E.: RAE to Utilize 750–1,000-ft. Antennas. Av. Wk., Sept. 27, 1965, p. 106.
27. STONE, R. G.: RAE—1500-ft. Antenna Satellite. Astronaut. Aeron., vol. 3, Mar. 1965, p. 46.
28. BROGLIO, L.: The San Marco 1–A Scientific Satellite. Paper at the 16th International Astronautical Congress, 1965.

Index

SCIENTIFIC SATELLITES

Date Due